VOLUME 24 / NUMBER 1
JANUARY 8, 1986
ACC. NOS. N86-10001 TO N86-11144

STAR
AN ABSTRACT JOURNAL

Scientific and Technical Aerospace Reports

PRODUCED BY THE
SCIENTIFIC AND TECHNICAL
INFORMATION
BRANCH

NASA

NATIONAL AERONAUTICS AND SPACE ADMINISTRATION

WHAT YOU CAN DO FOR *STAR*

All users of this abstract service are urged to forward reports to be considered for announcement in *STAR*. This will aid NASA in its efforts to provide the fullest possible coverage of all scientific and technical publications that might support aeronautics and space research and development. If you have prepared relevant reports (other than those that you will transmit to NASA, DoD, or DOE through the usual contract- or grant-reporting channels), please send them for consideration to the NASA Scientific and Technical Information Facility, P.O. Box 8757, B.W.I. Airport, Maryland 21240.

Reprints of journal articles, book chapters, and conference papers are also welcome. These will be considered for announcement in *STAR's* companion journal, *International Aerospace Abstracts*.

You may specify a particular source to be included in a report announcement if you wish; otherwise the report will be placed on public sale at the National Technical Information Service. Copyrighted publications will be announced but not distributed or sold.

PURCHASE OF *STAR*

The semimonthly issues are available for sale by the Superintendent of Documents, U.S. Government Printing Office, Washington, D.C. 20402.

PUBLISHED BY:

UNITED STATES GOVERNMENT
NATIONAL AERONAUTICS AND SPACE ADMINISTRATION
SCIENTIFIC AND TECHNICAL INFORMATION BRANCH
Scientific and Technical Aerospace Reports, Volume 24, is prepared by the NASA Scientific and Technical Information Facility operated for the National Aeronautics and Space Administration by RMS Associates.

The Administrator of the National Aeronautics and Space Administration has determined that the publication of this periodical is necessary in the transaction of the public business required by law of this Agency. Use of funds for printing this periodical has been approved by the Director of the Office of Management and Budget through March 22, 1988.

US ISSN 0036-8741

INTRODUCTION

Scientific and Technical Aerospace Reports (STAR) is a major component of a comprehensive National Aeronautics and Space Administration information system covering aeronautics, space, and supporting disciplines. *STAR* is issued on the 8th and 23rd of each month and announces current publications of the following types:

- NASA, NASA contractor, and NASA grantee reports
- Reports issued by other U.S. Government agencies, domestic and foreign institutions, universities, and private firms
- Translations in report form
- NASA-owned patents and patent applications
- Dissertations and theses

Cumulative index volumes are published annually.

Journal, book, and conference literature, cover-to-cover journal translations, and certain foreign dissertations are announced in a companion journal, *International Aerospace Abstracts (IAA)*, available on subscription from the American Institute of Aeronautics and Astronautics, Technical Information Service, 555 West 57th Street, 12th Floor, New York, New York 10019.

SUBJECT SCOPE

Subject scope of *STAR*, and *IAA* includes all aspects of aeronautics and space research and development, supporting basic and applied research, and applications. Aerospace aspects of earth resources, energy development, conservation, oceanography, environmental protection, urban transportation, and other topics of high national priority are also covered.

OTHER NASA PUBLICATIONS

Other NASA publications and information services are described in the publication, *The NASA Scientific and Technical Information System ... and How to Use It*, available without charge from the NASA Scientific and Technical Information Facility, P.O. Box 8757, B.W.I. Airport, Maryland 21240.

HOW TO USE *STAR* SUBJECT CATEGORIES

STAR is categorized by 10 major subject divisions divided into 74 specific subject categories and one general category/division. The major subject divisions are listed in the Table of Contents, together with a note for each that defines its scope and provides any cross-references. For example:

AERONAUTICS

Includes aeronautics (general); aerodynamics; air transportation and safety; aircraft communications and navigation; aircraft design, testing and performance; aircraft instrumentation; aircraft propulsion and power; aircraft stability and control; and research and support facilities (air).

For related information see also *Astronautics*.

Each major division is further divided into as many as nine specific categories, which are identified by category numbers.

Abstracts in *STAR* are grouped by specific category, the categories appearing in sequential order. Category breaks in the abstract section are identified by the category number and title, and a scope note. Cross-references to other categories are provided as appropriate. For example:

02 AERODYNAMICS

Includes aerodynamics of bodies, combinations, wings, rotors, and control surfaces; and internal flow in ducts and turbomachinery.

For related information see also *34 Fluid Mechanics and Heat Transfer.*

CROSS-REFERENCES

Individual *STAR* abstracts are not ordinarily cross-referenced, except for certain conference reports or book translations that have had separate abstracts written for their component papers or chapters. Citations and abstracts of the components follow immediately after those of the parent document. When the subject content of a component differs sufficiently from the general content of the parent, a cross-reference citation also is printed at the end of the category to which it normally would have been assigned if it were independent.

DOCUMENTS ON MICROFICHE

Documents on microfiche(1) are designated by a pound sign (#) following the accession number. The pound sign is used without regard to the source or quality of the microfiche.

AVAILABILITIES

One or more sources from which a document announced in *STAR* is available to the public is given in each citation. The most commonly indicated sources and their acronyms or abbreviations are listed below. If the publication is available from a source other than those listed, the publisher and his address will be displayed on the availability line or in combination with the corporate source line.

(1) A microfiche is a transparent sheet of film, 105 by 148 mm in size, containing as many as 60 to 98 pages of information reduced to micro images (not to exceed 26:1 reduction).

Avail: NTIS. Sold by the National Technical Information Service. Prices for hard copy (HC) and microfiche (MF) are indicated by a price code following the letters HC or MF in the *STAR* citation. Current values for the price codes are given in the tables on page vii.

Initially distributed microfiche under the NTIS SRIM (Selected Research in Microfiche) is available at greatly reduced unit prices. For this service and for information concerning subscription to NASA printed reports, consult the NTIS Subscription Section, Springfield, Va. 22161.

NOTE ON ORDERING DOCUMENTS: When ordering NASA publications (those followed by the * symbol), use the N accession number. NASA patent applications (only the specifications are offered) should be ordered by the US-Patent-Appl-SN number. Non-NASA publications (no asterisk) should be ordered by the AD, PB, or other *report* number shown on the last line of the citation, not by the N accession number. It is also advisable to cite the title and other bibliographic identification.

Avail: SOD (or GPO). Sold by the Superintendent of Documents, U.S. Government Printing Office, in hard copy. The current price and order number are given following the availability line. (NTIS will fill microfiche requests, as indicated above, for those documents identified by a # symbol.)

Avail: NASA Public Document Rooms. Documents so indicated may be examined at or purchased from the National Aeronautics and Space Adminstration, Public Documents Room (Room 126), 600 Independence Ave., S.W., Washington, D.C. 20546, or public document rooms located at each of the NASA research centers, the NASA Space Technology Laboratories, and the NASA Pasadena Office at the Jet Propulsion Laboratory.

Avail: DOE Depository Libraries. Organizations in U.S. cities and abroad that maintain collections of Department of Energy reports, usually in microfiche form, are listed in *Energy Research Abstracts*. Services available from the DOE and its depositories are described in a booklet, *DOE Technical Information Center - Its' Functions and Services* (TID-4660), which may be obtained without charge from the DOE Technical Information Center.

Avail: Univ. Microfilms. Documents so indicated are dissertations selected from *Dissertation Abstracts* and are sold by University Microfilms as xerographic copy (HC) and microfilm. All requests should cite the author and the Order Number as they appear in the citation.

Avail: USGS. Originals of many reports from the U.S. Geological Survey, which may contain color illustrations, or otherwise may not have the quality of illustrations preserved in the microfiche or facsimile reproduction, may be examined by the public at the libraries of the USGS field offices whose addresses are listed in this Introduction. The libraries may be queried concerning the availability of specific documents and the possible utilization of local copying services, such as color reproduction.

Avail: HMSO. Publications of Her Majesty's Stationery Office are sold in the U.S. by Pendragon House, Inc. (PHI), Redwood City, California. The U.S. price (including a service and mailing charge) is given, or a conversion table may be obtained from PHI.

Avail: BLL (formerly NLL): British Library Lending Division, Boston Spa, Wetherby, Yorkshire, England. Photocopies available from this organization at the price shown. (If none is given, inquiry should be addressed to the BLL.)

Avail: Fachinformationszentrum, Karlsruhe. Sold by the Fachinformationszentrum Energie, Physik, Mathematik GMBH, Eggenstein Leopoldshafen, Federal Republic of Germany, at the price shown in deutschmarks (DM).

Avail: Issuing Activity, or Corporate Author, or no indication of availability. Inquiries as to the availability of these documents should be addressed to the organization shown in the citation as the corporate author of the document.

Avail: U.S. Patent and Trademark Office. Sold by Commissioner of Patents and Trademarks, U.S. Patent and Trademark Office, at the standard price of 50 cents each, postage free. (See discussion of patents and patent applications below.)

Avail: ESDU. Pricing information on specific data, computer programs, and details on ESDU topic categories can be obtained from ESDU International Ltd. Requesters in North America should use the Virginia address while all other requesters should use the London address, both of which are on page vi.

NASA PATENTS AND PATENT APPLICATIONS

Patents and patent applications owned by NASA are announced in *STAR* under appropriate subject categories and are referenced in the *STAR* indexes. In the Report/Accession Number Index, patents are indexed by the NASA Case Number (which appears in lieu of the report number in other indexes), the U.S. Patent Number, the U.S. Patent Application Serial Number, and the U.S. Patent Class. Patent applications for which patents have not yet been issued are indexed by the NASA Case Number and the U.S. Patent Application Serial Number.

NASA *patent application specifications* are sold in paper copy by the National Technical Information Service at price code A02 ($9.95 domestic; $19.90 foreign). Microfiche are sold at price code A01 ($5.95 domestic; $11.90 foreign). The US-Patent-Appl-SN- number should be used in ordering either paper copy or microfiche from NTIS. Printed copies of *patents* (which are not microfiched) are available for purchase at 50 cents per copy from:

Commissioner of Patents and Trademarks
U.S. Patent and Trademark Office
Washington, D.C. 20231

When ordering patents, the U.S. Patent Number should be used, and payment must be remitted in advance, preferably by money order or check payable to the Commissioner of Patents and Trademarks. Prepaid purchase coupons for ordering are also available from the Patent and Trademark Office. The patents and patent applications announced in *STAR* are owned by NASA and are available for royalty-free licensing. Requests for licensing terms and further information should be addressed to:

Assistant General Counsel for Patent Matters/Code GP-1
National Aeronautics and Space Administration
Washington, D.C. 20546

ELIGIBILITY AND REGISTRATION FOR NASA INFORMATION PRODUCTS AND SERVICES

A variety of services is available to organizations of the following types that have registered with NASA to receive specific services or products:

1. NASA offices, research centers, contractors, subcontractors, grantees, and consultants;
2. Other U.S. Government agencies and their contractors;
3. Libraries in the United States that have arrangements with NASA to maintain collections of NASA documents for public reference;
4. Other organizations in the United States having a need for NASA documents in work related to aeronautics and space research;
5. Organizations abroad that have established reciprocal document exchange arrangements with NASA.

Only the central service points or central points of document acquisition and control within qualified organizations are eligible to register for NASA products and services. Domestic organizations that may be eligible to receive various classes of NASA publications and services should address their requests for registration or for further information to:

NASA Scientific and Technical Information Facility
ATTN: Registration Activity
P.O. Box 8757
B.W.I. Airport, Maryland 21240

Organizations abroad should direct requests to the same address, but to the attention of: International Exchange Program.

AVAILABILITY OF *STAR* ABSTRACTS ON MICROFICHE

Microfiche of the abstract sections of this issue and other issues of *STAR* are available on annual subscription from NTIS, Attn: Subscriptions, 5285 Port Royal Road, Springfield, Virginia 22161. Annual subscription rates are $60.00 North America; $120.00 foreign. Abstract sections for previous years retroactive to 1964 are available at the current rates. Microfiche for individual *STAR* issue abstract sections are not available.

PUBLIC COLLECTIONS OF NASA DOCUMENTS

DOMESTIC: NASA and NASA-sponsored documents and a large number of aerospace publications are available to the public for reference purposes at the library maintained by the American Institute of Aeronautics and Astronautics, Technical Information Service, 555 West 57th Street, 12th Floor, New York, New York 10019.

EUROPEAN: An extensive collection of NASA and NASA-sponsored publications is maintained by the British Library Lending Division, Boston Spa, Wetherby, Yorkshire, England for public access. The British Library Lending Division also has available many of the non-NASA publications cited in *STAR*. European requesters may purchase facsimile copy or microfiche of NASA and NASA-sponsored documents, those identified by both the symbols # and * from ESA - Information Retrieval Service European Space Agency, 8-10 rue Mario-Nikis, 75738 Paris CEDEX 15, France.

FEDERAL DEPOSITORY LIBRARY PROGRAM

In order to provide the general public with greater access to U.S. Government publications, Congress established the Federal Depository Library Program under the Government Printing Office (GPO), with 50 regional depositories responsible for permanent retention of material, inter-library loan, and reference services. Over 1,300 other depositories also exist. A list of the regional GPO libraries appears on the inside back cover of *STAR*.

ADDRESSES OF ORGANIZATIONS

American Institute of Aeronautics and Astronautics
Technical Information Service
555 West 57th Street, 12th Floor
New York, New York 10019

British Library Lending Division,
Boston Spa, Wetherby, Yorkshire,
England

Commissioner of Patents and Trademarks
U.S. Patent and Trademark Office
Washington, D.C. 20231

Department of Energy
Technical Information Center
P.O. Box 62
Oak Ridge, Tennessee 37830

ESA-Information Retrieval Service
ESRIN
Via Galileo Galilei
00044 Frascati (Rome) Italy

ESDU International, Ltd.
1495 Chain Bridge Road
McLean, Virginia 22101

ESDU International, Ltd.
251-259 Regent Street
London, W1R 7AD, England

Fachinformationszentrum Energie, Physik, Mathematik GMBH
7514 Eggenstein Leopoldshafen
Federal Republic of Germany

Her Majesty's Stationery Office
P.O. Box 569, S.E. 1
London, England

NASA Scientific and Technical Information Facility
P.O. Box 8757
B.W.I. Airport, Maryland 21240

National Aeronautics and Space Administration
Scientific and Technical Information Branch (NIT-1)
Washington, D.C. 20546

National Technical Information Service
5285 Port Royal Road
Springfield, Virginia 22161

Pendragon House, Inc.
899 Broadway Avenue
Redwood City, California 94063

Superintendent of Documents
U.S. Government Printing Office
Washington, D.C. 20402

University Microfilms
A Xerox Company
300 North Zeeb Road
Ann Arbor, Michigan 48106

University Microfilms, Ltd.
Tylers Green
London, England

U.S. Geological Survey Library
National Center – MS 950
12201 Sunrise Valley Drive
Reston, Virginia 22092

U.S. Geological Survey Library
2255 North Gemini Drive
Flagstaff, Arizona 86001

U.S. Geological Survey
345 Middlefield Road
Menlo Park, California 94025

U.S. Geological Survey Library
Box 25046
Denver Federal Center, MS 914
Denver, Colorado 80225

NTIS PRICE SCHEDULES

(Effective October 1, 1985)

Schedule A
STANDARD PRICE DOCUMENTS AND MICROFICHE

PRICE CODE	PAGE RANGE	NORTH AMERICAN PRICE	FOREIGN PRICE
A01	Microfiche	$ 5.95	$11.90
A02-A03	001-050	9.95	19.90
A04-A05	051-100	11.95	23.90
A06-A09	101-200	16.95	33.90
A10-A13	201-300	22.95	45.90
A14-A17	301-400	28.95	57.90
A18-A21	401-500	34.95	69.90
A22-A25	501-600	40.95	81.90
A99	601-up	*	*
NO1		$40.00	70.00
NO2		40.00	70.00

Schedule E
EXCEPTION PRICE DOCUMENTS AND MICROFICHE

PRICE CODE	NORTH AMERICAN PRICE	FOREIGN PRICE
E01	$ 7.50	15.00
E02	10.00	20.00
E03	11.00	22.00
E04	13.50	27.00
E05	15.50	31.00
E06	18.00	36.00
E07	20.50	41.00
E08	23.00	46.00
E09	25.50	51.00
E10	28.00	56.00
E11	30.50	61.00
E12	33.00	66.00
E13	35.50	71.00
E14	38.50	77.00
E15	42.00	84.00
E16	46.00	92.00
E17	50.00	100.00
E18	54.00	108.00
E19	60.00	120.00
E20	70.00	140.00
E99	*	*

*Contact NTIS for price quote.

IMPORTANT NOTICE

NTIS Shipping and Handling Charges (effective June 1, 1985)

U.S., Canada, Mexico — ADD $3.00 per TOTAL ORDER

All Other Countries — ADD $4.00 per TOTAL ORDER

Exceptions — Does NOT apply to:

ORDERS REQUESTING NTIS RUSH HANDLING

ORDERS FOR SUBSCRIPTION OR STANDING ORDER PRODUCTS *ONLY*

NOTE: Each additional delivery address on an order requires a separate shipping and handling charge.

VOLUME 24 NUMBER 1 / JANUARY 8, 1986

TABLE OF CONTENTS

AERONAUTICS

Includes aeronautics (general); aerodynamics; air transportation and safety; aircraft communications and navigation; aircraft design, testing and performance; aircraft instrumentation; aircraft propulsion and power; aircraft stability and control; and research and support facilities (air).

For related information see also *Astronautics.*

01 AERONAUTICS (GENERAL) 1

02 AERODYNAMICS 3

Includes aerodynamics of bodies, combinations, wings, rotors, and control surfaces; and internal flow in ducts and turbomachinery.

For related information see also *34 Fluid Mechanics and Heat Transfer*

03 AIR TRANSPORTATION AND SAFETY 6

Includes passenger and cargo air transport operations; and aircraft accidents.

For related information see also *16 Space Transportation* and *85 Urban Technology and Transportation.*

04 AIRCRAFT COMMUNICATIONS AND NAVIGATION N.A.

Includes digital and voice communication with aircraft; air navigation systems (satellite and ground based); and air traffic control.

For related information see also *17 Spacecraft Communications, Command and Tracking* and *32 Communications.*

05 AIRCRAFT DESIGN, TESTING AND PERFORMANCE 6

Includes aircraft simulation technology.

For related information see also *18 Spacecraft Design, Testing and Performance* and *39 Structural Mechanics.*

06 AIRCRAFT INSTRUMENTATION N.A.

Includes cockpit and cabin display devices; and flight instruments.

For related information see also *19 Spacecraft Instrumentation* and *35 Instrumentation and Photography.*

07 AIRCRAFT PROPULSION AND POWER N.A.

Includes prime propulsion systems and systems components, e.g., gas turbine engines and compressors; and on-board auxiliary power plants for aircraft.

For related information see also *20 Spacecraft Propulsion and Power, 28 Propellants and Fuels,* and *44 Energy Production and Conversion.*

08 AIRCRAFT STABILITY AND CONTROL 8

Includes aircraft handling qualities; piloting; flight controls; and autopilots.

09 RESEARCH AND SUPPORT FACILITIES (AIR) 9

Includes airports, hangars and runways; aircraft repair and overhaul facilities; wind tunnels; shock tube facilities; and engine test blocks.

For related information see also *14 Ground Support Systems and Facilities (Space).*

ASTRONAUTICS

Includes astronautics (general); astrodynamics; ground support systems and facilities (space); launch vehicles and space vehicles; space transportation; spacecraft communications, command and tracking; spacecraft design, testing and performance; spacecraft instrumentation; and spacecraft propulsion and power.

For related information see also *Aeronautics*

12 ASTRONAUTICS (GENERAL) 9

For extraterrestrial exploration see *91 Lunar and Planetary Exploration.*

13 ASTRODYNAMICS 35

Includes powered and free-flight trajectories; and orbit and launching dynamics.

14 GROUND SUPPORT SYSTEMS AND FACILITIES (SPACE) 35

Includes launch complexes, research and production facilities; ground support equipment, e.g., mobile transporters; and simulators.

For related information see also *09 Research and Support Facilities (Air).*

15 LAUNCH VEHICLES AND SPACE VEHICLES 36

Includes boosters; manned orbital laboratories; reusable vehicles; and space stations.

16 SPACE TRANSPORTATION 36

Includes passenger and cargo space transportation, e.g., shuttle operations; and rescue techniques.

For related information see also *03 Air Transportation and Safety* and *85 Urban Technology and Transportation.*

17 SPACECRAFT COMMUNICATION, COMMAND AND TRACKING 46

Includes telemetry; space communications networks; astronavigation; and radio blackout.

For related information see also *04 Aircraft Communications and Navigation* and *32 Communications.*

18 SPACECRAFT DESIGN, TESTING AND PERFORMANCE 46

Includes spacecraft thermal and environmental control; and attitude control.

For life support systems see *54 Man/System Technology and Life Support.* For related information see also *05 Aircraft Design, Testing and Performance* and *39 Structural Mechanics.*

19 SPACECRAFT INSTRUMENTATION 48

For related information see also *06 Aircraft Instrumentation* and *35 Instrumentation and Photography.*

20 SPACECRAFT PROPULSION AND POWER 48

Includes main propulsion systems and components, e.g., rocket engines; and spacecraft auxiliary power sources.

For related information see also *07 Aircraft Propulsion and Power, 28 Propellants and Fuels,* and *44 Energy Production and Conversion.*

CHEMISTRY AND MATERIALS

Includes chemistry and materials (general); composite materials; inorganic and physical chemistry; metallic materials; nonmetallic materials; and propellants and fuels.

23 CHEMISTRY AND MATERIALS (GENERAL) 49
Includes biochemistry and organic chemistry.

24 COMPOSITE MATERIALS 49
Includes laminates.

25 INORGANIC AND PHYSICAL CHEMISTRY 51
Includes chemical analysis, e.g., chromatography; combustion theory; electrochemistry; and photochemistry.
For related information see also *77 Thermodynamics and Statistical Physics.*

26 METALLIC MATERIALS 53
Includes physical, chemical, and mechanical properties of metals, e.g., corrosion; and metallurgy.

27 NONMETALLIC MATERIALS 57
Includes physical, chemical, and mechanical properties of plastics, elastomers, lubricants, polymers, textiles, adhesives, and ceramic materials.

28 PROPELLANTS AND FUELS 60
Includes rocket propellants, igniters, and oxidizers; storage and handling; and aircraft fuels.
For related information see also *07 Aircraft Propulsion and Power, 20 Spacecraft Propulsion and Power,* and *44 Energy Production and Conversion.*

ENGINEERING

Includes engineering (general); communications; electronics and electrical engineering; fluid mechanics and heat transfer; instrumentation and photography; lasers and masers; mechanical engineering; quality assurance and reliability; and structural mechanics.
For related information see also *Physics.*

31 ENGINEERING (GENERAL) 61
Includes vacuum technology; control engineering; display engineering; and cryogenics.

32 COMMUNICATIONS 62
Includes land and global communications; communications theory; and optical communications.
For related information see also *04 Aircraft Communications and Navigation* and *17 Spacecraft Communications, Command and Tracking.*

33 ELECTRONICS AND ELECTRICAL ENGINEERING 69
Includes test equipment and maintainability; components, e.g., tunnel diodes and transistors; microminiaturization; and integrated circuitry.
For related information see also *60 Computer Operations and Hardware* and *76 Solid-State Physics.*

34 FLUID MECHANICS AND HEAT TRANSFER 75
Includes boundary layers; hydrodynamics; fluidics; mass transfer; and ablation cooling.
For related information see also *02 Aerodynamics* and *77 Thermodynamics and Statistical Physics.*

35 INSTRUMENTATION AND PHOTOGRAPHY 80
Includes remote sensors; measuring instruments and gages; detectors; cameras and photographic supplies; and holography.
For aerial photography see *43 Earth Resources.* For related information see also *06 Aircraft Instrumentation* and *19 Spacecraft Instrumentation.*

36 LASERS AND MASERS 88
Includes parametric amplifiers.

37 MECHANICAL ENGINEERING 89
Includes auxiliary systems (non-power); machine elements and processes; and mechanical equipment.

38 QUALITY ASSURANCE AND RELIABILITY 92
Includes product sampling procedures and techniques; and quality control.

39 STRUCTURAL MECHANICS 92
Includes structural element design and weight analysis; fatigue; and thermal stress.
For applications see *05 Aircraft Design, Testing and Performance* and *18 Spacecraft Design, Testing and Performance.*

GEOSCIENCES

Includes geosciences (general); earth resources; energy production and conversion; environment pollution; geophysics; meteorology and climatology; and oceanography.
For related information see also *Space Sciences.*

42 GEOSCIENCES (GENERAL) N.A.

43 EARTH RESOURCES 97
Includes remote sensing of earth resources by aircraft and spacecraft; photogrammetry; and aerial photography.
For instrumentation see *35 Instrumentation and Photography.*

44 ENERGY PRODUCTION AND CONVERSION 105
Includes specific energy conversion systems, e.g., fuel cells and batteries; global sources of energy; fossil fuels; geophysical conversion; hydroelectric power; and wind power.
For related information see also *07 Aircraft Propulsion and Power, 20 Spacecraft Propulsion and Power, 28 Propellants and Fuels,* and *85 Urban Technology and Transportation.*

45 ENVIRONMENT POLLUTION 110
Includes air, noise, thermal and water pollution; environment monitoring; and contamination control.

46 GEOPHYSICS 112
Includes aeronomy; upper and lower atmosphere studies; ionospheric and magnetospheric physics; and geomagnetism.
For space radiation see *93 Space Radiation.*

47 METEOROLOGY AND CLIMATOLOGY 116
Includes weather forecasting and modification.

48 OCEANOGRAPHY 118
Includes biological, dynamic and physical oceanography; and marine resources.

LIFE SCIENCES

Includes sciences (general); aerospace medicine; behavioral sciences; man/system technology and life support; and planetary biology.

51 LIFE SCIENCES (GENERAL) 119
Includes genetics.

52 AEROSPACE MEDICINE 125
Includes physiological factors; biological effects of radiation; and weightlessness.

53 BEHAVIORAL SCIENCES 127
Includes psychological factors; individual and group behavior; crew training and evaluation; and psychiatric research.

54 MAN/SYSTEM TECHNOLOGY AND LIFE SUPPORT 129
Includes human engineering; biotechnology; and space suits and protective clothing.

55 PLANETARY BIOLOGY N.A.
Includes exobiology; and extraterrestrial life.

MATHEMATICAL AND COMPUTER SCIENCES

Includes mathematical and computer sciences (general); computer operations and hardware; computer programming and software; computer systems; cybernetics; numerical analysis; statistics and probability; systems analysis; and theoretical mathematics.

59 MATHEMATICAL AND COMPUTER SCIENCES (GENERAL) 130

60 COMPUTER OPERATIONS AND HARDWARE 130
Includes computer graphics and data processing.
For components see *33 Electronics and Electrical Engineering.*

61 COMPUTER PROGRAMMING AND SOFTWARE 134
Includes computer programs, routines, and algorithms.

62 COMPUTER SYSTEMS 138
Includes computer networks.

63 CYBERNETICS 139
Includes feedback and control theory.
For related information see also *54 Man/System Technology and Life Support.*

64 NUMERICAL ANALYSIS 139
Includes iteration, difference equations, and numerical approximation.

65 STATISTICS AND PROBABILITY 143
Includes data sampling and smoothing; Monte Carlo method; and stochastic processes.

66 SYSTEMS ANALYSIS 145
Includes mathematical modeling; network analysis; and operations research.

67 THEORETICAL MATHEMATICS 145
Includes topology and number theory.

PHYSICS

Includes physics (general); acoustics; atomic and molecular physics; nuclear and high-energy physics; optics; plasma physics; solid-state physics; and thermodynamics and statistical physics.
For related information see also *Engineering.*

70 PHYSICS (GENERAL) 146
For geophysics see *46 Geophysics.* For astrophysics see *90 Astrophysics.* For solar physics see *92 Solar Physics.*

71 ACOUSTICS 146
Includes sound generation, transmission, and attenuation.
For noise pollution see *45 Environment Pollution.*

72 ATOMIC AND MOLECULAR PHYSICS 148
Includes atomic structure and molecular spectra.

73 NUCLEAR AND HIGH-ENERGY PHYSICS 152
Includes elementary and nuclear particles; and reactor theory.
For space radiation see *93 Space Radiation.*

74 OPTICS 155
Includes light phenomena.

75 PLASMA PHYSICS 157
Includes magnetohydrodynamics and plasma fusion.
For ionospheric plasmas see *46 Geophysics.* For space plasmas see *90 Astrophysics.*

76 SOLID-STATE PHYSICS 166
Includes superconductivity.
For related information see also *33 Electronics and Electrical Engineering* and *36 Lasers and Masers.*

77 THERMODYNAMICS AND STATISTICAL PHYSICS 168
Includes quantum mechanics; and Bose and Fermi statistics.
For related information see also *25 Inorganic and Physical Chemistry* and *34 Fluid Mechanics and Heat Transfer.*

SOCIAL SCIENCES

Includes social sciences (general); administration and management; documentation and information science; economics and cost analysis; law and political science; and urban technology and transportation.

80 SOCIAL SCIENCES (GENERAL) **169**
Includes educational matters.

81 ADMINISTRATION AND MANAGEMENT **170**
Includes management planning and research.

82 DOCUMENTATION AND INFORMATION SCIENCE **171**
Includes information storage and retrieval technology; micrography; and library science.
For computer documentation see *61 Computer Programming and Software.*

83 ECONOMICS AND COST ANALYSIS **N.A.**
Includes cost effectiveness studies.

84 LAW AND POLITICAL SCIENCE **N.A.**
Includes space law; international law; international cooperation; and patent policy.

85 URBAN TECHNOLOGY AND TRANSPORTATION **172**
Includes applications of space technology to urban problems; technology transfer; technology assessment; and surface and mass transportation.
For related information see *03 Air Transportation and Safety*, *16 Space Transportation*, and *44 Energy Production and Conversion.*

SPACE SCIENCES

Includes space sciences (general); astronomy; astrophysics; lunar and planetary exploration; solar physics; and space radiation.
For related information see also *Geosciences.*

88 SPACE SCIENCES (GENERAL) **N.A.**

89 ASTRONOMY **174**
Includes radio and gamma-ray astronomy; celestial mechanics; and astrometry.

90 ASTROPHYSICS **178**
Includes cosmology; and interstellar and interplanetary gases and dust.

91 LUNAR AND PLANETARY EXPLORATION **180**
Includes planetology; and manned and unmanned flights.
For spacecraft design see *18 Spacecraft Design, Testing and Performance.* For space stations see *15 Launch Vehicles and Space Vehicles.*

92 SOLAR PHYSICS **180**
Includes solar activity, solar flares, solar radiation and sunspots.

93 SPACE RADIATION **181**
Includes cosmic radiation; and inner and outer earth's radiation belts.
For biological effects of radiation see *52 Aerospace Medicine.* For theory see *73 Nuclear and High-Energy Physics.*

GENERAL

99 GENERAL **N.A.**

Note: N.A. means that no abstracts were assigned to this category for this issue.

SUBJECT INDEX **I-1**
PERSONAL AUTHOR INDEX **I-69**
CORPORATE SOURCE INDEX **I-77**
CONTRACT NUMBER INDEX **I-91**
REPORT/ACCESSION NUMBER INDEX **I-95**

TYPICAL CITATION AND ABSTRACT

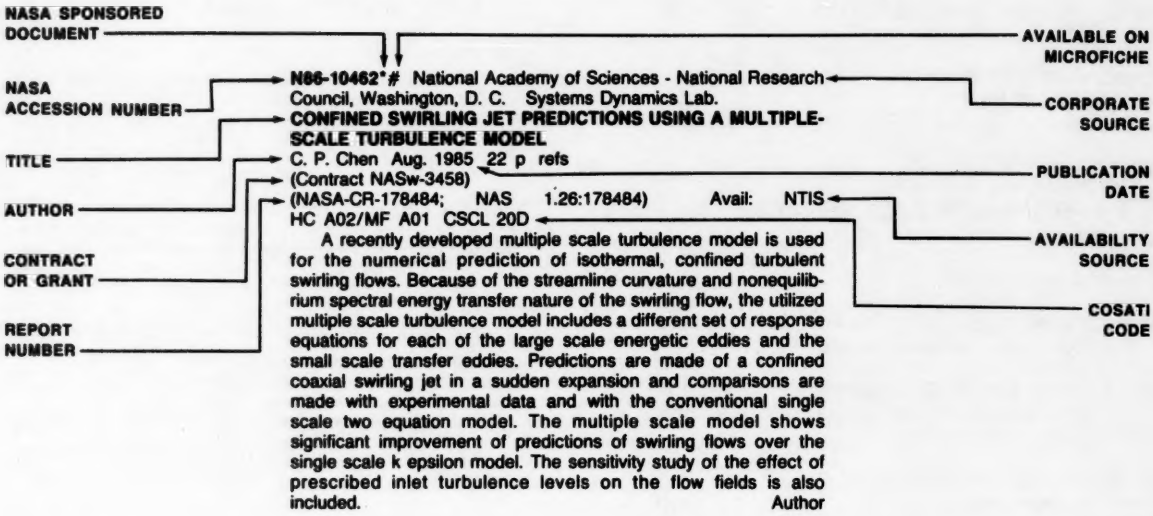
NASA SPONSORED DOCUMENT
NASA ACCESSION NUMBER
TITLE
AUTHOR
CONTRACT OR GRANT
REPORT NUMBER
AVAILABLE ON MICROFICHE
CORPORATE SOURCE
PUBLICATION DATE
AVAILABILITY SOURCE
COSATI CODE
N86-10462*# National Academy of Sciences - National Research Council, Washington, D. C. Systems Dynamics Lab.
CONFINED SWIRLING JET PREDICTIONS USING A MULTIPLE-SCALE TURBULENCE MODEL
C. P. Chen Aug. 1985 22 p refs
(Contract NASw-3458)
(NASA-CR-178484; NAS 1.26:178484) Avail: NTIS
HC A02/MF A01 CSCL 20D
A recently developed multiple scale turbulence model is used for the numerical prediction of isothermal, confined turbulent swirling flows. Because of the streamline curvature and nonequilibrium spectral energy transfer nature of the swirling flow, the utilized multiple scale turbulence model includes a different set of response equations for each of the large scale energetic eddies and the small scale transfer eddies. Predictions are made of a confined coaxial swirling jet in a sudden expansion and comparisons are made with experimental data and with the conventional single scale two equation model. The multiple scale model shows significant improvement of predictions of swirling flows over the single scale k epsilon model. The sensitivity study of the effect of prescribed inlet turbulence levels on the flow fields is also included.
Author

VOLUME 24 NUMBER 1 / JANUARY 8, 1986

Scientific and Technical Aerospace Reports

A Semimonthly Publication of the National Aeronautics and Space Administration

01 AERONAUTICS (GENERAL)

N86-10001# Air Force Systems Command, Wright-Patterson AFB, Ohio. Foreign Technology Div.

ACTA AERONAUTICA ET ASTRONAUTICA SINICA (SELECTED ARTICLES)

4 Oct. 1984 64 p refs Transl. into ENGLISH from Hangkong Xuebao (China), v. 4, no. 4, 1983 p 1-19, 11-19; 39-47; 101-104 (AD-A147304; FTD-ID(RS)T-1120-84) Avail: NTIS HC A04/MF A01 CSCL 01/2

Research in aeronautics and astronautics in China is discussed. Some areas of research are: (1) approximation method for transonic flow over swept wings; (2) shock turbulent interaction over a compression corner for supersonic flow; (3) optimum design of an aircraft wing; and (4) a simple estimation method for two phase flow in a nozzle of rocket ramjet engine. For individual titles, see N86-10002 through N86-10005.

N86-10002# Air Force Systems Command, Wright-Patterson AFB, Ohio. Foreign Technology Div.

SECOND ORDER APPROXIMATION METHOD FOR TRANSONIC FLOWS OVER SWEPT WINGS c02

Shen Keyang (Shanghai Aviation Industry Corp.) *In its* Acta Aeron. and Astronautica Sinica (FTD-ID(RS)T-1120-84) 4 Oct. 1984 p 1-17 refs Transl. into ENGLISH from Hangkong Xuebao (China), v. 4, no. 4, 1983 p 1-10 (For primary document see N86-10001 01-01)

Avail: NTIS HC A04/MF A01 CSCL 01/1

The TSDH equation is used to calculate the transonic flows over three dimensional swept wings. It considers the leading edge boundary conditions and leading edge velocity potential equation suitable for the blunt leading edge of wings. The expanded form of the Jameson scheme is used in the unequal step length grid for the discretization of the TSDH equation into a set of finite difference equations. A rarefied grid was arranged in the calculation space, then a dense grid was arranged near the wing and alternate iteration of the rarefied and dense meshes was carried out so as to accelerate convergence and raise calculation precision. Calculations of the supercritical without shock wave and with shock wave conditions of the ONERA M6 wing show that there is good agreement between the TSDH solution and the FVP solution and wind tunnel tests. Author

N86-10003# Air Force Systems Command, Wright-Patterson AFB, Ohio. Foreign Technology Div.

A NUMERICAL SOLUTION OF THE SHOCK-TURBULENT INTERACTION OVER A COMPRESSION CORNER FOR SUPERSONIC FLOW c02

Cao Qipeng (Nanjing Aeronautical Inst.) *In its* Acta Aeron. et Astronautica Sinica (FTD-ID(RS)T-1120-84) 4 Oct. 1985 p 18-33 refs Transl. into ENGLISH from Hangkong Xuebao (China), v. 4, no. 4, 1983 p 11-19 (For primary document see N86-10001 01-01)

Avail: NTIS HC A04/MF A01 CSCL 01/1

The shock turbulent boundary layer interaction over a compression corner for supersonic flow is calculated. The calculations use the Cebeci-Kellet box method; the turbulence model uses the algebraic eddy viscosity model; the pressure strength distribution uses the unified hypersonic and supersonic formulas of flowing over a wedge. Iteration correction is carried out of the shock turbulent boundary layer disturbance. The calculations predict the wall pressure distribution as well as the initial rise point location of the pressure. Author

N86-10004# Air Force Systems Command, Wright-Patterson AFB, Ohio. Foreign Technology Div.

OPTIMUM DESIGN OF AN AIRCRAFT WING STRUCTURE WITH MULTIPLE CONSTRAINTS BY THE DIRECT-VISION CRITERIA METHOD c05

Li Linang (Shenyang Aircraft Corp.) *In its* Acta Aeron. et Astronautica Sinica (FTD-ID(RS)T-1120-84) 4 Oct. 1984 p 34-52 refs Transl. into ENGLISH from Hangkong Xuebao (China), v. 4, no. 4, 1983 p 39-47 (For primary document see N86-10001 01-01)

Avail: NTIS HC A04/MF A01 CSCL 01/1

An optimized computer program (SAFDOP) is introduced which uses the direct vision criteria method for a wing surface structure with multiple constraints. This program can separately carry out analysis, optimization and synthetic optimization calculations of stress, displacement, flutter and static aeroelasticity. The alternate constraint method was used for synthetic optimization calculations. Aside from the stress constraints using the full stress method, each of the other constraints used the uniform derivative criteria. For practical purposes, the element linking weight was used as an independent design variable, in the optimum design the automatic sieve selection design variable and other methods were used and the automatic generation of initial numerical data was considered. This program was used to calculate a typical fighter wing and it proved to be feasible. Author

N86-10005# Air Force Systems Command, Wright-Patterson AFB, Ohio. Foreign Technology Div.

THEORETICAL SPECIFIC IMPULSE FOR TWO-PHASE FLOW IN NOZZLE OF ROCKET-RAMJET ENGINE: A SIMPLE ESTIMATION METHOD c20

Bi Shiguan (China Precision Machinery Co.) *In its* Acta Aeron. et Astronautica Sinica (FTD-ID(RS)T-1120-84) 4 Oct. 1984 p 53-60 refs Transl. into ENGLISH from Hangkong Xuebao (China), v. 4, no. 4, 1984 p 101-104 (For primary document see N86-10001 01-01)

Avail: NTIS HC A04/MF A01 CSCL 21/8

A theoretical specific impulse formula is derived for two phase flow in nozzle rocket ramjet engine on the basis of similarity to that used for rocket engines. Theoretically, it is proved that the properties of two phase flow in nozzle for these two types of engines can be analyzed with a common combined parameter which is equivalent to the exhaust velocity. A simple estimation method is introduced for specific impulse losses of two phase flow with variable lag. An approximate solution is proposed to deal with the problem of singularity. Author

N86-10006# Information Spectrum, Inc., Arlington, Va.
F-16X MSIP (MULTI-NATIONAL STAGED IMPROVEMENT PROGRAM) CASE EXAMPLE: OPERATING AND SUPPORT COST ESTIMATION USING VAMOSC (VISIBILITY AND MANAGEMENT OF OPERATING AND SUPPORT COSTS) Final Technical Report
W. C. Redeen 17 Aug. 1984 71 p
(Contract F33600-82-C-0543)
(AD-A156893; ISI-V-4859-02) Avail: NTIS HC A04/MF A01 CSCL 05/1

This case example of a hypothetical F-16X MSIP (Multi-National Staged Improvement Program) Operating and Support (O&S) cost estimate, sponsored by AFLC/MM (VAMOSC), has been prepared to demonstrate and test the capability of the Air Force Visibility and Management of Operating and Support Costs (VAMOSC) system to provide unique and detailed experience data suitable for credible and explicit O&S cost estimation for advanced Air Force aircraft systems and subsystems. The specific objective of this effort is: To produce a case example of VAMOSC applicability to O&S cost estimation which conforms to the following conditions: Is compatible with OSD/CAIG and USAF costing guidance. Is linkable to reported experience data for existing aircraft. Provided a VAMOSC-Supported Methodology which can be utilized to predict the impact of configuration changes on system O&S costs. Depicts a methodology which is applicable to O&S costing for any aircraft system in advanced conceptual development. Provides estimates which are verifiable by tests. Identifies areas of VAMOSC requiring enhancement or modification to improve system integrity and applicability. GRA

N86-10007# Air Force Systems Command, Wright-Patterson AFB, Ohio. Foreign Technology Div.
THREE ARTICLES ON NEW CALCULATION METHODS IN AERONAUTICS (SELECTED ARTICLES)
17 Aug. 1984 55 p refs Transl. into ENGLISH from Hangkong Xuebao (China), v. 4, no. 3, Sep. 1983 p 1-18, 56-62, and 102-104
(AD-A145745; FTD-ID(RS)T-0910-84) Avail: NTIS HC A04/MF A01 CSCL 01/2

Selected research topics are investigated in search of new calculation methods for aeronautics. Numerical solutions are sought for calculating hypersonic flow and unsteady supersonic aerodynamic forces. Methods for determining aerodynamic coefficients are discussed. Selected highlights of the third conference of the Aeronautical Society of China are also discussed. Shear layer effects on the stability of an axisymmetrical external compression air intake are investigated. For individual titles, see N86-10008 through N86-10011.

N86-10008# Air Force Systems Command, Wright-Patterson AFB, Ohio. Foreign Technology Div.
NUMERICAL SOLUTION OF HYPERSONIC FLOW NEAR LEADING EDGE OF A FLAT PLATE **c02**
Dexun Fu *In its* Three Articles on New Calculation Methods in Aeron. (Selected Articles) (FTD-ID(RS)T-0910-84) 17 Aug. 1984 p 1-14 refs Transl. into ENGLISH from Hangkong Xuebao (China), v. 4, no. 3, Sep. 1983 p 1-8 Original language document announced in IAA as A84-23903 (For primary document see N86-10007 01-01)
Avail: NTIS HC A04/MF A01 CSCL 01/2

A one-step difference scheme for solving two-dimensional steady state Navier-Stokes equations is proposed to handle supersonic and hypersonic viscous interaction problems near the leading edge of a flat plate. The scheme is considered and analyzed with a model equation. It has second-order accuracy in space for steady state problems and its stability condition is improved. The scheme is much simpler, compared to the commonly used two-step predictor-corrector difference scheme for N-S equations and also is convenient for programming. Two viscous interaction problems are solved with the proposed scheme; the solutions are valid throughout the boundary layer, shock-wave structure, and inviscid core. The results show good agreement with experimental data. The numerical solutions show that the nonslip conditions can be used for weak viscous interaction. C.D. (IAA)

N86-10009# Air Force Systems Command, Wright-Patterson AFB, Ohio. Foreign Technology Div.
A NEW METHOD FOR CALCULATING UNSTEADY SUPERSONIC AERODYNAMIC FORCES AND ITS APPLICATION **c02**
Xianxin Wang *In its* Three Articles on New Calculation Methods in Aeron. (Selected Articles) (FTD-ID(RS)T-0910-84) 17 Aug. 1984 p 15-31 refs Transl. into ENGLISH from Hangkong Xuebao (China), v. 4, no. 3, Sep. 1983 p 9-18 (For primary document see N86-10007 01-01)
Avail: NTIS HC A04/MF A01 CSCL 01/2

This paper proposes a new method for calculating supersonic unsteady aerodynamic forces. It combines the piston theory for unsteady supersonic flow with the conical flow theory for steady flow so that the interaction between points on a wing neglected in the piston theory is approximated by the conical flow theory. This method was used in this paper for flutter calculations of 29 cases for wings with 10 different types of plane forms. The results were compared with flutter test results obtained in wind tunnels and they were in satisfactory agreement. It was especially the case that the accuracy of flutter analysis improved by this method was noticeably higher than that obtained by the piston theory. This shows that this method is reliable and feasible for supersonic flutter analysis. It possesses the advantages of being a more succinct method and having higher calculation accuracy, less computing time and easier programming. Author

N86-10010# Air Force Systems Command, Wright-Patterson AFB, Ohio. Foreign Technology Div.
EFFECT OF A SHEAR LAYER ON THE STABILITY OF AN AXISYMMETRICAL EXTERNAL COMPRESSION AIR INTAKE **c02**
Kunyuan Zhang, Shaozhi Yu, and Chengyi Peng *In its* Three Articles on New Calculation Methods in Aeron. (Selected Articles) (FTD-ID(RS)T-0910-84) 17 Aug. 1984 p 32-42 refs Transl. into ENGLISH from Hangkong Xuebao (China), v. 4, no. 3, Sep. 1983 p 56-62 (For primary document see N86-10007 01-01)
Avail: NTIS HC A04/MF A01 CSCL 01/2

The influence of shear layers of various strengths on the stability of an axisymmetric compression supersonic air intake is studied. Strength is defined as the ratio of total pressure difference between the two sides of a shear layer to the total pressure of the incoming flow. Six central bodies with different cone angles were used to produce shear layers with strengths ranging from 5 to 11 percent of the total pressure of upstream flow inside a free stream wind tunnel with a fixed Mach number of 1.72. Shear layers with less than 10 percent strength were strong enough to cause separation of the boundary layer from the inside surface of the cowl. Shear layers of strength less than 11 percent failed to induce buzz in the axisymmetric intake. The influence of a shear layer depended on its distance from the lip of the cowl, and was most noticeable at a distance of 10 to 18 percent of the cowl radius. C.D. (IAA)

N86-10011# Air Force Systems Command, Wright-Patterson AFB, Ohio. Foreign Technology Div.
COMMENT ON DETERMINATION OF AERODYNAMIC COEFFICIENTS FOR A REENTRY BODY BY MEANS OF THE KALMAN FILTER METHOD **c02**
Jinshi Cai *In its* Three Articles on New Calculation Methods in Aeron. (Selected Articles) (FTD-ID(RS)T-0910-84) 17 Aug. 1984 p 43-46 Transl. into ENGLISH from Hangkong Xuebao (China), v. 4, no. 3, Sep. 1983 p 102-104 (For primary document see N86-10007 01-01)
Avail: NTIS HC A04/MF A01 CSCL 01/2

Research emphatically indicates that a mathematical model for aerodynamic parameter identification of a reentry body bases only on the data of angular rates and accelerations onboard but not on trajectory observation data. It can only determine the ratio

between aerodynamic coefficients of the reentry body but can't determine the aerodynamic coefficients directly. B.W.

02 AERODYNAMICS

Includes aerodynamics of bodies, combinations, wings, rotors, and control surfaces; and internal flow in ducts and turbomachinery.

For related information see also *34 Fluid Mechanics and Heat Transfer.*

N86-10012 Georgia Inst. of Tech., Atlanta.
A STUDY OF THE AERODYNAMIC PERFORMANCE OF WEIS-FOGH WINGS Ph.D. Thesis
Hsun Hu Chen 1985 145 p
Avail: Univ. Microfilms Order No. DA8510956

A general theory of aerodynamics developed on the basis of viscous flow equations, is utilized in an investigation of the Weis-Fogh problem. The general theory is ideally suited for nonlinear unsteady aerodynamic problems. It is also shown that the general theory permits the important flow elements dominating the aerodynamics of nonlinear unsteady flows to be identified and their contributions evaluated individually. The Weis-Fogh problem is a well known biofluiddynamics problem involving articulate lifting bodies. The present study has yielded useful results for the lift and drag acting on a wing undergoing the fling and the clap phases of the Weis-Fogh motion. Closed form expressions have been obtained for the unsteady aerodynamic forces and the power expenditure of the Weis-Fogh wing. These results have led to the identification of major contributions to aerodynamic performance of the Weis-Fogh wings and to an assessment of the relative importance of these contributions. Dissert. Abstr.

N86-10013 Princeton Univ., N. J.
ON THE DESIGN OF AIRFOILS IN TRANSONIC FLOW USING THE EULER EQUATIONS Ph.D. Thesis
John Foster Fay 1985 83 p
Avail: Univ. Microfilms Order No. DA8509636

This work falls naturally into two parts. One part describes a computer program that designs airfoils using the Lighthill method of conformal mappings. This program involves the use of the Euler equations to solve for the flow past a given initial shape, and also around intermediate shapes. The other part is a derivation of an extension of the Lighthill method to compressible flows with the assumptions of potential flow and small disturbances of the free stream. The description of the program speaks to its various aspects, namely the Euler solution formulation and the actual process of design. Several other topics are also mentioned; these include several factors affecting the rate of convergence of the design process, the importance of equaling the lift coefficients of the initial and final shapes; and the effect of using the same design velocity distribution at different freestream Mach numbers. There is a short appendix giving a plausible argument indicating that the interaction for small disturbance and arbitrary subsonic Mach number will converge to a desired shape. Dissert. Abstr.

N86-10014*# Vanderbilt Univ., Nashville, Tenn. Dept. of Mechanical and Materials Engineering.
THE ROLE OF FREESTREAM TURBULENCE SCALE IN SUBSONIC FLOW SEPARATION Interim Progress Report, 1 Jan. - 30 Jun. 1985
J. Leith Potter, W. R. Seebaugh, Carl E. Fisher, R. Joel Barnett, and Rajiv B. Gokhale 30 Jun. 1985 56 p
(Grant NAG1-483)
(NASA-CR-176237; NAS 1.26:176237; IPR-2) Avail: NTIS HC A04/MF A01 CSCL 01A

The clarification of the role of freestream turbulence scale in determining the location of boundary layer separation is discussed. Modifications to the test facility were completed. Wind tunnel flow characteristics, including turbulence parameters, were determined with two turbulence generating grids, as well as no grid. These results are summarized. Initial results on the role of scale on turbulent boundary layer separation on the upper surface of an airfoil model are also discussed. Author

N86-10015*# National Aeronautics and Space Administration. Ames Research Center, Moffett Field, Calif.
EVALUATION OF AN AERODYNAMIC-LOAD PREDICTION METHOD ON A STOL FIGHTER CONFIGURATION
Joseph Katz Aug. 1985 33 p refs Previously announced as N85-33121
(NASA-TM-86782; Rept-85358; NAS 1.15:86782) Avail: NTIS HC A03/MF A01 CSCL 01A

A three-dimensional panel method was used to compute the aerodynamic loads on a large-scale, powered wind tunnel model. The size of the computation grid was selected such that turnaround times, on present computers remained satisfactory. With this constraint, the STOL aircraft configuration was modeled and the capabilities and limitations of the prediction method were investigated. After this study, a similar numerical model was established for a forward-swept-wing aircraft configuration which is planned for large-scale, low-speed testing. The resulting aerodynamic-load predictions are discussed and will be utilized, together with the future experimental results, to obtain a broader validation of this method as well as to reduce the necessary size of the matrix of the test parameters. Author

N86-10016*# National Aeronautics and Space Administration. Langley Research Center, Hampton, Va.
OPERATING CHARACTERISTICS OF THE MULTIPLE CRITICAL VENTURI SYSTEM AND SECONDARY CALIBRATION NOZZLES USED FOR WEIGHT-FLOW MEASUREMENTS IN THE LANGLEY 16-FOOT TRANSONIC TUNNEL
Bobby L. Berrier, Laurence D. Leavitt, and Linda S. Bangert Sep. 1985 74 p refs
(NASA-TM-86405; L-15960; NAS 1.15:86405) Avail: NTIS HC A04/MF A01 CSCL 01A

An investigation has been conducted in the Langley 16 Foot Transonic Tunnel to determine the weight flow measurement characteristics of a multiple critical Venturi system and the nozzle discharge coefficient characteristics of a series of convergent calibration nozzles. The effects on model discharge coefficient of nozzle throat area, model choke plate open area, nozzle pressure ratio, jet total temperature, and number and combination of operating Venturis were investigated. Tests were conducted at static conditions (tunnel wind off) at nozzle pressure ratios from 1.3 to 7.0. Author

N86-10017*# National Aeronautics and Space Administration. Lewis Research Center, Cleveland, Ohio.
THREE-DIMENSIONAL INVISCID ANALYSIS OF RADIAL TURBINE FLOW AND A LIMITED COMPARISON WITH EXPERIMENTAL DATA
Y. K. Choo and K. C. Civinskas (Army Aviation Research and Technology Activity) [1985] 28 p refs To be presented at the ASME Winter Ann. Meeting, 3-Dimensional Flow Phenomena in Fluid Machinery Symp., Miami, Fla., 17-22 Nov. 1985
(NASA-TM-87091; E-2679; NAS 1.15:87091; USAAVSCOM-TR-85-C-12) Avail: NTIS HC A03/MF A01 CSCL 01A

The three-dimensional inviscid DENTON code is used to analyze flow through a radial-inflow turbine rotor. Experimental data from the rotor are compared with analytical results obtained by using the code. The experimental data available for comparison are the radial distributions of circumferentially averaged values of absolute flow angle and total pressure downstream of the rotor exit. The computed rotor-exit flow angles are generally underturned relative to the experimental values, which reflect the boundary-layer separation at the trailing edge and the development of wakes downstream of the rotor. The experimental rotor is designed for a higher-than-optimum work factor of 1.126 resulting in a nonoptimum positive incidence and causing a region of rapid flow adjustment and large velocity gradients. For this experimental rotor, the computed radial distribution of rotor-exit to turbine-inlet total

pressure ratios are underpredicted due to the errors in the finite-difference approximations in the regions of rapid flow adjustment, and due to using the relatively coarser grids in the middle of the blade region where the flow passage is highly three-dimensional. Additional results obtained from the three-dimensional inviscid computation are also presented, but without comparison due to the lack of experimental data. These include quasi-secondary velocity vectors on cross-channel surfaces, velocity components on the meridional and blade-to-blade surfaces, and blade surface loading diagrams. Computed results show the evolution of a passage vortex and large streamline deviations from the computational streamwise grid lines. Experience gained from applying the code to a radial turbine geometry is also discussed. Author

N86-10018*# National Aeronautics and Space Administration. Johnson (Lyndon B.) Space Center,
NUMERICAL PROCEDURE FOR THREE-DIMENSIONAL HYPERSONIC VISCOUS FLOW OVER AEROBRAKE CONFIGURATION
Chien-peng Li Aug. 1985 17 p refs
(NASA-TM-58269; S-549; NAS 1.15:58269) Avail: NTIS HC A02/MF A01 CSCL 01A

A numerical method, which is simpler and more efficient than others currently in use, is proposed for the computation of the full viscous flow over an aerobrake body in hypersonic stream at high altitude. It treats the shock layer surrounding the blunt forebody and the near wake behind the base simultaneously by formulating the Navier-Stokes equations in conformal and azimuthal-angle coordinates. The computational domain is confined by the body wall, outflow surface and the shock, which is adjusted along the coordinate normal to the wall in the course of iterations. Because of the optimal grid and a well developed alternating direction implicit factorization technique for the governing equations, reasonably accurate results can be obtained with a 28 x 36 x 7 grid and 400 time-marching iterations. Excellent agreement of shock location is found between the present result and the schlieren photograph. Details of the base flow and shear layer impingement on the cylindrical aft body are presented for an adiabatic wall case. Author

N86-10019*# National Aeronautics and Space Administration. Lewis Research Center, Cleveland, Ohio.
FORCED RESPONSE ANALYSIS OF AN AERODYNAMICALLY DETUNED SUPERSONIC TURBOMACHINE ROTOR
Daniel Hoyniak and Sanford Fleeter (Purdue Univ., West Lafayette, Ind.) 1985 24 p refs Presented at 10th Bien. Design Eng. Div. Conf. and Exhibit on Mech. Vibration and Noise, Cincinnati, 10-13 Sep. 1985; sponsored by ASME
(NASA-TM-87093; E-2685; NAS 1.15:87093) Avail: NTIS HC A02/MF A01 CSCL 01A

High performance aircraft-engine fan and compressor blades are vulnerable to aerodynamically forced vibrations generated by inlet flow distortions due to wakes from upstream blade and vane rows, atmospheric gusts, and maldistributions in inlet ducts. In this report, an analysis is developed to predict the flow-induced forced response of an aerodynamically detuned rotor operating in a supersonic flow with a subsonic axial component. The aerodynamic detuning is achieved by alternating the circumferential spacing of adjacent rotor blades. The total unsteady aerodynamic loading acting on the blading, as a result of the convection of the transverse gust past the airfoil cascade and the resulting motion of the cascade, is developed in terms of influence coefficients. This analysis is used to investigate the effect of aerodynamic detuning on the forced response of a 12-blade rotor, with Verdon's Cascade B flow geometry as a uniformly spaced baseline configuration. The results of this study indicate that, for forward traveling wave gust excitations, aerodynamic detuning is very beneficial, resulting in significantly decreased maximum-amplitude blade responses for many interblade phase angles. Author

N86-10020# Department of the Air Force, Washington, D.C.
SUBMERGED RAM AIR INLETS FOR ECM (ELECTRONIC COUNTERMEASURES) PODS Patent Application
Foxwell, inventor (to Air Force) Filed 27 Jun. 1985 15 p
(AD-D011801; US-Patent-Appl-SN-749333) Avail: NTIS HC A02/MF A01 CSCL 21/5

The present invention utilizes a substantially pear-shaped submerged air inlet duct in the surface of an electronic countermeasures (ECM) pod to provide cooling air for heat exchanger units which are utilized to cool electronic components in a ECM pod. The smaller opening is in the forward most position. GRA

N86-10021# Sandia Labs., Albuquerque, N. Mex.
INVISCID FLOW FIELD ANALYSIS OF MANEUVERING HYPERSONIC VEHICLES USING THE SCM FORMULATION AND PARABOLIC GRID GENERATION
R. W. Noack 1985 13 p Presented at the 18th Fluid Dyn., Plasma Dyn. and Lasers, Cincinnati, 16 Jul. 1985
(Contract DE-AC04-76DP-00789)
(DE85-013950; SAND-84-2670C; CONF-850717-1) Avail: NTIS HC A02/MF A01

The split-coefficient matrix (SCM) form of the Euler equations for a cylindrical base coordinate system is extended to allow the use of a generalized three-dimensional grid generation scheme. A grid generation scheme based on a parabolic partial differential equation is developed. Grids are obtained without iteration by marching from the body to the shock with body and shock points specified. The SCM type body boundary condition has been found to underpredict surface pressure for geometries with small radii of curvature. An improved method of characteristic (MOC) type body boundary condition has been developed which uses SMC type differencing in the crossflow direction. The improved MOC boundary condition has been found to have the robustness of the SCM type scheme while having superior accuracy. Solutions using the SCM form of the Euler equations with the parabolic grid generator and the improved MOC body boundary condition have been obtained for a hypersonic six fin missile. Generally good agreement is found in comparisons of the inviscid predictions with experimental data. DOE

N86-10022# Office National d'Etudes et de Recherches Aerospatiales, Paris (France). Direction Scientifique de la Resistance des Structures.
THEORETICAL STUDY OF THE UNSTEADY LINEAR PROBLEM FOR A RECTANGULAR WING WITH A PITCHING MOVEMENT Final Report [ETUDE THEORIQUE DU PROBLEME INSTATIONNAIRE LINEAIRE POUR UNE AILE RECTANGULAIRE ANIMEE D'UN MOUVEMENT DE TANGAGE]
C. Coneim Jun. 1984 35 p refs In FRENCH
(Contract DRET-83-34-135)
(ONERA-RT-17/1841-RY-010-R) Avail: NTIS HC A03/MF A01

The pressure distribution on a helicopter rectangular wing with a positive angle of attack and a harmonic pitching movement is computed. The flow separation is not taken in account as the incidence is assumed to be low. The treatment of the singularity is detailed. Results for relatively high frequencies and three profiles are presented. The three dimensional effects of the wing tip are shown. Author (ESA)

N86-10023# Societe Nationale Industrielle Aerospatiale, Toulouse (France). Div. Avions.
AERODYNAMICS OF HYPERLIFT SYSTEMS [AERODYNAMIQUE DES SYSTEMES HYPERSUSTENTATEURS]
P. Capbern, J. Javelle, N. Larger, A. J. Paut, and C. Bonnet 23 Jan. 1985 97 p refs In FRENCH
(Contract DRET-83-34-051-00-470-75-01)
(SNIAS-443.501/85) Avail: NTIS HC A05/MF A01

A method to compute two dimensional noncompressible viscous flow on multiprofile configurations is described. The potential flow and the viscous layers are solved interactively. The potential flow is obtained by a singularities method. The boundary layers are treated by integral equations. Evaluation using the ATR 42 configuration (narrow slots, separated flow) shows the robustness of the method when treating difficult problems and a good prediction of separation and pressure distribution. The computer

program is adapted to industrial utilization on CRAY 1 computer.
Author (ESA)

N86-10024# Societe Nationale Industrielle Aerospatiale, Toulouse (France).
ANALYSIS OF HYPERLIFT SYSTEMS. STUDY OF A SINGULARITIES METHOD [ANALYSE DES SYSTEMES HYPERSUSTENATATEURS. ETUDE D'UNE METHODE DE SINGULARITES]
N. Larger 10 Sep. 1984 42 p In FRENCH
(SNIAS-443.529/84; SNIAS-443.501/85) Avail: NTIS HC A03/MF A01

Singularity models are tested to solve problems imposed by narrow airfoil profiles commonly found in industrial configurations. Solutions including computation phases, skeleton and thick profile, and the adoption of vortices for either the skeleton or the full profile are described. The results obtained are better than those from classic methods. Author (ESA)

N86-10025# Deutsche Forschungs- und Versuchsanstalt fuer Luft- und Raumfahrt, Goettingen (West Germany). Abt. Hochgeschwindigkettsstroemungen.
INVESTIGATIONS ON A SUPERCRITICAL AIRFOIL WITH BOUNDARY LAYER SUCTION THROUGH A PERFORATED STRIP IN THE SHOCK REGION
Paul Krogmann Nov. 1984 56 p refs In GERMAN; ENGLISH summary Report will also be announced as translation (ESA-TT-940)
(DFVLR-FB-85-15; ISSN-0171-1342) Avail: NTIS HC A04/MF A01; DFVLR, Cologne DM 16.50

The effect of local boundary layer suction through a perforated strip on the flow development and aerodynamic characteristics of a transonic airfoil is investigated in a 1 m X 1 m transonic wind tunnel. In comparison with reference measurements on the same model with a solid surface, the results show that, aside from the improvements due to suction, the flow development in the non-suction case is most favorably affected by the arrangement of the perforated strip with a cavity underneath. Due to a secondary flow through the perforation and cavity, caused by the strong adverse pressure gradients occurring at higher angles of attack, the shock location as well as the flow field downstream of the shock are affected. Thus, considerable gain in maximum lift and drag reductions can be achieved. Author (ESA)

N86-10026# Deutsche Forschungs- und Versuchsanstalt fuer Luft- und Raumfahrt, Goettingen (West Germany). Forschungsbereich Stroemungsmechanik.
EXPERIMENTAL AND THEORETICAL INVESTIGATIONS OF THE FLOW AROUND AIRFOIL SYSTEMS WITH GROUND EFFECT
Dieter Steinbach Sep. 1984 63 p refs
(DFVLR-FB-85-17; ISSN-0171-1342) Avail: NTIS HC A04/MF A01; DFVLR, Cologne DM 21.50

For two rectangular wings with flaps (Q/R4 and NACA 4415) pressure distribution for plane flow and low flow velocities is measured. For ground simulation fixed ground boards adjustable in height are used. Reynolds and Mach numbers are 1.6 million and 0.15. For the NACA 4415 wing flow field measurements are carried out also. The surface singularity method with separation model used for the calculations is outlined. Agreement between experiment and theory is good to satisfactory, especially if flow separation is not too large. But even for large separated flow regions the separation model improves results. The presence of ground gives enlarged flow separation, higher pressure and base pressure values, and lower suction peaks. High-lift systems with positive camber line show considerable losses of lift near ground. A static instability of lift with respect to ground distance occurs. This effect becomes stronger as the angle of attack is increased.
Author (ESA)

N86-10027# Deutsche Forschungs- und Versuchsanstalt fuer Luft- und Raumfahrt, Goettingen (West Germany). Inst. fuer Experimentelle Stroemungsmechanik.
INVESTIGATION OF DENSITY GRADIENT FLUCTUATIONS IN A TURBULENT FREE JET BY MEANS OF THE LASER SCHLIEREN CROSSED-BEAM METHOD
Juergen Kompenhans, Hans R. Hoefer, and Sabine Rannenberg Dec. 1984 94 p refs In GERMAN; ENGLISH summay Report will also be announced as translation (ESA-TT-942)
(DFVLR-FB-85-19; ISSN-0171-1342) Avail: NTIS HC A05/MF A01; DFVLR, Cologne DM 25.50

Density gradient fluctuations within a round, turbulent jet were investigated at Mach numbers of 0.62 and 0.95 by laser schlieren photography. Cross spectral density, coherence function and phase velocity of the density gradient fluctuations were obtained using an arrangement of two crossed laser beams at various distances from the nozzle. Information on coherent structures in a jet was obtained, even at high Mach numbers. Author (ESA)

N86-10028# Max-Planck-Institut fuer Stroemungsforschung, Goettingen (West Germany).
OSCILLATIONS OF SUBSONIC FLOW IN AN ABRUPTLY EXPANDING CIRCULAR DUCT
W. C. Selerowicz, A. P. Szumowski, and G. E. A. Meier Sep. 1984 39 p refs
(MPIS-16/1984; ISSN-0436-1199) Avail: NTIS HC A03/MF A01; Fachinformationszentrum, Karlsruhe, West Germany DM 17

Subsonic flow in an abruptly expanding duct driven from a pressure reservoir, which shows self-excited oscillations of considerable amplitude was studied by visualization and acoustic pressure measurements. Depending on the pressure drop in the duct and its dimensions, three distinct types of flow oscillations are observed. These are characterized by symmetrical and antisymmetrical oscillations of the separated jet in the abruptly expanding section, and symmetrical oscillations of the jet periodically separating and reattaching to the wall. The oscillations are accompanied by intensive noise, with an intensity of 40 dB above the turbulence noise level. Author (ESA)

N86-10029# German-Dutch Wind Tunnel, North East Polder (Netherlands).
[ACTIVITIES REPORT OF THE GERMAN-DUTCH WIND TUNNEL] Annual Report, 1983
1984 18 p refs
Avail: NTIS HC A02/MF A01

Tests, maintenance, demonstrations, systems integration, and the 1983 accounts of the German-Dutch Wind tunnel are described. Installation of turbine powered simulators, and propeller simulation technology are outlined. Author (ESA)

N86-10002# Air Force Systems Command, Wright-Patterson AFB, Ohio. Foreign Technology Div.
SECOND ORDER APPROXIMATION METHOD FOR TRANSONIC FLOWS OVER SWEPT WINGS
Shen Keyang (Shanghai Aviation Industry Corp.) *In its* Acta Aeron. and Astronautica Sinica (FTD-ID(RS)T-1120-84) 4 Oct. 1984 p 1-17 refs Transl. into ENGLISH from Hangkong Xuebao (China), v. 4, no. 4, 1983 p 1-10 (For primary document see N86-10001 01-01)
Avail: NTIS HC A04/MF A01 CSCL 01/1

N86-10003# Air Force Systems Command, Wright-Patterson AFB, Ohio. Foreign Technology Div.
A NUMERICAL SOLUTION OF THE SHOCK-TURBULENT INTERACTION OVER A COMPRESSION CORNER FOR SUPERSONIC FLOW
Cao Qipeng (Nanjing Aeronautical Inst.) *In its* Acta Aeron. et Astronautica Sinica (FTD-ID(RS)T-1120-84) 4 Oct. 1985 p 18-33 refs Transl. into ENGLISH from Hangkong Xuebao (China), v. 4, no. 4, 1983 p 11-19 (For primary document see N86-10001 01-01)
Avail: NTIS HC A04/MF A01 CSCL 01/1

N86-10008# Air Force Systems Command, Wright-Patterson AFB, Ohio. Foreign Technology Div.
NUMERICAL SOLUTION OF HYPERSONIC FLOW NEAR LEADING EDGE OF A FLAT PLATE

Dexun Fu *In its* Three Articles on New Calculation Methods in Aeron. (Selected Articles) (FTD-ID(RS)T-0910-84) 17 Aug. 1984 p 1-14 refs Transl. into ENGLISH from Hangkong Xuebao (China), v. 4, no. 3, Sep. 1983 p 1-8 Original language document announced in IAA as A84-23903 (For primary document see N86-10007 01-01)
Avail: NTIS HC A04/MF A01 CSCL 01/2

N86-10009# Air Force Systems Command, Wright-Patterson AFB, Ohio. Foreign Technology Div.
A NEW METHOD FOR CALCULATING UNSTEADY SUPERSONIC AERODYNAMIC FORCES AND ITS APPLICATION
Xianxin Wang *In its* Three Articles on New Calculation Methods in Aeron. (Selected Articles) (FTD-ID(RS)T-0910-84) 17 Aug. 1984 p 15-31 refs Transl. into ENGLISH from Hangkong Xuebao (China), v. 4, no. 3, Sep. 1983 p 9-18 (For primary document see N86-10007 01-01)
Avail: NTIS HC A04/MF A01 CSCL 01/2

N86-10010# Air Force Systems Command, Wright-Patterson AFB, Ohio. Foreign Technology Div.
EFFECT OF A SHEAR LAYER ON THE STABILITY OF AN AXISYMMETRICAL EXTERNAL COMPRESSION AIR INTAKE
Kunyuan Zhang, Shaozhi Yu, and Chengyi Peng *In its* Three Articles on New Calculation Methods in Aeron. (Selected Articles) (FTD-ID(RS)T-0910-84) 17 Aug. 1984 p 32-42 refs Transl. into ENGLISH from Hangkong Xuebao (China), v. 4, no. 3, Sep. 1983 p 56-62 (For primary document see N86-10007 01-01)
Avail: NTIS HC A04/MF A01 CSCL 01/2

N86-10011# Air Force Systems Command, Wright-Patterson AFB, Ohio. Foreign Technology Div.
COMMENT ON DETERMINATION OF AERODYNAMIC COEFFICIENTS FOR A REENTRY BODY BY MEANS OF THE KALMAN FILTER METHOD
Jinshi Cai *In its* Three Articles on New Calculation Methods in Aeron. (Selected Articles) (FTD-ID(RS)T-0910-84) 17 Aug. 1984 p 43-46 Transl. into ENGLISH from Hangkong Xuebao (China), v. 4, no. 3, Sep. 1983 p 102-104 (For primary document see N86-10007 01-01)
Avail: NTIS HC A04/MF A01 CSCL 01/2

03 AIR TRANSPORTATION AND SAFETY

Includes passenger and cargo air transport operations; and aircraft accidents.

For related information see also *16 Space Transportation* and *85 Urban Technology and Transportation.*

N86-10030# Deutsche Forschungs- und Versuchsanstalt fuer Luft- und Raumfahrt, Cologne (West Germany). Hauptabt. Verkehrsforschung.
TENDENCIES TOWARD LIBERALIZATION IN EUROPEAN AIR TRAFFIC CONTROL
Rolf Juergen Haupt and Paul-Juergen Weber Mar. 1985 131 p refs In GERMAN; ENGLISH summary Report will also be announced as translation (ESA-TT-947)
(DFVLR-FB-85-23; ISSN-0171-1342) Avail: NTIS HC A07/MF A01; DFVLR, Cologne DM 37.50

Deregulation of European air transportation is discussed. Aim and content of proposed or decided regulations are considered, and proposals for the further development of the air transport system are offered. Aspects of competition, market entry and tariff regulations are presented and the fundamentals of air transport policy of Great Britain, Federal Republic of Germany and The Netherlands are described, indicating the points of view of the air transport managers (governments, airlines, and travel agencies) and of the users. Author (ESA)

N86-10031# Deutsche Forschungs- und Versuchsanstalt fuer Luft- und Raumfahrt, Cologne (West Germany). Haupabt. Verkehrsforschung.
THE AIR TRAFFIC DEMAND IN PASSENGER TRAVEL OF THE FEDERAL REPUBLIC OF GERMANY 1990 - 2000. UPDATE OF THE DFVLR AIR TRAFFIC FORECAST
Dieter Wilken and Klaus Bachmann Dec. 1984 125 p refs In GERMAN; ENGLISH summary
(DFVLR-Mitt-85-06; ISSN-0176-7739) Avail: NTIS HC A06/MF A01; DFVLR, Cologne DM 36

The future air transport demand for the Federal Republic of Germany was studied in order to update the demand part of the DFVLR air traffic forecast, with estimates of traffic at the German airports. The future demand volume was forecast with respect to trip purpose, region, and type of service. Reflecting a series of forecast hypotheses, especially regarding economic growth, demand for air travel is expected to grow from 16.3 million in 1982 to about 28 million air travellers in the year 2000. Primarily because of a strong growth of business travel, the demand for scheduled services will rise faster than the demand for charter services. Author (ESA)

04 AIRCRAFT COMMUNICATIONS AND NAVIGATION

Includes digital and voice communication with aircraft; air navigation systems (satellite and ground based); and air traffic control.

For related information see also *17 Spacecraft Communications, Command, and Tracking* and *32 Communications.*

No abstracts in this category.

05 AIRCRAFT DESIGN, TESTING AND PERFORMANCE

Includes aircraft simulation technology.

For related information see also *18 Spacecraft Design, Testing and Performance* and *39 Structural Mechanics.*

N86-10032 Department of the Air Force, Washington, D.C.
ATTACHMENT METHOD-CERAMIC RADOME TO METAL BODY Patent
J. S. Perry, inventor (to Air Force) Issued 28 May 1985 6 p Supersedes AD-D010270
(AD-D011778; US-Patent-4,520,364; US-Patent-Appl-SN-486603; US-Patent-Class-343-872) Avail: US Patent and Trademark Office CSCL 13/8

A radome assembly for an airframe and a method for attaching the assembly to an airframe are provided. The radome assembly comprises a ceramic shell with a polymeric transition section bonded thereto, which shell is adapted for mounting to a metal airframe. The transition section has a coefficient of thermal expansion intermediate between that of the ceramic shell and that of the metal airframe. The method of this invention comprises preloading the transition section in circumferential compression when the radome assembly is attached to the airframe.
Author (GRA)

N86-10033*# Virginia Polytechnic Inst. and State Univ., Blacksburg. Dept. of Chemistry.
A FUNDAMENTAL STUDY OF THE STICKING OF INSECT RESIDUES TO AIRCRAFT WINGS Annual Technical Report
N. S. Eiss, Jr., J. P. Wightman, D. R. Gilliam, and E. J. Siochi Apr. 1985 191 p refs
(Grant NAG1-300)
(NASA-CR-176231; NAS 1.26:176231) Avail: NTIS HC A09/MF A01 CSCL 01C

The aircraft industry has long been concerned with the increase

of drag on airplanes due to fouling of the wings by insects. The present research studied the effects of surface energy and surface roughness on the phenomenon of insect sticking. Aluminum plates of different roughnesses were coated with thin films of polymers with varying surface energies. The coated plates were attached to a custom jig and mounted on top of an automobile for insect collection. Contact angle measurements, X-ray photoelectron spectroscopy and specular reflectance infrared spectroscopy were used to characterize the surface before and after the insect impact experiments. Scanning electron microscopy showed the topography of insect residues on the exposed plates. Moments were calculated in order to find a correlation between the parameters studied and the amount of bugs collected on the plates. An effect of surface energy on the sticking of insect residues was demonstrated.
Author

N86-10034# Air Command and Staff Coll., Maxwell AFB, Ala.
THE DIRIGIBLE: A CATALYST FOR RESOURCE EXPLOITATION IN REMOTE AREAS?
J. C. Murphy Apr. 1985 80 p
(AD-A156518; ACSC-85-1950) Avail: NTIS HC A05/MF A01 CSCL 01/3

Many developing nations have considerable wealth in natural resources, but are unable to exploit it. Located in remote areas, the countries simply cannot afford to invest the enormous amounts required to build roads, railroads, or airfields to access the regions. The dirigible--modern day blimp--offers a potentially inexpensive, flexible, and capable method of of transporting minerals, timber, or crops in areas without traditional transportation support. Even more important, they can stimulate agricultural or industrial development a significant distance from principal roads thereby unlocking the wealth of the land for a nation. The airship can be the catalyst for colonization at the same time it strengthens the economy. This study provides a cost/benefit model to evaluate the relative benefits of different transportation systems in the exploitation of resources. Author (GRA)

N86-10035# Naval Postgraduate School, Monterey, Calif.
CONSTRUCTION AND USE OF A RADIO CONTROLLED MODEL HELICOPTER FOR RESEARCH M.S. Thesis
C. J. Hintze Mar. 1985 67 p
(AD-A156547) Avail: NTIS HC A04/MF A01 CSCL 01/3

This thesis examines the relationship that exists between a radio controlled model helicopter and a full-size helicopter. The construction of a radio controlled model helicopter and flight training involved is discussed. Initial hover performance testing of a radio controlled helicopter is evaluated. Author (GRA)

N86-10036# Aeronautical Research Labs., Melbourne (Australia).
A REVIEW OF AUSTRALIAN INVESTIGATIONS ON AERONAUTICAL FATIGUE DURING THE PERIOD APRIL 1983 TO MARCH 1985
G. S. Jost Mar. 1985 93 p
(AD-A156602; ARL/STRUC-TM-399) Avail: NTIS HC A05/MF A01 CSCL 01/3

A summary is presented of the aircraft fatigue research and associated activities which form part of the programs of the Aeronautical Research Laboratories, the Department of Aviation and the Australian aircraft industry. The major topics discussed include the fatigue of both civil and military aircraft structures, fatigue damage detection, analysis and repair and fatigue life monitoring and assessment. Author (GRA)

N86-10037# Aeronautical Research Labs., Melbourne (Australia).
REPORT ON AN OVERSEAS VISIT
C. M. Scala Nov. 1984 33 p
(AD-A156603; ARL/MAT-TM-388) Avail: NTIS HC A03/MF A01 CSCL 14/2

A report is given on an overseas visit by Dr C.M. Scala of Australia to the USA, U.K. and Switzerland for a period of thirty-two days departing Australia on 7 July 1984. The principal purposes of the visit were to: (1) attend and present a paper at the Review of Progress in Quantitative NDE held at the University of California, San Diego; (2) undertake updating visits to laboratories in the USA and U.K. to review current research in nondestructive evaluation (NDE) and to determine useful directions for future NDE research; and (3) coordinate progress (in both the USA and Switzerland) on the DSTO contract with Battelle Pacific Northwest Laboratories to monitor fatigue crack growth in a Mirage aircraft using acoustic emission (AE). GRA

N86-10038# Air Command and Staff Coll., Maxwell AFB, Ala.
RETROFIT OF SAC EC-135C AND RC-135 AIRCRAFT WITH CFM-56 ENGINES
W. N. Stooke, Jr. Apr. 1985 42 p
(AD-A156688; ACSC-85-2630) Avail: NTIS HC A03/MF A01 CSCL 15/5

This report is an analysis of the advantages and disadvantages of retrofitting SAC's EC-135C and RC-135 fleet with the CFM-56 engine package being used to convert the KC-135As to KC-135Rs. It reviews selected components of the modification package and compares the performance capabilities of current and modified aircraft during takeoff, cruise, receiver aerial refueling, and landing. The projected fuel savings on the investment dollar are calculated in Af Regulation 173-13, USAF Cost and Planning Factors, and could pay for the retrofit of the 31 aircraft in 18 years. Finally, the advantage of logistics commonality among all three aircraft is assessed. GRA

N86-10039# Aeronautical Research Labs., Melbourne (Australia).
PROPOSED MODIFICATIONS FOR THE RAAF AIRTRAINER CT-4A COCKPIT
K. W. Anderson and K. C. Hendy Dec. 1984 23 p
(AD-A156808; ARL/SYS-TM-75) Avail: NTIS HC A02/MF A01 CSCL 01/3

The design of the CT-4A Airtrainer cockpit is known to breach numerous ergonomics principles and several ASCC Air Standards. As a result, pilots report problems such as inadequate reach envelopes and obstruction of the control column by the left pilot's left knee. Consequently, the RAAF asked ARL to study the cockpit design and recommend simple changes. An anthropometric model was developed and used to evaluate several patterns of seat adjustment. The best of these (a ramp at 40 degrees to the fuselage reference line) was evaluated in practical trials with an experimental seat in a CT-4A fuselage. For each of the thirty pilot subjects, a sitting position with acceptable view, reach and clearance was found with the experimental arrangement. The ARL recommendations for cockpit modifications include: a smaller left side throttle quadrant with external pushrods, a seat adjustable along a 40 degree ramp, improved instrument lighting, pedals moved forwards, control column modifications, lowered lap belt anchor points, dual fuel gauges and a center transponder location. Incorporation of these recommendations is expected to enhance training effectiveness and improve flying safety. GRA

N86-10040# Air Command and Staff Coll., Maxwell AFB, Ala.
THE QUEST FOR A HELICOPTER SUITABLE FOR COMBAT RESCUE, 1967 - 1983
T. O. Jahnke Apr. 1985 30 p
(AD-A156842; AD-E301723; ACSC-85-1330) Avail: NTIS HC A03/MF A01 CSCL 01/3

This paper provides a concise, historical perspective of the quest for a helicopter suitable for combat rescue. Concentrating on the period 1967 to 1983, this report looks at the historical development, roles and missions, and analyzes the selection process of four different combat rescue helicopters. The study concludes that the unique mission requirements of combat rescue require aircraft designed from the ground on as pure rescue helicopters. Author (GRA)

N86-10041# Naval Postgraduate School, Monterey, Calif.
A COMPARATIVE ANALYSIS OF A CV HELICOPTER AND A JVX (JOINT SERVICES ADVANCED VERTICAL LIFT) TILT-ROTOR AIRCRAFT IN AN AIRCRAFT CARRIER BASED ASW (ANTI-SUBMARINE WARFARE) M.S. Thesis
R. L. Wilde Mar. 1985 134 p

(AD-A156871) Avail: NTIS HC A07/MF A01 CSCL 01/3

This thesis analyzes the environmental compatibility and the potential performance capabilities of two proposed types of vertical flight capable aircraft in an aircraft carrier Anti-Submarine role. The aircraft compared are the CV Helicopter(SH-60F) and an ASW variant of the Joint Services Advanced Vertical Lift (JVX) tilt-rotor aircraft. This thesis compares their adaptability and relative expected mission effectiveness by analyzing their physical dimensions and characteristics and their projected flight performance parameters. Their expected performance in a specific scenario, an ASW pouncer mission employing active dipping sonar, is analyzed using a simulation model. GRA

N86-10042*# Texas Technological Univ., Lubbock. Dept. of Electrical Engineering.

ELECTROMAGNETIC RESONANCES OF CYLINDERS AND AIRCRAFT MODEL WITH RESISTIVE WIRES Final Report, Apr. 1983 - Apr. 1984

G. W. Wood and T. F. Trost Apr. 1985 61 p

(Contract NAG1-28; DA Proj. 376-3)

(NASA-CR-176250; NAS 1.26:176250; AD-A156960;

AFWL-TR-84-90) Avail: NTIS HC A04/MF A01 CSCL 01C

Laboratory experiments were done to determine the natural frequencies of the electromagnetic resonances of conducting bodies with attached wires. The bodies include two cylinders and an approximate scale model of the NASA F-106B aircraft. All are three feet in length. Time-domain waveforms of B-dot and D-dot were obtained from a sampling oscilloscope, and Prony analysis was used to extract the natural frequencies. This work is an extension of previous work, but smaller, more resistive wires have been used. The first four natural frequencies of the cylinders (and wires) were determined, and a comparison with calculated results of other investigators show reasonable agreement. Seven natural frequencies were determined for the F-106B model (wire wires), and these have been compared with results obtained by NASA in 1982 during direct lightning strikes to the aircraft. The agreement between the corresponding natural frequencies of the model and the aircraft is fairly good and is better than that obtained in the previous work using wires with less resistance. The frequencies lie between 6.5 MHz and 41 MHz, and all of the normalized damping rates are between 0.14 and 0.27. GRA

N86-10043# European Space Agency, Paris (France).

SYSTEM MODELING AND IDENTIFICATION OF EQUIVALENT SYSTEMS WITH AND WITHOUT COMPENSATING TIME DELAY FOR CONTROL-AUGMENTED AIRCRAFT

Jean Skudridakis Oct. 1985 104 p refs Transl. into ENGLISH of "Systemmodellierung und Identifizierung von aequivalenten' Systemen mit und ohne Ersatztotleit fuer reglergestuetzte Flugzeuge' Rept. DFVLR-FB-83-36, DFVLR, Brunswick, 1983 Original language document was previously announced as N84-24570

(ESA-TT-852; DFVLR-FB-83-36) Avail: NTIS HC A06/MF A01; original German version available from DFVLR, Cologne DM 34

The identification of the aerodynamic and equivalent derivatives in the longitudinal and lateral motions of modern fighter aircraft is described. Determination of handling qualities parameters through reduced evaluation methods in order to fulfill the requirements of the MIL-F-8785 C calculation is discussed. To accomplish that goal, the highly complex method of observing aircraft motion was reduced by goal-oriented simplifications to a lower order system. The mathematical modeling for various control inputs with and without compensating time-delay, their influence on the results, and their accuracy are outlined. Author (ESA)

N86-10044# Fraunhofer-Inst. fuer Betriebsfestigkeit, Darmstadt (West Germany).

REVIEW OF INVESTIGATIONS ON AERONAUTICAL FATIGUE IN THE FEDERAL REPUBLIC OF GERMANY Review Period, May 1983 - April 1985

O. Buxbaum and H. Huth 1985 86 p refs Presented at 19th Intern. Comm. on Aeron. Fatigue (ICAF) Conf., Pisa, 1985

(LBF-S-173; ISSN-0721-5320) Avail: NTIS HC A05/MF A01; Fachinformationszentrum, Karlsruhe, West Germany DM 95

Measurement and analysis of operational loads on aircraft; metal fatigue (notch strength, low cycle fatigue, crack propagation and fracture mechanics); composites (fatigue, environmental influences, damage mechanisms); joints; fatigue life prediction; and component and full scale tests are summarized. Author (ESA)

N86-10045# Technische Hogeschool, Delft (Netherlands). Dept. of Aerospace Engineering.

FATIGUE, STATIC TENSILE STRENGTH AND STRESS CORROSION OF AIRCRAFT MATERIALS AND STRUCTURES

J. Schijve Oct. 1982 203 p refs Presented at Summer School Course, Bandung, Indonesia, Aug. 1982 Sponsored by Netherlands and Indonesian Governments

(VTH-LR-360-Pt-1) Avail: NTIS HC A10/MF A01

Failure modes in aircraft structures; stress concentration at notches; plastic deformation and residual stress; stress intensity factors of cracks; failure in tension; stress corrosion; material fatigue; fatigue under constant and variable amplitude loading; joint fatigue; fatigue loads on aircraft structures; and fatigue of aircraft structures are discussed. Author (ESA)

N86-10004# Air Force Systems Command, Wright-Patterson AFB, Ohio. Foreign Technology Div.

OPTIMUM DESIGN OF AN AIRCRAFT WING STRUCTURE WITH MULTIPLE CONSTRAINTS BY THE DIRECT-VISION CRITERIA METHOD

Li Linang (Shenyang Aircraft Corp.) *In its* Acta Aeron. et Astronautica Sinica (FTD-ID(RS)T-1120-84) 4 Oct. 1984 p 34-52 refs Transl. into ENGLISH from Hangkong Xuebao (China), v. 4, no. 4, 1983 p 39-47 (For primary document see N86-10001 01-01) Avail: NTIS HC A04/MF A01 CSCL 01/1

06 AIRCRAFT INSTRUMENTATION

Includes cockpit and cabin display devices; and flight instruments.

For related information see also *19 Spacecraft Instrumentation* and *35 Instrumentation and Photography.*

No abstracts in this category.

07 AIRCRAFT PROPULSION AND POWER

Includes prime propulsion systems and systems components, e.g., gas turbine engines and compressors; and on-board auxiliary power plants for aircraft.

For related information see also *20 Spacecraft Propulsion and Power, 28 Propellants and Fuels,* and *44 Energy Production and Conversion.*

No abstracts in this category.

08 AIRCRAFT STABILITY AND CONTROL

Includes aircraft handling qualities; piloting; flight controls; and autopilots.

N86-10046 Mississippi State Univ., State College.

GUIDANCE AND CONTROL OF A CABLE BASED PAYLOAD PICKUP SYSTEM Ph.D. Thesis

Young-whoon Jun 1984 130 p

Avail: Univ. Microfilms Order No. DA8507876

A payload capsule in a hostile environment can be retrieved by use of a cable attached to an aircraft. The free end of the cable may be guided to the payload capsule by a specially designed tug aircraft. To accomplish this mission successfully, a control law is needed to obtain the minimum miss-distance (less than .6 ft), optimal trajectory and minimum horizontal range which provides obstacle clearance for the tug. These objectives can be obtained by applying optimal control theory to a control system for the tug. A computer simulation study has been made to obtain the control law giving the minimum clearance range and optimal trajectory of the cable pickup system. The simulated tug has a sensor package which provides precise measurement information. With this information, the control can be generated to allow a hook engagement for a small target. Dissert. Abstr.

N86-10047# Deutsche Forschungs- und Versuchsanstalt fuer Luft- und Raumfahrt, Brunswick (West Germany). Abt. Flaechenflugzeuge.

CONTROL CONCEPTS FOR IN-FLIGHT SIMULATION INCLUDING ACTUATOR NONLINEARITIES AND TIME DELAYS

Frohmut Henschel Mar. 1985 69 p refs In GERMAN; ENGLISH summary Report will also be announced as translation (ESA-TT-948)

(DFVLR-FB-85-24; ISSN-0171-1342) Avail: NTIS HC A04/MF A01; DFVLR, Cologne DM 23.50

A model-following system was developed to study the dynamic behavior of transport aircraft with reduced longitudinal stability. The system is divided into two parts. The first consists of feedforward branches. If a linear description of the model and the basic aircraft is assumed an exact model-following is achieved by this part. For the control matrices algebraic expressions are derived. In the equations the influence of actuator dynamics is considered. A set of formulas in which all variables are assumed to be discretized for processing on a digital computer is developed. By the second subsystem an error suppression is achieved. The application of a cost vector method is demonstrated for one example. It is shown that nonlinearities and time lags can be included in the calculation of the feedback gains. Author (ESA)

09 RESEARCH AND SUPPORT FACILITIES (AIR)

Includes airports, hangars and runways; aircraft repair and overhaul facilities; wind tunnels; shock tube facilities; and engine test blocks.

For related information see also *14 Ground Support Systems and Facilities (Space).*

N86-10048*# National Aeronautics and Space Administration. Ames Research Center, Moffett Field, Calif.

MANNED FLIGHT SIMULATION: CHALLENGE AND RESPONSE

John C. Dusterberry Sep. 1985 10 p refs

(NASA-TM-86827; Rept-85392; NAS 1.15:86827) Avail: NTIS HC A02/MF A01 CSCL 14B

Early AGARD papers on manned flight simulation describe the status of an emerging test technique and then offer suggestions of problems that should be solved to advance the technique and predictions of the results that will be obtained by its use. Later AGARD literature is examined to determine how these challenges have been met, both in ground-based and in-flight simulation and how AGARD has played an important role in advancing the technique so that it is now an integral part of the aerospace vehicle design process. Author

N86-10049# Sandia Labs., Albuquerque, N. Mex.

SIMULATED DIRECT-STRIKE LIGHTNING TESTING AT SANDIA NATIONAL LABORATORIES

G. L. Maxam 1985 10 p Presented at the Intern. Symp. on Electromagnetic Compatibility, Wakefield, Miss., 20 Aug. 1985

(Contract DE-AC04-76DP-00789)

(DE85-012033; SAND-85-0063C; CONF-850884-1) Avail: NTIS HC A02/MF A01

The design of the Sandia Lightning Simulator is described and its capabilities are summarized. The approach generally used in testing components and systems including the instrumentation used for test item diagnostics and for data acquisition is also described. Several applications of the simulator test capabilities are examined including Sandia systems, Navy aircraft and an ALCM missile. Some future directions now envisioned are discussed. DOE

N86-10050# Eidgenoessisches Flugzeugwerk, Emmen (Switzerland).

INVESTIGATIONS TO IMPROVE THE SLOTTED-WALL TEST SECTION OF THE F+W TRANSONIC WIND TUNNEL

Gerard Capitaine Nov. 1984 29 p refs Presented at European Mech. Colloq. No. 137 on Adaptive Wall Wind Tunnels and Wall Interferences Correction Methods, Goettingen, West Germany, 15-17 Oct. 1984

(Grant LFP-955147)

(F+W-FO-1752) Avail: NTIS HC A03/MF A01

Efficiency of a slotted wind tunnel wall is improved; wall and wall interferences of the selected wall configuration for three dimensional models are estimated. The influence of the opening of the ventilated wall on the aerodynamic coefficients of tested models is investigated. The cross-flow characteristics of the ventilated wall are determined. Due to the particular test section design (deep slots, small plenum chamber) and the natural mass outflow removal, the precise determination of the wall characteristics is difficult. In order to assess the mass flow through the wall, direct measurements and an indirect method were used. The latter method is based on the simple one-dimensional channel flow equation, taking into account the boundary layer development along the test section walls. Direct and indirect method results agree. Author (ESA)

N86-10051# Deutsche Forschungs- und Versuchsanstalt fuer Luft- und Raumfahrt, Goettingen (West Germany). Abt. Hochgeschwindigkeitsstroemungen.

THE RUBBER TUBE TEST SECTION OF THE DFVLR IN GOETTINGEN, WEST GERMANY

Erich Wedemeyer and Alfred Heddergott Jul. 1984 45 p refs

(DFVLR-FB-85-18; ISSN-0171-1342) Avail: NTIS HC A03/MF A01; DFVLR, Cologne DM 13.50

To realize three-dimensional adaptative wind tunnel walls a test section is constructed from a thick walled rubber tube. Test section length = 240 cm, and circular cross section = 80 cm. It is installed in a high speed wind tunnel. The cylindrical walls of the test section can be adapted to interference free boundary conditions by a set of 64 jacks driven by stepping motors. The measurement and evaluation of wall pressures, the computation of the interference free wall contour, and the wall adaptation by the 64 jacks are computer-controlled and performed automatically. Model tests demonstrate the achievement of interference free flow. Author (ESA)

N86-10052# German-Dutch Wind Tunnel, North East Polder (Netherlands).

[ACTIVITIES REPORT OF THE GERMAN-DUTCH WIND TUNNEL] Annual Report, 1982

1983 18 p refs

Avail: NTIS HC A02/MF A01

Testing, calibrating, demonstrations and systems integration of a large, low speed wind tunnel are outlined. Rotor noise and automobile tests are described. Author (ESA)

12 ASTRONAUTICS (GENERAL)

For extraterrestrial exploration see *91 Lunar and Planetary Exploration.*

N86-10053*# National Aeronautics and Space Administration, Washington, D.C.

MICROGRAVITY SCIENCE AND APPLICATIONS PROGRAM TASKS

Elizabeth Pentecost, comp. May 1985 224 o refs
(NASA-TM-87568; NAS 1.15:87568) Avail: NTIS HC A10/MF A01 CSCL 22A

This report is a compilation of the active research tasks as of the end of the fiscal year 1984 of the Microgravity Science and Applications Program, NASA-Office of Space Science and Applications, involving several NASA centers and other organizations. The purpose of the document is to provide an overview of the program scope for managers and scientists in industry, university, and government communities. The report is structured to include an introductory description of the program, strategy and overall goal; identification of the organizational structures and people involved; and a description of each research task, together with a list of recent publications. The tasks are grouped into six categories: (1) electronic materials; (2) solidification of metals, alloys, and composites; (3) fluid dynamics and transports; (4) biotechnology; (5) glasses and ceramics; and (6) combustion. For individual titles, see N86-10054 through N86-10178.

N86-10054*# North Carolina State Univ., Raleigh.
PROCESSING OF COMPLEX COMPOUND SEMICONDUCTORS IN SPACE Abstract Only

Klaus Bachmann *In* NASA, Washington Microgravity Sci. and Appl. Program Tasks May 1985 p 7 (For primary document see N86-10053 01-12)
(Grant NAG1-354)
Avail: NTIS HC A10/MF A01 CSCL 22A

The purpose of this first year ground based research effort was to develop growth and characterization facilities for bulk single crystals of compound semiconductor alloys. As a system of 2-6 alloy crystal growth, C sub x Mn sub (1-x)Te was chosen since it has a relatively narrow solidus-liquidus separation serving as a suitable first model for zone melting and solution growth. Also, it allows, in principle, perfect lattice matching to Cd sub x Hg sub(1-x)Te that needs to be studied as a model for the investigation of heteroepitaxial growth from Te-solutions. A vertical zone melting furnace was built and used in the synthesis of Cd sub x Mn sub(1-x)Te from the elements and crystal growth in carbon coated fused silica crucibles of Bridgman growth geometry. Photoluminescence spectra of the crystals reveal band to band recombination at energies that agree with the reported literature data. In addition, deep luminescence is present at energies corresponding to proportional shifts from the 1.4 eV deep emission observed for bulk single crystals of CdTe. Author

N86-10055*# Massachusetts Inst. of Tech., Cambridge.
FLUID FLOW IN CRYSTAL GROWTH: ANALYSIS OF THE VERTICLE BRIDGMAN AND FLOATING ZONE PROCESS

Robert A. Brown *In* NASA, Washington Microgravity Sci. and Appl. Program Tasks May 1985 p 8-10 refs (For primary document see N86-10053 01-12)
(Grant NsG-7645)
Avail: NTIS HC A10/MF A01 CSCL 22A

Research is aimed at the fundamental understanding of the interactions of heat and mass transport and fluid mechanics in crystal growth from the melt, especially in how it pertains to experiments supported by the Microgravity Science and Applications program. Emphasis has been on studies of the vertical Bridgman system, on small-scale floating zone systems proposed for space flight, and on quantitative prediction of nonlinear transitions in melt/solid interface morphologies leading to the formation of dendrites in directional solidification. The analysis of vertical Bridgman growth has lead to the complete numerical analysis of transport phenomena in directional solidification and to a detailed comparison of calculations to the GaGe growth experiments of Wang and Witt. Calculations show the central role of the ampoule material in determining the radial temperature gradients in the melt and thus, the intensity of convection. Results indicate that diffusion-controlled growth can not be achieved on Earth with conventional growth systems, but are feasible in microgravity B.W.

N86-10056*# Massachusetts Inst. of Tech., Cambridge. Dept. of Materials Sciences and Engineering.
SOLUTAL CONVECTION AND ITS EFFECTS ON CRYSTAL GROWTH AND SEGREGATION IN BINARY AND PSEUDO-BINARY SYSTEM WITH LARGE LIQUIDUS-SOLIDUS SEPARATION

Robert A. Brown and August F. Witt *In* NASA, Washington Microgravity Sci. and Appl. Program Tasks May 1985 p 11 (For primary document see N86-10053 01-12)
(Grant NsG-7645)
Avail: NTIS HC A10/MF A01 CSCL 22A

This research program is composed of theoretical and experimental studies of solutal convection and its effects on crystal growth and segregation in binary and pseudo-binary systems with large liquidus-solidus separation. The theoretical program has resulted in the development of a transient simulation of the growth of concentrated alloys in microgravity and has been used to study the dynamics of GeSi, PbSnTe, HgCdTe growth. Finite element analysis has also been developed for studying the interactions of buoyancy-driven convection in the melt caused by temperature and concentration variations with melt-solid interface morphology and alloy segregation in the grown crystal. These calculations are being compared directly to experimental measurements of segregation and interface shape for GeSi growth and GaGe growth. The results for SiGe indicate that careful design of the thermal system can result in almost diffusion-controlled growth on Earth because of the stablizing influence of the concentration gradient ahead of the solidification front. B.W.

N86-10057*# National Aeronautics and Space Administration. Langley Research Center, Hampton, Va.
CRYSTAL GROWTH RESEARCH IN SPACE

R. K. Crouch and A. L. Fripp *In* NASA, Washington Microgravity Sci. and Appl. Program Tasks May 1985 p 12-13 refs (For primary document see N86-10053 01-12)
Avail: NTIS HC A10/MF A01 CSCL 22A

The objectives of this work are to develop growth techniques and theory leading to improved bulk growth of semiconductor single crystals. Ground based experiments will be complemented by experiments carried out in the low-g environment provided by the space shuttle. Analytical studies and laboratory investigations are being conducted to better define the causes of crystalline defects and inhomogeneities. The compound semiconductor lead-tin-telluride is being used as the modeling material. Theoretical techniques are being developed to predict the thermal and solutal fields which are present during bulk growth from a melt. Techniques for measuring the thermophysical properties of semiconductors at high temperatures have been developed. During the past year electrochemical etching techniques have been developed for delineation of inhomogeneous regions in crystals. Thermal diffusivity measurements have been completed for the solid and liquid phases of PbTe and PbSnTe. Preliminary results have been obtained on the effects on crystal morphology of gravity, interface shape and interaction between the melt and the container. B.W.

N86-10058*# National Aeronautics and Space Administration. Marshall Space Flight Center, Huntsville, Ala.
GROWTH OF ORGANIC CRYSTALS BY OSTWALD RIPENING Abstract Only

William Egbert (Minnesota Mining and Manufacturing Co.), Christopher Podsiadly (Minnesota Mining and Manufacturing Co.), and Robert Naumann *In* NASA, Washington Microgravity Sci. and Appl. Program Tasks May 1985 p 14 (For primary document see N86-10053 01-12)
Avail: NTIS HC A10/MF A01 CSCL 22A

The objective of this investigation is to evaluate the growth of various organic crystals by chemical precipitation and Ostwald ripening. Six precipitation reactors were flown on STS-51A. Five of the reactors contained proprietary materials. The sixth contained

urea dissolved in ethanol with toluene as the precipitating agent. The size distribution will be analyzed and compared with a similar model being developed. B.W.

N86-10059*# Stanford Univ., Calif. Center for Materials Research.
THE INFLUENCE OF LOW FREQUENCY MECHANICAL VIBRATIONS ON THE GROWTH OF SINGLE CRYSTALS
Robert S. Feigelson and Dennis Elwell *In* NASA, Washington Microgravity Sci. and Appl. Program Tasks May 1985 p 15 (For primary document see N86-10053 01-12)
(Contract NAS8-34872)
Avail: NTIS HC A10/MF A01 CSCL 22A

The optimum conditions for crystal growth are usually achieved either by suppressing convective fluid flows (e.g., by the use of a low-gravity environment) or by over-riding thermal and solutal convection by the use of a strong stirring action. A novel stirring technique has been developed which involves subjecting a vertical crucible to a circle in a horizontal plane (without rotation). Use of an amplitude of 3 mm at a frequency of approx 6 Hz produced complete mixing of a non-uniform aqueous liquid in a few seconds. The mixing action involved the downward flow of liquid in the outer annulus of the liquid, driven by surface waves. When the downward flowing liquid reaches the bottom of the crucible, it is reflected in a central, upward flowing spiral. This flow pattern should be beneficial for crystal growth by the Bridgman method since it will sweep impurities away from the walls and produce a more convex solid-liquid interface. Initial attempts to apply the new stirring technique to CdTe crystal growth did not show significant improvement in the number of crystals nucleated, but the interface shape appeared to be close to that predicted. B.W.

N86-10060*# Science Applications, Inc., Huntsville, Ala.
THE CONTROL OF FLOAT ZONE INTERFACES BY THE USE OF SELECTED BOUNDARY CONDITIONS
Larry M. Foster *In* NASA, Washington Microgravity Sci. and Appl. Program Tasks May 1985 p 16 (For primary document see N86-10053 01-12)
(Contract NAS8-35108)
Avail: NTIS HC A10/MF A01 CSCL 22A

Since the float zone process involves two solid-melt interfaces, possible gas interfaces, heat and mass transfers, various driving forces and complex heating sources, an analysis of the entire process would be very complex. For an initial investigation, a more feasible approach is to examine each component of the process separately. The three principal components are: (1) the shapes of the melt and solid-melt interfaces, (2) the heat and mass transfers, and (3) the heating and cooling sources. This study combined facets of all three components. The purpose of this effort was to study and compute the surface boundary conditions required to give flat (float zone) FZ solid-melt interfaces. This study was undertaken in two phases. The first phase was to investigate the solid zones surface boundary conditions required for flat solid-melt interfaces when given the melt zone surface boundary conditions. The second phase complemented the first and was to investigate the melt zone surface boundary conditions required for flat solid-melt interfaces if given the solid zones surface boundary conditions. Dual integral transform methods were used in both phases; in addition, the use of various numerical methods for differential equations and linear systems of equations were required. B.W.

N86-10061*# Massachusetts Inst. of Tech., Cambridge.
CRYSTAL GROWTH OF DEVICE QUALITY GaAs IN SPACE
Harry C. Gatos *In* NASA, Washington Microgravity Sci. and Appl. Program Tasks May 1985 p 17-18 refs (For primary document see N86-10053 01-12)
(Grant NsG-7331)
Avail: NTIS HC A10/MF A01 CSCL 22A

The GaAs research evolves about these key thrust areas. The overall program combines: (1) studies of crystal growth on novel approaches to engineering of semiconductor material (i.e., GaAs and related compounds); (2) investigation and correlation of materials properties and electronic characteristics on a macro- and microscale; and (3) investigation of electronic properties and phenomena controlling device applications and device performance. This effort is aimed at the essential ground-based program which would insure successful experimentation with and eventually processing of GaAs in near zero gravity environment. It is believed that this program addresses in a unique way materials engineering aspects which bear directly on the future exploitation of the potential of GaAs and related materials in device and systems applications. Author

N86-10062*# Massachusetts Inst. of Tech., Cambridge.
CRYSTAL MELTS UNDER REDUCED GRAVITY
Harvey P. Greenspan *In* NASA, Washington Microgravity Sci. and Appl. Program Tasks May 1985 p 19 (For primary document see N86-10053 01-12)
(Contract NAS8-35412)
Avail: NTIS HC A10/MF A01 CSCL 22A

To date, fluid motion due to thermocapillary convection and centrifugal buoyancy has been studied theoretically and numerically, by adapting specialized programs for rotating viscous fluids. It has been shown that by rotating the crystal melt, thermocapillary flow can be confined to a thin layer at the melt-gas interface even when the interfacial velocity is large enough for non-linear effects to be important. Theoretical analysis of the basic processes proceeds, but a much larger effort is now being devoted to the numerical simulation of the actual motion in a rotating crystal melt. A numerical program is under development for the study of the fully nonlinear problem. Although the flow is viewed, to start, as one of rapid rotation (in order that certain boundary layer simplifications can be invoked), a more general approach will allow consideration of the situations and conditions of real practical interest. B.W.

N86-10063*# Westech Systems, Inc., Phoenix, Ariz.
MICROGRAVITY SILICON ZONING INVESTIGATION
E. L. Kern *In* NASA, Washington Microgravity Sci. and Appl. Program Tasks May 1985 p 20 (For primary document see N86-10053 01-12)
(Contract NAS8-34920)
Avail: NTIS HC A10/MF A01 CSCL 22A

This research program is directed toward the understanding of the float zone crystal growth process, the melt interactions which lead to crystal inhomogeneities, and the influence of microgravity on reducing these inhomogeneities. Silicon was selected as the model crystal because its inhomogeneities lead to known variations in device performance, and because the mechanisms involved in its growth are understood better than for other high temperature crystals. The objective of the program is to understand the growth mechanisms in float zone growth and thereby determine the feasibility and advantages of float zone growth of silicon under microgravity conditions. This will be done by characterizing the growth at $g = 1$, projecting the changes in melt flows due to microgravity, observing these in space growth and determining the effects on defective inhomogeneities. A Thin Rod Zoner was constructed as a laboratory prototype for flight growth of 5 mm diameter silicon crystals, which can be done within the power and cooling capabilities of shuttle flights. A new method of zoning silicon, using resistance heating, has resulted in melting 5 mm diameter ingots. B.W.

N86-10064*# Alabama A & M Univ., Normal. Dept. of Physics and Mathematics.
SOLUTION GROWTH OF CRYSTALS IN ZERO-GRAVITY
R. B. Lal and R. L. Kroes *In* NASA, Washington Microgravity Sci. and Appl. Program Tasks May 1985 p 21-22 refs (For primary document see N86-10053 01-12)
(Contract NAS8-32945)
Avail: NTIS HC A10/MF A01 CSCL 22A

In a low-g environment, buoyancy driven convection effects in solution crystal growth are greatly reduced and, thus, one can study diffusion mass transport which in 1-g is masked by convective phenomena. Crystals of triglycine sulfate (TGS) will be grown

aboard the Spacelab 3 mission, using a specially developed Fluids Experiments System (FES). The objectives of the experiment are: (1) to develop a technique for solution crystal growth in a low-g environment, (2) to characterize the growth environment provided by an orbiting spacecraft and to determine the influence of the environment on the growth behavior, and (3) to determine how gravity in a low-gravity environment influences the properties of a resulting TGS crystal. Single crystals of TGS have been grown using conventional low-temperature solution crystal growth method and the growth process has been extensively characterized. Various physical properties of TGS solution have been measured. Also, a unique technique of growing solution growth crystals by extracting heat at a programmed rate from the crystal through a semi-insulating sting has been developed and tested in 1-g environment. B.W.

N86-10065*# National Aeronautics and Space Administration. Marshall Space Flight Center, Huntsville, Ala.

GROWTH OF SOLID SOLUTION CRYSTALS

S. L. Lehoczky, F. R. Szofran, and L. R. Holland (Wyle Labs., Inc., Huntsville, Ala.) *In* NASA, Washington Microgravity Sci. and Appl. Program Tasks May 1985 p 23-25 refs (For primary document see N86-10053 01-12)

Avail: NTIS HC A10/MF A01 CSCL 22A

The major objective of this program is to determine the conditions under which single crystals of solid solutions can be grown from the melt in a Bridgman configuration with a high degree of chemical homogeneity. The central aim is to assess the role of gravity in the growth process and to explore the possible advantages for growth in the absence of gravity. The alloy system being investigated is the solid solution semiconductor with x-values appropriate for infrared detector applications in Hg sub (1-x) Cd sub x Te the 8 to 14 micro m wavelength region. Both melt and Te-solvent growth are being considered. The study consists of an extensive ground-based experimental and theoretical research effort followed by flight experimentation where appropriate. Experimental facilities have been established for the purification, casting, and crystal growth of the alloy system. Facilities have been also established for the metallurgical, compositional, electric and optical characterization of the alloys. Crystals are being grown by the Bridgman-Stockbarger method and are analyzed by various experimental techniques to evaluate the effects of growth conditions on the longitudinal and radial compositional variations and defect densities in the crystals. B.W.

N86-10066*# Edgerton, Germeshausen and Grier, Inc., Goleta, Calif.

HgI SUB 2 CRYSTAL GROWTH FOR NUCLEAR DETECTORS

W. F. Schnepple and L. VandenBerg *In* NASA, Washington Microgravity Sci. and Appl. Program Tasks May 1985 p 26-27 refs (For primary document see N86-10053 01-12)

(NASA Order H-73830-B)

Avail: NTIS HC A10/MF A01 CSCL 22A

The objectives of this program are to obtain a benchmark quality sample grown at low-g conditions and to study vapor growth phenomena under space conditions. Ground-based crystals show a defect structure which impairs their performance as nuclear radiation detectors. These defects may be caused by the gravitational force acting on the crystal in its weakended state at the elevated growth temperature and by irregular convection patterns in the vapor during growth. Mechanical strength measurements have been performed (uniaxial compression tests) which show that the crystals exhibit slip parallel to the c-planes at stresses as low as 1/2 psi. Preliminary calculations using a simple linearized model indicate the oscillating instabilities in the convection part of the vapor transport system are unlikely, even at 1-g, provided that the utmost care is taken in the preparation of the crystal growth source material. Author

N86-10067*# Ames Lab., Iowa.

FLOAT ZONE EXPERIMENTS IN SPACE

John D. Verhoeven *In* NASA, Washington Microgravity Sci. and Appl. Program Tasks May 1985 p 28-29 refs (For primary document see N86-10053 01-12)

(NASA Order H-34328-B)

Avail: NTIS HC A10/MF A01 CSCL 22A

The objective of this work has been to evaluate whether or not Marangoni flow could be suppressed in molten metals by the presence of very thin oxide films. Experimental work has been carried out on molten Sn under UHV conditions. A disk floating zone arrangement was developed to allow in situ Auger examination of molten surfaces. An electron energy loss technique was developed which allows detection of continuous tin oxide films of 6 A or greater. Experiments were planned to detect the effects of oxide formation upon Marangoni flow by measuring: (1) temperature profiles, (2) solid liquid interface shapes, (3) macrosegregation, and (4) the onset of oscillatory Marangoni flow by detecting oscillating temperature variations. Work on (4) showed that oscillatory temperature variations of frequency $<$ or $=$ 10 Hz were not present in the disk float zone geometry under conditions of Ma $=$ 4300 with an oxide free molten surface. The disk float zone geometry was modeled with a finite element analysis and temperature and velocity profiles were determined. B.W.

N86-10068*# Rensselaer Polytechnic Inst., Troy, N. Y. Dept. of Chemistry.

FLUID DYNAMICS AND THERMODYNAMICS OF VAPOR PHASE CRYSTAL GROWTH

H. Wiedemeier *In* NASA, Washington Microgravity Sci. and Appl. Program Tasks May 1985 p 30-31 refs (For primary document see N86-10053 01-12)

(Contract NAS8-33562)

Avail: NTIS HC A10/MF A01 CSCL 22A

The ground-based research effort under this program is concerned with systematic studies of the effects of variations: (1) of the relative importance of buoyancy-driven convection, and (2) of diffusion and viscosity conditions on crystal properties. These experimental studies are supported by thermodynamic characterizations of the systems, based on which fluid dynamic parameters can be determined. The specific materials under investigation include: the GeSe-GeI4, Ge-GeI4, HgTe-HgI2, and Hg sub (1-x)Cd sub (x) Te-HgI2 systems. Mass transport rate studies of the GeSe-GeI system as a function of orientation of the density gradient relative to the gravity vector demonstrated the validity of flux anomalies observed in earlier space experiments. The investigation of the effects of inert gases on mass flux yielded the first experimental evidence for the existence of a boundary layer in closed ampoules. Combined with a thorough thermodynamic analysis, a transport model for diffusive flow including chemical vapor transport, sublimation, and Stefan flow was developed. B.W.

N86-10069*# Rensselaer Polytechnic Inst., Troy, N. Y. Dept. of Chemistry.

VAPOR GROWTH OF ALLOY-TYPE SEMICONDUCTOR CRYSTALS

H. Wiedemeier *In* NASA, Washington Microgravity Sci. and Appl. Program Tasks May 1985 p 32-33 refs (For primary document see N86-10053 01-12)

(Contract NAS8-32936)

Avail: NTIS HC A10/MF A01 CSCL 22A

The present effort is part of a continuing research program directed towards the investigation of basic vapor transport phenomena and of crystal growth properties of electronic materials. The primary purpose of ground-based studies is the development and definition of optimum experimental parameters for flight experiments. The ground-based effort includes the investigation of gravity-driven convection effects on mass transport rates and on crystal morphology for different orientations of the density gradient with respect to the gravity vector, and as a function of pressure and of temperature. In addition to the experimental tasks, theoretical efforts involve the quantitative thermodynamic analysis of the systems under investigation, the computation of fluid dynamic parameters, and the consideration of other possible effects on fluid flow under vertical, stabilizing and microgravity conditions. The specific experiments to be performed in a microgravity environment include the investigation of vapor transport and crystal

growth phenomena of the GeSe-Xenon system and of the mass flux and growth of bulk and layer-type crystals of Hg sub (1-x) Cd sub x Te using HgI as a transport agent. B.W.

N86-10070*# Clarkson Coll. of Technology, Potsdam, N.Y. Dept. of Chemical Engineering.
STUDY OF EUTECTIC FORMATION
W. R. Wilcox *In* NASA, Washington Microgravity Sci. and Appl. Program Tasks May 1985 p 34-35 refs (For primary document see N86-10053 01-12)
(Contract NAS8-34887)
Avail: NTIS HC A10/MF A01 CSCL 22A

The objectives of this program are to determine the influence of convection on the microstructure of eutectics and to develop a technique for revealing the longitudinal microstructure of the MnBi-Bi eutectic. Both objectives aim at trying to explain the observed influence of space processing on the microstructure of MnBi-Bi. A computer program was developed and used to determine the concentration field in front of a growing lamellar eutectic. From this the deviation of the interfacial concentration from the eutectic composition was calculated as a function of eutectic composition, freezing rate, convection, and lamellar spacing. B.W.

N86-10071*# Clarkson Coll. of Technology, Potsdam, N.Y. Dept. of Chemical Engineering.
MODELING DIRECTIONAL SOLIDIFICATION
W. R. Wilcox and T. Paptheodorou *In* NASA, Washington Microgravity Sci. and Appl. Program Tasks May 1985 p 36-37 ref (For primary document see N86-10053 01-12)
(Contract NAS8-34891)
Avail: NTIS HC A10/MF A01 CSCL 22A

The objective of the research is to develop tools of use in explaining the results of directional solidification experiments in space. These tools consist of mathematical and experimental models. Experiments are also being flown at low-g to validate the ground-based results. Many metals and semiconductors directionally solidified in space had a diameter less than that of the containing ampoule. In fact this occurred whenever the ampoule contained a gas space. This phenomenon has been attributed in a vague way to lack of wetting of the ampoule wall by the melt. The actual liquid behavior by use of low temperature analogs is being observed aboard the KC-135. In the first flight, water was placed in plastic ampoules (not wet) with ceramic end plugs which were wet by the water to simulate a solid-liquid interface. Unfortunately during storage prior to the flight the water began to wet the ampoule wall. Discrete bubbles formed down the axis of the ampoules. New ampoule materials are being used now, with testing for stability prior to the next flight. A theoretical model has also been developed for this phenomenon. B.W.

N86-10072*# Massachusetts Inst. of Tech., Cambridge.
HEAT FLOW AND SEGREGATION IN DIRECTIONAL SOLIDIFICATION
August F. Witt *In* NASA, Washington Microgravity Sci. and Appl. Program Tasks May 1985 p 38-39 refs (For primary document see N86-10053 01-12)
(Grant NsG-7645)
Avail: NTIS HC A10/MF A01 CSCL 22A

This research is composed of three major components: (1) development of interface morphology control for automated Bridgman growth of semiconductor systems; (2) comparative analysis of segregation during crystal growth in a reduced gravity environment and in the presence of magnetic fields; and (3) consequences of seeding by meltback in Bridgman growth under reduced gravity conditions. In attempts to optimize furnace design for crystal growth in a reduced gravity environment, an analytical approach to heat transfer was developed. It was thus found that charge confining crucibles diminish the ability to control the growth interface morphology through its position within the gradient zone. A heat pipe hot zone system for Bridgman growth, in reduced gravity environment, of crystal with diameters up to 16 mm was developed. For growth of Ga-doped germanium in the multipurpose (ASTP) furnace, it was found that the application of transverse magnetic fields (up to 36 kg) does not substantially increase the effective distribution coefficient; i.e., diffusion-controlled segregation observed in reduced gravity environment cannot be reached nor approached by magnetic field induced melt stabilization. B.W.

N86-10073*# Vanderbilt Univ., Nashville, Tenn. Dept. of Mechanical and Materials Engineering.
EFFECT OF UNDERCOOLING IN A LOW-GRAVITY CONTAINERLESS ENVIRONMENT ON THE STRUCTURE AND PROPERTIES OF ALLOYS
Robert J. Bayuzick *In* NASA, Washington Microgravity Sci. and Appl. Program Tasks May 1985 p 43-44 refs (For primary document see N86-10053 01-12)
(Contract NAS8-34676)
Avail: NTIS HC A10/MF A01 CSCL 22A

The 30 meter and 100 meter drop tubes at the Marshall Space Flight Center offer a unique opportunity to study solidification in a containerless, microgravity environment. Samples are melted in a furnace at the top of the drop tube and solidify during a 4.5 second free fall in the 100 meter drop tube or a 2.6 second free fall in the 30 meter drop tube. The cooling rate obtained in the drop tubes is lower than cooling rates in atomization and splat-quenching processes. Decoupling the rapid solidification process allows the study of the effects of undercooling and recalescence on alloy morphologies. The research therefore has a three-fold purpose. The first is examination of the limits of undercooling of niobium and niobium-base alloys in the drop tube. The second purpose is the observation of microstructures resulting from the solidification of samples at large undercoolings and moderate cooling rates. The third purpose is the observation of metastable phase formation in highly undercooled samples. B.W.

N86-10074*# National Bureau of Standards, Washington, D.C.
MEASUREMENT OF HIGH TEMPERATURE THERMOPHYSICAL PROPERTIES
D. W. Bonnell *In* NASA, Washington Microgravity Sci. and Appl. Program Tasks May 1985 p 45-46 refs (For primary document see N86-10053 01-12)
(NASA Order H-27954-B)
Avail: NTIS HC A10/MF A01 CSCL 22A

Technique development and the application of electromagnetic levitation to thermophysical property measurement, including determining heats of fusion, heat capacities, and enthalpy increment functions for extremely refractory materials are discussed. Tungsten properties and the development of an apparatus employing electromagnetic levitation and electron beam heating capable of melting levitating tungsten high temperature heat content measurements by drop calorimetry are emphasized. The development of a prototype microcomputer data acquisition system suitable for controlling the ground based system, with consequent improvement in system handling, which can serve as a model for the system needed for flight experiments is described, which include the development of techniques for imaging pyrometry at temperatures above 3500 K, a semiautomatic calorimeter system capable of handling liquid tungsten, and development of a two color imaging pyrometer system. E.A.K.

N86-10075*# Houston Univ., Tex. Dept. of Physics.
EFFECT OF UNDERCOOLING AND MODIFIED MICROSTRUCTURE ON THE PHYSICAL PROPERTIES OF MATERIAL SYNTHESIZED IN THE DROP TUBE AND DROP TOWER
C. W. Chu *In* NASA, Washington Microgravity Sci. and Appl. Program Tasks May 1985 p 47-48 refs (For primary document see N86-10053 01-12)
(Contract NAS8-35161)
Avail: NTIS HC A10/MF A01 CSCL 22A

The effects of undercooling and modified microstructure on the physical properties of synthesized materials were investigated. The objectives of this program are: (1) to determine the possible existence of metastable phases and novel physical processes on material prepared in a microgravity environment; and (2) to

investigate the feasibility of fabricating advanced electronic devices using material with microstructures obtainable in a microgravity environment. The specific alloys and compounds under study are Au-Ge and immiscible alloys Nb-Ge compounds, and Ga-Bi immiscible alloys, and Ba-Pb-Bi-O. The superconducting and normal state transport properties of the materials under different pressures and in different magnetic fields were determined. The simultaneous study on the physical properties and the microstructure of material will provide information about the potential applications of materials processed in a microgravity environment. E.A.K.

N86-10076*# Battelle Memorial Inst., Columbus, Ohio.
THE INFLUENCE OF CONTAINERLESS UNDERCOOLING AND RAPID SOLID-STATE QUENCHING ON THE SUPERCONDUCTIVE AND MAGNETIC PROPERTIES OF SOME CLUSTERING ALLOY SYSTEMS
E. W. Collings *In* NASA, Washington Microgravity Sci. and Appl. Program Tasks May 1985 p 49-50 refs (For primary document see N86-10053 01-12)
(Contract NAS8-35145)
Avail: NTIS HC A10/MF A01 CSCL 22A

The potential of the 100-meter drop-tube for producing materials with new and important properties by their rapid solidification containerless undercooling was investigated. Materials produced exhibit evidence of very rapid quenching. The importance of rapid quenching in producing materials of considerable scientific and technological interest is emphasized. It is indicated that containerless undercooling, using at first a drop tube and eventually a space-shuttle-serviced orbiting laboratory, will provide another powerful approach for rapid quenching. A special advantage of the drop tube is that the microgravity condition is imposed ballistically; it is therefore possible to obtain either spherical samples by allowing solidification to take place in flight, or splats by allowing the sample material while still in undercooled liquid form to impact a stationary quench plate. E.A.K.

N86-10077*# National Bureau of Standards, Washington, D.C.
CONVECTION DURING UNIDIRECTIONAL SOLIDIFICATION
S. R. Coriell, R. J. Schaefer, and G. B. McFadden *In* NASA, Washington Microgravity Sci. and Appl. Program Tasks May 1985 p 51-52 refs (For primary document see N86-10053 01-12)
(NASA Order H-27954-B)
Avail: NTIS HC A10/MF A01 CSCL 22A

The fluid flow and solute segregation which occur during directional solidification, including effects of gravity and microgravity were studied. The nature of the fluid flow, its effects on the shape of the crystal-metal interface and the resulting distribution of solutes are examined. During solidification of a binary alloy at constant velocity vertically upwards, thermosolutal convection occurs if the solute rejection or preferential incorporation at the crystal-melt interface decreases the density of the melt. Numerical calculations of the solute, temperature, and flow fields are carried out by using previously developed algorithms for Schmidt numbers Sc = 1, 10, 81. The time periodic flow, which occurs over a narrow range of parameters, is investigated. E.A.K.

N86-10078*# Massachusetts Inst. of Tech., Cambridge. Dept. of Materials Science and Engineering.
SIGNAL ANALYSIS OF GAS TUNGSTEN ARC WELDS
T. W. Eagar *In* NASA, Washington Microgravity Sci. and Appl. Program Tasks May 1985 p 53 (For primary document see N86-10053 01-12)
(Grant NsG-7645)
Avail: NTIS HC A10/MF A01 CSCL 22A

Gas tungsten arc welding is a process in which the input parameters such as current, voltage and travel speed, can be easily controlled and/or monitored. However, weld quality is not solely a function of these parameters. An adaptive method of observing weld quality is desired to improve weld quality assurance. The use of dynamic electrical properties of the welding arc as a weld quality monitor was studied. The electrical properties of the arc are characterized by the current voltage transfer function. The hardware and software necessary to collect the data at a maximum rate of 45 kHz and to allow the off-line processing of this data are tested. The optimum input current waveform is determined. Bead-on-plate welds to observe such characteristics of the weld as the fundamental frequency of the puddle are studied. Future work is planned to observe changes of the arc response with changes in joint geometry, base metal chemistry, and shielding gas composition are discussed. E.A.K.

N86-10079*# Commissariat a l'Energie Atomique, Grenoble (France). Center for Nuclear Studies.
MEPHISTO: INTERFACIAL DESTABILIZATION IN METAL ALLOYS
J. J. Favier and Y. Malmejac *In* NASA, Washington Microgravity Sci. and Appl. Program Tasks May 1985 p 54 (For primary document see N86-10053 01-12)
Avail: NTIS HC A10/MF A01 CSCL 22A

The destabilizing mechanisms at a solidification interface were studied to obtain information on the kinetics and morphologies in the transient and steady state, and to separate the influences of liquid phase instabilities from interfacial instabilities. A differential seebeck voltage measurements technique was developed to provide a continuous record of the solid-liquid interface temperature as the solidification rate is varied to determine the kinetic coefficients. Signal processing and noise suppression techniques allow nonovolt precision which corresponds to mK accuracy for the interfacial temperature. E.A.K.

N86-10080*# Massachusetts Inst. of Tech., Cambridge. Materials Processing Center.
UNDERCOOLING, REMELTING, AND COARSENING
Merton C. Flemings and Y. Shiohara *In* NASA, Washington Microgravity Sci. and Appl. Program Tasks May 1985 p 55-56 refs (For primary document see N86-10053 01-12)
(Grant NsG-7645)
Avail: NTIS HC A10/MF A01 CSCL 22A

Solidification of metal alloys with initial high undercoolings occurs with rapid recalescence due to rapid heat release of the latent heat of fusion. The recalescence temperature is usually higher than the solidus and/or the thermodynamic T sub o temperature of the alloy, depending on the initial undercooling and alloy composition. The rapid heating during recalescence alters the initially solidified structures, in ways that must include partial remelting, ripening, coarsening, and decomposition of the rapidly solidified primary metastable or supersaturated phases. New ways to study the solidification and remelting phenomena associated with the rapid heating during recalescence of undercooled alloys were developed. The phenomena are studied by using: (1) emulsions of iron and nickel base alloys in viscous liquid carriers; and (2) rapid heating of metal samples by electric discharge, using a technique similar to the exploding wire process (EWP), except with less power input. Experimental results are combined with theoretical analyses to better understand the solidification of levitated metal droplets with high undercooling, which relates to the solidification process. E.A.K.

N86-10081*# Gelles (S. H.) Associates, Columbus, Ohio.
LIQUID PHASE MISCIBILITY GAP MATERIALS
S. H. Gelles and A. J. Markworth (Battelle Columbus Lab.) *In* NASA, Washington Microgravity Sci. and Appl. Program Tasks May 1985 p 57-58 ref (For primary document see N86-10053 01-12)
(Contract NAS8-32952)
Avail: NTIS HC A10/MF A01 CSCL 22A

The manner in which the microstructural features of liquid-phase miscibility gap alloys develop was determined. This will allow control of the microstructures and the resultant properties of these alloys. The long-duration low gravity afforded by the shuttle will allow experiments supporting this research to be conducted with minimal interference from buoyancy effects and gravitationally driven convection currents. Ground base studies were conducted on Al-In, Cu-Pb, and Te-Tl alloys to determine the effect of cooling rate, composition, and interfacial energies on the phase separation and solidification processes that influence the development of micro-

structure in these alloys. Isothermal and directional cooling experiments and simulations are conducted. The ground based activities are used as a technological base from which flight experiments formulated and to which these flight experiments are compared. E.A.K.

N86-10082*# Rensselaer Polytechnic Inst., Troy, N. Y.
DENDRITIC GROWTH IN UNDERCOOLED MELTS
Martin E. Glicksman *In* NASA, Washington Microgravity Sci. and Appl. Program Tasks May 1985 p 59 (For primary document see N86-10053 01-12)
Avail: NTIS HC A10/MF A01 CSCL 22A

The kinetic and morphological behavior of systems solidifying at small undercooling were investigated with emphasis on the role of convective and diffusive transport and the influence of gravity. A data base was established for pure succinonitrile which permits a comprehensive check on diffusional dendrite growth theory and the development of scaling laws to extend the theory to other material systems. A departure from diffusional-controlled growth was observed which becomes more significant at smaller undercoolings. A shuttle experiment is prepared to test the theory at the low undercoolings where convective effects begin to dominate. E.A.K.

N86-10083*# Rensselaer Polytechnic Inst., Troy, N. Y.
INFLUENCE OF MELT CONVECTION ON SOLID-LIQUID INTERFACE UNDER TERRESTRIAL AND REDUCED GRAVITY ENVIRONMENTS
Martin E. Glicksman *In* NASA, Washington Microgravity Sci. and Appl. Program Tasks May 1985 p 60-62 refs (For primary document see N86-10053 01-12)
(Grant NAG3-333)
Avail: NTIS HC A10/MF A01 CSCL 22A

Solidification and crystal growth processes involve thermal and solutal gradients within a molten phase. In the presence of gravity, such gradients result in convective flows which interact with diffusion fields at the solid-liquid interface. Dendritic growth kinetics was studied in transparent model systems which freeze similarily to most metals. Succinonitrile shows a strong influence of convection at supercoolings below about 1K. Fluid flows adjacent to solid-liquid interfaces and the behavior of shear flows in vertical annular geometries are studied. Novel low-frequency eigenstates were discovered and classified as coupled modes, for their involvement with interfacial deformation coupled to the fluid flow, and are unknown in systems without deformable interfaces. The dependence of coupled convection modes on interfacial geometry, gravity, fluid properties, and transformation characteristics studied for several annual flow arrangements with nominally pure solid-liquid systems. E.A.K.

N86-10084*# Deere and Co., Moline, Ill.
CONTROL OF CAST IRON MICROSTRUCTURE
James Graham, Norman Lillybeck, Nick Franco, and Doru M. Stefanescu *In* NASA, Washington Microgravity Sci. and Appl. Program Tasks May 1985 p 63 (For primary document see N86-10053 01-12)
Avail: NTIS HC A10/MF A01 CSCL 22A

The use of microgravity for industrial research in the processing of cast iron was investigated. Solidification experiments were conducted using the KC-135 and F-104 aircraft, and an experiment plan was developed for follow-on experiments using the Shuttle. Three areas of interest are identified: (1) measurement of thermophysical properties in the melt; (2) understanding of the relative roles of homogeneous nucleation, grain multiplication, and innocultants in forming the microstructure; and (3) exploring the possibility of obtaining an aligned graphite structure in hypereutectic Fe, Ni, and Co. E.A.K.

N86-10085*# Massachusetts Inst. of Tech., Cambridge.
THE ROLE OF ENTRAINED SURFACE OXIDES IN RS-PM ALUMINUM ALLOYS ON RESULTANT STRUCTURES AND PROPERTIES
N. J. Grant *In* NASA, Washington Microgravity Sci. and Appl. Program Tasks May 1985 p 64 refs (For primary document see N86-10053 01-12)
(Grant NsG-7645)
Avail: NTIS HC A10/MF A01 CSCL 22A

The RS-PM aluminum alloys which show less than anticipated toughness properties were studied. After eliminating negative variables such as sodium and potassium in lithium containing alloys, hydrogen in all Al alloys, and trapped impurities from the atomization processing the data pointed to fine oxides, as the primary cause of poor toughness properties. The oxide content of aluminum powders increases with: decreasing powder size, deviations from spherical powder shapes, exposure to moist atmospheres either during atomization or in subsequent powder handling, and alloy compositions which contain significant amounts of lithium, magnesium, cerium, and other reactive elements. E.A.K.

N86-10086*# Michigan Technological Univ., Houghton. Dept. of Metallurgical Engineering.
THE DEVELOPMENT AND PREVENTION OF CHANNEL SEGREGATION DURING ALLOY SOLIDIFICATION
Angus Hellawell *In* NASA, Washington Microgravity Sci. and Appl. Program Tasks May 1985 p 65-66 refs (For primary document see N86-10053 01-12)
(Grant NAG3-560)
Avail: NTIS HC A10/MF A01 CSCL 22A

During alloy solidification, interdendritic microsegregation causes density differences between entrapped liquid and bulk liquid which provides a driving force for convection. One of the consequences of this effect is the formation of long, nearly vertical liquid channels, rich in solute, flowing through the solid-liquid mushy zone somewhat as a river and tributary system. In ingot castings where the heat flow is vertically downwards and the solute less dense than the solute the convective flow is antiparallel with the flow caused by contraction on freezing. Identification of the mechanisms involved in these two problems is discussed. It is known that certain types of bulk liquid movements can inhibit channel development and the mechanism by which they do so are examined. E.A.K.

N86-10087*# National Aeronautics and Space Administration. Marshall Space Flight Center, Huntsville, Ala.
STUDY OF THE REACTIVE-ELEMENT EFFECT IN OXIDATION OF Fe-Cr ALLOYS USING TRANSVERSE SECTION ANALYTICAL ELECTRON MICROSCOPY
Wayne E. King (Argonne National Lab.) and Edwin C. Ethridge *In* NASA, Washington Microgravity Sci. and Appl. Program Tasks May 1985 p 67-68 (For primary document see N86-10053 01-12)
Avail: NTIS HC A10/MF A01 CSCL 22A

The role of trace additions of reactive elements like Y, Ce, Th, or Hf to Cr bearing alloys was studied by applying a new developed technique of transverse section analytical electron microscopy. This reactive-element effect improves the high temperature oxidation resistance of alloys by strongly reducing the high temperature oxidation rate and enhancing the adhesion of the oxide scale, however, the mechanisms for this important effect remain largely unknown. It is indicated that the presence of yttrium affects the oxidation of Fe-Cr-Y alloys in at least two ways. The reactive element alters the growth mechanism of the oxide scale as evidenced by the marked influence of the reactive element on the oxide scale microstructure. The present results also suggest that reactive-element intermetallic compounds, which internally oxidize in the metal during oxidation, act as sinks for excess vacancies thus inhibiting vacancy condensation at the scale-metal interface and possibly enhancing scale adhesion. E.A.K.

N86-10088*# California Univ., Santa Barbara.
THEORETICAL PROBLEMS IN MATERIALS SCIENCE Inst. for Theoretical Physics.
J. S. Langer and M. E. Glicksman *In* NASA, Washington Microgravity Sci. and Appl. Program Tasks May 1985 p 69 (For primary document see N86-10053 01-12)
(Grant NSF PHY-77-27084)
Avail: NTIS HC A10/MF A01 CSCL 22A

Interactions between theoretical physics and material sciences to identify problems of common interest in which some of the powerful theoretical approaches developed for other branches of physics may be applied to problems in materials science are presented. A unique structure was identified in rapidly quenched Al-14% Mn. The material has long-range directed bonds with icosahedral symmetry which does not form a regular structure but instead forms an amorphous-like quasiperiodic structure. Finite volume fractions of second phase material is advanced and is coupled with nucleation theory to describe the formation and structure of precipitating phases in alloys. Application of the theory of pattern formation to the problem of dendrite formation is studied. E.A.K.

N86-10089*# Grumman Aerospace Corp., Bethpage, N.Y. Materials and Structural Mechanics Research.
ORBITAL PROCESSING OF ALIGNED MAGNETIC COMPOSITES
David J. Larson *In* NASA, Washington Microgravity Sci. and Appl. Program Tasks May 1985 p 70-71 (For primary document see N86-10053 01-12)
(Contract NAS8-35483)
Avail: NTIS HC A10/MF A01 CSCL 22A

Experiments will be conducted on the space shuttle in which aligned, two-phase magnetic composites will be grown by plane front directional solidification. The objectives are to: (1) identify and quantitatively evaluate the influences of gravitationally driven thermo-solutal convection on contained plane front solidification of binary, eutectic, off-eutectic, and peritectic magnetic composites; (2) to evaluate the effectiveness of micro-g processing as a means of damping convection; and (3) to evaluate the uniqueness of micro-g processing relative to the best of terrestrial convection damping. E.A.K.

N86-10090*# Case Western Reserve Univ., Cleveland, Ohio. Dept. of Metallurgy and Materials Science.
SOLIDIFICATION FUNDAMENTALS
V. Laxmanan and J. F. Wallace *In* NASA, Washington Microgravity Sci. and Appl. Program Tasks May 1985 p 72-73 refs (For primary document see N86-10053 01-12)
(Grant NAG3-417)
Avail: NTIS HC A10/MF A01 CSCL 22A

The fundamental aspects of a variety of solidification phenomena were studied, taking advantage of the unique opportunities offered by the microgravity environment of space. Containerless processing and an understanding of the role of fluids induced by gravitational effects are the two major objectives justifying an experimental program in reduced gravity. The solidification phenomena which are likely to benefit are: macro and microsegregation, columnar-equiaxed transition, pore formation, and undercooling. E.A.K.

N86-10091*# Rice Univ., Houston, Tex. Dept. of Chemistry.
MEASUREMENT OF THE PROPERTIES OF TUNGSTEN AT HIGH TEMPERATURES
John L. Margrave *In* NASA, Washington Microgravity Sci. and Appl. Program Tasks May 1985 p 74 (For primary document see N86-10053 01-12)
(Contract NAS8-33199)
Avail: NTIS HC A10/MF A01 CSCL 22A

The thermophysical properties of tungsten and other materials were measured using containerless techniques. Levitation of liquid silver, gallium and tungsten were studied. The studies of liquid aluminum are almost complete and are expected to derive new, reliable properties for liquid aluminum. E.A.K.

N86-10092*# Midwest Research Inst., Kansas City, Mo.
CONTAINERLESS HIGH TEMPERATURE PROPERTY MEASUREMENTS BY ATOMIC FLUORESCENCE
Paul C. Nordine *In* NASA, Washington Microgravity Sci. and Appl. Program Tasks May 1985 p 75 refs (For primary document see N86-10053 01-12)
Avail: NTIS HC A10/MF A01 CSCL 22A

Laser induced fluorescence (LIF) provides a noncontact method for measuring high temperature properties. It is used with aerodynamic and/or electromagnetic levitation, and electromagnetic and/or CW CO2 laser heating to develop new methods for containerless high temperature property measurements and process control. The capabilities and limitations of Earth-based experiments are demonstrated and the information necessary to design improved experiments in space is obtained. The LIF methods were developed to measure temperature and component activities, which will be applied to containerless property measurements on liquids and to process control in synthesis experiments. Component activities will be obtained from relative LIF intensities over a compound and its components at the same temperature. Author

N86-10093*# Wisconsin Univ., Madison. Dept. of Metallurgical and Mineral Engineering.
CONTAINERLESS PROCESSING OF UNDERCOOLED MELTS
John H. Perepezko *In* NASA, Washington Microgravity Sci. and Appl. Program Tasks May 1985 p 76 (For primary document see N86-10053 01-12)
(Grant NAG3-436)
Avail: NTIS HC A10/MF A01 CSCL 22A

The physical mechanisms controlling liquid undercooling were studied for application to solidification processing methods. The undercooling potential of containerless processing was assessed on droplet samples of high melting temperature metals drop tube and drop tower facilities and in a laboratory-scale apparatus. New insight into nucleation and crystal growth will be obtained in undercooled liquids of high melting temperature iron and nickel-base systems. The processing parameters include melt superheat, droplet size and particle statistics and droplet surface coating. The solidification behavior is determined by thermal analysis and by structural and metallographic characterization. E.A.K.

N86-10094*# Grumman Aerospace Corp., Bethpage, N.Y.
THERMAL AND SOLUTAL CONVECTION DAMPING USING AN APPLIED MAGNETIC FIELD
R. G. Pirich and J. L. DeCarlo *In* NASA, Washington Microgravity Sci. and Appl. Program Tasks May 1985 p 77-78 refs (For primary document see N86-10053 01-12)
Avail: NTIS HC A10/MF A01 CSCL 22A

Samples of eutectic Bi/Mn alloy were directionally solidified in the presence of a transverse magnetic field to determine if gravity-induced convection effects could be reduced or eliminated. The microstructure of Bi/MnBi is characterized by a regular, aligned-rod eutectic morphology that is sensitive to growth conditions. This, combined with ferromagnetism of one of the components, MnBi, can be used to eliminate whether convection effects are significant enough to be effected by the presence of a static, homogeneous, magnetic field. E.A.K.

N86-10095*# Johns Hopkins Univ., Baltimore, Md.
METALLIC FOAMS
Robert B. Pond *In* NASA, Washington Microgravity Sci. and Appl. Program Tasks May 1985 p 79 (For primary document see N86-10053 01-12)
(Contract NAS8-33021)
Avail: NTIS HC A10/MF A01 CSCL 22A

The formation of metallic foams by use of a blowing agent in the melt was investigated. It was attempted to produce a metallic foam by melting a mixture of Cu powder and graphite in a SPAR rocket. The graphite combines with the oxide on the copper to form Co and acts as a blowing agent. No foam was formed, and it could not be determined whether the foam fails to form, forms but was lost to surface tension instabilities, or is destroyed by incomplete solidification before reentry. E.A.K.

N86-10096*# Johns Hopkins Univ., Baltimore, Md.
DIFFUSION IN IMMISCIBLE MELTS
Robert B. Pond *In* NASA, Washington Microgravity Sci. and Appl. Program Tasks May 1985 p 80 (For primary document see N86-10053 01-12)
(Contract NAS8-35620)

Avail: NTIS HC A10/MF A01 CSCL 22A

The objective of this program is to measure the diffusion coefficients for molten Pb in Zn in the immiscible liquid-phase region. Diffusion couples of pure Pb and Zn were prepared using a shear cell. These have been placed in graphite crucibles and encapsulated in stainless steel cartridges and are awaiting the next Materials Experiment Assembly (MEA) flight opportunity. In flight, one couple will be soaked for 40 minutes at 440 deg C (just above the monotectic temperature) and the second couple will be soaked for 40 minutes 820 deg C (just above the consolute temperature). After the soak both samples will be rapidly quenched by flowing He to minimize redistribution of the immiscible phases. Post flight compositional analysis will be accomplished using X-ray fluorescence in the scanning electron microscopy. Author

N86-10097*# Commissariat a l'Energie Atomique, Grenoble (France). Centre d'Etudes Nucleaires.

DIRECTIONAL SOLIDIFICATION OF MONOTECTIC AND HYPERMONOTECTIC ALUMINUM-INDIUM ALLOYS UNDER MICRON-G

Claude Potard *In* NASA, Washington Microgravity Sci. and Appl. Program Tasks May 1985 p 81-82 (For primary document see N86-10053 01-12)

Avail: NTIS HC A10/MF A01 CSCL 22A

The objective of this program is to analyze the mechanisms involved in the composite solid structure formation obtained from a miscibility gap alloy under microgravity. The metallic system aluminum-indium was chosen for its low critical temperature, broad miscibility gap, and rather well-known thermodynamic properties. The experiment was performed aboard the Salyut-7 spacecraft. The theories of capture of particulates by an advancing front were not able to explain the observations made on SPAR and Salyut-7 experiments. A new model was developed based on the filtration theory considering the globules population: the solid/liquid interface is like a filter of negligible thickness for the globules and its efficiency is limited by a pressure barrier measured for Al-In alloys by ground based experiments. The Materials Experiment Assembly (MEA)-3 experiment was consequently adjusted to take into account the new model. The behavior of the globules in an interacting population on the solid front is, of course, an essential factor in the theory. The theory is at present being completed by results obtained by the Laboratoire d'Aerothermique of Meudon. The hydrodynamic and thermal interactions between pairs of globules placed in a temperature gradient have been calculated showing a large reduction of the Marangoni effect compared to the isolated globule. Physico-chemical properties of metallic liquid interface are currently being investigated. R.J.F.

N86-10098*# Massachusetts Inst. of Tech., Cambridge. Materials Processing Center.

METALS ELECTROPROCESSING IN MOLTEN SALTS

D. R. Sadoway *In* NASA, Washington Microgravity Sci. and Appl. Program Tasks May 1985 p 83 (For primary document see N86-10053 01-12)

(Grant NsG-7645)

Avail: NTIS HC A10/MF A01 CSCL 22A

The present study seeks to explain the poor quality of solid electrodeposits in molten salts through a consideration of the effects of fluid flow of the electrolyte. Transparent cells allow observation of electrolyte circulation by a laser schlieren optical technique during the electrodeposition of solid zinc from the molten salt electrolyte, $ZnCl_2$ - LiCl-KCl. Experimental variables are current, density, electrolyte composition, and cell geometry. Based on the results of earlier electrodeposition studies as well as reports in the literature, these parameters are identified as having the primary influence on cell performance and deposit quality. Experiments are conducted to measure the fluid flow patterns and the electrochemical cell characteristics, and to correlate this information with the morphology of the solid electrodeposit produced. Specifically, cell voltage, cell current, characteristic time for dendrite evolution, and dendrite growth directions are noted. Their relationship to electrolyte flow patterns and the morphology of the resulting electrodeposit are derived. Results to date indicate that laser schlieren imaging is capable of revealing fluid flow patterns in a molten salt electrolyte. R.J.F.

N86-10099*# Syracuse Univ., N. Y. Dept. of Chemical Engineering and Materials Science.

ENVIRONMENTAL DEGRADATION OF MATERIALS: SURFACE CHEMISTRY RELATED TO STRESS CORROSION CRACKING

James A. Schwarz *In* NASA, Washington Microgravity Sci. and Appl. Program Tasks May 1985 p 84 (For primary document see N86-10053 01-12)

(Grant NAGw-466)

Avail: NTIS HC A10/MF A01 CSCL 22A

Parallel experiments have been performed in order to develop a comprehensive model for stress cracking (SCC) in structural materials. The central objective is to determine the relationship between the activity and selectivity of the microstructure of structural materials to their dissolution kinetics and experimentally measured SCC kinetics. Zinc was chosen as a prototype metal system. The SCC behavior of two oriented single-crystal disks of zinc in a chromic oxide/sodium sulfate solution (Palmerton solution) were determined. It was found that: (1) the dissolution rate is strongly (hkil)-dependent and proportional to the exposure time in the aggressive environment; and (2) a specific slip system is selectively active to dissolution under applied stress and this slip line controls crack initiation and propagation. As a precursor to potential microgrvity experiments, electrophoretic mobility measurements of zinc particles were obtained in solutions of sodium sulfate (0.0033 M) with concentrations of dissolved oxygen from 2 to 8 ppm. The equilibrium distribution of exposed oriented planes as well as their correlation will determine the particle mobility. Author

N86-10100*# Alabama Univ., Huntsville. College of Engineering.

GRAPHITE FORMATION IN CAST IRON

D. M. Stefanescu *In* NASA, Washington Microgravity Sci. and Appl. Program Tasks May 1985 p 85 (For primary document see N86-10053 01-12)

(Grant NAGw-469)

Avail: NTIS HC A10/MF A01 CSCL 22A

In the first phase of the project it was proven that by changing the ratio between the thermal gradient and the growth rate for commercial cast iron samples solidifying in a Bridgman type furnace, it is possible to produce all types of graphite structures, from flake to spheroidal, and all types of matrices, from ferritic to white at a certain given level of cerium. KC-135 flight experiments have shown that in a low-gravity environment, no flotation occurs even in spheroidal graphite cast irons with carbon equivalent as high as 5%, while extensive graphite flotation occurred in both flake and spheroidal graphite cast irons, in high carbon samples solidified in a high gravity environment. This opens the way for production of iron-carbon composite materials, with high carbon content (e.g., 10%) in a low gravity environment. By using KC-135 flights, the influence of some basic elements on the solidification of cast iron will be studied. The mechanism of flake to spheroidal graphite transition will be studied, by using quenching experiments at both low and one gravity for different G/R ratios. R.J.F.

N86-10101*# Ohio State Univ., Columbus. Dept. of Physics.

THEORETICAL STUDIES OF THE SURFACE TENSION OF LIQUID METAL SYSTEM Report, Jul. 1984 - Jul. 1987

David G. Stroud and Wei-Heng Shih *In* NASA, Washington Microgravity Sci. and Appl. Program Tasks May 1985 p 86-87 (For primary document see N86-10053 01-12)

(Grant NAG-483)

Avail: NTIS HC A10/MF A01 CSCL 22A

A major goal of this project is to understand the surface tension and other thermophysical properties of liquid metals and alloys from a fundamental viewpoint. The approach is to calculate these quantities by a first principles technique which combines the statistical-mechanical theory of the liquid state with an electronic pseudopotential theory of electrons in metals. The inhomogeneity of the surface is treated using an ionic-density-functional formalism developed with the support of NASA. Of particular interest

are the variation of surface tension with temperature and impurity concentration: such variations strongly influence the types of convection which make take place in a low-gravity environment. Some progress has already been achieved in computing the reduction of surface tension due to the presence of low-surface-tension impurities, and the corresponding surface segregation of such impurities. In the coming year, it is planned to concentrate on the surface properties of materials of particular interest to the MSA program: Si, Ga and GaSn alloys. An additional goal is to gain some theoretical understanding of the high temperature thermophysical properties of liquid metals, particularly high melting point materials which have not been studied extensively from a theoretical viewpoint. Author

N86-10102*# Jet Propulsion Lab., California Inst. of Tech., Pasadena.
CONTAINERLESS STUDIES OF NUCLEATION AND UNDERCOOLING Abstract Only
Eugene H. Trinh *In* NASA, Washington Microgravity Sci. and Appl. Program Tasks May 1985 p 88 (For primary document see N86-10053 01-12)
(Contract NAS7-918)
Avail: NTIS HC A10/MF A01 CSCL 22A

The long term research goals are to perform experiments to determine the achievable limits of undercooling, the characteristics of heterogeneous nucleation, and the physical properties of significantly undercooled melts. The techniques used are based on the newly developed containerless manipulation methods afforded by acoustic levitation. Ground based investigations involved 0.1 to 2 mm specimens of pure metals and alloys (In, Ga, Sn, Ga-In, ...) as well as glass-forming organic compounds (O-Terphenyl). A currently operating ultrasonic high temperature apparatus has allowed the ground-based levitation of 1 to 2 mm samples of solid aluminum at 550 deg C in an argon atmosphere. Present work is concentrating on the undercooling of pure metal samples (In, Sn), and on the measurements of surface tension and viscosity of the undercooled melts via shape oscillation techniques monitored through optical detection methods. The sound velocity of undercooled O-Terphenyl is being measured in an immiscible liquid levitation cells. R.J.F.

N86-10103*# National Aeronautics and Space Administration. Marshall Space Flight Center, Huntsville, Ala.
CLOUD MICROPHYSICS BY THERMAL WAVE METHODS
B. Jeffrey Anderson, David A. Bowdle (Universities Space Research Association), and Michael Reischel (Universities Space Research Association) *In* NASA, Washington Microgravity Sci. and Appl. Program Tasks May 1985 p 91-92 (For primary document see N86-10053 01-12)
Avail: NTIS HC A10/MF A01 CSCL 22A

This experiments series is the first application of a low-gravity experimental technique to the study of cloud microphysics. The low-gravity environment is provided by the parabolic maneuver of NASA's KC-135 aircraft. The primary objective is to compare experimental observations of cloud droplet growth and evaporation in a convection free environment with a numerical model of the process. Beyond that, the work also involves the development and testing of low-gravity research techniques. In particular, passive methods of thermal control have been devised and used effectively. The study to date has shown that the method is particularly suitable for looking at interactions between adjoining portions of the cloud drop field and interactions of the drop field with a solid interface. After final analysis of the data, it is expected the results will shed light on the development of cloud droplet size spectra in natural clouds as well as the performance of certain types of cloud physics instrumentation, particularly continuous flow diffusion chambers and loud condensation nuclei counters. R.J.F.

N86-10104*# National Aeronautics and Space Administration. Marshall Space Flight Center, Huntsville, Ala.
EXTENSION OF OSTWALD RIPENING THEORY
James Baird (Alabama Univ., Huntsville) and Robert Naumann *In* NASA, Washington Microgravity Sci. and Appl. Program Tasks May 1985 p 93 (For primary document see N86-10053 01-12)
Avail: NTIS HC A10/MF A01 CSCL 22A

The objective is to develop models based on the mean field approximation of Ostwald ripening to describe the growth of second phase droplets or crystallites. The models will include time variations in nucleation rate, control of saturation through addition of solute, precipitating agents, changes in temperature, and various surface kinetic effects. Numerical integration schemes have been developed and tested against the asymptotic solution of Liftshitz, Slyozov and Wagner (LSW). A second attractor (in addition to the LSW distribution) has been found and, contrary to the LSW theory, the final distribution is dependent on the initial distribution. A series of microgravity experiments is being planned to test this and other results from this work. Author

N86-10105*# Massachusetts Inst. of Tech., Cambridge. Dept. of Chemical Engineering.
MODELLING OF LASER-ENHANCED CHEMICAL VAPOR DEPOSITION
Robert A. Brown *In* NASA, Washington Microgravity Sci. and Appl. Program Tasks May 1985 p 94 (For primary document see N86-10053 01-12)
(Grant NsG-7645)
Avail: NTIS HC A10/MF A01 CSCL 22A

Research is directed at development of a detailed model of mass and heat transfer and chemical reaction in the pyrolysis of silane for the growth of thin amorphous silicon substrates incorporating laser heating of the gas phase above the film. The model will be the basis for evaluation of the relative importances of the decomposition of SiH4 in the vapor phase, mass transfer of the intermediate species, e.g., SiH2, and the evolution of hydrogen gas. Plans are also underway for developing a model for homogeneous nucleation of Si in the vapor phase to model the rate limitations observed at high gas-phase temperatures and high partial pressures of silane. Work was concentrated on an almost one-dimensional model for the coupling of the CO2 laser beam for heat transfer of the vapor phase with simple kinetic models for SiH4 decomposition and subsequent absorption of Si vapor on the substrate. Mass transfer in the vapor phase is assumed to be solely by diffusion. The role of convection in the vapor phase caused by the large changes in density in and around the center of the laser beam will be analyzed to evaluate the potential of microgravity experiments for increasing the uniformity of the film and the deposition rate. Author

N86-10106*# National Bureau of Standards, Washington, D.C.
DYNAMIC THERMOPHYSICAL MEASUREMENTS IN SPACE
Ared Cezairliyan, A. P. Miller, M. S. Morse, and L. A. Schmid *In* NASA, Washington Microgravity Sci. and Appl. Program Tasks May 1985 p 95 (For primary document see N86-10053 01-12)
(NASA Order H-27954-B) Avail: NTIS HC A10/MF A01 CSCL 22A

The objective is to develop techniques for the dynamic measurement of selected thermophysical properties (e.g., heat of fusion, heat capacity, electrical resistivity) of solids and liquids at temperatures above 2000 K in a near zero-gravity environment. The first phase involves establishing the stability (geometrical) limits of specimens when rapidly heated to temperatures beyond their melting point. A test equipment package was designed and constructed for this purpose, consisting of removable specimen cartridge cells, a battery-bank power supply, a high-speed framing camera, a single-wavelength pyrometer, and electronic switching and control equipment. The operation of the equipment package was tested in the laboratory in preparation for near zero-gravity experiments to be performed during a KC-135 flight in September, 1984. Author

N86-10107*# National Aeronautics and Space Administration. Lewis Research Center, Cleveland, Ohio.
TRANSPORT PROCESSES IN SOLUTION CRYSTAL GROWTH
A.-T. Chai *In* NASA, Washington Microgravity Sci. and Appl. Program Tasks May 1985 p 96 (For primary document see N86-10053 01-12)

Avail: NTIS HC A10/MF A01 CSCL 22A

The objective of this effort is to conduct fundamental research in reduced gravity on transport processes occurring during solution crystal growth. Experimental techniques will be developed to monitor and control key parameters at the interface between a growing crystal and the solution from which it grows. Techniques developed will lead to an in-space experiment in the Shuttle. The focus will be on non-incursive ground-based laboratory measurements of model systems and the definition of requirements for space experimentation. Initially, aqueous solutions will be used for easier control and instrumentation. Model systems with imposed steady flows and simplified boundary conditions will be studied for characterization. Various nonincursive measurement techniques are being investigated for proper applications in a newly built laboratory capable of flow visualization, laser Doppler velocimetry, Schlieren photography, specklegram, holographic interferometry, and Raman spectroscopy. Author

N86-10108*# California Univ., Berkeley.

FREE SURFACE PHENOMENA UNDER LOW- AND ZERO-GRAVITY CONDITIONS

Paul Concus, D. Coles (California Inst. of Tech.), R. Finn (Stanford Univ.), and L. Hesselink (Stanford Univ.) *In* NASA, Washington Microgravity Sci. and Appl. Program Tasks May 1985 p 97 (For primary document see N86-10053 01-12)

(Grant NAG3-147)

Avail: NTIS HC A10/MF A01 CSCL 22A

In a low- or zero-gravity environment the free surface of a liquid can behave in striking, unexpected ways. For example, in a partially filled container, a free surface that is well behaved under terrestrial conditions can rise to an arbitrarily large height or even fail to exist when gravity is absent. An answer is sought to the central mathematical questions: Under what conditions can free surfaces exist and what are their properties? -- and experimental questions of what means can be devised to observe and to measure the surfaces quantitatively. Current activity focuses on material selection and the design of optical diagnostic methods for in-space experiments. These experiments will test mathematical predictions of discontinuous transition from existence to nonexistence of capillary free surfaces in certain geometric configurations under zero gravity conditions. Liquids and container materials suitable for achieving the required contact-angle range and optical properties are being investigated, as well as the effects of contaminants and fluid motion on contact angle. The optical diagnostic technique investigation concerns laser-induced fluorescence, including emphasis on data on acquisition, sources and detectors, reliability, data management, and computer control. Author

N86-10109*# Northwestern Univ., Evanston, Ill. Dept. of Engineering Sciences and Applied Mathematics.

THERMOCAPILLARY FLOWS AND THEIR STABILITY: EFFECTS OF SURFACE LAYERS AND CONTAMINATION

S. H. Davis and G. M. Homsey (Stanford Univ.) *In* NASA, Washington Microgravity Sci. and Appl. Program Tasks May 1985 p 98-99 (For primary document see N86-10053 01-12)

(Contract NAS8-33881)

Avail: NTIS HC A10/MF A01 CSCL 22A

The objective is to study quantitatively thermocapillary flows in two-dimensional and axisymmetric geometries in order to learn the impact of such flows on float-zone refining configurations. The work begins with the analytical study of steady flows in slots and zones to obtain predictions of surface curvature, flow and heat transport. It then examines the instability of such flows. Three new instability mechanisms have been identified and the results show that thermocapillary flows of high Prandtl number fluid become convectively unstable while those of low Prandtl number fluid become hydrodynamically unstable. The work includes numerical simulations of steady, high Marangoni number flows in unit aspect ratio boxes and asymptotic solutions in large boxes. Furthermore, the effect of surface contamination on the steady thermocapillary flows was examined. This fundamental study focused on fluid dynamical systems used to understand events in the flow of melts in float-zone geometries both on Earth and in microgravity environments. Author

N86-10110*# Toledo Univ., Ohio.

MASS TRANSPORT PHENOMENA BETWEEN BUBBLES AND DISSOLVED GASES IN LIQUIDS UNDER REDUCED GRAVITY CONDITIONS

Kenneth J. DeWitt and J. L. Brockwell (Union Carbide Technical Center) *In* NASA, Washington Microgravity Sci. and Appl. Program Tasks May 1985 p 100-101 (For primary document see N86-10053 01-12)

(Grant NAG3-34)

Avail: NTIS HC A10/MF A01 CSCL 22A

The long term objective of the experiment is to observe the dissolution of isolated, immobile gas bubbles of specified size and composition in a solvent liquid of known concentration in the reduced gravity environment of earth orbit. Preliminary bubble dissolution experiment conducted both in the NASA Lewis 2.2 sec drop tower and in normal gravity using SO2 - Toluene system were not completely successful in their objective. The method of gas injection and lack of bubble interface stabiliy experienced due to the extreme solubility of SO in Toluene has the effects of changing the problem from that of bubble dissolution to one of bubble formation stability and subsequent dissolution in a liquid of unknown initial solute concentration. Current work involves further experimentation in order to refine the bubble injection system and to investigate the concept of having a bubble with a critical radius in a state of unstable equilibrium. R.J.F.

N86-10111*# George Washington Univ., Washington, D.C.

SUPPRESSION OF MARANGONI CONVECTION IN FLOAT ZONES

Robert F. Dressler *In* NASA, Washington Microgravity Sci. and Appl. Program Tasks May 1985 p 102-103 (For primary document see N86-10053 01-12)

Avail: NTIS HC A10/MF A01 CSCL 22A

The basic purpose of this program is to demonstrate by means of an Earth-based 1-g experiment that the undesirable Marangoni (surface tension) convection can be suppressed or significantly reduced by means of gas jets directed tangentially to the free surface of the liquid in a float zone. These jets will establish the tangential shear stress field over the surface which must be adjusted to equal the counter-stress resultant of the Marangoni shear stress which causes the convection. For proposed materials processing in space (o-g), particularly of important, highly reactive semiconductor materials, e.g., silicon, microgravity will virtually eliminate the unwanted thermal-buoyancy convection in the liquid silicon, but will have no effect in reducing the Marangoni convection. Unless this can be sufficiently suppressed by other means, there may be no significant advantages to the proposed space processing of reactive semiconductors. Although some inert gas such as argon must be used for the corrosive liquid silicon, the Earth-based experiment uses air jets and various transparent oils, since the basic principle involved is the same. The first float zone is enclosed in a very small rectangular box with a quasi-planar free surface. Stable Marangoni convection has been achieved and velocities measured photographically. The air jet system with variable velocity and temperature is under construction. Three independent parameters must be optimized to attain maximum suppression: the gas velocity, angle of attack, and gas temperature. R.J.F.

N86-10112*# National Aeronautics and Space Administration. Marshall Space Flight Center, Huntsville, Ala.

STUDIES OF MODEL IMMISCIBLE SYSTEMS

Donald O. Frazier, B. R. Facemire, W. K. Witherow, U. Fanning, and William F. Kaukler (Universities Space Research Association) *In* NASA, Washington Microgravity Sci. and Appl. Program Tasks May 1985 p 104-105 (For primary document see N86-10053 01-12)

Avail: NTIS HC A10/MF A01 CSCL 22A

The objectives are to use model transparent monotectics to obtain fundamental information applicable to two-phase systems

in general, to apply this understanding to materials of interest in the Microgravity Science and Applications program, and to interpret results of flight experimental involving monotectic alloys. A number of model immiscible systems are in use to study various aspects of two-phase behavior within the miscibility gap and during solidification. Particle growth, coalescence and particle motions are under investigation using a holographic microscopy system. The system is capable of working with particle densities up to 10 to the 7th power particles/cubic centimeters through a 100 micron depth and can resolve particles of the order of 2 to 3 micron in diameter throughout the entire cell volume. Particle size, distribution changes with respect to time and temperature are observable from sequential holograms. Initial experiments using diethylene glycol/ethyl salicylate (DEG/ES) have demonstrated the usefulness of the technique. The thermal system controls temperature to at least plus or minus 0.001 K over the course of an experiment. A time-lapse film, made from holograms, of a succinonitrile/water solution shows particle size and number distribution changes with time under isothermal conditions. The observations are consistent with Ostwald ripening theory. Author

N86-10113*# Maryland Univ., College Park.
LIGHT SCATTERING TESTS OF FUNDAMENTAL THEORIES OF TRANSPORT PROPERTIES IN THE CRITICAL REGION
R. W. Gammon and M. R. Moldover (NBS, Washington, D.C.) *In* NASA, Washington Microgravity Sci. and Appl. Program Tasks May 1985 p 106 (For primary document see N86-10053 01-12)
(Grant NAG3-470)
Avail: NTIS HC A10/MF A01 CSCL 22A

The objective of this program is to measure the decay rates of critical density fluctuations in a simple fluid (xenon) very near its liquid-vapor critical point using laser light scattering and photon correlation spectroscopy. Such experiments have been severely limited on Earth by the presence of gravity which causes large density gradients in the sample when the compressibility diverges approaching the critical point. The goal is to measure decay rates deep in the critical region where the scaled wavevector is the order of 1000. This will require loading the sample to 0.01% of the critical density and taking data as close as 3 microKelvin to the critical temperature (Tc = 289.72 K). Other technical problems have to be addressed such as multiple scattering and the effect of wetting layers. The ability to avoid multiple scattering by using a thin sample (100 microns) was demonstrated, as well as a temperature history which can avoid wetting layers satisfactory temperature control and measurement, and accurate sample loading. Thus the questions of experimental art are solved leaving the important engineering tasks of mounting the experiment to maintain alignment during flight and automating the state-of-the-art temperature bridges for microcomputer control of the experiment. R.J.F.

N86-10114*# National Bureau of Standards, Boulder, Colo.
TRANSIENT HEAT TRANSFER IN ZERO GRAVITY ENVIRONMENT
P. G. Giarratano, Vincent D. Arp, and A. Kumakawa (National Aerospace Lab., Mijagi, Japan) *In* NASA, Washington Microgravity Sci. and Appl. Program Tasks May 1985 p 107 (For primary document see N86-10053 01-12)
(NASA Order H-27954B) Avail: NTIS HC A10/MF A01 CSCL 22A

The objective is to provide computer codes and/or correlations for application in the design of transient heat transfer systems. The mathematical models in the computer codes are being tested by experimental data obtained in the laboratory using optical techniques. The elimination of natural convection (buoyancy) in the experimental data obtained in zero-g (KC-135) facilitates the study of thermal expansion effects which is of interest in the development and testing of the mathematical models of the transient heat transfer. Initial flight in the KC 135 (June 1983) suggested some modifications to the experimental apparatus and the data acquisition technique (high speed video will replace high speed movies for recording optical records generated during the experiments). A series of KC-135 flights with this experiment on board are scheduled for summer/fall 1984. The acquisition of the aforementioned data using interferometry and beam deflection optical techniques is anticipated. The measurements provide time dependent temperature fields above a horizontal heater surface submerged in a static fluid (Freon 13). The heater surface is electrically heated for a time interval approximately < 0.100 sec. during which the data are optically recorded. Author

N86-10115*# National Bureau of Standards, Washington, D.C. Inst. for Materials Research.
SURFACE TENSIONS AND THEIR VARIATIONS WITH TEMPERATURE AND IMPURITIES
S. C. Hardy and J. Fine *In* NASA, Washington Microgravity Sci. and Appl. Program Tasks May 1985 p 108 (For primary document see N86-10053 01-12)
(NASA Order H-27954b) Avail: NTIS HC A10/MF A01 CSCL 22A

The surface tensions in this work were determined using the sessile drop technique. This method is based on a comparison of the profile of a liquid drop with the profile calculated by solving the Young-Laplace equation. The comparison can be made in several ways; the traditional Bashforth-Adams procedure was used in conjunction with recently calculated drop shape tables which virtually eliminate interpolation errors. Although previous study has found little difference in measurements with pure and oxygen doped silicon, there is other evidence suggesting that oxygen in dilute concentrations severely depresses the surface tension of silicon. The surface tension of liquid silicon in purified argon atmospheres was measured. A temperature coefficient near -0.28 mJ/square meters K was found. The experiments show a high sensitivity of the surface tension to what is believed are low concentrations of oxygen. Thus one cannot rule out some effect of low levels of oxygen in the results. However, the highest surface tension values obtained in conditions which minimized the residual oxygen pressure are in good agreement with a previous measurement in pure hydrogen. Therefore, depression of the surface tension by oxygen is insignificant in these measurements. R.J.F.

N86-10116*# Alabama Univ., Huntsville.
DIRECT OBSERVATION OF CRITICAL POINT WETTING IN MICROGRAVITY
William F. Kaukler *In* NASA, Washington Microgravity Sci. and Appl. Program Tasks May 1985 p 109 (For primary document see N86-10053 01-12)
Avail: NTIS HC A10/MF A01 CSCL 22A

The objective of this program is to observe the interface shape in single and multicomponent systems at the onset of critical wetting in microgravity using the MSFC drop tower and KC-135 aircraft. Test cells for the drop facility were built and tested up to critical point of CCl. Low temperature drops were conducted for two-component systems near the critical consolute point. Contact angle seems to approach 90 deg near the critical consolute temperature contrary to expectations. It is suspected that since the interfacial energy becomes vanishingly small at the critical consolute temperature, the interface shape has not reached equilibrium in the available low-gravity time. Author

N86-10117*# National Aeronautics and Space Administration. Lewis Research Center, Cleveland, Ohio.
SURFACE TENSION INDUCED INSTABILITIES IN REDUCED GRAVITY: THE BENARD PROBLEM
E. Koschmieder (Texas Univ., Austin) and A.-T. Chai *In* NASA, Washington Microgravity Sci. and Appl. Program Tasks May 1985 p 110 (For primary document see N86-10053 01-12)
(Grant NAG3-303)
Avail: NTIS HC A10/MF A01 CSCL 22A

A Benard convection experiment has been set up, and the onset of convection in shallow layers of silicone oil two millimeters or less deep has been studied. The onset has been observed visually or has been determined by the break in the heat transfer curve which accompanies the onset of convection. The outcome of these experiments has been very surprising, from the point of view of theoretical expectations. The onset of convection at

temperature differences far below the critical value for fluid depths smaller than 2mm was observed. The discrepancy between experiments and theory increases with decreasing fluid depth. According to theoretical considerations, the effects of surface tension become more important as the fluid depth is decreased. Actually, one observes that the onset of convection tales place in two stages. There is first an apparently surface tension driven instability, occuring at subcritical temperature differences according to conventional theory. If then the temperature difference is increased, a second instability occurs which transform the first pattern into conventional strong hexagonal Benard cells. The second instability is in agreement with the critical temperature gradients predicted by Nield. R.J.F.

N86-10118*# Stanford Univ., Calif. Dept. of Physics.
LAMBDA POINT EQUIPMENT
John A. Lipa and William M. Fairbank *In* NASA, Washington Microgravity Sci. and Appl. Program Tasks May 1985 p 111-112 (For primary document see N86-10053 01-12)
(Contract JPL-955057; Grant NAG2-62)
Avail: NTIS HC A10/MF A01 CSCL 22A

A compilation of the active research tasks as of the end of the fiscal year 1984 of the Microgravity Science and Applications Program, NASA-Office of Space Science and Applications, involving several NASA centers and other organizations is presented. The purpose is to provide an overview of the program scope for managers and scientists in industry, university, and government communities. An introductory description of the program, strategy and overall goal; identification of the organizational structures and people involved; and a description of each research task, together with a list of recent publications is presented. The tasks are grouped into six categories: Electronic Materials; Solidification of Metals, Alloys, and Composites; Fluid Dynamics and Transports; Biotechnology; Glasses and Ceramics; and Combustion. Author

N86-10119*# Duke Univ., Durham, N. C. Dept. of Physics.
CRITICAL TRANSPORT PHENOMENA IN FLUID HELIUM UNDER LOW GRAVITY
Horst Meyer and Robert P. Behringer *In* NASA, Washington Microgravity Sci. and Appl. Program Tasks May 1985 p 113 (For primary document see N86-10053 01-12)
(Grant NAG4-379)
Avail: NTIS HC A10/MF A01 CSCL 22A

The feasibility of carrying out measurements of certain critical transport properties of pure fluid under conditions of low gravity was studied. These properties are the thermal conductivity, kappa, the shear viscosity zeta and the diffusive relaxation time tau, which are predicted to diverge (tend to infinity) as the liquid-vapor critical point is approached. However, in this critical region, the Earth's gravity effect becomes very important. As the critical point is approached, the gravity effects increasingly distort the results. The reason for this is that the compressibility of the fluid also diverges and under the influence of gravity causes a vertical density gradient in the fluid, which is significant even when very thin fluid layers (typically 1 mm high) are being used. The result is that the temperature dependence of kappa, zeta, and tau tends to flatten off as T sub c is approached instead of continuing to increase, and therefore the predictions from the renormalization group and mode coupling theories cannot be subjected to a satisfactory test. G.L.C.

N86-10120*# National Bureau of Standards, Washington, D.C.
PRECISE VISCOSITY MEASUREMENTS VERY CLOSE TO CRITICAL POINTS
M. R. Moldover and B. Berg *In* NASA, Washington Microgravity Sci. and Appl. Program Tasks May 1985 p 114 (For primary document see N86-10053 01-12)
(NASA Order C-86129D) Avail: NTIS HC A10/MF A01 CSCL 22A

A torsion oscillator is being developed to measure the viscosity of fluids at moderate temperatures (0-100 C) and pressures (0-10 MPa) at very low frequencies (0.5 Hz) and very low shear rates (0.05/sec). These conditions are required to measure the shear viscosity of fluids extremely close to the critical point. The oscillator, thermostat, vacuum system, and instrumentation were assembled and are undergoing debugging. Preliminary measurements indicate that the system has a noise corresponding to 0.2% of the viscosity of methanol-cyclohexane mixtures near the consolute point. Author

N86-10121*# National Bureau of Standards, Washington, D.C.
EXPERIMENTAL AND THEORETICAL STUDIES OF WETTING AND MULTILAYER ADSORPTION
M. R. Moldover, J. W. Schmidt, J. W. Cahn, and R. F. Kayser *In* NASA, Washington Microgravity Sci. and Appl. Program Tasks May 1985 p 115 (For primary document see N86-10053 01-12)
(NASA Order H-27954B) Avail: NTIS HC A10/MF A01 CSCL 22A

The recent work with partially miscible binary liquid mixtures has established that the structure of the liquid-vapor interface can undergo a first-order phase transition from incomplete to complete wetting of the vapor as the temperature is raised. A discontinuity in the change of interfacial tension as a function of temperature at the phase transition has been predicted to occur in many systems and to play an important role in the growth of uniform composites from alloy melts at monotectic points. These measurements are the first to establish the order of the transition. Studies of capillary rise in SF6 in a unique interferometer have led to the first measurements of the thickness of wetting layers (or equivalently, multilayer adsorbed films) on a solid surface near a liquid-vapor critical point. Instabilities in wetting layers were observed. A theory for the instabilities is being developed and will be checked by both static and dynamic optical experiments. The effect of gravity on the apparent thickness of interfaces (as measured by ellipsometry) is under study. Author

N86-10122*# National Bureau of Standards, Washington, D.C. Thermophysics Div.
IMPURITY EXTRACTION BY DROPLETS
Graham Morrison and J. M. Kincaid *In* NASA, Washington Microgravity Sci. and Appl. Program Tasks May 1985 p 116-117 (For primary document see N86-10053 01-12)
Avail: NTIS HC A10/MF A01 CSCL 22A

The goals are to model and to measure the phase equilibrium properties of a finely divided fluid containing a large number of chemically similar species. The objective is to develop an accurate, usable model for such phenomena as pollutant extraction of rain clouds, industrial separation in spray towers, and separation in emulsions. The project was designed as a hierarchy of complementary theoretical and experimental steps. A theory was developed to describe the segregation of complex impurities at the interface of a solvent. This phenomenon is important in phase behavior when a large fraction of molecules in a material are near an interface, the situation in a finely divided material. The theory will be modified to account for the effect of surface curvature on the surface tension. The study of mixtures differs from pure fluids not only because of the surface effects but also because composition differences between the droplet and the surrounding vapor can stabilize a droplet with respect to a bulk phase. G.L.C.

N86-10123*# Arizona State Univ., Tempe. Dept. of Mechanical and Aerospace Engineering.
ENERGY STABILITY OF THERMOCAPILLARY CONVECTION IN MODELS OF THE FLOAT ZONE PROCESS Abstract Only
G. Paul Neitzel and Daniel F. Jankowski *In* NASA, Washington Microgravity Sci. and Appl. Program Tasks May 1985 p 118 (For primary document see N86-10053 01-12)
(Grant NAG3-568)
Avail: NTIS HC A10/MF A01 CSCL 22A

The energy-stability of thermocapillary convection in models of the float-zone, crystal-growing process was studied. Stability limits, as functions of pertinent parameters, that will identify conditions which will not allow the existence of an undesirable oscillatory flow instability were determined. Such instabilities may occur in the space processing of semiconductor materials. The determination of the stability limits will involve two sets of numerical

computations: (1) solution of the nonlinear governing equations together with the appropriate boundary conditions to determine the basic state (in general, velocity, pressure and temperature fields and the displacement of free surfaces and interfaces); and (2) solution of a nonlinear Euler-Lagrange systems for the energy-stability limit. Both computations, while difficult, should be within the scope of available computer capability and available concepts in numerical analysis. Finite-element methods are attractive candidates for the numerical work. G.L.C.

N86-10124*# Case Western Reserve Univ., Cleveland, Ohio. Dept. of Mechanical and Aerospace Engineering.
SURFACE-TENSION DRIVEN CONVECTION
S. Ostrach and Y. Kamotani *In* NASA, Washington Microgravity Sci. and Appl. Program Tasks May 1985 p 119-120 (For primary document see N86-10053 01-12)
(Grant NAG3-570)
Avail: NTIS HC A10/MF A01 CSCL 22A

The present experiments are directed to examine surface-tension gradients. The surface-tension induced convection under reduced gravity it's comparison with normal gravity convection with all other identical conditions are studied. The intensities of such flows and their penetration depth below the free surface are also determined. In this way, the dominant role of a free surface in a reduced-gravity environment is indicated. The interface between two fluid phases can influence the motion of fluids when either the interface has finite curvature or when the interfacial tension varies from point to point. In both cases, forces appear in the interfacial region that can affect or generate fluid motions. G.L.C.

N86-10125*# National Aeronautics and Space Administration. Lewis Research Center, Cleveland, Ohio.
THERMOCAPILLARY MOTION RESEARCH
Todd T. Peterson and A.-T. Chai *In* NASA, Washington Microgravity Sci. and Appl. Program Tasks May 1985 p 121 (For primary document see N86-10053 01-12)
Avail: NTIS HC A10/MF A01 CSCL 22A

Fundamental microgravity research on interfacial surface tension driven motion by a linear temperature gradient was conducted. A vertical linear temperature gradient will be established within a test container filled with a host fluid. The thermal gradient will be positive in the upward vertical direction to avoid any free convective currents. With minimal disturbance, a single immisible fluid droplet will be introduced into the host fluid. As predicted by existing theory, the droplet will move in the direction of higher temperature due to tangential shear stresses created by surface tension variations along the periphery of the droplet. G.L.C.

N86-10126*# Utah Univ., Salt Lake City.
MORPHOLOGICAL STABILITY AND FLUID DYNAMICS OF VAPOR CRYSTAL GROWTH
Franz Rosenberger *In* NASA, Washington Microgravity Sci. and Appl. Program Tasks May 1985 p 122-124 (For primary document see N86-10053 01-12)
(Grant NsG-1534)
Avail: NTIS HC A10/MF A01 CSCL 22A

A fundamental understanding of the conditions under which crystals can retain morphological stability, i.e., shape stability of the advancing interface, during growth from vapors was studied. Morphological stability (MS) is a necessary condition for the growth of homogeneous single crystals required for numerous device applications. For crystallization from melts, the MS concepts are well developed and are essentially based on heat and mass transfer conditions about the advancing interface. For crystallization from vapors, the MS requirements are more complex and not well understood. The added complexity arises from the fact that anisotropies in interfacial kinetics are typically stronger in crystallization from vapors than from melts. These pronounced anisotropies root in the distinctly lower atomic roughness of most vapor-solid interfaces. G.L.C.

N86-10127*# Massachusetts Inst. of Tech., Cambridge. Materials Processing Center.
AUTOMATIC PROCESSING OF REACTIVE POLYMERS
David Roylance *In* NASA, Washington Microgravity Sci. and Appl. Program Tasks May 1985 p 125 (For primary document see N86-10053 01-12)
(Grant NsG-7645)
Avail: NTIS HC A10/MF A01 CSCL 22A

A series of process modeling computer codes were examined. The codes use finite element techniques to determine the time-dependent process parameters operative during nonisothermal reactive flows such as can occur in reaction injection molding or composites fabrication. The use of these analytical codes to perform experimental control functions is examined; since the models can determine the state of all variables everywhere in the system, they can be used in a manner similar to currently available experimental probes. A small but well instrumented reaction vessel in which fiber-reinforced plaques are cured using computer control and data acquisition was used. The finite element codes were also extended to treat this particular process. G.L.C.

N86-10128*# Colorado Univ., Boulder. Dept. of Chemical Engineering.
THERMOCAPILLARY AND DIFFUSOCAPILLARY MIGRATION OF A FLUID DROP
Robert L. Sani *In* NASA, Washington Microgravity Sci. and Appl. Program Tasks May 1985 p 126 (For primary document see N86-10053 01-12)
(Grant NAG3-493)
Avail: NTIS HC A10/MF A01 CSCL 22A

The migration of bubbles, or drops, plays an important role in many engineering science and space manufacturing problems. In material science processes as in the manufacturing of glasses, etc., gas bubbles can be formed from the by-products of chemical reactions or gas trapped in the interstices of the raw material. In the low-g environment of space, forces other than gravitational must be utilized as a bubble separation technique. It is well-known that gradients in interfacial tension on the bubbles' surface can promote droplet motion in the direction of decreasing interfacial tension and hence provide such a separation mechanism. Thus, the role of thermocapillary and diffusocapillary migration of a bubble, or drop, can be of paramount interest in materials processing in space. G.L.C.

N86-10129*# Princeton Univ., N. J. Dept. of Chemical Engineering.
TRANSPORT PROCESSES RESEARCH
Dudley A. Saville and W. B. Russel *In* NASA, Washington Microgravity Sci. and Appl. Program Tasks May 1985 p 127 (For primary document see N86-10053 01-12)
(Grant NAG3-447)
Avail: NTIS HC A10/MF A01 CSCL 22A

Fundamental research in reduced gravity on transport processes occurring during crystallization and/or during solidification processes was studied. The details of the transport processes in various materials processing modes will be systematically studied. A Shuttle experiment will be planned to provide a better understanding of the role of fluid motion on the formation of morphological patterns and roles of these patterns in solid composition. The approach to the research will involve theoretical modeling of transport processes, non-incursive ground-based laboratory measurements of model systems, and the definition of requirements for space experimentation. Author

N86-10130*# Princeton Univ., N. J. Dept. of Chemical Engineering.
ELECTROHYDRODYNAMICS
Dudley A. Saville *In* NASA, Washington Microgravity Sci. and Appl. Program Tasks May 1985 p 128 (For primary document see N86-10053 01-12)
(Grant NAG3-259)
Avail: NTIS HC A10/MF A01 CSCL 22A

Models of electrohydrodynamic processes involving liquids with poorly ionized solutes at high (applied) field strengths were developed and tested. Extant theories which account for the details

of physico-chemical processes associated with charged interfaces deal mainly with low field strengths and fully ionized solutes. The model used to describe processes at high field strengths--the leaky dielectric--omits consideration of electric double-layers, adsorption at interfaces, and chemical processes involved in the dissociation and recombination of solute species. Thus, even though the model depicts some features associated with bulk fluid motion, it fails to give a comprehensive picture. One example of the shortcomings of both the classical model of eletrokinetics at low field strengths and the leaky-dielectric model for high field strengths is found in the field strength dependence of the mobility of small particles in apolar liquids. The research will provide a more general model of electrohydrodynamic phenomena capable of application in diverse circumstances. G.L.C.

N86-10131*# National Bureau of Standards, Washington, D.C. Thermophysics Div.
MISCIBILITY GAP SYSTEMS
L. A. Schmid *In* NASA, Washington Microgravity Sci. and Appl. Program Tasks May 1985 p 129 (For primary document see N86-10053 01-12)
(NASA Order H-27954B) Avail: NTIS HC A10/MF A01 CSCL 22A

Immiscible droplets embedded in a host fluid in which a temperature gradient exists migrate toward the hot end of the host fluid because of the temperature dependence of the interfacial energy of the droplet. This thermocapillary migration effect was exploited in the design of a controllable heat valve which is the thermal analog of the electronic vacuum triode. Studies have also been made of test cells that could use thermocapillary migration to facilitate the study of condensation and dissolution kinetics in miscibility-gap solutions. Author

N86-10132*# Aerodyne Research, Inc., Billerica, Mass.
EXPERIMENTAL AND THEORETICAL ANALYSIS OF CHEMICAL VAPOR DEPOSITION WITH PREDICTION OF GRAVITY EFFECTS
Charter D. Stinespring and Karl E. Spear (Pennsylvania State Univ.) *In* NASA, Washington Microgravity Sci. and Appl. Program Tasks May 1985 p 130 (For primary document see N86-10053 01-12)
(Contract NAS3-23934)
Avail: NTIS HC A10/MF A01 CSCL 22A

A combined experimental and theoretical study to characterize the effects of gravitationally-induced transport on atmospheric pressure silicon epitaxy by SiH4 pyrolysis is planned. Experimentally, flow regimes in which free convective transport contributes to the Chemical Vapor Deposition (CVD) process will be identified, and, for these conditions, the flow and deposition process will be characterized. Specifically, this will include measurements of three dimensional temperature variations using in situ Rayleigh scattering, gas phase composition profiles using laser absorption and fluorescence techniques, and deposition rates and defect densities. Subsequently, the free convective transport contribution to the CVD process will be minimized and/or altered while leaving deposition chemistry unaltered, and the characterization will be repeated. Based on these analyses, the effects of gravitationally-induced transport on atmospheric pressure CVD will be assessed. G.L.C.

N86-10133*# Massachusetts Inst. of Tech., Cambridge.
ROLE OF CONVECTION IN GRAIN REFINING
Julian Szekely, Merton C. Flemings, N. El-Kaddah, and Y. Shiohara *In* NASA, Washington Microgravity Sci. and Appl. Program Tasks May 1985 p 131-132 (For primary document see N86-10053 01-12)
(Grant NsG-7645)
Avail: NTIS HC A10/MF A01 CSCL 22A

A quantitative representation of the heat and fluid flow fields in electromagnetically levitated (positioned) metallic specimens is examined. Experimental studies as well as modelling of those studies on undercooling and solidification of levitated metal droplets are also considered. Thermal measurements will be made of the undercooling and solidification of levitated metal droplets. Thermal measurements will be made of the undercooling and of the details of the ultra-rapid recalescence. This levitation technique combined with quenching will be used to aid in the development of coherent model for the solidification process related to structural studies, including thermodynamics and kinetics for nucleation and metastable solute partition, kinetics for solid/liquid interface velocity with high undercooling, and heat flow consideration. G.L.C.

N86-10134*# Michael Reese Research Foundation, Chicago, Ill.
BIOCHEMICAL ASSAYS OF CULTURED CELLS
Grant H. Barlow *In* NASA, Washington Microgravity Sci. and Appl. Program Tasks May 1985 p 135 (For primary document see N86-10053 01-12)
(Contract NAS9-16389)
Avail: NTIS HC A10/MF A01 CSCL 22A

Subpopulations of human embryonic kidney cells isolated from continuous flow electrophoresis experiments performed at McDonnell Douglas and on STS-8 have been analyzed. These analyses have included plasminogen activator assays involving indirect methodology on fibrin plated and direct methodology using chromogenic substrates. Immunological studies were performed and the conditioned media for erythropoietin activity and human granulocyte colony stimulating (HGCSF) activity was analyzed. G.L.C.

N86-10135*# Arizona Univ., Tucson. Dept. of Microbiology.
HORMONE PURIFICATION BY ISOELECTRIC FOCUSING
Milan Bier *In* NASA, Washington Microgravity Sci. and Appl. Program Tasks May 1985 p 136-137 (For primary document see N86-10053 01-12)
(Contract NAS8-32950)
Avail: NTIS HC A10/MF A01 CSCL 22A

Various ground-based research approaches are being applied to a more definitive evaluation of the natures and degrees of electroosmosis effects on the separation capabilities of the Isoelectric Focusing (IEF) process. A primary instrumental system for this work involves rotationally stabilized, horizontal electrophoretic columns specially adapted for the IEF process. Representative adaptations include segmentation, baffles/screens, and surface coatings. Comparative performance and development testing are pursued against the type of column or cell established as an engineering model. Previously developed computer simulation capabilities are used to predict low-gravity behavior patterns and performance for IEF apparatus geometries of direct project interest. Three existing mathematical models plus potential new routines for particular aspects of simulating instrument fluid patterns with varied wall electroosmosis influences are being exercised. G.L.C.

N86-10136*# Oregon Health Sciences Univ., Portland. Dept. of Neurology.
CELL PARTITION IN TWO POLYMER AQUEOUS PHASES
Donald E. Brooks *In* NASA, Washington Microgravity Sci. and Appl. Program Tasks May 1985 p 138-139 (For primary document see N86-10053 01-12)
(Contract NAS8-35333)
Avail: NTIS HC A10/MF A01 CSCL 22A

In a reduced gravity environment the two polymer phases will not separate via density driven settling in an acceptably short length of time. It is to be expected that a certain amount of phase separation will take place, however, driven by the reduction in free energy gained when the interfacial area is reduced. This stage of separation process will therefore depend directly on the magnitude of the interfacial tension between the phases. In order to induce complete phase separation in a short time, electric field-induced separation which occurs because the droplets of one phase in the other have high electrophoretic mobilities which increase with droplet size was investigated. These mobilities are significant only in the presence of certain salts, particularly phosphates. The presence of such salts, in turn has a strong effect on the cell partition behavior in dextran-poly (ethylene glycol) (PEG) systems. The addition of the salts necessary to produce phase drop mobilities has a large effect on the interfacial tensions in the systems. G.L.C.

N86-10137*# Sydney Univ. (Australia). Dept. of Medicine.
A STUDY OF BLOOD FLOW AND OF AGGREGATION OF BLOOD CELLS UNDER CONDITIONS OF ZERO GRAVITY: ITS RELEVANCE TO THE OCCLUSIVE DISEASES AND CANCER
Leopold Dintenfass *In* NASA, Washington Microgravity Sci. and Appl. Program Tasks May 1985 p 140 (For primary document see N86-10053 01-12)
Avail: NTIS HC A10/MF A01 CSCL 22A

The objectives of this program are: (1) to determine whether the size of red cell aggregates, kinetics and morphology of these aggregates are influenced by near-zero gravity; (2) whether viscosity, especially at low shear rate, is afflicted by near-zero gravity (the latter preventing sedimentation of red cells); (3) whether the actual shape of red cells changes; and (4) whether blood samples obtained from different donors (normal and patients suffering from different disorders) react in the same manner to near-zero gravity. G.L.C.

N86-10138*# Alabama Univ., Huntsville.
NEW INSTRUMENTATION FOR PHASE PARTITIONING
J. Milton Harris *In* NASA, Washington Microgravity Sci. and Appl. Program Tasks May 1985 p 141-142 (For primary document see N86-10053 01-12)
(Contract NAS8-35334)
Avail: NTIS HC A10/MF A01 CSCL 22A

Cells and molecules can be purified by partitioning between the two immiscible liquid phases formed by aqueous solutions of poly/ethylene glycol and dextran. Such purification can be more selective, higher yielding, and less destructive to sensitive biological materials than other available techniques. Earth's gravitational field is a hindering factor as it causes sedimentation of particles to be purified and shear-induced particle randomization. The present proposal is directed toward developing new instrumentation for performing phase partitioning both on Earth and in microgravity. G.L.C.

N86-10139*# Alabama Univ., Huntsville.
CELL PARTITION IN TWO POLYMER AQUEOUS PHASES
J. Milton Harris *In* NASA, Washington Microgravity Sci. and Appl. Program Tasks May 1985 p 143 (For primary document see N86-10053 01-12)
(Contract NAS8-35362)
Avail: NTIS HC A10/MF A01 CSCL 22A

Partition of biological cells in two phase aqueous polymer systems is recognized as a powerful separation technique which is limited by gravity. The synthesis of new, selective polymer ligand conjugates to be used in affinity partition separations is of interest. The two most commonly used polymers in two phase partitioning are dextran and polyethylene glycol. A thorough review of the chemistry of these polymers was begun, particularly in the area of protein attachment. Preliminary studies indicate the importance in affinity partitioning of minimizing gravity induced randomizing forces in the phase separation process. The PEG-protein conjugates that were prepared appear to be ideally suited for achieving high quality purifications in a microgravity environment. An interesting spin-off of this synthetic work was the observation of catalytic activity for certain of our polymer derivatives. Author

N86-10140*# National Aeronautics and Space Administration. Johnson (Lyndon B.) Space Center,
PURIFICATION AND CULTIVATION OF HUMAN PITUITARY GROWTH HORMONES SECRETING CELLS
Wesley C. Hymer (Pennsylvania State Univ., University Park), Paul Todd (Pennsylvania State Univ., University Park), Richard Grindeland (Pennsylvania State Univ., University Park), Wayne Lanham (Pennsylvania State Univ., University Park), and Dennis Morrison *In* NASA, Washington Microgravity Sci. and Appl. Program Tasks May 1985 p 144-145 refs (For primary document see N86-10053 01-12)
(Contract NAS9-15566)
Avail: NTIS HC A10/MF A01 CSCL 22A

The rat and human pituitary gland contains a mixture of hormone producing cell types. The separation of cells which make growth hormone (GH) is attempted for the purpose of understanding how the hormone molecule is made within the pituitary cell; what form(s) it takes within the cell; and what form(s) GH assumes as it leaves the cell. Since GH has a number of biological targets (e.g., muscle, liver, bone), the assessment of the activities of the intracellular/extracellular GH by new and sensitive bioassays. GH cells contained in the mixture was separated by free flow electrophoresis. These experiments show that GH cells have different electrophoretic mobilities. This is relevant to NASA since a lack of GH could be a prime causative factor in muscle atrophy. Further, GH has recently been implicated in the etiology of motion sickness in space. Continuous flow electrophoresis experiment on STS-8 showed that GH cells could be partially separated in microgravity. However, definitive cell culture studies could not be done due to insufficient cell recoveries. Author

N86-10141*# National Aeronautics and Space Administration. Johnson (Lyndon B.) Space Center,
CELL SEPARATIONS IN MICROGRAVITY AND DEVELOPMENT OF A SPACE BIOREACTOR
Dennis R. Morrison *In* NASA, Washington Microgravity Sci. and Appl. Program Tasks May 1985 p 146-147 refs (For primary document see N86-10053 01-12)
Avail: NTIS HC A10/MF A01 CSCL 22A

A bioreactor optimized for operations in space is now being developed. The current research is focused on determining the optimum cell-bead ratios, medium content and proper maintenance conditions required to keep living cell specimens alive and healthy for the entire flight. The bioreactor development project has recently added a microprocessor/computer to the JSC prototype for control and data analysis. Appropriate new technology is being combined with the current bioreactor designs and tested to determine what specific features must be included in the fabrication of a bioreactor designed to operate for STS demonstration tests. Considerations include: (1) circulation and resupply of culture media; (2) sensors required to monitor temperature, cell growth, mass transport, and oxygen consumption; and (3) inflight control of shear stress on cells, gas transfer in microgravity, diffusion, and intracellular transport. These data and results from the JSC prototype bioreactor test will be used for the design and construction of a small space bioreactor for the Orbiter middeck. Author

N86-10142*# National Aeronautics and Space Administration. Johnson (Lyndon B.) Space Center,
CELL MAINTENANCE SYSTEMS
Dennis R. Morrison *In* NASA, Washington Microgravity Sci. and Appl. Program May 1985 p 148 (For primary document see N86-10053 01-12)
Avail: NTIS HC A10/MF A01 CSCL 22A

Living human cells require attachment to a suitable surface and special culture conditions in order to grow. These requirements are modified and amplified when cells are taken into a weightless environment. Special handling and maintenance systems are required for routine laboratory procedures conducted in the Orbiter and in the Spacelab. Methods were developed to maintain cells in special incubators designed for the Orbiter middeck, however, electrophoresis and other experiments require cells to be harvested off of the culture substrate before they can be processed or used. The cell transport assembly (CTA) was flown on STS-8, and results show that improvements are required to maintain adequate numbers of cells in this device longer than 48 hours. The life sciences middeck centrifuge probably can be used, but modifications will be required to transfer cells from the CTA and keep the cells sterile. Automated systems such as the Skylab SO-15 flight hardware and crew operated systems are being evaluated for use on the Space Shuttle, Spacelab, and Space Station research modules. Author

N86-10143*# National Aeronautics and Space Administration. Marshall Space Flight Center, Huntsville, Ala.
MATHEMATICAL MODELS OF CONTINUOUS FLOW ELECTROPHORESIS
D. A. Saville (Princeton Univ.) and R. S. Snyder *In* NASA,

Washington Microgravity Sci. and Appl. Program Tasks May 1985 p 149-150 refs (For primary document see N86-10053 01-12)
(Contract NAS8-32614)
Avail: NTIS HC A10/MF A01 CSCL 22A

Development of high resolution continuous flow electrophoresis devices ultimately requires comprehensive understanding of the ways various phenomena and processes facilitate or hinder separation. A comprehensive model of the actual three dimensional flow, temperature and electric fields was developed to provide guidance in the design of electrophoresis chambers for specific tasks and means of interpreting test data on a given chamber. Part of the process of model development includes experimental and theoretical studies of hydrodynamic stability. This is necessary to understand the origin of mixing flows observed with wide gap gravitational effects. To insure that the model accurately reflects the flow field and particle motion requires extensive experimental work. Another part of the investigation is concerned with the behavior of concentrated sample suspensions with regard to sample stream stability particle-particle interactions which might affect separation in an electric field, especially at high field strengths. Mathematical models will be developed and tested to establish the roles of the various interactions. Author

N86-10144*# National Aeronautics and Space Administration. Marshall Space Flight Center, Huntsville, Ala.
ELECTROPHORESIS TECHNOLOGY
R. S. Snyder *In* NASA, Washington Microgravity Sci. and Appl. Program Tasks May 1985 p 151-152 refs (For primary document see N86-10053 01-12)
Avail: NTIS HC A10/MF A01 CSCL 22A

A new high resolution apparatus designed for space was built as a laboratory prototype. Using a moving wall with a low zeta potential coating, the major sources of flow distortion for an electrophoretic sample stream are removed. Highly resolved fractions, however, will only be produced in space because of the sensitivity of this chamber to buoyancy-induced convection in the laboratory. The second and third flights of the McDonnell Douglas Astronautics Corporation continuous flow electrophoresis system carried samples developed at MSFC intended to evaluate the broad capabilities of free flow electrophoresis in a reduced gravity environment. Biological model materials, hemoglobin and polystyrene latex microspheres, were selected because of their past use as electrophoresis standards and as visible markers for fluid flow due to electroosmosis, spacecraft acceleration or other factors. The dependence of the separation resolution on the properties of the sample and its suspension solution was assessed. Author

N86-10145*# Pennsylvania State Univ., University Park.
KIDNEY CELL ELECTROPHORESIS
Paul Todd *In* NASA, Washington Microgravity Sci. and Appl. Program Tasks May 1985 p 153 (For primary document see N86-10053 01-12)
(Contract NAS9-15584)
Avail: NTIS HC A10/MF A01 CSCL 22A

Materials and procedures for microgravity electrophoresis of living human embryonic kidney cells were evaluated, ground support in the form of analytical cell electrophoresis and flow cytometry was provided and cells returned from space flight were analyzed. Preflight culture media, electrophoresis buffer, fraction collection media, temperature profiles, and urokinase assay procedures were tested prior to flight. Electrophoretic mobility distributions of aliquots of the cell population to be fractionated in flight were obtained. The protocol established and utilized is given. Author

N86-10146*# National Aeronautics and Space Administration. Marshall Space Flight Center, Huntsville, Ala.
PRODUCTION OF LARGE-PARTICLE-SIZE MONODISPERSE LATEXES IN MICROGRAVITY
J. W. Vanderhoff (Lehigh Univ.), F. J. Micale (Lehigh Univ.), M. S. El-Aasser (Lehigh Univ.), and M. Kornfeld *In* NASA, Washington Microgravity Sci. and Appl. Program Tasks May 1985 p 154-155 refs (For primary document see N86-10053 01-12)
(Contract NAS8-32951)
Avail: NTIS HC A10/MF A01 CSCL 22A

A latex is a suspension of very tiny (micrometer-size) plastic spheres in water, stabilized by emulsifiers. The growth of billions of these tiny plastic spheres to sizes larger than can be grown on Earth is attempted while keeping all of them exactly the same size and perfectly spherical. Thus far on several of the Monodisperse Latex Reactor (MLR) flights, the latex spheres have been returned to Earth with standard deviations of better than 1.4%. In microgravity the absence of buoyancy effects has allowed growth of the balls up to 30 micrometers in diameter thus far. The MLR has now flown 5 times on the Shuttle. The MLR has now produced the first commercial space product; that is the first commercial material ever manufactured in space and marketed on Earth. Once it is demonstrated that these large-size-monodisperse latexes can be routinely produced in quantity and quality, they can be marketed for many types of scientific applications. They can be used in biomedical research for such things as drug carriers and tracers in the body, human and animal blood flow studies, membrane and pore-sizing in the body, and medical diagnostic tests. Author

N86-10147*# Massachusetts Inst. of Tech., Cambridge.
COLLOIDAL OXIDE PROPERTIES AND KINETIC STUDIES
I-Wei Chen *In* NASA, Washington Microgravity Sci. and Appl. Program Tasks May 1985 p 159 (For primary document see N86-10053 01-12)
(Grant NSG-7645)
Avail: NTIS HC A10/MF A01 CSCL 22A

Silica based oxide particles prepared by various methods are compared in terms of their gellation kinetics, densification kinetics, and microable structural evolutions begin at very low temperature. Additional work reported in literature further suggested that the colloidal behaviors and the dried gel structures of the same oxide from different preparation techniques differ fundamentally. These differences significantly affect the densification kinetics and the product microstructure. Gravitational segregation of particles of different sizes in a gravitational field is modelled as a diffusion/segregation problem. A structural free volume model was used to describe the activation process of jump statistics. The sizes of the particles, the interstices, and their packing topology are accounted for in the estimation of the free volume. An attempt frequency is ascribed to particles to account for the vibrational rearrangement during powder packing. Author

N86-10148*# Missouri Univ., Rolla.
CONTAINERLESS PROCESSING OF GLASS FORMING-MELTS IN SPACE
Delbert D. Day *In* NASA, Washington Microgravity Sci. and Appl. Program Tasks May 1985 p 160-161 refs (For primary document see N86-10053 01-12)
(Contract NAS8-34758)
Avail: NTIS HC A10/MF A01 CSCL 22A

The major objectives of this work are: (1) obtain quantitative evidence for the suppression of heterogeneous nucleation/crystallization in containerless melts in micro-g; (2) study melt homogenization in the absence of gravity driven convection; (3) develop the procedures for preparing precursor samples suitable for flight experiments; (4) perform comparative property analysis of glasses melted on Earth and in micro-g; (5) determine the feasibility of preparing glass shells in micro-g for use as laser fusion targets; and (6) assess the operational performance of the single axis acoustic levitator/furnace apparatus for processing multicomponent, glass forming melts in micro-g. Ways of obtaining these goals are discussed. Author

N86-10149*# Rensselaer Polytechnic Inst., Troy, N. Y.
CRYSTALLIZATION, OPTICAL AND CHEMICAL PROPERTIES OF FLUORIDE GLASSES
Robert H. Doremus *In* NASA, Washington Microgravity Sci. and Appl. Program Tasks May 1985 p 162 (For primary document see N86-10053 01-12)
(Contract JPL-955870)
Avail: NTIS HC A10/MF A01 CSCL 22A

Fluoride glasses have great promise as infrared optical components, especially fibers, because they are transparent to 8 micrometers and higher. In order to optimize properties, different glass compositions are needed. Some are hard to form in a container, and may possibly be formable in a containerless furnace. Understanding of crystallization with and without a container could lead to glasses with optimum properties. Chemical durability (attack by water) can limit or extend the applicability of fluoride glasses. Progress to date is given. Author

N86-10150*# KMS Fusion, Inc., Ann Arbor, Mich.
GEL PRECURSORS AS GLASS AND CERAMIC STARTING MATERIALS FOR SPACE PROCESSING APPLICATIONS RESEARCH
Raymond L. Downs and Wayne J. Miller *In* NASA, Washington Microgravity Sci. and Appl. Program Tasks May 1985 p 163 (For primary document see N86-10053 01-12)
(Contract NAS7-100)
Avail: NTIS HC A10/MF A01 CSCL 22A

The crystallization kinetics and glass forming ability of reluctant glass formers is investigated. This could ultimately aid the formation of bulk samples of unique glass compositions outside of normal glass forming regions allowing the optimization of certain properties of the glass. One important aspect of processing in space is the containerless undercooling of molten substances. Theoretically, the extent of undercooling can be greatly enhanced by solidifying in the absence of heterogeneous nucleation resulting from contact with crucibles or molds. Techniques were established for the measurement of crystallization kinetics and critical cooling rates. The glass formation ability and crystallization kinetics of Ga2O-43CaO and several Al2O3-CaO compositions were measured. An apparatus was set up to measure the temperature of spherical samples on a thermocouple at large cooling rates. The time and temperature of nucleation is recorded and the probability of nucleation at various cooling rates can be measured. Author

N86-10151*# National Aeronautics and Space Administration. Marshall Space Flight Center, Huntsville, Ala.
GLASS FORMATION IN RELUCTANT GLASS FORMERS
E. C. Ethridge *In* NASA, Washington Microgravity Sci. and Appl. Program Tasks May 1985 p 164-165 refs (For primary document see N86-10053 01-12)
Avail: NTIS HC A10/MF A01 CSCL 22A

The crystallization kinetics and glass forming ability of reluctant glass formers is investigated. This could ultimately aid the formation of bulk samples of unique glass compositions outside of normal glass forming regions allowing the optimization of certain properties of the glass. One important aspect of processing space is the containerless undercooling of molten substances. Theoretically, the extent of undercooling can be greatly enhanced by solidifying in the absence of heterogeneous nucleation resulting from contact with crucibles or molds. Techniques were established for the measurement of crystallization kinetics and critical cooling rates. The glass formation ability and crystallization kinetics of Ga2O-43CaO and several Al2O3-CaO compositions were measured. An apparatus was set up to measure the temperature of spherical samples on a thermocouple at large cooling rates. The time and temperature of nucleation is recorded and the probability of nucleation at various cooling rates can be measured. Author

N86-10152*# Massachusetts Inst. of Tech., Cambridge. Materials Processing Center.
RAPID SOLIDIFICATION OF MAGNETIC OXIDES
G. Kalonji and M. R. DeGuire *In* NASA, Washington Microgravity Sci. and Appl. Program Tasks May 1985 p 166 (For primary document see N86-10053 01-12)
(Grant NSG-7645)
Avail: NTIS HC A10/MF A01 CSCL 22A

The enhanced control over microstructural evolution inherent in rapid solidification processing techniques are exploited to create novel ceramic magnetic materials. The great sensitivity of magnetic properties to local structure provides a powerful probe both for the study of structure and of microscopic solidification mechanisms. The first system studied is the SrO-Fe2O3 binary, which contains the commercially important hard magnetic compound strontium hexaferrite. The products were analyzed by transmission electron microscopy, Mossbauer spectroscopy, magnetic measurements, and differential thermal analysis. As-quenched ribbons contain high concentrations of super-paramagnetic particles, 80 to 250 Angstroms in diameter, in a glassy matrix. This suggests the possibility of crystallizing monodomain strontium hexaferrite during subsequent heat treatment, with a resulting increase in coercivity over conventionally processed ferrite magnets. That magnetic properties can be controlled in solidification processing by varying the quench rate is demonstrated. Author

N86-10153*# Jet Propulsion Lab., California Inst. of Tech., Pasadena.
SOL-GEL GLASSES
S. P. Mukherjee *In* NASA, Washington Microgravity Sci. and Appl. Program Tasks May 1985 p 167-169 (For primary document see N86-10053 01-12)
Avail: NTIS HC A10/MF A01 CSCL 22A

Multicomponent homogeneous, ultrapure noncrystalline gels/gel derived glasses are promising batch materials for the containerless glass melting experiments in microgravity. Hence, ultrapure, homogeneous gel precursors could be used to: (1) investigate the effect of the container induced nucleation on the glass forming ability of marginally glass forming compositions; and (2) investigate the influence of gravity on the phase separation and coarsening behavior of gel derived glasses in the liquid-liquid immiscibility zone of the nonsilicate systems having a high density phase. The structure and crystallization behavior of gels in the SiO2-GeO2 as a function of gel chemistry and thermal treatment were investigated. As are the chemical principles involved in the distribution of a second network former in silica gel matrix being investigated. The procedures for synthesizing noncrystalline gels/gel-monoliths in the SiO2-GeO2, GeO2-PbO systems were developed. Preliminary investigations on the levitation and thermal treatment of germania silicate gel-monoliths in the Pressure Facility Acoustic Levitator were done. Author

N86-10154*# Harvard Univ., Cambridge, Mass.
BULK FORMATION OF METALLIC GLASSES AND AMORPHOUS SILICON FROM THE MELT
Frans Spaepen *In* NASA, Washington Microgravity Sci. and Appl. Program Tasks May 1985 p 170-171 refs (For primary document see N86-10053 01-12)
(Contract NAS8-35416)
Avail: NTIS HC A10/MF A01 CSCL 22A

By using metallic glass compositions with a high relative glass transition temperature, such as Pd40Ni40P20, homogeneous nucleation also becomes negligible. Large (5g) masses of this alloys were obtained using a molten B2O3 flux. Presently, bulk glass formation in iron based glasses is being investigated. It is expected that if an undercooling of about 250K can be achieved in a Ge or Si melt, formation of the amorphous semiconductor phase (rather than the crystal) may be kinetically favored. The volumetric behavior of undercooled liquid Ga droplet dispersion is investigated by dilatometry. A theoretical model (both analytical and numerical) was developed for transient nucleation in glass forming melts. The model, originally designed for isothermal conditions, was extended to continuous quenching. It is being applied to glass formation in various metallic and oxide systems. A further refinement will be the inclusion of diffusion controlled interfacial rearrangements governing the growth of the crystal embryos. Author

N86-10155*# Clarkson Coll. of Technology, Potsdam, N.Y. Dept. of Chemical Engineering.
PHYSICAL PHENOMENA IN CONTAINERLESS GLASS PROCESSING
R. S. Subramanian and Robert Cole *In* NASA, Washington Microgravity Sci. and Appl. Program Tasks May 1985 p 172-173 refs (For primary document see N86-10053 01-12)

Avail: NTIS HC A10/MF A01 CSCL 22A

An investigation into the various physical phenomena of importance in the space experiments is under way. Theoretical models of thermocapillary flow in drops, thermal migration of bubbles and droplets, the motion of bubbles inside drops, and the migration of bubbles in rotating liquid bodies are being developed. Experiments were conducted on the migration of bubbles and droplets to the axis of a rotating liquid body, and the rise of bubbles in molten glass. Also, experiments on thermocapillary motion in silicone oils as well as glass melts were performed. Experiments are currently being conducted on the migration of bubbles in a thermal gradient, and on their motion inside unconstrained liquid drops in a rotating liquid. Author

N86-10156*# Jet Propulsion Lab., California Inst. of Tech., Pasadena.

FUSION TARGET TECHNOLOGY

T. G. Wang *In* NASA, Washington Microgravity Sci. and Appl. Program Tasks May 1985 p 174 refs (For primary document see N86-10053 01-12)

Avail: NTIS HC A10/MF A01 CSCL 22A

In order to produce the high quality spherical shells that are required, three parameters must be controlled accurately: the shell dimensions, shell sphericity and concentricity, and the surface topology of the shell. Attempts to conduct experiments on the dynamics of liquid bubbles (molten shells) in laboratories are limited by a strong coupling among the three parameters, time, gravity, and temperature. These limitations are circumvented and detailed study of each of the important processes is carried out through the use of low gravity environments collectively available in drop towers, in KC-135 flights, in a neutrally buoyant immiscible system, and in an acoustic levitation system. Author

N86-10157*# Jet Propulsion Lab., California Inst. of Tech., Pasadena.

GLASS RESEARCH

Michael C. Weinberg *In* NASA, Washington Microgravity Sci. and Appl. Program Tasks May 1985 p 175-176 refs (For primary document see N86-10053 01-12)

Avail: NTIS HC A10/MF A01 CSCL 22A

Research efforts span three general areas of glass science: glass refining, gel-derived glasses, and nucleation and crystallization of glasses. Gas bubbles which are present in a glass product are defects which may render the glass totally useless for the end application. For example, optical glasses, laser host glasses, and a variety of other specialty glasses must be prepared virtually defect free to be employable. Since a major mechanism of bubble removal, buoyant rise, is virtually inoperative in microgravity, glass fining will be especially difficult in space. On the other hand, the suppression of buoyant rise and the ability to perform containerless melting experiments in space allows the opportunity to carry out several unique bubble experiments in space. Gas bubble dissolution studies may be performed at elevated temperatures for large bubbles with negligible bubble motion. Also, bubble nucleation studies may be performed without the disturbing feature of heterogeneous bubble nucleation at the platinum walls. Ground based research efforts are being performed in support of these potential flight experiments. Author

N86-10158*# Massachusetts Inst. of Tech., Cambridge. Materials Processing Center.

OXIDATION BEHAVIOR OF GLASSY ALLOYS

G. Yurek *In* NASA, Washington Microgravity Sci. and Appl. Program Tasks May 1985 p 177 (For primary document see N86-10053 01-12)

(Grant NSG-7645)

Avail: NTIS HC A10/MF A01 CSCL 22A

The oxidation behavior of high temperature glassy alloys produced by rapid solidification processing is investigated and the effects of processing and composition on oxidation behavior is studied. Glassy Ta-44.5at%Ir, Ta-40at%Ir-10at%B and Nb-45at%Ir oxidized rapidly at 700 to 800 C at an oxygen partial pressure of .001 atm. The alloys were embrittled during the oxidation process. No apparent oxidation or embrittlement of the Ta-Ir alloy occurred after oxidation for 4h at 500 C at an oxygen partial pressure of .001 atm. Embrittlement occurred, however, after 100h of exposure under the latter conditions. Alloy embrittlement is associated with the partial or full conversion of the metallic glass to a mixture of crystalline beta-Ta2O5 and metallic iridium. Hot compaction of glassy alloys of this type must be limited to relatively low temperatures (approx. 500 C) and short times at the low temperatures unless extremely low oxygen partial pressures can be achieved during the compaction process. Author

N86-10159*# Kentucky Univ., Lexington. Dept. of Mechanical Engineering.

SOLID SURFACE COMBUSTION AT REDUCED GRAVITY

Robert A. Altenkirch *In* NASA, Washington Microgravity Sci. and Appl. Program Tasks May 1985 p 181 refs (For primary document see N86-10053 01-12)

Avail: NTIS HC A10/MF A01 CSCL 22A

The spread of a flame in the gas over the surface of a solid combustible involves in an essential way the transfer of heat from the flame to the solid fuel immediately ahead of it. This heat transfer is affected by the character of the gas phase flame, and so the phenomenon of flame spreading under reduced gravity, in which the flow is generated by gasification of the solid combustible, is apt to be different from what occurs under the Earth's normal gravitational acceleration where the flow is largely buoyancy driven. An experiment is being designed for the Middeck of the Space Shuttle to aid us in understanding the process of flame spreading in the absence of a buoyancy driven flow. A chamber approximately 0.35 cu.m. in volume is to contain either a thin sample of a cellulosic material or a thick sample of polymethyl-methacrylate and an oxidizing environment of O2 and N2. Samples will be ignited at one end, and the ensuing flame spread will be filmed. The spread rate can be determined from the films, and surface and gas-phase temperatures just above the surface will also be recorded. These data will help to clarify the mechanism of forward heat transfer in the low gravity flames. Author

N86-10160*# California Univ., San Diego, La Jolla. Energy Center.

PARTICLE CLOUD COMBUSTION EXPERIMENT

A. L. Berlad *In* NASA, Washington Microgravity Sci. and Appl. Program Tasks May 1985 p 182 refs (For primary document see N86-10053 01-12)

(Grant NAG3-381)

Avail: NTIS HC A10/MF A01 CSCL 22A

Preparation of flight experiment designs is supported by experimental studies of acoustically induced mixing process, optical transmissivities of particle cloud distributions, wall saturation effects and their control through the use of electrically neutral flame tube materials and surfaces, and the pyrolysis-vaporization kinetics of selected organic particulates. Drop tower tests of stabilized particle cloud flames have allowed valuable comparison of g = 0 and g = 1 (upwards and downwards) stabilized flame propagation. These stabilized flame data will be valuable assists in dealing with the freely propagating particle cloud flame data anticipated through Space Shuttle experimentation. Supporting theoretical studies emphasize comprehensive flame propagation and extinction relations among premixed single phase (gaseous) flames and premixed particle cloud flames, for both stabilized and freely propagating flames. Author

N86-10161*# Science Applications, Inc., Chatsworth, Calif. Combustion Science and Advanced Technology Dept.

BUOYANCY EFFECTS UPON VAPOR FLAME AND EXPLOSION PROCESSES

Raymond B. Edelman and Phillip T. Harsha *In* NASA, Washington Microgravity Sci. and Appl. Program Tasks May 1985 p 183 ref (For primary document see N86-10053 01-12)

(Contract NAS3-22822)

Avail: NTIS HC A10/MF A01 CSCL 22A

The objective of this microgravity project is to develop an experimental and theoretical analyses critical to the understanding

of the coupling of buoyancy and turbulence generation and its effect on fuel-air mixing, flame intensity and flame propagation in jet diffusion flames. The experiment is designed to examine certain effects of buoyancy acting on a diffusion flame in which the flame is directed either upward or downward. This change from negative to positive g is observed to significantly alter the flame shape although all other operating conditions are the same for both configurations. However, to perform this experiment a significant coaxial secondary air flow is needed in order to prevent flow reversal when the flame is inverted. The theoretical analysis that has been developed handles the secondary air flow and the extreme change in gravity vector direction. Thus the data will provide a measure of credibility of the analysis which will then be used to assist in the design of the actual zero-g experiment.

F.M.R.

N86-10162*# California Univ., Berkeley.

A FUNDAMENTAL STUDY OF SMOLDERING WITH EMPHASIS ON EXPERIMENTAL DESIGN FOR ZERO-g

Patrick J. Pagni and A. Carlos Fernandez-Pello *In* NASA, Washington Microgravity Sci. and Appl. Program Tasks May 1985 p 184 (For primary document see N86-10053 01-12)

(Grant NAG3-443)

Avail: NTIS HC A10/MF A01 CSCL 22A

The objective of this section of the microgravity project is to identify key sets of low-gravity experiments which would critically compliment a larger set of more easily performed normal-gravity experiments to explain the phenomena found in smoldering combustion. It is planned to follow through on the conceptual design of these experiments by participating in the future in the fabrication of the refined apparatus and in the data collection and interpretation. Low-gravity experiments are appropriate for smoldering combustion because of the complexity of smoldering which requires every means possible to discriminate among the many chemical and physical mechanisms active in most smoldering combustion scenarios. Efforts will be primarily analytical, attempting to identify appropriate approximations and dominant dimensionless groups based on existing data and state-of-the-art combustion modelling. Transient stability questions such as ignition, extinction and the choices among charring, tarring, or flaming modes will be included.

F.M.R.

N86-10163*# Carnegie-Mellon Univ., Pittsburgh, Pa.

IGNITION AND FLAME SPREAD ABOVE LIQUID FUEL POOLS

William A. Sirignano *In* NASA, Washington Microgravity Sci. and Appl. Program Tasks May 1985 p 185 (For primary document see N86-10053 01-12)

(Grant NAG3-404)

Avail: NTIS HC A10/MF A01 CSCL 22A

Phenomena of ignition and flame spread above liquid fuel pools are studied and factors that can improve fire safety are determined. Dominant mechanisms for convective heat transfer and impact on ignition and flame spread above liquid fuel pools will be determined from these efforts. The approach is: (1) analytical and computational studies to evaluate scaling factors; (2) experimental design, development, and operation in laboratory at Earth's gravity; (3) experimental design for drop towers at NASA Lewis Research Center; (4) development and operation of drop tower experiments together with NASA Lewis Research personnel and; (5) develop recommendations for Lear Jet and/or Space Shuttle experiments. Through this research, a mathematical model of two-phase systems is formulated and is being coded for the computer.

F.M.R.

N86-10164*# Illinois Univ., Urbana.

FLAMMABILITY LIMITS OF GASES UNDER LOW GRAVITY CONDITIONS

Roger A. Strehlow *In* NASA, Washington Microgravity Sci. and Appl. Program Tasks May 1985 p 186-187 refs (For primary document see N86-10053 01-12)

(Contract NAS3-23770)

Avail: NTIS HC A10/MF A01 CSCL 22A

The purpose of this combustion science investigation is to determine the effect of zero, fractional, and super gravity on the flammability limits of a premixed methane air flame in a standard 51 mm diameter flammability tube and to determine, if possible, the fluid flow associated with flame passage under zero-g conditions and the density (and hence, temperature) profiles associated with the flame under conditions of incipient extinction. This is accomplished by constructing an appropriate apparatus for placement in NASA's Lewis Research Center Lear Jet facility and flying the prescribed g-trajectories while the experiment is being performed. Data is recorded photographically using the visible light of the flame. The data acquired is: (1) the shape and propagation velocity of the flame under various g-conditions for methane compositions that are inside the flammable limits, and (2) the effect of gravity on the limits. Real time accelerometer readings for the three orthogonal directions are displayed in full view of the cameras and the framing rate of the cameras is used to measure velocities.

F.M.R.

N86-10165*# Princeton Univ., N. J.

FUNDAMENTAL STUDIES OF DROPLET COMBUSTION AT REDUCED GRAVITY

Forman A. Williams *In* NASA, Washington Microgravity Sci. and Appl. Program Tasks May 1985 p 188 (For primary document see N86-10053 01-12)

(Grant NAG3-380)

Avail: NTIS HC A10/MF A01 CSCL 22A

Reduced gravity is used to carry out scientific investigations of droplet combustion. In earlier work a preliminary conceptual design had been developed for droplet burning experiments for Spacelab. Refinements of the earlier work with special consideration given to possible experiments for Mid-Deck Modules of the Space Shuttle is discussed. A re-evaluation of suitable experiments on droplet combustion is done to ascertain whether influences of reduced buoyancy on time-dependent processes of heat and mass transfer in the gas or in the liquid on extinction processes or on disruptive burning phenomena are best suited for further investigation. Components of the experimental apparatus, which include a droplet dispensing system, a droplet positioning system, a droplet ignition system and provision for recording, primarily photographically, the combustion of the individual droplet in a chamber having a controlled gas atmosphere, are studied to determine optimal approaches to the experimental design. Methods for data reduction and interpretation are being made more specific, particularly in the context of an objective to calculate overall gas-phase chemical-kinetic parameters for the combustion from observations of extinction conditions in different atmospheres.

F.M.R.

N86-10166*# National Aeronautics and Space Administration. Marshall Space Flight Center, Huntsville, Ala.

DEVELOPMENT OF MATERIALS PROCESSING SYSTEMS FOR USE IN SPACE ON LOW-g SIMULATION DEVICES

B. R. Aldrich and W. D. Whitt *In* NASA, Washington Microgravity Sci. and Appl. Program May 1985 p 191 (For primary document see N86-10053 01-12)

Avail: NTIS HC A10/MF A01 CSCL 22A

Advanced furnace systems are being developed for use in space. Systems are being tested for current experiment applications and modified for future experiment requirements. Future projects are: (1) fabrication and testing of the Advanced Automated Directional Solidification Furnace (AADSF) flight hardware; (2) development of a Heat Pipe Furnace (HPF) for use in space. Heat pipes will be tested for space flight qualification in conjunction with the furnace development. The HPF design will be based on the AADSF development and will be of modular design including capabilities of operating with or without heat pipes; and (3) the AADSF furnace will be modified and tested to operate at temperatures up to 1700 C in the heated cavity. This will be accomplished by developing a new hot end heating module and insulation package for the existing AADSF. Refurbishment of the Drop Tower Furnace (DTF) is under way. The DTF can operate at temperatures up to 1700 C. The sample size will be approximately 3/8 in. dia. x 5/8 in. long. Design improvements for the General Purpose

Rocket Furnace (GPFR) for use in the Material Experiment Assembly (MEA) are to be accomplished. F.M.R.

N86-10167*# Jet Propulsion Lab., California Inst. of Tech., Pasadena.
MULTIMODE ACOUSTIC RESEARCH
Martin Barmatz *In* NASA, Washington Microgravity Sci. and Appl. Program Tasks May 1985 p 192 refs (For primary document see N86-10053 01-12)
(Contract NAS7-918)
Avail: NTIS HC A10/MF A01 CSCL 22A

There is a need for high temperature containerless processing facilities that can efficiently position and manipulate molten samples in the reduced gravity environment of space. The goal of the research is to develop sophisticated high temperature manipulation capabilities such as selection of arbitrary axes rotation and rapid sample cooling. This program will investigate new classes of acoustic levitation in rectangular, cylindrical and spherical geometries. The program tasks include calculating theoretical expressions of the acoustic forces in these geometries for the excitation of up to three acoustic modes (multimodes). These calculations are used to: (1) determine those acoustic modes that produce stable levitation, (2) isolate the levitation and rotation capabilities to produce more than one axis of rotation, and (3) develop methods to translate samples down long tube cylindrical chambers. Experimental levitators will then be constructed to verify the stable levitation and rotation predictions of the models. F.M.R.

N86-10168*# Bjorksten Research Labs., Inc., Madison, Wis.
CONTINUOUS FIBERIZATION OF SILICON-CARBIDE-NITRIDE PRECURSOR RESIN
Stanley A. Dunn *In* NASA, Washington Microgravity Sci. and Appl. Program Tasks May 1985 p 193 (For primary document see N86-10053 01-12)
(Contract NAS8-34648)
Avail: NTIS HC A10/MF A01 CSCL 22A

The objective of this project is to design and build a laboratory scale extruder and with it to fiberize 5000 continuous feet of silicon-carbide-nitride precursor resin. Subsequently the objective is extended to include the cross-linking and pyrolysis of approximately 100 feet of the resin fiber. The extruder is designed to accommodate approximately 1 cubic centimeter samples at accurately controllable rates corresponding to take-up from a single orifice of a 25 micron fiber at speeds in the 1000 feet/minute region. Positive feed delivery is achieved with a cylinder and piston driven by a geared down electric motor. Gear reduction is achieved primarily with off-the-shelf parts. Over 5000 feet of fiber, 20 to 30 micron diameter, are spun from precursor resin samples. The formation of continuous silicon carbide/silicon nitride fiber appears to be feasible. F.M.R.

N86-10169*# Bjorksten Research Labs., Inc., Madison, Wis.
LEVITATING FURNANCE FOR CONTAINERLESS PROCESSING IN SPACE
Stanley A. Dunn *In* NASA, Washington Microgravity Sci. and Appl. Program Tasks May 1985 p 194 (For primary document see N86-10053 01-12)
(Contract NAS8-33513)
Avail: NTIS HC A10/MF A01 CSCL 22A

The purpose of this project is to design, construct and test a levitator which would function reliably in a radiant heated cold wall furnace in a reduced gravity environment. A prototype levitating/positioning device termed the Sonic Pump Levitator is designed, built and successfuiiy tested in full gravity and in the reduced gravity of the parabolic flight regime of the KC-135. Positioning is achieved by timely and appropriate application of gas momentum from one or more of six sonic pumps. The sonic pumps, which are arranged orthogonally in opposed pairs about the levitation region, are activated by an electro-optical, computer controlled, feedback system. The Sonic Pump Levitator is a promising candidate for containerless processing in microgravity. Being a null point device, it imposes minimal perturbation on the levitated, or positioned, target. Functioning as it does by optical feedback controlled jets of air, it would be expected to be free from disturbance caused by high temperature. This expectation is now being examined experimentally. F.M.R.

N86-10170*# Bjorksten Research Labs., Inc., Madison, Wis.
ELECTRIC FIELD CONTAINERLESS PROCESSING TECHNOLOGY
D. D. Elleman and W. K. Rhim *In* NASA, Washington Microgravity Sci. and Appl. Program Tasks May 1985 p 195 refs (For primary document see N86-10053 01-12)
Avail: NTIS HC A10/MF A01 CSCL 22A

The objective of this task is to develop the science and technology base required to design and construct a high temperature electric field positioning module that could be used by materials scientists to conduct containerless science experiments in a low gravity environment. Containerless science modules that employ electric fields to position and manipulate samples offer several advantages over acoustic or electromagnetic systems. The electric field system will operate not only at atmospheric pressures but also in a vacuum, in contrast to the acoustic modules which can only operate in atmosphere where the acoustic forces are sufficient. The electric field technique puts minimum energy into the sample, whereas the electromagnetic system can deposit energy into the sample through eddy current heat as well as physical mixing in the sample. Two types of electric field modules have been constructed and tested to date. One employs a charged sample and uses electrostatic forces to position and control the sample. The second type of module induces electrical polarization of the sample and electric field gradients to position and control the sample. F.M.R.

N86-10171*# Stanford Univ., Calif. Lab. of Physics.
CRYOGENIC EQUIVALENCE PRINCIPLE EXPERIMENT
C. W. F. Everitt and Paul W. Worden *In* NASA, Washington Microgravity Sci. and Appl. Program Tasks May 1985 p 196-197 refs (For primary document see N86-10053 01-12)
Avail: NTIS HC A10/MF A01 CSCL 22A

The purpose of this project is to test the equivalence of inertial and passive gravitational mass in an Earth-orbiting satellite. A ground-based experiment is now well developed. It consists of comparing the motions of two cylindrical test masses suspended in precision superconducting magnetic bearings and free to move along the horizontal (axis) direction. The masses are made of niobium and lead-plated aluminum. A position detector based on a SQUID magnetometer measures the differential motion between the masses. The periods of the masses are matched by adjustment of the position detector until the system is insensitive to common mode signals, and so that the experiment is less sensitive to seismic vibration. The apparatus is contained in a twelve inch helium dewar suspended in a vibration isolation stand. The stand achieves 30 db isolation from horizontal motions between 0.1 and 60 Hz, by simulating the motion of a 200 meter long pendulum with an air bearing. With this attenuation of seismic noise and a common mode rejection ratio of 10 to the 5th power in the differential mode, the ground based apparatus should have a sensitivity to equivalence principle violations of one part in 10 to the 13th power; the satellite version might have a sensitivity of one part in 10 to the 17th power. F.M.R.

N86-10172*# General Electric Co., Philadelphia, Pa.
MODIFICATION OF THE ELECTROMAGNETIC LEVITATOR (EML) HARDWARE
R. T. Frost *In* NASA, Washington Microgravity Sci. and Appl. Program Tasks May 1985 p 198 (For primary document see N86-10053 01-12)
(Contract NAS8-34321)
Avail: NTIS HC A10/MF A01 CSCL 22A

The goals of this project are: (1) to study the upgrade requirements and approaches needed for incorporation of an Electromagnetic Levitator (EML) into the shuttle orbiter, (2) to work with members of the Electromagnetic Containerless Processing science working group (SWG) to define future experiments for the EML, and (3) to assist these investigators in further development

of ground-based experiment techniques to the limits possible in the terrestrial gravitational environment. Present work is directed toward: (1) upgrading the EML flight apparatus to meet requirements of safety and integration interfaces with the MSL orbiter carrier, (2) development of new experiment components required to carry out approved experiments in undercooled solidification and associated fluid flow studies directed by MIT, and (3) construction, test, qualification and integration assistance for the EML MSL flight package. Author

N86-10173*# National Aeronautics and Space Administration. Lewis Research Center, Cleveland, Ohio.
MICROGRAVITY MATERIALS SCIENCE LABORATORY
S. J. Grisaffe *In* NASA, Washington Microgravity Sci. and Appl. Program Tasks May 1985 p 199 (For primary document see N86-10053 01-12)
Avail: NTIS HC A10/MF A01 CSCL 22A

A Microgravity Materials Science Laboratory (MMSL) has been planned, designed, and is being developed. This laboratory will support related efforts to define the requirements for the Microgravity and Materials Processing Laboratory (MMPF) and the MMPF Test Bed for the Space Station. The MMSL will serve as a check out and training facility for science mission specialists for STS, Spacelab and Space Station prior to the full operation of the MMPF Test Bed. The focus of the MMSL will be on experiments related to the understanding of metal/ceramic/glass solidification, high perfection crystal growth and fluid physics. This ground-based laboratory will be used by university/industry/government researchers to examine and become familiar with the potential of new microgravity materials science concepts and to conduct longer term studies aimed at fully developing a l-g understanding of materials and processing phenomena. Such research will help create new high quality concepts for space experiments and will provide the basis for modeling, theories, and hypotheses upon which key space experiments can be defined and developed.
Author

N86-10174*# National Aeronautics and Space Administration. Marshall Space Flight Center, Huntsville, Ala.
ADVANCED OPTICAL MEASUREMENT TECHNIQUES
R. B. Owen, M. H. Johnston, and W. K. Witherow *In* NASA, Washington Microgravity Sci. and Appl. Program Tasks May 1985 p 200 (For primary document see N86-10053 01-12)
Avail: NTIS HC A10/MF A01 CSCL 22A

This research analyzes four areas: (1) Improved Techniques for Optical Measurement; (2) KC-135 Low Gravity Simulation Flight Preparation; (3) In-Line Holographic Microscopy; and (4) Holographic Optical Schlieren System (HOSS). The first task provides for laboratory breadboarding of advanced optical measurement techniques which appear promising for use in Material Processing System (MPS) flight experiments. A laboratory schlieren system has been constructed which simulates a similar optical system on the Fluids Experiment System (FES) which is to be flown on Spacelab 3. The second task allows improved optical systems and breadboards to be built for experiments and hardware tests on the KC-135 aircraft. A new, more stable Mach-Zehnder interferometer has been developed and components have been ordered. The third task is concerned with improvements on the optical system being used to study immiscible fluids. Experiments studying the dynamics of nucleation and the separation of immiscible fluids have been conducted. The four task involves building breadboard reconstruction systems for holograms taken in the HOSS. The HOSS is an early prototype of the Fluids Experiments System (FES) which is scheduled to fly on Spacelab 3. F.M.R.

N86-10175*# National Aeronautics and Space Administration. Marshall Space Flight Center, Huntsville, Ala.
DESIGN, FABRICATION AND TESTING OF AN EXPERIMENTAL APPARATUS FOR DETERMINING PARTICLE BEHAVIOR UNDER VERY LOW INTERGRANULAR STRESSES
Stein Sture and Nicholas Costes *In* NASA, Washington Microgravity Sci. and Appl. Program Tasks May 1985 p 201-202 (For primary document see N86-10053 01-12)
(Contract NAS8-35668)
Avail: NTIS HC A10/MF A01 CSCL 22A

Because the constitutive laws for soils are governed mainly by interparticle friction, all aspects of their mechanical behavior depend strongly on gravitational body forces. This fact poses serious limitations on the formulation of a materially objective soil constitutive theory, based on experimentation performed on Earth. In particular, the presence of the Earth's gravity prohibits the design of controlled experiments to properly simulate a variety of critical phenomena associated with the dynamic response of soils to seismic excitation in a very low effective confining stress field. For these reasons, laboratory-controlled experiments in the Space Shuttle, under essentially zero-gravity conditions, could offer invaluable opportunities for developing a quantitative understanding of fundamental aspects of soil behavior during or after an earthquake, which, in turn, could result in significant technological advances in geotechnical earthquake engineering. Author

N86-10176*# Jet Propulsion Lab., California Inst. of Tech., Pasadena.
ADVANCED CONTAINERLESS PROCESSING TECHNOLOGY
T. G. Wang *In* NASA, Washington Microgravity Sci. and Appl. Program Tasks May 1985 p 203 refs (For primary document see N86-10053 01-12)
Avail: NTIS HC A10/MF A01 CSCL 22A

Breadboards for high temperature containerless processing systems are to be developed, the principles of operation are to be studied, the performance is to be characterized, the limitations identified, and the influence of the acoustic field on the samples established. The subjects to be addressed are experimental and theoretical studies of: (1) acoustic positioning and manipulation capabilities in a high temperature gradient environment (from 26 C to 990 C); (2) acoustic waveforms, harmonic contents, power transfer, sample transport and stability associated with high temperature gradient system; (3) high temperature ground based levitation systems which will allow melting, processing, and solidifying samples without crucibles in the laboratory, (4) KC-135 and laboratory tests of various acoustic geometries which may have spherical applications in the Materials Processing in Space Program; and (5) provide technical information to Acoustics Containerless Experimental System (ACES) engineering team and establish the operation conditions for ACES. F.M.R.

N86-10177*# Intersonics, Inc., Northbrook, Ill.
ACOUSTIC LEVITATION CONTAINERLESS PROCESSING
R. R. Whymark and C. A. Rey *In* NASA, Washington Microgravity Sci. and Appl. Program Tasks May 1985 p 204 refs (For primary document see N86-10053 01-12)
(Contract NAS8-33742)
Avail: NTIS HC A10/MF A01 CSCL 22A

This research program consists of the development of acoustic containerless processing systems with applications in the areas of research in material sciences, as well as the production of new materials, solid forms with novel and unusual microstructures, fusion target spheres, and improved optical fibers. Efforts have been focused on the containerless processing at high temperatures for producing new kinds of glasses. Also, some development has occurred in the areas of containerlessly supporting liquids at room temperature, with applications in studies of fluid dynamics, potential undercooling of liquids, etc. The high temperature area holds the greatest promise for producing new kinds of glasses and ceramics, new alloys, and possibly unusual structural shapes, such as very uniform hollow glass shells for fusion target applications. High temperature acoustic levitation required for containerless processing has been demonstrated in low-g environments as well as in ground-based experiments. Future activities include continued development of the signals axis acoustic levitator. F.M.R.

N86-10178*# National Aeronautics and Space Administration. Johnson (Lyndon B.) Space Center,
HIGH-TEMPERATURE CONTROLLED REDOX CRYSTALLIZATION STUDIES

Richard J. Williams *In* NASA, Washington Microgravity Sci. and Appl. Program Tasks May 1985 p 205 (For primary document see N86-10053 01-12)
Avail: NTIS HC A10/MF A01 CSCL 22A

The crystallization of silicates containing redox sensitive ions (e.g., Fe, Ti, Ce) must be performed under controlled and known redox conditions in order to obtain the maximum scientific benefit from experimental study. Furthermore, many compositions crystallize dense phases which settle during ground-based experiments. This settling influences the texture and chemical evolution of the crystallizing system. The purpose of this investigation is to develop a test system in which controlled redox experiments can be performed in the microgravity environment. The system will use solid ceramic oxygen electrolyte cells for control, measurements, and production of the required redox conditions. A preliminary design for a prototype is developed, the electrolyte and furnace tested, and a tentative protocol for experiment developed. The control parameter is to be established and a laboratory prototype built. F.M.R.

N86-10179*# National Aeronautics and Space Administration, Washington, D. C.
PROJECT VESTA, EXPLORATORY MISSION TO THE ASTEROIDS: SCIENTIFIC OBJECTIVES AND TECHNICAL SPECIFICATIONS
Sep. 1985 13 p Transl. into ENGLISH of "Project VESTA, Interet Scientifique d'une Mission d'Exploration vers les Petits Corps" Paris, CNES, 1985 p 1-14 Transl. by The Corporate Word, Inc., Pittsburgh, Pa.
(Contract NASw-4006)
(NASA-TM-77669; NAS 1.15:77669) Avail: NTIS HC A02/MF A01 CSCL 22A

The VESTA project, a Franco-Soviet collaboration, is described. The VESTA probe will be launched and will pass through the asteroid belts before encountering comets. The probe will be an autonomous vehicle. The scientific objectives are to obtaining information on asteroids, comets, solar system formation, meteorites and other sources of extraterrestrial material. The surface morphology, mineral composition and internal structure of asteroids will be studied. E.A.K.

N86-10180# Bundesministerium fuer Forschung und Technologie, Bonn (West Germany).
SATELLITE USE FOR MEN [SATELLITENNUTZUNG FUER DEN MENSCHEN]
1985 39 p In GERMAN
Avail: NTIS HC A03/MF A01

Research satellites with German participation are listed. Satellite image maps for the Antartic region Neuschwaben land, for the Dodoma region in Tanzania, and for Upper Volta (Burkina) were made. Sondes to study trace gases in the atmosphere and the Earth radiation budget were developed. A modem for highly exact satellite position determination was developed. Large single protein crystals were grown in space. For individual titles, see N86-10181 through N86-10186.

N86-10181# Bundesministerium fuer Forschung und Technologie, Bonn (West Germany).
HOW ANTARCTICA WAS UNVEILED. MASTERPIECES OF FRANKFURT TOPOGRAPHIC SURVEYORS. A PART OF THE GERMAN ANTARCTICA RESEARCH PROGRAM [WIE DIE ANTARKTIS ENTSCHLEIERT WIRD. MEISTERSTUECKE FRANKFURTER ERDVERMESSER. EIN TEIL DES DEUTSCHEN ANTARKTIS-FORSCHUNGSPROGRAMMS] c43
Ruediger Jungblutth *In its* Satellite Use for Men 1985 p 5-10 In GERMAN (For primary document see N86-10180 01-12)
Avail: NTIS HC A03/MF A01

Satellite image maps for the Antartic region were produced, the most important of which is a 1:6 million map covering the Atlantic half of Antartic, made from NOAA and LANDSAT data. The way in which the digital satellite data were converted into analog representations is described. An optimal gray scale discrimination is obtained for the most important continental areas. Distortion effects are compensated by adding several pictures to a mosaic. Author (ESA)

N86-10182# Bundesministerium fuer Forschung und Technologie, Bonn (West Germany).
SATELLITE DATA EVEN FOR A POULTRY FARM. A DEVELOPMENT FOR TANZANIA. IMAGE EVALUATION FOLLOWING NEW WAYS [SATELLITENDATEN SELBST FUER EINE HUEHNERFARM. EIN ENTWICKLUNGSPROJEKT FUER TANSANIA. BILDAUSWERTUNG AUF NEUEN WEGEN] c43
Philip Erdoes *In its* Satellite Use for Men 1985 p 11-16 In GERMAN (For primary document see N86-10180 01-12)
Avail: NTIS HC A03/MF A01

Maps of the 11,000 sq km Dodoma region in Tanzania were made using LANDSAT-3 data. Multispectral scanner data were processed using Intensity-Saturation color theory. The intensity gives information about the relief. The ratio images give information about the type of soil and vegetation. A classification of 14 geographically homogeneous land units, and a ground water map were made. Author (ESA)

N86-10183# Bundesministerium fuer Forschung und Technologie, Bonn (West Germany).
WITH ARGUS EYES FROM SPACE. SATELLITE DIAGNOSIS FOR UPPER VOLTA. SEVEN MAPS WITHOUT MYSTERY [MIT ARGUSAUGEN AUS DEM ALL. SATELLITEN-DIAGNOSE FUER OBERVOLTA. SIEBEN KARTEN OHNE SIEBEN SIEGEL] c43
Uwe Andresen *In its* Satellite Use for Men 1985 p 17-21 In GERMAN (For primary document see N86-10180 01-12)
Avail: NTIS HC A03/MF A01

Maps of Upper Volta (Burkina) were made using LANDSAT images. It is shown that the interpretation of satellite data is by far superior to any other method if these interpretations are checked in situ by sampling tests. Maps giving information on geology, soil science, land use, and hydrogeology were made. A map which provides detailed information about settlement density, cultivation possibilities of the soil, and ground water expectations is discussed. The results show substantial perturbations of the vegetation structure due to extended livestock and agricultural methods such as overgrazing, uncontrolled deforestation, and burnt cleared land. Author (ESA)

N86-10184# Bundesministerium fuer Forschung und Technologie, Bonn (West Germany).
THE AIR OF LIFE OF THE BLUE PLANET. ATMOSPHERE RESEARCH FROM SPACE USING DATA AND FACTS AGAINST CLIMATE SPECULATIONS [DIE LEBENSLUFT DES BLAUEN PLANETEN. ATMOSPHAERENFORSCHUNG VOM WELTRAUM AUS DATEN UND FAKTEN GEGEN KLIMA-SPEKULATIONEN] c47
Dieter Schwab *In its* Satellite Use for Men 1984 p 22-25 In GERMAN (For primary document see N86-10180 01-12)
Avail: NTIS HC A03/MF A01

Three satellite-borne sondes to provide exact data on trace gases in the atmosphere between 20 and 100 km height, and on the Earth radiation budget are described. The sondes predict changes in the climate due to trace gases and the reduction of the ozone concentration. The Michelson Interferometer for Passive Atmospheric Sounding analyzes the light spectrum and is based on interference phenomena. The Microwave Atmospheric Sounder analyzes the characteristic electromagnetic waves emitted by trace gases. The Conical Scan Radiometer CSR measures the sunlight on Earth as well as the heat radiation from the Earth in several directions. Author (ESA)

N86-10185# Bundesministerium fuer Forschung und Technologie, Bonn (West Germany).
A NANOSECOND OR THIRTY CENTIMETERS: WHY ATOMIC CLOCKS HAVE TO BE SYNCHRONIZED. MITREX OPENS NEW

DIMENSIONS FOR MEASURING ACCURACY [EINE MILLIARDSTELSEKUNDE ODER 30 ZENTIMETER: WESHALB ATOMUHREN WELTWEIT GLEICHLAUFEN MUESSEN. MITREX OEFFENT NEUE DIMENSIONEN DER MESSGENAUIGKEIT] **c35**

Hans-Dieter Wolz *In its* Satellite Use for Men 1985 p 26-29 In GERMAN (For primary document see N86-10180 01-12)
Avail: NTIS HC A03/MF A01

Microwave Time and Ranging Experiment was developed to enable highly exact satellite position determination. The measurement is performed in ground stations. The portable system allows position measurements with an accuracy as high as 30 cm, and is planned to be long term tested in order to be introduced as a standard. The required signal strength is very low. The processing of the electromagnetic signals allows reliable statements about the time of flight and about perturbations. The application possibilities of the MITREX-system are presented. Author (ESA)

N86-10186# Bundesministerium fuer Forschung und Technologie, Bonn (West Germany).
GROWTH OF LARGER SINGLE CRYSTALS [ZUECHTUNG VON GROESSEREN EINKRISTALLEN] **c76**

Ruediger Jungbluth *In its* Satellite Use for Men 1985 p 30-32 In GERMAN (For primary document see N86-10180 01-12)
Avail: NTIS HC A03/MF A01

Large single protein crystals were grown during the Spacelab 1 flight in order to study metabolism phenomena. For X-ray structural analysis the single crystals have to be sufficiently large (about 1 mm in all 3 directions). The crystals grown under weightlessness conditions (excluding convection effects) in a few minutes are comparable to those grown on Earth after several days. Two model proteins were grown: the high-molecular enzyme beta-galactosidasis and the low-molecular enzyme lysozyme. The testing of a large number of protein species is necessary in order to allow a definitive prognosis about this technique. Author (ESA)

N86-10187# Deutsche Forschungs- und Versuchsanstalt fuer Luft- und Raumfahrt, Cologne (West Germany).
THE FIRST GERMAN SPACELAB MISSION D1 REPORTS Progress Report [ERSTE DEUTSCHE SPACELAB-MISSION D1-REPORT]
Oct. 1984 4 p In GERMAN
(PR-1) Avail: NTIS HC A02/MF A01

The Spacelab mission; Spacelab specifications and technical concept; Spacelab history, and scheduling from December 1984 to October 1985 are discussed. Author (ESA)

N86-10188# Deutsche Forschungs- und Versuchsanstalt fuer Luft- und Raumfahrt, Cologne (West Germany).
THE FIRST GERMAN SPACELAB MISSION D1 REPORTS Progress Report [ERSTE DEUTSCHE SPACELAB-MISSION D1-REPORT]
Dec. 1984 8 p In GERMAN
(PR-2) Avail: NTIS HC A02/MF A01

Spacelab D1 payload integration; aerospace medicine in weightlessness; process technology; NAVEX program: Earth observation, communication and navigation; project management; the environmental control and life support systems; the MEDEA, Biorack payloads; and the Mirror heating facility are discussed. Author (ESA)

N86-10189# Deutsche Forschungs- und Versuchsanstalt fuer Luft- und Raumfahrt, Cologne (West Germany).
THE FIRST GERMAN SPACELAB MISSION D1 REPORTS Progress Report [ERSTE DEUTSCHE SPACELAB-MISSION D1-REPORT]
Feb. 1985 7 p In GERMAN
(PR-3) Avail: NTIS HC A02/MF A01

Astronaut preparation with the Spacelab training simulator; project planning for the Columbus and Ariane 5 programs; the D1 - Transport platforms: a 4 m wide and 6.5 m long special container for integral payload transport; milestones of the European space programs since 1969; and opinions against manned space flights are discussed. Author (ESA)

N86-10209# Hamburg Univ. (West Germany).
INFLUENCES AFFECTING SEPARATION IN MONOTECTIC ALLOYS UNDER MICROGRAVITY
H. Ahlborn and K. Loehberg (Technische Univ., Berlin) *In* ESA Fifth European Symp. on Mater. Sci. under Microgravity. Results of Spacelab 1 Dec. 1984 p 55-61 refs (For primary document see N86-10200 01-16)
Avail: NTIS HC A21/MF A01

N86-10210# Max-Planck-Inst. fuer Metallforschung, Stuttgart (West Germany).
PARTICLE COARSENING IN IMMISCIBLE ZINC-LEAD ALLOYS UNDER MICROGRAVITY
A. Kneissel (Montanuniv. Leoban, Austria) and H. Fischmeister *In* ESA Fifth European Symp. on Mater. Sci. under Microgravity. Results of Spacelab 1 Dec. 1984 p 63-68 refs Sponsored by Austrian Ministry of Science and Research (For primary document see N86-10200 01-16)
Avail: NTIS HC A21/MF A01

N86-10211# Katholieke Universiteit te Leuven (Belgium). Dept. Metaalkunde und Toegepaste Materiaalkunde.
MELTING AND SOLIDIFICATION OF METAL MATRIX COMPOSITES UNDER MICROGRAVITY
L. Froyen and A. Deruyttere *In* ESA Fifth European Symp. on Mater. Sci. under Microgravity. Results of Spacelab 1 Dec. 1984 p 69-78 refs (For primary document see N86-10200 01-16)
Avail: NTIS HC A21/MF A01

N86-10212# Technische Hogeschool, Delft (Netherlands). Dept. of Metals Science.
UNIDIRECTIONAL SOLIDIFICATION OF CAST IRON: EXPERIMENT ES-325
H. Nieswaag, T. Luyendijk, and W. H. M. Alsem *In* ESA Fifth European Symp. on Mater. Sci. under Microgravity. Results of Spacelab 1 Dec. 1984 p 79-85 refs Sponsored by Netherlands State Department (For primary document see N86-10200 01-16)
Avail: NTIS HC A21/MF A01

N86-10213# Maschinenfabrik Augsburg-Nuernberg A.G., Munich (West Germany).
SKIN CASTING OF ALLOYS AND COMPOSITES: RESULTS OF SPACELAB (SL)-1 AND TEXUS EXPERIMENTS
H. Sprenger *In* ESA Fifth European Symp. on Mater. Sci. under Microgravity. Results of Spacelab 1 Dec. 1984 p 87-94 refs Sponsored by Bundesministerium fuer Forschung und Technologie (For primary document see N86-10200 01-16)
Avail: NTIS HC A21/MF A01

N86-10214# Technische Univ., Vienna (Austria).
VACUUM BRAZING UNDER MICROGRAVITY
K. Frieler, R. Stickler (Bundesanstalt fuer Materialpruefung.), and E. Siegfried *In* ESA Fifth European Symp. on Mater. Sci. under Microgravity. Results of Spacelab 1 Dec. 1984 p 95-99 refs (For primary document see N86-10200 01-16)
Avail: NTIS HC A21/MF A01

N86-10215# Bologna Univ. (Italy). Dipt. di Fisica.
MELTING AND SOLIDIFICATION IN O-g OF SINTERED ALLOYS: EXPERIMENTS ES 311 A AND B BUBBLE REINFORCED MATERIALS
F. Barbier, C. Patuelli, P. Gonndi (Rome Univ.), and R. Montanari (Rome Univ.) *In* ESA Fifth European Symp. on Mater. Sci. under Microgravity. Results of Spacelab 1 Dec. 1984 p 101-107 refs (For primary document see N86-10200 01-16)
Avail: NTIS HC A21/MF A01

N86-10216# Technische Univ., Clausthal-Zellerfeld (West Germany). Arbeitsgruppe Glas.
INTERDIFFUSION IN THE GLASS MELT SYSTEM (Na_2O+Rb_2O) .$3SiO_2$
M. Braedt, V. Braetsch, and G. H. Frischat *In* ESA Fifth European Symp. on Mater. Sci. under Microgravity. Results of Spacelab 1 Dec. 1984 p 109-112 refs Sponsored by Bundesministerium fuer Forschung und Technologie (For primary document see N86-10200 01-16)
Avail: NTIS HC A21/MF A01

N86-10218# Commissariat a l'Energie Atomique, Grenoble (France). Dept. de Metallurgie.
DIRECTIONAL SOLIDIFICATION OF AN ALUMINUM-ZINC VAPOR EMULSION IN MICROGRAVITY
C. Potard and P. Morgand *In* ESA Fifth European Symp. on Mater. Sci. under Microgravity. Results of Spacelab 1 Dec. 1984 p 121-125 (For primary document see N86-10200 01-16)
Avail: NTIS HC A21/MF A01

N86-10219# Commissariat a l'Energie Atomique, Grenoble (France). Dept. de Metallurgie.
DIRECTIONAL SOLIDIFICATION OF EUTECTIC ALLOYS
J. J. Favier and J. deGoer *In* ESA Fifth European Symp. on Mater. Sci. under Microgravity. Results of Spacelab 1 Dec. 1984 p 127-133 refs (For primary document see N86-10200 01-16)
Avail: NTIS HC A21/MF A01

N86-10220# Centre National de la Recherche Scientifique, Meudon-Bellevue (France). Equipe de Technologie de la Croissance Cristalline.
LEAD TELLURIDE CRYSTALS GROWN IN MICROGRAVITY: EXPERIMENT ES 318 [CRISTAUX DE TELLURURE DE PLOMB ELABORES EN MICROGRAVITE EXPERIENCE ES 318]
H. Rodot and O. Tottereau *In* ESA Fifth European Symp. on Mater. Sci. under Microgravity. Results of Spacelab 1 Dec. 1984 p 135-139 refs In FRENCH (For primary document see N86-10200 01-16)
Avail: NTIS HC A21/MF A01

N86-10221# Erlangen-Nuremberg Univ. (West Germany). Inst. fuer Werkstoffwissenschaften.
DIRECTIONAL SOLIDIFICATION OF InSb-NiSb EUTECTIC
G. Mueller and P. Kyr *In* ESA Fifth European Symp. on Mater. Sci. under Microgravity. Results of Spacelab 1 Dec. 1984 p 141-146 refs Sponsored by DFVLR and Bundesministerium fuer Forschung und Technologie (For primary document see N86-10200 01-16)
Avail: NTIS HC A21/MF A01

N86-10222# Commissariat a l'Energie Atomique, Grenoble (France). Dept. de Metallurgie.
THERMOMIGRATION OF COBALT IN LIQUID TIN: EXPERIMENT 1 ES 320
Y. Malmejac and J. P. Praizey *In* ESA Fifth European Symp. on Mater. Sci. under Microgravity. Results of Spacelab 1 Dec. 1984 p 147-152 refs (For primary document see N86-10200 01-16)
Avail: NTIS HC A21/MF A01

N86-10224# Stuttgart Univ. (West Germany). Inst. fuer Physikalisches.
GaSb-SEMICONDUCTOR CRYSTALS UNDER MICROGRAVITY: EXPERIMENT ES 323
K. W. Benz and G. Nagel *In* ESA Fifth European Symp. on Mater. Sci. under Microgravity. Results of Spacelab 1 Dec. 1984 p 157-161 refs (For primary document see N86-10200 01-16) (Contract DFVLR-01-QV-698)
Avail: NTIS HC A21/MF A01

N86-10225# Freiburg Univ. (West Germany). Inst. fuer Kristollographisches.
SOLUTION GROWTH OF CADMIUM TELLURIDE: EXPERIMENT ES 322
R. Schoenholz, R. Dian, and R. Nitsche *In* ESA Fifth European Symp. on Mater. Sci. under Microgravity. Results of Spacelab 1 Dec. 1984 p 163-167 refs Sponsored by Bundesministerium fuer Forschung und Technologie (For primary document see N86-10200 01-16)
Avail: NTIS HC A21/MF A01

N86-10226# Wacker-Chemie G.m.b.H. Burghausen (West Germany).
CRYSTALLIZATION OF A SILICON SPHERE
H. Koelker *In* ESA Fifth European Symp. on Mater. Sci. under Microgravity. Results of Spacelab 1 Dec. 1984 p 169-172 refs (For primary document see N86-10200 01-16)
Avail: NTIS HC A21/MF A01

N86-10227# Freiburg Univ. (West Germany). Inst. fuer Kristollographisches.
CRYSTAL GROWTH OF SILICON IN SPACELAB 1: EXPERIMENT ES-321
A. Eyer, H. Leiste, and R. Nitsche *In* ESA Fifth European Symp. on Mater. Sci. under Microgravity. Results of Spacelab 1 Dec. 1984 p 173-182 refs (For primary document see N86-10200 01-16)
Avail: NTIS HC A21/MF A01

N86-10228# Freiburg Univ. (West Germany). Chemisches Lab.
PROTEIN SINGLE CRYSTAL GROWTH UNDER MICROGRAVITY
W. Littke and C. John *In* ESA Fifth European Symp. on Mater. Sci. under Microgravity. Results of Spacelab 1 Dec. 1984 p 185-188 refs Original language document previously announced as A85-39084 Sponsored by Bundesministerium fuer Forschung und Technologie (For primary document see N86-10200 01-16)
Avail: NTIS HC A21/MF A01

N86-10229# Technical Univ. of Denmark, Lyngby. Physics Lab. 3.
CRYSTAL GROWTH FROM SOLUTION
G. Galster and K. F. Nielsen *In* ESA Fifth European Symp. on Mater. Sci. under Microgravity. Results of Spacelab Dec. 1984 p 189-191 refs Sponsored by Danish Space Board (For primary document see N86-10200 01-16)
Avail: NTIS HC A21/MF A01

N86-10230# Paris VI Univ. (France). Lab. de Mineralogie et Cristallographie.
GROWTH AND CHARACTERIZATION OF BRUSHITE AND LEAD MONETITE, SIMULATION AND RESULTS
M. C. Robert, F. Lefaucheux, and A. Authier *In* ESA Fifth European Symp. on Mater. Sci. under Microgravity. Results of Spacelab 1 Dec. 1984 p 193-199 refs Sponsored by CNES (For primary document see N86-10200 01-16)
Avail: NTIS HC A21/MF A01

N86-10231# Technische Univ., Berlin (West Germany). Inst. fuer Metallforschung.
SELF DIFFUSION OF Sn112 AND Sn124 IN LIQUID TIN
G. Frohberg, K.-H. Kraatz, and H. Wever *In* ESA Fifth European Symp. on Mater. Sci. under Microgravity. Results of Spacelab 1 Dec. 1984 p 201-205 refs (For primary document see N86-10200 01-16)
Avail: NTIS HC A21/MF A01

N86-10232# Politecnico di Milano (Italy).
ADHESION OF METALS: EXPERIMENT 1 ES-340
F. Rossitto and G. Ghersini (Centro Informazioni Studi Esperienze) *In* ESA Fifth European Symp. on Mater. Sci. under Microgravity. Results of Spacelab 1 Dec. 1984 p 207-217 refs Sponsored by CNR (For primary document see N86-10200 01-16)
Avail: NTIS HC A21/MF A01

N86-10233*# Harvard Univ., Cambridge, Mass. Div. of Applied Sciences.
CRYSTAL NUCLEATION AND GLASS FORMATION IN METALLIC ALLOY MELTS
F. Spaepen *In* ESA Fifth European Symp. on Mater. Sci. under Microgravity. Results of Spacelab 1 Dec. 1984 p 215-219 refs (For primary document see N86-10200 01-16)

(Contract NAS8-36516)
Avail: NTIS HC A21/MF A01

N86-10234*# Massachusetts Inst. of Tech., Cambridge.
CRYSTAL GROWTH OF GaAs IN SPACE
H. C. Gatos, J. Lagowski, L. M. Pawlowicz, F. Dabkowski, and C.-J. Li *In* ESA Fifth European Symp. on Mater. Sci. under Microgravity. Results of Spacelab 1 Dec. 1984 p 221-225 refs (For primary document see N86-10200 01-16)
Avail: NTIS HC A21/MF A01

N86-10236# Academy of Sciences (USSR), Moscow. Inst. for Problems in Mechanics.
MATHEMATICAL SIMULATION OF DISTURBING FORCES AND MATERIAL SCIENCE PROCESSES UNDER LOW GRAVITY
V. I. Polezhaev, A. P. Lebedev, and S. A. Nikitin *In* ESA Fifth European Symp. on Mater. Sci. under Microgravity. Results of Spacelab 1 Dec. 1984 p 237-243 refs (For primary document see N86-10200 01-16)
Avail: NTIS HC A21/MF A01

N86-10246*# National Aeronautics and Space Administration. Marshall Space Flight Center, Huntsville, Ala. Space Science Lab.
SEPARATION OF AQUEOUS TWO-PHASE POLYMER SYSTEMS IN MICROGRAVITY
J. M. VanAlstine, J. M. Harris (Alabama Univ., Huntsville), S. Synder, P. A. Curreri, S. B. Bamberger (Oregon Health Sciences Univ.), and D. E. Brooks (Oregon Health Sciences Uni.) *In* ESA Fifth European Symp. on Mater. Sci. under Microgravity. Results of Spacelab 1 Dec. 1984 p 309-312 refs Sponsored by Universities Space Research Association (For primary document see N86-10200 01-16)
(Contracts NAS8-35333; NAS8-35334; NAS8-35362)
Avail: NTIS HC A21/MF A01 CSCL 22A

N86-10247*# National Aeronautics and Space Administration. Marshall Space Flight Center, Huntsville, Ala. Dept. of Pathology and Chemistry.
RATIONALE FOR TWO PHASE POLYMER SYSTEM MICROGRAVITY SEPARATION EXPERIMENTS
D. E. Brooks (British Columbia Univ.), S. B. Bamberger (Oregon Health Sciences Univ.), J. M. Harris (Alabama Univ., Huntsville), and J. VanAlstine *In* ESA Fifth European Symp. on Mater. Sci. under Microgravity. Results of Spacelab 1 Dec. 1984 p 315-318 refs Sponsored in part by NASA (For primary document see N86-10200 01-16)
(Grant USPN-HL-23374)
Avail: NTIS HC A21/MF A01 CSCL 22A

N86-10248# Alabama Univ., Huntsville. Dept. of Chemistry.
APPLICATION OF THE THEORY OF OSTWALD RIPENING TO MICROGRAVITY PHASE SEPARATION EXPERIMENTS
J. K. Baird *In* ESA Fifth European Symp. on Mater. Sci. under Microgravity. Results of Spacelab 1 Dec. 1984 p 319-321 refs Sponsored by Alabama University (For primary document see N86-10200 01-16)
Avail: NTIS HC A21/MF A01

N86-10254# Technische Univ., Clausthal-Zellerfeld (West Germany). Inst. fuer Nichtmetallische Werkstoffe.
SHRINKING OF A GAS BUBBLE IN A GLASS MELT UNDER MICROGRAVITY CONDITIONS
V. Rosenkranz and G. H. Frischat *In* ESA Fifth European Symp. on Mater. Sci. under Microgravity. Results of Spacelab 1 Dec. 1984 p 353-357 refs Sponsored by Bundesministerium fuer Forschung und Technologie (For primary document see N86-10200 01-16)
Avail: NTIS HC A21/MF A01

N86-10255# Technische Univ., Munich (West Germany).
PHYSICAL AND CHEMICAL PROPERTIES OF A NICKEL CATALYST PROCESSED UNDER MICROGRAVITY
H. Riepl *In* ESA Fifth European Symp. on Mater. Sci. under Microgravity. Results of Spacelab 1 Dec. 1984 p 359-363 refs (For primary document see N86-10200 01-16)
Avail: NTIS HC A21/MF A01

N86-10256# Royal Inst. of Tech., Stockholm (Sweden). Dept. of Casting Metals.
A PRELIMINARY REPORT ON FLOATING ZONE EXPERIMENTS WITH GERMANIUM CRYSTALS IN A SOUNDING ROCKET
T. Carlberg *In* ESA Fifth European Symp. on Mater. Sci. under Microgravity. Results of Spacelab 1 Dec. 1984 p 367-373 refs (For primary document see N86-10200 01-16)
Avail: NTIS HC A21/MF A01

N86-10257# Deutsche Forschungs- und Versuchsanstalt fuer Luft- und Raumfahrt, Cologne (West Germany). Inst. for Space Simulation.
TRANSPORT PROCESSES IN DIRECTIONAL SOLIDIFICATION DURING SPACE SHUTTLE FLIGHT
H. Klein, R. Naehle, and K. Wanders *In* ESA Fifth European Symp. on Mater. Sci. under Microgravity. Results of Spacelab 1 Dec. 1984 p 375-378 refs (For primary document see N86-10200 01-16)
Avail: NTIS HC A21/MF A01

N86-10258# Deutsche Forschungs- und Versuchsanstalt fuer Luft- und Raumfahrt, Cologne (West Germany). Inst. for Space Simulation.
STABILITY OF METALLIC DISPERSIONS
H. Otto *In* ESA Fifth European Symp. on Mater. Sci. under Microgravity. Results of Spacelab 1 Dec. 1984 p 379-388 refs (For primary document see N86-10200 01-16)
Avail: NTIS HC A21/MF A01

N86-10259# Deutsche Forschungs- und Versuchsanstalt fuer Luft- und Raumfahrt, Cologne (West Germany). Inst. for Space Simulation.
UNDERCOOLING INVESTIGATIONS ON THE EASY GLASS FORMER Pd-Cu-Si
D. M. Herlach, R. Willnecker, and F. Gillessen *In* ESA Fifth European Symp. on Mater. Sci. under Microgravity. Results of Spacelab 1 Dec. 1984 p 389-397 refs (For primary document see N86-10200 01-16)
Avail: NTIS HC A21/MF A01

N86-10260# Deutsche Forschungs- und Versuchsanstalt fuer Luft- und Raumfahrt, Cologne (West Germany). Inst. for Space Simulation.
CONTAINERLESS UNDERCOOLING OF Ni
D. M. Herlach, R. Willnecker, and F. Gillessen *In* ESA Fifth European Symp. on Mater. Sci. under Microgravity. Results of Spacelab 1 Dec. 1984 p 399-402 refs (For primary document see N86-10200 01-16)
Avail: NTIS HC A21/MF A01

N86-10261*# National Aeronautics and Space Administration. Lewis Research Center, Cleveland, Ohio.
DENDRITIC SOLIDIFICATION IN A BINARY ALLOY MELT: STEADY-STATE VERSUS MORPHOLOGICAL STABILITY THEORIES
V. Laymanan *In* ESA Fifth European Symp. on Mater. Sci. under Microgravity. Results of Spacelab 1 Dec. 1984 p 403-407 refs Sponsored in part by NASA (For primary document see N86-10200 01-16)
Avail: NTIS HC A21/MF A01

N86-10262# Commissariat a l'Energie Atomique, Grenoble (France). Lab. d'Etude de la Solidification.
CELLULAR MORPHOLOGIES IN LEAD-THALLIUM ALLOYS
B. Billia (Faculte des Sciences St-Jerome, Marseille), H. Jamgotchian (Faculte des Sciences St.-Jerome, Marseille), J. J. Favier, and D. Camel *In* ESA Fifth European Symp. on Mater. Sci. under Microgravity. Results of Spacelab 1 Dec. 1984 p 409-412 refs Sponsored by CNES (For primary document see N86-10200 01-16)
Avail: NTIS HC A21/MF A01

N86-10264*# Gelles (S. H.) Associates, Columbus, Ohio.
SPACE SHUTTLE EXPERIMENTS ON Al-In LIQUID PHASE

MISCIBILITY GAP (LPMG) ALLOYS
S. H. Gelles and A. J. Markworth (Battelle Columbus Labs., Columbus) *In* ESA Fifth European Symp. on Mater. Sci. under Microgravity. Results of Spacelab 1 Dec. 1984 p 417-422 refs (For primary document see N86-10200 01-16)
(Contract NAS8-32952)
Avail: NTIS HC A21/MF A01

N86-10267# Eidgenoessische Technische Hochschule, Zurich (Switzerland).
CRYSTAL GROWTH FROM SOLUTIONS AND NUCLEATION FROM THE VAPOR PHASE
E. Kaldis *In* ESA Fifth European Symp. on Mater. Sci. under Microgravity. Results of Spacelab 1 Dec. 1984 p 439-441 refs (For primary document see N86-10200 01-16)
Avail: NTIS HC A21/MF A01

N86-10396*# Jet Propulsion Lab., California Inst. of Tech., Pasadena. TDA Planning Office.
A VLA EXPERIMENT: PLANNING FOR VOYAGER AT NEPTUNE
J. W. Layland, P. J. Napier (National Radio Astronomy Observatory), and A. R. Thompson (National Radio Astronomy Observatory) *In its* The Telecommun. and Data Acquisition Progr. Rept. 15 Aug. 1985 p 136-142 refs (For primary document see N86-10382 01-32)
Avail: NTIS HC A10/MF A01 CSCL 22A

13 ASTRODYNAMICS

Includes powered and free-flight trajectories; and orbit and launching dynamics.

N86-10190# Royal Aircraft Establishment, Farnborough (England).
LUMPED GEOPOTENTIAL HARMONICS OF ORDER 14, FROM THE ORBIT OF 1967-11G
D. G. King-Hele Jan. 1985 20 p
(AD-A156627; RAE-TR-85002; DRIC-BR-95198) Avail: NTIS HC A02/MF A01 CSCL 08/5

The satellite 1967-11G, which had an orbital inclination of 40 deg, passed through 14th-order resonance with the Earth's gravitational field in 1974. The changes in its orbital inclination at resonance were analyzed to obtain values for four lumped 14th-order harmonics in the geopotential, with accuracies equivalent to about 5 cm in geoid height. Analysis of the eccentricity was also attempted, but did not yield useful results. As no previous satellite analyzed at 14th-order resonance has had an inclination near 40 deg., the results have proved to be valuable in determining individual 14th-order harmonics in the geopotential. GRA

14 GROUND SUPPORT SYSTEMS AND FACILITIES (SPACE)

Includes launch complexes, research and production facilities; ground support equipment, e.g., mobile transporters; and simulators.

For related information see also *09 Research Support Facilities (Air).*

N86-10191# Armament Development and Test Center, Eglin AFB, Fla.
DYNAMIC ANALYSIS OF A SLED TRAVELING ALONG A ROUGH RAIL Final Report, Nov. 1983 - May 1985
G. L. Ferguson 15 May 1985 317 p
(AF Proj. TKSI)
(AD-A156589; AD-TR-85-39) Avail: NTIS HC A14/MF A01 CSCL 12/1

Rocket sleds are commonly used for simulation of special environments for testing purposes. The motion of a sled on the track induces large quasi-steady-state and dynamic forces on the sled. Design of sleds requires knowledge of these forces and of established techniques for application of measured and theoretical forcing functions to proven mathematical structural simulations. The prediction of the quasi-steady-state sled loads is relatively straight-forward and requires few specialized techniques. Dynamic force prediction on the other hand is somewhat of a black art. Several techniques have been theorized but the results have been extremely marginal at best. This research is intended to find a reliable force prediction tool that is not extremely cumbersome to use. GRA

N86-10192# Sandia Labs., Albuquerque, N. Mex.
LASER GENERATION AND TRANSPORT OF A RELATIVISTIC ELECTRON BEAM
S. L. Shope, C. A. Frost, G. T. Leifeste, C. E. Crist, P. D. Kiekel, J. W. Poukey, and B. B. Godfrey 1985 14 p Presented at the Particle Accelerator Conf., Vancouver, British Columbia, 13 May 1985 Prepared in cooperation with Mission Research Corp., Albuquerque, N. Mex.
(Contract DE-AC04-76DP-00789)
(DE85-011709; SAND-85-0042C; CONF-850504-30) Avail: NTIS HC A02/MF A01

A foilless diode usually requires an externally applied magnetic field to control expansion and transport of a relativistic electron beam. A new foilless diode was developed that does not require an external magnetic field. A low pressure organic gas is introduced into the diode and the transport region. A UV laser beam is injected through the transport region and is terminated at the cathode. The laser photoionizes the low pressure gas forming an ionized channel that captures the electron beam near the cathode. The electron beam is focused and guided by electrostatic attraction to the ionized channel. A 1.5-MeV, 20-kA electron beam was generated and transported 1 m using this technique. The laser is replaced by an 800 V, 250 ma, low energy electron beam which is used to guide the relativistic electron beam 4 m through a 90 bend. E.A.K.

N86-10193# Virginia Univ., Charlottesville. Dept. of Materials Science.
SIMULATING THE CTR ENVIRONMENT IN THE HVBM Final Report, 1 Sep. 1975 - 31 Aug. 1984
W. A. Jesser 1984 18 p
(Contract DE-AS05-76ET-52023)
(DE85-011745; DOE/ET-52023/34) Avail: NTIS HC A02/MF A01

The first high voltage electron microscope-ion accelerator facility in the world was established in 1976. Through use of this facility, helium embrittlement as revealed through intergranular fracture was shown to be independent of helium bubble content in the grain boundaries. This result is contrary to most current thinking and theories of helium embrittlement. The most likely mechanism of helium embrittlement is a plastic deformation assisted distribution of helium in finely dispersed helium-vacancy clusters. The key to overcoming helium embrittlement should lie in preventing the fine dispersion by providing benign sinks or treatments that agglomerate the helium. DOE

N86-10194# Kanner (Leo) Associates, Redwood City, Calif.
RFQ-FUNNELING
A. Schempp 1985 11 p Transl. into ENGLISH of rept. Int. Rep. 85-6 Inst. fuer Angewandte Physik der Univ. Frankfurt/Main, Feb. 1985 Prepared for LASL
(Contract W-7405-eng-36)
(DE85-012483; LA-tr-85-21) Avail: NTIS HC A02/MF A01

Funneling which is the joining of beams in a zipper arrangement while doubling the frequency to increase the beam current, to utilize the acceptance of the linear accelerator even at the higher frequency is discussed. Funneling is necessary to obtain higher current, higher brilliance. No experiments were conducted although it is one of the prerequisites for the realization of this high current accelerator. Several divergent ideas on funneling are compiled and presented. DOE

N86-10195# Sandia Labs., Albuquerque, N. Mex.
COMPACT, LOW JITTER, TRIGGERED SPARK GAP
W. K. Tucker, E. E. Jones, T. L. Franklin, I. F. Bennett, and G. Reber 10 Jun. 1985 4 p Presented at the 5th IEEE Pulsed Power Conf., Washington, D.C., 10 Jun. 1985
(Contract DE-AC04-76DP-00789)
(DE85-012812; SAND-84-2395C; CONF-850616-18) Avail: NTIS HC A02/MF A01

High energy particle accelerators using compact, high gradient cavities will require small, highly reliable, triggered spark gaps. This paper will discuss the design and development of V/N triggered spark gaps operating from 520 kV to 1280 kV. Spark gap jitter of < ns has been obtained with trigger voltages of 60 kV. Capacitively balancing the trigger blade electrode, coupled with a trigger voltage rise time of 10 ns, produces three or more arcs across the main electrode gaps. A 2.3 (UC OMEGA) injector using 12 parallel spark gaps operating at 1280 kV has been successfully tested. The total number of shots on this injector exceeds 700 without having to refurbish the gaps. A C.44 (UC OMEGA) accelerating cavity with 24 parallel spark gaps and operating at 520 kV charge voltage has also been tested. DOE

N86-10196# Department of Energy, Washington, D. C.
COUNTERPULSE RAILGUN ENERGY RECOVERY CIRCUIT Patent Application
E. M. Honig, inventor (to DOE (LASL) Filed 28 Sep. 1985 16 p
(DE85-011603; US-Patent-Appl-SN-655490) Avail: NTIS HC A02/MF A01

The invention presented relates to a high-power pulsing circuit and more particularly to a repetitive pulse inductive energy storage and transfer circuit for an electromagnetic launcher. In an electromagnetic launcher such as a railgun for propelling a projectile at high velocity, a counterpulse energy recovery circuit is employed to transfer stored inductive energy from a source inductor to the railgun inductance to propel the projectile down the railgun. Switching circuitry and an energy transfer capacitor are used to switch the energy back to the source inductor in readiness for a repetitive projectile propelling cycle. DOE

N86-10197# Department of Energy, Washington, D. C.
OVERPULSE RAILGUN ENERGY RECOVERY CIRCUIT Patent Application
E. M. Honig, inventor (to DOE) (LASL) Filed 28 Sep. 1984 17 p
(DE85-011607; US-Patent-Appl-SN-655593) Avail: NTIS HC A02/MF A01

A high power pulsing circuit is presented and more particularly a repetitive pulse inductive energy storage and transfer circuit for an electromagnetic launcher. In an electromagnetic launcher such as a railgun for propelling a projectile at high velocity, an overpulse energy recovery circuit is employed to transfer stored inductive energy from a source inductor to the railgun inductance to propel the projectile down the railgun. Switching circuitry and an energy transfer capacitor are used to switch the energy back to the source inductor in readiness for a repetitive projectile propelling cycle. DOE

N86-10394*# Jet Propulsion Lab., California Inst. of Tech., Pasadena. TDA Mission Support and DSN Operations Office.
JPL EMERGENCY SUPPORT OF TDRSS AND COMPATIBLE SATELLITES
N. A. Fanelli *In its* The Telecommun. and Data Acquisition Progr. Rept. 15 Aug. 1985 p 120-124 (For primary document see N86-10382 01-32)
Avail: NTIS HC A10/MF A01 CSCL 14B

N86-10395*# Jet Propulsion Lab., California Inst. of Tech., Pasadena. TDA Planning Office.
PLANNING FOR VLA/DSN ARRAYED SUPPORT TO THE VOYAGER AT NEPTUNE
J. W. Layland and D. W. Brown *In its* The Telecommun. and Data Acquisition Progr. Rept. 15 Aug. 1985 p 125-135 refs (For primary document see N86-10382 01-32)
Avail: NTIS HC A10/MF A01 CSCL 14B

N86-10399*# Jet Propulsion Lab., California Inst. of Tech., Pasadena. TDA Engineering Section.
THE GCF MARK 4 IMPLEMENTATION AND BEYOND
R. A. Crowe *In its* The Telecommun. and Data Acquisition Progr. Rept. 15 Aug. 1985 p 163-172 refs (For primary document see N86-10382 01-32)
Avail: NTIS HC A10/MF A01 CSCL 14B

15 LAUNCH VEHICLES AND SPACE VEHICLES

Includes boosters; manned orbital laboratories; reusable vehicles; and space stations.

N86-10198# Department of the Navy, Washington, D. C.
IMPROVED ARRESTING AND RECOVERY SYSTEM FOR TEST MISSILES Patent Application
R. E. Kennedy and J. D. Neef, inventors (to Navy) Filed 2 Aug. 1984 18 p
(AD-D011743; US-Patent-Appl-SN-637238) Avail: NTIS HC A02/MF A01 CSCL 16/1

A system for arresting and recovering test ballistic missiles is adaptable for use in an existing facility and with the existing arresting engine. A long loop of cable encircles a sheave on the nose-end of the test missile and is supported by sheaves mounted on the support structure. The ends of the cable loop are terminated on one side of a singletree device. The other side is connected by a single cable to the arresting engine. One end of the cable loop slidably engages with the singletree and has an end cap. As the test missile is launched the cable loop and singletree are drawn toward a ratchet mechanism which grasp the end cap. An intermittent pulling machine is disposed for anchoring one leg of the cable loop whereby the test missile may be later raised or lowered for recovery. The system effectively doubles the load carrying capacity of an existing arresting engine by providing mechanical advantage. GRA

N86-10199# Air Command and Staff Coll., Maxwell AFB, Ala.
AN ANTHOLOGY: RATIONALE FOR A US BALLISTIC MISSILE DEFENSE (1969 - 1984) Student Report
E. C. Tircuit Apr. 1985 122 p
(AD-A156781; ACSC-85-2715) Avail: NTIS HC A06/MF A01 CSCL 15/3

This anthology is a selection and short synopsis of representative articles on the rationale for a US ballistic missile defense (BMD). Unclassified articles and documents were reviewed and analyzed to identify and include nine representative articles in the anthology. The anthology reduces the search for quality material on the subject and documents the fundamental rationale for a BMD. The author concluded that the fundamental rationale for a US BMD is to deter nuclear war. In addition, specific rationale for a US BMD is provided in the anthology. Finally, an extensive bibliography is included in the anthology to enhance further research on the subject. GRA

16 SPACE TRANSPORTATION

Includes passenger and cargo space transportation, e.g., shuttle operations; and rescue techniques.

For related information see also *03 Air Transportation and Safety* and *85 Urban Technology and Transportation.*

N86-10200# European Space Agency, Paris (France).
FIFTH EUROPEAN SYMPOSIUM ON MATERIAL SCIENCES UNDER MICROGRAVITY. RESULTS OF SPACELAB 1
T. D. Guyenne, comp. and J. J. Hunt, comp. Dec. 1984 489 p refs Partly in ENGLISH and FRENCH Proc. held at Schloss Elmau, West Germany, 5-7 Nov. 1984; sponsored by DFVLR, ESA, Bundesministerium fuer Forschung und Technologie, Bonn, West

Germany, European Low-Gravity Research Association, CNES, Dornier-Werke GmbH, Friedrichshafen, West Germany, Erno GmbH, Bremen, West Germany, and Kodak Ltd., Harrow, England
(ESA-SP-222; ISSN-0379-6566) Avail: NTIS HC A21/MF A01

Spacelab Fluid Physics Module; isothermal furnace; gradient furnace; and mirror furnace experiments were discussed. The experiments include investigations of composite materials; metallurgy; melt and solution growth experiments involving semiconductors; nucleation from the vapor phase; and liquids and interfaces. For individual titles, see N86-10201 through N86-10268.

N86-10201# European Space Agency. European Space Research and Technology Center, ESTEC, Noordwijk (Netherlands).
THE FLUID PHYSICS MODULE: A TECHNICAL DESCRIPTION **c34**
A. Gonfalone *In its* Fifth European Symp. on Mater. Sci. under Microgravity. Results of Spacelab 1 Dec. 1984 p 3-7 refs (For primary document see N86-10200 01-16)
Avail: NTIS HC A21/MF A01

The Spacelab Fluid Physics Module (FPM) is a multipurpose facility for investigations on the behavior of fluids in a microgravitational environment. It can establish a floating zone between two parallel coaxial disks, allowing for disturbance to be applied to the liquid, whose behavior is filmed. The stimuli can be mechanical (rotation, vibration or lateral displacement) or thermal (heating). Experiments on fluid motions induced by differences in surface tension, bubble motions, and fluid dynamics can be performed. The FPM is mounted in the Material Science Double Rack.
Author (ESA)

N86-10202# Kodak Ltd., London (England).
CAPILLARY FORCES IN A LOW GRAVITY ENVIRONMENT **c34**
J. E. Padday *In* ESA Fifth European Symp. on Mater. Sci. under Microgravity. Results of Spacelab 1 Dec. 1984 p 9-14 refs Sponsored by Kodak Ltd. and England Department of Industry (For primary document see N86-10200 01-16)
Avail: NTIS HC A21/MF A01

The capillary properties of a liquid (silicone oil) attached to a large circular solid surface (titanium) and held in the form of an axisymmetric liquid zone by a second smaller solid disk were studied on Spacelab. The unperturbed shapes and stability properties of these (zero-g) axisymmetric zones were obtained from the Laplace capillary equation. The principle by which a Laplace shape may be distorted by external force fields is described and the features of the method by which solid-liquid disjoining pressure is measured, are given. Experimental methods, image recording, image processing and the antispread treatment are described. It is found that the antispread works nominally and that the electrical field shows no effects. Equilibrium is reached very quickly and zone breakage was recorded. Thirteen data points were obtained with capillary pressures in the range -0.4 to -0.009 N/sqcm. At the lower pressure, very thick liquid films form; at higher pressures the films are thin. Author (ESA)

N86-10203# Naples Univ. (Italy). Inst. of Aerodynamics Umberto Nobile.
SOME RESULTS OF THE MARANGONI FREE CONVECTION EXPERIMENT **c34**
L. G. Napolitano, R. Monti, and G. Russo *In* ESA Fifth European Symp. on Mater. Sci. under Microgravity. Results of Spacelab 1 Dec. 1984 p 15-22 refs (For primary document see N86-10200 01-16)
(Contract CNR-PSN-83-070)
Avail: NTIS HC A21/MF A01

Thermally induced Marangoni flows in a floating zone under a variety of imposed boundary conditions were investigated on Spacelab. Problems in measuring the velocity in the bulk fluid, and the implications of the values obtained that confirm the attainment of a Marangoni boundary layer regime are discussed. Heat transferred across the floating zone is considered. The method used to determine, from the measured temperature of the hot disk, the time evolution of the temperature of the cold disk and its steady state Nusselt number is given, and results obtained from one run are presented. Author (ESA)

N86-10204# Centre National de la Recherche Scientifique, Meudon-Bellevue (France). Equipe de Technologie de la Croissance Cristalline.
OSCILLATIONS OF SEMI-FREE LIQUIDS IN MICROGRAVITY: SPACELAB 1 EXPERIMENT ES 326 [OSCILLATIONS DE VOLUMES LIQUIDES SEMI-LIBRES EN MICROGRAVITE: EXPERIENCE ES 326 DANS SPACELAB 1] **c34**
H. Rodot and C. Bisch *In* ESA Fifth European Symp. on Mater. Sci. under Microgravity. Results of Spacelab 1 Dec. 1984 p 23-29 refs In FRENCH (For primary document see N86-10200 01-16)
Avail: NTIS HC A21/MF A01

The effects of axial vibration on semi-free liquid in microgravity were studied on Spacelab 1. Amplitude, resonant frequencies, and oscillation damping of the liquid spheres were determined, using silicone oil injected onto a vibrating plate. Results confirm theoretical models and show that the liquid is very sensitive to vibrations in the 0.2 to 2 Hz range. To prevent strong resonance, e.g., during crystal growth, a small support/sphere diameter ratio is recommended. It is difficult to evaluate wetting factors.
Author (ESA)

N86-10205# Universidad Politecnica de Madrid (Spain). Dept. of ETSI Aeronautics.
LIQUID COLUMN STABILITY: EXPERIMENT 1 ES-331 **c34**
T. Martinez *In* ESA Fifth European Symp. on Mater. Sci. under Microgravity. Results of Spacelab 1 Dec. 1984 p 31-36 refs Sponsored by Spanish Commission for Space Research (For primary document see N86-10200 01-16)
Avail: NTIS HC A21/MF A01

The Spacelab floating zone stability in zero gravity experiment to form a long cylindrical liquid bridge (10 cm), between 2 solid coaxial disks, to study the surface deformation and inner liquid motion resulting from the application of mechanical disturbances is described. The scheduled investigations were not accomplished due to the impossibility of holding the liquid interface anchored at the nominal disk edge, but considerable knowledge on experiment design, e.g., on the difficulty of getting a clean start, and on the role of inertia in bridge formation was acquired. Author (ESA)

N86-10206# National Aerospace Lab., Amsterdam (Netherlands).
AXISYMMETRIC FREE SURFACE BEHAVIOR OF MOVING LIQUID IN A CYLINDER IN MICROGRAVITY **c34**
J. P. B. Vreeburg *In* ESA Fifth European Symp. on Mater. Sci. under Microgravity. Results of Spacelab 1 Dec. 1984 p 37-42 refs (For primary document see N86-10200 01-16)
Avail: NTIS HC A21/MF A01

The behavior of silicone oil during spin-up and spin-down of the container, and liquid response to forced oscillations, in stationary and steadily rotating states were studied on Spacelab. Nonlinear growth and decay of the half subharmonic resonance of the free liquid surface were examined. A diagnostic method for the determination of free liquid surface shape is outlined. The free liquid surface is included as a reflecting or refracting optical surface by which an illuminated line is observed. Via ray tracing and analysis, shape parameters of the surface are determined from the images of this line. The extreme wetting behavior of the oil produces a bubble of the air in the container rather than the formation of a spherical meniscus with a defined contact line (with zero contact angle). The excitation of capillary surface resonances is difficult. Most easily generated is a zero order mode in which the undeformed bubble oscillates. Author (ESA)

N86-10207# Bristol Univ. (England). School of Chemistry.
KINETICS OF SPREADING OF LIQUIDS IN MICROGRAVITY: EXPERIMENT 1 ES 327 **c34**
J. M. Haynes *In* ESA Fifth European Symp. on Mater. Sci. under Microgravity. Results of Spacelab 1 Dec. 1984 p 43-46 refs (For primary document see N86-10200 01-16)
Avail: NTIS HC A21/MF A01

The phenomenology of spreading of a tethered liquid drop is reviewed, and compared with the data obtained in microgravity experiments conducted in the fluid physics module during the Spacelab 1 mission. Recommendations for conduct of experiments of this kind are made. Author (ESA)

N86-10208# Deutsche Forschungs- und Versuchsanstalt fuer Luft- und Raumfahrt, Cologne (West Germany). Inst. fuer Raumsimulation.

THE ISOTHERMAL HEATING FACILITY c18

K. Wittmann *In* ESA Fifth European Symp. on Mater. Sci. under Microgravity. Results of Spacelab 1 Dec. 1984 p 49-54 refs (For primary document see N86-10200 01-16)

Avail: NTIS HC A21/MF A01

The Spacelab Isothermal Heating Facility (IHF) is a resistance heated vacuum furnace integrated in the Material Science Double Rack (MSDR). In the first Spacelab Mission the IHF was used for heating (Tmax = 1500 c) and rapid cooling of a wide range of sample material enclosed in standard sample container in 12 experiments. Besides the isothermal mode with low temperature gradients within the sample, the IHF can establish time variable axial temperature gradients in special gradient samples. The IHF heating and cooling cycles are performed automatically, controlled by the central computer of the MSDR. Author (ESA)

N86-10209# Hamburg Univ. (West Germany).

INFLUENCES AFFECTING SEPARATION IN MONOTECTIC ALLOYS UNDER MICROGRAVITY c12

H. Ahlborn and K. Loehberg (Technische Univ., Berlin) *In* ESA Fifth European Symp. on Mater. Sci. under Microgravity. Results of Spacelab 1 Dec. 1984 p 55-61 refs (For primary document see N86-10200 01-16)

Avail: NTIS HC A21/MF A01

Specimens from the monotectic systems Zn-Bi, Zn-Pb, and Zn-Bi-Pb were cooled (30 K/min) through the miscibility gap in microgravity on Spacelab to study separation. Results are contradictory, and it is not possible to decide if the separation process in monotectic alloys under microgravity is determined by one or more processes, and which of these is the most efficient. To obtain a homogeneous distribution of small sized droplets of the minority phase in a liquid matrix, its volume portion should not exceed 5%, and a low interfacial energy between the droplets and the matrix, and a high viscosity of the matrix are required.

Author (ESA)

N86-10210# Max-Planck-Inst. fuer Metallforschung, Stuttgart (West Germany).

PARTICLE COARSENING IN IMMISCIBLE ZINC-LEAD ALLOYS UNDER MICROGRAVITY c12

A. Kneissel (Montanuniv. Leoban, Austria) and H. Fischmeister *In* ESA Fifth European Symp. on Mater. Sci. under Microgravity. Results of Spacelab 1 Dec. 1984 p 63-68 refs Sponsored by Austrian Ministry of Science and Research (For primary document see N86-10200 01-16)

Avail: NTIS HC A21/MF A01

Spacelab experiments on the liquid-liquid system Zn-Pb are described. Using alloys consisting of a low volume fraction of Pb-rich droplets in a Zn-rich matrix, it was demonstrated that a homogeneous dispersion of fine droplets can be maintained under microgravity and solidified into a homogeneous dispersion structure at the cooling rates available in the isothermal furnace of Spacelab. The particle coarsening which occurs during a hold in the two-liquid region is compatible with known data for the Pb-Zn system within the error limits of the measurements. Disturbance of the Ostwald process by Marangoni and residual g convection is unimportant.

Author (ESA)

N86-10211# Katholieke Universiteit te Leuven (Belgium). Dept. Metaalkunde und Toegepaste Materiaalkunde.

MELTING AND SOLIDIFICATION OF METAL MATRIX COMPOSITES UNDER MICROGRAVITY c12

L. Froyen and A. Deruyttere *In* ESA Fifth European Symp. on Mater. Sci. under Microgravity. Results of Spacelab 1 Dec. 1984 p 69-78 refs (For primary document see N86-10200 01-16)

Avail: NTIS HC A21/MF A01

Particulate composites with Al-matrix were melted, held during 40 min at 800C and solidified in the Spacelab Isothermal Heating Facility. Comparison with ground processed reference samples shows that the space processed samples are much more homogeneous, for coarse and fine dispersed particles. Higher homogeneity leads to an important increase of the uniformity of macro-Vickers hardness. The abrasive wear resistance of the Al-SiC composite after melting and solidification in space is as good as in samples prepared by powder metallurgy. The particle rearrangements in the 1 g-reference and micro g-samples can be explained by interfacial energy considerations, sedimentation, and convection.

Author (ESA)

N86-10212# Technische Hogeschool, Delft (Netherlands). Dept. of Metals Science.

UNIDIRECTIONAL SOLIDIFICATION OF CAST IRON: EXPERIMENT ES-325 c12

H. Nieswaag, T. Luyendijk, and W. H. M. Alsem *In* ESA Fifth European Symp. on Mater. Sci. under Microgravity. Results of Spacelab 1 Dec. 1984 p 79-85 refs Sponsored by Netherlands State Department (For primary document see N86-10200 01-16)

Avail: NTIS HC A21/MF A01

Eutectic cast iron with 3.9%C-1.5%Si-0.01%P-0.025%S was solidified unidirectionally in the Spacelab isothermal furnace at 4 growth rates between 0.1 and 1.0 mm/min to study graphite growth and the sulfur transport in the liquid during solidification under microgravity. From the sulfur concentration profile it is concluded that a stronger convection occurs in space. Transients in the sulfur concentration at changing solidification rate prove, however, that a narrow diffusive boundary layer must be present. The graphite flakes are not better aligned than at 1 g. The flight specimen is separated into two parts in a more pronounced way than observed under terrestrial conditions. Cavities are found in the micro g sample at the position where the solid-liquid interface stopped after melting. The plasma-sprayed alumina skin was rigid enough to keep the liquid specimen in its original shape, although cracks are observed. Author (ESA)

N86-10213# Maschinenfabrik Augsburg-Nuernberg A.G., Munich (West Germany).

SKIN CASTING OF ALLOYS AND COMPOSITES: RESULTS OF SPACELAB (SL)-1 AND TEXUS EXPERIMENTS c12

H. Sprenger *In* ESA Fifth European Symp. on Mater. Sci. under Microgravity. Results of Spacelab 1 Dec. 1984 p 87-94 refs Sponsored by Bundesministerium fuer Forschung und Technologie (For primary document see N86-10200 01-16)

Avail: NTIS HC A21/MF A01

Shape stability of alumina skin coated cast iron specimens during heat-up, melting, hold time, and directional solidification were studied in TEXUS sounding rocket and Spacelab experiments. It is shown that the main contributions to skin deformation come from the volume change during melting and from interfacial tension forces between melt and skin. In the Spacelab experiment, the cast iron sample shows unexpected behavior due to strong deviation of the experiment run from the intended time temperature profile. The appearance of pores and the separation of the melt into two parts, caused by gas formation, influences the resulting thermal gradient and solidification rate. There is evidence, however, that these parameters are also influenced by the strongly reduced convection during the directional solidification phase. Author (ESA)

N86-10214# Technische Univ., Vienna (Austria).

VACUUM BRAZING UNDER MICROGRAVITY c12

K. Frieler, R. Stickler (Bundesanstalt fuer Materialpruefung.), and E. Siegfried *In* ESA Fifth European Symp. on Mater. Sci. under Microgravity. Results of Spacelab 1 Dec. 1984 p 95-99 refs (For primary document see N86-10200 01-16)

Avail: NTIS HC A21/MF A01

Gravity dependent vacuum brazing process control parameters including thermal history, geometry of brazing gaps, and flow patterns were studied in the Spacelab Isothermal Heating Facility

under microgravity. Gap filling, braze mixing, and microstructure as a function of joint hardness were examined. Only the liquid phase of the braze is gravity dependent. More pronounced mixing occurs for micro-g than for 1 g cases. While all the gaps of the 1 g specimen are filled to the degree indicated by the equilibrium of hydrostatic and capillary pressure, only the outer 200 micron gap of the micro-g sample is filled completely. Microgravity increases porosity. The segregation of CuNi dendrites and melt at 1100 K seen at 1 g is absent in micro-g. Author (ESA)

N86-10215# Bologna Univ. (Italy). Dipt. di Fisica.
MELTING AND SOLIDIFICATION IN O-g OF SINTERED ALLOYS: EXPERIMENTS ES 311 A AND B BUBBLE REINFORCED MATERIALS c12
F. Barbier, C. Patuelli, P. Gonndi (Rome Univ.), and R. Montanari (Rome Univ.) *In* ESA Fifth European Symp. on Mater. Sci. under Microgravity. Results of Spacelab 1 Dec. 1984 p 101-107 refs (For primary document see N86-10200 01-16)
Avail: NTIS HC A21/MF A01

The behavior after melting and solidification in O and 1 g of sintered Cu-Ag and Al alloys was compared in Spacelab experiments. Oxide films are efficient in maintaining the initial shape after melting and solidification in O g. After melting and solidification in O g the bubble distribution appears to be connected with sweeping phenomena, and to phase and grain boundaries, along the solidification front. The eutectics in O g present larger lamella spacings, depending on smaller solidification rates, larger diffusion coefficients, and/or smaller nucleation rates. The Al alloys show reduced coalescence in O g, leading to uniform distribution of aggregates of limited size, much smaller than the one of the aggregates forming in 1 g and depending on Brownian motion. No evidence for effects of convective motions depending on the surface tension gradients in these liquid metals with oxide film coating is found. Author (ESA)

N86-10216# Technische Univ., Clausthal-Zellerfeld (West Germany). Arbeitsgruppe Glas.
INTERDIFFUSION IN THE GLASS MELT SYSTEM (Na2O+Rb2O) .3SiO2 c12
M. Braedt, V. Braetsch, and G. H. Frischat *In* ESA Fifth European Symp. on Mater. Sci. under Microgravity. Results of Spacelab 1 Dec. 1984 p 109-112 refs Sponsored by Bundesministerium fuer Forschung und Technologie (For primary document see N86-10200 01-16)
Avail: NTIS HC A21/MF A01

An investigation of the interdiffusion between Na2O.3SiO2 and Rb2O.3SiO2 glass melts and the corrosion of SiO2 glass by alkalisilicate glass melts at 1200 C was planned for Spacelab. The temperature-time program, planned to maintain a 30 min period of constant temperature of 1200 C was quite different. Only the interdiffusion experiment can be evaluated for an effective temperature of 1180 C, with an effective time of 1730 sec. Despite the problems, the micro-g diffusion profiles result in a concentration-dependent interdiffusion coefficient with typical mixed-alkali effect behavior. For a composition of 0.5 Na2O.0.5 Rb2O.3SiO2 the D value approaches (1.1 + or - 0.3) 0.00001 sqcm/sec, and fits the order of data obtained earlier. The 1 g reference experiment was totally disturbed by convection effects. Author (ESA)

N86-10217# Centre National d'Etudes Spatiales, Toulouse (France).
GRADIENT HEATING FACILITY BEHAVIOR c18
G. Cambon, B. Castets, O. Boutemy, J. P. Gicquel, R. Aubron, M. Boddaert, and J. Benoit *In* ESA Fifth European Symp. on Mater. Sci. under Microgravity. Results of Spacelab 1 Dec. 1984 p 115-119 refs (For primary document see N86-10200 01-16)
Avail: NTIS HC A21/MF A01

The Spacelab Gradient Heating Facility (GHF) is a furnace with 3 heating zones with cooled heat sink permitting the control of unidirectional solidification without pulling device at temperatures up to 1250 C. The GHF can run three 0.7 gr cartridges simultaneously. The experiment and the furnace can be cooled together very rapidly after helium injection at low partial pressure. Flight data analysis shows that only a maximum of 50% of data are available. It is difficult to have a complete assurance of the correct working of the GHF plus Materials Science Double Rack and in particular, to understand the reasons for the oxydizing of GHF cartridges during the heating. Author (ESA)

N86-10218# Commissariat a l'Energie Atomique, Grenoble (France). Dept. de Metallurgie.
DIRECTIONAL SOLIDIFICATION OF AN ALUMINUM-ZINC VAPOR EMULSION IN MICROGRAVITY c12
C. Potard and P. Morgand *In* ESA Fifth European Symp. on Mater. Sci. under Microgravity. Results of Spacelab 1 Dec. 1984 p 121-125 (For primary document see N86-10200 01-16)
Avail: NTIS HC A21/MF A01

A Spacelab experiment tested a method of creating solid structures in which aluminum-zinc alloys are directionally solidified under controlled partial pressure of zinc and thermal conditions. Destabilization of interfacial liquid zone was expected to give rise to vapor phase nucleation growth and trapping by the advancing solid-liquid front. This was partially realized during the space processing of the specimens: bubble populations are present in the sample. This is due to a nonwetting effect in space not observed on the ground. The microstructures of samples processed in space and on the ground are compared. Author (ESA)

N86-10219# Commissariat a l'Energie Atomique, Grenoble (France). Dept. de Metallurgie.
DIRECTIONAL SOLIDIFICATION OF EUTECTIC ALLOYS c12
J. J. Favier and J. deGoer *In* ESA Fifth European Symp. on Mater. Sci. under Microgravity. Results of Spacelab 1 Dec. 1984 p 127-133 refs (For primary document see N86-10200 01-16)
Avail: NTIS HC A21/MF A01

Eutectic alloys Ag-Ge, Al3Ni-Al, Al2Cu-Al forming respectively, under ground conditions, irregular, fiberlike and lamelar structures were directionally solidified under well defined thermal conditions in the Spacelab Gradient Heating Facility. The microstructures are compared with those obtained under the same conditions on the ground. The major difference appears with the fiberlike Al-Ni system, for which the main spacing between the needles is larger in space than on Earth, confirming TEXUS results. An explanation taking into account off-eutectic considerations is proposed.
Author (ESA)

N86-10220# Centre National de la Recherche Scientifique, Meudon-Bellevue (France). Equipe de Technologie de la Croissance Cristalline.
LEAD TELLURIDE CRYSTALS GROWN IN MICROGRAVITY: EXPERIMENT ES 318 [CRISTAUX DE TELLURURE DE PLOMB ELABORES EN MICROGRAVITE EXPERIENCE ES 318] c12
H. Rodot and O. Tottereau *In* ESA Fifth European Symp. on Mater. Sci. under Microgravity. Results of Spacelab 1 Dec. 1984 p 135-139 refs In FRENCH (For primary document see N86-10200 01-16)
Avail: NTIS HC A21/MF A01

Three lead telluride monocrystals grown in the Spacelab Gradient Heating Facility under microgravity (two from seeds, one without by the Bridgman method) were compared with crystals grown on the ground. Results show that it is possible to grow large (17 mm diameter) lead telluride crystals in space, with better quality than those on Earth, which have defects due to gravity induced convection. The rate and stability of acceleration are the main factors for successful crystal growth in space, and exclude manned vehicles or those with multiple payloads incompatible with these requirements. Author (ESA)

N86-10221# Erlangen-Nuremberg Univ. (West Germany). Inst. fuer Werkstoffwissenschaften.
DIRECTIONAL SOLIDIFICATION OF InSb-NiSb EUTECTIC c12
G. Mueller and P. Kyr *In* ESA Fifth European Symp. on Mater. Sci. under Microgravity. Results of Spacelab 1 Dec. 1984 p 141-146 refs Sponsored by DFVLR and Bundesministerium fuer Forschung und Technologie (For primary document see N86-10200 01-16)

Avail: NTIS HC A21/MF A01

The InSb-NiSb quasi binary eutectic was directionally solidified under microgravity and Earth-gravity conditions in the Spacelab Gradient Heating Facility by the power down technique. Comparison of space and Earth processed samples reveals a 30% decrease in the spacing of the SiSb fibers in the samples grown under microgravity. Author (ESA)

N86-10222# Commissariat a l'Energie Atomique, Grenoble (France). Dept. de Metallurgie.

THERMOMIGRATION OF COBALT IN LIQUID TIN: EXPERIMENT 1 ES 320 **c12**

Y. Malmejac and J. P. Praizey *In* ESA Fifth European Symp. on Mater. Sci. under Microgravity. Results of Spacelab 1 Dec. 1984 p 147-152 refs (For primary document see N86-10200 01-16)

Avail: NTIS HC A21/MF A01

Thermomigration of cobalt in liquid tin was studied on the spacelab by heating capillary samples of liquid tin containing 0.5% cobalt in a thermal gradient of 200 deg/cm. When chemical steady state is reached, the liquid alloy is sampled, and the cobalt concentration analyzed by activation. On Earth, a constant concentration profile is obtained. In microgravity relative concentration of cobalt varies from 0.7 at the cold end to 1.4 at the hot end. The heat of transport can be expressed by: Q cal/mole = -(3,72 + or - 0,08) T (K) for 593 to 933 K. Soret coefficient is 0.024/K at 773 K. Convection calculations explain why thermomigration effects are measurable in microgravity but not on Earth in the configuration considered. Author (ESA)

N86-10223# Freiburg Univ. (West Germany). Inst. fuer Kristallographisches.

THE MIRROR HEATING FACILITY: PERFORMANCE AND EXPERIENCES **c18**

R. Nitsche *In* ESA Fifth European Symp. on Mater. Sci. under Microgravity. Results of Spacelab 1 Dec. 1984 p 155-156 refs (For primary document see N86-10200 01-16)

Avail: NTIS HC A21/MF A01

The Spacelab Mirror Heating Facility (MHF) is a multiuser furnace of low thermal inertia, providing high local temperatures (up to 2000 deg C) at relatively low power consumption. The sample is radiation heated by two 400 W halogen lamps, situated in the foci of a double ellipsoid mirror. The mirror can be translated relative to the stationary, but rotatable, sample. This makes the MHF especially suited for crystal growth from the melt by the floating zone method and for solution growth by the traveling heater method. The MHF was part of the Materials Science Double Rack (MSDR). The MHF was activated eight times, with varying success, before breakdown of the MSDR cooling system crippled it. Author (ESA)

N86-10224# Stuttgart Univ. (West Germany). Inst. fuer Physikalisches.

GaSb-SEMICONDUCTOR CRYSTALS UNDER MICROGRAVITY: EXPERIMENT ES 323 **c12**

K. W. Benz and G. Nagel *In* ESA Fifth European Symp. on Mater. Sci. under Microgravity. Results of Spacelab 1 Dec. 1984 p 157-161 refs (For primary document see N86-10200 01-16) (Contract DFVLR-01-QV-698)

Avail: NTIS HC A21/MF A01

The Traveling-heater method was used to grow the III-V compound GaSb on Spacelab. Convective transport phenomena and the origins of dopant inhomogeneities under Earth and space conditions were studied. Earth grown crystals show strong dopant variations mainly due to convective flow phenomena. The Spacelab experiment reveals an increase of dopant homogeneity in the space grown crystal because of the absence of natural convection. Author (ESA)

N86-10225# Freiburg Univ. (West Germany). Inst. fuer Kristollographisches.

SOLUTION GROWTH OF CADMIUM TELLURIDE: EXPERIMENT ES 322 **c12**

R. Schoenholz, R. Dian, and R. Nitsche *In* ESA Fifth European Symp. on Mater. Sci. under Microgravity. Results of Spacelab 1 Dec. 1984 p 163-167 refs Sponsored by Bundesministerium fuer Forschung und Technologie (For primary document see N86-10200 01-16)

Avail: NTIS HC A21/MF A01

Microgravity growth of CdTe from Te solution by the traveling heater method was achieved on Spacelab. The experiment was terminated after 6 instead of 17 hr of growth, due to breakdown of the cooling system. The tiny layer of material grown in this time could not be analyzed satisfactorily. It was severely cracked by thermal stress since the slow cooling phase was not carried out. Author (ESA)

N86-10226# Wacker-Chemie G.m.b.H. Burghausen (West Germany).

CRYSTALLIZATION OF A SILICON SPHERE **c12**

H. Koelker *In* ESA Fifth European Symp. on Mater. Sci. under Microgravity. Results of Spacelab 1 Dec. 1984 p 169-172 refs (For primary document see N86-10200 01-16)

Avail: NTIS HC A21/MF A01

Directional solidification of silicon was investigated in the spacelab under zero gravity to see if surface driven flow exists in liquid silicon. After solidification, the Si-crystal was sliced, polished and etched, and the striation pattern studied with a microscope. The result clearly suggests the existence of time dependent surface driven flow. Author (ESA)

N86-10227# Freiburg Univ. (West Germany). Inst. fuer Kristollographisches.

CRYSTAL GROWTH OF SILICON IN SPACELAB 1: EXPERIMENT ES-321 **c12**

A. Eyer, H. Leiste, and R. Nitsche *In* ESA Fifth European Symp. on Mater. Sci. under Microgravity. Results of Spacelab 1 Dec. 1984 p 173-182 refs (For primary document see N86-10200 01-16)

Avail: NTIS HC A21/MF A01

A phosphorus doped silicon crystal of 10 mm diameter and 112 mm length was grown by the floating zone method at a rate of 5 mm/min aboard Spacelab 1. Zone forms and interface shapes of the microgravity and the terrestrial reference sample differ considerably, but the patterns of (nonrotational) striations are very similar. Thus, time dependent thermocapillary flows, driven by gravity independent surface tension gradients in the molten zone, appear to be the dominant cause for these dopant inhomogeneities in space as well as on Earth. Author (ESA)

N86-10228# Freiburg Univ. (West Germany). Chemisches Lab.

PROTEIN SINGLE CRYSTAL GROWTH UNDER MICROGRAVITY **c12**

W. Littke and C. John *In* ESA Fifth European Symp. on Mater. Sci. under Microgravity. Results of Spacelab 1 Dec. 1984 p 185-188 refs Original language document previously announced as A85-39084 Sponsored by Bundesministerium fuer Forschung und Technologie (For primary document see N86-10200 01-16)

Avail: NTIS HC A21/MF A01

Single crystals of Beta galactosidase and Lysozyme were grown in Spacelab for X-ray diffraction studies of three dimensional crystal structure. The Beta galactosidase shows a 27-fold, Lysozyme a 1000-fold increase in volume compared with crystals grown under terrestrial conditions. The crystalline material is well shaped and microscopic examinations under polarized light show good quality. Wide fronts of diffusion favor the formation of large crystals. Applying an increasing temperature gradient improves crystallization of galactosidase. Perfect habit is found with crystals grown free floating out of the solution without touching the wall. The equipment and procedures are described. Author (ESA)

N86-10229# Technical Univ. of Denmark, Lyngby. Physics Lab. 3.

CRYSTAL GROWTH FROM SOLUTION **c12**

G. Galster and K. F. Nielsen *In* ESA Fifth European Symp. on Mater. Sci. under Microgravity. Results of Spacelab Dec. 1984 p 189-191 refs Sponsored by Danish Space Board (For primary

document see N86-10200 01-16)
Avail: NTIS HC A21/MF A01

Experiments on crystal growth using the method of opposite oriented diffusion growth in Spacelab 1 are described. The growth of calcium-tartrate crystals demonstrates that filters between the three chambers of a growth reactor are necessary even in the low gravity environment of the Spacelab. Attempts to grow low-dimensional, electrically conducting crystals failed due to chemical disintegration during the prolonged waiting period prior to launch. Author (ESA)

N86-10230# Paris VI Univ. (France). Lab. de Mineralogie et Cristallographie.
GROWTH AND CHARACTERIZATION OF BRUSHITE AND LEAD MONETITE, SIMULATION AND RESULTS c12
M. C. Robert, F. Lefaucheux, and A. Authier *In* ESA Fifth European Symp. on Mater. Sci. under Microgravity. Results of Spacelab 1 Dec. 1984 p 193-199 refs Sponsored by CNES (For primary document see N86-10200 01-16)
Avail: NTIS HC A21/MF A01

Single crystals obtained in Spacelab experiments of solution growth by coprecipitation were characterized by optical and X-ray topographic techniques. It is shown how gel growth simulation experiments can be used to select the parameters for space experiments and to analyze the growth features of the crystals. Author (ESA)

N86-10231# Technische Univ., Berlin (West Germany). Inst. fuer Metallforschung.
SELF DIFFUSION OF Sn112 AND Sn124 IN LIQUID TIN c12
G. Frohberg, K.-H. Kraatz, and H. Wever *In* ESA Fifth European Symp. on Mater. Sci. under Microgravity. Results of Spacelab 1 Dec. 1984 p 201-205 refs (For primary document see N86-10200 01-16)
Avail: NTIS HC A21/MF A01

The temperature dependence of self diffusion and isotope effect in molten tin under micro-g and 1 g conditions were investigated on the Spacelab. Eight cartridges, 16 tin samples were isothermally annealed at 8 diffusion temperatures between 240 and 1250 C. The penetration profiles were analyzed. Significantly lower diffusion coefficients than under 1 g indicate the absence of gravity-driven microconvections. Accuracy is typically 0.5%. An isotope effect of 0.1 (400 C) and 0.9 (810 C) is reported. Author (ESA)

N86-10232# Politecnico di Milano (Italy).
ADHESION OF METALS: EXPERIMENT 1 ES-340 c12
F. Rossitto and G. Ghersini (Centro Informazioni Studi Esperienze) *In* ESA Fifth European Symp. on Mater. Sci. under Microgravity. Results of Spacelab 1 Dec. 1984 p 207-217 refs Sponsored by CNR (For primary document see N86-10200 01-16)
Avail: NTIS HC A21/MF A01

The characterization of stainless steel surface forces and interface energies at the contact between real surfaces, was studied in the Spacelab ultrahigh vacuum (UHV) chamber. In spite of the malfunctions during the experiment and in the output data, it can be affirmed that most of the objectives of the experiment are reached. The flight shows the nominal performance of the UHV Chamber, and single pulse analysis is able to explore the adhesion mechanisms, to characterize the interaction model between the colliding bodies, and to evaluate dynamically the interface energy. Author (ESA)

N86-10233*# Harvard Univ., Cambridge, Mass. Div. of Applied Sciences.
CRYSTAL NUCLEATION AND GLASS FORMATION IN METALLIC ALLOY MELTS c12
F. Spaepen *In* ESA Fifth European Symp. on Mater. Sci. under Microgravity. Results of Spacelab 1 Dec. 1984 p 215-219 refs (For primary document see N86-10200 01-16)
(Contract NAS8-36516)
Avail: NTIS HC A21/MF A01

Homogeneous nucleation, containerless solidification, and bulk formation of metallic glasses are discussed. Homogeneous nucleation is not a limiting factor for metallic glass formation at slow cooling rates if the reduced glass transition temperature is high enough. Such glasses can be made in bulk if heterogeneous nucleants are removed. Containerless processing eleminates potential sources of nucleants, but as drop tube experiments on the Pd-Si alloys show, the free surface may still be a very effective heterogeneous nucleant. Combination of etching and heating in vacuum or fluxing can be effective for cleaning fairly large ingots of nucleants. Reduced gravity processing has a potentially useful role in the fluxing technique, for example to keep large metallic ingots surrounded by a low density, low fluidity flux if this proved difficult under ground conditions. For systems where heterogeneous nucleants in the bulk of the ingot need gravity to segregate to the flux-metal interface, reduced gravity processing may not be appropriate for bulk glass formation. Author (ESA)

N86-10234*# Massachusetts Inst. of Tech., Cambridge.
CRYSTAL GROWTH OF GaAs IN SPACE c12
H. C. Gatos, J. Lagowski, L. M. Pawlowicz, F. Dabkowski, and C.-J. Li *In* ESA Fifth European Symp. on Mater. Sci. under Microgravity. Results of Spacelab 1 Dec. 1984 p 221-225 refs (For primary document see N86-10200 01-16)
Avail: NTIS HC A21/MF A01

It is shown that stoichiometry variations in the GaAs melt during growth constitute the most critical parameter regarding defect formations and their interactions; this defect structure determines all relevant characteristics of GaAs. Convection in the melt leads to stoichiometric variations. Growth in axial magnetic fields reduces convection and permits the study of defect structure. In order to control stoichiometry in space and to accommodate expansion during solidification, a partially confined configuration was developed. A triangular prism is employed to contain the growth melt. This configuration permits the presence of the desired vapor phase in contact with the melt for controlling the melt stoichiometry. Author (ESA)

N86-10235# Naples Univ. (Italy). Inst. of Aerodynamics Umberto Nobile.
THE TEXUS FLIGHT RESULTS ON CONVECTIVE FLOWS AND HEAT TRANSFER IN SIMULATED FLOATING ZONES c34
R. Monti, L. G. Napolitano, and G. Mannara *In* ESA Fifth European Symp. on Mater. Sci. under Microgravity. Results of Spacelab 1 Dec. 1984 p 229-236 refs (For primary document see N86-10200 01-16)
Avail: NTIS HC A21/MF A01

On TEXUS 9 sounding rocket flight, a cylindrical liquid bridge between 2 circular disks was created and 1 of the disks then heated with an assigned temperature time profile. The experiment collected data on the thermofluidynamic fields that prevail at high Peclet number and unsteady thermal conditions. Thermocouple failure caused problems in heat transfer data reduction, and in numerical correlation. Author (ESA)

N86-10236# Academy of Sciences (USSR), Moscow. Inst. for Problems in Mechanics.
MATHEMATICAL SIMULATION OF DISTURBING FORCES AND MATERIAL SCIENCE PROCESSES UNDER LOW GRAVITY c12
V. I. Polezhaev, A. P. Lebedev, and S. A. Nikitin *In* ESA Fifth European Symp. on Mater. Sci. under Microgravity. Results of Spacelab 1 Dec. 1984 p 237-243 refs (For primary document see N86-10200 01-16)
Avail: NTIS HC A21/MF A01

A model of microgravity aboard an unmanned Earth satellite is suggested. The results of microgravity calculation of unmanned spacecraft in gravity stabilized flight are presented. The thermal convection and impurity distribution in germanium melt in time-dependent microgravity cases on the base of Boussinesq equations mathematical models are studied. It is shown that in the cases of the low-frequencies microgravity oscillations when average microgravity is not zero, there is a sharply pronounced maximum in the macroinhomogeneity. It is also shown that high frequency

convection has a small effect on impurity distribution in crystal, but low frequency convection results in striations like the ones in terrestrial conditions. Author (ESA)

N86-10237# Goettingen Univ. (West Germany). Inst. fuer Angewandte Mechanik und Stroemungsphysik.
THE INFLUENCE OF THERMOCAPILLARITY ON THE MIGRATION OF DROPLETS IN A LIQUID POSSESSING A UNIFORM TEMPERATURE GRADIENT c34
V. Delitzsch, H. Eckelmann, and W. Wuest (Deutsche Forshungs- und Versuchsanstalt fuer Luft- und Raumfahrt, Goettingen, West Germany) *In* ESA Fifth European Symp. on Mater. Sci. under Microgravity. Results of the Spacelab 1 Dec. 1984 p 245-249 refs (For primary document see N86-10200 01-16)
Avail: NTIS HC A21/MF A01

The influence of thermocapillarity on the migration of water droplets in butylbenzoate and fluorobenzene is investigated at low Reynolds and Marangoni numbers. The two components of both liquid systems are immiscible with one another and have the same density at 32 and 50 C respectively. At temperature gradients of 1 C/cm in stratified butylbenzoate and 4 C/cm in stratified fluorobenzene in equilibrium, gravity is reduced to a hundredth of the interfacial force. Water droplets injected into the test cell are sorted out in the gravity field dependent on their diameters. Under these conditions the smaller droplets migrate to higher temperature than the bigger ones. The final position of a droplet is determined by the balance of Marangoni and gravity forces both of which depend on droplet diameter. The positions of the droplets in the test cell are evaluated photographically. The interface tension gradients are 0.000001 N/cm for both systems. Author (ESA)

N86-10238# Naples Univ. (Italy). Inst. of Aerodynamics Umberto Nobile.
NUMERICAL SIMULATION OF UNSTEADY THERMAL MARANGONI FLOWS c34
L. G. Napolitano, C. Golia, and A. Viviani *In* ESA Fifth European Symp. on Mater. Sci. under Microgravity. Results of Spacelab 1 Dec. 1984 p 251-258 refs (For primary document see N86-10200 01-16)
(Contract CNR-PSN-83-070)
Avail: NTIS HC A21/MF A01

A two-dimensional numerical code for the analysis of unsteady thermal Marangoni flows which solves the full Navier-Stokes equation for natural, Marangoni, or combined free convection in plane and axisymmetric geometries and arbitrary variations of surface tension with temperature is developed. The equations are discretized using a semi-implicit finite difference scheme that preserves conservative and transport properties within cell mesh and allows the use of time-steps much larger than those relative to a purely explicit technique. Results pertain to a plane configuration with surface tension varying linearly with temperature. The time evolution of the velocity and temperature fields, and the assessement of the range of validity of the so-called shallow-cavity approximation for steady state are discussed. Author (ESA)

N86-10239# Canadian Astronautics Ltd., Ottawa (Ontario).
NUMERICAL SIMULATION OF CONVECTIONS IN THE MICROGRAVITY ENVIRONMENT c34
R. Boudreault *In* ESA Fifth European Symp. on Mater. Sci. under Microgravity. Results of Spacelab 1 Dec. 1984 p 259-264 refs (For primary document see N86-10200 01-16)
Avail: NTIS HC A21/MF A01

A numerical simulation program to study g-jitter and Marangoni convection in the liquid phase under microgravity were produced. The program solves the Navier-Stokes equations in the derived variable configuration. An alternative direction implicit method is used to solve the finite differences equations representing flow in the cavity. The resulting flow field and mixing characteristic are analyzed at different dimensionless times. Author (ESA)

N86-10240# Hochschule der Bundeswehr, Munich (West Germany). Inst. fuer Raumfahrttechnik.
OSCILLATIONS OF A VISCOELASTIC LIQUID DROP IN ZERO-GRAVITY c34
H. F. Bauer *In* ESA Fifth European Symp. on Mater. Sci. under Microgravity. Results of Spacelab 1 Dec. 1984 p 265-270 refs (For primary document see N86-10200 01-16)
Avail: NTIS HC A21/MF A01

The transcendental frequency equation for a viscoelastic spherical liquid drop is presented. For small viscoelasticity the viscous effect dominates, where the oscillation ceases to exist for small relaxation time, while for large viscoelasticity of the liquid the elastic effects dominate the vibrational behavior, producing oscillations again. A viscoelastic liquid drop subjected to a fluctuating temperature gradient also produces oscillations, which may disintegrate the system. The response of the drop with surface tension, viscosity and relaxation time as parameters is presented. Author (ESA)

N86-10241# Gesamthochschule, Essen (West Germany).
VERIFICATION OF TURBULENCE DEVELOPING FROM THE OSCILLATORY MARANGONI CONVECTION IN A LIQUID COLUMN c34
Ch.-H. Chun *In* ESA Fifth European Symp. on Mater. Sci. under Microgravity. Results of Spacelab 1 Dec. 1984 p 271-280 refs (For primary document see N86-10200 01-16)
Avail: NTIS HC A21/MF A01

A microgravity experiment during the TEXUS 7 rocket flight investigated whether the Marangoni convection of a liquid column at Marangoni numbers of 94,000 and 124,000 (far beyond the critical values for the first oscillatory instability) remains oscillatory or goes into the turbulent state, and studied the role of the aspect ratio of the liquid column on the instabilities. Oscillatory turbulent states are found. A physical model concept, criteria for the higher oscillation mode occurrence, and their development into turbulent nonperiodic structure are discussed. Author (ESA)

N86-10242# Giessen Univ. (West Germany). Inst. fuer Physkikalisches.
MEASUREMENTS OF THE CRITICAL MARANGONI NUMBER OF THE LAMINAR-OSCILLATORY TRANSITION OF THERMOCAPILLARY CONVECTION IN FLOATING ZONES c34
D. Schwabe and A. Scharmann *In* ESA Fifth European Symp. on Mater. Sci. under Microgravity. Results of Spacelab 1 Dec. 1984 p 281-289 refs (For primary document see N86-10200 01-16)
(Contract BMFT-01-QV-148-ZA-SN-SLN-7786)
Avail: NTIS HC A21/MF A01

The critical Marangoni number of the transition point from laminar to oscillatory thermocapillary convection in a liquid bridge with free cylindrical surface (floating zone) is measured under microgravity. The critical Marangoni numbers of NaNO3-zones with 6 mm diameter and length 4.00 and 4.79 mm are compared with measurements under normal Earth gravity. Data on the dependence of the oscillation frequency on the Marangoni number are given. Frequency jumps and beat frequencies are found in microgravity and normal gravity. Author (ESA)

N86-10243# Ishikawajima-Harima Heavy Industries Co. Ltd., Yokohama (Japan).
EXPERIMENTAL STUDY ON MARANGONI CONVECTION c34
J. Ochiai, K. Kuwahara, M. Morioka, S. Enya, K. Sezaki, T. Maekawa (Ioyo Univ., Japan), and I. Tanasawa (Tokyo Univ.) *In* ESA Fifth European Symp. on Mater. Sci. under Microgravity. Results of Spacelab 1 Dec. 1984 p 291-295 refs Sponsored by Japanese Science and Technology Agency (For primary document see N86-10200 01-16)
Avail: NTIS HC A21/MF A01

The natural convection in a rectangular container driven by surface tension gradient is investigated in the laboratory and the Marangoni effect under microgravity is estimated. The flow patterns are visualized and the velocity distributions are obtained under various thermal conditions and aspect ratios. The flow and the temperature fields of the Marangoni convection strongly depend on the coupled buoyant convection and the aspect ratio of the

liquid layer. Thin wires placed on the free surface and the external magnetic field reduce the convective motion considerably and are expected to be effective means for obtaining desirable flow conditions. Author (ESA)

N86-10244# Universidad Politecnica de Madrid (Spain). Lab. de Aerodinamica.
STABILITY OF LONG LIQUID COLUMNS c34
J. Meseguer *In* ESA Fifth European Symp. on Mater. Sci. under Microgravity. Results of Spacelab 1 Dec. 1984 p 297-300 refs (For primary document see N86-10200 01-16)
Avail: NTIS HC A21/MF A01

Analytical expressions for minimum volume stability limits of long liquid bridges having cylindrical volume are reviewed and compared with numerical results. These expressions show the dependence of stability limits on the length of the liquid column and the microgravity level. Unequal disk effects are added, and the resulting expression extended to the case of noncylindrical volume configurations through a linear analysis of interface equilibrium shapes. Author (ESA)

N86-10245# Mons Univ. (Belgium). Faculty of Sciences.
RAYLEIGH-BENARD INSTABILITY IN SYSTEMS PRESENTING A MINIMUM IN SURFACE TENSION c34
D. Villers and J. K. Platten *In* ESA Fifth European Symp. on Mater. Sci. under Microgravity. Results of Spacelab 1 Dec. 1984 p 301-305 refs (For primary document see N86-10200 01-16)
Avail: NTIS HC A21/MF A01

It is shown that in the Benard configuration, when the temperature of the upper surface is exactly Tmin, the Marangoni number is equal to zero and therefore Marangoni convection should be suppressed. The rest state (linearly stable) is unstable with respect to at least one particular type of perturbation, provided that the curvature of surface tension is important and, simultaneously, the initial temperature fluctuation exceeds a critical threshold. Author (ESA)

N86-10246*# National Aeronautics and Space Administration. Marshall Space Flight Center, Huntsville, Ala. Space Science Lab.
SEPARATION OF AQUEOUS TWO-PHASE POLYMER SYSTEMS IN MICROGRAVITY c12
J. M. VanAlstine, J. M. Harris (Alabama Univ., Huntsville), S. Synder, P. A. Curreri, S. B. Bamberger (Oregon Health Sciences Univ.), and D. E. Brooks (Oregon Health Sciences Uni.) *In* ESA Fifth European Symp. on Mater. Sci. under Microgravity. Results of Spacelab 1 Dec. 1984 p 309-312 refs Sponsored by Universities Space Research Association (For primary document see N86-10200 01-16)
(Contracts NAS8-35333; NAS8-35334; NAS8-35362)
Avail: NTIS HC A21/MF A01 CSCL 22A

Phase separation of polymer systems in microgravity is studied in aircraft flights to prepare shuttle experiments. Short duration (20 sec) experiments demonstrate that phase separation proceeds rapidly in low gravity despite appreciable phase viscosities and low liquid interfacial tensions (i.e., 50 cP, 10 micro N/m). Ostwald ripening does not appear to be a satisfactory model for the phase separation mechanism. Polymer coated surfaces are evaluated as a means to localize phases separated in low gravity. Contact angle measurements demonstrate that covalently coupling dextran or PEG to glass drastically alters the 1-g wall wetting behavior of the phases in dextran-PEG two phase systems.
Author (ESA)

N86-10247*# National Aeronautics and Space Administration. Marshall Space Flight Center, Huntsville, Ala. Dept. of Pathology and Chemistry.
RATIONALE FOR TWO PHASE POLYMER SYSTEM MICROGRAVITY SEPARATION EXPERIMENTS c12
D. E. Brooks (British Columbia Univ.), S. B. Bamberger (Oregon Health Sciences Univ.), J. M. Harris (Alabama Univ., Huntsville), and J. VanAlstine *In* ESA Fifth European Symp. on Mater. Sci. under Microgravity. Results of Spacelab 1 Dec. 1984 p 315-318 refs Sponsored in part by NASA (For primary document see N86-10200 01-16)
(Grant USPN-HL-23374)
Avail: NTIS HC A21/MF A01 CSCL 22A

The two-phase systems that result when aqueous solutions of dextran and poly(ethylene glycol) are mixed at concentrations above a few percent are discussed. They provide useful media for the partition and isolation of macromolecules and cell subpopulations. By manipulating their composition, separations based on a variety of molecular and surface properties are achieved, including membrane hydrophobic properties, cell surface charge, and membrane antigenicity. Work on the mechanism of cell partition shows there is a randomizing, nonthermal energy present which reduces separation resolution. This stochastic energy is probably associated with hydrodynamic interactions present during separation. Because such factors should be markedly reduced in microgravity, a series of shuttle experiments to indicate approaches to increasing the resolution of the procedure are planned.
Author (ESA)

N86-10248# Alabama Univ., Huntsville. Dept. of Chemistry.
APPLICATION OF THE THEORY OF OSTWALD RIPENING TO MICROGRAVITY PHASE SEPARATION EXPERIMENTS c12
J. K. Baird *In* ESA Fifth European Symp. on Mater. Sci. under Microgravity. Results of Spacelab 1 Dec. 1984 p 319-321 refs Sponsored by Alabama University (For primary document see N86-10200 01-16)
Avail: NTIS HC A21/MF A01

A heuristic derivation of the theory of Ostwald ripening which is correct up to constants of the order of unity is applied to the separation of aqueous solutions of dextran and polyethylene glycol, used in the phase partitioning of biological cells. In the absence of gravity, it is calculated that the suspension should be stable for > 1 yr. Author (ESA)

N86-10249# Deutsche Forschungs- und Versuchsanstalt fuer Luft- und Raumfahrt, Cologne (West Germany). Inst. for Space Simulation.
HOLOGRAPHIC INTERFEROMETRY NEAR GAS/LIQUID CRITICAL POINTS: GROUND-BASED STUDY OF A D1 EXPERIMENT c34
H. Klein and K. Wanders *In* ESA Fifth European Symp. on Mater. Sci. under Microgravity. Results of Spacelab 1 Dec. 1984 p 323-325 refs (For primary document see N86-10200 01-16)
Avail: NTIS HC A21/MF A01

Ground-based investigations for a Spacelab Holographic Optics Laboratory study of density distribution in three cells filled with SF6 at different near-critical densities cycled through the critical temperature are described. Results show that cooling is so fast that gravity-induced free convection can develop in the sample. As a result, temperature gradients are formed which, via thermal expansion coefficient, cause density gradients, like gravity via compressibility. At the critical point, thermal expansion coefficient and compressibility are singular; the density gradients caused by temperature gradients and gravity are large. For small cooling rates and gravitational effects, density distribution is greatly affected by temperature gradients produced from outside or by temperature gradients produced as a result of adiabatic mass rearrangements inside the sample. Author (ESA)

N86-10250# Technische Univ., Munich (West Germany). Lehrstuhl A fuer Thermodynamik.
NUCLEATE POOL BOILING IN SUBCOOLED LIQUID UNDER MICROGRAVITY: RESULTS OF TEXUS EXPERIMENTAL INVESTIGATIONS c34
M. Zell, J. Straub, and A. Weinzierl *In* ESA Fifth European Symp. on Mater. Sci. under Microgravity. Results of Spacelab 1 Dec. 1984 p 327-333 refs Sponsored by Bundesministerium fuer Forschung und Technologie (For primary document see N86-10200 01-16)
Avail: NTIS HC A21/MF A01

Experiments on subcooled nucleate pool boiling in microgravity were carried out to separate gravity driven effects on heat

transfer within the boiling process. A ballistic trajectory by sounding rocket flight (TEXUS 5 and 10) achieved a gravity level of a/g = 0.0001 for 360 sec. For determination of geometrical effects on heat transport two different experimental configurations (platinum wire and flat plate) were employed. Boiling curves and bubble dynamics recorded by cinematography lead to gravity independent modelling of the boiling phenomena. The results ensure the applicability and high efficiency of nucleate pool boiling for heat exchangers in space laboratories. Author (ESA)

N86-10251# Technische Univ., Munich (West Germany). Lehrstuhl A fuer Thermodynamik.

ISOCHORIC SPECIFIC HEAT OF SULFUR HEXAFLUORIDE AT THE CRITICAL POINT. A SPACELAB EXPERIMENT FOR THE GERMAN D1-MISSION IN 1985 **c18**

K. Nitsche, J. Straub, and R. Lange *In* ESA Fifth European Symp. on Mater. Sci. under Microgravity. Results of Spacelab 1 Dec. 1984 p 335-340 refs Sponsored by Bundesministerium fuer Forschung und Technologie (For primary document see N86-10200 01-16)

Avail: NTIS HC A21/MF A01

The mechanical and functional concept of a space qualified scanning ratio calorimeter for measuring the isochoric specific heat of SF6 near the critical point is presented. The microgravity relevance of this experiment is discussed and underlined by laboratory measurements, the hydrostatic height of the specimen being varied. In 1-g reference experiments the critical exponent and parameters for cv are determined. Critical relaxation effects are taken into account by a functional time profile for the Spacelab experiment. Author (ESA)

N86-10252# Milan Univ. (Italy).

SURFACE FORCES IN CONTACTING SOLIDS **c26**

G. Poletti and D. Cambiaghi (Centrotecnica) *In* ESA Fifth European Symp. on Mater. Sci. under Microgravity. Results of Spacelab 1 Dec. 1984 p 341-346 refs (For primary document see N86-10200 01-16)

Avail: NTIS HC A21/MF A01

A dynamic experiment on surface forces in contacting solids to be performed within the TEXUS rocket program is discussed. It measures surface force and surface energy in the contact area between real bodies and assesses their dependence on mechanical, physical and geometrical parameters. A small metallic sphere impacts against a metal target and time behavior of contact force, contact time, and restitution coefficient are measured as a function of the incoming sphere velocity. Computer simulation of the experiment indicates that suitable conditions exist in which surface force effects can be measured. To fulfill these conditions the experiment must be carried out in microgravity under ultrahigh vacuum. The experimental device is discussed together with the value of the parameters chosen for the experiment. Author (ESA)

N86-10253# Lyon-1 Univ. (France).

SPACE EXPERIMENT ON THERMAL DIFFUSION. PREPARATION AND THEORETICAL ANALYSIS **c34**

J. Bert, D. Henry, P. Layani, G. Chuzeville, J. Dupuy, and B. Roux (Marseille Univ.) *In* ESA Fifth European Symp. on Mater. Sci. under Microgravity. Results of Spacelab 1 Dec. 1984 p 347-352 refs Sponsored by CNES (For primary document see N86-10200 01-16)

Avail: NTIS HC A21/MF A01

A spaceborne experiment on the Soret coefficient of a binary solution is suggested. Analysis of the experimental problems in measuring emf variations induced by thermal diffusion on a AgIxKI(1-x) system indicates a thermodiffusion cell design. A mathematical treatment of the convective problem in a case close to experimental conditions, and with two microgravity levels is outlined. The separations (normalized to 1 for pure Soret effect) are 0.46 and 0.98 for g = 0.001 and 0.0001, respectively, indicating that 0.0001 is a threshold for the separation regime (corresponding to an unperturbed separation). A cell size decrease to check the measurement validity is proposed. Author (ESA)

N86-10254# Technische Univ., Clausthal-Zellerfeld (West Germany). Inst. fuer Nichtmetallische Werkstoffe.

SHRINKING OF A GAS BUBBLE IN A GLASS MELT UNDER MICROGRAVITY CONDITIONS **c12**

V. Rosenkranz and G. H. Frischat *In* ESA Fifth European Symp. on Mater. Sci. under Microgravity. Results of Spacelab 1 Dec. 1984 p 353-357 refs Sponsored by Bundesministerium fuer Forschung und Technologie (For primary document see N86-10200 01-16)

Avail: NTIS HC A21/MF A01

Shrinking of a helium bubble in a glass melt at 1100 C was observed under microgravity for 93 min by taking photographs every minute. The diffusion coefficient was determined from the radius-time data. The bubble shrinks almost linearly with time to a residual volume of 10%, while its center remains stationary. No motion due to Marangoni convection or residual gravity is observed. The experiment ran fully automatically in a MAUS container during the STS-11 mission. Author (ESA)

N86-10255# Technische Univ., Munich (West Germany).

PHYSICAL AND CHEMICAL PROPERTIES OF A NICKEL CATALYST PROCESSED UNDER MICROGRAVITY **c12**

H. Riepl *In* ESA Fifth European Symp. on Mater. Sci. under Microgravity. Results of Spacelab 1 Dec. 1984 p 359-363 refs (For primary document see N86-10200 01-16)

Avail: NTIS HC A21/MF A01

A nickel catalyst processed under microgravity was compared with a reference sample produced on Earth. The examination methods are hydrogen peroxide decomposition, stereoselective hydrogenation with hydrazine, and physical methods. An abnormal thermal behavior of the microgravity processed catalyst is found. Kinetic data differ from normal. Electron microscopy and X-ray indicate analysis a different structure of the payload catalyst. Author (ESA)

N86-10256# Royal Inst. of Tech., Stockholm (Sweden). Dept. of Casting Metals.

A PRELIMINARY REPORT ON FLOATING ZONE EXPERIMENTS WITH GERMANIUM CRYSTALS IN A SOUNDING ROCKET **c12**

T. Carlberg *In* ESA Fifth European Symp. on Mater. Sci. under Microgravity. Results of Spacelab 1 Dec. 1984 p 367-373 refs (For primary document see N86-10200 01-16)

Avail: NTIS HC A21/MF A01

Dopant homogeneity was studied in floating zone experiments in a sounding rocket. It is found that convective mixing occurs in space and on Earth. Fluid dynamic analysis shows that Marangoni convection causes mixing in the space samples. Results from samples processed on Earth indicate stronger convection. Author (ESA)

N86-10257# Deutsche Forschungs- und Versuchsanstalt fuer Luft- und Raumfahrt, Cologne (West Germany). Inst. for Space Simulation.

TRANSPORT PROCESSES IN DIRECTIONAL SOLIDIFICATION DURING SPACE SHUTTLE FLIGHT **c12**

H. Klein, R. Naehle, and K. Wanders *In* ESA Fifth European Symp. on Mater. Sci. under Microgravity. Results of Spacelab 1 Dec. 1984 p 375-378 refs (For primary document see N86-10200 01-16)

Avail: NTIS HC A21/MF A01

The conditions for producing solid metallic dispersions from the melt under microgravity were studied during STS-7. The system CsCl with second phase inclusions (air bubbles and Pb drops) was selected as transparent model material for a solidifying metal. About 200 photographs were taken during melting and directional solidification of the CsCl matrix. Results confirm metal-like solidification of CsCl. Features identified in the photographs include solidification front distortions induced by Marangoni convection, air bubble and Pb drop motions caused by gravitationally driven convection, and particle pushing by the solidification front. Author (ESA)

N86-10258# Deutsche Forschungs- und Versuchsanstalt fuer Luft- und Raumfahrt, Cologne (West Germany). Inst. for Space Simulation.

STABILITY OF METALLIC DISPERSIONS c12

H. Otto *In* ESA Fifth European Symp. on Mater. Sci. under Microgravity. Results of Spacelab 1 Dec. 1984 p 379-388 refs (For primary document see N86-10200 01-16)

Avail: NTIS HC A21/MF A01

An experiment to investigate the stability of metallic dispersions was flown aboard STS-7 in 2 MAUS containers mounted on the carrier OSTA-2. The gallium-mercury with a miscibility gap in the liquid state was used to form the dispersed state in a sample under microgravity conditions. The sample was cooled into the miscibility gap with different cooling rates but no solidification was attempted. The appearance of the liquid/liquid dispersion of mercury droplets in a gallium matrix was recorded by X-ray transmission photography. About 100 X-ray photographs were obtained for evaluation of homogenization, precipitation, aging, and droplet growth. Author (ESA)

N86-10259# Deutsche Forschungs- und Versuchsanstalt fuer Luft- und Raumfahrt, Cologne (West Germany). Inst. for Space Simulation.

UNDERCOOLING INVESTIGATIONS ON THE EASY GLASS FORMER Pd-Cu-Si c12

D. M. Herlach, R. Willnecker, and F. Gillessen *In* ESA Fifth European Symp. on Mater. Sci. under Microgravity. Results of Spacelab 1 Dec. 1984 p 389-397 refs (For primary document see N86-10200 01-16)

Avail: NTIS HC A21/MF A01

The undercooling behavior of the easy glass former Pd77.5Cu6Si16.5 was studied under high vacuum. Formation of the intermetallic phase Pd3Si initiates the solidification of the undercooled melt. Reducing this heterogeneous nucleation within the volume extends undercooling up to 310K enabling the formation of 2 distinct metastable phases both crystalline and nucleated at the surface. Transformation kinetics of heterogeneous nucleation is estimated and compared with homogeneous nucleation rates as determined within nucleation theory. Author (ESA)

N86-10260# Deutsche Forschungs- und Versuchsanstalt fuer Luft- und Raumfahrt, Cologne (West Germany). Inst. for Space Simulation.

CONTAINERLESS UNDERCOOLING OF Ni c12

D. M. Herlach, R. Willnecker, and F. Gillessen *In* ESA Fifth European Symp. on Mater. Sci. under Microgravity. Results of Spacelab 1 Dec. 1984 p 399-402 refs (For primary document see N86-10200 01-16)

Avail: NTIS HC A21/MF A01

An electromagnetic levitation apparatus for containerless melts and solidification of metallic systems is described. Undercooling experiments on Ni within an Al2O3 crucible and in containerless state show that eliminating heterogeneous nucleation due to container walls enables an enlargement of undercooling by a factor of 4. However, the electromagnetic levitation technique is limited to high melting point metals. A lower limit in attainable temperature of 1000K in the containerless process can be given due to the high power absorption necessary to levitate heavy samples as metals with densities of > several g/cc under 1 g conditions. The only possibility to overcome this limitation is the use of a reduced gravity environment. Author (ESA)

N86-10261*# National Aeronautics and Space Administration. Lewis Research Center, Cleveland, Ohio.

DENDRITIC SOLIDIFICATION IN A BINARY ALLOY MELT: STEADY-STATE VERSUS MORPHOLOGICAL STABILITY THEORIES c12

V. Laymanan *In* ESA Fifth European Symp. on Mater. Sci. under Microgravity. Results of Spacelab 1 Dec. 1984 p 403-407 refs Sponsored in part by NASA (For primary document see N86-10200 01-16)

Avail: NTIS HC A21/MF A01

A model for dendritic growth in a binary alloy melt, in the presence of a positive temperature gradient in the liquid, is presented. The model describes satisfactorily the transition from a dendritic interface to a planar interface at very low and very large growth rates. A dendrite tip stability parameter is derived, strictly from steady state considerations, without resorting to a perturbation analysis. The estimates of the parameter agree with those obtained by models based on perturbation analyses. Author (ESA)

N86-10262# Commissariat a l'Energie Atomique, Grenoble (France). Lab. d'Etude de la Solidification.

CELLULAR MORPHOLOGIES IN LEAD-THALLIUM ALLOYS c12

B. Billia (Faculte des Sciences St-Jerome, Marseille), H. Jamgotchian (Faculte des Sciences St.-Jerome, Marseille), J. J. Favier, and D. Camel *In* ESA Fifth European Symp. on Mater. Sci. under Microgravity. Results of Spacelab 1 Dec. 1984 p 409-412 refs Sponsored by CNES (For primary document see N86-10200 01-16)

Avail: NTIS HC A21/MF A01

Unidirectionally grown lead-thallium alloys were chosen for a comparative study of the cellular strucutres obtained on Earth with cells solidified under microgravity during the Spacelab D1 mission. Results show that whatever the orientation of growth with respect to the gravity field, on Earth there is convection in the liquid phase. Thus only under reduced gravity is it possible to lower convection enough for transport in the melt to be essentially by diffusion. Author (ESA)

N86-10263# Ceskoslovenska Akademie Ved, Prague. Inst. of Physics.

EXPERIMENTAL FACILITY FOR MATERIALS RESEARCH IN SPACE (CSK-1) c18

C. Barta, A. Triska, J. Trinka, and L. L. Regel (Academy of Sciences, Moscow) *In* ESA Fifth European Symp. on Mater. Sci. under Microgravity. Results of Spacelab 1 Dec. 1984 p 413-415 (For primary document see N86-10200 01-16)

Avail: NTIS HC A21/MF A01

Equipment designed for studying material solidification and crystallization processes under zero-gravity conditions was developed. A series of 19 pre-programmed experiments can be performed without the direct presence of an operator. Each experiment has its own temperature and movement control and can be run in any sequence. The next series of experiments can be run after exchange of the chamber with specimens and of the cassette of the recorder tape where program and data of previous series of experiments are recorded. Author (ESA)

N86-10264*# Gelles (S. H.) Associates, Columbus, Ohio.

SPACE SHUTTLE EXPERIMENTS ON Al-In LIQUID PHASE MISCIBILITY GAP (LPMG) ALLOYS c12

S. H. Gelles and A. J. Markworth (Battelle Columbus Labs., Columbus) *In* ESA Fifth European Symp. on Mater. Sci. under Microgravity. Results of Spacelab 1 Dec. 1984 p 417-422 refs (For primary document see N86-10200 01-16)

(Contract NAS8-32952)

Avail: NTIS HC A21/MF A01

Massive phase separation observed at low-g was studied during the phase separation process while cooling through the miscibility gap under a controlled thermal gradient was investigated. The molten drops which form during the phase separation process appear to move in a direction opposite to that predicted by the theory of thermocapillary droplet motion. A second experiment utilized a plunger arrangement designed to eliminate the surface tension driven convection currents originating at a free surface. This experiment suggests that the free surface does contribute to the coalescence process but that there are other mechanisms which are more important. Author (ESA)

N86-10265# European Space Agency, Paris (France).

FIRST SPACELAB PAYLOAD (FSLP) EXPERIMENTS ON COMPOSITE MATERIALS c24

H. U. Walter *In its* Fifth European Symp. on Mater. Sci. under

Microgravity. Results of Spacelab 1 Dec. 1984 p 425-433 refs (For primary document see N86-10200 01-16)
Avail: NTIS HC A21/MF A01

Liquid phase processing of composite materials in the First Spacelab Payload is summarized. It is shown that spinodal decomposition is not a feasible approach to produce homogeneous composites. Dispersions formed by solidifying heterogeneous mixtures prepared by mixing or formed by nucleation and growth of nuclei are only homogeneous at low volume fractions. Capillarity phenomena play a dominant role in determining the equilibrium configuration under microgravity conditions. Transport of inclusions due to Marangoni flow is observed in many systems; temperature gradients should be kept minimal during cooling and solidification. The influence of added impurities that lower interfacial tension and reduce Marangoni flow should be studied. Ostwald ripening can be studied under diffusion controlled conditions and the interaction of the solidification front with inclusions can be studied without the interference of sedimentation and buoyancy.
Author (ESA)

N86-10266# Commissariat a l'Energie Atomique, Grenoble (France). Lab. d'Etude de la Solidification.
FIRST SPACELAB PAYLOAD (FSLP) EXPERIMENTS IN METALLURGY **c26**
J. J. Favier *In* ESA Fifth European Symp. on Mater. Sci. under Microgravity. Results of Spacelab 1 Dec. 1984 p 435-436 (For primary document see N86-10200 01-16)
Avail: NTIS HC A21/MF A01

The First Spacelab Payload metallurgy experiments consisted of tests of metallurgical technologies in space for direct space application (e.g., vacuum brazing under microgravity); measurement of thermophysical and physical parameters in better conditions, and tests of theories; and elaboration of new or better materials (composites, emulsions, special crystals). The best results emerge from the first two groups of experiments, because the background resulting from ground-based studies is more developed in these cases. Author (ESA)

N86-10267# Eidgenoessische Technische Hochschule, Zurich (Switzerland).
CRYSTAL GROWTH FROM SOLUTIONS AND NUCLEATION FROM THE VAPOR PHASE **c12**
E. Kaldis *In* ESA Fifth European Symp. on Mater. Sci. under Microgravity. Results of Spacelab 1 Dec. 1984 p 439-441 refs (For primary document see N86-10200 01-16)
Avail: NTIS HC A21/MF A01

First Spacelab Payload studies of protein crystallization; growth of insoluble crystals by homogeneous nucleation via precipitation; and nucleation and growth experiments from the vapor phase with the model substance HgJ2 are summarized. Author (ESA)

N86-10268# Battelle Inst., Frankfurt am Main (West Germany).
LIQUIDS AND INTERFACES **c34**
D. Langbein *In* ESA Fifth European Symp. on Mater. Sci. under Microgravity. Results of Spacelab 1 Dec. 1984 p 443-447 (For primary document see N86-10200 01-16)
Avail: NTIS HC A21/MF A01

Spacelab Fluid Physics Module experiments are summarized. The experiments studied capillarity (menisci, drops, wetting, contact angle, coalescence); and interface convection, including bubble/drop migration and growth fronts. Author (ESA)

N86-10269# Weston Observatory, Mass.
VIBRO-ACOUSTIC FORECAST FOR SPACE SHUTTLE LAUNCHES AT VANDENBERG AFB: THE PAYLOAD CHANGEOUT ROOM AND THE ADMINISTRATION BUILDING
F. A. Crowley and E. B. Hartnett Hanscom AFB, Mass. AFGL 31 Oct. 1984 71 p
(Contract F19628-84-C-0011)
(AD-A156944; AFGL-TR-84-0322; SR-2) Avail: NTIS HC A04/MF A01 CSCL 22/4

The Payload Changeout Room and Administration Building vibro-acoustic environment is simulated for Shuttle launches at Vandenberg AFB using local responses and a source term founded on Kennedy Space Center launch pressures. Overpressure emanating from above the Launch Mount at VAFB is materially altered in form and level by site reverberations. Motion produced in simulations regularly approaches or exceeds velocity and acceleration thresholds cited for other launch support structures. Forecasts call for PCR roof displacements toward the PPR exceeding 2.0 cm for most launches. The expected maximum displacement after 5 launches is 3.5 cm. An exceedance of 5 cm can be anticipated over the facility life cycle (about 100 launches). Author (GRA)

17 SPACECRAFT COMMUNICATIONS, COMMAND AND TRACKING

Includes telemetry; space communications networks; astronavigation; and radio blackout.

For related information see also *04 Aircraft Communications and Navigation* and *32 Communications.*

N86-10270# Technische Hogeschool, Eindhoven (Netherlands). Div. of Telecommunications.
DIGITAL TRANSMISSION EXPERIMENTS WITH THE ORBITAL TEST SATELLITE
J. Dijk, A. P. Verlijsdonk, and J. C. Arnbak Oct. 1984 50 p refs (EUT-84-E-144; ISBN-90-6144-144-7; ISSN-0167-9708) Avail: NTIS HC A03/MF A01

Digital satellite communication experiments in the 11/14 GHz band were performed on a 115 km link by OTS (ESA). Equipment was developed and tested via a translator loop. For transmission and reception of RF signals, paraboloid antennas of 3 and 8 m diameter were used. Digital transmission tests were carried out via the OTS-A and OTS-B transponders. Spectra of the transmitted and received signals were measured for different QPSK modulation and demodulation strategies at bit rates of 4 and 8.448 Mbit/sec. Videophone and single channel per carrier digital telephony demonstrations in satellite loop operation were given. Bit error rate was measured for QPSK modulation at bitrates of 4 and 8.448 and 32 kbit/sec. Author (ESA)

18 SPACECRAFT DESIGN, TESTING AND PERFORMANCE

Includes spacecraft thermal and environmental control; and attitude control.

For life support systems see *54 Man/System Technology and Life Support.* For related information see also *05 Aircraft Design, Testing and Performance* and *39 Structural Mechanics.*

N86-10271*# Massachusetts Inst. of Tech., Cambridge. Space Systems Lab.
ROBUST FAILURE DETECTION FILTERS M.S. Thesis
Alejandro Miguel SanMartin 1 Jul. 1985 135 p refs
(Grant NAG1-126)
(NASA-CR-176232; NAS 1.26:176232; SSL-17-85) Avail: NTIS HC A07/MF A01 CSCL 22B

The robustness of detection filters applied to the detection of actuator failures on a free-free beam is analyzed. This analysis is based on computer simulation tests of the detection filters in the presence of different types of model mismatch, and on frequency response functions of the transfers corresponding to the model mismatch. The robustness of detection filters based on a model of the beam containing a large number of structural modes varied dramatically with the placement of some of the filter poles. The dynamics of these filters were very hard to analyze. The design of detection filters with a number of modes equal to the number of sensors was trivial. They can be configured to detect any number

of actuator failure events. The dynamics of these filters were very easy to analyze and their robustness properties were much improved. A change of the output transformation allowed the filter to perform satisfactorily with realistic levels of model mismatch.
Author

N86-10272*# University of Southern California, Los Angeles.
EVALUATION OF A PULSE CONTROL LAW FOR FLEXIBLE SPACECRAFT Final Technical Report, 1 Jun. 1984 - 31 May 1985
Jun. 1985 40 p
(Grant NAG1-471)
(NASA-CR-176233; NAS 1.26:176233) Avail: NTIS HC A03/MF A01 CSCL 22B

The following analytical and experimental studies were conducted: (1) A simple algorithm was developed to suppress the structural vibrations of 3-dimensional distributed parameter systems, subjected to interface motion and/or directly applied forces. The algorithm is designed to cope with structural oscillations superposed on top of rigid-body motion: a situation identical to that encountered by the SCOLE components. A significant feature of the method is that only local measurements of the structural displacements and velocities relative to the moving frame of reference are needed. (2) A numerical simulation study was conducted on a simple linear finite element model of a cantilevered plate which was subjected to test excitations consisting of impulsive base motion and of nonstationary wide-band random excitation applied at its root. In each situation, the aim was to suppress the vibrations of the plate relative to the moving base. (3) A small mechanical model resembling an aircraft wing was designed and fabricated to investigate the control algorithm under realistic laboratory conditions.
G.L.C.

N86-10273*# National Aeronautics and Space Administration, Washington, D. C.
X-RAY SATELLITE Status Report, second quarter 1985
Sep. 1985 44 p Transl. into ENGLISH of "Roentgen Satellit Statusbericht, 2. Quartal 1985" rept. DFVLR-WF2/8734 DFVLR, Cologne, 30 Jun. 1985 p 1-63 Transl. by The Corporate Word, Inc., Pittsburgh, Pa.
(Contract NASw-4006)
(NASA-TM-77923; NAS 1.15:77923; DFVLR-WF2/8734) Avail: NTIS HC A03/MF A01 CSCL 22B

An overview of the second quarter 1985 development of the X-ray satellite project is presented. It is shown that the project is proceeding according to plan and that the projected launch date of September 9, 1987 is on schedule. An overview of the work completed and underway on the systems, subsystems, payload, assembly, ground equipment and interfaces is presented. Problem areas shown include cost increases in the area of focal instrumentation, the star sensor light scattering requirements, and postponements in the data transmission subsystems.
Author

N86-10274*# Lockheed Missiles and Space Co., Palo Alto, Calif.
TEST AND EVALUATE PASSIVE ORBITAL DISCONNECT STRUTS (PODS 3)
R. T. Parmley, W. C. Henninger, S. A. Katz, and I. Spradley Aug. 1985 83 p refs
(Contract NAS2-11946)
(NASA-CR-177368; NAS 1.26:177368) Avail: NTIS HC A05/MF A01 CSCL 22B

The objectives of the Passive Orbital Disconnect Struts (PODS) test are to evaluate modal resonance of the PODS-III supports to obtain engineering data required for use of PODS-III on flight systems; determine possible performance improvements in large LO2/LH2 space applications. (1) Modal Vibration Tests. A modal resonance survey is performed on a set of six PODS-III struts assembled in a dewar simulator. The survey conditions simulate both launch and orbital loadings of the struts. The orbital load range spans a full to an empty tank. The frequencies surveyed cover the range consistent with Shuttle qualification requirements and the principal resonant modes of the strut system. (2) Benefit study. The benefit of using PODS-III supports on OTV and Space Station LO sub 2 and LH sub 2 reference tanks was compared to nondisconnect supports. Four LO sub 2 and LH sub 2 tanks were studied under various conditions: (1) holding the launch resonance at 35 Hz and varying the orbit resonance; (2) analyzing both full and emtpy tanks at launch; (3) varying orbit boundary temperaure; (4) varying the number of struts; (5) varying orbit times; and (6) using or not using vapor cooling.
Author

N86-10275# Air Force Inst. of Tech., Wright-Patterson AFB, Ohio.
NONLINEAR METHODS FOR SPACECRAFT ATTITUDE MANEUVERS Ph.D. Thesis
A. L. Batten 1985 152 p
(AD-A156956; AFIT/CI/NR-85-51D) Avail: NTIS HC A08/MF A01 CSCL 22/1

Spacecraft attitude control is described by a nonlinear dynamic mathematical model. When Euler parameters are used to define the orientation of a spacecraft with respect to an inertial frame, the model takes a certain form where the components of one factor are quadratic or higher order functions of the state vehicles. Large-angle maneuvers have traditionally been accomplished as a succession of small-angle rotations from a sequence of defined operating points about which the model is linearized. Alternatively, a sequence of single axis rotations are performed. These processes are computationally burdensome and are unable to produce fast multi-axial rotational maneuvers.
GRA

N86-10208# Deutsche Forschungs- und Versuchsanstalt fuer Luft- und Raumfahrt, Cologne (West Germany). Inst. fuer Raumsimulation.
THE ISOTHERMAL HEATING FACILITY
K. Wittmann *In* ESA Fifth European Symp. on Mater. Sci. under Microgravity. Results of Spacelab 1 Dec. 1984 p 49-54 refs (For primary document see N86-10200 01-16)
Avail: NTIS HC A21/MF A01

N86-10217# Centre National d'Etudes Spatiales, Toulouse (France).
GRADIENT HEATING FACILITY BEHAVIOR
G. Cambon, B. Castets, O. Boutemy, J. P. Gicquel, R. Aubron, M. Boddaert, and J. Benoit *In* ESA Fifth European Symp. on Mater. Sci. under Microgravity. Results of Spacelab 1 Dec. 1984 p 115-119 refs (For primary document see N86-10200 01-16)
Avail: NTIS HC A21/MF A01

N86-10223# Freiburg Univ. (West Germany). Inst. fuer Kristallographisches.
THE MIRROR HEATING FACILITY: PERFORMANCE AND EXPERIENCES
R. Nitsche *In* ESA Fifth European Symp. on Mater. Sci. under Microgravity. Results of Spacelab 1 Dec. 1984 p 155-156 refs (For primary document see N86-10200 01-16)
Avail: NTIS HC A21/MF A01

N86-10251# Technische Univ., Munich (West Germany). Lehrstuhl A fuer Thermodynamik.
ISOCHORIC SPECIFIC HEAT OF SULFUR HEXAFLUORIDE AT THE CRITICAL POINT. A SPACELAB EXPERIMENT FOR THE GERMAN D1-MISSION IN 1985
K. Nitsche, J. Straub, and R. Lange *In* ESA Fifth European Symp. on Mater. Sci. under Microgravity. Results of Spacelab 1 Dec. 1984 p 335-340 refs Sponsored by Bundesministerium fuer Forschung und Technologie (For primary document see N86-10200 01-16)
Avail: NTIS HC A21/MF A01

N86-10263# Ceskoslovenska Akademie Ved, Prague. Inst. of Physics.
EXPERIMENTAL FACILITY FOR MATERIALS RESEARCH IN SPACE (CSK-1)
C. Barta, A. Triska, J. Trinka, and L. L. Regel (Academy of Sciences, Moscow) *In* ESA Fifth European Symp. on Mater. Sci. under Microgravity. Results of Spacelab 1 Dec. 1984 p 413-415 (For primary document see N86-10200 01-16)
Avail: NTIS HC A21/MF A01

19 SPACECRAFT INSTRUMENTATION

For related information see also *06 Aircraft Instrumentation* and *35 Instrumentation and Photography.*

N86-10276# Defence Research Establishment, Ottawa. (Ontario).
SARSAT LUC (LOCAL USER TERMINAL) TO CMCC (CANADIAN MISSION CONTROL CENTRE) ALERT DATA INTERFACE: A CRITICAL REVIEW
W. R. McPherson and S. Y. Slinn Dec. 1984 47 p
(AD-A156881; DREO-TN-84-24) Avail: NTIS HC A03/MF A01 CSCL 17/2

The transfer of beacon alert data from the SARSAT Local User Terminal (LUT) to the Canadian Mission Control Center (CMCC) has shortcomings. On the one hand, the LUT provides alert data quality indicators which during the SARSAT Demonstration and Evaluation have been demonstrated to be inadequate, while on the other hand, it retains data descriptors which are required by operational personnel. The purpose of this report is to critically review data available at the LUT, determine its operational utility and outline a definition of transfer from the LUT to the CMCC. The potential impact of implementing this definition will be assessed with the aid of historical data. The subject work is documented in terms of the background to the problem, an outline of approach and analytical tools developed, validation of the approach, summary comments and recommendations. GRA

20 SPACECRAFT PROPULSION AND POWER

Includes main propulsion systems and components, e.g., rocket engines; and spacecraft auxiliary power sources.

For related information see also *07 Aircraft Propulsion, 28 Propellants and Fuels,* and *44 Energy Production and Conversion.*

N86-10277 Department of the Air Force, Washington, D.C.
SMALL CARTRIDGE HEATER Patent
F. L. Merritt and C. H. Taylor, inventors (to Air Force) Issued 9 Apr. 1985 5 p Supersedes AD-D010971
(AD-D011784; US-Patent-4,510,377; US-Patent-Appl-SN-577391) Avail: US Patent and Trademark Office CSCL 21/8

A cylindrical core of a ceramic such as alumina (Al2O3) has grooves in the form of a double lead thread. A coil of Nichrome V is placed in the grooves, starting in one lead of the thread and returning in the other. A coil of Nichrome V is placed in the grooves, starting in one lead of the thread and returning in the other. A split ring of a ceramic such as beryllia surrounds the core. The heater is enclosed in a housing of a metal such as Inconel 600. The entire cartridge is only one inch long and 3/16 inch diameter. It is used as a catalyst bed heater for a satellite thruster. GRA

N86-10278*# National Aeronautics and Space Administration. Marshall Space Flight Center, Huntsville, Ala.
ANALYTICAL INVESTIGATION OF SOLID ROCKET NOZZLE FAILURE
Kenneth E. McCoy and J. Hester Aug. 1985 24 p ref
(NASA-TM-86513; NAS 1.15:86513) Avail: NTIS HC A02/MF A01 CSCL 21H

On April 5, 1983, an Inertial Upper Stage (IUS) spacecraft experienced loss of control during the burn of the second of two solid rocket motors. The anomaly investigation showed the cause to be a malfunction of the solid rocket motor. This paper presents a description of the IUS system, a failure analysis summary, an account of the thermal testing and computer modeling done at Marshall Space Flight Center, a comparison of analysis results with thermal data obtained from motor static tests, and describes some of the design enhancement incorporated to prevent recurrence of the anomaly. Author

N86-10279*# National Aeronautics and Space Administration. Lewis Research Center, Cleveland, Ohio.
COMPATIBILITY OF GRAIN-STABILIZED PLATINUM WITH CANDIDATE PROPELLANTS FOR RESISTOJETS
Margaret V. Whalen and Stanley P. Grisnik [1985] 21 p refs Presented at the 18th Intern. Elec. Propulsion Conf., Alexandria, Va., 30 Sep. - 2 Oct. 1985; cosponsored by AIAA, DGLR and JSASS
(NASA-TM-87118; E-2725; NAS 1.15:87118; AIAA-85-2014) Avail: NTIS HC A02/MF A01 CSCL 21I

Resistojets are candidates for space station auxiliary propulsion, and should be characterized by both long life and multipropellant operations, requirements limited by available materials. Grain stabilized platinum is examined for use as a resistojet thruster material. Use of platinum in other applications indicates it can be used at moderately high temperatures for extended periods of time. Past results indicate that grain-stabilized platinum should be sufficiently inert in candidate propellant environments. Therefore, compatibility of platinum-yttria (P/Y2O3) and platinum-zirconia (Pt/ZrO2) with carbon dioxide, methane, hydrogen and ammonia is examined. A series of 1000 hr tests in CO2, H2, and NH3 is conducted at 1400 C and a series of 1000 hr tests in CH4 is conducted at about 500 C. Scanning electron microscopy, Auger electron spectroscopy and depth profiling analysis are then used to determine the effects of propellants on the material surface, to evaluate possible material contamination and to evaluate grain growth. The results indicate that there is carbon deposition on the surface of the Pt/Y2O3 and Pt/ZrO2 in both the CO2 and CH4 environments. In the H2 environment, the Pt/Y2O3 and Pt/ZrO2 specimen surfaces are roughened. After exposure to the NH3 environment, the Pt/Y2O3 and Pt/ZrO2 are roughened and pitted over the entire heated area with some pitted areas along the grain boundaries. SEM photos show grain growth in cross-sectional views of all the Pt/Y2O3 samples and the Pt/ZrO2 samples, except that tested in methane. Mass loss measurements indicate that Pt/Y2O3 and Pt/ZrO2 would last in excess of 200,000 hr in each propellant environment. However, in NH3 both Pt/Y2O3 and Pt/ZrO2 are severely pitted, with voids up to 50 percent into the material. Pt/Y2O3 and Pt/ZrO2 are not recommended for high temperature service in NH3. Author

N86-10280*# National Aeronautics and Space Administration. Lewis Research Center, Cleveland, Ohio.
RAPID EVALUATION OF ION THRUSTER LIFETIME USING OPTICAL EMISSION SPECTROSCOPY
Brian A. Rock (Arizona State Univ.), Maris A. Mantenieks (Arizona State Univ.), and Michael L. Parsons 1985 47 p refs Presented at the 18th Intern. Elec. Propulsion Conf., Alexandria, Va., 30 Sep. - 2 Oct. 1985; cosponsored by AIAA, JSASS, and DGLR
(NASA-TM-87103; E-2700; NAS 1.15:87103; AIAA-85-2011) Avail: NTIS HC A03/MF A01 CSCL 21H

A major life-limiting phenomenon of electric thrusters is the sputter erosion of discharge chamber components. Thrusters for space propulsion are required to operate for extended periods of time, usually in excess of 10,000 hr. Lengthy and very costly life-tests in high-vacuum facilities have been required in the past to determine the erosion rates of thruster components. Alternative methods for determining erosion rates which can be performed in relatively short periods of time at considerably lower costs are studied. An attempt to relate optical emission intensity from an ion bombarded surface (screen grid) to the sputtering rate of that surface is made. The model used a kinetic steady-state (KSS) approach, balancing the rates of population and depopulation of ten low-lying excited states of the sputtered molybdenum atom (MoI) with those of the ground state to relate the spectral intensities of the various transitions of the MoI to the population densities. Once this is accomplished, the population density can be related to the sputtering rate of the target. Radiative and collisional modes of excitation and decay are considered. Since actual data has not been published for MoI excitation rate and decay constants, semiempirical equations are used. The calculated sputtering rate and intensity is compared to the measured intensity and sputtering rates of the 8 and 30 cm ion thrusters. Author

N86-10281*# National Aeronautics and Space Administration. Lewis Research Center, Cleveland, Ohio.
EXPERIMENTAL PERFORMANCE OF A 1-KILOWATT ARCJET THRUSTER
Shigeo Nakanishi 1985 30 p refs
(NASA-TM-87131; E-2744; NAS 1.15:87131) Avail: NTIS HC A03/MF A01 CSCL 21C

A formerly unused cathode and anode/nozzle assembly from a flight model arcjet was tested with nitrogen, hydrogen, and nitrogen-hydrogen mixture simulating ammonia decomposition products at arc power levels from about 300 to 950 W. Two different power sources and two nozzle configurations were tested at low back-ground pressures to exclude facility effects. Increased nozzle expansion ratio improved cold flow nozzle efficiency from 0.8 to 0.9. Hydrogen thrust efficiency of 0.26 at 872 sec specific impulse matched some 1964 performance on a similar device. Simulated ammonia thrust efficiency was 0.31 at 422 sec. Spontaneously occurring voltage mode changes at constant arc current could be partially stabilized with appropriate power source characteristics. In the higher voltage mode specific impulse was higher, but thrust efficiency changed only slightly from that of the lower voltage mode. Sustained tests of up to 2 hr duration exhibited no apparent performance degradation with time. Author

N86-10005# Air Force Systems Command, Wright-Patterson AFB, Ohio. Foreign Technology Div.
THEORETICAL SPECIFIC IMPULSE FOR TWO-PHASE FLOW IN NOZZLE OF ROCKET-RAMJET ENGINE: A SIMPLE ESTIMATION METHOD
Bi Shiguan (China Precision Machinery Co.) *In its* Acta Aeron. et Astronautica Sinica (FTD-ID(RS)T-1120-84) 4 Oct. 1984 p 53-60 refs Transl. into ENGLISH from Hangkong Xuebao (China), v. 4, no. 4, 1984 p 101-104 (For primary document see N86-10001 01-01)
Avail: NTIS HC A04/MF A01 CSCL 21/8

23 CHEMISTRY AND MATERIALS (GENERAL)

Includes biochemistry and organic chemistry.

N86-10282 Department of the Army, Washington, D. C.
RECOVERY OF ALCOHOL FROM A FERMENTATION SOURCE BY SEPARATION RATHER THAN DISTILLATION Patent
D. C. Sayles, inventor (to Army) Issued 2 Apr. 1985 5 p
(AD-D011782; US-Patent-4,508,929; US-Patent-Appl-SN-455362; US-Patent-Class-568-923) Avail: US Patent and Trademark Office CSCL 07/3

Ethanol is recovered from fermentation products by a countercurrent extraction process which employs diethyl ether as the extraction process which employs diethyl ether as the extraction solvent to form a diethyl ether-ethanol mixture. The ethanol is salted out by adding calcium chloride to the mixture, and the diethyl ether layer is separated and recycled. The calcium chloride in ethanol solution is removed by adding sodium carbonate to form the solids calcium carbonate and sodium chloride which are removed by filtration. The ethanol is recovered as the filtrate.
Author (GRA)

N86-10283# Columbia Univ., New York. Dept. of Chemistry.
A PROCEDURE IDENTIFYING A POLYACETYLENE INITIATOR OF OLEFIN METATHESIS. THE REACTIVITIES OF METAL-CARBENES TOWARD ALKENES AND ALKYNES
C. C. Han and T. J. Katz 10 Jul. 1985 63 p
(Contract N00014-79-C-0683)
(AD-A156997; AD-E950724; TR-11) Avail: NTIS HC A04/MF A01 CSCL 07/3

When phenylacetylene plus tungsten hexachloride initiate the metathesis of cyclopentene, poly(phenylacetylene) is found attached to the resulting polypentenamer chains. The average amount of this poly(phenylacetylene) does not vary as the growth of the polypentenamer chains is checked by added diphenylacetylene, showing it to be present as a block at their start. The implication is that the metathesis is initiated by the growning acetylene writing with the olefin, strong evidence for the hypothesis that the acetylene polymerizatrion is propagated by metal-carbenes. The variations that occur in the length of the chains and the amount of poly(phenylacetylene) attached to the average chain as the acetylene concentration is varied are analyzed for the underlying kinetic parameters. The stabilized metal-carbenes propagating the phenylacetylene polymerization react 3,000 times more quickly with phenylacetylene than with cyclopentene, whereas the less stabilized metal-carbenes propagating the cyclopentene, metathesis select 17-fold in the opposite direction. Diphenylacetylene is 26 times more effective than phenylacetylene in quenching the metathesis, and 2.4 times more effective than phenylmethylacetylene. The key to the experiments is the observation that diphenylacetylene in minute amounts quenches metathesis but does not initiate the reaction. GRA

24 COMPOSITE MATERIALS

Includes laminates.

N86-10284 Yale Univ., New Haven, Conn.
THE MECHANICS OF DELAMINATION IN COMPOSITE MATERIALS Ph.D. Thesis
William Joseph Bottega 1984 114 p
Avail: Univ. Microfilms Order No. DA8509687

A growth law is derived which governs the propagation of an arbitrary shaped delamination embedded in a layered plate, where the plate is of an arbitrary shape as well and is considered to be subjected to edge loading. The phenomenon of delamination buckling and growth is then analyzed to a compressively loaded two layer circular plate containing an initial penny shaped delamination and for a compressively loaded two layer rectangular plate containing an initial thru delamination. An asymptotic technique is used for the postbuckling analysis and the influence of imperfections is also examined. The dynamics of delamination growth in layered plates as a result of delamination buckling is studied in the context of the aforementioned circular plate problem. The interaction of delamination buckling and normal impact is modeled through the application of a uniform transverse tension pulse, simulating the effect of wave front passing through the layer interface, in conjunction with the radial loading. The interfacial response of multilayered plates subject to a time dependent normal point load is found by way of an eigenfunction expansion technique. Dissert. Abstr.

N86-10285 Delaware Univ., Newark.
MECHANICS OF COATED FIBER COMPOSITES Ph.D. Thesis
Yozo Mikata 1984 159 p
Avail: Univ. Microfilms Order No. DA8511217

The mechanics of coated fiber composites were studied. Two types of coated fiber composite are considered: coated short fiber composite, which is modeled as an infinite medium containing two confocal spheroidal inhomogeneities, and coated continuous fiber composite, which is modeled as an infinite medium containing three concentric long circular cylinders. Interaction of fibers is included in the formulation for coated continuous fiber composites, while it is not for coated short fiber composites. Stress fields are obtained for both types of coated fiber composites under thermo-mechanical loadings. A possibility of cracking in coating layer is discussed. Dissert. Abstr.

N86-10286 Illinois Univ., Chicago.
THREE-DIMENSIONAL STRESS SINGULARITIES IN ANISOTROPIC MATERIALS AND COMPOSITES Ph.D. Thesis
Nihal Somaratna 1985 96 p
Avail: Univ. Microfilms Order No. DA8511281

The simplified case of a transversely isotropic material bounded

by one or two axisymmetric conical boundaries is studied analytically. Eigenequations for delta are obtained in terms of Legendre functions of the first and second kind. These results are subsequently used as benchmark tests for the more general numerical method proposed. A finite element scheme is developed for the more general case of a notch/inclusion of an arbitrary shape in a completely anisotropic material. The method is tested against some known results for the stress singularity at the tip of a quarter infinite crack in an isotropic half space and also against the results for the axisymmetric conical notch/inclusion in a transversely isotropic material obtained. Excellent agreement is evident. Then the finite element scheme is used to study the possible existence of stress singularities at 3-d corners in anisotropic materials and also at the free surface tip of a crack normal to the interface of a laminated composite. Dissert. Abstr.

N86-10287 Georgia Inst. of Tech., Atlanta.
THE EFFECT OF DEBOND GROWTH ON CRACK PROPAGATION IN COMPOSITE PLATES REINFORCED WITH ADHESIVELY BONDED COMPOSITE STRINGERS Ph.D. Thesis
Catherine Ann Bigelow 1984 153 p
Avail: Univ. Microfilms Order No. DA8510952

A general solution for the problem of the adhesively bonded stringer was developed. A fundamental analysis was used, assuming that the adherends were in a state of plane stress and the adhesive was in pure shear. Using Green's functions and the complex variable theory of elasticity developed by Lekhnitski, a set of integral equations were solved numerically to produce the shear stress distribution in the adhesive layer. Using these adhesive stresses, equations for the crack tip stress intensity factors were also found. The solution of the integral equations assuming a linear adhesive was presented. The most critical parameter for reducing the stress intensity factors was found to be the distance from the centerline of the crack to the edge of the stringer. The effect of debonding in the adhesive on the stress intensity factors was also examined. In the cases studied, adding a nonlinear adhesive to the debonding decreased the stress intensity factors relative to the linear solution and increased the stress levels necessary to cause debonding. Dissert. Abstr.

N86-10288 Case Western Reserve Univ., Cleveland, Ohio.
FUNDAMENTAL STUDIES OF LOW VELOCITY IMPACT RESISTANCE OF GRAPHITE FIBER REINFORCED POLYMER MATRIX COMPOSITES Ph.D. Thesis
Kenneth James Bowles 1985 255 p
Avail: Univ. Microfilms Order No. DA8510096

A study was conducted to relate the impact resistance of graphite fiber reinforced composites with matrix properties through gaining an understanding of the basic mechanics involved in the deformation and fracture process, and the effect of the polymer matrix structure on these mechanisms. It was found that the resin matrix structure influences the composite impact resistance in at least two ways. The integration of flexibilizers into the polymer chain structure tends to reduce the T sub g and the mechanical properties of the polymer. The reduction in the mechanical properties of the matrix does not enhance the composite impact resistance because it allows matrix controlled failure to initiate impact damage. It was found that when the instrumented drop-weight impact tester is used as a means for assessing resin toughness, the resin toughness is enhanced by the ability of the clamped specimen to deflect enough to produce sufficient membrane action to support a significant amount of the load. The results of this study indicate that crossplied composite impact resistance is very much dependent on the matrix mechanical properties. Dissert. Abstr.

N86-10289 Department of the Air Force, Washington, D.C.
EROSION-RESISTANT NOSETIP CONSTRUCTION Patent
A. R. Taverna and W. S. Thompson, inventors (to Air Force) Issued 7 May 1985 6 p Supersedes AD-D011346; N85-15797
(AD-D011787; US-Patent-4,515,847; US-Patent-Appl-SN-643140; US-Patent-Class-428-107) Avail: US Patent and Trademark Office CSCL 22/2

A pierced fabric carbon-carbon structure is selectively loaded with a particulate material to provide resistance to erosion.
Author (GRA)

N86-10290*# National Aeronautics and Space Administration. Lewis Research Center, Cleveland, Ohio.
PROGRESSIVE DAMAGE, FRACTURE PREDICTIONS AND POST MORTEM CORRELATIONS FOR FIBER COMPOSITES
1985 21 p refs Presented at Intern. Conf.: Post Failure Anal. Tech. Fiber Reinforced Composites, Dayton, Ohio, 1-3 Jul. 1985; sponsored by Air Force
(NASA-TM-87101; E-2695; NAS 1.15:87101) Avail: NTIS HC A02/MF A01 CSCL 11D

Lewis Research Center is involved in the development of computational mechanics methods for predicting the structural behavior and response of composite structures. In conjunction with the analytical methods development, experimental programs including post failure examination are conducted to study various factors affecting composite fracture such as laminate thickness effects, ply configuration, and notch sensitivity. Results indicate that the analytical capabilities incorporated in the CODSTRAN computer code are effective in predicting the progressive damage and fracture of composite structures. In addition, the results being generated are establishing a data base which will aid in the characterization of composite fracture. Author

N86-10291# Michigan Univ., Ann Arbor. Dept. of Materials and Metallurgical Engineering.
PRELIMINARY REPORTS, MEMORANDA AND TECHNICAL NOTES OF THE MATERIALS RESEARCH COUNCIL SUMMER CONFERENCE, LA JOLLA, CALIFORNIA
M. J. Sinnott Jul. 1984 242 p Conf. held at La Jolla, Calif.
(Contract MDA903-84-K-0232; DARPA Order 4000)
(AD-A156776) Avail: NTIS HC A11/MF A01 CSCL 11/4

Papers provided for workshops on the following topics include: Bulk Crystal Growth of Electronic Materials - Strengthening and structure of semiconducting crystals, Formation of new phases from systems that are not in metastable Equilibrium, A mechanism for the reduction in dislocation Density in as-grown GaAs crystals by Indium additions, and Analysis of the potential of a reduced gravity environment for growth of electronic materials; Structure and Properties of Solid Interfaces Relevant to Electronic Materials - Electronic properties of interfaces, Organometallic chemical vapor deposition, Edge cracking of multilayer strained superlattices, Damage of strained superlattices by dislocation injection, and Epitaxial methods for preparing thin semiconducting layers; Integration of Solid State Electronics and Chemical and Biological Systems; Mitigation of Coupling and Shock Waves from Intense Single Pulse Lasers; Optical Interconnects in Computer Networks - Interconnections and VLSI; Fracture Toughness of Advanced Fibrous Composites -Metal matrix composites, Matrix cracking in ceramic-matrix composites, and Shear strength of brittle matrix fiber composites. GRA

N86-10292# Dayton Univ., Ohio.
PROCESS MODELS FOR 3D COMPOSITES Interim Technical Report, 1 Sep. 1981 - 1 Dec. 1983
S. R. Soni and N. J. Pagano Wright-Patterson AFB, Ohio AFWAL Mar. 1985 148 p
(Contract F33615-81-C-5056)
(AD-A156889; AFWAL-TR-85-4002) Avail: NTIS HC A07/MF A01 CSCL 11/4

This work deals with the process environment modeling of carbon-carbon composites. Capabilities of the process environment model (PEM) computer code developed by Science Application Incorporated, California, have been discussed. Users instructions for PEM code have been given. Illustrative examples for different phases of processing of carbon-carbon composites are presented. Close form analytical solutions for impregnation analysis have been derived. A comparison between close from solution results and PEM results has been given. The primary purpose of the PEM is to predict the pressure and temperature environment for the mechanical model. GRA

N86-10265# European Space Agency, Paris (France).
FIRST SPACELAB PAYLOAD (FSLP) EXPERIMENTS ON COMPOSITE MATERIALS
H. U. Walter *In its* Fifth European Symp. on Mater. Sci. under Microgravity. Results of Spacelab 1 Dec. 1984 p 425-433 refs (For primary document see N86-10200 01-16)
Avail: NTIS HC A21/MF A01

N86-10389*# Jet Propulsion Lab., California Inst. of Tech., Pasadena. Ground Antennas and Facilities Engineering Section.
LOAD-DEFLECTION TESTS AND COMPUTER ANALYSES OF A HIGH-PRECISION ADHESIVE-BONDED ANTENNA REFLECTOR PANEL
C. T. Chian and R. Levy *In its* The Telecommun. and Data Acquisition Progr. Rept. 15 Aug. 1985 p 68-81 (For primary document see N86-10382 01-32)
Avail: NTIS HC A10/MF A01 CSCL 11D

25 INORGANIC AND PHYSICAL CHEMISTRY

Includes chemical analysis, e.g., chromatography; combustion theory; electrochemistry; and photochemistry.

For related information see also *77 Thermodynamics and Statistical Physics.*

N86-10293*# National Aeronautics and Space Administration, Washington, D. C.
DETERMINATION OF THERMOPHYSICAL CHARACTERISTICS OF SOLID MATERIALS BY ELECTRICAL MODELLING OF THE SOLUTIONS TO THE INVERSE PROBLEMS IN NONSTEADY HEAT CONDUCTION
L. A. Kozdoba and F. A. Krivoshei Sep. 1985 7 p refs Transl. into ENGLISH from "Thermophysical Properties of Solid Materials" Moscow, Izdatelstvo Nauk, 1973 p 28-31 Original language document announced in IAA as A74-45335 Transl. by Kanner (Leo) Associates, Redwood City, Calif.
(Contract NASw-4005)
(NASA-TM-77907; NAS 1.15:77907) Avail: NTIS HC A02/MF A01 CSCL 07D

The solution of the inverse problem of nonsteady heat conduction is discussed, based on finding the coefficient of the heat conduction and the coefficient of specific volumetric heat capacity. These findings are included in the equation used for the electrical model of this phenomenon. IAA

N86-10294# Defence Research Establishment, Ottawa. (Ontario).
DESIGN AND CALIBRATION OF A FLAT-FLAME BURNER USING LINE REVERSAL TECHNIQUES
D. R. Snelling and M. Fischer Apr. 1985 40 p Original contains color illustrations
(AD-A156724; DREO-TN-85-4) Avail: NTIS HC A03/MF A01 CSCL 21/2

A premixed methane/air flat-flame burner is described. The burner was designed to have a central flame which can be seeded with sodium, and an annular guard flame which ensured a flat temperature profile in the seeded region. The burner produced a well behaved flat flame for linear gas velocities of 20 to 30 cm/s and air to fuel ratios within 15% of stoichiometric. The temperature distribution in the flame was measured for a range of operating conditions using the sodium line-reversal technique. The temperatures measured were within the range 2000 to 2100 K, slightly lower than the adiabatic methane/air flame temperature. This burner will be used as a calibration tool in the development of CARS (Coherent Antistokes Raman Spectroscopy). GRA

N86-10295# National Bureau of Standards, Boulder, Colo. Time and Frequency Div.
COOLED ION FREQUENCY STANDARD Annual Summary Report, FY 1985
D. J. Wineland 1 Jul. 1985 21 p
(Contract N00014-85-F-0004; RR0-1103)
(AD-A156813) Avail: NTIS HC A02/MF A01 CSCL 04/2

The purpose of this work is to develop techniques to overcome the fundamental limits of present frequency standards,the second and residual first-order Doppler shifts. To this end we study suitable frequency reference transitions in ions which are stored on electromagnetic traps and cooled by radiation pressure to $> 1K$. GRA

N86-10296# California Univ., Livermore. Lawrence Livermore Lab.
NEW DIRECTIONS IN CHEMICAL ANALYSIS
T. B. Hirschfeld May 1985 35 p Presented at the IUCCP Symp., College Station, Tex., 1 Apr. 1985
(Contract W-7405-eng-48)
(DE85-012930; UCRL-92731; CONF-8504138-1) Avail: NTIS HC A03/MF A01

The last twenty years have seen a steady increase in the work load of analytical chemistry. A number of procedures have evolved in the analytical laboratory to deal with this increase in work load. By far, the most important one of these is the preponderance of lab automation. Because of the entrance of computers in the laboratories, we can achieve productivity increases that would have been inconceivable without them. The second new procedure that has evolved in analytical chemistry to cope with the work load increase has been the incorporation of systems engineering as a part of the analytical laboratory practice. This paper discusses in depth the role of personal computers and systems engineering in analytical chemistry. DOE

N86-10297# Pacific Northwest Lab., Richland, Wash.
RAPID ANALYSIS USING CAPILLARY SUPERCRITICAL FLUID CHROMATOGRAPHY
B. W. Wright and R. D. Smith Mar. 1985 10 p Presented at the 6th Intern. Symp. on Capillary Chromatography, Riva del Garda, Italy, 16 May 1985
(Contract DE-AC06-76RL-01830)
(DE85-012460; PNL-SA-12698; CONF-8505151-1) Avail: NTIS HC A02/MF A01

Capillary supercritical fluid chromatography (SFC) is proving to be a viable and useful separation method for thermally labile and nonvolatile materials. As with other capillary chromatographic techniques, very fast separations can be accomplished by sacrificing total efficiency and optimizing the conditions for rapid analysis. This is achieved using short, small-bore capillary columns, increased mobile phase linear velocities and very fast pressure programming rates. These principles are demonstrated for the rapid separation of selected component systems. DOE

N86-10298# Sandia Labs., Albuquerque, N. Mex.
THEORETICAL COMPARISON OF CLASSICAL (K-MATRIX) AND INVERSE (P-MATRIX) LEAST-SQUARES METHODS FOR QUANTITATIVE INFRARED SPECTROSCOPY
D. M. Raaland 1985 9 p Presented at the Intern. Conf. on Fourier and Computerized Infrared Spectry., Ottawa, 24 Jun. 1985
(Contract DE-AC04-76DP-00789)
(DE85-012827; SAND-85-02980; CONF-8506118-1) Avail: NTIS HC A02/MF A01

Both classical and inverse least-squares methods have been applied to the quantitative IR spectra analysis of multicomponent samples. The two methods are presented and compared in this paper. The classical method is capable of higher precision and accuracy since it can use all of the data in a spectrum. Its ability to obtain full-spectrum residuals provides methods for identifying problems in the spectral data. The inverse method has the potential advantage that it can be applied even if only one component in the sample is known. DOE

N86-10299# Pacific Northwest Lab., Richland, Wash.
DETERMINING A PHYSICALLY APPROPRIATE NEUTRON SPECTRUM FROM MULTISPHERE DATA
R. I. Scherpelz and I. W. Brackenbush Apr. 1985 22 p Presented at the Health Phys. Soc. Ann. Meeting, Chicago, 26 May 1985

(Contract DE-AC06-76RL-01830)
(DE85-013045; PNL-SA-12888; CONF-8505103-3) Avail: NTIS HC A02/MF A01

The multisphere (or Bonner Sphere) spectrometer system is widely used for the characterization of neutron radiation fields due to its good sensitivity over a wide range of energies. The multisphere data must first be processed by an unfolding code to determine the neutron parameters, and this code must select the spectrum from an infinite number of mathematically correct possibilities. Recent studies have shown that the neutron spectra determined by an unfolding code can be influenced by features of the code such as the choice of initial spectra or the method of smoothing. This study further explores the characteristics of a multisphere measurement and unfolding code that can influence the calculated spectrum and its approximation of a physical realistic neutron spectrum. The use of data from another spectrometer system for setting the initial spectrum is shown to be a very promising technique for generating physically meaningful results. Other factors discussed in this study include the detector response functions and the convergence criteria and duration of iteration. The study shows that the determination of a physically appropriate neutron spectrum can only be accomplished with proper attention to these factors. DOE

N86-10300# New Mexico Univ., Albuquerque.
CATALYTIC ACTIVITY OF SHOCK MODIFIED ZnO FOR CO OXIDATION AND METHANOL SYNTHESIS
F. L. Williams, Y. K. Lee, B. Morosin, and R. A. Graham 22 Jul. 1985 8 p refs Presented at Am. Phys. Soc. Topical Conf. on Shock Waves in Condensed Matter, Spokane, Wash., 22 Jul. 1985
(Contract DE-AC04-76DP-00789)
(DE85-014704; SAND-85-0721C; CONF-850736-19) Avail: NTIS HC A02/MF A01

Alteration of the catalytic activity of inorganic powders by dynamic shock compression has been reported in the literature. Previous work on the effect of shock compression on ZnO catalysis revealed an enhanced activity for CO oxidation that decreased during the rate measurements. Steady-state rate measurements of CO oxidation and methanol synthesis over shock compressed ZnO powers under reaction conditions believed to be transport limitation free is reported. The best explanation of the enhanced catalytic activity of ZnO powders is that shock compression modified the ability of the particle surface to form active centers under reaction conditions. The shock compression probably does not itself put long lived active centers at the surface or major changes in activation energies or selectivity would be observed. However, if local strain or defects were induced in the surface, it would be possible for atomic rearrangement of the surface to result in additional sites like those on unshocked ZnO. In that way, the catalytic chemistry of all the powders would only be different in the number of sites available for catalysis. The minima may then result from a surface distortion in the unshocked powder that is released by a relatively mild shock compression. DOE

N86-10301# Exxon Research and Engineering Co., Annandale, N.J.
LASER RAMAN SPECTROSCOPY STUDY OF THE ZINC AND BROMIDE ION COMPLEX EQUILIBRIUM IN ZINC/BROMINE BATTERY ELECTROLYTES
P. G. Grimes and J. A. Larrabee 1985 5 p Presented at the 168th Meeting of the Electrochem. Soc., Las Vegas, Nev., 13 Oct. 1985
(Contract DE-AC04-76DP-00789)
(DE85-011820; SAND-85-71960; CONF-851048-2) Avail: NTIS HC A02/MF A01

Laser Raman spectroscopy is used to study the zinc and bromide ion complex equilibrium in zinc bromine battery model electrolytes. Solutions of zinc bromide with added KBr, HBr and N-methyl, N-ethyl morpholinium (MEM) bromide are examined and compared. Solutions studied ranged from 1 to 3 molar in zinc and from 2.5 to 8 molar in bromide. A typical Raman spectrum of a zinc bromide solution is shown. Each of the zinc species is identified, Zn(++) (aq), ZnBr(+), ZnBr2 (aq), ZnBr3(-) and ZnBr4(2-). By the use of peak heights or deconvolution/integration along with published Raman cross sections, the amount of each zinc species could be quantitatively determined. The addition of bromide ions to the zinc bromide solutions will shift the equilibrium toward higher bromide complexes. The added cations will influence the shifts. It is noted that the conductivity of the electrolyte decreases when the quaternary ammonium ions are present compared to cations such as potassium or hydrogen. Significantly more free zinc is present in zinc bromide solutions with added KBr than with either MEMBr or HBr. Shifts are also noted with the other zinc ion containing species. It appears that the quaternary ammonium ions and possibly the pH could have a stabilizing effect on zinc bromide complex ion formation. DOE

N86-10302# National Bureau of Standards, Washington, D.C. Center for Fire Research.
SELF-HEATING TO IGNITION MEASUREMENTS AND COMPUTATION OF CRITICAL SIZE FOR SOLAR ENERGY COLLECTOR MATERIALS Final Report
J. J. Loftus Mar. 1985 37 p
(Contract DE-AT01-77DP-70032)
(DE85-011449; NBSIR-85-3122) Avail: NTIS HC A03/MF A01

Kinetic constants of the self-heating reaction are determined for plywood, a retardant treated plywood, and eight samples of polyurethane foam representing possibly two different kinds of foam materials. Under the assumption that self-heating follows a first order reaction, these constants are used to calculate the critical half thickness of slabs of these materials for surface temperatures likely to be experienced during long term use in solar energy collectors. Based on these calculations, estimates are provided on the self-heating or ignition hazards associated with the size and use of these materials in solar energy systems. DOE

N86-10303# Arizona Univ., Tucson. Dept. of Chemistry.
EXTRACTION OF LANTHANIDE IONS BY 2-METHYL-8-QUINOLINOL
S. Taguchi and H. Freiser 1985 14 p refs
(Contract DE-AC02-76ER-04073)
(DE85-014277; DOE/ER-04073/18) Avail: NTIS HC A02/MF A01

The equilibrium extraction behavior of a series of tervalent lanthanides (La, Pr, Eu, Ho, and Yb) with 2-methyl-8-quinolinol (HL) in chloroform has been studied. Although the sterically hindered extractant does not form neutral LnL3 complexes, ion pair complexes of intermediate chelates with either perchlorate or thiocyanate ions are extractable. The extraction constants of such species are smaller than those of other 8-quinolinols and closer together because the adverse steric influence of the 2-methyl group is greater on the heavier lanthanide ions. DOE

N86-10304# Sandia Labs., Albuquerque, N. Mex.
CHEMICAL KINETICS AND CELLULAR STRUCTURE OF DETONATIONS IN HYDROGEN SULPHIDE AND AIR
J. E. Shepherd, A. Sulmistras, A. J. Saber, and I. O. Moen 25 Feb. 1985 31 p refs Presented at the 10th Intern. Colloq. on Dyn. of Explosions and Reactive Systems, Berkeley, Calif., 4 Aug. 1985 Prepared in cooperation with Concordia Univ., Montreal, Quebec
(Contract DE-AC04-76DP-00789)
(DE85-009408; SAND-85-0258C; CONF-850830-2) Avail: NTIS HC A03/MF A01

Analyses of hydrogen sulphide oxidation have been used to characterize the reaction zone structure at temperatures and pressures typical of detonations in mixtures of hydrogen sulphide and air. Detonation reaction zone lengths are calculated for a wide range of compositions, and the variation of these lengths with initial pressure and water vapor dilution are calculated. Estimates of detonation cell size lambda are made based on scaling factors established for other fuel-air systems. These estimates are compared with results obtained in an experimental investigation of the detonability of mixtures of hydrogen sulphide and air. The predicted cell size of 10 cm at stoichiometric composition and standard initial conditions is in excellent agreement with the

experimental results. The predicted variation of cell size also agrees well with the experimental observations over a concentration range of 10 to 20% (by volume) hydrogen sulphide. Based on the d(sub c) = 12lambda estimate of critical tube diameter d(sub c), the minimun critical tube diameter (for a stoichiometric mixture) is 1.3 m. Mixtures of hydrogen sulphide and air are therefore slightly less sensitive to detonation than propane-air mixtures, which have a minimum critical tube diameter of 0.9 m. DOE

N86-10305# Michigan Univ., Ann Arbor. Dept. of Aerospace Engineering.
EFFECTS OF CHEMISTRY AND SWIRL ON THE PRODUCTION OF TURBULENCE IN A FLAME Annual Report, Dec. 1983 - Nov. 1984
J. F. Driscoll Mar. 1985 29 p refs
(PB85-219632; GRI-85/0064) Avail: NTIS HC A03/MF A01 CSCL 13A

The goal of this project is to measure the gas velocity, temperature, and turbulence levels within a swirl stabilized flame while independently varying the swirl number and the air-fuel ratio. The measurements are used to identify how much turbulence and recirculation are needed to obtain a stable flame of a desired length; results are also used to improve current computer models of turbulent combustion so that they can better handle swirl and thus be more useful for the design of practical burners. The measurements are used to assess several computer models. Laser velocimetry and laser Rayleigh scattering diagnostics are used. GRA

26 METALLIC MATERIALS

Includes physical, chemical, and mechanical properties of metals, e.g., corrosion; and metallurgy.

N86-10306 Metals Society, London (England).
MECHANISM OF THE FORMATION OF BORONISED LAYERS ON HIGH CARBON STEEL
A. Galibois, O. Boutenko, and B. Voyzelle Sep. 1984 19 p refs Transl. into ENGLISH from Acta Met., no. 28, 1980 p 1753-1763 Original language document announced in IAA as A81-15771
(BLL-BISI-Trans-23036-(9022.06)) Avail: British Library Lending Div., Boston Spa, Engl.: £13.00; overseas $30.00

The coating of steels and alloys by boronizing is used to improve their resistance to wear and corrosion. Several types of processes used, which differ according to the media, are solid, liquid, or gaseous. The solid medium is the most widespread for technological and economic reasons. Within the solid media, a choice is made between the technology of pastes or powders. The pastes obtain thicker layers for the same duration of treatment, and it is preferred to attain the principal objective, which is to study the composition of the different sections of boronized layers and the mechanism of their formation on the surface of industrial high-carbon steel. E.A.K.

N86-10307 Metals Society, London (England).
BORONISING OF IRON AND STEEL BY IONIC BOMBARDMENT BY DIBORANE
P. Casadesus and C. Frantz Sep. 1984 17 p refs Transl. into ENGLISH from Mem. Sci. Rev. Met. (Paris), v. 75, no. 2, 1978 p 81-91 Original language document announced in IAA as A78-29273
(BLL-BISI-Trans-23034-(9022.06)) Avail: British Library Lending Div., Boston Spa, Engl.: £10.00; overseas $22.50

The possibilities of boronizing iron and steel by ionic bombardment with diborane are discussed. The influence of the principal parameters: composition of atmosphere, nature of substrate, temperature, and length of treatment on the composition and thickness of boronized layers and on their morphology and structure was studied. Various layer arrangements, characterized by different proportions of the borides of iron, FeB and Fe2B, are obtained. The suitability of various types of steel for boronizing over a wide temperature range is studied. The growth rate of the boronized layers, which are produced by the process of ionic bombardment is analyzed. E.A.K.

N86-10308 Metals Society, London (England).
APPLICATION OF THE UNLOADING COMPLIANCE METHODS IN FRACTURE TOUGHNESS MEASUREMENTS OF A QUENCHED AND TEMPERED STEEL
J. Albrecht and C. Wuethrich Oct. 1984 17 p refs Transl. into ENGLISH from Z. Werkstofftech. (West Germany), no. 13, 1982 p 96-103
(BLL-BISI-Trans-21628-(9022.06)) Avail: British Library Lending Div., Boston Spa, Engl.: £13.00; overseas $30.00

The application of the J-integral leads to a considerable reduction of material needed for establishing toughness data. The number of specimens is further reduced by measuring the crack resistance curve in a single specimen. This requires monitoring the crack extension during the experiment. A comparison of several methods showed that the unloading compliance technique is particularly suitable for that purpose. This method was applied for measuring the toughness as a function of location in a large forging of a steel 25 NiCrMo 145. Good toughness values (about 200 MPam sup 1/2) with little scatter were found over the whole cross section of the forging. Author

N86-10309 British Aerospace Aircraft Group, Bristol (England).
PRE-BOND TREATMENT FOR TITANIUM ALLOYS
A. Kennedy, comp. and R. Kohler, comp. 26 Jan. 1984 82 p refs
(Contract MIN-DEF-A93b/1034)
(BAe-AL/MAT/3864; BR91991) Avail: NTIS

Pre-bond surface preparations were investigated to optimize the initial strength and durability properties of 6A1 4V (BS TA10) and CP (BS TA6) titanium metal to metal adhesive joints exposed under conditions of heat, moisture and stress. Anodizing in sodium hydroxide solutions and in sodium hydroxide/hydrogen peroxide mixtures, and treatment in sodium hydroxide/hydrogen peroxide mixtures catalyzed by the additon of heavy metal ions were assessed. It is shown that 10V anodizing at ambient temperature for 30 min in 5M sodium hydroxide solution gives surfaces which form highly durable bonds with epoxy adhesives. This process presents very low operating and environmental hazards and is suitable for large scale continuous production use. The presence of hydrogen peroxide is not necessary and can reduce adhesive bond durability. Titanium/epoxy adhesive joints with acceptable durability can be produced by treating the titanium at ambient temperature in a mixture of 1M sodium hydroxide and 0.5M hydrogen peroxide catalyzed by the addition of 160 mg/l of manganese sulfate. Author (ESA)

N86-10310*# Analytical Services and Materials, Inc., Tabb, Va.
A SIMPLE METHOD OF OBTAINING CONCENTRATION DEPTH-PROFILES FROM X-RAY DIFFRACTION
K. E. Wiedemann and J. Unnam Warrendale, Pa. Metallurgical Society of AIME 1984 13 p refs
(NASA-CR-176262; NAS 1.26:176262; TMS-Paper-F8415) Avail: NTIS HC A02/MF A01 CSCL 11F

The construction of composition profiles from X-ray intensity bands was investigated. The intensity band-to-composition profile transformation utilizes a solution which can be easily evaluated. The technique can be applied to thin films and thick speciments for which the variation of lattice parameters, linear absorption coefficient, and reflectivity with composition are known. A deconvolution scheme with corrections for the instrumental broadening and ak-alfadoublet is discussed. E.A.K.

N86-10311*# National Aeronautics and Space Administration. Lewis Research Center, Cleveland, Ohio.
CREEP-FATIGUE BEHAVIOR OF NiCoCrAlY COATED PWA 1480 SUPERALLOY SINGLE CRYSTALS
Robert V. Miner, John Gayda, and Mohan G. Hebsur 1985 20 p refs Presented at the Symp. on Low-Cycle Fatigue Directions for the Future, Bolton Landing, N.Y., 30 Sep. - 4 Oct. 1985; sponsored

by American Society for Testing Materials
(NASA-TM-87110; E-2710; NAS 1.15:87110) Avail: NTIS HC A02/MF A01 CSCL 11F

Single crystal specimens of a Ni base superalloy, PWA 1480, with a low pressure plasma sprayed NiCoCrAlY coating were tested in various 0.1 Hz fatigue and creep fatigue cycles both at 1015 and 1050 C. Creep fatigue tests of the cp, pc, and cc types were conducted with various constant total strain ranges employing creep dwells at various constant stresses. Considerable cyclic softening occurred as was evidenced particularly by rapidly increasing creep rates in the creep fatigue tests. The cycle time in the creep fatigue tests typically decreased by more than 80 percent at 0.5 N sub f. Though cyclic life did correlate with delta epsilon sub in a better correlation existed with sub f for both the fatigue and creep fatigue tests, and poor correlations were observed with either sigma sub max or the average cycle time. A model containing both delta sigma and delta sigma (sub in), N sub f = alpha delta sigma (sub in) beta delta sigma gamma, with best fit values of sigma for each cycle type, but the same values of beta and gamam, was found to provide good correlations. Life lines were not greatly different among the cycle types, differing only by a factor of about three. The cp cycle life line was lowest for both test temperatures, however among the other three cycle types there was no consistent ranking. For all test types failure occurred predominately by multiple internal cracking originating at pores. The strong correlation of life with delta sigma may reflect a significant crack growth period in the life of the specimens. B.W.

N86-10312*# Spectrolab, Inc., Sylmar, Calif.
DEVELOPMENT OF METALLIZATION PROCESS Final Report
A. Garcia, III Apr. 1985 99 p
(Contracts NAS7-100; JPL-956205)
(NASA-CR-176209; DOE/JPL/956205-85/8; NAS 1.26:176209; DE85-013585; DRL-175) Avail: NTIS HC A05/MF A01 CSCL 11F

The object of this contract is the optimization, evaluation, and demonstration of a novel metallization applied by a screen printing process. A paste consisting of molybdenum, tin, and titanium hydride is selected as the promising composition. No satisfactory cells are made using any of the molybdenum/tin pastes used as a complete replacement for conventional silver pastes. The major problem is the inability to form a bond between the pastes and silicon that withstands soldering. This problem can be overcome by using a two step process where any interconnection to the cell is done at small pads of conventional screen printed silver. The most promising use of the molybdenum/tin metallization system would be this two step process with a silver paste serving as the soldering pad. The Mo/Sn system would compete with silver economically if silver prices rose and could serve as a backup process. The use of a heated stage SEM with reactive gases is a great help in elucidating problems and suggesting solutions. DOE

N86-10313# Department of the Navy, Washington, D. C.
RUSTY BOLT INTERMODULATION INTERFERENCE REDUCER Patent Application
R. Panayappan and J. C. Cooper, inventors (to Navy) Filed 12 Apr. 1985 13 p
(AD-D011748; US-Patent-Appl-SN-722579) Avail: NTIS HC A02/MF A01 CSCL 09/1

In the preferred embodiment of the invention about 20 percent by weight of copper-pyrrolidine-chloride, about 5 percent by weight of polyvinyl pyrrodlidinone, and about 75 percent by weight of ethylene gylcol are mixed to form a viscious green solution which can be applied to metal surfaces by any common means, preferably painting or spraying. The chelating functional groups in PVP and pyrrolidine incorporate the metal of the metal oxide into their structure thus removing the metal oxide from the MOM junction. The PVP is cross-linked by metal ions removed from the metal oxide thus producing a structurally strong, hard material that sets in place and remains there to provide structural integrity at the junction. The PVP is also a mild reducing agent which prevents future oxidative or electrolytic corrosion. GRA

N86-10314# Department of the Navy, Washington, D. C.
PASSIVATION OF STEEL WITH AQUEOUS AMINE SOLUTIONS Patent Application
P. J. Hearst, inventor (to Navy) Filed 3 May 1985 13 p
(AD-D011749; US-Patent-Appl-SN-729849) Avail: NTIS HC A02/MF A01 CSCL 11/6

This is a process that allows previously cleaned steel (which may have been cleaned in any of several different ways) to be passivated with a rinse of almost pure water, that is made slightly alkaline to inhibit corrosion, and flash rusting such that any small residue remaining of the steel surface after drying of the water will itself evaporate and in such a manner that any remaining residue will be incorporated into a subsequently applied non-aqueous protective coating without leaving any water-soluble or ionic residue on the surface of the steel that will cause corrosion or affect adhesion of the protective coating. GRA

N86-10315# Army Materials and Mechanics Research Center, Watertown, Mass.
DEVELOPMENT OF A SHEATH FOR SENSOR PROTECTION IN MOLTEN STEEL APPLICATIONS Final Report
G. G. Bryant, T. V. Hynes, and J. J. Swab May 1985 109 p
(AD-A156764; AMMRC-TR-85-9) Avail: NTIS HC A06/MF A01 CSCL 13/8

Studies were performed to select appropriate candidate materials for development of thermal sensor protective sheaths for liquid steel processing systems. Samples of refractory ceramics were tested in laboratory scale melts and the best ceramic, boron nitride (BN), was tested at industrial scale in a continuous casting tundish. Industrial tests were performed on a prototype sensor sheath system at 1565 + or - 40 C for six tests of approximately five hours each, beginning with cold immersion. The sensor sheath system performed as a temperature monitor and demonstrated a high survivability rate due to the chemical inertness, low wetability high thermal conductivity, and low thermal expansion of the boron nitride. Materials studies included development of representative laboratory test environments, evaluation of failure mechanisms of materials, measurement of erosion/corrosion and wetting/penetration, and compatibility of materials and sensor systems. Analyses included optical microscopy, X-ray diffraction of reaction interface materials, and electron probe detection of the penetration of iron. GRA

N86-10316# Department of the Air Force, Washington, D.C.
LIQUID CRYSTAL NON-DESTRUCTIVE INSPECTION OF METALS Patent Application
G. J. Pech, inventor (to Air Force) Filed 14 Jun. 1985 23 p
(AD-D011772; US-Patent-Appl-SN-744593) Avail: NTIS HC A02/MF A01 CSCL 14/2

This patent application pertains to a non-destructive visual inspection arrangement for ferrous and non-ferrous metallic workpieces. The inspection arrangement employs a liquid crystal indicator medium and electrical current flow through the workpiece to develop potential differences across work surface flaws that are to be detected. The concepts of direct application of the liquid crystal medium to the work area surface and containment of the liquid crystal medium within a viewing device are also included. Author (GRA)

N86-10317# California Univ., Livermore. Lawrence Livermore Lab.
HUGONIOT MEASUREMENTS IN ALUMINUM TO 420 GPa USING THE LLNL TWO-STAGE LIGHT-GAS GUN
G. R. Gathers and A. C. Mitchell Jun. 1985 6 p refs Presented at the Am. Phys. Soc. Topical Conf. on Shock Waves in Condensed Matter, Spokane, 22 Jul. 1985
(Contract W-7405-eng-48)
(DE85-013821; UCRL-92204; CONF-850736-4) Avail: NTIS HC A02/MF A01

Aluminum is a standard material for shock wave experiments.

The increased velocity of our two-stage light-gas gun has been used to extend the range of previous aluminum measurements in order to reduce the gap between laboratory data and the data obtained with the nuclear driven shock inpedance match methods. The experiments reported include direct collision Hugoniot measurements with tantalum impactors and reshock measurements using tantalum impactors and both platinum and copper anvils. DOE

N86-10318# McElroy (Ralph) Co., Austin, Tex.
NONLINEAR PROPAGATION OF ELASTOPLASTIC WAVES IN Ke PENETRATORS (EXCERPTS)
G. F. Kuscher May 1985 143 p Transl. into ENGLISH of "Nicht-Lineare Ausbreitung Elasto-Plastischer Wellen in Ke-Penetratoren" rept. 2/85 Ernst-Mach Inst., Freiburg, West Germany, Feb. 1985 Prepared for California Univ., Livermore, Lawrence Livermore Lab.
(Contract W-7405-eng-48)
(DE85-011450; UCRL-Trans-12061) Avail: NTIS HC A07/MF A01

The characteristic principles of the approximation models are discussed briefly. As a result of the present study, it has been possible for the first time to obtain experimental confirmation of the basic hypotheses of the theory of elastic as well as elastoplastic wave propagation and to obtain dynamic material data corresponding to the theoretical definitions. The one-dimensional elastic and elastoplastic theory of wave propagation is discussed in detail. In general, all authors assume a one-dimensional treatment of wave propagation as the basis for an experimental study of elastoplastic properties of materials in bars. Within the resent study, no experimental findings were obtained, such as boundary influences or dispersion of the elastic wave, which would not justify this type of analysis. DOE

N86-10319# Du Pont de Nemours (E. I.) and Co., Aiken, S.C. Savannah River Lab.
MULTIPURPOSE PAN DEVELOPMENT
G. C. Rodrigues 1985 14 p Presented at the 9th Ann. Actinide Separations Workshop, Richland, Wash., 22 May 1985
(Contract DE-AC09-76SR-00001)
(DE85-012326; DP-MS-85-57; CONF-8505139-2) Avail: NTIS HC A02/MF A01

Savannah River Plant presently uses separate pans for filtration and roasting PuF3 precipitates in the Pu metal finishing line. Savannah River Laboratory has developed a multipurpose pan which uses platinum filter media for filtration and roasting. DOE

N86-10320# Edgerton, Germeshausen and Grier, Inc., Idaho Falls, Idaho.
FRACTURE TOUGHNESS AND STRESS RELIEF RESPONSE OF IRRADIATED TYPE 347/348 STAINLESS STEEL
F. M. Haggag 1985 7 p refs Presented at 8th Intern. Conf. on Struct. Mech. in Reactor Technol., Brussels, 19 Aug. 1985
(Contract DE-AC07-76ID-01570)
Avail: NTIS HC A02/MF A01

A test program has experimentally determined: (1) The fracture toughness of Type 347/348 stainless steel (SS) specimens with high values of irradiation fluence (2.3 to 4.8 x 10 to the 22nd power n/sq. cm. (2), E > 1.0 MeV) and experiencing different levels of irradiation creep (0.0, 0.6, 1.1, 1.8%), (2) the effect of thermal stress relief on fracture toughness recovery for the highly irradiated material, and (3) the mechanisms associated with fracture toughness recovery due to thermal stress relief. The postirradiation fracture toughness tests and tensile tests were conducted at 427 C. DOE

N86-10321# California Univ., Berkeley. Lawrence Berkeley Lab.
ELECTRONIC AND MAGNETIC PROPERTIES OF NOBLE-METAL AND TRANSITION-METAL ALLOYS, INTERFACES AND OVERLAYERS
L. M. Falicov May 1985 12 p refs Presented at 114th AIME Ann. Meeting (includes Soc. of Mining Engr.), New York, 24 Feb. 1985
(Contract DE-AC03-76SF-00098)
(DE85-014532; LBL-19695; CONF-850211-10) Avail: NTIS HC A02/MF A01

The electronic and magnetic properties of noble-metal and transition-metal alloys, interfaces and overlayers are examined theoretically. In particular, results are reported on the electronic and magnetic structure of: (1) nickel-copper alloys; (2) cobalt-iron alloys; (3) nickel-copper interfaces; and (4) chromium, cobalt, nickel and copper overlayers on a variety of substrates. General trends are examined and qualitative rules derived. DOE

N86-10322# Argonne National Lab., Ill.
PORTEVIN-LE CHATELIER EFFECT. 1: MODEL FOR THE TYPE-E SERRATIONS
R. B. Schwarz Jan. 1985 7 p Presented at the 7th Intern. Conf. on the Strength of Met. and Alloys, Montreal, 12 Aug. 1985
(Contract W-31-109-eng-38)
(DE85-006879; CONF-850823-3) Avail: NTIS HC A02/MF A01

A model is advanced for the discontinuous propagation of a Pottevin-Le Chatelier deformation band in tensile tests. The glide resistance is assumed to be a superposition of a time-independent strain hardening component and a time-dependent solute hardening component. The amplitude of the stress serrations, the strain increment across the band, and the propagation of the band per serration are calculated as a function of the work-hardening parameter, and material and machine parameters. The predictions of the model are found in good agreement with measurements. DOE

N86-10323# California Univ., Livermore. Lawrence Livermore Lab.
WORK-HARDENING AND EFFECTIVE VISCOSITY IN SOLID BERYLIUM
D. Steinberg, D. Breithaupt, and C. Honodel Jun. 1985 9 p refs Presented at 10th High Pressure Conf. on Res. in High Pressure Sci. and Technol., Amsterdam, 8 Jul. 1985
(Contract W-7405-eng-48)
(DE85-013978; UCRL-91892; CONF-850759-2) Avail: NTIS HC A02/MF A01

Results from Hopkinson split-bar, plate-impact, and cylinder deceleration experiments on beryllium are compared with hydrodynamic computer code simulations. By substantially increasing the beryllium work-hardening in the Steinberg-Guinan constitutive model, excellent agreement between the experiments and the calculations is achieved. A model to estimate effective viscosity is also proposed and the resultant calculations are in reasonable agreement with those derived from another model advanced by Asay, Chhabildas and Wise. DOE

N86-10324# Sandia Labs., Albuquerque, N. Mex.
WELD METAL HOT-CRACKING OF HASTELLOY ALLOYS C-22 AND C-276: A STUDY BY ANALYTICAL ELECTRON MICROSCOPY
M. J. Cieslak, A. D. Romig, Jr., and T. J. Headley 1985 25 p Presented at the Joint Meeting of the Electron Microscopy Soc. of Am. and the Microbeam Anal. Soc., Lousiville, Ky., 5 Aug. 1985
(Contract DE-AC04-76DP-00789)
(DE85-009437; SAND-85-0098C; CONF-850840-2) Avail: NTIS HC A02/MF A01

Weld metal hot-cracking in multi-component alloys systems is often the result of the formation of small volume fractions of nonequilibrium constituents along solidification grain boundaries. These constituents arise as a result of the segregation phenomenon accompanying weld solidification and often serve to extend the solidification temperature range well below the equilibrium solidus. Purpose of this study is to identify and characterize (crystal structure and composition) by analytical electron microscopy (AFM) the phases associated with weld metal hot-cracking in Hastelloy alloys O-22 and O-276. DOE

N86-10325# Rockwell International Corp., Golden, Colo.
METALLURGY AND METALLOGRAPHY OF BRAZE JOINTS

M. M. McDonald 1985 59 p Presented at the Intern. Metal. Soc. Conf., Denver, 21 Jul. 1985
(Contract DE-AC04-76DP-03533)
(DE85-014563; RFP-3848; CONF-850753-2) Avail: NTIS HC A04/MF A01

Metallographic examination of braze joints involves standard metallographic procedures with a need for special attention to some unique characteristics of braze joints. These unique characteristics include very thin joints and dissimilar metal combinations. The thin joint geometry sometimes requires special sectioning techniques. The dissimilar metal combinations, usually involving soft and hard metals, can result in problems during polishing and etching. Imperfections that one should be on the lookout for in the metallographic examination of braze joints include cracks, entrapped flux, porosity, intermetallics phases, incomplete joining, corrosion, and erosion. In investigating possible origins of failure of braze joints, nonmetallurgical factors should not be overlooked. Improper design, particularly those that result in poor distribution of stress or improper clearances are often responsible for failures of braze joints. inadequate cleaning or protection of parts and incorrect choices of heating process, filler metal and flux may all lead to a poor braze joint. DOE

N86-10326# Battelle Columbus Labs., Ohio.
RESEARCH NEEDS FOR CORROSION CONTROL AND PREVENTION IN ENERGY CONSERVATION SYSTEMS
E. W. Brooman and J. W. Hurwitch Jun. 1985 107 p
(Contract DE-AC06-76RL-01830)
(DE85-014852; PNL-5457) Avail: NTIS HC A06/MF A01

A group of 28 electrochemists, materials scientists, and corrosion engineers is brought together to determine if the government could have a role as a focal point for corrosion R and D, discuss opportunities in fundamental research and solving corrosion problems, and develop a research agenda. Participants from government, industry and academia assembled into four technical discussion groups: localized corrosion, general corrosion, high temperature corrosion, and corrosion control and prevention. Research needs are identified, discussed, then assigned a figure of merit. Some 44 corrosion control and prevention topics are identified as having a high priority for consideration for funding. Another 35 topics are identified as having a medium priority for funding. When classified according to corrosion phenomenon, the areas which should receive the most attention are molten salt attack, crevice corrosion, stress-corrosion cracking, erosion-corrosion, pitting attack, intergranular attack and corrosion fatigue. When classified according to the sector or system involved, those which should receive the most attention are chemical processes, transportation, buildings and structures, electric power generation, and batteries and fuel cells. DOE

N86-10327# California Inst. of Tech., Pasadena. Lab. of Engineering Materials
FORMATION AND CHARACTERIZATION OF AMORPHOUS ERBIUM-BASED ALLOYS PREPARED BY NEAR-ISOTHERMAL COLD-ROLLING OF ELEMENTAL COMPOSITES
M. Atzmon, K. M. Unruh, and W. L. Johnson Jul. 1985 27 p
(Contract DE-AT03-81ER-10870)
(DE85-014853; DOE/ER-10870/156) Avail: NTIS HC A3/MF A01

The formation of bulk single phase amorphous Cu-Er and Ni-Er alloys by extensive cold rolling of elemental foils is reported. The reaction is driven by the negative enthalpies of mixing of the constituent elements and occurs near ambient temperature. The crystallization behavior of the alloys obtained is studied by means of differential scanning calorimetry and found to agree closely with that of the corresponding sputtered and liquid quenched alloys. Radial distribution functions are measured for sputtered and rolled Cu72Er28 and are found to be in good agreement. DOE

N86-10328# Nooter Corp., St. Louis, Mo.
FABRICATION AND METALLURGICAL PROPERTIES OF MODIFIED 9Cr-1 Mo STEEL
M. Jawad, V. K. Sikka, and P. Patriarca 1985 24 p refs Presented at the Am. Petroleum Inst. Midyear Refining Meeting, Kansas City, Mo., 14 May 1985 Prepared in cooperation with ORNL
(Contract DE-AC05-84CR-21400)
(DE85-012885; CONF-8505145-1) Avail: NTIS HC A02/MF A01

A newly developed modified 9 Cr-1 Mo steel has good potential as a replacement for 2 1/4 Cr-1 Mo steel because of its high strength and creep rupture properties at elevated temperatures. Melting, fabrication, mechanical properties, and operating experience in power plants are discussed. Cost comparisons between modified 9 Cr-1 Mo and 2 1/4 Cr-1 Mo steel are also presented. DOE

N86-10329# Oak Ridge National Lab., Tenn.
SWELLING AND TENSILE PROPERTIES OF EBR-2-IRRADIATED TANTALUM ALLOYS FOR SPACE REACTOR APPLICATIONS
M. I. Grossbeck and F. W. Wiffen 1985 34 p refs Presented at the 2nd Symp. on Space Nucl. Power Systems, Albuquerque, N. Mex., 14 Jan. 1985
(Contract DE-AC05-84OR-21400)
(DE85-012887; CONF-850103-10) Avail: NTIS HC A03/MF A01

The tantalum alloys T-111, ASTAR-811C, Ta-10 W, and unalloyed tantalum are examined following EBR-II irradiation to a fluence of 1.7 x 10(26) neutrons/m(2) ($E > 0.1$ MeV) at temperatures from 650 to 950 K. Swelling is found to be negligible for all alloys; only tantalum is found to exhibit swelling, 0.36%. Tensile testing reveals that irradiated T-111 and Ta-10 W are susceptible to plastic instability, but ASTAR-881C and tantalum are not. The tensile properties of ASTAR-811C appear adequate for current SP-100 space nuclear reactor designs. Irradiated, oxygen-doped T-111 exhibits no plastic deformation, and the abrupt failure is intergranular in nature. The absence of plastic instability in ASTAR-811C is encouraging for alloys containing carbide precipitates. These fine precipitates might prevent dislocation channeling, which leads to plastic instability in many bcc metals after irradiation. DOE

N86-10330# Oak Ridge Y-12 Plant, Tenn.
ALUMINUM ION PLATING FOR CORROSION PROTECTION OF URANIUM, REVISION 1
C. M. Egert 25 Apr. 1985 12 p Presented at the US Army Corps of Eng. Ion Plating Workshop, Champaign, Ill., 12 Dec. 1984
(Contract DE-AC05-84OS-21400)
(DE85-012419; Y/DV-404-Rev-1; CONF-841267-1) Avail: NTIS HC A02/MF A01

This report discusses the coating structure and corrosion resistance for two methods of ion plating aluminum on uranium subject to a 100 C temperature limit. The first method is an evaporative technique using aluminum on resistivity heated tungsten filaments. This technique is presented used in production at the Oak Ridge Y-12 Plant for uranium coating processes. Another technique, presently under development, is magnetron bias sputter deposition where a magnetron sputter source replaces the filaments as the source of aluminum. This new technique results in considerable improvement in coating structure and consequently the corrosion resistance. DOE

N86-10331# Sandia Labs., Albuquerque, N. Mex.
METASTABLE PHASE FORMATION IN NI-IMPLANTED AI: AN ANALYTICAL ELECTRON MICROSCOPE INVESTIGATION
D. M. Follstaedt and A. D. Romig, Jr. 1985 17 p Presented at the Joint Meeting of the Electron Microscopy Soc. of Am. and the Microbeam Anal. Soc., Louisville, Ky., 5 Aug. 1985
(Contract DE-AC04-76DP-00789)
(DE85-009105; SAND-85-0262C; CONF-850840-3) Avail: NTIS HC A02/MF A01

By athermally injecting ions with energies from a few keV up to several MeV, virtually any atomic species can be alloyed into any host metal, independently of many of the thermodynamic constraints which apply to thermal alloying processes. Implanted alloy microstructures are currently being extensively investigated

in attempts to arrive at a more general understanding of the phases that are produced. The phase types include metastable solid solutions, amorphous phases and second crystalline phases. DOE

N86-10332# European Space Agency, Paris (France).
LOW TEMPERATURE PLASTIC DEFORMATION MECHANISMS OF ALPHA-TITANIUM SINGLE CRYSTALS
Shigehisa Naka Apr. 1985 226 p refs Transl. into ENGLISH of "Etude des Mechanisms de Deformation Plastique a Basse Temperature de Monocristaux de Titane Alpha" rept. ONERA-NT-1983-7 ONERA, Paris, 1983
(ESA-TT-871; ONERA-NT-1983-7) Avail: NTIS HC A11/MF A01

The importance of the Peierls mechanism in the plastic deformation behavior of titanium is emphasized, as is the case of BCC metals. A non-planar core structure of screw dislocations was proposed; the core is dissociated simultaneously in one prismatic plane (10 bar 10) and two 1st order pyramidal planes (10 bar 11) and (10 bar 1 bar 1). The model of the core structure permitted qualitative explanation of various experimental results associated with the movement of screw dislocations (macro yield stress) which needs a recombination of the partials lying out of the slip plane. The hardening effect of inertial impurities was explained by introducing a modification of the core structure by the presence of impurities in the form of clusters (chemical interaction). This modification makes the recombination of the core more difficult. The presence of stage 2 on the stress vs strain curve at 77 K was explained by the fact that the micro yield stress corresponding to the propagation of edge dislocations was relatively high. That seems to be a particularity of titanium, at least, within the purity range of the titanium used. Author (ESA)

N86-10252# Milan Univ. (Italy).
SURFACE FORCES IN CONTACTING SOLIDS
G. Poletti and D. Cambiaghi (Centrotecnica) *In* ESA Fifth European Symp. on Mater. Sci. under Microgravity. Results of Spacelab 1 Dec. 1984 p 341-346 refs (For primary document see N86-10200 01-16)
Avail: NTIS HC A21/MF A01

N86-10266# Commissariat a l'Energie Atomique, Grenoble (France). Lab. d'Etude de la Solidification.
FIRST SPACELAB PAYLOAD (FSLP) EXPERIMENTS IN METALLURGY
J. J. Favier *In* ESA Fifth European Symp. on Mater. Sci. under Microgravity. Results of Spacelab 1 Dec. 1984 p 435-436 (For primary document see N86-10200 01-16)
Avail: NTIS HC A21/MF A01

27 NONMETALLIC MATERIALS

Includes physical, chemical, and mechanical properties of plastics, elastomers, lubricants, polymers, textiles, adhesives, and ceramic materials.

N86-10333 Massachusetts Univ., Amherst.
ELECTRICALLY CONDUCTING POLYMERS Ph.D. Thesis
John Robert Reynolds 1985 237 p
Avail: Univ. Microfilms Order No. DA8509598

A thorough investigation of the electronic properties of perchlorate doped polyacetylene was carried out. The conductivity of the polymer changes from semiconducting to values greater than 10(-2)Scn(-1) with doping and shows a distinct semiconductor to metal transition .0001 <y< .001. The polyacetylene films were doped using either electrochemical oxidation or a novel oxidation by ferric perchlorate allowing comparison of the two techniques. The changes in the electronic properties of a variety of arylenevinylene compounds, including poly(phenylene vinylene) (PPV), were examined with oxidation by AsF5. Conductivities as high as 1 Scm(-1) were observed for heavily doped PPV. Specific electron paramagnetic resonance characteristics were closely studied and a possible mechanism for conduction proposed. To overcome some of the limitations of the doped conjugated organic polymers a series of poly(metal tetrathiooxalates) (MTTO) were synthesized for the first time. Dissert. Abstr.

N86-10334 Massachusetts Univ., Amherst.
POLYACETYLENE POLYMERIZATION, STRUCTURE, AND ELECTRICAL TRANSPORT PROPERTIES Ph.D. Thesis
Michael Alan Schen 1985 344 p
Avail: Univ. Microfilms Order No. DA8509602

The field of highly conducting polymeric charge transfer complexes has focused principally on conjugated polymers with polyacetylene [CH] sub x, receiving the greatest attention. From an electrical transport properties view, much is known about polyacetylene. However, due to its insolubility and intractability, some of the most fundamental polymeric aspects of polyacetylene have not been addressed. The aim of this dissertation has been to elucidate the interrelationships which exist between polyacetylene molecular weight and the observed structural and electrical transport properties. Polyacetylene was polymerized using the Ziegler-Natta catalyst T(OBu) sub 4/A(Et) sub 3. Using radioactive c-14 labeled carbon monoxide and carbon dioxide as specific labels and h3 labeled methanol as a nonspecific label, the polymerization kinetics were fully elucidated. Simultaneously, the number average molecular weight, M sub n, of [CH] sub x obtained under a wide range of reaction conditions have been determined. Dissert. Abstr.

N86-10335 Georgia Inst. of Tech., Atlanta.
STEADY STATE FRICTIONAL BEHAVIOR OF THIN FILM COATINGS Ph.D. Thesis
Yutaka Shimazaki 1985 255 p
Avail: Univ. Microfilms Order No. DA8510973

Steady state frictional behavior of thin film coatings were studied and the effect of the applied coating thickness was emphasized. Four coating materials are studied, of which three are solid lubricants and one is wear resistance material. Film thickness, substrate roughness, applied load and substrate hardness were studied. The effect of these parameters on the transition and steady state friction coefficients are evaluated. It is shown that the steady state friction coefficients of MoS2 WSe2 WSe2/In/Ga coatings vary with the applied coating thicknesses. With the thicker coatings the wear track is fully covered with deformed coating material and the friction coefficients become higher. The steady state friction coefficient of WSe2/In/Ga coatings are determined by the behavior of the debonded and resmeared coating material. The substrate hardness seems to play the most dominant role upon the behavior of the resmeared film.
Dissert. Abstr.

N86-10336 Rensselaer Polytechnic Inst., Troy, N. Y.
FUEL AND LUBRICANT BEHAVIOR IN BOUNDARY LAYERS ANALYZED BY INFRARED EMISSION FOURIER TRANSFORM SPECTROMETRY Ph.D. Thesis
Peter Vogel 1984 188 p
Avail: Univ. Microfilms Order No. DA8509671

Thin films on metal surfaces were analyzed by Fourier transform infrared emission microspectrophotometry. The theory of thin films on a reflector was further developed to explore the possibilities of determining molecular alignment, film thickness and temperature from the emission spectra. The mechanism of deposit formation seems to be a two-stage process. Lubricants, used on magnetic recording media to minimize damage in case of a head crash, were studied by infrared emission spectrophotometry. The spectra of very thin layers of the lubricant directly on a mirror finished metal surface were quite different compared to the spectra of the bulk fluid. It is possible to detect the lubricant on top of the magnetic coating, which has strong bands in the same spectral region as the lubricant. A linear relationship between spectral intensity and lubricant concentration is found. Infrared emission spectrophotometry is a powerful tool for characterizing the lubricant as well as determine its concentration in a noncontact nondestructive way. Dissert. Abstr.

N86-10337 Johns Hopkins Univ., Baltimore, Md.
ELASTIC PROPERTIES AND THERMAL STABILITY CHARACTERIZATION OF METALLIC GLASSES BY GUIDED WAVE TECHNIQUES Ph.D. Thesis
Carl Lee Friant 1985 113 p
Avail: Univ. Microfilms order No. DA8510413

This study utilizes guided wave techniques for the determination of the isotropic elastic moduli of several metallic glass alloys. In addition, structural relaxation in the amorphous state that occurs during annealing below the crystallization temperature was monitored through changes in the elastic moduli using these methods. Metallic glasses unlike their crystalline counterparts are thermodynamically nonequilibrium structures. Consequently, knowledge of their thermal stability is of great importance from both a scientific and commercial standpoint. Structural relaxation of the asquenched structure manifests itself in the form of elastic moduli and density changes at temperatures well below that required for crystallization. Traditional techniques for characterizing the crystallization of metallic glssses such as X-ray diffraction and differential scanning and calorimetry are not effective for monitoring changes that take place in the wholly amorphous condition.
Dissert. Abstr.

N86-10338 Department of the Air Force, Washington, D.C.
SYNTHESIS OF ARYLENE SILOXANYLENE POLYMERS AND COPOLYMERS Patent
H. Rosenberg and T. T. Tsai, inventors (to Air Force) Issued 21 May 1985 11 p Supersedes AD-D009359
(AD-D011780; US-Patent-4,518,759; US-Patent-Appl-SN-343032; US-Patent-Class-528-35) Avail: US Patent and Trademark Office CSCL 07/3

This invention is directed to the preparation of certain arylene bis-silanols in highly purified form and to the preparation of five new arylene bis-silanols in particular, along with a procedure for ploymerizing these and other arylene-type bis-silanols using phosgene as a polymerization promotor or catalyst, to obtain highly purified, high molecular weight arylenesiloxanylene polymers. Preferred polymers are those which, when laminated to polycarbonate sheets or glass maintain their transparency, stability and adherence to said substrates at temperatures of up to and including 400 F. Such polymers are useful for the formulation of high temperature interlayers for windshields and canopies for aircraft and related aerospace vehicles.
GRA

N86-10339 Imperial Metal Industries Ltd., Kidderminster (England).
[CARBON FIBER REINFORCED POLYMIDE FILAMENT WOUND TUBE MANUFACTURING] Quarterly Progress Report
M. W. Jones Jun. 1974 9 p
(Contract MIN-DEF-K80B/33)
(BR64172; QPR-6) Avail: Issuing Activity

Progress in the development of a manufacturing process for information surveys of holes, joints, sandwich and open pattern structures; a design study on preferred joint designs; the formulation of a mathematical analysis to predict buckling; and test programs using glass reinforced polymide, filament wound tubes to validate theoretical analyses covering the prediction of strain distributions and buckling is summarized. Tube testing of glass polymide tubes was completed. Practical and theoretical data show good correlation for the winding angles most likely to be required for structures designed on flexural type loadings although at other winding patterns agreement is poor. Test data show the previous design study assessment of glass reinforced polymide tubes to be conservative for ambient temperature.
Author (ESA)

N86-10340*# Martin Marietta Aerospace, Denver, Colo. Mechanical Materials Engineering Section.
EVALUATION AND PREDICTION OF LONG-TERM ENVIRONMENTAL EFFECTS ON NON METALLIC MATERIALS Final Report
Harold Papazian Jan. 1985 26 p refs Addendum to N85- 19137
(NASA-CR-178495; NAS 1.26:178495; MCR-85-506-Addn) Avail: NTIS HC A03/MF A01 CSCL 11G

Predictive modeling of environmental conditions on nonmetallic materials was studied. The in-flight data of the atomic oxygen reaction with carbon and osmium, the laboratory and in-flight data of the atomic oxygen reaction with polymeric films and the effect of electron irradiation on the rates of oxidation are discussed. No information is found that can be used to model such effects on composites. The effects of the space environment on thermal control coatings and its effect on the space station are examined.
Author

N86-10341*# National Aeronautics and Space Administration. Lewis Research Center, Cleveland, Ohio.
TRIBOLOGICAL PROPERTIES OF STRUCTURAL CERAMICS
Donald H. Buckley and Kazuhisa Miyoshi Sep. 1985 103 p refs Submitted for publication
(NASA-TM-87105; E-2649; NAS 1.15:87105) Avail: NTIS HC A06/MF A01 CSCL 11B

The tribological and lubricated behavior of both oxide and nonoxide ceramics are reviewed in this chapter. Ceramics are examined in contact with themselves, other harder materials and metals. Elastic, plastic and fracture behavior of ceramics in solid state contact is discussed. The contact load necessary to initiate fracture in ceramics is shown to be appreciably reduced with tangential motion. Both friction and wear of ceramics are anisotropic and relate to crystal structure as has been observed with metals. Grit size effects in two and three body abrasive wear are observed for ceramics. Both free energy of oxide formation and the d valence bond character of metals are related to the friction and wear characteristics for metals in contact with ceramics. Surface contaminants affect friction and adhesive wear. For example, carbon on silicon carbide and chlorine on aluminum oxide reduce friction while oxygen on metal surfaces in contact with ceramics increases friction. Lubrication increases the critical load necessary to initiate fracture of ceramics both in indentation and with sliding or rubbing. Ceramics compositions both as coatings and in composites are described for the high temperature lubrication of both alloys and ceramics.
Author

N86-10342# Plant Resources Inst., Salt Lake City, Utah.
WHOLE PLANT UTILIZATION OF SUNFLOWERS AS A RENEWABLE SOURCE OF STRATEGIC MATERIALS (RUBBER) Final Report, 1 May 1983 - 30 Apr. 1984
M. F. Balandrin, J. R. Martineau, and G. A. Stone 14 Apr. 1985 14 p
(Contract DAAG29-83-C-0016)
(AD-A155833; ARO-20679.1-MS-S) Avail: NTIS HC A02/MF A01 CSCL 06/3

In an attempt to discover and develop new domestic sources of natural rubber (NR), 143 population of 47 species of sunflowers were collected and analyzed for their content of NR. Yields of crude NR obtained ranged from traces to 2.15% of the dry weight of the plant material. These quantities of NR are significantly lower (by approximately one order of magnitude) than those obtainable from domestic guayule plants. In addition, samples of sunflower NR were examined using chromatographic and spectroscopic techniques and were found to have low molecular weight elastomeric properties unsuitable for use in traditional Hevea latex or guayule NR applications. Thus, because of low yields, low NR molecular weights and quality, and relatively narrow genetic diversity in sunflower NR production characteristics, it is highly unlikely that sunflowers could serve as a domestic source of NR in the foreseeable future.
GRA

N86-10343# Royal Aircraft Establishment, Farnborough (England).
CALCULATION OF THE GLASS TRANSITION TEMPERATURES OF LINEAR POLYMERS. PART 1: RULES FOR HIERARCHICAL ORDERING OF THE DATA SET
W. A. Lee Nov. 1984 17 p
(AD-A156584; RAE-TR-84109-Pt-1; DRIC-BR-94287-Pt-1) Avail: NTIS HC A02/MF A01 CSCL 07/3

The rational ordering of polymers in a large data set for the correlation of glass transition temperature (Tg) with structure requires the establishment of seniority criteria. An extension of

polymer nomenclature rules published by the International Union of Pure and Applied Chemistry is proposed and applied, with examples, to the groups in a large polymer data set. The rules can be extended to cover new polymers without upsetting the original order. GRA

N86-10344# Naval Air Systems Command, Washington, D. C.
POLYMER ENGINEERING: POLYMERIC AND MOLECULAR ELECTRONIC, DIELECTRIC AND OPTICAL PROPERTIES FOR DEVICE APPLICATIONS
T. W. Barrett 1985 68 p
(AD-A156671) Avail: NTIS HC A04/MF A01 CSCL 09/3

In the first five chapters the theoretical physics and chemistry which underpin device function is introduced. Chapters six to nine address the problems of material organization. Chapters ten to fifteen address applications. An attempt has been made in these chapters to indicate the possibilities and opportunities in this emerging field, but, at the same time, to indicate the difficulties. Chapter headings include the following: Polymer Semiconductors; Physical Bases of Excitons; Soliton Physics and Quantum Engineering; Photon Molecular Switching; Properties of Bioconductors; Langmuir-Blodgett Films for Oriented Mono and Multilayers; Organization of Polymeric Conductors; Devices: Material Considerations; Polymer Interfaces; Applications; Application of Advanced Devices; Architectures; Other Applications including Advanced Sensors; Defense and Aerospace Applications; Defense and Aerospace Market Considerations. GRA

N86-10345# Lockheed Missiles and Space Co., Palo Alto, Calif.
BINDER-FILLER INTERACTION IN ENERGETIC POLYMERS Final Report, May 1983 - Dec. 1984
R. H. Martinson 31 Mar. 1985 88 p
(Contract N00014-83-C-0271)
(AD-A156752; LMSC/F035789) Avail: NTIS HC A05/MF A01 CSCL 07/3

The objective of this study was to measure the kinetics of the dewetting process in a variety of filled energetic polymers being studied as candidates for improved solid rocket and gun propellants in the Office of Naval Research ONR Power Program. By studying the dewetting process in detail, correlations between surface energetics and dewetting behavior would be obtained. Specific questions addressed in this document are: (1) What is the relation, if any, between the particle size of RDX and the voids created by dewetting? (2) Does the number density of voids caused by strain vary with solids loading in the same binder? (3) What is the influence of plasticizers on the size and number density of voids? (4) What is the relative number density of voids in compositions that fracture at different strains? The size? and (5) What do the growth curves of voids look like as functions of strain? By combining Small Angle X-Ray Scattering (SAXS) and ultrasonic wave scattering (UWS) data with existing theories of scattering, partial answers to these questions can be derived. GRA

N86-10346# Northwestern Univ., Evanston, Ill. Dept. of Civil Engineering.
FINITE DEFORMATION CRACK-LINE FIELDS IN A THIN ELASTO-PLASTIC SHEET Interim Report
N. Nishimura and J. D. Achenbach Feb. 1985 39 p
(Contract N00014-76-C-0063)
(AD-A156757; NU-SML-TR-85-2) Avail: NTIS HC A03/MF A01 CSCL 20/11

Finite deformation in the crack-tip zone of plastic deformation is investigated for Mode-1 opening of a crack in a thin sheet of elasto-plastic material. The materials obeys the Von Mises yield criterion in the true stresses, and the stretching tensor satisfies a flow law of the Prandtl-Reuss type. Incompressibility and a state of generalized plane stress are assumed. It is assumed that linearized elasticity applies outside the zone of plastic deformation. On the crack line between the crack tip and the elastic-plastic boundary, two distinct regions were recognized: the near tip zone and the intermediate region. In the near tip zone the fields are controlled by the radius of curvature of the blunted crack tip. Here the stress field was approximated by classical plane stress results. It was that the crack-line stresses may be taken as uniform in the intermediate region. In each region, deformation variables were determined by the use of the constitutive relations, and the results were matched to the corresponding quantities in the neighboring region(s). In this manner expressions were constructed for the deformation gradients on the crack line, in terms of the distance to the crack tip in the deformed configuration, the yield stress in shear and the stress-intensity factor of linear elastic fracture mechanics. GRA

N86-10347# Materials Research Labs., Ascot Vale (Australia).
AGE-LIFE PREDICTION OF NYLON 66 PARACHUTE MATERIALS. PART 2: CHANGES IN THE CHEMICAL AND PHYSICAL PROPERTIES OF MATERIALS ON AGING
G. T. Egglestone and G. A. George Jan. 1985 31 p
(AD-A156909; MRL-R-950-Pt-2) Avail: NTIS HC A03/MF A01 CSCL 11/5

Changes in the chemical properties of nylon 66 taffeta material and olive drab ripstop material on accelerated thermal aging are reported. The thermooxidative changes that occurred were used to measure rates and degree of polymer degradation. Relationships between tensile strength, molecular weight and other chemical changes were established and found to be applicable for in-service parachutes. The nylon 66 materials were also examined for photochemical degradation after outdoor exposure. No photoendering was found for the dyed material and the difference in the degradation rates was attributed to different stabilizers being used during fiber manufacture. GRA

N86-10348# Du Pont de Nemours (E. I.) and Co., Aiken, S.C.
RECIRCULATION WITHIN A GLASS MIXTURE SUBJECTED TO EXTERNAL AND RESISTIVE HEATING
D. W. Pepper 1985 15 p refs Presented at the 4th Intern. Conf. on Numerical Methods in Laminar and Turbulent Flow, Swansea, England, 8 Jul. 1985
(Contract DE-AC09-76SF-00001)
(DE85-010068; DP-MS-85-29; CONF-850745-8) Avail: NTIS HC A02/MF A01

Convective motion within a glass mixture undergoing external and resistive (joule) heating is numerically simulated. A time-split finite element technique and a pseudo-pressure formulation are used to solve the two and three-dimensional primitive equations of motion. The viscosity, thermal diffusivity, and electrical conductivity vary as a function of temperature; the temperature varies from ambient to 1150 C. DOE

N86-10349# Los Alamos National Lab., N. Mex.
MIXED-MODE FRACTURE OF CERAMICS
J. J. Petrovic 1985 10 p Presented at the 4th Intern. Symp. on the Fracture Mech. of Ceram., Blacksburg, Va., 18 Jun. 1985
(Contract W-7405-eng-36)
(DE85-014087; LA-UR-85-2195; CONF-8506128-2) Avail: NTIS HC A02/MF A01

The mixed-mode fracture behavior of ceramic materials is of importance for monolithic ceramics in order to predict the onset of fracture under generalized loading conditions and for ceramic composites to describe crack deflection toughening mechanisms. Experimental data on surface flaw mixed-mode fracture in various ceramics indicate that the flaw-plane normal stress at fracture decreases with increasing in-flaw-plane shear stress, although present data exhibit a fairly wide range in details f this sigma-tau relationship. Fracture from large cracks suggests that mode 2 has a greater effect on Mode 1 fracture than Mode 3. A comparison of surface flaw and large crack mixed-mode 1-2 fracture responses indicated that surface flaw behavior is influenced by shear resistance effects. DOE

N86-10350# Sandia Labs., Albuquerque, N. Mex.
ANALYSIS OF TRANSITIONS BETWEEN FERROELECTRIC AND ANTIFERROELECTRIC STATES UNDER CONDITIONING OF UNIAXIAL STRAIN
S. T. Montgomery 1985 11 p Presented at the Am. Phys. Soc. Topical Conf. on Shock Waves in Condensed Matter, Spokane,

22 Jul. 1985
(Contract DE-AC04-76DP-00789)
(DE85-014468; SAND-85-0554C; CONF-850736-14) Avail: NTIS HC A02/MF A01

The ferroelectric ceramic PZT 95/5, formed as a solid solution from the antiferroelectric, PbZrO3, and the ferroelectric PbTiO3, is known to transform to an antiferroelectric state under pressure. This transition can be used to convert mechanical energy to electrical energy under shock conditions. A mathematical model for this transformation has been developed for conditions of uniaxial strain. It uses two order parameters as internal state variables to reflect the microscopic state of the material. One order parameter corresponds to the spontaneous lattice polarization. The other represents the microscopic alignment of the spontaneous polarization within the lattice with parallel alignment corresponding to a ferroelectric state and anti-parallel alignment corresponding to an antiferroelectric state. A numerical method for solution is used to illustrate dynamic material response from the transition. DOE

N86-10351# Sandia Labs., Albuquerque, N. Mex.
THERMAL EXPANSION OF GLASSES IN THE SOLID AND LIQUID PHASES
W. D. Drotning 1985 18 p Presented at the 9th Symp. on Thermophys. Properties, Boulder, Colo., 24 Jun. 1985
(Contract DE-AC04-76DP-00789)
(DE85-013953; SAND-84-2342C; CONF-850617-1) Avail: NTIS HC A02/MF A01

The thermal expansion of a number of mixed oxide glasses is measured in the solid and liquid regions by gamma densitometry. Dead borate glasses are examined in the range 27 to 42 mol % PbO. The liquid phase volumetric thermal expansion coefficient is observed to decrease with increasing PbO content, in contrast to the solid phase linear thermal expansion coefficients, which displays some increase with increasing PbO composition. At 33.3 and 42 mol % PbO, these glasses display crystallization behavior during cooling from the melt, depending on the cooling rate. In soda-baria phosphate glasses (50 mol % P2O5), liquid phase volumetric expansion coefficients. For those phosphates with Na2O, crystallization is observed on cooling from the melt. Measurements on a lithia-aluminosilicate glass ceramic are obtained by this method to approximately 400 C above the limit of conventional dilatometry, thereby allowing the measurement of the thermal expansion of high temperature crystalline phases, as well as the liquid phase density. The gamma densitometry technique can yeild density, thermal expansion, T(sub g) and crystallization information, and quenching rate dependence data on glasses to temperatures in excess of 1500 C, and thus provides a means for high temperature characterization of glasses which complements conventional dilatometry, calorimetry, and thermal analysis. DOE

N86-10352# Karlsruhe Univ. (West Germany). Inst. fuer Werkstoffkunde 2.
HIGH TEMPERATURE PROPERTIES AND CHARACTERIZATION OF S3-N4 MATERIALS Final Report, Dec. 1983
Georg Grathwohl and Franz Porz Bonn Bundesministerium fuer Forschung und Technologie May 1985 145 p refs In GERMAN; ENGLISH summary Sponsored by Bundesministerium fuer Forschung und Technologie
(BMFT-FB-T-85-046; ISSN-0340-7608) Avail: NTIS HC A07/MF A01; Fachinformationszentrum, Karlsruhe, West Germany DM 30.50

The applicability of reaction-bonded silicon nitrides (RBSN) at high temperatures (up to 1,500 C) is studied by investigating their high temperature characteristics, creep strength and long term stability as well as their oxidation behavior depending on the size and distribution of the material pores. The variations in RBSN strength induced by static and cyclic oxidation treatment are measured. Failure at high temperatures and under lower stresses is due to creep rupture, slow crack growth, creep strain and creep damage explaining the differences in the lifetimes of silicon nitrides. Author (ESA)

N86-10353# Karlsruhe Univ. (West Germany). Inst. fuer Werkstoffkunde 2.
HIGH TEMPERATURE PROPERTIES OF SiC MATERIALS Final Report, Dec. 1983
Henri Cohrt, Rainer Hamminger, and Georg Grathwolh Bonn Bundesministerium fuer Forschung und Technologie May 1985 141 p refs In GERMAN; ENGLISH summary Sponsored by Bundesministerium fuer Forschung und Technologie
(BMFT-FB-T-85-047; ISSN-0340-7608) Avail: NTIS HC A07/MF A01; Fachinformationszentrum, Karlsruhe, West Germany DM 30

The oxidation and creep properties as well as the microstructural parameters and grain boundaries of several SiSiC and SSiC materials were studied to determine their applicability at high temperatures. Stress distributions in the bending specimens are calculated. Creep deformation occurs in a transient mode approaching zero creep in long term tests. Further improvement of SiSiC materials can be achieved by optimizing the microstructure of the green compact, that of SSiC materials by optimizing the processing and sintering techniques. Inclusions and segregations with high concentrations of impurities and additives were analyzed. Thin grain boundary films were studied with high resolution Auger electron spectroscopy. Author (ESA)

28 PROPELLANTS AND FUELS

Includes rocket propellants, igniters, and oxidizers; storage and handling; and aircraft fuels.

For related information see also *07 Aircraft Propulsion and Power, 20 Spacecraft Propulsion and Power,* and *44 Energy Production and Conversion.*

N86-10354# Army Armament Research and Development Command, Dover, N. J. Large Caliber Weapon Systems Lab.
EMACK RAILGUN FIRING TEST REPORT NUMBER 9 Final Technical Report, for period ending 20 Dec. 1983
A. E. Zielinski, J. A. Pappas, W. Williams, and G. Zsidisin Jun. 1985 44 p
(AD-A156661; AD-E401349; ARLCD-TR-85009; Test-9) Avail: NTIS HC A03/MF A01 CSCL 20/3

The test firing of the EMACK railgun test bed was successfully conducted on 20 December 1983 at a peak system current of 430 kiloamperes and 1.6 megajoules stored inertially in the homopolar generator. Current was successfully commutated into the launcher in 800 microseconds. The D1.1 projectile in-flight shadowgraphs were taken with a 150 KV Hewlett Packard flash X-ray system and a motion picture of the muzzle arc was taken with a 5000 frame-per-second high speed camera. The projectile weighed 566 grams and reached a velocity of 506 m/s in the 5 meter-long barrel. The improved armature design left the barrel intact and acceptable for EMACK shot no. 10. GRA

N86-10355# Department of the Air Force, Washington, D.C.
GAS GENERATOR FUEL FLOW THROTTLE CONTROL SYSTEM Patent Application
W. H. Miller, inventor (to Air Force) Filed 21 Mar. 1984 30 p
(AD-D011797; US-Patent-Appl-SN-591715) Avail: NTIS HC A03/MF A01 CSCL 21/8

In this patent application, a gas generator fuel flow throttle control system provides a fuel rich gas to a propellant grain of a small diameter rocket. An adaptive iterative gain technique allows the throttle to closely follow a commanded fuel flow rate as required by a missile processor. GRA

N86-10356# Los Alamos Scientific Lab., N. Mex.
DEVELOPMENT OF NEW AMMONIUM NITRATE COMPOSITE EXPLOSIVES Final Report, Oct. 1982 - Jan. 1984
K. Y. Lee Mar. 1985 10 p refs
(Contract W-7405-eng-36)
(DE85-014252; LA-10276) Avail: NTIS HC A02/MF A01

Studies of several ammonium nitrate (AN) based composite

explosive systems were continued from earlier work. The critical temperature (T(sub c)) of AN/ANT, AN/ENT, and AN/DETN systems were measured and their thermal stabilities evaluated. We have also studied the effect of ENT on the melt temperature of EA (EDD/AN) and found that ENT forms a eutectic with EA. The eutectic temperature of the ternary system AN/EDD/ENT (AENT) is 89C. Results from an initial pahse-diagram study of the quaternary system AN/KN/EDD/DETN (DEAK) are also presented. DOE

N86-10357# Sandia Labs., Albuquerque, N. Mex.
EXPLOSIVE INITIATION BY VERY SMALL CONICAL SHAPED CHARGE JETS
M. G. Vigil 1985 11 p refs Presented at the 8th Intern. Symp. on Detonation, Albuquerque, N. Mex., 15 Jul. 1985
(Contract DE-AC04-76DP-00789)
(DE85-009443; SAND-84-18440; CONF-850706-9) Avail: NTIS HC A02/MF A01

Very small conical shaped charge (CSC) jets are used to initiate four different secondary explosives. The liner thicknesses vary between 0.076 and 0.17 mm. LX-13 (80% PETN and 20% SYLGARD) explosive is used to drive the conical liners to form the CSC jets. The CSC jet velocities vary between 3.6 and 6.5 mm/(MU)s. The jet tip diameters range from 0.041 and 1.10 mm. The explosive acceptor or target diameters vary between 1.90 19.1 mm. The lateral confinement of the acceptor explosives is minimal. Relationships for critical jet initiation energy and dimensionless explosive/jet parameter as a function of initiation parameters is developed. The jet initiation data from this investigation as well as previously published data are shown to be consistent with the developed relationships. The threshold initiation parameter (jet velocity squared times jet diameter) for LX-13, PETN, PBX-9407, and TETRYI were experimentally determined to be 0.011, 0.0130, 0.041, and 0.044 cucm/(MU)s(2), respectively, for copper jets impacting bare explosive acceptors. The lower values for the LX-13 and PETN indicate these two explosives are more sensitive to shock initiation than PBX-9407 and TETRYL explosives. Author

N86-10358# Heller (Jean), Los Alamos, N. Mex.
PROPERTIES OF PLASTIC-BONDED NITROGUANIDINE
H. Dong, Y. Tian, X. Chen, F. Meng, and Q. Wang 1985 14 p refs Transl. into ENGLISH from Baozha yu Chongji (China), no. 1, 1981 p 77-83
(Contract W-7405-eng-36)
(DE85-015316; LA-tr-85-30) Avail: NTIS HC A02/MF A01

The formulation of bonded nitroguanidine used is Nq/TnT/PVB 97.5/1/1/5, which is designated as PB-NQ-1. Various properties of PB-NQ-1 were determined. Its detonation parameters were measured with 100-mm-diameter charges, initiated by a plane wave lens and a 100-mm-diameter by 10-mm-thick Comp. B booster. The detonation velocity is 8.159 mm/(MU)s, and the effective C-J detonation pressure is 26.2 GPa at rho0 = 1.676 g/cm(3). The energy of the one-dimensional plate push test is 65% that of PBX 9704. Experimental data show the performance of nitroguanidine, insensitivity characteristics and stability under normal temperatures, are comparable to those of TATB. Hence nitroguanidine may be used as a cheaper substitute for the latter. DOE

N86-10359# California Univ., Livermore. Lawrence Livermore Lab.
COMPOSITE EXPLOSIVES FOR METAL ACCELERATION: THE EFFECT OF DETONATION TEMPERATURE
R. R. McGuire and M. Finger 10 Jun. 1985 9 p refs Presented at the 8th Intern. Symp. on Detonation, Albuquerque, N. Mex., 15 Jul. 1985
(Contract W-7405-eng-48)
(DE85-013982; UCRL-91482; CONF-850706-21) Avail: NTIS HC A02/MF A01

Previous work in the area of composite explosives has emphasized the necessity of small particle size and intimate contact between fuel and oxidizer in obtaining prompt performance from fuel/oxidizer mixtures. This work has provided a basis for the definition of a composite explosive as an explosive system that requires the transport, mixing and subsequent reaction of the initial decomposition products of the system components in order to achieve the predicted detonation performance. A general working model and present experimental evidence demonstrating the importance of detonation temperature in achieving performance from composite explosives in metal acceleration experiments is presented. DOE

N86-10360# Research Inst. of National Defence, Umea (Sweden). ABC Research Dept.
METHOD FOR DETERMINING ELEMENTAL SULFUR IN JET FUEL
Birgitta Olofsson and Roger Roffey Jan. 1985 38 p refs In SWEDISH; ENGLISH summary
(FOA-C-40211-B4; ISSN-0347-2124) Avail: NTIS HC A03/MF A01; Research Institute of National Defence, KR 50

A method to determine elemental sulfur in jet fuel, based on differential pulse polarography, which needs smaller sample size, and is more sensitive than older methods is developed. The detection limit is 0.1 mg/l and the analytical range tested 0.1 to 10 mg/l. The test can be reproduced with a precision better than 10% for samples above 1 mg/l, and 15% to 20% near the detection limit. Accuracy is $> 5\%$. The influence on the polarographic peak of interferences is studied. Author (ESA)

31 ENGINEERING (GENERAL)

Includes vacuum technology; control engineering; display engineering; and cryogenics.

N86-10361 North Carolina State Univ., Raleigh.
FREEZER MODEL USING A POPULATION BALANCE APPROACH FOR STEADY-STATE, DIRECT-CONTACT, SECONDARY REFRIGERANT, FREEZE DESALINATION Ph.D. Thesis
Larry Wayne Byrd 1984 131 p
Avail: Univ. Microfilms Order No. DA8507355

A study of the secondary refrigerant, direct-contact, freeze desalination process is presented. In the study, a mathematical analysis of crystallization which occurs in the freezer is carried out and pilot plant data interpreted in light of the analytically implied behavior. The mathematical model assumes that refrigerant drop sizes are dispersed at any instant of time according to a scaled beta distribution. The inlet liquid refrigerant drops have a mondisperse size distribution while the ice crystal distribution has the form f sub c(r sub c) = (beta G)exp(-BETA r sub c/G) where BETA and G are empirical relations describing crystal nucleation and growth respectively. Agglomeration and breakage of droplets and crystals is included in the theory, although excluded in calculations. A number conservation equation, equations describing well-mixed behavior, a heat and mass balance, a salt balance, a volume constraint, and brine property relations are used to describe freezer operation. Author

N86-10362 Rensselaer Polytechnic Inst., Troy, N. Y.
MODELING AND CONTROL OF NONLINEAR SYSTEMS Ph.D. Thesis
Soleyman Mohseni 1984 125 p
Avail: Univ. Microfilms Order No. DA8509661

A method is presented for modeling a class of nonlinear systems by a linear combination of a library of differentiable, independent, and continuous functions that are possible suspects for inclusion in the model. While each possible model structure is represented by a node in a tree, it is shown that searching the tree for the optimal n-term model structure can be done in n stages using an algorithm based on conjungate direction ideas. The essential feature of the technique is that it generates a sequence of projection matrices such that the original vector-valued functions become conjugate directions. This leaves the original nonlinear terms intact and allows the structure for the optimal n-term model to be assembled in n selections from the library. It

is also shown that if applied to the quadratic optimization problem, the method obtains the extremum of the quadratic objective function after n stages without any explicit line search and/or matrix inversion. Dissert. Abstr.

N86-10363# Office National d'Etudes et de Recherches Aerospatiales, Paris (France).
LA RECHERCHE AEROSPATIALE, BIMONTHLY BULLETIN, NO. 1984-5, SEPTEMBER-OCTOBER 1985
Claude Sevestre, ed. Paris ESA Apr. 1985 81 p refs Transl. into ENGLISH of 'La Rech. Aerospatiale, Bull. Bimensuel. No. 1984-5, Sep. - Oct. 1984" France, ONERA
(ESA-TT-899) Avail: NTIS HC A05/MF A01; print copy in ENGLISH available at ONERA, Paris FF 70; original report in FRENCH available at ONERA, Paris FF 70

A numerical optimization method for airfoil design; noncentered numerical schemes in two-dimensional gas dynamics; a chemical laser by oxygen-iodine excitation transfer; a model for quantitative X-ray microanalysis (application to in-depth analysis of heterogeneous samples); a multidimensional case of an etropic variational formulation of conservative hyperbolic systems; and a radar signature analysis facility are discussed. Author (ESA)

N86-10364# Research Inst. of National Defence, Stockholm (Sweden).
REPORT ON A VISIT TO ENGLAND
Gunilla Derefeldt and Ulf Berggrund Mar. 1985 46 p refs Partly in ENGLISH, SWEDISH, and FRENCH Proc. of Nato Workshop on Color Coded VS Monochrome Electron. Displays, Farnborough, England, 28 Feb. - 1 Mar. 1984
(FOA-C5-85-0006-H2; ISSN-0347-7665) Avail: NTIS HC A03/MF A01

Color and monochrome display cost and system effectiveness; color displays in aircraft cockpits; digitally generated maps for aircraft; subjective reactions to color displays; and raster graphics were discussed. Author (ESA)

N86-10365# Nationaal Inst. voor Kernfysica en Hoge Energiefysica, Amsterdam (Netherlands). Sectie-H.
[ACTIVITIES REPORT IN SAFETY] Annual Report, 1983 [VEILIGHEIDSJAARVERSLAG 1983]
1984 38 p In DUTCH
Avail: NTIS HC A03/MF A01

Conventional and radiation aspects of safety management, and safety programs at a nuclear research institute are presented. The design of the laboratory is described. The technical execution of the safety management is outlined. Author (ESA)

32 COMMUNICATIONS

Includes land and global communications; communications theory; and optical communications.

For related information see also *04 Aircraft Communications and Navigation* and *17 Spacecraft Communications, Command and Tracking.*

N86-10366 British Broadcasting Corp., Kingswood (England). Engineering Div.
AN EVALUATION OF THE USE OF MICROPHONE ARRAYS FOR STUDIO RECORDING
P. S. Gaskell, C. Eng, and K. A. Bradbury Aug. 1985 20 p refs (BBC-RD-1985/8; PH-273) Avail: BBC, Kingswood Warren, Tadworth, Surrey, Engl.

The feasibility of using arrays of microphones as a studio recording technique in those situations where it is difficult to site the microphone close to the source was assessed.It was shown that the reverberant field, present in all studios, imposes severe demands on the performance of the array. It is estimated that the minimum number of microphones needed for a practical array is of the order of 100. The array would have to be constructed to stringent practical tolerances and would need considerable signal processing hardware for cophasing and beam steering. This technique therefore is unlikely to be appropriate for studio recording except in special circumstances. E.A.K.

N86-10367 Maryland Univ., College Park.
TOPICS IN NONLINEAR WAVE THEORY WITH APPLICATIONS Ph.D. Thesis
Eugene Raymond Tracy 1984 232 p
Avail: Univ. Microfilms Order No. DA8510466

Selected topics in nonlinear wave theory are discussed and applications to the study of modulational instabilities are presented. A historical survey is given of topics relating to solitons and modulational problems. A method is then presented for generating exact periodic and quasiperiodic solutions to several nonlinear wave equations which have important physical applications. The method is then specialized for the purposes of studying the modulated instability of a plane wave solution of the nonlinear Schrodinger equation, an equation with general applicability in one dimensional modulational problems. Some numerical results obtained in conjunction with the analytic study are presented. The analytic approach explains the recurrence phenomena seen in our numerical studies, and the numerical work of other authors. The method of solution (related to the Inverse Scattering Method) is then analyzed within the context of Hamiltonian dynamics. The construction of closed form solutions of these nonlinear wave equations, via the solution of Jacobi's Inversion Problem, is surveyed briefly. Dissert. Abstr.

N86-10368 Delaware Univ., Newark.
THE INTERPOLATION OF SIGNALS SAMPLED AT LESS THAN THE NYQUIST RATE Ph.D. Thesis
Khan Lutful Kabir 1984 126 p
Avail: Univ. Microfilms Order No. DA8511213

To obtain analog information by digitally processing uniformly spaced samples depends on the interpolation scheme. The constraints for the usual Shannon-Whittaker interpolation is to sample such signals at or above the Nyquist rate of twice the highest frequency present. This interpolation scheme produces poor reconstruction for signals with no highest frequency. In this dissertation, a new sampling theorem is developed based on the Newton-Gregory interpolation formula which is applicable to signals produced by stable physical systems with rational transfer functions. According to this theorem, such a signal is uniquely specified by its samples whenever the poles of the system transfer function all have frequencies less than one-sixth the sampling rate. A direct application of the Newton-Gregory interpolation scheme is made to numerically evaluate the spectra of poorly bandlimited signals at frequencies well above the sampling rate. Dissert. Abstr.

N86-10369 Case Western Reserve Univ., Cleveland, Ohio.
THEORETICAL AND NUMERICAL INVESTIGATION OF DIPOLE RADIATION OVER A FLAT EARTH Ph.D. Thesis
George Konstantin Karawas 1985 204 p
Avail: Univ. Microfilms Order No. DA8510121

The electromagnetic problem of dipole radiation in the presence of a conducting half-space is old and has been treated extensively in the literature. Various writers, including such prominent names as H. Weyl and B. van der Pol, have given different but equivalent presentations of the solution. A short derivation, similar to that of van der Pol, is given in an appendix for the field along the surface of the earth. It is then shown how this representation can be used to derive a new form of an asymptotic expansion, whose first term is identical with the one to be found in the literature. A recurrence relation is derived for calculating the higher order terms of the expansion and a tight bound is derived which permits an easy estimate of the truncation error. A discussion is presented about the numerical computation of the complementary error function which figures prominently in the present problem. Two methods are presented, one in form of the solution of a simple system of ordinary differential equations of the first order and another in form of continued fractions. Dissert. Abstr.

N86-10370 Georgia Inst. of Tech., Atlanta.
THE MEASUREMENT AND APPLICATION OF TRANSPORT

PROPERTIES OF ION SWARMS IN GASES Ph.D. Thesis
Franklin Benton Holleman 1984 179 p
Avail: Univ. Microfilms Order No. DA8510962

The drift velocities, mobilities, and longitudinal diffusion coefficients of the ion-gas combinations Tl + in He, Ne, Ar, and O2, Cl in N2 and NO + in N2 were measured at constant room temperature as a function of E/N, where E is the electric field strength and N is the number density of the neutral gas. T measured mobilities of Tl + in Ar were used to determine the ion-neutral interaction potential. The measured mobilities of Cl-in N2 were used to determine an effective ion-neutral interaction potential. Cross sections for momentum transfer were calculated as a function of ion-neutral collision energy in the center-of-mass frame from the directly determined ion-neutral interaction potentials for the Tl + in Ar and Cl-in N2 gas combinations. The data taken as a function of E/N were obtained in a low pressure drift tube mass spectrometer. For this study the Tl + ions were obtained by thermionic emission from a specially coated filament while the Cl- and NO+ ions were generated by electron bombardment of trace gases. Arrival time histograms were built up for the mass-selected ions. Dissert. Abstr.

N86-10371 Department of the Air Force, Washington, D.C.
ANGLE SET-ON APPARATUS Patent
R. R. Willmore, inventor (to Air Force) Issued 14 May 1985 6 p Supersedes AD-D009406
(AD-D011766; US-Patent-4,517,568; US-Patent-Appl-SN-347749; US-Patent-Class-343-18) Avail: US Patent and Trademark Office CSCL 17/9

An angle set on apparatus for an electronic countermeasure system utilizing a single dual mode phased array antenna which is operated under receiver/processor control to serve as both a transmit and receive element thereby avoiding the need for a separate direction finding system and, since transmit and receive functions share the same antenna, eliminating the need for precision pointing accuracy. The receiver/processor unit would continue to identify emitters using the jamming unit's receive antenna element and, where appropriate, PRI trackers would be assigned. The time of arrival window would be assigned. The time of arrival window would then be used to blank the transmitter signal and to switch the phased array to the receive mode. During sequential time of arrival windows the receiver/processor would vary the pointing angle of the phase array until the emitter angle of arrival is determined and stored in memory. At periodic intervals in the future, the receiver/processor unit would be pointed to the stored angle of arrival value for high effective radiated power jamming. GRA

N86-10372 Department of the Air Force, Washington, D.C.
METHOD FOR TUNING A PHASED ARRAY ANTENNA Patent
R. P. Gray, Jr., inventor (to Air Force) Issued 14 May 1985 5 p Supersedes AD-D010172
(AD-D011768; US-Patent-4,517,570; US-Patent-Appl-SN-471550; US-Patent-Class-343-372) Avail: US Patent and Trademark Office CSCL 09/6

During installation or maintenance of a phased array antenna system in which the transmission line to each element includes an adjustable phase shift device, it is required that the effective electrical lengths of the lines be adjusted to be equal, or alternatively that the phase errors be determined and stored as correction data for use during normal operation. One way of doing this is to phase modulate by + or - 90 deg the phase shift device of one element at a time, while applying a test signal to all elements. The signal is radiated by the array, received via a test antenna, and supplied to and envelope has different amplitudes at + 90 deg and - 90 deg of the modulation. The element is tuned by adjusting the length of its transmission line or line or the adjustment of its phase shift device to obtain a null at the amplitude detector. In an improved technique, to reduce certain errors, sum tuning is used, in which the + or 90 deg phase modulation is applied to all of the phase shift devices, except for that of the element being tuned. GRA

N86-10373 Department of the Air Force, Washington, D.C.
HIGH SENSITIVITY MILLIMETER-WAVE MEASUREMENT APPARATUS Patent
T. T. Mori, R. B. Dybdal, and R. D. Etcheverry, inventors (to Air Force) Issued 9 Apr. 1985 5 p Supersedes AD-D009697
(AD-D011786; US-Patent-4,510,622; US-Patent-Appl-SN-388327; US-Patent-Class-455-67) Avail: US Patent and Trademark Office CSCL 09/5

A millimeter wave measurement apparatus utilizing a phase-locked transmitter to generate a millimeter wave signal and a phase-locked local oscillator receiver to receive the transmitted millimeter wave signal. A conventional microwave receiver unit receives the IF signal from the millimeter wave receiver and downconverts the IF signal for detectiona and measurement. GRA

N86-10374 Department of the Air Force, Washington, D.C.
SAMPLE DATA PHASE LOCKED LOOP FOR ADAPTIVE DOPPLER TRACKER Patent
A. W. Roeder, inventor (to Air Force) Issued 23 Apr. 1985 9 p Supersedes AD-D010534
(AD-D011788; US-Patent-4,513,429; US-Patent-Appl-SN-329558; US-Patent-Class-375-120) Avail: US Patent and Trademark Office CSCL 09/5

Precise phase acquisition and tracking of a data modulated pulse signal in order to recover the data in a low signal to noise ratio environment is achieved by a sample data phase locked loop that is adaptive, second order, and uses baseband polar coordinate processing. The circuit utilizes an adaptive second order loop where the loop bandwidth can be adjusted by a coherence measurement. This provides wide bandwidths during initial acquisition, medium bandwidths during acquisition/track transition and narrow bandwidth during tracking. GRA

N86-10375 Department of the Navy, Washington, D. C.
PHASE-CODED PULSE EXPANDER-COMPRESSOR Patent
B. L. Lewis, inventor (to Navy) Issued 2 Apr. 1985 11 p Supersedes AD-D009914
(AD-D011812; US-Patent-4,509,051; US-Patent-Appl-SN-420209; US-Patent-Class-343-17.2PC) Avail: US Patent and Trademark Office CSCL 17/9

A pulse expansion and compression system, especially useful for radar ranging, comprising a pulse coder for expanding an input pulse and a pulse compressor of the matched-filter type. The coder consists of a plurality of delay stages into which the input pulse is fed, a discrete Fourier transform (DFT) circuit to which the output signals of the delay stages are fed by way of respective phase weights and for which every other frequency port is inverted prior to entry to a time-dispersion-means (TDM) comprising an arrangement of adders interconnected by delay stages for differently delaying the output signals from the DFT. The adders are connected in N/2-fold cyclically permutated order to the frequency ports, where N is the number of frequency ports if that number is even, and N is the number of frequency ports less one if that number is odd. The TDM output is fed to a phase modulator and then to the transmitter. The echo signals are conjugated, time-inverted, and passed through the same DFT as the input pulse signal by way of the phase weights. The outputs of the DFT are then inverted at every other frequency port and passed through the TDM, but this time in time-inverted order. The outputs of the TDM are fed through an envelope detector to provide a cross-correlated facsimile of the original input pulse. Author (GRA)

N86-10376 Department of the Navy, Washington, D. C.
PHASE CODED PULSE EXPANDER-COMPRESSOR Patent
B. L. Lewis, inventor (to Navy) Issued 18 Jun. 1985 8 p Supersedes AD-D009614
(AD-D011817; US-Patent-4,524,362; US-Patent-Appl-SN-377107; US-Patent-Class-17.2-PC) Avail: US Patent and Trademark Office CSCL 17/9

A pulse expansion and compression system, especially useful for radar ranging, comprising a pulse coder for expanding an input pulse and a pulse compressor of the matched-filter type. The coder consists of a plurality of delay stages into which the input

pulse is fed, a discrete Fourier transform (DFT) circuit to which the output signals of the delay stages are fed by way of respective phase weights and for which every other frequency port is inverted prior to entry to a time-dispersion means (TDM) comprising an arrangement of adders interconnected by delay stages for differently delaying the output signals from the DFT. The TDM output is fed to a phase modulator and then to the transmitter. The echo signals are conjugated, time-inverted, and passed through the same DFT as the input pulse signal by way of the phase weights. The outputs of the DFT are then inverted at every other frequency port and passed through the TDM, but this time in time-inverted order. The outputs of the TDM are fed through an envelope detector to provide a cross-correlated facsimile of the original input pulse. Author (GRA)

N86-10377*# Illinois Univ., Urbana. Electromagnetics Lab.
NUMERICAL METHODS FOR ANALYZING ELECTROMAGNETIC SCATTERING Semannual Report, 25 Mar. - 24 Sep. 1985
S. W. Lee, Y. T. Lo, S. L. Chuang, and C. S. Lee 24 Sep. 1985 176 p refs
(Grant NAG3-475)
(NASA-CR-176141; NAS 1.26:176141) Avail: NTIS HC A09/MF A01 CSCL 20N

Attenuation properties of the normal modes in an overmoded waveguide coated with a lossy material were analyzed. It is found that the low-order modes, can be significantly attenuated even with a thin layer of coating if the coating material is not too lossy. A thinner layer of coating is required for large attenuation of the low-order modes if the coating material is magnetic rather than dielectric. The Radar Cross Section (RCS) from an uncoated circular guide terminated by a perfect electric conductor was calculated and compared with available experimental data. It is confirmed that the interior irradiation contributes to the RCS. The equivalent-current method based on the geometrical theory of diffraction (GTD) was chosen for the calculation of the contribution from the rim diffraction. The RCS reduction from a coated circular guide terminated by a PEC are planned schemes for the experiments are included. The waveguide coated with a lossy magnetic material is suggested as a substitute for the corrugated waveguide. E.A.K.

N86-10378*# National Aeronautics and Space Administration, Washington, D. C.
DISCUSSION ON THE PROGRESS AND FUTURE OF SATELLITE COMMUNICATION (JAPAN)
M. Ogata, H. Mizusawa, and K. Irie Sep. 1985 20 p refs Transl. into ENGLISH from Mitsubishi Gunki Giho (Japan), v. 59, no. 6, 1985 p 408-412 Transl. by The Corporate Word, Inc. Pittsburgh, Pa.
(Contract NASw-4006)
(NASA-TM-77672; NAS 1.15:77672) Avail: NTIS HC A02/MF A01 CSCL 17B

The current status of communications satellite development in Japan is presented. It is shown that beginning with research on satellite communucations in the late 1950's, progress was made in the areas of communications, remote sensing, and technology experimentation. The current status of communication satellites is presented, stressing development in the areas of CFRP construction elements, the use of LSI and MIC circuits, advanced multibeam antenna systems, Ku and Ka band transmission systems, and the shift to small-scale earth stations. Methods for reducing costs and increasing transmission efficiency are shown. The technical specifications of all satellite projects currently under development are given. Users of Japanese communications satellite are presented. E.A.K.

N86-10379*# National Aeronautics and Space Administration. Lewis Research Center, Cleveland, Ohio.
TEST RESULTS FOR 20-GHz GaAs FET SPACECRAFT POWER AMPLIFIER
Kurt A. Shalkhauser Aug. 1985 22 p refs
(NASA-TM-87072; E-2573; NAS 1.15:87072) Avail: NTIS HC A02/MF A01 CSCL 09C

Test were conducted to measure the performance of the 20-GHz solid state, proof-of-concept amplifier. The amplifier operates over the 17.7 to 20.2-GHz frequency range and uses high power gallium arsenide field effect transistors. The amplifier design and test methods are briefly described. NASA and contractor performance data are compared. Author

N86-10380*# National Aeronautics and Space Administration. Lewis Research Center, Cleveland, Ohio.
A DUAL FREQUENCY MICROSTRIP ANTENNA FOR Ka BAND
Richard Q. Lee and Maurice F. Baddour 1985 12 p refs Presented at 1985 Antenna Appl. Symp., 18-20 Sep. 1985; Sponsored by Illinois Univ. and RADC, Monticello, Ill.
(NASA-TM-87124; E-2737; NAS 1.15:87124) Avail: NTIS HC A02/MF A01 CSCL 20N

For fixed satellite communication systems at Ka band with downlink at 17.7 to 20.2 GHz and uplink at 27.5 to 30.0 GHz, the focused optics and the unfocused optics configurations with monolithic phased array feeds have often been used to provide multiple fixed and multiple scanning spot beam coverages. It appears that a dual frequency microstrip antenna capable of transmitting and receiving simultaneously is highly desirable as an array feed element. This paper describes some early efforts on the development and experimental testing of a dual frequency annular microstrip antenna. The antenna has potential application for use in conjunction with a monolithic microwave integrated circuit device as an active radiating element in a phased array of phased array feeds. The antenna is designed to resonate at TM sub 12 and TM sub 13 modes and tuned with a circumferential microstrip ring to vary the frequency ratio. Radiation characteristics at both the high and low frequencies are examined. Experimental results including radiating patterns and swept frequency measurements are presented. Author

N86-10381*# National Aeronautics and Space Administration. Lewis Research Center, Cleveland, Ohio.
A NUMERICAL METHOD FOR APPROXIMATING ANTENNA SURFACES DEFINED BY DISCRETE SURFACE POINTS
Richard Q. Lee and Roberto Acosta 1985 10 p refs Presented at 1985 Antenna Appl. Symp., 18-20 Sep. 1985; sponsored by Illinois Univ. and RADC, Monticello, Ill.
(NASA-TM-87125; E-2738; NAS 1.15:87125) Avail: NTIS HC A02/MF A01 CSCL 20N

A simple numerical method for the quadratic approximation of a discretely defined reflector surface is described. The numerical method was applied to interpolate the surface normal of a parabolic reflector surface from a grid of nine closest surface points to the point of incidence. After computing the surface normals, the geometrical optics and the aperture integration method using the discrete Fast Fourier Transform (FFT) were applied to compute the radiaton patterns for a symmetric and an offset antenna configurations. The computed patterns are compared to that of the analytic case and to the patterns generated from another numerical technique using the spline function approximation. In the paper, examples of computations are given. The accuracy of the numerical method is discussed. Author

N86-10382*# Jet Propulsion Lab., California Inst. of Tech., Pasadena.
THE TELECOMMUNICATIONS AND DATA ACQUISITION REPORT Progress Report, Apr. - Jun. 1985
E. C. Posner, ed. 15 Aug. 1985 218 p refs
(Contract NAS7-918)
(NASA-CR-176203; NAS 1.26:176203; TDA-PR-42-82) Avail: NTIS HC A10/MF A01 CSCL 17B

Deep Space Network (DSN) progress in flight project support, tracking and data acquisition research and technology, network engineering, hardware and software implementation, and operation is discussed. In addition, developments in Earth-based radio technology as applied to geodynamics, astrophysics and the radio search for extraterrestrial intelligence are reported. For individual titles, see N86-10383 through N86-10402.

N86-10383*# Jet Propulsion Lab., California Inst. of Tech., Pasadena. Tracking Systems and Applications Section.
A VLBI SURVEY AT 2.29 GHz
D. D. Morabito, R. A. Preston, J. G. Williams, J. Faulkner, D. L. Jauncey (CSIRO, Sydney, Australia), and G. D. Nicolson (Council for Scientific and Industrial Research, Johannesburg, South Africa) *In its* The Telecommun. and Data Acquisition Progr. Rept. 15 Aug. 1985 p 1-10 refs (For primary document see N86-10382 01-32)
Avail: NTIS HC A10/MF A01 CSCL 20N

The Deep Space Network (DSN) is establishing a high-accuracy VLBI celestial reference frame. The results of a search for suitable radio sources to be used in constructing this frame are given. The VLBI observations using DSN baselines at 2.29 GHz with fringe spacings of about 3 milliarcseconds have been performed on 1398 radio sources spread over the entire sky. Of those, 917 sources were detected including 93% of the identifed BL Lacertae objects, 86% of Quasars and 36% of galaxies. The resulting catalog of compact radio sources is also useful for various astrophysical studies and in the formation of VLBI celestial reference frames. Author

N86-10384*# Jet Propulsion Lab., California Inst. of Tech., Pasadena. Tracking Systems and Applications Section.
COMPARISON OF THE CALIBRATION OF IONOSPHERIC DELAY IN VLBI DATA BY THE METHODS OF DUAL FREQUENCY AND FARADAY ROTATION
J. A. Scheid *In its* The Telecommun. and Data Acquisition Progr. Rept. 15 Aug. 1985 p 11-23 refs (For primary document see N86-10382 01-32)
Avail: NTIS HC A10/MF A01 CSCL 20N

When both S-band and X-band data are recorded for a signal which has passed through the ionosphere, it is possible to calculate the ionospheric contribution to signal delay. In Very Long Baseline Interferometry (VLBI) this method is used to calibrate the ionosphere. In the absence of dual frequency data, the ionospheric content measured by Faraday rotation, using a signal from a geostationary satellite, is mapped to the VLBI observing direction. The purpose here is to compare the ionospheric delay obtained by these two methods. The principal conclusions are: (1) the correlation between delays obtained by these two methods is weak; (2) in mapping Faraday rotation measurements to the VLBI observing direction, a simple mapping algorithm which accounts only for changes in hour angle and elevation angle is better than a more elaborate algorithm which includes solar and geomagnetic effects; (3) fluctuations in the difference in total electron content as seen by two antennas defining a baseline limit the application of Faraday rotation data to VLBI. Author

N86-10385*# Jet Propulsion Lab., California Inst. of Tech., Pasadena. Ground Antennas and Facilities Engineering Section.
A NEW 70-METER ANTENNA QUADRIPOD WITH REDUCED RF BLOCKAGE
J. J. Cucchissi *In its* The Telecommun. and Data Acquisition Progr. Rept. 15 Aug. 1985 p 24-30 refs (For primary document see N86-10382 01-32)
Avail: NTIS HC A10/MF A01 CSCL 20N

The new subreflector mount (quadripod) for the 64-meter to 70-meter antenna extension project was the result of many trial designs aimed at reducing radio frequency spherical and plane wave blockage and minimizing structural weight while satisfying strength and natural frequency requirements. An optimum design emerged which has a gain improvement of 0.32 dB over the present 64-meter design. Some of the trial designs made and the final optimum configuration selected are described. Author

N86-10386*# Jet Propulsion Lab., California Inst. of Tech., Pasadena. Ground Antennas and Facilities Engineering Section.
SEISMIC ANALYSIS OF THE LARGE 70-METER ANTENNA, PART 1: EARTHQUAKE RESPONSE SPECTRA VERSUS FULL TRANSIENT ANALYSIS **c46**
K. Kiedron and C. T. Chian *In its* The Telecommun. and Data Acquisition Progr. Rept. 15 Aug. 1985 p 31-42 ref (For primary document see N86-10382 01-31)
Avail: NTIS HC A10/MF A01 CSCL 08K

As a check on structure safety aspects, two approaches in seismic analysis for the large 70-m antennas are presented. The first approach, commonly used by civil engineers, utilizes known recommended design response spectra. The second approach, which is the full transient analysis, is versatile and applicable not only to earthquake loading but also to other dynamic forcing functions. The results obtained at the fundamental structural frequency show that the two approaches are in good agreement with each other and both approaches show a safe design. The results also confirm past 64-m antenna seismic studies done by the Caltech Seismology Staff. Author

N86-10387*# Jet Propulsion Lab., California Inst. of Tech., Pasadena. Radio Frequency and Microwave Subsystems Section.
AN EXPERIMENTAL TE SUB 12 - TE SUB 11 CIRCULAR WAVEGUIDE MODE CONVERTER **c33**
D. Hoppe *In its* The Telecommun. and Data Acquisition Progr. Rept. 15 Aug. 1985 p 43-56 refs (For primary document see N86-10382 01-32)
Avail: NTIS HC A10/MF A01 CSCL 09C

Theoretical and experimental results for a prototype TE sub 12 to TE sub 11 circular waveguide mode converter are discussed. The system which requires such device, the high power Ka-Band transmitter is described briefly. A short review of coupled mode theory is given, and the theoretical performance of the final converter design is given. Experimental results for the fabricated converter are presented and compared with theory. A method of identifying the various circular waveguide modes in a multimode device is described. Given the close agreement between the theoretical predictions and experimental results, the computer code may be used with confidence in the design of future multimode tapers and mode converters. Author

N86-10388*# Jet Propulsion Lab., California Inst. of Tech., Pasadena. Radio Frequency and Microwave Subsystems Section.
PROPAGATION AND RADIATION CHARACTERISTICS OF A MULTIMODE CORRUGATED WAVEGUIDE FEEDHORN
D. Hoppe *In its* The Telecommun. and Data Acquisition Progr. Rept. 15 Aug. 1985 p 57-67 refs (For primary document see N86-10382 01-32)
Avail: NTIS HC A10/MF A01 CSCL 20N

A prototype of the multimode corrugated feedhorn which will be used in the 400 kW CW Ka-band radar system is described. A rough design is done using coupled mode theory and standard corrugated waveguide modes. A more exact analysis using mode matching techniques is then used which takes into account the effect of a finite number of corrugations per wavelength and determines the modes which are reflected from the device. A prototype feedhorn has been constructed and measured. These experimental results are then compared to the theoretical predictions which agree satisfactorily closely. Author

N86-10389*# Jet Propulsion Lab., California Inst. of Tech., Pasadena. Ground Antennas and Facilities Engineering Section.
LOAD-DEFLECTION TESTS AND COMPUTER ANALYSES OF A HIGH-PRECISION ADHESIVE-BONDED ANTENNA REFLECTOR PANEL **c24**
C. T. Chian and R. Levy *In its* The Telecommun. and Data Acquisition Progr. Rept. 15 Aug. 1985 p 68-81 (For primary document see N86-10382 01-32)
Avail: NTIS HC A10/MF A01 CSCL 11D

New adhesive-bonded panels are being investigated as a part of an effort to extend and upgrade the 64-m to a 70-m antenna network. Load-deflection tests were conducted on a sample high-precision adhesive-bonded panel for comparison with design criteria. Two computerized structural models were developed in order to predict the deformation patterns under different types of distributed and concentrated loadings. The main purpose was to obtain empirical stiffness factors for the slit beams and girders in the panel structure. With determination and use of the empirical

stiffness factors, there is a good agreement between the theoretically predicted deflections and the test measurements. It was also found that the new bonded panels satisfy the stringent design specifications and surface tolerance bounds. Author

N86-10390*# Jet Propulsion Lab., California Inst. of Tech., Pasadena. Communications Systems Research Section.
A SEQUENTIAL DECODING PERFORMANCE ANALYSIS FOR INTERNATIONAL COMET EXPLORER c61
D. Divsalar *In its* The Telecommun. and Data Acquisition Progr. Rept. 15 Aug. 1985 p 82-91 refs (For primary document see N86-10382 01-32)
Avail: NTIS HC A10/MF A01 CSCL 09B

The effect of a noisy reference carrier on the performance of International Comet Explorer (ICE) Sequential decoder is analyzed. Ideal reference models for frame deletion probability are given for the Telemetry Processing Assembly (TPA) and the Linkabit (LS4815) sequential decoders. Based on these ideal reference models the deletion probability in the presence of noisy reference carrier is computed for both the high and the low data rate cases. A medium data rate performance model is then derived using an interpolation method. The derived medium rate performance model depends on the phase locked loop bandwidth-integration time product. Results are obtained for frame length 1024 bits, data bit rates of 1024 bps and 512 bps, modulation index of 60 deg, and threshold loop bandwidths of 10 Hz and 3 Hz. The medium rate model agrees with experimental data to within measurement uncertainty. For the 10 Hz loop bandwidth and modulation index of 60 deg at frame deletion rate of 0.0001, the required total received power to noise ratio is 36 dB. The analysis given is general and applicable to any sequential decoder, provided that the ideal reference model of the decoder is available. Author

N86-10391*# Jet Propulsion Lab., California Inst. of Tech., Pasadena. Communications System Research Section.
THE VLSI DESIGN OF ERROR-TRELLIS SYNDROME DECODING FOR CONVOLUTIONAL CODES c64
I. S. Reed (Univ. of Southern California, Los Angeles), J. M. Jensen (Univ. of Southern California, Los Angeles), T. K. Truong, and I. S. Hsu *In its* The Telecommun. and Data Acquisition Progr. Rept. 15 Aug. 1985 p 92-107 refs (For primary document see N86-10382 01-32)
Avail: NTIS HC A10/MF A01 CSCL 12A

A recursive algorithm using the error-trellis decoding technique is developed to decode convolutional codes (CCs). An example, illustrating the very large scale integration (VLSI) architecture of such a decode, is given for a dual-K CC. It is demonstrated that such a decoder can be realized readily on a single chip with metal-nitride-oxide-semiconductor technology. Author

N86-10392*# Jet Propulsion Lab., California Inst. of Tech., Pasadena. Communications Systems Research Section.
HIGH-RATE CONVOLUTIONAL CODE CONSTRUCTION WITH THE MINIMUM REQUIRED SNR CRITERION c64
P. J. Lee *In its* The Telecommun. and Data Acquisition Progr. Rept. 15 Aug. 1985 p 108-112 refs (For primary document see N86-10382 01-32)
Avail: NTIS HC A10/MF A01 CSCL 12A

New short constraint length, high-rate convolutional codes which minimize the required signal to noise ratios (SNR) are found and tabulated for rates 2/3, 3/4, and 4/5, and for constraint length K up to 10. When compared with previously reported codes, most of the new codes reduce the required SNR only slightly. However, there are some pairs of K and code rate for which the new codes require considerably less SNR. The most significant one is the new K = 8, ate 4/5 code which requires 1.2 dB less SNR than the known code with the same parameters, for a desired bit error rate of 0.000001. Author

N86-10393*# Jet Propulsion Lab., California Inst. of Tech., Pasadena. TDA Engineering Section.
DSN FREQUENCY AND TIMING SYSTEM, MARK 4-85
B. W. Falin *In its* The Telecommun. and Data Acquisition Progr. Rept. 15 Aug. 1985 p 113-119 (For primary document see N86-10382 01-32)
Avail: NTIS HC A10/MF A01 CSCL 20N

As part of the Deep Space Network (DSN) Mark IVA implementation program, the DSN frequency and timing system is currently undergoing changes. With the implementation of signal processing centers (SPC) at each deep space communications complex (DSCC), major changes to the frequency and timing distribution equipment were necessary. A functional description of the Mark IVA frequency and timing system (FTS) as it exists today and planned capabilities through 1988 is given. Author

N86-10394*# Jet Propulsion Lab., California Inst. of Tech., Pasadena. TDA Mission Support and DSN Operations Office.
JPL EMERGENCY SUPPORT OF TDRSS AND COMPATIBLE SATELLITES c14
N. A. Fanelli *In its* The Telecommun. and Data Acquisition Progr. Rept. 15 Aug. 1985 p 120-124 (For primary document see N86-10382 01-32)
Avail: NTIS HC A10/MF A01 CSCL 14B

The Tracking and Data Relay Satellite System (TDRSS) will consist of three identical satellites in geosynchronous orbits and a dedicated ground receiving station. The first two satellites (TDRS East and TDRS West) will form the operational TDRS service network providing near-global real-time user satellite coverage. The third TDRS satellite will act as an in-orbit spare. Since the TDRSS satellite are supported by a single ground station, a method of providing emergency support for TDRS and user satellites is needed. The support to be provided by JPL's Deep Space Network is described. Author

N86-10395*# Jet Propulsion Lab., California Inst. of Tech., Pasadena. TDA Planning Office.
PLANNING FOR VLA/DSN ARRAYED SUPPORT TO THE VOYAGER AT NEPTUNE c14
J. W. Layland and D. W. Brown *In its* The Telecommun. and Data Acquisition Progr. Rept. 15 Aug. 1985 p 125-135 refs (For primary document see N86-10382 01-32)
Avail: NTIS HC A10/MF A01 CSCL 14B

Preplanning for the use of the National Radio Astronomy Observatory's Very Large Array (VLA) in support of Voyager at Neptune has been underway since early 1982. When arrayed with the Deep Space Network (DSN) antennas at Goldstone, CA, the VLA more than doubles the potential data return over the American longitude for the 1989 Voyager encounter. The background, rationale and current status of planning for VLA-DSN Arrayed Support to the Voyager at Neptune are discussed. Author

N86-10396*# Jet Propulsion Lab., California Inst. of Tech., Pasadena. TDA Planning Office.
A VLA EXPERIMENT: PLANNING FOR VOYAGER AT NEPTUNE c12
J. W. Layland, P. J. Napier (National Radio Astronomy Observatory), and A. R. Thompson (National Radio Astronomy Observatory) *In its* The Telecommun. and Data Acquisition Progr. Rept. 15 Aug. 1985 p 136-142 refs (For primary document see N86-10382 01-32)
Avail: NTIS HC A10/MF A01 CSCL 22A

A very large array (VLA) engineering experiment was conducted on the night of July 22, 1983 to explore one aspect of the potential for the VLA to support Voyager at its Neptune encounter in August of 1989. Specifically, the experiment tested the abiliy of the VLA to self-calibrate on a natural radio source whose effective signal strength is the same as Voyager's will be at its Neptune encounter. The experiment was successful and supported the belief that the VLA would be able to be self-calibrated with Voyager's signal. Author

N86-10397*# Jet Propulsion Lab., California Inst. of Tech., Pasadena. Reliability Engineering Section.
PERIODIC BINARY SEQUENCES WITH VERY GOOD AUTOCORRELATION PROPERTIES c64
S. Tyler and J. Loftsson *In its* The Telecommun. and Data

Acquisition Progr. Rept. 15 Aug. 1985 p 143-158 refs (For primary document see N86-10382 01-32)
Avail: NTIS HC A10/MF A01 CSCL 12A

Computer searches were performed using both an 8086 microprocessor and a Cyber 750 mainframe to find repeated binary phase coded waveforms with very good matched and mismatched autocorrelation properties. The best results for every period up to 64 are given. Sequences with optimal peak sidelobes were discovered for each of these periods. These sequences have extensive applications in radar and communications, particularly in situations when there are very unfavorable signal-to-noise ratios. The best sequence of period 64 when processed using a mismatched filter giving no sidelobes has a reduction in the main lobe of less than 0.23 dB. Author

N86-10398*# Jet Propulsion Lab., California Inst. of Tech., Pasadena. Reliability Engineering Section.
A BINARY SEQUENCE OF PERIOD 60 WITH BETTER AUTOCORRELATION PROPERTIES THAN THE BARKER SEQUENCE OF PERIOD 13 **c64**
J. Watkins (TRW, Inc., Redondo Beach, Calif.), J. Loftsson, and S. Tyler *In its* The Telecommun. and Data Acquisition Progr. Rept. 15 Aug. 1985 p 159-162 refs (For primary document see N86-10382 01-32)
Avail: NTIS HC A10/MF A01 CSCL 12A

A binary sequence of period 60 has been discovered which in some respects has better autocorrelation properties than the Barker sequence of period 13. When both sequences are processed using appropriate sidelobe-eliminating mismatched filters, the Barker sequence's main lobe is reduced by a factor of 1.040 or 0.17 dB, while the new sequence's main lobe is reduced by a factor of only 1.035 or 0.15 dB. This sequence is the first counterexample known to the authors of the hypothesis that the autocorrelation properties of all sequences of periods greater than 13 are inferior to those of the Barker period-13 sequences. Sequences of this type are very useful in radar and deep space communications, especially in situations where there is an adverse signal to noise ratio. Author

N86-10399*# Jet Propulsion Lab., California Inst. of Tech., Pasadena. TDA Engineering Section.
THE GCF MARK 4 IMPLEMENTATION AND BEYOND **c14**
R. A. Crowe *In its* The Telecommun. and Data Acquisition Progr. Rept. 15 Aug. 1985 p 163-172 refs (For primary document see N86-10382 01-32)
Avail: NTIS HC A10/MF A01 CSCL 14B

A brief overview is given of the major subsystems that comprise the Mark IVA ground communication facility (GCF) along with key information on basic functionality that may be inadequately or imperfectly understood. The evolving GCF System as it is currently being designed is described. Author

N86-10400*# Jet Propulsion Lab., California Inst. of Tech., Pasadena. Communications Systems Research Section.
SETI RADIO SPECTRUM SURVEILLANCE SYSTEM
B. Crow, A. Lokshin, M. Marina, and L. Ching *In its* The Telecommun. and Data Acquisition Progr. Rept. 15 Aug. 1985 p 173-184 (For primary document see N86-10382 01-32)
Avail: NTIS HC A10/MF A01 CSCL 20N

The SETI Radio Spectrum Surveillance System (SRSSS) will provide a data base for assessing the radio frequency interference (RFI) environment for SETI and minimizing RFI disruptions during the search. The system's hardware and software are described and the sensitivity of the system is discussed. Author

N86-10401*# Jet Propulsion Lab., California Inst. of Tech., Pasadena. Tracking Systems and Applications Section.
MOBILE VLBI AND GPS MEASUREMENT OF VERTICAL CRUSTAL MOTION **c46**
P. M. Kroger, J. M. Davidson, and E. C. Gardner (Kalamazoo Coll.) *In its* The Telecommun. and Data Acquisition Progr. Rept. 15 Aug. 1985 p 185-198 refs (For primary document see N86-10382 01-32)
Avail: NTIS HC A10/MF A01 CSCL 08E

Mobile Very Long Base Interferometry (VLBI) and Global Positioning System (GPS) geodetic measurements have many error sources in common. Calibration of the effects of water vapor on signal transmission through the atmosphere, however, remains the primary limitation to the accuracy of vertical crustal motion measurements made by either technique. The two primary methods of water vapor calibration currently in use for mobile VLBI baseline measurements were evaluated: radiometric measurements of the sky brightness near the 22 GHz emission line of free water molecules and surface meteorological measurements used as input to an atmospheric model. Based upon a limited set of 9 baselines, it is shown that calibrating VLBI data with water vapor radiometer measurements provides a significantly better fit to the theoretical decay model than calibrating the same data with surface meteorological measurements. The effect of estimating a systematic error in the surface meteorological calibration is shown to improve the consistency of the vertical baseline components obtained by the two calibration methods. A detailed error model for the vertical baseline components obtained indicates current mobile VLBI technology should allow accuracies of order 3 cm with WVR calibration and 10 cm when surface meteorological calibration is used. Author

N86-10402*# Jet Propulsion Lab., California Inst. of Tech., Pasadena. Communications Systems Research Section.
IMPROVED MAPPING OF RADIO SOURCES FROM VLBI DATA BY LEAST-SQUARE FIT
E. R. Rodemich *In its* The Telecommun. and Data Acquisition Progr. Rept. 15 Aug. 1985 p 199-210 refs (For primary document see N86-10382 01-32)
Avail: NTIS HC A10/MF A01 CSCL 20N

A method is described for producing improved mapping of radio sources from Very Long Base Interferometry (VLBI) data. The method described is more direct than existing Fourier methods, is often more accurate, and runs at least as fast. The visibility data is modeled here, as in existing methods, as a function of the unknown brightness distribution and the unknown antenna gains and phases. These unknowns are chosen so that the resulting function values are as near as possible to the observed values. If researchers use the radio mapping source deviation to measure the closeness of this fit to the observed values, they are led to the problem of minimizing a certain function of all the unknown parameters. This minimization problem cannot be solved directly, but it can be attacked by iterative methods which we show converge automatically to the minimum with no user intervention. The resulting brightness distribution will furnish the best fit to the data among all brightness distributions of given resolution. Author

N86-10403# Weapons Systems Research Lab., Adelaide (Australia).
A SIMPLIFIED METHOD OF ESTIMATION OF THE SPECULAR COMPONENTS OF RADAR CROSS SECTION FOR SOME RE-ENTRANT CONDUCTORS
L. A. Nicholls Dec. 1984 34 p
(AD-A156573; WSRL-0389-TM) Avail: NTIS HC A03/MF A01 CSCL 17/9

Methods of ray optics are used to describe the wavefronts emerging from the specular lines or specular rings on three separate irradiated reentrant conductors for short radar wavelengths. The conductors are a biconical reflector, a hollow circular cylinder with a far flat termination, and a thin spherical shell with a circular hole. The associated far fields and hence their Radar Cross Section (RCS) components are then found from evaluation of the associated simple field integrals using Huygen's Principle. GRA

N86-10404# Naval Weapons Center, China Lake, Calif.
RADOME ANALYSIS AND DESIGN CAPABILITIES OF THE RF AND MICROWAVE TECHNOLOGY BRANCH Interim Report, Fiscal Year 1982 - 1984
P. L. Overfelt Apr. 1985 39 p
(AD-A156662; AD-E900475; NWC-TP-6636) Avail: NTIS

HC A03/MF A01 CSCL 17/9

A description of computer codes covering boresight error prediction, flat panel reflection and transmission properties, Von Karman geometry parameters, and spherical wave propagation for radomes is presented. The theoretical basis for each code is discussed, and examples of inputs and outputs are given. Comparison of theory with experimental data shows reasonable correlation. Thus, these codes can predict many interesting and useful properties needed for adequate initial radome design without resorting to expensive and time-consuming test procedures. GRA

N86-10405# Mission Research Corp., Santa Barbara, Calif.
ACOUSTIC GRAVITY WAVE CHEMISTRY MODEL FOR THE RAYTRACE CODE Technical Report, 30 Jun. 1983 - 31 Jul. 1984
T. E. Old 1 Mar. 1984 38 p
(Contract DNA001-80-C-0022)
(AD-A156850; AD-E301723; MRC-R-815; DNA-TR-84-127) Avail: NTIS HC A03/MF A01 CSCL 20/14

This report discusses the implementation of F-region electron chemistry in the acoustic gravity wave model of the code RAYTRACE. The chemistry consists of three dominant reactions that control electron depletion in an F-region parcel that is pushed down into the higher density E-region atmosphere by the passage of a large amplitude gravity wave. The effect of electron depletion on the propagation of high frequency radio waves is shown by comparison of RAYTRACE radio propagation calculations with and without chemistry. GRA

N86-10406# Naval Research Lab., Washington, D. C.
ON THE USE OF X-BAND CW NANOSECOND AIRBORNE RADAR FOR TERRAIN PROFILING Final Report, Oct. 1984 - Apr. 1985
D. T. Chen and E. A. Uliana 25 Jun. 1985 21 p
(DA Proj. W05-270)
(AD-A156886; NRL-MR-5599) Avail: NTIS HC A02/MF A01 CSCL 17/9

Terrain profile sensed by a 10 GHz X-band airborne nanosecond radar has been compared against the terrain profile sensed simultaneously by a pulse laser profilometer. Several facts can be observed from a series of inter-comparisons between these two profiles. First, under the condition of comparable sampling intervals, the terrain profile sensed by radar is almost the same as that sensed by the laser profilometer except radar sensed profile does not contain information of narrow and tall objects above the ground surface. Second, a radar range resolution finer than 4 nanoseconds and a better algorithm on return waveform analysis for identifying narrow and tall objects in addition to the ground surface are going to improve accuracy and precision of radar's capability in terrain profiling. Third, for a short flight track, the removal of the effects on radar range measurements due to aircraft motion can not be achieved with knowing three ground surface elevations whose locations are well separated along the flight track. Last, the limit at which radar range tracking circuitry loses its lock and, thus, its ability in resolving ranging is higher for aftside range slopes than for foreside range slopes. GRA

N86-10407# Politecnico di Torino (Italy). Dept. di Elettronica.
COMPUTATIONAL TECHNIQUES FOR THE ANALYSIS AND DESIGN OF DIGITAL COMMUNICATION SYSTEMS Final Technical Report, 28 Jan. 1982 - 28 Mar. 1985
E. Biglieri Mar. 1985 107 p
(Contract DAJA37-80-C-0011; DA Proj. 1L1-61102-BH-57)
(AD-A156945; AD-E750985) Avail: NTIS HC A06/MF A01 CSCL 12/1

In this report we introduce some computational techniques for the analysis and design of digital communication systems, possibly operating over a nonlinear channel (a typical example is a digital satellite system, with the transponder amplifier working at or near saturation for better efficiency). We first consider evaluation of error probabilities when the disturbances are only incompletely known. Then we describe a combined simulation-and-analytical technique to evaluate the power density spectrum of a digital signal passed through a nonlinear channel. Next, we consider the problem of designing and evaluating the performance of the optimum linear receiving filter for transmission over a nonlinear channel. Finally, we consider Ungerboeck codes; a new class of multidimensional codes is introduced, its applications discussed, and an important property concerning their power spectral densities is shown. GRA

N86-10408# Sandia Labs., Albuquerque, N. Mex.
METHODS FOR DEVELOPING JAM-RESISTANT SECURITY COMMUNICATIONS NETWORKS AT FIXED-SITE FACILITIES
D. J. Gangel, J. E. Heustess, and M. K. Snell 1985 5 p Presented at the 1st Ann. AFCEA Symp. and Exposition on Phys. and Electron. Security, Philadelphia, 19 Aug. 1985
(Contract DE-AC04-76DP-00789)
(DE85-012032; SAND-85-0200C; CONF-850885-1) Avail: NTIS HC A02/MF A01

Considerable work has been done identifying and developing equipment and procedures that can be used to improve the survivability of a security communications network during a jamming assault. Insight is given into alternate communications methods that can be used to develop resistance to jamming by supplementing existing radio communications. The spatial properties of jamming are then discussed and examples of how these properties can be explocited are examined. Also discussed are spread-spectrum radios that are highly resistant to jamming and the importance of jamming exercises. DOE

N86-10409# California Univ., Livermore. Lawrence Livermore Lab.
MICROWAVE EVALUATION OF MATERIALS
R. J. King and V. R. Latorre May 1985 14 p
(Contract W-7405-eng-48)
(DE85-013183; UCID-20437) Avail: NTIS HC A02/MF A01

Modern microwave tools and measurement techniques show considerable promise for evaluating the electrical and physical properties of materials. These techniques are particularly useful for measuring the dielectric and conductive properties in situ. From these measurements, it is possible to infer many physical parameters such as moisture content, porosity, state of cure or aging, the presence of surface cracks, surface roughness, fiber/filler ratio, bulk fiber orientation, and some constitutent parameters such as graphite. While the wavelength of microwaves (centimeters) limits the spatial resolution required to locate small flaws (deep cracks, voids, etc.), microwaves are ideally suited to measure small variations in density and semiconductive properties of nonmetals. This is best accomplished using coherent techniques which are highly sensitive and capable of measuring the phase as well as the amplitude of the microwave signals being coupled to the test material. Moreover, since microwaves are polarized vector fields, they are highly sensitive to the anisotropy of materials. DOE

N86-10410# Allied Bendix Aerospace, Kansas City, Mo.
MINIATURE RADAR PACKAGING Final Report
G. W. Andrews Jun. 1985 105 p
(Contract DE-AC04-76DP-00613)
(DE85-014598; BDX-613-3266) Avail: NTIS HC A06/MF A01

Several concepts of interconnections between coaxial cables and RF HMCs were evaluated resulting in two approaches that function well electrically and mechanically and that are easily processed. Methods of attaching various configurations of large ceramic substrates into assemblies were investigated, yielding a better understanding of why breakage occurs, and to find ways to reduce the occurrence of breakage. An evaluation of several materials for use as gaskets to shield against RF interference between RF circuit compartments resulted in two suitable possibilities. Resistive film and microwave absorber liners were evaluated on the inside of RF circuit compartment covers, with favorable results obtained from one that reduced the effect of the lid proximity on the circuit performance. DOE

N86-10411# Research Inst. of National Defence, Linkoeping (Sweden).

DIGITAL RADIO LINK: METHOD AND A MEASURING SYSTEM FOR STUDYING THE RADIO CHANNEL DURING FREQUENCY SELECTIVE FADING

Stefan Mattsson Mar. 1985 57 p refs In SWEDISH; ENGLISH summary
(FOA-C-30386-E2; ISSN-0347-3708) Avail: NTIS HC A04/MF A01; Research Institute of National Defence, Stockholm KR 50

Methods to calculate propagation parameters during multipath propagation on microwave line-of-sight paths are reviewed. Spectrum measurements to verify a channel model for Swedish conditions, in the 7 and 13 GHz frequency bands are described. The measurements are controlled, in the sense that received power spectra are recorded if the discrepancy from a reference exceeds a given threshold. The program is described, and methods based on the characteristic frequency dependent attenuation during frequency selective fading are outlined. Author (ESA)

N86-10412# Deutsche Forschungs- und Versuchsanstalt fuer Luft- und Raumfahrt, Oberpfaffenhofen (West Germany). Inst. fuer Hochfrequenztechnik.

DIRECT-COUPLED CAVITY FILTERS WITH IRISES OF ARBITRARY THICKNESS

Manfred Weisser and Karl Hans Waegel Jan. 1985 67 p refs In GERMAN; ENGLISH summary Report will also be announced as translation (ESA-TT-939)
(DFVLR-FB-85-14; ISSN-0171-1342) Avail: NTIS HC A04/MF A01; DFVLR, Cologne DM 21

The transmission characteristics of symmetrical waveguide filters are investigated. The thickness of the irises is taken into account. The calculations are based on an exact mode matching method. In the frequency range of the X-band one-, two-, three-, four-, and six-cavity filters are analyzed and parameters such as aperture, thickness of irises, and cavity length are changed. The results of the measurements are in good agreement with the computed transmission characteristics. Author (ESA)

N86-10413# Deutsche Forschungs- und Versuchsanstalt fuer Luft- und Raumfahrt, Oberpfaffenhofen (West Germany). Abteilung HF-Verfahren.

SAR IMAGE QUALITY: A REVIEW

Timonthy K. Pike Mar. 1985 41 p refs
(DFVLR-Mitt-85-07; ISSN-0176-7739) Avail: NTIS HC A03/MF A01; DFVLR, Cologne DM 14

The necessities and applications of Synthetic Aperture Radar (SAR) image quality measurement, and the common SAR image quality parameters including spatial resolution, radiometric resolution, radiometric accuracy, energy distribution, and geometric distortion are discussed. Measurement techniques are described and supplemented with examples from SAR campaigns. Author (ESA)

N86-10616*# Jet Propulsion Lab., California Inst. of Tech., Pasadena.

RADAR SYSTEM DESCRIPTION

D. N. Held and W. E. Brown *In its* NASA/JPL Aircraft SAR Workshop Proc. 15 Jun. 1985 p 5-12 Original contains color illustrations (For primary document see N86-10615 01-43)
Avail: NTIS HC A05/MF A01 CSCL 17I

N86-10617*# Jet Propulsion Lab., California Inst. of Tech., Pasadena.

CV-990 L-BAND SAR: A CALIBRATION EXPERIMENT

D. N. Held and C. Werner *In its* NASA/JPL Aircraft SAR Workshop Proc. 15 Jun. 1985 p 17-20 ref Original contains color illustrations (For primary document see N86-10615 01-43)
Avail: NTIS HC A05/MF A01 CSCL 17I

33 ELECTRONICS AND ELECTRICAL ENGINEERING

Includes test equipment and maintainability; components, e.g., tunnel diodes and transistors; microminiaturization; and integrated circuitry.

For related information see also *60 Computer Operations and Hardware* and *76 Solid-State Physics.*

N86-10414 Department of the Air Force, Washington, D.C.

PROTECTION CIRCUITRY FOR HIGH VOLTAGE DRIVERS Patent

G. H. Frank, inventor (to Air Force) Issued 14 May 1985 5 p Supersedes AD-D010559
(AD-D011781; US-Patent-4,517,618; US-Patent-Appl-SN-529412; US-Patent-Class-361-58) Avail: US Patent and Trademark Office CSCL 09/1

Protection circuitry interposed between a power source and a load is arranged to gradually apply high voltage has attained a predetermined percentage of its nominal value. In the event that the load current exceeds a prescribed maximum limit, or in the absence of additional load voltages, the high voltage supply is disconnected from the load. GRA

N86-10415 Department of the Navy, Washington, D. C.

AMPLITUDE AND PHASE MODULATION IN FIN-LINES ELECTRICAL TUNING Patent

C. Vittoria, inventor (to Navy) Issued 19 Mar. 1985 6 p
(AD-D011813; US-Patent-4,506,234; US-Patent-Appl-SN-505569; US-Patent-Class-332-16R) Avail: US Patent and Trademark Office CSCL 09/1

A fin-line waveguide device for modulating signals passing there through, was discussed. The device comprises a fin-line waveguide including two channel members longitudinally extending in the direction of signal propagation through the device. The channel members are physically and electrically separated by a ferrite dielectric slab which is oriented in a longitudinally extending plane parallel to the electric field lines of the signal passing through the device. A magnetic field is applied to the ferrite slab to magnetically bias the slab to ferromagnetic resonance. A voltage is applied across the ferrite slab to alter the ferromagnetic resonance characteristics of the slab. The phase and amplitude of the signal processing through the waveguide are modulated in response to the applied voltage. GRA

N86-10416 Department of the Navy, Washington, D. C.

P-N JUNCTION CONTROLLED FIELD EMITTER ARRAY CATHODE Patent

R. F. Greene and H. F. Gray, inventors (to Navy) Issued 23 Apr. 1985 11 p Supersedes AD-D009923
(AD-D011815; US-Patent-4,513,308; US-Patent-Appl-SN-421766; US-Patent-Class-357-55) Avail: US Patent and Trademark Office CSCL 09/1

A Field Emitter Array comprising a semiconductor substrate with an emitter surface formed thereon. A plurality of emitter pyramids is disposed on the emitter surface for emitting an electron current. The magnitude of the electron current emitted by each emitter pyramid 1 max, is controlled by a reverse-biased p-n junction associated with each emitter pyramid where 1 max = j sat X A p-n, j sat being the saturation current density and A p-n being the area of the reverse-biased p-n junction associated with each emitter pyramid. A grid, positively biased relative to the emitter surface and the emitter pyramids, is disposed above the emitter surface for creating a electric field that induces the emission of the electron current from the emitter tips. Author (GRA)

N86-10417 Department of the Navy, Washington, D. C.

PULSE COMPRESSION SYSTEM Patent

B. L. Lewis, inventor (to Navy) Issued 4 Jun. 1985 14 p Supersedes AD-D007318
(AD-D011833; US-Patent-4,521,779; US-Patent-Appl-SN-143399; US-Patent-Class-343-17.2PC) Avail: US Patent and Trademark

Office CSCL 09/4

This patent desribes a system for polyphase encoding transmitted pulses of energy and for decoding the received signals to enhance returns from the range interval being examined during a particular processing period and attenuate returns from contiguous range intervals (pulse compression). The system includes a decoding device which comprises a delay circuit having N distributed outputs including its input for producing a uniform delay between adjacent outputs corresponding to N inputted elements of received phase-coded signal of length N squared; a conjugator circuit coupled to the first N/2 successive outputs of the delay circuit; a first signal-combining circuit coupled to the conjugator circuit and to the last N/2 successive outputs of the delay circuit; a multiplier circuit coupled to the first signal-combining circuit; and a second signal-combining circuit coupled to the multiplier circuit. The decoding device provides a decoding phase shift to the signal elements of the phase-coded signal. GRA

N86-10418*# National Aeronautics and Space Administration, Washington, D. C.

DESIGN AND CONSTRUCTION OF A FARADAY CUP FOR MEASUREMENT OF SMALL ELECTRONIC CURRENTS

Andre Veyssiere Sep. 1985 35 p refs Transl. into ENGLISH of "Etudes et Realisation d'une Coupe de Faraday pour les Mesures de Faibles Courants Electroniques" Saclay, CEA, Oct. 1967 p 1-28 Original language document announced as N68-25321 Transl. by Scientific Translation Service, Santa Barbara, Calif.
(Contract NASw-4004)
(NASA-TM-77915; NAS 1.15:77915; CEA-R-3276) Avail: NTIS HC A03/MF A01 CSCL 09A

The design of a device to measure and integrate very small currents generated by the impact of a charged particle beam upon a Faraday cut is described. The main component is a graphite block capable of stopping practically all the incident changes. The associated electronic apparatus required to measure better than 10/13 ampere with a precision of 10/0 is described. E.A.K.

N86-10419# Defence Research Establishment Valcartier (Quebec).

AN ACTIVE TRACKING BAND-PASS FILTER

A. Morin and P. Labbe May 1985 50 p
(AD-A156559; DREV-4347/85) Avail: NTIS HC A03/MF A01 CSCL 09/5

A frequency-agile tracking filter, which operates over a wide frequency range with a high immunity to noise and interference, has been designed. It consists of a second-order bandpass filter which is continuously tunable over the 5 to 140-kHz band. The resonant frequency of the filter is adjusted by means of a feedback loop to the frequency component of greatest amplitude in the input signal. The loop includes a fast AGC amplifier, a fast frequency-to-voltage converter and a low-pass filter. The components of the tracking filter are described and analyzed. Analysis of the tracking filter, as regards its immunity to noise and interference, its frequency agility and the stability of its control loop, is also presented to optimize system parameters. Finally, the performance of the processor is shown by experimental measurements. GRA

N86-10420# Washington Univ., St. Louis, Mo. Dept. of Electrical Engineering.

CRITERIA FOR THE DESIGN OR SELECTION OF A BIOELECTROMAGNETICS EXPERIMENT Final Technical Report, 1 Sep. 1984 - 31 May 1985

W. F. Pickard 28 Jun. 1985 15 p
(Contract N00014-84-K-0457)
(AD-A156575) Avail: NTIS HC A02/MF A01 CSCL 06/19

By athermal, one normally means an effect which: (1) has been explained explicitly and unambiguously in terms of mechanisms other than increased random molecular motion (i.e., heating), or (2) occurs at absorbed power levels so low that a thermal mechanism seems unlikely, or (3) displays so unexpected a dependence upon some experimental variable that it is hard to see how heating could lie behind it. The aim of this report is to discuss guidelines by which and experiment directed toward the discovery or elucidation of an athermal effect might be designed or evaluated. It will consist of three main sections. First, the great commandment of athermal bioelectromagnetics will be discussed; that any reported, putatively athermal bioeffect be robustly reproducible. Six criteria are propounded for judging the credibility of a reported experiment in athermal bioelectromagnetics. It is concluded that experimentation in athermal bioelectromagnetics would be markedly facilitated by the identification of the mechanisms underlying the observed effects. GRA

N86-10421# Department of the Navy, Washington, D. C.

CONSTANT RISE AGC (AUTOMATIC GAIN CONTROL) DEVICE Patent Application

R. A. Slack, inventor (to Navy) Filed 25 Mar. 1985 19 p
(AD-D011744; US-Patent-Appl-SN-715992) Avail: NTIS HC A02/MF A01 CSCL 09/5

The invented device provides automatic gain control (AGC) of incoming signals over a large dynamic range of input levels with a constant rise time. The constant rise AGC device includes a primary AGC loop for receiving the incoming or input signal and splitting the input signal to input and output components of the primary AGC loop. The input signal to the input component is processed within the primary AGC loop to control the gain of the input signal at the output component of the primary AGC loop. The primary AGC loop has a slow detector. A secondary AGC loop is provided within the primary AGC loop, and this secondary AGC loop includes the aforementioned input component and has its output connected to the slow detector. The secondary AGC loop has a fast detector for preventing self-imposed saturation. With this arrangement the secondary AGC loop can be utilized to provide a constant AGC buildup signal for any input signal which is greater than a predetermined dB range, and the remainder of the primary AGC loop, which receives the constant AGC buildup signal from the secondary AGC loop, can be optimized for desired rise and fall times so that the latter's output signal can be relatively unaffected by interference bursts, signal gaps, and fading in the input signal. Author (GRA)

N86-10422# Department of the Navy, Washington, D. C.

EXTENDED PRECISION IN VIDEO BANDWIDTH ANALOG TO DIGITAL CONVERTER USING OPTICAL TECHNIQUES Patent Application

H. F. Taylor, inventor (to Navy) Filed 28 Mar. 1985 19 p
(AD-D011745; US-Patent-Appl-SN-717365) Avail: NTIS HC A02/MF A01 CSCL 09/5

Two interferometric electro-optic modulators formed from single mode waveguides in a single crystal substrate of pockels (linear) electro-optic material is used in conjunction with optical sampling techniques and conventional Analog-to-Digital technology to convert analog signals to a binary representation. Author (GRA)

N86-10423# Department of the Navy, Washington, D. C.

HIGH OUTPUT PROGRAMMABLE SIGNAL CURRENT SOURCE FOR LOW OUTPUT IMPEDANCE APPLICATIONS Patent Application

D. G. Jablonski and R. W. Watkins, inventors (to Navy) Filed 10 May 1985 10 p
(AD-D011751; US-Patent-Appl-SN-732330) Avail: NTIS HC A02/MF A01 CSCL 09/5

The present invention relates to a high output programmable current source. Complementary output stages are connected between appropriate power supply polarities for driving a low impedance load which is connected to circuit ground. An operational amplifier is connected between the input and emitter of each of the complementary stages providing negative feedback for virtually eliminating in the input offset voltage of the respective output stage. A programmable function signal source is connected to the operational amplifiers for driving a programmable signal current to the extent possible through the load resistance from a limited voltage supply. Author (GRA)

N86-10424# Department of the Air Force, Washington, D.C.
TOTAL INTERNAL REFLECTION MODULATOR/DEFLECTOR Patent Application
Birnbaum, inventor (to Air Force) Filed 22 Apr. 1985 21 p
(AD-D011757; US-Patent-Appl-SN-726872) Avail: NTIS HC A02/MF A01 CSCL 20/3

This document refers to a total internal reflection modulator/deflector assembly for use with a focused beam of polarized incident laser light. The application of a low direct current voltage (e.g., less than 50 volts) to a pair of identical stacked crystals exhibiting the Pockel's effect produces an index of refraction difference at their interface. Since the index changes are small, the incidence angle of the impinging polarized laser light is large, e.g., 89 degrees. In the preferred embodiment, one crystal is rotated relative to the other, such that the applied electric field causes and index changes of +(delta)n in one crystal and of -(delta)n in the other crystal. As a result, the impinging polarized laser light is refraction into two portions, one of which is totally internal reflected, and transmitted in the desired modulated conditions. Two electrode members are used to apply the low direct current voltage to the interface of the crystals, with the electrodes arranged to face each other across the crystals, and also positioned such that the incident light need not traverse them. GRA

N86-10425# Department of the Air Force, Washington, D.C.
INSTANTANEOUS FREQUENCY MEASUREMENT RECEIVER WITH DIGITAL PROCESSING Patent Application
J. B. Y. Tsui, inventor (to Air Force) Filed 30 May 1985 13 p
(AD-D011759; US-Patent-Appl-SN-739413) Avail: NTIS HC A02/MF A01 CSCL 14/2

The receiver comprises a 90 deg hybrid and analog-to-digital converters between the RF section and digital processing: which makes it possible to eliminate a phase correlator, four diode detectors and two differential amplifiers used in previous IFM (Instantaneous Frequency Measurement) receivers to obtain the sine and cosine signal samples at an initial time and at a delayed time. GRA

N86-10426# Department of the Air Force, Washington, D.C.
PHOTOIONIZATION TECHNIQUE FOR GROWTH OF METALLIC FILMS Patent Application
J. G. Eden, inventor (to Air Force) Filed 29 May 1985 21 p
(AD-D011760; US-Patent-Appl-SN-738817) Avail: NTIS HC A02/MF A01 CSCL 13/8

A novel method and system for depositing films of selected metallic or semiconductor materials, and particularly of the group 3, 4, and 5 elements, is described which comprises heating a halide compound of the material to produce vapor within a substantially closed chamber, irradiating the vapor with light of preselected wavelength to dissociatively photoionize the vapor with light of preselected wavelength to dissociatively photoionize the vapor into the constituent positive ions of the material and negative halogen ions, and subjecting the photoionized vapor to an electric field to selectively remove the positive ions of the material for plating as a film. GRA

N86-10427# Department of the Air Force, Washington, D.C.
SIGNAL ANALYSIS RECEIVER WITH ACOUSTO-OPTIC DELAY LINES Patent Application
J. B. Y. Tsui, inventor (to Air Force) Filed 10 Jun. 1985 15 p
(AD-D011761; US-Patent-Appl-SN-742825) Avail: NTIS HC A02/MF A01 CSCL 09/1

The system makes use of an interferometric Bragg cell for the time delays needed by the multiple antenna inputs in an angle-of-arrival (AOA) measurement system, for accurate measurements over wide bandwidths. A signal Bragg cell is modulated with a selected band of the EW signal environment, using a separate transducer coupled to each quadrant antenna element. A reference Bragg cell is modulated with a chirp signal. Coherent light from a laser is split and directed to both the signal. Coherent light from a laser is split and directed to both the signal cell and the reference cell. The output light beams from the reference Bragg cell and signal Bragg cell are combined and focused onto photo detectors having a one-dimensional array for each quadrant antenna element. The reference and signals are heterodyned at the photodetectors, which results in a channelized spectral output with each channel at the same intermediate frequency (IF). The outputs of the photodetectors are used by a phase comparison unit, cued by a frequency measurement receiver to the correct detectors, to provide the AOA measurement. GRA

N86-10428# Electronics Research Lab., Adelaide (Australia).
A COMPACT BULK ACOUSTO-OPTIC TIME INTEGRATING CORRELATOR
D. A. B. Fogg Nov. 1984 48 p
(AD-A156608; ERL-0323-TR) Avail: NTIS HC A03/MF A01 CSCL 09/3

This report describes the design and testing of a prototype correlator using lead molybdate Bragg cells. It indicates the suitability of this design for cells made of materials with longer transition times, such as tellurium dioxide. Compactness and simplicity are achieved by the use of a specially designed prism. An analysis of the AO, TIC process and performance parameters is given. GRA

N86-10429# Stanford Univ., Calif. Electronics Lab.
INVESTIGATION OF METALLIC IMPURITIES INTRODUCED INTO SiO2 AND SILICON BY VARIOUS CANDIDATE VLSI METALLIZATION SYSTEMS: CHEMICAL REACTIONS, DIFFUSION, AND ELECTRICAL PROPERTIES Final Report
T. W. Sigmon and R. M. Swanson Apr. 1985 17 p
(Contract MDA903-82-K-0412; DARPA Order A04541)
(AD-A156609) Avail: NTIS HC A02/MF A01 CSCL 09/5

The main objectives of this project were to investigate the diffusion of various gate metals into SiO2 and the diffusion of metals into silicon from contact metallization. The bulk of the work was performed on SiO2, and experimental diffusion results were obtained for Ag, Cu, Pd, Au, Ta, and Ti. From these results, a model for interstitial diffusion in SiO2 was developed that predicts both the ionization state and activation energy for diffusion and solid solubility as a function of temperature. The work concluded that Pd, Au, Mo, Ta, W, Pt, Ti, and Al are suitable candidates for VLSI gate and interconnect metallizations, whereas Ag, Cu, Na, Ni, Mn, Fe, Mg, and Ga are not. This report covers work performed to detect and measure the diffusion of contact metals into crystalline Si. This effort encountered more experimental problems than the SiO2 case, partially because in VLSI technology there are both different types on contacts and varying junction depths present below the contacts. Realizing the importance of these points enabled us to choose a suitable mask set to take these parameters into account. The parameters on interest in this work are; junction depth, junction conductivity type; overlapped or enclosed junction geometry, and contact metallization. Junctions with different combinations of these parameters are subjected to Bias Current Temperature Stressing (BJTS) at elevated temperatures to simulate a long Dt diffusion. The various diodes are packaged to avoid direct probing, and to make sure the temperature is constant for all diodes undergoing BJTS. GRA

N86-10430# Weapons Systems Research Lab., Adelaide (Australia).
A COMPARISON OF SWEPT FREQUENCY AND FFT METHODS USED TO CALIBRATE ARRAY TEST MODULES
G. B. Gillman Oct. 1984 47 p
(AD-A156629; WSRL-0383-TR) Avail: NTIS HC A03/MF A01 CSCL 20/1

A description is given of swept frequency and Fast Fournier Transform (FFT) methods used to calibrate array test modules. The FFT method is shown to give sensitivity versus frequency plots with relative ease and known accuracy. The swept frequency method is capable of giving similar results but only after operator interpretation of the mean of fluctuating signals and calculations on a point to point basis. A digital filtering method is briefly described which can be used to process the signals obtained in swept frequency calibration obviating the need for operator interpretation. The accuracy of the FFT method is discussed and

an overall accuracy figure is obtained for the derived sensitivity of the test array. A summary of the FFT method is given as a guide for future hydrophone calibration experiments. GRA

N86-10431# Virginia Polytechnic Inst., Blacksburg.
INTRINSIC MECHANISMS OF MULTILAYER CERAMIC CAPACITOR FAILURE Annual Report, 15 Mar. 1984 - 13 Mar. 1985
L. C. Burton Apr. 1985 53 p
(Contract N00014-83-K-0168)
(AD-A156638) Avail: NTIS HC A04/MF A01 CSCL 09/1

The possible role of grain boundaries (GB) in MLC capacitors, with respect to insulation resistance and its degradation, is reviewed. Activation energy (E sub A) can be related directly to GB barrier height, Phi sub B. The voltage dependent activation energies for poly-Si, ZnO varistors and PTC devices has been attributed directly to E sub A. Varistor and PTC device degradation is caused GB passivation. A similar voltage dependence is reported here for barrier layer and COG capacitor types where E sub A decreases from 0.91 to 0.44eV and from 1.61 to 0.90eV respectively, with concurrent super-ohmic increases in leakage current. Such a voltage dependent E sub A is not seen for X7R devices, even though the current is super-ohmic. Reasons to account for this are discussed. It is concluded that the GB potential barrier may offer a major source of impedance to leakage current for MLC capacitors, and its decrease may result in failure. It has been ascertained that E sub A decreases for degraded X7R devices, with an increase in the I-V slope. These results are consistent with our earlier reports on degraded devices, and with the space charge limited current model for emission from electrodes. X7R chips with no internal electrodes exhibit both ohmic and super-ohmic characteristics, with activation energies independent of voltage. A near-exponential rate of current increase with time, accompanied by a linear decrease in E sub A, was seen for both X7R and Z5U capacitors. GRA

N86-10432# Carnegie-Mellon Inst. of Research, Pittsburgh, Pa. Dept. of Computer Science.
IMPLEMENTATION ISSUES FOR ALGORITHMIC VLSI (VERY LARGE SCALE INTEGRATION) PROCESSOR ARRAYS Ph.D. Thesis
A. L. Fisher Oct. 1984 108 p
(Contracts F33615-81-K-1539; N00014-76-C-0370; N00014-80-C-0236)
(AD-A156699) Avail: NTIS HC A06/MF A01 CSCL 09/5

Advances in very large scale integration (VLSI) have led to a great deal of interest in highly parallel cellular architectures as high-performance solutions to computational bottlenecks. These architectures pose a number of novel implementation issues not encountered in traditional designs. This thesis investigates and resolves some of the most important of these issues, taking both practical and theoretical points of view. Chapter 2 considers the subject of programmability for arrays of processors. It describes some of the advantages and disadvantages of flexible implementations, and discusses processor design issues in light of the requirements of the array environment. In particular, it describes the design of PSC, a chip designed for systolic array implementations, which has been realized in nMOS. It also discusses alternative combinations of processors and memories for the implementation of systolic algorithms. Chapter 3 examines the question of synchronization in large arrays of processors. It gives asymptotic upper and lower bounds for the speed of clocked arrays of differing topologies under differing models of clock stew, and also makes some observations on practical issues of synchronization in large systems. Chapter 4 concentrates on implementations in which arithmetic is broken up into serial bit or subword steps; it shows how systolic serialized systems can be designed, and discusses some practical issues of cost and performance. Finally, Chapter 5 presents a case study of architectures for a family of information retrieval tasks. GRA

N86-10433# Reliability Analysis Center, Griffiss AFB, N. Y.
MICROCIRCUIT DEVICE RELIABILITY FIELD EXPERIENCE DATABASE. VOLUME 1. FIELD DATA. VOLUME 2. FAILURE EVENT/ANALYSIS DATA
D. J. Mahar and M. J. Rossi 11 Feb. 1985 715 p
(Contract F30602-84-C-0162)
(AD-A156836; AD-E301723; MDR-21A-Vol-1/2) Avail: NTIS HC A99/MF A02 CSCL 09/5

MDR-21a is a Structured presentation of Field Experience Reliability Data which covers Digital, Linar, Interface, Memory and VLSI Device Types. GRA

N86-10434# Air Force Inst. of Tech., Wright-Patterson AFB, Ohio.
CONTACT EFFECTS IN LIGHT ACTIVATED GaAs SWITCHES M.S. Thesis
P. S. Durkin May 1985 41 p
(AD-A156957; AFIT/CI/NR-85-40T) Avail: NTIS HC A03/MF A01 CSCL 09/5

The purpose of this work was to examine the effects of various types of contacts on the switching behavior of a light-triggered power switch. The switch was constructed from a homogeneous wafer of chromium-doped gallium arsenide; the contacts were either ohmic, non-ohmic, or Schottky barriers. These were formed on the wafer in two geometries; both contacts on one side, and one contact spacings were used to permit the effects of the location of the existing laser pulse to be studied. A high voltage power supply (zero to 20 kV) was employed as the bias supply. A Nd:YAG laser, in the pulsed mode, was used to trigger the switch, which was mounted on a cold finger cooled to near liquid nitrogen temperature. Cooling reduced the dark current to manageable values (less than 1 micro A), and also reduced the avalanche breakdown voltage. The results of the measurements indicate that ohmic contacts produced more reliable switching than the non-ohmic or Schottky contacts, in as much as the shape of the output current pulse was better, and the number of pulses which the switches could sustain before the pulse shape deteriorated was greater, for the ohmic contacts. Surface discharge between the one-sided contacts obscured any differences in switching characteristics which might have depended on the location of the pulsed light excitation, so that no correlation between position and behavior could be obtained. GRA

N86-10435# Department of the Air Force, Washington, D.C.
APPARATUS FOR LOCATING PASSIVE INTERMODULATION INTERFERENCE SOURCES Patent Application
J. C. Mantovani, inventor (to Air Force) Filed 4 Apr. 1985 24 p
(AD-D011798; US-Patent-Appl-SN-719792) Avail: NTIS HC A02/MF A01 CSCL 20/1

An apparatus for locating passive interference sources by using a pair of different RF signals in conjunction with an acoustic signal to generate intermodulation products in metal-to-metal junctions. The acoustic tagging technique utilizes a focused, high power beam of acoustic energy to mechanically vibrate the suspected offending junction. This mechanical vibration causes the level of intermodulation products that are generated in the junction to become amplitude modulated at the frequency of the acoustic illumination. The detection of the AM sidebands with a low noise RF receiver that is tuned to a particular intermodulated component, permits the offending junction to be located. Author (GRA)

N86-10436# Department of the Air Force, Washington, D.C.
INTERDIGITAL SCHOTTKY BARRIER CAPACITOR APPARATUS Patent Application
Bierig, inventor (to Air Force) Filed 7 May 1985 19 p
(AD-D011799; US-Patent-Appl-SN-731223) Avail: NTIS HC A02/MF A01 CSCL 09/1

The present invention relates broadly to Schottky barrier capacitors, and in particular to an interdigital Schottky barrier capacitor apparatus. In the prior art, the Schottky barrier diode is rather well known. In general, a Schottky barrier device comprises a semiconductor substrate layer that is formed by a first layer of heavily doped materials and a second layer of lightly doped materials upon which a layer of barrier metal is deposited thereon. The maximum reverse bias voltage which can be appplied to the Schottky barrier device is determined by the thickness of the lightly doped layer of semiconductive material which is deposited upon

the substrate layer. This is only one of the factors that determined the reverse bias voltage, When a guardring is diffused into the lightly doped layer of semiconductive substrate material, the thickness of the layer is reduced, and therefore, the reverse bias voltage that can be applied to the Schottky device is reduced. GRA

N86-10437# Department of the Air Force, Washington, D.C.
MULTI-ROW CONNECTOR WITH GROUND PLANE BOARD Patent Application
J. C. Cunningham, inventor (to Air Force) Filed 6 Mar. 1985 12 p
(AD-D011803; US-Patent-Appl-SN-708909) Avail: NTIS HC A02/MF A01 CSCL 09/1

The present invention relates to electrical connectors and particularly to a multi-row connector having a printed circuit ground plane board associated there with for grounding the outer shields of conductors at the connector. This patent application discloses a multi-row connector having a ground plane board mounted between rows of connector pins on the backside of the connector. Conductor shields of individual wires are soldered directly to conductor strips on the printed circuit ground plane board, and the strips are jumpered to a grounding pin on the connector. GRA

N86-10438# Brookhaven National Lab., Upton, N. Y. School of Chemical Engineering Practice.
STREAMING POTENTIALS IN CONDUCTIVE AND NONCONDUCTIVE TUBING
A. Fung, R. Conti, and J. Ruszkay Sep. 1984 73 p refs
(Contract DE-AC02-76CH-00016)
(DE85-012984; BNL-51875; MIT/BNL-84-4) Avail: NTIS HC A04/MF A01

The feasibility of using streaming potentials measured in blood flow for diagnostic purposes (electroarteriograms) was studied by flowing electrolyte solutions in both nonconductive and conductive tubings as model systems. Streaming potentials measured for 10 to the minus 4 power M and 10 to the minus 5 power M sodium chloride solutions in nonconductive polyethylene tubing obeyed the published theoretical relationships between potential and velocity. Under the same conditions, tubes constructed from conductive Nafion and a cationic exchange material which possessed the same ion-exchange group did not exhibit measurable streaming potentials while an apparent streaming potential was observed with an anionic exchange tubing. Electroarteriogram signals may not represent streaming potentials since blood electrolyte concentrations yield a conductivity that may be too high to cause a measurable effect. DOE

N86-10439# Sandia Labs., Albuquerque, N. Mex.
CALIBRATED FARADAY CURRENT AND MAGNETIC FIELD SENSOR
B. T. Neyer, J. Chang, G. J. Lockwood, and L. E. Ruggles 1985 10 p Presented at the 5th IEEE Pulsed Power Conf., Washington, D.C., 10 Jun. 1985
(Contract DE-AC04-76DP-00789)
(DE85-013438; SAND-84-2544C; CONF-850616-38) Avail: NTIS HC A02/MF A01

A calibrated optical fiber Faraday rotation current sensor is developed. This sensor has a gigahertz response, is immune to electromagnetic interference, and is constructed entirely of dielectric material. All of these advantages make the sensor ideal for pulsed power measurements. DOE

N86-10440# Washington Univ., St. Louis, Mo.
NON-EMPIRICAL INTERATOMIC POTENTIALS FOR TRANSITION METALS Progress Report
7 Jun. 1985 7 p
(Contract DE-FG02-84ER-45130)
(DE85-013448; DOE/ER-45130/T1) Avail: NTIS HC A02/MF A01

Research is reported in the study of metallic bonding and interatomic potential functions. Topics covered include many-atom interactions and the notion of an effective pair potential in a metal, interactions between transition metal ions in semiconductors and insulators, mathematical techniques for extrapolation from incomplete information about atomic distribution functions, and bonding and electronic structure of filled d-band tetrahedral compounds. DOE

N86-10441# Westinghouse Research and Development Center, Pittsburgh, Pa.
DELAY TIMES AND JITTER IN TRIGGERED VACUUM SPARK GAPS USING METAL VAPOR AND SURFACE FLASHOVER TYPES OF TRIGGERS
R. E. Voshall, D. Bhasavanich, J. G. Gorman, and M. T. Buttram (Sandia Labs., Albuquerque, N. Mex.) 1985 5 p refs Presented at 5th IEEE Pulsed Power Conf., Washington, D.C., 10 Jun. 1985
(Contract DE-AC04-76DP-00789)
(DE85-013966; CONF-850616-46) Avail: NTIS HC A02/MF A01

Triggered vacuum spark gap experiments were performed in a demountable arc chamber with a pressure of 10/2 to 10/4 m torr. Planar copper electrodes were used in which one electrode contained the trigger. Metal vapor spark triggers and surface flash-over types of triggers were explored. The delay time between the trigger breakdown and the conduction of the main gap, and the jitter in this time, were measured as a function of main gap voltage ranging from 3 to 20 kV and main gap separations of 13 to 19 mm. Main gap current following breakdown ranged from 3 to 15 kA. Using the metal vapor trigger, delay times as long as 500 ns were observed for a gap field of 500 V/mm while using the surface flashover type of triggers, delay times of 300 ns were observed for a similar main gap field strength. When the trigger was in the cathode electrode and the trigger was pulsed negatively, the operation of the gap was more consistent and the delay times were observed to increase with main gap voltage. The experimental data are interpreted on the basis of plasma expansion models. DOE

N86-10442# California Univ., Berkeley. Lawrence Berkeley Lab.
DEFECT IDENTIFICATION IN HIGH-ENERGY SEMICONDUCTORS
E. E. Haller May 1985 14 p Presented at the 2nd Spring Meeting of the Mater. Res. Soc., San Francisco, 15 Apr. 1985
(Contract DE-AC03-76SF-00098)
(DE85-014533; LBL-19218; CONF-850421-01) Avail: NTIS HC A02/MF A01

The elemental semiconductors silicon and germanium can be purified to electrically active impurity concentrations as low as approx. 10(10) cm(-3). Highly sensitive, energy dispersive analytical techniques have been developed to identify and measure the concentration of the residual elemental impurities. The application of these techniques to very pure materials has also resulted in the discovery of a large number of new levels which are due to impurity/defect complexes. Photothermal ionization spectroscopy using uniaxial stress or a magnetic field, electron paramagnetic resonance, and doping experiments using stable and radioactive elements have been used in combination to identify the composition and the structure of some of the new centers. DOE

N86-10443# Argonne National Lab., Ill.
SOUDAN 2 DATA ACQUISITION AND TRIGGER ELECTRONICS
J. Dawson, R. Iaird, E. May, N. Mondal, J. Schlereth, N. Solomey, J. Thron, and S. Heppelman 1985 5 p refs Presented at 4th Topical Conf. on Computerized Data Acquisition in Particle and Nucl. Phys., Chicago, 19 May 1985
(Contract W-31-109-eng-38)
(DE85-013864; CONF-850579-3) Avail: NTIS HC A02/MF A01

The 1.1 kton Soudan 2 detector is read out by 15 K anode wires and 3 2 K cathode strips. Preamps from each wire or strip are bussed together in groups of 8 to reduce the number of ADC channels. The resulting 6144 channels of ionization signals are flash-digitized every 150 ns and stored in RAM. The raw data hit patterns are continually compared with programmable trigger multiplicity and adjacency conditions. The data acquisition process is managed in a system of 24 parallel crates each containing

an Intel 8086 microprocessor, which supervises a pipe-lined data compactor, and allows transfer of the compacted data via CAMAC to the host computer. The 8086's also manage the local trigger conditions and can perform some parallel processing of the data. Due to the scale of the system and multiplicity of identical channels, semi-custom gate array chips are used for much of the logic, utilizing 2.5 micron CMOS technology. DOE

N86-10444# Physical Sciences, Inc., Andover, Mass.
FUEL CELL TECHNOLOGY ASSESSMENT PROGRAM, WORK ELEMENT NO. 6 Final Report, 30 Sep. 1981 - 30 Sep. 1984
D. Bloomfield and H. Piperopoulou Sep. 1985 187 p
(Contract DE-AC21-81FE-15078)
(DE85-008228; DOE/FE-15078/6-1; PSI-TR-451) Avail: NTIS HC A09/MF A01

The Fuel Cell Technology Assessment Program (FCTAP) developed at Physical Sciences Inc. (PSI) is a set of four computer codes which may be used to determine the effect of advances in fuel cell technology on the distribution of energy in the United States. The four codes are written for use on IBM/PC microcomputers (or equivalent) and are summarized. DOE

N86-10445# Department of Energy, Washington, D. C.
ALUMINUM BATTERY ALLOYS Patent Application
D. S. Thompson, inventor (to DOE) (California Univ., Livermore, Lawrence Livermore Lab.) and D. H. Scott, inventor (to DOE) (California Univ., Livermore, Lawrence Livermore Lab.) Filed 28 Sep. 1984 25 p
(Contract W-7405-eng-48)
(DE85-011599; US-Patent-Appl-SN-655486) Avail: NTIS HC A02/MF A01

Aluminum alloys suitable for use as anode structures in electrochemical cells are disclosed. These alloys include iron levels higher than previously felt possible, due to the presence of controlled amounts of manganese, with possible additions of magnesium and controlled amounts of gallium. DOE

N86-10446# California Univ., Berkeley. Lawrence Berkeley Lab.
EFFECT OF H2S AND COS IN THE FUEL GAS ON THE PERFORMANCE OF AMBIENT PRESSURE PHOSPHORIC ACID FUEL CELLS
P. N. Ross, Jr. Apr. 1985 40 p refs
(Contract DE-AC03-76SF-00098)
(DE85-013913; LBL-18001) Avail: NTIS HC A03/MF A01

The objective of this project was to determine in laboratory cells the tolerance of phosphoric acid fuel cells (PAFC) to hydrogen sulfide and carbonyl sulphide impurities in the anode feed gas. The study was conducted in three phases: the first was testing in a small (1 sq cm) free electrolyte cell to examine the effect of electrode structure on cell tolerance and to determine the order of magnitude of sulfur causing failure in cells at zero utilization; the second was testing in standard 2' x 2' PAFC laboratory hardware at ambient pressure to examine the effect of hydrogen utilization on tolerance and the possible effect of fuel impurities on cathode performance; the final phase was testing with a 2' x 2' cell in a pressure vessel to determine the effect of pressurized operation on cell tolerance. The poisoning effect of hydrogen sulfide was characteristically different from the effects of carbon monoxide, in that it was not manifested by a marginal (e.g., 0 to 50 mV) increase in anode potential but either had no effect or caused catastrophic polarization. Critical levels were derived for hydrogen sulfide as related to cell operating conditions. DOE

N86-10447# Institute of Gas Technology, Chicago, Ill.
EFFECTS OF H2S ON MOLTEN CARBONATE FUEL CELLS Progress Report, 1 Jul. - 30 Sep. 1984
R. J. Remick Jun. 1985 41 p refs
(Contract DE-AC21-83MC-20212)
(DE85-014052; DOE/MC-20212/1850) Avail: NTIS HC A03/MF A01

Phase 2 work was directed toward determination of the impact of H2S contaminants upon the ability of nickel-10% chromium anodes to catalyze the steam reforming reaction. Small amounts of three hydrocarbons representative of three homologous series were added to the fuel. These series were the paraffin series with methane as its representative, the olefin series with ethylene and the aromatics with toluene. Results indicated that the nickel-10% chromium anode had little catalytic activity toward the steam reforming of methane, but the steam reform did have 70% of the ethylene and about 30% of the toluene. The addition of 5 ppM hydrogen sulfide to the fuel totally poisoned all steam reforming activity. Phase 3 work addressed the impact on cell performance of SO2 in the oxidant gases. The cell was operated for 200 hours on clean fuel and oxidant. After baseline data had been collected, the cell was switched to an oxidant supply that contained 2 ppM of SO2. After 170 hours of operation on contaminated oxidant, no SO2 could be detected in the oxidant exhaust although 200 ppM of H2S were present in the fuel exhaust steam. DOE

N86-10448# Tennessee Univ., Knoxville. Dept. of Chemical and Metallurgical Engineering.
THERMODYNAMIC CONSTRAINTS ON ION BEAM MIXING OF METALS ON INSULATORS
G. C. Farlow, B. R. Appleton, L. A. Boatner, C. J. McHargue, C. W. White, G. J. Clark, and J. E. F. Baglin 1985 10 p Presented at the 2nd Spring Meeting of the Mater. Res. Soc., San Francisco, 15 Apr. 1985 Prepared in cooperation with IBM Research Lab., Yorktown Heights, N.Y.
(Contract DE-AC05-84OR-21400)
(DE85-013628; CONF-850421-10) Avail: NTIS HC A02/MF A01

Several different insulating substrates are coated with various metal films and ion beams irradiated using either Xe or Kr ions. These are then examined by Rutherford backscattering spectroscopy and scanning electron microscopy to determine if interfacial mixing has taken place. These results are compared with the sign of the reaction enthalpy of the metal and substrate to test the proposition that metals mix on insulators if the reaction enthalpy is negative and do not mix if it is positive. The enthalpy rule is, in general, valid. Two exceptions are found: Cr on SiO2 and Zr on Al2O3; however, these exceptions contain ambiguous features. Irradiation with a light, reactive ion is found to produce no mixing. DOE

N86-10449# Messwandler-Bau G.m.b.H., Bamberg (West Germany).
HIGH VOLTAGE INSTRUMENT TRANSFORMERS FOR OUTDOOR SERVICE WITH AN INSULATION OF LOW PRESSURE SF6 GAS AND PLASTIC FOILS Final Report, Jul. 1984
Uwe Brand Bonn Bundesministerium fuer Forschung und Technologie Apr. 1985 40 p refs In GERMAN; ENGLISH summary Sponsored by Bundesministeriun fuer Forschung und Technologie
(BMFT-FB-T-85-034; ISSN-0340-7608) Avail: NTIS HC A03/MF A01; Fachinformationszentrum, Karlsruhe, West Germany DM 8.50

Gas-insulated failsafe high voltage instrument transformers with system voltages in the range of 123 to 420 kV for outdoor service were developed. The basic physics and high power tests performed on gas-filled instrument transformer housings are discussed. Construction and design of gas-insulated voltage transformers are explained. The insulation of the 123 kV model consists of low pressurized SF6 gas and plastic foils. The 245 kV unit has the same principal design; however, a higher SF6 pressure is used and the apparatus is fitted with a hollow composite insulator made of a fiber reinforced plastics tube and silicone casing. For the 420 kV model the same insulator type is used and a design for the voltage grading along the insulator is developed. The transformers show good performance in service; they are a safe and environment-protecting alternative to oil insulated equipment.
Author (ESA)

N86-10450# Kernforschungsanlage, Juelich (West Germany). Inst. fuer Grenzflaechenforschung und Vakuumphysik.
DIELECTRIC PROPERTIES OF SILICON SURFACES AND SILVER THIN FILMS Thesis - Technische Hochchule, Aachen [DIELEKTRISCHE EIGENSCHAFTEN VON SILIZIUMOBERF-

LAECHEN UND DUENNEN SILBERFILMEN]
U. Backes Jan. 1985 85 p refs In GERMAN; ENGLISH summary
(JUEL-1968; D-82; ISSN-0366-0885) Avail: NTIS HC A05/MF A01

The metallic behavior of silicon (111) 7x7-surfaces with different misorientation angles is investigated. Its contribution to quasielastic peak broadening and to high background of inelastically scattered electrons is quantitatively shown using High Resolution Electric Energy Loss Spectroscopy (HREELS) by measuring the scattering cross sections for multiple plasmon excitation localized within a thin layer at the surface. The theoretical assumptions are confirmed by the spectra detected on the silver film-silicon substrate whose presence is explained by plasmon theory. Author (ESA)

N86-10451# Valvo Roehren- und Halbleiterwerke der Philips G.m.b.H., Hamburg (West Germany). Produktber. MOS-ICS.
INCREASE OF THE PACKAGING DENSITY OF VERY LARGE SCALE INTEGRATION (VLSI) CIRCUITS USING AUTOMATIC ALIGNMENT Final Report, Dec. 1983
Heino Fehling Bonn Bundesministerium fuer Forschung und Technologie Mar. 1985 104 p refs In GERMAN; ENGLISH summary Sponsored by Bundesministerium fuer Forschung und Technologie
(BMFT-FB-T-85-020; ISSN-0340-7608) Avail: NTIS HC A06/MF A01; Fachinformationszentrum, Karlsruhe, West Germany DM 22

Experiments in a production line were conducted to investigate the possible reduction of safety distances in VLSI circuits when an automatic alignment system is used. The test setup is described. With the very accurate alignment system of the Philips silicon repeater, the safety distance between a contact hole and a polysilicon-gate in a modified microcomputer circuit is reduced 0.7 micron without any yield loss. Design rules based on these experiments, and on lithography investigations were applied to redesign a 4 k static read-only memory. The area of a single memory cell in this redesign is 825 59 microns, compared to 1800 sq microns in the original version, and the final chip area is reduced to 8 sq mm compared to 13 sq mm. Author (ESA)

N86-10452# Nationaal Inst. voor Kernfysica en Hoge Energiefysica, Amsterdam (Netherlands). Sectie-K.
RENOVATED COOLING AT PIMU [VERNIEUWDE KOELING BY PIMU]
P. deGroen 18 Apr. 1985 27 p In DUTCH
(LINO-122) Avail: NTIS HC A03/MF A01

An electronic temperature control system for the cool water circuit at the PIMU section is described. The system consists of a temperature reader, control, offset and switch print, a programmable logic circuit (plc) and a motor speed control unit for the ventilators. From 21 to 6 C, with every 1.4 C temperature increase an extra cooling unit is switched on up to 30 C; every unit is switched off 1.4 C lower than its switching on temperature. Switching on a unit, an air value is opened and a ventilator starts on 10% of its maximum power and is regulated with the temperature increase within the 1.4 C step. Author (ESA)

N86-10453# National Bureau of Standards, Gaithersburg, Md. Electricity Div.
INVESTIGATION OF THE UNCERTAINTIES OF THE NBS (NATIONAL BUREAU OF STANDARDS) THERMAL VOLTAGE AND CURRENT CONVERTERS Final Report
F. L. Hermach Apr. 1985 124 p refs
(PB85-200178; NBSIR-84-2903) Avail: NTIS HC A06/MF A01 CSCL 14B

The uncertainties of the NBS reference and working standards for ac-dc current and voltage transfer measurements have been redetermined, to 50 and 100 kHz, respectively, by means of a set of multijunction thermal converters (MJTCs), an improved emf comparator, and extensive series of intercomparisons. As a result the accuracy of the NBS standards and the output of its calibration service for ac-dc current and voltage transfer are considered to be on a much firmer and better documented basis. Improvement by factors of two to five in the calibration accuracy for high-quality, single-range thermoelements and thermal voltage converters is possible for certain ranges of current, voltage, and frequency. For very special tests, such as international comparisons, accuracies approaching 1 ppm are within reach. GRA

N86-10387*# Jet Propulsion Lab., California Inst. of Tech., Pasadena. Radio Frequency and Microwave Subsystems Section.
AN EXPERIMENTAL TE SUB 12 - TE SUB 11 CIRCULAR WAVEGUIDE MODE CONVERTER
D. Hoppe *In its* The Telecommun. and Data Acquisition Progr. Rept. 15 Aug. 1985 p 43-56 refs (For primary document see N86-10382 01-32)
Avail: NTIS HC A10/MF A01 CSCL 09C

N86-10814# Joint Publications Research Service, Arlington, Va.
COMPACT, HIGH-SPEED ALGORITHM FOR LAYING OUT PRINTED CIRCUIT BOARD RUNS
D. Ye. Zapolotskiy *In its* USSR Rept.: Cybernetics, Computers and Automation Technol. (JPRS-UCC-85-006) 5 Sep. 1985 p 59-67 refs Transl. into ENGLISH from Upravlyayushchiye Sistemy i Mashiny (Kiev), no. 2, Mar. - Apr. 1985 p 33-37 (For primary document see N86-10809 01-60)
Avail: NTIS HC A08

34 FLUID MECHANICS AND HEAT TRANSFER

Includes boundary layers; hydrodynamics; fluidics; mass transfer; and ablation cooling.

For related information see also *02 Aerodynamics* and *77 Thermodynamics and Statistical Physics.*

N86-10454 Purdue Univ., Lafayette, Ind.
ON THE METHOD OF CHARACTERISTICS AND ITS APPLICATION TO THE CALCULATIONS OF ANNULAR NOZZLE FLOWFIELDS Ph.D. Thesis
Ber Nien Wang 1984 154 p
Avail: Univ. Microfilms Order No. DA8507772

A new, simple and effective approach to deriving the characteristic equations of gas dynamics is proposed. The compatibility equation is derived in vector form, which is valid for any coordinate system. The concepts of this derivation are clearer than previous derivations. A general form of the energy equation which contains the speed of sound directly is obtained. This form, which is valid for either ideal or real gases, is particularly useful for the method of characteristics. Coordinate transformation by algebraic methods is studied in detail. It is found that this method may be the only practical method for solving moving boundary problems, such as the free jet boundary problem. Using the basic concepts of coordinate transformations, all the viscous force terms and the dissipative terms in a curved coordinate system are obtained. Thus, the method of characteristics can be used to solve either real viscous flowfields or flowfields with artificial viscosity for smearing shock waves. Dissert. Abstr.

N86-10455 Arizona Univ., Tucson.
MEAN TURBULENCE STRUCTURE IN STRONGLY HEATING AIR FLOWS Ph.D. Thesis
Ahmed-Mohsen Tawfick Mohamed Shehata 1984 272 p
Avail: Univ. Microfilms Order No. DA8510896

Measurements of mean velocity and mean temperature fields and wall parameters for air flowing in a smooth, vertical tube at low entry Reynolds numbers are presented for heating with constant wall heat flux along the heated length. Two entry Reynolds numbers of approximately 6000 and 4000 were employed with three heating rates of approximately 0.0018, 0.0035 and 0.0045. The flow development was measured by obtaining internal profiles along the heated length at axial locations from $x/D = 3.17$ to $x/D = 24.54$. An adiabatic entry of 50 diameters preceded the

heated region. The three heating rates caused slight, large and severe property variations of the air. The highest heating rate was found to cause significant buoyancy effects. The internal measurements were obtained using constant temperature hot wire anemometry and resistance thermometry for velocity and temperature, respectively, employing a single short wire probe. The measurements are compared to numerical predictions employing two simple versions of the van Driest mixing length turbulence model. Dissert. Abstr.

N86-10456 Maryland Univ., College Park.
ANALYSIS OF COMBINED NATURAL AND FORCED CONVECTION AROUND CYLINDERS AND SPHERES Ph.D. Thesis
Soung Hong Moon 1984 310 p
Avail: Univ. Microfilms Order No. DA8510267

Combined natural and forced convection around cylinders and spheres was numerically investigated using stream function, vorticity formulations with hybrid (central and upwind) differences and nonuniform grid spacing for gases having a Prandtl number of 0.7. A successive overrelaxation method was employed to solve the stream, vorticity and temperature equations. For recovery of the pressure distribution, the pressure Poisson's equation was solved after convergence of stream and vorticity solutions. Numerical results were found to be functions of Reynolds number, Grashof number and Froude number. Local and average Nusselt numbers were obtained at various Grashof numbers. The mixed convection boundaries were defined: (1) when the buoyancy force of natural convection is significant in forced convection, and (2) when forced convection is significant in natural convection. Temperature and velocity distributions around cylinders and spheres were obtained and the effects of Reynolds and Grashof numbers and the separation point, drag coefficient and pressure were found. Dissert. Abstr.

N86-10457 Virginia Polytechnic Inst. and State Univ., Blacksburg.
FINITE ELEMENT SOLUTION OF THE NAVIER-STOKES EQUATIONS FOR 3-D TURBULENT FREE SHEAR FLOWS Ph.D. Thesis
Dominique Henri Pelletier 1984 228 p
Avail: Univ. Microfilms Order No. DA8507209

A half-equation model of turbulence has been developed to describe three-dimensional turbulent free shear flows. The model is used in a general purpose finite element procedure using primitive variables. The penalty function method is used, in a generalized Galerkin weak formulation of the Navier-Stokes equations, to enforce the conservation of mass. In this procedure the pressure does not explicitly appear, thus significantly reducing the computation time when compared to the velocity-pressure approach. Numerical solutions are obtained for four problems: a round jet issuing from a wall into still surroundings, a three-dimensional square jet issuing from a wall into still surroundings, a uniform flow past a free running propeller, and a shear flow past a free running propeller. An actuator disk with variable radial distribution of thrust and torque is used to model the propeller. Very good agreement between prediction and experiments is observed for the jet problems. Dissert. Abstr.

N86-10458 Washington Univ., Seattle.
RADIATIVE HEAT TRANSFER IN NONISOTHERMAL COMBUSTION PRODUCTS Ph.D. Thesis
Mohammed Ahmed Hamdan 1985 166 p
Avail: Univ. Microfilms Order No. DA8510851

Radiative heat transfer plays a significant and sometimes dominant role within combustion systems. Heat flux measurements in such systems are sometimes economically disadvantaged and difficult, if not impractical to perform. To demonstrate a feasible alternative, a simplified numerical model using total transmittance data, TTNH, was developed for predicting the heat flux from nonisothermal combustion systems containing variable concentrations of water vapor, carbon dioxide, and methane. Total and spectral experimental measurements were carried out, to test the numerical model, using nonisothermal mixtures of water vapor/carbon dioxide and methane/ethene, and using isothermal mixtures of methane and ethene. In general, the TTNH model was found to be reliable to predict the total emitted energy by nonisothermal mixtures of carbon dioxide and water vapor within 10%. However, the model was found not reliable to predict the theoretical emittance of methane. Dissert. Abstr.

N86-10459 Dartmouth Coll., Hanover, N.H.
ANALYSIS OF ANNULAR TWO-PHASE FLOW WITH LIQUID ENTRAINMENT Ph.D. Thesis
Mohamed Abdelfatah Abolfadl 1985 195 p
Avail: Univ. Microfilms Order No. DA8509840

A differential model for adiabatic annular gas-liquid to phase flow with liquid entrainment was developed by postulating a mixing length distribution in the turbulent flow region, across both the liquid and the core phases. The model is based on a modified form of the single phase mixing length function to account for turbulence intensity attenuation due to the presence of entrained liquid droplets in the gas core and the presence of the core film interface. The shear stress velocity gradient relationships are integrated numerically by using the complete shear stress distribution to produce the velocity profile which in turn is integrated to obtain the flow rates of each phase. A nondimensional form of the model is used to handle different fluids and tube diameters. Predicted velocity profiles in the core region also compare well with data. The model includes a new treatment of the characteristic shear stress in the laminar wall layer that makes it possible to predict flow rates in vertical flow at the point of zero wall shear stress in agreement with limited experimental results.
Dissert. Abstr.

N86-10460*# Universities Space Research Association, Columbia, Md.
A ROOT-MEAN-SQUARE PRESSURE FLUCTUATIONS MODEL FOR INTERNAL FLOW APPLICATIONS
Y. S. Chen Washington NASA Sep. 1985 17 p refs
(Contract NAS8-35918)
(NASA-CR-3928; NAS 1.26:3928) Avail: NTIS HC A02/MF A01 CSCL 20D

A transport equation for the root-mean-square pressure fluctuations of turbulent flow is derived from the time-dependent momentum equation for incompressible flow. Approximate modeling of this transport equation is included to relate terms with higher order correlations to the mean quantities of turbulent flow. Three empirical constants are introduced in the model. Two of the empirical constants are estimated from homogeneous turbulence data and wall pressure fluctuations measurements. The third constant is determined by comparing the results of large eddy simulations for a plane channel flow and an annulus flow. Author

N86-10461*# Stanford Univ., Calif. Thermosciences Div.
FILM COOLING ON A CONVEX WALL: HEAT TRANSFER AND HYDRODYNAMIC MEASUREMENTS FOR FULL AND PARTIAL COVERAGE Final Report
K. Furuhama, R. J. Moffat, J. P. Johnston, and W. M. Kays Aug. 1985 170 p refs
(Grant NAG3-3)
(NASA-CR-174964; NAS 1.26:174964) Avail: NTIS HC A08/MF A01 CSCL 20D

Turbine-blade cooling is an important issue for high-efficiency turbine engines, and discrete-hole injection is widely used as a cooling method. In the present study, detailed measurements were made of the heat transfer and hydrodynamics of a film-cooled flow on a convex wall, both for full and partial coverage. Two important parameters were altered: the blowing ratio, m, and the number of rows of injection holes. Three values of m were tested: $m = 0.2$, 0.4, and 0.6. In the blown region, $m = 0.4$ results in the lowest Stanton numbers of the three blowing ratios tested. This indicates that the value of $m = 0.4$ is near optimum on the convex wall from the point of view of cooling effect by injection. In the recovery region, Stanton numbers gradually approach the no injection values. Although the heat-transfer behavior during recovery from injection looks relatively complicated, the behavior of Stanton number can be explained in terms of two mechanisms:

recovery from the thermal effect of injection and recovery from the turbulence augmentation. This interpretation of the data is supported by the hydrodynamic and temperture-profile measurements. For partial blowing cases, the data follow the full-coverage values inside the blown region. In the unblown region, both in the curved and in the flat plate, the effect of the number of blown rows is clearly seen. Hydrodynamic boundary-layer profiles were measured with the aid of a triple hot-water probe. Three mean-velocity components and six turbulence quantities were simultaneously measured, and inside the blown region strong three-dimensionality was observed. Author

N86-10462*# National Academy of Sciences - National Research Council, Washington, D. C. Systems Dynamics Lab.
CONFINED SWIRLING JET PREDICTIONS USING A MULTIPLE-SCALE TURBULENCE MODEL
C. P. Chen Aug. 1985 22 p refs
(Contract NASw-3458)
(NASA-CR-178484; NAS 1.26:178484) Avail: NTIS HC A02/MF A01 CSCL 20D

A recently developed multiple scale turbulence model is used for the numerical prediction of isothermal, confined turbulent swirling flows. Because of the streamline curvature and nonequilibrium spectral energy transfer nature of the swirling flow, the utilized multiple scale turbulence model includes a different set of response equations for each of the large scale energetic eddies and the small scale transfer eddies. Predictions are made of a confined coaxial swirling jet in a sudden expansion and comparisons are made with experimental data and with the conventional single scale two equation model. The multiple scale model shows significant improvement of predictions of swirling flows over the single scale k epsilon model. The sensitivity study of the effect of prescribed inlet turbulence levels on the flow fields is also included. Author

N86-10463*# National Aeronautics and Space Administration. Lewis Research Center, Cleveland, Ohio.
THEORETICAL MODELING OF THE VAPOR CAVITATION IN DYNAMICALLY LOADED JOURNAL BEARINGS
David E. Brewe [1985] 35 p refs Presented at the Tribology Conf., Atlanta, 8-10 Oct. 1985; cosponsored by Am. Soc. of Lubrication Engr., and ASME Sponsored in part by Army
(NASA-TM-87076; E-2651; USAAVSCOM-TR-85-C-15; NAS 1.15:87076) Avail: NTIS HC A03/MF A01 CSCL 13I

A theoretical investigation is made of the evolution of a vapor-bubble for a submerged journal bearing under dynamically loaded conditions using the Elrod algorithm. This method conserves mass throughout the computational domain. A comparison study is performed to determine some of the consequences of applying a nonconservative theory (pseudo-Gumbel BC) to a dynamic problem. A complete dynamic cycle of a journal whirling in a circular path is chosen for the basis of comparison. Significant differences are observed in the load components near the end of the cycle. Further, good agreement with experiment is found for stationary and nonstationary cavitation. Author

N86-10464*# National Aeronautics and Space Administration. Ames Research Center, Moffett Field, Calif.
LARGE EDDY INTERACTIONS IN A TURBULENT CHANNEL FLOW
S. K. Hong Sep. 1985 66 p refs
(NASA-TM-86757; Rept-85265; NAS 1.15:86757) Avail: NTIS HC A04/MF A01 CSCL 20D

The dynamic processes of large eddies in a turbulent channel flow have been examined by utilizing an orthogonal expansion of the velocity fluctuation, known in the literature as the Proper Orthogonal Decomposition Theorem. The mathematical form of these functions is unknown in contrast to the Fourier analysis. Attention is focused on the nonlinear, turbulence-turbulence interaction process in the dynamical equation for large eddies (the first term in the expansion). The nonlinear interactions of the components of the first mode are treated exactly, but influences of higher modes are modeled. This requires adjustment of both the skewness and the effective Reynolds number so that the energy equilibrium of the large eddies is ensured when the mean velocity distribution is assumed known for experiments. Computational results show that the first mode contributes significantly to turbulent intensities and possesses a structural and statistical character similar to that of the entire flow. Author

N86-10465# IBM Research Lab., San Jose, Calif.
CHARACTERIZATION OF VAPOR AND AEROSOL FLOWS BY PHOTOTHERMAL METHODS
H. Sontag and A. C. Tam 25 Jun. 1985 8 p
(Contract N00014-83-C-0170)
(AD-A156601; TR-19) Avail: NTIS HC A02/MF A01 CSCL 20/4

Pulsed laser heating is used to label aerosols or absorbing vapors which can be detected by optical means yielding flow and spectroscopic information. Author (GRA)

N86-10466# California Univ., Livermore. Lawrence Livermore Lab.
ANGLE OF INCIDENCE EFFECTS FOR UNDERWATER SHOCK USING GENERIC COMPUTATIONAL MODELS
C. E. Rosenkilde and J. H. Ginsberg Feb. 1985 23 p Presented at the 55th Shock and Vibration Symp., Dayton, Ohio, 23 Oct. 1984 Prepared in cooperation with Georgia Inst. of Tech. 2 Vol.
(Contract W-7405-eng-48)
(DE85-012936; UCRL-91078-2; CONF-8410159-2) Avail: NTIS HC A02/MF A01

The computer programs for three models which provide the ability to perform damage assessments, particularly regarding the significance of angle of incidence are described. Each computer code evaluates the temporal response of the structure for an explosive source situated at a specified angle relative to the axis. Responses are displayed as temporal histories of the velocity and acceleration components relative to a body fixed coordinate system. Such results are evaluated for the center of mass and points at each end of the cylindrical segment. When a sequence of heading angles covering a quarter circle are input, the magnitude of the instantaneous (vector) velocity and acceleration at each point is monitored for its maximum value. In conjunction with the evaluation of the structural motion, in TDEF, a simple model is used to correlate the shock severity of the structural motion to that experienced by a small piece of equipment. This model consists of a one-degree-of-freedom oscillator whose base motion is obtained from the motion arising from any of the aforementioned structural models. DOE

N86-10467# California Univ., Livermore. Lawrence Livermore Lab.
ANGLE OF INCIDENCE EFFECTS FOR UNDERWATER SHOCK USING GENERIC COMPUTATIONAL MODELS, REV. 1
C. E. Rosenkilde and J. H. Ginsberg Feb. 1985 33 p Presented at the 55th Shock and Vibration Symp., Dayton, Ohio, 23 Oct. 1984 Prepared in cooperation with Georgia Inst. of Tech. 2 Vol.
(Contract W-7405-eng-48)
(DE85-012921; UCRL-91078-Rev-1; CONF-8410159-2-Rev-1) Avail: NTIS HC A03/MF A01

The modeling techniques used to develop several generic models of the shock response of submarines are described. The result is three overlapping models: (1) CAPS, in which the directly arriving shock wave is applied to a rigid capped cylinder that contains a large spring supported mass; (2) REFLECT, in which a rigid cylinder capped by hemispheres is subjected to direct and reflected shock waves resulting from an explosive source at an arbitrary location; and (3) TDEF, in which the directly arriving shock wave drives a deformable capped cylinder that is modeled by a combination of rigid body modes, beam modes, and axisymmetric shell modes. How the computer programs for these models provide the ability to perform damage assessments, is described, particularly regarding the significance of angle of incidence. Each computer code evaluates the temporal response of the structure for an explosive source situated at a specified angle relative to the axis. Results are evaluated for the center of mass and points

at each end of the cylindrical segment. When a sequence of heading angles covering a quarter circle is input, the magnitude of the instantaneous (vector) velocity and acceleration at each point is monitored for its maximum value. DOE

N86-10468# GA Technologies, Inc., San Diego, Calif.
HIGH EFFICIENCY HEAT TRANSPORT AND POWER CONVERSION SYSTEM FOR CASCADE
I. Maya, R. F. Borque, R. I. Creedon, and K. R. Schultz Feb. 1985 8 p Presented at the 6th Topical Meeting on the Technol. of Fusion Energy, San Francisco, 3 Mar. 1985
(Contract W-7405-eng-48)
(DE85-012959; UCRL-15640; CONF-850310-110) Avail: NTIS HC A02/MF A01

The cascade ICF reactor features a flowing blanket of solid BeO and LiAlO2 granules with very high temperature capability (up to approx. 2300 K). Presented here are the design of a high temperature granule transport and heat exchange system, and two options for high efficiency power conversion. The centrifugal throw transport system uses the peripheral speed imparted to the granules by the rotating chamber to effect granule transport and requires no additional equipment. The heat exchanger design is a vacuum heat transfer concept utilizing gravity induced flow of the granules over ceramic heat exchange surfaces. A reference Brayton power cycle is presented which achieves 55% net efficiency with 1300 K peak helium temperature. A modified Field steam cycle (a hybrid Rankine/Brayton cycle) is presented as an alternate which achieves 56% net efficiency. DOE

N86-10469# Los Alamos Scientific Lab., N. Mex.
KRAK: A COMPUTER PROGRAM FOR TWO-PHASE, TWO-COMPONENT POROUS FLOW AND FRACTURE PROPAGATION, REVISION
B. J. Travis, A. H. Davis, T. D. Kunkle, and R. G. Deupree Apr. 1985 96 p
(Contract W-7405-eng-36)
(DE85-014264; LA-9703-Rev) Avail: NTIS HC A05/MF A01

The KRAK code models the mass, momentum, and energy flow of steam liquid water, and a noncondensable gas in a porous medium. It can model the initiation and propagation of hydrofracture in this medium by any or all of the fluid components using finite difference techniques. The interaction of the flow and the cracking is self-consistently performed. Furthermore, flow in the crack is treated by a full-momentum equation, which allows rapid fracturing. The code has been used in studies of the underground containment of radioactive gases produced by nuclear explosions and of siting underground nuclear power reactors. The code could also be applied to a wide variety of geophysical situations such as geothermal energy extraction, geysers, convection in a fractured medium, and explosive well stimulation. The physical model includes heat transfer between the porous medium and the flowing fluid, an equation of state that allows fluid condensation and evaporation, a model for the viscosity of each fluid component and the composite viscosity, and a permeability model that successfully treats interfaces of greatly differing permeabilities (produced by either different materials or different states of the same material). Cracking is controlled by a simple fracture mechanics model. DOE

N86-10470# California Univ., Livermore. Lawrence Livermore Lab.
SPONTANEOUS RAMAN SPECTROSCOPY OF SHOCKED H2O
N. C. Holmes, W. J. Nellis, W. B. Graham, and G. E. Walrafen Jun. 1985 13 p refs Presented at 10th High Pressure Conf. on Res. in High Pressure Sci. and Technol., Amsterdam, 8 Jul. 1985
(Contract W-7405-eng-48)
(DE85-014557; UCRL-92895; CONF-850759-3) Avail: NTIS HC A02/MF A01

A new Raman spectroscopic system for recording spontaneous Raman spectra from shocked mater at high pressure and temperature during shock passage has been developed. This system is applied to the study of the OH-stretch band of water shocked to pressures between 7.5 and 25.7 GPa. The spectra indicate that strong intermolecular hydrogen-bonding persists to 12 GPa and decreases in strength at higher pressures. A two-component mixture model fits the data well under shock conditions. DOE

N86-10471# California Univ., Livermore. Lawrence Livermore Lab.
TIME-IMPLICITY SIMULATION OF PARTICLE-FLUID SYSTEMS
J. Denavit 17 Jan. 1985 20 p Presented at the 2nd Intern. School for Space Simulation, Honolulu, 3 Feb. 1985
(Contract W-7405-eng-48)
(DE85-012944; UCRL-91642; CONF-850266-6) Avail: NTIS HC A02/MF A01

One-dimensional particle-fluid hybrid simulations are presented in which the strongly collisional components of the plasma (e.g., ions and thermal electrons with nu(sub cf) (DELTA) t $>$ 1) are treated as fluids and the weakly collisional components (e.g., energetic electrons with nu(sub cp) (DELTA) t $<$ 1) are treated as particles. Here nu(sub cf) denotes the fluid ion and electron collision frequencies, nu(sub cp) is the energetic between particle and fluid components are treated by a Monte-Carlo method and mass transfers between the particle and fluid electron computed implicitly to allow time steps with (LC OMEGA) (sub p) (DELTA) t $>$ 1 ((LC OMEGA) (sub p): plasma frequency). DOE

N86-10472# Oak Ridge National Lab., Tenn.
ENGINE-DRIVEN AND ABSORPTION HEAT PUMP PROGRAMS
G. T. Privon 1984 4 p Presented at the DOE/ORNL Heat Pump Conf., Washington, D.C., 10 Dec. 1984
(Contract DE-AC05-84OR-21400)
(DE85-013930; CONF-841231-21) Avail: NTIS HC A02/MF A01

The development of energy efficient, thermally activated heat pumps for heating and cooling is reported. A breadboard system with a 32.5%-BHP-efficient linear engine in the final phase of steady state was tested. The absorption heat pump advanced cycle program is in progress. Analysis confirms the level of potential and preferred cycles and fluids are selected. Reliability for the linear engine heat pump and long life of the shaft seal must be established. The advanced absorption systems each require high performance from an internal counterflow heat exchanger and the development of reliable, high performance fluid pumps. DOE

N86-10473# Oak Ridge National Lab., Tenn.
LABORATORY EXPERIMENTS OF HEAT PUMP DYNAMIC LOSSES
W. A. Miller 1985 6 p refs Presented at the DOE/ORNL Heat Pump Conf., Washington, D.C., 10 Dec. 1984
(Contract DE-AC05-84OR-21400)
(DE85-013931; CONF-841231-22) Avail: NTIS HC A02/MF A01

Air-source heat pump experiments at ORNL: (1) provide detailed system and component performance data usable in understanding dynamic loss phenomena, and (2) enable formulation and evaluation of methods that could reduce dynamic losses. Results presented herein are from a series of laboratory experiments performed at ORNL aimed at providing detailed characterization steady-state performance data. Continuous modulation heat pump experiments to observe dynamic loss trends under part-load heat pump operation will follow. DOE

N86-10474# Sandia Labs., Albuquerque, N. Mex.
EFFECTS OF SCALE AND GEOMETRY ON HYDROGEN-AIR DETONATIONS
M. Berman 1985 56 p refs Presented at the Natl. Heat Transfer Conf., Denver, 4 Aug. 1985
(Contract DE-AC04-76DP-00789)
(DE85-006762; SAND-85-0171C; CONF-850810-6) Avail: NTIS HC A04/MF A01

Recent experiments have investigated the influence of scale and geometry on the ability of a fuel-air mixture to propagate or sustain a detonation, and on the probability that a deflagration will undergo a transition to detonation. The data show that many past concepts concerning detonations need to be revised. In particular, the occurrence of detonations may not be as unlikely as previously considered, especially in large-scale industrial

environments. This paper reviews some of the important recent experimental research, and provides some qualitative ideas concerning the interpretation of the experiments and their implications for improving safety. DOE

N86-10475# Kernforschungsanlage, Juelich (West Germany). Inst. fuer Reaktorbauelemente.
DUST DEPOSITION IN REGIONS OF SEPARATED FLOW [STAUBABLAGERUNG IN GEBIETEN ABGELOESTER STROEMUNG]
R. Griemert Mar. 1985 150 p refs In GERMAN; ENGLISH summary
(JUEL-1985; ISSN-0336-0885) Avail: NTIS HC A07/MF A01

A numerical assessment of the forces on dust grains in a closed duct is made as well as a measurement of the wall shear stress distribution and of fluid velocity and fluid fluctuations in the main flow direction at forward and backward facing steps. The deposition conditions were determined from photographs of copper, tin, and rubber dust to provide manufacturers of high temperature reactors with data on optimal hot gas pipe shapes and fluid dynamical data under determined pressure, temperature and geometrical conditions so that dust deposition in recirculation region can be avoided. Operating parameters can also be selected so that former dust deposition is not reentrained and does not fill the recirculation region. Author (ESA)

N86-10476# Stuttgart Univ. (West Germany). Inst. fuer Kernenergetik und Energiesysteme.
LAMINAR FILM CONDENSATION IN VERTICAL CLOSED TWO-PHASE THERMOSIPHONS Ph.D. Thesis [LAMINARE FILMKONDENSATION IM VERTIKALEN GESCHLOSSENEN SWEIPHASEN-THERMOSIPHON]
Thomas Spendel Feb. 1985 111 p refs In GERMAN; ENGLISH summary
(IKE-5-220; ISSN-0173-6892) Avail: NTIS HC A06/MF A01

The influence of the vapor flow on laminar film condensation heat transfer in closed two-phase thermosiphons is studied. The calculation of the vapor flow is based on the conservative equations for steady incompressible two-dimensional flow for which a finite difference method is applied to solve the system of equations. The influence of the vapor flow on heat transfer depends on the value of the Froude number. The influence of temperature-dependent material parameters and the condensation parameter on heat transfer are examined. Author (ESA)

N86-10477# Technische Hogeschool, Delft (Netherlands). Lab. of Fluid Mechanics.
EXPERIMENTS AND COMPUTATIONS ON UNSTEADY SEPARATING FLOW IN AN EXPANDING FLUME
G. S. Stelling (Netherlands Department of Transport and Public Works) and L.-X. Wang (Water Conservancy and Hydroelectric Power Research Institute, Beijing, China) 1984 62 p refs
(Rept-2-84) Avail: NTIS HC A04/MF A01

An unsteady, separating, flume flow with a free surface was investigated with a physical model and a numerical model. To simulate tidal flow, the prescribed flow rate at the inflow boundary was a half-period sine function of time. Velocities and wave heights were measured by a laser Doppler velocimeter and a wave-height meter in a straight open channel with a sudden widening and a nonreflective outlet. Distributions of depth-averaged velocities at different times were obtained. Numerical simulation of this flow was carried out using a computer program of second-order accuracy. The development of the recirculation region in course of time was well simulated, and the observed splitting of the main eddy in a later phase and the secondary eddy in the concave corner were reproduced. The computational results are markedly influenced by the boundary conditions at closed boundaries and the eddy viscosity applied. Author (ESA)

N86-10201# European Space Agency. European Space Research and Technology Center, ESTEC, Noordwijk (Netherlands).
THE FLUID PHYSICS MODULE: A TECHNICAL DESCRIPTION
A. Gonfalone *In its* Fifth European Symp. on Mater. Sci. under Microgravity. Results of Spacelab 1 Dec. 1984 p 3-7 refs (For primary document see N86-10200 01-16)
Avail: NTIS HC A21/MF A01

N86-10202# Kodak Ltd., London (England).
CAPILLARY FORCES IN A LOW GRAVITY ENVIRONMENT
J. E. Padday *In* ESA Fifth European Symp. on Mater. Sci. under Microgravity. Results of Spacelab 1 Dec. 1984 p 9-14 refs Sponsored by Kodak Ltd. and England Department of Industry (For primary document see N86-10200 01-16)
Avail: NTIS HC A21/MF A01

N86-10203# Naples Univ. (Italy). Inst. of Aerodynamics Umberto Nobile.
SOME RESULTS OF THE MARANGONI FREE CONVECTION EXPERIMENT
L. G. Napolitano, R. Monti, and G. Russo *In* ESA Fifth European Symp. on Mater. Sci. under Microgravity. Results of Spacelab 1 Dec. 1984 p 15-22 refs (For primary document see N86-10200 01-16)
(Contract CNR-PSN-83-070)
Avail: NTIS HC A21/MF A01

N86-10204# Centre National de la Recherche Scientifique, Meudon-Bellevue (France). Equipe de Technologie de la Croissance Cristalline.
OSCILLATIONS OF SEMI-FREE LIQUIDS IN MICROGRAVITY: SPACELAB 1 EXPERIMENT ES 326 [OSCILLATIONS DE VOLUMES LIQUIDES SEMI-LIBRES EN MICROGRAVITE: EXPERIENCE ES 326 DANS SPACELAB 1]
H. Rodot and C. Bisch *In* ESA Fifth European Symp. on Mater. Sci. under Microgravity. Results of Spacelab 1 Dec. 1984 p 23-29 refs In FRENCH (For primary document see N86-10200 01-16)
Avail: NTIS HC A21/MF A01

N86-10205# Universidad Politecnica de Madrid (Spain). Dept. of ETSI Aeronautics.
LIQUID COLUMN STABILITY: EXPERIMENT 1 ES-331
T. Martinez *In* ESA Fifth European Symp. on Mater. Sci. under Microgravity. Results of Spacelab 1 Dec. 1984 p 31-36 refs Sponsored by Spanish Commission for Space Research (For primary document see N86-10200 01-16)
Avail: NTIS HC A21/MF A01

N86-10206# National Aerospace Lab., Amsterdam (Netherlands).
AXISYMMETRIC FREE SURFACE BEHAVIOR OF MOVING LIQUID IN A CYLINDER IN MICROGRAVITY
J. P. B. Vreeburg *In* ESA Fifth European Symp. on Mater. Sci. under Microgravity. Results of Spacelab 1 Dec. 1984 p 37-42 refs (For primary document see N86-10200 01-16)
Avail: NTIS HC A21/MF A01

N86-10207# Bristol Univ. (England). School of Chemistry.
KINETICS OF SPREADING OF LIQUIDS IN MICROGRAVITY: EXPERIMENT 1 ES 327
J. M. Haynes *In* ESA Fifth European Symp. on Mater. Sci. under Microgravity. Results of Spacelab 1 Dec. 1984 p 43-46 refs (For primary document see N86-10200 01-16)
Avail: NTIS HC A21/MF A01

N86-10235# Naples Univ. (Italy). Inst. of Aerodynamics Umberto Nobile.
THE TEXUS FLIGHT RESULTS ON CONVECTIVE FLOWS AND HEAT TRANSFER IN SIMULATED FLOATING ZONES
R. Monti, L. G. Napolitano, and G. Mannara *In* ESA Fifth European Symp. on Mater. Sci. under Microgravity. Results of Spacelab 1 Dec. 1984 p 229-236 refs (For primary document see N86-10200 01-16)
Avail: NTIS HC A21/MF A01

N86-10237# Goettingen Univ. (West Germany). Inst. fuer Angewandte Mechanik und Stroemungsphysik.
THE INFLUENCE OF THERMOCAPILLARITY ON THE MIGRATION OF DROPLETS IN A LIQUID POSSESSING A UNIFORM

TEMPERATURE GRADIENT
V. Delitzsch, H. Eckelmann, and W. Wuest (Deutsche Forshungs- und Versuchsanstalt fuer Luft- und Raumfahrt, Goettingen, West Germany) *In* ESA Fifth European Symp. on Mater. Sci. under Microgravity. Results of the Spacelab 1 Dec. 1984 p 245-249 refs (For primary document see N86-10200 01-16)
Avail: NTIS HC A21/MF A01

N86-10238# Naples Univ. (Italy). Inst. of Aerodynamics Umberto Nobile.
NUMERICAL SIMULATION OF UNSTEADY THERMAL MARANGONI FLOWS
L. G. Napolitano, C. Golia, and A. Viviani *In* ESA Fifth European Symp. on Mater. Sci. under Microgravity. Results of Spacelab 1 Dec. 1984 p 251-258 refs (For primary document see N86-10200 01-16)
(Contract CNR-PSN-83-070)
Avail: NTIS HC A21/MF A01

N86-10239# Canadian Astronautics Ltd., Ottawa (Ontario).
NUMERICAL SIMULATION OF CONVECTIONS IN THE MICROGRAVITY ENVIRONMENT
R. Boudreault *In* ESA Fifth European Symp. on Mater. Sci. under Microgravity. Results of Spacelab 1 Dec. 1984 p 259-264 refs (For primary document see N86-10200 01-16)
Avail: NTIS HC A21/MF A01

N86-10240# Hochschule der Bundeswehr, Munich (West Germany). Inst. fuer Raumfahrttechnik.
OSCILLATIONS OF A VISCOELASTIC LIQUID DROP IN ZERO-GRAVITY
H. F. Bauer *In* ESA Fifth European Symp. on Mater. Sci. under Microgravity. Results of Spacelab 1 Dec. 1984 p 265-270 refs (For primary document see N86-10200 01-16)
Avail: NTIS HC A21/MF A01

N86-10241# Gesamthochschule, Essen (West Germany).
VERIFICATION OF TURBULENCE DEVELOPING FROM THE OSCILLATORY MARANGONI CONVECTION IN A LIQUID COLUMN
Ch.-H. Chun *In* ESA Fifth European Symp. on Mater. Sci. under Microgravity. Results of Spacelab 1 Dec. 1984 p 271-280 refs (For primary document see N86-10200 01-16)
Avail: NTIS HC A21/MF A01

N86-10242# Giessen Univ. (West Germany). Inst. fuer Physikalisches.
MEASUREMENTS OF THE CRITICAL MARANGONI NUMBER OF THE LAMINAR-OSCILLATORY TRANSITION OF THERMOCAPILLARY CONVECTION IN FLOATING ZONES
D. Schwabe and A. Scharmann *In* ESA Fifth European Symp. on Mater. Sci. under Microgravity. Results of Spacelab 1 Dec. 1984 p 281-289 refs (For primary document see N86-10200 01-16)
(Contract BMFT-01-QV-148-ZA-SN-SLN-7786)
Avail: NTIS HC A21/MF A01

N86-10243# Ishikawajima-Harima Heavy Industries Co. Ltd., Yokohama (Japan).
EXPERIMENTAL STUDY ON MARANGONI CONVECTION
J. Ochiai, K. Kuwahara, M. Morioka, S. Enya, K. Sezaki, T. Maekawa (Ioyo Univ., Japan), and I. Tanasawa (Tokyo Univ.) *In* ESA Fifth European Symp. on Mater. Sci. under Microgravity. Results of Spacelab 1 Dec. 1984 p 291-295 refs Sponsored by Japanese Science and Technology Agency (For primary document see N86-10200 01-16)
Avail: NTIS HC A21/MF A01

N86-10244# Universidad Politecnica de Madrid (Spain). Lab. de Aerodinamica.
STABILITY OF LONG LIQUID COLUMNS
J. Meseguer *In* ESA Fifth European Symp. on Mater. Sci. under Microgravity. Results of Spacelab 1 Dec. 1984 p 297-300 refs (For primary document see N86-10200 01-16)
Avail: NTIS HC A21/MF A01

N86-10245# Mons Univ. (Belgium). Faculty of Sciences.
RAYLEIGH-BENARD INSTABILITY IN SYSTEMS PRESENTING A MINIMUM IN SURFACE TENSION
D. Villers and J. K. Platten *In* ESA Fifth European Symp. on Mater. Sci. under Microgravity. Results of Spacelab 1 Dec. 1984 p 301-305 refs (For primary document see N86-10200 01-16)
Avail: NTIS HC A21/MF A01

N86-10249# Deutsche Forschungs- und Versuchsanstalt fuer Luft- und Raumfahrt, Cologne (West Germany). Inst. for Space Simulation.
HOLOGRAPHIC INTERFEROMETRY NEAR GAS/LIQUID CRITICAL POINTS: GROUND-BASED STUDY OF A D1 EXPERIMENT
H. Klein and K. Wanders *In* ESA Fifth European Symp. on Mater. Sci. under Microgravity. Results of Spacelab 1 Dec. 1984 p 323-325 refs (For primary document see N86-10200 01-16)
Avail: NTIS HC A21/MF A01

N86-10250# Technische Univ., Munich (West Germany). Lehrstuhl A fuer Thermodynamik.
NUCLEATE POOL BOILING IN SUBCOOLED LIQUID UNDER MICROGRAVITY: RESULTS OF TEXUS EXPERIMENTAL INVESTIGATIONS
M. Zell, J. Straub, and A. Weinzierl *In* ESA Fifth European Symp. on Mater. Sci. under Microgravity. Results of Spacelab 1 Dec. 1984 p 327-333 refs Sponsored by Bundesministerium fuer Forschung und Technologie (For primary document see N86-10200 01-16)
Avail: NTIS HC A21/MF A01

N86-10253# Lyon-1 Univ. (France).
SPACE EXPERIMENT ON THERMAL DIFFUSION. PREPARATION AND THEORETICAL ANALYSIS
J. Bert, D. Henry, P. Layani, G. Chuzeville, J. Dupuy, and B. Roux (Marseille Univ.) *In* ESA Fifth European Symp. on Mater. Sci. under Microgravity. Results of Spacelab 1 Dec. 1984 p 347-352 refs Sponsored by CNES (For primary document see N86-10200 01-16)
Avail: NTIS HC A21/MF A01

N86-10268# Battelle Inst., Frankfurt am Main (West Germany).
LIQUIDS AND INTERFACES
D. Langbein *In* ESA Fifth European Symp. on Mater. Sci. under Microgravity. Results of Spacelab 1 Dec. 1984 p 443-447 (For primary document see N86-10200 01-16)
Avail: NTIS HC A21/MF A01

35 INSTRUMENTATION AND PHOTOGRAPHY

Includes remote sensors; measuring instruments and gages; detectors; cameras and photographic supplies; and holography.

For aerial photography see *43 Earth Resources.* For related information see also *06 Aircraft Instrumentation,* and *19 Spacecraft Instrumentation.*

N86-10478 State Univ. of New York, Buffalo.
DIGITAL DECODING OF IN-LINE HOLOGRAMS Ph.D. Thesis
Levent Onural 1985 151 p
Avail: Univ. Microfilms Order No. DA8510353

In-line holography is a useful tool in the study of dynamic objects in three-dimensional space. A hologram is a specific non-linear coding which is recorded in the presence of coherent illumination. The physical reconstruction is done by reilluminating the hologram, and the resulting image is contaminated by the interfering twin-image. Here in this dissertation, a system of digital

filters is presented, which is applied directly to the in-line hologram and maps the hologram into an image of the boundaries (edges) of the objects encoded in it, provided that the object distribution function is real. This technique bypasses physical reconstruction completely and gives a clear decoding of the objects. In the first stage of the system, the hologram is approximated as the dc shifted output of a linear system. An approximation inverse filter is used to obtain the desired object distribution from the hologram since the exact inverse is not realizable. The linear approximate inverse filter is a truncated series expansion of the inverse filter in the Fourier transform domain. Dissert. Abstr.

N86-10479 Texas Christian Univ., Fort Worth.
REAL-TIME HOLOGRAPHY BY STIMULATED RAMAN AND BRILLOUIN SCATTERING Ph.D. Thesis
Swati Roy 1984 99 p
Avail: Univ. Microfilms Order No. DA8510382

Experimental investigations on the quality of real image reconstruction by stimulated Brillouin scattering (SBS) and stimulated Raman scattering (SRS) are reported here. The quality of real image reconstruction under two separate experimental conditions was found to be highly dependent on: (1) the amplitude modulations of the laser radiation, (2) the input laser power and (3) the position of the lens-focus. The best quality of reconstruction was observed when the lens focus was in front of the cell and the real image of the object formed by the lens was located inside the nonlinear medium, within 3 cm of the entrance window of the cell. Also, this experimental condition reconstructed a smaller area of the illuminated object than the inside focus condition. According to existing theory, when the lens-focus is inside the nonlinear medium, the complex interference pattern near the entrance window of the cell plays the role of a real-time hologram. Dissert. Abstr.

N86-10480 Department of the Air Force, Washington, D.C.
SENSOR SYSTEM Patent
J. E. Heath and H. W. Swenson, inventors (to Air Force) Issued 14 May 1985 6 p Supersedes AD-D011242; N85-11828
(AD-D011767; US-Patent-4,517,464; US-Patent-Appl-SN-431866; US-Patent-Class-250-370) Avail: US Patent and Trademark Office CSCL 17/5

An infrared sensor system for use on satellites comprising dual arrays of mercury cadmium tellurice semiconductor elements is described. One array of conventional photovoltaic detectors is wired in parallel with a novel array of HdCdTe material in which the n-type region of each mesa and the resulting p-n junction is considerably smaller than that utilized in the conventional detector. As the cumulative dose of incident radiation is increased, type conversion in both arrays occurs resulting in degraded performance in the conventional array but an increase in performance caused by the now effective p-n junction area in the novel array. An electronic switching device, coupled with a dosimeter, alternately selects the conventional array or the novel array depending upon the total dose of radiation received. GRA

N86-10481 Department of the Air Force, Washington, D.C.
STEREOSCOPIC VIDEO IMAGERY GENERATION Patent
G. G. Kuperman and F. R. Bodine, inventors (to Air Force) Issued 9 Apr. 1985 5 p Supersedes AD-D009489
(AD-D011785; US-Patent-4,510,525; US-Patent-Appl-SN-361016; US-Patent-Class-358-88) Avail: US Patent and Trademark Office CSCL 14/5

Flying spot scanner technology is combined with stereo photography in motion to produce two channels of video imagery which can be optically combined to produce the perception of dynamic stereoscopic detail. The scanner generates alternate lines with lateral offset corresponding to the physical separation between stereo photographic pairs to provide two rasters. Author (GRA)

N86-10482 Department of the Air Force, Washington, D.C.
FALL VELOCITY INDICATOR/VIEWER Patent
R. O. Berthel, V. G. Plank, S. H. Jones, and A. J. Matthews, inventors (to Air Force) Issued 30 Apr. 1985 8 p Supersedes AD-D010045
(AD-D011789; US-Patent-4,514,758; US-Patent-Appl-SN-442496; US-Patent-Class-358-93) Avail: US Patent and Trademark Office CSCL 04/2

A fall velocity indicator/viewer having a sampling compartment, a camera system, and an elongated tunnel for interconnecting the camera system to the sampling compartment is described. The camera system includes a video camera for continuously monitoring snowflakes as they naturally fall through a viewing area in the sampling compartment. The snowflakes are illuminated by a pair of strobe lights directly and in combination with reflected light from a pair of mirrors. In addition, a mirror in the tunnel provides a reflected view from the top of the snowflakes. The video camera is capable of thereby monitoring multiple views of snowflakes in a single video frame and provide sufficient data to analyze the physical characteristics of the snowflakes as well as aid in making velocity determinations and other observations of naturally falling snowflakes. Author (GRA)

N86-10483 Department of the Navy, Washington, D. C.
PRECISE BEARING SUPPORT DITHERER WITH PIEZOELECTRIC DRIVE MEANS Patent
G. L. Assard and A. L. Moorcroft, inventors (to Navy) Issued 11 Jun. 1985 6 p
(AD-D011819; US-Patent-4,523,120; US-Patent-Appl-SN-617049; US-Patent-Class-310-323) Avail: US Patent and Trademark Office CSCL 13/9

A relatively solid mounting surface, which may be part of a leveling gimbal, supports a piezoelectric bearing mount which has the properties of an acoustic transducer. The transducer has electrodes thereon which are powered from multi-phase electrical sources causing the bearing mount, and a bearing jewel which is rigid therewith, to move so as to dither the jewel in a rotary or other preselected fashion, thereby reducing bearing friction. Bandwidth, level and phasing sequence of the power sources are adjustable permitting optimized average dynamic motion and corresponding increased readout accuracy. Author (GRA)

N86-10484*# Illinois Univ., Urbana-Champaign. Dept. of Electrical and Computer Engineering.
SEMICONDUCTOR SUPERLATTICE PHOTODETECTORS Semi-annual Report, Jan. - 30 Jun. 1985
S. L. Chuang, K. Hess, J. J. Coleman, and J. P. Leburton Jun. 1985 23 p refs
(Grant NAG1-500)
(NASA-CR-176249; NAS 1.26:176249) Avail: NTIS HC A02/MF A01 CSCL 14B

Two novel types of superlattice photodetectors were studied. The first was a superlattice photomultiplier and the second a photodetector based on the real space transfer mechanism. A summary of the results is presented. G.L.C.

N86-10485# European Space Agency, Paris (France).
METRIC CAMERA WORKSHOP
T. D. Guyenne, ed. and J. J. Hunt, ed. Apr. 1985 210 p refs Workshop held in Oberpfaffenhofen, West Germany, 11-13 Feb. 1985; sponsored by DFVLR and ESA
(ESA-SP-209; ISSN-0379-6566) Avail: NTIS HC A10/MF A01

Photogrammetry, photomapping, geological surveys, and thematic mapping with the Spacelab metric camera were discussed. For individual titles, see N86-10486 through N86-10522.

N86-10486# Stuttgart Univ. (West Germany). Inst. of Photogrammetry.
DIGITAL ELEVATION MODEL FROM SPACELAB METRIC CAMERA PHOTOGRAPHS
F. Ackermann and E. Stark *In* ESA Metric Camera Workshop Apr. 1985 p 9-12 (For primary document see N86-10485 01-35)
Avail: NTIS HC A10/MF A01

In two different pairs of Spacelab metric camera photographs terrain elevations were measured in an area of fluvioglacial morphology. The derived digital terrain model and contour lines are compared with each other and absolutely checked against

topographic maps. The results show that height accuracy is 20m, with 15m accuracy possible, giving a contour interval of 50m. A slower film and image motion compensation are recommended. Doubts about the suitability of metric camera photography for line mapping are expressed. Author (ESA)

N86-10487# Technische Univ., Hanover (West Germany). Inst. for Photogrammetry and Engineering Surveys.
ORTHOPHOTOMAPPING FROM METRIC CAMERA IMAGERY
H. Engel and G. Konecny *In* ESA Metric Camera Workshop Apr. 1985 p 13-18 refs (For primary document see N86-10485 01-35)
Avail: NTIS HC A10/MF A01

The advantages and techniques of orthophoto generation for topographic mapping from Spacelab metric camera imagery are outlined. The technique combines high efficiency and precision, minimized loss of information caused by the involved direct photographic process, independence of interpretation, and possible application of and common photogrammetric instruments. Preprocessing involves densification of control points and determination of the parameters of exterior orientation by aerotriangulation with bundle block adjustment, and generating digital terrain models for differential rectification. Author (ESA)

N86-10488# Technische Univ., Vienna (Austria). Inst. of Photogrammetry.
STEREO-ORTHOPHOTOS IN VARIOUS MAP PROJECTIONS
G. Fritze, J. Jansa, and K. Kraus *In* ESA Metric Camera Workshop Apr. 1985 p 19-24 refs (For primary document see N86-10485 01-35)
Avail: NTIS HC A10/MF A01

The production of stereo-orthophoto maps from aerial and spaceborne photographs is discussed. When making orthophotos from satellite images, Earth curvature and map projections have to be taken into account. There are also problems having control points all determined in one homogenous coordinate system. The terrain data of the large area belong to different systems, and have to be transformed to the map coordinate system in which the orthophoto is produced. With stereo-orthophotos, users are given additional information on terrain heights without having to apply complicated photogrammetric compilation techniques.
Author (ESA)

N86-10489# Karlsruhe Univ. (West Germany). Inst. fuer Photogrammetrie und Topographie.
RESTITUTION OF SPACELAB PHOTOGRAPHY BY ANALOG STEREOPLOTTER
H. P. Baehr *In* ESA Metric Camera Workshop Apr. 1985 p 25-28 refs (For primary document see N86-10485 01-35)
Avail: NTIS HC A10/MF A01

Analog restitution of Spacelab metric camera photography using conventional instrumentation was chosen to meet the needs and capacities of Third World users. Absolute orientation of a whole stereomodel is not possible because of distortion between geocentric and geodetic coordinate systems. Limiting the restored area to 40 km x 30 km, height errors from system distortion stay below 15 m. Test results correspond to theory for single height points. On-line plotting of contour lines, however, seems critical, though analog orthophoto production is done without any problems for graphical presentation. Author (ESA)

N86-10490# Politecnico di Milano (Italy). Ist. di Topografia Fotogrammetria e Geofisica.
EVALUATION OF THE ACCURACY OF THE METRIC CAMERA IMAGES FOR THE PRODUCTION OF LINE MAPS AND ORTHOPHOTOS
G. Togliatti and A. Moriondo *In* ESA Metric Camera Workshop Apr. 1985 p 29-34 (For primary document see N86-10485 01-35)
Avail: NTIS HC A10/MF A01

The accuracy of Spacelab metric camera black and white images was analyzed on stereomodels. The heights of 1500 trigonometric vertices and the planimetric position of 150 points were measured. Pointing errors in planimetry and height were computed by a comparison with the coordinates of the national trigonometric grids. For selected areas repeated drawing of contours were checked against 1:25,000 scale maps. Accuracy is best in altimetry (20 m) and contours, good as expected in planimetry (N = 13 m, E = 12 m), poor in detail identification due to lack of illumination and of image motion compensator. The production of orthophotos on the scale 1:100,000 is completely successful. Accuracy evaluated on 50 photographic points is the same as obtained for line maps derived from stereomodels.
Author (ESA)

N86-10491# Heidelberg Univ. (West Germany). Inst. fuer Geographie.
PHOTOMAPPING IN DIFFERENT CLIMATIC ZONES
K. P. Wiesner and F. E. Fezer *In* ESA Metric Camera Workshop Apr. 1985 p 37-41 ref (For primary document see N86-10485 01-35)
Avail: NTIS HC A10/MF A01

Use of Spacelab metric camera color infrared images for updating topographic maps and developing thematic maps was assessed. Test areas included the Alps, Brittany, Sudan, Zimbabwe, and Qinghai (China). Scales of 1:250,000 in all vegetation zones; and 1:100,000 in arid zones were used. For map revision urban growth; new roads, railways, mines, man-made lakes; cropped and wooded areas expanding or reducing were studied. For thematic maps landforms and vegetation were examined. Although photo quality is generally poor because of the weather, objects not represented on conventional maps show up well. Organic materials cannot be distinguished from scrub, and manmade patterns are difficult to find, but objects such as railroads can be identified.
Author (ESA)

N86-10492# Mainz Univ. (West Germany).
A GEOLOGICAL STRUCTURAL ANALYSIS OF THE SOUTHEASTERN ZAGROS (IRAN) RANGES BASED ON METRIC CAMERA PHOTOS
M. Fuerst *In* ESA Metric Camera Workshop Apr. 1985 p 43-46 refs (For primary document see N86-10485 01-35)
Avail: NTIS HC A10/MF A01

Spacelab metric photography was used to make a tetonic inventory of the southeastern Zagros Ranges on the Persian Gulf. Photogeological structural analysis shows that the fold mountains are cut by overthrust faults and by major faults. The latter strike at a right or an acute angle to the folds. They are inferred to be associated with the rigid competent basement and punch through the sedimentary cover. Active and inactive salt plugs together with collapse structures occur along these overthrust faults and along major faults, which represent intricate plate tectonic movement planes. The salt plugs are confined to the intersections of areas of pressure maximum and salt concentration with these tectonic elements. Author (ESA)

N86-10493# Ecole Polytechnique Federale de Lausanne (Switzerland). Inst. des Mensurations.
EROSION CONTROL AND WATERSHED MANAGEMENT BY SPACELAB PHOTOGRAPHY
O. Koelbl and P. dePury *In* ESA Metric Camera Workshop Apr. 1985 p 47-52 (For primary document see N86-10485 01-35)
Avail: NTIS HC A10/MF A01

The interpretability of false color Spacelab photographs for erosion control and water shed management was assessed using photos taken over Nepal and the Mount Everest Massif. The thematic interpretation was done by a geologist working in this region. Scale limitations, image reproduction, and filtering of the photographs are discussed. Results show that much information can be extracted using relatively simple means. Color infrared photography must be used since panchromatic imagery does not show enough detail. Author (ESA)

N86-10494# Geological Survey, Reston, Va.
HIGH-RESOLUTION IMAGE DATA FROM THE SPACE SHUTTLE
F. J. Doyle *In* ESA Metric Camera Workshop Apr. 1985 p 55-58

(For primary document see N86-10485 01-35)
Avail: NTIS HC A10/MF A01

Shuttle Mission STS-41G carried the Large Format Camera with its stellar Attitude Reference System, and the Shuttle Imaging Radar. Exceptional photographs which should permit compilation of 1:50,000 scale image and topographic maps were obtained. The photographs will be made available through the United States Geological Survey EORS data center. The radar, though plagued with operational problems, also produced images useful for Earth science and development of radar mapping procedures.
Author (ESA)

N86-10495# University Coll., London (England). School of Oriental and African Studies.
EVALUATION OF METRIC CAMERA IMAGES AT THE UNIVERSITY OF LONDON
I. J. Downman, A. Meneguette, and J. A. Allan *In* ESA Metric Camera Workshop Apr. 1985 p 59-64 ref (For primary document see N86-10485 01-35)
Avail: NTIS HC A10/MF A01

Methods to determine coordinates and produce maps using a stereo comparator and an analytical stereo plotter as the measuring devices, and interpretation and plotting of data for land use studies with Spacelab metric camera image are discussed. Photogrammetric procedures of space resection, orientation and plotting are outlined. Results which indicate the inherent precision of the data and the accuracy which may be obtained when carrying out mapping or map revision are given. The type of detail which may be correctly interpreted and land use interpretation in arid areas are considered. Author (ESA)

N86-10496# Bonn Univ. (West Germany).
PARTIAL IN-FLIGHT CALIBRATION OF THE METRIC CAMERA Interim Report
G. Kupfer *In* ESA Metric Camera Workshop Apr. 1985 p 65-66 refs (For primary document see N86-10485 01-35)
Avail: NTIS HC A10/MF A01

Black and white, and color infrared photographs were used to assess whether in-flight calibration of the Spacelab metric camera is possible. Results suggest that it is feasible given sufficient geodetic control. Author (ESA)

N86-10497# Institut Geographique National, Paris (France).
IDENTIFICATION OF PLANIMETRIC FEATURES FROM THE METRIC CAMERA
A. Baudoin *In* ESA Metric Camera Workshop Apr. 1985 p 69-73 refs (For primary document see N86-10485 01-35)
Avail: NTIS HC A10/MF A01

The Spacelab metric camera flight over the southeast of France where many maps and aerial photographs exist and where a strip of 1:60,000 aerial photos was acquired the same day of the Shuttle flight was studied. It was possible to measure the percentage of planimetric features visible on the Spacelab images. This percentage depends on the kind of features (road, railways, hedges, rivers etc.), on their size (width, surface) and on their contrast. The results show that these space images could be helpful to revise medium scale topographic maps (1:100,000 or 1:50,000).
Author (ESA)

N86-10498# Technische Univ., Munich (West Germany). Lehrstuhl fuer Geographie und Geographische Fernerkundung.
ANALYSIS OF METRIC CAMERA IMAGES FROM THE USA AND THEIR SUITABILITY FOR TOPOGRAPHIC AND THEMATIC MAPPING
K. R. Dietz *In* ESA Metric Camera Workshop Apr. 1985 p 75-80 refs (For primary document see N86-10485 01-35)
Avail: NTIS HC A10/MF A01

Spacelab metric camera images of the Black Hills and the Mississippi Valley were analyzed to assess their suitability for topographic and thematic mapping. Ground checks in the respective areas were carried out in 1982 and 1984. Although both selected photos permit the delimitation of larger natural units, they are only of restricted value for topographic and thematic mapping, as their information content is unevenly distributed. Due to the unfavorable illumination conditions during the data acquisition many details required for topographic mapping are lost, through shadow effects or lacking contrast. The illumination also negatively affects attempts at thematic mapping on the 1:100,000 scale.
Author (ESA)

N86-10499# Rennes Univ. (France). Equipe Aerogeographie.
LONG RANGE TRANSLOCATIONS ASHORE TO OFFSHORE USING SPACELAB-1 METRIC CAMERA IMAGERY IN THE PERSPECTIVE OF INTEGRATED GEOPHYSICAL SURVEYS
G. Galibert *In* ESA Metric Camera Workshop Apr. 1985 p 81-85 refs (For primary document see N86-10485 01-35)
Avail: NTIS HC A10/MF A01

It is shown that long range translocations ashore to offshore of points or objects are possible (up to 150,000 m, X and Y) using Spacelab metric camera imagery when conventional methods of positioning by triangulation, Doppler satellites or radio-electric hyperbolic systems are unusable. Experiments in the Saint Malo coastal area along the French side of the English Channel are described. Dimensional measurements of colored crystals give an accuracy of 8 to 20 m through analog or digital methods, X and Y, with a possible transfer on topographical maps or charts at scales of 1:25000 or 1:15560. Transfers of digitized images on helicopter head up displays (theoretical accuracy 1 m) is also possible to prepare airborne coastal surveys over shallow waters.
Author (ESA)

N86-10500# Deutsche Forschungs- und Versuchsanstalt fuer Luft- und Raumfahrt, Oberpfaffenhofen (West Germany). Inst. of Optoelectronics.
LINE MAPPING AND RESOLUTION TESTS WITH METRIC CAMERA DATA
M. Schroeder, W. Schuhr (Technische Univ., Hanover), and A. Schuering (Technische Univ., Hanover) *In* ESA Metric Camera Workshop Apr. 1985 p 87-90 refs (For primary document see N86-10485 01-35)
Avail: NTIS HC A10/MF A01

The utility of Spacelab metric camera imagery for topographic mapping was assessed. The edge gradient analysis applied to derive modulation transfer function curves is described. The resolution on the ground for a line pair is equivalent up to 20 m for high contrast. Samples for line map production and updating are shown for conventional medium scale maps by analytical plotters as well as for quasi-line maps by digital image processing. Author (ESA)

N86-10501# United Nations Economic Commission for Africa, Addis Ababa (Ethiopia).
ROLE OF THE ECONOMIC COMMISSION FOR AFRICA AS A PRINCIPAL INVESTIGATOR IN THE METRIC CAMERA EXPERIMENT AND REPORTS OF THE RESULT OF THE ASSESSMENT FOR TOPOGRAPHIC AND REVISION OF MAPS IN POPULATED AND DEVELOPED AREAS OF THE WORLD
OluFunso Olujohungbe *In* ESA Metric Camera Workshop Apr. 1985 p 91-93 (For primary document see N86-10485 01-35)
Avail: NTIS HC A10/MF A01

Spacelab metric camera photographs of the irrigation areas of the Al Gezira region of Sudan were used to assess the feasibility of using the camera for map revision and making in Africa. Results confirm the high resolution of the images, particularly details registered in the infrared, favorable for observation and identification of features, and rapid stereoplotting from space photographs for topographic and small scale mapping. Author (ESA)

N86-10502# Parma Univ. (Italy). Ist. di Geologia.
THE ROLE OF VERY SMALL SCALE METRIC IMAGES IN MODERN GEOLOGY
M. Sgavetti *In* ESA Metric Camera Workshop Apr. 1985 p 97-102 refs (For primary document see N86-10485 01-35)
Avail: NTIS HC A10/MF A01

The suitability of the Spacelab metric camera stratigraphic resolution for the construction of models for sedimentary basins

and the structural analysis of tectonically complex areas was assessed. Metric camera images, large scale aerial photos, and seismic profiles are compared, in terms of resolution of physical surfaces (bed pattern). The Spacelab images give good results in structural analysis of tectonically complex areas. Author (ESA)

N86-10503# Technische Hochschule, Graz (Austria). Inst. of Image Processing and Computer Graphics.
GEOLOGICAL MAPPING OF REMOTE MOUNTAINOUS REGIONS USING METRIC CAMERA IMAGERY
M. F. Buchroithner *In* ESA Metric Camera Workshop Apr. 1985 p 103-108 refs (For primary document see N86-10485 01-35)
Avail: NTIS HC A10/MF A01

The applicability of colored infrared Spacelab metric camera photography for geological reconnaissance mapping and for more detailed studies up to scales larger than 1:100,000 is demonstrated with mountainous regions of different geological structure in Western Saudi Arabia, in the Afghan Hindu Kush, and in the East Nepalese Himalayas. Advantages and drawbacks for geological mapping in remote areas are discussed. Author (ESA)

N86-10504# Technische Univ., Munich (West Germany). Inst. fuer Geographie.
INTERPRETATION OF METRIC CAMERA CONCERNING HYDROLOGIC STRUCTURES OF THE RHONE DELTA
K. Halm *In* ESA Metric Camera Workshop Apr. 1985 p 109-114 (For primary document see N86-10485 01-35)
Avail: NTIS HC A10/MF A01

Hydrological maps are made visually using Spacelab metric camera (MC) imagery after contrast enhancement, edge enhancement, and enlargements 8 x and 16 x as transparencies and prints. Field-work is carried out simultaneously with the MC data acquisition time (landcover mapping, object recording, terrestrial photo documentation, sediment and water samples) to check MC mapping. Linear elements cannot be clearly classified (watercourses, roads, paths, field boundaries). In a lagoon zone, it is possible to differentiate 6 classes using the MC image. Water basins can be classified into five classes. It is impossible to differentiate agricultural acreage. This should be possible using a combined system of panchromatic and multispectral recording, as shown on example of the double exposure of MC and MSS-LANDSAT. Author (ESA)

N86-10505# Topographical Survey Branch, Kathmandu (Nepal). Survey Dept.
TEST ON MAPPING APPLICATION OF METRIC CAMERA IMAGERY
K. R. Adhikary *In* ESA Metric Camera Workshop Apr. 1985 p 115-118 refs (For primary document see N86-10485 01-35)
Avail: NTIS HC A10/MF A01

The accuracy reliability, production difficulties, and costs of Spacelab metric camera imagery for topographic mapping of the eastern Himalayas in Nepal are compared with existing maps. It appears possible to extract sufficient cartographic details from Spacelab imagery for mapping at the scale of 1:100,000, however, an extensive field completion is required for all the hidden details due to very small original negative scale of the imagery. This costs more time and money than conventional topographic mapping. Using identifiable points in existing maps (1 in = 1 mile) as control, accuracy of planimetric details is 50 m, a little larger than the map accuracy standard for 1:100,000 of 34 m. Proper identification and post-pointing of geodetic control is possible to meet the accuracy standard of topographic mapping. Author (ESA)

N86-10506# Deutsche Forschungs- und Versuchsanstalt fuer Luft- und Raumfahrt, Cologne (West Germany). Beretch fuer Projektraegerschaften.
STATUS OF PREPARATION ACTIVITIES FOR METRIC CAMERA REFLIGHT ON EOM-1/2
A. Langner *In* ESA Metric Camera Workshop Apr. 1985 p 121-123 (For primary document see N86-10485 01-35)
Avail: NTIS HC A10/MF A01

In autumn 1986 the Metric Camera will be reflown in the Earth Observation Shuttle Mission. The implementation of a forward motion compensation mechanism and the use of high resolution films will increase ground resolution by a factor of 2. Hardware refurbishment and modifications are nearly completed and the system is ready for integration into the FOM-1/2 payload. Mission objective is to demonstrate the mapping capability of high resolution space photography for compiling topographic and thematic maps for unpopulated or less developed regions of the world, and updating and revising topographic and thematic maps in populated and developed areas of the world. Images will be taken with 60% or 80% overlap for stereoscopic evaluation. Author (ESA)

N86-10507# University Coll., London (England).
OEEPE PARTICIPATION IN TESTING METRIC CAMERA PHOTOGRAPHY
I. J. Downman *In* ESA Metric Camera Workshop Apr. 1985 p 125-126 (For primary document see N86-10485 01-35)
Avail: NTIS HC A10/MF A01

A test program for the Spacelab metric camera is outlined. Image content, image accuracy, man compilation and revision, orthophoto production, and aerial triangulation are tested. Position on photograph, mode of viewing (monoscopic or stereoscopic), amount of overlap for stereo viewing, and emulsion (color infrared or panchromatic) are investigated. Author (ESA)

N86-10508# Technische Univ., Berlin (West Germany). Dept. of Photogrammetry and Cartography.
TOPOGRAPHIC INTERPRETATION OF METRIC CAMERA IMAGES: AN EXAMPLE IN SOMALIA
J. Albertz and A. A. Gulaid *In* ESA Metric Camera Workshop Apr. 1985 p 129-133 refs (For primary document see N86-10485 01-35)
Avail: NTIS HC A10/MF A01

An extremely arid area of Somalia was used to test the Spacelab metric camera's ability to distinguish topographic map elements such as landforms, drainage, planimetric elements and vegetation. Landforms (except small valleys and ridges) the sea, wadis, and watersheds are identified well. Vegetation, small streams, paths, and settlements are hard or impossible to distinguish. Identification strongly depends on contrast, object size, and their relative arrangement. Interpretation experience gained in other regions cannot simply be transferred to arid zones.
Author (ESA)

N86-10509# Institut Geographique National, Paris (France).
THEMATIC INVESTIGATIONS IN FRANCE BASED ON METRIC CAMERA IMAGERY
P.-Y. Lecordix *In* ESA Metric Camera Workshop Apr. 1985 p 135-137 In FRENCH; ENGLISH summary (For primary document see N86-10485 01-35)
Avail: NTIS HC A10/MF A01

Spacelab metric camera images were used to study geological features, land use, and forestry, and were compared with other data sources used in cartography. For geological surveys, the metric camera is comparable to SPOT satellite, and better than LANDSAT. For land use, Spacelab images are unsatisfactory in urban areas; woodland and scrub is over-represented due to shadow effects and inclusion of water covered with aquatic plants; forest distribution is well reproduced; sandy features are well identified. For forest inventories, results are surprisingly good, e.g., only 4% error in distinguishing resinous and leafy trees.
Author (ESA)

N86-10510# Technische Univ., Munich (West Germany). Inst. fuer Geographie.
THEMATIC MAPPING OF METRIC CAMERA COLOR INFRARED AND BLACK AND WHITE PHOTOGRAPHS FOR LAND USE CLASSIFICATION
H. G. Gierloff-Emden *In* ESA Metric Camera Workshop Apr. 1985 p 139-145 (For primary document see N86-10485 01-35)
Avail: NTIS HC A10/MF A01

The use of Spacelab metric camera black and white, and color infrared photography for land use and thematic mapping

was tested for a mountainous region, interspersed with very flat features in Mexico (black and white) and a coastal zone in France (color). Ground checks were carried out in both regions, though not during the time of the flight. Results show that black and white is superior concerning line detection and minimum visibility. Both images could serve as auxiliary means for thematic mapping on scales of 1:100,000. Author (ESA)

N86-10511# Technische Univ., Hanover (West Germany). Inst. fuer Photogrammetrie und Ingenieurvermessungen.
DIGITAL IMAGE PROCESSING OF METRIC CAMERA IMAGERY
P. Lohmann *In* ESA Metric Camera Workshop Apr. 1985 p 147-152 refs (For primary document see N86-10485 01-35)
Avail: NTIS HC A10/MF A01

The use of digitized Spacelab metric camera imagery for map updating is demonstrated for an area of Germany featuring agricultural and industrial areas, and a region of the White Nile. LANDSAT and Spacelab images were combined, and digital image processing techniques used for image enhancement. Updating was achieved by semiautomatic techniques, but for many applications manual editing may be feasible. Author (ESA)

N86-10512# Silsoe Coll., Bedford (England).
LAND EVALUATION SUCCESSES WITH THE METRIC CAMERA
M. A. Keech *In* ESA Metric Camera Workshop Apr. 1985 p 153-156 refs (For primary document see N86-10485 01-35)
Avail: NTIS HC A10/MF A01

The Spacelab metric camera as a data source for land resource planning was demonstrated using stereophotographs of Oman (after cloud covered most of the proposed areas in Brazil and the Andes). The photographs show drainage patterns, vegetation patterns, roads, and settlements. The scale variation is small, the resolution is adequate for all but the most detailed survey work, and for geologist, agriculturalist, or forest planner the images provide the most useful synoptic view of an area, which the human eye and brain can interpret without further image processing. Author (ESA)

N86-10513# Freiburg Univ. (West Germany). Abteilung Luftbildmessung und Fernerkundung.
REQUIREMENTS AND POSSIBILITIES OF SPACELAB METRIC CAMERA PHOTOS USAGE FOR INVENTORIES OF LARGE AREAS OF EXTENSIVELY MANAGED FORESTS
W. Forstreuter *In* ESA Metric Camera Workshop Apr. 1985 p 157-160 (For primary document see N86-10485 01-35)
Avail: NTIS HC A10/MF A01

LANDSAT MSS and Spacelab metric camera coverage, spectral and geometric resolution, data handling, and results for forest are compared. Discrimination of vegetation types is poor for both sensors in a test area of wet forest. Mapping of a very small stream was very difficult, and it could not even be seen in LANDSAT images. Author (ESA)

N86-10514# Technische Univ., Munich (West Germany). Inst. fuer Geographie.
TOPOGRAPHIC AND THEMATIC MAPPING: ANALYSIS OF METRIC CAMERA BLACK AND WHITE PHOTOGRAPHS OF THE RHONE DELTA
W. Stolz *In* ESA Metric Camera Workshop Apr. 1985 p 161-166 refs (For primary document see N86-10485 01-35)
Avail: NTIS HC A10/MF A01

A Spacelab Metric Camera (MC) black and white photograph of the Rhone Delta was analyzed concerning the information content of the image for topographic and thematic mapping. Ground check was carried out at the same time of the flight. The interpretation shows that the image meets the standards of medium scale topographic maps with limitations. For thematic mapping the image could serve as auxiliary means in scales around 1:100,000. Comparison with aerial photographs demonstrates the information loss caused by enlargement of the MC-image.
Author (ESA)

N86-10515# Zurich Univ. (Switzerland). Dept. of Geography.
EVALUATION OF METRIC CAMERA PHOTOS
H. Haefner and F. Hugentobler *In* ESA Metric Camera Workshop Apr. 1985 p 169-171 (For primary document see N86-10485 01-35)
Avail: NTIS HC A10/MF A01

The resolution of linear features, and the mapping of the transient snowline and the snow cover on Spacelab metric camera photographs of the Alps were investigated. Forest, shrubland, settlements and roads can be identified. Snowlines on glaciers cannot be identified, but the transient snow line is clear. Small features, including moraines and crevasses can be seen. Shadow and vegetation cover can cause problems in identifying snowfree areas. The main advantage of the photos is the synoptic view of large areas and the possibility to determine correlations between various features and/or regions. Single features may be recognized and mapped in great detail. The resolution capability, and the density and variety of the information for studies of larger areas is unmatched by other remote sensing systems, including LANDSAT MSS. Author (ESA)

N86-10516# Indian Space Research Organization, Ahmedabad. Space Applications Center.
CREATION OF GROUND CONTROL POINTS (GCP) LIBRARY USING ESA SPACELAB METRIC CAMERA IMAGERY
P. K. Srivastava, S. N. Jha, P. M. Udani, A. K. S. Gopalan, and D. S. Kamat *In* ESA Metric Camera Workshop Apr. 1985 p 173-174 ref (For primary document see N86-10485 01-35)
Avail: NTIS HC A10/MF A01

Using standard software for aerial triangulation and coordinates of ground control from 1:250,000 scale maps, the ground coordinates of ground control points for precision processing of remote sensing data were obtained. With 10 points for control, coordinates of test points are found to be off by as much as 200 m. A digital image restitution model is presented. It is hoped to obtain 30 to 40 m accuracy. Author (ESA)

N86-10517# Technische Univ., Munich (West Germany). Inst. fuer Geographie.
UPDATING OF TOPOGRAPHIC MAPS BY MEANS OF METRIC CAMERA PHOTOS EXAMPLE: HALLERTAU (BAVARIA)
P. Kammerer *In* ESA Metric Camera Workshop Apr. 1985 p 175-180 refs (For primary document see N86-10485 01-35)
Avail: NTIS HC A10/MF A01

The environmental changes (land use, settlements, roads) in a Spacelab metric camera test region are described and the suitability of metric camera photos for the updating of topographic maps is analyzed. The photos allow updating of forest on the scale 1:100,000 in combination with ground truth. Because of the snow cover and the low Sun elevation, the possibilities for the mapping of settlements and roads are limited. Author (ESA)

N86-10518# Technische Univ., Munich (West Germany).
INTERPRETATION OF SPACELAB-1 PHOTOGRAPHS FOR THE GENERATION OF 1:200000 TOPOGRAPHIC MAP
R. Finsterwalder *In* ESA Metric Camera Workshop Apr. 1985 p 181-182 (For primary document see N86-10485 01-35)
Avail: NTIS HC A10/MF A01

The interpretation of Spacelab metric camera photographs for the generation of a 1:200 000 topographic map was assessed for an area of 1,100 sq km, in a densely populated area. Forests, water, roads, and settlements were mapped from photographic enlargements (diapositives) 1:100,000, partly with the help of stereoscopic viewing. The reliability of the interpretation was examined by comparing with the official topographic map (1:200,000). The semantic information of the Spacelab photographs is not sufficient to produce a topographic map from a densely populated region which corresponds to the quality of the official map. Author (ESA)

N86-10519# Technische Univ., Munich (West Germany). Inst. fuer Geographie.
METRIC CAMERA IMAGE OF MUNICH AS ADDITIONAL MEANS FOR URBAN CARTOGRAPHY

F. W. Strathmann *In* ESA Metric Camera Workshop Apr. 1985 p 183-189 refs (For primary document see N86-10485 01-35)
Avail: NTIS HC A10/MF A01

The utilization of Spacelab metric camera (MC) image photointerpretation for urban mapping was tested in a snow covered townscape. Because of information gaps in areas with little contrast, small-scale urban maps (overview maps/basic maps) cannot be produced by MC-images, nor can they be updated completely in a revision interval. Because the gray tone combinations often allow several interpretations of the urban land use, an extensive mapping of real land use without evaluation of maps and aerial photos and/or additional ground truth is not feasible. In the quality of the first MC mission the image detail for the city can only be a limited help for further data acquisition.
Author (ESA)

N86-10520# Hosei Univ., Tokyo (Japan). Coll. of Engineering.
AN EXAMPLE OF SINGLE MODEL ORIENTATION OF METRIC CAMERA STEREOPHOTOGRAPHS
T. Oshima, K. Miyashita, M. Yoshimura, S. Tanaka (Remote Sensing Technology Center of Japan), and T. Sugiura (Remote Sensing Technology Center of Japan) *In* ESA Metric Camera Workshop Apr. 1985 p 191-192 (For primary document see N86-10485 01-35)
Avail: NTIS HC A10/MF A01

Accuracy of the model orientation of Spacelab metric camera photographs was evaluated. Control points on the map were read using the map scale 1:200,000 giving a distinguishable limit of the naked eye is of 20 m in actual size. The results are within the permissible range of errors and the results of height errors are also effective for actual use. Mean square errors are: mx = + or - 39.9 m; my = + or -37.2 m; mz = + or - 29.6 m.Author (ESA)

N86-10521# Technische Univ., Munich (West Germany). Arbeitsgruppe Geowissenschaftliche.
TECTONIC ANALYSIS OF TYPICAL FOLD STRUCTURES IN THE ZAGROS MOUNTAINS (IRAN) BY THE APPLICATION OF QUANTITATIVE PHOTOGRAMMETRIC METHODS ON METRIC CAMERA DATA
J. Bodechtel, M. Kley, and U. Muenzer *In* ESA Metric Camera Workshop Apr. 1985 p 193-197 refs (For primary document see N86-10485 01-35)
Avail: NTIS HC A10/MF A01

Photometric methods were applied on 1:850,000 scale metric camera data for the evaluation of tectonic values on typical fold structures in arid selective eroded Zagros ridges in Iran. The black and white photographs clearly reveal a frequent bending of anticlinal structures, and improve qualitative interpretation. Author (ESA)

N86-10522# Mapping and Charting Establishment, Ottawa (Ontario).
TEST RESULTS USING METRIC CAMERA PHOTOGRAPHY FOR 1:250,000 MAPPING
G. G. Dalgity and E. A. Fleming *In* ESA Metric Camera Workshop Apr. 1985 p 199-206 (For primary document see N86-10485 01-35)
Avail: NTIS HC A10/MF A01

Spacelab metric camera photography over a region in southern Alberta, Canada was used to compile a map at the scale of 1:250,000. Culture, drainage and contours were drawn using an analytical plotter. Map accuracy tests were applied and content was compared with that of the published 1:250,000 map of the area. Notwithstanding the faults of the photography, a map accuracy classification of NATO B-1 is achieved. Map content is not as great as that of the published map. Author (ESA)

N86-10523# Advanced Engineering Lab., Adelaide (Australia).
SPECIFICATION FOR THE PERFORMANCE, DESIGN, DEVELOPMENT AND TEST REQUIREMENTS FOR A SEVERE ENVIRONMENT CARTRIDGE RECORDER. ISSUE 4
S. J. Caldecott and N. J. Phillis 20 Nov. 1984 17 p
(AD-A156637; AEL-0125-SD) Avail: NTIS HC A02/MF A01 CSCL 14/3

This specification establishes the performance, design, development and test requirements for a Severe Environment Cartridge Recorder (SECR). The SECR shall consist of a magnetic tape cartridge recorder intended for recording analog or digital data in high vibration, high acceleration and wide temperature range environments. The SECR shall comprise a single assembly in which shall be housed an electric motor, a means of securing and driving a magnetic tape cartridge, electronic speed control circuitry and a four-track magnetic recording tape head. No signal-conditioning electronics shall be contained within the SECR. Replay of magnetic tape cartridges shall be accomplished with the Cartridge Replay Machine (CRM). GRA

N86-10524# Science Applications International Corp., McLean, Va.
HIGH FLUX CALORIMETRY
M. McDonnell, N. Olson, and S. Woods 5 May 1984 147 p
(Contract DNA001-82-C-0185)
(AD-A156852; AD-E301731; SAIC-84/1104; DNA-TR-84-183)
Avail: NTIS HC A07/MF A01 CSCL 14/2

Four basic radiant energy sensing concepts were examined for applicability to high flux calorimetry measurement. Calorimeters were cross calibrated using five radiant energy sources. Commercial availability was an important criterion. A commercial calorimeter with a specially designed and fabricated adapter appears to be an acceptable calorimeter for High Flux Measurements. GRA

N86-10525# Department of the Air Force, Washington, D.C.
CAPTIVE VOLUME DEVICE AS A SAFE LIFE MONITOR Patent Application
Borgardt, inventor (to Air Force) Filed 27 Jun. 1985 15 p
(AD-D011802; US-Patent-Appl-SN-749335) Avail: NTIS HC A02/MF A01 CSCL 21/9

The present invention utilizes a closed chamber or structure to enclose a small of amount of a solid propellant whose useful life is to be measured or sensed. The closed chamber forms a captive volume device in which there is included a detecting means. The useful life detecting means may comprise either colorimetric material which change color or a differential pressure device which changes its position in relationship to the useful life of the solid propellant material. A visual viewing port is provided in the captive volume device to allow the state of the detecting means to be observed. GRA

N86-10526# Oak Ridge National Lab., Tenn.
AUTOMATED ANALYSIS OF DIGITAL IMAGES GENERATED BY TWO-DIMENSIONAL GEL ELECTROPHORESIS
R. C. Mann, B. K. Mansfield, and J. K. Selkirk 1985 11 p refs Presented at the 2nd Intern. Congr. of Appl. Pattern Recognition, Amsterdam, 19 Jun. 1985
(Contract DE-AC05-84OR-21400)
(DE85-011906; CONF-8506115-1) Avail: NTIS HC A02/MF A01

Two-dimensional gel electrophoresis is a method to separate proteins according to their molecular weights and mobilities in an electric field at a certain pH value. The presence of a radioactively or fluorescently labeled protein in a preparation is indicated by a spot that is produced on a film with the intensity of the spot indicative of the amount of protein. This article presents algorithms that accomplish automated quantitative analysis of digitized gel images. The limits of currently available analysis systems are discussed. The methods are implemented by software on a commercially available digital image processor that uses a minicomputer host. DOE

N86-10527# Pacific Northwest Lab., Richland, Wash.
ELCAP INSTRUMENTATION
G. J. Schuster and S. D. Tomich Apr. 1985 7 p Presented at the EPRI End-Use Metering Workshop, Seattle, 15 Jan. 1985
(Contracts DE-AC06-76RL-01830; DE-AC79-83BP-13795)
(DE85-013042; PNL-SA-12863; CONF-850175-1) Avail: NTIS HC A02/MF A01

Over the past few years Pacific Northwest Laboratory has developed a series of data loggers. The most recently completed logger, designed to meet these requirements, is currently being deployed in the End-Use Load and Conservation Assessment

Program (ELCAP), an end-use metering study of 1000 residential and commercial structures in BPA's service territory. This document provides a functional description of the data logger, describing both the main hardware components and the system's software. Application of the logger to power measurements and meteorological and interior condition measurements is discussed along with experience on field performance. A table is provided showing approximate data logger, sensor, and installation costs as experienced in this study. DOE

N86-10528# Edgerton, Germeshausen and Grier, Inc., Goleta, Calif.

PARALLEL PULSE PROCESSING FOR MERCURIC IODIDE GAMMA-RAY DETECTORS

A. Beyerle, V. Gerrish, and K. Hull 1985 19 p Presented at the 8th Symp. on X- and Gamma-Ray Sources and Appl., Ann Arbor, Mich., 21 May 1985

(Contract DE-AC08-83NV-10282)

(DE85-013391; EGG/10282-2055; CONF-850533-9) Avail: NTIS HC A02/MF A01

Mercuric iodide (HgI2) is a semiconductor material of interest for use as a gamma ray detector because of its wide band-gap and high atomic number. The current work is with detectors of intermediate thickness (2 to 5mm), to be used to get good energy resolution with some reasonable gamma ray efficiency. The work reported covers the parallel pulse processing to obtain interaction depth information which is used to extend the usable thickness through resolution enhancements, and to obtain better detector performance from selected portions of the thicker detectors through pulse rejection techniques. A sample spectrum from a 2.5-mm-thick detector is shown. Resolution is about 10% and peak-to-valley ratio about 4:1. After taking advantage of the enhancement techniques described, resolution of 5% and peak-to-valley ratios of 8:1 are common. Poor hole mobility has been used to advantage to obtain interaction depth information. Two techniques are demonstrated for extracting conventional energy spectra from two-parameter spectra - the spectral enhancement technique which corrects for hole losses in every interaction in the detector and increases the number which fall under the full energy peak, and the pulse rejection technique which selects only those pulses which need no correction. DOE

N86-10529# Heller (Jean), Los Alamos, N. Mex.

TYPE OF NEW CHINESE-PRODUCED HIGH-SPEED CAMERA AND ITS UTILIZATION IN DETONATION PHYSICS EXPERIMENTS

Y. Sang 1985 7 p Transl. into ENGLISH from Baozha yu Chongji (China), no. 2, 1981 p 113-115

(Contract W-7405-eng-36)

(DE85-015191; LA-tr-85-31) Avail: NTIS HC A02/MF A01

This paper introduces the technological capability and special features of the new, domestically produced, Type SJZ-15 high-speed rotating mirror scanning camera and its utilization in detonation physics experiments. The camera uses an axial flow gas turbine and a two-stage internal blower for cooling. The turbine and blower use the same group of nozzles. The structure is simple, has good axial balance, and improves the cooling capability of the driving bearing housing. The two ends of the rotating mirror use three elastic bearing supporters. The axial bearings have 0-type elastic rubber balls, which are automatically centered and absorb vibration very well. The rotating mirror does not use an axial vacuum system, but the picture quality is excellent. The first objective lens Fujica type and permits use as a split-range camera. The operation handles are located on the same side of the camera. The operation handles for the rotating mirror and the main objective lens are not as convenient as the micrometer adjustment. Detonation experimental tests, technology evaluations, and actual usage prove the operation is simple and reliable, the quality of optical image formation is excellent, the light strength is appropriate, and it is an instrument of comparatively great potential. DOE

N86-10530# Edgerton, Germeshausen and Grier, Inc., Idaho Falls, Idaho.

VELOCITIES OF GAS AND PLASMAS FROM REAL TIME HOLOGRAPHIC INTEROGRAMS

V. A. Deason, L. D. Reynolds, and M. E. McIlwain 1985 9 p refs Presented at Soc. of Photo-Opt. Instr. Engr. Symp., Los Angeles, Calif., 21 Jan. 1985

(Contract DE-AC07-76ID-01570)

(DE85-014618; EGG-M-27084; CONF-850137-4) Avail: NTIS HC A02/MF A01

A truly noninvasive measurement technique for plasma velocity has not been demonstrated. Plasma velocities have been inferred using laser Doppler anemometry or photographic analysis of the position of smoke or small particles. An alternate method based on the refractive index change created in a plasma by a gaseous probe material injected into the plasma is described. This disturbance of the refractive index can be monitored using interferometry. A multipass real time holographic interferometry system is used to follow the changes of the interferometric pattern, and the data is recorded using high speed cinematography. A transparent model of an industrial plasma torch is employed in these studies, and a number of different types of trace gas materials are used to track the plasma flow. Using a combination of multipass interferometry and a laser line absorbing gas, sufficient interferometric sensitivity is obtained to determine plasma velocities in the 100 m/s range. Based on these results, a working plasma torch is constructed. Further studies are planned using this torch and actual plasmas. DOE

N86-10531# Sandia Labs., Albuquerque, N. Mex.

GEOTHERMAL LOST CIRCULATION ZONE MAPPING TOOL

T. J. Bauman 1985 7 p refs Presented at the Intern. Symp. on Geothermal Energy, Kailua Kona, Hawaii, 26 Aug. 1985

(Contract DE-AC04-76DP-00789)

(DE85-008696; CONF-850801-7) Avail: NTIS HC A02/MF A01

Lost circulation is an expensive and often encountered problem when drilling into geothermal formations. A method is needed to more accurately describe loss zones encountered during geothermal drilling to allow for more realistic testing since present testing techniques are inadequate. A Lost Circulation Zone Mapping Tool (LCZMT) is being developed that will quickly locate a loss zone and then provide a visual image of this zone as it interesects the wellbore. A modified Sandia high temperature Acoustic Borehole Televiewer should allow modeling of geothermal loss zones, which would in turn lead to testing that can be performed to evaluate lost circulation materials under simulated downhole conditions. DOE

N86-10532# California Univ., Livermore. Lawrence Livermore Lab.

IMPROVED PARTICLE-VELOCITY TRANSDUCER FOR EQUATION-OF-STATE EXPERIMENTS

S. J. Spataro 30 May 1985 21 p Presented at the 13th Transducer Workshop, Monterey, Calif., 4 Jun. 1985

(Contract W-7405-eng-48)

(DE85-013204; UCRL-92648; CONF-8506131-1) Avail: NTIS HC A02/MF A01

An improved particle velocity transducer was developed for use in equation of state experiments in the low(sub-kilobar) stock region. In low amplitude shock experiments, the standard one turn transducer generated voltages so low that signal to noise problems limited the resolution. By using multiple turns in the new transducer, an increase in signal proportional to the number of turns, with no apparent increase in noise. The complete experiment system consists of passive, multiple turn current loop transducers, a Helmholtz pair of electromagnets, a firing and timing system, a data recording system, the material under study, and a small explosive charge. Each current loop is actually a narrow linear strip of very thin copper foil, which is embedded in the test material. The shock wave from the emplaced explosive charge moves the element across an orthogonal magnetic field causing, for a brief period, a voltage output proportional to the velocity of the element. The theory and design of a new three turn transducer, its advantages, its error sources, and some typical test results are

presented. The magnetic field generator, the data recording system, and data processing are also described. DOE

N86-10533# Societe Crouzet, Valence (France).
ELASTIC WAVE GYROMETER. EXPERIMENTS WITH A PARAMETRIC WAVE DEVICE [GYROMETRE A ONDES ELASTIQUES. EXPERIMENTATION D'UN DISPOSITIF A ONDES PARAMETRIQUES]
21 Feb. 1985 15 p In FRENCH
(Contract DRET-83-056)
(Rept-26/5005/HF/AR) Avail: NTIS HC A02/MF A01

The sensitivity of a parameter wave generator to detect Coriolis acceleration is tested. The generator is built using a quartz crystal with metal electrodes and two high frequency quartz generators. A rotating table is used in experiments at angular velocities of + or - 300 deg/sec. Electronic circuits and filters, a phase meter with 0.1 deg sensitivity, and an HP 85 minicomputer are used. The results are negative, showing that the sensitivity of the device is inferior to the phase meter resolution. Author (ESA)

N86-10534# Technische Hogeschool, Eindhoven (Netherlands). Vakgroep Meten en Regelen.
MEASUREMENT OF WORKPIECE TEMPERATURE DURING WELDING FOR WELDING ROBOT CONTROL Progress Report, Mar. 1982 - Mar. 1983 [HET METEN VAN WERKSTUKTEMPERATUREN BIJ HET LASSEN OM EEN LASROBOT TE STUREN]
P. F. A. Illegrams 1983 98 p refs In DUTCH
Avail: NTIS HC A05/MF A01

MIG/MAG welding robot seam tracking system based on a symetrically noncontact temperature measurement is presented. Using literature in formation on temperature distribution during welding, a model for the prediction of the behavior of a pyrometer twin is constructed. The temperature difference between the measuring points constitutes the signal for a position control of the twin holding welding torch. As temperature measurement is made impossible by radiation originating from the welding arc, this is done during intermittent welding in time intervals in which the welding arc is switched off. Author (ESA)

N86-10185# Bundesministerium fuer Forschung und Technologie, Bonn (West Germany).
A NANOSECOND OR THIRTY CENTIMETERS: WHY ATOMIC CLOCKS HAVE TO BE SYNCHRONIZED. MITREX OPENS NEW DIMENSIONS FOR MEASURING ACCURACY [EINE MILLIARDSTELSEKUNDE ODER 30 ZENTIMETER: WESHALB ATOMUHREN WELTWEIT GLEICHLAUFEN MUESSEN. MITREX OEFFENT NEUE DIMENSIONEN DER MESSGENAUIGKEIT]
Hans-Dieter Wolz *In its* Satellite Use for Men 1985 p 26-29 In GERMAN (For primary document see N86-10180 01-12)
Avail: NTIS HC A03/MF A01

36 LASERS AND MASERS

Includes parametric amplifiers.

N86-10535 Tennessee Univ., Knoxville.
DETERMINATION OF OPTICAL PROPERTIES BY THIRD-HARMONIC GENERATION IN NOBLE GASES IN UNFOCUSED LASER BEAMS Ph.D. Thesis
Wanda Randall Ferrell 1985 124 p
Avail: Univ. Microfilms Order No. DA8511381

A new laser technique involving phase-matched third-harmonic generation in unfocused laser beams has been used to determine vacuum ultraviolet (VUV) oscillator strengths in xenon, VUV indices of refraction for the buffer gas (krypton or argon), and the VUV absorption coefficients were determined through total ionization measurements in the frequency regions of phase matching resulting from the interaction of unfocused linearly polarized light with mixtures of xenon and positively dispersive buffer gases. Since the multiphoton ionization mechanism is sharply dominated by the dimer absorption of third-harmonic photons, the ionization signal provides an excellent probe for determination of these optical parameters. Absolute ionization measurements were made through the use of a proportional counter which was calibrated by the ionization resulting from an internal Fe-55 source. Dissert. Abstr.

N86-10536 Department of the Air Force, Washington, D.C.
LASER TARGET SPECKLE ELIMINATOR Patent
C. N. Scully, inventor (to Air Force) Issued 16 Apr. 1985 5 p Supersedes AD-D010049
(AD-D011775; US-Patent-4,511,220; US-Patent-Appl-SN-452601; US-Patent-Class-350-403) Avail: US Patent and Trademark Office CSCL 20/6

An apparatus for eliminating the phenomenon of speckle with regard to laser light reflected from a distant target whose roughness exceeds the wavelength of the laser light. The apparatus includes a half plate wave member, a first polarizing beam splitter member, a totally reflecting right angle prism, and a second polarizing beam splitter member, all of which are in serial optical alignment, that are used in combination to convert a linearly (i.e., vertically) polarized light beam, which is emitted by a laser having a known coherence length, into two coincident, orthogonally polarized, beams that are not coherent with each other, and that have an optical path difference which exceeds the known coherence length of the emitting laser, to eliminate the speckle. Author (GRA)

N86-10537 Department of the Navy, Washington, D. C.
DEVICE FOR CRYOGENICALLY FABRICATING SOURCE MATERIAL FOR PLASMA X-RAY LASERS Patent
R. C. Elton, R. H. Dixon, and J. L. Ford, inventors (to Navy) Issued 2 Apr. 1985 6 p Supersedes AD-D010383
(AD-D011814; US-Patent-4,508,055; US-Patent-Appl-SN-500725; US-Patent-Class-118-724) Avail: US Patent and Trademark Office CSCL 20/5

This patent describes a device for fabricating a target of a lasing material and a pump material for lasing at X-ray wavelengths wherein one of the materials occurs naturally as a gas. A substrate of the other material is cooled below the freezing point of the one material occuring naturally as a gas. Then a gaseous atmosphere of the latter material is supplied to the cooled substrate so that a frozen layer of the latter material condenses onto the substrate to form the target. GRA

N86-10538 Department of the Navy, Washington, D. C.
W-SHAPED DIFFUSED STRIPE GaAs/AlGaAs LASER Patent
Y. Z. Liu, C. S. Hong, and D. Dapkus, inventors (to Navy) Issued 4 Jun. 1985 7 p Supersedes AD-D009849
(AD-D011818; US-Patent-4,521,887; US-Patent-Appl-SN-415639; US-Patent-Class-372-45) Avail: US Patent and Trademark Office CSCL 20/5

This patent describes a w-shaped diffused stripe GaAs/AlGaAs laser and a method for making the same. A double heterostructure layered structure includes a p-type GaAs active layer in contact with a p-type AlGaAss current blocking layer. These layers are sandwiched between two N-type AlGaAs confinement layers. A p-type zinc diffused stripe region having a w-shaped diffusion front extends longtudinally between two reflective surfaces located on respective ends of the device and extends vertically from the surface of the upper confinement layer and through a portion of the lower confinement layer and through portions of the various intervening layers. In a method of forming the device, the various layers are formed by epitaxial growth or by metalorganic chemical vapor deposition. The stripe region is formed by diffusing zinc into the device from a source through a pair of parallel slots in a diffusion mask. The zinc diffused into the device is further driven-in by heating the device on the absence of the zinc source. GRA

N86-10539*# Florida Univ., Gainesville. Dept. of Nuclear Engineering Sciences.
RESEARCH ON SOLAR PUMPED LIQUID LASERS Final Report
John D. Cox, Ulrich H. Kurzweg, Neil H. Weinstein, and Richard T. Schneider Apr. 1985 67 p refs
(Grant NAG1-135)
(NASA-CR-176235; NAS 1.26:176235) Avail: NTIS

HC A04/MF A01 CSCL 20E

A solar pumped liquid laser that can be scaled up to high power (10 mW CW) for space applications was developed. Liquid lasers have the advantage over gases in that they provide much higher lasant densities and thus high-power densities. Liquids also have advantages over solids in that they have much higher damage thresholds and are much cheaper to produce for large scale applications. Among the liquid laser media that are potential candidates for solar pumping, the POC13: Nd sup 3+:ZrC14 liquid was chosen for its high intrinsic efficiency and its relatively good stability against decomposition due to protic contamination. The development of a manufacturing procedure and performance testing of the laser, liquid and the development of an inexpensive large solar concentrator to pump the laser are examined. E.A.K.

N86-10540*# Washington Univ., Seattle. Aerospace and Energetics Research Program.

SCALING STUDIES OF SOLAR PUMPED LASERS Semiannual Progress Report, 1 Jan. - 30 Jun. 1985

W. H. Christiansen and J. Chang Aug. 1985 8 p refs

(Grant NAG1-176)

(NASA-CR-176240; NAS 1.26:176240) Avail: NTIS HC A02/MF A01 CSCL 20E

A progress report of scaling studies of solar pumped lasers is presented. Conversion of blackbody radiation into laser light has been demonstrated in this study. Parametric studies of the variation of laser mixture composition and laser gas temperature were carried out for CO2 and N2O gases. Theoretical analysis and modeling of the system have been performed. Reasonable agreement between predictions in the parameter variation and the experimental results have been obtained. Almost 200 mW of laser output at 10.6 micron was achieved by placing a small sapphire laser tube inside an oven at 1500 K the tube was filled with CO2 laser gas mixture and cooled by longitudinal nitrogen gas flow. B.W.

N86-10541# IBM Research Lab., San Jose, Calif.

TIME RESOLVED FLOW VELOCITY AND CONCENTRATION MEASUREMENTS USING A TRAVELLING THERMAL LENS

H. Sontag and A. C. Tam 25 Jun. 1985 17 p

(Contract N00014-83-C-0170)

(AD-A156706; TR-18) Avail: NTIS HC A02/MF A01 CSCL 05/9

The travelling thermal lens technique is a new all optical method for probing concentration and velocity patterns in flowing media. A thermal lens created by absorption of a short laser pulse moves with the flow and can be probed by a CW laser beam further downstream as a deflection signal. This technique enables optical measurements of the flow velocity component perpendicular to the probe laser at high spatial resolution. Its application requires no seeding with particulates as needed in most other optical techniques. GRA

N86-10542# RAND Corp., Santa Monica, Calif.

SOVIET FREE-ELECTRON LASER RESEARCH Interim Report

S. Kassel May 1985 92 p

(Contract MDA903-85-C-0030)

(AD-A156898; RAND/R-3259-ARPA) Avail: NTIS HC A05/MF A01 CSCL 20/5

The purpose of this report is to evaluate free-electron laser (FEL) research and development in the Soviet Union and to compare it with the corresponding activity in the U.S. In presenting this material, the intention is to acquaint U.S. researchers with the objectives, techniques, and results of their Soviet counterparts, as well as to provide the broad context of this area of Soviet R&D that consists of the organization, facilities, personalities, and leadership involved. The U.S. Soviet comparison has focused on the experimental programs, the most important area of this new technology. Section 2 compares individual experiments conducted by the USSR and the United States. In Section 3 the history of the theoretical development of FEL is presented, providing an insight into the conceptual issues that shaped FEL research in both countries. The remainder of the report is devoted primarily to the Soviet side of FEL research. Section 4 describes the organizational features of this research in terms of the performer institutes and leadership, focusing on the role of the Academy of Sciences, USSR. Section 5 analyzes the scientific objectives of Soviet FEL research, for the most part as discussed by Soviet reviewers of their research program. Section 6 presents conclusions. GRA

N86-10543# Spectra Technology, Inc., Bellevue, Wash.

DESIGN, FABRICATE AND TEST A 1.06(MU) REPETITIVELY PULSED LASER Final Report

J. M. Eggleston and E. A. Crawford 28 Jun. 1985 71 p

(Contract DE-AC06-83FR-53157)

(DE85-014439; DOE/ER-53157/T1) Avail: NTIS HC A04/MF A01

The results of a program to develop the Thomson scattering diagnostic laser are described. Background material and technical justification for the design approach are given. Principal results of the developmental program were the construction of a rep rated slab glass amplifier, and the accumulation of the design knowledge necessary to build such amplifiers for maximum performance. Significant advances are made in reducing second order optical distortions. DOE

N86-10544# Deutsche Forschungs- und Versuchsanstalt fuer Luft- und Raumfahrt, Oberpfaffenhofen (West Germany). Abt. Lasertechnik.

EXPERIMENTAL INVESTIGATIONS OF PULSE-PULSE INTERFERENCE IN HETERODYNE DETECTION

Friedrich Malota May 1984 25 p refs In GERMAN; ENGLISH summary Report will also be announced as translation (ESA-TT-949)

(DFVLR-FB-85-26; ISSN-0171-1342) Avail: NTIS HC A02/MF A01; DFVLR, Cologne DM 10

The interference of two laser pulses originating from the same source and thus having a constant frequency difference was investigated. The calculation of the heterodyne currents in the interference of two pulses is described. It is shown that a coherent pulse-pulse interference is possible in a pulse heterodyne system. Experimental data are in good agreement with theoretical predictions, especially the determination of the intermediate frequency. Author (ESA)

37 MECHANICAL ENGINEERING

Includes auxiliary systems (non-power); machine elements and processes; and mechanical equipment.

N86-10545 Purdue Univ., Lafayette, Ind.

DYNAMIC ANALYSIS OF ROBOTIC MANIPULATIONS WITH FLEXIBLE LINKS Ph.D. Thesis

Liang-Wey Chang 1984 189 p

Avail: Univ. Microfilms Order No. DA8507666

The development dynamic model for flexible manipulator systems and a solution method to solve the equations of motion efficiently is discussed. The model describes the global motion of the flexible manipulators as a large motion and a small motion. The large motion is represented by the Equivalent Rigid Link System (ERLS) which is kinematically equivalent to the real rigid link system. The small motion represents deformations of the system relative to the ERLS. A sequential integration method is applied to integrate the equations of motion numerically to obtain significant improvement in computation efficiency. The sequential integration method is particularly efficient for solving the equations of motion of the manipulator system which possesses a wide range of frequencies of which only the lower frequencies are excited. Robotic dynamics of the flexible mannipulator is useful in the design and the control areas. Procedures are proposed to solve the robotic dynamics. A planar manipulator is used as an example to demonstrate the simulation results. Dissert. Abstr.

N86-10546 United Kingdom Atomic Energy Authority, Risley (England).

THE INFLUENCE OF THE SUBSTRATE ON THE PRACTICAL MACHINING APPLICATIONS OF CUTTING EDGES COATED WITH DIFFERENT MATERIALS

K.-E. Klemme 25 Nov. 1984 11 p refs Transl. into ENGLISH from Werkstatt und Betrieb (West Germany), v. 114, no. 5, 1981 p 291-293

(BLL-Risley-TR-5039-(9091.9F)) Copyright. Avail: British Library Lending Div., Boston Spa, Engl.

Coated cutting edges were employed to extend tool life and to increase the volume of the material. The coatings are applied to the hardmetal substrate very largely using the Chemical Vapor Deposition (CVD) method. The application of these coatings from the gasous phase is no problems. The influence of the substrate, irrespective of the coating, on the service life attained by a cutting edge is studied. The manner in which the machining character of a cutting edge is altered is examined. E.A.K.

N86-10547 Johns Hopkins Univ., Baltimore, Md.

STIFFENED AND PRESTRESSED COMPOSITE OVERWRAPPED PRESSURE VESSELS Ph.D. Thesis

Mostefa Djamel Boussouf 1985 246 p

Avail: Univ. Microfilms Order No. DA8510402

A structural analysis of a stiffened inner metal layer strengthened by two unidirectional composite overwrapped layers in which the fibers have a ring winding. One layer covers the structure completely and provides reinforcement in the axial direction, while another covers the cylindrical part only with a circumferential composite overwrap. Methods are developed for deriving equivalent flexural rigidity, and interaction influence stiffness. Analytical solutions and numerical results for vessels with and without edge stiffeners are presented. This study is confined to the isotropic/orthotropic thin shell theory and uses load sharing liners, it also assumes that there is no adhesive between layers, thus no shear coupling. The analysis takes into consideration the variation in the radii of individual layers. It is assumed that fiber winding of the composite layers are coincident with the principal directions of the structure, that is the axial and circumferential for the cylinder and only meridional for the spherical cap. Dissert. Abstr.

N86-10548 Ohio State Univ., Columbus.

DIGITAL CONTROL OF THE HYDRAULIC ACTUATORS OF AN ADAPTIVE SUSPENSION VEHICLE Ph.D. Thesis

Joseph Alan Dworak 1985 498 p

Avail: Univ. Microfilms Order No. DA8510565

A series-bypass hydraulic power circuit is evaluated for use on a six-legged walking vehicle. This vehicle will be totally autonomous and have the capability to carry a man and 500 lbs. payloads. This hydraulic circuit is part of a closed loop feedback system which uses microprocessors to control the vehicle trajectory. The series-bypass circuit combines features of pump and valve controlled hydraulic circuits to achieve high energy efficiency and maximize the closed loop bandwidth. The circuit is mathematically modeled and analyzed using linearized symbolic and frequency response transfer functions and a nonlinear time domain simulation. These methods are used to select and test controller designs. The control architecture is primarily designed by using classical transfer function methods. Due to the nature of the series-bypass circuit and performance objectives, it is also necessary to employ multivariable techniques in designing and analyzing the closed loop systems. Based on the simulation and linearized studies, controller designs are experimentally evaluated on a microprocessor controlled prototype series-bypass circuit. Dissert. Abstr.

N86-10549 Ohio State Univ., Columbus.

COMPUTER CONTROL OF AN ELECTRIC HYDRAULIC ROBOT LEG WITH PROXIMITY RANGING SYSTEM Ph.D. Thesis

Chi-Keng Tsai 1985 286 p

Avail: Univ. Microfilms Order No. DA8510647

Real-time control was implemented using an Intel 8086 microprocessor-based microcomputer. State Feedback Control with a simplified Inverse Plant feedforward term was implemented to improve the joint servo performance of high speed leg motion and to solve the highly underdampled system problem. In particular, filtered pressure feedback is used to speed up the response and improve the damping characteristics. The new approaches based on the Jacobian were implemented as the basis for finding the joint positions associated with a constrained foot position. Two proximity sensors mounted on the Prototype Leg were successfully used for the purpose of stepping over an object during the leg transfer phase. The control algorithm developed is of general form so as to be appropriate for other tasks and configurations of sensors. Dissert. Abstr.

N86-10550 Westland Helicopters Ltd., Yeovil (England).

TRIALS ON THE ASPERITY COUNTING MONITORING SYSTEM Final Report

R. Wordsworth (Imperial Coll. of Science and Technology) and P. B. MacPherson May 1984 32 p refs

(Contract A12/1347)

(Res-Paper-670; BR93962) Avail: Issuing Activity

A monitoring system, based on asperity contacts within a loaded and lubricated pair of metal surfaces, was evaluated in a mini disk machine. Results confirm the sensitivity of the system to changes in surface topography. With additional storage capacity available in microcomputers, a tool for laboratory test running normally undertaken in a mechanical research laboratory is available. The monitor could also be applied in a gearbox test rig for studying the performance of a specific bearing or gear set. Although interest in grease as a gearbox lubricant waned an effective system for routine monitoring of helicopter tail and intermediate gearboxes is feasible. Author (ESA)

N86-10551*# National Aeronautics and Space Administration. Lewis Research Center, Cleveland, Ohio.

MEASUREMENT OF THE DENSITY OF BASE FLUIDS AT PRESSURES 0.422 TO 2.20 GPa

Bernard J. Hamrock, Bo O. Jacobson (Lulea Univ.), and Sten-Ivar Bergstroem (Lulea Univ.) [1985] 22 p refs Presented at the Ann. Meeting of the Am. Soc. of Lubrication Engrs., Toronto, 12-15 May 1986

(NASA-TM-87114; E-2650; NAS 1.15:87114) Avail: NTIS HC A02/MF A01 CSCL 20D

The influence of pressure on the density of six base fluids is experimentally studied for a range of pressures from 0.422 to 2.20 GPa. An important parameter used to describe the results is the change in relative volume with change in pressure dv sub r/dp. For pressures less than the solidification pressure ($p < ps$) a small change in pressure results in a large change in dv sub r/ps. For pressures greater than the solidification pressure ($p > ps$) there is no change in dv sub r/dp with changing pressure. The solidification pressures of the base fluids varies considerably, as do the slopes that the experimental data assumes for $p < ps$. A new formula is developed that describes the effect of pressure on density in terms of four constants. These constants vary for the different base fluids tested. Author

N86-10552*# National Aeronautics and Space Administration. Lewis Research Center, Cleveland, Ohio.

THE MECHANISM OF EROSION OF METALLIC MATERIALS UNDER CAVITATION ATTACK

B. C. S. Rao (Case Western Reserve Univ.) and D. H. Buckley 1985 18 p refs Proposed for presentation at the Intern. Symp. on Cavitation, Sendai, 16-19 Apr. 1986; sponsored by Japan Society of Mechanical Engineers, ASME, Institution of Mechnanical Engineers (British), JSCE and International Association for Hydraulic Research

(NASA-TM-87133; E-2684; NAS 1.15:87133) Avail: NTIS HC A02/MF A01 CSCL 11F

The mean depth of penetration rates (MDPRs) of eight polycrystalline metallic materials, Al 6061-T6, Cu, brass, phosphor bronze, Ni, Fe, Mo, and Ti-5Al-2.5Sn exposed to cavitation attack in a viscous mineral oil with a 20 kHz ultrasonic oscillator vibrating at 50 micron amplitude are reported. The titanium alloy followed by molybdenum have large incubation periods and small MDPRs.

The incubation periods correlate linearly with the inverse of hardness and the average MDPRs correlate linearly with the inverse of tensile strength of materials. The linear relationships yield better statistical parameters than geometric and exponential relationships. The surface roughness and the ratio of pit depth to pit width (h/a) increase with the duration of cavitation attack. The ratio h/a varies from 0.1 to 0.8 for different materials. Recent investigations (20) using scanning electron microscopy to study deformation and pit formation features are briefly reviewed. Investigations with single crystals indicate that the geometry of pits and erosion are dependent on their orientation. Author

N86-10553# Admiralty Marine Technology Establishment, Teddington (England).
THE GENERATION AND TRANSMISSION OF VIBRATION IN PLAIN CYLINDRICAL BEARINGS. PART 2. EXPERIMENT
L. V. Embling, C. J. Jenkins, and P. Meyer Sep. 1984 67 p
(AD-A156577; AMTE(N)/R84009-Pt-2; DRIC-BR-95691-Pt-2) Avail: NTIS HC A04/MF A01 CSCL 13/9

The vibration transmission characteristics of hydrodynamic bearings have been investigated at frequencies well above the out of balance frequency. Part 1 of this report developed theories to predict the linear transfer functions of bearings and to examine the effects of nonlinearities in modulating the response to external forces. This part of the report describes an experimental investigation on a bearing test rig aimed at validating the theories. It is concluded that: (1) bearings are not always rigid to vibration, the frequency range over which the rigidity applies being determined by the bearing parameters; (2) transfer functions across the bearing in the direction of the applied force are reciprocal; and (3) the bearing can introduce modulation in the response to a single-frequency force. GRA

N86-10554# Department of the Navy, Washington, D. C.
AIRBOC (AIR RAPID BLOOM OFFBOARD CHAFF) CHAFF DEPLOYMENT SYSTEM Patent Application
W. Humphries, J. Bryant, R. C. Eklund, D. C. Hayes, and P. Ferko, inventors (to Navy) Filed 1 Apr. 1985 14 p
(AD-D011746; US-Patent-Appl-SN-718399) Avail: NTIS HC A02/MF A01 CSCL 17/4

An AIRBOC (Air Rapid Bloom Offboard Chaff) chaff deployment apparatus comprising a canister with a wind flap attached externally to the canister and connected to a drogue chute that is housed inside the canister. The drogue chute is situated atop a main chute that is atop a release mechanism, which is atop a fuze and that is atop a chaff payload, all of which is housed inside the canister. When the AIRBOC is dropped from a plane, the wind flap extends, pulling out the drogue chute. The drogue chute in turn activates the release mechanism which frees the drogue chute to pull out the main chute to which the drogue chute is connected. The deployment of the main chute causes a force greater than 40 lbs to be applied to the release mechanism, resulting in the chaff payload being released from the canister and the fuze being activated, consequently detonating the released chaff payload. GRA

N86-10555# Department of the Navy, Washington, D. C.
MARGINAL-TERRAIN STRADDLE-LIFT CONTAINER HANDLER Patent Application
C. I. Skaalen, H. G. Lange, and P. S. Springston, inventors (to Navy) Filed 11 Apr. 1985 29 p
(AD-D011752; US-Patent-Appl-SN-718762) Avail: NTIS HC A03/MF A01 CSCL 13/6

A highly maneuverable straddle carrier vehicle structure is provided for handling various sizes of containers and outsized loads over rough, unleveled, weak and unprepared soils to meet austere requirements which are beyond the capability of commercial straddle lifts that normally operate on prepared surfaces within specific boundaries of yards and docks. Features include high flotation tires capable of operation over marginal terrain, fording capability, all wheel 360 degree steering and offset wheel yokes which permits automatic changing of wheelbase dimensions for rugged sloping terrain operations and wheel positioning for optimum mobility including lateral and oblique movement and vehicle rotation within its own length for a variety of close quarters operations. Load stabilization devices permit container securing during transit and hinged transverse members operate to reduce torsion and bending moments on the vehicle structure over severe terrain. GRA

N86-10556# Department of the Air Force, Washington, D.C.
OVER-CENTER TOGGLE LATCH Patent Application
F. T. Hinds, inventor (to Air Force) Filed 14 Aug. 1984 12 p
(AD-D011753; US-Patent-Appl-SN-640623) Avail: NTIS HC A02/MF A01 CSCL 13/5

This patent application discloses an improved low profile over-center toggle latch arm with an internally threaded latch barrel nut for adjustable cooperation with a threaded latched draw bolt. The bolt is pivotally coupled to a latch handle assembly. The latter comprises projecting sidewalls and a grip end. The latch handle assembly is mounted by means of integral flanges cooperating with journals defined in a mounting stirrup, the latter being mounted on the container body. GRA

N86-10557# Air Force Inst. of Tech., Wright-Patterson AFB, Ohio.
A TRANSFORMATION METHOD FOR THE EVALUATION OF THE RESPONSE MOMENTS OF ELASTIC STRUCTURES WITH RANDOM PROPERTIES Ph.D. Thesis
R. H. Bennett Apr. 1985 169 p
(AD-A156882; AFIT/CI/NR-85-46D) Avail: NTIS HC A08/MF A01 CSCL 20/11

In this investigation a new method for computing the first and second moments of the displacement response of linear elastic structures with random stiffness and damping is developed. The method accurately computes the mean and variance of the displacement of a dynamically loaded structure as functions of time. The probability that the displacement will be greater than a specified value is also computed. The results of the transformation method are compared to exact solutions for a number of cases. The influence of the randomness in the underlying parameters on the randomness of the response is discussed. Author (GRA)

N86-10558# Department of the Air Force, Washington, D.C.
TERMINATION LOAD CARRYING DEVICE Patent Application
J. N. Tervo, inventor (to Air Force) Filed 19 Jun. 1985 11 p
(AD-D011800; US-Patent-Appl-SN-746617) Avail: NTIS HC A02/MF A01 CSCL 13/9

A follower nut assembly is attached to a load carrying nut all of which is threaded onto a ball screw of a drive actuator. The actuator drive causes a load attached to said load carrying nut to be translated to a fully extended position. At about the fully extended position, a run-off end without threads of the ball screw is positioned in the load carrying nut. This causes the translating force to be fully applied to a follower nut which is normally shear pinned to the load carrying nut. Because of the inertia of the load, the follower nut shears the pin and then rotates within a cage of the follower nut assembly. The translation of the load stops when the shear pin is broken. A thrust bearing is positioned between the follower nut and the load carrying nut to provide the necessary support when the load is fully extended. Author (GRA)

N86-10559# Princeton Univ., N. J. Dept. of Mechanical and Aerospace Engineering.
MODELING OF ENGINE SPRAYS
F. V. Bracco 1985 24 p
(Contract DE-AC04-81AL-16338)
(DE85-010020; DOE/AL-16338/T1) Avail: NTIS HC A02/MF A01

Atomization and full-cone sprays from single cylindrical orifices were considered. The following subjects are reviewed: the structure of the breakup region; the structure of the far field; modern models that, given the outcome of the breakup process, compute the steady and transient of sprays; some comparison with detailed measurements; and some practical applications. It is concluded that the spray breakup and the development regions are the most relevant in engine applications, the inner structure of the breakup

region is still largely unknown, two and three-dimensional spray models are available, but remain mostly untested, particularly in their vaporization and combustion components, in part because of a lack of accurate measurements in controlled engine-type environments, engine applications of such models are recommended for learning, interpretative, and exploratory studies, but not for predictions. DOE

N86-10560# Deutsche Gold- und Silber-Scheideanstalt, Frankfurt am Main (West Germany). Fertigungstechnik Metall.
REDUCTION OF NOBLE METAL STOCK AND NOBLE METAL LOSS DURING WIRE PRODUCTION WITH THE CONFORM EXTRUSION PROCESS Final Report, Dec. 1983
Wolfgang Diem Bonn Bundesministerium fuer Forschung und Technologie May 1985 34 p refs In GERMAN; ENGLISH summary Sponsored by Bundesministerium fuer Forschung und Technologie
(BMFT-FB-T-85-049; ISSN-0340-7608) Avail: NTIS HC A03/MF A01; Fachinformationszentrum, Karlsruhe, West Germany DM 7

The conform continuous extrusion process used in wire production was tested to optimize the process and facilities and to determine its economical use in copper and silver hard solder production taking into account a reduction of the noble metal stock and noble metal loss during production. The Conform extrusion process allows a reduction in the amount of noble metals recycled and in the material loss during production resulting from a reduction in the number of production steps and thus in the mean production time. However, the Conform process cannot be economically used in copper and silver hard solder production because of quality control and tool durability problems.
Author (ESA)

N86-10587# Indian Inst. of Science, Bangalore. Dept. of Mechanical Engineering.
RECENT ADVANCES IN THE ANALYSIS OF EXHAUST MUFFLERS
M. L. Munjal *In* Shock and Vibration Information Center The Shock and Vibration Digest, Vol. 17, No. 3 Mar. 1985 p 3-16 refs (For primary document see N86-10585 01-39)
Avail: SVIC, Code 5804, Naval Research Lab., Washington, D.C. 20375 CSCL 13/9

38 QUALITY ASSURANCE AND RELIABILITY

Includes product sampling procedures and techniques; and quality control.

N86-10561*# National Aeronautics and Space Administration. Lewis Research Center, Cleveland, Ohio.
ULTRASONIC EVALUATION OF MECHANICAL PROPERTIES OF THICK, MULTILAYERED, FILAMENT WOUND COMPOSITES
Harold E. Kautz Sep. 1985 36 p refs
(MASA-TM-87088; E-2676; NAS 1.15:87088) Avail: NTIS HC A03/MF A01 CSCL 14D

A preliminary investigation is conducted to define capabilities and limitations of ultrasonic and acousto-ultrasonic measurements related to mechanical properties of filament wound graphite/epoxy composite structures. The structures studied are segments of filament wound cylinders formed of multiple layers of hoop and helical windings. The segments consist of 24 to 35 layers and range from 3.02 to 3.34 cm in wall thickness. The resultant structures are anisotropic, heterogeneous, porous, and highly attenuating to ultrasonic frequencies greater than 1 MHz. The segments represent structures to be used for space shuttle booster cases. Ultrasonic velocity and acousto-ultrasonic stress wave factor measurement approaches are discussed. Correlations among velocity, density, and porosity, and between the acousto-ultrasonic stress wave factor and interlaminar shear strength are presented.
Author

N86-10562# Laboratorio de Acustica e Sonica, Sao Paulo (Brazil).
ULTRASONIC INSPECTION OF WELDMENTS IN LARGE SIZE SPIRAL BOX FOR HYDROELECTRIC PLANT
L. X. Nepomuceno and A. Vendetti 19 Jul. 1985 51 p In PORTUGUESE; ENGLISH summary
(AS-701/85) Avail: NTIS HC A04/MF A01

The adopted procedures, the criteria established for acceptance of the inspected weldments and the observed results are described. The detected discontinuities are corrected, the weld is reinspected and applied to the acceptance criteria. E.A.K.

N86-10563# Army Test and Evaluation Command, Aberdeen Proving Ground, Md.
TEST, MEASUREMENT, AND DIAGNOSTIC EQUIPMENT (SYSTEM PECULIAR) Final Report
30 May 1985 15 p Supersedes report dated 7 May 1974, AD-781946
(AD-A156669; TOP-6-2-335) Avail: NTIS HC A02/MF A01 CSCL 14/2

This Test Operations Procedure (TOP) provides guidance for planning tests of system-peculiar test, measurement, and diagnostic equipment (TMDE) including Test Program Sets (TPS) needed to support a system, to ensure its conformance with requirements documents, Acquisition Plan (AP), Test Program Set Management Plan (TPSMP), and Item Integrated Logistics Support Plan (ILSP). Subtests to satisfy the requirements for the particular TMDE and test type (DT 2 and 3) can be selected or supplemented from those listed in the test procedures. GRA

N86-10564# Societe Nationale Industrielle Aerospatiale, Suresnes (France). Lab. Central.
NONDESTRUCTIVE CONTROL OF THICK STRUCTURES MADE WITHOUT DISASSEMBLING [CONTROLE NON DESTRUCTIF D'ASSEMBLAGE DE FORTES EPAISSEURS SANS DEMONTAGE DES FIXATIONS, PROCES VERBAL 43-954/F/3]
D. Lecuru 21 Jan. 1985 43 p refs In FRENCH
(Contract STPA-82-96-006)
(PV-43-954/F/3) Avail: NTIS HC A03/MF A01

Ultrasonic and Foucault current methods to inspect aircraft structures in places were plate superposition gives a total thickness > 5 to 7 mm were studied. The feasibility of the ultrasonic is demonstrated for external plates, while that of the Foucault current method is shown for the inner plates up to 20 mm thickness.
Author (ESA)

39 STRUCTURAL MECHANICS

Includes structural element design and weight analysis; fatigue; and thermal stress.

For applications see *05 Aircraft Design, Testing and Performance* and *18 Spacecraft Design, Testing and Performance.*

N86-10565 Iowa Univ., Iowa City.
DESIGN SENSITIVITY ANALYSIS AND OPTIMIZATION OF BUILT-UP STRUCTURES Ph.D. Thesis
Hee Gag Lee 1984 184 p
Avail: Univ. Microfilms Order No. DA8507953

Design sensitivity analysis and optimization of built-up structures are formulated, analyzed, and solved numerically. A variational approach is used to incorporate both finite dimensional and distributed state and design variables in the same energy equation. Kinematic and natural boundary conditions at the interfaces between structural components of built-up structures are defined. Variation of the energy equation with the material derivative idea from continuum mechanics and introduction of an adjoint variational equation yield design sensitivity vectors and functions with respect to conventional and shape design variables. A unified method of shape design sensitivity analysis for static and eigenvalue problems, to complement the finite element method of structural analysis is developed. Standard shape design sensitivity forms are derived

for structural components and may be applied to various kinds of built-up structures to obtain design sensitivity forms at the interfaces between structural components of built-up structures. This method provides potential for shape optimization of complex built-up structures. Dissert. Abstr.

N86-10566 Clemson Univ., S.C.
AN ANALYTICAL AND NUMERICAL STUDY OF THE BUCKLING BEHAVIOR OF FIBER-REINFORCED BEAMS Ph.D. Thesis
Hossam Nasser Mohamed-Aly 1984 189 p
Avail: Univ. Microfilms Order No. DA8507587

A nonlinear theory suitable for determining bifurcation loads, or limit point loads, for straight beams with thin-walled open cross sections that are made from midplane symmetric, fiber-reinforced laminates is presented. A computer code is developed that computes requisite section properties for six different cross-sectional shapes. It can be used to compute bifurcation or limit point loads for three different loading conditions under a variety of boundary conditions and any midplane symmetrical, angle ply fiber pattern. The nonlinear equilibrium equations and boundary conditions associated with limit point buckling, or bifurcation buckling, are solved iteratively using Newton's method. First order finite-difference formulas are used to obtain a numerical analogue for the system of lienar correctional equations obtained by the Newton method. This system of equations is solved using Potter's algorithm. An interval halfing procedure is used to refine the accuracy of a buckling load so that a sign change in the buckling determinant occurs between load levels for which the load increment is less than one percent. Dissert. Abstr.

N86-10567 Florida Univ., Gainesville.
ANALYTICAL AND EXPERIMENTAL STUDY OF CRACKS EMANATING FROM AN ELLIPTICAL HOLE IN UNIDIRECTIONAL COMPOSITE MATERIAL Ph.D. Thesis
Said Abdel-Maaboud Khalil 1984 214 p
Avail: Univ. Microfilms Order No. DA8509948

A fundamental study of stress fields around an elliptical hole, with and without cracks emanating from it, in unidirectional composite materials is presented. The first part deals with stress concentration factors. The second part discusses stress intensity factors and energy release rate. The fracture mechanics part starts with a discussion of the application of different energy principles to the finite element technique. This discussion is followed by the introduction of a new mathematical formulation of a finite element model. This model is based on the modified complementary energy principle in conjunction with the anisotropic elasticity and complex variable techniques. Calculations of stress intensity factors for single mode and mixed mode fractures are included. Analytical and experimental evaluations of the strain energy release rate are determined. Analytical evaluation of the energy release rate is based on the finite element solution. The experimental part of this evaluation is based on the compliance calibration technique. Dissert. Abstr.

N86-10568 Yale Univ., New Haven, Conn.
STRENGTH OF SHELLS UNDER LOCAL TRANSVERSE LOADS Ph.D. Thesis
Mandayam Anandanpillai Srinivasan 1984 293 p
Avail: Univ. Microfilms Order No. DA8509786

This thesis is concerned with the estimation of the limit load of thin shells composed of ductile materials and subjected to local transverse loads which are quasi-static and monotonically increasing. Two problems are considered: an axisymmetric spherical dome with a cutout and a cylindrical shell under a rigid punch. Application of the theorems of limit analysis to the suitably nondimensionalized governing equations supplied by shell theory lead to constrained optimization problems in the presence of two parameters measuring the load size and the thickness of the shell, where the latter is very small. One of the main purposes is to devise systematic analytical procedures that take advantage of the presence of this small parameter in obtaining close bounds to the optimum, the limit load. The spherical dome is loaded radially along the circumference of the circular cut-out. The complete solution (i.e., the limit load and the associated velocity and stress resultant fields) of the problem covering a wide range of parameter values is obtained. Dissert. Abstr.

N86-10569 Akron Univ., Ohio.
FINITE ELEMENT ANALYSIS OF METALS AT ELEVATED TEMPERATURE USING UNIFIED CONSTITUTIVE THEORIES Ph.D. Thesis
Jium-Pang Chang 1985 242 p
Avail: Univ. Microfilms Order No. DA8511183

The present study is aimed at the finite element formulation of a family of viscoplastic models intended for inelastic analysis of structures deformed at elevated temperatures. The constitutive theories considered in this dissertation represent the state of the art approach in high-temperature applications. That is, the inelastic strains are treated as unified quantities (no distinction between creep and plastic strains), which are the functions of stress, temperature and state variables. The approach is capable of representing creep, stress relaxation, plasticity, cyclic behavior, and creep-plasticity interaction of metals. In order to effectively investigate the uniaxial responses of various viscoplastic models, an interactive computerized procedure with extensive graphic display features has been developed. Its applications include the predictions of cyclic stress-strain response, creep, stress relaxation, and thermomechanical fatigue loop. It also serves as a tool for the parametric study of a given material model and the evaluation of numerical integration schemes. Dissert. Abstr.

N86-10570 Johns Hopkins Univ., Baltimore, Md.
LOAD SPACE FORMULATION OF RELIABILITY FOR NONLINEAR RANDOM STRUCTURAL SYSTEMS Ph.D. Thesis
Tzyy Shan Lin 1985 216 p
Avail: Univ. Microfilms Order No. DA8510428

A technique is proposed for determining the reliability of redundant ductile framed structures. A nonlinear structural analysis program and incremental load procedure are used to find the limit state function in load space for fixed structural properties. The failure probability of this deterministic structure is then computed by integrating the joint distribution function of loads over the failure region in load space. The procedure is extended to include randomness in the strength of the structure by introducing a random resistance variable unique to each load path. The statistics of this variable can be found by relating magnitudes of the load vector to successive component failure. The load space formulation of system reliability appears applicable to realistic structures of reasonable complexity. Dissert. Abstr.

N86-10571 Case Western Reserve Univ., Cleveland, Ohio.
FINITE ELEMENT ANALYSIS OF STATICS AND DYNAMIC STRUCTURAL ENGINEERING PROBLEMS USING SEMI-EXPLICIT METHODS Ph.D. Thesis
Rupasiri Purasinghe 1985 116 p
Avail: Univ. Microfilms Order No. DA8510102

Improved semi-explicit methods to solve static and dynamic structural engineering problems are presented which have computer implementation advantages in large and small systems. In solving structural dynamic problems in large systems an unsymmetric splitting method of the stiffness matrix is presented. This technique has the advantage of an explicit method that no matrix factorization of the effective stiffness matrix is necessary at each time step. Besides this method has the advantage of an implicit method that a large time step, larger than that provided in a classical explicit formulation is achieved. In solving static and dynamic problems on small systems, improved iterative techniques which have less storage requirements are presented. These improved iterative techniques are based on a projection of the residuals using a partial Choleski decomposition of the global stiffness matrix. A use of line search to accelerate convergence is included. Dissert. Abstr.

N86-10572 Illinois Univ., Chicago.
OPTIMAL DESIGN OF PORTAL FRAMES AGAINST BUCKLING Ph.D. Thesis

Naser Rezaie-Keyvan 1985 100 p
Avail: Univ. Microfilms Order No. DA8511278

The application of standard stationarity conductions to the optimal design of a structure against buckling may actually lead to a reduction of its real strength in the sense that the optimized structure has been weakened with respect to higher modes to the extent that these have now become fundamental. In this case, a true optimum occurs when the magnitudes of several eigenvalues coalesce, and the corresponding optimality condition is then no longer stationary, but singular. The relevant equations are developed, and an analytical solution is obtained for the case of a symmetric portal frame under symmetric loading for various height-to-span ratios. As expected, and in conformity with the know solution to the fixed-fixed column problem, The correct optimal design exhibits no hinges. Unlike the column problem, however, the value of the associated optimal load parameter is appreciably below the one corresponding to a single-mode solution.
Dissert. Abstr.

N86-10573 Florida Univ., Gainesville.
INELASTIC ANALYSIS OF FRAME STRUCTURES INCLUDING MEMBER AND JOINT SHEARS Ph.D. Thesis
Vinayagamoorthy Balachandran 1984 435 p
Avail: Univ. Microfilms Order No. DA8509902

A computer program, FRAME82, is developed to perform inelastic static and dynamic analyses of plane frame structures including member and joint shear deformations. The effects of parameters such as inelastic material properties and member and joint supports, nonlinear geometry, cyclic loading, mass dependent viscous damping, etc., are also included in the program, FRAME82 utilizes a newly developed Discrete (Finite) Element Shear Model to incorporate the effects of member shear, in addition to the Discrete Element Flexural Model that considers only flexural and axial deformations. Joint shear panels are assumed to have only shear deformations, and flexural and axial deformations are ignored. Besides the three regular degrees of freedom, namely, horizontal, vertical, and rotational displacement, the program requires an additional rotational degree of freedom, namely, horizontal, vertical, and rotational displacement, the program requires an additional rotational degree of freedom for each joint to include the joint shear deformation effects. The structure stiffness is formulated from the stress-stain level and several inelastic models including Masing are incorporated. The program updates the structure stiffness after each iteration within each time step and adds any unbalance in dynamic equilibrium as a corrective load at the beginning of the subsequent iteration. Dissert. Abstr.

N86-10574 Georgia Inst. of Tech., Atlanta.
THE USE OF NEW PATH INDEPEDENT INTEGRALS IN ELASTIC-PLASTIC AND CREEP FRACTURE Ph.D. Thesis
Frederick William Brust, Jr. 1984 262 p
Avail: Univ. Microfilms Order No. DA8510953

A new path independent integral referred to as T* is presented and critically examined with respect to its ability to characterize nonlinear fracture mechanics. T* can characterize nonlinear fracture since it is equivalent to the currently established parameters, which are theoretically valid under limited circumstances. The application of T* to nonlinear fracture includes elastic-plastic stable crack growth, creep fracture, low cycle fatigue situations, and even in a situation where time dependent and time independent material behavior prevail. Experimental data on elastic-plastic stable crack growth in steel is modeled via the finite element method. The ability of T* to characterize the fracture process under these circumstances, and the corresponding inability of the currently established plastic fracture parameters is established. Finite element analyses were performed to evaluate the effectiveness of the T* parameter under creep conditions. This is done, in part, by modeling experimental data of creep crack growth.
Dissert. Abstr.

N86-10575 Testwell Ltd., Daventry (England).
FRACTURE TOUGHNESS TESTING OF CENTRIFUGALLY CAST NICKEL ALUMINIUM BRONZE
May 1984 43 p
(Contract AMTE-NSM42D/1611)
(Rept-MAT/720; BR94518) Avail: NTIS

Fracture toughness of a large centrifugally cast component was assessed by testing 49 specimens from various locations of the component. The AC-PD technique was used to detect the initiation of ductile tearing and show stable crack growth. Metallographic examination was carried out on five specimens, one from each of the test locations, in order to investigate any correlation of grain size with the initiation of ductile tearing. A J resistance curve for each location was determined with a minimum of five specimens in each case; J IC was evaluated by extrapolation of the resistance curve to a blunting line. The J initiation was estimated from the AC-PD measurements and J resistance curves were derived. Author (ESA)

N86-10576 Sussex Univ., Brighton (England). School of Chemistry and Molecular Sciences.
THE PREPARATION AND TESTING OF TITANIUM AND ZIRCONIUM COUPLING AGENTS Final Report
Rowena Lalanandham, Paul D. Calvert, and David R. M. Walton Feb. 1984 47 p refs
(Contract MIN-DEF-ERC/9/4/2120/034)
(SJ70; BR91279) Avail: NTIS

A series of titanium and zirconium-based coupling agents containing isopropoxy and epoxy or amine-functional carboxylate groups selected so as to promote bonding between epoxy resins and aluminum or iron oxide surfaces were prepared. Infrared spectral studies show that titanium and zirconium alkoxides form strong water-stable bonds with aluminum, iron, and silica surfaces. Carboxylates carrying epoxide or amino functions can bond to epoxy resins. Titanium and zirconium isopropoxy tricarboxylates were tested as coupling agents on epoxy-aluminum bonds exposed to water. Only small strength improvements result, but fracture is found to be in the oxide layer rather than interfacial. Author (ESA)

N86-10577*# Old Dominion Univ., Norfolk, Va. Dept. of Civil Engineering.
PASSIVE DAMPING CONCEPTS FOR SLENDER COLUMNS IN SPACE STRUCTURES Progress Report, 1 Feb. - 1 Jul. 1985
Zia Razzaq and Rajendra K. Ekhelikar May 1985 137 p refs
(Grant NAG1-336)
(NASA-CR-176234; NAS 1.26:176234) Avail: NTIS HC A07/MF A01 CSCL 20K

An experimental and theoretical study of three different passive damping concepts is conducted for a slender member with partial rotational end restraints. Over a hundred full-scale natural vibration experiments were conducted to evaluate the effectiveness of mass-string, polyethylene tubing, and chain damping concepts. The damping properties obtained from the experiments were used in the approximate analyses based on the partial differential equation of motion for the problem. The comparison of the experimental and the theoretical deflection-time relations shows that the velocity-dependent damping model used in the theory is adequate. From the experimental results, the effect of end connection friction and induced axial forces on damping is identified. The definition of an efficiency index is proposed based on the damping ratio and the mass of a given passive damping device. Using this definition, the efficiencies of the three damping devices are compared. The polyethylene tubing concept resulted into a low damping efficiency. B.W.

N86-10578*# College of William and Mary, Williamsburg, Va.
STUDY OF STATIS AND DYNAMIC STRESS EFFECTS IN NONLINEAR SOLIDS Semiannual Progress Report, 15 Dec. 1984 - 15 Jun. 1985
Min Namkung 15 Jun. 1985 19 p refs
(Grant NCC1-75)
(NASA-CR-176236; NAS 1.26:176236) Avail: NTIS HC A02/MF A01 CSCL 20K

As the basic physical principles behind the low-field magnetoacoustic interactions have been unfolded, a new step in the present research had to be taken. First, the stress measurements

began in samples obtained in real railroad wheel and rail materials. Second, the effect of texture, which is the prime obstacle of conventional NDE techniques, has been investigated. The first stage shows experimental results on these subjects again confirmed that the present technique is most suited for nondestructive stress characterization in steel components. The stress effects on the magnetoacoustic interaction obtained in a sample made from railroad rail which were very similar to those obtained previously in 1045 steel. These results being somewhat different from the results with low (1020) and high (1095) carbon steels, there seemed to be certain range of medium carbon steels having the same characteristics. Also, as expected from the model, the stress information obtained by this technique has been confirmed to be least affected by the presence of texture. Author

N86-10579*# National Aeronautics and Space Administration. Lewis Research Center, Cleveland, Ohio.
JOINT RESEARCH EFFORT ON VIBRATIONS OF TWISTED PLATES, PHASE 1: FINAL RESULTS
Robert E. Kielb, Arthur W. Leissa, James C. MacBain, and Kelly S. Carney Washington Sep. 1985 100 p refs
(NASA-RP-1150; E-2576; NAS 1.61:1150) Avail: NTIS HC A05/MF A01 CSCL 20K

The complete theoretical and experimental results of the first phase of a joint government/industry/university research study on the vibration characteristics of twisted cantilever plates are given. The study is conducted to generate an experimental data base and to compare many different theoretical methods with each other and with the experimental results. Plates with aspect ratios, thickness ratios, and twist angles representative of current gas turbine engine blading are investigated. The theoretical results are generated by numerous finite element, shell, and beam analysis methods. The experimental results are obtained by precision matching a set of twisted plates and testing them at two laboratories. The second and final phase of the study will concern the effects of rotation. Author

N86-10580*# National Aeronautics and Space Administration. Langley Research Center, Hampton, Va.
THREE-DIMENSIONAL VIBRATION ANALYSIS OF A UNIFORM BEAM WITH OFFSET INERTIAL MASSES AT THE ENDS
Daniel K. Robertson (Cincinnati Univ.) Sep. 1985 71 p refs
(NASA-TM-86393; NAS 1.15:86393) Avail: NTIS HC A04/MF A01 CSCL 20K

Analysis of a flexible beam with displaced end-located inertial masses is presented. The resulting three-dimensional mode shape is shown to consist of two one-plane bending modes and one torsional mode. These three components of the mode shapes are shown to be linear combinations of trigonometric and hyperbolic sine and cosine functions. Boundary conditions are derived to obtain nonlinear algebraic equations through kinematic coupling of the general solutions of the three governing partial differential equations. A method of solution which takes these boundary conditions into account is also presented. A computer program has been written to obtain unique solutions to the resulting nonlinear algebraic equations. This program, which calculates natural frequencies and three-dimensional mode shapes for any number of modes, is presented and discussed. Author

N86-10581*# National Aeronautics and Space Administration. Langley Research Center, Hampton, Va.
FATIGUE OF GRAPHITE/EPOXY BUFFER STRIP PANELS WITH CENTER CRACKS
C. A. Bigelow Aug. 1985 32 p refs
(NASA-TM-87595; NAS 1.15:87595) Avail: NTIS HC A03/MF A01 CSCL 20K

The effects of fatigue loading on the behavior of graphite/epoxy panels with either S-Glass or Kevlar-49 buffer strips is studied. Buffer strip panels are fatigued and tested in tension to measure their residual strength with crack-like damage. Panels are made with [45/0/-45/90] sub 2s layup with either S-Glass or Kevlar-49 buffer strip material. The buffer strips are parallel to the loading direction and made by replacing narrow strips of the 0-degree graphite plies with strips of either 0-degree S-Glass/epoxy or Kevlar-49/epoxy on a one-for-one basis. The panels are subjected to a fatigue loading spectrum MINITWIST, the shortened version of the standardized load program for the wing lower surface of a transport aircraft. Two levels of maximum strain are used in the spectrum with three durations of the fatigue spectrum. One group of panels is preloaded prior to the application of the fatigue cycling. The preload consists of statistically loading the spectrum in tension until the crack-tip damage zone reaches the ajacent buffer strips. After fatigue loading, all specimens are statistically loaded in tension to failure to determine their residual strengths. Author

N86-10582*# National Aeronautics and Space Administration. Lewis Research Center, Cleveland, Ohio.
IMPROVED STUD CONFIGURATIONS FOR ATTACHING LAMINATED WOOD WIND TURBINE BLADES Final Report
James R. Fadoul Sep. 1985 29 p refs
(Contract DE-AI01-76ET-20320)
(NASA-TM-87109; DOE/NASA/20320-66; E-2709; NAS 1.15:87109) Avail: NTIS HC A03/MF A01

A series of bonded stud design configurations was screened on the basis of tension-tension cyclic tests to determine the structural capability of each configuration for joining a laminated wood structure (wind turbine blade) to a steel flange (wind turbine hub). Design parameters which affected the joint strength (ultimate and fatigue) were systematically varied and evaluated through appropriate testing. Two designs showing the most promise were used to fabricate addiate testing. Two designs showing the most promise were used to fabricate additional test specimens to determine ultimate strength and fatigue curves. Test results for the bonded stud designs demonstrated that joint strengths approaching the 10,000 to 12,000 psi ultimate strength and 5000 psi high cycle fatigue strength of the wood epoxy composite could be achieved. Author

N86-10583# Technion - Israel Inst. of Tech., Haifa. Dept. of Aeronautical Engineering.
EFFECT OF SEQUENCE OF LOADING ON INTERACTION CURVES FOR BUCKLING OF STIFFENED SHELLS
T. Weller and H. Abramovich Sep. 1984 89 p refs Sponsored in part by DFG in cooperation with RWTH Aachen
(TAE-536) Avail: NTIS HC A05/MF A01

The effect of order of loading on the behavior of stringer-stiffened circular cylindrical shells, on the way to and at buckling under combined axial compression and external pressure was studied. The feasibility of deriving more realistic interaction buckling curves for repeatedly buckled shells by use of the nondestructive vibration correlation technique for definition of boundary conditions was demonstrated. It was shown that the method is feasible, provided that the shell is subjected to an appropriate sequence of loading-constant axial compression first and the external pressure is increased until buckling occurs. Reversing the order of loading, and applying a constant external pressure first, reduced the axial load carrying capacity of the shell. E.A.K.

N86-10584# Technion - Israel Inst. of Tech., Haifa. Dept. of Aeronautical Engineering.
CORRELATION BETWEEN VIBRATIONS AND BUCKLING OF CYLINDRICAL SHELLS STIFFENED BY SPOT-WELDED AND RIVETED STRINGERS
T. Weller, H. Abramovich, and J. Singer Jan. 1985 81 p refs Sponsored in part by DFG in cooperation with RWTH Aachen
(TAE-537) Avail: NTIS HC A05/MF A01

The Vibration Correlation Techniques (VCT) was successfully applied, as a nondestructive tool for definition of actual boundary conditions and better prediction of buckling loads, to shells with spot-welded and riveted stringer stiffeners. It was demonstrated that the effective boundary conditions of the shells are fairly well by this technique, and that the lumping effects of the initial imperfection in the definition of the equivalent restraints are relatively small. Measurements of initial geometrical imperfections were conducted prior to testing of each shell. It is shown that calculation of their degrading effect on the buckling load serves

as a complementary tool for improved predictions of actual buckling loads. When combined with the more precisely defined boundary conditions, yielded by the VCT, the agreement between predictions and tests is significantly improved. E.A.K.

N86-10585# Shock and Vibration Information Center (Defense), Washington, D. C.
THE SHOCK AND VIBRATION DIGEST, VOLUME 17, NO. 3 Monthly Report
Judith Nagle-Eshleman, ed. Mar. 1985 105 p refs
(AD-A154144) Avail: SVIC, Code 5804, Naval Research Lab., Washington, D.C. 20375 CSCL 20/11

Abstracts, book reviews, current news, and literature reviews concerning themselves with shock and vibration are presented. The featured articles is on the analysis of exhaust mufflers and vibration problems in jet engines. For individual titles, see N86-10586 through N86-10587.

N86-10586# Shock and Vibration Information Center (Defense), Washington, D. C.
EDITORS RATTLE SPACE c85
Ronald E. Eshleman, ed. *In its* The Shock and Vibration Digest, Vol. 17, No. 3 Mar. 1985 p 2 (For primary document see N86-10585 01-39)
Avail: SVIC, Code 5804, Naval Research Lab., Washington, D.C. 20375 CSCL 05/2

The technology transfer process has developed rapidly during the past ten years to provide more knowledge to engineers at a faster rate. However, the distillation of the literature into handbooks and monographs has lagged the progress on information retrieval and short course performance. Up to now there is no magical, fast way to transform specialized technology from journals and reports into handbooks, tables, and computer data bases. The problem always arises on who will organize and pay for it. It is obvious that it requires joint efforts with the cost spread out over many companies. Today, no good means has been found to accomplish this process on a large scale basis. Author

N86-10587# Indian Inst. of Science, Bangalore. Dept. of Mechanical Engineering.
RECENT ADVANCES IN THE ANALYSIS OF EXHAUST MUFFLERS c37
M. L. Munjal *In* Shock and Vibration Information Center The Shock and Vibration Digest, Vol. 17, No. 3 Mar. 1985 p 3-16 refs (For primary document see N86-10585 01-39)
Avail: SVIC, Code 5804, Naval Research Lab., Washington, D.C. 20375 CSCL 13/9

Recent advances are reviewed in three major approaches to the analysis of exhaust mufflers: aeroacoustic, finite element, and finite wave. Contributions in the last four years are assessed in the context of earlier work as well as contemporary work. Emphasis is on application and usefulness in design of exhaust mufflers. Author

N86-10588*# Georgia Inst. of Tech., Atlanta.
ANALYSIS OF LARGE, NON-ISOTHERMAL ELASTIC-VISCO-PLASTIC DEFORMATIONS
R. Riff, R. L. Carlson, and G. J. Simitses [1984] 4 p refs
(Grant NAG3-534)
(NASA-CR-176220; NAS 1.26:176220) Avail: NTIS HC A02/MF A01 CSCL 20K

The development of a general mathematical model and solutions of test problems to analyze large nonisothermal elasto-visco-plastic deformatisms of structures is discussed. Geometric and material type nonlinearities of higher order are present in the development of the mathematical model and in the developed solution methodology. DOE

N86-10589*# Southwest Research Inst., San Antonio, Tex.
CONSTITUTIVE MODELING FOR ISOTROPIC MATERIALS (HOST) Annual Status Report
U. S. Lindholm, K. S. Chan, S. R. Bodner, R. M. Weber, K. P. Walker, and B. N. Cassenti 20 Aug. 1985 185 p refs
(Contract NAS3-23925)
(NASA-CR-174980; NAS 1.26:174980; SwRI-7576/30; ASR-2) Avail: NTIS HC A09/MF A01 CSCL 20K

This report presents the results of the second year of work on a problem which is part of the NASA HOST Program. Its goals are: (1) to develop and validate unified constitutive models for isotropic materials, and (2) to demonstrate their usefulness for structural analyses of hot section components of gas turbine engines. The unified models selected for development and evaluation are that of Bodner-Partom and Walker. For model evaluation purposes, a large constitutive data base is generated for a B1900 + Hf alloy by performing uniaxial tensile, creep, cyclic, stress relation, and thermomechanical fatigue (TMF) tests as well as biaxial (tension/torsion) tests under proportional and nonproportional loading over a wide range of strain rates and temperatures. Systematic approaches for evaluating material constants from a small subset of the data base are developed. Correlations of the uniaxial and biaxial tests data with the theories of Bodner-Partom and Walker are performed to establish the accuracy, range of applicability, and integability of the models. Both models are implemented in the MARC finite element computer code and used for TMF analyses. Benchmark notch round experiments are conducted and the results compared with finite-element analyses using the MARC code and the Walker model. Author

N86-10590# Southwest Research Inst., San Antonio, Tex.
CHARACTERIZATION OF MECHANICAL DAMAGE MECHANISMS IN CERAMIC COMPOSITE MATERIALS Interim Technical Report, 24 May 1984 - 23 May 1985
J. Lankford Jun. 1985 68 p
(Contract N00014-84-C-0123)
(AD-A156574) Avail: NTIS HC A04/MF A01 CSCL 11/4

This report summarizes research performed on two distinctly different ceramic composite materials. One was SiC-fiber reinforced LAS glass, while the other was an yttrium partially-stabilized, tetragonal-cubic phase zirconia. Silicon carbide fiber reinforced glass-ceramic matrix composite material has been tested in compression over a wide range in temperature. Both unidirectionally and multiaxially reinforced composites were tested. Compressive strength was measured, and pre-failure damage mechanisms characterized using acoustic emission and optical and scanning electron microscopy. Results are contrasted with corresponding tensile failure modes, and interpreted in terms of matrix microfracture, fiber kinking, and fiber orientation. Deformation and failure mechanisms are characterized for fully and partially yttria-stabilized single crystals tested in compression from 23 C to 1150 C. It is found that both types of material exhibit extensive plastic flow with increasing temperature. Tetragonal to monoclinic transformation-induced plasticity is not observed; rather, plastic flow is related solely to dislocation activity. Evidence is found for apparent cubic to rhombohedral transformation during polishing, and reverse rhombohedral to cubic transformation during imposed compressive stress. GRA

N86-10591# California Univ., Los Angeles. School of Engineering and Applied Science.
HIGH TEMPERATURE MECHANICAL TESTING OF A CYLINDRICAL WEAVE CARBON-CARBON COMPOSITE
S. Mack and G. Sines 1 Jul. 1985 84 p
(Contract N00014-77-C-0505)
(AD-A156639; UCLA-ENG-85-20) Avail: NTIS HC A05/MF A01 CSCL 11/4

The goal is to provide the material property information that is needed to decide whether radial bundles can reduce the stress in the circumferential bundles during the thermal processing of billets. Testing consisted of bundle pull-out experiments at room temperature, 1000 C, and 1500 C on coupons excised from as billet and of rupture and creep experiments on bundles processed to different degrees. The pull-out specimens showed increasing shear strength with temperature and the data showed a decrease in the coefficient of variation with temperature. The average bundle-matrix bond strength at 1500 C had a value of 1940 ksi with a coefficient

variation of 4.9%. The tests at 1000 C and room temperature had a coefficient variation of 7.9% and 19.2 % respectively. The tensile strengths of the bundles were relatively insensitive to processing and varied from 190 to 260 ksi. No creep was observed at the maximum available temperature of 1800 C. Author (GRA)

N86-10592# Naval Weapons Center, China Lake, Calif.
FRACTURE TOUGHNESS OF HYDROGEN-EMBRITTLED PRECIPITATION-HARDENED STAINLESS STEELS Final Report, 1982 - 1983
K. F. Hayes Apr. 1985 25 p
(AD-A156664; AD-E900472; NWC-TP-6488) Avail: NTIS HC A02/MF A01 CSCL 11/6

The chevron-notched specimen method was used to determine the fracture toughness of precipitation-hardened (PH) stainless steels possessing a range of microstructures. The specimens were tested while immersed in various aggressive environments (air, salt water, acidified salt water, or after cathodic polarization). GRA

N86-10593# Northwestern Univ., Evanston, Ill. Structural Mechanics Lab.
RESISTANCE CURVES FOR CRACK GROWTH UNDER PLANE-STRESS CONDITIONS IN AN ELASTIC PERFECTLY-PLASTIC MATERIAL Interim Report
J. D. Achenbach and Z. L. Li Jan. 1985 15 p
(Contract N00014-76-C-0063)
(AD-A156778; NU-SML-TR-85-1) Avail: NTIS HC A02/MF A01 CSCL 20/11

A recently developed solution for a plastic strain on the crack line is used in conjunction with a critical strain criterion to construct curves for K sub R (a) versus a, where a is the increase in crack length. Resistance curves have been computed for various values of the critical plastic strain. They show a monotonic increase of K sub R (a) with increase in crack length, to a constant steady-state value. Author (GRA)

N86-10594# Societe Nationale Industrielle Aerospatiale, Suresnes (France). Lab. Central.
NONDESTRUCTIVE CORROSION TEST OF ALUMINUM ALLOY STRUCTURES [CONTROLE NON DESTRUCTIF DE LA CORROSION DANS LES ASSEMBLAGES EN ALLIAGES D'ALUMINIUM, PROCES VERBAL PV 43-954/F2]
D. Lecuru 21 Jan. 1985 63 p refs In FRENCH
(Contract STPA-82-96006)
(PV-43-954/F/2) Avail: NTIS HC A04/MF A01

In order to avoid maintenance cost penalties, aluminum aircraft structure nondestructive test methods are studied, including ultrasonics, radiography, neutronography and Foucault currents. The results show that pitting corrosion is easy to detect, but intergranular corrosion is better detected by ultrasonics or neutronography. The best solution to inspect real aircraft structures is a method based on multiparameter analysis of ultrasonic signals. Author (ESA)

N86-10595# Kernforschungsanlage, Juelich (West Germany). Dept. for Reactor Materials.
EXPERIMENTS WITH TUBULAR PROBES MADE OF INCOLOY 800 H UNDER UNIAXIAL AND MULTIAXIAL STRAIN
M. Roedig, H. J. Penkalla, K. Franzke, F. Schubert, and H. Nickel Feb. 1985 65 p refs In GERMAN; ENGLISH summary
(JUEL-1979; ISSN-0366-0885) Avail: NTIS HC A04/MF A01

The transferability of material data and constitutive equations in the high temperature region is verified by performing uniaxial and multiaxial creep tests on heat exchanger tubes made of INCOLOY 800 H from the same master heat and exposed to various combinations of tension, internal pressure, and torsion at 950 C. Under strain combinations with the same deviatoric stress the different tube lifetimes measured can be explained by constitutive equations. Their deformation under multiaxial strain cannot be predicted exactly with the mathematical model. The tubes under superposed strain conditions failed by leak formation or fracture but never spontaneously. The transfer methods may be improved with the application of extensometers for expansion measures. Author (ESA)

N86-10596# Fraunhofer Inst. fuer Werkstoffmechanik, Freiburg (West Germany).
NUMERICAL SIMULATION OF CRACK ARREST EXPERIMENTS ON ARALDITE B USING THE FINITE DIFFERENCE METHOD
H. Stoeckl Dec. 1982 52 p refs In GERMAN; ENGLISH summary
Sponsored by Bundesministerium fuer Forschung und Technologie
(Rept-W-9/82) Avail: NTIS HC A04/MF A01

A program based on the finite difference method was developed on an HP 1000 computer to simulate crack arrest experiments on rectangular double cantilever beam specimens made of Araldite B. The program solves the equations of motion for linear elastic plane models by explicit time integration. The values of the stress intensity factor influencing crack propagation are calculated from a path integral corrected for dynamic effects. The values are compared with experimental values determined with the shadow optical method. The results confirm the experimental method. The numerical method can be applied for dynamic propagation with at most small plastic fracture mechanisms. Author (ESA)

42 GEOSCIENCES (GENERAL)

No abstracts in this category.

43 EARTH RESOURCES

Includes remote sensing of earth resources by aircraft and spacecraft; photogrammetry; and aerial photography.

For instrumentation see *35 Instrumentation and Photography.*

N86-10597* Pacific Northwest Lab., Richland, Wash.
LANDSAT TM IMAGE DATA QUALITY ANALYSIS FOR ENERGY-RELATED APPLICATIONS Final Report
G. E. Wukelic, H. P. Foote, G. M. Petrie, J. C. Barnard, and J. R. Eliason Aug. 1985 21 p refs Original contains color imagery; Original photography may be purchased from the EROS Data Center, Sioux Falls, S.D. 57198 ERTS
(NASA Order S-12402-C)
(E85-10109; NASA-CR-176268; NAS 1.26:176268; PNL-5572) Avail: NTIS HC A02 CSCL 08G

This project represented a no-cost agreement between National Aeronautic Space Administration Goddard Space Flight Center (NASA GSFC) and the Pacific Northwest Laboratory, a Department of Energy (DOE) national laboratory. The objective of the investigation was to evaluate LANDSAT's thematic mapper (TM) data quality and utility characteristics from an energy research and technological perspective. Of main interest was the extent to which repetitive TM data might support DOE efforts relating to siting, developing, and monitoring energy-related facilities, and to basic geoscientific research. The investigation involved: (1) both LANDSAT 4 and 5 TM data, (2) qualitative and quantitative use consideration, and (3) NASA P (corrected) and A (uncorrected) CCT analysis for a variety of sites of DOE interest. All results substantiate the consistent performance of the LANDSAT TM system, and the added application value associated with the increased spectral and spatial capabilities of the TM. Such data are being incorporated into several DOE programs involving continental scientific drilling, acid rain, wind energy, contaminant transport, geologic studies, and environmental/ecological research. Author

N86-10598 Yale Univ., New Haven, Conn.
MODELING GROUNDWATER FLOW INTO LAKES Ph.D. Thesis

John F. Dowo 1984 338 p
Avail: Univ. Microfilms Order No. DA8509696

Groundwater flow into a lake was investigated for conditions similar to those found is a deep kettle hole pond in glacial outwash material. Steady state conditions were used, based upon observed and extrapolated lake elevations and piezometer observations for annual and seasonal averaging times. The finite element procedure operated in a transformed space using smooth basis functions that were formed as one-dimensional cubic B-splines. The effects of anisotropy, but not heterogeneity, of hydraulic conductivity were investigated. Both constant head and noflow were used for boundary conditions on the watertable. The nonlinear problem, where the watertable location was found as part of the solution, was also examined. The flux decreases rapidly with distance from the lake margin, although this decrease was less rapid for anisotropic conditions. For most cases, the integrated least squares exponential fit to the model solution was similar to the direct integration of the finite element results using Gauss-Legendre quadrature. Numerical instability was increased when the aquifer domain boundary and lake boundary were relatively close to the lake margin. The finite element procedure provides an efficient method for obtaining groundwater flux along a lake bottom. Integration of these fluxes provides a useful estimate of average groundwater contributions to a lake. Dissert. Abst.

N86-10599*# Jet Propulsion Lab., California Inst. of Tech., Pasadena.
REPORT OF THE WORKSHOP ON GEOLOGIC APPLICATIONS OF REMOTE SENSING TO THE STUDY OF SEDIMENTARY BASINS
Harold R. Lang, ed. 1 Aug. 1985 81 p refs Workshop held in Lakewood, Colo., 10-11 Jan. 1985 ERTS
(Contract NAS7-918)
(E86-10002; NASA-CR-176211; JPL-Pub-85-44; NAS 1.26:176211) Avail: NTIS HC A05/MF A01 CSCL 08G

The Workshop on Geologic Applications of Remote Sensing to the Study of Sedimentary Basins, held January 10 to 11, 1985 in Lakewood, Colorado, involved 43 geologists from industry, government, and academia. Disciplines represented ranged from vertebrate paleontology to geophysical modeling of continents. Deliberations focused on geologic problems related to the formation, stratigraphy, structure, and evolution of foreland basins in general, and to the Wind River/Bighorn Basin area of Wyoming in particular. Geological problems in the Wind River/Bighorn basin area that should be studied using state-of-the-art remote sensing methods were identified. These include: (1) establishing the stratigraphic sequence and mapping, correlating, and analyzing lithofacies of basin-filling strata in order to refine the chronology of basin sedimentation, and (2) mapping volcanic units, fracture patterns in basement rocks, and Tertiary-Holocene landforms in searches for surface manifestations of concealed structures in order to refine models of basin tectonics. Conventional geologic, topographic, geophysical, and borehole data should be utilized in these studies. Remote sensing methods developed in the Wind River/Bighorn Basin area should be applied in other basins. For individual titles, see N86-10600 through N86-10609.

N86-10600*# Geological Survey, Sioux Falls, S. Dak. EROS Data Center.
SOME OPINIONS ON REMOTE SENSING AND GEOLOGIC STUDIES **c46**
G. Bryan Bailey *In* JPL Rept. of the Workshop on Geol. Appl. of Remote Sensing to the Study of Sedimentary Basins 1 Aug. 1985 p 29-30 ERTS (For primary document see N86-10599 01-43)
Avail: NTIS HC A05/MF A01 CSCL 08G

The principal role of remote sensing data in geologic studies is as a source of geologic information from which meaningful geologic interpretations can be made. Remote sensing data are important in sedimentary basin analysis and other geologic studies as independent and sometimes unique sources of important lithologic and structural information; however, their greatest benefit to exploration-oriented investigations may come when these data are used with other relevant data in a digital database approach to exploration. Modern computer technology facilitates the rapid integration and synthesis of satellite, topographic, gravity, aeromagnetic, geochemical, and other data collected from a given region. Once such data are geometrically registered, they can be digitally processed, within the constraints of defined geologic models, to rapidly identify, and focus further exploration efforts on, target areas that have the greatest potential for success. R.J.F.

N86-10601*# Hawaii Univ., Honolulu. Planetary Geosciences Div.
POSITION PAPER: WORKSHOP ON GEOLOGIC APPLICATIONS OF REMOTE SENSING TO THE STUDY OF SEDIMENTARY BASINS **c46**
Pamela L. Blake, Robert B. Singer, and Eileen Bruckenthal *In* JPL Rept. of the Workshop on Geol. Appl. of Remote Sensing to the Study of Sedimentary Basins 1 Aug. 1985 p 31-32 ERTS (For primary document see N86-10599 01-43)
Avail: NTIS HC A05/MF A01 CSCL 08G

The utility of LANDSAT Multispectral Scanner (MSS) and Thematic Mapper (TM) data for providing regional coverage has been demonstrated. Information derived from LANDSAT spectral data is varied, but has primarily been used for distinguishing materials in a scene. Because of the limited number and width of the MSS and TM bands, LANDSAT data has only limited utility for actual identification of materials. The new advanced sensors (currently airborne, but eventually shuttle-based) have more limited areal extent than LANDSAT, but greater spatial and spectral resolution. The Airborne Imaging Spectrometer (AIS) has spectral resolution of about .01 microns and, typically, has 10m/pixel spatial resolution. This improved spectral resolution means that diagnostic spectral features may now be identified, which in turn means that actual identification of mineral phases present can be addressed (of either monominerallic or composite materials). Another new sensor, the Thermal Infrared Multispectral Scanners (TMS), obtains data in the 8 to 12 micron range. The information from the various sensors (e.g., LANDSAT, AIS, and TIMS) is complementary, covering different wavelength regions and consequently sensitive to different materials or physical properties of materials. In addition, the new sensors also produce a higher volume of data, which must be cleverly and efficiently handled. R.J.F.

N86-10602*# University of Southern California, Los Angeles. Dept. of Geological Sciences.
CHRONOLOGIC ANALYSIS OF TERRESTRIAL SEDIMENTS AND BASIN EVOLUTION **c46**
Douglas Burbank *In* JPL Rept. of the Workshop on Geol. Appl. of Remote Sensing to the Study of Sedimentary Basins 1 Aug. 1985 p 33-36 ERTS (For primary document see N86-10599 01-43)
Avail: NTIS HC A05/MF A01 CSCL 08G

The use of magnetic-polarity stratigraphy to provide detailed chronologies of numerous areas within a sedimentary basin is discussed. Sediments suitable for magnetostratigraphic studies are identified. Sets of figures intended to illustrate some of the applications of magnetic-polarity stratigraphy to various aspects of basin analysis are given. Most of the examples are drawn from the Himalayan molasse (Indo-Gangetic foredeep) in northern Pakistan and northwestern India. Each of the figures illustrates an example of how detailed chronologies can be utilized in enhancing and refining models of basin analysis and tectonic deformation. R.J.F.

N86-10603*# Jet Propulsion Lab., California Inst. of Tech., Pasadena.
TERTIARY AND QUATERNARY RESEARCH WITH REMOTE SENSING METHODS **c46**
James E. Conel *In its* Rept. of the Workshop on Geol. Appl. of Remote Sensing to the Study of Sedimentary Basins 1 Aug. 1985 p 37-40 refs ERTS (For primary document see N86-10599 01-43)
Avail: NTIS HC A05/MF A01 CSCL 08G

Problems encountered in mapping the Quaternary section of the Wind River Region using remote sensing methods are discussed. Analysis of the stratigraphic section is a fundamental aspect of the geologic study of sedimentary basins. Stratigraphic analysis of post-Cretaceous rocks in the Wind River Basin encounters problems of a distinctly different character from those involved in studying the pre-Cretaceous section. The interior of the basin is predominantly covered by Tertiary and Quaternary sediments. These rocks, except on the basin margin to the north, are mostly flat lying or gently dipping. The Tertiary section consists of sandstones, siltstones, and tuffaceous sediments, some variegated, but in general poorly bedded and of great lithologic similarity. The Quaternary sediments consist of terrace, fan, and debris tongue deposits, unconsolidated alluvium occupying the bottoms of modern watercourses, deposits of eolian origin and tufa. Terrace and fan deposits are compositionally diverse and reflect the lithologic diversity of the source terranes. R.J.F.

N86-10604*# Jet Propulsion Lab., California Inst. of Tech., Pasadena.

MULTISENSOR DATA INTEGRATION TECHNIQUES

Diane L. Evans, Pamela L. Blake (Hawaii Univ., Honolulu), James E. Conel, Harold R. Lang, Thomas L. Logan, Barbara A. McGuffie, Ernest D. Paylor, Robert B. Singer (Hawaii Univ., Honolulu), and Leslie R. Schenck *In its* Rept. of the Workshop on Geol. Appl. of Remote Sensing to the Study of Sedimentary Basins 1 Aug. 1985 p 41 ERTS (For primary document see N86-10599 01-43)

Avail: NTIS HC A05/MF A01 CSCL 05B

The availability of data from sensors operating in several different wavelength regions had led to the development of new techniques and strategies for both data management and image analysis. Work is ongoing to develop computer techniques for analysis of integrated data sets. These techniques include coregistration of multisensor images, rectification of radar images in areas of topographic relief to ensure pixel to pixel registration with planimetric data sets, calibration of data so that signatures can be applied to remote areas, normalization of data acquired with disparate sensors and determination of extended spectral signatures of surface units. In addition, software is being developed to analyze coregistrated digital terrain and image data so that automated stratigraphic and structural analyses can be performed. These software procedures include: strike and dip determination, terrain profile generation, stratigraphic column generation, stratigraphic thickness measurements, structural cross-section generation, and creation of 3-D block diagrams. These techniques were applied to coregistered LANDSAT 4 Thematic Mapper (TM), Thermal Infrared Multispectral Scanner (TIMS), and multipolarization synthetic aperture radar (SAR) data of the Wind River Basin in Wyoming. R.J.F.

N86-10605*# Washington Univ., St. Louis, Mo. McDonnell Center for the Space Sciences.

[ANALYSIS OF REMOTE SENSING DATA] **c46**

E. A. Guiness, M. Sultan, and R. E. Arvidson *In* JPL Rept. of the Workshop on Geol. Appl. of Remote Sensing to the Study of Sedimentary Basins 1 Aug. 1985 p 45-46 ERTS (For primary document see N86-10599 01-43)

Avail: NTIS HC A05/MF A01 CSCL 08G

A brief assessment of remote sensing applied to geological studies is given. An analysis of thematic mapping data on oak-hickory forests in southern Missouri is discussed. It was found that there is a control on the infrared reflectance (bands 4, 5, and 7 of the Thematic Mapper (TM) of the forests that correlates with rock and soil types. During the growing season, soils with low water retention capacities correlate with high infrared (band 4, lesser with band 5 and 7) signatures. A metamorphic core complex called the Meatiq located in the Eastern Desert of Egypt was studied. The dome provides exposure of most of the rock units of the Arabian-Nubian Precambrian Shield. The dome bears many resemblances to Cordilleran metamorphic complexes. LANDSAT TM data was used to improve on reconnaissance maps of the dome. The remote sensing data was interpreted in the context of field observations, petrographic, and chemical analysis of rock units in the dome, in order to map similar domes in the Eastern Desert from TM data. Mapping projects such as the one just described will help constrain the geologic evolution of the Arabian-Nubian Shield. Two particular hypotheses that researchers hope to test for the development of the shield are: (1) closure of a proto-Red Sea; and (2) accretion of a primitive island arc system onto the shield. R.J.F.

N86-10606*# Jet Propulsion Lab., California Inst. of Tech., Pasadena.

REMOTE STRATIGRAPHIC AND STRUCTURAL ANALYSIS: MULTISENSOR RESULTS IN THE WIND RIVER/BIGHORN BASIN AREA, WYOMING **c46**

Harold R. Lang, Earnest D. Paylor, and James E. Conel *In its* Rept. of the Workshop on Geol. Appl. of Remote Sensing to the Study of Sedimentary Basins 1 Aug. 1985 p 51-52 ERTS (For primary document see N86-10599 01-43)

Avail: NTIS HC A05/MF A01 CSCL 08G

A brief survey is given of research on the San Juan Basin located in northwest New Mexico and Southern Colorado. Seismic, LANDSAT multispectral scanner and geologic data will be examined in order to understand the changing structural configuration of the basin. Several questions concerned with the discrimination of lithology using LANDSAT multispectral scanner data are posed. R.J.F.

N86-10607*# Lamont-Doherty Geological Observatory, Palisades, N. Y.

STRUCTURAL MAPPING OF FOLDED SEDIMENTARY ENVIRONMENTS FROM SATELLITE IMAGES: AN EXAMPLE FROM CENTRAL ASIA **c46**

William Leith *In* JPL Rept. of the Workshop on Geol. Appl. of Remote Sensing to the Study of Sedimentary Basins 1 Aug. 1985 p 53-54 refs ERTS (For primary document see N86-10599 01-43)

Avail: NTIS HC A05/MF A01 CSCL 08G

In the Tadjik Depression, in Soviet Central Asia, in the absence of existing geologic or topographic maps, an enhanced LANDSAT multispectral scanner image was used in combination with field data to produce a 1:250000 geologic map of the Vakhsh fold-and-thrust belt and adjacent autochthon. Several structural conclusions are reached as a result of this mapping. Deformation of the Cretaceous and Tertiary strata of the fold-and-thrust belt is, in the central Tadjik Depression, conspicuously absent north of a buried basement fault that marks the hinge-zone of the Late Mesozoic passive margin. But, in the eastern half of the depression, thrusting has moved coherent sheets northward, over the block fault, these sheets now lie flat atop the autochthon to the north. The crustal structure inherited from the Mesozoic extensional phase has strongly influenced the Late Cenozoic pattern of deformation, producing the fold-and-thrust belt that is markedly asymmetric. The development of the thrust system has included the progressive overlapping of thrust: the later thrusts apparently formed internal to the older thrusts, and subsequently overrode them. R.J.F.

N86-10608*# Jet Propulsion Lab., California Inst. of Tech., Pasadena.

FORELAND BASIN STRUCTURES AND REMOTE SENSING **c46**

Earnest D. Paylor *In its* Rept. of the Workshop on Geol. Appl. of Remote Sensing to the Study of Sedimentary Basins 1 Aug. 1985 p 55-56 ERTS (For primary document see N86-10599 01-43)

Avail: NTIS HC A05/MF A01 CSCL 08G

Rocky Mountain foreland basins are somewhat unique in that the basins may exhibit a variety of structural styles. It is generally agreed that shortening has occurred in the foreland basement but the cause is controversial: vertical vs compressional horizontal tectonics. Even when shortening is attributed to compression, the attitude (dip) of the fault plane and whether the horizontal or vertical component of movement is dominant is unconstrained. The controversy is difficult to resolve from surface data alone due

to the variety of possible interpretations. Detailed surface mapping and geologic modeling are needed to constrain subsurface interpretations. In many areas of the Wind River and Bighorn basins detailed geologic maps do not exist. State-of-the-art remote sensing data could potentially provide an efficient means of mapping surface geology. State-of-the-art remote sensing systems now provide geometrically correct data at 30 meter pixel size and increased spectral coverage, capable of more detailed geologic analyses. These data can be photographically enlarged to 1:24, 000 scale and combined with 7 1/2' uses topographic quads to provide an excellent base map for geologic interpretations. R.J.F.

N86-10609*# Carnegie Museum of Natural History, Pittsburgh, Pa. Section of Vertebrate Fossils.
PALEOGENE VERTEBRATE PALEONTOLOGY, GEOLOGY AND REMOTE SENSING IN THE WIND RIVER BASIN c46
Richard K. Stucky and Leonard Krishtalka *In* JPL Rept. of the Workshop on Geol. Appl. of Remote Sensing to the Study of Sedimentary Basins 1 Aug. 1985 p 59-60 refs ERTS (For primary document see N86-10599 01-43)
Avail: NTIS HC A05/MF A01 CSCL 08G

Biostratigraphic and lithostratigraphic studies were used to correlate different events in the geologic evolution of the northeastern part of the Wind River Basin and have suggested several conclusions. Laterally equivalent exposures of the Lysite member from Cedar Ridge to Bridger Creek show a gradation in lithology from interbedded boulder conglomerates and sandstones to interbedded lenticular sandstones and mudstones to interbedded carbonaceous shales, coals and tabular sandstones. This gradation suggests a shift from alluvial fan to braided stream to paludal or lacustrine sedimentary environments during the late early Eocene. The Lysite and Lost Cabin members of the Wind River Formation are in fault contact in the Bridger Creek area and may intertongue to the east along Cedar Ridge. Ways in which remote sensing could be used in these studies are discussed. R.J.F.

N86-10610*# Purdue Univ., Lafayette, Ind. Lab. for Applications of Remote Sensing.
VEGETATION AND SOILS FIELD RESEARCH DATA BASE: EXPERIMENT SUMMARIES
L. L. Biehl, C. S. T. Daughtry, and M. E. Bauer Dec. 1984 24 p refs Revised ERTS
(Contract NAS9-16528)
(E85-10110; NASA-CR-171894; NAS 1.26:171894;
LARS-TR-042382) Avail: NTIS HC A02/MF a01 CSCL 05B

Understanding of the relationships between the optical, spectral characteristics and important biological-physical parameters of earth-surface features can best be obtained by carefully controlled studies over fields and plots where complete data describing the condition of targets are attainable and where frequent, timely spectral measurement can be obtained. Development of a vegetation and soils field research data base was initiated in 1972 at Purdue University's Laboratory for Applications of Remote Sensing and expanded in the fall of 1974 by NASA as part of LACIE. Since, then over 250,000 truck-mounted and helicopter-borne spectrometer/multiband radiometer observations have been obtained of more than 250 soil series and 20 species of crops, grasses, and trees. These data are supplemented by an extensive set of biophysical and meteorological data acquired during each mission. Experiment summaries are given in table form. In addition, separate tables are presented which include specifications of the spectroradiometers and multiband radiometers used for obtaining the spectral data, and the vegetation for which data have been acquired. M.G.

N86-10611*# National Aeronautics and Space Administration, Washington, D. C.
MAXIMUM WATER RESERVES IN THE SNOW COVER IN THE EUROPEAN TERRITORY OF THE USSR ACCORDING TO DATA FOR 1892-1960
V. D. Komarov and Ye. S. Sinegub Aug. 1985 18 p refs Transl. into ENGLISH from Trudy Psi. (USSR), no. 148, 1966 p 150-160 Transl. by Kanner (Leo) Associates, Redwood City, Calif.
(Contract NASw-4005)
(NASA-TM-77901; NAS 1.15:77901) Avail: NTIS HC A02/MF A01 CSCL 08H

The snow cover of the European territory of the U.S.S.R. is examined. Maps of the average greatest and least magnitudes of the maximum water reserves are given, as well as a map of the coefficient of variation of the maximum reserve. E.A.K.

N86-10612*# National Aeronautics and Space Administration, Washington, D. C.
REPRESENTATION OF THE DISTRIBUTION OF THE SNOW COVER ON THE SURFACE OF THE EARTH'S DRY LAND
G. D. Rikhter and L. A. Petrova Aug. 1985 6 p Transl. into ENGLISH from "Geografia Snezhnogo Pokrova" Moscow, Academy of Sciences of the Soviet Union Press, 1960 p 5-7 Transl. by Kanner (Leo) Associates, Redwood City, Calif.
(Contract NASw-4005)
(NASA-TM-77909; NAS 1.15:77909) Avail: NTIS HC A02/MF A01 CSCL 08L

The distribution of the snow cover on the surface of the Earth's dry land, is discussed. The general laws of this distribution and the influencing factors are determined. E.A.K.

N86-10613*# National Aeronautics and Space Administration, Washington, D. C.
OBSERVATIONS OF THE SNOW COVER IN THE SOUTHERN PART OF THE BURYAT AUTONOMOUS SOVIET SOCIALIST REPUBLIC
Ye. A. Nefedeva Aug. 1985 16 p refs Transl. into ENGLISH from "Geografia Snezhnogo Pokrova" Moscow, Academy of Sciences of the Soviet Union Press, 1960 p 37-44 Transl. by Kanner (Leo) Associates, Redwood City, Calif.
(Contract NASw-4005)
(NASA-TM-77910; NAS 1.15:77910) Avail: NTIS HC A02/MF A01 CSCL 08L

The characteristics of the snow cover, as a function of various natural factors, in sectors of the southern part of the Buryat Autonomous Soviet Socialist Republic were examined. The thawing process is also discussed. E.A.K.

N86-10614*# National Aeronautics and Space Administration, Washington, D. C.
LAWS OF DISTRIBUTION OF THE SNOW COVER ON THE GREATER CAUCASUS (SOVIET UNION)
Ye. Ye. Gurtovaya, G. K. Sulakvelidze, and A. V. Yashina Aug. 1985 24 p refs Transl. from "Geografia Snezhnogo Pokrova" Moscow, Academy of Sciences of the Soviet Union Press, 1960 p 7-20 Transl. by Kanner (Leo) Associates, Redwood City, Calif.
(Contract NASw-4005)
(NASA-TM-77911; NAS 1.15:77911) Avail: NTIS HC A02/MF A01 CSCL 08L

The laws of the distribution of the snow cover on the mountains of the greater Caucasus are discussed. It is shown that an extremely unequal distribution of the snow cover is caused by the complex orography of this territory, the diversity of climatic conditions and by the difference in altitude. Regions of constant, variable and unstable snow cover are distinguished because of the clearly marked division into altitude layers, each of which is characterized by climatic differences in the nature of the snow accumulation. E.A.K.

N86-10615*# Jet Propulsion Lab., California Inst. of Tech., Pasadena.
NASA/JPL AIRCRAFT SAR WORKSHOP PROCEEDINGS
N. Donovan, ed., D. L. Evans, ed., and D. N. Held, ed. 15 Jun. 1985 82 p refs Workshop held in Pasadena, Calif., 4-5 Feb. 1985 Original contains color illustrations
(Contract NAS7-918)
(NASA-CR-176204; NAS 1.26:176204; JPL-Pub-85-39) Avail: NTIS HC A05/MF A01 CSCL 17I

Speaker-supplied summaries of the talks given at the NASA/JPL Aircraft SAR Workshop on February 4 and 5, 1985, are provided. These talks dealt mostly with composite quadpolarization

imagery from a geologic or ecologic prespective. An overview and summary of the system characteristics of the L-band synthetic aperture radar (SAR) flown on the NASA CV-990 aircraft are included as supplementary information. Other topics ranging from phase imagery and interferometric techniques classifications of specific areas, and the potentials and limitations of SAR imagery in various applications are discussed. For individual titles, see N86-10616 through N86-10629.

N86-10616*# Jet Propulsion Lab., California Inst. of Tech., Pasadena.
RADAR SYSTEM DESCRIPTION c32
D. N. Held and W. E. Brown *In its* NASA/JPL Aircraft SAR Workshop Proc. 15 Jun. 1985 p 5-12 Original contains color illustrations (For primary document see N86-10615 01-43)
Avail: NTIS HC A05/MF A01 CSCL 17I

A brief overview is given of the hardware and software utilized to generate the CV-990 synthetic aperture radar's image products. The on-board hardware is described, then the operational processing software, and finally the image products that are routinely available. Author

N86-10617*# Jet Propulsion Lab., California Inst. of Tech., Pasadena.
CV-990 L-BAND SAR: A CALIBRATION EXPERIMENT c32
D. N. Held and C. Werner *In its* NASA/JPL Aircraft SAR Workshop Proc. 15 Jun. 1985 p 17-20 ref Original contains color illustrations (For primary document see N86-10615 01-43)
Avail: NTIS HC A05/MF A01 CSCL 17I

Calibrated image data is required by most users of synthetic aperture radar (SAR) data particularly those attempting to classify targets based upon their radar backscatter signature as a function of frequency polarization or incidence angle. In this experiment, the backscatter derived by calibrating the NASA/JPL CV-990 L-band SAR, and the backscatter reported from a pass of the NASA/JSC C-130 scatterometer as the two instruments flew over the same site at different times are compared. Author

N86-10618*# Jet Propulsion Lab., California Inst. of Tech., Pasadena.
NEOGENE COMPRESSIONAL DEFORMATION AND POSSIBLE THRUST FAULTING IN SOUTHWEST DOMINICAN REPUBLIC Abstract Only
M. P. Golombek, P. Goreau, and T. H. Dixon *In its* NASA/JPL Aircraft SAR Workshop Proc. 15 Jun. 1985 p 21 (For primary document see N86-10615 01-43)
Avail: NTIS HC A05/MF A01 CSCL 08B

Analysis of regional and high resolution remote sensing data coupled with detailed field investigations indicates Neogene compressional deformation in the southwest Dominican Republic. Airborne synthetic aperture radar data and high resolution near infrared photography show folds in Tertiary sediments and possible thrust fault scarps implying NE to SW compression in the region. Large road cuts through the scarps allow study of otherwise poorly accessible, heavily vegetated karst terrain. Deformation increases toward scrap fronts where small bedding-plane thrust faults become more numerous. Analysis of mesoscopic faults with slickensides indicates compression oriented between N to S and E to W. The lowermost scarp has highly sheared fault breccia and undeformed frontal talus breccias implying it is the basal thrust into which the higher thrust faults sole. Thus, the scarps probably formed in a regional NE to SW compressional stress regime and are the toes of thrust sheets. Previous workers have suggested that these scarps are ancient shorelines. However, the gross morphology of the scarps differs substantially from well known erosional terraces on the north coast. Author

N86-10619*# National Aeronautics and Space Administration. Goddard Space Flight Center, Greenbelt, Md.
THE EFFECT OF VEGETATION TYPE, MICRORELIEF, AND INCIDENCE ANGLE ON RADAR BACKSCATTER
Manfred Owe, Peggy E. ONeill, Thomas J. Jackson, and Thomas J. Schmugge *In* JPL NASA/JPL Aircraft SAR Workshop Proc. 15 Jun. 1985 p 25-29 Original contains color illustrations (For primary document see N86-10615 01-43)
Avail: NTIS HC A05/MF A01 CSCL 17E

The NASA/JPL Synthetic Aperture Radar (SAR) was flown over a 20 x 110 km test site in the Texas High Plains regions north of Lubbock during February/March 1984. The effect of incidence angle was investigated by comparing the pixel values of the calibrated and uncalibrated images. Ten-pixel-wide transects along the entire azimuth were averaged in each of the two scenes, and plotted against the calculated incidence angle of the center of each range increment. It is evident from the graphs that both the magnitudes and patterns exhibited by the corresponding transect means of the two images are highly dissimilar. For each of the cross-poles, the uncalibrated image displayed very distinct and systematic positive trends through the entire range of incidence angles. The two like-poles, however, exhibited relatively constant returns. In the calibrated image, the cross-poles exhibited a constant return, while the like-poles demonstrated a strong negative trend across the range of look-angles, as might be expected. Author

N86-10620*# Jet Propulsion Lab., California Inst. of Tech., Pasadena.
AGE-DATING VOLCANIC AND ALLUVIAL SURFACES WITH MULTIPOLARIZATION DATA c46
Tom G. Farr *In its* NASA/JPL Aircraft SAR Workshop Proc. 15 Jun. 1985 p 31-36 refs Original contains color illustrations (For primary document see N86-10615 01-43)
Avail: NTIS HC A05/MF A01 CSCL 08G

A false-color multipolarization version of one of the images of Owens Valley area acquired by the JPL Synthetic Aperture Radar (SAR) is given. A geologic map of the alluvial fans there (Gillespie, 1982) is also given for comparison. In general, brightness in the multipolarization images can be seen to be inversely proportional to the age of the surfaces. A more detailed investigation of the relationship between backscatter and age of the surfaces was undertaken with calibrated aircraft SAR data. The quantitative relationship between backscatter coefficient and age for the three polarizations is shown. The straight lines connecting the measured data points imply a steady-state process, although the process or processes leading to this relationship may have operated at rates that varied with climate fluctuations, such as the glacial ages. It is expected that the relationship between radar brightness and age is a consistent one, and that with the wider availability of calibrated radar backscatter data, these relationships can be less well-known areas. The effect of variable such as past climate fluctuations, tectonic disturbance, and rock type must be understood before extension beyond the Mojave Desert region can be attempted. R.J.F.

N86-10621*# National Aeronautics and Space Administration. Goddard Space Flight Center, Greenbelt, Md.
THE EFFECTS OF MERGING TM AND A/C RADAR ON WETLAND CLASSIFICATION
James P. Ormsby and Patricia J. Mulligan *In* JPL NASA/JPL Aircraft SAR Workshop Proc. 15 Jun. 1985 p 37-38 refs (For primary document see N86-10615 01-43)
Avail: NTIS HC A05/MF A01 CSCL 08B

While radar does not provide detailed begetation discrimination, it provide the means to separate areas of different moisture conditions. Thus, the use of LANDSAT Thematic Mapper (TM) in conjunction with the microwave data was attempted. If successful, information on shoreline cover, emergent wetland vegetation and extent, and submerged grassbeds would provide much needed data for planning and maintenance of wetlands. Originally, the goal was to determine the accuracy with which one could categorize various types of vegetation and land use within an inland wetland using LANDSAT TM data. First, a Level 1/2 supervised classification was performed. Following a more detailed ground trust survey, a Level 3 classification was done. Aircraft L-band radar data were received and the decision was made to merge the TM and L-band data and assess whether vegetation catagories within the wetland areas could be better defined. Preliminary results indicate vegeta-

tion delineation is improved for open agricultural areas and water, but other features are more confused. R.J.F.

N86-10622*# Jet Propulsion Lab., California Inst. of Tech., Pasadena.
TOPOGRAPHIC MAPPING FROM INTERFEROMETRIC SYNTHETIC APERTURE RADAR OBSERVATIONS
Howard A. Zebker and Richard M. Goldstein *In its* NASA/JPL Aircraft SAR Workshop Proc. 15 Jun. 1985 p 41-44 refs Original contains color illustrations (For primary document see N86-10615 01-43)
Avail: NTIS HC A05/MF A01 CSCL 08B

The production of high-resolution topographic maps derived from interferometric synthetic aperture radar observations of the Earth is reported. Topographic maps are typically determined from stereo-pair optical photographs. Vertical relief causes the same terrain to appear in a slightly different projection for differing look angles, and this shift in appearance is interpreted in terms of the height of the terrain. The radar interferometric approach is related to the stereo technique in that the terrain is viewed at two different angles; however, in this case, the angular separation of the antennas is extremely small, on the order of a milliradian or less, as compared to tens of degrees for the optical case. Thus, the geometrical distortion and subsequent rectification correction algorithms are much less severe in the reduction of interferometric data. R.J.F.

N86-10623*# Washington Univ., Seattle.
STRATEGIES FOR ANALYZING MIXED PIXELS IN REMOTELY SENSED IMAGERY
Milton Smith and John Adams *In* JPL NASA/JPL Aircraft SAR Workshop Proc. 15 Jun. 1985 p 47-48 (For primary document see N86-10615 01-43)
Avail: NTIS HC A05/MF A01 CSCL 05B

Two uncalibrated synthetic aperture radar (SAR) scenes from Death Valley, California, and two uncalibrated scenes from Owens Valley, California, were used to test a technique to identify and separate the primary factors associated with multipolarized radar image sets. Unique to the technique is the concept that varied types of radar polarization signatures are a result of the interaction of a few physical factors (e.g., roughness, volume scattering, and dielectric constant). Thus, the varied signatures observed in an image reflect the interaction between these factors. The objectives are to first separate the interaction of factors directly influencing the measurement and to attempt to identify these factors. Interpretation of the SAR image sets proceeds by testing models that hypothesize the cause and effect relations between those factors directly affecting the radar measurement and those features of interest to the interpreter. The results of our analysis indicated two consistent endmember types over all four image scenes. These types are defined by a high flat polarized signature near a level of 255 DN and a low level flat signature near 0 DN for all polarizations. Four other endmember types were also isolated. The spatial distribution of these endmember types indicates possible correspondence to surface volume scattering and changes in surface dielectric. However, the shapes of these endmember types were different from scene to scene. R.J.F.

N86-10624*# Jet Propulsion Lab., California Inst. of Tech., Pasadena.
LITHOLOGIC MAPPING IN A SEDIMENTARY ENVIRONMENT USING MULTIPOLARIZATION SAR IMAGES
Diane L. Evans and Leslie R. Schenck *In its* NASA/JPL Aircraft SAR Workshop Proc. 15 Jun. 1985 p 49-50 refs Original contains color illustrations (For primary document see N86-10615 01-43)
Avail: NTIS HC A05/MF A01 CSCL 08B

Multipolarization Synthetic Aperture Radar (SAR) data from the NASA/JPL aircraft SAR were used in conjunction with LANDSAT Thematic Mapper (TM), Thermal Infrared Multispectral Scanner (TIMS), and Airborne Imaging Spectrometer (AIS) data as part of a three-year research program to evaluate the utility of remote sensing measurements for analysis of sedimentary basins. The purpose of this research effort is to construct stratigraphic columns, map variations in the lithology, geometry, and structure of sedimentary rocks in the Wind River/Bighorn Basin area, Wyoming, and to integrate remote sensing data with conventional rain models of basin formation and evolution. Author

N86-10625*# Jet Propulsion Lab., California Inst. of Tech., Pasadena.
MAPPING DIVERSE FOREST COVER WITH MULTIPOLARIZATION AIRBORNE RADAR
J. P. Ford, D. E. Wickland, and R. R. Sharitz (Dupont de Nemours (E. I.) and Co., Aiken, S.C.) *In its* NASA/JPL Aircraft SAR Workshop Proc. 15 Jun. 1985 p 53-54 ref Original contains color illustrations (For primary document see N86-10615 01-43)
Avail: NTIS HC A05/MF A01 CSCL 02F

Imaging radar backscatter in continuously forested areas contains information about the forest canopy; it also contains data about topography, landforms, and terrain texture. For purposes of radar image interpretation and geologic mapping researchers were interested in identifying and separating forest canopy effects from geologic or geomorphic effects on radar images. The objectives of this investigation was to evaluate forest canopy variables in multipolarization radar images under conditions where geologic and topographic variables are at a minimum. A subsidiary objective was to compare the discriminatory capabilities of the radar images with corresponding optical images of similar spatial resolution. It appears that the multipolarization images discriminate variation in tree density, but no evidence was found for discrimination between evergreen and deciduous forest types. R.J.F.

N86-10626*# National Aeronautics and Space Administration. National Space Technology Labs., Bay Saint Louis, Miss.
POTENTIAL APPLICATIONS OF MULTIPOLARIZATION SAR FOR PINE PLANTATION BIOMASS ESTIMATION
S. T. Wu *In* JPL NASA/JPL Aircraft SAR Workshop Proc. 15 Jun. 1985 p 59-61 (For primary document see N86-10615 01-43)
Avail: NTIS HC A05/MF A01 CSCL 02F

This study was conducted as a part of the research tasks under the Radar Land Cover Analysis Program. The Radar Land Cover Analysis objective is, through utilization of multisensor data, to gain a basic understanding of the measurements and data characteristics in the visible-IR-microwave regions of the electromagnetic spectrum associated with specific surface features and cover types. Since the results of analysis of data acquired by Shuttle Imaging Radar (SIR-A) and LANDSAT Thematic Mapper (TM) over the study area were reported (NSTL/ERL Report No. 228, December 1984), this study focused on the analysis and evaluation of the L-band multipolarization airborne SAR data acquired over a southeastern pine forest scene. The data acquisition mission was flown on September 8 and 9, 1983. The HH, HV polarizations and the VV, VH polarizations were used on the first and the second day, respectively. Due to instrumentation difficulties, the digital recorder recorded only the second day's data. Because of this, only the VV and VH polarization data were used in this analysis. However, the HH and HV polarization images were available for visual comparison. It appears that SAR digital numbers correlate with the index of green biomass. Author

N86-10627*# Jet Propulsion Lab., California Inst. of Tech., Pasadena.
ON THE USE OF L-BAND MULTIPOLARIZATION AIRBORNE SAR FOR SURVEYS OF CROPS, VINEYARDS, AND ORCHARDS IN A CALIFORNIA IRRIGATED AGRICULTURAL REGION
Jack F. Paris *In its* NASA/JPL Aircraft SAR Workshop Proc. 15 Jun. 1985 p 63 Original contains color illustrations (For primary document see N86-10615 01-43)
Avail: NTIS HC A05/MF A01 CSCL 02C

The airborne L-band synthetic aperture radar (SAR) collected multipolarization calibrated image data over an irrigated agricultural test site near Fresno, CA, on March 6, 1984. The conclusions of the study are as follows: (1) the effects of incidence angle on the measured backscattering coefficients could be removed by using a correction factor equal to the secant of the angle raised to the

1.4 power, (2) for this scene and time of year, the various polarization channels were highly correlated such that the use of more than one polarization added little to the ability of the radar to discriminate vegetation type or condition; the exception was barley which separated from vineyards only when a combination of like and cross polarization data were used (polarization was very useful for corn identification in fall crops), (3) an excellent separation between herbaceous vegetation (alfalfa, barley, and oats) or bare fields and trees in orchards existed in brightness was well correlated to alfalfa height or biomass, especially for the HH polarization combination, (5) vineyards exhibited a narrow range of brightnesses with no systematic effects of type or number of stakes nor of number of wires in the trellises nor of the size of the vines, (6) within the orchard classes, areal biomass [characterized by basal area] differences caused radar image brightness differences for small to medium trees but not for medium to large trees. Author

N86-10628*# Jet Propulsion Lab., California Inst. of Tech., Pasadena.
VEGETATION CANOPY DISCRIMINATION AND BIOMASS ASSESSMENT USING MULTIPOLARIZED AIRBORNE SAR
F. T. Ulaby (Michigan Univ.), M. C. Dobson (Michigan Univ.), and D. N. Held *In its* NASA/JPL Aircraft SAR Workshop Proc. 15 Jun. 1985 p 67-75 Original contains color illustrations (For primary document see N86-10615 01-43)
Avail: NTIS HC A05/MF A01 CSCL 02C

Multipolarized airborne Synthetic Aperture Radar (SAR) data were acquired over a largely agricultural test site near Macomb, Illinois, in conjunction with the Shuttle Imaging Radar (SIR-B) experiment in October 1984. The NASA/JPL L-band SAR operating at 1.225 GHz made a series of daily overflights with azimuth view angles both parallel and orthogonal to those of SIR-B. The SAR data was digitally recorded in the quadpolarization configuration. An extensive set of ground measurements were obtained throughout the test site and include biophysical and soil measurements of approximately 400 agricultural fields. Preliminary evaluation of some of the airborne SAR imagery indicates a great potential for crop discrimination and assessment of canopy condition. False color composites constructed from the combination of three linear polarizations (HH, VV, and HV) were found to be clearly superior to any single polarization for purposes of crop classification. In addition, an image constructed using the HH return to modulate intensity and the phase difference between HH and VV returns to modulate chroma indicates a clear capability for assessment of canopy height and/or biomass. In particular, corn fields heavily damaged by infestations of corn borer are readily distinguished from noninfested fields. Author

N86-10629*# Jet Propulsion Lab., California Inst. of Tech., Pasadena.
MODELLING OF VEGETATION VOLUMES
Jakob J. vanZyl (California Inst. of Tech.), Charles H. Papas (California Inst. of Tech.), Nader Engheta, and Charles Elachi *In its* NASA/JPL Aircraft SAR Workshop Proc. 15 Jun. 1985 p 77-79 (For primary document see N86-10615 01-43)
Avail: NTIS HC A05/MF A01 CSCL 02C

The purpose is to describe work that is being done to find theoretical models to describe radar backscatter from vegetation layers. The geometry of the problem is shown. The information that one would like to find through the application of the results of these models would include: the thickness of the layer; the absorption in the layer (i.e., density, moisture content, and biomass); the geometry of the scatterers (i.e., shape and orientation); how much of the received power is due to volume scattering only; and a way to enhance the ratio of scattering that has some interaction with the ground surface. The proposed ways to find this information are discussed. R.J.F.

N86-10630# Army Engineer Topographic Labs., Fort Belvoir, Va.
ANALYSIS OF EDGE DETECTION ALGORITHMS ON DIAL (DIGITAL IMAGE ANALYSIS LABORATORY)
J. M. Brown Jan. 1985 38 p
(DA Proj. 4A7-62707-A-855)
(AD-A156735; ETL-0371) Avail: NTIS HC A03/MF A01 CSCL 12/1

As part of an effort to deliver to the Defense Mapping Agency in FY85 a semiautomated feature extraction system, the Engineer Topographic Laboratories is conducting a feature extraction study. One of the objectives of this study is to determine whether selected edge-finding algorithms can be used to find such lineal features as roads and boundaries. The purpose of this document is to report on progress to date on an analysis of several edge-detection algorithms that exist on ETL's Digital Image Analysis Laboratory image-processing facility. In addition to evaluating the algorithms, this study investigated the possibilities of integrating the algorithms' resultant edges with other feature classification algorithms. Three fundamental edge-detection methods were compare: (1) a nonlinear edge-enhancement operator; (2) a directional edge operator; and (3) an extraction of the zero-crossings from filtering an image with the Laplacian of a symmertric Gaussian function. GRA

N86-10631# Pacific Northwest Lab., Richland, Wash.
ENERGY BALANCE IN A DEEP COLORADO VALLEY: ASCOT 84
J. R. Simpson, L. J. Fritschen, C. D. Whiteman, and M. M. Orgill Jan. 1985 5 p refs Presented at the 17th Conf. on Agr. and Forest Meteorol., Phoenix, Ariz., 20 May 1985 Prepared in cooperation with Washington Univ., Seattle
(Contract DE-AC06-76RL-01830)
(DE85-012441; PNL-SA-12990; CONF-850581-3) Avail: NTIS HC A02/MF A01

Five portable, battery-operated energy balance stations were installed and operated in the deep, semiarid Brush Creek Valley of western Colorado for 22 days. Surface energy budget data from these stations are presented for the clear day of September 29, 1984. DOE

N86-10632# California Univ., Livermore. Lawrence Livermore Lab.
APPLICATION OF THE RUTHENIUM AND TECHNETIUM THERMODYNAMIC DATA BASES USED IN THE EQ3/6 GEOCHEMICAL CODES
D. Isherwood Apr. 1985 63 p
(Contract W-7405-eng-48)
(DE85-013766; UCRL-53594) Avail: NTIS HC A04/MF A01

Based on a critical review of the available thermodynamic data, computerized data bases for technetium and ruthenium were created for use with the EQ3/6 geochemical computer codes. The technetium data base contains thermodynamic data for 8 aqueous species and 15 solids; 26 aqueous species and 9 solids were included in the ruthenium data base. The EQ3NR code was used to calculate solubility limits for ruthenium (8 x 10(-16) M) in ground water from Yucca Mountain, a potential nuclear waste repository site near the Nevada Test Site (NTS). The code confirmed the essentially unlimited solubility of technetium in oxidizing conditions, such as those that are believed to exist in the unsaturated zone at Yucca Mountain and the Cambric Nuclear event site at the NITS. Ruthenium migration observed from the Cambric site was evaluated. The solubility limit for ruthenium (as the aqueous species RuO4(-)) when constrained by BuO2 is approximately equal to the concentration of ruthenium found in the cavity ground water (i.e., 2.1 x 10(-11) vs 4.5 x 10(-11) M). Differences in ruthenium solubility limits between Yucca Mountain and Cambric are primarily due to differences in ground-water pH. Technetium solubility (3 x 10(-8) M) for moderately reducing conditions (Eh = -0.1 V) using the metastable oxide, TcO2.2H2O, as the solubility constraint is within the range of experimental values. DOE

N86-10633# Rockwell International Corp., Richland, Wash.
TIME-TERM ANALYSIS OF UPPER CRUSTAL STRUCTURE IN THE COLUMBIA BASIN, WASHINGTON
A. C. Rohay, D. W. Glover, and S. D. Malone Apr. 1985 24 p Presented at the Seismological Soc. of Am. Conf., Austin, Tex.,

14 Apr. 1985
(Contract DE-AC06-77RL-01030)
(DE85-012390; RHO-BW-SA-435P; CONF-8504151-1) Avail: NTIS HC A02/MF A01

Arrival time data from existing permanent networks and supplementary portable stations were collected during the US Geological Survey (USGS) refraction program in August 1984. Reduced travel time plots of these data and USGS record sections were used to select data from two branches of the travel time curve. Sixty-six arrival times selected in the distance range 3 to 63 km were fit to a velocity of 5.16 km/s (plus or minus 0.02 km/s). Time terms determined at 31 stations range from -0.10 to +0.15 s (plus or minus 0.05 s) and show correlations with elevation and near-surface geology. The four intercept times range from 0.15 to 0.22 s (plus or minus 0.05 s), implying an average depth of 0.5 km to the 5.16-km/s refracting horizon within the basalt. Eighty-three arrival times selected in the distance range 50 to 145 km were fit to a velocity of 6.16 km/s (plus or minus 0.02 km/s). Time terms calculated at 40 stations range from -0.6 to +0.6 s (plus or minus 0.1 s), with the four intercept times ranging from 1.4 to 2.0 s (plus or minus 0.1 s). These show a systematic regional pattern consistent with previous studies (Malone and Rohay 1983) but extended by portable-station coverage. Conversion of the time terms to basement depth is dependent upon the lateral extent of an inferred low-velocity layer beneath the basalts, which is suggested by deep-borehole logs and magnetotelluric data. DOE

N86-10634# Western Research Inst., Laramie, Wyo.
GEOLOGIC EVALUATION AND RESERVOIR PROPERTIES OF THE PR SPRING TAR SAND DEPOSIT, UINTAH AND GRAND COUNTIES, UTAH
D. J. Sinks Jan. 1985 197 p refs
(Contract DE-FC21-83FE-60177)
(DE85-013248; DOE/FE-60177/1883) Avail: NTIS HC A09/MF A01

A seven-corehole drilling program at the PR Spring tar sand deposit, southeastern Uinta Basin, Utah was completed. The data were integrated with other resource information to complete lithologic correlations, to evaluate general reservoir property trends for each major tar sand zone, and to identify areas of potential in situ processing. Five distinct arkoses (sandstones) of lacustrine origin have definable areal extents and are variable saturated with bitumen. Two newly recognized zones stratigraphically lower than the other five, were tentatively identified in one core from the southeast portion of the deposit. Core descriptions and analytical data were used to generate computerized maps to identify general areal trends in resource parameters for the five major zones. Two pairs of zones exhibit similar areal trends, indicating similar depositional conditions. Insufficient data for zone E inhibited the identification of any resemblance to other zones. Direction of increase for some reservoir properties were noted for all zones. Portions of all five zones are suitable for surface mining. DOE

N86-10635# Argonne National Lab., Ill.
APPROACHES TO CUMULATIVE IMPACT ASSESSMENT
G. W. Witmer 1985 15 p refs Presented at the Natl. Wetland Assessment Symp., Portland, Oreg., 17 Jun. 1985
(Contract W-31-109-eng-38)
(DE85-013891; CONF-8506146-1) Avail: NTIS HC A02/MF A01

The quantity and quality of North American wetlands were reduced this century. Growing concern over the social and ecological effects lead to studies of wetlands ecology and efforts to classify, monitor, and predict impacts to wetlands. Assessing and predicting land use and developmental activity impacts particularly cumulative impacts to wetlands is difficult because of their diverse, complex, and dynamic nature. The methods allow for multiple projects or land uses, an extended time frame, the aggregation of impacts, a flexibility in geographic boundaries, and adaptability to new techniques and sources of information. Nine categories of existing methods are reviewed. It is probable that a combination of these methods can be used for cumulative impact assessment. To do so effectively, some additional concepts must be incorporated. DOE

N86-10636# Deutsche Forschungs- und Versuchsanstalt fuer Luft- und Raumfahrt, Oberpfaffenhofen (West Germany). Abt. Fernerkundung.
CALIBRATION OF THE MULTISPECTRAL SCANNER (MSS) SATELLITE DATA TO EVALUATE CHANGE IN THE REFLECTION OF CONIFEROUS STOCKS Ph.D. Thesis - Technische Univ., Berlin
Gerd-Peter Fehlert Sep. 1984 184 p refs In GERMAN; ENGLISH summary Report will also be announced as translation (ESA-TT-938) Original contains color illustrations
(DFVLR-FB-84-44; ISSN-0171-1342) Avail: NTIS HC A09/MF A01; DFVLR, Cologne DM 71

A relative calibration is performed in order to allow a comparative, multitemporal analysis of MSS satellite data and hence the detection of reflectory changes with regard to selected object classes. By applying the method to the class wood, the age of a coniferous stock can be determined, and during the stage of growth distinct age groups show locally differing reflectory properties. The latter suggests disorders of the proliferation of young sprouts. This method can be an early indicator for the detection of damaged forest areas. The atmospheric influence on satellite data is determined by a multilayer atmospheric model. Author (ESA)

N86-10637# Delft Hydraulics Lab. (Netherlands).
THE RHINE-MEUSE ESTUARY HYDRAULIC SCALE MODEL. EXPERIENCES WITH COMPUTER CONFIGURATION AND SOFTWARE
W. Scholten Feb. 1985 8 p refs Presented at 21st Intern. Assoc. for Hydraulic Res. Congr., Melbourne, 19-23 Aug. 1985
(Publ-335) Avail: NTIS HC A02/MF A01

The hardware and software configurations of the Rhine-Meuse estuary hydraulic model are described. The system for real time processing consists of a PDP 11/24 computer and a FOX digital control system. A PDP 11/44 performs offline processing. The RSX-11M system is used. Programs to simulate tidal movements, acquire measurement data, prepare boundary conditions, administer measurements, and process measurements were created. Adjustment of tidal flows at sea boundanes takes 1 day; salinity measurements are free from initial conditions after 3 hr. Programming is time consuming because of the relatively limited free space available (48 kbytes). Author (ESA)

N86-10638# Instituut voor Culturrtechniek en Waterhuishouding, Wageningen (Netherlands).
REMOTE SENSING
G. J. A. Nieuwenhuis and J. M. M. Bouwmans (Landinrichtingsdienst) May 1984 46 p In DUTCH
(NOTA-1535) Avail: NTIS HC A03/MF A01

Electromagnetic radiation, and remote sensors are introduced. Color and false color, multispectral and stereophotography, multispectral and infrared line scanning, and microwave techniques are described. The impact of wave length, and the way the images are obtained and compiled on the resulting image content is discussed. Interpretation and analog and digital procedures are surveyed. Applications such as crop identification and meteorological research are reviewed. Author (ESA)

N86-10639# Instituut voor Culturrtechniek en Waterhuishouding, Wageningen (Netherlands).
REMOTE SENSING STUDY PROJECT EAST GELDERLAND (NETHERLANDS). PART 2: REMOTE SENSING FLIGHTS IN 1982 AND 1983; ORGANIZATION ASPECTS [REMOTE SENSING STUDIEPROJECT OOST-GELDERLAND. DEELRAPPORT 2: REMOTE SENSING VLUCHTEN IN 1982 EN 1983: ORGANISATORISCHE ASPECTEN]
G. J. A. Nieuwenhuis Jun. 1983 30 p refs In DUTCH
Avail: NTIS HC A03/MF A01

Photographs of 2 strips of peatland of 8 x 40 km at 5000 m altitude and detailed studies at 800 to 2000 m were made under different weather conditions with visibility from 5 to 15 km. As

infrared photography is visibility and cloud independent and quality can be improved by repeating a trajectory and processing afterwards, it is concluded that flights should go on even under bad navigation circumstances. Author (ESA)

N86-10640# Haskoning, Consulting Engineers, Nijmegen (Netherlands).
UTILIZATION OF SATELLITE REMOTE SENSING FOR THE MONITORING OF OIL POLLUTION AND MARINE ECOSYSTEMS IN INDONESIA. A TROPICAL EARTH RESOURCES SATELLITE PROGRAM (TERS) CASE STUDY IMPLEMENTED FOR THE NLR, DELFT
Nov. 1983 67 p refs
Avail: NTIS HC A04/MF A01

The suitability of a remote sensing satellite for environmental monitoring in tropical zones with considerable cloud cover was assessed in a case study of the impact of an oil refinery extension on coastal and mangrove swamp ecology. It is concluded that the Tropical Earth Resources Satellite (TERS) program panchromatic and spectral bands in the wavelength interval between 40 to 1000 nm are suitable for the detection of the mangrove zone, dead tree zones, the location and drift of oil spills, and the location of sources of pollution-like drilling and production platforms, tanker traffic, and pipeline traces. The TERS system can be used as a first stage waring system, with follow-up by aerial and ground surveys. Author (ESA)

N86-10641# Texas Dept. of Water Resources, Austin.
EVALUATING THE GROUND-WATER RESOURCES OF THE HIGH PLAINS OF TEXAS, VOLUME 4
T. Knowles, P. Nordstrom, and W. B. Klemt Dec. 1984 393 p (PB85-191625; TDWR/R-288-Vol-4) Avail: NTIS HC A17/MF A01; also avail: in set of 4 reports HC E99 as PB85-191583 CSCL 08H

This report is prepared in four volumes. Volume 4 contains the basic data for the counties in the southern third of the study area as shown on the accompanying map. GRA

N86-10181# Bundesministerium fuer Forschung und Technologie, Bonn (West Germany).
HOW ANTARCTICA WAS UNVEILED. MASTERPIECES OF FRANKFURT TOPOGRAPHIC SURVEYORS. A PART OF THE GERMAN ANTARCTICA RESEARCH PROGRAM [WIE DIE ANTARKTIS ENTSCHLEIERT WIRD. MEISTERSTUECKE FRANKFURTER ERDVERMESSER. EIN TEIL DES DEUTSCHEN ANTARKTIS-FORSCHUNGSPROGRAMMS]
Ruediger Jungblutth *In its* Satellite Use for Men 1985 p 5-10 In GERMAN (For primary document see N86-10180 01-12)
Avail: NTIS HC A03/MF A01

N86-10182# Bundesministerium fuer Forschung und Technologie, Bonn (West Germany).
SATELLITE DATA EVEN FOR A POULTRY FARM. A DEVELOPMENT FOR TANZANIA. IMAGE EVALUATION FOLLOWING NEW WAYS [SATELLITENDATEN SELBST FUER EINE HUEHNERFARM. EIN ENTWICKLUNGSPROJEKT FUER TANSANIA. BILDAUSWERTUNG AUF NEUEN WEGEN]
Philip Erdoes *In its* Satellite Use for Men 1985 p 11-16 In GERMAN (For primary document see N86-10180 01-12)
Avail: NTIS HC A03/MF A01

N86-10183# Bundesministerium fuer Forschung und Technologie, Bonn (West Germany).
WITH ARGUS EYES FROM SPACE. SATELLITE DIAGNOSIS FOR UPPER VOLTA. SEVEN MAPS WITHOUT MYSTERY [MIT ARGUSAUGEN AUS DEM ALL. SATELLITEN-DIAGNOSE FUER OBERVOLTA. SIEBEN KARTEN OHNE SIEBEN SIEGEL]
Uwe Andresen *In its* Satellite Use for Men 1985 p 17-21 In GERMAN (For primary document see N86-10180 01-12)
Avail: NTIS HC A03/MF A01

44 ENERGY PRODUCTION AND CONVERSION

Includes specific energy conversion systems, e.g., fuel cells and batteries; global sources of energy; fossil fuels; geophysical conversion; hydroelectric power; and wind power.

For related information see also *07 Aircraft Propulsion and Power, 20 Spacecraft Propulsion and Power, 28 Propellants and Fuels,* and *85 Urban Technology and Transportation.*

N86-10642 Department of the Air Force, Washington, D.C.
NICKEL-CADMIUM BATTERY CONDITIONER AND TESTER APPARATUS Patent
D. C. Kinney, inventor (to Air Force) Issued 14 May 1985 5 p Supersedes AD-D009945
(AD-D011770; US-Patent-4,517,517; US-Patent-Appl-SN-431434; US-Patent-Class-324-433) Avail: US Patent and Trademark Office CSCL 14/2

This provides a battery test apparatus for determining the state of quality of a nickel-cadmium battery. The battery test apparatus provides a battery discharge circuit that discharges the battery under test until a specified terminal voltage level is reached wherein the discharge cycle is automatically terminated. Since a visual indication is provided at the initiation of the discharge cycle and visual indication is provided at the end of the test cycle, the elapsed time for the discharge test is accurately measured. If the time required to discharge the battery to the predetermined level exceeds a certain value, such as 48 minutes the level exceeds a certain value, such as 48 minutes the quality of the battery is acceptable. The battery test apparatus also includes a reconditioning switch for recharging acceptable batteries to full charge capacity. GRA

N86-10643*# National Aeronautics and Space Administration. Lewis Research Center, Cleveland, Ohio.
PHOTOVOLTAIC SYSTEMS IN REMOTE LOCATIONS: AN EXPERIENCE SUMMARY Final Report
A. F. Ratajczak [1985] 19 p refs Presented at the Solar Appl. in Remote Locations Workshop, Las Cruces, N. Mex., 11-14 Mar. 1985
(Contract DE-AI01-79ET-20485)
(NASA-TM-87106; E-2703; DOE/NASA/20485-20; NAS 1.15:87106) Avail: NTIS HC A02/MF A01 CSCL 10A

Since 1979, the NASA Lewis Research Center has been responsible for the design, installation and operational support of 58 photovoltaic systems located in 27 countries. Together these systems contain 77.1 kW of photovoltaic modules and provide power for a variety of loads ranging from single low-power street light systems to a utility type power system for a village of over 150 people. Systems installation, reliability, operation, maintenance and repair experience is given and major problem areas are listed. Experience indicates that photovoltaic system technology is a proven technology, but that developing countries need to better posture themselves to acquire and utilize the technology. Recommendations are given. Author

N86-10644# Sandia Labs., Albuquerque, N. Mex.
CHARACTERIZATION OF CATHODIC CORROSION PRODUCTS IN THE Ca/CaCrO4 THERMAL BATTERY
R. A. Guidott, F. W. Reinhardt, E. L. Venturini, J. W. Rogers, Jr., and W. N. Cathey May 1985 35 p Prepared in cooperation with Nevada Univ., Reno
(Contract DE-AC04-76DP-00789)
(DE85-013442; SAND-84-1098) Avail: NTIS HC A03/MF A01

Using thermal analysis techniques, the corrosion process resulting from the reaction of iron, nickel, and stainless steel (used as current collectors in Ca/CaCrO4 thermal batteries) with CaCrO4 dissolved in LiCl-KCl eutectic was investigated. The reaction product for iron was synthesized in bulk external to the battery and was characterized by chemical analysis, X-ray diffraction,

Moessbauer spectroscopy, X-ray photoelectron spectroscopy, static magnetization, and electrical conductivity. This characterization provides a better understanding of the cathodic corrosion processes that occur in the Ca/CaCrO4 thermal battery, and how the properties of the reaction layer at the catholyte-current collector interface influence battery performance. DOE

N86-10645# Midwest Research Inst., Golden, Colo. Solar Energy Research Inst.

IDENTIFICATION OF CHEMICAL AND PHYSICAL PHENOMENA AFFECTING THE DURABILITY OF SILVERED POLYMER (PMMA) MIRRORS

P. Schissel, H. H. Neidlinger, and A. W. Czanderna May 1985 42 p

(Contract DE-AC02-83CH-10093)

(DE85-012131; SERI/PR-255-2493) Avail: NTIS HC A03/MF A01

Mirrors are the device of choice in concentrating solar radiation for solar thermal applications. Efficiency requirements and economic factors dictate that the mirrors maintain high reflectance for many years. The mirrors must have such surface perfection that they can deliver all their reflected energy into an angle of 1 to 5 milliradians (mrad). Other design factors such as weight, flexibility, and cost make silvered polymer films highly desirable for solar thermal use. Factors that affect the durability and performance of silvered polymer films in outdoor exposure are reported. The results presented are based on laboratory analyses of various polymers silvered by various processes. The crucial role in degradation played by ultraviolet (UV) light is shown. The screens in the polymer improve weatherability and inconel uv blockers improve adhesive performance. Weather-Ohmeter studies comparing exposures with and without UV radiation show more rapid degradation due to UV. Fourier transform infrareds (FT-IR) show synergistic effects with UV, Chlorine, and silver. DOE

N86-10646# Conservation and Renewable Energy Inquiry and Referral Service, Silver Spring, Md.

GEOTHERMAL ENERGY TECHNOLOGY PROGRAM SUMMARY

May 1985 4 p

(Contract DE-AC01-83CE-30780)

(DE85-013101; DOE/CE-0111) Avail: NTIS HC A02/MF A01

The progress to date of the geothermal energy program of the US Department of Energy is briefly summarized. Federal/industry cooperation, program focus, and a budget are discussed. DOE

N86-10647# Oak Ridge National Lab., Tenn.

SIMPLIFIED ANALYSIS OF STIRLING ENGINES AND HEAT PUMPS

N. C. J. Chen, F. P. Griffin, and C. D. West 12 Dec. 1984 9 p Presented at the DOE/ORNL Heat Pump Conf., Washington, D.C., 10 Dec. 1984

(Contract DE-AC05-84OR-21400)

(DE85-005366; CONF-841231-5) Avail: NTIS HC A02/MF A01

Because most of the parameters describing the instantaneous state of the working fluid in a Stirling engine (i.e., the pressure, mass and temperature of the gas in the various parts of the engine) are time dependent, the mass and energy conservation equations must be expressed as differential equations. Generally, the equations are nonlinear and can only be solved by numerical approximations. Such solutions are plaqued by both instabilities and by numerical artifacts, although given sufficient computer time and programming effort, satisfactory results can usually be obtained. There is, however, a simpler approach that is not only much more economical but also more revealing. In the new method all of the relevant quantities are represented by linear combinations of sine and cosine terms. Because the differentials of harmonic functions are also harmonic functions (the sine and cosine are the only periodic functions for which this is true), when they are substituted into the differential equations, the equations become simple algebraic ones. DOE

N86-10648# Conservation and Renewable Energy Inquiry and Referral Service, Silver Spring, Md.

PASSIVE AND HYBRID SOLAR TECHNOLOGIES PROGRAM SUMMARY

May 1985 3 p

(Contract DE-AC01-83CE-30780)

(DE85-013100; DOE/CE-0109) Avail: NTIS HC A02/MF A01

The goal of the national energy policy is to foster an adequate supply of energy at reasonable prices. This policy recognizes that adequate supply requires flexibility, with no undue reliance on any single source of supply. The goal of reasonable prices suggests economic efficiency so that consumers, individuals, commercial and industrial users alike, are not penalized by government regulation or subside. The strategies for achieving this energy policy goal are: (1) to minimize federal regulation in energy pricing while maintaining public health and safety and environmental quality, and (2) to promote a balanced and mixed energy resource system through research and development. One of the keys to energy sufficiently is the scientific application of passive solar energy techniques. DOE

N86-10649# Brookhaven National Lab., Upton, N. Y.

IMPROVED BLUE RESPONSE AND EFFICIENCY OF A-Si:H SOLAR CELLS DEPOSITED FROM DISILANE USING A DUAL-CHAMBER PLASMA SYSTEM

G. Rajeswaran, P. E. Vanier, R. R. Corderman, and F. J. Kampas 1985 10 p Presented at the 18th IEEE Photovoltaic Spec. Conf., Las Vegas, Nev., 21 Oct. 1985

(Contract DE-AC02-76CH-00016)

(DE85-013289; BNL-36577; CONF-851043-1) Avail: NTIS HC A01/MF A01

Thin film amorphous silicon solar cells with glass/SnO2/p/i/n/A1 structures and 6 to 7% AM1 conversion efficiencies were fabricated at rapid deposition rates in a dual-chamber glow discharge deposition system. Parameters such as electrode spacing, Si2H6 partial pressure and flow rate were optimized to produce uniform deposition over large areas. Identical solar cells were deposited in either the single-chamber mode or the dual-chamber mode for comparison. Single-chamber mode cells perform poorly over the visible wavelengths and hence produce low short circuit currents. The dual-chamber mode cells show a significant improvement in blue response and a factor of two increase in short circuit current over the single-chamber mode cells. Under short circuit conditions, 15 mA sq cm was generated from rapidly deposited cells from disilane and 18 MA/sq cm was generated from rapidly deposited cells from disilane and 18 MA/sq cm from low deposition rate monosilane cells. DOE

N86-10650# Tennessee Univ., Knoxville.

GROUND-COUPLED HEAT PUMP RESEARCH AT THE UNIVERSITY OF TENNESSEE WASHINGTON, D.C., 10 DEC. 1984

W. S. Johnson, B. A. McGraw, R. N. Baugh, and W. A. Griffith 1984 10 p refs Presented at DOE/ORNL Heat Pump Conf.,

(Contract DE-AC05-84OR-21400)

(DE85-005357; CONF-841231-7) Avail: NTIS HC A02/MF A01

The seasonal performance of a horizontal-coil ground-coupled heat pump system in both the heating and cooling mode was evaluated to determine its potential for use in the Knoxville, TN area. The effects of the significant parameters on performance were determined with the required data to develop an optimized system. The ground-coupled heat pump system was installed in TECH House I. The following conclusions are presented: (1) the data indicate that the ground coil heat exchanger is undersized for summer operation, operation during the winter season was acceptable with an overall seasonal performance factor of 2.6 which is higher than a typical air-air heat pump; (2) an undersized ground coil in a ground-coupled heat pump system will produce a significant performance penalty; (3) backfilling with clay must be carefully done to avoid having air pockets in the ground due to the tendency of clay to agglomerate; (4) backfilling with sand around the ground coil produced improved performance of the system during the initial summer of operation; (5) during winter operation, no electric resistance backup heating is required;

(6) a ground-coupled heat pump in this area of the country must be sized based on the cooling peak which will normally result in an overdesign for the winter season, such as overdesign maybe, desirable because of reduced need for backup resistance heat. DOE

N86-10651# United Technologies Corp., South Windsor, Conn. Power Systems Div.
PHOSPHORIC AND ELECTRIC UTILITY FUEL TECHNOLOGY DEVELOPMENT Technical Progress Report, quarter ending Dec. 1984
R. D. Breault, T. A. Briggs, J. V. Congdon, R. L. Geltig, G. J. Goller, W. L. Luoma, M. W. McCloske, A. P. Mientek, J. J. OBrien, and S. A. Randall 1985 69 p refs
(Contract DE-AC21-83FE-60338)
(DE85-014741; FCR-6948P; TPR-20) Avail: NTIS HC A04/MF A01

Seventeen hundred hours and 11 thermal cycles were accumulated on the second 10 sq ft short stack at 120 psia and 405 F. A subscale cell out from 10 sq ft electrodes in the same batch used for the second 10 sq ft short stack accumulated over 4100 hours with performance conforming close to the E-line goal at 120 psia and 400 F. Over 14,870 hours and 42 thermal cycles were accumulated on the 3.7 sq ft, 30-cell short stack at 120 psia and 405 F. A subscale cell with GSB-18 catalyst completed over 10,000 hours of operation at 120 psia, 400 F. The full-size, 10 sq ft stack containment vessel and reactant gas manifolds were observed. The improved edge seal decreased leakage by more than 50% from the conventional edge seal. Cross-pressure tolerance also improved. Continuous automatic operation of the substrate forming machine was demonstrated by producing substrates at a 50% faster rate with high yields and low material loss. The cooler bonding cycle was significantly reduced by using a cold press in conjunction with the hot press. A lower cost stainless steel tubing is identified that could reduce cooler array cost by up to 50%. Assembly of the automated cell fill and assembly machine is initiated. DOE

N86-10652# United Technologies Corp., South Windsor, Conn. Power Systems Div.
PHOSPHORIC AND ELECTRIC UTILITY FUEL CELL TECHNOLOGY DEVELOPMENT Technical Progress Report, Jan. 1985
R. D. Breault, T. A. Briggs, J. V. Congdon, R. L. Gelting, G. J. Goller, W. L. Luoma, M. W. McCloskey, A. P. Mientek, J. J. OBrien, S. A. Randall et al Jan. 1985 35 p refs
(Contract DE-AC21-83FE-60338)
(DE85-014552; FCR-6956P; TPR-21) Avail: NTIS HC A03/MF A01

A subscale cell containing GSB-18, dry mix catalyst has accumulated over 6500 hours with performance 10 mV above E-line at 120 psia and 400 F. Over 150 thick separator plates were molded for use in cooler assemblies. The full-size 10-ft, 460 cell structural work-up is completed. All repeat components for the next 10-ft short stack are formed and processed. DOE

N86-10653# Oak Ridge National Lab., Tenn.
COMPARATIVE ANALYSIS OF SINGLE AND CONTINUOUSLY VARIABLE-CAPACITY HEAT PUMP CONCEPTS
C. K. Rice and S. K. Fischer 1984 9 p refs Presented at the DOE/ORNL Heat Pump Conf., Washington,D. C., 10 Dec. 1984
(Contract DE-AC05-84OR-21400)
(DE85-004089; CONF-841231-23) Avail: NTIS HC A02/MF A01

An initial assessment is given of the potential benefits of continuous-capacity-modulation in electric-driven, air to air heat pumps for residential application. The purpose was to provide a quantitative estimate of the possible annual performance gains of advanced continuously modulating heat pumps relative to single-speed designs at comparable levels of development. Seasonal (heating and cooling) and annual performance factor (APF) analysis capability was added to earlier design work to allow direct evaluation of annual energy use from heat pump performance data generated by the ORNL heat pump model. A modulating version of the heat pump model was developed to provide a means for simulating the steady state performance of continuously variable-speed (CVS) systems. With these tools, the APFs of both single and continuously variable-capacity (CVC) concepts could be studied as basic heat pump design variables were varied. DOE

N86-10654# Carrier Corp., Syracuse, N.Y.
ADVANCED ABSORPTION HEAT PUMP CYCLES
R. C. Reimann 1984 3 p ref Presented at the DOE/ORNL Heat Pump Conf., Washington, D.C., 10 Dec. 1984
(Contract DE-AC05-84OR-21400)
(DE85-003914; CONF-841231-20) Avail: NTIS HC A02/MF A01

The main goal is the development of significantly improved absorption machinery. This was to be directed specifically towards the development of a direct natural gas-fired absorption heat pump with both heating and cooling efficiencies advanced beyond current commercial offerings. These were to be accomplished through the use of novel and superior cycles, or by improved component performance. To keep the focus on machinery, the stipulation was agreed that candidate absorbent-refrigerant combinations were to be selected from among those whose properties were adequately known to permit cycle calculations and preliminary machine layouts. DOE

N86-10655# Purdue Univ., Lafayette, Ind. School of Electrical Engineering.
THEORY OF ADVANCED, HIGH-EFFICIENCE CONCENTRATOR CELLS Final Report
M. S. Lundstrom, R. J. Schwartz, C. M. Maziar, and P. D. DeMoulin 1985 195 p
(Contract DE-AC02-83CH-10093)
(DE85-008821; SERI/STR-211-2687) Avail: NTIS HC A09/MF A01

The goal of this project was to begin developing accurate, and ultimately predictive, device models for 3-V concentrator cells. The project consisted of extending a one-dimensional numerical device model previously developed at Purdue to 3-V solar cells. The accuracy of the code was verified by comparing computed and measured solar cell characteristics. Gallium arsenide was selected because it is the most mature 3-V technology and because GaAs solar cells have demonstrated high conversion efficiency. Materials models for GaAs solar cells were compiled, evaluated, and in some cases extended. These materials models were then implemented into the numerical device model. The device mode as also extended to analyze optical absorption and reflection from bare and anti-reflection (AR) coated cells. To test the GaAs cell model, its predictions were compared to measured results for an N(+)P cell (the shallow homojunction cell reported by Fan and co-workers) and a P(+)N cell (fabricated by Borrego and co-workers). In general, good agreement between theory and experiment was obtained for both concentrated and unconcentrated conditions. DOE

N86-10656# Bonneville Power Administration, Portland, Oreg. Solar Utilization Network.
PASSIVE SOLAR DESIGN HANDBOOK
M. S. Baker Apr. 1985 28 p
(DE85-014263; DOE/BP-2) Avail: NTIS HC A03/MF A01

A basic introduction to solar energy is provided in this manual. The most common passive solar heating designs are described very briefly. The designs presented fall under three passive heating classifications: direct gain, indirect gain, and isolated gain. Design considerations for buildings are included along with considerations for: thermal storage walls, thermal storage roofs, attached sunspaces, and convectiv loops. A glossary of solar energy related terms is included. DOE

N86-10657# Midwest Research Inst., Golden, Colo.
SOLAR THERMAL TECHNICAL INFORMATION GUIDE
May 1985 180 p
(Contract DE-AC02-83CH-10093)
(DE85-002941; SERI/SP-271-2511) Avail: NTIS HC A09/MF A01

This guide is designed to help investigators search for

information in the solar thermal technology field. The information ranges from history and technology basics to the latest in research and develoment. It is written to help several audiences, including engineers and scientists who may be unfamiliar with a particular aspect of solar thermal energy, university researchers who are interested in the field, manufacturers needing to learn more about specific topics, and librarians who provide information to their clientele. The guide is divided into ten chapters, with Chapters 1 to 8 providing background on solar thermal energy development (including its history and current status) by topic. Within each topic, an overview is provided with references to relevant publications or information sources. Chapters 9 and 10 contain directories listing research centers and major technical information sources, respectively. DOE

N86-10658# Midwest Research Inst., Golden, Colo.
PHOTOVOLTAICS: REPORT, 1984 Annual Progress Report, 1984
Jun. 1985 39 p refs
(Contract DE-AC02-83CH-10093)
(DE85-014713; DOE/CE-0128) Avail: NTIS HC A03/MF A01

Progress on the research and development of photovoltaics in 1984 is summarized. Some of the achievements in materials, collector, and systems research are presented. The major materials research activity in 1984 was the single junction thin films research which received over 12 million dollars in funding. The Flat Plate Solar Array Project was yet another major recipient of research funding with just over seven million dollars. Other research achievements are briefly discussed and include: multijunction and innovative concepts, silicon materials, concentrator collectors, module reliability, and balance of system developments. DOE

N86-10659# Argonne National Lab., Ill.
ADVANCED FUEL CELL DEVELOPMENT Progress Report, Jul. - Sep. 1984
R. D. Pierce, N. Q. Minh, J. L. Smith, G. H. Kucera, F. C. Mrazek, J. R. Stapay, J. Moreschi, R. Herceq, R. B. Poeppel, and J. Routhort Jun. 1985 31 p ref
(Contract W-31-109-eng-38)
(DE85-014550; ANL-85-7) Avail: NTIS HC A03/MF A01

Fuel cell research and development activities at Argonne National Laboratory (ANL) during the period July through September 1984 are discussed. These efforts were directed toward seeking alternative cathode materials to NiO for molten carbonate fuel cells. Particular emphasis was placed on studying the relationship of synthesis and sintering conditions on the resistivity of doped and undoped LiFeO2 and Li2MnO3 and on achieving a better understanding of the crystalline defect structures of phases that are thermodynamically stable at 1- and 10-atm pressure. To this end, several experimental assemblies (including synthesis, solubility, and sintering vessels and a high-pressure thermogravimetric analyzer) were constructed to permit 10-atm operation. Methods to improve the corrosion resistance of stainless steel components in ion-migration test cells are under assessment. A study to provide improved understanding of anode creep and densification occuring under fuel cell conditions is under way. DOE

N86-10660# Los Alamos Scientific Lab., N. Mex.
GENERAL-PURPOSE HEAT SOURCE DEVELOPMENT: SAFETY VERIFICATION TEST PROGRAM. BULLET/FRAGMENT TEST SERIES
T. G. George, R. E. Tate, and K. M. Axler May 1985 38 p
(Contract W-7405-eng-36)
(DE85-014262; LA-10364-MS) Avail: NTIS HC A03/MF A01

The radioisotope thermoelectric generator (RTG) that will provide power or space missions contains 18 General-Purpose Heat Source (GPHS) modules. Each module contains four (238) PuO2-fueled clads and generates 250 W sub (t). Because a launch-pad or post-launch explosion is always possible, the ability of GPHS fueled clads within a module to survive fragment impact needs to be determined. The bullet/fragment test series, part of the Safety Verification Test Plan, was designed to provide information on clad response to impact by a compact, high-energy, aluminum-alloy fragment and to eestablish a threshold value of fragment energy required to breach the iridium cladding. Test results show that a velocity of 555 m/s (1820 ft/s) with an 18-g bullet is at or near the threshold value of fragment velocity that will cause a clad breach. Results also show that an exothermic Ir/Al reaction occurs if aluminum and hot iridium are in contact, a contact that is possible and most damaging to the clad within a narrow velocity range. The observed reactions between the iridium and the aluminum were studied in the laboratory and are reported. DOE

N86-10661# Oak Ridge National Lab., Tenn.
STIRLING-ENGINE-DRIVEN HEAT PUMP PROGRAM OVERVIEW
F. C. Chen 1984 5 p Presented at the DOE/ORNL Heat Pump Conf., Washington, D.C., 10 Dec. 1984
(Contract DE-AC05-84OR-21400)
(DE85-004796; CONF-841231-10) Avail: NTIS HC A02/MF A01

A brief summary is given of the Stirling-engine-driven heat pump project being carried out by Oak Ridge National Laboratory (ORNL) for the Department of Energy. The Objective and approach, early development effort, current status and accomplishments, and future technology options are discussed. DOE

N86-10662# Midwest Research Inst., Golden, Colo. Solar Energy Research Inst.
SOME ASPECTS OF LONG-RANGE, HIGH-RISK PHOTOVOLTAIC RESEARCH AT SERI
S. K. Deb Jul. 1985 13 p Presented at the SPIE Tech. Symp. East '85, Arlington, Va., 8 Apr. 1985
(Contract DE-AC02-83CH-100983)
(DE85-012144; SERI/TP-212-2749; CONF-8504109-2) Avail: NTIS HC A02/MF A01

The work described includes some aspects of the long-range, high-risk research being conducted at the Solid State Photovoltaic Research Branch at SERI. The areas covered include: amorphous silicon, high efficiency, multijunction solar cells, CdS/CuInSe2 thin films, crystal growth research and solid state theory. In each of these areas specific research projects which have long-range implications are highlighted. DOE

N86-10663# Los Alamos Scientific Lab., N. Mex.
RECENT DEVELOPMENT IN THE HOT DRY ROCK GEOTHERMAL ENERGY PROGRAM
P. R. Franke and G. J. Nunz 1985 5 p Presented at the Intern. Symp. on Geothermal Theory, Kailua Kona, Hawaii, 26 Aug. 1985
(Contract W-7405-eng-36)
(DE85-009562; LA-UR-85-934; CONF-850801-24) Avail: NTIS HC A02/MF A01

The hot dry rock programs effort has focused on the extraction technology development effort. The pair of approximately 400 m wells for the phase 2 engineering system of the Fenton Hill Project were completed. Hydraulic fracture operations were carried out to develop the geothermal reservoir. Advances were made in fracture identification techniques and instrumentation. To develop a satisfactory interwellbore flow connection the next step is to redrill the lower section of one of the wells into the fractured region. Chemically reactive tracer techniques are developed to determine the effective size of the reservoir area. Hot dry rock resource are estimated based upon geothermal gradiant data. DOE

N86-10664# Phillips Engineering Co., St. Joseph, Mich.
ANALYSIS OF ADVANCED RESIDENTIAL ABSORPTION HEAT PUMP CYCLES
B. A. Phillips 1985 22 p Presented at the DOE/ORNL Heat Pump Conf., Washington, D.C., 10 Dec. 1984
(Contract DE-AC05-84OR-21400)
(DE85-005244; CONF-841231-17) Avail: NTIS HC A02/MF A01

The development and proof testing of advanced absorption refrigeration cycle concepts is reported. The purpose is to develop a gas fired absorption heat pump for residential and small commercial applications that will produce a coefficient of perfor-

mance of at least 1.6 Btu heating and .7 Btu of cooling per Btu of gas input. The goals refer to air-to-air heat pump operation at the rating conditions of 47 F outdoor ambient in heating mode and 95 F ambient in cooling mode. For year-round residential and small commerical use other requirements were added. One was that the heat pump itself will provide all the heating and cooling required by the building over the majority of temperatures experienced in the United States (from -10 F to 110 F) without resource to supplemental heat. The means of making major improvements in gas fired absorption systems include the following categories: higher efficiency cycles, better fluids, and higher flues efficiencies. High efficiency absorption cycles were evaluated and the cycle and working fluid combination preferred for development of an advanced absorption test unit of residential size is selected. DOE

N86-10665# Sandia Labs., Albuquerque, N. Mex.
PHOTOVOLTAIC CONCENTRATOR ARRAY EVALUATION
A. B. Maish 1985 5 p Presented at INTERSOL '85 Solar Energy: The Diverse Solution, Montreal, 23 Jun. 1985
(DE85-013789; SAND-84-1775C; CONF-850604-6) Avail: NTIS HC A02/MF A01

Photovoltaic (PV) concentrator arrays are tested at the Sandia PV test facility in order to characterize the performance of the array subsystems during baseline tests and to evaluate array performance during extended operation. Array testing is designed to evaluate the complete array system (modules, structure, drives, and tracking controls) following module development and qualification testing and preceding full field tests. The major baseline tests characterize array electrical and thermal efficiency, sensitivity to tracking errors, full day tracking accuracy and array power requirements. DOE

N86-10666# Pacific Northwest Lab., Richland, Wash.
OVERVIEW OF WIND TURBINE SITING RESEARCH: PROSPECTING TO MICROSITING
L. L. Wendell May 1985 9 p Presented at the Delphi Workshop of Wind Energy Appl., Delphi, Greece, 20 May 1985
(Contract DE-AC06-76RL-01830)
(DE85-013496; PNL-SA-13032; CONF-8505171-1) Avail: NTIS HC A02/MF A01

The Federal Wind Energy Program of the United States' Department of Energy has directed research in wind behavior relevant to the economic extraction of power from the wind. The variability of the wind in time and space is important in this process. Topics of research related to wind turbine siting have included resource assessment, siting techniques, and techniques for documenting the variability of wind over space and time and the impact of this variability on energy capture. Siting techniques were developed to select areas most promising for wind energy development. The evaluation of candidate sites within these areas included a period of direct wind measurement so that long-term and hourly or subhourly time variability of the wind could be analyzed. In the study of spatial wind variability, turbine placement strategy has sought to minimize adverse effects of terrain or upwind machine wakes. Modeling techniques were developed to examine the variability of the wind over time and space and to correlate wind variability with turbine power output. Developments in terrain digitization and visual depiction and refined numerical flow modeling show promise of becoming operational tools that can be used in arrangement of turbines in clusters for maximum energy capture in complex terrain. DOE

N86-10667# Argonne National Lab., Ill.
CHEMICAL/HYDROGEN ENERGY SYSTEMS Annual Report, 1 Jan. - 31 Dec. 1984
May 1985 126 p
(Contract DE-AC02-76CH-00016)
(DE85-012742; BNL-51865) Avail: NTIS HC A07/MF A01

Activities conducted in 1984 within the Chemical/Hydrogen Energy Systems Program are described. Progress made is summarized for work in electrolytic hydrogen production, hydrogen storage materials, and transport systems. During 1984 the development of a technology base for hydrogen which would be used for coupling the abundant/renewable energy resources to the demand sector uses in the far term is emphasized. Hydrogen generation via water vapor electrolysis, three novel hydrogen storage concepts, hydrogen embrittlement of pipeline steels, and operational testing of advanced hydrogen systems in the hydrogen technology evaluation center (HTEC) are reported. Related International Energy Agency cooperative efforts and plans and major activities scheduled for 1985 are summarized. DOE

N86-10668# Chronar Corp., Princeton, N.J.
PHOTOVOLTAIC DEVICES USING A Si:H FROM HIGHER ORDER SILANES Final Subcontract Report, 1 Sep. 1983 - 31 Aug. 1984
A. E. Delahoy Mar. 1985 59 p
(Contract DE-AC02-83CH-10093)
(DE85-008804; SERI/STR-211-2637) Avail: NTIS HC A04/MF A01

The preparation of hydrogenated amorphous silicon (a-Si:H) films and photovoltaic devices by chemical vapor deposition (CVD) from higher silanes, and the properties of such films and devices are described. The motivation for this research is the prospect of preparing by a new technique a-Si:H having electronic properties similar to material prepared by the well-known glow discharge technique. Possible advantages of thermal CVD are the absence of ion bombardment, high deposition rates, efficient utilization of feedstock gases, lower levels of impurity incorporation, absence of pinholes, and greater material stability. Photochemical vapor deposition of a-Si:H from disilane is described and yield higher efficiency solar cells than thermal CVD. DOE

N86-10669# Centronic Ltd., Croydon (England).
MAKING THE RIGHT CHOICE
J. O. Miller 1985 5 p
Avail: NTIS HC A02/MF A01

Performance and cost criteria for choosing silicon photodiodes are given. Spectral response, response time, minimum detectable power, diode configuration, temperature effects, and operating circuits are discussed. Author (ESA)

N86-10670# Fachhochschule, Giessen (West Germany). Labor fuer Elektrische Messtechnik.
CONTRIBUTION OF WIND ENERGY TO THE ENERGY BALANCE OF A COMBINED SOLAR AND WIND ENERGY SYSTEM. PART 1: SYSTEM DESCRIPTION, DATA ACQUISITION AND SYSTEM PERFORMANCE Final Report, Jun. 1984
Rainer Ferger and Uwe Machens Bonn Bundesministerium fuer Forschung und Technologie May 1985 95 p refs In GERMAN; ENGLISH summary Sponsored by Bundesministerium fuer Forschung und Technologie 2 Vol.
(BMFT-FB-T-85-051-Vol-1; ISSN-0340-7608) Avail: NTIS HC A05/MF A01; Fachinformationszentrum, Karlsruhe, West Germany DM 20

A one-family house was equipped with a combined solar and wind energy system plus a night storage heater to measure the seasonal complementary contribution of wind and solar energy to energy demand. Project implementation, problems encountered and modifications to the initial system are described. Meteorological and operational data and house consumption data were recorded on computer-based measuring system. Data on the combined effects of and interdependence between solar collector and wind energy converter are discussed. Author (ESA)

N86-10671# Kernforschungsanlage, Juelich (West Germany). Programmgruppe.
CONTRIBUTION OF WIND ENERGY TO THE ENERGY BALANCE OF A COMBINED SOLAR AND WIND ENERGY SYSTEM. PART 2: COMPUTER-ASSISTED INVESTIGATIONS Final Report, Jun. 1984
Peter Wilhelm Wensierski Bonn Bundesministerium fuer Forschung und Technologie May 1985 141 p refs In GERMAN; ENGLISH summary Sponsored by Bundesministerium fuer Forschung und Technologie 2 Vol.
(BMFT-FB-T-85-052-Vol-2; ISSN-0340-7608) Avail: NTIS

HC A07/MF A01; Fachinformationszentrum, Karlsruhe, West Germany DM 29.50

A mathematical simulation model of the combined solar and wind energy system was used to determine the weak points of a wind-solar energy domestic system and to analyze the thermodynamic behavior of its different components and regulation functions. The simulation results are compared with the measured data to collect data for the optimization of the system for economical use and for determining the optimal complementarity of both energy sources. Different system configurations are studied for a better supply utilization according to regional climatology. Recommendations to improve the system performance are given taking into account an unchanged and a modified system configuration and the selection of the wind energy system. Author (ESA)

N86-10672# Groningen Rijksuniversiteit (Netherlands). Vrije Studierichting Scheikunde.

WIND ENERGY IN AGRICULTURE, A PROMISE [WINDENERGIE IN DE LANDBROUW, EEN BELOFTE]

Johan Koops Aug. 1982 43 p refs In DUTCH

(SS-45; B8476135) Avail: NTIS HC A03/MF A01

The investment possibilities of windpowered generators on dairy-farms in the northern Netherlands are investigated. Data concerning the energy consumption of five farms are statistically correlated with wind velocity distributions and the characteristics of a 10 kWh windmill. Using the buying and selling energy prices of the local power stations and the investment costs, the feasibility is estimated. The attitude of 105 farmers is assessed. Unless special energy storage provisions are made, the investment will not pay within 10 years, so is not interesting enough.

Author (ESA)

N86-10673# Groningen Rijksuniversiteit (Netherlands). Vrije-Studierichting Scheikunde.

WIND ENERGY, A FEASIBILITY INVESTIGATION FOR WIND MILLS IN AGRICULTURE [WINDENERGIE EEN HAALBAARHEIDSONDERZOEK NAAR WINDMOLLENS IN DE LANDBOUW]

Johan Koops Jan. 1982 33 p refs In DUTCH

(SS-45A; B8475856) Avail: NTIS HC A03/MF A01

The investment possibilities of windpowered generators on dairy-farms in the northern Netherlands are investigated. Data concerning the energy consumption of four farms are statistically correlated with wind velocity distribution data and the characteristics of a 10 kWh windmill. Using the buying and selling energy prices of the local power stations and the investment costs, the feasibility is estimated. Unless special energy storage provisions are made, the investment will not pay within 10 years. Author (ESA)

45 ENVIRONMENT POLLUTION

Includes air, noise, thermal and water pollution; environment monitoring; and contamination control.

N86-10674 Department of the Air Force, Washington, D.C.

MULTIPLE SITE LASER EXCITED POLLUTION MONITORING SYSTEM Patent

J. A. Gelbwachs, inventor (to Air Force) Issued 14 May 1985 6 p Supersedes AD-D009407

(AD-D011769; US-Patent-4,516,858; US-Patent-Appl-SN-347391; US-Patent-Class-356-437) Avail: US Patent and Trademark Office CSCL 13/2

A multiple site laser excited pollution monitoring system having a single laser located at a central location capable of providing a laser output beam, deflected in timed sequence, in a plurality of distinct different directions. Transmitting means, preferably in the form of a plurality of optical fibers, transmit the laser output beam in timed sequence to a plurality of remotely located laser excited pollution detectors (photoacoustic detector heads). Signals from the pollution detectors are transmitted to a signal processor and display unit also located at the central location. As a consequence thereof, a single laser can provide power for a plurality of laser excited detectors at a multiplicity of remote sites and thereby greatly reduce the expense involved in detecting the presence of pollutants at each of the plurality remote locations. Author (GRA)

N86-10675# California Univ., Irvine, Dayton, Ohio.

EVALUATION OF THE 90-DAY INHALATION TOXICITY OF PETROLEUM AND OIL SHALE JP-5 JET FUEL Technical Report, Jul. 1977 - Jul. 1983

C. L. Gaworski, J. D. MacEwen, E. H. Vernot, C. C. Haun, and H. F. Leahy Wright-Patterson AFB, Ohio AFAMRL Apr. 1985 40 p Prepared in cooperation with Naval Medical Research Inst.

(Contract F33615-80-C-0512)

(AD-A156815; AFAMRL-TR-85-035) Avail: NTIS HC A03/MF A01 CSCL 06/20

Subchronic 90-day inhalation studies were conducted to compare the toxicity of Petroleum and Oil Shale derived JP-5 jet fuel. Beagle dogs, Fischer 344 rats, and C57BL/6 mice were continuously exposed to JP-5 at concentrations of 150 mg/m cum and 750 mg/cum 3. Unexposed control groups were also maintained. All dogs and a portion of each rodent group were sacrificed and examined at exposure termination. Remaining rodents were held for observation up to 21 months postexposure. The most significant exposure related effect occurred in male rats, where JP-5 produced nephropathy characterized by hyaline droplets, necrosis, and intratubular casts. Accentuated tubular degeneration and medullary mineralization were noted in exposed rats held for long-term postexposure observation. Female rats were free of significant JP-5 related renal damage. Consistent with the pathologic changes in male rats exposed to 750 mg/cu m 3 were increased kidney weight and increased serum creatinine and BUN levels. Reduced body weight gains also occurred in male rats exposed to JP-5. No pathologic lesions were observed in dogs exposed to JP-5. Hepatocellular vacuolization and fatty change occurred in mice exposed to JP-5 from either source and in rats exposed to Shale JP-5. The results of this study suggest that there are no substantial differences between Petroleum and Shale JP-5. GRA

N86-10676# Argonne National Lab., Ill. Energy and Environmental Systems Div.

DEVELOPMENT OF THE MULTI-ATTRIBUTE HAZARD ASSESSMENT SYSTEM (MAHAS) AND ITS APPLICATION TO ENERGY-RELATED WASTE STREAMS

Donald J. Fingleton, Loren J. Habegger, Shen-Yann Chiu, Susan G. Barisas, and Ray H. Petersen (Illinois Inst. of Tech., Chicago) Apr. 1985 12 p refs Presented at the Air Pollution Control Assoc. Ann. Meeting and Exhibition, Detroit, 16 Jun. 1985

(Contract W-31-109-eng-38)

(DE85-010278; CONF-850612-2) Avail: NTIS HC A02/MF A01

The Multi-Attribute Hazard Assessment System (MAHAS), which determines the relative health risk associated with various waste streams, is described. The degree of hazard for several waste streams is presented. DOE

N86-10677# Oak Ridge National Lab., Tenn.

EXAMPLES OF REGIONAL ENVIRONMENTAL ASSESSMENT USING ACID DEPOSITION DATA

R. J. Olson, R. S. Turner, and L. J. Allison 1985 27 p refs Presented at the Natl. Conf. on Hazardous Wastes and Environ. Emergencies, Cincinnati, 14 May 1985

(Contract DE-AC05-84OR-21400)

(DE85-012903; CONF-8505149-1) Avail: NTIS HC A03/MF A01

Integrated assessments of acid deposition impacts require data on pollutant emissions, pollutant deposition, air quality, aquatic resources, crops, forests, and manmade materials. These data must have common spatial and temporal attributes that can be readily accessed for statistical analysis, modeling, and display purposes. The Acid Deposition Assessment Staff of Task Group I established the Acid Deposition Data Network (ADDNET) at Oak Ridge National Laboratory to provide accurate and reliable data to conduct assessment and policy analysis for the National Acid Precipitation Assessment Program (NAPAP). Two applications of

the ADDNET Data Base to assessment activities are described: estimation of the extent of sensitive lakes at risk to high atmospheric deposition and the mapping of regional soil properties according to hypothesized sensitivity criteria. Both examples cover New York and the New England states and show the integration of data from diverse sources for analyses. DOE

N86-10678# Oak Ridge National Lab., Tenn.
NATIONAL PERSPECTIVE ON ENVIRONMENTAL CONSTRAINTS TO HYDROELECTRIC DEVELOPMENT
S. G. Hildebrand, M. J. Sale, G. F. Cada, and J. M. Loar 1985 12 p Presented at the Natl. Conf. on Perspectives on Nonpoint Source Pollution, Kansas City, Mo., 19 May 1985
(Contract DE-AC05-84OR-21400)
(DE85-013111; CONF-8505148-1) Avail: NTIS HC A02/MF A01

Two issues are analyzed relative to problems associated with the concentration of dissolved oxygen in tailwaters below dams and instream flow requirements for fisheries. The need for and technical challenges related to assessment of the environmental effects of multiple-project development in river basins are discussed. Although the focus of the DOE program is on small-scale hydroelectric development, the issues discussed here are applicable to large-scale facilities as well. DOE

N86-10679# Oak Ridge National Lab., Tenn.
DEVELOPMENT AND EVALUATION OF MULTISPECIES TEST PROTOCOLS FOR ASSESSING CHEMICAL TOXICITY
C. T. Garten, Jr., ed., G. W. Suter, Jr., ed., and B. G. Blaylock, ed. Jun. 1985 158 p refs
(Contract DE-AC05-84OR-21400)
(DE85-013526; ORNL/TM-9225; Environ-Sci-Div-2354) Avail: NTIS HC A08/MF A01

Toxicity testing is a tool to assist in evaluating the hazards of chemicals to individual biological species. Multispecies toxicity tests are well developed. Three test systems were examined: the legume-Rhizobium symbiosis for N-fixation, soil microbial populations, and algal multispecies interactions. Test protocols were developed and tested using several different chemicals. Test protocols for the legume-Rhizobium and soil microorganisms systems were developed and are presented. DOE

N86-10680# Tennessee Valley Authority, Knoxville. Office of Natural Resources and Economic Development.
SEDIMENT CHARACTERIZATION. TASK 2: INSTREAM CONTAMINANT STUDY. VOLUME 2: APPENDICES
Apr. 1985 453 p
(Contract DE-AI05-84CR-21444)
(DE85-013503; DOE/OR-21444/T2-Vol-2) Avail: NTIS HC A20/MF A01

Data are appended for mercury concentration and particle size, and for Cesium 137 radionuclide concentrations. Quality control and sampling procedures are detailed. DOE

N86-10681# Department of Energy, Pittsburgh, Pa. Energy Technology Center.
MICROCOMPUTER AIDED CALCULATIONS OF PARAMETERS FOR SPRAY DRYER OPERATION
J. T. Yeh, D. F. Gyorke, H. W. Pennline, and C. J. Drummond 1985 31 p Presented at the Air Pollution Control Assoc. Ann. Meeting and Exhibition, Detroit, 16 Jun. 1985
(DE85-013468; CONF-850612-4) Avail: NTIS HC A03/MF A01

This paper provides a series of practical microcomputer programs that can be used as a tool by engineers and researchers working with spray dryers for combustion process effluent control. The microcomputer programs calculate flue gas composition (CO_2, N_2, O_2, H_2O, and SO_2) from the composition of the fuel. The residence time of the flue gas in a spray dryer can be estimated, and using values provided by the user for the flow of water and absorbent slurry in the spray dryer, the program recalculates the flue gas composition and heat capacity at the exit of the spray dryer without accounting for any SO_2 removal that could occur in the spray dryer. From these values and the system pressure, the dew point and flue gas temperature at the spray dryer exit are calculated, providing the approach to saturation resulting from this choice of operating parameters. This computer code would enable a process engineer to quickly evaluate effects of important process parameters, such as flue gas temperature at the inlet to the spray dryer, atomizer water feed rate, and absorbent slurry concentration and feed rate, on the operation of a spray dryer. DOE

N86-10682# Membrane Technology and Research, Inc., Menlo Park, Calif.
MEMBRANE RESEARCH IN ENERGY AND SOLVENT RECOVERY FROM INDUSTRIAL EFFLUENT STREAMS Annual Report, 5 Nov. 1983 - 31 Jan. 1985
R. W. Baker 1985 46 p
(Contract DE-AC07-83ID-12379)
(DE85-014583; DOE/ID-12379/T2) Avail: NTIS HC A03/MF A01

The overall feasibility of using membranes to separate organic vapors from effluent air streams was demonstrated. High-performance, ultrathin composite membranes were prepared and incorporated into small spiral wound membrane modules. The modules were evaluated on a series of organic solvent-air mixtures. Typical solvent fluxes with silicone rubber membranes were 2 to 10 litres sq. m day. An economic analysis of the process based on these fluxes and using reasonable values for the costs of the membrane modules and pump and system components shows that a process using these membranes would be economical with a number of effluent air streams. Process payback times vary from 4 to 10 months. Particularly suitable feed streams are those containing 0.5 to 2% of high value solvents that can be reused in the plant producing the stream. DOE

N86-10683# Tennessee Valley Authority, Knoxville. Office of Natural Resources and Economic Development.
SEDIMENT CHARACTERIZATION. TASK 2: INSTREAM CONTAMINANT STUDY, VOLUME 1
Apr. 1985 87 p refs
(DE85-013502; DOE/OR-21444/T2-Vol-1) Avail: NTIS HC A05/MF A01

The instream contaminant study is presented. The results of laboratory analyses of sediment samples collected downstream of the DOE facilities are analyzed. The samples were collected from June through November 1984. The sediment data and the procedures for the collecting, handling, and analyzing the samples are reported. Results are summarized in graphs and tables that include available criteria, standards, and background levels. The procedures and data are discussed but not evaluated. DOE

N86-10684# Pacific Northwest Lab., Richland, Wash.
RADIONUCLIDE COMPLEXATION IN XYLEM EXUDATES OF PLANTS
D. A. Cataldo, D. M. McFadden, T. R. Garland, and R. R. Wildung Apr. 1985 14 p refs Presented at the Seminar on the Speciation of Fission Prod. in the Environ., Oxford, England, 16 Apr. 1985
(Contract DE-AC06-76RL-01830)
(DE85-013446; PNL-SA-12549; CONF-850473-3) Avail: NTIS HC A02/MF A01

The plant xylem is the primary avenue for transport of nutrient and pollutant elements from the roots of aerial portions of the plant. It is proposed that the transport of reactive or hydrolyzable ions is facilitated by the formation of stable/soluble complexes with organic metabolites. The xylem exudates of soybean were characterized as to their inorganic and organic components, complexation patterns for radionuclides, both in vivo and in vitro, and for class fractions of exudates using thin-layer electrophoresis. The radionuclides Pu-238 and Fe-59 were found primarily as organic acid complexes, while Ni-63 and Cd-109 were associated primarily with components of the amono acid fraction. Technetium-99 was found to be uncomplexed and transported as the pertechnetate ion. It was not possible to duplicate fully complexes formed in vivo by back reaction with whole exudates or class fractions, indicating the possible importance of plant induction processes, reaction kinetics and/or the formation of mixed ligand complexes. DOE

N86-10685# Deutsche Forschungs- und Versuchsanstalt fuer Luft- und Raumfahrt, Oberpfaffenhofen (West Germany). Inst. fuer Physik der Atmosphaere.

AIRBORNE MEASUREMENTS OF THE BORDER-CROSSING AIR POLLUTION IN THE AREA BETWEEN WEIDEN AND HOF/ BAVARIA

Dieter Paffrath Feb. 1985 79 p refs In GERMAN; ENGLISH summary

(DFVLR-FB-85-25; ISSN-0171-1342) Avail: NTIS HC A05/MF A01; DFVLR, Cologne DM 19.50

An airborne measuring system was used under various weather conditions to determine the air pollution in an area of the German-Czechoslovakian frontier where pollution is particularly high due to exhaust gases produced by Czechoslovakian sources. Mass fluxes of SO2, NOx and NO were determined by airborne measurements of horizontal and vertical distributions of concentrations, and by wind profile measurements. The results show that the mass fluxes vary to a large extent depending on the fluctuating emission rate, on the weather situation, and on the season of the year. Author (ESA)

N86-10686# Radian Corp., Morrisville, N.C.

PROCEEDINGS: FIRST ANNUAL ACID DEPOSITION EMISSIONS INVENTORY SYMPOSIUM Report, Sep. 1984 - Apr. 1985

James B. Homolya, comp. May 1985 147 p refs Symp. held at Raleigh, N. Car., 3-4 Dec. 1984

(Contract EPA-68-02-3994)

(PB85-200004; EPA-600/9-85-015) Avail: NTIS HC A07/MF A01 CSCL 13B

The proceedings document a 2-day symposium on the progress in implementing the National Acid Precipitation Assessement Program (NAPAP) Task Group B's emission inventory programs. Topics included the development of emission factors for a wide range of pollutant emissions and the use of detailed emission inventories for atmospheric transport, transformation, and deposition modeling. The meeting:(1) provided detailed presentation and information transfer of the NAPAP emission inventory program; (2) illustrated and strengthened the relationship between the emission inventory data base and its users; and (3) compared and contrasted the NAPAP emission inventory with other on-going emission inventory development programs. GRA

N86-10687# Environmental Protection Agency, Research Triangle Park, N.C. Environmental Monitoring Systems Lab.

VOLATILE ORGANIC COMPOUNDS IN INDOOR AIR: A SURVEY OF VARIOUS STRUCTURES

J. D. Pleil, K. Oliver, and W. A. McClenny 1985 15 p refs Prepared in cooperation with Northrop Services, Inc.

(PB85-198356; EPA-600/D-85-100) Avail: NTIS HC A02/MF A01 CSCL 07D

Co-workers collected indoor air samples in their homes in SUMMA polished canisters. The whole air samples were analyzed for volatile organic compounds (VOCs) using cryogenic sample preconcentration and subsequent capillary column chromatography. Simultaneous flame ionization and electron capture detection yielded quantitative concentration data in a range 0.1 to 10 ppbv for 19 calibration compounds, vinyl chloride, vinyllidene chloride. Freon 113, chloroform, 1,2-dichloroethane, methyl chloroform, benzene, carbon tetrachlonide, trichloroethylene, cis-1,3-dichloropropene, trans-1,3-dichloropropene, toluene, 1,2-dibromoethane, tetrachloroethylene, chlorobenzene, b-xylene, benzyl chloride and hexachlorobutadiene. These data are presented in three sample groups: summer indoor samples, winter indoor samples, and combined summer and winter outdoor samples. GRA

N86-10688# Engineering-Science, Inc., Fairfax, Va.

EMISSIONS OF NOx, SOx AND VOC FROM ANTROPOGENIC SOURCES

D. A. Toothman and J. D. Mobley 1985 9 p refs

(Contract EPA-68-02-3996)

(PB85-193530; EPA-600/D-85-106) Avail: NTIS HC A02/MF A01 CSCL 05B

A 1980 emisssions inventory for use in the National Acid Precipitation Assessment Program (NAPAP) is discussed. The current inventory contains point source data for 50,200 plants with more than 201,000 emission points and area source data for the 3,069 counties in the 48 contiguous States and the District of Columbia. Emissions of SO2, NOx, VOC, sulfates, ammonia, CO, and particulates are included in the inventory, but the paper focuses on SO2, NOx, and VOC which are of primary interest for acid deposition research. NAPAP Version 4.0 emissions of SO2, NOx, and VOC are 27.1, 23.7 and 23.3 million tons per year, respectively. The NAPAP report represents the best detailed inventory of emissions on a national scale that has been developed to date. Nevertheless, additional improvements are planned, focusing on major point sources. GRA

N86-10689# Battelle Columbus Labs., Ohio.

EVALUATION OF PASSIVE SAMPLING DEVICES (PSDS)

R. W. Coutant Apr. 1985 74 p refs

(Contract EPA-68-02-3487)

(PB85-196418; EPA-600/4-85-034) Avail: NTIS HC A04/MF A01 CSCL 14B

This study is to evaluate the performance of the EPA passive sampling device (PSD) for ambient level volatile organic compounds (VOC's); to develop an understanding of the mechanics of passive sampling using reversible adsorption; and to apply this understanding to development of an improved PSO that is usable for sampling of VOC's over periods of 8 to 24 hours. Laboratory and limited field evaluations of the standard and modified RSD's were conducted and a model relating sorbent properties and device design to samplining rates was developed. The results show the standard PSD's to be useful for sampling of VOC's having large retention volumes. Modified PSD's having greatly reduced sampling rates show promise for sampling compounds having retention volumes as low as 5 to 10 L/g over 8 to 24 hour sampling periods. GRA

46 GEOPHYSICS

Includes aeronomy; upper and lower atmosphere studies; ionospheric and magnetospheric physics; and geomagnetism.

For space radiation see *93 Space Radiation.*

N86-10690 North Carolina Univ., Chapel Hill.

CRETACEOUS AND CENOZOIC STRATIGRAPHY OF THE UPPER AND MIDDLE COASTAL PLAIN, HARNETT COUNTY AREA, NORTH CAROLINA Ph.D. Thesis

Suellen Cabe 1984 121 p

Avail: Univ. Microfilms Order No. DA8508571

Criteria for differenting and correlating Cretaceous sediments and younger surficial deposits were determined. The results indicate that each of the units can be distinguished by a particular set of grain size and clay mineral characteristics. The Cretaceous units in the study area are the Cape Fear and Middendorf Formations. The Cape Fear Formation is characterized by smectite in the < 0.002 mm fraction and by finer sand size and higher percentages of silt and clay than the Middendorf Formation, which contains no smectite and is dominated by kaolinite in the clay fraction. Dissert. Abstr.

N86-10691 Iowa Univ., Iowa City.

STRATIGRAPHY, PETROLOGY, DEPOSITIONAL AND POST-DEPOSITIONAL HISTORIES AND THEIR EFFECTS UPON RESERVOIR PROPERTIES OF THE PARKMAN FORMATION OF THE MESA VERDE GROUP, POWDER RIVER BASIN, WYOMING Ph.D. Thesis

Ahmet Umran Dogan 1984 282 p

Avail: Univ. Microfilms Order No. DA8507934

The depositional system within which deposition of the Upper Cretaceous Parkman Formation (= Parkman Sandstone Member

of the Mesaverde Formation) in the Wyoming portion of the Powder River Basin took place, was delineated using a combination of data from outcrops, subsurface cores, and geophysical well logs. The post-depositional history of these rocks was determined, semi-quantitative compositional analyses of authigenic components were made, and paragenetic sequences were established with the aid of scanning electron microscope and transmission electron microscope both equipped with energy dispersive X-ray micro-analyzer. Dissert. Abstr.

N86-10692 California Univ., Santa Barbara.
PALEONTOLOGY AND STRATIGRAPHY OF LOWER CAMBRIAN AND UPPER PROTEROZOIC SEDIMENTS, CABORCA REGION, NORTHWESTERN SONORA, MEXICO Ph.D. Thesis
Mark Allan Schulte McMenamin 1984 229 p
Avail: Univ. Microfilms Order No. DA8509445

Shelly fossils from a homoclinal sequence of sediments spanning the Precambrian-Cambrian transition in the Caborca region of northwestern Sonora, Mexico, are among the oldest in North America. These fossils, together with new finds of Lower Cambrian trilobites and trace fossils, permit correlations between the Caborca sequence and Lower Cambrian sediments of Nevada and eastern California (USA). The Lower Cambrian Nevadella and Fallotaspis zones of Fritz (1972) can now be recognized in the La Cienega and Puerto Blanco Formations of the Caborca sequence. Because of the abundant fossils, the stratigraphic interval between the top of the Nevadella zone and the lowest shelly fossils can be subdivided into six new assemblages (in ascending stratigraphic order): the (1) Sinotubulites, (2) Monomorphichnus multilineatus, (3) Fallotaspis cf. F. tazemmourtensis, (4) Fallotaspis-Judomia, (5) Nevadia, and (6) Nevadella assemblages. Dissert. Abstr.

N86-10693 Pittsburgh Univ., Pa.
DYNAMIC LITHOSTRATIGRAPHY AND PALEECOLOGY OF UPPER MISSISSIPPI (CHESTERIAN) STRATA OF THE NORTH-CENTRAL APPALACHIAN BASIN Ph.D. Thesis
David Kevin Brezinski 1984 132 p
Avail: Univ. Microfilms Order No. DA8504406

Chesterian strata of the northcentral Appalachians consist of intertonguing marine carbonates and paralic to terrestrial clastics. The basal unit, the Loyalhanna, rests unconformably upon lower Mississippian Pocono sandstones and accumulated under conditions of episodic sea level transgression. The Loyalhanna, in most places is a festoon cross-bedded, sandy lime grainstone, but a nearshore interbedded carbonate-shale facies is also recognized. Minor oscillations in sea level resulted in a vertical repetition of marine and nonmarine rocks after which a major episodic marine transgression began which resulted in the deposition of the Wymps Gap Limestone. Two facies of the Wymps Gap developed; a calcareous sandstone and thinly interbedded wackestone and shale. Topographic relief created by a thick lobe of underlying clastics resulted in the formation of a local carbonate platform along the edge of which developed a carbonate sand shoal, containing grainstone. Dissert. Abstr.

N86-10694 Ohio State Univ., Columbus.
A NUMERICAL MODEL FOR THE ESTIMATION OF SOLAR RADIATION ON RUGGED TERRAIN Ph.D. Thesis
Evelyn Carole Anderson 1985 252 p
Avail: Univ. Microfilms Order No. DA8510545

A physically-based numerical model has been developed to estimate the recepit of solar radiation for high-altitude, rugged terrain. Previously, similar models have been developed and tested for locations with surface elevations well below 1000 m, and their usefulness has not before been shown for higher elevations. The model was employed to estimate the daily receipt of solar radiation on a horizontal surface for three high-altitude stations: Albuquerque, NM; El Paso, TX; and Great Falls, MT. The results of this simulation indicate that, for both clear and cloudy conditions, the model produced results as accurate as those which have been obtained using a similar algorithm for low-altitude locations. The use of the model for non-horizontal terrain was demonstrated using several idealized surfaces including a valley with a north-south axis and a bowl-shaped depression. Dissert. Abstr.

N86-10695 Wisconsin Univ., Milwaukee.
ALTITUDINAL DISTRIBUTION OF GRANITIC LANDFORMS IN THE SOUTH CENTRAL SIERRA NEVADA, CALIFORNIA Ph.D. Thesis
Mark F. Windsor 1984 498 p
Avail: Univ. Microfilms Order No. DA8509271

The study verifies three hypotheses relating weathered and exhumed granitic landforms to altitude in the Sierra Nevada. (1) Granitic landform types are distributed in distinctive patterns related to altitude. (2) Assemblages of these landform types are regionalized by altitude. (3) These landform distributions reflect the altitudinally differentiated morphogenetic environments. The study focuses on unglaciated granitic landform distributions in three sample transects on the western slope; theories of origins and ages of landforms and paleo-morphogenetic environments provide supportive evidence for interpretation of the distributions. Three regions of wheatered granitic landform assemblages are identified; the Grusified Corestone - Tor Region at low altitudes, the Tor and Dome region at intermediate altitudes and the Felsburg - Felsenmeer Highland Region at high altitudes. Dissert. Abstr.

N86-10696 Johns Hopkins Univ., Baltimore, Md.
ULTRAVIOLET SPECTROSCOPY OF THE EARTH'S DAYGLOW AND MAGNETOSPHERE CLEFT Ph.D. Thesis
Richard Wayne Eastes 1985 230 p
Avail: Univ. Microfilms Order No. DA8510411

Separate observations, made from sounding rockets, of the ultraviolet photon spectrum emitted by the Earth's dayglow and the magnetospheric cleft are described. The two sets of observations are complementary. In the dayglow, excitation is by photoelectron impact and ultraviolet solar photons, while in the cleft, excitation by energetic particle impact dominates. The different excitation mechanisms and energy spectra of the exciting particles results in significantly different spectra. These differences lead to a better understanding of the excitation mechanisms responsible for emissions in the Earth's atmosphere. The dayglow spectra are at higher resolution than any previous observations over a broad range of ultraviolet wavelengths. The observation of the cleft's emissions are the first sounding rocket measurements of the ultraviolet emissions from this regional of the atmosphere. Dissert. Abstr.

N86-10697 State Univ. Coll. of New York, Buffalo.
GEOTHERMAL INFLUENCES ON THE LONG-TERM THICKNESS OF THE MECHANICAL LITHOSPHERE DURING FLEXURE Ph.D. Thesis
Robert F. DeRito 1985 111 p
Avail: Univ. Microfilms Order No. DA8510323

The fundamental relationship between temperature and the thickness of the mechanical lithosphere may be demonstrated by combining realsistic rock rheology with a simple flexure model. The temperature dependent, nonlinear Maxwell law is the simplest rheology capable of reconciling experimental creep data with the apparently elastic behavior of the lithosphere in the long term. The Maxwell model attains effective thicknesses that are consistent with those obtained empirically using elastic flexure models, since the former reaches a quasi-steady state in the long term. Rheological zones develop in the model lithosphere due to the increase of temperature with depth. An upper, predominantly elastic or lithospheric zone yields to a lower, predominantly viscous, or asthenospheric zone through a narrow vicoelastic transition zone. The initial thickness of the lithospheric plate is relatively unimportant during the long term. Dissert. Abstr.

N86-10698 Columbia Univ., New York.
FUNDAMENTAL STUDY OF THE CLOSURE PROPERTY OF JOINTS Ph.D. Thesis
Stephen Ray Brown 1984 242 p
Avail: Univ. Microfilms Order No. DA8511484

In three papers, the results of a fundamental study of joint

closure are presented. Considering the joint surfaces to have random topography, which remains elastic during deformation, paper 1 presents a derivation of the constitutive law relating the joint closure to the applied normal stress. The theory shows that the joint closure depends as much on the topography of the contacting surfaces as on the elastic properties of the material. Paper 2 also discusses the application of the theory to mated joints, where the surfaces are highly correlated. The results of papers 1 and 2 show that the elastic joint closure depends only on a limited band of topographic features, which is defined by the correlation between the surfaces and the onset of plastic flow. Paper 3 presents the results of a general study of the topography of natural rock surfaces, including surfaces of tension fractures, a frictional wear surface, and a bedding pine surface.Dissert. Abstr.

N86-10699 California Univ., Santa Barbara.
STRUCTURAL DISCONTINUITY WITHIN THE SOUTHERN CALIFORNIA CONTINENTAL MARGIN: SEISMIC AND GRAVITY MODELS OF THE WESTERN TRANSVERSE RANGES Ph.D. Thesis
Barry Ruland Keller 1984 108 p
Avail: Univ. Microfilms Order No. DA8509435

Crustal models of P wave velocity structure and bulk density along a north-south profile across the western Transverse Ranges of California are based on published seismic reflection profiles, a seismic refraction experiment using shots at sea to receivers on land and at sea, Pn and teleseismic arrivals at permanent seismic stations, and published gravity data on land and at sea. The seismic ray trace model is further constrained by two intersecting east-west crustal refraction profiles. The density model is constrained by an auxiliary profile tying the outer Borderland to oceanic lithosphere. A range of density models is evaluated based on the range of densities reported for particular P wave velocities and the preferred model is selected by regional seismic criteria. Lateral variations in the crust are resolved to greater than 10 km depth. Variations observed in teleseismic arrival times are substantially accounted for by the crustal velocity model. The western Transverse Ranges are not in isostatic balance, the south side being heavier than the north side. Dissert. Abstr.

N86-10700 Texas Univ., El Paso.
CRUSTAL STRUCTURE OF THE SOUTHERN RIO GRANDE RIFT DETERMINED FROM SEISMIC REFRACTION, SURFACE WAVE DISPERSION, AND GRAVITY DATA Ph.D. Thesis
Yehia Ahmed Sinno 1984 195 p
Avail: Univ. Microfilms Order No. DA8509026

A series of seismic refraction profiles have been recorded in south central New Mexico with the goal of determining the crustal structure in the southern Rio Grande rift. These lines consist of three regional profiles a reversed E-W line across the rift, an unreversed N-S axial line, and an unreversed NW-SE line. The reversed E-W line shows no significant dip along the Moho (approx. 32 km thick crust) and 7.7 km/sec Pn velocity. Results from the N-S axial line and the NW-SE line indicate an apparent Pn velocity of 7.95 km/sec and significant dip along the Moho in the south and southeast directions, respectively. When interpreted together, these data indicate a crustal thinning in the southern rift of 4 to 6 km with respect to the northern rift and the adjacent Basin and Range province. The regional Pn velocity is approximately 7.7 km/sec. An analysis of regional Bouguer gravity anomalies in the area is consistent with these seismic results and indicate the crust is thinnest (approx. 26 km) within a oval N-S trending area near El Paso, Texas. Dissert. Abstr.

N86-10701 Hawaii Univ., Honolulu.
A BOUNDARY LAYER FLOW MODEL FOR AREAS OF COMPLEX TERRAIN Ph.D. Thesis
David Andre Eramus 1984 153 p
Avail: Univ. Microfilms Order No. DA8508776

In areas of complex terrain, the topography affects the boundary layer wind field. When the basic flow is at least of moderate strength, mechanical effect will dominate thermal effects in determining the topographically modified wind field. A boundary layer flow model is developed for application under these conditions. The model is applied to a complex terrain area on the island of Oahu, Hawaii. Objective and subjective analyses of the observed and modeled winds are performed to evaluate the model. These analyses show that the model is able to simulate the topographically modified wind field successfully when conditions for which the model is developed prevail. The results also suggest that the model may be applied successfully in other complex terrain areas with wind regimes similar to that in the experimental area. Dissert. Abstr.

N86-10702 Tennessee Univ., Knoxville.
THE EFFECTS OF OROGRAPHY ON LAND-ATMOSPHERE TURBULENT EXCHANGE PROCESSES Ph.D. Thesis
John Speridon Theon 1985 232 p
Avail: Univ. Microfilms Order No. DA8511404

An experimental investigation of the effects of orography on the boundary layer was conducted in February 1984 in the vicinity of Boulder, Colorado. Wind and thermodynamic data were acquired principally by the NASA B-57B aircraft but also with rawinsondes, the Boulder Atmospheric Observatory meteorological tower, the PROFS Mesonet surface stations, the radar wind profiler network, and the Boulder wind network. The aircraft, which was instrumented to measure 3-axis mean winds and turbulence fluctuations as well as temperature and moisture information, was flown in a box-like pattern at multiple levels from approximately 305m (1000 ft) to 3140m (10,300 ft) above the surface. These data provided a three-dimensional view of the flow in the lee of the Rocky Mountains, including the front range, the Flat Irons. Separation of the flow from the sharp edges of orographic features was detected. Indication of flow reattachment and even reverse flows on the plain downstream of the mountain range was evident. Dissert. Abstr.

N86-10703 Instituut TNO voor Bouwmaterialen en Bouwconstructies, Delft (Netherlands).
SIMULATION OF THE ATMOSPHERIC BOUNDARY LAYER IN THE LARGE WIND TUNNEL OF THE TNO INSTITUTE FOR BUILDING MATERIALS AND CONSTRUCTIONS (IBBC). PART 1: THEORY [SIMULATIE VAN DE ATMOSFERISCHE GRENSLAAG IN DE GROTE WINDTUNNEL VAN HET IBBC. DEEL 1: THEORIE]
P. Vermeulen 1983 80 p refs In DUTCH
(BI-76-39/08.7.23100-Pt-1) Avail: Issuing Activity

The turbulence structures describing of wind tunnel simulated and real atmospheric boundary layers (ABL) were compared, to determine the flow around and dynamic load on buildings. A 1 m thick wind tunnel boundary layer was formed on a rough foreground of 17 m length. The scale value between prototype and wind tunnel model was determined. Author (ESA)

N86-10704 Instituut TNO voor Bouwmaterialen en Bouwconstructies, Delft (Netherlands).
SIMULATION OF THE ATMOSPHERIC BOUNDARY LAYER IN THE LARGE WIND TUNNEL OF THE TNO INSTITUTE FOR BUILDING MATERIALS AND CONSTRUCTION (IBBC). PART 2: EXPERIMENTS [SIMULATIE VAN DE ATMOSFERISCHE GRENSLAAG IN DE GROTE WINDTUNNEL VAN HET IBBC. DEEL 2: EXPERIMENTEN]
P. Vermeulen 1983 60 p ref In DUTCH 2 Vol.
(BI-76-39/08.7.23100-Pt-2) Avail: Issuing Activity

Experiments to create a workable simulation of the atmospheric boundary layer and to verify the derived relation between the power law exponent and roughness height were performed. Using a power law exponent x = 0.26, a foreground consisting of 3.75 x 2.5 x 2.5 cm cubes with a 0.17 density and 1.5 slenderness, and a scale value of 1:300, it is shown that turbulence intensity, energy spectra, longitudinal integral length scales and coherences are in quantitatively and qualitatively well simulated. Author (ESA)

N86-10705*# Roberts Associates, Inc., Vienna, Va.
COMPUTATION OF FLOW REGIMES IN PARAMETER SPACE FOR THE AGCE Final Report, 13 Sep. 1984 - 13 Jul. 1985

Glyn O. Roberts 27 Jul. 1985 20 p refs
(NASA Order H-78181-B)
(NASA-CR-178480; NAS 1.26:178480; RAI-84-AG-4) Avail: NTIS HC A02/MF A01 CSCL 04A

This report describes the results of a small study program in support of the design studies for NASA's proposed Atmospheric General Circulation Experiment (AGCE). The proposed experiment will model the atmosphere using a hemispherical layer of a dielectric fluid such as silicone oil, heated at the equator, and with a large radial AC electric field producing a temperature-dependent radial body force similar to radial gravity. The effect of terrestrial gravity on the experiment can be eliminated by doing the experiment in space flight. The author developed a series of three computer models to support these design studies. The first two calculate axisymmetric solutions and their stability to small non-axisymmetric perturbations. The third computes three-dimensional solutions. These codes allow the option of solving problems in a cylindrical geometry as well as a rather generally defined spherical layer.
B.W.

N86-10706# Universite des Sciences et Techniques du Languedoc, Montpellier (France). Dept. de Physique Mathematique.
FORMATION OF WAVES BY GROUND MOTION
Pierre C. Sabatier [1984] 102 p refs Submitted for publication (PM/84/09) Avail: NTIS HC A06/MF A01

Models devised for understanding the formation of water waves by ground motion were surveyed. The models which are used to understand the formation of water waves by ground motion are described. Theoretical models, real events, and a survey of secondary effects are presented.
EAK

N86-10707*# Jet Propulsion Lab., California Inst. of Tech., Pasadena.
CHEMICAL KINETICS AND PHOTOCHEMICAL DATA FOR USE IN STRATOSPHERIC MODELING
W. B. DeMore, J. J. Margitan, M. J. Molina, R. T. Watson, D. M. Golden, R. F. Hampson, M. J. Kurylo, C. J. Howard, and A. R. Ravishankara 1 Jul. 1985 226 p refs
(Contract NAS7-918)
(NASA-CR-176198; NAS 1.26:176198; JPL-Pub-85-37) Avail: NTIS HC A11/MF A01 CSCL 04A

Rate constants and photochemical cross sections are presented. The primary application of the data is for modeling of the stratospheric processes, with particular emphasis on the ozone layer and its possible perturbation by anthropogenic and natural phenomena.
E.A.K.

N86-10708# Aerospace Corp., El Segundo, Calif. Space Sciences Lab.
POTENTIAL STRUCTURES AND PARTICLE ACCELERATION ON AURORAL FIELD LINES
D. J. Gorney 1 May 1985 31 p
(Contract F04701-83-C-0084)
(AD-A156694; TR-0084A(5940-05)-6; SD-TR-85-12) Avail: NTIS HC A03/MF A01 CSCL 04/1

In the 1970's major advances in the understanding of auroral processes were brought about by observations of plasmas and electric fields within the regions of space responsible for auroral particle acceleration. The major contribution of these observations was the verification of the existence of electric fields with components parallel to the magnetic field over large regions of altitude (1000 to 20000 kilometers). These electric fields constitute potential drops of several kilovolts, accelerating magnetospheric electrons downward to form the aurora and ionospheric ions upward, where they contribute significantly to the magnetospheric hot ion population. Perpendicular spatial scales of about 100 kilometers are most common, although finer scales have been observed embedded, and individual small amplitude double layers occur on much smaller parallel spatial scales. More recently, the same data sets have revealed the existance of about 100 V electric potential drops directed downward in return current regions. Downward electric fields are in a direction to accelerate electrons out of the ionsphere and tend to retard the propagation of ions upward. An association between upflowing electron beams and transversely heated ions at low altitude has been noted, and a casual relationship between downward electric fields and ion conics is suggested.
GRA

N86-10709# Kiruna Geophysical Inst. (Sweden).
[ACTIVITIES REPORT IN GEOPHYSICS] Annual Report, 1984
1984 53 p refs Sponsored by Swedish Governement and Swedish Board for Space Activities
(KGI-188; ISSN-0347-6405) Avail: NTIS HC A04/MF A01

Acceleration mechanisms for auroral particles; magnetospheric wave-particle interactions as observed primarily in the particle populations; composition measurements in the hot magnetospheric plasma; convection electric field effects on magnetospheric particle populations; and EISCAT related research are discussed. Rocket and satellite sounding are described.
Author (ESA)

N86-10710# Systems Applications, Inc., San Rafael, Calif.
TECHNICAL CONSIDERATIONS IN REGIONAL AEROSOL MODELING
C. Seigneur and H. M. Barnes 1985 39 p refs
(Contract EPA-68-02-4076)
(PB85-193027; EPA-600/D-85-083) Avail: NTIS HC A03/MF A01 CSCL 04A

This work addresses the theoretical aspects of the behavior of aerosol particles in the atmosphere. In particular, it focuses on mathematical modeling of atmospheric aerosols at the regional scale (3001000 km). The paper discusses the evolution of the model in a stepwise fashion. First is considered the mathematical formulation of the transport mechanisms used. Second is a synopsis of the physical processes that affect aerosol dynamics of the aerosol population. Then a review of the pertinent chemistry of atmospheric aerosols is given. Various mathematical models of aerosol dynamics and chemistry and the formulation of the complete aerosol model are discussed. Concluding remarks include suggestions for future work such as the treatment of aerosols in clouds and model evaluation with data.
Author (GRA)

N86-10386*# Jet Propulsion Lab., California Inst. of Tech., Pasadena. Ground Antennas and Facilities Engineering Section.
SEISMIC ANALYSIS OF THE LARGE 70-METER ANTENNA, PART 1: EARTHQUAKE RESPONSE SPECTRA VERSUS FULL TRANSIENT ANALYSIS
K. Kiedron and C. T. Chian *In its* The Telecommun. and Data Acquisition Progr. Rept. 15 Aug. 1985 p 31-42 ref (For primary document see N86-10382 01-31)
Avail: NTIS HC A10/MF A01 CSCL 08K

N86-10401*# Jet Propulsion Lab., California Inst. of Tech., Pasadena. Tracking Systems and Applications Section.
MOBILE VLBI AND GPS MEASUREMENT OF VERTICAL CRUSTAL MOTION
P. M. Kroger, J. M. Davidson, and E. C. Gardner (Kalamazoo Coll.) *In its* The Telecommun. and Data Acquisition Progr. Rept. 15 Aug. 1985 p 185-198 refs (For primary document see N86-10382 01-32)
Avail: NTIS HC A10/MF A01 CSCL 08E

N86-10600*# Geological Survey, Sioux Falls, S. Dak. EROS Data Center.
SOME OPINIONS ON REMOTE SENSING AND GEOLOGIC STUDIES
G. Bryan Bailey *In* JPL Rept. of the Workshop on Geol. Appl. of Remote Sensing to the Study of Sedimentary Basins 1 Aug. 1985 p 29-30 ERTS (For primary document see N86-10599 01-43)
Avail: NTIS HC A05/MF A01 CSCL 08G

N86-10601*# Hawaii Univ., Honolulu. Planetary Geosciences Div.
POSITION PAPER: WORKSHOP ON GEOLOGIC APPLICATIONS

OF REMOTE SENSING TO THE STUDY OF SEDIMENTARY BASINS
Pamela L. Blake, Robert B. Singer, and Eileen Bruckenthal *In* JPL Rept. of the Workshop on Geol. Appl. of Remote Sensing to the Study of Sedimentary Basins 1 Aug. 1985 p 31-32 ERTS (For primary document see N86-10599 01-43)
Avail: NTIS HC A05/MF A01 CSCL 08G

N86-10602*# University of Southern California, Los Angeles. Dept. of Geological Sciences.
CHRONOLOGIC ANALYSIS OF TERRESTRIAL SEDIMENTS AND BASIN EVOLUTION
Douglas Burbank *In* JPL Rept. of the Workshop on Geol. Appl. of Remote Sensing to the Study of Sedimentary Basins 1 Aug. 1985 p 33-36 ERTS (For primary document see N86-10599 01-43)
Avail: NTIS HC A05/MF A01 CSCL 08G

N86-10603*# Jet Propulsion Lab., California Inst. of Tech., Pasadena.
TERTIARY AND QUATERNARY RESEARCH WITH REMOTE SENSING METHODS
James E. Conel *In its* Rept. of the Workshop on Geol. Appl. of Remote Sensing to the Study of Sedimentary Basins 1 Aug. 1985 p 37-40 refs ERTS (For primary document see N86-10599 01-43)
Avail: NTIS HC A05/MF A01 CSCL 08G

N86-10605*# Washington Univ., St. Louis, Mo. McDonnell Center for the Space Sciences.
[ANALYSIS OF REMOTE SENSING DATA]
E. A. Guiness, M. Sultan, and R. E. Arvidson *In* JPL Rept. of the Workshop on Geol. Appl. of Remote Sensing to the Study of Sedimentary Basins 1 Aug. 1985 p 45-46 ERTS (For primary document see N86-10599 01-43)
Avail: NTIS HC A05/MF A01 CSCL 08G

N86-10606*# Jet Propulsion Lab., California Inst. of Tech., Pasadena.
REMOTE STRATIGRAPHIC AND STRUCTURAL ANALYSIS: MULTISENSOR RESULTS IN THE WIND RIVER/BIGHORN BASIN AREA, WYOMING
Harold R. Lang, Earnest D. Paylor, and James E. Conel *In its* Rept. of the Workshop on Geol. Appl. of Remote Sensing to the Study of Sedimentary Basins 1 Aug. 1985 p 51-52 ERTS (For primary document see N86-10599 01-43)
Avail: NTIS HC A05/MF A01 CSCL 08G

N86-10607*# Lamont-Doherty Geological Observatory, Palisades, N. Y.
STRUCTURAL MAPPING OF FOLDED SEDIMENTARY ENVIRONMENTS FROM SATELLITE IMAGES: AN EXAMPLE FROM CENTRAL ASIA
William Leith *In* JPL Rept. of the Workshop on Geol. Appl. of Remote Sensing to the Study of Sedimentary Basins 1 Aug. 1985 p 53-54 refs ERTS (For primary document see N86-10599 01-43)
Avail: NTIS HC A05/MF A01 CSCL 08G

N86-10608*# Jet Propulsion Lab., California Inst. of Tech., Pasadena.
FORELAND BASIN STRUCTURES AND REMOTE SENSING
Earnest D. Paylor *In its* Rept. of the Workshop on Geol. Appl. of Remote Sensing to the Study of Sedimentary Basins 1 Aug. 1985 p 55-56 ERTS (For primary document see N86-10599 01-43)
Avail: NTIS HC A05/MF A01 CSCL 08G

N86-10609*# Carnegie Museum of Natural History, Pittsburgh, Pa. Section of Vertebrate Fossils.
PALEOGENE VERTEBRATE PALEONTOLOGY, GEOLOGY AND REMOTE SENSING IN THE WIND RIVER BASIN
Richard K. Stucky and Leonard Krishtalka *In* JPL Rept. of the Workshop on Geol. Appl. of Remote Sensing to the Study of Sedimentary Basins 1 Aug. 1985 p 59-60 refs ERTS (For primary document see N86-10599 01-43)
Avail: NTIS HC A05/MF A01 CSCL 08G

N86-10620*# Jet Propulsion Lab., California Inst. of Tech., Pasadena.
AGE-DATING VOLCANIC AND ALLUVIAL SURFACES WITH MULTIPOLARIZATION DATA
Tom G. Farr *In its* NASA/JPL Aircraft SAR Workshop Proc. 15 Jun. 1985 p 31-36 refs Original contains color illustrations (For primary document see N86-10615 01-43)
Avail: NTIS HC A05/MF A01 CSCL 08G

47 METEOROLOGY AND CLIMATOLOGY

Includes weather forecasting and modification.

N86-10711 Royal Netherlands Meteorological Inst., De Bilt. Werkgroep Grenslag.
LIST OF PUBLICATIONS ON THE 200 m METEOROLOGICAL MAST AT CABAUW, THE NETHERLANDS
A. G. M. Driedonks Feb. 1985 16 p refs
(KNMI-FM-85-6) Avail: Issuing Activity
About 120 publications on the site and installation, and impact of a 200 m tower used to study atmospheric boundary layer phenomena are listed. Author (ESA)

N86-10712# Naval Weapons Center, China Lake, Calif.
SURFACE WINDS AT NWC (NAVAL WEAPONS CENTER): 1964 - 1982 Final Report
A. R. Kelso and R. W. Evert Feb. 1985 75 p
(AD-A156660; AD-E900456; NWC-TP-6572) Avail: NTIS HC A04/MF A01 CSCL 04/2
This report contains surface wind data for the China Lake Complex of the Naval Weapons Center (NWC), China Lake, California. The data, collected from 1964 through 1982, are presented in graphs and tables. These illustrations depict monthly as well as daily time segment compilations of wind directional frequencies and average speeds. This information will be useful to Center personnel in planning, scheduling, and evaluating mission-related tests. GRA

N86-10713# Air Command and Staff Coll., Maxwell AFB, Ala.
ROTARY-WING OPERATIONS IN A MICROBURST ENVIRONMENT
E. E. Mace Apr. 1985 43 p
(AD-A156695; ACSC-85-1670) Avail: NTIS HC A03/MF A01 CSCL 04/2
Microburst wind shear has been directly or indirectly involved in 28 aircraft incidents or accidents since 1964. Following the last major aircraft accident attributed to microburst wind shear in 1982, a major effort was undertaken to study the hazard. The majority of the work that has been accomplished deals with the publicity of the phenomenon to the aviation community and with acceptable methods of detecting it before it occurs. This study explores the background, detection systems and special considerations of helicopter operations in relation to microburst induced wind shear. Included are subjective hazards, aircraft response and recommended pilot actions to successfully penetrate the wind shear if inadvertently encountered. The study recommends that it be used as an interim measure to supplement existing microburst wind shear information and that additional helicopter microburst testing be conducted. Author (GRA)

N86-10714# Naval Research Lab., Washington, D. C.
THE LIU, KATSAROS, AND BUSINGER (1979) BULK ATMOSPHERIC FLUX COMPUTATIONAL ITERATION PROGRAM IN FORTRAN AND BASIC
W. T. Liu and T. V. Blanc 8 May 1984 19 p
(RR0-3302)
(AD-A156736; NRL-MR-5291) Avail: NTIS HC A02/MF A01 CSCL 04/2
The computer program described by Liu, Katsaros, and

Businger (1979) for calculating the bulk-derived atmospheric fluxes, stability, and roughness is presented in both the FORTRAN and BASIC versions. The results of 12 test calculations are presented to ensure that the program has been properly encoded. The program requires seven input parameters: (1) wind speed; (2) air temperature; (3) specific humidity; (4) water temperature at the surface; (5) altitude of the wind-speed measurement; (6) altitude of the air-temperature measurement; and (7) altitude of the humidity measurement. GRA

N86-10715# Air Force Inst. of Tech., Wright-Patterson AFB, Ohio.
A COMPOSITE CLIMATOLOGICAL STUDY OF THE FREQUENCY AND DISTRIBUTION OF SEVERE WEATHER ASSOCIATED WITH SPRING SEASON COLORADO CYCLOGENESIS M.S. Thesis
J. H. Peters 1985 95 p
(AD-A156981; AD-E950724; AFIT/CI/NR-85-52T) Avail: NTIS HC A05/MF A01 CSCL 04/2

A composite approach is used to investigate the evolution and distribution of severe weather events for 39 cases of spring season Colorado cyclogenesis. The study also examined the incidence of severe weather during a jet streak subsample of 15 cases, based on the presence of a 300 mb wind maximum over the New Mexico-Texas area on the day of cyclogenesis, and a complement subsample of the cyclogenetic cases not included in the jet streak subsample. Composites were constructed of the normalized frequency of: (1) tornadoes, (2) high winds, (3) large hail, (4) funnel clouds and (5) total severe weather events for the total sample of 39 cases and the two subsamples for three 24 hour intervals with the first interval coinciding with the day of cyclogenesis. Distribution and frequency of severe weather for the three days was consistent with the mean synoptic features as the composite cyclone developed and moved away from its lee side development site in the southern Rockies. The area where severe weather occurred significantly broadened and moved northeastward on the two days following cyclogenesis. For each of the three samples, the maximum frequency of total severe storm events was highest on the day after cyclogenesis. GRA

N86-10716# Sandia Labs., Albuquerque, N. Mex.
ESTIMATING WIND SPEED AS A FUNCTION OF HEIGHT ABOVE GROUND: AN ANALYSIS OF DATA OBTAINED AT THE SOUTHWEST RESIDENTIAL EXPERIMENT STATION, LAS CRUCES, NEW MEXICO
D. F. Menicucci and I. J. Hall May 1985 24 p
(Contract DE-AC04-76DP-00789)
(DE85-013262; SAND-84-2530) Avail: NTIS HC A02/MF A01

Thermel modelling of photovoltaic arrays requires accurate estimates of wind speed at the level of the arrays. Wind speed data are normally recorded by an anemometer at the 30-foot level. To estimate the relationship between wind speed and height, wind speed data were acquired at various heights in the range of 10 to 30 feet and a nonlinear regression analysis was performed. This analysis shows that, over the range of conditions covered by the present data, the predictive relationship given by the Mechanical Engineer's Handbook is quite accurate; wind velocity can generally be estimated to within plus or minus 1.5 mph. DOE

N86-10717# California Univ., Livermore. Lawrence Livermore Lab.
SMOKE INPUTS TO CLIMATE MODELS: OPTICAL PROPERTIES AND HEIGHT DISTRIBUTION FOR NUCLEAR WINTER STUDIES
J. E. Penner and I. C. Haselman, Jr. Apr. 1985 27 p refs Presented at the Intern. Conf. on Nucl. War, Erice, Sicily, 19 Aug. 1984
(Contract W-7405-eng-48)
(DE85-011363; UCRI-92523; CONF-8408122-3) Avail: NTIS HC A03/MF A01

Smoke from fires produced in the aftermath of a major nuclear exchange has been predicted to cause large decreases in land surface temperatures. The extent of the decrease and even the sign of the temperature change depend on the optical characteristics of the smoke and how it is distributed with altitude. The height distribution of smoke over a fire is determined by the amount of buoyant energy produced by the fire and the amount of energy released by the latent heat of condensation of water vapor. The optical properties of the smoke depend on the size distribution of smoke particles which changes due to coagulation within the lofted plume. Calculations are presented demonstrating these processes and estimate their importance for the smoke source term input for climate models. For high initial smoke densities and for absorbing smoke (m = 1.75 - 0.3i), coagulation of smoke particles within the smoke plume is predicted to first increase, then decrease, the size-integrated extinction cross section. DOE

N86-10718# California Univ., Livermore. Lawrence Livermore Lab.
MICROPHYSICAL/MESOSCALE ASPECTS OF NUCLEAR WINTER AND NEW DIRECTIONS IN ASSESSMENTS
J. B. Knox Jun. 1985 13 p refs Presented at the 4th Intern. Conf. on Nucl. War, Erice, Italy, 19 Aug. 1984
(Contract W-7405-eng-48)
(DE85-013479; UCRL-91359; CONF-8408122-5) Avail: NTIS HC A02/MF A01

Recent results of model studies and sensitivity tests have shown the degree to which the intensity and duration of nuclear winter depends on the mass of soot and dust suspended, its optical properties, its vertical distribution in the atmosphere, and the residence time. The soot from urban fires is viewed as evolving during its dispersion from the early fire induced plumes, to cloud scale systems, to the mesoscale and large systems. Micro-physical processes are perceived as operating within these systems in a manner to enhance removal from the troposphere, and to alter the vertical distribution of the soot or its subsequent, aging or evolving aerosol. Relevant observations and studies of these processes are presented and discussed. Critical inputs to the climate simulation models may well be altered significant by these process effects, many of which are in need of better definition. Appropriate research needs to be initiated to address and better define these microphysical/mesoscale processes of potential importance in the altered atmospheric system after a major nuclear exchange. DOE

N86-10719# Brookhaven National Lab., Upton, N. Y.
SEASONAL VARIATIONS IN ATMOSPHERIC CHEMISTRY IN THE ADIRONDACKS
T. J. Kelly, R. L. Tanner, S. E. McLaren, and M. V. DuBois Mar. 1985 11 p refs Presented at the Air Pollution Control Assoc. Ann. Meeting and Exhibition, Detroit, 16 Jun. 1985 Prepared in cooperation with the State Univ. of New York, Albany
(Contract DE-AC02-76CH-00016)
(DE85-014227; BNL-36671; CONF-850612-5) Avail: NTIS HC A02/MF A01

The results of continuous real-time measurements of aerosol composition, HNO3, and SO2, performed at the summit of Whiteface Mountain, New York, during 1984 are reported. The purpose was to shed light on the seasonal variation in atmospheric acidity in this ecologically sensitive area. DOE

N86-10720# Deutsche Forschungs- und Versuchsanstalt fuer Luft- und Raumfahrt, Oberpfaffenhofen (West Germany). Abt. fuer Physik der Atmosphaere.
COMPARATIVE FLIGHT MEASUREMENT OF ICING PARAMETERS FOR THE PROPELLER AIRCRAFT Do-28D2 OF THE TEST STATION 61 OF THE DFVLR AND FOR THE DFVLR AIRCRAFT FALON 20e IN STRATUS CLOUDS
Klaus-Peter Schickel and Kurt Uwira (Bundesamt fuer Wehrtechnik und Beschaffung, Landsberg/Lech, West Germany) Dec. 1984 52 p refs In GERMAN; ENGLISH summary Report will also be announced as translation (ESA-TT-941)
(DFVLR-FB-85-16; ISSN-0171-1342) Avail: NTIS HC A04/MF A01; DFVLR, Cologne DM 15.50

Two aircraft of different types and instrumentation were compared during a flight operation in icing stratus clouds. The results of the measurements are comparable. It is established

that differences between icing and nonicing stratus clouds can be detected in infrared satellite pictures; possible causes of these differences are given. The improvement of forecasts of icing stratus clouds is planned. Author (ESA)

N86-10721# Deutsche Forschungs- und Versuchsanstalt fuer Luft- und Raumfahrt, Oberpfaffenhofen (West Germany). Abteilung Wolkenphysik.
USER MANUAL FOR THE FALCON SYSTEM
Feb. 1985 134 p refs In GERMAN; ENGLISH summary Report will also be announced as translation (ESA-TT-936)
(DFVLR-Mitt-85-08; ISSN-0176-7739) Avail: NTIS HC A07/MF A01; DFVLR, Cologne DM 36.50

The user manual for the meteorological research aircraft Falcon E, operated by DFVLR, is presented. The system and its technical data are described. The meteorological mission possibilities are discussed, and measuring campaigns are reviewed. Basic and special equipment is described. The onboard data acquisition system and the operational data evaluation programs are discussed. Author (ESA)

N86-10722# GKSS-Forschungszentrum Geesthacht (West Germany). Inst. fuer Physik.
THE BOUNDARY CONDITION IN A NUMERICAL MODEL OF ATMOSPHERIC FLOWS OVER FIXED INTERFACES [DIE UNTERE RANDBEDINGUNG IN EINEM NUMERISCHEN MODELL ATMOSPHAERISCHER STROEMUNGEN UEBER UNBEWEGTEN GRENZFLAECHEN]
M. Claussen 1985 35 p refs In GERMAN; ENGLISH summary (GKSS-85-E-10; ISSN-0344-9629) Avail: NTIS HC A03/MF A01

The boundary conditions of wind velocity, temperature and humidity are formulated in a numerical model of atmospheric flows to calculated wind velocity taking into account the roughness length. Different models of surface temperature and humidity taking into account surface energy balance, heat and water transfer within the soil are compared with each other. Strongly simplified models are inappropriate for medium range temperature forecasts. For short range forecasts soil moisture prediction can be omitted if the surface humidity is properly diagnosed from synoptic parameters. The calculation of a boundary value of the wind velocity is reduced to the determination of a roughness length and the problems related to that reduction are discussed. Author (ESA)

N86-10723# National Oceanic and Atmospheric Administration, Boulder, Colo. Atmospheric Observatory.
FIELD COMPARISON OF IN SITU METEOROLOGICAL SENSORS
J. C. Kaimal, J. E. Gaynor, P. L. Finkelstein (EPA, Research Triangle Park, N. C.), M. E. Graves (Northrup Services, Inc., Research Triangle Park, N. C.), and T. J. Lockhart (Meteorology Research, Inc., Altadena, Calif.) Dec. 1984 105 p refs Sponsored in part by EPA
(PB85-196988; BAO-6) Avail: NTIS HC A06/MF A01 CSCL 04B

Measurements of wind speed, wind direction, and the vertical wind component from five conventional in situ meteorological systems were compared with similar measurements from a fast response sonic anemometer. The systems tested were an orthogonal three axis propeller anomometer, a light bivane and cup anemometer, a bivane propeller anemometer, a light cup and vane with a vertical propeller, and a vane mounted propeller anemometer with a vertical propeller. Computed accuracy and field precision variables measured by each system are presented. GRA

N86-10724# National Weather Service, Washington, D.C. Climate Analysis Center.
MONTHLY AND SEASONAL WEATHER OUTLOOK FOR MID-APRIL TO MID-MAY 1985, VOLUME 39, NUMBER 8
13 Apr. 1985 11 p
(PB85-195345) Avail: NTIS HC A02/MF A01 CSCL 04B

The report gives the precipitation and temperature weather outlook for periodic and seasonal variations for North America. GRA

N86-10184# Bundesministerium fuer Forschung und Technologie, Bonn (West Germany).
THE AIR OF LIFE OF THE BLUE PLANET. ATMOSPHERE RESEARCH FROM SPACE USING DATA AND FACTS AGAINST CLIMATE SPECULATIONS [DIE LEBENSLUFT DES BLAUEN PLANETEN. ATMOSPHAERENFORSCHUNG VOM WELTRAUM AUS DATEN UND FAKTEN GEGEN KLIMA-SPEKULATIONEN]
Dieter Schwab *In its* Satellite Use for Men 1984 p 22-25 In GERMAN (For primary document see N86-10180 01-12)
Avail: NTIS HC A03/MF A01

48 OCEANOGRAPHY

Includes biological, dynamic and physical oceanography; and marine resources.

N86-10725 Columbia Univ., New York.
IN-SITU GEOPHYSICAL INVESTIGATIONS INTO THE NATURE OF THE OCEANIC CRUST Ph.D. Thesis
Robin L. Newmark 1985 236 p
Avail: Univ. Microfilms Order No. DA8511536

The layered structure of the oceanic crust is characterized by changes in geophysical gradients. Correlation of geophysical logs and cores recovered from DSDP Hole 504B provides some insight into the physical properties which control these gradient changes. Physical characteristics of crustal layers 2A, 2B and 2C such as the detailed sonic velocity and lithostratigraphic structure and variations of porosity with depth are obtained through analysis of the sonic, borehold televiewer, electrical resistivity and other logs. Several well logs which are sensitive to the presence of fractures and open porosity in the formation indicate many zones of fracturing. Interpretation of these observations suggests that there may be a fundamental pattern of cooling-induced structure in the oceanic crust. Synthetic seismograms in the tau-p domain, constructed using a detailed velocity model derived from the sonic logs run in Hole 504B are used to examine the evidence of narrow low-velocity channels in the shallow crust at seismic wavelengths. Dissert. Abstr.

N86-10726 Columbia Univ., New York.
A QUANTITATIVE METHOD FOR ANALYZING THE ROUGHNESS OF THE SEAFLOOR Ph.D. Thesis
Christopher Gene Fox 1985 233 p
Avail: Univ. Microfilms Order No. DA8511501

A method has been developed which allows a valid statistical model of the variability of oceanic depths to be derived from digital bathymetric soundings. Existing bathymetric contour charts represent low-frequency, deterministic models of the seafloor. To describe the higher frequency variability, or roughness, of the seafloor requires the development of a valid stochastic model. The statistical model of seafloor roughness is also a valuable tool for predicting acoustic scattering and in addition contains a wealth of geological information for interpreting deep-sea processes. To allow the variability of depths to be described as a function of scale (spatial frequency), the amplitude spectrum is employed as the fundamental statistic underlying the model. Since the validity of the amplitude spectrum depends upon the assumption of a statistically stationary sample space, a computer algorithm operating in the spatial domain was developed which delineates geographic provinces of limited statistical heterogeneity. Dissert. Abstr.

N86-10727# Polar Research Lab., Inc., Carpinteria, Calif.
LONG TERM STATISTICAL MEASUREMENTS OF ENVIRONMENTAL ACOUSTICS PARAMETERS IN THE ARCTIC. AEAS REPORT NUMBER 2. LOW FREQUENCY TRANSMISSION LOSS MEASUREMENTS IN THE CENTRAL ARCTIC OCEAN
B. M. Buck 15 Jan. 1985 105 p
(Contract N00014-84-C-0394)
(AD-A156576; PRL-TR-55; AEAS-2) Avail: NTIS HC A06/MF A01 CSCL 20/1

Propagation loss data were taken using manned ice camps and aircraft and ambient noise levels were measured using arctic data buoys that operated through the NIMBUS 6 and NOAA series satellites. The present report of the series addresses propagation loss in deep water (i.e., over 1000 m) of the Central Arctic Ocean at low frequencies (10 - 500 Hz). The data were taken primaily for underwater shots, although some CW data are included, at source depths between 18.3 m and 243.8 m. Receiving hydrophones were at depths between 18.3 m and 243.8 m. Receiving hydrophones were at depths between 9 and 91 m. Other data in the tabulations include for the source: station name, type, depth below sea level and below the ice, nominal TNT yield, measured yield, latitude and longitude, water depth, and source energy at the analysis frequencies. For the receiver: station name, hydrophone depth below sea level and below the ice, nominal TNT yield, measured yield, latitude and longitude, water depth, and source energy at the analysis frequencies. For the receiver: station name, hydrophone depth below sea level and below the ice, latitude and longitude, water depth, and received signal energy at the analysis frequencies. For the path: range, bottomside ice roughness, % of path less than 1000 m deep, % of path over an abyssal plain, mean path depth, and minimum depth in the path. GRA

N86-10728# Coastal Engineering Research Center, Vicksburg, Miss.
APPLICATION OF THE DUTCH METHOD FOR ESTIMATING STORM-INDUCED DUNE EROSION Final Report
F. E. Sargent and W. A. Birkemeier May 1985 46 p
(AD-A156717; CERC-IR-85-2) Avail: NTIS HC A03/MF A01 CSCL 08/3

The Delft Hydraulics Laboratory of the Netherlands has developed a reasonable and simple method for estimating dune and beach erosion caused by severe storms. The method requires knowledge of the sediment size, wave height, and surge level. Major assumptions are that the expected shape of the poststorm beach profile can be predicted by the incident deepwater wave height and sediment size, and that the amount of material eroded will equal the deposition (i.e., cross-shore transport). The method has been verified for the Dutch coast based on both field measurements and laboratory experiments. An evaluation using a limited amount of data for the Atlantic and Gulf coasts of the United States found quantitative agreement with the method, justifying its application to storm conditions in the United States. This report discusses the method and identifies its inherent limitations. The procedure may be solved graphically or by using the included FORTRAN computer program. GRA

N86-10729# Naval Postgraduate School, Monterey, Calif.
EVALUATION OF SURFACE EXCHANGE COEFFICIENTS FROM MILDEX OCEAN/ATMOSPHERE MIXED LAYER DATA M.S. Thesis
H. S. Rosner Mar. 1985 75 p
(AD-A156765) Avail: NTIS HC A04/MF A01 CSCL 08/3

This thesis evaluates a coupled oceanic-atmospheric boundary (ABL/OBL) model which provides single-station prediction capability relative to wind stress and oceanic mixed layer depth observations. The model is initialized and verified using data obtained during the 1983 Mixed Layer Dynamics Experiment (MILDEX). Model computation of friction velocity and oceanic mixed layer depth are compared with observations from both atmospheric frontal and non-frontal synoptic situations. Favorable results of model predictions are achieved although in some cases they are slightly higher than observed turbulence values. Mixed layer predictions are very close to the observed except in frontal regions. Proper ABL/OBL model initialization of boundary layer values is critical in order to achieve favorable results. GRA

N86-10730# Naval Research Lab., Washington, D. C.
A PROCESSOR FOR THE STUDY OF OCEAN FINE-SCALE PATCHES
L. J. Rosenblum, G. O. Marmorino, and J. P. Dugan 17 Jul. 1985 48 p
(AD-A157019; NRL-MR-5573) Avail: NTIS HC A03/MF A01 CSCL 08/10

When a vertical array of temperature sensors is towed through the upper thermocline, patches of high temperature variance of considerable horizontal length can be observed. The Ocean Dynamics Branch at NRL has developed a towed thermistor array system which is extremely useful in obtaining finely detailed data on the horizontal/vertical structure of small-scale temperature fluctuations in the upper ocean. This report documents an algorithm for using towed thermistor array data to study these patches. Briefly, the algorithm detrends the temperature data and computes the FFT of the windowed data for 16 second data blocks. An estimate of the temperature variance is thus obtained within a user-selected band, typically 1 to 3 m. A normalization is generally performed to remove the effects of a changing vertical temperature gradient. Shades of gray plots are then used to display the patch structure. The algorithm is applied to data from a 1981 Atlantic Ocean experiment near the Sargasso Sea. Many examples of patch processor output are shown, along with other results. It will be seen that the patch processor algorithm provides an effective medium for the portrayal of high variance of ocean fine structure. GRA

N86-10731# Conservation and Renewable Energy Inquiry and Referral Service, Silver Spring, Md.
OCEAN ENERGY TECHNOLOGY PROGRAM SUMMARY
May 1985 4 p
(Contract DE-AC01-83CE-30780)
(DE85-013102; DOE/CE-0114) Avail: NTIS HC A02/MF A01

One of the possible ways to achieve national energy sufficiency is to recycle the solar energy stored within the world's oceans in the form of thermal energy, waves and currents. The Department of Energy's (DOE) Ocean Energy Technology (OET) Program was instituted in 1978 to develop technologies which could exploit these resources in an economically viable and environmentally acceptable manner. Presently, the OET Program is investigating Ocean Thermal Energy Conversion (OTEC) Pneumatic Wave Energy Conversion (PWEC), and Hybrid Geothermal1/OTEC (GEOTEC) technologies. DOE

N86-10732# Royal Netherlands Meteorological Inst., De Bilt. Div. of Oceanographic Research.
MONTHLY BULLETIN NORTH SEA: VOLUME 2, JANUARY 1985
F. B. Koek, ed., C. G. Korevaar, ed., and R. A. vanMoerkerken, ed. Jan. 1985 25 p
(KNMI-167-Vol-2; ISSN-0168-8332) Avail: NTIS HC A02/MF A01

Weather charts and graphs of the North Sea in January 1985 covering visibility; height of cloud base; dewpoint temperature; air temperature; sea surface temperature; wind direction; wind speed; and wave height are some discussion areas presented. Author (ESA)

51 LIFE SCIENCES (GENERAL)

Includes genetics.

N86-10733# Committee on Energy and Commerce (U. S. House).
BIOTECHNOLOGY REGULATION
Washington GPO 1985 186 p Hearing before the Subcomm. on Oversight and Invest. of the Comm. on Energy and Com., 98th Congr., 2nd Sess., 11 Dec. 1984
(GPO-43-778) Avail: Subcommittee on Oversight and Investigations

Testimony and hearings in support of biotechnology regulation. Before The Subcommittee On Oversight And Investigations Of The Committee On Energy And Commerce House Of Representatives are presented. Special consideration is given to the regulation of genetic engineering. B.W.

N86-10734*# National Aeronautics and Space Administration. Ames Research Center, Moffett Field, Calif.
LIFE SCIENCES RESEARCH ON THE SPACE STATION: AN INTRODUCTION
Sep. 1985 18 p refs
(NASA-TM-86836; Rept-85408; NAS 1.15:86836) Avail: NTIS HC A02/MF A01 CSCL 06B

The Space Station will provide an orbiting, low gravity, permanently manned facility for scientific research, starting in the 1990s. The facilities for life sciences research are being designed to allow scientific investigators to perform research in Space Medicine and Space Biology, to study the consequences of long-term exposure to space conditions, and to allow for the permanent presence of humans in space. This research, using humans, animals, and plants, will provide an understanding of the effects of the space environment on the basic processes of life. In addition, facilities are being planned for remote observations to study biologically important elements and compounds in space and on other planets (exobiology), and Earth observations to study global ecology. The life sciences community is encouraged to plan for participation in scientific research that will be made possible by the Space Station research facility. Author

N86-10735# Federation of American Societies for Experimental Biology, Bethesda, Md.
[LSRO/ONR AD HOC REVIEW PROCESS] Annual Progress Report, 1 May 1984 - 30 Apr. 1985
13 Jun. 1985 14 p
(Contract N00014-83-C-0196)
(AD-A156590) Avail: NTIS HC A02/MF A01 CSCL 06/1

This annual progress report covers the ad hoc review process. Efforts are continuing to increase the number of peer reviewers who are experienced in the LSRO/ONR review process. The LSRO/FASEB Proposal Rating Form, the form used for the ad hoc peer review evaluation activity, has been reorganized so that it can, if required, be used by all programs of the Biological Sciences Division. The LSRO Oversight Panel on the Office of Naval Research Molecular Biology Program has continued to function with further refinement. In performing evaluations of certain aspects of the Molecular Biology Program, selected members of the LSRO Oversight Panel attended a meeting with selected contractors of the Molecular Biology Program whose research focuses on biotechnology and protein engineering. Non-contract Activities; Contract Problems Encountered and Resolved; Review Process Time; Contract Modifications; LSRO Oversight Panel Reorganization are discussed. GRA

N86-10736# Edgerton, Germeshausen and Grier, Inc., Idaho Falls, Idaho.
KINETICS OF BIOLOGICAL FERROUS IRON OXIDATION
P. I. Wichlacz and H. Olem 1985 15 p refs Presented at the 114th AIME Ann. Meeting, New York, 24 Feb. 1985; sponsored in cooperation with Society of Mining Engineers Prepared in cooperation with Tennessee Valley Authority, Chattanooga
(Contract DE-AC07-76ID-01570)
(DE85-014616; EGG-M-27484; CONF-850211-12) Avail: NTIS HC A02/MF A01

A mathematical model of growth and ferrous iron oxidation for attached bacteria was applied to rotating biological contactor (RBC) units treating acidic mine drainage. The model describes attached bacterial growth as a saturation function, where the rate of substrate utilization is determined by a maximum substrate oxidation rate constant, a half saturation constant, and the concentration of substrate within the RBC. The maximum oxidation rate constant was proportional to flow rate and the substrate concentration in the reactor varied with influent substrate concentration. The model was tested at three separate sites and with three different size RBC units. The ability of the model to predict the rate of iron oxidation under all test conditions was significant. The accuracy of the model was found to be affected by unit size and vary with specific test site. DOE

N86-10737# California Univ., Livermore. Lawrence Livermore Lab.
SOMATIC CELL AND MOLECULAR GENETICS APPROACH TO DNA REPAIR AND MUTAGENESIS
L. H. Thompson 14 Jun. 1985 10 p Presented at the 4th Intern. Conf. on Environ. Mutagens, Stockholm, 24 Jun. 1985
(Contract W-7405-eng-48)
(DE85-014181; UCRL-92834; CONF-8506137-4) Avail: NTIS HC A02/MF A01

In the CHO cell line, UV-sensitive mutants representing five genetic complementation groups were identified. Mutants from each of these groups were shown to be defective in performing the incision step of repair after exposure to UV. It is questioned whether the large number of complementation groups of xeroderma pigmentosa mutations of these groups all correspond to single gene loci. The same issue applies to the five groups of UV-sensitive CHO mutants. The human karyotype of the genes that complement the defects in the CHO mutants were localized. By marking CHO/human cell hybrids under the appropriate selective conditions, each of the complementing human genes are mapped. The mutation in strain UV20 (Group 2) was complemented by human chromosome 19. Preliminary evidence suggests that UV5 may also be complemented by human chromosome 19 while each of the other 3 groups involves a different human chromosome. Mutant EM9 is also complemented by a gene on chromosome 19. DOE

N86-10738# Joint Publications Research Service, Arlington, Va.
USSR REPORT: LIFE SCIENCES. BIOMEDICAL AND BEHAVIORAL SCIENCES
18 Sep. 1985 103 p Transl. into ENGLISH from various Russian articles
(JPRS-UBB-85-023) Avail: NTIS HC A06

Progress in research in the life sciences, with emphasis on biomedical and behavioral sciences is reported. Topics discussed include: aerospace medicine, biotechnology; military medicine, nonionizing electromagnetic radiation effects, and physiology. For individual titles, see N86-10739 through N86-10767.

N86-10739# Joint Publications Research Service, Arlington, Va.
HEMODYNAMICS DURING GRAVITATIONAL OVERLOADS (MATHEMATICAL MODELING) Abstract Only **c52**
B. L. Palets, A. A. Popov, M. A. Tikhonov, and D. Yu. Arkhangelskiy *In its* USSR Rept.: Life Sci. Biomed. and Behavioral Sci. (JPRS-UBB-85-023) 18 Sep. 1985 p 1 Transl. into ENGLISH from Fiziol. Cheloveka (Moscow), v. 11, no. 2, Mar. - Apr. 1985 p 185-191 Original language document announced in IAA as A85-33952 (For primary document see N86-10738 01-51)
Avail: NTIS HC A06

A mathematical model is developed for the regulation of human blood circulation under +Gz acceleration in the head-pelvis direction. A digital-computer study of the model shows that it is adequate to experimental data with respect to indices of systemic hemodynamics in the entire +Gz acceleration range up to the tolerance limit. Regulatory processes detemining changes in the central blood volume are shown to play an important role in the pattern of circulation response to +Gz acceleration; the role of active venomotor responses is relatively small. B.J. (IAA)

N86-10740# Joint Publications Research Service, Arlington, Va.
STUDY OF HYPOKINESIA AND ACCELERATION EFFECTS ON HUMAN CHROMOSOMES Abstract Only **c52**
N. N. Bobkova *In its* USSR Rept.: Life Sci. Biomed. and Behavioral Sci. (JPRS-UBB-85-023) 18 Sep. 1985 p 1 Transl. into ENGLISH from Fiziol. Cheloveka (Moscow), v. 11, no. 2, Mar. - Apr. 1985 p 300-302 (For primary document see N86-10738 01-51)
Avail: NTIS HC A06

A thirty-day antiorthostatic hypokinesia with an -8 deg angle to horizontal position followed by laterally-directed 8 g accelerations for 40 s did not lead to any chromosomal damage in peripheral blood lymphocytes of adult subjects with arthereosclerosis and vegetative vascular dystonia. E.A.K.

N86-10741# Joint Publications Research Service, Arlington, Va.
ROMANIAN PLANT PRODUCES PROTEIN CONCENTRATE FROM PARAFFIN-NOURISHED YEASTS
In its USSR Rept.: Life Sci. Biomed. and Behavioral Sci. (JPRS-UBB-85-023) 18 Sep. 1985 p 17-18 Transl. into ENGLISH from Nauka i Tekhn. (Riga), no. 6, May 1985 p 28-29 (For primary document see N86-10738 01-51)
Avail: NTIS HC A06

Protein concentrate production from paraffin nourished yeasts is reported. Abioprotein plant converts candida type yeasts microorganisms into flour which contains protein concentrate used on cattle and animal feed. The culture growth medium contains sulfates and phosphates. Paraffin supplies the carbon essential to the microorganisms' viability. The development of a technology to produce proteins from methanol is considered. E.A.K.

N86-10742# Joint Publications Research Service, Arlington, Va.
BIOTECHNOLOGY: SCIENCE AND PRACTICE
A. Ilyaletdinov *In its* USSR Rept.: Life Sci. Biomed. and Behavioral Sci. (JPRS-UBB-85-023) 18 Sep. 1985 p 19-21 Transl. into ENGLISH from Kazakhstansk. Pravda (Alma-Ata), Jun. 1985 p 3 (For primary document see N86-10738 01-51)
Avail: NTIS HC A06

The development of scientific research and the introduction of biotechnology's achievements into production are discussed. The development of an antibiotics industry, based upon the use of pure microorganism cultures under sterile conditions, and a microbiological industry, producing feed protein for animal husbandry and microbiological means for fighting agricultural pests is outlined. Industrial microbiology is related. A technology for culturing feed yeasts directly in feed shops by using media containing starch preliminary subjected to fermentation with the malt of germinated grain--barley or other cereal grains is proposed. The method of fermenting starch-containing stock with malt amylase, is turned into feed production. Special species of yeast, produced by our staff members, are used to obtain the feed protein. The contributions of microbiology and virology to the development of biological Science and Scientific and technical progress are outlined. E.A.K.

N86-10743# Joint Publications Research Service, Arlington, Va.
DYNAMICS OF CHANGES OF STATISTICAL INDICATORS OF HEART RHYTHM OF PERSONS WITH DIFFERENT DEGREE OF MOTION SICKNESS Abstract Only **c52**
S. S. Markaryan, A. V. Igrevskiy, and Yu. A. Korotkov *In its* USSR Rept.: Life Sci. Biomed. and Behavioral Sci. (JPRS-UBB-85-023) 18 Sep. 1985 p 46 Transl. into ENGLISH from Fiziol. Cheloveka (Moscow), v. 11, no. 1, Jan. - Feb. 1985 p 157-158 (For primary document see N86-10738 01-51)
Avail: NTIS HC A06

The possibility of using variation pulsometry to reveal latent forms of motion sickness, in seamen who participate in long voyages was studied. It was shown that this procedure could detect latent motion sickness in seamen. It is found that there are definite differences of adaptation to motion sickness in persons with different levels of resistance of Coriolis acceleration. Subjects resistant to vestibular effects revealed only a slight tendency toward insignificant changes of heart rhythm. E.A.K.

N86-10744# Joint Publications Research Service, Arlington, Va.
EFFECT OF SINGLE ACTIONS OF WEAK ELECTROMAGNETIC FIELDS OF ULTRALOW FREQUENCY ON INDICES OF ENDOCRINE SYSTEM Abstract Only **c52**
Ye. A. Zagorskaya *In its* USSR Rept.: Life Sci. Biomed. and Behavioral Sci. (JPRS-UBB-85-023) 18 Sep. 1985 p 50 Transl. into ENGLISH from Fiziol. Cheloveka (Moscow), v. 11, no. 2, Mar. - Apr. 1985 p 293-299 (For primary document see N86-10738 01-51)
Avail: NTIS HC A06

Functions of the human endocrine system was studied after a single exposure to weak electromagnetic field of ultralow frequency with a tension close to the real geomagnetic background and one approaching the alpha rhythm of human EEG. A single 5 hr exposure of healthy male subjects led to decreased activity of hypophysis-adrenal system manifested by lower levels of urinary 17-keto steroids, lower plasma cortisol and corticosterone and increased ACTH levels, accompanied by increased levels of circulating blood testosterone which in some cases exceeded the normal physiological range. Increased levels of TSH and free and total thyroxin in blood was noted in some subjects. The findings represent adaptable compensatory reactions of the regulatory systems showing that this system is highly sensitive to the effect of a magnetic field. E.A.K.

N86-10745# Joint Publications Research Service, Arlington, Va.
EFFECT OF EMOTIONAL STRESS ON HEMOSTASIS SYSTEM OF HEALTHY PERSONS Abstract Only **c53**
Ye. I. Sokolov, T. P. Khovanskaya, I. V. Novikov, and M. V. Baluda *In its* USSR Rept.: Life Sci. Biomed. and Behavioral Sci. (JPRS-UBB-85-023) 18 Sep. 1985 p 62 Transl. into ENGLISH from Fiziol. Cheloveka (Moscow), v. 11, no. 1, Jan. - Feb. 1985 p 79-82 (For primary document see N86-10738 01-51)
Avail: NTIS HC A06

The effect of emotional stress on activity of the sympatho-adrenal system and of some indicators of the system of thrombocytic-vascular and plasma links of hemostasis was studied. Emotional stress of the subjects caused increase of catecholamines in the blood and increases of excretion of them in the urine and activation of the anticoagulation system and increase of the blood heparin level while the fibrinolytic activity increased and the fibrogen concentration in the blood decreased. Thromboelastograms recorded in the first phase of coagulation showed a tendency toward hypocoagulation in the subjects, under emotional stress. Emotional stress shows a tendency toward the increase of heparin tolerance of the plasma but does not change the ADP-induced aggregation of thrombocytes. E.A.K.

N86-10746# Joint Publications Research Service, Arlington, Va.
ASSESSMENT OF STATE OF CHRONOTROPIC AND INOTROPIC HEART FUNCTION AT DIFFERENT DEGREES OF PHYSICAL FITNESS Abstract Only **c52**
V. V. Aksenov and I. G. Tazetdinov *In its* USSR Rept.: Life Sci. Biomed. and Behavioral Sci. (JPRS-UBB-85-023) 18 Sep. 1985 p 62-63 Transl. into ENGLISH from Fiziol. Cheloveka (Moscow), v. 11, no. 1, Jan. - Feb. 1985 p 96-101 Original language document announced in IAA as A85-27781 (For primary document see N86-10738 01-51)
Avail: NTIS HC A06

An approach to the mathematical analysis of cardiosignals is developed which makes it possible to quantitatively evaluate the chronotropic and inotropic functions of the heart from a systems point of view. Combining statistical, cross-correlation, and frequency analyses, this approach makes it possible to assess physical-training level in aerospace and sports medicine. As an example, cardiosignals from the flight commanders and engineers on the Salyut-5 and Salyut-6 orbital stations were analyzed. It is concluded that the mathematical analysis of cardiosignals recorded in conditions of rest makes it possible to evlauate physical-training level as the potential readiness of regulatory systems to provide for the required high level of body functioning under physical loads. B.J. (IAA)

N86-10747# Joint Publications Research Service, Arlington, Va.
CAPACITY FOR WORK AND HEMODYNAMICS IN MALES RESIDING AT MIDDLE AND HIGH LATITUDES Abstract Only **c52**
L. N. Matveyev *In its* USSR Rept.: Life Sci. Biomed. and Behavioral Sci. (JPRS-UBB-85-023) 18 Sep. 1985 p 63 Transl. into ENGLISH from Fiziol. Cheloveka (Moscow), v. 11, no. 1, Jan. - Feb. 1985 p 113-120 (For primary document see N86-10738 01-51)
Avail: NTIS HC A06

The reaction of the cardiovascular system to physical exertion of various intensity was studied. Fitness for physical work of nonindigenous population of the Northeast is closely associated with length of stay in the North. Performance of work analogous to that performed by men from Moscow produces a significant

hyperenergic reaction of the cardovascular system. Persons staying in the North for up to 5 years have adequate metabolic requirements from hyper-dynamia which provides adequate capacity for physical work and rapid recovery rates but a stay of more than 5 years gives lesser capacity for phyiscal work and slowing of recovery rates, due to an approach to the limits of adaptational capacities of the cardiovascular system. Men born in the North have some limitation on their capacity for physical work but have rather rapid recovery rates, indicating a whole complex of adaptational changes. E.A.K.

N86-10748# Joint Publications Research Service, Arlington, Va.
INDIVIDUAL TYPOLOGICAL FEATURES OF AUTONOMIC REACTIONS DURING AUTOGENIC TRAINING IN POLAR EXPEDITION MEMBERS IN PERIOD OF WINTERING IN ANTARCTICA Abstract Only **c52**
Yu. A. Sidorov *In its* USSR Rept.: Life Sci. Biomed. and Behavioral Sci. (JPRS-UBB-85-023) 18 Sep. 1985 p 64 Transl. into ENGLISH from Fiziol. Cheloveka (Moscow), v. 11, no. 1, Jan. - Feb. 1985 p 121-128 (For primary document see N86-10738 01-51)
Avail: NTIS HC A06

Subjects at a coastal Antarctic station underwent autotraining sesions in individual rooms, seated in a comfortable position. Autotraining sessions to achieve relaxation were most effectiv in the expedition members with average or low level of adaptive plasticity, beginning in the second half of wintering at the station. Intersystem inter-relationships of central and peripheral links for providing adaptive reconstructions during autotraining of the expedition members depended on individual parameters of cerebral neurodynamics. Autotraining proved to be an adequate nonmedical method for preventing and correcting disadaptational disturbances in the expedition members during their stay in Antarctica. Individual differences in the plasticity of neurodynamic processes determine the nature of autonomic reactions of the body to autotraining. E.A.K.

N86-10749# Joint Publications Research Service, Arlington, Va.
EFFECT OF INCLUSION OF SUPPLEMENTARY ASCORBIC ACID IN DAILY DIET ON DEGREE OF VITAMIN SATURATION OF BODY AND THERMORESISTANCE OF ERYTHROCYTES WHILE WORKING IN ARID ZONE Abstract Only **c52**
I. M. Mommadov, V. A. Grafova, and G. A. Tupikova *In its* USSR Rept.: Life Sci. Biomed. and Behavioral Sci. (JPRS-UBB-85-023) 18 Sep. 1985 p 64-65 Transl. into ENGLISH from Fiziol. Cheloveka (Moscow), v. 11, no. 1, Jan. - Feb. 1985 p 129-133 Original language document announced in IAA as A85-27786 (For primary document see N86-10738 01-51)
Avail: NTIS HC A06

The physiological needs for ascorbic acid and of the effect of vitamin C supplements at the rate of 150 mg/day on human resistance to heat in arid zones were studied. Ascorbic acid sufficiency was determined by its level in the fasting morning urine. Subjects ate a dragee containing 50 mg of ascorbic acid 3 times a day immediately after meals which increased the vitamin C level in the morning urine. The 150 mg/day dosage normalized the studies ascorbic acid level. The vitamin C supplement increases erythrocytes resistance to heat when working in high temperatures with high insolation. E.A.K.

N86-10750# Joint Publications Research Service, Arlington, Va.
EFFECT OF VARIOUS DOSES OF SOME VITAMINS ON NONSPECIFIC MECHANISMS OF ADAPTATION OF MAN Abstract Only **c52**
V. S. Novikov and V. N. Bortnovskiy *In its* USSR Rept.: Life Sci. Biomed. and Behavioral Sci. (JPRS-UBB-85-023) 18 Sep. 1985 p 65 Transl. into ENGLISH from Fiziol. Cheloveka (Moscow), v. 11, no. 1, Jan. - Feb. 1985 p 134-137 Original language document announced in IAA as A85-27787 (For primary document see N86-10738 01-51)
Avail: NTIS HC A06

An experimental study was conducted to investigate the effect of vitamin additions on the state of the vascular system in the nonspecific resistance of the body in persons working in unfavorable environmental conditions. Thirty operators 19 to 23 years of age were studied whose work was characterized by high work strain, hypokinesia, and environmental discomfort (e.g., high air temperature). One group of 10 subjects received the following vitamins daily: retinol acetate (0.00172 g), thiamine bromide (0.0026 g), riboflavin (0.002 g), nicotinamide (.015 g) pyridoxin hydrochloride (0.002 g), and ascorbic acid (0.07 g). A second group of 10 subjects received a double dose of the same vitamins, while a third group (the control) received placebos. Administration of the vitamins in a double dose was found to prevent the development of deadaptive changes. It is concluded that vitamin additions can prevent a reduction in the nonspecific resistance of the body under extreme environmental conditions. E.A.K.

N86-10751# Joint Publications Research Service, Arlington, Va.
ADAPTATION OF MAN TO EXTREME CONDITIONS OF ANTARCTICA Abstract Only **c52**
S. I. Soroko, A. L. Matusov, and Yu. A. Sidorov *In its* USSR Rept.: Life Sci. Biomed. and Behavioral Sci. (JPRS-UBB-85-023) 18 Sep. 1985 p 66 Transl. into ENGLISH from Fiziol. Cheloveka (Moscow), v. 10, no. 6, Nov. - Dec. 1984 p 907-920 (For primary document see N86-10738 01-51)
Avail: NTIS HC A06

An effort is made to clarify the problem of human adaptation to Antarctic conditions on the basic of multiyear complex ecological-physiological studies. These studies include the investigation of: (1) the ecological factors (natural and anthropogenic) of Antarctica; (2) individual features of the adaptive plasticity of central and vegetative mechanisms of regulation under various factors of the winter stay; (3) the dynamics of analyzer systems; (4) the work capacity of polar workers; (5) the psychoneural status of workers; and (6) the health of expedition members. It is concluded that the complex of extreme factors of Antarctica makes severe demands on the nervous, vegetative, and psychoemotional elements of human beings, calling forth all the reserve capacities of the body. B.J. (IAA)

N86-10752# Joint Publications Research Service, Arlington, Va.
INDIVIDUAL TYPOLOGICAL SELF-REGULATION OF CARDIOVASCULAR SYSTEM Abstract Only **c52**
Ye. G. Vashchillo, M. A. Konstantinov, and D. N. Menitskiy *In its* USSR Rept.: Life Sci. Biomed. and Behavioral Sci. (JPRS-UBB-85-023) 18 Sep. 1985 p 67 Transl. into ENGLISH from Fiziol. Cheloveka (Moscow), v. 10, no. 6, Nov. - Dec. 1984 p 929-936 Original language document announced in IAA as A85-19936 (For primary document see N86-10738 01-51)
Avail: NTIS HC A06

New data are reported pertaining to individual expological differences in the guided self-regulation of heart rate (HR) and arterial pressure (AP) in a visual feedback tracking study. Particular attention is given to individual differences in the latency of effects from baroreceptors at different levels of CNS regulation, these differences being manifested in differences in the amplitude-phase characteristics of guided oscillations of HR and AP rhythms with respect to a sinusoidal control signal. It is concluded that the proposed technique can be used as a training tool in alternating-load exercise and to study the possibility of destabilizing a regulation system with the aim of changing its state. Author

N86-10753# Joint Publications Research Service, Arlington, Va.
CONDITIONING POTENTIALITIES OF RESPIRATORY APPARATUS Abstract Only **c52**
F. T. Agarkov *In its* USSR Rept.: Life Sci. Biomed. and Behavioral Sci. (JPRS-UBB-85-023) 18 Sep. 1985 p 69 Transl. into ENGLISH from Fiziol. Cheloveka (Moscow), v. 10, no. 6, Nov. - Dec. 1984 p 981-987 (For primary document see N86-10738 01-51)
Avail: NTIS HC A06

The temperature of expired alveolar air sublingual, axillary and rectal temperature with temperature of the environment at -30 up to +30 C +50, +60 and +70 C in a heat chamber. Temperature of expired alveolar air at the height of maximally deep exhalation has the same value. Heat or cold, disturbing the isothermy, caused destabilization and an increasing change of the temperature of

exhaled alveolar air. Exogenous heat effects disturb isothermy of the organism and destabilize the temperature of the alveolar air. Factors which limit the conditionaing potentials of the respiratory apparatus in the presence of intense heat include the air temperature, the air humidity and developing hypothermia, the degree of pronouncement of which determines the degree of increase of temperature of the alveolar air, to the greatest extent. It is assumed that the respiratory apparatus is not an ideal conditioner and the existing idea about the constancy and the conformity of the temperature of the alveolar air to the temperature of the core of the body is reconsidered. E.A.K.

N86-10754# Joint Publications Research Service, Arlington, Va.
SHORT TERM HEAT EFFECT ON ADRENO- AND CHOLINO-SENSITIVITY OF RAT'S SMALL INTESTINE Abstract Only
Kh. A. Mezidova, B. N. Manukhin, and F. F. Sultanov *In its* USSR Rept.: Life Sci. Biomed. and Behavioral Sci. (JPRS-UBB-85-023) 18 Sep. 1985 p 70 Transl. into ENGLISH from Fiziol. Zh. SSSR Im. I. M. Sechenov (Leningrad), v. 71, no. 2, Feb. 1985 p 195-199 (For primary document see N86-10738 01-51)
Avail: NTIS HC A06

The dynamics of adreno and choline sensitivity of the smooth muscles of rat's small intestine were studied at various times after exposure to 45 C for 30 or 60 minutes. The body temperature of test animals increased rapidly under the influence of the external temperature. Sensitivity of the intestine to noradrenaline also increased under conditions of hyperthermia, following the pattern of body temperature. Sensitivity of acetylcholine was less initial heating resulted in a slight decrease followed by an increase after a 1 hr exposure; after termination of the experiment, the sensitivity remained below that of control values for about 5 days. It is shown that changes in adrenoreceptor sensitivity could be controlled by the altering of environmental temperature. E.A.K.

N86-10755# Joint Publications Research Service, Arlington, Va.
CLASSIFICATION OF CHANGES IN ELECTROCARDIOGRAM DURING MUSCULAR EXERTION OF HEALTHY INDIVIDUALS Abstract Only **c52**
A. I. Zavyalov *In its* USSR Rept.: Life Sci. Biomed. and Behavioral Sci. (JPRS-UBB-85-023) 18 Sep. 1985 p 73 Transl. into ENGLISH from Fiziol. Cheloveka (Moscow), v. 11, no. 2., Mar. - Apr. 1985 p 201-207 (For primary document see N86-10738 01-51)
Avail: NTIS HC A06

The determination of human endurance during physical stress is one of the most important tasks in aviation, space, work and in sport physiology. Bodily fuctioning depends on the cardio-respiratory system and evaluation of the myocardium during exertion is achieved by study of the electric activity of the heart. The dynamics of EKG were studied on subjects while applying various stress loads. Advanced athletes and sedentary individuals were examined during exercise and in rest periods. Telemetric and conductive EKG seismography, photoplethysmography and arterial pressure were studied. The data statistically leading to comparative analysis was analyzed. Appearance of overstress signals on EKG was accompanied by decreased frequency of heart contractions, a drop in systolic arterial pressure, lowered blood supply, decreased amplitude of seismocardiac signals and of the photoplethysmography wave, indicating a disorder in the contractural function of the myocardium. E.A.K.

N86-10756# Joint Publications Research Service, Arlington, Va.
EYE-MOVEMENT ACTIVITY AS INDEX OF FUNCTIONAL STATE OF BRAIN Abstract Only **c52**
Ye. D. Khomskaya and I. V. Yefimova *In its* USSR Rept.: Life Sci. Biomed. and Behavioral Sci. (JPRS-UBB-85-023) 18 Sep. 1985 p 73 Transl. into ENGLISH from Fiziol. Cheloveka (Moscow), v. 11, no. 2., Mar. - Apr. 1985 p 235-240 (For primary document see N86-10738 01-51)
Avail: NTIS HC A06

Two types of eye movements slow or tracing movements and fast, saccadic movements with different control mechanisms were studied. Rhythmic saccadic eye movements were studied in relationship to mental fatigue which develops during the day and the characteristics of eye movements in individuals with varying degree of motor activity. A definite correlation between the parameters of eye movement reactions and general motor activity of the subjects with their functional state was found. Fatigue and emotional stress resulted in increased frequency of eye movements especially in the more sedentary individuals. It is suggested that eye movement reactions could be used as diagnostic tools in determining the functioning state of the brain. E.A.K.

N86-10757# Joint Publications Research Service, Arlington Va
MECHANISM OF ADAPTOGENIC ACTION OF PRICKLY ELEUTHEROCOCCUS ON MAN DURING HEAT STRESS Abstract Only **c52**
G. N. Novozhilov and K. K. Silchenko *In its* USSR Rept.: Life Sci. Biomed. and Behavioral Sci. (JPRS-UBB-85-023) 18 Sep. 1985 p 74 Transl. into ENGLISH from Fiziol. Cheloveka (Moscow), v. 11, no. 2., Mar. - Apr. 1985 p 303-306 Original language document announced in IAA as A85-33964 (For primary document see N86-10738 01-51)
Avail: NTIS HC A06

The application of eleutherococcus extract in the course of 10 days prior to applied heat stress was found to have a favorable effect on body thermoregulation; body temperature was 0.73 C lower in test subjects than in the control group. However, a high biological cost for the heat adaptation was observed, expressed in two effects: (1) a significantly higher energy cost of enhanced thermal stability under eleutherococcus administration than in the control group; and (2) a more pronounced mobilization of proteins, manifested in the growth of the fraction of protein consumed in the energy metabolism and in a higher level of excretion of nitrogen compounds in the sweat and urine. Author

N86-10758# Joint Publications Research Service, Arlington, Va.
VESTIBULAR RESISTANCE AND BLOOD CIRCULATION CHANGES IN ORTHOSTATIC POSITION DURING HYPERTHERMIA Abstract Only **c52**
V. I. Sobolevskiy *In its* USSR Rept.: Life Sci. Biomed. and Behavioral Sci. (JPRS-UBB-85-023) 18 Sep. 1985 p 74-75 Transl. into ENGLISH from Fiziol. Cheloveka (Moscow), v. 11, no. 2., Mar. - Apr. 1985 p 327-330 (For primary document see N86-10738 01-51)
Avail: NTIS HC A06

Vestibular and orthostatic stability of the body under various environmental conditions in applied human physiology especially under conditions of progressive exogenic hyperthermia was studied. Thermogenic changes of arterial pressure, volume of circulating blood and peripheral resistance were studied in gravitational and vestibular loads. It was shown that with limited internal hyperthermia the vestibular and orthostatic stabilities of men are unaffected. The principal mechanism of lowering resistance to vestibular and gravitational irritants is the disturbance in the blood circulating system and in cardiac activity. E.A.K.

N86-10759# Joint Publications Research Service, Arlington, Va.
HEAT TRANSFER MECHANISM IN HUMAN EXTREMITIES Abstract Only **c52**
T. G. Raygorodskaya, V. N. Koshelev, and O. L. Pertsov *In its* USSR Rept.: Life Sci. Biomed. and Behavioral Sci. (JPRS-UBB-85-023) 18 Sep. 1985 p 75 Transl. into ENGLISH from Fiziol. Cheloveka (Moscow), v. 11, no. 2., Mar. - Apr. 1985 p 336-338 (For primary document see N86-10738 01-51)
Avail: NTIS HC A06

The possible effects of conductive and convective forms of heat transfer on the formation of the skin temperature field in the lower extremities during exercise of the muscles are assessed by a comparison of experimental data with numerical results obtained on the basis of the mathematical model of Koshelev and Pertsov (1978). Results indicate that the role of heat conduction in the transfer of heat from deep muscles to extremity surfaces is insignificant, while most of the heat dissipation in the tissues and heat transfer to the surfaces occurs convectively. B.J. (IAA)

N86-10760# Joint Publications Research Service, Arlington, Va.
REACTION OF RABBIT RESPIRATION SYSTEM TO HYPOXIC STIMULUS IN NITROGEN-OXYGEN MEDIUM AT ELEVATED PRESSURE Abstract Only
Zh. A. Donina *In its* USSR Rept.: Life Sci. Biomed. and Behavioral Sci. (JPRS-UBB-85-023) 18 Sep. 1985 p 75 Transl. into ENGLISH from Fiziol. Zh. SSSR Im. I. M. Sechenov (Leningrad), v. 71, no. 3, Mar. 1985 p 316-319 Original language document announced in IAA as A85-33968 (For primary document see N86-10738 01-51)
Avail: NTIS HC A06

Respiratory changes in exposed animals to increasing hypoxia was investigated on rabbits under normal conditions and in nitrogen-oxygen mixture at elevated pressure. While remaining at atmospheric pressure in air, the oxygen pressure in arterial blood dropped gradually during recycled breathing from a bag, resulting in hyperventilation. The largest increase in respiratory volume is observed when oxygen pressure in blood drops to 44.9 mm Hg; this occurred while the respiration becomes deeper and more frequent. During hyperbaria, the requency of breathing decreases while the depth of the respiration increases. The increase in respiratory volume and lung ventilation is accompanied by increased pressure in the lungs and by more labored breathing.
E.A.K.

N86-10761# Joint Publications Research Service, Arlington, Va.
INDICES OF BLOOD OXYGEN TRANSPORTING PROPERTIES AND ERYTHROPOIESIS IN RATS AFTER PROLONGED STAY IN NITROGEN-OXYGEN MIXTURE AT ELEVATED PRESSURE Abstract Only
A. M. Volzhskaya, G. V. Troshikhin, and T. Ye. Shumilova *In its* USSR Rept.: Life Sci. Biomed. and Behavioral Sci. (JPRS-UBB-85-023) 18 Sep. 1985 p 76 Transl. into ENGLISH from Fiziol. Zh. SSSR Im. I. M. Sechenov (Leningrad), v. 71, no. 3, Mar. 1985 p 320-323 (For primary document see N86-10738 01-51)
Avail: NTIS HC A06

Principal blood indices determining the oxygen transport properties and the intensity of erythropoiesis in rats exposed for different times to elevated pressure in a mixed nitrogen-oxygen atmosphere were investigated. After decompression, the animals showed increased concentration of hemoglobin, elevated levels of hematocrit and higher quantities of erythrocytes, which persisted for 4 hrs; after 24 hrs the values returned to normal. The concentration of 2,3-diphosphoglycerate in erythrocytes increased and remained that way for 72 hrs. The erythropoietic activity was intensified through the 72 hrs. Mechanisms aimed at improving delivery of oxygen to the tissue and representing compensatory reactions to hypoxia are indicated. E.A.K.

N86-10762# Joint Publications Research Service, Arlington, Va.
HOMOCARNOSIN IN RAT BRAIN DURING ADAPTATION TO COLD Abstract Only
T. I. Bondarenko, A. A. Krichevskaya, and G. N. Koshchiy *In its* USSR Rept.: Life Sci. Biomed. and Behavioral Sci. (JPRS-UBB-85-023) 18 Sep. 1985 p 76 Transl. into ENGLISH from Fiziol. Zh. SSSR Im. I. M. Sechenov (Leningrad), v. 71, no. 3, Mar. 1985 p 333-336 (For primary document see N86-10738 01-51)
Avail: NTIS HC A06

Homocarnosin (gamma-aminobutyryl-1-histidine) is a peptide neuromediator of the central nervous system; its content in white rate brain was studied during cold adaptation process lasting from 1 to 45 days. It was shown that the homocarnosin level dropped progressively with exposure to this temperature. During the stress period, peroxide oxidation intensified and the hemoglobin in serum was elevated. Stimulation of the peroxide oxidation damaged some enzymes and the structure of the membranes and some of their properties were altered. Adaptation time to the cold varied in different animals. At that time the level of homocarnosin in cold-adapted animals was 56% lower than controls. The exposure to low temperature led to decrease in homocarnosin-carnosynthetase activity which explained the lower levels of homocarnosin in cold adapted animals. E.A.K.

N86-10763# Joint Publications Research Service, Arlington, Va.
EFFICIENCY OF MUSCULAR WORK IN WHITE RATS DURING ADAPTATION TO COLD Abstract Only
Ye. Ya. Tkachenko and M. A. Yakimenko *In its* USSR Rept.: Life Sci. Biomed. and Behavioral Sci. (JPRS-UBB-85-023) 18 Sep. 1985 p 77 Transl. into ENGLISH from Fiziol. Zh. SSSR Im. I. M. Sechenov (Leningrad), v. 71, no. 3, Mar. 1985 p 337-341 (For primary document see N86-10738 01-51)
Avail: NTIS HC A06

The relationship between heat production and muscle work performed under various work loads by adult rats adapted to a cold medium was investigated to determine the maximum of work ability and its energetic optimum. Temperature increase in the contracting muscle per unit work (delta/A) was plotted as a function of the magnitude of completed work by cold-adapted and control rats. It is shown that work effectiveness changed with adaptation in cold: optimum performance was achieved by cold adapted animals with loads of 200 to 250 g as compared to controls which showed a 320 to 380 g loads. E.A.K.

N86-10764# Joint Publications Research Service, Arlington, Va.
INTRADIURNIAL ORGANIZATION OF WAKEFULNESS-SLEEP SEQUENCE AND ENERGY METABOLISM IN RATS EXPOSED TO LOW AMBIENT TEMPERATURE Abstract Only
V. S. Sazonov and Yu. F. Pastukhov *In its* USSR Rept.: Life Sci. Biomed. and Behavioral Sci. (JPRS-UBB-85-023) 18 Sep. 1985 p 77 Transl. into ENGLISH from Fiziol. Zh. SSSR Im. I. M. Sechenov (Leningrad), v. 71, no. 3, Mar. 1985 p 342-347 Original language document announced in IAA as A85-36611 (For primary document see N86-10738 01-51)
Avail: NTIS HC A06

Sleep characteristics were studied as a function of energy exchange under conditions of acute and chronic exposure to low ambient temperature. Two sleep phases were identified in all animals regardless of the temperature; (1) slow wave sleep, further subdivided into surface and deep subgroups; and (2) paradoxial sleep. Three control rats were used and five cold-adapted ones. At low ambient temperature, controls had a lighter, shorter and often interrupted sleep. After cold adaptation daily sleeping period increased both at low and ambient temperatures. It is assumed that after prolonged cold the sleep initiation mechanisms continue to be active, while those of the sleep development arrested.
E.A.K.

N86-10765# Joint Publications Research Service, Arlington, Va.
TV MONITORING CONTROL SYSTEM IN ELECTROPHYSIOLOGICAL STUDIES Abstract Only **c52**
Yu. G. Kratin, Ye. P. Popechitelev, A. N. Solovyev, and Yu. I. Buch *In its* USSR Rept.: Life Sci. Biomed. and Behavioral Sci. (JPRS-UBB-85-023) 18 Sep. 1985 p 78 Transl. into ENGLISH from Fiziol. Zh. SSSR Im. I. M. Sechenov (Leningrad), v. 71, no. 3, Mar. 1985 p 381-383 (For primary document see N86-10738 01-51)
Avail: NTIS HC A06

In electrophysiological experiments and during determination of EEG curves, the flow of formation must be filtered to isolate most important indices to be able to follow the functional state of the brain. A special monitor was constructed which consists of a TV camera, video-control unit and an image synthesizer consisting of synchronous impulse selector, round figure contructor and a coloring block. The degree of brain activity is converted to the background color scheme, to study the subject concurrently with the observation of brain activation. This apparatus can be modified for other clinical applications. E.A.K.

N86-10766# Joint Publications Research Service, Arlington, Va.
EFFECT OF COLD ON BRAIN SEROTONIN SYSTEM AND PLASMA CORTICOSTEROID LEVEL IN DIFFERENT STRAINS OF MICE Abstract Only
L. A. Koryakina, A. V. Kulikov, M. Yu. Figurova, and N. K. Popova *In its* USSR Rept.: Life Sci. Biomed. and Behavioral Sci. (JPRS-UBB-85-023) 18 Sep. 1985 p 78-79 Transl. into ENGLISH from Fiziol. Zh. SSSR Im. I. M. Sechenov (Leningrad), v. 71, no. 3,

Mar. 1985 p 422-427 (For primary document see N86-10738 01-51)
Avail: NTIS HC A06

The activity of tryptophan hydroxylase in brain and was evaluated the plasma corticosteroid levels in male mice while exposed to +4 C for 1 or 6 hrs. It is shown that the activity of tryptophan hydroxylase dropped during the cooling process, and it is assumed that the activity of the entire serotonin system in brain lowered. Decreased synthesis of serotonin supported temperature homeostasis and increased the resistance of animals to cold. The changes in the serotonin system were of an adaptive nature. No linear relationship is noted between the degree of activation of hypothalamo-hypophyseal-adrenal systems and the drop in body temperature of the experimental animals. It is assumed that the observed changes in the synthesis of biogenic amine represent a specific reaction of the body to the cooling process and are caused by participation of brain serotonin in central thermoregulation. E.A.K.

N86-10767# Joint Publications Research Service, Arlington, Va.
DYNAMICS OF GENERAL RESISTANCE OF RATS DURING READAPTATION PERIOD AFTER TRAINING IN ALTERED GAS ENVIRONMENT Abstract Only
Ye. Ye. Zverkova *In its* USSR Rept.: Life Sci. Biomed. and Behavioral Sci. (JPRS-UBB-85-023) 18 Sep. 1985 p 79 Transl. into ENGLISH from Fiziol. Zh. SSSR Im. I. M. Sechenov (Leningrad), v. 71, no. 4, Apr. 1985 p 523-526 (For primary document see N86-10738 01-51)
Avail: NTIS HC A06

The duration of retained resistance of animals to external conditions was studied on 330 white rats as a function of adaptive training and specific conditions of altered gas medium. The adaptation training to combined hypoxia and hypercapnia or to pure hypoxia lasted 15 and 30 days for each modality. It was shown that a 15-day training by either of above methods had an insignificant effect on high altutide resistance. The animals exposed to 30 day treatment showed significant increase in resistance to acute hypoxia. The high altitude resistance was higher at all times in the groups exposed to a combination of hypoxia and hypercapnia training. This type of resistance lasted for up to 60 days after thre readaptation period. E.A.K.

52 AEROSPACE MEDICINE

Includes physiological factors; biological effects of radiation; and weightlessness.

N86-10768* National Aeronautics and Space Administration, Washington, D. C.
AEROSPACE MEDICINE AND BIOLOGY: A CONTINUING BIBLIOGRAPHY WITH INDEXES (SUPPLEMENT 275)
Sep. 1985 99 p
(NASA-SP-7011(275); NAS 1.21:7011(275)) Avail: NTIS HC $7.00 (special price) CSCL 06E

This bibliography lists 321 reports, articles, and other documents introduced into the NASA scientific and technical information system in August 1985. E.A.K.

N86-10769 Maryland Univ., College Park.
DETERMINATION OF SYMMETRY AND PHASE IN HUMAN VISUAL RESPONSE FUNCTIONS: THEORY AND EXPERIMENTS Ph.D. Thesis
David Geoffrey Stork 1984 189 p
Avail: Univ. Microfilms Order DA8510459

Several mathematical and experimental techniques to deduce the temporal impulse response and static line spread function of the human visual system were employed. The problem of linearity in the visual system near threshold is recieved and the mathematical foundations of different experimental approaches are discussed. It is found that the method of constant (threshold) output avoids certain difficulties associated with other methods. The use of harmonic stimuli in vision, and the inherent phase or symmetry ambiguities associated with it are described. Physiological data on cat responses are analyzed. It is demonstrated that a spatially antisymmetric line spread function explains this data better that a spatially symmetric one. A novel stimulus segconverging and diverging stimuli is introduced and show how it can be used to probe spatial symmetry of the line spread function.It is demonstrated that the sensitivity to converging and diverging stimuli are equal. It is shown that adaptation to velocity stimuli at one retinal position can affect (reduce) sensitivity at spatially separated positions. Dissert. Abstr.

N86-10770*# Pennsylvania Univ., Philadelphia. Dept. of Computer and Information Service.
STRENGTH MODELING REPORT
Norman I. Badler, Philip Lee, and Sui Wong 30 May 1985 79 p refs
(Contract NAS9-16634)
(NASA-CR-171896; NAS 1.26:171896) Avail: NTIS HC A05/MF A01 CSCL 06P

Strength modeling is a complex and multi-dimensional issue. There are numerous parameters to the problem of characterizing human strength, most notably: (1) position and orientation of body joints; (2) isometric versus dynamic strength; (3) effector force versus joint torque; (4) instantaneous versus steady force; (5) active force versus reactive force; (6) presence or absence of gravity; (7) body somatotype and composition; (8) body (segment) masses; (9) muscle group envolvement; (10) muscle size; (11) fatigue; and (12) practice (training) or familiarity. In surveying the available literature on strength measurement and modeling an attempt was made to examine as many of these parameters as possible. The conclusions reached at this point toward the feasibility of implementing computationally reasonable human strength models. The assessment of accuracy of any model against a specific individual, however, will probably not be possible on any realistic scale. Taken statistically, strength modeling may be an effective tool for general questions of task feasibility and strength requirements. G.L.C.

N86-10771# Federal Aviation Administration, Washington, D.C. Office of Aviation Medicine.
THE EFFECTS OF AGE, SLEEP DEPRIVATION, AND ALTITUDE ON COMPLEX PERFORMANCE
H. W. Mertens and W. E. Collins May 1985 22 p
(AD-A156987; AD-E950724; FAA-AM-85-3) Avail: NTIS HC A02/MF A01 CSCL 06/19

Little research has been concerned with the combined effects on performance of age, sleep deprivation, and altitude. This study examined their potential interaction with laboratory tasks measuring aviation-related psychological functions. Healthy men in two age groups, 30-39 yr (N=16) and 60-69 yr (N=14), were evaluated for complex (time-shared) performance in the four possible combinations of two altitudes (ground level vs. 3,810 m (12,500 ft)) and two sleep conditions (sleep permitted vs. sleep deprived). Following training, performance was evaluated during 3-h test sessions in the morning and afternoon of each of 4 test days. Complex performance, measured by the Multiple Task Performance Battery (MTPB), included: monitoring of warning lights and meters, mental arithmetic, problem solving, target identification, and tracking. Workload was varied within each hour by varying the tasks performed simultaneously. Performance was significantly lower in the older subjects, but age did not interact significantly with sleep deprivation or altitude. When subjects were rested, altitude had no effect. When subjects were sleep deprived, performance was significantly lower in general, and the greatest decrement in performance occurred at altitude. Increasing workload enhanced the interaction of sleep deprivation and altitude. The performance of older subjects tended to be more affected by increases in workload, but decrements induced by sleep deprivation and altitude did not appear to interact with age. These findings provide empirical evidence in support of warnings in the aeromedical literature concerning greater effects of sleep deprivation as altitude increases within the general aviation range. GRA

N86-10772# Pacific Northwest Lab., Richland, Wash.
APPROACHES TO QUANTITATIVE EXPRESSION OF DOSE RESPONSE
E. S. Gilbert Apr. 1985 16 p refs Presented at the Symp. on Epidemiol. and Health Risk Assessment, Columbia, Md., 14 May 1985
(Contract DE-AC06-76RL-01830)
(DE85-013498; PNL-SA-13193; CONF-850577-1) Avail: NTIS HC A02/MF A01

Quantifying risks experienced by populations been exposed to relatively low levels of harmful agents for substances are discussed. DOE

N86-10773# Hauptverband der Gewerblichen Berufsgenossenschaften, e. V., Bonn (West Germany).
REPORT ON THE RESEARCH ACTIVITIES ON WHOLE-BODY VIBRATIONS. HUMAN STRAIN DUE TO MECHANICAL VIBRATIONS [BEANSPRUCHUNG DES MENSCHEN DURCH MECHANISCHE SCHWINGUNGEN. KENNTNISSTAND ZUR WIRKUNG VON GANZ-KOERPER-SCHWINGUNGEN]
H. Dupuis (Mainz Univ., West Germany) and G. Zerlett (Rheinische Braunkohlenwerke AG) May 1984 148 p refs In GERMAN
(ISBN-3-88383-107-7) Avail: NTIS HC A07/MF A01

Knowledge of whole-body vibration effects on man was surveyed to give authorities a guide for decision-making and judgement regarding occupational problems. The acute effects of mechanical vibrations on man's organism and physiological functions are reported as well as the chronic effects of whole-body vibrations and the influence of specific strain factors. Prevention measures are listed together with West German legislation and guidelines regarding the protection against mechanical vibrations at work. Author (ESA)

N86-10774# Amsterdam Univ. (Netherlands). Lab. voor Medischefysica.
VARIABILITY ANALYSIS OF VISUALLY INDUCED RESPONSES IN THE MIDST OF NOISE Ph.D. Thesis [VARIABILITEITS ANALYSE VAN VISUEEL OPGEWEKTE RESPONSIES TE MIDDEN VAN RUIS]
M. F. vanLoon Apr. 1984 91 p refs In DUTCH
(B8564052) Avail: NTIS HC A05/MF A01

The variability of EEG responses to visual stimuli, and possible relations between variations in latency and amplitude are investigated. A matched filter to detect and estimate the magnitude of variabilities on series of recordings until a 20% signal to noise ratio is reached was applied to responses of two subjects. Measurements show that in case of variability no relation exists between stimulus and the magnitude of the variability in latency or amplitude. Variability seems mainly to depend on the condition of the subject. Author (ESA)

N86-10739# Joint Publications Research Service, Arlington, Va.
HEMODYNAMICS DURING GRAVITATIONAL OVERLOADS (MATHEMATICAL MODELING) Abstract Only
B. L. Palets, A. A. Popov, M. A. Tikhonov, and D. Yu. Arkhangelskiy *In its* USSR Rept.: Life Sci. Biomed. and Behavioral Sci. (JPRS-UBB-85-023) 18 Sep. 1985 p 1 Transl. into ENGLISH from Fiziol. Cheloveka (Moscow), v. 11, no. 2, Mar. - Apr. 1985 p 185-191 Original language document announced in IAA as A85-33952 (For primary document see N86-10738 01-51)
Avail: NTIS HC A06

N86-10740# Joint Publications Research Service, Arlington, Va.
STUDY OF HYPOKINESIA AND ACCELERATION EFFECTS ON HUMAN CHROMOSOMES Abstract Only
N. N. Bobkova *In its* USSR Rept.: Life Sci. Biomed. and Behavioral Sci. (JPRS-UBB-85-023) 18 Sep. 1985 p 1 Transl. into ENGLISH from Fiziol. Cheloveka (Moscow), v. 11, no. 2, Mar. - Apr. 1985 p 300-302 (For primary document see N86-10738 01-51)
Avail: NTIS HC A06

N86-10743# Joint Publications Research Service, Arlington, Va.
DYNAMICS OF CHANGES OF STATISTICAL INDICATORS OF HEART RHYTHM OF PERSONS WITH DIFFERENT DEGREE OF MOTION SICKNESS Abstract Only
S. S. Markaryan, A. V. Igrevskiy, and Yu. A. Korotkov *In its* USSR Rept.: Life Sci. Biomed. and Behavioral Sci. (JPRS-UBB-85-023) 18 Sep. 1985 p 46 Transl. into ENGLISH from Fiziol. Cheloveka (Moscow), v. 11, no. 1, Jan. - Feb. 1985 p 157-158 (For primary document see N86-10738 01-51)
Avail: NTIS HC A06

N86-10744# Joint Publications Research Service, Arlington, Va.
EFFECT OF SINGLE ACTIONS OF WEAK ELECTROMAGNETIC FIELDS OF ULTRALOW FREQUENCY ON INDICES OF ENDOCRINE SYSTEM Abstract Only
Ye. A. Zagorskaya *In its* USSR Rept.: Life Sci. Biomed. and Behavioral Sci. (JPRS-UBB-85-023) 18 Sep. 1985 p 50 Transl. into ENGLISH from Fiziol. Cheloveka (Moscow), v. 11, no. 2, Mar. - Apr. 1985 p 293-299 (For primary document see N86-10738 01-51)
Avail: NTIS HC A06

N86-10746# Joint Publications Research Service, Arlington, Va.
ASSESSMENT OF STATE OF CHRONOTROPIC AND INOTROPIC HEART FUNCTION AT DIFFERENT DEGREES OF PHYSICAL FITNESS Abstract Only
V. V. Aksenov and I. G. Tazetdinov *In its* USSR Rept.: Life Sci. Biomed. and Behavioral Sci. (JPRS-UBB-85-023) 18 Sep. 1985 p 62-63 Transl. into ENGLISH from Fiziol. Cheloveka (Moscow), v. 11, no. 1, Jan. - Feb. 1985 p 96-101 Original language document announced in IAA as A85-27781 (For primary document see N86-10738 01-51)
Avail: NTIS HC A06

N86-10747# Joint Publications Research Service, Arlington, Va.
CAPACITY FOR WORK AND HEMODYNAMICS IN MALES RESIDING AT MIDDLE AND HIGH LATITUDES Abstract Only
L. N. Matveyev *In its* USSR Rept.: Life Sci. Biomed. and Behavioral Sci. (JPRS-UBB-85-023) 18 Sep. 1985 p 63 Transl. into ENGLISH from Fiziol. Cheloveka (Moscow), v. 11, no. 1, Jan. - Feb. 1985 p 113-120 (For primary document see N86-10738 01-51)
Avail: NTIS HC A06

N86-10748# Joint Publications Research Service, Arlington, Va.
INDIVIDUAL TYPOLOGICAL FEATURES OF AUTONOMIC REACTIONS DURING AUTOGENIC TRAINING IN POLAR EXPEDITION MEMBERS IN PERIOD OF WINTERING IN ANTARCTICA Abstract Only
Yu. A. Sidorov *In its* USSR Rept.: Life Sci. Biomed. and Behavioral Sci. (JPRS-UBB-85-023) 18 Sep. 1985 p 64 Transl. into ENGLISH from Fiziol. Cheloveka (Moscow), v. 11, no. 1, Jan. - Feb. 1985 p 121-128 (For primary document see N86-10738 01-51)
Avail: NTIS HC A06

N86-10749# Joint Publications Research Service, Arlington, Va.
EFFECT OF INCLUSION OF SUPPLEMENTARY ASCORBIC ACID IN DAILY DIET ON DEGREE OF VITAMIN SATURATION OF BODY AND THERMORESISTANCE OF ERYTHROCYTES WHILE WORKING IN ARID ZONE Abstract Only
I. M. Mommadov, V. A. Grafova, and G. A. Tupikova *In its* USSR Rept.: Life Sci. Biomed. and Behavioral Sci. (JPRS-UBB-85-023) 18 Sep. 1985 p 64-65 Transl. into ENGLISH from Fiziol. Cheloveka (Moscow), v. 11, no. 1, Jan. - Feb. 1985 p 129-133 Original language document announced in IAA as A85-27786 (For primary document see N86-10738 01-51)
Avail: NTIS HC A06

N86-10750# Joint Publications Research Service, Arlington, Va.
EFFECT OF VARIOUS DOSES OF SOME VITAMINS ON NONSPECIFIC MECHANISMS OF ADAPTATION OF MAN Abstract Only
V. S. Novikov and V. N. Bortnovskiy *In its* USSR Rept.: Life Sci. Biomed. and Behavioral Sci. (JPRS-UBB-85-023) 18 Sep. 1985 p 65 Transl. into ENGLISH from Fiziol. Cheloveka (Moscow), v. 11, no. 1, Jan. - Feb. 1985 p 134-137 Original language

document announced in IAA as A85-27787 (For primary document see N86-10738 01-51)
Avail: NTIS HC A06

N86-10751# Joint Publications Research Service, Arlington, Va.
ADAPTATION OF MAN TO EXTREME CONDITIONS OF ANTARCTICA Abstract Only
S. I. Soroko, A. L. Matusov, and Yu. A. Sidorov *In its* USSR Rept.: Life Sci. Biomed. and Behavioral Sci. (JPRS-UBB-85-023) 18 Sep. 1985 p 66 Transl. into ENGLISH from Fiziol. Cheloveka (Moscow), v. 10, no. 6, Nov. - Dec. 1984 p 907-920 (For primary document see N86-10738 01-51)
Avail: NTIS HC A06

N86-10752# Joint Publications Research Service, Arlington, Va.
INDIVIDUAL TYPOLOGICAL SELF-REGULATION OF CARDIOVASCULAR SYSTEM Abstract Only
Ye. G. Vashchillo, M. A. Konstantinov, and D. N. Menitskiy *In its* USSR Rept.: Life Sci. Biomed. and Behavioral Sci. (JPRS-UBB-85-023) 18 Sep. 1985 p 67 Transl. into ENGLISH from Fiziol. Cheloveka (Moscow), v. 10, no. 6, Nov. - Dec. 1984 p 929-936 Original language document announced in IAA as A85-19936 (For primary document see N86-10738 01-51)
Avail: NTIS HC A06

N86-10753# Joint Publications Research Service, Arlington, Va.
CONDITIONING POTENTIALITIES OF RESPIRATORY APPARATUS Abstract Only
F. T. Agarkov *In its* USSR Rept.: Life Sci. Biomed. and Behavioral Sci. (JPRS-UBB-85-023) 18 Sep. 1985 p 69 Transl. into ENGLISH from Fiziol. Cheloveka (Moscow), v. 10, no. 6, Nov. - Dec. 1984 p 981-987 (For primary document see N86-10738 01-51)
Avail: NTIS HC A06

N86-10755# Joint Publications Research Service, Arlington, Va.
CLASSIFICATION OF CHANGES IN ELECTROCARDIOGRAM DURING MUSCULAR EXERTION OF HEALTHY INDIVIDUALS Abstract Only
A. I. Zavyalov *In its* USSR Rept.: Life Sci. Biomed. and Behavioral Sci. (JPRS-UBB-85-023) 18 Sep. 1985 p 73 Transl. into ENGLISH from Fiziol. Cheloveka (Moscow), v. 11, no. 2., Mar. - Apr. 1985 p 201-207 (For primary document see N86-10738 01-51)
Avail: NTIS HC A06

N86-10756# Joint Publications Research Service, Arlington, Va.
EYE-MOVEMENT ACTIVITY AS INDEX OF FUNCTIONAL STATE OF BRAIN Abstract Only
Ye. D. Khomskaya and I. V. Yefimova *In its* USSR Rept.: Life Sci. Biomed. and Behavioral Sci. (JPRS-UBB-85-023) 18 Sep. 1985 p 73 Transl. into ENGLISH from Fiziol. Cheloveka (Moscow), v. 11, no. 2., Mar. - Apr. 1985 p 235-240 (For primary document see N86-10738 01-51)
Avail: NTIS HC A06

N86-10757# Joint Publications Research Service, Arlington, Va.
MECHANISM OF ADAPTOGENIC ACTION OF PRICKLY ELEUTHEROCOCCUS ON MAN DURING HEAT STRESS Abstract Only
G. N. Novozhilov and K. K. Silchenko *In its* USSR Rept.: Life Sci. Biomed. and Behavioral Sci. (JPRS-UBB-85-023) 18 Sep. 1985 p 74 Transl. into ENGLISH from Fiziol. Cheloveka (Moscow), v. 11, no. 2., Mar. - Apr. 1985 p 303-306 Original language document announced in IAA as A85-33964 (For primary document see N86-10738 01-51)
Avail: NTIS HC A06

N86-10758# Joint Publications Research Service, Arlington, Va.
VESTIBULAR RESISTANCE AND BLOOD CIRCULATION CHANGES IN ORTHOSTATIC POSITION DURING HYPERTHERMIA Abstract Only
V. I. Sobolevskiy *In its* USSR Rept.: Life Sci. Biomed. and Behavioral Sci. (JPRS-UBB-85-023) 18 Sep. 1985 p 74-75 Transl. into ENGLISH from Fiziol. Cheloveka (Moscow), v. 11, no. 2., Mar. - Apr. 1985 p 327-330 (For primary document see N86-10738 01-51)
Avail: NTIS HC A06

N86-10759# Joint Publications Research Service, Arlington, Va.
HEAT TRANSFER MECHANISM IN HUMAN EXTREMITIES Abstract Only
T. G. Raygorodskaya, V. N. Koshelev, and O. L. Pertsov *In its* USSR Rept.: Life Sci. Biomed. and Behavioral Sci. (JPRS-UBB-85-023) 18 Sep. 1985 p 75 Transl. into ENGLISH from Fiziol. Cheloveka (Moscow), v. 11, no. 2., Mar. - Apr. 1985 p 336-338 (For primary document see N86-10738 01-51)
Avail: NTIS HC A06

N86-10765# Joint Publications Research Service, Arlington, Va.
TV MONITORING CONTROL SYSTEM IN ELECTROPHYSIOLOGICAL STUDIES Abstract Only
Yu. G. Kratin, Ye. P. Popechitelev, A. N. Solovyev, and Yu. I. Buch *In its* USSR Rept.: Life Sci. Biomed. and Behavioral Sci. (JPRS-UBB-85-023) 18 Sep. 1985 p 78 Transl. into ENGLISH from Fiziol. Zh. SSSR Im. I. M. Sechenov (Leningrad), v. 71, no. 3, Mar. 1985 p 381-383 (For primary document see N86-10738 01-51)
Avail: NTIS HC A06

53 BEHAVIORAL SCIENCES

Includes psychological factors; individual and group behavior; crew training and evaluation; and psychiatric research.

N86-10775 Institute for Perception RVO-TNO, Soesterberg (Netherlands).
STUDIES ON HUMAN VEHICLE CONTROL
Hans Godthelp 1984 159 p refs
(B8563352) Avail: Issuing Activity

The accuracy of closed and open loop steering were measured in a reproduction task. Precognitive control aspects of open and closed loop steering in a lane change maneuver were studied. Preview control in open and closed loop steering on entering a bend was investigated. Straight lane keeping compensatory control and the limits of error neglecting in lane keeping were examined. For closed loop conditions, amplitude accuracy is linearly dependent on movement velocity, illustrating the validity of Fitts/ law for continuous, closed loop movements. However, for open loop conditions the results indicate the amplitude accuracy to depend only on movement amplitude and not on velocity. Driver's self-chosen occlusion times correspond closely with time of lane crossing. Author (ESA)

N86-10776 Institute for Perception RVO-TNO, Soesterberg (Netherlands).
CAR DRIVING AS A SUPERVISORY CONTROL TASK
Gerard Jan Blaauw 1984 139 p refs
(B8563351) Avail: Issuing Activity

Car driving was analyzed using a supervisory driver model. The driver is assumed to supervise single tasks like lateral and longitudinal vehicle control, each of which is assumed to be autonomously controlled. The driver only intervenes when the conditions of a single task force him to. An integral description of multitask performance in driving is possible. An observation/ prediction block, a control block and a decision-making block are distinguished. Results suggest that lateral control does not need continuous foveal visual information. In conditions creating a minimum level of attention for lateral control, skilled and unskilled drivers show an acceptable stay within their lane, although variations in lateral control are larger than in other conditions. Performance during occlusion is not much affected in relation to multitask or deteriorated driving conditions. However, skilled drivers choose longer occlusion times than the unskilled drivers for comparable levels of driving performance. Author (ESA)

N86-10777*# National Aeronautics and Space Administration. Ames Research Center, Moffett Field, Calif.

THE SYNTHESIS AND ANALYSIS OF COLOR IMAGES

Brian A. Wandell Sep. 1985 37 p refs

(NASA-TM-86844; Rept-85419; NAS 1.15:86844) Avail: NTIS HC A03/MF A01 CSCL 05I

A method is described for performing the synthesis and analysis of digital color images. The method is based on two principles. First, image data are represented with respect to the separate physical factors, surface reflectance and the spectral power distribution of the ambient light, that give rise to the perceived color of an object. Second, the encoding is made efficient by using a basis expansion for the surface spectral reflectance and spectral power distribution of the ambient light that takes advantage of the high degree of correlation across the visible wavelengths normally found in such functions. Within this framework, the same basic methods can be used to synthesize image data for color display monitors and printed materials, and to analyze image data into estimates of the spectral power distribution and surface spectral reflectances. The method can be applied to a variety of tasks. Examples of applications include the color balancing of color images, and the identification of material surface spectral reflectance when the lighting cannot be completely controlled.

Author

N86-10778# Department of the Air Force, Washington, D.C.

VISION TEST CHART AND METHOD USING GAUSSIANS Patent Application

H. L. Task, inventor (to Air Force) Filed 23 Jan. 1985 19 p

(AD-D011756; US-Patent-Appl-SN-693927) Avail: NTIS HC A02/MF A01 CSCL 06/12

A novel vision test device and method for measuring the ability of a subject to perceive contrasts is described, which comprises a chart for display to the subject having a plurality of visual test shapes systematically organized thereover in a predetermined array on a background of preselected luminance or reflectance level, each test shape having a preselected luminance level providing maximum contrast relative to background at its center and substantially zero contrast relative to background at its edges, the luminance (or reflectance) level of each test shape varying radially from its preselected distribution factor.

GRA

N86-10779# Office of Naval Research, Arlington, Va. Psychological Sciences Div.

PSYCHOLOGICAL SCIENCES DIVISION 1984 PROGRAMS Annual Report, 1 Jan. - 1 Dec. 1984

M. A. Tolcott 1 Dec. 1984 184 p

(AD-A156631; Rept-442-4) Avail: NTIS HC A09/MF A01 CSCL 05/10

This booklet describes research carried out under the Psychological Sciences Division of ONR during Fiscal Year 1984. The booklet is divided into three programmatic research area: Engineering Psychology; Personnel and Training; and Organizational Effectiveness - the last area will be re-named Group Psychology in Fiscal Year 1985. Specific study areas are: Man-Machine System Interfaces, Perception, Decision Making, Distributed Tactical Decision Making, Special Projects. Man-Machine Systems Technology, Defense Small Business Advanced Technology Program, Effective Heterogeneous Groups, personnel Turnover and Retention, Productivity in Organizations, Manpower R&D Programs, Theory-Based Personnel Assessment, Information-Processing Abilities, Attention and Action, Instructional Theory and Methods, Cognitive Processes. Each report within these sections gives specific objectives, approach, progress, potential applications.

GRA

N86-10780# Deutsche Forschungs- und Versuchsanstalt fuer Luft- und Raumfahrt, Hamburg (West Germany). Abt. Flugphysiologie und Psychologie.

EXTENDED ANALYSIS OF THE STRUCTURE OF ERROR SCORES IN PSYCHOLOGICAL APTITUDE TESTS

Klaus-Martin Goeters Mar. 1985 50 p refs In GERMAN; ENGLISH summary Report will also be announced as translation (ESA-TT-943)

(DFVLR-FB-85-20; ISSN-0171-1342) Avail: NTIS HC A03/MF A01; DFVLR, Cologne DM 16.50

A series of psychological aptitude tests was analyzed with respect to human performance and reliability. A factor analysis of the test scores reveals five components of performance. Three independent error components are extracted: errors in quick visual detection of targets; difficulties in mental processing of numbers and symbols; and erroneous actions under performance stress. All three factors are the expression of a deficient control of performance. They are discussed as functional aspects of decision making and human information processing.

Author (ESA)

N86-10781# Deutsche Forschungs- und Versuchsanstalt fuer Luft- und Raumfahrt, Hamburg (West Germany). Abt. Flugphysiologie und Psychologie.

SPEED OF WORK AND ERROR RATE: ANALYSES OF INDIVIDUAL DIFFERENCES IN A CHOICE REACTION SERIES WITH A COGNITIVE COMPONENT

Klaus-Martin Goeters Mar. 1985 27 p refs In GERMAN; ENGLISH summary Report will also be announced as translation (ESA-TT-944)

(DFVLR-FB-85-21; ISSN-0171-1342) Avail: NTIS HC A03/MF A01; DFVLR, Cologne DM 10.50

A visual choice reaction test with a cognitive component was introduced to measure response processes in more detail than is possible with summarizing scoring of paper pencil tests. For each reaction the following information was registered: stimulus (light), reaction (right/wrong), reaction time, and omission (yes/no). Each subject had to react on 320 successive signals without pause. From the reaction protocol of each subject indices for speed of work, oscillation of performance, error disposition, and reaction inhibition were computed. The main result is that in this reaction test speed of work and error disposition are not coupled. Errors are not a consequence of quick reactions. The observed errors seem to be the expression of an increased variation in performance. The results are discussed with a view to a psychophysiological model of activation.

Author (ESA)

N86-10782# Institute for Perception RVO-TNO, Soesterberg (Netherlands). Afd. Psychologie.

STANDARDIZATION OF TASKS: APPROACH PLANNING

A. W. K. Gaillard and L. C. Boer Jul. 1984 19 p In DUTCH; ENGLISH summary

(Contract A83/K/045)

(IZF-1984-19; TDCK-79518) Avail: NTIS HC A02/MF A01

Ten information processing tasks were grouped on a microcomputer for use in, e.g., personnel selection, the registration of pyschological fitness (combat readiness) and assessing mental workload. Testing areas are: reaction time, (continuing) memory searching, selective attention, pursuit-tracking, serial memory, word classification, logical arguing, and response-conflict situations. The program is developped to be administered by personnel with 1 week training.

Author (ESA)

N86-10783# Institute for Perception RVO-TNO, Soesterberg (Netherlands). Traffic Behavior Group.

PATH ERROR-NEGLECTION IN STRAIGHT LANE DRIVING

J. Godthelp Oct. 1984 21 p refs

(IZF-1984-32; TDCK-79698) Avail: NTIS HC A02/MF A01

Decision rules, describing how drivers switch from error-neglection to error-correction when approaching the edge of a lane, were derived for a straight lane keeping task. Drivers were instructed to neglect the vehicle path error and to switch over to error-correction only at that moment. The vehicle motion still could comfortably be corrected to prevent a crossing of the lane boundary. The results show that the lateral distance from the lance boundary at which drivers switch to error-correction increases linearly with the lateral approach speed. This mechanism results in a constant time to lane crossing distance at this decision moment, this result being consistant for a broad range of speeds.

Author (ESA)

N86-10745# Joint Publications Research Service, Arlington, Va.
EFFECT OF EMOTIONAL STRESS ON HEMOSTASIS SYSTEM OF HEALTHY PERSONS Abstract Only
Ye. I. Sokolov, T. P. Khovanskaya, I. V. Novikov, and M. V. Baluda *In its* USSR Rept.: Life Sci. Biomed. and Behavioral Sci. (JPRS-UBB-85-023) 18 Sep. 1985 p 62 Transl. into ENGLISH from Fiziol. Cheloveka (Moscow), v. 11, no. 1, Jan. - Feb. 1985 p 79-82 (For primary document see N86-10738 01-51)
Avail: NTIS HC A06

54 MAN/SYSTEM TECHNOLOGY AND LIFE SUPPORT

Includes human engineering; biotechnology; and space suits and protective clothing.

N86-10784 Ohio State Univ., Columbus.
THE INFLUENCE OF TACTUAL SEAT-MOTION CUES ON TRAINING AND PERFORMANCE IN A ROLL-AXIS COMPENSATORY TRACKING TASK SETTING Ph.D. Thesis
Edward Albert Martin 1985 327 p
Avail: Univ. Microfilms Order No. DA8510600

A considerable body of knowledge exists regarding the influence of whole-body motion on the control behavior and task performance of a vehicle operator required to compensate for the effects of unexpected external disturbances. The research described was conducted to determine whether similar effects would be observed if the motion information were tactually displayed through the seat pan, rather than in a whole-body motion environment. The experiment was designed such that the transfer of training from a tactual dynamic seat display to a whole-body motion environment could also be evaluated. The environmental task required subjects to regulate for a random-appearing, roll-axis disturbance in a simulated vehicle having aircraft-like dynamics. A centrally located compensatory display, subtending about nine degrees, provided visual roll error information. Control inputs were made via a right side-arm isometric controller. The two-phase experiment included a training phase and a criterion phase. The data clearly demonstrate that a dynamic sea pan can effectively impart motion information. Dissert. Abstr.

N86-10785*# Pennsylvania Univ., Philadelphia. Dept. of Computer and Information Science.
TEMPUS: SIMULATING PERSONNEL AND TASKS IN A 3-D ENVIRONMENT Final Report
Norman I. Badler and Jon D. Korein 31 May 1985 18 p
(Contract NAS9-16634)
(NASA-CR-171901; NAS 1.26:171901) Avail: NTIS HC A02/MF A01 CSCL 05H

The latest TEMPUS installation occurred in March, 1985. Another update is slated for early June, 1985. An updated User's Manual is in preparation and will be delivered approximately mid-June, 1985. NASA JSC has full source code listings and internal documentation for installed software. NASA JSC staff has received instruction in the use of TEMPUS. Telephone consultations have augmented on-site instruction. G.L.C.

N86-10786# Defence Research Establishment, Ottawa. (Ontario).
EFFECT OF INCREASED BODY CLOTHING INSULATION ON HAND TEMPERATURE IN A COLD ENVIRONMENT
S. D. Livingstone, R. W. Nolan, and S. W. Cattroll Dec. 1984 17 p
(AD-A156597; DREO-TN-84-26) Avail: NTIS HC A02/MF A01 CSCL 06/17

Thermal protection of personnel who must remain relatively inactive while performing tasks outdoors in the cold is a continuing problem. Provision of comfort and allowing for mobility are design difficulties experienced by persons working in the cold at tasks for which manual dexterity is required is In such situations only very light handwear can be worn and often, mitts or gloves must be removed in order to perform the task. A particular example of such a task exists at the CF Satellite Tracking and Identification Unit at St. Margaret's, New Brunswick. The telescope which is used for tracking satellites is located outdoors when operational. To minimize optical interference, the area around the telescope cannot be heated in winter. During the course of the tracking sequence, which takes about 30 minutes, the operator must be in contact with the large metal mass of the telescope. In addition, the operation of the steering control button requires that if any handwear is worn, it must be very thin. Operating temperatures as low as -20 C are often experienced. It was found that, as predicted, if additional insulation was applied to the whole body of the man, the temperature of his hands could be maintained for a longer period of time. GRA

N86-10787# Air Force Inst. of Tech., Wright-Patterson AFB, Ohio.
MILD HYPOXIA AND VISUAL PERFORMANCE WITH NIGHT VISION GOGGLES M.S. Thesis
L. L. Leber May 1985 57 p
(AD-A156969; AD-E950724; AFIT/CI/NR-85-35T) Avail: NTIS HC A04/MF A01 CSCL 06/5

Pilots have frequently reported an apparent darkening of the visual field while flying at high altitude without supplemental oxygen, and subsequent exposure to oxygen resulted in marked increases in the brightness of lights. Likewise, at low light intensities visual acuity is greatly decreased during oxygen deprivation. In contrast, at high light intensities, the effect of moderate oxygen deprivation on visual acuity is slight. Even though the Night Vision Goggles (NVGs) amplify low night illumination, the interaction between amplified illumination and high altitude effects may provide to be important factors in visual performance. The objective of this research was to investigate the effects of mild hypoxid aon monocular visual performance with NVGs. This study revealed that mild oxygen deprivation significantly affects unaided square-0wave grating visual acuity but does not significantly affect NVG-augmented performance. Large differences between visual sensitivities at different spatial frequencies were not differentially affected by mild hypoxia. Supplemental oxygen did significantly improve naked-eye but not NVG-augmented night resolution acuity up to an altitude of 13,000 feet (3,692 m) above sea level (ASL). GRA

N86-10788# Aeronautical Research Labs., Melbourne (Australia).
A GRAPHIC ANTHROPOMETRIC AID FOR SEATING AND WORKPLACE DESIGN
K. C. Hendy, K. W. Anderson, and D. M. Drumm Apr. 1984 60 p
(AD-A156988; AD-E950724; ARL/SYS-R-29) Avail: NTIS HC A04/MF A01 CSCL 06/14

In recent workplace design projects at ARL, a procedure for the use of anthropometric information has be developed which relies on the use of sets of anthropometric data from individuals rather than the conventionally used pooled data. This report describes a graphic anthropometric design aid which has been devised to assist in the implementation of this procedure. The aid predicts the positions, in side elevation, of certain cardinal points which are considered to be important to the design process, viz, the eye, thumb tip reach, knee point, seat reference point and heel point. This report also contains details of the design aid's validation, the concept of the aid's use and the fidelity of the aid within the design process. GRA

N86-10789# Institute for Perception RVO-TNO, Soesterberg (Netherlands). Afd. Thermofysiologie.
THE WEARING COMFORT OF THE PVC: COMBAT BACK PACK
F. J. G. vanderlinde and H. VanMiddendorp Nov. 1984 24 p In DUTCH; ENGLISH summary
(Contract A79/KL/097)
(IZF-1984-34; TDCK-79782) Avail: NTIS HC A02/MF A01

A PVC coated back pack was compared to canvas ones. Wearing comfort, particularly with regard to sweat build-up, body temperatures, and thermal sensation were studied. Data from two subjects walking on a treadmill in a climate chamber were

obtained. The PVC prototype scores slighthy better the canvas rucksack. Author (ESA)

55 PLANETARY BIOLOGY

Includes exobiology; and extraterrestrial life.

No abstracts in this category.

59 MATHEMATICAL AND COMPUTER SCIENCES (GENERAL)

N86-10790# IIT Research Inst., Rome, N.Y.
CATALOG OF RESOURCES FOR EDUCATION IN Ada (TRADEMARK) AND SOFTWARE ENGINEERING (CREASE). VERSION 3.0
May 1985 334 p
(Contract MDA903-83-C-0306)
(AD-A156687) Avail: NTIS HC A15/MF A01 CSCL 05/9

Over the last twenty-five years, software technology has made enormous strides. The Ada program serves as a focal point for the consolidation of state-of-the-art thinking about this technology. Proper use of the technology can contribute significantly to controlling the cost and improving the quality of software. However, this is a sophisticated technology, and its proper use depends upon sophisticated education and training for the people applying it. The effectiveness of the Ada programming language will be determined by the degree to which people are able to use it to implement software engineering practices in applications programming. A carefully planned education and training program, which teaches both fundamental software engineering concepts and the effective use of the Ada language, is therefore essential. This publication is intended to serve as a source of information about resources available to those who are planning such programs, with the hope that it will not only serve as a ready reference, but will also increase awareness of the many aspects of education in Ada and Software Engineering. GRA

60 COMPUTER OPERATIONS AND HARDWARE

Includes computer graphics and data processing.

For components see *33 Electronics and Electrical Engineering.*

N86-10791# Naval Postgraduate School, Monterey, Calif.
COMPUTER-BASED TRAINING FOR THE US COAST GUARD STANDARD TERMINAL MICROCOMPUTER: A BASIS FOR IMPLEMENTATION UTILIZING THE ELABORATION THEORY OF INSTRUCTIONAL DESIGN M.S. Thesis
S. E. Johnson Mar. 1985 81 p
(AD-A156548) Avail: NTIS HC A05/MF A01 CSCL 09/2

Various factors concerning the U.S. Coast Guard Standard Terminal microcomputer, including the large number of installation sites, steady turnover of user personnel, and conflicting demands of operational commitments indicate that computer-based training is a desirable approach for indoctrinating new users of the computer system. Any such instructional computer program developed for this purpose should consider the characteristics of the trainee audience, particularly the varied levels of procedural detail desired and constraints on time available for training. The elaboration theory of instructional design provides an excellent framework for creating a viable computer-based course of instruction. A Pascal computer program and demonstration lesson modules utilize the macro-strategy components of Elaboration Theory in an introductory course on computer procedures. Course presentation is controlled by special characters imbedded in the lesson text files and interpreted by the program. Author (GRA)

N86-10792# Department of the Navy, Washington, D. C.
PARALLEL LOCAL INTERFACE BUS Patent Application
G. J. Palatucci, C. M. Nowicki, and R. Whitsel, inventors (to Navy)
Filed 29 Nov. 1984 20 p
(AD-D011742; US-Patent-Appl-SN-677136) Avail: NTIS HC A02/MF A01 CSCL 09/2

A modular parallel local interface bus provides a two-way interface between a microprocessor and a plurality of distributed signal processing units which are controlled by the microprocessor. Likewise, the microprocessor is enabled to read operational parameter data from sensors in the signal processing units. In this way, a plurality of discrete signal processing units may be controlled to perform required RF transmit-receive functions. The units may also be monitored for any operational problems which could develop. Author (GRA)

N86-10793# Royal Signals and Radar Establishment, Malvern (England).
SPECIAL PURPOSE HARDWARE ARCHITECTURES FOR LANGUAGE RECOGNITION
R. A. Evans and J. D. Morison Mar. 1985 22 p
(AD-A156634; RSRE-Memo-3806; DRIC-BR-95704) Avail: NTIS HC A02/MF A01 CSCL 09/2

Two distinct chip architectures for language recognition are presented. THe first allows a recogniser for any regular expression to be constructed by simply assembling predefined cells linto a linear array. The cells correspond to the symbols which can occur in a regular expression, and the appropriate cells are placed in a line in the same order as the expression. The recogniser is then correct by construction, and all inter-cell connections are made automatically. The second architecture can be programmed to recognize any LL(1) context-free language by loading it with the appropriate grammar rules. The grammar rules are embodied within and array of identical cells, which, in conjunction with a standard LIFO stack, form the recognition hardware. Author (GRA)

N86-10794# Yale Univ., New Haven, Conn. Dept. of Computer Science.
ALTERNATING DIRECTION METHODS ON MULTIPROCESSORS: AN EXTENDED ABSTRACT
Y. Saad and M. H. Schultz Apr. 1985 7 p
(Contract N00014-82-K-0184)
(AD-A156722; Yaleu/DCS/RR-381) Avail: NTIS HC A02/MF A01 CSCL 09/2

We propose a few implementations of the Alternating Direction Method for solving parabolic partial differential equations on multiprocessors. A careful complexity analysis of these implementations shows that, contrary to what is generally believed, the method can be made highly efficient on parallel architectures by using pipelining and variations of the classical Gaussian elimination algorithm for solving tridiagonal systems. GRA

N86-10795# Yale Univ., New Haven, Conn. Dept. of Computer Science.
EFFICIENT SYSTOLIC ARRAYS FOR THE SOLUTION OF TOEPLITZ SYSTEMS: AN ILLUSTRATION OF A METHODOLOGY FOR THE CONSTRUCTION OF SYSTOLIC ARCHITECTURES IN VLSI (VERY LARGE SYSTEMS INTEGRATION)
J. M. Delosme and I. C. F. Ipsen Jun. 1985 25 p
(Contracts N00014-82-K-0184; N00014-84-K-0092)
(AD-A156767; Yaleu/DCS/RR-370) Avail: NTIS HC A02/MF A01 CSCL 09/2

Advanced high resolution methods for real-time signal processing require fast multiprocessor architectures, realized as Very Large Scale Integrated systems, for their implementation. A class of parallel structures, systolic arrays, fulfills the demands of signal processing and at the same time conforms to the limitations of

VLSI technology. The design of efficient systems of systolic arrays is an iterative process in which the information gathered from mapping algorithms onto hardware is influential in the development of the algorithms. Presently, the absence of mapping tools makes it extremely difficult to find good systolic implementations for many important problems. Often, one cannot do better than implementing structurally simple but numerically inferior algorithms, which is undesirable for most signal processing tasks. A methodology is proposed that automates the mapping of recurrence equations to processor arrays. Two aspects distinguish our methodology from extant work: (1) complex coupled systems of recurrence equations can be systematically treated, and (2) the resulting systolic systems are optimal. The methodology takes as input recurrence equations describing the algorithm, along with certain desirable hardware features. GRA

N86-10796# Naval Postgraduate School, Monterey, Calif.
INITIAL DESIGN OF A RELATIONAL DATABASE SYSTEM FOR NPS COMPUTER ASSET IDENTIFICATION AND VALUATION FOR RISK ASSESSMENT M.S. Thesis
F. W. Thompson Mar. 1985 124 p
(AD-A156847; AD-E301723) Avail: NTIS HC A06/MF A01 CSCL 09/2

Relational database technology is examined as a means to support computer Risk Assessment at the Naval Postgraduate School. The current methodology for conducting computer Risk Assessment within the Department of the Navy is used to construct an initial design for a relational database system. The initial design focuses on computer asset identification and valuation as the first step of the computer Risk Assessment process. GRA

N86-10797# Naval Postgraduate School, Monterey, Calif.
DEVELOPMENT OF IS2100: AN INFORMATION SYSTEMS LABORATORY M.S. Thesis
C. S. D. Witten Mar. 1985 41 p
(AD-A156848; AD-E301723) Avail: NTIS HC A03/MF A01 CSCL 09/2

On the premise that fundamental concepts and uses of microcomputers can be better taught in a hands-on environment, the Administrative Science Department Instructional Laboratory was established. IS 2100, an Information Systems Laboratory uses these facilities to reinforce material taught in the first two quarters of the Computer System Management Curriculum. Its purpose and objective is to develop computer literacy and introduce the student to microcomputers and the facilities of the developing laboratory. This thesis is the report of the development of IS 2100 as first taught during Winter 1985. GRA

N86-10798# Air Force Inst. of Tech., Wright-Patterson AFB, Ohio.
APPLICATIONS FOR THREE-DIMENSIONAL COMPUTER GRAPHIC CLOUD REPRESENTATIONS PRODUCED FROM SATELLITE IMAGERY M.S. Thesis
A. C. Meade 1985 112 p
(AD-A156903; AFIT/CI/NR-85-50T) Avail: NTIS HC A06/MF A01 CSCL 04/2

In this research process, two-dimensional satellite topographic images are used to produce 3-D, mathematically defined, cloud-topography models. This research focuses on applications for three-dimensional cloud representations which are displayed above a topographic surface. The computer graphic cloud-topography displays are produced using actual GOES satellite data, Defense Mapping Agency topography data, and rawinsonde upper air data. Data from these three sources is used to generate three-dimensional models which mathematically define cloud cover and topography for a given area. By applying computer graphics techniques, these three-dimensional models can be displayed as continuous tone images or perspective line drawings. Satellite data and topography data, displayed in this manner, produces a realistic depiction of cloud cover displayed above a topographic surface. As for applications, these displays can be used for cloud studies, briefing aids, and flight simulations. GRA

N86-10799# Department of the Air Force, Washington, D.C.
HARMONIC DISTORTION REDUCTION TECHNIQUE FOR DATA ACQUISITION Patent Application
W. P. Evans, inventor (to Air Force) Filed 12 Jun. 1985 18 p
(AD-D011771; US-Patent-Appl-SN-743853) Avail: NTIS HC A02/MF A01 CSCL 09/2

An analog to digital converter (ADC) is presented which uses a calibration technique to reduce harmonic distortion in data acquisition systems. This mechanization also allows faster conversion rates than previously possible for high resolution analog-to-digital converters. This converter makes use of a subrange or half Flash architecture where the subrange digital-to-analog converter (DAC) is augmented with a software calibrated DAC which removes system nonlinearities. The advantage of this system is that it allows the building of higher speed data acquisition systems with higher spurious free dynamic range than would be possible with conventional techniques. By adding the correction to the input of the subrange ADC, correction resolution can be a fraction of a quanta. A second approach using the same mathematics places at the output of the ADC a RAM or ROM look up table which linearizes the transfer function. Author (GRA)

N86-10800# Department of the Air Force, Washington, D.C.
ARITHMETIC PIPELINE FOR IMAGE PROCESSING Patent Application
W. R. Steiner, inventor (to Air Force) Filed 6 Jun. 1985 77 p
(AD-D011773; US-Patent-Appl-SN-741644) Avail: NTIS HC A05/MF A01 CSCL 09/2

The arithmetic pipeline processor (which is used for computer graphics such as a flight simulator) is a group of boards capable of solving an equation of a certain form. It includes a digital logarithmic calculator using shifters and stored tables to perform arithmetic functions such as multiplication, division, squares, square roots, and fourth roots. It comprises two imput ports each capable of receiving digital data N bits wide. Included are a log transform unit, a log sum or difference unit and an antilog unit. Following these is an M-bit Ariithmetic Logic Unit and circuitry for converting between fixed point and floating numbers. It uses piece wise linear approximation in conjunction with stored slope information in tables to do the transform calculation of logarithms and antilogarithms. The M-bit arithmetic unit performs accumulation of up to k terms. In a specific embodiment, N=32, M-36, and K=128. Note that a pipeline processor has no central processing unit or software in itself, but it may interface with a computer for inputs and outputs including control information. GRA

N86-10801# Stanford Linear Accelerator Center, Calif.
DISSECTING THE COW
E. Linstadt Apr. 1985 3 p Presented at the Particle Accelerator Conf., Vancouver, British Columbia, 13 May 1985
(Contract DE-AC03-76SF-00515)
(DE85-013369; SU-SLAC-PUB-3638; CONF-850504-69) Avail: NTIS HC A02/MF A01

The COW, or Console On Wheels, is the primary operator interface to the Stanford Linear Collider (SLC) accelerator control system. A hardware and oftware description of the COW, a microcomputer based system with a color graphics display output and touch-panel and knob inputs, is given. The ease of development and expandability, due to both the modular nature of the hardware and the multitasking, interrupt driven software running in the COW, are described. Integration of the COW into the SLCNET communications network and SLC Control system is detailed.DOE

N86-10802# Technische Hogeschool, Eindhoven (Netherlands). Digital Systems Group.
DESIGN OF A MULTIFUNCTION INPUT-OUTPUT (I/O) CONTROLLER
M. P. J. Stevens and M. P. M. vanLoon Aug. 1984 63 p refs In FRENCH; ENGLISH summary
(EUT-84-E-143; ISBN-90-6144-143-9; ISSN-0167-9708) Avail: NTIS HC A04/MF A01

A multifunction I/O-controller used for the exchange of data between a microcomputer and a peripheral was designed. Design

strategies for the realization of (V)LSI-circuits are discussed. By partitioning the controller into subsystems and carefully defining the interaction between these subsystems, the design can be implemented in a number of technologies like custom designed NMOS or gate-arrays. The controller can be used with many Intel and Motorola processors and it has four programmable modes: direct I/O, handshake I/O, three wire I/O and bidirectional I/O. Author (ESA)

N86-10803# Technische Hogeschool, Eindhoven (Netherlands). Digital Systems Group.
MINIMIZATION OF PROGRAMMABLE LOGIC ARRAYS
M. J. M. vanWeert Nov. 1984 48 p refs In DUTCH; ENGLISH summary
(EUT-84-E-145; ISBN-90-6144-145-5; ISSN-0167-9708) Avail: NTIS HC A03/MF A01

The efforts undertaken to minimize four programmable logic arrays (PLA) and so to define part of the control section of a multifunction I/O controller, are described. The silicon area occupied by the minimized PLA is equal to 65% of the original area. It is shown that searching for and recognizing terms as don't care terms, and inverting one or more output functions contribute a lot to the final result. The functional behavior of the PLA was simulated before and after minimization, and is found to be correct. Author (ESA)

N86-10804# Technische Hogeschool, Eindhoven (Netherlands). Digital Systems Group.
REALIZATION OF A MULTIFUNCTION INPUT/OUTPUT (I/O) CONTROLLER BY MEANS OF A GATE ARRAY
L. T. Rozendaal, M. P. J. Stevens, and P. M. C. M. vandenEijnden Jan. 1985 110 p refs In DUTCH; ENGLISH summary
(EUT-85-E-147; ISBN-90-6144-147-1; ISSN-0167-9708) Avail: NTIS HC A06/MF A01

The implementation process of a multifunction I/O controller using a gate consisting of Schottky TTL gates is described. This process is straightforward if during the logic design (analysis) of the chip, care is given to a modular construction and when the logic in the chip is defined using regular structures like programmable logic arrays instead of so-called wild logic. The software package used to define, simulate, and test the design of the I/O controller, is described. Author (ESA)

N86-10805# Technische Hogeschool, Eindhoven (Netherlands). Digital Systems Group.
A COURSE ON FIELD PROGRAMMABLE LOGIC
P. M. C. M. vandenEijnden Apr. 1985 122 p refs
(EUT-85-E-148; ISBN-90-6144-148-X; ISSN-0167-9708) Avail: NTIS HC A06/MF A01

Programmable logic components that can be used to realize both combinational and sequential logic circuits are reviewed. A general structure for these components starting with boolean equations and state diagrams is determined. The considerations with respect to optimization and decomposition of a circuit, important in designs with these components, are discussed. Commercially available products are included. Author (ESA)

N86-10806# Technische Hogeschool, Delft (Netherlands). Lab. voor Schakeltechniek en Techniek van de Informatieverwerkende Machines.
THE LOCAL DISK CONTROLLER
G. E. Houtekamer 7 Feb. 1985 20 p refs
(Rept-1-68430-44(1985)01) Avail: NTIS HC A02/MF A01

The performance of the input/output (I/O) subsystem in the the IBM 370-XA architecture was increased considerably by a modified of the new channel subsystem, as compared to the System/370. The emphasis in the 370-XA architecture is on reducing the CPU load associated with I/0, and on reducing the contention in multi-CPU, shared systems, by redesigning the channel system. It is shown that a reallocation of the control unit logic may triple channel subsytem capacity, while still using the same disk drives. The performance gain is achieved by adding intelligence and local buffer memory to each disk drive, creating a local disk controller. The proposed system remains fully software compatible with the 370-XA architecture. Author (ESA)

N86-10807# Technische Hogeschool, Delft (Netherlands). Lab. voor Schakeltechniek en Techniek van de Informatieverwerkende Machines.
PERFORMANCE ANALYSIS OF THE IBM DIRECT ACCESS STORAGE DEVICE (DASD) SUBSYSTEM, AND SOME SUGGESTIONS FOR IMPROVED SYSTEMS
G. E. Houtekamer 7 Feb. 1985 19 p refs
(Rept-1-68430-44(1985)02) Avail: NTIS HC A02/MF A01

The IBM 370-XA input/output (I/O) architecture is described. The I/O response time consists of several components, such as the seek and rotational delay. All access time components are analyzed, and suggestions to improve the system are given. The buffered disk system and local disk controller system are discussed. After modifications to the hardware of the 370-XA I/O subsystem they provide a much better performance. The local disk controller system allows access rate of the order of 60 SIOs per disk per second. The performance improvements achievable with caching for the control unit based system, and for the local disk controller system are investigated. Author (ESA)

N86-10808# Technische Hogeschool, Delft (Netherlands). Lab. voor Schakeltechniek en Techniek van de Informatieverwerkende Machines.
AN INTELLIGENT LOCAL DISK CONTROL SYSTEM
G. E. Houtekamer 1 May 1984 131 p refs
(Rept-051560-28(1984)08) Avail: NTIS HC A07/MF A01

A disk input/output (I/O) system for IBM 30xx series main frames was developed. The system is based on the utilization of an intelligent local control for each disk pack. The disks are connected to the central computer via a high-speed bus (32 MB/sec). Every disk is equipped with an Intel iAPx 286 microprocessor, which controls the disk hardware and executes the I/O programs. The system is designed so that the most expensive components of the I/O system; the top model from the IBM disk-series (3380); and the present software (IBM/MUS operating system) can be used without adaptation. Author (ESA)

N86-10809# Joint Publications Research Service, Arlington, Va.
USSR REPORT: CYBERNETICS, COMPUTERS AND AUTOMATION TECHNOLOGY
5 Sep. 1985 153 p refs Transl. into ENGLISH from various Russian articles
(JPRS-UCC-85-006) Avail: NTIS HC A08

Progress is reported in U.S.S.R. cybernetics, computers and automation technology. Topics discussed include: (1) general automation technology; (2) hardware; (3) software; (4) computer applications; (5) computer networks; (6) computation theory; (7) education; and (8) automation organizations. For individual titles, see N86-10810 through N86-10818.

N86-10810# Joint Publications Research Service, Arlington, Va.
PROSPECTS FOR CREATION OF OPTICAL DIGITAL HIGH-PERFORMANCE COMPUTERS
V. M. Yegorov and E. G. Kostsov *In its* USSR Rept.: Cybernetics, Computers and Automation Technol. (JPRS-UCC-85-006) 5 Sep. 1985 p 22-36 refs Transl. into ENGLISH from Avtometriya (Novosibirsk), no. 1, Jan. - Feb. 1985 p 114-126 (For primary document see N86-10809 01-60)
Avail: NTIS HC A08

The technological feasibility of creating optical digital high-performance computers is investigated. The need for increased computer productivity in solving large-scale problems in space research and mathematical physics is established. General advances in microelectronic technology are discussed in the area of optical data processing. Specifically, the possibility of fabricating a thin film electrooptic light modulator is explored. B.W.

N86-10811# Joint Publications Research Service, Arlington, Va.
ELEKTRONIKA MS 1603 HIGH-SPEED PERIPHERAL PROCESSOR

V. A. Dyboy, V. V. Kashtanov, V. O. Lazarev, and A. A. Fokin *In its* USSR Rept.: Cybernetics, Computers and Automation Technol. (JPRS-UCC-85-006) 5 Sep. 1985 p 39-43 Transl. into ENGLISH from Avtometriya (Novosibirsk), no. 2, Mar. - Apr. 1985 p 88-90 (For primary document see N86-10809 01-60)
Avail: NTIS HC A08

High-speed peripheral processors, with their high computation speed, high reliability, compact design and low power requirement, have found wide application in recent years. An example of such a system is the Elektronika MT-70 high-speed peripheral processor, series-produced by domestic industry for many years. The Elektronika MS 1603 was developed on the basis of operational experience with the MT-70 and is compatible with the latter at the application program level. The Elektronika MSS 1603 high-speed peripheral processor can be used in conjunction with any computer having a common-bus type parallel bus interface between modules. Its primary purpose in operation with an Elektronia 60 computer system is the execution of a large number of vector multiplication and addition operations. The technical specifications of the Elektronika MS 1603 high-speed peripheral processor are given. B.W.

N86-10812# Joint Publications Research Service, Arlington, Va.
DIAGNOSTICS OF PERIPHERAL PROCESSORS AND CONTROLLERS
V. A. Dyboy, O. S. Semenova, and A. A. Fokin *In its* USSR Rept.: Cybernetics, Computers and Automation Technol. (JPRS-UCC-85-006) 5 Sep. 1985 p 48-53 Transl. into ENGLISH from Avtometriya (Novosibirsk), no. 2, Mar. - Apr. 1985 p 90-93 (For primary document see N86-10809 01-60)
Avail: NTIS HC A08

One of the problems facing computer system manufacturers and users is that of calibration and maintenance. The problem is caused by the increasing complexity of equipment combined with the inflexible nature of the methods of testing employed. These methods are based on component troubleshooting (the location and correction of failed components) according to indirect signs generated as the result of operational monitoring. Under these conditions, the introduction of more progressive and higher quality (and more complex) equipment is inefficient due to the concomitant need for hiring or training highly qualified specialists to calibrate (during production) or repair (during operation) this equipment. A diagnostic method using built-in diagnostic hardware is described which allows a significant increase in the scope of trouble-shooting. B.W.

N86-10813# Joint Publications Research Service, Arlington, Va.
AN APPROACH TO IMPLEMENTING CAMAC MICROPROCESSOR MODULES
Ye. M. Bazarnyy, A. N. Vystavkin, L. Z. Pososhenko, V. P. Reztsov, and A. B. Furshchik *In its* USSR Rept.: Cybernetics, Computers and Automation Technol. (JPRS-UCC-85-006) 5 Sep. 1985 p 54-58 refs Transl. into ENGLISH from Upravlyayushchiye Sistemy i Mashiny (Kiev), no. 2, Mar. - Apr. 1985 p 106-108 (For primary document see N86-10809 01-60)
Avail: NTIS HC A08

CAMAC (computer automated measurement and control) hardware is widely used in the creation of systems for automating scientific research. The use of microprocessors in CAMAC hardware allows substantial improvement in functional characteristics and increases in system efficiency. In addition to the design of multicontroller microprocessor systems, a generation of smart modules needs to be developed to enable preliminary data processing directly in the control subprogram execution module and to perform a number of auxiliary tasks (automonitoring, parameter correction, etc.). This article discusses one possible architecture for a new generation of CAMAC modules based on microprocessor components and points out the superior properties of these modules. Author

N86-10814# Joint Publications Research Service, Arlington, Va.
COMPACT, HIGH-SPEED ALGORITHM FOR LAYING OUT PRINTED CIRCUIT BOARD RUNS c33
D. Ye. Zapolotskiy *In its* USSR Rept.: Cybernetics, Computers and Automation Technol. (JPRS-UCC-85-006) 5 Sep. 1985 p 59-67 refs Transl. into ENGLISH from Upravlyayushchiye Sistemy i Mashiny (Kiev), no. 2, Mar. - Apr. 1985 p 33-37 (For primary document see N86-10809 01-60)
Avail: NTIS HC A08

A high speed printed circuit connection layout algorithm is described which was developed within the framework of an interactive system for designing two-sided printed circuit broads. For this reason, algorithm speed was considered, a priori, as a requirement equally as important as the inherent demand for minimizing circuit run lengths and the number of junction openings. This resulted from the fact that, in order to provide psychological man/machine compatibility in the design process, real-time dialog during the layout phase is possible only within limited time frames (on the order of several seconds) for each circuit run. The work was carried out for use on an ARM-R automated work site complex based on an SM-4 minicomputer with a 32K-word memory. This limited memory capacity heightened the demand for algorithm speed and also tightened data file structure and size requirements. The layout algorithm's design logic is analyzed. The structure and organization of the data files are described. B.W.

N86-10815# Joint Publications Research Service, Arlington, Va.
CLASSIFICATION OF REAL-TIME PROGRAM TESTING TASKS AND METHODS c61
I. N. Dolganyuk and Ye. Ya. Karpovskiy *In its* USSR Rept.: Cybernetics, Computers and Automation Technol. (JPRS-UCC-85-006) 5 Sep. 1985 p 70-83 refs Transl. into ENGLISH from Upravlyayushchiye Sistemy i Mashiny (Kiev), no. 2, Mar. - Apr. 1985 p 57-62 (For primary document see N86-10809 01-60)
Avail: NTIS HC A08

The testing of real-time programs, one of the most important steps in program debugging, is a critical problem in modern programming theory. Usually debugging is understood as the group of activities involved in detecting (identifying) and correcting errors in programs. These activities are grouped in stages: establishing the presence of an error, identifying the error and, finally, correcting the error. In the course of debugging programs, developers are faced with a number of questions involving the determination of current test method capabilities and suitability. An understanding of the nature of the testing process is essential in classifying the methods and tasks involved in seeking errors in programs. The research suggests that the presence of an error in a program is detected by means of the following sequence of actions: (1) test objective definition; (2) tactical goal assignment; (3) criteria selection; (4) test design and generation; (5) test introduction and program execution; (6) program result processing to determine the existence of errors; and (7) testing cutoff point determination. B.W.

N86-10816# Joint Publications Research Service, Arlington, Va.
DBS/R DATABASE CONTROL SYSTEM
Yu. Sharr *In its* USSR Rept.: Cybernetics, Computers and Automation Technol. (JPRS-UCC-85-006) 5 Sep. 1985 p 84-92 Transl. into ENGLISH from Upravlyayushchiye Sistemy i Mashiny (Kiev), no. 2, Mar. - Apr. 1985 p 97-101 (For primary document see N86-10809 01-60)
Avail: NTIS HC A08

The Robotron combine (GDR) is producing YeS- and SM-series computers and developing a wide assortment of system and application software. This paper highlights the database software developed at the Robotron combine which includes database management systems (DBMS) and information retrieval system. One system in particular is examined, the DBS/R Data Base Management System. The general features, functions and languages; applications, and economic effects of the DBS/R are discussed in detail. B.W.

N86-10817# Joint Publications Research Service, Arlington, Va.
COLLECTIVE USE COMPUTER SYSTEM FOR THE ACADEMY OF SCIENCES KaSSR
U. M. Sultangazin, I. T. Pak, M. A. Bulakh, G. T. Manabayev, and

V. A. Tsay *In its* USSR Rept.: Cybernetics, Computers and Automation Technol. (JPRS-UCC-85-006) 5 Sep. 1985 p 105-111 refs Transl. into ENGLISH from Upravlyayushchiye Sistemy i Mashiny (Kiev), no. 2, Mar. - Apr. 1985 p 108-111 (For primary document see N86-10809 01-60)
Avail: NTIS HC A08

At this time electronic computer technology is penetrating many branches of industry at various levels and is solving increasing complex problems. A number of automated control systems for production and engineering processes have been created and are being developed to solve these types of problems. The role and place of the computer in automated control systems has quite definitely grown because of this. A particularly promising field for computer application are automated systems for scientific research which are oriented toward automating labor-intensive processes and which facilitate the establishment of principles behind the phenomena studied. The critical need for computer technology in scientific research has been clearly pointed out in this research. A computer network known as VSKP is described which is intended to increase scientific research efficiency at the Academy of Sciences KaSSR. B.W.

N86-10818# Joint Publications Research Service, Arlington, Va.
DIGITAL PROCESSING OF IMAGES IN TRACKING A MOVING OBJECT **c61**
B. A. Alpatov, A. A. Selyayev, and A. I. Stapashkin *In its* USSR Rept.: Cybernetics, Computers and Automation Technol. (JPRS-UCC-85-006) 5 Sep. 1985 p 123-127 refs Transl. into ENGLISH from Proborostr. (Leningrad), no. 2, Feb. 1985 p 39-43 (For primary document see N86-10809 01-60)
Avail: NTIS HC A08

A digital algorithm for digital processing images in tracking a moving object is proposed. The results of computer simulation are given which confirm the expediency of using the preliminary smoothing of images to increase the precision of evaluating coordinates. Author

61 COMPUTER PROGRAMMING AND SOFTWARE

Includes computer programs, routines, and algorithms.

N86-10819*# Informatics, Inc., Palo Alto, Calif.
LANES 1 USERS' GUIDE
Joe Jordan Feb. 1985 21 p
(Contract NAS2-11555)
(NASA-CR-177334; NAS 1.26:177334; TN-84-7104-925-46) Avail: NTIS HC A02/MF A01 CSCL 09B

This document is intended for users of the Local Area Network Extensible Simulator, version I. This simulator models the performance of a Fiber Optic network under a variety of loading conditions and network characteristics. The options available to the user for defining the network conditions are described in this document. Computer hardware and software requirements are also defined. Author

N86-10820*# Pennsylvania Univ., Philadelphia. Dept. of Computer and Information Science.
USER INTERFACE ENHANCEMENT REPORT
Norman I. Badler, Jeffrey Gangel, Gwen Shields, and Glenn Fala 31 May 1985 50 p refs
(Contract NAS9-16634)
(NASA-CR-171898; NAS 1.26:171898) Avail: NTIS HC A03/MF A01 CSCL 09B

The existing user interfaces to TEMPUS, Plaid, and other systems in the OSDS are fundamentally based on only two modes of communication: alphanumeric commands or data input and grapical interaction. The latter are especially suited to the types of interaction necessary for creating workstation objects with BUILD and with performing body positioning in TEMPUS. Looking toward the future application of TEMPUS, however, the long-term goals of OSDS will include the analysis of extensive tasks in space involving one or more individuals working in concert over a period of time. In this context, the TEMPUS body positioning capability, though extremely useful in creating and validating a small number of particular body positions, will become somewhat tedious to use. The macro facility helps somewhat, since frequently used positions may be easily applied by executing a stored macro. The difference between body positioning and task execution, though subtle, is important. In the case of task execution, the important information at the user's level is what actions are to be performed rather than how the actions are performed. Viewed slightly differently, the what is constant over a set of individuals though the how may vary. G.L.C.

N86-10821*# Pennsylvania Univ., Philadelphia. Dept. of Computer and Information Science.
SYSTEM INTEGRATION REPORT
Norman I. Badler, Jon D. Korein, Craig Meyer, Kamran Manoochehri, Jane Rovins, Jeffrey Beale, and Brian Barr 31 May 1985 42 p refs
(Contract NAS9-16634)
(NASA-CR-171900; NAS 1.26:171900) Avail: NTIS HC A03/MF A01 CSCL 09B

Several areas that arise from the system integration issue were examined. Intersystem analysis is discussed as it relates to software development, shared data bases and interfaces between TEMPUS and PLAID, shaded graphics rendering systems, object design (BUILD), the TEMPUS animation system, anthropometric lab integration, ongoing TEMPUS support and maintenance, and the impact of UNIX and local workstations on the OSDS environment. E.A.K.

N86-10822*# New Orleans Univ., La. Dept. of Physics.
STUDY OF ONE- AND TWO-DIMENSIONAL FILTERING AND DECONVOLUTION ALGORITHMS FOR A STREAMING ARRAY COMPUTER Final Report
George E. Ioup [1985] 6 p
(Grant NsG-1648)
(NASA-CR-176221; NAS 1.26:176221) Avail: NTIS HC A02/MF A01 CSCL 09B

The development of vector processing computers of the streaming array architectures has made possible a dramatic decrease in the time required for the solution of problems, i.e., for those algorithms which readily lend themselves to sequential operations on long vectors. There has concurrently been rapid growth in the applications of the techniques generally known as mathematical digital filtering, also called signal analysis, digital signal processing, time series analysis, and digital image processing. The best known applications of these techniques is to seismic data and two-dimensional images, data types consisting of very large collections of numbers. A major limitation for these cases is the size and speed of the computer available. Therefore, a move to the streaming array architecture can result in marked improvement in the data analysis techniques which may be employed. Author

N86-10823*# New Orleans Univ., La. Dept. of Physics.
A STUDY OF MORRISON'S ITERATIVE NOISE REMOVAL METHOD Final Report M. S. Thesis
George E. Ioup and Karin Ann Ringer Wright Oct. 1985 165 p refs
(Grant NsG-1648)
(NASA-CR-176222; NAS 1.26:176222) Avail: NTIS HC A08/MF A01 CSCL 09B

Morrison's iterative noise removal method is studied by characterizing its effect upon systems of differing noise level and response function. The nature of data acquired from a linear shift invariant instrument is discussed so as to define the relationship between the input signal, the instrument response function, and the output signal. Fourier analysis is introduced, along with several pertinent theorems, as a tool to more thorough understanding of the nature of and difficulties with deconvolution. In relation to such difficulties the necessity of a noise removal process is

discussed. Morrison's iterative noise removal method and the restrictions upon its application are developed. The nature of permissible response functions is discussed, as is the choice of the response functions used. Author

N86-10824*# New Orleans Univ., La. Dept. of Physics.
ALWAYS-CONVERGENT ITERATIVE NOISE REMOVAL AND DECONVOLUTION FOR IMAGE DATA Final Report M.S. Thesis
George E. Ioup and Mark A. Whitehorn Dec. 1981 143 p refs (Contract NsG-1648)
(NASA-CR-176223; NAS 1.26:176223) Avail: NTIS HC A07/MF A01 CSCL 09B

Linear filtering techniques currently used for the restoration of noisy, blurred or otherwise degraded image data are discussed and new techniques related to the iterative techniques of Morrison and van Cittert are developed and implemented. Programs written for the implementation are discussed in the appendices. It is shown that the new techniques are convergent for any system response function, and they are applied to the task of restoring a severely blurred image. Author

N86-10825*# New Orleans Univ., La. Dept. of Physics.
A STUDY OF DERIVATIVE FILTERS USING THE DISCRETE FOURIER TRANSFORM Final Report M. S. Thesis
George E. Ioup May 1980 105 p refs
(Grant NsG-1648)
(NASA-CR-176224; NAS 1.26:176224) Avail: NTIS HC A06/MF A01 CSCL 09B

Important properties of derivative (difference) filters using the discrete Fourier transform are investigated. The filters are designed using the derivative theorem of Fourier analysis. Because physical data are generally degraded by noise, the derivative filter is modified to diminish the effects of the noise, especially the noise amplification which normally occurs while differencing. The basis for these modifications is the reduction of those Fourier components for which the noise most dominates the data. The various filters are tested by applying them to find differences of two-dimensional data to which various amounts of signal dependent noise, as measured by a root mean square value, have been added. The modifications, circular and square ideal low-pass filters and a cut-off pyramid filter, are all found to reduce noise in the derivative without significantly degrading the result. Author

N86-10826*# New Orleans Univ., La. Dept. of Physics.
COORDINATE AXES, LOCATION OF ORIGIN, AND REDUNDANCY FOR THE ONE AND TWO-DIMENSIONAL DISCRETE FOURIER TRANSFORM Final Report
George E. Ioup and Juliette W. Ioup [1985] 24 p refs
(Grant NsG-1648)
(NASA-CR-176225; NAS 1.26:176225) Avail: NTIS HC A02/MF A01 CSCL 09B

Appendix 4 of the Study of One- and Two-Dimensional Filtering and Deconvolution Algorithms for a Streaming Array Computer discusses coordinate axes, location of origin, and redundancy for the one- and two-dimensional Fourier transform for complex and real data. F.M.R.

N86-10827*# New Orleans Univ., La. Dept. of Physics.
STUDY OF ONE- AND TWO-DIMENSIONAL FILTERING AND DECONVOLUTION ALGORITHMS FOR A STREAMING ARRAY COMPUTER Final Report
George E. Ioup [1985] 10 p refs
(Grant NsG-1468)
(NASA-CR-176226; NAS 1.26:176226) Avail: NTIS HC A02/MF A01 CSCL 09B

Appendix 5 of the Study of One- and Two-Dimensional Filtering and Deconvolution Algorithms for a Streaming Array Computer includes a resume of the professional background of the Principal Investigator on the project, lists of this publications and research papers, graduate thesis supervised, and grants received. F.M.R.

N86-10828*# National Aeronautics and Space Administration. Langley Research Center, Hampton, Va.
USER'S GUIDE FOR LANGLEY RESEARCH CENTER ORBITAL LIFETIME PROGRAM
Lynne H. Orr Sep. 1985 65 p refs
(NASA-TM-87587; NAS 1.15:87587) Avail: NTIS HC A04/MF A01 CSCL 09B

A FORTRAN program used by Langley Research Center for analyzing orbital lifetimes of spacecraft is described. Calculations can, at the user's option, take into account perturbations in the orbit due to atmospheric drag, solar radiation pressure, and gravitation effects of the Sun, the Moon, and Earth oblateness. Instructions are provided for access and use of the program, and several sample cases are included with detailed descriptions of their associated input and output. Author

N86-10829# Institute for Defense Analyses, Alexandria, Va.
Ada (TRADEMARK) PROGRAMMING SUPPORT ENVIRONMENT (APSE) EVALUATION AND VALIDATION (E AND V) WORKSHOP REPORT HELD AT AIRLIE, VIRGINIA ON 2-6 APRIL 1984 Final Report
V. L. Castor, C. M. Anderson, T. E. Lindquist, and J. F. Kramer, Jr. Dec. 1984 128 p Workshop held at Airlie, Va., 2-6 Apr. 1984
(Contract MDA903-84-C-0031)
(AD-A156667; AD-E500721; IDA-M-34; IDA/HQ-84-29295) Avail: NTIS HC A07/MF A01 CSCL 09/2

The Evaluation & Validation (E&V) Task has been established by the AJPO to develop technology necessary to assess the quality of software tools that will be included in an Ada Programming Support Environment (APSE). An E&V Workshop convened April 2 to 6, 1984, consisted of government and industry representatives who developed draft documents in three E&V subject areas--Task Recommendations, Task Requirements, and the APSE Evaluation Reference Manual. This report contains an account of the plenary sessions and the papers that address the three subject areas under discussion during this workshop. GRA

N86-10830# Geological Survey, Reston, Va. Water Resources Div.
SUTRA (SATURATED-UNSATURATED TRANSPORT). A FINITE-ELEMENT SIMULATION MODEL FOR SATURATED-UNSATURATED, FLUID-DENSITY-DEPENDENT GROUND-WATER FLOW WITH ENERGY TRANSPORT OR CHEMICALLY-REACTIVE SINGLE-SPECIES SOLUTE TRANSPORT Final Report, 29 Dec. 1982 - 30 Jan. 1985
C. I. Voss 30 Dec. 1984 427 p
(Contract MIPR-N-83-18; AF Proj. 2103)
(AD-A156779; USGS/WRI/84-4369; AFESC/ESL-TR-85-10) Avail: NTIS HC A19/MF A01 CSCL 09/2

SUTRA (Saturated-Unsaturated Transport) is a computer program which simulates fluid movement and the transport of either energy or dissolved substances in a subsurface environment. The mathematical model employs a two-dimensional hybrid finite-element and integrated-finite-difference method to approximate the governing equations that describe the two interdependent processes that are simulated by SUTRA: (1) fluid density-dependent saturated or unsaturated ground-water flow, and either; (2a) transport of a solute in the ground water, in which the solute may be subject to: equilibrium adsorption on the porous matrix, and both first-order and zero-order production or decay, or, (2b) transport of thermal energy in the ground water and solid matrix of the aquifer. SUTRA provides, as the primary calculated result, fluid pressures and either solute concentrations or temperatures, as they vary with time, everywhere in the simulated subsurface system. SUTRA may also be used to simulate simpler subsets of the above process. Author (GRA)

N86-10831# Air Command and Staff Coll., Maxwell AFB, Ala.
LET'S GET SERIOUS ABOUT SOFTWARE
J. R. Hegland Apr. 1985 47 p
(AD-A156819; ACSC-85-1130) Avail: NTIS HC A03/MF A01 CSCL 09/2

This guide translates applicable Air Force and TAC data processing requirements into language and examples fighter crews can relate to and understand. It provides information on methods of programming, documenting, and submitting software to TAC. It is designed to help get fighter squadron software into TAC-wide distribution and prevent wasted efforts. Author (GRA)

N86-10832# Army Military Personnel Center, Alexandria, Va.
SUPERVISORY CONTROL OF THE RIGHT ARM OF THE BEAM ASSEMBLY TELEOPERATOR Final Report
A. J. Manganiello 10 May 1985 173 p
(AD-A156856) Avail: NTIS HC A08/MF A01 CSCL 13/9

This thesis develops a method of supervisory control of the five-degree-of-freedom dexterous right arm of the Beam Assembly Teleoperator (BAT). The thesis imposes a constraint that the end effector of the right arm or manipulator must move in a straight line. The joint angles are used to transform the position of the end effector into cylindrical coordinates. With the initial and final position known, an equation for a straight line is obtained and the cylindrical coordinates of the end effector for each point on the straight line are found. The cylindrical coordinates are then transformed back into joint angles for each point and the joint angles are used to control the BAT's right arm. The method of moving the end effector in a straight line is implemented in two ways. The first implementation uses an unknown starting position and moves to a known finish point. Here the previously developed BAT software is used to input the starting position of the arm. Then the straight line path method uses this starting point and drives the arm to the known finish point. In the second implementation, a method is developed in which a set of points is remembered by the BAT and the straight line path method is used to drive the arm from any start point, through all the stored points and return to the original point. Further extensions using this method are discussed. GRA

N86-10833# Yale Univ., New Haven, Conn. Dept. of Computer Science.
THE DUCK MANUAL
D. McDermott Jun. 1985 95 p
(Contract N00014-83-K-0281; Grant NSF DCR-84-07077)
(AD-A156936; YALEU/DCS/RR-399) Avail: NTIS HC A05/MF A01 CSCL 09/2

Duck is deductive database designed to work as an adjunct to Artificial-Intelligence application programs written in Lisp. It provides the following features: Backward chaining logic interpreter; Forward chaining; Data dependencies and reason maintenance; Integration of deduction with Lisp computation; Multiple databases; Syntax checking for deductive rules; Trace package; Interactive examination of successful and failed deductions; and Generation of quasi-English versions of rules. Author (GRA)

N86-10834# Colorado Univ., Boulder. Dept. of Computer Science.
COMPLEXITY OF HIGHER-ORDER PROGRAMS
J. Shultis Jan. 1985 31 p refs
(Contract DE-FG02-84ER-13283)
(DE85-012776; DOE/ER-13283/2) Avail: NTIS HC A03/MF A01

A logic for analyzing the time complexity of programs using higher-order functions is presented. A simple functional language with static binding and call-by-value as its only parameter discipline was studied. The language is defined by denotational semantics that model both the functionality and cost of programs. The logic is derived from the semantic model, and tested against an implementation of the language based directly on the semantics. The use of the logic is demonstrated for a number of examples including data structure omparison and higher-order recursive functions. DOE

N86-10835# Los Alamos Scientific Lab., N. Mex.
NEW PROBABILISTIC MODELING AND SIMULATION METHODS FOR COMPLEX TIME-DEPENDENT SYSTEMS
R. J. Bartholomew 1985 13 p Presented at the 7th Intern. System Safety Conf., San Jose, Calif., 25 Jul. 1985
(Contract W-7405-eng-36)
(DE85-009575; LA-UR-85-828; CONF-850723-2) Avail: NTIS HC A02/MF A01

This paper is a tutorial that presents a new method of modeling the probabilistic description of failure mechanisms in complex, time-dependent systems. The method of modeling employs a state vector differential equation representation of cumulative failure probabilities derived from Markov models associated with certain generic fault trees, and the method automatically includes common cause/common mode statistical dependences, as well as time-related dependencies not considered in the literature previously. Simulations of these models employ a population dynamics representation of a probability space involving probability particle transitions among the Markov disjoint states. The particle transitions are governed by a random, Monte Carlo selection process. DOE

N86-10836# Stanford Linear Accelerator Center, Calif.
KLYSTRON CONTROL SOFTWARE IN THE SIC
R. K. Jobe, K. Thompson, and N. Phinney May 1985 3 p Presented at the Particle Accelerator Conf., Vancouver, British Columbia, 13 May 1985
(Contract DE-AC03-76SF-00515)
(DE85-013068; SU-SLAC-PUB-3667; CONF-850504-79) Avail: NTIS HC A02/MF A01

Triggering, control, and monitoring of 240 high-power klystrons will be supported by the Stanford Linear Collider (SLC) control system. The control software is distributed among a VAX host computer, a local microprocessor cluster, and a dedicated intelligent CAMAC module. The functions performed by these three components and the algorithms used are discussed. DOE

N86-10837# Los Alamos National Lab., N. Mex.
REVISION OF AND DOCUMENTATION FOR THE STANDARD VERSION OF THE POISSON-GROUP CODES
J. L. Warren, G. P. Boicourt, M. T. Menzel, G. W. Rodenz, and M. C. Vasquez 1985 4 p Presented at the Particle Accelerator Conf., Vancouver, British Columbia, 13 May 1985
(Contract W-7405-eng-36)
(DE85-012659; LA-UR-85-1618; CONF-850504-62) Avail: NTIS HC A02/MF A01

The main applications are in the design of electromagnets (POISSON and PANDIRA) and RF cavities (SUPERFISH). Other applications include electrostatics heat transport, and finding mathematical surfaces of minimum area. The standard version was revised and corrected and a comprehensive manual containing many examples and a summary of the theory behind the codes is written. Some of the capabilities of the codes are illustrated and the manual is summarized. DOE

N86-10838# Department of Energy, Oak Ridge, Tenn. Office of Scientific and Technical Information.
COMPUTER CODES: A BIBLIOGRAPHY, SUPPLEMENT 1
G. H. Thoeming, ed. Jun. 1985 987 p
(DE85-008721; DOE/TIC-3386-Suppl-1) Avail: NTIS HC A99/MF E04

Included are 3964 citations to literature on computer codes contained in the DOE Energy Data Base for the period March 1981 through January 1985. The citations represent all Energy Data Base subject categories and include reports, journal articles, books, conference papers, and monographs. Corporate, personal Author, Subject, and Report Number Indexes are provided. DOE

N86-10839# Los Alamos Scientific Lab., N. Mex.
GUIDELINES FOR A THERMOCHEMICAL KINETICS COMPUTER PROGRAM
J. I. Janney May 1985 11 p
(Contract W-7405-eng-36)
(DE85-014266; LA-10361-MS) Avail: NTIS HC A02/MF A01

Guidelines are given for an interactive computer program that will analyze thermochemical decomposition rate data obtained by isothermal differential-scanning calorimetry. Data from any portion of the rate curve may be analyzed, and either normal or autocata-

lytic rate laws may be used. The computer calculates and displays normalized data listings, rate curves, order plots, and autocatalytic rate law plots. It calculates rate constants by linear regression treatment of data from curve segments chosen by the user. Many options are available, and many forms of the rate laws may be selected. This program was designed primarily for research rather than routine use. DOE

N86-10840# Oak Ridge National Lab., Tenn.
BOX METHOD FOR FINDING INTERSECTIONS OF A TRAJECTORY WITH AXISYMMETRIC FLUX SURFACES
S. E. Attenberger and W. A. Houlberg May 1985 43 p
(Contract DE-AC05-84OR-21400)
(DE85-013525; ORNL/TM-9483) Avail: NTIS HC A03/MF A01

Computer routines were developed for handling a difficult geometry problem which frequently occurs in the analysis of toroidal plasmas. It is assumed that the plasma may be described in terms of a set of nested toroidal magnetic flux surfaces. Presented here is a set of algorithms that determine the intersections of a given trajectory with a given set of flux surfaces. DOE

N86-10841# Los Alamos Scientific Lab., N. Mex.
FRAMEWORK FOR GENERATING EXPERT SYSTEMS TO PERFORM COMPUTER SECURITY RISK ANALYSIS
S. T. Smith and J. J. Lim 1985 8 p Presented at the 1st Ann. AFCEA Symp. and Exposition on Phys. and Electron. Security, Philadelphia, 19 Aug. 1985
(Contract W-7405-eng-36)
(DE85-014134; LA-UR-85-1933; CONF-850885-2) Avail: NTIS HC A02/MF A01

A framework to generate knowledge based expert systems for performing automated risk analyses upon a subject system was developed. The expert system is a computer program that models experts' knowledge about A topic, including facts, assumptions, insights, and decision rationale. The subject system is a member of the class of systems with three identifying characteristics: (1) a set of desirable assets (or targets); (2) a set of adversaries (or threats) desiring to obtain or to do harm to the assets; and (3) a set of protective mechanisms to safeguard the assets from the adversaries. Risk analysis evaluates both vulnerability to and the impact of successful threats against the targets by determining the overall effectiveness of the subject system safeguards, identifying vulnerabilities in that set of safeguards, and determining cost effective improvements to the safeguards. The inherent vulnerabilities and risks in a system of computer security safeguards are evaluated. The method considers safeguards protecting four generic targets. The automated procedure to assess the effectiveness of computer security safeguards differs from traditional risk analysis methods. DOE

N86-10842# Allied Bendix Aerospace, Kansas City, Mo.
SOFTWARE FOR AN AUTOMATED GAGING SYSTEM Final Report
R. E. Hines May 1985 100 p
(Contract DE-AC04-76DP-00613)
(DE85-013322; BDX-613-3268) Avail: NTIS HC A05/MF A01

Gaging software was developed for an automated gaging system. The system acquires and processes dimensional data from product that is inspected on multi-probe rotary gages. Speed and flexibility are major advantages of the gaging system. For example, it collects 60 readings each from 40 probes on a part, analyzes the data for 90 characteristics, compares against tolerance limits, and prints a detailed report in 8 minutes. This would take over 8 hours to do with manual methods. The software and hardware are general purpose, which allows the system to be easily re-programmed for different gaging applications. The system is currently operating at Bendix Kansas City with seven different gages. The software, which is programmed in both FORTRAN (about 80%) and assembly anguages, is to read, interpret, and process the keyword commands from user-defined control files. Routines are available for 12 varieties of feature analysis: contour, radius, wall thickness, diameter, dimension, position, concentricity, perpendicularity, runout, parallelism, surface angle, and the difference between two probes. The results from the feature analysis routines can then be compared to either product, guardband, or monitor unit limit files. DOE

N86-10843# Oak Ridge Gaseous Diffusion Plant, Tenn.
HALFBREED: AN EXTENDED CAPABILITY VERSION OF THE YAQUI CODE
J. E. Park Jun. 1985 21 p
(Contract DE-AC05-84CT-21400)
(DE85-014237; K/CSD/INF-85/4) Avail: NTIS HC A02/MF A01

Several special modifications to the ICE-ALE computer code, UAQUI, are described. The modified code was dudded HALFBREED. DOE

N86-10844# Technische Hogeschool, Eindhoven (Netherlands). Dept. of Electrical Engineering.
THE IDENTIFICATION PACKAGE SATER
A. J. W. vandenBoom and R. Bollen 1983 7 p refs
(ER-83/08) Avail: NTIS HC A02/MF A01

Structure and identification methods of an interactive program package for identification of linear single-input systems are described. The computer package is meant for inexperienced users of (application of) identification methods and for students. Interaction is very user friendly. The package contains parameter estimation routines, order testing routines, a program for converting discrete models into continuous models, simulation and test signal generation modules, facilities for preprocessing measured signals, as well as modules for analyzing continuous systems based on Nyquist, Bode and root-locus diagrams. Author (ESA)

N86-10845# Technische Hogeschool, Eindhoven (Netherlands). Vakgroep Automatischen Systeemontwerpen.
COMPACT: COMPACTION OF HIERARCHICAL CHIP LAYOUTS BASED ON A CONSTRAINT GRAPH METHOD WITH DOUBLE-SIDED CONSTRAINTS Progress Report, Jun. 1982-May 1983
X. I. M. Timmermans 1983 45 p refs
Avail: NTIS HC A03/MF A01

The compaction program COMPACT used in interactive computer aided design of integrated circuit layouts is described. The compaction method is based on a constraint graph. Compaction is achieved in one or more subsequent steps by grouping the layout elements into features and then shifting these features together in horizontal or vertical direction. The nodes and edges of the graph represent the features and the constraints between the features. The compaction algorithm can handle one-sided and two-sided constraints. The two-sided constraints are resolved by backtracking. Constraints on the shift of layout elements which overlap each other are determined with a linear method. For determination of constraints of nonoverlapping elements, windowing and shadowing techniques are used to reduce computation time. Author (ESA)

N86-10846# Technische Hogeschool, Eindhoven (Netherlands). Digital Systems Group.
STATE ASSIGNMENT IN SEQUENTIAL CIRCUITS
Jan. 1985 22 p refs In DUTCH; ENGLISH summary
(EUT-85-E-146; ISBN-90-6144-146-3; ISSN-0167-9708) Avail: NTIS HC A02/MF A01

An algorithm for optimizing the code assignement in sequential digital circuits is described. Source for this algorithm are three heuristic rules. These rules aim to find the largest block of 1-s in a Karnaugh-diagram. The algorithm starts with a state table and ends with the excitation tables. During the code assignement the user is asked to choose between several alternatives, after which the excitation tables are settled. Author (ESA)

N86-10847# National Bureau of Standards, Gaithersburg, Md.
NBSGSC: A FORTRAN PROGRAM FOR QUANTITATIVE X-RAY FLUORESCENCE ANALYSIS Final Technical Note
G. Y. Tao, P. A. Pella, and R. M. Rousseau Apr. 1985 124 p Prepared in cooperation with Geological Survey of Canada
(PB85-206068; NBS/TN-1213) Avail: NTIS HC A06/MF A01; also Avail: SOD as SN003-003-02653-1 CSCL 07D

A FORTRAN program (NBSGSC) is developed for performing quantitative analysis of bulk specimens by X-ray fluorescence spectrometry. This program corrects for X-ray absorption/enhancement phenomena using the comprehensive alpha coefficient algorithm proposed by Lachance (COLA). Part one of the program (CALCO) performs the calculation of theoretical alpha coefficients, and part two (CALCOMP) computes the composition of the analyte specimens. The analysis of alloys, pressed minerals, and fused specimens can currently be treated by the program. In addition to using measured X-ray tube spectral distributions, spectra from seven commonly used X-ray tube targets could also be calculated with an NBS algorithm included in the program. GRA

N86-10390*# Jet Propulsion Lab., California Inst. of Tech., Pasadena. Communications Systems Research Section.
A SEQUENTIAL DECODING PERFORMANCE ANALYSIS FOR INTERNATIONAL COMET EXPLORER
D. Divsalar *In its* The Telecommun. and Data Acquisition Progr. Rept. 15 Aug. 1985 p 82-91 refs (For primary document see N86-10382 01-32)
Avail: NTIS HC A10/MF A01 CSCL 09B

N86-10815# Joint Publications Research Service, Arlington, Va.
CLASSIFICATION OF REAL-TIME PROGRAM TESTING TASKS AND METHODS
I. N. Dolganyuk and Ye. Ya. Karpovskiy *In its* USSR Rept.: Cybernetics, Computers and Automation Technol. (JPRS-UCC-85-006) 5 Sep. 1985 p 70-83 refs Transl. into ENGLISH from Upravlyayushchiye Sistemy i Mashiny (Kiev), no. 2, Mar. - Apr. 1985 p 57-62 (For primary document see N86-10809 01-60)
Avail: NTIS HC A08

N86-10818# Joint Publications Research Service, Arlington, Va.
DIGITAL PROCESSING OF IMAGES IN TRACKING A MOVING OBJECT
B. A. Alpatov, A. A. Selyayev, and A. I. Stapashkin *In its* USSR Rept.: Cybernetics, Computers and Automation Technol. (JPRS-UCC-85-006) 5 Sep. 1985 p 123-127 refs Transl. into ENGLISH from Proborostr. (Leningrad), no. 2, Feb. 1985 p 39-43 (For primary document see N86-10809 01-60)
Avail: NTIS HC A08

62 COMPUTER SYSTEMS

Includes computer networks.

N86-10848*# Carnegie-Mellon Univ., Pittsburgh, Pa.
FAULT-FREE BEHAVIOR OF RELIABLE MULTIPROCESSOR SYSTEMS: FTMP EXPERIMENTS IN AIRLAB
Ed Clune, Zary Segall, and Daniel Siewiorek Aug. 1985 33 p refs
(Grant NAG1-190)
(NASA-CR-177967; NAS 1.26:177967) Avail: NTIS HC A03/MF A01 CSCL 09B

This report describes a set of experiments which were implemented on the Fault tolerant Multi-Processor (FTMP) at NASA/Langley's AIRLAB facility. These experiments are part of an effort to formulate and evaluate validation methodologies for fault-tolerant computers. This report deals with the measurement of single parameters (baselines) of a fault free system. The initial set of baseline experiments lead to the following conclusions: (1) The system clock is constant and independent of workload in the tested cases; (2) the instruction execution times are constant; (3) the R4 frame size is 40mS with some variation; (4) the frame stretching mechanism has some flaws in its implementation that allow the possibility of an infinite stretching of frame duration. Future experiments are planned. Some will broaden the results of these initial experiments. Others will measure the system more dynamically. The implementation of a synthetic workload generation mechanism for FTMP is planned to enhance the experimental environment of the system. Author

N86-10849# Naval Postgraduate School, Monterey, Calif.
SHIPBOARD NON-TACTICAL COMPUTER SYSTEMS OF THE US NAVY M.S. Thesis
W. J. McMican and J. J. Richards Mar. 1985 129 p
(AD-A156769) Avail: NTIS HC A07/MF A01 CSCL 09/2

This thesis reviews the development and application of current non-tactical shipboard ADP systems in the U.S. Navy, and provides an analysis of each systems' strengths and weaknesses. The primary focus of this review includes Perq/ZOG, WANG installations, and SNAP II. The methodologies of procurement, development and implementation vary as widely as the scope and complexity of the various systems. This analysis provides insight into some primary management issues, limitations, and constrait encountered in providing non-tactical automatic data processing to the fleet. Author (GRA)

N86-10850# Yale Univ., New Haven, Conn. Dept. of Computer Science.
TOPOLOGICAL PROPERTIES OF HYPERCUBES
Y. Saad and M. H. Schultz Jun. 1985 19 p
(Contract N00014-82-K-0184)
(AD-A156777; Yaleu/DCS/RR-389) Avail: NTIS HC A02/MF A01 CSCL 12/1

The n-dimensional hypercube or n-cube is a highly concurrent multiprocessor architecture consisting of 2 to the nth nodes each connected or n neighbors. Such machines have been advocated as ideal ensemble architectures because of their powerful interconnection. In this paper we examine the hypercube architecture from the graph theory point of view and we consider those features which make the hypercube interconnection so appealing. Among other things, we propose a theoretical characterization of the hypercube as a graph and show how to map various other architectures into a hypercube. The hypercube is a loosely coupled parallel multiprocessor based on a binary n-cube network and introduced under different names (for example, cosmic cube, n-cube, binary n-cube, and boolean n-cube). A few machines based on the hypercube topology have been implemented by several groups, see (7) for references, and others are now being built. An n-cube parallel multiprocessor consists of (2) identical processors, each provided with its own sizable memory, and connected to n neighbors in the form of a binary n-cube network. There are essentially two broad classes of MIMD parallel multiprocessor processor designs with large number of processors. The first type of architecture consists of a large number of identical processors connected to one another according to some convenient pattern. In these machines there is no shared memory and no global synchronization. The second important class of parallel multiprocessors consists of those systems with N identical processors connected via a large switching network to N memories. GRA

N86-10851# Technische Hogeschool, Eindhoven (Netherlands). Computing Center.
STOCK-TAKING OF DATA BASE MANAGEMENT SYSTEMS CHOICE CONSIDERATIONS FOR THE EINDHOVEN TECHNICAL UNIVERSITY COMPUTING CENTER (THE-RC) [INVENTARISATIE VAN DATA BASE MANAGEMENT SYSTEMEN EN KEUZE-OVERWEGINGEN VOOR HET THE-RC]
Th. H. Bruning Dec. 1983 38 p In DUTCH
(Comp-Cent-Note-18; B8562872) Avail: NTIS HC A03/MF A01

Nine data base management systems, namely: DMS II (Burroughs), SQL/DS (IBM), IDMS (Cullinane), ORACLE (Relational Software), RAPPORT (Logica), TOTAL (Cincom Systems), ADABAS (Software AG), BASIS (Batelle), and MIMER (Savant) are examined. Systems for administrative purposes are distinguished from technico scientific systems, and aspects such as data base structure, integration of the functions, transfer possibilities, user friendliness, facilities, and costs are discussed. A definitive selection is not made. Author (ESA)

63 CYBERNETICS

Includes feedback and control theory.

For related information see also *54 Man/System Technology and Life Support.*

N86-10852 Wyoming Univ., Laramie.
SPILLOVER MINIMIZATION IN SELF-ADJOINT DISTRIBUTED-PARAMETER SYSTEMS WITH DIRECT OUTPUT FEEDBACK Ph.D. Thesis
David Steven Barker 1984 142 p
Avail: Univ. Microfilms Order No. DA8508862

Control of a high-dimensional system by a low-dimensional controller is intriguing problem. High-dimensional systems (distributed-parameter systems) and low-dimensional controllers (lumped-parameter controllers) are mismatched due to their different dimensionality. The question which is addressed here is whether a low-dimensional controller can be designed for a high-dimensional system. Several control strategies exist and none is simpler than direct output feedback which multiplies sensor outputs by constants and adds the results to form the actuator inputs. Optimum sensor and actuator placement schemes for a direct output feedback controller which gives significant damping to a few modes of oscillation and minimally interacts with the higher modes of oscillation is discussed. Unwanted interaction among modes of oscillation which occurs through the controller is commonly referred to as spillover. The results for the Euler-Bernoulli beam (a self-adjoint distributed parameter system) will provide bench marks for other controllers. Dissert. Abstr.

N86-10853 Case Western Reserve Univ., Cleveland, Ohio.
OPTIMAL CONTROL MODELING OF LOWER EXTREMITY MUSCULOSKELETAL MOTION Ph.D. Thesis
Musa Latangrang Audu 1985 233 p
Avail: Univ. Microfilms Order No. DA8510114

The application of optimal control theory in the study of musculoskeletal motion was investigated. The research includes a comparative study of muscle models of varying complexity. Four such models ranging in complexity from simple input-output models to very sophisticated phenomenological models were examined. A model was developed which was able to strike a compromise between model complexity and practicability in musculoskeletal motion applications. Dissert. Abstr.

N86-10854# Oxford Univ. (England). Dept. of Engineering Science.
IDENTIFICATION OF A PLANT'S WEIGHTING SEQUENCE
D. W. Clarke 1984 40 p refs
(OUEL-1534/84) Avail: NTIS HC A03/MF A01

The mathematical foundation of the weighting sequence model and a set of algorithms which can estimate its parameters are described. It is shown how a multi-input single-output plant (e.g., a single loop with known load-disturbances) can be modelled. The algorithms are designed to cope with offsets, noise, and drift of the plant output, and provide compromises between rapid estimation and possible effects of noisy data on the results. The UDU implementation of recursive least squares which is the optimal method but which involves considerable computations, and the recursive learning method as used by the IDCOM controller design which is simple but which can be sensitive to noise are recommended. Author (ESA)

64 NUMERICAL ANALYSIS

Includes iteration, difference equations, and numerical approximation.

N86-10855 State Univ. of New York, Buffalo.
ADVANCED DEVELOPMENT OF BEM FOR TWO AND THREE DIMENSIONAL NONLINEAR ANALYSIS Ph.D. Thesis
S. T. Raveendra 1985 149 p
Avail: Univ. Microfilms Order No. DA8510358

Application of the boundary element method are applied to solve nonlinear problems. The material behavior is idealized by elasto-plastic and viscoplastic models. The boundary element method formulation of the governing equations of elastoplasticity developed makes use of an initial stress approach in which the incremental solutions are modified by the presence of initial stresses. The viscoplastic model which describes the time-dependent inelastic deformation of solids is used to solve creep problems as well as elastoplastic problems since steady state viscoplasticity can be conceived as an alternative description of elastoplastic behavior. The iterative procedure is accelerated by extrapolating the past plastic history which reduces the computing time substantially. A new formulation to solve problems in elastoplasticity is developed by exploiting some of the characteristics of the constitutive relationships. This approach is equivalent to the variable stiffness method employed in finite element algorithms in which no iterative procedure is necessary. Dissert. Abstr.

N86-10856# Tata Inst. of Fundamental Research, Bombay (India).
PRINCIPAL BUNDLES ON THE AFFINE LINE
M. S. Raghunathan and A. Ramanthan 20 Feb. 1985 16 p refs
Avail: NTIS HC A02/MF A01

Assume that G is connected and reductive. Let B be an element of A be a principal G-bundle on A such that B sub(Spec k) x Spec k subs is trivial over Spec k subs [T] where k subs is the separable closure of k. Then there is a principal G-bundle B sub 0 over Spec k such that B is K-isomorphic to the pull back of B sub 0 by the structure morphism A be an element of Spec k. If k is algebraically closed it follows from a theorem of Steinberg that all G-bundles on A, with G connected, are trivial. Thus if k is perfect (in particular if the characteristic of k is zero) the assumption of triviality over k sub s is always satisfied. On the other hand Knus, Ojanguren and Saltman have shown that for separably closed non-perfect fields k there exist non-trivial PGL(n)-bundles on A. However it seems likely that for simply connected groups G such a phenomenon does not occur. G.L.C.

N86-10857# Tata Inst. of Fundamental Research, Bombay (India). School of Mathematics.
COINCIDENCE DENSITIES AND SPECTRA OF A CLASS OF SUBSTITUTION MINIMAL SETS
S. Muralidharan 17 May 1985 24 p refs
Avail: NTIS HC A02/MF A01

For any primitive substitution theta on (0,1) such that the theta-matrix is singular, we show that the coincidence density D(theta) exists and is rational. We also prove that the associated minimal dynamical system has discrete spectrum if and only if D(theta) = 1; this verifies a conjecture of Michel for the class of substitutions as above. Author

N86-10858# Universite des Sciences et Techniques du Languedoc, Montpellier (France). Lab. de Physique Mathematique.
WELL-POSED QUESTIONS AND EXPLORATION OF THE SPACE OF PARAMETERS IN LINEAR AND NONLINEAR INVERSION
Pierre C. Sabatier [1984] 22 p refs Sponsored in part by CNRS
(PN-84/13) Avail: NTIS HC A02/MF A01

Solving inverse problems is defining convenient routes, in the space of parameters, towards those called solutions of the problem. Thus methods for solving inverse problems are primarily related to the existence of routes in a space rather than to statistical, algebraic, or other considerations. After a brief survey of the local routes which yield for instance least square inversion, global routes obtained by using geometric transforms are dealt with. One shows on examples how to construct these routes, how to use them, what questions can be answered which escape the range of local routes. These methods apply at least to all inverse problems related with exact solutions of nonlinear partial differential equations, and in particular to the inverse problems of wave equations. They yield efficient algorithms. The case in which localization of the desired solutions is only obtained through some extreme points of a domain is then reviewed. In this method of analysis, one replaces

the ill-posed problem of finding solutions that correspond to actual measurements by a set of well-posed questions whose answers are inequalities on theoretical measurements of the set of solutions and enable decision in applied problems. Several applications in engineering and geophysical research were given in the last few years. Author

N86-10859# Universite des Sciences et Techniques du Languedoc, Montpellier (France). Lab. de Physique Mathematique.
A MODIFIED MODIFIED KORTEWEG-DEVRIES EQUATION
F. Calogero (Rome Univ.) and A. Degasperis (Rome Univ.) Dec. 1984 18 p refs Sponsored in part by Italian Ministry of Education Submitted for publication
(PN-84/27) Avail: NTIS HC A02/MF A01

The solution of the Cauchy problem, an infinite set of conserved quantities, a variational formulation, the auto-Backlund transformations and the soliton phenomenology (featuring singly and doubly humped solitons, as well as breathers) are tersely surveyed, for the integrable nonlinear evolution partial differential equation known as the modified-modified Kortwege-deVries equation. Author

N86-10860*# Georgia Inst. of Tech., Atlanta. School of Engineering Science and Mechanics.
BOUNDING SOLUTIONS OF GEOMETRICALLY NONLINEAR VISCOELASTIC PROBLEMS
John M. Stubstad and George J. Simitses [1985] 3 p refs
(Grant NAG3-534)
(NASA-CR-176219; NAS 1.26:176219) Avail: NTIS HC A02/MF A01 CSCL 12A

Integral transform techniques, such as the Laplace transform, provide simple and direct methods for solving viscoelastic problems formulated within a context of linear material response and using linear measures for deformation. Application of the transform operator reduces the governing linear integro-differential equations to a set of algebraic relations between the transforms of the unknown functions, the viscoelastic operators, and the initial and boundary conditions. Inversion either directly or through the use of the appropriate convolution theorem, provides the time domain response once the unknown functions have been expressed in terms of sums, products or ratios of known transforms. When exact inversion is not possible approximate techniques may provide accurate results. The overall problem becomes substantially more complex when nonlinear effects must be included. Situations where a linear material constitutive law can still be productively employed but where the magnitude of the resulting time dependent deformations warrants the use of a nonlinear kinematic analysis are considered. The governing equations will be nonlinear integro-differential equations for this class of problems. Thus traditional as well as approximate techniques, such as cited above, cannot be employed since the transform of a nonlinear function is not explicitly expressible. Author

N86-10861# Carnegie-Mellon Univ., Pittsburgh, Pa. Management Sciences Research Group.
TWO ALGORITHMS FOR WEIGHTED MATROID INTERSECTION
C. Brezovec, G. Cornuejols, and F. Glover Mar. 1985 26 p
(Contract N00014-82-K-0329; Grant NSF ECS-82-05425)
(AD-A156525; MSRR-517; WP-29-84-85) Avail: NTIS HC A03/MF A01 CSCL 12/1

Consider a finite set E, a weight function w:E approaches R, and two matroids M1 and M2 defined on E. The weighted matroid intersection problem consists of finding a set of E, independent in both matroids, that maximizes sigma E w(e): e in 1. This improves the complexity of earlier algorithms by a factor r, when c < or = O(n), and by a factor n when max(c, log n) < or = O(r). A related problem is to find a maximum weight set, independent in both matroids, and of given cardinality k (if one exists). Our algorithm also solves this problem. In addition, we present a second algorithm which, given a feasible solution of cardinality k, finds an optimal one of the same cardinality. A sensitivity analysis on the weights is easy to perform using this approach. GRA

N86-10862# Maryland Univ., College Park. Lab. for Numerical Analysis.
THE h, p AND h-p VERSIONS OF THE FINITE ELEMENT METHOD IN DIMENSION. PART 1: THE ERROR ANALYSIS OF THE p-VERSION Final Report
W. Gui and I. Babuska Apr. 1985 60 p
(Contract N00014-85-K-0169; Grant NSF DMS-83-15216)
(AD-A156600; BN-1036) Avail: NTIS HC A04/MF A01 CSCL 12/1

This paper is the first one in the series of three which are addressing in detail the properties of the three basic versions of the finite element method in the one dimensional setting. The main emphasis is placed on the analysis when the (exact) solution has singularity of x sub alpha type. The first part analyzes the p-version, the second the h-version and general h-p version and the final third part addresses the problems of the adaptive h-p version. Author (GRA)

N86-10863# Naval Underwater Systems Center, New London, Conn.
AN IMPROVED FFT (FAST FOURIER TRANSFORM) FOR A FOUR PARALLEL PIPE SIMD ARITHMETIC PROCESSOR Progress Report
T. T. Tylaska and T. C. Choinski 1 May 1985 35 p
(S14-40)
(AD-A156625; NUSC-TR-7363) Avail: NTIS HC A03/MF A01 CSCL 12/1

An algorithm is derived that reduces the execution time of a fast Fourier transform (FFT) by a factor of 4 utilizing a loosely coupled four parallel pipe processor that a single instruction, multiple data (SIMD) stream architecture. This algorithm distributes the FFT computations among the four parallel pipes for the radix-4 and the mixed radix-2/-4 cases. The algorithm is demonstrated specifically for both a 16- and 32-point FFT. In addition, the radix-4 FFT algorithm is derived in detail, along with formulas for the execution times and a method that computes the inverse FFT. The necessity for prescrambling the input data is explained and a simple hardware implementation is given. Author (GRA)

N86-10864# Maryland Univ., College Park. Lab. for Numerical Analysis.
THE h, p AND h-p VERSIONS OF THE FINITE ELEMENT METHOD IN 1 DIMENSION. PART 3. THE ADAPTIVE h-p VERSION Final Report
W. Gui and I. Babuska Jun. 1985 50 p
(Contract N00014-85-K-0169; Grant NSF DMS-83-15216)
(AD-A156626; BN-1038) Avail: NTIS HC A03/MF A01 CSCL 12/1

The paper is the third and final part in the series of three devoted to the detailed analysis of the three basic versions of the finite element method in one dimension. The first part analyzed the p-version, and the second part concentrated on the h and h-p version. This paper analyzes a theoretical frame of the adaptive h-p version and based on it the authors provide a concrete algorithm for the one dimensional problem. It is proven that in the case that the solution has x sub alpha-type singularity, the adaptive algorithm give an exponential rate of convergence, very close to the optimal one analyzed in the second part of the paper. GRA

N86-10865# Defence Research Establishment Valcartier (Quebec).
ACCELERATION-INVARIANT APPROXIMATION METHOD FOR RECURSIVE DIGITAL FILTERS
A. Morin and P. Labbe May 1985 23 p
(AD-A156655; DREV-4371/85) Avail: NTIS HC A02/MF A01 CSCL 12/1

This document describes a procedure for designing recursive digital filters from continuous-time filters when the ratio of the sampling frequency to the pole frequency is small. The discrete-time transfer function of digital filters obtained by this method, called the acceleration-invariant transformation, has been derived from the partial fraction expansion of the continuous-time transfer function. An error function between the digital and analog transfer

functions has also been deduced. Finally, the performance of the proposed method is demonstrated by plotting the frequency response of high-order Butterworth and elliptic filters.
Author (GRA)

N86-10866# Rensselaer Polytechnic Inst., Troy, N. Y.
A MESH MOVING TECHNIQUE FOR TIME DEPENDENT PARTIAL DIFFERENTIAL EQUATIONS IN TWO SPACE DIMENSIONS Final Technical Report
D. C. Arney and J. E. Flaherty Jun. 1985 41 p Presented at 2nd Army Conf. on Appl. Math and Computing (2nd), 22-24 May 1984, Troy, NY
(Contract DAAG29-82-K-0197; Grant AF-AFOSR-0192-80)
(AD-A156663; AD-E440287; ARLCB-TR-85016) Avail: NTIS HC A03/MF A01 CSCL 12/1

We discuss an adaptive mesh moving technique that can be used with a finite difference or finite element scheme to solve initial-boundary value problems for vector systems or partial differential equations in two space dimensions and time. The mesh moving technique is based on an algebraic node movement function determined from the propagation of significant error regions. The algorithm is designed to be flexible, so that it can be used with many existing finite difference and finite element methods. To test the algorithm, we implemented the mesh mover in a system code along with an initial mesh generator and a MacCormack finite volume integrator on quadralateral cells to solve hyperbolic vector systems. Results are presented for several computational examples. This moving mesh reduces dispersion errors near shocks and wave fronts and thereby reduces the grid requirements necessary to compute accurate solutions while increasing efficiency. GRA

N86-10867# Yale Univ. Observatory, New Haven, Conn. Dept. of Computer Science.
PARTIAL EIGENSOLUTIONS OF LARGE NONSYMMETRIC MATRICES
Y. Saad Jun. 1985 28 p
(Contract N00014-82-K-0184)
(AD-A156711; Yaleu/DCS/RR-397) Avail: NTIS HC A03/MF A01 CSCL 12/1

We propose several methods based on combinations of deflation techniques and polynomial iteration methods, for computing small invariant subspaces of large matrices, associated with the eigenvalues with largest (or smallest) real parts. We consider both Chebyshev polynomials and least-squares polynomials for the acceleration scheme and we propose a deflation technique which is a variant of Wielandt's deflation that does not require the left eigenvectors of the matrix. As an application we compare our methods on an example issued from a bifurcation problem and show their efficiency when the number of eigenvalues required is small. GRA

N86-10868# Yale Univ. Observatory, New Haven, Conn. Dept. of Computer Science.
ON THE LANCZOS METHOD FOR SOLVING SYMMETRIC LINEAR SYSTEMS WITH SEVERAL RIGHT-HAND-SIDES
Y. Saad 13 Jun. 1985 14 p
(Contracts N00014-82-K-0184; DE-AC02-81ER-10996; Grant AF-AFOSR-0193-81)
(AD-A156816; Yaleu/DCS/RR-396) Avail: NTIS HC A02/MF A01 CSCL 12/1

This paper analyses two methods based on the Lanczos algorithm for solving large sparse symmetric linear systems with several right hand sides. The methods examined are suitable for the case where the right sides are not too different from one another as is often the case in time dependent or parameter dependent problems. We will show in particular that a modified Lanczos algorithm, introduced by Parlett is in some sense equivalent to the block Lanczos algorithm. Author (GRA)

N86-10869# Maryland Univ., College Park. Lab. for Numerical Analysis.
THE h, p AND h-p VERSIONS OF THE FINITE ELEMENT METHOD IN 1 DIMENSION. PART 2. THE ERROR ANALYSIS OF THE H AND h-p VERSIONS Final Report
W. Gui and I. Babuska 1 May 1985 77 p
(Contract N00014-85-K-0169; Grant NSF DMS-83-15216)
(AD-A156835; AD-E301723; BN-1037-Pt-2) Avail: NTIS HC A05/MF A01 CSCL 12/1

This paper is the second part in a series of three parts which address in detail the properties and performance of the h, p and h--p versions of the finite element method in one dimensional setting. In general the h-version of FEM has the degree of elements fixed and the convergence is achieved by the refinement of the mesh. The p-version fixes the mesh and increases the degree of elements. The h-p version combines both approaches. This part investigates the h and h-p version. GRA

N86-10870# Michigan Univ., Ann Arbor.
TEST OF A MULTILEVEL COMPUTATIONAL THEORY OF STEREOSCOPIC VISUAL IMAGE PROCESSING Final Report, 1 Dec. 1984 - 31 May 1985
W. R. Uttal 1 Jun. 1985 16 p
(Contract N00014-85-K-0131; RR0-4209)
(AD-A157011; PERLAB-6) Avail: NTIS HC A02/MF A01 CSCL 12/1

The scientific objective of this contract was to develop and test a computational model of human detection, discrimination, recognition, and reconstruction of dotted forms. Both computer programming and psychophysical research efforts were necessary to fulfill this goal. The dotted form continues to be a powerful vehicle with which to study visual perception by human observes as well as by computer image processors. Several experiments comparing detection, discrimination, and recognition are reported and the current status of the mathematical model describing these visual processes is presented. GRA

N86-10871# Argonne National Lab., Ill.
COMPUTING THE STRUCTURAL INDEX
I. S. Duff and C. W. Gear Mar. 1985 13 p
(Contract W-31-109-eng-38)
(DE85-014370; ANL/MCS-TM-50) Avail: NTIS HC A02/MF A01

The index of many differential/algebraic equations is determined by the tructure of the system, that is, by the pattern of nonzero entries in the Jacobians. It is important to be able to determine if the index is two or less because such problems can be solved numerically. An algorithm that determines if the index is one, two, or greater, based only on the sturcture is presented. The algorithm can be exponential in its execution time. However, in many practical problems, this algorithm will execute in polynomial time. DOE

N86-10872# Chalmers Univ. of Technology, Goteborg (Sweden). Dept. of Mathematics.
ERROR ESTIMATES AND AUTOMATIC TIME STEP CONTROL FOR NUMERICAL METHODS FOR STIFF ORDINARY DIFFERENTIAL EQUATIONS
Claes Johnson 1984 45 p refs
(CTH-Math-1984-27; ISSN-0347-2809) Avail: NTIS HC A03/MF A01

Numerical methods for initial value problems for stiff ordinary differential equations (ODE) are considered. Runge-Kutta methods (RKM) resulting from discretizing in time of a discontinuous Galerkin method (DGM) are studied. A special class of RKM given satisfactory error estimates for monotone ODE, is discussed. This technique is suggested as the basis for rational methods for automatic time step control. This error estimate can be extended to nonlinear ODE when linear autonomous parabolic problems of DGM are analyzed. Author (ESA)

N86-10873# Chalmers Univ. of Technology, Goteborg (Sweden). Dept. of Mathematics.
ON THE ABSOLUTE CONTINUITY OF ELLIPTIC MEASURES
Bjoern E. J. Dahlberg 1984 27 p refs
(CTH-Math-1984-28; ISSN-0347-2809) Avail: NTIS HC A03/MF A01

The Dirichlet for elliptic equations in divergence form with bounded measurable coefficients into n-dimensional space, is studied. It is proven that conditions on the coefficients of partial differential elliptic operators imply the existence of elliptic measures which are absolutely continuous. Author (ESA)

N86-10874# Chalmers Univ. of Technology, Goteborg (Sweden). Dept. of Mathematics.
ESTIMATES FOR MAXIMAL FUNCTIONS ALONG HYPERSURFACES
Hasse Carlsson and Peter Joergen 1984 25 p refs
(CTH-Math-1984-29; ISSN-0347-2809) Avail: NTIS HC A02/MF A01

Maximal function operator (MFO) of a surface in the n-dimensional real space, is considered. The fact that boundaries and regularity conditions of the Hessian at origin on the surface gives an MFO bounded, in the sense of L supp function space, is proven. Author (ESA)

N86-10875# Chalmers Univ. of Technology, Goteborg (Sweden). Dept. of Mathematics.
ON MAXIMAL AND DISTRIBUTIONAL COUPLING
Hermann Thorisson 1984 8 p refs
(CTH-Math-1984-30; ISSN-0347-2809) Avail: NTIS HC A02/MF A01

A method for the construction of maximal coupling (MC) of discrete time stochastic processes, is given. This method does not consider topological restriction on state space. Maximal coupling is given by way of a distributional coupling concept. The MC of continuous time stochastic processes is considered. Author (ESA)

N86-10876# Chalmers Univ. of Technology, Goteborg (Sweden). Dept. of Mathematics.
POISSON SEMIGROUPS AND SINGULAR INTEGRALS
Bjoern E. J. Dahlberg 1985 15 p refs
(CTH-Math-1985-05; ISSN-0347-2809) Avail: NTIS HC A02/MF A01

The Dirichlet problem of the Laplace operator in Lipschitz domain (LD) is discussed. Properties on L sq-function space of the solution operator that corresponds to Dirichlet Problem in LD are given. Author (ESA)

N86-10877# Chalmers Univ. of Technology, Goteborg (Sweden). Dept. of Mathematics.
BRAUER-SEVERI SCHEMES OF ORDERS
Juliusz Brzezinski 1985 36 p refs
(CTH-Math-1985-06; ISSN-0347-2809) Avail: NTIS HC A03/MF A01

Algebraic properties of orders over a Dedekind ring in a central simple algebra over its quotient field and geometric properties of its Brauer-Severi Scheme (BS) are discussed. Explicit description of the BS schemes for orders in quaternion algebra is given. Gorenstein orders (Bass and hereditary properties) are equivalent to BS integral schemes (Normal and Regular properties). It is proved that the singularites of normal BS schemes are rational double points (quaternion case). Author (ESA)

N86-10878# Centre d'Etudes Aerodynamiques et Thermiques, Poitiers (France). Lab. d'Etudes Aerodynamiques.
SPECTRAL METHODS IN ADAPTED CURVED GRIDS Final Report [METHODES SPECTRALES EN MAILLAGE CURVILIGNE ADAPTE]
T. Alziary deRoquefort and A. Farcy Dec. 1984 70 p refs In FRENCH
(Contract DRET-81-668)
Avail: NTIS HC A04/MF A01

Two dimensional problems are studied using single domain transformations based on Chebyshev polynomials developed in two directions. Grid generation and the possibility of creating orthogonal grids are examined. The transformation of partial differential equations and the calculation of the derivatives in the transformed plans are analyzed. The Poisson equation with Dirichlet limit conditions is developed. The solution confirms method efficiency. Author (ESA)

N86-10879# Technische Hogeschool, Eindhoven (Netherlands). Dept. of Electrical Engineering.
MULTIVARIABLE PARTIAL REALIZATION AND THE ASPECT OF UNIQUENESS
Paul VandenHof, Ad Damen, and Andrzej Hajdasinski (Tilburg Univ., Netherlands) 1983 7 p refs
(ER-83/09) Avail: NTIS HC A02/MF A01

The realization of a finite sequence of Markov parameters is handled by exact and approximate realization. For the partial realization problem, a necessary and sufficient condition for the existence of a unique realization which can always be evaluated using the Ho-Kalman algorithm is introduced. A class of finite generic sequences containing sequences constructed from noisy data is defined. When such a sequence is considered, the criterion for uniqueness of a minimal partial realization takes a very simple form. A straightforward algebraic test on the length of the available sequence shows uniqueness or nonuniqueness of the extension sequence. This unique extension is important when trying to find an approximate realization of prescribed low dimension, which fits the original sequence as well as possible. The problem of approximate partial realization is defined, and it is shown how a unique solution to this problem may be obtained. Author (ESA)

N86-10880# Technische Hogeschool, Eindhoven (Netherlands). Dept. of Electrical Engineering.
NAIVE APPROXIMATE REALIZATION OF NOISY DATA
Andrzej Hajdasinski (Tilburg Univ.), Paul VandenHof, and Ad Damen 1983 7 p refs
(ER-83/10) Avail: NTIS HC A02/MF A01

Suboptimal solutions to the problem of approximate partial realization: given a multivariable formal power series of finite length, a state space description has to be constructed with limited dimension, in such a way that it approximates the available matrix sequence with respect to a criterion are presented. Methods based on the Ho-Kalman algorithm and employing a Hankel matrix or an alternative to it, a Page matrix, fail theoretically but appear to be practically quite useful. Results of the simulations allow cases in which the Hankel or Page matrix approach is more appropriate to be determined. Author (ESA)

N86-10881# Groningen Rijksuniversiteit (Netherlands). Dept. of Mathematics.
A MODIFIED SUCCESSIVE OVER-RELAXATION (SOR) METHOD FOR THE POISSON EQUATION IN UNSTEADY FREE-SURFACE FLOW CALCULATIONS
Eugen F. F. Botta and Marcel H. M. Ellenbroek 1985 27 p refs
(TW-264) Avail: NTIS HC A03/MF A01

Convergence difficulties that occur if the successive over relaxation (SOR) method is applied to the Poisson equation on a region with irregular free boundaries are analyzed. It is shown that these difficulties are related to the treatment of the free boundaries and caused by the appearance of complex eigenvalues in the system of discrete equations, when standard centered differences are used. After a modification of this system of equations such that the complex eigenvalues become small, a modified SOR method where two relaxation factors are used alternately is presented. The method leads to fast convergence without requiring specific information about the complex eigenvalues. Author (ESA)

N86-10882# Nationaal Inst. voor Kernfysica en Hoge Energiefysica, Amsterdam (Netherlands). Sectie-H.
ON THE ANALYTICAL EVALUATION OF THE PARTITION FUNCTION FOR UNIT HYPERCUBES IN FOUR DIMENSIONS
N. D. Hari Dass Oct. 1984 34 p refs
(NIKHEF-H/84-12) Avail: NTIS HC A03/MF A01

The group integrations required for the analytic evaluation of the partition function for unit hypercubes in four dimensions are carried out. Modifications of the graphical rules for SU(2) group integrations are developed. A complete classification of all surfaces

that can be embedded in the unit hypercube is given and their individual contribution to the partition function worked out. Applications are discussed. Author (ESA)

N86-10883# Nationaal Inst. voor Kernfysica en Hoge Energiefysica, Amsterdam (Netherlands). Sectie-H.
VARIATIONAL ESTIMATES FOR THE MASS GAP OF SU(2) EUCLIDEAN LATTICE GAUGE THEORY
N. D. Hari Dass Oct. 1984 14 p refs
(NIKHEF-H/84-13; B8561677) Avail: NTIS HC A02/MF A01

The application of variational techniques to the Euclidean SU(2) lattice gauge theories is reviewed. Variational results based on the single plaquette ansatz augmented with larger Wilson loops as glueball creation operators support many of the qualitative features of the Monte Carlo studies of SU(2) glueball mass. The most salient of these are the relative unimportance of the plaquettes in higher representations; the importance of the extended operators; and the trend for the mass gap to start increasing again immediately after the crossover region. The improvement of the mass gap estimates with the effective dimensionality has a simple interpretation; when the effective dimensionality is lower the glueball is squeezed more, resulting in a higher mass. Author (ESA)

N86-10884# Center for Mathematics and Computer Science, Amsterdam (Netherlands). Department of Computer Science.
PARTIAL EVOLUTION AND OMEGA COMPLETENESS OF ALGEBRAIC SPECIFICATIONS
J. Heering Jan. 1985 17 p refs Submitted for publication
(CWI-CS-R8501) Avail: NTIS HC A02/MF A01

The concept of partial evaluation (or mixed computation) is introduced. Suppose P(x,y) is a program with two arguments, whose first argument has a known value c, but whose second argument is not yet known. Partial evaluation of P(c,y) should result in a specialized residual program Pc(y) in which as much as possible is computed on the basis of c. This is expressed by saying that partial evaluation amounts to making maximal use of incomplete information. A precise meaning is given to this notion in the context of initial algebra specifications and term rewriting systems. It turns out that, if maximal propagation of incomplete information is to be achieved, as a first step it is necessary to add equations to the algebraic specification in question until it is omega-complete (if ever). The basic properties of omega-complete specifications are discussed, and examples of omega-complete specifications and specifications that do not have a finite omega-complete enrichment are given. Author (ESA)

N86-10391*# Jet Propulsion Lab., California Inst. of Tech., Pasadena. Communications System Research Section.
THE VLSI DESIGN OF ERROR-TRELLIS SYNDROME DECODING FOR CONVOLUTIONAL CODES
I. S. Reed (Univ. of Southern California, Los Angeles), J. M. Jensen (Univ. of Southern California, Los Angeles), T. K. Truong, and I. S. Hsu *In its* The Telecommun. and Data Acquisition Progr. Rept. 15 Aug. 1985 p 92-107 refs (For primary document see N86-10382 01-32)
Avail: NTIS HC A10/MF A01 CSCL 12A

N86-10392*# Jet Propulsion Lab., California Inst. of Tech., Pasadena. Communications Systems Research Section.
HIGH-RATE CONVOLUTIONAL CODE CONSTRUCTION WITH THE MINIMUM REQUIRED SNR CRITERION
P. J. Lee *In its* The Telecommun. and Data Acquisition Progr. Rept. 15 Aug. 1985 p 108-112 refs (For primary document see N86-10382 01-32)
Avail: NTIS HC A10/MF A01 CSCL 12A

N86-10397*# Jet Propulsion Lab., California Inst. of Tech., Pasadena. Reliability Engineering Section.
PERIODIC BINARY SEQUENCES WITH VERY GOOD AUTOCORRELATION PROPERTIES
S. Tyler and J. Loftsson *In its* The Telecommun. and Data Acquisition Progr. Rept. 15 Aug. 1985 p 143-158 refs (For primary document see N86-10382 01-32)
Avail: NTIS HC A10/MF A01 CSCL 12A

N86-10398*# Jet Propulsion Lab., California Inst. of Tech., Pasadena. Reliability Engineering Section.
A BINARY SEQUENCE OF PERIOD 60 WITH BETTER AUTOCORRELATION PROPERTIES THAN THE BARKER SEQUENCE OF PERIOD 13
J. Watkins (TRW, Inc., Redondo Beach, Calif.), J. Loftsson, and S. Tyler *In its* The Telecommun. and Data Acquisition Progr. Rept. 15 Aug. 1985 p 159-162 refs (For primary document see N86-10382 01-32)
Avail: NTIS HC A10/MF A01 CSCL 12A

65 STATISTICS AND PROBABILITY

Includes data sampling and smoothing; Monte Carlo method; and stochastic processes.

N86-10885# Maryland Univ., College Park. Dept. of Management Sciences and Statistics.
A MODIFIED REPAIR STRATEGY FOR TWO-COMPONENT SYSTEMS WITH REVEALED AND UNREVEALED FAULTS Technical Report, Feb. - May 1985
N. L. Johnson and S. Kotz May 1985 15 p
(Contract N00014-84-K-0301)
(AD-A156715; UMD-DMSS-85/5) Avail: NTIS HC A02/MF A01 CSCL 12/1

Some consequences of a modified repair system for Phillips' model for a two component system are discussed. In the original model, both components are repaired whenever a revealed fault occurs; in the modified model only faulty components are repaired. Specifically: (1) the distribution of time from the initial state up to discovery of an unrevealed fault, (2) the expected propagation of the time during which there exists an unrepaired fault, and (3) the distribution of number of revealed faults up to and including the one which leads to a discovery of an unrevealed fault, are obtained. The theory is illustrated by examples, based on specific distributions for the times between repairs and occurrences of the two types of faults. A characterization of the exponential distribution is indicated. GRA

N86-10886# Maryland Univ., College Park. Dept. of Management Sciences and Statistics.
ESTIMATION BY MOMENTS IN A MODEL OF FAULTY INSPECTION Technical Report, Mar. - Jun. 1985
M. Shisong, S. Kotz, and N. L. Johnson Jun. 1985 9 p
(Contract N00014-84-K-0301)
(AD-A156754; UMD-DMSS-85/6) Avail: NTIS HC A02/MF A01 CSCL 12/1

Methodology developed by Blischke is applied to estimate the parameters in a model of faulty inspection, and to obtain approximate formulae for the variances of these estimators. GRA

N86-10887# Yale Univ., New Haven, Conn. Dept. of Computer Science.
RANK REVEALING QR-FACTORIZATIONS
T. F. Chan Jun. 1985 13 p
(Contracts N00014-82-K-0184; DAAG29-83-K-0177; DE-AC02-81ER-10996)
(AD-A156756; Yaleu/DCS/RR-398) Avail: NTIS HC A02/MF A01 CSCL 12/1

An algorithm is presented for computing a column permutation Pi and a QR-factorization (A)(Pi) = QR of an m by n (m > or = n) matrix A such that a possible rank deficiency of A will be revealed in the triangular factor R having a small lower right block. For low rank deficient matrices, the algorithm is guaranteed to reveal the rank of A and the cost is only slightly more than the cost of one regular QR-factorization. A posteriori upper and lower bounds on the singular values of A are derived and can be used to infer the numerical rank of A. GRA

N86-10888# Technische Hogeschool, Eindhoven (Netherlands). Computing Center.
ADAPTIVE DISTRIBUTION-FREE TEST FOR THE K RANDOM SAMPLING PROBLEM, PART 1 [ADAPTIEVE VERDELINGSVRIJE TOETS VOOR HET K-STEEKPROEVENPROBLEEM]
T. Smeulders, R. Doornbos, and J. B. Dijkstra Jan. 1983 25 p refs In DUTCH 2 Vol.
(Comp-Cent-Note-14-Pt-1; THE-RC-51408-Pt-1) Avail: NTIS HC A02/MF A01

A rank test adapted to random sample data distributions is developed. Knowing that for the double-exponential and normal distributions the median and Van der Waerden tests have a bigger power and using the Hogg compartimentator to estimate the distribution, the test is derived. In case of a small random sample the Kruskal and Wallis test is used. However, results show that the distinguishing power of the adaptive test is not greater than that of Kruskal and Wallis. Author (ESA)

N86-10889# Technische Hogeschool, Eindhoven (Netherlands). Computing Center.
ADAPTIVE DISTRIBUTION FREE TEST FOR THE K RANDOM SAMPLING PROBLEM, PART 2 [ADAPTIEVE VERDELINGSVRIJE TOETS VOOR HET K-STEEKPROEVENPROBLEEM, DEEL 2]
R. V. H. Rooijakkers, R. Doornbos, and J. B. Dijkstra Feb. 1983 18 p refs In DUTCH 2 Vol.
(Comp-Cent-Note-15-Pt-2; THE-RC-52082-Pt-2) Avail: NTIS HC A02/MF A01

The power of an adaptive distribution-free test is compared with the power of each of the three distribution-free tests, from which it is derived. (Van der Waerden, Kruskal Wallis and Mood Brown test). Starting from 4 random samples of the same size at 15, 300 samplings are taken for certain sample shiftings. This is done on normal, log and double-exponential distributions. For each test the number of rejections of the null hypothesis is calculated. Next this is done for the value of 40. Results show that the Kruskal Wallis test is the most powerful. Author (ESA)

N86-10890# Technische Hogeschool, Eindhoven (Netherlands). Computing Center.
ROBUSTNESS OF MULTIPLE COMPARISONS AGAINST VARIANCE HETEROGENEITY
Jan B. Dijkstra 1983 15 p refs Presented at Conf. on Robustness of Statistical Methods and Nonparametric Statistics, Schwerin, East Germany, 29 May - 4 Jun. 1983
(Comp-Cent-Note-17; B8562871) Avail: NTIS HC A02/MF A01

The source of differences when the null hypothesis mu1 = ... muk is rejected for normal populations with classical one way analysis of variance is discussed. If the population variances are equal, the: (1) least significant difference test, (2) multiple range test for equal sample sizes, (3) an adaptation for unequal sample sizes (4) multiple F-test, or (5) multiple Comparisons test can be considered. For all these methods (including the one way analysis of variance) alternatives that are robust against variance heterogeneity exist. A modification of (3) has unattractive properties if the variances and the sample sizes differ greatly. The adaptations for unequal variances of (4) and (5) seem better than (1) for cases with many samples. Test (2) is rather robust in itself if the variances are not too different. Modifications that allow slight unequalities in the sample sizes exist. Author (ESA)

N86-10891# Technische Hogeschool, Eindhoven (Netherlands). Computing Center.
NONPARAMETRIC COMPARISON OF SEVERAL MEAN VALUES WITH MILD ADAPTATION TO SOME SAMPLE CHARACTERISTICS
Jan B. Dijkstra 1984 16 p refs Presented at Computation Statistics (COMPSTAT) Conf., Prague, 27-31 Aug. 1984
(Comp-Cent-Note-20; B8562873) Avail: NTIS HC A02/MF A01

Criteria for choosing between rank tests for log, double exponential, and normal distributions are considered. For certain criteria, the principle of taking the combined sample and ignoring the origin of individual values is seriously violated, so that the resulting tests do not remain permutation tests. A simulation study to find out how much this violation affects control over the chosen size is performed. Powers are estimated for various alternatives, also by using simulation techniques. It is concluded that mild adaptation is possible in this situation without serious harm in the sense of size-control. Extra power can be gained by it, though not for small samples. Author (ESA)

N86-10892# Groningen Rijksuniversiteit (Netherlands). Dept. of Mathematics.
ON THE NUMERICAL DETERMINATION OF THE DIMENSION OF AN ATTRACTOR
F. Takens 1985 11 p refs
(ZW-8415) Avail: NTIS HC A02/MF A01

The convergence of an algorithm to estimate the correlation dimension from experimental data (i.e., errors to be expected when using a finite part of the data sequence) is discussed. The method consists of reconstruction of the phase space in IRn and second the determination of the correlation dimension of a bounded subset in IRn with a probability measure. Using ideas from mathematical statistics, particularly Fischer's maximum likelihood rule, the algorithm is extended to minimize errors. Author (ESA)

N86-10893# Tilburg Univ. (Netherlands). Dept. of Business and Economics.
SUPEREFFICIENT ESTIMATION OF POWER FUNCTIONS IN SIMULATION EXPERIMENTS
J. P. C. Kleijnen 1985 16 p refs
(B8562445) Avail: NTIS HC A02/MF A01

A superefficient procedure that computes the extreme parameter value that would still be accepted under the null hypothesis, given the sample outcome is outlined. This transforms the estimation of the power function into the estimation of a distribution function. Comparing power functions becomes straightforward. The power function is contrasted with Schruben's (1980) coverage function. Author (ESA)

N86-10894# Tilburg Univ. (Netherlands). Dept. of Business and Economics.
THE POWER OF WEIGHTED AND ORDINARY LEAST SQUARES WITH ESTIMATED UNEQUAL VARIANCES IN EXPERIMENTAL DESIGN
J. P. C. Kleijnen, P. Cremers, and F. vanBelle 1985 21 p refs
(B8562446) Avail: NTIS HC A02/MF A01

Response variances are estimated using replications for each experimental condition. The resulting estimated variances can be used to derive the correct variances of the Ordinary Least Squares (OLS) estimators. The estimates can also be used to compute the Estimated Least Squares (EWLS) estimators. The asymptotic covariance formula for EWLS might be used to test the EWLS estimators. The type 1 and 7 errors of this test procedure are compared with those for the OLS estimations. If the variances are constant, EWLS should not be used, but with strong heterogeneity EWLS is more efficient if the variance can be estimated from more than two observations. Author (ESA)

N86-10895# Tilburg Univ. (Netherlands). Dept. of Business and Economics.
REGRESSION ANALYSIS: ASSUMPTIONS, ALTERNATIVES, APPLICATIONS
J. P. C. Kleijnen 1985 51 p refs
Avail: NTIS HC A04/MF A01

The use of a regression model to summarize the reaction of the output of a simulation program to changes in the input is considered. The applicability, testing, and alternatives to six assumptions are discussed: a non-singular matrix of independent variables; a regression model with linear parameters; responses with constant variances; independent responses; normally distributed responses; and a valid or correctly specified regression model. Author (ESA)

66 SYSTEMS ANALYSIS

Includes mathematical modeling; network analysis; and operations research.

N86-10896*# Pennsylvania Univ., Philadelphia. Dept. of Computer and Information Science.
MOTION ANALYSIS REPORT
Norman I. Badler 31 May 1985 33 p refs
(Contract NAS9-16634)
(NASA-CR-171897; NAS 1.26:171897) Avail: NTIS HC A03/MF A01 CSCL 12B

Human motion analysis is the task of converting actual human movements into computer readable data. Such movement information may be obtained though active or passive sensing methods. Active methods include physical measuring devices such as goniometers on joints of the body, force plates, and manually operated sensors such as a Cybex dynamometer. Passive sensing de-couples the position measuring device from actual human contact. Passive sensors include Selspot scanning systems (since there is no mechanical connection between the subject's attached LEDs and the infrared sensing cameras), sonic (spark-based) three-dimensional digitizers, Polhemus six-dimensional tracking systems, and image processing systems based on multiple views and photogrammetric calculations. G.L.C.

N86-10897*# Pennsylvania Univ., Philadelphia. Dept. of Computer and Information Science.
ZERO-GRAVITY MOVEMENT STUDIES
Norman I. Badler, Paul Fishwick, Nina Taft, and Mukul Agrawala 31 May 1985 113 p refs
(Contract NAS9-16634)
(NASA-CR-171899; NAS 1.26:171899) Avail: NTIS HC A06/MF A01 CSCL 12B

The use of computer graphics to simulate the movement of articulated animals and mechanisms has a number of uses ranging over many fields. Human motion simulation systems can be useful in education, medicine, anatomy, physiology, and dance. In biomechanics, computer displays help to understand and analyze performance. Simulations can be used to help understand the effect of external or internal forces. Similarly, zero-gravity simulation systems should provide a means of designing and exploring the capabilities of hypothetical zero-gravity situations before actually carrying out such actions. The advantage of using a simulation of the motion is that one can experiment with variations of a maneuver before attempting to teach it to an individual. The zero-gravity motion simulation problem can be divided into two broad areas: human movement and behavior in zero-gravity, and simulation of articulated mechanisms. G.L.C.

N86-10898# Massachusetts Inst. of Tech., Cambridge. Lab. for Computer Science.
REACHING APPROXIMATE AGREEMENT IN THE PRESENCE OF FAULTS Interim Research Report
D. Dolev, N. A. Lynch, S. S. Pinter, E. W. Stark, and W. E. Weihl Mar. 1985 27 p
(Contract N00014-83-K-0125)
(AD-A156541; MIT/LCS/TM-276) Avail: NTIS HC A03/MF A01 CSCL 12/1

This paper considers a variant on the Byzantine Generals problem, in which processes start with arbitrary real values rather than Boolean values or values from some bounded range, and in which approximate, rather than exact, agreement is the desired goal. Algorithms are presented to reach approximate agreement in asynchronous, as well as synchronous systems. The asynchronous agreement algorithm is an interesting contrast to a result of Fischer, Lynch, and Patterson, who show that exact agreement in not attainable in an asynchronous system with a provable convergence rate that depends on the ratio between the number of faults and the number of processes. Lower bounds on the convergence rate for algorithms of this form are proven, and the algorithms presented are shown to be optimal. GRA

N86-10899# Carnegie-Mellon Univ., Pittsburgh, Pa. Dept. of Computer Science.
DERIVATIONAL ANALOGY: A THEORY OF RECONSTRUCTIVE PROBLEM SOLVING AND EXPERTISE ACQUISITION
J. G. Carbonell 5 Mar. 1985 26 p
(Contracts N00014-79-C-0661; N00014-82-C-5076)
(AD-A156817; CMU-CS-85-115) Avail: NTIS HC A03/MF A01 CSCL 05/10

Derivational analogy, a method of solving problems based on the transfer of past experience to new problem situations, is discussed in the context of other general approaches to problem solving. The experience transfer process consists of recreating lines of reasoning, including decision sequences and accompanying justifications, that proved effective in solving particular problems requiring similar initial analysis. The role of derivational analogy in case-based reasoning and in automated expertise acquisition is discussed. Author (GRA)

N86-10900# Air Force Inst. of Tech., Wright-Patterson AFB, Ohio.
GENERATION OF FLIGHT PATHS USING HIERARCHICAL PLANNING M.S. Thesis
K. B. Kline 1985 265 p
(AD-A156905; AFIT/CI/NR-85-37T) Avail: NTIS HC A12/MF A01 CSCL 12/2

This thesis examines the use of an artificial intelligence technique, hierarchical planning, to solve the problem of generating an aircraft route and finding a path through various hostile environments. A route or path is evaluated by the number and type of threats the aircraft encounters on the route and the route length. An algorithm using hierarchical planning is presented and tested against several hostile environments. Specifically, the algorithms will divide the problem space or grid into smaller spaces or boxes. These boxes are then assigned values based upon the input hostile environment. Block paths are then constructed and evaluated based on the values in the boxes. An exhaustive search is performed on the two best block paths to find a flight path for the aircraft. Test results are compared to previous results obtained using heuristic search and indicate an improvement in solution quality. Although specific plans are incorporated into the algorithm to obtain test results, many other plans within the realm of hierarchical planning certainly exist and could be used to solve this problem. GRA

N86-10901# Technische Hogeschool, Eindhoven (Netherlands). Dept. of Industrial Engineering.
OPERATIONS RESEARCH APPLICATIONS [OPERATIONS-RESEARCH TOEPASSINGEN]
C. B. Tilanus Mar. 1983 27 p refs In DUTCH Submitted for publication
(ARW-03-THE-BDK/ORS/83-08) Avail: NTIS HC A03/MF A01

The essentials of operations research (OR) are illustrated. The term OR, and similarities and differences with related terms are elucidated. The OR applications in the Netherlands are classified by economic sector, problem area, methods and computer languages. As an example of the long way from mathematical methods, via standardized programs to the utilization in concerns and other organizations, vice versa, linear programming is treated and standard programs are presented. Author (ESA)

67 THEORETICAL MATHEMATICS

Includes topology and number theory.

N86-10902# Chalmers Univ. of Technology, Goteborg (Sweden). Dept. of Mathematics.
SOME REMARKS ABOUT CUSP FORMS: HOLOMORPHIC AND NON-HOLOMORPHIC
Dennis A. Hejhal 1984 35 p refs
(CTH-Math-1984-26; ISSN-0347-2809) Avail: NTIS HC A03/MF A01

Cusp forms on a modular group and its congruence sub-

groups are considered. It is proven that estimations and properties of Fourier coefficients of nonholomorphic cusp forms depending on the norm of the fundamental region, the level, and other constants can be handled by the Kloosterman-Estermann (KE) approach. The KE approach is an analog of the Ramanujan-Peterson conjecture. Author (ESA)

N86-10903# Chalmers Univ. of Technology, Goteborg (Sweden). Dept. of Mathematics.
ON CLASS GROUPS OF LATTICES
Juliusz Brzezinski 1985 22 p refs
(CTH-Math-1985-08; ISSN-0347-2809) Avail: NTIS HC A03/MF A01

General formulas for spinor class groups of orders are given. The formulas are analogous to the formulas for the locally free class groups of a subring of a central simple algebra over the quotient of a Dedekind ring. Author (ESA)

N86-10904# Chalmers Univ. of Technology, Goteborg (Sweden). Dept. of Mathematics.
GALOIS DESCENT AND CLASS GROUPS OF ORDERS
Per Salberger 1985 19 p refs
(CTH-Math-1985-09; ISSN-0347-2809) Avail: NTIS HC A02/MF A01

It is proved that class groups are finite for maximal order over polynomial rings with coefficients in the field of finite transcendence degree over its prime fields, in a central simple K(t) algebras over the algebra of rational functions. The Galois descent method is used. The best-results are obtained for number fields K. Author (ESA)

N86-10905# Groningen Rijksuniversiteit (Netherlands). Dept. of Mathematics.
A NOTE ON THE DIFFERENCIABILITY OF CENTER MANIFOLDS
Floris Takens 1985 7 p refs
(ZW-8414) Avail: NTIS HC A02/MF A01

Center manifold theorem is discussed. An example of a center manifold that cannot be smoothed by restricting it to a small neighborhood of the origin is studied. An explicit construction on four dimensional space is given. Author (ESA)

70 PHYSICS (GENERAL)

For geophysics see *46 Geophysics*. For astrophysics see *90 Astrophysics*. For solar physics see *92 Solar physics*.

N86-10906 Department of the Air Force, Washington, D.C.
INFRARED SYSTEM WITH COMPUTERIZED IMAGE DISPLAY Patent
R. P. Walker, J. D. Rex, and J. H. Schummers, inventors (to Air Force) Issued 28 May 1985 15 p Supersedes AD-D009774 (AD-D011777; US-Patent-4,520,504; US-Patent-Appl-SN-403246; US-Patent-Class-382-1) Avail: US Patent and Trademark Office CSCL 17/5

An object of this invention is to provide a system in which detected signals from an infrared scanner can be used to provide a calibrated display, and by which the data can be stored for later use. In the system according to the invention, image signals originating from an infrared scanner are transformed into a digitized form for storage in a computer and manipulated to produce a calibrated display. This transforms the merely qualitative utility of such a scanner into a quantitative capability allowing analysis of heat energy losses from structures of interest with only modest investments in capital equipment. GRA

N86-10907# California Univ., Livermore. Lawrence Livermore Lab.
NEW APPROACH TO MULTIPHASE EQUILIBRIA: APPLICATION TO HIGH-PRESSURE PHYSICS PROBLEMS
F. H. Ree Jun. 1985 19 p refs Presented at 10th High Pressure Conf. on Res. in High Pressure Sci. and Technol., Amsterdam, 8 Jul. 1985
(Contract W-7405-eng-48)
(DE85-013820; UCRL-92121; CONF-850759-1) Avail: NTIS HC A02/MF A01

A multiphase, multicomponent equation-of-state (EOS) model based on first principles of statistical mechanics is described. The model was used to study fluid-fluid phase separations in binary (H2-He, Ar-Ne, Xe-He, and N2-H20) and ternary or more complex systems involving species with C, H, N, and O atoms. Results of these calculations and a brief description of a new theory which can simultaneously describe both solid and fluid EOS properties are given. DOE

N86-10908# California Univ., Livermore. Lawrence Livermore Lab.
CRYOGENIC STRUCTURAL MATERIALS FOR SUPERCONDUCTING MAGNETS
E. N. C. Dalder and J. W. Morris, Jr. 22 Feb. 1985 19 p Presented at the 8th Intern. Conf. on Struct. Mech. in Reactor Technol., Brussels, 19 Aug. 1985
(Contract W-7405-eng-48)
(DE85-008026; UCRL-92161; CONF-850809-19) Avail: NTIS HC A02/MF A01

Research in the United States and Japan on structural materials for high-field superconducting magnets is reviewed. Superconducting magnets are used for magnetic fusion energy devices and for accelerators that are used in particle-physics research. The cryogenic structural materials that were reviewed are used for magnet cases and support structures. Increased materials requirements are expected in the future. DOE

71 ACOUSTICS

Includes sound generation, transmission and attenuation. For noise pollution see *45 Environment Pollution*.

N86-10909 ESDU International Ltd., London (England).
SUMMARY OF WORK ON JET NOISE PREDICTION
R. F. Lambert Apr. 1985 38 p refs
(ESDU-BR-62636; ESDU-AN-36B) Copyright. Avail: ESDU

Design data for aircraft noise, which include the estimation of subsonic far-field jet mixing noise are presented. It is proposed to extend the existing far field jet mixing noise to supersonic jet velocity conditions. The theories which form the basis for jet exhaust noise prediction are summarized. Measured and predicted overall and spectrum noise levels are compared. The existing data item, the theoretical basis for extending the item into the supersonic jet velocity region, and comparison with jet noise predictions are assessed. E.A.K.

N86-10910 North Carolina State Univ., Raleigh.
SOUND RADIATION FROM REPETITIVE TRANSIENT VIBRATIONS USING MULTI-CHANNEL DIGITAL SIGNAL PROCESSING WITH APPLICATION TO IMPACT MACHINERY Ph.D. Thesis
Ronald Bruce Coleman 1984 242 p
Avail: Univ. Microfilms Order No. DA8507359

Sound radiation from repetitive transient vibrations has been investigated both experimentally and analytically to determine techniques capable of ranking acoustic sources on transient impact machinery. Several of the difficulties encountered in analyzing transient impact noise have been overcome through advanced digital signal processing techniques. These digital signal processing techniques indicated for the first time that traditional multiple input/single output modes of the sound radiation froeXcomplex machinery, characterized by omnidirectional energy flow and/or high spatial coherence throughout the structure, will fail to accurately rank acoustic sources. The utility of cepstral analysis in deconvolving contaminated pressure signals from repetitive transient machinery tested under semi-anechoic conditions, and acoustic intensity measurements in the near- and far-field have also been demonstrated. Approximate and analytical models of

repetitive transient vibrations and sound radiation have been investigated. Dissert. Abstr.

N86-10911 Johns Hopkins Univ., Baltimore, Md.
PHYSICAL ACOUSTICS: INVESTIGATION OF CHEMICAL KINETIC AND THERMODYNAMIC PROPERTIES OF FLUIDS Ph.D. Thesis
Timothy Scott Margulies 1984 146 p
Avail: Univ. Microfilms Order No. DA8501663

Measurement of the absorption and dispersion of forced acoustic waves propagating in fluids in equilibrium have been used to determine thermostatic properties and the kinetics of reactions. A theoretical treatment of this problem using the linearized (or first-order) balance equations of mass, linear momentum, energy and chemical kinetics is presented. General results are obtained in the form of a characteristic equation for the complex propagation variable x= - (alpha + i omega/c) where alpha is the attenuation coefficient, c is the phase speed for the progressive wave, and omega = 2 pi F is the angular frequency. Dissert. Abstr.

N86-10912*# Purdue Univ., Lafayette, Ind.
A STUDY OF METHODS TO PREDICT AND MEASURE THE TRANSMISSION OF SOUND THROUGH THE WALLS OF LIGHT AIRCRAFT. INTEGRATION OF CERTAIN SINGULAR BOUNDARY ELEMENT INTEGRALS FOR APPLICATIONS IN LINEAR ACOUSTICS
Dan Zimmerle and Robert J. Bernhard Jul. 1985 40 p
(Grant NAG1-58)
(NASA-CR-176229; NAS 1.26:176229; HL-85-21; Rept-0226-16) Avail: NTIS HC A03/MF A01 CSCL 20A

An alternative method for performing singular boundary element integrals for applications in linear acoustics is discussed. The method separates the integral of the characteristic solution into a singular and nonsingular part. The singular portion is integrated with a combination of analytic and numerical techniques while the nonsingular portion is integrated with standard Gaussian quadrature. The method may be generalized to many types of subparametric elements. The integrals over elements containing the root node are considered, and the characteristic solution for linear acoustic problems are examined. The method may be generalized to most characteristic solutions. E.A.K.

N86-10913*# National Aeronautics and Space Administration. Langley Research Center, Hampton, Va.
INVESTIGATION OF COMPOSITE MATERIALS PROPERTY REQUIREMENTS FOR SONIC FATIGUE RESEARCH
Howard V. L. Patrick (Embry-Riddle Aeronautical Univ.) Aug. 1985 37 p refs
(NASA-TM-87601; NAS 1.15:87601) Avail: NTIS HC A03/MF A01 CSCL 20A

Experimental techniques for determining the extensional and bending stiffness characteristics for symmetric laminates are presented. Vibrational test techniques for determining the dynamic modulus and material damping are also discussed. Partial extensional stiffness results intially indicate that the laminate theory used for predicting stiffness is accurate. It is clearly shown that the laminate theory can only be as accurate as the physical characteristics describing the lamina, which may vary significantly. It is recommended that all of the stiffness characteristics in both extension and bending be experimentally determined to fully verify the laminate theory. Dynamic modulus should be experimentally evaluated to determine if static data adequately predicts dynamic behavior. Material damping should also be ascertained because laminate damping is an order of magnitude greater than found in common metals and can significantly effect the displacement response of composite panels. Author

N86-10914# Naval Postgraduate School, Monterey, Calif.
FIBER OPTIC GRADIENT HYDROPHONE CONSTRUCTION AND CALIBRATION FOR SEA TRIAL M.S. Thesis
G. E. MacDonald Mar. 1985 125 p
(AD-A156469) Avail: NTIS HC A06/MF A01 CSCL 17/1

A Mach-Zehnder interferometric fiber optic gradient hydrophone, for operation at 632.8 nm wavelength, was designed and constructed for testing in the laboratory. Two individual fiber optic hydrophone sensing coils with 10 m of fiber each were wound and potted on an epoxy mandrel and their respective sensitivities were obtained. They then were mounted on a rigid bar, separated by 10 cm, to form a gradient hydrophone. The sensitivity of this arrangement then was obtained in a calibrator which allowed the coil pair to be rotated 360 deg. Since the laboratory interferometric system was too large to be used in the sea trial tests, a second interferometric system, operating at 830 nm wavelength, using diode lasers was designed and constructed. This was mounted in an experimental apparatus designed and constructed for sea trial. A sea trial of a standard Navy type DIFAR hydrophone was conducted to test the effectiveness of the experimental apparatus. The results of the laboratory tests are summarized and discussed and recommendations for further studies are presented. GRA

N86-10915# Department of the Air Force, Washington, D.C.
TUNABLE ACOUSTO-OPTIC FILTER WITH IMPROVED SPECTRAL RESOLUTION AND INCREASED APERTURE Patent Application
I. C. Chang, inventor (to Air Force) Filed 26 Apr. 1985 21 p
(AD-D011758; US-Patent-Appl-SN-727507) Avail: NTIS HC A02/MF A01 CSCL 09/5

This document refers to a transverse configuration, electronically tunable acousto-optic filter assembly with improved spectral resolution and increased aperture. The crystal prism member is made of TeO(2) and has a large prism angle (i.e., close to 90 degrees). An acoustic prism coupler member made of material with low acoustic velocity (such as TeO(2), AsS(3), or GeAsSe), to avoid total internal reflection of the interface, is bonded in optical contact with a face of the crystal prism member which defines one extreme of the large prism angle, and which is not traversed by a polarized light beam that is transmitted through the crystal prism member and that interacts with a generated, perpendicularly directed, acoustic wave. The use of the acoustic prism couple member, together with the use of a large prism angle in the crystal prism member, result in high spectral resolution and large aperture of the filter assembly and its desired usability in the infrared region. GRA

N86-10916# Southwest Research Inst., San Antonio, Tex.
EXPLORATORY DEVELOPMENT FOR A HIGH RELIABILITY FLAW CHARACTERIZATION MODULE Final Report, 31 Aug. 1981 - 31 Jan. 1985
G. J. Gruber, G. J. Hendrix, and T. A. Mueller Wright-Patterson AFB, Ohio AFWAL Mar. 1985 155 p
(Contract F33615-81-C-5066)
(AD-A156632; AFWAL-TR-84-4172) Avail: NTIS HC A08/MF A01 CSCL 14/2

Two sets of ultrasonic characterization procedures were applied under blind test conditions to 42 manufacturing flaws (inclusions and voids) embedded in titanium and IN100 alloy specimens. The Born inversion procedures (BIP) resulted in size estimates that were independent of not only flaw composition, but also shape, size, and orientation. Instead, the Born diameters were determined to be directly related to the period of the incident wave. For this reason, the BIP results could not be reproduced with different transducers. The Born inversion algorithm correctly treats the first half-cycle of the impulse response of a volumetric flaw as the front-surface echo, but mistakes its third half-cycle for a back-surface (internal satellite pulse) or a creeping-wave return (external satellite pulse). The characterization procedures based on the satellite-pulse observation technique (SPOT) proved to be insensitive to the period of the employed high-frequency transducers and, as expected, the practically constant separation between the front-surface echo and the satellite pulse was found to be directly related to flaw size. Semiautomated satellite analysis procedures (SSAP) that waive the requirement for a highly trained ultrasonic examiner were developed and qualified on 32 test flaws. GRA

N86-10917# Human Engineering Labs., Aberdeen Proving Ground, Md.

PROPOSED AURAL NONDETECTABILITY LIMITS FOR ARMY MATERIEL Final Report
G. R. Garinther, J. T. Kalb, D. C. Hodge, and G. R. Price Mar. 1985 61 p
(AD-A156704; HEL-TM-3-85) Avail: NTIS HC A04/MF A01 CSCL 20/1

The parameters which affect the propagation and detectability of sound are discussed and assessed for the purpose of revising the aural nondetectability limits of MIL-STD-1474 (1979). The factors considered are geometric spreading, atmospheric absorption, ground effect, atmospheric turbulence, refraction due to wind and temperature gradients, barriers, foliage, threshold of hearing, psychoacoustic factors, and background noise at the listener's location. Examples are given of the effect on sound propagation of varying the parameters, and several suggestions are offered for field expedient measures to control or detect sound. Standard conditions for sound propagation and detectability are proposed, along with two assumed background noise levels. These conditions and background noise levels form the basis for two proposed nondetectability limits. These limits, expressed in 1/3-octave bands, are provided for critical and typical military scenarios and a rationale for selecting between them is developed. Measurement procedures for determining conformance with the limits and an explanation of the methods and rationale used in computing the limits are also presented. The proposed limits are intended to provide nondetectability under most conditions likely to be encountered. However sound propagation conditions are identified which might allow materiel meeting the limits to be detected. Author (GRA)

N86-10918# Mississippi Univ., University. Physical Acoustics Research Lab.
ACOUSTIC CAVITATION AND BUBBLE DYNAMICS
A. A. Atchley and L. A. Crum 15 Jun. 1985 126 p
(Contract N00014-84-C-0193)
(AD-A156888; TR-2-85) Avail: NTIS HC A07/MF A01 CSCL 20/1

The topic of this chapter, acoustic cavitation, is but one of several possible mechanisms through which ultrasound can interact with a liquid medium. Acoustic cavitation can affect a liquid through two possible avenues. The first is the bubble itself. The liquid is disrupted by the inhomogeneous presence of the bubble. The second avenue through which bubbles affect a fluid is through bubble dynamics. The bubble's interior and the liquid immediately surrounding the bubble are regions which undergo continual change. The bubble-liquid interface continually changes shape and size; liquid molecules diffuse into and out of the bubble; the concentration of gas in the surrounding liquid varies; acoustic streaming occurs in the liquid in the vicinity of the bubble often resulting in severe shear stresses; the interior pressure and temperature fluctuate rapidly; the bubble radiates acoustic energy as it oscillates; thermal and viscous damping hinder the bubble oscillations. GRA

N86-10919# Royal Aircraft Establishment, Farnborough (England).
MEASUREMENTS OF THE ACOUSTIC INTERFERENCE BETWEEN ADJACENT MICROPHONES
R. W. Copplestone Aug. 1984 26 p
(AD-A156892; RAE-TM-P-1030; DRIC-BR-94556) Avail: NTIS HC A03/MF A01 CSCL 20/1

An experimental technique is described to determine the disturbance to the response of one microphone due to the presence of a second identical microphone. The measurements were carried out in a free field environment using plane waves incident normally onto the microphones and protection grids were used. The microphone diaphragms were coplanar and the spacing between the microphone centers was varied from one to sixteen microphone diameters. Amplitude deviations up to 1 dB and phase deviations up to 7 degrees have been measured. The magnitudes of the disturbances have been found to be in good agreement with theory. Author (GRA)

N86-10920# Sandia Labs., Albuquerque, N. Mex.
UNDERSTANDING AND IMPROVING ACOUSTIC TO SEISMIC COUPLING AS IT PERTAINS TO SANDIA'S HELICOPTER DETECTOR
G. Elliott and R. J. Fogler 18 Mar. 1985 22 p
(Contract DE-AC04-76DP-00789)
(DE85-009440; SAND-85-0841C) Avail: NTIS HC A02/MF A01

The basic physics of the acoustic-to-seismic coupling phenomenon involved in the operation of a helicopter detector under development are reported. A series of tests were conducted near Albuquerque, New Mexico, investigating the coupling phenomenon using an impulsive noise source and two different helicopters. Results of the tests including the evaluation of a new microphone windscreen design are presented. DOE

72 ATOMIC AND MOLECULAR PHYSICS

Includes atomic structure and molecular spectra.

N86-10921 Maryland Univ., College Park.
MATTER-ANTIMATTER TRANSITION OPERATORS: A MANUAL FOR MODELING Ph.D. Thesis
Janko Milutinovic 1984 171 p
Avail: Univ. Microfilms order No. DA8510265

With the advent of grand unified theories of strong and electroweak interactions, some previously sacred principles, like baryon and lepton number conservation, have had to be abandoned. New interactions have rendered possible several processes which violate these conservation laws. The two most important and most extensively discussed such processes are proton decay and neutron-antineutron (NN) oscillations. Dissert. Abstr.

N86-10922 Pittsburgh Univ., Pa.
CHARGE EXCHANGE IN SLOW COLLISIONS OF ATOMS AND MOLECULES Ph.D. Thesis
Pradip Kumar Gangopadhyay 1984 90 p
Avail: Univ. Microfilms Order No. DA8511041

The cross section for symmetric charge transfer in ion-atom collisions is usually determined by the adiabatic theory. In this work the adiabatic theory is extended to very low energies taking into account the curvature of the nuclear motion due to polarization forces. At the very high energy end the Demkov-Ostrovskii theory is used to compare with the experimental results. The Coulomb force is incorporated into the standard adiabatic theory to determine the cross section for charge transfer between multiply charged ions. The results obtained are in very good agreement with the experimental results. The slight discrepancy between the modified asymptotic theory and the quantum result, in the case of HE^{*}-He+, is studied numerically. Ion-molecule charge transfer is studied numerically. Ion-molecule charge transfer is studied using the close-coupling method. The relative importance of short and long range electron transfer mechanism is studied. The merits and demerits of a surface crossing model are discussed. The importance of including the strong electronic-vibrational coupling in any theory dealing with molecular charge transfer is emphasized. Dissert. Abstr.

N86-10923# National Bureau of Standards, Gaithersburg, Md. Office of Standard Reference Data.
SELECTED TABLES OF ATOMIC SPECTRA. ATOMIC ENERGY LEVELS AND MULTIPLET TABLE O3
Charlotte E. Moore Jul. 1985 35 p refs Prepared in cooperation with NRL
(NBS/NSRDS-3/11; LC-64-60074) Avail: NTIS HC A03/MF A01

The present publication is the eleventh section of a series being prepared in response to the need for a current revision of two sets of the author's tables containing data on atomic spectra as derived from analyses of optical spectra. As in the previous Sections, Part A contains the atomic energy levels and Part B the multiplet tables. Section 11 includes these data for O3. Author

N86-10924# Naval Research Lab., Washington, D. C.
ELECTRON MOMENTUM TRANSFER COLLISION FREQUENCY

IN N(2), O(2) AND AIR Interim Report, 1984 - 1985
S. Slinker and A. W. Ali 26 Jul. 1985 30 p
(ARPA Order 4395)
(AD-A157030; NRL-MR-5614) Avail: NTIS HC A03/MF A01 CSCL 20/8

The electron momentum transfer collision frequencies in N2, O2 and air are calculated for a Maxwellian electron velocity distribution using several definitions of nu sub m (the momentum transfer collision frequency). Author (GRA)

N86-10925# Rochester Univ., N. Y. Dept. of Chemistry.
COOPERATIVE EMISSION BY TWO DIFFERENT ATOMS INTO SURFACE PLASMONS Interim Report
K. C. Liu and T. F. George Jul. 1985 36 p Prepared in cooperation with State Univ. of New York, Buffalo
(Contract N00014-80-C-0472)
(AD-A157033; URochester/DC/85/TR-68) Avail: NTIS HC A03/MF A01 CSCL 07/4

The interaction between surface plasmons and two atoms with different electronic transition frequencies near a metal or doped semiconductor surface is considered. The atom-atom and atom-surface separations are assumed to be smaller than the corresponding mean resonance wavelength. The time evolution of the emission rate of such an atomic pair into surface plasmon modes is calculated in a fully quantum-mechanical manner. Explicit results are given for various initial states of the diatomic system. As the frequency difference Delta < or = gamma, where gamma is the mean half-width of the atomic resonance lines, the emission behaves as if there are two identical atoms. On the other hand, when Delta > gamma, oscillations are found in the emission rate as a function of time in all cases as a manifestation of beating. The oscillations are especially pronounced when the diatomic system is initially in a coherent state. For the form of the particular state corresponding to complete photon trapping in the case of two identical atoms, a pair of two different atoms exhibits oscillating emission into the superadiant region before eventual decay to zero. Author (GRA)

N86-10926# Oak Ridge National Lab., Tenn. Physics Div.
THE 1984 BIBLIOGRAPHY OF ATOMIC AND MOLECULAR PROCESSES
C. F. Barnett, comp., H. B. Gilbody, comp. (Queen's Univ., Belfast), D. C. Gregory, comp., P. M. Griffin, comp., C. C. Havener, comp., A. M. Howard, comp., M. I. Kirkpatrick, comp., E. W. McDaniel, comp. (Georgia Tech. Research Inst.), F. W. Meyer, comp., T. J. Morgan, comp. (Wesleyan Univ.) et al Apr. 1985 209 p
(Contract DE-AC05-84OR-21400)
(DE85-010583; ORNL-6157) Avail: NTIS HC A10/MF A01

This annotated bibliography includes papers on atomic and molecular processes published during 1984. Sources include scientific journals, conference proceedings, and books. Each entry is designated by one or more of the 114 categories of atomic and molecular processes used by the Controlled Fusion Atomic Data Center, Oak Ridge National Laboratory to classify data. Also indicated is whether the work was experimental or theoretical, what energy range was covered, what reactants were investigated, and the country of origin of the first author. Following the bibliographical listing, the entries are indexed according to the categories and according to reactants within each subcategory. DOE

N86-10927# Los Alamos National Lab., N. Mex.
THEORY OF DENSE MOLECULAR FLUID EQUATIONS OF STATE WITH APPLICATION TO DETONATION PRODUCTS
M. S. Shaw, J. D. Johnson, and B. L. Holian 1984 4 p Presented at the 8th Intern. Symp. on Detonation, Albuquerque, N. Mex., 15 Jul. 1985
(Contract W-7405-eng-36)
(DE84-016822; LA-UR-84-2753; CONF-850706-1) Avail: NTIS HC A02/MF A01

Because of the uncertainty in using spherical potentials, a series of benchmark calculations was made using molecular dynamics with realistic anisotropic potentials. The configurational part of the Helmholtz free energy for an anisotropic molecular system can be obtained by using an equivalent spherical potential. Such potentials were obtained for N2, O2, NO, CO, and CO2. DOE

N86-10928# Sandia Labs., Albuquerque, N. Mex.
PROVIDING AUTOMATED CONTROL FOR PBFA-2
V. M. Italiano 1985 10 p Presented at the 5th IEEE Pulsed Power Conf., Washington, D.C., 10 Jun. 1985
(Contract DE-AC04-76DP-00789)
(DE85-012867; SAND-84-2434C; CONF-850616-1D) Avail: NTIS HC A02/MF A01

Four levels of control which are available to the operator in the particle beam fusion accelerator 2 (PBFA-2) control/monitor system are discussed. At the lowest control level, remote manual, the operator is responsible for all accelerator control and coordination and for interpreting sensor and actuator values to determine the state of the accelerator. At the highest control level, autostaging, the computer integrates the sensor and actuator values into reports. The operator controls several accelerator subsystems with single autostaging commands which the control/monitor system interprets into sequences of integrated functions. The control system is implemented from the bottom up, from remote manual to autostaging. Control action tasks are integrated with no major changes to the control/monitor design. Once the control action tasks are completely implemented no more changes are expected in the design. The control/monitor system is reviewed. DOE

N86-10929# Los Alamos National Lab., N. Mex.
HIGH-BRIGHTNESS PHOTOEMITTER INJECTOR FOR ELECTRON ACCELERATORS
J. S. Fraser, R. L. Sheffield, E. R. Gray, and G. W. Rodenz 1985 4 p refs Presented at the Particle Accelerator Conf., Vancouver, British Columbia, 13 May 1985
(Contract W-7405-eng-36)
(DE85-012673; LA-UR-85-1632; CONF-850504-96) Avail: NTIS HC A02/MF A01

A free-electron laser (FEL) oscillator, driven by an RF linac, requires a train of electron bunches delivered to an undulator. The electron-beam brightness requirement exceeds that available from a conventional buncher. The demonstrated high peak brightness of laser-illuminated photoemitters indicates that the conventional buncher system might be eliminated entirely without the usual large loss in beam brightness that occurs in bunchers. A photoemitter with a current density of about 200 A/cm (2) is located on an end wall of an RF cavity to accelerate a 60-ps bunch of electrons to 1 MeV as rapidly as possible. Preliminary experimental work and simulation calculations are presented. DOE

N86-10930# Los Alamos National Lab., N. Mex.
MEASUREMENT AND RESULTING FIRST AND SECOND ORDER APPROXIMATIONS FOR A 9 DEG BENDING MAGNET IN LAMPF'S 750-keV TRANSPORT
J. W. Hurd 1985 4 p Presented at the Particle Accelerator Conf., Vancouver, British Columbia, 13 May 1985
(Contract W-7405-eng-36)
(DE85-012691; LA-UR-85-1528; CONF-850504-118) Avail: NTIS HC A02/MF A01

The three Cartesian components of magnetic field are measured for a 9 degree bending magnet. Measurement errors are corrected and the data is fit to a polynomial which satisfies Maxwell's equations. Particle paths through the magnet are calculated by numerical integration and the corresponding first and second order particle transformation matrices are generated. A parameterization for the first order transformation matrix is developed and the resulting approximations for predicting particle motion in the magnet are compared to the results of the numerical integration. DOE

N86-10931# Brookhaven National Lab., Upton, N. Y.
METHOD FOR DETERMINING THE POSITION, ANGLE AND OTHER INJECTION PARAMETERS OF A SHORT PULSED BEAM IN THE BROOKHAVEN AGS

C. Gardner and L. Ahrens 1985 4 p Presented at the Particle Accelerator Conf., Vancouver, British Columbia, 13 May 1985
(Contract DE-AC02-76CH-00016)
(DE85-012523; BNL-36490; CONF-850504-135) Avail: NTIS HC A02/MF A01

As part of the effort to improve the monitoring of the injection process at the Brookhaven Alternating Gradient Synchrotron (AGS), a beam diagnostics package has been developed which processes the signals from the plates of a pick-up electrode (PUE) located near the injection region of the AGS and provides measurements of the position and angle (with respect to the equilibrium orbit) of the injected beam at the stripping foil where the incident H(-) beam is converted into protons. In addition the package provides measurements of the tune and chromaticity of the AGS at injection, and a measurement of the momentum spread of the injected beam. The diagnostics package is referred to as PIP which stands for Pulsed Injection Parameters. DOE

N86-10932# North Carolina Univ., Charlotte.
INITIAL INCREASE, PEAKING EFFECT, IN THE INTERNAL FRICTION OF COPPER FOLLOWING PULSED NEUTRON AND ELECTRON IRRADIATION
H. M. Simpson, D. M. Parkin, J. A. Goldstone, and J. W. Hemsky 1985 6 p Presented at the Conf. on Internal Friction and Ultrasonic Attenuation in Solids, Urbana, Ill., 3 Jun. 1985 Prepared in cooperation with LASL and Wright State Univ., Dayton, Ohio
(Contract W-7405-eng-36)
(DE85-012767; LA-UR-85-1829; CONF-8506125-2) Avail: NTIS HC A02/MF A01

Under certain experimental conditions the internal friction in metals can first increase and following prolonged irradiation decrease. Many models have been proposed to account for this peaking effect; however, in many of the cases, no effort is made to distinguish between the influence of interstitials and/or vacancies. To determine the nature of the point defect responsible for the peaking effect in high purity copper, a series of pulsed irradiations using neutrons and electrons were performed. In all of the experiments an initial very rapid rise in the internal friction and Young's modulus was observed. These data show that a fast diffusing defect is responsible for the peaking effect: i.e., the interstitial. DOE

N86-10933# Brookhaven National Lab., Upton, N. Y.
METHOD FOR COMPENSATING BELLOWS PRESSURE LOADS WHILE ACCOMMODATING THERMAL DEFORMATIONS
M. H. Woodle 1985 3 p Presented at the Particle Accelerator Conf., Vancouver, British Columbia, 13 May 1985
(Contract DE-AC02-76CH-00016)
(DE85-013306; BNL-36572; CONF-850504-144) Avail: NTIS HC A02/MF A01

Many metal bellows are used on storage ring vacuum chambers. They allow the ring to accommodate deformations with alignment, mechanical assembly and thermal expansion. The national synchrotron light source (NSLS) has two such electron storage rings, the VUV ring and the X-ray ring. Both rings utilize a number of welded metal bellows within the ring and at every beam port. There are provisions for 16 beam ports on the VUV and 28 ports in the X-ray ring. At each of these locations the bellows are acted on by an external pressure of 1 atmosphere, which causes a 520 lb reaction at the vacuum chamber beam port and at the beamline flange downstream of the bellows. The use of rigid tie rods across the bellows flanges to support this load is troublesome because most storage ring vacuum chambers are baked in situ to achieve high internal vacuum. Significant forces can develop on components if thermal deformation is restrained and damage could occur. DOE

N86-10934# Argonne National Lab., Ill.
USE OF THE MURA TRANSFORMATION TO GENERATE THE FIELDS AND CALCULATE THE MOTION OF PROTONS IN THE DESIGNED ARGONNE MINI-ASPUN FFAG SPIRAL SECTOR ACCELERATOR
E. A. Crosbie 13 May 1985 3 p refs Presented at the Particle Accelerator Conf., Vancouver, British Columbia, 13 May 1985
(Contract W-31-109-eng-38)
(DE85-011477; ANL-HEP-CP-85-34) Avail: NTIS HC A02/MF A01

As a long range goal for the production of high intensity neutrons, Argonne National Laboratory has proposed the construction of a 1.5 GeV FFAG Spiral Sector Accelerator called ASPUN. The 500-MeV injector for this proposed accelerator is a smaller FFAG Spiral Sector Accelerator named Mini-ASPUN. Until such a time as the larger machine could be built, it was planned that Mini-ASPUN would replace the present RCS now being used for the IPNS program at Argonne. In order to obtain an accurate estimation of the orbits and betatron oscillations in such a machine, it is necessary that realistic field values be used in the equations of motion. Obtaining these fields from 3-dimensional relaxation calculations is both time consuming and costly. However, because of the required scaling of the machine, the field-generating potential of three variables can be separated into a known function of the radius and a function of two variables. The second order differential equation satisfied by this function can be solved by ordinary relaxation methods. The fields generated from a mesh of values for this function will be accurate except for the extreme inside and outside orbits, which will be affected by the necessary termination of the inside and outside ends of the magnet. DOE

N86-10935# Brookhaven National Lab., Upton, N. Y.
AGS POLARIZED H(-) SOURCE
A. Kponcu, J. G. Alessi, and T. Sluyters 1985 7 p Presented at the Particle Accelerator Conf., Vancouver, British Columbia, 13 May 1985
(Contract DE-AC02-76CH-00016)
(DE85-013296; BNL-36486; CONF-850504-142) Avail: NTIS HC A02/MF A01

The AGS polarized H(-) source is now operational. During a month-long experimental physics run in July 1984, pulses equivalent to 15 (MU)A x 300 (MU)s (approx. 3 x 10 the 10 protons) were injected into the RFQ preaccelerator. Beam polarization, measured at 200 MeV, was approx. 75%. After the run, a program to increase the H(-) yield of the source was begun and significant progress was made. The H(-) current is now frequently 20 to 30 (MU)A. DOE

N86-10936# Oak Ridge National Lab., Tenn.
EXPERIMENTAL X-RAY SCATTERING CROSS SECTIONS FOR H2 AND RARE ATOMIC GASES
G. E. Ice 1985 23 p Presented at the New Directions in X-ray Scattering Workshop, Asilomar, Calif., 3 Apr. 1985
(Contract DE-AC05-84OR-21400)
(DE85-011572; CONF-8504136-1) Avail: NTIS HC A02/MF A01

Slides are presented for a talk on X-ray scattering from rare gases as an unambiquous test of ab initio wave functions and theoretical X-ray scattering cross sections. DOE

N86-10937# Brookhaven National Lab., Upton, N. Y.
METHANE-BUBBLE FORMATION IN HYDROGEN-CHARGED Fe-30 ppM C
C. L. Snead, Jr., K. G. Lynn, and M. Suenaga 1985 4 p refs Presented at the 7th Intern. Conf. on Positron Annihilation, New Delhi, 6 Jan. 1985
(Contract DE-AC02-76CH-00016)
(DE85-012526; BNL-36414; CONF-850169-13) Avail: NTIS HC A02/MF A01

Positrons were used as a probe of the early-stage growth of methane bubbles in hydrogen-charged polycrystalline Fe. Ferrovac E (30 ppM C) was charged at 900 psi of H2 at 475(0)C for various times to generate the methane internally. It is known that this process generates methane bubbles. Results show that, even at very early bubble-growth stages, dislocations are generated. A lifetime definitely associated with trapping at bubbles is not observed, due either to trapping by dislocations that are generated and which can screen the bubbles, or by passivation of the bubbles as positron traps by the presence of hydrogen or methane in them. DOE

N86-10938# Pacific Northwest Lab., Richland, Wash.
SECONDARY STANDARDS LABORATORIES FOR IONIZING RADIATION CALIBRATIONS: THE NATIONAL LABORATORY INTERESTS
P. I. Roberson and G. W. Campbell Nov. 1984 8 p ref Presented at the Workshop on Radiation Survey Instruments and Calibrations, Gaithersburg, Md., 10 Jul. 1985 Prepared in cooperation with Rockwell International Corp.
(Contract DE-AC06-76RL-01830)
(DE85-007046; PNL-SA-12423; CONF-850726-1) Avail: NTIS HC A02/MF A01

The national laboratories are probable candidates to serve as secondary standards laboratories for the federal sector. Representatives of the major Department of Energy laboratories were polled concerning attitudes toward a secondary laboratory structure. Generally, the need for secondary laboratories was recognized and the development of such a program was encouraged. The secondary laboratories should be reviewed and inspected by the National Bureau of Standards. They should offer all of the essential, and preferably additional, calibration services in the field of radiological health protection. The selection of secondary laboratories should be based on economic and geographic criteria and/or be voluntary. DOE

N86-10939# Atlanta Univ., Ga.
THEORETICAL INVESTIGATION OF ELECTRON-POSITIVE ION-ATOM INTERACTIONS Progress Report, 1 Jul. 1984 - 20 Mar. 1985
A. Z. Msezane 1985 6 p
(Contract DE-FG05-84FR-13266)
(DE85-013019; DOE/ER-13266/T1) Avail: NTIS HC A02/MF A01

Research involved investigations of e-positive ion/atom collisions and photoionization of excited atomic states. The latter is useful in determining appropriate wave functions for use in weakly bound systems which characterize excited states. Accurate differential cross sections for ZnII, MgII and Cu, integral cross sections for MgII, CdII, and Cu, and innershell excitation cross sections for Ti(3+) by electron impact were obtained. The close-coupling approximation was used with accurate configuration interaction wave functions. Also, photoionization cross sections for excited Na 3p, Na 4d and Ag 5d subshells are obtained in Hartree-Fock approximation using accurate wave functions. The purpose was to provide benchmark results to guide measurements. Differential cross section measurements for ions are very difficult owing to low target ion densities. Multi-minima in photoionization of excited states were not observed experimentally because of the lack of reliable predictions. DOE

N86-10940# Sandia Labs., Albuquerque, N. Mex.
PHOTONIC DIAGNOSTICS AND PULSED POWER RESEARCH
J. Chang, G. Allen, W. F. Filter, G. J. Lockwood, and B. T. Neyer 10 Jun. 1985 9 p Presented at the 5th IEEE Pulsed Power Conf., Washington, D.C., 10 Jun. 1985
(Contract DE-AC04-76DP-00789)
(DE85-013752; SAND-84-2500C; CONF-850616-44) Avail: NTIS HC A02/MF A01

Photonic methods offer a powerful approach to pulsed power diagnostics. The use of photon analog signals rather than the conventional electrical analog signals to make pulsed power measurements is a fundamental change that promises to evolutionize pulsed power research. This new approach uses inherently broadband optical components, and a picosecond streak camera to perform high speed measurements. We have developed sensors that use photonics principles to monitor voltages and currents, methods of using optical fibers to transmit the photon analog signals, and a High Speed Multi-Channel Data Recorder to economically record them. This system not only offers economy, compactness, high bandwidth, and EMI resistance, but it also accesses high field regions previously impossible to reach with metallic electrical monitors. The Photonic system will greatly reduce the complexity of pulsed power diagnostics. DOE

N86-10941# Argonne National Lab., Ill.
THE 20 keV UNDULATORS FOR A 6-GeV STORAGE RING
S. H. Kim and Y. Cho 1985 4 p refs Presented at the Particle Accelerator Conf., Vancouver, British Columbia, 13 May 1985
(Contract W-31-109-eng-38)
(DE85-013867; CONF-850504-177) Avail: NTIS HC A02/MF A01

The main goal of the future 6-GeV electron storage ring is to provide 20-keV fundamental harmonic radiations from insertion devices. Parameter restrictions of REC-Vanadium permendur hybrid undulators were examined. The critical factor is the achievable minimum gap of the undulator. Variations of the spectral brilliance for different beam parameters are also shown. DOE

N86-10942# Argonne National Lab., Ill.
NEW PARTICLE SEARCHES
M. Derrick 1985 39 p Presented at the PEP High Luminosity Workshop, Stanford, Calif., 5 Apr. 1985
(Contract W-31-109-eng-38)
(DE85-014073; ANL-HEP-CP-85-44; CONF-8504155-2) Avail: NTIS HC A03/MF A01

The Standard Model is a remarkable result of decades of work in particle physics, but it is clearly an incomplete representation of the world. Exploring possibilities beyond the Standard Model is a major preoccupation of both theorists and experimentalists. Despite the many suggestions that are extant about the missing links within the Standard Model as well as extensions beyond it, no hard experimental evidence exists. In particular, in more than five years of experimentation both at PETRA and PEP no new particles have been found that would indicate new physics. Several reasons are possible for these negative results: the particles may be too heavy; the experiments may not be looking in the proper way; the cross sections may be too small or finally the particles may not exist. A continuing PEP program, at high luminosity will ensure that the second and third reason continue to be addressed. The higher energy e(+)e(-) storage rings such as TRISTAN and LEP will extend the mass limits. High mass particles can also be produced at the CERN collider and soon with the Tevatron collider. A concise summary of the mass limits from the PETRA experiments was given in a recent Mark J publication. The results shown provide a convenient yardstick against which to measure future search experiments. DOE

N86-10943# Los Alamos Scientific Lab., N. Mex.
ANGULAR DISTRIBUTION OF NEUTRAL HYDROGEN FOLLOWING COLLISIONAL ELECTRON DETACHMENT FROM H(-)
J. D. Moses, D. Holtkamp, J. D. King, P. W. Lisowski, and J. E. Simmons Mar. 1985 16 p
(Contract W-7405-eng-36)
(DE85-014258; LA-10326-ML) Avail: NTIS HC A02/MF A01

The angular distribution of neutral hydrogen following electron detachment from H(-) was measured for H(-) on nitrogen and hydrogen gas, both for neutral atoms left in the 2S state, and for all neutrals independent of the state of excitation. The results are essentially in agreement with calculations based on the Born approximation, although there is some disagreement in detail. DOE

N86-10944# Los Alamos Scientific Lab., N. Mex.
PRELIMINARY INVESTIGATION OF CHANGES IN X-RAY MULTILAYER OPTICS SUBJECTED TO HIGH RADIATION FLUX
M. P. Hockaday, R. L. Blake, J. S. Grosso, M. M. Selph, M. M. Klein, W. Matuska, Jr., M. A. Palmer, and R. J. Liefeld 1985 9 p refs Presented at the SPIE Intern. Tech. Symp. on Optical and Electro-Optical Eng., San Diego, Calif., 18 Aug. 1985 Prepared in cooperation with Sandia National Labs., Albuquerque, N. Mex. and New Mexico State Univ., Las Cruces
(Contract W-7405-eng-36)
(DE85-014074; LA-UR-85-2265; CONF-850887-4) Avail: NTIS HC A02/MF A01

A variety of metal multilayers was exposed to high X-ray flux using Sandia National Laboratories' PROTO II machine in the gas

puff mode. Fluxes incident on the multilayers above 700 MW/sq.cm. in total radiation, in nominal 20 ns pulses, were realized. The neon hydrogen- and helium-like resonance lines were used to probe the X-ray reflectivity properties of the mulitlayers as they underwent change of state during the heating pulse. A fluorescer-fiber optic-streak camera system was used to monitor the changes in X-ray reflectivity as a function of time and irradiance. Preliminary results are presented for a W/C multilayer. DOE

N86-10945# Texas Univ., Austin.
NATURE OF PHOTOEMISSION INTO DIELECTRIC FLUIDS Progress Report
Dec. 1984 29 p
(Contract DE-FG05-84ER-45064)
(DE85-013017; DOE/ER-40561/1) Avail: NTIS HC A03/MF A01

The photoyield was measured in pure ammonia using a pulsed technique. It has been measured as a function of bias, temperature, and photon energy, in order to study the density of electron states in NH3 and the photo-injection process into the ammonia. The photoyield versus reference potential shows a much greater range of response than previous CW techniques. A strong temperature dependence was observed in the yield and a two slope behavior in the yield, observations which are consistent with our idea that there is a significant tail of localized states just below the conduction band in polar fluids. A systematic variation was found in the decay mode of the injected current as a function of reference potential, temperature, and impurity concentration giving us a new tool with which to examine the photo-injection process. DOE

N86-10946# Fermi National Accelerator Lab., Batavia, Ill.
HYPERON POLARIZATION: AN UNRESOLVED PROBLEM
J. Lach 10 Mar. 1985 7 p Presented at the 20th Recontre de Moriond, Les Arcs, France, 10 Mar. 1985
(Contract DE-AC02-76CH-03000)
(DE85-012298; FNAL/C-85/65; CONF-850375-1) Avail: NTIS HC A02/MF A01

Hyperons produced in high energy collisions have polarizations as large as 20%. These polarizations allowed high precision measurements of most hyperon magnetic moments and a confirmation of the Cabibbo theory involving semileptonic hyperon decays. However, a satisfactory quantitative explanation of hyperon polarization is still lacking. The question of whether the omega(-) is produced with significant polarization is crucial to the measurement of its magnetic moment. Present data are inconclusive as to whether the omega(-) is produced polarized. Phenomenological models and data on antihyperon production may not be useful guides in predicting the omega(-) polarization. DOE

N86-10947# Brookhaven National Lab., Upton, N. Y.
BEAM PROFILE MONITOR FOR THE NSLS VUV RING EMPLOYING LINEAR PHOTODIODE ARRAYS
R. J. Nawrocky, J. Galayda, L. H. Yu, and D. M. Shu 1985 4 p Presented at the Particle Accelerator Conf., Vancouver, British Columbia, 13 May 1985
(Contract DE-AC02-76CH-00016)
(DE85-012184; BNL-36497; CONF-850504-172) Avail: NTIS HC A02/MF A01

Among the most important parameters of a storage accelerator are the position and size of the particle beam. In an electron machine, these parameters can be derived from measurements of the emitted synchroton radiation. A system which monitors the two-dimensional profile of the synchrotron light in the NSLS VUV ring commercially available high-resolution linear photosensitive diode arrays is discussed. The optical system was designed to match the size of the image space to the dimensions of the diode sensor area. The scanning rate is automatically adjusted to hold the peaks of the profiles constant over a wide range of beam intensity variations. Video signals from the diode sensors can be readily interfaced to a computer for beam diagnostic purposes. Optics and factors determining the overall resolution of the system are discussed. Preliminary results of beam observations are presented. DOE

N86-10948# Brookhaven National Lab., Upton, N. Y.
SURFACE CONDITIONING OF SYNCHROTRON RADIATION SOURCE TO IMPROVE BEAM LIFETIME
T. S. Chou 1985 3 p Presented at the Particle Accelerator Conf., Vancouver, British Columbia, 13 May 1985
(Contract DE-AC02-76CH-00016)
(DE84-012185; BNL-36546; CONF-850504-170) Avail: NTIS HC A02/MF A01

Surface cleanliness is of prime importance to achieve the desirable vacuum condition for long beam lifetime in all synchrotron radiation sources. The Photon Factory at KEK resolved the severe gas load from synchrotron radiation by in-situ Ar glow discharging the whole storage ring. Sufficient experience was gained in the past two years operation on the synchrotron radiation source, especially on the VUV ring of the National Synchrotron Light Source (NSLS), to allow a decision to glow discharge the VUV ring. In hoping to obtain higher circulating current and to reveal the cause of lifetime limitation, a better understanding of the beam loss mechanism is needed. Photo desorption is the major gas load in all existing electron (position) storage rings. It is generally believed that these photodesorbed species (neutral and charged) provide the major loss mechanism to lessen the beam lifetime. The interaction of these species to the beam give rise to the various loss mechanisms, such as multiple Coulomb scattering, single scattering, bremsstrahlung and ion trapping. All these mechanisms were under intense study at NSLS. The result of surface condition and beam lifetime are described. DOE

N86-10949# Oak Ridge National Lab., Tenn.
EXPERIMENTAL STUDIES OF TRANSITION RADIATION AND OPTICAL BREMSSTRAHLUNG
E. T. Arakawa 1985 19 p refs Presented at the Penetration Phenomena Workshop, Oak Ridge, Tenn., 14 Apr. 1985
(Contract DE-AC05-84OR-21400)
(DE85-0135637; CONF-850484-1) Avail: NTIS HC A02/MF A01

Research on the optical emission from thin films and bulk metals bombarded by 25 to 120 keV electrons carried out at Oak Ridge National Laboratory is presented. Measurements were carried out on the dependence of the emitted spectra on angle of observation, polarization, sample thickness, surface roughness, surface contamination, and incident electron energy. DOE

N86-10950# Los Alamos National Lab., N. Mex.
WIDE DYNAMIC RANGE BEAM PROFILE MONITOR
D. M. Lee, D. Brown, R. A. Hardekopf, J. R. Bilskie, and O. B. V. vanDyck 1985 4 p Presented at the Particle Accelerator Conf., Vancouver, British Columbia, 13 May 1985
(Contract W-7405-eng-36)
(DE85-012709; LA-UR-85-1651; CONF-850504-134) Avail: NTIS HC A02/MF A01

An economical harp multiplexer system was developed to achieve a wide dynamic range. The harp system incorporates a pneumatically actuated harp detector with ceramic boards and carbon wires; a high-sensitivity multiplexer packaged in a double-wide NIM module; and flat, shielded ribbon cable consisting of individual twisted pairs. The system multiplexes 30 wires in each of the x and y planes simultaneously and operates with or without computer control. The system has operated in beams of 100 nA to 1 mA, 1- to 120-Hz repetition rate, with a signal-to-noise ratio of greater than 10/1. DOE

73 NUCLEAR AND HIGH-ENERGY PHYSICS

Includes elementary and nuclear particles; and reactor theory.

For space radiation see *93 Space Radiation.*

N86-10951# Army Military Personnel Center, Alexandria, Va.
THE DEVELOPMENT OF A NEUTRON EVAPORATION THEORY CODE FOR THE THERMAL FISSION OF URANIUM-235 Final

Report. M.S. Thesis
T. J. Rosener 3 May 1985 116 p
(AD-A156593) Avail: NTIS HC A06/MF A01 CSCL 20/8

The thermal fission of Uranium-235 has been studied by developing a computer code that used evaporation theory based on the Weisskopf model for neutron emission from individual fission fragments. This computer code calculates a prompt neutron spectrum for the thermal fission of Uranium-235, calculates the total gamma ray energy for the fission of Uranium-235, and calculates the average prompt neutron kinetic energy. Until now, evaporation theory codes used average values of mass and energy in determining prompt neutron spectra, and this code was developed to use all possible fission fragment combinations in order to eliminate this averaging. This approach is necessary to compute certain measured data such as the probability that 0,1,2,... neutrons are emitted per fission. This code uses subroutines to calculate rest masses, to correct the calculated rest mass to agree with experiment, and to determine the emitted neutron kinetic energies. Evaporation theory codes have predicted low total gamma energy release in fission, but agree quite favorably with experiments in predicting the average prompt neutron kinetic energy. The prompt neutron spectrum obtained in this code has a high tail region, that is, below 0.5 MeV. The average kinetic energy of the neutrons agree very well with experiment, and the total gamma energy is lower than experiment, as previous evaporation theory codes have been. GRA

N86-10952# Argonne National Lab., Ill.
SCOPING STUDIES OF VAPOR BEHAVIOR DURING A SEVERE ACCIDENT IN A METAL-FUELING REACTOR
B. W. Spencer and J. F. Marchaterre 15 Apr. 1985 17 p refs Presented at ANS/ENS Fast Reactor Safety Meeting, Knoxville, Tenn., 21 Apr. 1985
(Contract W-31-109-eng-38)
(DE85-011474; CONF-850410-47) Avail: NTIS HC A02/MF A01

The consequences of fuel melting and pin failures for a reactivity-insertion type accident in a sodium-cooled, pool-type reactor fueled with a metal alloy fuel were examined. The principal gas and vapor species released are shown to be Xe, Cs, and bond sodium contained within the fuel porosity. Condensation of sodium vapor as it expands into the upper sodium pool in a jet mixing regime may occur as rapidly as the vapor emerges from the disrupted core. If the predictions of rapid direct-contact condensation can be verified experimentally for the sodium system, the ability of vapor expansion to perform appreciable work on the system and the ability of an expanding vapor bubble to transport fuel and fission produce species to the cover gas region where they may be released to the containment are largely eliminated. The radionuclide species except for fission gas are largely retained within the core and sodium pool. DOE

N86-10953# Department of Energy, Argonne, Ill.
EVALUATION OF THE INTERNATIONAL ATOMIC ENERGY AGENCY (IAEA) SAFEGUARDS ANALYTICAL LABORATORY QUALITY ASSURANCE PROGRAM
C. E. Pietri and J. T. Bracey Feb. 1985 58 p refs Prepared in cooperation with Martin Marietta Energy Systems, Paducah, Ky.
(Contract DE-AC05-84OU-21400)
(DE85-012078; NBL-312; ISPO-232) Avail: NTIS HC A04/MF A01

Destructive analysis is used to verify the inventory of nuclear materials at nuclear facilities. The reliability and quality of these measurements must be assured in a systematic manner. The development and implementation for the quality assurance measures for the analytical procedures used in the destructive analysis of these safeguards samples are discussed. The procedures used for the destructive analysis of safeguards samples and the statistical evaluation of the resulting measurement data are evaluated. The procedures include analytical methods, quality control measures, and the treatment of data from these activities. Modifications to the system, which would provide routine assurance to management that these procedures are functioning properly to achieve safeguards objectives are recommended. The sample handling procedures, measurement control activities, analytical methods, reference materials, calibration procedures, statistical analysis of data, and data management system are evaluated. The degree to which laboratory quality assurance is achieved is assessed by comparing it to accepted standards of quality assurance. DOE

N86-10954# Idaho National Engineering Lab., Idaho Falls.
ON-LINE GAMMA-RAY DATA ACQUISITION AT THE POWER BURST FACILITY
J. K. Hartwell and E. W. Killian 1985 16 p refs Presented at the 6th Symp. on X- and Gamma-Ray Sources and Appl., Ann Arbor, Mich., 21 May 1985
(Contract DE-AC07-76ID-01570)
(DE85-011957; EGG-M-08985; CONF-850533-5) Avail: NTIS HC A02/MF A01

The PBF (Power Burst Facility) Fission Product Detection System (FPDS) incorporates four on-line gamma ray spectrometers controlled by operators one kilometer distant. The FPDS is uniquely designed to monitor the high fission product concentrations generated when reactor fuel rods are severely damaged. Through the use of variable collimators, fast analog electronics, a pulser subsystem, and a carefully designed shield, this system has monitored samples with dose rate readings greater than 900 R/h. The spectral data acquired by the FPDS have provided fission product release and transport behavior information not previously available from off-line or gross radiation monitoring methods. DOE

N86-10955# Los Alamos Scientific Lab., N. Mex.
POLARIZATION TRANSFER IN INELASTIC SCATTERING AND PIONIC MODELS OF THE EMC EFFECT
J. M. Moss 1985 13 p refs Presented at the Conf. on Antinucleon and Nucleon-Nucleus Interactions, Tessuride, Colo., 18 Mar. 1985
(Contract W-7503-eng-36)
(DE85-010738; LA-UR-85-1450; CONF-850315-2) Avail: NTIS HC A02/MF A01

A measurement of the sigma vector . q vector or spin-longitudinal nuclear response function was discussed. A LAMPF experiment was proposed. The European Muon Collaboration (EMC) effect, and the possibility that this ultrahigh-energy physics result may be related to nuclear pions and, the isovector sigma vector . q vector nuclear response function was investigated. The EMC effect and its interpretation in terms of excess nuclear pions is discussed. This model establishes a connection between the vastly different scales of the EMC experiment and the Los Alamos experiment. The Los Alamos experiment and its interpretation in terms of excess nuclear pions is described. Quark effects in nuclei based on the EMC and Los Alamos experimental results are analyzed. DOE

N86-10956# California Univ., Livermore. Lawrence Livermore Lab.
MEAN LIFE OF THE 2p(4)((1)S)3s (2)S STATE IN FLUORINE
K. T. Cheng and M. H. Chen 17 May 1985 5 p refs Presented at the Workshop on Autoionization of Atoms and Small Molecules, Argonne, Ill., 2 May 1985
(Contract W-7405-eng-48)
(DE85-012929; UCRL-92713; CONF-850560-5) Avail: NTIS HC A02/MF A01

The radiationless as well as the radiative decay rates for the 2p(4)((1)S)3s (2)S state are calculated. For comparison purposes similar calculations for the 2p(4)((1)D)4s (2)D state were also made. Calculations are based on the multi-configuration Dirac-Fock (MCDF) method. As spin-orbit interaction is built in, this method is capable of studying LS forbidden Auger transitions. Details of the Auger transition calculations have been given before. DOE

N86-10957# Georgia Inst. of Tech., Atlanta. School of Mechanical Engineering.
DEVELOPMENT AND APPLICATION OF THE ELECTROCHEMICAL ETCHING TECHNIQUE
M. E. Sanders Jul. 1984 119 p
(Contract DE-AS05-76FV-04814)

(DE85-010302; DOE/EV-04814/T<) Avail: NTIS HC A06/MF A01

The advances achieved in the development and application of several etched damage track plastic dosimeters that can be used to measure dose-equivalent from neutrons with energies from thermal to 20 MeV are discussed. The project was initiated with the design of a rem-responding dosimeter that measured fast (> 1 Mev) neutron dose-equivalent as a function of the damage track density directly induced within the volume of polycarbonate foils amplified by electrochemical etching. The thermal neutron dosimeter was composed of an external radiator tablet made of (7)LiF in contact with a polycarbonate foil and utilized the thermal neutron-induced (6) Li(n, (Alpha)) (3)H reaction to give a dose-equivalent response as a function of alpha track density registered in the detector foil. An intermediate (1 eV-1 MeV) neutron dosimeter was developed and was shown to give an approximately dose-equivalent response to neutrons with energies from 1 eV to 17 MeV. The intermediate neutron dosimeter consists of (6)LiF-Teflon/CR-3-9 Polymer foil assembly which is enclosed by a (Cd + In) neutron filter. The neutron dose-equivalent is measured as a variable function of these damage track density registered in the CR-39 detector foil to alpha particles from the 1/v dependent (6)Li(n, (ALPHA))(3)H reaction, recoil H, C, O nuclei from neutron-induced elastic scattering within the foil volume, and protons from the (6)Li(n, p) reaction for neutron energies above 2 MeV. DOE

N86-10958# Oak Ridge National Lab., Tenn.

ORR CORE RE-CONFIGURATION MEASUREMENTS TO INCREASE THE FAST NEUTRON FLUX IN THE MAGNETIC FUSION ENERGY (MFE) EXPERIMENTS

R. W. Hobbs, R. M. Stinnett, and T. M. Sims Jun. 1985 73 p
(Contract DE-AC05-84CR-21400)
(DE85-013520; ORNL/TM-9615) Avail: NTIS HC A04/MF A01

The relative increases obtainable in the fast neutron flux in the Magnetic Fusion Energy (MFE) experiment positions were studied by reconfiguring the current ORR core. The percentage increase possible in the current displacement per atom (dpa) rate was examined. The principle methods to increase the fast flux, consisted of reducing the current core size (number of fuel elements), to increase the core average power density and arrangement of the fuel elements in the reduced-size core to tilt the core power distribution towards the MFE positions were investigated. It is concluded that fast fluxes in the E-3 core position can be increased by approximately 15 to 20% over current values and in E-5 by approximately 45 to 55%. DOE

N86-10959# California Univ., Livermore. Lawrence Livermore Lab.

IMPACT OF LONG-LIVED RADIONUCLIDES ON WASTE CLASSIFICATION FOR FUSION

R. C. Maninger 10 May 1985 13 p Presented at the Ann. Meeting of the Am. Nucl. Soc., Boston, 9 Jun. 1985
(Contract W-7405-eng-48)
(DE85-013205; UCRL-91885; CONF-850610-30) Avail: NTIS HC A02/MF A01

A major goal for commercial applications of fusion reactors is to minimize radioactive wastes and to dispose of them by near surface burial. There currently are no regulations specifically applicable to fusion wastes but those in force for fission wastes furnish a framework for expected fusion regulations. It is recommended that all nuclides with half lives greater than five years be assigned concentration limits as done in 10CFR61 for fission wastes. Approximate limits for all the significant long half life sources of gamma radiation in the currently known periodic table are given. In the absence of working fusion reactors, computer models must be used to estimate the expected actual concentrations of radioactive nuclides. These estimates are needed to guide design parameters to achieve minimum radioactivity in fusion reactors. It is believed that the computer models and nuclear libraries must be much more comprehensive than ordinarily used today to do activation calculations. DOE

N86-10960# Oak Ridge National Lab., Tenn.

EVOLUTION OF THE FUSION POWER DEMONSTRATION TANDEM MIRROR REACTOR CONFIGURATION

J. A. OToole and D. C. Lousteau 1985 6 p Presented at the 6th Top. Meeting on the Technol. of Fusion Energy, San Francisco, 3 Mar. 1985
(Contract DE-AC05-84OR-21400)
(DE85-012889; CONF-850310-109) Avail: NTIS HC A02/MF A01

A presentation of the evolution of configurations proposed for tandem mirror Fusion Power Demonstration (FPD) machines is presented. The FPD study was undertaken to scope the mission as well as the technical and design requirements of the next tandem mirror device. Three configurations, entitled FPD I, II, and III were studied. During this process new systems were conceived and integrated into the design, resulting in a significantly changed overall machine configuration. The machine can be divided into two areas. A new center cell configuration, minimizing magnetic field ripple and thus maximizing center cell fusion power, features a semicontinuous solenoid. A new end cell has evolved which maintains the required thermal barrier in a significantly reduced axial length. The reduced end cell effective length leads to a shorter central cell length being required to obtain minimum ignition conditions. Introduced is the concept of an electron mantle stabilized octopole arrangement. The engineering features of the new end cell and maintenance concepts developed are influenced to a great extent by the octopole-based design. The new ideas introduced during the FPD study have brought forth a new perspective of the size, design, and maintenance of tandem mirror reactors, making them more attractive as commercial power sources. DOE

N86-10961# Argonne National Lab., Ill.

INFORMATION ON CONTINUUM STATES FROM FEEDING TIMES AND TOTAL (GAMMA) SPECTRA MEASURED WITH BGO SUPPRESSED DETECTORS

T. L. Khoo, I. Ahmad, P. Chowdhury, D. Frekers, R. Holzmann, R. V. F. Janssens, D. C. Radford, N. Azqui, H. Emling, and M. W. Drigert [1985] 14 p Prepared in cooperation with Gesellschaft fuer Schwerionenforschung m.b.H., Notre Dame Univ., Lappeenrannan Teknillinen and Purdue Univ., Lafayette, Ind.
(Contract W-31-109-eng-38)
(DE85-013868; DOE/NBM-5013868) Avail: NTIS HC A02/MF A01

The shape of nuclei is influenced by the occupation of Nilsson-orbitals, which changes with nucleon number, spin and temperature. The shape variation with neutron (or proton) number and spin in the N = 90 transitional region is now well understood for the cold yrast line. In contrast, the structural evolution with increasing temperature above the yrast line remains an open problem. To probe this evolution, to establish the link between yrast and continuum states, and to identify the collective modes built on high-spin aligned particle states, we have measured: (1) the feeding times of yrast states in /sup 152, 154/Dy (N = 86,88), and (2) the total GAMMA spectrum in Ho-153 (N = 86) with Compton-suppressed Ge detectors. Author

N86-10962# California Univ., Berkeley. Lawrence Berkeley Lab.

REPORT ON THE ENGINEERING TEST OF THE LBL 30 SECOND NEUTRAL BEAM SOURCE FOR THE MFTF-B PROJECT

M. C. Vella, P. A. Pincosy, C. A. Hauck, and R. V. Pyle Aug. 1985 58 p
(Contract DE-AC03-76SF-00098)
(DE85-013317; LBL-17550) Avail: NTIS HC A04/MF A01

Positive ion based neutral beam development has centered on the long pulse, advanced positive ion source (APIS). The APIS focused on development of 30 second sources for MFTF-B. The engineering test was part of competitive testing of the LBL and ORNL long pulse sources carried out for the NFTF-E Project. The test consisted of 500 beam shots with 80kV, 30 second deuterium. The results of LBL testing, in which the LBL APIS demonstrated that it would meet the requirements for MFTF-B 30 second sources are summarized. The LBL design was found to be suitable

as the baseline for a common long pulse source design for MFTF-B, TFTR, and doublet upgrade. DOE

N86-10963# Los Alamos Scientific Lab., N. Mex.
DIRECT MASS MEASUREMENTS IN THE LIGHT NEUTRON-RICH REGION USING A COMBINED ENERGY AND TIME-OF-FLIGHT TECHNIQUE
C. Pillai, I. W. Swenson, D. J. Vieira, G. W. Butler, J. M. Woutes, S. H. Rokni, K. Vaziri, and I. P. Remsberg 1985 6 p Presented at the Intern. Conf. on Nucl. Data for Basic and Appl. Sci., Santa Fe, N. Mex., 13 May 1985 Prepared in cooperation with Oregon State Univ., Corvallis
(Contract W-7405-eng-36)
(DE85-012758; LA-UR-85-1923; CONF-850507-40) Avail: NTIS HC A02/MF A01

This experiment has demonstrated that direct mass measurements can be performed (albeit of low precision in this first attempt) using the M proportional to ET(2) method. This technique has the advantage that many particle-bound nuclei, produced in fragmentation reactions can be measured simultaneously, independent of their N or Z. The main disadvantage of this approach is that both energy and time-of-flight must be measured precisely on an absolute scale. Although some mass walk with N and Z was observed in this experiment, these uncertainties were largely removed by extrapolating the smooth dependence observed for known nuclei which lie closer to the valley of (BETA)-stability. Mass measurements for several neutron-rich light nuclei ranging from C-17 to NE-26 have been performed. In all cases these measurements agree with the latest mass compilation of Wapstra and Audi. The masses of N-20 N and F-24 have been determined for the first time. DOE

N86-10964# Stanford Linear Accelerator Center, Calif.
PARASITIC MODE LOSSES VERSUS SIGNAL SENSITIVITY IN BEAM POSITION MONITORS
J. C. Denard, K. L. Bane, J. Bijleveld, A. M. Hutton, J. I. Pellegrin, L. Rivkin, P. Wang, and J. N. Weaver Apr. 1985 4 p Presented at the Particle Accelerator Conf., Vancouver, British Columbia, 13 May 1985
(Contract DE-AC03-76SF-00515)
(DE85-014367; SU-SLAC-PUB-3654; CONF-850504-190) Avail: NTIS HC A02/MF A01

A beam position monitor (BPM) for a storage or damping ring may be subject to heating problems due to the parasitic mode (PM) losses, beam interception and synchrotron radiation interception. In addition, high PM losses can cause beam instabilities under some conditions. Recessing and/or masking the BPM may increase the PM losses in the process of solving the latter two problems. Three complementary methods for estimating the PM losses and for improving the design of a stripline directional coupler type of BPM: bench measurements, computer modeling (TBCI), and an equivalent circuit representation are presented. These methods lead to a decrease in PM losses without significant reduction in output signal for the north Stanford Linear Collider (SLC) damping ring BPMs. DOE

N86-10965# Stanford Linear Accelerator Center, Calif.
BEAM-BEAM DEFLECTIONS TO MEASURE SIZE SPOT AND OFFSET AT SLC IP
P. Bambade 10 Jun. 1985 17 p
(Contract DE-AC03-76SF-00515)
(DE85-014285; SU-SLAC-CN-303) Avail: NTIS HC A02/MF A01

As soon as two SLC beams make it to the intersection region, both transverse offsets, spot sizes and shapes can be extracted from the pattern of angular deflections produced by the electromagnetic interaction of the two beams, as one is scanned across the other. These deflections, measured in two high resolution Beam Position Monitors (BPM) mounted symmetrically on both sides of the intersection point, will produce detectable signals allowing spot sizes to be tuned, even with the very low luminosities expected at turn on. They will also furnish a good signal to monitor beam centering and will therefore become an important part of the FFS feedback system. Summarized are the formulae which will allow us to correlate BPM offset readings with the properties of the two beams, and described are the range and limitations of the technique in the case of SLC. DOE

N86-10966# Rice Univ., Houston, Tex.
SUPERSONIC METAL CLUSTER BEAMS Technical Progress Report, 15 Mar. 1984 - 1 Apr. 1985
R. E. Smalley 1985 15 p
(Contract DE-AS05-78ER-06035)
(DE85-014321; DOE/ER-06035/7) Avail: NTIS HC A02/MF A01

Four major areas of bare metal cluster beams were studied: neutral cluster, chemical reactivity, cold cluster ion source development (both positive and negative), bare cluster ion ICR (ion cyclotron resonance) development, and photofragmentation studies of bare metal cluster ions. DOE

N86-10967# Nationaal Inst. voor Kernfysica en Hoge Energiefysica, Amsterdam (Netherlands). Sectie-K.
REPORT ON A VISIT TO CERN IN FEBRUARY 1985. NOTES ON BUNCH MONITORS, HIGH-FREQUENCY SYSTEMS, LINACS, KICKERS, MAGNETS, VACUUM AND BUNCH EXTRACTION [VERSLAG CERN BEZOEK FEBRUARI 1985. NOTITIES OVER BUNDELMONITOREN, HOOGFREQUENTSYSTEMEN, LINACS, KICKERS, MAGNETEN, VACUUM- EN BUNDELEXTRACTIE]
E. B. Kroes, G. Luijckx, R. Maas, and J. Noomen 1985 16 p ref In DUTCH
(LINO-119) Avail: NTIS HC A02/MF A01

The CERN Super Proton Synchrotor (SPS) vacuum installation, the development of magnets, and lamped element kickers with resonance built-in pulse generators are discussed. High resonance frequencies, computer programs, transmitters, cavities and construction aspects of linear accelerators are reported. The SPS monitors, Q-meter methods, and a stochastic extraction method are presented. Author (ESA)

N86-10968# Nationaal Inst. voor Kernfysica en Hoge Energiefysica, Amsterdam (Netherlands). Sectie-K.
THE MEA VACUUM SYSTEM [MEA VAKUUM SYSTEEM]
R. Stroo, H. Schwebeke, and E. Heine 31 Dec. 1984 18 p refs In DUTCH
(LINO-120) Avail: NTIS HC A02/MF A01

The leak security system and multiple pump unit with turbomolecular pump of the MEA vacuum system, consisting of a klystron system with diode pump and a bunch-conducting system with triode pump, is described. The triode pump has better pump capacities for rare gases but as it only works from 0.0001 Torr the pump unit has to be used. To replace the klystrons the two systems are coupled by two windows with nitrogen in between for high frequencies. To safeguard the system, slow isolation valves with Pirami gages, fast valves with ionization gages, and residual gas analyzers are installed. Hand valves and residual gas analyzer heads are used for the pump unit. The vacuum level is better than 0.0000001 Torr. Author (ESA)

N86-10969# Nationaal Inst. voor Kernfysica en Hoge Energiefysica, Amsterdam (Netherlands).
THE NETHERLANDS INSTITUTE FOR NUCLEAR AND HIGH ENERGY PHYSICS (NIKHEF) TRAVELING WAVE MONITOR USER GUIDE
I. Sluijk 27 Nov. 1984 15 p
(LINO-121) Avail: NTIS HC A02/MF A01

Instructions for operating a traveling wave monitor to measure beam displacement are given. Author (ESA)

74 OPTICS

Includes light phenomena.

N86-10970 Maryland Univ., College Park.
LIE ALGEBRAIC METHODS FOR CHARGED PARTICLE BEAMS AND LIGHT OPTICS Ph.D. Thesis
Joseph Cham Eugene Patrice Etienne Forest 1984 334 p

Avail: Univ. Microfilms Order No. DA8509163

The motion of a charged particle or the propagation of a ray in an optical system can be described in many cases by a Hamiltonian. One is often interested in deviation from a certain ideal trajectory. For this problem, the Lie algebraic methods are ideal tools. It has been shown that the Lie operators offer a very efficient parameterization of Hamiltonian maps. Along these lines, the parameterization of optical interaces is examined. It is shown that their Lie algebraic polynomials aere made of irreducible representations of the symplectic group. Our methods are also ideally suited for tracking particles in small and large rings. A complete theory of the computation of Lie algebraic maps is presented. Dissert. Abstr.

N86-10971 Arizona Univ., Tucson.
OPTICAL TESTING OF LARGE TELESCOPES USING MULTIPLE SUBAPERTURES Ph.D. Thesis
Tilman Werner Stuhlinger 1984 218 p
Avail: Univ. Microfilms Order No. DA8504134

The construction of telescope systems with large apertures (approx. 10 meters) is currently being planned. These entire telescope systems should be optically tested in a double-pass configuration. The high cost of manufacturing optical flats large enough to test a large telescope has stimulated research on a new type of testing in which several smaller flats, or subapertures, are distributed over the telescope aperture. The problem is to combine the partial data obtained only over the subapertures in order to obtain the wavefront over the entire aperture. The question of the necessity of phasing the subapertures relative to each other was specifically addressed in the experiment. Dissert. Abstr.

N86-10972 Department of the Air Force, Washington, D.C.
KALMAN FILTER PREPROCESSOR Patent
M. K. Giles and R. B. Rogers, inventors (to Air Force) Issued 16 Apr. 1985 7 p Supersedes AD-D009695
(AD-D011774; US-Patent-4,511,219; US-Patent-Appl-SN-388574; US-Patent-Class-350-388) Avail: US Patent and Trademark Office CSCL 09/2

This document describes an optical signal preprocessor for computing the input functions required to utilize an extended Kalman filter algorithm. An incoming stream of time-varying images is integrated to form a reference image, which is then subtracted from each subsequently sampled image. The result is digitized for use with the extended Kalman filter algorithm. The reference image is also fed through a spatial filter and then put into two light valve image subtraction systems to produce difference image approximations of two partial derivatives. These derivative functions are then digitized and utilized as inputs to the extended Kalman filter algorithm. Author (GRA)

N86-10973 Department of the Air Force, Washington, D.C.
MEASUREMENT OF VISUAL CONTRAST SENSITIVITY Patent
H. E. VonGierke and A. R. Marko, inventors (to Air Force) Issued 16 Apr. 1985 10 p Supersedes AD-D010599
(AD-D011776; US-Patent-4,511,228; US-Patent-Appl-SN-403247; US-Patent-Class-351-243) Avail: US Patent and Trademark Office CSCL 06/16

This invention involves measurement of the visual contrast sensitivity (modulation transfer) function of a human subject by means of linear or circular spatial frequency pattern on a cathode ray tube whose contrast is automatically decreasing or increasing depending on the subject pressing or releasing a hand-switch button. The threshold of detection of the pattern modulation is found by the subject by adjusting the contrast to values which vary about the subject's threshold thereby determining the threshold and also providing by the magnitude of the contrast fluctuations between reversals some estimate of the variability of the subject's absolute threshold. The invention also involves the slow automatic sweeping of the spatial frequency of the pattern over the spatial frequencies after preset time intervals or after threshold has been defined at each frequency by a selected number of subject-determined threshold crossings; i.e., contrast reversals.
Author (GRA)

N86-10974 Department of the Air Force, Washington, D.C.
OPTICAL DISC TRANSPORT SYSTEM Patent
A. P. Gilson, inventor (to Air Force) Issued 21 May 1985 7 p Supersedes AD-D010276
(AD-D011779; US-Patent-4,519,055; US-Patent-Appl-SN-486477; US-Patent-Class-369-37) Avail: US Patent and Trademark Office CSCL 14/3

A carrousel disc transport system has a donut shaped cartridge storage module, a changer and a record/read station. The changer is centrally located in said donut shaped module and selectively removes or replaces selected cartridges. A carrier of the changer has a carriage that is translated along a ball screw to be positioned over the storage module. A pair of transporting arms connected to drive means engages the selected cartridge in the module. The driving means of the ball screw transfer the carriage with the arms to move the cartridge to a transfer location where a second transporting means moves the cartridge to the record/read station. The reverse is required to replace the selected cartridge in the module. GRA

N86-10975 Department of the Navy, Washington, D. C.
SPATIAL FREQUENCY MULTIPLEXED COHERENT OPTICAL PROCESSOR FOR CALCULATING GENERALIZED MOMENTS Patent
J. A. Blodgett, H. H. Szu, C. L. Giles, and R. Athale, inventors (to Navy) Issued 19 Mar. 1985 6 p Supersedes AD-D010312
(AD-D011816; US-Patent-4,505,544; US-Patent-Appl-SN-387133; US-Patent-Class-350-162.13) Avail: US Patent and Trademark Office CSCL 20/6

An optical processor that can compute the moments of a two-dimensional image in parallel is discussed. The image is placed at the plane of a holographic mask which is diposed in the front focal plane of a Fourier-transforming lens and each of the desired moments is found at a respective one of a plurality of photodetectors arrayed in the back focal plane of the lens. Author (GRA)

N86-10976 Department of the Navy, Washington, D. C.
FIBER OPTIC SYSTEM FOR MEASURING ELECTRIC FIELDS Patent
L. C. Bobb, inventor (to Navy) Issued 18 Jun. 1985 5 p Supersedes AD-D010483
(AD-D011830; US-Patent-4,524,322; US-Patent-Appl-SN-442497; US-Patent-Class-324-72) Avail: US Patent and Trademark Office CSCL 14/2

A fiber optic sensor system and associated technique is disclosed for measuring an electric field wherein a sensor arm of optical fiber cable is wound about a core member of piezoelectric material. A reference arm of optical fiber cable substantially equal in optical path length to the sensor arm is isolated and connected in parallel to the sensor arm so that coherent light generated by a single model laser source may be split through the fiber-optic arms and recombined after passage there through for phase comparison. When subjected to a local electric field, the core member of piezoelectric material varies in dimensions and thereby causes a change in the strain in the optical fiber cable of the sensor arm. Relative phase changes in the coherent light caused by the resulting optical path length change of the strained homodyne demodulator and deterministic of the value of the local electric field. A vane-type shield is adapted to be rotated about the core member for periodically reducing the local electric field to near zero thereby providing a reference level for field measurement. GRA

N86-10977# IBM Research Lab., San Jose, Calif.
OPTICAL DETECTION OF PHOTOACOUSTIC PULSES IN THIN SILICON WAFERS
H. Sontag and A. C. Tam 25 Jun. 1985 11 p
(Contract N00014-83-C-0170)
(AD-A156705; TR-20) Avail: NTIS HC A02/MF A01 CSCL 20/6

A probe beam deflection method is used to study the propagation of photoacoustic longitudinal waves and plate modes in silicon wafers. Nanosecond acoustic pulses are produced in thin silicon

wafers by absorption of weak nitrogen laser pulses causing no sample ablation. A HeNe probe laser is tightly focused on the same or on the opposite side of the wafer. Deflections of this probe beam are monitored by a photodiode located in the Gaussian wing of the reflected, diverging beam. The transient deflection signal can be observed on a Tektronix Mod. 7104 oscilloscope in a single shot mode at nanosecond time resolution. The absorption of the pump laser pulse causes a permanent surface distortion, which is the source of longitudinal and shear wave pulses propagating into the sample. In conclusion, the probe beam deflection technique is shown to be a fast and simple method for measuring acoustic pulse propagation in solids. It does not require elaborate servo mechanisms as the interferometric detection scheme while offering similar sensitivity. GRA

N86-10978# California Univ., Berkeley. Lawrence Berkeley Lab.
INTEGRATING SPHERE MEASUREMENTS OF DIRECTIONAL-HEMISPHERICAL TRANSMITTANCE OF WINDOW SYSTEMS
J. Kessel and S. Selkowitz 5 Aug. 1984 23 p refs Presented at Illuminating Eng. Soc. Ann. Conf., St. Louis, 5 Aug. 1984
(Contract DE-AC03-76SF-00098)
(DE85-013926; LBL-17284; CONF-840817-3; EEB-W-84-22) Avail: NTIS HC A02/MF A01

Equations are presented that express the directional-hemispherical transmittance of window systems in terms of the experimental parameters of an integrating sphere. The construction and operation of a 2-meter-diameter sphere is described. Experimental results are given for both conventional and novel window systems. DOE

N86-10979# Argonne National Lab., Ill.
BEAM STABILITY IN A 6 GeV SYNCHROTRON LIGHT SOURCE
J. Norem, M. Knott, and A. Rauchas 1985 4 p Presented at the Particle Accelerator Conf., Vancouver, British Columbia, 13 May 1985
(Contract W-31-109-eng-38)
(DE85-013850; CONF-850504-175) Avail: NTIS HC A02/MF A01

Future synchrotron radiation sources designed to produce low emittance electron beams for wigglers and undulators will present beam position control problems essentially similar to those encountered by users of existing accelerators, however tolerances will be tighter due to: (1) the small emittance (7 x 10 to the 9th mrad) proposed for the electron beam and the correspondingly small emittences (sizes) of secondary photon beams, (2) the sensitivity of the electron beam closed orbit to quadrupole motion and dipole roll, (3) the high power levels associated with undulator and wiggler beams which will permit (and probably require) high precision and stability of the photon beam position measurements, in addition, (4) the large number of users on the roughly sixty beam lines will demand beams capable of producing the best experimental results. The effects of motion of beam components (quads, RF cavities and dipoles) on the beam is described and the properties of a compensation system from the perspective of users is considered. The system departs from standard particle in considering active perturbation of the electron beam to verify beam corrections. The effects of local closed orbit perturbations to direct undulator beams at different experimental setups are also considered. DOE

N86-10980# Research Inst. of National Defence, Linkoeping (Sweden).
INFORMATION TECHNIQUE 1985: OPTICAL TECHNOLOGY AND ELECTRO-OPTICS, A DEFENSE TECHNICAL COMPONENT REVIEW
Lars Bohman, Olof Engstroem, Ingmar Renhorn, and Soeren Svensson May 1985 62 p refs In SWEDISH; ENGLISH summary
(FOA-A-30037-E; ISSN-0281-0212) Avail: NTIS HC A04/MF A01; Research Institute of National Defence, Stockholm KR 50

Microelectronic image sensors for visible radiation and for IR wavelengths; laser applications, e.g., high energy lasers, lasers with a weapon effect, investigation lasers, excimer lasers, Q-switched lasers, copper vapor lasers, diode lasers; adaptive optics; optical information retrieval; optical data storage, e.g., storage of large quantities of information; electro-optical crystals; and optical fibers, e.g., IR fiber techniques, fluoride fibers, and optical fiber sensors. Author (ESA)

N86-10981# Deutsche Forschungs- und Versuchsanstalt fuer Luft- und Raumfahrt, Oberpfaffenhofen (West Germany).
SCATTERING BY COMPLICATED STRUCTURES: CALCULATION OF THE RADAR PROPERTIES OF METALLIC TARGETS BY MEANS OF PHYSICAL OPTICS
Dieter Klement Mar. 1985 55 p refs In GERMAN; ENGLISH summary Report will also be announced as translation (ESA-TT-946)
(DFVLR-FB-85-22; ISSN-0171-1342) Avail: NTIS HC A04/MF A01; DFVLR, Cologne DM 19.50

Theory and computer program for the determination of the radar cross section of metallic targets are described. The geometry of complicated targets is represented by plane quadrangles. The calculation of the radar cross section is carried out by the method of physical optics. Computer results of simple targets are compared with rigorous solutions, approximations and measurements. The influence of surface shaping is demonstrated. Author (ESA)

75 PLASMA PHYSICS

Includes magnetohydrodynamics and plasma fusion.
For ionospheric plasmas see *46 Geophysics*. For space plasmas see *90 Astrophysics*.

N86-10982# State Univ. of New York at Buffalo, Amherst. Dept. of Physics.
TWO-DIMENSIONAL ELECTRONS Annual Report, 1 Jun. 1984 - 31 May 1985
A. Isihara 31 May 1985 3 p
(Contract N00014-84-K-0387)
(AD-A156894) Avail: NTIS HC A02/MF A01 CSCL 20/8

Papers Submitted: Two-Dimensional Electrons in Strong Magnetic Field, Low-temperature Properties of Two-Dimensional Electrons. Effects of Level Broadening on the Magnetothermal Oscillations in Two-Dimensional Electron Systems; Magnetothermal Oscillations in a Two-Dimensional Electron System; Elementary Excitations and Energy Dispersion in TTF-TCNQ, Magnetoconductivity of 2D Conductors; Memory Function for Cyclotron Resonance of Two-Dimensional Electron Systems; and Quantum Oscillations of 2D Electron Systems. GRA

N86-10983# Naval Research Lab., Washington, D. C.
DYNAMICS OF IMPLODING NEON GAS PUFF PLASMAS. 1 Memorandum Report, Oct. 1984 - Oct. 1985
R. W. Clark and J. Davis 19 Jul. 1985 40 p
(T99-QMXL)
(AD-A156916; NRL-MR-5613) Avail: NTIS HC A03/MF A01 CSCL 20/9

The implosion of a cylindrical neon puff-gas plasma on a low density central core is investigated using a 1D non-LTE radiation-hydrodynamic model. Radiation transports energy into the core plasma and produces heating deep within the puff-gas. The implosion very efficiently converts kinetic energy into soft X-rays; about two-thirds of the initial plasma energy is radiated away. Comparison is made with a neon puff-gas implosion without a central core and with pure hydrodynamic calculations. For each case, detailed self-consistent emission spectra and energy partitioning are discussed. Author (GRA)

N86-10984# California Univ., Livermore. Lawrence Livermore Lab.
THEORETICAL ASPECTS OF MAGNETIC HELICITY
J. H. Hammer 15 Apr. 1985 12 p refs Presented at IAEA Tech. Comm. Meeting on Advan. in Compact Toroid Res., Sydney, 4 Mar. 1985

(Contract W-7405-eng-48)
(DE85-011846; UCRL-92538; CONF-8503137-1) Avail: NTIS HC A02/MF A01

Magnetic helicity, a function of the vector potential and the magnetic field, measures the topological linkage of magnetic fluxes. It also manifests itself in the twistedness and knottedness of flux tubes. The significance of helicity in plasma physics is that it is an ideal MHD invariant -- the linkage of a flux tube with all other flux tubes is preserved when the tubes are filled with infinitely conducting plasma. Even when finite resistivity and magnetic reconnection are allowed, one finds that the global magnetic helicity (accounting for all linkages) is still approximately preserved on the reconnection time scale. Local topological changes (tearing, etc.) that destroy local helicity invariance are allowed as long as the global linkage is preserved. F.M.R.

N86-10985# Los Alamos Scientific Lab., N. Mex.
BEAM LINE WINDOWS AT LAMPF
R. D. Brown, D. L. Grisham, and J. E. Lambert 1985 4 p refs Presented at Particle Accelerator Conf., Vancouver, British Columbia, 13 May 1985
(Contract W-7405-eng-26)
(DE85-012723; LA-UR-85-1737; CONF-850504-113) Avail: NTIS HC A02/MF A01

The A-6 main beam-line window at LAMPF separates the vacuum of the main beam line from the isotope production station, proton irradiation ports, and the beam stop, which operate in air. This window must withstand the design beam current of 1 mA at 800 MeV for periods of at least 3000 hours without failure. The window is water cooled and must be strong enough to withstand the 2.1 MPa (300 psig) cooling water pressure, as well as beam-induced thermal stresses. Two designs have been used to meet these goals, a stepped-plate window and a hemispherical window, both made from a precipitation-hardened nickel base alloy, Alloy 718. Calculations of the temperatures and stresses in each of these windows are presented. DOE

N86-10986# Los Alamos Scientific Lab., N. Mex.
PROPOSED BUNCHING SCHEME FOR A POLARIZED H(-) INJECTOR
G. R. Swain and A. A. Browman 1985 4 p Presented at the Particle Accelerator Conf., Vancouver, British Columbia, 13 May 1985
(Contract W-7405-eng-36)
(DE85-012648; LA-UR-85-1640; CONF-850504-48) Avail: NTIS HC A02/MF A01

Improvements to the polarized H(-) injector at LAMPF which will include a two-stage buncher and beam chopper are discussed. The buncher scheme will permit the compression of a major part of the current in 20 RF cycles of the drift-tube linac (100 nsec) into a single RF cycle (5 nsec), making possible time-of-flight experiments with the polarized H(-) beam. A proposed first buncher stage would use a ramp drive waveform; the second stage, a sinusoidal waveform. Design and sensitivity calculations are summarized, including beam energy considerations, buncher and chopper drive requirements, and longitudinal and transverse beam dynamics. It is indicated that about 70% of the beam from the source may be bunched in the 1-nsec acceptance region of the linac, with less than 0.1% of the beam in neighboring RF cycles. DOE

N86-10987# Los Alamos Scientific Lab., N. Mex.
BEAM-CAVITY INTERACTION MEASUREMENTS IN A DAW STRUCTURE
Y. Iwashita, S. O. Schriber, J. M. Potter, D. A. Swenson, and G. S. Mavrogenes 1985 4 p refs Presented at the Particle Accelerator Conf., Vancouver, British Columbia, 13 May 1985
(Contract W-7405-eng-36)
(DE85-012660; LA-74-85-1617; CONF-850504-56) Avail: NTIS HC A02/MF A01

Mode excitations induced by relativistic electron beams have been measured in a disk and washer (DAW) structure. The structure had three washers, each with four radial support stems, and half disk end terminations. The design DAW operating frequency was 1300 MHz, the same as that used to accelerate the electron beam. Both short pulse (35-ps, 800-Hz, 17-nC/pulse) and long pulse (10-(MU)s, 2-A average) conditions were used in the beam excitation experiments. Mode spectra were measured and identified using low power techniques employed after the high power beam measurements. Mode frequency calculations for the complete three washer geometry were performed using URMEL for up to m = 7. Calculated results are compared with data determined from low power and beam driven excitation of the DAW structure. DOE

N86-10988# Los Alamos Scientific Lab., N. Mex.
INCREASED PARTICLE CONFINEMENT WITH THE USE OF EXTERNAL dc BIAS FIELD IN THE CTX SPHEROMAK
C. W. Barnes, H. W. Hoida, I. Henins, J. C. Fernandez, T. R. Jarboe, and G. J. Marklin 1985 6 p Presented at the 7th US Symp. on Compact Toroid Res., Santa Fe, N. Mex., 21 May 1985
(Contract W-7405-eng-36)
(DE85-012744; LA-UR-85-1789; CONF-8505100-5) Avail: NTIS HC A02/MF A01

Spheromaks are formed in a mesh flux conserver in the presence of an external dc bias field. The spheromaks remain stable to tilt instabilities with ratios of bias to spheromak flux of up to 47 + or - 7%. Normally applied bias flux puts the spheromak separatrix inside the metal mesh and improves the particle confinement. DOE

N86-10989# Brookhaven National Lab., Upton, N. Y.
SEPARATED K(-) BEAMS (10 GeV AND ABOVE)
G. M. Bunce 1985 4 p refs Presented at the Intern. Conf. on Hadron Spectroscopy, College Park, Md., 20 Apr. 1985
(Contract DE-AC02-76CH-00016)
(DE85-012527; BNL-36450; CONF-8504133-2) Avail: NTIS HC A02/MF A01

Separated kaon beams with intensity similar to present pion beams are, in fact, possible to build now, with the potential of even high kaon flux in the future. It is particularly attractive to work with a kaon minus beam due to the large number of final state combinations which would be available, due to the strange quark. Cason and Donoghue showed that a kaon beam combined with a complete spectrometer capable of observing both neutral and charged particles would increase the available states for spectroscopy for masses from 1 to 3 GeV by a factor of 10. They urged a complete mapping of states, using a sky survey as an analogy. The present capability is similar to scans of the sky made only in the optical range. They also point out that the specific subject of confinement - whether there can be combinations of quarks and gluons not yet seen - is an exciting topic which is beginning to get theoretical guidance from QCD calculations on a lattice. This confluence of technical advance (intensity) and physics interest (confinement) makes a separated kaon beam particularly compelling. DOE

N86-10990# Los Alamos Scientific Lab., N. Mex.
TREATMENT PLANNING WITH ION BEAMS
M. H. Foss 1985 4 p Presented at the Particle Accelerator Conf., Vancouver, British Columbia, 13 May 1985
(Contract W-7405-eng-36)
(DE85-012661; LA-UR-85-1616; CONF-850504-54) Avail: NTIS HC A02/MF A01

Ions have higher linear energy transfer (LET) near the end of their range and lower LET away from the end of their range. Mixing radiations of different LET complicates treatment planning because radiation kills cells in two statistically independent ways. In some cases, cells are killed by a single-particle, which causes a linear decrease in log survival at low dosage. When the linear decrease is subtracted from the log survival curve, the remaining curve has zero slope at zero dosage. This curve is the log survival curves for cells that are killed only by two or more particles. These two mechanisms are statistically independent. To calculate survival these two kinds of doses must be accumulated separately. The effect of each accumulated dosage must be read from its survival curve, and the logarithms of the two effects added to get

the log survival. Treatment plans for doses of protons, He(3) ions, and He(4) ions suggest that these ions will be useful therapeutic modalites. DOE

N86-10991# Argonne National Lab., Ill.
PERFORMANCE OF THE H(-) ION SOURCE FOR THE INTENSE PULSED NEUTRON SOURCE
V. Stipp and A. DeWitt 1985 3 p Presented at the Particle Accelerator Conf., Vancouver, British Columbia, 13 May 1985
(Contract W-31-109-eng-38)
(DE85-012368; CONF-850504-117) Avail: NTIS HC A02/MF A01

In January of 1983, a magnetron type H(-) ion source was installed in the intense Pulse Neutron Source (IPNS) at Argonne National Laboratory. The higher available H(-) current has helped enable the weekly average intensity of the Rapid Cycling Synchrotron (RCS) to be increased from 8 (MU)A to over 12 (MU)A. After two years of operation, the reliability of the source producing 40 mA of H(-) ions at a 30 Hz repetition rate continues to be excellent. DOE

N86-10992# Los Alamos Scientific Lab., N. Mex.
NONINTERCEPTIVE TECHNIQUES FOR THE MEASUREMENT OF LONGITUDINAL PARAMETERS FOR INTENSE H(-) BEAMS
W. B. Cottingame, G. P. Boicourt, J. H. Cortez, W. W. Higgins, O. R. Sander, and D. P. Sandoval 1985 4 p refs Presented at the Particle Accelerator Conf., Vancouver, British Columbia, 13 May 1985
(Contract W-7405-eng-36)
(DE85-012662; LA-UR-85-1615; CONF-850504-53) Avail: NTIS HC A02/MF A01

With increasing brightness, beam diagnostic techniques requiring interception of the beam become impractical. For H(-) particle beams, solutions for this problem based on the phenomenon of photodissociation are currently under investigation at the Los Alamos National Laboratory accelerator test stand (ATS). A laser can be used to selectively neutralize portions of the beam that can be characterized after the charged particles have been swept away. This technique has been used for the measurement of current density versus longitudinal phase and the longitudinal phase-space distribution at the output of the ATS radio frequency quadrupole (RFQ). The results of our measurement are compared with the predictions of the particle-dynamics code, PARMTEQ. DOE

N86-10993# Los Alamos Scientific Lab., N. Mex.
HIGH-POWER RF CONTROLS FOR THE NBS-LOS ALAMOS RACETRACK MICROTRON
I. M. Young and R. S. Biddle 1985 4 p refs Presented at the Particle Accelerator Conf., Vancouver, British Columbia, 13 May 1985
(Contract W-7405-eng-36)
(DE85-012658; LA-UR-85-1619; CONF-850504-61) Avail: NTIS HC A02/MF A01

The high power RF system for the National Bureau of Standards (NBS) Los Alamos racetrack microtron (RTM) uses waveguide power splitters and waveguide phase shifters to distribute RF power from a single 500-kW CW klystron to four side-coupled accelerating structures. The amplitude and phase of each structure is controlled by a feedback system that uses the waveguide variable power splitters, waveguide phase shifters, and klystron drive as the active control elements. A block diagram of this system is shown, as is a subset of the complete system on which the measurements reported in this paper were performed. The feedback controls on the capture section use low level RF amplitude and phase controls on the RF drive to the klystron. These controls are very fast with an open loop gain bandwidth of approximately 40 kHz. DOE

N86-10994# Stanford Linear Accelerator Center, Calif.
APPLICATIONS OF THE SECOND-ORDER ACHROMAT CONCEPT TO THE DESIGN OF PARTICLE ACCELERATORS
K. L. Brown and R. V. Servranckx May 1985 3 p Presented at the Particle Accelerator Conf., Vancouver, British Columbia, 13 May 1985 Prepared in cooperation with European Organization for Nuclear Research, Geneva, and Saskatchewan Univ.
(Contract DE-AC03-76SF-00515)
(DE85-013072; SU-SLAC-PUB-3675; CONF-850504-77) Avail: NTIS HC A02/MF A01

A property of the second-order achromat, whereby dipole and sextupole families may be inserted into a lattice for chromatic corrections without introducing second-order geometrical (on momentum) optical distortions, has been incorporated in several new particle accelerator designs. These include the SLC at SLAC, LEP at CERN, the EROS pulse stretcher ring at Saskatoon, the CEBAF ring at SURA, and the MIT ring. DOE

N86-10995# Stanford Linear Accelerator Center, Calif.
SUPERCONVERGENT TRACKING AND INVARIANT SURFACES IN PHASE SPACE
R. D. Ruth, T. Raubenheimer, and R. L. Warnock Apr. 1985 4 p Presented at the Particle Accelerator Conf., Vancouver, British Columbia, 13 May 1985 Prepared in cooperation with California Univ., Berkeley, Lawrence Berkeley Lab.
(Contracts DE-AC03-76SF-00515; DE-AC03-76SF-00098)
(DE85-013051; SU-SLAC-PUB-3660; CONF-850504-75) Avail: NTIS HC A02/MF A01

Long term beam stability in very large storage rings presents an extraordinary challenge in nonlinear dynamics. Current computational methods seem less than adequate on the long time scales involved, and several methods that either are new or have not yet tried in accelerator problems heretofore were evaluated. The methods we investigate fall into two categories: (1) iteration of maps describing concatenated machine elements, for tracking of single particles; and (2) infinite-time methods for direct computation of invariant surfaces in phase space. DOE

N86-10996# Los Alamos National Lab., N. Mex.
FERRITE KICKER MAGNET FOR THE IAMPF SWITCHYARD UPGRADE
R. A. Hardekopf, E. F. Higgins, and J. S. Lunsford 1985 4 p refs Presented at the Particle Accelerator Conf., Vancouver, British Columbia, 13 May 1985
(Contract W-7405-eng-36)
(DE85-012657; IA-UR-85-1620; CONF-850504-60) Avail: NTIS HC A02/MF A01

The IAMPF switchyard requires a kicker magnet as the first element in the transport line leading to the proton storage ring (PSR). The magnet must produce 1-ms-long pulses with 40-(MU)s rise time and $<$ 0.3% flat-top regulation to deflect the 800-MeV H(-) beam by 1.2(0). Two 1-m-long, single-turn ferrite magnets, each powered by a modulator supplying up to 2400 A at a maximum rate of 24 Hz were constructed. The modulators use a transistor amplifier/regulator, a dual pulse-forming-network (PFN), and a compensating circuit driven by a function generator to achieve a total 0.1% current variation in the pulse. The system also produces an alternate kicking mode consisting of 150-(MU)s-long pulses at a maximum rate of 120 Hz; the two modes can be multiplexed within the charging power-supply limitations. DOE

N86-10997# Fermi National Accelerator Lab., Batavia, Ill.
FIELD-INDEPENDENT NORMALIZATION OF SSC COLLIDER RING COSTS
T. E. Toohig 25 Mar. 1985 3 p
(Contract DE-AC02-76CH-03000)
(DE85-012425; FNAL-TM-1306) Avail: NTIS HC A02/MF A01

The SSC Collider Ring represents the dominating cost element of the SSC project. The number of variables involved in optimizing the facility is very large so it is helpful to try to parameterize them in a way that allows a straightforward comparison of primary options. Cost information was drawn from the Reference Designs Study. Various studies indicate that a 9' to 10' tunnel seems optimal from a construction and operation viewpoint and is adequate for installation. According to both studies cited a tunnel of this size in reasonable geology will cost approximately $800 per linear foot. For the purposes of this analysis this is adopted as the standard tunnel. DOE

N86-10998# Los Alamos National Lab., N. Mex.
LOCAL DRIFT PARAMETER, J/N SUB E AND RESISTIVITY ANOMALY MEASUREMENTS IN CTX SPHEROMAKS
H. W. Hoida, C. W. Barnes, I. Henins, T. R. Jarboe, C. J. Buchenauer, and G. J. Marklin 1985 7 p Presented at the 7th U.S. Symp. on Compact Toroid Res., Santa Fe, N. Mex., 21 May 1985
(Contract W-7405-eng-36)
(DE85-012740; LA-UR-85-1791; CONF-8505100-12) Avail: NTIS HC A02/MF A01

The ratio of the electron drift velocity to the electron thermal velocity, also known as the drift parameter (streaming parameter), and j/n sub e (approx. V sub d) have been measured locally at the magnetic axis in CTX spheromaks at Los Alamos. The drift parameter and j/n sub e appear to be correlated with local measurements of the resistivity anomaly (eta/eta sub Spitz) at the magnetic axis. The drift parameter and j/n sub e are varied by changing the background fill pressure. Data is presented for three cases: high density (6 mT fill), medium density (4mT fill) and low density (0 mT fill). DOE

N86-10999# Los Alamos National Lab., N. Mex.
INTRODUCTION TO THE M = 1 HELICITY SOURCE
D. A. Platts, T. R. Jarboe, and B. L. Wright 1985 6 p Presented at the 7th U.S. Symp. on Compact Toroid Res., Santa Fe, N. Mex., 21 May 1985
(Contract W-7405-eng-36)
(DE85-012771; LA-UR-85-1820; CONF-8505100-11) Avail: NTIS HC A02/MF A01

The m = 1 Helicity Source, formerly called the Kinked 2-pinch, was developed as part of the Electrode Studies program at Los Alamos. The Electrode Studies program was initiated to study the control of electrode erosion in long discharge duration spheromak sources. Erosion control is necessary to reduce plasma impurities and to obtain adequate electrode lifetimes. The first task of the Electrode Studies program is to determine, from among a variety of configurations including the coaxial one, a helicity source geometry with good prospects for erosion control. The more efficient the helicity source the easier it will be to control erosion, but the source must also be easy to diagnose and modify if it is to be a useful test bed. The various erosion control techniques which were proposed will require extensive experimentation to evaluate and optimize. Proposed techniques include, using refractory metals, profiling of the electrodes and magnetic fields, and various gas injection schemes including porous electrodes. It is considered necessary to do these experiments on an optimized helicity source so that the electrode geometries and plasma properties will be relevant. Therefore the present Electrode Studies program is aimed at developing an improved helicity source design. DOE

N86-11000# Massachusetts Inst. of Tech., Cambridge. Plasma Fusion Center.
US SUPERCONDUCTING MAGNET DATA BASE ASSESSMENT FOR INTOR
J. H. Schultz and D. B. Montgomery 10 Dec. 1984 20 p
(Contract DE-AC02-78ET-51013)
(DE85-013648; PFC/RR-84-19; DOE/ET-51013/139) Avail: NTIS HC A02/MF A01

Because of its size, performance requirements and exposure to neutron and gamma irradiation, the superconducting magnet system for INTOR would represent a significant advance in superconducting magnet technology. US programs such as LCP, MFTF-B and others provide a significant data base for the INTOR application. The assessment of the adequacy of the US data base for the INTOR magnets is largely generic, and applies to the superconducting magnet systems for other magnetic confinement fusion reactors. Assessments of the data base generated by other national magnet technology programs are being prepared by the other INTOR participants. DOE

N86-11001# Los Alamos National Lab., N. Mex.
BEGINNINGS OF REMOTE HANDLING AT THE RAL SPALLATION NEUTRON SOURCE
D. J. Liska and J. Hirst 1985 4 p Presented at the Particle Accelerator Conf., Vancouver, British Columbia, 13 May 1985
(Contract W-7405-eng-36)
(DE85-012681; LA-UR-85-1585; CONF-850504-109) Avail: NTIS HC A02/MF A01

Expenditure of funds and resources for remote maintenance systems traditionally are delayed until late in an accelerator's development. However, simple remote-surveillance equipment can be included early in facility planning to set the stage for future remote-handling needs and to identify appropriate personnel. Some basic equipment that serves this function and was used to monitor beam loss during commissioning is described. A photograph of this equipment, positioned over the extractor septum magnet, is shown. This method can serve as a pattern approach to the problem of initiating remote-handling activities in other facilities. DOE

N86-11002# Los Alamos National Lab., N. Mex.
ANALYTIC EVALUATION OF LAMPF 2 BOOSTER CAVITY DESIGN
C. C. Friedrichs 1985 4 p Presented at the Particle Accelerator Conf., Vancouver, British Columbia, 13 May 1985
(Contract W-7405-eng-36)
(DE85-012680; LA-UR-85-1586; CONF-850504-108) Avail: NTIS HC A02/MF A01

Through the past few decades, a great deal of sophistication has evolved in the numeric codes used to evaluate electromagnetically resonant structures. The numeric methods are extremely precise, even for complicated geometries, whereas analytic methods require a simple uniform geometry and a simple, known mode configuration if the same precision is to be obtained. The code SUPERFISH, which is near the present state of the art of numeric methods, does have the following limitations: No circumferential geometry variations are permissible; there are no provisions for magnetic or dielectric losses; and finally, it is impractical (because of the complexity of the code) to modify it to extract particular bits of data one might want that are not provided by the code as written. SUPERFISH was used as an aid in derivating an analytic model of the Los Alamos Meson Physics Facility (LAMPF) II Booster Cavity. One a satisfactory model was derived, simple FORTRAN codes were generated to provide whatever data was required. The analytic model is made up of TEM and radial mode transmission line sections, as well as lumped elements where appropriate. Radial transmission line equations, which include losses, were not found in any literature, and the extension of the lossless equations to include magnetic and dielectric losses are included. DOE

N86-11003# Los Alamos Scientific Lab., N. Mex.
ENERGY EFFICIENCY OF THE CTX MAGNETIZED COAXIAL PLASMA SOURCE
J. C. Fernandez, C. W. Barnes, T. R. Jarboe, S. O. Knox, D. A. Platts, and K. F. McKenna 1985 5 p Presented at the 7th US Symp. on Compact Toroid Res., Santa Fe, N. Mex., 21 May 1985
(Contract W-7405-eng-36)
(DE85-012735; LA-UR-85-1818; CONF-8505100-2) Avail: NTIS HC A02/MF A01

The energy efficiency of the CTX coaxial plasma source in creating spheromaks is determined experimentally to be in agreement with the theoretical prediction of lambda sub sp/lambda g, where del x B = lambda sub sp B in the spheromak, and lambda sub g identical with (MU) 0I sub g// phi sub g with I sub g the source current and phi sub g the magnetic flux through either source electrode. This is shown to be equivalent to magnetic helicity conservation. The spheromak impurity radiation was measured using an absolutely calibrated single chord bolometer system. The theoretical efficiency is within the experimental uncertainty of the ratio of spheromak radiated energy to source input energy in a group of dirty discharges. The radiation measurement uncertainty is too large to determine whether a substantial part of the excess source energy not used in the production of

spheromak magnetic energy is radiated from the spheromak volume. DOE

N86-11004# Stanford Linear Accelerator Center, Calif.
ELECTRON WIND IN STRONG WAVE GUIDE FIELDS
F. Krienen Mar. 1985 4 p Presented at the Particle Accelerator Conf., Vancouver, British Columbia, 13 May 1985
(Contract DE-AC03-76SF-00515)
(DE85-013062; SU-SLAC-PUB-3616; CONF-850504-110) Avail: NTIS HC A02/MF A01

The X-ray activity observed near highly powered waveguide structures is usually caused by local electric discharges originating from discontinuities such as couplers, tuners or bends. In traveling waves electrons move in the direction of the power flow. Seed electrons can multipactor in a traveling wave, the moving charge pattern is different from the multipactor in a resonant structure and is self-extinguishing. The charge density in the wave guide will modify impedance and propagation constant of the wave guide. The radiation level inside the output wave guide of the SLAC, 50 MW, S-band, klystron is estimated. Possible contributions of radiation to window failure are discussed. DOE

N86-11005# Sandia Labs., Albuquerque, N. Mex.
RADIATION FIELD RESULTS FROM THE SPEED TRIAXIODE, A LARGE AREA, HIGH DOSE RATE, SHORT PULSE 1MV BREMSSTRAHLUNG SOURCE
M. A. Hedemann, A. L. Pregenzer, L. D. Posey, D. C. Evans, and P. W. Spence 1985 5 p refs Presented at the 22nd Ann. Conf. on Nucl. and Space Radiation Effects, Monterey, Calif., 22 Jul. 1985 Prepared in cooperation with Pulse Sciences, Inc., San Leandro, Calif.
(Contract DE-AC04-76DP-00789)
(DE85-009438; SAND-85-0459C; CONF-850711-7) Avail: NTIS HC A02/MF A01

Measurements and calculations were performed which characterize a short pulse-width (10 to 18 ns) fast rise-time (12 ns) source which provides more than 5 x 10 to the 11) Rad(Si)/sec over an area larger than 150 sq.cm. DOE

N86-11006# Kanner (Leo) Associates, Redwood City, Calif.
ION SOURCES FOR HIGH-FREQUENCY ACCELERATORS
R. Keller 1985 45 p refs Transl. into ENGLISH of "Ionenquellen fuer Hochfrequenzbeschleuniger" rept. VDI-Bildungswerk 41-18-02 Gesellschaft fuer Schweionenforschung m.b.H, Darmstadt, West Germany, 3 May 1982
(Contract W-7405-eng-36)
(DE85-012992; LA-tr-85-16) Avail: NTIS HC A03/MF A01

Ion sources are being applied increasingly in many areas of physics and technology, from basic research in nuclear and atomic physics to energy research, isotope separation, implantation technology, surface processing and analysis all the way to biomedicine. The function and problems of the types important for high-frequency accelerators are explained using a few individual examples in order to stimulate a basic understanding for this technically sophisticated and little-known equipment. The sources discussed here supply single or multiple positively charged ions. DOE

N86-11007# GA Technologies, Inc., San Diego, Calif.
GA THEORY NEWS, JANUARY-MARCH 1985
B. Harvey, ed. May 1985 12 p
(Contract DE-AT03-84ER-53158)
(DE85-012572; GA-A-17995) Avail: NTIS HC A02/MF A01

GA Theory News is a quarterly publication presenting condensed versions of recent research reports printed by the Fusion Theory Group at GA Technologies. This issue contains the following three summaries: (1) neoclassical transport in tokamaks with divertors, (2) how a swing behaves, and (3) subcritical MHD turbulence. DOE

N86-11008# California Univ., Berkeley. Lawrence Berkeley Lab.
PROCEEDINGS OF A WORKSHOP ON ELECTROWEAK SYMMETRY BREAKING
I. Hinchliffe Oct. 1984 87 p Proc. held at Berkeley, Calif., 4-22 Jun. 1984
(Contract DE-AC03-76SF-00098; Grant NSF PHY-84-01063)
(DE85-004444; LBL-18571; CONF-8406190) Avail: NTIS HC A05/MF A01

A theoretical workshop on electroweak symmetry breaking at the Superconducting Supercollider was held at Lawrence Berkeley Laboratory, June 4-22, 1984. The purpose of the workshop was to focus theoretical attention on the ways in which experimentation at the SSC could reveal manifestations of the phenomenon responsible for electroweak symmetry breaking. This issue represents, at present, the most compelling scientific argument for the need to explore the energy region to be made accessible by the SSC, and a major aim of the workshop was to involve a broad cross section of particle theoretists in the ongoing process of sharpening the requirements for both accelerator and detector design that will ensure detection and identification of meaningful signals, whatever form the electroweak symmetry breaking phenomenon should actually take. DOE

N86-11009# Stanford Linear Accelerator Center, Calif.
EFFECTS OF SLOTS/HOLES IN DISKS ON FREQUENCIES OF TM01 AND EH11 WAVES IN THE DISK-LOADED WAVEGUIDE
C. G. Yao Mar. 1985 4 p Presented at the Particle Accelerator Conf., Vancouver, British Columbia, 13 May 1985 Prepared in cooperation with Nanjing Univ.
(Contract DE-AC03-76SF-00515)
(DE85-013376; SU-SLAC-PUB-3599; CONF-850504-150) Avail: NTIS HC A02/MF A01

The increase in the BBU threshold current is very important for the high and medium energy electron linacs because of the larger operating current attainable or a smaller emittance available at certain operating current. For this purpose, many means can be used, among which the improvement in the accelerating structure itself is always fundamental. SLAC's three-meter long section is unique with truly constant gradient performance. The theoretical analyses and operating experiences at SLAC have indicated that detuning the Nos. 3, 4 and 5 cavities of some sections by 2 or 4 MHz for TM01 wave had considerably raised the BBU threshold current. A method of opening four holes symmetrically distributed on disks as described in detail will get the benefits in improvement of BBU threshold current. DOE

N86-11010# Brookhaven National Lab., Upton, N. Y.
MICROWAVE INSTABILITY ACROSS THE TRANSITION ENERGY
S. Y. Lee and J. M. Wang 1985 4 p Presented at the Particle Accelerator Conf., Vancouver, British Columbia, 13 May 1985
(Contract DE-AC02-76CH-00016)
(DE85-013304; BNL-36564; CONF-850504-146) Avail: NTIS HC A02/MF A01

It is well known that during the acceleration of hadrons in a storage ring, the beam always goes above the microwave instability threshold near the transition energy (GAMMA)sub t. The reason is that the longitudinal revolution frequency spread of the beam which otherwise provides landau damping vanishes at the transition energy. The amount of the beam dilution near the transition energy is determined by tau sub th, the length of time when the beam stays unstable, and the growth rate of the instability. It is pointed out that tau sub th is proportional to the fourth power of (GAMMA) sub t, and thus the choice of a large (GAMMA) sub t is not desirable from this point of view. An analysis is also given of the microwave instability induced heat dilution for the proposed Relativistic Heavy Ion Collider at Brookhaven National Laboratory. DOE

N86-11011# Sandia Labs., Albuquerque, N. Mex.
ADVANCES IN DATA ACQUISITION SYSTEM TECHNOLOGY FOR PBFA 2
W. B. Boyer, F. A. Bouchier, T. F. Ezell, C. B. Mattson, and C. C. Newcom 1985 14 p Presented at the 5th IEEE Pulsed Power Conf., Washington, D.C., 10 Jun. 1985
(Contract DE-AC04-76DP-00789)

(DE85-012860; SAND-8402519C; CONF-850616-30) Avail: NTIS HC A02/MF A01

The data acquisition system being built for particle beam fusion accelerator (PBFA) II incorporates several new advanced technology features. The system will have 80 new waveform recorders with a 1.35 GHz sampling rate, 250 MHz bandwidth and 10,000 sample record length. A fast analog multiplexer will be used to enable recording multiple signals on each recorder. The accelerator performance monitor system will use time interval digitizers with a time window of + or - 8 msec. This long window and the pretrigger feature will provide data for a thorough analysis of accelerator prefires. The calibration system will automatically route precision dc levels, sine waves and fast rise pulses to the waveform recorders. The waveform recording system is being characterized using special multichannel, high level simultaneous pulse generators. The system computer has a 32 bit CPU, 350 Mbytes of disc storage and a virtual memory operating system. All software is being written in FORTRAN 77. DOE

N86-11012# Stanford Linear Accelerator Center, Calif.
HIGH-RESOLUTION PHOSPHOR SCREEN BEAM PROFILE MONITOR
S. Yencho and D. R. Walz May 1985 4 p refs Presented at the Particle Accelerator Conf., Vancouver, British Columbia, 13 May 1985
(Contract DE-AC03-76SF-00515)
(DE85-013074; SU-SLAC-PUB-3671; CONF-850504-83) Avail: NTIS HC A02/MF A01

A high resolution luminescent screen beam profile monitor was developed to allow viewing of both conventional large diameter SLAC e(+)/e(-) beams, and also collider RF bunches having small transverse spatial extent, with one instrument. The principal features of the monitor are described. They include the two power magnification system offering magnifications of 12 and 78X, respectively; the reticle grid which is optically superimposed on the screen image by a cube beam splitter; selection of a suitable camera; and the Al2O3(Cr) phosphor screen. A simplified version of the monitor for viewing of only micron sized beams for applications in the collider arcs and final focus regions and achieving a magnification of approx. 40X, coupled with a resolution of approx. 20(MU)m is also presented. DOE

N86-11013# Sandia Labs., Albuquerque, N. Mex.
ENGINEERING HIGH RELIABILITY, LOW-JITTER MARX GENERATORS
L. X. Schneider and G. J. Lockwood 1985 4 p refs Presented at 5th IEEE Pulsed Power Conf., Washington, D.C., 10 Jun. 1985
(Contract DE-AC04-76DP-00789)
(DE85-012811; SAND-84-2499C) Avail: NTIS HC A02/MF A01

Multimodule pulsed power accelerators typically require high module reliability and nanosecond simultaneity between modules. Energy storage using bipolar Marx generators can meet these requirements. Experience gained from computer simulations and the development of the DEMON II Marx generator led to a fundamental understanding of the operation of these multistage devices. As a result of this research, significant improvements in erection time jitter and reliability were realized in multistage, bipolar Marx generators. Erection time jitter was measured as low as 2.5 nanoseconds for the 3.2 MV, 16-stage PBFA I Marx and 3.5 nanoseconds for the 6.0 MV, 30-stage PBFA II (DEMON II) Marx, while maintaining exceptionally low prefire rates. Performance data are presented from the DEMON II Marx research program, as well as discussions on the use of computer simulations in designing low-jitter Marx generators. DOE

N86-11014# Stanford Linear Accelerator Center, Calif.
SLC POSITRON DAMPING RING OPTICS DESIGN
J. P. Delahaye and I. Rivkin Apr. 1985 4 p refs Presented at Particle Accelerator Conf., Vancouver, British Columbia, 13 May 1985
(Contracts DE-AC03-76SF-00515; DE-AC03-81ER-40050)
(DE85-013054; SU-SLAC-Pub-3649; CONF-850504-99) Avail: NTIS HC A02/MF A01

The basic SLAC Linear Collider operation scheme assumes the use of two damping rings, one for the e(-), one for the e(+), in order to reduce the colliding beam normalized emittances to 30 (PI) radm hence raising the corresponding luminosity by a factor 170. The e(-) damping ring optics, designed by H. Wiedemann, were extensively studied and modelled since it's completion at the end of 1982. The e(+) damping ring being built will be based on the same design except for some modifications resulting from the studies on the e(-) damping ring which clearly pointed out two major weak points as far as the optics is concerned. Basic modifications of the ring lattice and main equipment positions in order to improve the situation in the Positron Damping Ring are described. DOE

N86-11015# Stanford Univ., Calif.
COMPUTER CONTROL OF RF AT SLAC
H. D. Schwarz Mar. 1985 6 p refs Presented at Particle Accelerator Conf., ancouver, British Columbia, 13 May 1985
(Contract DE-AC03-76SF-00515)
(DE85-013065; ; SU-SLAC-PUB-3600) Avail: NTIS HC A02/MF A01

The Stanford Linear Accelerator is upgrading for the SLAC Linear Collider project. The energy will be increased from approximately 31 GeV to 50 GeV. Two electron beams and one positron beam will be accelerated with high demands on the quality of the beams. The beam specifications are shown. To meet these specifications, all parameters influencing the beams have to be under tight control and continuous surveillance. This task is accomplished by a new computer system implemented at SLAC which has, among other functions, control over RF accelerating fields. DOE

N86-11016# California Univ., Livermore. Lawrence Livermore Lab.
COMPACT TORUS COMPRESSION OF MICROWAVES
D. W. Hewett and A. B. Langdon 17 May 1985 6 p refs Presented at 7th Symp. on Compact Toroid Res., Santa Fe, N.Y., 21 May 1985
(Contract W-7405-eng-48)
(DE85-012919; UCRL-92690; CONF-8505100-6) Avail: NTIS HC A02/MF A01

The possibility that a compact torus (CT) might be accelerated to large velocities was suggested by Hartman and Hammer. If this is feasible one application of these moving CTs might be to compress microwaves. The proposed mechanism is that a coaxial vacuum region in front of a CT is prefilled with a number of normal electromagnetic modes on which the CT impinges. A crucial assumption of this proposal is that the CT excludes the microwaves and therefore compresses them. Should the microwaves penetrate the CT, compression efficiency is diminished and significant CT heating results. MFE applications in the same parameters regime have found electromagnetic radiation capable of penetrating, heating, and driving currents. DOE

N86-11017# California Univ., Livermore. Lawrence Livermore Lab.
APPLICATION OF STRUCTURAL-MECHANICS METHODS TO THE DESIGN OF LARGE TANDEM-MIRROR FUSION DEVICES (MFTF-B)
V. N. Karpenko and D. S. Ng 4 Mar. 1985 14 p Presented at the 8th Intern. Conf. on Struct. Mech. in Reactor Technol., Brussels, 19 Aug. 1985
(Contract W-7405-eng-48)
(DE85-008960; UCRL-92246; CONF-850809-29) Avail: NTIS HC A02/MF A01

The Mirror Fusion Test Facility (MFTF-B) at Lawrence Livermore National Laboratory requires state-of-the-art structural-mechanics methods to deal with access constraints for plasma heating and diagnostics, alignment requirements, and load complexity and variety. Large interactive structures required an integrated analytical approach to achieve a reasonable level of overall system optimization. The Tandem Magnet Generator (TMG) creates a magnet configuration for the EFFI calculation of electromagnetic-field forces

that, coupled with other loads, form the input loading to magnet and vessel finite-element models. The analytical results provide the data base for detailed design of magnet, vessel, foundation, and interaction effects. DOE

N86-11018# Brookhaven National Lab., Upton, N. Y.
THEORY OF NON-PLANAR ORBITS
A. Anitllon and M. Month 1985 4 p refs Presented at the Particle Accelerator Conf., Vancouver, British Columbia, 13 May 1985
(Contract DE-AC02-76CH-00016)
(DE85-013284; BNL-36495; CONF-850504-160) Avail: NTIS HC A02/MF A01

The basic dynamics of a planar accelerator is extended to the non-planar case. This is one using the geometrical concept of torsion and extending the Hamiltonian formalism. A generalized non-planar reference orbit is adopted which introduces torsion in appropriately chosen drift spaces. The parameters of the reference orbit are associated with uncoupled and coupled betatron parameters currently in use. DOE

N86-11019# Sandia Labs., Albuquerque, N. Mex.
PHOTOACTIVATION OF PBFA-2
T. N. Simmons and J. B. Mashburn 1985 5 p Presented at the 5th IEEE Pulsed Power Conf., Washington, D.C., 10 Jun. 1985
(Contract DE-AC04-76DP-00789)
(DE85-013439; SAND-84-2576C; CONF-850616-35) Avail: NTIS HC A02/MF A01

A 30 MV peak output voltage will be produced. A substantial portion of the output energy will be lost as free electrons which produce hard X-rays. Many X-rays will have energies within the photoneutron giant resonance. A PBFA-2 shot will produce about 5 x 10 E14 photoneutrons. These photoneutron reactions will induce radioactivity in and about PBFA-2. Activation structural components in the center section will be limited by substituting aluminum for stainless steel in regions of high X-ray intensity. Air will be activated above and below the center section after shots; however, X-ray shielding will limit initial concentrations to five times health guidelines. The short half-lives of air radioactivity will permit reentry following simple decay without ventilation. Some radioactive material will be eroded by arcing, but the resulting contamination whould be small. Miniscule concentrations of radioactivity will be produced in the water surrounding the center section. DOE

N86-11020# Massachusetts Inst. of Tech., Cambridge. Plasma Fusion Center.
CONDUCTING WALL AND PRESSURE PROFILE EFFECT ON MHD STABILIZATION OF AXISYMMETRIC MIRROR
X. Z. Li, J. Kesner, and B. Lane 1985 37 p
(Contract DE-AC02-78ET-51013)
(DE85-013647; DOE/ET-51013/135; PFC/RR-84-15) Avail: NTIS HC A03/MF A01

The MHD Energy Princple is used to examine the stabilization effect of a conducting wall located near to the plasma surface. The stabilization effect is maximized when the normal components of the perturbed magnetic field approaches zero (Q sub n = 0) at the plasma surface. Under this boundary condition, the eigen-equation of the plasma displacement is solved for a two-step flat pressure profile model, which can include both the non-hollow and a hollow pressure profile. Only the rigid m-1 mode is considered due to the FLR effect. For an isotropic pressure component it is found that a hollow profile has better stability than a uniform pressure when the integral of the radial pressure profile is fixed. The implication for plasma experiments and fusion reactors is discussed. DOE

N86-11021# Brookhaven National Lab., Upton, N. Y.
THERMAL AND STRUCTURAL ANALYSIS OF RING COMPONENTS BY THE FINITE ELEMENT METHOD
R. Alforque and S. Sharma 1985 4 p Presented at the Particle Accelerator Conf., Vancouver, British Columbia, 13 May 1985
(Contract DE-AC02-76CH-00016)
(DE85-013305; BNL-36573; CONF-850504-145) Avail: NTIS HC A02/MF A01

In a previous report, a thermal study was made in order to determine the effects of a shift in the electron vertical orbital plane, and the resulting displacement of the wiggler photon beam striking the inner surface of the vacuum chamber. Since then, due to some changes in the physical parameters of the vacuum chamber, a new design has been developed. The new geometry is quite different from the one described earlier, due primarily to an increase in the chamber vertical aperture which was opened to 23 mm. from an initial opening of 6 mm. A new study is conducted for this new chamber design that includes a structural analysis in order to determine the stresses and deflections of the vacuum chamber due to the combined thermal and mechanical loading. It should be noted that various geometrical models are analyzed before the final geometry is decided. This report describes in detail the results of the thermal and structural analysis of the final geometry using the finite element code. DOE

N86-11022# Brookhaven National Lab., Upton, N. Y.
UNICELL STRUCTURE FOR SUPERCONDUCTING STORAGE RINGS
G. Danby, B. DeVito, J. Jackson, G. Keohane, Y. Y. Lee, R. Phillips, S. Plate, L. Repeta, J. Skaritka, and L. Smith 1985 4 p Presented at the Particle Accelerator Conf., Vancouver, British Columbia, 13 May 1985
(Contract DE-AC02-76CH-00016)
(DE85-013303; BNL-36559; CONF-850504-147) Avail: NTIS HC A02/MF A01

Mechanically integrated, magnetically decoupled storage rings were designed for a heavy ion collider for 100 GeV/amu Au, at B - 2.7T. New concepts were developed, including detailed engineering design and cost estimates. A unicell contains a half-cell of both rings within a single He vessel. The unicell design is optimized for economical mass production. Survey pads welded to the laminations provide external fiducials to locate the magnet cores. Roller bearing self aligning supports accommodate cool-down shrinkage. The design tolerates relative motion of components resulting from longitudinal shrinkage in the approx. 15 m long unicell without affecting performance. Magnetic and physical lengths are the same, eliminating waste space. Archomatic quadrupoles with sextupoles at both ends are located on a common precision beam tube which aligns and supports a pick-up electrode. The unicell accommodates longer dipoles compared to conventional designs, reducing B sub max, stored energy, and the volume of iron and superconductor. DOE

N86-11023# Brookhaven National Lab., Upton, N. Y.
TRACKING STUDIES ON THE EFFECTS OF MAGNET MULTIPOLES ON THE APERTURE OF THE RHIC HEAVY ION COLLIDER
G. F. Dell and G. Parzen 13 May 1985 4 p refs Presented at the Particle Accelerator Conf., Vancouver, British Columbia, 13 May 1985
(Contract DE-AC02-76CH-00016)
(DE85-013282; BNL-36566; CONF-850504-157) Avail: NTIS HC A02/MF A01

Tracking studies including the effects of random multipoles resulting from construction errors have been made for Relativistic Heavy Ion collider (RHIC) at Brookhaven National Laboratory (NHIC) with two independent tracking programs at three different tunes. The studies were made using ten different sets of random errors for each of the programs. The aperture was defined as the worst case, and the results of the two programs are in good agreement. A second set of studies was made for which the number of dipoles was doubled to determine whether doubling the number of independent random errors results in a reduction of the effects or random multipoles. The results for the two cases, one dipole per half cell and two dipoles per half cell, indicate there is little difference in dynamic aperture. DOE

N86-11024# Stanford Linear Accelerator Center, Calif.
TIMING SYSTEM CONTROL SOFTWARE IN THE SLC
K. Thompson and N. Phinney Apr. 1985 3 p Presented at the

Particle Accelerator Conf., Vancouver, British Columbia, 13 May 1985
(Contract DE-AC03-76SF-00515)
(DE85-013380; SU-SLAC-PUB-3651; CONF-850504-87) Avail: NTIS HC A02/MF A01

A new timing system that allows precision (approx. 1 to 2 ns) control of the trigger times of klystrons, beam position monitors, and other devices on a pulse-to-pulse basis at up to 360 Hz is in operation in the first third of the SLAC linear accelerator. The control software is divided between a central host VAX and local Intel 8086-based microprocessor clusters. Facilities exist to set up and adjust the timing of devices or groups of devices independently for beam pulses having different destinations and purposes, which are run in an interlaced fashion during normal machine operation. Upgrading of the system is currently underway, using a new version of the Programmable Delay Unit CAMAC module to allow pipelining of timing information for three machine pulses. An overview of the current state of the system is presented with an emphasis on software control. DOE

N86-11025# Stanford Linear Accelerator Center, Calif.
BEAM STEERING IN THE SLC LINAC
J. C. Sheppard, M. J. Lee, M. C. Ross, J. T. Seeman, R. F. Stiening, and M. D. Woodley Feb. 1985 3 p Presented at the Particle Accelerator Conf., Vancouver, British Columbia, 13 May 1985
(Contract DE-AC03-76SF-00515)
(DE85-013370; SU-SLAC-PUB-3583; CONF-850504-70) Avail: NTIS HC A02/MF A01

In order to control emittance growth due to transverse wakefields it will be necessary to transport electrons and positrons through the Stanford Linear Collider (SLC) linac to within a hundred (MU)m of the centers of the linac irises. Beam centering will be accomplished using computer routines to read stripline beam position monitors and in turn correct the orbits with dipole magnets. Several different steering algorithms have been investigated using electrons in the first third of the SLC linac lattice. The most promising scheme is a cascade of modified three-bumps in conjunction with long spanning harmonic corrections. General features of the orbit correcting software are discussed along with the mathematical recipes for correction. Experimental results and a discussion of future plans are presented. DOE

N86-11026# Brookhaven National Lab., Upton, N. Y.
RHIC LATTICE
S. Y. Lee, J. Claus, E. D. Courant, H. Hahn, and G. Parzen 1985 4 p refs Presented at the Particle Accelerator Conf., Vancouver, British Columbia, 13 May 1985
(Contract DE-AC02-76CH-00016)
(DE85-013289) Avail: NTIS HC A02/MF A01

An antisymmetric lattice for the proposed Relativistic Heavy Ion Collider at Brookhaven National Laboratory is presented, which was designed to have (1) an energy range from 7 GeV/amu up to 100 GeV/amu; (2) a good tunability of (BETA) and betatron tune; (3) freedom in the choice of crossing angle between beams; and (4) capability of operating unequal species, for example, proton on gold. Suppression of structure resonances is achieved by a proper choice of the phase advances across the insertion and the arc cells. DOE

N86-11027# Los Alamos Scientific Lab., N. Mex.
GENERALIZED HELICITY AND ITS TIME DERIVATIVE
T. R. Jarboe and G. J. Marklin 1985 8 p Presented at the 7th US Symp. on Compact Toroid Res., Santa Fe, N. Mex., 21 May 1985
(Contract W-7405-eng-36)
(DE85-012770; LA-UR-85-1821; CONF-8505100-15) Avail: NTIS HC A02/MF A01

Spheromaks can be sustained against resistive decay by helicity injection because they tend to obey the minimum energy principle. A plasma-laden magnetic configuration will relax to a state of minimum energy subject to the constraint that the magnetic helicity is conserved. Use of helicity as a constraint on the minimization of energy was proposed in connection with astrophysical phenomena. Helicity does decay on the resistive diffusion time. However, if helicity is created and made to flow continuously into a confinement geometry, these additional linked fluxes can relax and sustain the configuration indefinitely against the resistive decay. An extension of the definition of helicity to include systems where B vector can penetrate the boundary and the penetration can be varying in time is presented. The sustainment of RFPs and spheromaks in terms of helicity injection is discussed. DOE

N86-11028# Los Alamos Scientific Lab., N. Mex.
RECENT HELICITY SOURCE AND POWER SUPPLY IMPROVEMENTS IN CTX
I. Henins, S. O. Knox, T. R. Jarboe, and C. W. Barnes 1985 6 p Presented at the 7th US Symp. on Compact Toroid Res., Santa Fe., N. Mex., 21 May 1985
(Contract W-7405-eng-36)
(DE85-012741; LA-UR-1790; CONF-8505100-4) Avail: NTIS HC A02/MF A01

Since the last CT Symposium, two major changes in CTX have been the introduction of pulse forming networks (PFNs) to drive the coaxial electrode helicity source, and the very recent installation of a larger source with electrode diameters about twice the previous ones. The power supplies used for CTX have ranged from the simple connection of the capacitor bank across the electrode collector plates (slow mode) to the more sophisticated PFNs, described here, which optimize the energy transfer from the capacitor bank to the magnetic fields of the spheromak. Using the PFNs, the formation and sustainment phase to peak toroidal plasma current lasts longer (approx. = 0.7 ms) than in the slow mode (approx. = 0.05 ms), thus lowering the peak current that must flow through the electrode surfaces. Also, by supplying the source electrodes with both a square pulse current waveform and a quasi-steady source flux, phi sub g, one can generate helicity at a constant source lambda sub g parameter. The use of a larger diameter helicity source will improve the energy efficiency of helicity injection and allow higher source current for the same surface current density because of the larger electrode surface area. DOE

N86-11029# Los Alamos Scientific Lab., N. Mex.
EQUILIBRIUM OF THE KINK SOURCE EXPERIMENT
G. Marklin 1985 5 p Presented at the 7th US Symp. on Compact Toroid Res., Santa Fe, N. Mex., 21 May 1985
(Contract W-7405-eng-36)
(DE85-012764; LA-UR-85-1837; CONF-8505100-14) Avail: NTIS HC A02/MF A01

The kink source experiment (KSX) was conceived of as a method of injecting helicity into a spheromak making special use of the m = 1 helical Taylor state. It has a Z pinch as a helicity generating source, connected to a flux conserver through an entrance region. Since the entrance region is a long (length > diameter) cyclinder, the magnetic field should be close to the helical Taylor state, which is the minimum energy configuration of a magnetized plasma in an infinite cylinder with no net flux. Modeling the actual fields in the entrance region of the KSX using zer-beta ideal MHD equilibrium theory is described. DOE

N86-11030# California Univ., Livermore. Lawrence Livermore Lab.
LIQUID TO GAS LEAK RATIOS WITH LIQUID NITROGEN AND LIQUID HELIUM
T. H. Batzer and W. R. Call 26 Feb. 1985 4 p Presented at the 6th Topical Meeting on the Technol. of Fusion Energy, San Francisco, 3 Mar. 1985
(Contract W-7405-eng-48)
(DE85-012950; UCRL-91953; CONF-850310-112) Avail: NTIS HC A02/MF A01

To predict the leak rates of liquid helium and liquid nitrogen containers at operating conditions we need to know how small leaks 10 to the -8 to 10 to the -5 atm cc air/sec, measured at standard conditions, behave when flooded with these cryogens. Two small leaks were measured at ambient conditions (approx. 750 Torr and 295 K), at the normal boiling points of LN2 and

LHe, and at elevated pressures above the liquids. The ratios of the leak rates of the liquids at ambient pressure to the gases (G) at ambient pressure and room temperature were: GN2(1), LN2(18), GHe(1), and LHe(172). The leak rate ratio of LN2 at elevated pressure was linear with pressure. The leak rate ratio of LHe at elevated pressure was also linear with pressure. DOE

N86-11031# Los Alamos Scientific Lab., N. Mex.
ALTERNATIVE FUSION CONCEPTS AND THE PROSPECTS FOR IMPROVED REACTORS
R. A. Krakowski 1985 9 p Presented at the 20th Intersoc. Energy Conversion Eng. Conf., Miami Beach, Fla., 18 Aug. 1985
(Contract W-7405-eng-36)
(DE85-009622; LA-UR-85-1035; CONF-850808-3) Avail: NTIS HC A02/MF A01

Past trends, present status, and future directions in the search for an improved fusion reactor are reviewed, and promising options available to both the principle tokamak and other supporting concept are summarized. DOE

N86-11032# TRW Space Technology Labs., Redondo Beach, Calif. Energy Div.
SYMMETRIC TANDEM MIRROR PROGRAM Annual Progress Report
1985 56 p
(Contract DE-AC03-79ET-51017)
(DE85-012352; DOE/ET-51017/T2) Avail: NTIS HC A04/MF A01

The overall objective was to examine confinement of high-(BETA) plasmas in an axisymmetric mirror configuration which is stabilized by the presence of a plasma produced, annular magnetic well (ELMO-ring). To accomplish this objective, the high-(BETA) mirror-confined plasmas were generated by ICRH. The annular wells result from diamagnetism of hot electrons generated by ECRH. The development of techniques for controlling the spatial and energy distributions of these electrons was an esential ingredient in the program. The culmination of this work is the successful generation of hot-ion plasmas by ICRH with anti n approx. 1 x to the 13th/cc and T sub i approx. 300 eV corresponding to anti (BETA) approx. = 5%. DOE

N86-11033# Stanford Linear Accelerator Center, Calif.
PROGRAMMABLE DELAY UNIT INCORPORATING A SEMI-CUSTOM INTEGRATED CIRCUIT
E. Linstadt Apr. 1985 3 p Presented at the Particle Acclerator Conf., Vancouver, British Columbia, 13 May 1985
(Contract DE-AC03-76SF-00515)
(DE85-013379; SU-SLAC-PUB-3637; CONF-850504-72) Avail: NTIS HC A02/MF A01

The synchronization of Stanford Linear Collider (SLC) accelerator control and monitoring functions is realized by a CAMAC module, the PDU II (Programmable Delay Unit II, SLAC 253-002), which includes a semi-custom gate array integrated circuit. The PDU II distributes 16 channels of independently programmable delayed pulses to other modules within the same CAMAC crate. The delays are programmable in increments of 8.4 ns. Functional descriptions of both the module and the semi-custom integrated circuit used to generate the output pulses are given. Author

N86-11034# Los Alamos Scientific Lab., N. Mex.
HEATING AND GENERATION OF SUPRATHERMAL PARTICLES AT COLLISIONLESS SHOCKS
M. F. Thomsen 1985 28 p refs Presented at the Am. Inst. of Phys. Conf., Taos, N. Mex., 6 Aug. 1984
(Contract W-7405-eng-36)
(DE85-014114; LA-UR-85-2073; CONF-8408121-4) Avail: NTIS HC A03/MF A01

Collisionless plasma shocks are different from ordinary collisional fluid shocks in several important respects. They do not in general heat the electrons and ions equally, nor do they produce Maxwellian velocity distributions downstream. Furthermore, they commonly generate suprathermal particles which propagate into the upstream region, giving advance warning of the presence of the shock and providing a seed population for further acceleration to high energies. Recent space observations and theory have revealed a great deal about the heating mechanisms which occur in collisionless shocks and about the origin of the various suprathermal particle populations which are found in association with them. An overview of the present understanding of these subjects is presented. DOE

N86-11035# Stanford Linear Accelerator Center, Calif.
SEARCH FOR HEAVY NEUTRINES PRODUCED IN e(+)e(-) ANNIHILATION
G. J. Feldman May 1985 6 p refs Presented at the 20th Recontre de Moriond, Les Arcs, France, 10 Mar. 1985
(Contract DE-AC03-76SF-00515)
(DE85-013372; SU-SLAC-PUB-3684; CONF-850375-4) Avail: NTIS HC A02/MF A01

A search for long-lived heavy neutrinos produced by the neutral weak current in e(+)e(-) annihilation at 29 GeV at PEP was conducted. Data from the Mark II detector are examined for evidence of events with one or more separated vertices in the radial range of 2 mm to 10 cm. No events were found that were consistent with the hypothesis of heavy neutrino production, eliminating the possibility of heavy neutrinos with decay lengths of 1 to 20 cm in mass range 1 to 13 GeV/c(2). DOE

N86-11036# Argonne National Lab., Ill.
EXPERIMENTAL INVESTIGATIONS OF THERMAL RADIATION FROM POTASSIUM ATOMS AND DESIGN APPLICATIONS
C. S. Wang and L. S. H. Chow 1985 8 p refs Presented at the Natl. Heat Transfer Conf., Denver, 4 Aug. 1985
(Contract W-31-109-eng-38)
(DE85-004086; CONF-850810-3) Avail: NTIS HC A02/MF A01

Theoretical models of thermal radiation from potassium-laden combustion gases show that thermal radiation from potassium atoms can contribute significantly to the radiant heat flux in radiant furnaces of steam generating systems. The potassium radiation is being investigated experimentally at Argonne National Laboratory. Experimental data were interpreted by a radiant heat transfer model that calculates the total gas emissivity and absorptivity from the spectral properties of CO2, H2O, and potassium atoms. The model was applied to provide design data for radiant furnaces of coal-fired magnetohydrodynamic (MHD) power generation systems, where considerable amount of potassium atoms would be present. DOE

N86-11037# Oak Ridge National Lab., Tenn.
HOT CELL FACILITY DESIGN FOR LARGE FUSION DEVICES
R. J. Barrett and G. T. Bussell 1985 6 p Presented at the 6th Topical Meeting on the Technol. of Fusion Energy, San Francisco, 3 Mar. 1985 Prepared in cooperation with Burns and Roe, Inc., Oradell, N.J. and Stone and Webster Engineering Corp., Boston, Mass.
(Contract DE-AC05-84OR-21400)
(DE85-012893; CONF-850310-104) Avail: NTIS HC A02/MF A01

Large hot cell facilities will be necessary to support the operation of large fusion devices. The supporting hot cells will be needed to serve a variety of different functions and tasks, which include reactor component maintenance, tool and maintenance equipment repair, and preparation of radioactive material for shipment and disposal. This paper discusses hot cell facility functions, requirements, and design issues and techniques. Suggested solutions and examples are given. DOE

N86-11038# Nationaal Inst. voor Kernfysica en Hoge Energiefysica, Amsterdam (Netherlands). Sectie-H.
TWO-LOOP LARGE HIGGS MASS CORRECTIONS TO VECTOR BOSON SELF-COUPLINGS
J. J. vanderBij Oct. 1984 20 p refs
(NIKHEF-H/84-15; B8561680) Avail: NTIS HC A02/MF A01

The two-loop corrections to the three-vector boson vertices are calculated in the limit of large Higgs mass. Corrections growing quadratically with the Higgs mass appear in the anomalous

magnetic moment of the charged vector boson and the corresponding W0W+W- coupling. The weak coupling constant in the W0W+W- vertex receives a correction compared to the coupling in mu-decay. The results suggest a breakdown of perturbation theory for a Higgs mass of 3.4 TeV and larger. Author (ESA)

N86-11039# FOM-Inst. voor Plasmafysica, Rijnhuizen, Jutphaas (Netherlands).
[ACTIVITIES REPORT IN PLASMA PHYSICS] Annual Status Report, 31 Dec. 1984
Apr. 1985 140 p refs Sponsored by Euratom and Nederlandse Organisatie voor, Zuiver-Wetenschappelijk Onderzoek (ZWO)
Avail: NTIS HC A07/MF A01

Some areas of study were plasma pinches, turbulent heating in TORTUR tokamak and diagnostical studies, numerical calculations on cold plasma blankets, and electron cyclotron resonance heating. Plasma diagnostics, fusion reactor technology, magnetohydrodynamics, wave dynamics, and transport problems were also studied. Author (ESA)

76 SOLID-STATE PHYSICS

Includes superconductivity.

For related information, see also *33 Electronics and Electrical Engineering* and *36 Lasers and Masers.*

N86-11040 Rutgers - The State Univ., New Brunswick, N. J.
AN INVESTIGATION OF VORTEX DYNAMICS IN 2-DIMENSIONAL SUPERFLUID FILMS OF HELIUM-4 Ph.D. Thesis
Mokyang Kim 1985 198 p
Avail: Univ. Microfilms Order No. DA8510811

Recently the superfluidity in 2-dimensional helium film has been actively investigated theoretically and experimentally. By measuring the third sound damping associated with the amplitude of the oscillation and/or with the externally driven rotation, the vortex dynamics in 2-dimensional superfluid films of helium-4 was systematically investigated. Firstly, the effective vortex density when the present pair-breakings of bound pairs was measured for the both situations when the net vorticity of the system is zero and nonzero. The measured effective vortex density for the former case was compared with the theoretical predictions and that for the latter case was used to determine an empirical relation between the effective density of rotation-induced vortices from pair breaking. Secondly, the effective diffusion constant was measured and fitted experimentally. Thirdly, the decay of persistent current was measured in an open geometry when vortices leave the film and enter the film. Dissert. Abstr.

N86-11041 Columbia Univ., New York.
A SUPERCONDUCTING TUNNEL JUNCTION RECEIVER FOR MILLIMETER-WAVE ASTRONOMY Ph.D. Thesis
Shing-Kuo Pan 1984 245 p
Avail: Univ. Microfilms Order No. DA8511539

The development and construction of an ultra-low noise heterodyne receiver for millimeter wavelength ratio astronomy, and its use for spectral line observations of the 115.3 GHz rotational transition of interstellar CO is described. The receiver uses a Superconductor - Insulator - Superconductor (SIS) quasiparticle tunnel junction mixer to convert the millimeter wavelength signal to a microwave intermediate frequency. Experiments aimed at quantitative verification of J. R. Tucker's newly published quantum mixer theory are described. Experimental results were in excellent agreement with theory, assuming the 3-frequency approximation. Infinite available gain and negative output resistance were observed for the first time. Using this SIS receiver on the Columbia-GISS 4-ft telescope, 7 well separated large molecular clouds were observed at velocities between -80 and -20 km/sec towards the Cygnus-X region. The kinematic distances of these clouds lie between 6.5 and 12.7 kpc corresponding to galactocentric radii of 11 to 14.7 kpc. The total mass of these clouds is about 2 x 10 to the 6th power solar mass. Dissert. Abstr.

N86-11042 Illinois Inst. of Tech., Chicago.
FREE CARRIER ABSORPTION FROM ELECTRONS IN CONFINED SYSTEMS Ph.D. Thesis
Halina Adamska 1984 82 p
Avail: Univ. Microfilms Order No. DA8510285

A calculation of the free carrier absorption for two-dimensional quantum well structures and ultrathin wires fabricated from III-V semiconducting materials, where the carriers are scattered either by polar optical phonons or acoustic phonons is presented. The free carrier absorption coefficient is found to be an oscillatory function of the photon frequency when the carriers are confined in quasi-low-dimensional structures such as superlattice heterostructures, quantum wells or thin wires. The absorption in quasi-low-dimensional structures is enhanced by going to layers of decreasing widths or to wires of decreasing widths or to wires of smaller transverse dimensions over its value in the bulk III-V semiconducting materials. In addition, it was found that in quasi-low-dimensional structures made from these materials the electron - polar optical phonon interaction gives greater contribution to the absorption than the electron - acoustic phonon interaction. Dissert. Abstr.

N86-11043 Yale Univ., New Haven, Conn.
ELECTRON TUNNELING IN METAL/TUNNEL-OXIDE/DEGENERATE SILICON JUNCTIONS Ph.D. Thesis
Izak Bencuya 1984 176 p
Avail: Univ. Microfilms Order No. DA8509683

Electron tunneling through very thin oxides (approx. 20 angstroms) on degenerate silicon was studied at room, liquid nitrogen and liquid helium temperatures. Metal, silicon and silicon dioxide vibrational modes were identified by the method of inelastic tunneling spectroscopy at liquid helium temperatures. Variations of the tunneling conductance and location of the silicon phonon peaks with orientation and carrier type of the semiconductor, and the shape of the lead superconducting gap in the tunneling conductance, centered about zero bias, show that the current flow is predominantly by direct, band-to-band, momentum-conserving tunneling. Dissert. Abstr.

N86-11044 Maryland Univ., College Park.
ADSORPTION OF OXYGEN ON SINGLE CRYSTAL TIN AT LIQUID HELIUM TEMPERATURES Ph.D. Thesis
John Michael Cavallo 1984 132 p
Avail: Univ. Microfilms Order No. 8509150

The initial stages of oxygen adsorption on single crystal tin surfaces were studied at liquid helium temperatures. The low temperatures slowed the reaction of the oxygen with the tin so that stages, which pass quickly at room temperature, could be studied. The reactions were studied by monitoring changes in the work function and in low energy electron transmission spectra. Dissert. Abstr.

N86-11045 Harvard Univ., Cambridge, Mass.
TOPICS IN THE ELECTRONIC THEORY OF DISORDERED SEMICONDUCTORS Ph.D. Thesis
Kenneth Charles Hass 1984 305 p
Avail: Univ. Microfilms, Order No. DA8503535

Two topics in the electronic theory of disordered semiconductors are discussed. First various aspects of the electronic theory of zincblende pseudobinary alloys are developed. The effects of chemical and bond-length disorder are modeled using the empirical tight binding method (ETBM). The choice of parameters is given special emphasis. A relativistic ETEM-CPA formalism is developed for systems with pure substitutional disorder. Its implementation is simplified through the development of a novel computational scheme (based on analytic continuation) which is also applicable in other types of green's function calculations. Secondly, the theory of interband optical absorption is discussed. A new method is presented for testing models of the electronic structure and chemical bonding in amorphous semiconductors based on a comparative analysis of moments of e2 in amorphous materials and related crystals. An application to published data is shown to provide insight into (1) bonding differences between various classes

of amorphous semiconductors and (2) the validity of the independent band model. Dissert. Abstr.

N86-11046 Maryland Univ., College Park.
CRITICAL DYNAMICS IN SUPERFLUID HELIUM Ph.D. Thesis
Michael Steven Korth 1984 222 p
Avail: Univ. Microfilms Order No. DA8510254

The properties of liquid He-4 were very extensively studied and are, consequently, fairly well characterized. This, together with the capability of approaching the lambda-temperature (T sub lambda) closely and making high-precision measurements, accounts for the superiority of this system as a proving ground for any theory of critical phenomena. Thus when recent experiments on the thermal conductivity and the light-scattering spectrum near T sub lambda both manifested clear deviations from the predictions of dynamic scaling theory, the theory was seriously questioned. A mode-coupling type approach was used to calculate these two quantities. Non-critical background terms are included in a natural way. In the first three-term epsilon-expansion in critical dynamics, the asymptotic region (in which dynamic scaling ideas apply) is found to be very small--beyond the range of current experiments. Proper inclusion of these two effects (the non-critical and the non-asymptotic) are shown to be the key to reconciling the theory and experiments. Dissert. Abstr.

N86-11047*# Eloret Corp., Sunnyvale, Calif.
THE INTERACTION OF SMALL METAL PARTICLES WITH REFRACTORY OXIDE SUPPORTS Final Technical Report
Ch. Park and Klaus Heinemann 4 Mar. 1985 85 p refs
(NASA Order R05-030-001; Grant NCC2-248)
(NASA-CR-176228; NAS 1.26:176228) Avail: NTIS HC A05/MF A01 CSCL 20L

Islands and continuous layers of Pd were grown in UHV on Mo and MoO subtrates. As-deposited Pd islands and layers exhibited bulk Pd adsorption properties for CO when the Pd had been deposited at RT and at thicknesses exceeding 3 ML. However, CO adsorption was drastically reduced upon annealing. This deactivation was interpreted in terms of substrate/support interaction involving the diffusion of substrate species toward the Pd surface, using AES, TPD, and work function measurement techniques. A study of the growth and annealing behavior of Pd on Mo(110) was made for thicknesses up to 12 monolayers and substrate temperatures up to 1300K, using AES, XPS, LEED, and work function measurements. At low tempertures Pd formed a monolayer without alloying. In thick layers (12 ML) annealed about 700 K, Mo diffusion into the Pd layer and alloying were noted. Such layers remained continuous up to 1100 K. Thinner Pd layers were less stable and started coalescing upon annealing to as little as 550 K. Significant changes in Pd Auger peak shape, as well as shifts of Pd core levels, were observed during layer growth and annealing. Author

N86-11048*# National Aeronautics and Space Administration. Lewis Research Center, Cleveland, Ohio.
ION BEAM SPUTTER DEPOSITED ZINC TELLURIDE FILMS
Daniel A. Gulino 1985 19 p refs Proposed for presentation at 32nd Natl. Symp. of the Am. Vacuum Soc., Houston, Tex., 18-22 1985
(NASA-TM-87119; E-2726; NAS 1.15:87119) Avail: NTIS HC A02/MF A01 CSCL 20L

Zinc telluride is of interest as a potential electronic device material, particularly as one component in an amorphous superlattice, which is a new class of interesting and potentially useful materials. Some structural and electronic properties of ZnTe films deposited by argon ion beam sputter depoairion are described. Films (up to 3000 angstroms thick) were deposited from a ZnTe target. A beam energy of 1000 eV and a current density of 4 mA/sq. cm. resulted in deposition rates of approximately 70 angstroms/min. The optical band gap was found to he approximately 1.1 eV, indicating an amorphous structure, as compared to a literature value of 2.26 eV for crystalline material. Intrinsic stress measurements showed a thickness dependence, varying from tensile for thicknesses below 850 angstroms to compressive for larger thicknesses. Room temperature conductivity measurement also showed a thickness dependence, with values ranging from 1.86 x to to the -6/ohm. cm. for 300 angstrom film to 2.56 x 10 to the -1/ohm. cm. for a 2600 angstrom film. Measurement of the temperature dependence of the conductivity for these films showed complicated behavior which was thickness dependent. Thinner films showed at least two distinct temperature dependent conductivity mechanisms, as described by a Mott-type model. Thicker films showed only one principal conductivity mechanism, similar to what might be expected for a material with more crystalline character. Author

N86-11049# Naval Research Lab., Washington, D. C.
RENORMALIZATION OF AN INVERSE SCATTERING THEORY FOR INHOMOGENEOUS DIELECTRICS Memorandum Report
H. D. Ladouceur and A. K. Jordan Apr. 1985 28 p
(DA Proj. RR0-3302)
(AD-A156636) Avail: NTIS HC A03/MF A01 CSCL 20/3

Renormalized solutions are obtained for an inverse scattering problem that are equivalent to the second-order regular perturbation approximations for the exact theory (Gelfand-Levitan-Marchenko). We have developed an inversion method for reconstructing the permitivity profiles of inhomogeneous dielectric slabs from reflection coefficient data. Solutions with increased radii of convergence are obtained. Numerical examples are demonstrated for simulated scattering data from Gaussian, homogeneous slab and parabolic profiles. GRA

N86-11050# Oregon Graduate Center for Study and Research, Beaverton.
TRANSIENT VELOCITY ASSESSMENT IN GALLIUM ARSENIDE, AND OF OTHER GaAs CHARACTERISTICS RELATED TO DEVICE FUNCTIONS Semiannual Technical Report, Aug. 1984 - Feb. 1985
J. S. Blakemore and R. E. Kremer 10 Jun. 1985 41 p
(Contract MDA903-84-K-0374; ARPA Order 5020)
(AD-A156983; AD-E950724; Rept-71-521-SA-1) Avail: NTIS HC A03/MF A01 CSCL 20/12

Reports on the first six months of the program, with four tasks in two general areas. Concerning submicron GaAs devices and the possibility of high speed operation by velocity overshoot or ballistic mechanisms, tasks were to assemble the pertinent literature (now essentially done), and evaluate this - on which an interim evaluation is provided in the report to the effect that newly recognized scattering mechanisms make ballistic transport unlikely unless electron transit distances can be made less than some 100nm. This looks more feasible with vertically-oriented devices. The other two tasks were an assessment of literature and information concerning EL2 and other significant defect states in GaAs (for which a substantial data base has been assembled), and participation in collaborative activities directed towards optimization of evaluation techniques for GaAs wafers to be used for FET and related integrated circuit purposes. Work to date indicates that the local population of the EL2 midgap donor is likely to have a direct effect on FET properties. GRA

N86-11051# Stanford Linear Accelerator Center, Calif.
SUPERCONDUCTORS FOR PULSED RF ACCELERATORS
I. E. Campisi and Z. D. Parkas Apr. 1985 4 p Presented at the Particle Accelerator Conf., Vancouver, British Columbia, 13 May 1985
(Contract DE-AC03-76SF-00515)
(DE85-013378; SU-SLAC-PUB-3617; CONF-850504-67) Avail: NTIS HC A02/MF A01

The choice of superconducting materials for accelerator RF cavities has been determined in the past only in part by basic properties of the superconductors, such as the critical field, and to a larger extent by criteria which include fabrication processes, surface conditions, heat transfer capabilities and so on. For CW operated cavities the trend has been toward choosing materials with higher critical temperatures and lower surface resistance, from lead to niobium, from niobium to Nb3Sn. This trend has been dictated by the specific needs of storage ring CW system and by

the relatively low fields which could be reached without breakdown. The work performed on superconducting cavities using microsecond long high power RF pulses has shown that in Pb, Nb, and Nb3Sn, fields close to the critical magnetic fields can be reached without magnetic breakdown. DOE

N86-11052# Argonne National Lab., Ill.
FERMI SURFACE STUDY OF CeSb IN THE FERROMAGNETIC AND ANTIFERROMAGNETIC PHASES
H. Aoki, G. W. Crabtree, W. Joss, and F. Hulliger Feb. 1985 12 p Presented at the 5th Intern. Conf. on Crystalline Field Effects in f-Electron Systems: ICCF5
(Contract W-31-109-eng-38)
(DE85-012122; CONF-8504115-4) Avail: NTIS HC A02/MF A01

A de Haas-van Alphen effect study of CeSb in the intermediate field antiferromagnetic phase and in the high field ferromagnetic phase is reported. The results are discussed in the light of the p-f mixing model and a new weak coupling model based on a band structure calculation with localized f-orbitals. DOE

N86-11053# City Univ. of New York, N.Y.
MAGNETIC PROPERTIES OF DOPED SEMICONDUCTORS Progress Report, 1 Aug. 1984 - 31 Jul. 1985
M. P. Sarachik 1985 5 p
(Contract DE-FG02-84ER-45153)
(DE85-012090; DOE/ER-45153/1) Avail: NTIS HC A02/MF A01

The susceptibility of a series of boron-doped silicon samples with concentrations spanning the metal-nonmetal transition has been measured between 1.25K and 300K, and the magnetization has been measured to 50 kG. The magnetization of an insulating phosphorus-doped silicon sample is investigated, and the results are analyzed using the scaling theory of Bhatt and Lee. The assembly and testing of a Faraday balance is planned, as well as measurements of the Hall effect and magnetoresistance in pumped helium 4, and studies of thermoelectric power at low temperatures. DOE

N86-11054# Sandia Labs., Albuquerque, N. Mex.
SHOCK LOADING AND RELEASE BEHAVIOR OF X-CUT QUARTZ
L. C. Chabildas 1985 5 p refs Presented at Am. Phys. Soc. Topical Conf. on Shock Waves in Condensed Matter, Spokane, Wash., 22 Jul. 1985
(Contract DE-AC04-76DP-00789)
(DE85-013954; SAND-85-0149C; CONF-850736-6) Avail: NTIS HC A02/MF A01

Results of release-adiabat measurements are reported for shock-loaded x-cut quartz over the stress range of 15 GPa to 110 GPa. Release paths determined from a shock stress of 15 GPa indicate a return to the original density, while measurements of release adiabats from shock stresses over 50 GPa suggest release to be occurring primarily from and in the high density phase. Significant hysteretic effects are observed upon release and a retransformation to a low density phase is observed at lower stresses. Measurements of wave speeds in shocked quartz at stresses over 50 GPa indicate a decrease in wave speeds over the stress regime 71 to 108 GPa. DOE

N86-11055# Sandia Labs., Albuquerque, N. Mex.
HIGH-PRESSURE RELEASE-WAVE MEASUREMENTS AND PHASE TRANSFORMATION IN CaCO3
D. E. Grady 1985 13 p refs Presented at the Am. Phys. Soc. Topical Conf. on Shock Waves in Condensed Matter, Spokane, 22 Jul. 1985
(Contract DE-AC04-76DP-00789)
(DE85-012592; SAND-85-0148C; CONF-850736-2) Avail: NTIS HC A02/MF A01

Release-wave measurements on theoretical-density single crystal calcium carbonate from Hugoniot states of 11.5-, 17.0- and 26.5-GPa shock pressure were performed using time-resolved laser velocity interferometry diagnostics. Samples were subjected to planar impact with metal discs accelerated to high velocity using a powder gun facility. Motion was measured at a diffusely reflecting interface between the sample and lithium fluoride window material. Evidence for a high-pressure phase transformation between 12 and 14 GPa was provided from the 17.0- and 26.5-GPa experiments in terms of a well-defined rarefaction shock wave. The new phase may be a further metastable phase of calcite or identical to the high pressure state of argonite. DOE

N86-11056# Argonne National Lab., Ill.
ANELASTIC RELAXATION IN IRRADIATED Cu-Be
L. E. Rehn, H. Wiedersich, and A. V. Granato May 1985 5 p Presented at the Internal Friction and Ultrasonic Attenuation in Solids Conf., Urbana, Ill., 3 Jun. 1985 Prepared in cooperation with Illinois Univ., Urbana
(Contract W-31-109-eng-38)
(DE85-013893; CONF-8506125-3) Avail: NTIS HC A02/MF A01

Ultrasonic velocity measurements were made after thermal neutron irradiation of single-crystal Cu specimens containing 700 or 3700 appM Be. Ultrasonic attenuation was measured in similar specimens after 3 MeV electron irradiation. Three inelastic relaxation processes due to self-interstitial-Be complexes were observed. Cu-Be 1 was found to occur near liquid helium temperature; the temperature dependence of the velocity change suggests that reorientation of the Cu-Be 1 complex may involve quantum mechanical tunneling. Cu-Be produced an attenuation peak at approx. 2.5 K at a frequency of 10 MHz. Cu-Be 3 appeared simultaneously with 2 as a shoulder on the high temperature side of the 2.5 K attenuation peak. DOE

N86-11057# California Univ., Berkeley. Lawrence Berkeley Lab.
SURFACE SCIENCE AND CATALYSIS
G. A. Somorjai Feb. 1985 46 p refs Presented at the Royal Soc. Discussion Meeting, London, 28 Feb. 1985
(Contract DE-AC03-76SF-00098)
(DE85-013922; LBL-19139; CONF-850286-1) Avail: NTIS HC A03/MF A01

Modern surface science studies have explored a large number of metal catalyst systems. Three classes of catalytic reactions can be identified: (1) those that occur over the metal surface; (2) reactions that take place on top of a strongly adsorbed overlayer and (3) reactions that occur on co-adsorbate modified surfaces. Case histories for each class are presented. DOE

N86-10186# Bundesministerium fuer Forschung und Technologie, Bonn (West Germany).
GROWTH OF LARGER SINGLE CRYSTALS [ZUECHTUNG VON GROESSEREN EINKRISTALLEN]
Ruediger Jungbluth *In its* Satellite Use for Men 1985 p 30-32 In GERMAN (For primary document see N86-10180 01-12)
Avail: NTIS HC A03/MF A01

77 THERMODYNAMICS AND STATISTICAL PHYSICS

Includes quantum mechanics; and Bose and Fermi statistics.

For related information see also *25 Inorganic and Physical Chemistry* and *34 Fluid Mechanics and Heat Transfer.*

N86-11058 Rensselaer Polytechnic Inst., Troy, N. Y.
HEAT TRANSFER IN CONDENSING AND EVAPORATING TWO-COMPONENT, TWO-PHASE FLOW INSIDE A HORIZONTAL TUBE Ph.D. Thesis
Walter M. B. Duval 1984 111 p
Avail: Univ. Microfilms Order No. DA8509649

The effect of adding a small amount of oil to condensing and evaporation refrigerant R-12 following inside a horizontal tube is investigated both experimentally and analytically. Analytically, the problem is addressed assuming annular flow inside the tube. The analysis is based on the momentum and energy equations with the heat transfer in the liquid film determined using the Reynolds

analogy between turbulent heat and momentum transfer. Two separate methods are developed for extending this model to include the effects of the two-component nature of the flow. Experimentally, two-phase local heat transfer measurements and flow pattern visualization are made for both condensation and evaporation. From the measurements, correlations are developed to predict two-phase heat transfer for the range of 0%, 2% and 5% oil fraction by mass flow. Dissert. Abstr.

N86-11059*# Virginia Univ., Charlottesville. Dept. of Materials Science.
A STUDY OF THE APPLICABILITY OF NUCLEATION THEORY TO QUASI-THERMODYNAMIC TRANSITIONS OF SECOND AND HIGHER EHRENFEST-ORDER Annual Report
R. E. Barker, Jr. and K. W. Campbell Jul. 1985 75 p refs
(Grant NAG1-419)
(NASA-CR-176238; NAS 1.26:176238; UVA/528230/MS86/101) Avail: NTIS HC A04/MF A01 CSCL 20M

The applicability of classical nucleation theory to second (and higher) order thermodynamic transitions in the Ehrenfest sense has been investigated and expressions have been derived upon which the qualitative and quantitative success of the basic approach must ultimately depend. The expressions describe the effect of temperature undercooling, hydrostatic pressure, and tensile stress upon the critical parameters, the critical nucleus size, and critical free energy barrier, for nucleation in a thermodynamic transition of any general order. These expressions are then specialized for the case of first and second order transitions. The expressions for the case of undercooling are then used in conjunction with literature data to estimate values for the critical quantities in a system undergoing a pseudo-second order transition (the glass transition in polystyrene). Methods of estimating the interfacial energy gamma in systems undergoing a first and second order transition are also discussed. Author

N86-11060*# Virginia Univ., Charlottesville. Dept. of Materials Science.
A STUDY OF THE APPLICABILITY OF NUCLEATION THEORY TO QUASI-THERMODYNAMIC TRANSFORMATIONS OF SECOND AND HIGHER EHRENFEST-ORDER Status Report, 15 Dec. 1984 - 14 Jun. 1985
R. E. Barker, Jr. 14 Jun. 1985 31 p refs
(Grants NAG1-419; AF-AFOSR-0290-82)
(NASA-CR-176230; NAS 1.26:176230; UVA/5-28230; SAPR-2) Avail: NTIS HC A03/MF A01 CSCL 20M

Transient and steady-state phenomena in temperature, stress, and electric, field intensity in ferroelectric polymers were investigated. The application and extension of the theory in the primary stage to the polarization domain nucleation and growth in ferroelectric polymers were developed. The kinetics of this growth were investigated. Expressions describing nucleation under the influence of an electric field were found through the expansion of the Gibbs' free energy in a Maclaurin series. The series was expanded in the electric field strength rather than the degree of undercooling. The resulting expressions were manipulated and applied to the case of nucleation of polarized domains in ferroelectric polymers. The kinetics of the nucleation and growth of polarized domains are also investigated. This was accomplished through the modification of the Johnson-Mehl-Avrami treatment of crystallization kinetics to be applicable to the growth of polarization domains in ferroelectric materials. E.A.K.

N86-11061# Johns Hopkins Univ., Baltimore, Md. Dept. of Chemical Engineering.
THERMODYNAMICS OF POLYMER-SUPERCRITICAL SOLVENT MIXTURES Final Technical Report, Jul. 1983 - Jun. 1985
M. A. McHugh 3 Jul. 1985 6 p
(Contract N00014-83-K-0613)
(AD-A157038) Avail: NTIS HC A02/MF A01 CSCL 07/4

The objectives of this research are to experimentally investigate the high pressure fluid phase behavior of polymer solutions and to characterize the resultant phase behavior using contemporary polymer solution theories. The polymer solutions of interest are of three types: (1) a binary mixture of polymer and organic solvent; (2) a binary mixture of polymer and supercritical fluid (SCF) solvent; and (3) a ternary mixture of polymer, organic solvent, and SCF solvent. There are three goals of the experimental phase of this project. The first goal is to determine the effect of high pressure on the lower critical solution temperature (LCST) of the polymer-organic solvent mixture at conditions close to the critical point of the organic solvent. The second goal is to study the phase behavior of polymer - SCF solvent mixtures. The final experimental goal is to study the high pressure phase behavior of tenary mixtures consisting of a polymer, an organic solvent, and an SCF solvent. GRA

N86-11062# Massachusetts Univ., Amherst. Dept. of Physics and Astronomy.
RELATIVISTIC WAVEFUNCTION AT THE ORIGIN AND THE PION DECAY CONSTANT
E. Hagg and H. Suura [1985] 13 p Prepared in cooperation with Minnesota Univ., Minneapolis
(Contract DE-AC02-83ER-40105)
(DE85-012392; DOE/ER-40105/T3; COO-1764-408) Avail: NTIS HC A02/MF A01

A hybrid Breit-Salpeter amplitude related to f sub (PI) is finite at the origin if the full relativistic equation is solved. This leads to an unambiguous calculation of f sub (PI). It is shown that this finiteness of the wavefunction is due to a suppression of the Coulomb potential whereby the 1/r singularity at the origin is reduced to a logarithmic one. DOE

N86-11063# Texas Univ., Austin. Inst. for Fusion Studies.
LOCAL CONSERVATION LAWS FOR THE MAXWELL-VLASOV AND COLLISIONLESS KINETIC GUIDING CENTER THEORIES
D. Pfirsch and P. J. Morrison Apr. 1985 17 p
(Contract DE-FG05-80ET-53088)
(DE85-013122; DOE/ET-53088/177; IFSR-177) Avail: NTIS HC A02/MF A01

Using one of the recent variational formulations of the Maxwell-Vlasov and guiding center theories, the energy momentum and angular momentum tensors for such theories are derived and the corresponding local conservation laws are proven. The energy momentum tensor is shown to be symmetric in its spatial components while the angular momentum density is naturally antisymmetric. DOE

80 SOCIAL SCIENCES (GENERAL)

Includes educational matters.

N86-11064*# Old Dominion Univ., Norfolk, Va.
NASA/AMERICAN SOCIETY FOR ENGINEERING EDUCATION (ASEE) SUMMER FACULTY FELLOWSHIP PROGRAM, 1985
G. Goglia, comp. Sep. 1985 156 p refs
(Grant NGT-47-003-029)
(NASA-CR-177972; NAS 1.26:177972) Avail: NTIS HC A08/MF A01 CSCL 05I

Since 1964, the National Aeronautics and Space Administration (NASA) has supported a program of summer faculty fellowships for engineering and science educators. In a series of collaborations between NASA research and development centers and nearby universities, engineering faculty members spend 10 weeks working with professional peers on research. The Summer Faculty Program Committee of the American Society for Engineering Education supervises the programs. The objectives of this program are: (1) to further the professional knowledge of qualified engineering and science faculty members; (2) to simulate and exchange ideas between participants and NASA; (3) to enrich and refresh the research and teaching activities of participants institutions; and (4) to contribute to the research objectives of the NASA center. College or university faculty members will be appointed as research fellows to spend 10 weeks in cooperative research and study at the NASA Langley Research Center. The fellows will devote

approximately 90 percent of the time to a research problem and the remaining time to a study program. The study program will consist of lectures and seminars on topics of general interest or that are directly relevant to the fellows' research project. The lecturers and seminar leaders will be distinguished scientists and engineers from NASA, the educational community, or industry.
Author

N86-11065# George Mason Univ., Fairfax, Va. Dept. of Psychology.
AN ANNOTATED BIBLIOGRAPHY OF ABSTRACTS ON THE USE OF SIMULATORS IN TECHNICAL TRAINING
A. Ayres, R. T. Hays, M. J. Singer, and m. Heinicke Oct. 1984 555 p
(Contract MDA903-83-M-2646)
(AD-A156792; ARI-RP-84-21) Avail: NTIS HC A24/MF A01 CSCL 05/9

This document contains annotated abstracts of 149 selected papers from the literature on simulator training devices and programs. The abstracts are organized into two sections: abstracts of 83 empirical articles and abstracts of 66 theoretical articles. Each abstract is organized according to a standardized format, with the following headings: Authors; Title; Source; Topic keywords; Short summary; Device; Institution; Type of article. The purpose of these annotated abstracts is to effectively summarize, and not merely to describe or identify, the contents of the papers under review. The abstract will be entered into a computerized data base for future analyses. GRA

N86-11066# Amsterdam Univ. (Netherlands). Research Group for Science Dynamics.
MISSION ORIENTATION IN SCIENCE
W. vandenDaele May 1984 155 p refs Sponsored by Netherlands Ministry of Education and Sciences
Avail: NTIS HC A08/MF A01

A program to study social orientation and political direction of scientific development particularly in chemistry and ecology is outlined. Projects include adjustment of technological potentials to social priorities; technology development within universities; mission orientation in ecology; polyunsaturated fats; hybrid forms in the development of chemical toxicology; the conception of nature in ecosystems; and the concept of normative science.
Author (ESA)

81 ADMINISTRATION AND MANAGEMENT

Includes management planning and research.

N86-11067# Bundesministerium fuer Forschung und Technologie, Bonn (West Germany).
SPACE UTILIZATION [NUTZUNG DES WELTRAUMS]
Jan. 1985 64 p refs In GERMAN
Avail: NTIS HC A04/MF A01

The perspectives of the commercial utilization of space sciences are discussed. The scientific-technical user requirements in the field of astronautics till the end of the century are considered. The expenses of the Federal Ministry of Research and Technology (BMFT) in the field of space sciences are reviewed for the period 1983-1985. For individual titles, see N86-11068 through N86-11070.

N86-11068# Bundesministerium fuer Forschung und Technologie, Bonn (West Germany).
SPACE SCIENCES: PERSPECTIVES OF COMMERCIAL UTILIZATION FOR THE GERMAN INDUSTRY [WELTRAUMFORSCHUNG: PERSPEKTIVEN DER KOMMERZIELLEN NUTZUNG FUER DIE DEUTSCHE INDUSTRIE]
H. L. Jordan *In its* Space Utilization Jan. 1985 p 2-16 In GERMAN Presented at BDI Ausschuss fuer Forsch.- u. Wissenschaftspolitik, Bonn, 19 Oct. 1984 (For primary document see N86-11067 01-81)
Avail: NTIS HC A04/MF A01

Space sciences and their possible utilization by industry are presented. The development of astronautics and applications in observation techniques, communication, and navigation are reviewed. Utilization of reduced gravitational force effects: diffusion phenomena, crystal growth, production process for metals and composite materials, biochemistry, biotechnology, and biosciences are considered. Author (ESA)

N86-11069# Bundesministerium fuer Forschung und Technologie, Bonn (West Germany).
DFVLR, STRATEGIC STUDY OF ASTRONAUTICS 1984, USER REQUIREMENTS [DFVLR: STRATEGIESTUDIE RAUMFAHRT 1984, NUTZERBEDARF]
In its Space Utilization Jan. 1985 p 17-50 In GERMAN (For primary document see N86-11067 01-81)
Avail: NTIS HC A04/MF A01

In order to determine the scientific-technical requirements in the field of astronautics till the end of the century the disciplines which are used or are going to use astronautics are considered: extraterrestrial research, Earth observation, biosciences, materials sciences, telecommunication, navigation, and new applications. Astronomy, astrophysics, solar terrestrial relations, Sun and solar system, planets, and comets are discussed. Atmospheric physics and climate, meteorology, cartography and land use, oceans and ice geodesy, and reconnaissance are treated. Human physiology and medicine, space biology, gravity, radiology, exobiology, and biotechnology (bioprocessing) are discussed. Materials research and its applications; and the commercial market and technology program for telecommunication and navigation are presented. Solar energy utilization in orbit, waste treatment, orbital flow test stand, orbital laboratory for planet surface, and quarantine station for planet materials are discussed. Author (ESA)

N86-11070# Bundesministerium fuer Forschung und Technologie, Bonn (West Germany).
SPACE RESEARCH EXPENSES OF THE FEDERAL MINISTRY OF RESEARCH AND TECHNOLOGY (BMFT) IN THE PERIOD 1983-1985 [WELTRAUMFORSCHUNGSAUSGABEN DES BMFT IN 1983-1985]
In its Space Utilization Jan. 1985 p 51-62 In GERMAN (For primary document see N86-11067 01-81)
Avail: NTIS HC A04/MF A01

The expenses of the BMFT in space flight techniques, utilization of space laboratories and satellites, royalties for space transport, extraterrestrial basic research, operation of test stands, contribution to ESA, development of communication satellites, and DFVLR research are shown. Author (ESA)

N86-11071# Institute for Defense Analyses, Alexandria, Va.
REPORT OF THE AD HOC COMMITTEE TO REVIEW THE PROGRAM OF THE SDI DIRECTORATE ON INNOVATIVE SCIENCE AND TECHNOLOGY (IST) Final Report, Feb. - Apr. 1985
B. Balko Apr. 1985 16 p
(Contract MDA903-84-C-0031)
(AD-A156668; AD-E500720; IDA-M-83; IDA/HQ-85-29861) Avail: NTIS HC A02/MF A01 CSCL 15/3

Deliberations and conclusions are summarized of an ad hoc Committee to review the Innovative Science and Technology (IST) Directorate. Areas for programmatic emphasis, proposal selection, funding for individuals and consortia, and desirable budgetary levels are discussed. GRA

N86-11072# Research Inst. of National Defence, Stockholm (Sweden).
MANAGEMENT OF ORGANIZATIONAL OPERATIONS IN DYNAMIC ENVIRONMENTS TOWARDS A FRAME OF REFERENCE.
Roger Hagafors and Robert Allard Feb. 1985 25 p refs
(FOA-C5-85-0003-H2; ISSN-0347-7665) Avail: NTIS HC A02/MF A01

The premises, the structure and the process of managing

organizations are discussed. The organization is regarded as an open system and a dynamic environment model is assumed. The implications of the assumptions are described, and a frame of reference for analyzing the management situation is put forward. The hierarchical structure of organizations, the dimension of time in the management process, and the role of the management task, are discussed. Author (ESA)

N86-11073# Technische Hogeschool, Eindhoven (Netherlands). Dept. of Industrial Engineering.
ON THE STRUCTURE OF MANPOWER PLANNING, A CONTRIBUTION OF SIMULATION EXPERIMENTS WITH DECOMPOSITION METHODS
J. D. vanderBij, J. Wessels, and J. Wijngaard Aug. 1983 19 p refs
(Manpower-Planning-28) Avail: NTIS HC A02/MF A01

Manpower planning in a personnel system consisting of one personnel group, located in different organizational units is considered. The ease with which personnel availability can be matched to personnel requirement, when the flexibility within the personnel group is used is analyzed. This is done by comparing the performance of integrated planning, coordinated planning, and decomposed planning. Results are derived by simulation experiments. Author (ESA)

N86-11074# Technische Hogeschool, Eindhoven (Netherlands). Dept. of Industrial Engineering.
ASPECTS OF MANPOWER PLANNING AT A DUTCH UNIVERSITY, AN EXAMPLE OF AGGREGATION AND DECOMPOSITION METHODS IN MANPOWER PLANNING
N. Aerts, J. D. vanderBij, and J. Wessels Dec. 1983 41 p refs (Manpower-Planning-29) Avail: NTIS HC A03/MF A01

The choice of the categories for the medium term manpower planning in an organization is considered in a system with a simple personnel structure, consisting of two function groups on different hierarchical levels. An example of such a system is the research and teaching staff of a university, when only the two lowest function groups are considered. In this system the question can be posed whether two or more categories have to be distinguished for the medium term manpower planning or whether it is sufficient to distinguish one aggregate category. If two or more categories are distinguished, another question is which relationships between the categories are important for the medium term manpower planning. Simulation experiments with aggregation and decomposition methods show that model choice depends on costs. Author (ESA)

N86-11075# Technische Hogeschool, Eindhoven (Netherlands). Dept. of Industrial Engineering.
ON THE STRUCTURE OF MANPOWER PLANNING, A CONTRIBUTION OF SIMULATION EXPERIMENTS WITH AGGREGATION METHODS
J. D. vanderBij, J. Wessels, and J. Wijngaard Aug. 1983 24 p refs
(Manpower-Planning-30) Avail: NTIS HC A02/MF A01

Two ways to estimate the possibilities of matching manpower availability to manpower requirement in the organization activity plan of a task oriented unit of an organization are considered. One estimation procedure is based on detailed information about the personnel groups which are located in the task oriented unit. The other procedure is based on aggregate information about total availability and total personnel requirement in the whole unit. A situation for the case that steps are taken on the basis of detailed information and for the case that steps are taken on the basis of aggregate information was analyzed. Results show that use of aggregate information in drawing up personnel plans causes no extra problems if the maximum potential mobility is high or if future manpower requirements in personnel groups is highly correlated. Author (ESA)

N86-11076# Technische Hogeschool, Eindhoven (Netherlands). Dept. of Industrial Engineering.
FAILURES AND SUCCESSES OF QUANTITATIVE METHODS IN MANAGEMENT
C. B. Tilanus May 1984 18 p refs Presented at ORSA/TIMS Joint Natl. Meeting, San Diego, CA., 25-27 Oct. 1982, 15th Operational Res. Soc. of India Ann. Conv., Kharagpur, India, 9-11 Dec. 1982, and Netherlands Soc. of Statistics and Operations Res. Ann. Conf., Eindhoven, Netherlands, 31 Mar. 1983 Revised (ARW-03-THE-BDK/ORS/83-06) Avail: NTIS HC A02/MF A01

About 60 cases of failures and successes of quantitative methods in management, collected in industry, business and government are analyzed for features determining failure or success. Author (ESA)

N86-11077# Institute for Perception RVO-TNO, Soesterberg (Netherlands). Experimental Psychology Group.
RISK PROPENSITY, ACTION READINESS AND THE ROLES OF SOCIETAL AND INDIVIDUAL DECISION MAKERS
S. Lichtenstein, W. A. Wagenfar, G. B. Keren, and T. W. vanderSchaaf Aug. 1984 21 p refs Sponsored by Central Organization TNO
(IZF-1984-27; TDCK-79524) Avail: NTIS HC A02/MF A01

Decision making by public officials and citizens was compared by eliminating different socio-economic backgrounds and different available information; to investigate the effects of adopting one role or the other (societal vs individual). Dependent measures were the willingness to choose a risky option vs a sure outcome, and the readiness to take explicit action or not. A total of 478 student subjects read the same cover story which deals with the decision problem of how to limit the number of victims of an epidemic. The results (choices and reasons) show that societal decision makers are less likely than individuals to take explicit action. Taking action is more often preferred when associated with the risky option than with the sure outcome. The large majority of subjects justify their choice on the basis of the number of victims. Results are discussed in terms of framing. Author (ESA)

82 DOCUMENTATION AND INFORMATION SCIENCE

Includes information storage and retrieval technology; micrography; and library science.

For computer documentation see *61 Computer Programming and Software.*

N86-11078# R-K Research and System Design, Malibu, Calif.
ANNOTATED BIBLIOGRAPHY OF PUBLICATIONS DEALING WITH OCCUPATIONAL HEALTH AND MEDICAL INFORMATION SYSTEMS, COST ANALYSIS PROCEDURES, EVALUATION METHODOLOGY AND RELATED LEGAL ISSUES
1984 43 p
(Contract N00014-84-C-0601)
(AD-A156650) Avail: NTIS HC A03/MF A01 CSCL 06/10

The purpose of this selective bibliography is to provide a sense of the scope of the literature relevant to the subject matter of interest in this project to test and evaluate the Navy Occupational Health Information Management System (NOHIMS). The intent has been to describe the contents of each reference in sufficient detail so that a decision could be made whether or not to obtain a copy of the complete article. Articles are taken from journals such as The New England Journal of Medicine, Proceedings of the Fifth Annual Symposium on Computer Applications in Medical Care, Journal of Occupational Medicine, Navy Lifeline and Science. Topics cover a variety of topics such as liability for personal injuries caused by defective medical computer programs, computers in medical care, mental health information systems, COSTAR, Environmental Health Systems, and Medical surveillance requirements. GRA

N86-11079# Naval Postgraduate School, Monterey, Calif.
A SYSTEMS DEVELOPMENT LIFE CYCLE STUDY OF THE INFORMATION CENTER M.S. Thesis
M. L. Lechleitner Mar. 1985 133 p

(AD-A156977; AD-E950724) Avail: NTIS HC A07/MF A01 CSCL 05/2

End user computing has penetrated most large organizations in an uncontrolled fashion. The newness of the technology, the lack of management expertise, and the inability to gain corporate-wide control under the traditional organizational structure have often resulted in inefficiency, incompatibility, and missed opportunities. One solution to this situation is the Information Center (IC). ICs are centralized coordination centers for end user computing and offer end user computer expertise. ICs may be any combination of consulting services, training services, mainframe computer terminals, or microcomputers. This thesis examines the IC concept from the viewpoint of the manager tasked with implementation and provides a methodology, the Systems Development Life Cycle, to evaluate and implement an IC. Each phase of the methodology is explained and some innovative ideas on IC implementation and operation are provided. Examples of past successes and mistakes are also presented. GRA

N86-11080# California Univ., Livermore. Lawrence Livermore Lab.

WRITER/EDITOR AND THE COMPUTER

B. R. Smith Apr. 1985 7 p Presented at Forum 85, Helsingor, Denmark, 26 Aug. 1985

(Contract W-7405-eng-48)

(DE85-011843; UCRL-92525; CONF-850864-1) Avail: NTIS HC A02/MF A01

Computer development in the publications process is discussed. Authors and editors of scientific and engineering documents felt the impact in adverse and beneficial ways. When the computer entered the scene, the writer/editor had to learn different hardware systems to try to keep up with the software explosion. An innate flexibility and specialized knowledge of how to get a document into the best form for its specific audience quaranteed the writer/editor's survival. The experiences of writer/editors in one scientific laboratory are reviewed. The experiences typify challenges the forward-moving manager of a technical document production system can expect to encounter. DOE

N86-11081# Technische Hogeschool, Delft (Netherlands). Afd. der Scheikundige Technologie.

ACQUAINTANCE WITH ON LINE LITERATURE RESEARCH. AN INTRODUCTION FOR EDUCATION AT THE CHEMICAL TECHNOLOGY SECTION [KENNISMAKING MET ONLINE LITERATUUR-ONDERZOEK. EEN INLEIDING BIJ HET ONDERWIJS AAN DE AFDELING PER SCHEIKUNDIGE TECHNOLOGIE]

L. Maat, C. A. G. Konings, and M. VandenHondel Feb. 1985 39 p In DUTCH

Avail: NTIS HC A03/MF A01

A manual for automated information retrieval in international (bio-) chemical data banks is presented. The indexing elements (keywords, classification systems), searching language and search profile are discussed and explained. Accessible databanks (Chemical- and Biological Abstracts, Science Citation Index) are surveyed. Author (ESA)

N86-11082# Executive Office of the President, Washington, D.C.

PUBLICATION OF THE EXECUTIVE OFFICE OF THE PRESIDENT, JANUARY 20, 1981 - DECEMBER 31, 1984

1985 7 p

(PB85-187110) Avail: NTIS HC A02/MF A01 CSCL 05B

The bibliography lists the documents issued by the components of the Executive Office of the President, and are available for sale to the public. GRA

83 ECONOMICS AND COST ANALYSIS

Includes cost effectiveness studies.

No abstracts in this category.

84 LAW AND POLITICAL SCIENCE

Includes space law; international law; international cooperation; and patent policy.

No abstracts in this category.

85 URBAN TECHNOLOGY AND TRANSPORTATION

Includes applications of space technology to urban problems; technology transfer; technology assessment; and surface and mass transportation.

For related information see *03 Air Transportation and Safety, 16 Space Transportation,* and *44 Energy Production and Conversion.*

N86-11083*# Jet Propulsion Lab., California Inst. of Tech., Pasadena.

ADVANCED VEHICLE SYSTEMS ASSESSMENT. VOLUME 2: SUBSYSTEMS ASSESSMENT

K. Hardy Mar. 1985 167 p refs For Volume 1, see N85-28887 5 Vol.

(Contract NAS7-918; JPL Proj. 5030-573; Contract DE-AI01-78CS-54209)

(NASA-CR-176205; JPL-5030-573-Vol-2; JPL-Pub-84-79-Vol-2; NAS 1.26:176205; DOE/CS-54209/22-Vol-2) Avail: NTIS HC A08/MF A01 CSCL 13F

Volume 2 (Subsystems Assessment) is part of a five-volume report entitled Advanced Vehicle Systems Assessment. Volume 2 presents the projected performance capabilities and cost characteristics of applicable subsystems, considering an additional decade of development. Subsystems of interest include energy storage and conversion devices as well as the necessary powertrain components and vehicle subsystems. Volume 2 also includes updated battery information based on the assessment of an independent battery review board (with the aid of subcontractor reports on advanced battery characteristics). Author

N86-11084*# Jet Propulsion Lab., California Inst. of Tech., Pasadena.

ADVANCED VEHICLE SYSTEMS ASSESSMENT. VOLUME 3: SYSTEMS ASSESSMENT

K. Hardy Mar. 1985 292 p refs For Volume 1, see N85-28887 5 Vol.

(Contract NAS7-918; JPL Proj. 5030-573; Contract DE-AI01-78CS-54209)

(NASA-CR-176206; JPL-5030-573-Vol-3; JPL-Pub-84-79-Vol-3; NAS 1.26:176206; DOE/CS-54209/22-Vol-3) Avail: NTIS HC A08/MF A01 CSCL 13F

The systems analyses integrate the advanced component and vehicle characteristics into conceptual vehicles with identical performance (for a given application) and evaluates the vehicles in typical use patterns. Initial and life-cycle costs are estimated and compared to conventional reference vehicles with comparable technological advances, assuming the vehicles will be in competition in the early 1990s. Electric vans, commuter vehicles, and full-size vehicles, in addition to electric/heat-engine hybrid and fuel-cell powered vehicles, are addressed in terms of performance

and economics. System and subsystem recommendations for vans and two-passenger commuter vehicles are based on the economic analyses in this volume. Author

N86-11085*# Jet Propulsion Lab., California Inst. of Tech., Pasadena.
ADVANCED VEHICLE SYSTEMS ASSESSMENT. VOLUME 4: SUPPORTING ANALYSES
K. Hardy Mar. 1985 125 p refs For Volume 1, see N85-28887 5 Vol.
(Contract NAS7-918; JPL Proj. 5030-573; Contract DE-AI01-78CS-54209)
(NASA-CR-176207; JPL-5030-573-Vol-4; JPL-Pub-84-79-Vol-4; NAS 1.26:176207; DOE/CS-54209/22-Vol-4) Avail: NTIS HC A08/MF A01 CSCL 13F

Volume 4 (Supporting Analyses) is part of a five-volume report, Advanced Vehicle Systems Assessment. Thirty-nine individuals, knowledgeable in advanced technology, were interviewed to obtain their preferences. Rankings were calculated for the eight groups they represented, using multiplicative and additive utility models. The four topics for consideration were: (1) preferred range for various battery technologies; (2) preferred battery technology for each of a variety of travel ranges; (3) most promising battery technology, vehicle range combination; and (4) comparison of the most preferred electric vehicle with the methanol-fuled, spark-ignition engine vehicle and with the most preferred of the hybrid vehicles. G.L.C.

N86-11086*# Jet Propulsion Lab., California Inst. of Tech., Pasadena.
ADVANCED VEHICLE SYSTEMS ASSESSMENT. VOLUME 5: APPENDICES
K. Hardy Mar. 1985 615 p For Volume 1, see N85-28887 5 Vol.
(Contract NAS7-918; JPL Proj. 5030-573; Contract DE-AI01-78CS-54209)
(NASA-CR-176208; JPL-5030-573-Vol-5; JPL-Pub-84-79-Vol-5; NAS 1.26:176208; DOE/CS-54209/22-Vol-5) Avail: NTIS HC A08/MF A01 CSCL 13F

An appendix to the systems assessment for the electric hybrid vehicle project is presented. Included are battery design, battery cost, aluminum vehicle construction, IBM PC computer programs and battery discharge models. G.L.C.

N86-11087*# Garrett Mfg. Ltd., Rexdale (Ontario).
ADVANCED GAS TURBINE (AGT) POWERTRAIN SYSTEM DEVELOPMENT FOR AUTOMOTIVE APPLICATIONS REPORT Semiannual Progress Report, Jan. - Jun. 1984
Dec. 1984 112 p refs
(NASA-CR-174886; DOE/NASA/0167-9; NAS 1.26:174886; Rept-31-3725(9); SAPR-9) Avail: NTIS HC A06/MF A01 CSCL 13F

This report describes progress and work performed during January through June 1984 to develop technology for an Advanced Gas Turbine (AGT) engine for automotive applications. Work performed during the first eight periods initiated design and analysis, ceramic development, component testing, and test bed evaluation. Project effort conducted under this contract is part of the DOE Gas Turbine Highway Vehicle System Program. This program is oriented at providing the United States automotive industry the high-risk long-range techology necessary to produce gas turbine engines for automobiles with reduced fuel consumption and reduced environmental impact. Technology resulting from this program is intended to reach the marketplace by the early 1990s. B.W.

N86-11088# Westat Research, Inc., Rockville, Md.
ACADEMIC RESEARCH EQUIPMENT IN SELECTED SCIENCE-ENGINEERING FIELDS, 1982-83. AN ANALYSIS OF FINDINGS FROM THE BASELINE NATIONAL SURVEY OF ACADEMIC RESEARCH INSTRUMENTS AND INSTRUMENTATION NEEDS
Kenneth Burgdorf and Howard J. Hausman Aug. 1985 221 p refs
(Grant NSF SRS-80-17873)
Avail: NTIS HC A10/MF A01

This report presents information from the two-phase baseline cycle of the National Science Foundation's (NSF's) National Survey of Academic Research Instruments and Instrumentation Needs. Phase 1, conducted in early 1983 with reference to instrumentation existing on December 31, 1982, involved collection of instrument-related data from physical and computer science and engineering departments at a stratified probability sample of 43 universities. The following year, in phase 2 data pertaining to 1983 instrumentation were collected for the agricultural, biological and environmental sciences at the same 43 universities. Phase 2 also included biological science departments (not clinical departments) at a stratified probability sample of 24 medical schools. In each phase, (1) department and facility administrators were surveyed to ascertain their equipment-related activities, needs and priorities, and (2) samples of existing research equipment were selected and the responsible faculty investigators were asked to provide information about each item's age, condition, cost, usage, etc. The resulting data bases contain questionnaire responses from over 900 department and facility heads and for over 10,000 individual items of research equipment. B.W.

N86-11089# National Aerospace Lab., Amsterdam (Netherlands).
AEROSPACE RESEARCH AT NLR
1984 39 p Original contains color illustrations
Avail: NTIS HC A03/MF A01

The NLR fluid dynamics, flight, structures and materials, space, and engineering and technical services divisions activities are presented. Research covers wind tunnel tests, computational aerodynamics, unsteady aerodynamics, aeroacoustics, propulsion systems, flight tests, aircraft performance assessment, human factors engineering, aircraft structures, aircraft loads, fatigue and corrosion, engine tests, satellite attitude control and ground operations, microgravity effects, robotics, and signal processing. Author (ESA)

N86-11090# National Aerospace Lab., Amsterdam (Netherlands). Ruimtevaartlab.
[ACTIVITIES REPORT OF THE SPACE FLIGHT LABORATORY] Annual Report, 1982 [VERSLAG OVER HET JAAR]
1983 127 p refs In DUTCH; ENGLISH summary Original contains color illustrations
Avail: NTIS HC A07/MF A01

Aerodynamics, flight, structures and materials, spaceflight technology, computer, remote sensing, and environment and energy supply research is summarized. Wind tunnel model investigations with turbo-powered simulators and remote sensing data processing are described. Activities in the German Dutch Windtunnel, European Transonic Windtunnel, the Group for Aeronautical Research and Technology in Europe, and cooperation with Indonesia are discussed. Author (ESA)

N86-11091# National Aerospace Lab., Amsterdam (Netherlands). Ruimtevaartlab.
[ACTIVITIES REPORT OF THE SPACE FLIGHT LABORATORY] Annual Report, 1983 [VERSLAG OVER HET JAAR 1983]
1984 126 p refs In DUTCH; ENGLISH summary Original contains color illustrations
Avail: NTIS HC A07/MF A01

Aerodynamics, flight, structures and materials, spaceflight and remote sensing, applied informatics, and environment and energy supply research is summarized. Helicopter-ship qualification testing, and design and manufacture of large wind-tunnel models are described. Activities of the Netherlands Agency of Aerospace Programs, and international cooperation such as the Advisory Group for Aerospace Research and Development, the German Dutch Windtunnel, European Transonic Windtunnel, the Group for Aeronautical Research and Technology in Europe and cooperation with Indonesia are discussed. Author (ESA)

N86-10586# Shock and Vibration Information Center (Defense), Washington, D. C.

EDITORS RATTLE SPACE
Ronald E. Eshleman, ed. *In its* The Shock and Vibration Digest, Vol. 17, No. 3 Mar. 1985 p 2 (For primary document see N86-10585 01-39)
Avail: SVIC, Code 5804, Naval Research Lab., Washington, D.C. 20375 CSCL 05/2

88 SPACE SCIENCES (GENERAL)

No abstracts in this category.

89 ASTRONOMY

Includes radio and gamma-ray astronomy; celestial mechanics; and astrometry.

N86-11092 Wyoming Univ., Laramie.
THE TWO MICRON SPECTRUM OF R SCUTI Ph.D. Thesis
David Mozurkewich 1984 195 p
Avail: Univ. Microfilms Order No. DA8508874

High-resolution two micron spectrograms of R Scuti, the brightest RV Tauri variable, were obtained to study the mass loss rate and the kinematics of the star's circumstellar material. These observations include atomic lines as well as molecular bands of CO, H2O and OH. There are four major results of this research. (1) The atomic velocities execute a continuous velocity curve with a period of 145 days, twice the period of the discontinuous velocity curve determined from the visible spectrum. (2) The star is surrounded by two circumstellar layers. One is at a temperature of 2200K and is falling toward the star at 13 Km/s. The second is at 1000K and is stationary. The mass of the infalling layer is about 10 to the -5 power solar mass. The stationary shell is a factor of ten larger. (3) Atomic and molecular emission are visible in most of the spectra, apparently originating in an extended envelope surrounding the star. This envelope is at approximately 3000K and contains 3 x 10 to the -7 power solar mass. (4) There are occasional outbursts during which material is expelled from the star at less than escape velocity. This material presumably fuels both the infalling layer of CO and the circumstellar emission. Dissert. Abstr.

N86-11093 Brandeis Univ., Waltham, Mass.
RADIO STUDIES OF A COMPLETE SAMPLE OF QUASARS Ph.D. Thesis
Robert Ira Potash 1985 195 p
Avail: Univ. Microfilms Order No. DA8509832

Fifty-seven quasars were observed with the NRAO 3 element interferometer. Fifty-two of the quasars comprise a complete radio/optical sample, consisting of all quasars in a particular area of sky with radio and optical flux denities above specified limits (Schmidt 1976). Radio structures were determined at lambda 3.7 and 11.1 cm. These data were combined with data from other complete samples to perform statistical studies of quasar linear sizes. The correlation between size and redshift is demonstrated. The quasar distribution is assumed separable into a space density function, optical, and radio (color) distributions. These distributions are derived for different linear size ranges. The results favor but do not prove an underlying size-radio luminosity relation. Dissert. Abstr.

N86-11094# Royal Observatory, Edinburgh (Scotland).
OPTICAL/IR TELESCOPE ARRAYS: A STUDY OF THEIR POTENTIAL FOR SATISFYING OBSERVATIONAL REQUIREMENTS IN ASTRONOMY FOR A LARGE APERTURE SYSTEM IN THE 1990s AND BEYOND
C. M. Humphries, D. J. Walshaw, V. C. Reddish, and A. H. Greenaway 1984 140 p refs
(Rept-15; ISSN-0309-099X) Avail: NTIS HC A07/MF A01

The diffuse light received from the sky background and the angular proximity of resolved faint sources both act as constraints against which astronomical observations are made. Existing ground-based optical telescopes operate successfully at source faintness levels where at visible wavelengths the signal to be extracted is only about one per cent of that due to the sky background. At infrared wavelengths, where sky background levels are much higher, sky-chopping allows this ratio to be extended to approx. 10 to 3d power - 10 to the 6th power. The rate at which such information can be obtained is determined almost entirely by telescope aperture and it is unlikely that telescopes being used today will continue to satisfy observational needs. Large aperture optical telescopes improve angular resolution. The sensitivity (i.e., limiting magnitude) at which ground-based interferometric measurements are made, is also dependent on telescope aperture, whereas angular resolution is determined by the length of the baseline between separate phased apertures. With an array (or multiple-mirror) telescope, the aperture synthesis technique used routinely in radioastronomy becomes a possibility also at optical and infrared wavelengths. F.M.R.

N86-11095*# Alabama Univ., Birmingham. Dept. of Physics.
THEORETICAL ANALYSIS OF WOLTER/LSM X-RAY TELESCOPE SYSTEMS Final Report, 1 Oct. 1984 - 26 May 1985
D. L. Shealy and S. Chao 26 May 1985 57 p refs
(NASA Order H-78183-B)
(NASA-CR-176244; NAS 1.26:176244) Avail: NTIS HC A04/MF A01 CSCL 03A

A ray tracing analysis has been performed for the spectral slicing zoom X-ray telescope for configurations in which a convex layered synthetic microstructure (LSM) optic is placed in front of the prime focus or a concave LSM optic is placed behind the prime focus. The analysis has considered the geometrical shape of the LSM optic to be either a hyperboloid, sphere, ellipsoid or constant optical path aspheric element for two configurations of the glancing incidence X-ray telescope: the ATM Experimental S-056 Wolter I system and the Stanford/MSFC Wolter-Schwarzchild nested system. For the different systems the RMS blur circle radii, the point spread function (PSF), the full width half maximum (FWHM) of the PSF have been evaluated as a function of field angle and magnification of the secondary to determine resolution of the system. The effects of decentration and tilt of the selected LSM element on the performance of the system have been studied to determine mounting and alignment tolerances. B.W.

N86-11096# European Space Agency, Paris (France).
COLLOQUIUM ON KILOMETRIC OPTICAL ARRAYS IN SPACE
N. Longdon, ed. and O. Melita, ed. Apr. 1985 196 p refs Proc. held at Cargese, Corsica, 23-25 Oct. 1984; sponsored by ESA and Centre d'Etudes et de Recherches Geodynamiques et Astronomiques
(ESA-SP-226; ISSN-0379-6566) Avail: NTIS HC A09/MF A01

The use of configurations of two or three satellites to constitute a kilometric optical array in space was discussed. Scientific goals, image reconstruction, aperture synthesis, and lessons from radio astronomy were considered. For individual titles, see N86-11097 through N86-11126.

N86-11097# Centre d'Etudes et de Recherches Geodynamiques et Astronomiques, St. Vallier de Thiey (France).
RESULTS AND LIMITATIONS OF GROUND-BASED OPTICAL ARRAYS
A. Labeyrie *In* ESA Colloq. on Kilometric Opt. Arrays in Space Apr. 1985 p 1-6 refs (For primary document see N86-11096 01-89)
Avail: NTIS HC A09/MF A01

The usefulness and limits of ground based interferometers for astronomy are discussed, and current and planned systems are described. While optical arrays do work on the ground, and can probably reach baselines on the order of 300 m, their observing

efficiency and limiting magnitude are greatly affected by the turbulent atmosphere, as well as their capability to generate reconstructed images. At a cost comparable to the planned VLT array, floating arrays of two or more small apertures in space can reach higher limiting magnitudes and produce more results in a given time. With large component apertures, and many of them, floating arrays are bound to enormously increase optical penetration into the universe. The wider spectral window in space is also of interest in image reconstruction. Author (ESA)

N86-11098# Padua Univ. (Italy). Ist. di Astronomia.
EXTRAGALACTIC OBSERVATIONS WITH OPTICAL SPACE ARRAYS
E. Bertola *In* ESA Colloq. on Kilometric Opt. Arrays in Space Apr. 1985 p 7-9 refs (For primary document see N86-11096 01-89)
Avail: NTIS HC A09/MF A01

Results achievable by optical arrays in space with resolution of 0.000001 arcsec are assessed from theoretical models predicting small scale features, and VLBI radio domain results. Extragalactic topics which could be investigated by a space interferometer allowing, in addition to high resolution imaging, the possibility of precise measurements of proper motions and parallaxes in nearby galaxies, are reviewed. Objects such as HII regions and supernovae in external galaxies, as well as the broad line region in Seyfert's and QSO's are good candidates for interferometric observations, while interesting effects caused by gravitational lenses can be detected. Author (ESA)

N86-11099# Cambridge Univ. (England). Inst. of Astronomy.
ASTRONOMICAL CRITERIA FOR INTERFEROMETRIC ARRAYS
Edward Kibblewhite *In* ESA Colloq. on Kilometric Opt. Arrays in Space Apr. 1985 p 13-16 (For primary document see N86-11096 01-89)
Avail: NTIS HC A09/MF A01

The effect of Michelson stellar interferometric arrays on spacecraft design is discussed. Almost all sources that can be resolved by kilometer baseline interferometers are bright. Most active galaxies and QSO's contain a compact object which enables the amplitude and phase of features in weak spectral lines to be measured to a few per cent even with the simplest spacecraft. Many of the most interesting stars and binary systems need at least kilometer baselines to obtain adequate spatial resolution across their disks but also rotate with periods of hours or days. This greatly complicates the design of the spacecraft and means two telescope interferometers may only have limited usefulness in obtaining star spot pictures. However, accurate diameters can be measured in a few hours and the spacecraft could obtain submicroarcsecond astrometry on certain classes of object. Other considerations dictate the use of high orbits and relatively long observation times for first generation interferometers in space. Author (ESA)

N86-11100# Paris VII Univ. (France).
HIGH ANGULAR RESOLUTION IN THE INFRARED: PROSPECTS FOR SPACE OBSERVATIONS
P. Lena *In* ESA Colloq. on Kilometric Opt. Arrays in Space Apr. 1985 p 17-21 refs (For primary document see N86-11096 01-89)
Avail: NTIS HC A09/MF A01

The growth of high angular resolution (sub arc second) programs in infrared astronomy (from 1 to 1000 microns) is discussed. Ground based programs (speckle or two-telescope interferometry) are reviewed. It is shown that interferometry in space will improve the sensitivity, extend the wavelength coverage, and open a new field in astrophysics, even with current detector and system performances, and with only a 50 m baseline. Author (ESA)

N86-11101# Centre d'Etudes et de Recherches Geodynamiques et Astronomiques, St. Vallier de Thiey (France).
STRATEGY FOR THE DEVELOPMENT OF SPACE ARRAYS
A. Labeyrie *In* ESA Colloq. on Kilometric Opt. Arrays in Space Apr. 1985 p 23-25 refs (For primary document see N86-11096 01-89)
Avail: NTIS HC A09/MF A01

The development of large telescopes in space is discussed. Rigid and floating arrays are attractive. For a modest price increase, a four aperture floating array is much faster, more reliable, and considerably facilitates image reconstruction. Rather than waiting for support from the space agencies, a World Agency for Space Observatories should be created and provided with funds for developing space arrays. Technology tests should start as soon as possible aboard shuttle flights. Author (ESA)

N86-11102# Centre d'Etudes et de Recherches Geodynamiques et Astronomiques, St. Vallier de Thiey (France).
TRIO: A KILOMETRIC ARRAY STABILIZED BY SOLAR SAILS
A. Labeyrie, B. Authier, Th. Degraauw, E. Kibblewhite, and G. Weigelt *In* ESA Colloq. on Kilometric Opt. Arrays in Space Apr. 1985 p 27-33 refs (For primary document see N86-11096 01-89)
Avail: NTIS HC A09/MF A01

A spaceborne optical array (TRIO) consisting of 2 to 4 telescopes spaced up to 1000 m apart, at Lagrange point 5 of the Earth-Moon trajectory is described. For kilometric baselines and variable aperture patterns allowing image reconstructions, TRIO has free flying telescopes and a focal station. Small solar sails point and stabilize the system. Electrostatic mounts support the telescopes. Many apertures can be utilized in later versions. Author (ESA)

N86-11103*# National Aeronautics and Space Administration. Goddard Space Flight Center, Greenbelt, Md.
SAMSI: AN ORBITING SPATIAL INTERFEROMETER FOR MICRO-ARC SECOND ASTRONOMICAL OBSERVATIONS
R. V. Stachnik (Harvard Smithsonian Center for Astrophysics, Cambridge, Mass.) and D. Y. Gezari *In* ESA Colloq. on Kilometric Opt. Arrays in Space Apr. 1985 p 35-42 refs (For primary document see N86-11096 01-89)
(Contract NASw-3755; Grant NsG-7176)
Avail: NTIS HC A09/MF A01 CSCL 03A

The concept and performance of (SAMSI) Spacecraft Array for Michelson Spatial Interferometry, an orbiting spatial interferometer comprised of three free-flying spacecraft, two collector telescopes and a central mixing station are described. In the one-dimensional interferometry mode orbits exist which provide natural scanning of the baseline. These orbits place extremely small demands on thrusters and fuel consumption. Resolution of 0.00001 arcsecond and magnitude limits of mv = 15 to 20 are achievable in a single orbit. In the imaging mode, SAMSI could synthesize images equivalent to those produced by equal diameter filled apertures in space, making use of the fuel resupply capability of a space station. Simulations indicate that image reconstruction can be performed with milliarcsecond resolution to a visual magnitude 12 in 12 hr of spiral scanning integration time. Author (ESA)

N86-11104*# Harvard-Smithsonian Center for Astrophysics, Cambridge, Mass.
COSMIC: A HIGH RESOLUTION, LARGE COLLECTING AREA TELESCOPE
W. A. Traub and N. P. Carleton *In* ESA Colloq. on Kilometric Opt. Arrays in Space Apr. 1985 p 43-48 refs (For primary document see N86-11096 01-89)
(Grant NsG-7176)
Avail: NTIS HC A09/MF A01 CSCL 03A

The spaceborne Coherent Optical System of Modular Imaging Collectors (COSMIC) is presented. It has high angular resolution and can produce images of complex, low-surface-brightness objects such as distant galaxies. If configured as a 36 m filled linear array, COSMIC can have 15 times better angular resolution and 10 times greater collecting area than the Space Telescope. Alternatively, if the collecting area is spread out to create an unfilled two-dimensional array, there is the additional advantage of not needing to rotate the array in order to build up a reconstructed image. Considerations which led to the design

concept, scientific goals, and the potentially useful role of a space station for assembly are discussed. Author (ESA)

N86-11105# Centre National de la Recherche Scientifique, Verrieres-Le Buisson (France). Service d'Aeronomie.
A FIBER-LINKED VERSION OF PROJECT TRIO
P. Connes, Cl. Froehly (Limoges University, France), and P. Facq (Limoges University, France) *In* ESA Colloq. on Kilometric Opt. Arrays in Space Apr. 1985 p 49-61 refs (For primary document see N86-11096 01-89)
Avail: NTIS HC A09/MF A01

It is shown that the TRIO spaceborne telescope array can be simplified by using two equal-length single-mode fibers to connect the two telescopes to the central station. The price to be paid is mostly a reduction of base-length at the short wavelength end of the spectrum. The number of parameters to be accurately controlled is much reduced: one merely has to guide telescopes and null path-difference. All motions of the central station become irrelevant. Star acquisition is performed in a docked configuration of all three elements. The necessary cables may also be used to feed power to the two telescopes; hence these require neither power generating nor propulsion devices. Possible base line scanning methods either in high orbits (e.g., at the Lagrange points) or in low orbits are discussed. Author (ESA)

N86-11106# Royal Greenwich Observatory, Herstmonceux (England).
OASIS: OPTICAL APERTURE SYNTHESIS IN SPACE
J. E. Noordam, P. D. Atherton (Groningen University, Netherlands), and A. H. Greenaway (Royal Signals and Radar Establishment, Malvern, UK) *In* ESA Colloq. on Kilometric Opt. Arrays in Space Apr. 1985 p 63-69 (For primary document see N86-11096 01-89)
Avail: NTIS HC A09/MF A01

Techniques necessary to accomplish optical aperture synthesis in space (OASIS) are described. The purpose of OASIS is to obtain reliable, high resolution images of astronomical sources, in emission lines, absorption lines, and the continuum, with high dynamic range. Redundant spacing calibration allows the identification of phase and amplitude errors associated with a particular telescope in an array. This requires the separate availability of the visibility phase and amplitude for all interferometers (telescope pairs). Issues which determine the design and feasibility of the technique are discussed. Author (ESA)

N86-11107# Perkin-Elmer Corp., Danbury, Conn.
FUTURE SPACE TELESCOPE DESIGN CONCEPTS
Alan N. Bunner *In* ESA Colloq. on Kilometric Opt. Arrays in Space Apr. 1985 p 71-76 refs (For primary document see N86-11096 01-89)
Avail: NTIS HC A09/MF A01

Five generically-different approaches to a high resolution, high sensitivity space telescope covering the options of focal and afocal collectors, filled apertures and dilute apertures and one-dimensional and two-dimensional arrays are described. These concepts are compared, given equal collecting area and equal observing time, on the basis of angular resolution and sensitivity to faint point sources and extended sources in the presence of photon statistics, zodical background light, and other sources in the field. Technology development issues involved in the realization of advanced telescopes are listed. Author (ESA)

N86-11108# Centre National de la Recherche Scientifique, Marseilles (France). Lab. d'Astronomie Spatiale.
TRIO OPTICS
B. Authier, P. Rabout, and A. Labeyrie *In* ESA Colloq. on Kilometric Opt. Arrays in Space Apr. 1985 p 79-84 refs (For primary document see N86-11096 01-89)
Avail: NTIS HC A09/MF A01

The optical train of the TRIO spaceborne stellar interferometer is discussed. Thermal variation and their effect on the Cassegrain telescopes are calculated. Designs for the beam recombiner in the central station are considered. The main difficulty is to utilize efficiently the wide spectral range available, with a 2-D formatting of the fringe information versus wavelength, using as few pixels as possible. Stray light in the coude beams, generated by structure lighting rather than by meteoritic dust, may affect the limiting magnitude if it is not efficiently baffled. Author (ESA)

N86-11109# Centre National de la Recherche Scientifique, Marseilles (France).
SOLAR PROPULSION FOR THE TRIO INTERFEROMETER [PROPULSION SOLAIRE POUR L'INTERFEROMETRE TRIO]
J. L. Boit *In* ESA Colloq. on Kilometric Opt. Arrays in Space Apr. 1985 p 85-90 refs In FRENCH; ENGLISH summary (For primary document see N86-11096 01-89)
Avail: NTIS HC A09/MF A01

A solar sailing device was designed to cope with the large displacement and high accuracy positioning of each of the three satellites of the TRIO interferometer, which require a long-service-life, clean, modulated propulsion system. The six Euler movements must be uncoupled. An articulated link between the solar sail and the satellite is necessary, and electrostatic devices are proposed. Problems related to mechanics, thermal behavior, celestial mechanics, attitude correction strategy, and positioning error detection, are discussed. Author (ESA)

N86-11110# European Space Agency. European Space Research and Technology Center, ESTEC, Noordwijk (Netherlands). Mathematical Support Div.
PRELIMINARY STUDIES OF A SPINNING TETHER-CONNECTED TRIO CONCEPT
E. B. Crellin *In* ESA Colloq. on Kilometric Opt. Arrays in Space Apr. 1985 p 91-94 refs (For primary document see N86-11096 01-89)
Avail: NTIS HC A09/MF A01

Use of a slowly spinning interferometer configuration with the telescopes attached to the central station using tethers of equal length, including tether configuration, mass and storage is discussed. Slow rotation allows measurements of each source at different baseline angles. When the maximum baseline length is reached, the tethers can be retracted (stopping at intermediate lengths for further measurements, if required) and the telescopes recaptured by the central station. The attitude change to another source can be performed with the rigid configuration. Author (ESA)

N86-11111# Centre National de la Recherche Scientifique, Marseilles (France). Lab. d'Astronomie Spatiale.
TRIO INTERFEROMETER POSITIONING
B. Authier *In* ESA Colloq. on Kilometric Opt. Arrays in Space Apr. 1985 p 95-97 refs (For primary document see N86-11096 01-89)
Avail: NTIS HC A09/MF A01

The high accuracy positioning of each of the three satellites of the TRIO interferometer, with respect to the others and to the reference stars, is discussed. Based on ground interferometer experience, strategy guidelines are presented with related recommendations for spacecraft design. After star pointing, the two telescopes are aligned with respect to the central station so that the star images are within the central station field of view while optical path difference is smaller than the coherence length. Fine guidance is obtained from image superimposition on the central station focal plane, and from fringe contrast measurement. Author (ESA)

N86-11112# Centre d'Etudes et de Recherches Geodynamiques et Astronomiques, St. Vallier de Thiey (France). Observation de Calern.
FRINGE DRIFT COMPENSATION IN COMPUTER MEMORY
L. Koechlin *In* ESA Colloq. on Kilometric Opt. Arrays in Space Apr. 1985 p 99-105 refs (For primary document see N86-11096 01-89)
Avail: NTIS HC A09/MF A01

Fringe detection and contrast measurement techniques used on a groundbased 6 to 67m baseline Michelson interferometer are described. Very faint object interferometric observation with spacecraft such as TRIO is proposed. Author (ESA)

N86-11113# Centre d'Etudes et de Recherches Geodynamiques et Astronomiques, St. Vallier de Thiey (France). Synthese d'Ouverture Optique.

TRIANGLE: A DIFFERENT DESIGN FOR A THREE SATELLITE INTERFEROMETER IN SPACE

Farrokh Vakili *In* ESA Colloq. on Kilometric Opt. Arrays in Space Apr. 1985 p 107-111 (For primary document see N86-11096 01-89)
Avail: NTIS HC A09/MF A01

A design for the optical and geometrical arrangement of a TRIO-type array made up of three spacecraft is proposed. Instead of having two telescopes and a central station, TRIANGLE consists of three identical satellites, each acting as a telescope and a central station. The satellites are maintained on the summits of an equilateral triangle and provide a triple baseline interferometer. The configuration of the system is presented. Problems concerning the optics, imaging efficiency, and stabilization are discussed. Author (ESA)

N86-11114# European Space Agency. European Space Operations Center, Darmstadt (West Germany).

MISSION ANALYSIS ASPECTS

E. A. Roth *In* ESA Colloq. on Kilometric Opt. Arrays in Space Apr. 1985 p 113-116 refs (For primary document see N86-11096 01-89)
Avail: NTIS HC A09/MF A01

Astrodynamical problems associated with projects where the baseline of the interferometer is represented by two (or more) free-flying satellites are considered. High terrestrial orbits, quasi-periodic orbits around the triangular libration points (L4, L5) in the Earth-Moon system, or orbits near these points in the Earth-Sun system are considered. It is shown that constraints imposed on the baseline and on the attitude control of the satellites require considerably more detailed investigations before the feasibility of the project can be assessed. The number of problems is multiplied if the number of satellites is increased for optical arrays in space. Author (ESA)

N86-11115# Centre d'Etudes et de Recherches Geodynamiques et Astronomiques, St. Vallier de Thiey (France).

PROBLEMS IN IMAGE RECONSTRUCTION WITH OPTICAL ARRAYS

A. Labeyrie *In* ESA Colloq. on Kilometric Opt. Arrays in Space Apr. 1985 p 117-119 refs (For primary document see N86-11096 01-89)
Avail: NTIS HC A09/MF A01

Ways of reconstructing images with space arrays are discussed. With 2 apertures, the 0.1' field makes it difficult to obtain phase information, but the readily available multicolor phases can help phaseless reconstruction algorithms. With three or more apertures, phases are obtained through phase-closure algorithms. A four aperture system for a first generation optical array in space is recommended to reduce observation time. Author (ESA)

N86-11116# Harvard-Smithsonian Center for Astrophysics, Cambridge, Mass.

NUMERICAL EXPERIMENTS IN IMAGE RECONSTRUCTION

M. Faucherre, R. V. Stachnik, and S. Aram (Wellesley College, MA.) *In* ESA Colloq. on Kilometric Opt. Arrays in Space Apr. 1985 p 121-127 refs Sponsored in part by ESA (For primary document see N86-11096 01-89)
Avail: NTIS HC A09/MF A01

An approach to Fourier transform phase recovery which can work for two-element interferometers and does not require a reference star is described. It depends on the fact that, for many small, bounded, realistic sources, the Fourier transform amplitude and phase structure is dominated by the edges. Numerical experiments which illustrate the Fourier amplitude and phase structure associated with realistic sources; produce reconstructions by simple Fourier inversion for sources of varying brightness; simulate degradation in the recovered image due to reference phase errors; and show the consequence of invoking the simplest of a number of more sophisticated image recovery algorithms, phase array relaxation are presented. Author (ESA)

N86-11117# Mullard Radio Astronomy Observatory, Cambridge (England). Cavendish Lab.

RADIO ASTRONOMY EXPERIENCE IN IMAGE RECONSTRUCTION. A HISTORY LESSON FOR OPTICAL ASTRONOMERS

P. J. Warner *In* ESA Colloq. on Kilometric Opt. Arrays in Space Apr. 1985 p 129-131 refs (For primary document see N86-11096 01-89)
Avail: NTIS HC A09/MF A01

The difficulties faced by radio astronomers in reconstructing images without phase information are reviewed. Very long baseline interferometry investigations of the Sun and radio sources show that mistakes can arise if assumptions about brightness distribution are inaccurate. If baselines are not small enough to include all the flux density, objects can be missed. There appear to be fundamental difficulties in reconstructing images of complicated objects without phase. Author (ESA)

N86-11118# Harvard-Smithsonian Center for Astrophysics, Cambridge, Mass.

COSMIC IMAGE RECONSTRUCTION

M. G. Lacasse and W. A. Traub *In* ESA Colloq. on Kilometric Opt. Arrays in Space Apr. 1985 p 133-140 refs (For primary document see N86-11096 01-89)
(Grant NsG-7176)
Avail: NTIS HC A09/MF A01 CSCL 03A

Numerical methods of image reconstruction for use with an orbiting array of optical telescopes in which a rotating rectangular aperture mimics a large circular aperture are discussed. Numerical simulations to test the robustness of algorithms in the presence of photon noise are described. Measures of the quality of the reconstructed image as a function of total photon count are presented. Results of laboratory simulations using relatively bright, complex images and broad band optical filters are also presented. Good quality images are readily reconstructed from the numerical and laboratory simulations. Author (ESA)

N86-11119# Groningen Rijksuniversiteit (Netherlands).

THE OASIS CORRELATOR

P. D. Atherton, A. H. Greenaway (Royal Signals and Radar Establishment, Malvern, UK), and J. E. Noordam (Royal Greenwich Observatory, Hertsmonceux, UK) *In* ESA Colloq. on Kilometric Opt. Arrays in Space Apr. 1985 p 141-144 (For primary document see N86-11096 01-89)
Avail: NTIS HC A09/MF A01

The principle of nonredundant recombination of a redundant array of telescopes is described. The design of the Optical Aperture Synthesis in Space correlator is presented. Advantages of pupil plane over image plane interference are summarized. Author (ESA)

N86-11120# Erlangen-Nuremberg Univ. (West Germany). Inst. fuer Physik.

IMAGING SPECKLE INTERFEROMETER IN SPACE: DIGITAL SIMULATIONS OF IMAGE RECONSTRUCTION AND PHOTON NOISE

K.-H. Hofmann and G. Weigelt *In* ESA Colloq. on Kilometric Opt. Arrays in Space Apr. 1985 p 145-151 refs (For primary document see N86-11096 01-89)
Avail: NTIS HC A09/MF A01

Image reconstruction for the Imaging Speckle Interferometer (ISI) a space-based multiple mirror interferometer which can produce high-resolution images is discussed. At short UV wavelengths a multiple mirror interferometer produces speckle interferograms caused by aberrations of the interferometer. From the speckle interferograms true images can easily be reconstructed with the speckle masking method. In speckle masking no point source is required near the object. Digital simulations of image reconstruction from ISI data, in which various multiple mirror pupil functions and various amounts of photon noise (1000 to 10 photons per pixel) were simulated are shown. Speckle spectroscopy with ISI, and image reconstruction from 2-telescope interferograms are considered. Author (ESA)

N86-11121# Centre d'Etudes et de Recherches Geodynamiques et Astronomiques, St. Vallier de Thiey (France). Observatoire du Calern.
ON LINE ASTRONOMICAL IMAGE PROCESSING USING MICROCOMPUTERS
C. Thom *In* ESA Colloq. on Kilometric Opt. Arrays in Space Apr. 1985 p 153-154 refs (For primary document see N86-11096 01-89)
Avail: NTIS HC A09/MF A01

A microprocessor based system for reducing images on a large astronomical interferometer was built for use as an autocorrelator. It consists of three standard VME boards (two CPU boards and a graphic visualization controller) and a board built for image acquisition. The CPU 1 is a 128 kbyte, MC 68000 with 8 MHz clock. It does photon centroiding and image cleaning; CPU 2 is a 512 kbyte, MC 68000 with 10 MHz clock. It does image autocorrelation and integration, but can be adapted to user needs. The graphic controller is 256 x 256 pixels in 16 colors. Images are stored in two fast flip-flop RAMs to allow the processor to work on the last image without interference with acquisition of the next one.
Author (ESA)

N86-11122# Centre d'Etudes et de Recherches Geodynamiques et Astronomiques, St. Vallier de Thiey (France).
THE INTENSIFIED MULTI CCD CAMERA
A. Blazit *In* ESA Colloq. on Kilometric Opt. Arrays in Space Apr. 1985 p 155-156 (For primary document see N86-11096 01-89)
Avail: NTIS HC A09/MF A01

A photon counting 40 mm diameter TV camera for a space interferometer is described. It is an intensified mosaic of 4 CCD: CCD pixels are subdivided in 4 x 4 subpixels by a photon centroiding processor, yielding a total of 7,000,000 image elements. Its main advantage over a CCD camera is that it does not require perfect compensation of fringe drifts. Author (ESA)

N86-11123# Joint Inst. for Lab. Astrophysics, Boulder, Colo.
SPACE ANTENNA FOR GRAVITATIONAL WAVE ASTRONOMY
J. E. Faller, P. L. Bender, J. L. Hall, D. Hils, and M. A. Vincent *In* ESA Colloq. in Kilometric Opt. Arrays in Space Apr. 1985 p 157-163 refs Prepared in cooperation with National Bureau of Standards, Boulder, Colorado (For primary document see N86-11096 01-89)
Avail: NTIS HC A09/MF A01

Designs for a laser gravitational wave antenna in space using free test masses and heterodyne (interferometric) detection were investigated. Use of 1 million km baselines between three spacecraft in nearly circular 1 yr solar orbit is considered. With milliwatt-transmitted laser power levels and 50 cm diameter optics, a strain sensitivity of 10 to the minus 19th power per sq root Hz over at least the period range from 10 to 10,000 sec is feasible. The measurements observe gravitational radiation associated with present or past interactions of supermassive objects. Binary sources can also be studied. For periods <10 sec the sensitivity for a baseline length of 1 million km degrades as a result of multiple gravitational wavelengths being contained in the arm lengths. For longer periods, the main limitation is likely to come from spurious accelerations due to forces other than the gravitational attraction of the Sun and planetary bodies.
Author (ESA)

N86-11124# Centre National de la Recherche Scientifique, Toulouse (France).
APERTURE SYNTHESIS WITH OR WITHOUT PHASE INFORMATION FOR KILOMETRIC ARRAYS INTERPOLATION ALGORITHMS FOR STABILIZED IMAGE RECONSTRUCTION
A. Lannes *In* ESA Colloq. on Kilometric Opt. Arrays in Space Apr. 1985 p 165-169 refs (For primary document see N86-11096 01-89)
Avail: NTIS HC A09/MF A01

Reconstructing high resolution images from a sparsely sampled two dimensional frequency plane with synthetic aperture spaceborne interferometers is discussed. At the cost of compromise between resolution and robustness, the problem must be stated in terms of interpolation. Using the steepest descent method a very simple and powerful algorithm for interpolation with or without phase data is introduced. The constraint of nonnegativity on limited field is taken into consideration. The Fienup algorithm can be retrieved as a special case and improved by modifying its constraint operator and the implicit choice of its relaxation parameter.
Author (ESA)

N86-11125# Centre d'Etudes et de Recherches Geodynamiques et Astronomiques, St. Vallier de Thiey (France).
THE DUO: FAR INFRARED HETERODYNE CONCEPT FOR SPACE INTERFEROMETRY
J. Gay and Y. Rabbia *In* ESA Colloq. on Kilometric Opt. Arrays in Space Apr. 1985 p 171-176 refs (For primary document see N86-11096 01-89)
Avail: NTIS HC A09/MF A01

The direct Michelson technique and heterodyning are compared for spaceborne far infrared interferometer design. Constraints for space interferometry are recalled. The high spectral selectivity; diffraction-limited field of view; handling of electrical signals for correlation; low sensitivity to background radiation; and heavy and sophisticated equipment involved in heterodyning are discussed. The greatest advantage of heterodyning is the need for two satellites instead of three. Author (ESA)

N86-11126# California Inst. of Tech., Pasadena.
VLBI AT OPTICAL AND RADIO WAVELENGTHS: CONGRUENCES AND CONTRASTS
Bernard F. Burke *In* ESA Colloq. on Kilometric Opt. Arrays in Space Apr. 1985 p 177-183 refs (For primary document see N86-11096 01-89)
Avail: NTIS HC A09/MF A01

It is pointed out that conceptually there are few distinctions between aperture synthesis interferometry at radio, infrared, or optical wavelengths, and the experience and software developed in the radio domain should be largely applicable to the optical case. Coherence time is a vital consideration for radio and optical cases. Radio VLBI practice requires use of phase closure and amplitude closure relations; this may be the case for optical interferometric systems as well. This means that the optical aperture synthesis interferometer will consists of many elements. In the near term (10 to 20 yr) there will be orbiting devices; if a manned lunar base is established, an optical equivalent of the VLA might be constructed and operated on the Moon. Author (ESA)

90 ASTROPHYSICS

Includes cosmology; and interstellar and interplanetary gases and dust.

N86-11127 Texas Univ., Austin.
A METHOD FOR NUMERICAL RELATIVITY: SIMULATION OF AXISYMMETRIC GRAVITATIONAL COLLAPSE AND GRAVITATIONAL RADIATION GENERATION Ph.D. Thesis
Charles Ross Evans, II 1984 285 p
Avail: Univ. Microfilms Order No. DA8508264

A method is presented which allows fully self-consistent numerical simulation of asymptotically flat axisymmetric nonrotating general relativistic systems. These techniques have been developed to model and understand resulting relativistic effects in gravitational core collapse and gravitational radiation generation. Both vacuum (Brill) spacetimes and matter-filled configurations can be treated. The (3 + 1) decomposition of Arnowitt, Deser and Misner is used to write general relativity in a dynamical form. The conformal approach, including the transverse-traceless decomposition of extrinsic curvature due to York, is used to solve the initial value problem. In addition, these techniques are extended to provide a fully constrained evolution scheme. Several new boundary conditions, applied at large but finite radius, are derived for the elliptic constraint equations. This method uses a simplifying

three-gauge, placing the metric in quasi-isotropic form.
Dissert. Abstr.

N86-11128 Texas Univ., Austin.
INITIAL DATA FOR N BLACK HOLES Ph.D. Thesis
Anil Dattatray Kulkarni 1984 111 p
Avail: Univ. Microfilms Order No. DA8508294

The N-body problem in general relativity is of enormous difficulty, especially in the nonlinear regime where radiation is important. It is now possible to study this problem by treating it as a Cauchy problem and by using large-scale computers to develop numerical models. With this motivation, the Cauchy formulation of Einstein equations is described. It consists of the Hamiltonian and momentum constraint equations, and the evolution equations. The constraints are analyzed using the conformal technique. The first step in this approach is to set up initial data compatible with the constraints. The N-body data, in general, will depend on the stress-energy tensor of the bodies. Hence this issue is bypassed by considering the matter free representation of particles in terms of the geometries of certain non-Euclidean manifolds, such as the Einstein-Rosen manifold M sub n and the (N + 1)-sheeted manifold (sigma sub-n). Among these possibilities, the Einstein-Rosen manifold is of special interest because of its symmetry. Dissert. Abstr.

N86-11129 Boston Univ., Mass.
GRAVITATIONAL COLLAPSE OF A SCALAR FIELD Ph.D. Thesis
Tara Maithreyan 1985 90 p
Avail: Univ. Microfilms Order No. DA8508916

A self-similar collapse of massless scalar waves is considered, and the Einstein field equations in classical general relativity are solved to obtain the metric for the collapse. These scalar waves satisfy the massless wave equation and the energy momentum tensor associated with them is derived from their Lagrangian density. The collapse begins at t = 0 before which spacetime is flat, empty spacetime described by the Minkowski metric. Self similarity assumes that a homothetic Killing vector exists for the collapse, which satisfies the corresponding homothetic Killing equation. The solution obtained contains a constant c2 whose value determines the nature of the collapse and the kind of singularity formed by the collapsing scalar waves. The three different cases are outlined and the corresponding Penrose diagrams are given. The apparent horizons, defined by Hawking as the limit of the trapped surfaces surrounding the singularity are calculated for each case. Dissert. Abstr.

N86-11130 Washington Univ., Seattle.
PHYSICAL CONDITIONS IN GIANT EXTRAGALACTIC H2 REGIONS Ph.D. Thesis
Evan David Skillman 1984 223 p
Avail: Univ. Microfilms Order No. DA8508091

Giant Extragalactic H2 Regions (GEHRs) in nearby galaxies have been observed at both radio and optical wavelengths. Narrow band optical imaging, large and small aperture optical spectrophotometry, radio continuum imaging at lambda 6 cm and lambda 21 cm, and lambda 21 cm H1 spectral line mapping have been employed to investigate the point to point variations of the physical conditions within and surrounding the GEHRs. Measurement of reddening and extinction were found to be strongly dependent on resolution. Variations in extinction as measured by the optical method were not found to correlate with those measured with the optical-radio method. In at least one case this was due to the presence of a nonthermal radio continuum source. Significant differences in optical line strength ratios exist between different points in a single GEHR. These differences point to variations of the physical conditions within the GEHR. Dissert. Abstr.

N86-11131 Princeton Univ., N. J.
THE DYNAMICS AND STELLAR CONTENT OF GLOBULAR STAR CLUSTERS Ph.D. Thesis
Robert Hugh Lupton 1985 175 p
Avail: Univ. Microfilms Order No. DA8509640

Models are rpesented of rotating globular clusters with an anisotropic velocity dispersion, based upon the assumption that the total angular momentum is a good integral even for systems with slightly flattened potentials. Such models are given of the cluster M13 and M29, using both photometry and stellar radial velocities to constrain the fits. It is shown that the data is satisfactorily represented by models with anisotropy radii of about 5 and 20 core radii respectively, and mass functions of Salpeter index about 2.25. These models predict mass segregation, with the lighter stars which contribute a negligible proportion of the light being found futher from the cluster center. A computer program is presented to do star counts in crowded fields complete to about 23.5th magnitude, and the conversion from the Gunn gri photometric system to mass for pop 2 main sequence stars, based on published infrared photometry. To within the errors in the star counts no evidence is found of mass segregation, which is consistent with the published models of M3 and the model presented for M13. Dissert. Abstr.

N86-11132 Pittsburgh Univ., Pa.
ELECTRON-ION RECOMBINATION STUDIES OF PLANETARY IONOSPHERIC AND ASTROPHYSICAL IONS Ph.D. Thesis
Bishwajit Ganguli 1984 104 p
Avail: Univ. Microfilms Order No. DA8511040

The rates of rcombination of HCO +, H2CN + and H2CN + HCN ions with electrons were determined as a function of electron temperature T sub e using a microwave afterglow/mass spectrometer apparatus employing microwave electron heating. In addition, an investigation was carried out to obtain qualitatively the inelastic energy loss frequency Nu sub e sup' inel (T sub e) of electrons in dilute N2-Ne mixtures using microwave techniques.
Dissert. Abstr.

N86-11133*# Atmospheric and Environmental Research, Inc., Cambridge, Mass.
COMETARY ATMOSPHERES: MODELING THE SPATIAL DISTRIBUTION OF OBSERVED NEUTRAL RADICALS Interim Report, Jun. - Aug. 1985
Michael R. Combi Oct. 1985 8 p refs
(Contract NASw-3950)
(NASA-CR-176242; NAS 1.26:176242) Avail: NTIS HC A02/MF A01 CSCL 03B

The analysis of observed brightness profiles for the C2 radical in comets with Haser's model implies that the parent scale length varies as the square of the heliocentric distance. The use of new Haser scale lengths for C2 and CN determined under this project appears to explain the apparent drop in the C2-to-CN ratio with increasing heliocentric distance. Author

N86-11134# California Univ., Livermore. Lawrence Livermore Lab.
STELLAR s-PROCESS DIAGNOSTICS
G. J. Mathews, R. A. Ward, K. Takahashi, and W. M. Howard May 1985 10 p Presented at the 20th Recontre de Moriond, Les Arcs, France, 10 Mar. 1985
(Contract W-7405-eng-48)
(DE85-012926; UCRL-92724; CONF-850375-5) Avail: NTIS HC A02/MF A01

The solar-system sigma-N curve is best understood if the s-process is largely produced by stars in the mass range of M approx. 2 to 4 M0. Observations were studied as indicators of the validity of this hypothesis. It is found that isotopic Zr abundances and elemental (Ba/Sr) vs (Ba/Nd) ratios are consistent with these conditions. It is found that the elemental (Tc/Nb) ratio is not an indicator of temperature as was suggested but rather a measure of the age of an AGB star in the third dredge-up phase. DOE

N86-11135# European Southern Observatory, Munich (West Germany).
[ACTIVITIES REPORT OF THE EUROPEAN SOUTHERN OBSERVATORY] Annual Report, 1984
1985 86 p refs In ENGLISH, FRENCH, and GERMAN Original contains color illustrations

Avail: NTIS HC A05/MF A01

Observations of a ring around Neptune, Halley's comet, asteroids, stellar atmospheres, stellar chromospheres, stellar oscillations, binary stars, the interstellar medium, and galaxies are summarized. Gamma, X-ray, infrared, ultraviolet, and satellite-borne astronomy are discussed. Facilities at the European Southern Observatory are described. Author (ESA)

91 LUNAR AND PLANETARY EXPLORATION

Includes planetology; and manned and unmanned flights. For spacecraft design see *18 Spacecraft Design Testing, and Performance*. For space stations see *15 Launch Vehicles and Space Vehicles*.

N86-11136 Arizona State Univ., Tempe.
CONTEMPORARY AEOLIAN PROCESSES ON MARS: LOCAL DUST STORMS Ph.D. Thesis
Alan Richard Peterfreund 1985 263 p
Avail: Univ. Microfilms Order No. DA8510680

Local and major dust storms play a dominant role in contemporary aeolian processes on Mars. As a means of better documenting the role of dust storms on the surface, a record of their occurrence during the four years of the Viking Mission has been established using thermal infrared and visual observations. The dust storm record was then compared to observations of the Martian surface. Particle transport, source region characteristics, and effects of dust storms, proximal and distal to their source are considered for both the Earth and Mars. Basic elements necessary for a dust storm on Earth and Mars (i.e., adequate winds, sufficient sediment supply, and surface susceptible to erosion) are similar. The frequency, intensity, and geologic impact of dust storms, however, differ due to variations in these elements. On Mars, large temporal and spatial variations in atmospheric pressure and temperature are the primary control. On Earth, sediment supply and surface conditions appear to be the more variable factors. On both planets these conditions are related to climatic cycles. Dissert. Abstr.

N86-11137*# Jet Propulsion Lab., California Inst. of Tech., Pasadena.
GALILEO: EXPLORATION OF JUPITER'S SYSTEM
T. V. Johnson, C. M. Yeates, L. Colin (NASA. Ames Research Center), F. P. Fanale (Hawaii Univ.), L. Frank (Iowa Univ.), and D. M. Hunten (Arizona Univ.) Jun. 1985 179 p refs
(NASA-SP-479; NAS 1.12/6:479) Avail: NTIS HC A09/MF A01 CSCL 03B

The scientific objectives of the Galileo mission to the Jovian system is presented. Topics discussed include the history of the project, our current knowledge of the system, the objectives of interrelated experiments, mission design, spacecraft, and instruments. The management, scientists, and major contractors for the project are also given. Author

N86-11138*# National Aeronautics and Space Administration. Goddard Space Flight Center, Greenbelt, Md.
PHOTOGRAPHIC CATALOG OF SELECTED PLANETARY SIZE COMPARISONS
Stephen Paul Meszaros Sep. 1985 130 p refs
(NASA-TM-86207; Rept-85B0346; NAS 1.15:86207) Avail: NTIS HC A07/MF A01 CSCL 03B

Photographs taken by NASA spacecraft, and cartographic products based on these photos, are used to illustrate size comparisons of the planets and moons of the solar system. Global views and prominent geographical features are depicted at the same scale, allowing size relationships to be studied visually. Author

N86-11139*# Jet Propulsion Lab., California Inst. of Tech., Pasadena.
A MODELING ANALYSIS PROGRAM FOR THE JPL TABLE MOUNTAIN Io SODIUM CLOUD Interim Report, 1 Jun. - 31 Aug. 1985
William H. Smyth (Atmospheric and Environmental Research, Inc., Cambridge, Mass.) and Bruce A. Goldberg Dec. 1984 23 p refs (Contract NASw-3949)
(NASA-CR-176241; NAS 1.26:176241) Avail: NTIS HC A02/MF A02 CSCL 03B

A data quality review for the entire set of the 1981 Region B/C images has been completed and is presented. The review indicates that almost all images are of sufficient quality to be valuable in our analysis of this data set. Five data-correlation studies for the same data set have also been completed and are useful in classifying and studying the sodium cloud morphology and its interactions with solar radiation pressure and the plasma torus. Additional progress in developing new image processing techniques and in improving the Io sodium cloud model is also discussed. Author

N86-11140# Technische Univ., Berlin (West Germany). Inst. fuer Luft- und Raumfahrt.
A LOGISTICS SCENARIO FOR AN EARLY LUNAR BASE
H. H. Koelle and B. Johenning 10 Dec. 1984 47 p refs
(ILR-Mitt-143) Avail: NTIS HC A03/MF A01

Mission, base, and logistics models were used to assess the feasibility of a lunar base. It is shown that a heavy lift launch vehicle (HLLV) using the present space shuttle main engine can serve as the backbone of such a lunar logistics system. A typical launch schedule reaching 24 flights in its 7th operational year is developed. This HLLV can carry 300 metric tons to the 530Km space station orbit or 70 metric tons directly to the lunar surface. The lunar base model suggests landing the first 20 people on the Moon in 1999 and reaches a level of 120 people on the lunar base, plus 20 people in lunar orbit in its 8th year of operation. The lunar base facilities have a total mass of 4000 metric tons in its 10th year. Author (ESA)

92 SOLAR PHYSICS

Includes solar activity, solar flares, solar radiation and sunspots.

N86-11141*# National Aeronautics and Space Administration. Goddard Space Flight Center, Greenbelt, Md.
DIRECTIONALITY OF BREMSSTRAHLUNG FROM RELATIVISTIC ELECTRONS IN SOLAR FLARES
Charles D. Dermer and Reuven Ramaty Sep. 1985 40 p refs Submitted for publication
(NASA-TM-87509; NAS 1.15:87509) Avail: NTIS HC A03/MF A01 CSCL 03B

Angular and energy spectra of bremsstrahlung have been calculated from anisotropic electron distributions in solar flares. Results have been compared to observations of gamma-ray limb-brightening and to data on the variation of the gamma-ray spectrum with flare position on the sun. Author

N86-11142# Louisiana State Univ., Baton Rouge. Dept. of Physics and Astronomy.
SOLAR FLARES AND MAGNETOSPHERIC PARTICLES: INVESTIGATIONS BASED UPON THE ONR-602 EXPERIMENT Annual Letter Report, 1 Apr. 1984 - 30 Jun. 1985
J. P. Wefel 28 Jun. 1985 14 p
(Contract N00014-83-K-0365)
(AD-A156583) Avail: NTIS HC A02/MF A01 CSCL 03/2

The work performed during the past year can be divided into three areas: (1) data reduction/processing and instrument response; (2) solar flare studies, and (3) magnetospheric particles. Our analysis effort had been divided between obtaining an overview of the entire ONR-602 (Phenix 1) dataset, identifying data processing/analysis problems and locating scientifically interesting effects for additional study, and studying specific areas or fully

understand the operation of the ONR-602 instrument in the space environment and the complicated particle flux variations over the spacecraft orbit. GRA

93 SPACE RADIATION

Includes cosmic radiation; and inner and outer Earth's radiation belts.

For biological effects of radiation see *52 Aerospace Medicine*. For theory see *73 Nuclear and High-Energy Physics*.

N86-11143 New Hampshire Univ., Durham.
SOLAR MODULATION OF GALACTIC COSMIC RAYS: TECHNIQUES AND APPLICATIONS Ph.D. Thesis
John Steven Perko 1984 78 p
Avail: Univ. Microfilms Order No. DA8510482

The time dependent, spherically symmetric, solar modulation of galactic cosmic rays is discussed. A numerical technique was introduced for the solution of this problem. A model for the solar cycle variation in cosmic ray intensity illustrated this method, using enhanced particle scattering regions. An attempt to explain recent observations which show that cosmic ray electrons are returning to higher intensities, characteristic of solar minimum, faster than cosmic ray protons of about the same energy, the reverse of the previous eleven year cycle is presented. The solar modulation of galactic antiprotons is explained. It appears that a recent low energy measurement of these particles has given cosmic ray theorists trouble devising an interstellar spectrum to fit the observations. A spherically symmetric, stead state calculation of the effects of a strong termination shock in the heliosphere is also presented. The overall effect of a shock on the near-Earth spectra seems negligible. Dissert. Abstr.

N86-11144 Rutgers - The State Univ., New Brunswick, N. J.
EXTRA-GALACTIC X-RAY SOURCES AND THE DIFFUSE X-RAY BACKGROUND Ph.D. Thesis
Chris R. Shrader 1985 170 p
Avail: Univ. Microfilms Order No. DA8510828

The source of the isotropic, diffuse X-ray background (DXRB) is considered in the context of observational data obtained by the HEAO-1 and HEAO-2 spacecraft. Attempts are made to determine the contribution to the DXRB by unresolved discrete sources. Several different approaches are followed. QSO optical and X-ray luminosities were correlated and optical luminosity functions were used to estimate faint X-ray counts. Results are consistent with those previously published. Dissert. Abstr.

99 GENERAL

No abstracts in this category.

Typical Subject Index Listing

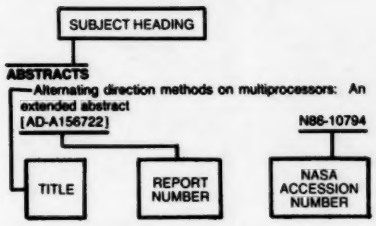

The subject heading is the key to the subject content of the document. Titles, report numbers, and accession numbers of pertinent documents are provided under each subject heading. When the title is insufficiently descriptive of the document content, a title extension has been added, separated from the title by three hyphens. The report number helps to indicate the type of document cited (e.g., NASA report, NASA translation, NASA contractor report). The NASA accession number is the number by which the document abstracts are arranged in this journal and by which the document is sold or requested. The titles, with title extensions if present, are arranged under each subject heading in ascending accession number order. The subject headings have been selected from the latest revision of the *NASA Thesaurus* (NASA SP-7051).

A

ABSORPTION
Engine-driven and absorption heat pump programs [DE85-013930] N86-10472
The interaction of small metal particles with refractory oxide supports [NASA-CR-176228] N86-11047

ABSORPTION COOLING
Analyses of advanced residential absorption heat pump cycles [DE85-005244] N86-10664

ABSTRACTS
Alternating direction methods on multiprocessors: An extended abstract [AD-A156722] N86-10794
An annotated bibliography of abstracts on the use of simulators in technical training [AD-A156792] N86-11065

ABUNDANCE
Physical conditions in giant extragalactic H2 regions N86-11130

ACCELERATION (PHYSICS)
Composite explosives for metal acceleration: The effect of detonation temperature [DE85-013982] N86-10359

ACCELERATION STRESSES (PHYSIOLOGY)
Hemodynamics during gravitational overloads (mathematical modeling) N86-10739
Study of hypokinesia and acceleration effects on human chromosomes N86-10740
Dynamics of changes of statistical indicators of heart rhythm of persons with different degree of motion sickness N86-10743

ACCELERATION TOLERANCE
Hemodynamics during gravitational overloads (mathematical modeling) N86-10739

ACCELERATORS
Simulating the CTR environment in the HVBM [DE85-011745] N86-10193

ACCIDENT PREVENTION
Activities report in safety N86-10365

ACCIDENTS
Scoping studies of vapor behavior during a severe accident in a metal-fueling reactor [DE85-011474] N86-10952

ACCURACY
A nanosecond or thirty centimeters: Why atomic clocks have to be synchronized. MITREX opens new dimensions for measuring accuracy N86-10185
A comparison of swept frequency and FFT methods used to calibrate array test modules [AD-A156629] N86-10430
Investigation of the uncertainties of the NBS (National Bureau of Standards) thermal voltage and current converters [PB85-200178] N86-10453

ACID RAIN
Examples of regional environmental assessment using acid deposition data [DE85-012903] N86-10677
Proceedings: First Annual Acid Deposition Emissions Inventory Symposium [PB85-200004] N86-10686
Emissions of NOx, SOx and VOC from Antropogenic sources [PB85-193530] N86-10688
Seasonal variations in atmospheric chemistry in the Adirondacks [DE85-014227] N86-10719

ACIDITY
Phosphoric and electric utility fuel technology development [DE85-014741] N86-10651

ACIDS
Kinetics of biological ferrous iron oxidation [DE85-014616] N86-10736

ACOUSTIC ATTENUATION
Physical acoustics: Investigation of chemical kinetic and thermodynamic properties of fluids N86-10911

ACOUSTIC EMISSION
Report on an overseas visit [AD-A156603] N86-10037
Multimode acoustic research N86-10167

ACOUSTIC LEVITATION
Containerless studies of nucleation and undercooling N86-10102
Multimode acoustic research N86-10167
Advanced containerless processing technology N86-10176
Acoustic levitation containerless processing N86-10177

ACOUSTIC MEASUREMENT
Long term statistical measurements of environmental acoustics parameters in the arctic. AEAS report number 2. Low frequency transmission loss measurements in the central arctic ocean [AD-A156576] N86-10727
Sound radiation from repetitive transient vibrations using multi-channel digital signal processing with application to impact machinery N86-10910
Understanding and improving acoustic to seismic coupling as it pertains to Sandia's helicopter detector [DE85-009440] N86-10920

ACOUSTIC SCATTERING
Exploratory development for a high reliability flaw characterization module [AD-A156632] N86-10916

ACOUSTIC VELOCITY
On the method of characteristics and its application to the calculations of annular nozzle flowfields N86-10454
Tunable acousto-optic filter with improved spectral resolution and increased aperture [AD-D011758] N86-10915

ACOUSTICS
Vibro-acoustic forecast for space shuttle launches at Vandenberg AFB: The payload changeout room and the administration building [AD-A156944] N86-10269
Ultrasonic inspection of weldments in large size spiral box for hydroelectric plant [AS-701/85] N86-10562
A study of methods to predict and measure the transmission of sound through the walls of light aircraft. Integration of certain singular boundary element integrals for applications in linear acoustics [NASA-CR-176229] N86-10912
Proposed aural nondetectability limits for Army materiel [AD-A156704] N86-10917
Measurements of the acoustic interference between adjacent microphones [AD-A156892] N86-10919

ACOUSTO-OPTICS
Signal analysis receiver with acousto-optic delay lines [AD-D011761] N86-10427
A compact bulk acousto-optic time integrating correlator [AD-A156608] N86-10428
Fiber optic gradient hydrophone construction and calibration for sea trial [AD-A156469] N86-10914
Tunable acousto-optic filter with improved spectral resolution and increased aperture [AD-D011758] N86-10915

ACQUISITION
Derivational analogy: A theory of reconstructive problem solving and expertise acquisition [AD-A156817] N86-10899

ACTIVATION
Contact effects in light activated GaAs switches [AD-A156957] N86-10434

ACTUATORS
Control concepts for in-flight simulation including actuator nonlinearities and time delays [DFVLR-FB-85-24] N86-10047
Robust failure detection filters [NASA-CR-176232] N86-10271
Soudan 2 data acquisition and trigger electronics [DE85-013864] N86-10443
Termination load carrying device [AD-D011800] N86-10558

ADA (PROGRAMMING LANGUAGE)
Ada (trademark) Programming Support Environment (APSE) Evaluation and Validation (E and V) workshop report held at Airlie, Virginia on 2-6 April 1984 [AD-A156667] N86-10829

ADAPTATION
The rubber tube test section of the DFVLR in Goettingen, West Germany --- wind tunnel walls [DFVLR-FB-85-18] N86-10051
Dynamics of changes of statistical indicators of heart rhythm of persons with different degree of motion sickness N86-10743
Dynamics of general resistance of rats during readaptation period after training in altered gas environment N86-10767

ADAPTIVE CONTROL
Gas generator fuel flow throttle control system [AD-D011797] N86-10355

ADDITIVES
Magnetic properties of doped semiconductors [DE85-012090] N86-11053

ADHESION
Development of metallization process [NASA-CR-176209] N86-10312
Tribological properties of structural ceramics [NASA-TM-87105] N86-10341

ADHESION TESTS
Adhesion of metals: Experiment 1 ES-340 --- Spacelab N86-10232

ADHESIVE BONDING
The effect of debond growth on crack propagation in composite plates reinforced with adhesively bonded composite stringers N86-10287
Pre-bond treatment for titanium alloys [BAE-AL/MAT/3864] N86-10309
Load-deflection tests and computer analyses of a high-precision adhesive-bonded antenna reflector panel N86-10389
The preparation and testing of titanium and zirconium coupling agents [SJ70] N86-10576

ADIABATIC EQUATIONS
Charge exchange in slow collisions of atoms and molecules N86-10922
ADIRONDACK MOUNTAINS (NY)
Seasonal variations in atmospheric chemistry in the Adirondacks
[DE85-014227] N86-10719
ADSORPTION
Evaluation of Passive Sampling Devices (PSDs)
[PB85-196418] N86-10689
Adsorption of oxygen on single crystal tin at liquid helium temperatures N86-11044
AERIAL PHOTOGRAPHY
Remote sensing study project East Gelderland (Netherlands). Part 2: Remote sensing flights in 1982 and 1983; organization aspects N86-10639
AEROACOUSTICS
Recent advances in the analysis of exhaust mufflers N86-10587
AEROBRAKING
Numerical procedure for three-dimensional hypersonic viscous flow over aerobrake configuration
[NASA-TM-58269] N86-10018
AERODYNAMIC CHARACTERISTICS
Three articles on new calculation methods in aeronautics (selected articles)
[AD-A145745] N86-10007
Theoretical study of the unsteady linear problem for a rectangular wing with a pitching movement
[ONERA-RT-17/1841-RY-010-R] N86-10022
AERODYNAMIC COEFFICIENTS
Comment on Determination of Aerodynamic Coefficients for a Reentry Body by Means of the Kalman Filter Method N86-10011
AERODYNAMIC CONFIGURATIONS
Aerodynamics of hyperlift systems
[SNIAS-443.501/85] N86-10023
Analysis of hyperlift systems. Study of a singularities method
[SNIAS-443.529/84] N86-10024
AERODYNAMIC DRAG
A fundamental study of the sticking of insect residues to aircraft wings
[NASA-CR-176231] N86-10033
AERODYNAMIC FORCES
A new method for calculating unsteady supersonic aerodynamic forces and its application N86-10009
AERODYNAMIC INTERFERENCE
The rubber tube test section of the DFVLR in Goettingen, West Germany — wind tunnel walls
[DFVLR-FB-85-18] N86-10051
AEROELASTICITY
Forced response analysis of an aerodynamically detuned supersonic turbomachine rotor
[NASA-TM-87093] N86-10019
AERONAUTICAL ENGINEERING
A review of Australian investigations on aeronautical fatigue during the period April 1983 to March 1985
[AD-A156602] N86-10036
AEROSOLS
Characterization of vapor and aerosol flows by photothermal methods
[AD-A156601] N86-10465
Technical considerations in regional aerosol modeling
[PB85-193027] N86-10710
AEROSPACE ENGINEERING
Aerospace research at NLR N86-11089
Activities report of the Space Flight Laboratory N86-11090
Activities Report of the Space Flight Laboratory N86-11091
AEROSPACE ENVIRONMENTS
Influence of melt convection on solid-liquid interface under terrestrial and reduced gravity environments N86-10083
Control of cast iron microstructure N86-10084
Solidification fundamentals N86-10090
Life sciences research on the space station: An introduction
[NASA-TM-86836] N86-10734
AEROSPACE INDUSTRY
Space utilization N86-11067
Space sciences: Perspectives of commercial utilization for the German industry N86-11068
AEROSPACE MEDICINE
Aerospace medicine and biology: A continuing bibliography with indexes (supplement 275)
[NASA-SP-7011(275)] N86-10768
The effects of age, sleep deprivation, and altitude on complex performance
[AD-A156987] N86-10771
AEROSPACE SCIENCES
Space utilization N86-11067
Space sciences: Perspectives of commercial utilization for the German industry N86-11068
Space research expenses of the Federal Ministry of Research and Technology (BMFT) in the period 1983-1985 N86-11070
AEROSPACE SYSTEMS
Aerospace research at NLR N86-11089
AEROSPACE TECHNOLOGY TRANSFER
Activities Report of the Space Flight Laboratory N86-11091
AEROSPACE VEHICLES
Manned flight simulation: Challenge and response
[NASA-TM-86827] N86-10048
AFRICA
Role of the Economic Commission for Africa as a principal investigator in the metric camera experiment and reports of the result of the assessment for topographic and revision of maps in populated and developed areas of the world N86-10501
AGGLOMERATION
Cell partition in two polymer aqueous phases N86-10136
New instrumentation for phase partitioning N86-10138
AGING (BIOLOGY)
The effects of age, sleep deprivation, and altitude on complex performance
[AD-A156987] N86-10771
AGING (MATERIALS)
Age-life prediction of nylon 66 parachute materials. Part 2: Changes in the chemical and physical properties of materials on aging
[AD-A156909] N86-10347
Microwave evaluation of materials
[DE85-013183] N86-10409
AGRICULTURE
Wind energy in agriculture, a promise
[SS-45] N86-10672
Wind energy, a feasibility investigation for wind mills in agriculture
[SS-45A] N86-10673
AIR
Chemical kinetics and cellular structure of detonations in hydrogen sulphide and air
[DE85-009408] N86-10304
Effects of scale and geometry on hydrogen-air detonations
[DE85-006762] N86-10474
AIR COOLING
Submerged ram air inlets for ECM (electronic countermeasures) pods
[AD-D011801] N86-10020
AIR FLOW
Mean turbulence structure in strongly heating air flows N86-10455
AIR INTAKES
Three articles on new calculation methods in aeronautics (selected articles)
[AD-A145745] N86-10007
Effect of a shear layer on the stability of an axisymmetrical external compression air intake N86-10010
Submerged ram air inlets for ECM (electronic countermeasures) pods
[AD-D011801] N86-10020
AIR LAW
Tendencies toward liberalization in European air traffic control
[DFVLR-FB-85-23] N86-10030
AIR POLLUTION
Airborne measurements of the border-crossing air pollution in the area between Weiden and Hof/Bavaria
[DFVLR-FB-85-25] N86-10685
Proceedings: First Annual Acid Deposition Emissions Inventory Symposium
[PB85-200004] N86-10686
Evaluation of Passive Sampling Devices (PSDs)
[PB85-196418] N86-10689
AIR QUALITY
Proceedings: First Annual Acid Deposition Emissions Inventory Symposium
[PB85-200004] N86-10686
Emissions of NOx, SOx and VOC from Antropogenic sources
[PB85-193530] N86-10688
AIR SAMPLING
Emissions of NOx, SOx and VOC from Antropogenic sources
[PB85-193530] N86-10688
Evaluation of Passive Sampling Devices (PSDs)
[PB85-196418] N86-10689
AIR TRAFFIC
Tendencies toward liberalization in European air traffic control
[DFVLR-FB-85-23] N86-10030
The air traffic demand in passenger travel of the Federal Republic of Germany 1990 - 2000. Update of the DFVLR air traffic forecast
[DFVLR-MITT-85-06] N86-10031
AIR TRANSPORTATION
Tendencies toward liberalization in European air traffic control
[DFVLR-FB-85-23] N86-10030
The dirigible: A catalyst for resource exploitation in remote areas?
[AD-A156518] N86-10034
AIR WATER INTERACTIONS
The Liu, Katsaros, and Businger (1979) bulk atmospheric flux computational iteration program in FORTRAN and BASIC
[AD-A156736] N86-10714
Evaluation of surface exchange coefficients from mildex ocean/atmosphere mixed layer data
[AD-A156765] N86-10729
AIRBORNE EQUIPMENT
Airborne measurements of the border-crossing air pollution in the area between Weiden and Hof/Bavaria
[DFVLR-FB-85-25] N86-10685
AIRCRAFT ACCIDENTS
Rotary-wing operations in a microburst environment
[AD-A156695] N86-10713
AIRCRAFT CARRIERS
A comparative analysis of a CV helicopter and a JVX (Joint Services Advanced Vertical Lift) tilt-rotor aircraft in an aircraft carrier based ASW (Anti-Submarine Warfare)
[AD-A156871] N86-10041
AIRCRAFT CONSTRUCTION MATERIALS
Review of investigations on aeronautical fatigue in the Federal Republic of Germany
[LBF-S-173] N86-10044
Fatigue, static tensile strength and stress corrosion of aircraft materials and structures
[VTH-LR-360-PT-1] N86-10045
AIRCRAFT CONTROL
Control concepts for in-flight simulation including actuator nonlinearities and time delays
[DFVLR-FB-85-24] N86-10047
AIRCRAFT DESIGN
Acta Aeronautica et Astronautica Sinica (selected articles)
[AD-A147304] N86-10001
Optimum design of an aircraft wing structure with multiple constraints by the direct-vision criteria method N86-10004
Summary of work on jet noise prediction
[ESDU-BR-62636] N86-10909
AIRCRAFT ENGINES
Retrofit of SAC EC-135C and RC-135 aircraft with CFM-56 engines
[AD-A156688] N86-10038
AIRCRAFT HAZARDS
Electromagnetic resonances of cylinders and aircraft model with resistive wires
[NASA-CR-176250] N86-10042
AIRCRAFT MANEUVERS
System modeling and identification of equivalent systems with and without compensating time delay for control-augmented aircraft
[ESA-TT-852] N86-10043
AIRCRAFT MODELS
Evaluation of an aerodynamic-load prediction method on a STOL fighter configuration
[NASA-TM-86782] N86-10015
Electromagnetic resonances of cylinders and aircraft model with resistive wires
[NASA-CR-176250] N86-10042
System modeling and identification of equivalent systems with and without compensating time delay for control-augmented aircraft
[ESA-TT-852] N86-10043
AIRCRAFT RELIABILITY
A review of Australian investigations on aeronautical fatigue during the period April 1983 to March 1985
[AD-A156602] N86-10036
AIRCRAFT SAFETY
Proposed modifications for the RAAF Airtrainer CT-4A cockpit
[AD-A156808] N86-10039
Rotary-wing operations in a microburst environment
[AD-A156695] N86-10713
AIRCRAFT STRUCTURES
Review of investigations on aeronautical fatigue in the Federal Republic of Germany
[LBF-S-173] N86-10044
Fatigue, static tensile strength and stress corrosion of aircraft materials and structures
[VTH-LR-360-PT-1] N86-10045
Nondestructive control of thick structures made without disassembling
[PV-43-954/F/3] N86-10564

Nondestructive corrosion test of aluminum alloy structures
[PV-43-954/F/2] N86-10594

AIRFOIL PROFILES
Analysis of hyperlift systems. Study of a singularities method
[SNIAS-443.529/84] N86-10024
La Recherche Aerospatiale, bimonthly bulletin, no. 1984-5, September-October 1985
[ESA-TT-899] N86-10363

AIRFOILS
A new method for calculating unsteady supersonic aerodynamic forces and its application N86-10009
On the design of airfoils in transonic flow using the Euler equations N86-10013
A fundamental study of the sticking of insect residues to aircraft wings
[NASA-CR-176231] N86-10033

AIRFRAMES
Attachment method-ceramic radome to metal body
[AD-D011778] N86-10032
A review of Australian investigations on aeronautical fatigue during the period April 1983 to March 1985
[AD-A156602] N86-10036

AIRLINE OPERATIONS
Tendencies toward liberalization in European air traffic control
[DFVLR-FB-85-23] N86-10030

AIRSHIPS
The dirigible: A catalyst for resource exploitation in remote areas?
[AD-A156518] N86-10034

ALGAE
Development and evaluation of multispecies test protocols for assessing chemical toxicity
[DE85-013526] N86-10679

ALGEBRA
Computing the structural index
[DE85-014370] N86-10871
Brauer-Severi schemes of orders
[CTH-MATH-1985-06] N86-10877

ALGORITHMS
Automatic processing of reactive polymers N86-10127
Modeling and control of nonlinear systems N86-10362
The VLSI design of error-trellis syndrome decoding for convolutional codes N86-10391
Acoustic gravity wave chemistry model for the RAYTRACE code
[AD-A156850] N86-10405
Implementation issues for algorithmic VLSI (Very Large Scale Integration) processor arrays
[AD-A156699] N86-10432
Automated analysis of digital images generated by two-dimensional gel electrophoresis
[DE85-011906] N86-10526
Analysis of edge detection algorithms on DIAL (Digital Image Analysis Laboratory)
[AD-A156735] N86-10630
A processor for the study of ocean fine-scale patches
[AD-A157019] N86-10730
Alternating direction methods on multiprocessors: An extended abstract
[AD-A156722] N86-10794
Compact, high-speed algorithm for laying out printed circuit board runs N86-10814
Coordinate axes, location of origin, and redundancy for the one and two-dimensional discrete Fourier transform
[NASA-CR-176225] N86-10826
State assignment in sequential circuits
[EUT-85-E-146] N86-10846
Identification of a plant's weighting sequence — self-tuning control
[OUEL-1534/84] N86-10854
Two algorithms for weighted matroid intersection
[AD-A156525] N86-10861
An improved FFT (Fast fourier transform) for a four parallel pipe SIMD arithmetic processor
[AD-A156625] N86-10863
The h, p and h-p versions of the finite element method in 1 dimension. Part 3. The adaptive h-p version
[AD-A156626] N86-10864
A mesh moving technique for time dependent partial differential equations in two space dimensions
[AD-A156663] N86-10866
On the lanczos method for solving symmetric linear systems with several right-hand-sides
[AD-A156816] N86-10868
Error estimates and automatic time step control for numerical methods for stiff ordinary differential equations
[CTH-MATH-1984-27] N86-10872
Rank revealing QR-Factorizations
[AD-A156756] N86-10887
Generation of flight paths using hierarchical planning
[AD-A156905] N86-10900
Exploratory development for a high reliability flaw characterization module
[AD-A156632] N86-10916

ALIGNMENT
Parasitic mode losses versus signal sensitivity in beam position monitors
[DE85-014367] N86-10964
Beam steering in the SLC linac
[DE85-013370] N86-11025

ALKENES
A procedure identifying a polyacetylene initiator of olefin metathesis. The reactivities of metal-carbenes toward alkenes and alkynes
[AD-A156997] N86-10283

ALKYL COMPOUNDS
Synthesis of arylene siloxanylene polymers and copolymers
[AD-D011780] N86-10338

ALLOYS
Microgravity Science and Applications Program tasks
[NASA-TM-87568] N86-10053
The influence of containerless undercooling and rapid solid-state quenching on the superconductive and magnetic properties of some clustering alloy systems N86-10076
Undercooling, remelting, and coarsening N86-10080
Liquid phase miscibility gap materials N86-10081
The development and prevention of channel segregation during alloy solidification N86-10086
Theoretical problems in materials science N86-10088
Lambda point equipment N86-10118
Acoustic levitation containerless processing N86-10177
Portevin-Le Chatelier effect. 1: Model for the type-E serrations
[DE85-006879] N86-10322
Weld metal hot-cracking of hastelloy alloys C-22 and C-276: A study by analytical electron microscopy
[DE85-009437] N86-10324
Constitutive modeling for isotropic materials (HOST)
[NASA-CR-174980] N86-10589

ALPHA PARTICLES
Development and application of the electrochemical etching technique
[DE85-010302] N86-10957

ALPS MOUNTAINS (EUROPE)
Evaluation of metric camera photos — Spacelab; alpine snow cover N86-10515

ALTERNATING CURRENT
Investigation of the uncertainties of the NBS (National Bureau of Standards) thermal voltage and current converters
[PB85-200178] N86-10453

ALTITUDE
Laws of distribution of the snow cover on the greater Caucasus (Soviet Union)
[NASA-TM-77911] N86-10614
Altitudinal distribution of granitic landforms in the south central Sierra Nevada, California N86-10695
The effects of age, sleep deprivation, and altitude on complex performance
[AD-A156987] N86-10771

ALTITUDE TOLERANCE
Dynamics of general resistance of rats during readaptation period after training in altered gas environment N86-10767

ALUMINUM
Theoretical problems in materials science N86-10088
Containerless studies of nucleation and undercooling N86-10102
Hugoniot measurements in aluminum to 420 GPa using the LLNL two-stage light-gas gun
[DE85-013821] N86-10317
Aluminum ion plating for corrosion protection of uranium, revision 1
[DE85-012419] N86-10330
Metastable phase formation in Ni-implanted Al: An analytical electron microscope investigation
[DE85-009105] N86-10331
The mechanism of erosion of metallic materials under cavitation attack
[NASA-TM-87133] N86-10552
An analytical and numerical study of the buckling behavior of fiber-reinforced beams N86-10586

ALUMINUM ALLOYS
The role of entrained surface oxides in RS-PM aluminum alloys on resultant structures and properties N86-10085
Directional solidification of monotectic and hypermonotectic aluminum-indium alloys under micron-g N86-10097
Space shuttle experiments on Al-In liquid phase miscibility gap (LPMG) alloys N86-10264
Metastable phase formation in Ni-implanted Al: An analytical electron microscope investigation
[DE85-009105] N86-10331
Aluminum battery alloys
[DE85-011599] N86-10445
Nondestructive corrosion test of aluminum alloy structures
[PV-43-954/F/2] N86-10594

ALUMINUM COMPOUNDS
Directional solidification of an aluminum-zinc vapor emulsion in microgravity — Spacelab N86-10218

ALUMINUM GALLIUM ARSENIDES
W-shaped diffused stripe GaAs/AlGaAs laser
[AD-D011818] N86-10538

ALUMINUM OXIDES
High efficiency heat transport and power conversion system for cascade
[DE85-012959] N86-10468

ALUMINUM SILICATES
Thermal expansion of glasses in the solid and liquid phases
[DE85-013953] N86-10351

ALVEOLAR AIR
Conditioning potentialities of respiratory apparatus N86-10753

AMBIENCE
Evaluation of Passive Sampling Devices (PSDs)
[PB85-196418] N86-10689

AMINES
Passivation of steel with aqueous amine solutions
[AD-D011749] N86-10314
Development of new ammonium nitrate composite explosives
[DE85-014252] N86-10356

AMMETERS
Calibrated Faraday current and magnetic field sensor
[DE85-013438] N86-10439

AMMONIA
Nature of photoemission into dielectric fluids
[DE85-013017] N86-10945

AMMONIUM NITRATES
Development of new ammonium nitrate composite explosives
[DE85-014252] N86-10356

AMORPHOUS MATERIALS
Bulk formation of metallic glasses and amorphous silicon from the melt N86-10154
Formation and characterization of amorphous erbium-based alloys prepared by near-isothermal cold-rolling of elemental composites
[DE85-014853] N86-10327
Photovoltaic devices using a Si:H from higher order silanes
[DE85-008804] N86-10668
Ion beam sputter deposited zinc telluride films
[NASA-TM-87119] N86-11048

AMORPHOUS SEMICONDUCTORS
Topics in the electronic theory of disordered semiconductors N86-11045

AMPLIFIERS
Instantaneous frequency measurement receiver with digital processing
[AD-D011759] N86-10425

AMPLITUDE MODULATION
Amplitude and phase modulation in fin-lines electrical tuning
[AD-D011813] N86-10415

AMPLITUDES
Forced response analysis of an aerodynamically detuned supersonic turbomachine rotor
[NASA-TM-87093] N86-10019
Real-time holography by stimulated Raman and Brillouin scattering N86-10479
Measurements of the acoustic interference between adjacent microphones
[AD-A156892] N86-10919

ANALOG DATA
Restitution of Spacelab photography by analog stereoplotter N86-10489

ANALOG TO DIGITAL CONVERTERS
Extended precision in video bandwidth analog to digital converter using optical techniques
[AD-D011745] N86-10422
Instantaneous frequency measurement receiver with digital processing
[AD-D011759] N86-10425
Digital image processing of metric camera imagery — Spacelab N86-10511
Harmonic distortion reduction technique for data acquisition
[AD-D011771] N86-10799

ANALOGIES
Derivational analogy: A theory of reconstructive problem solving and expertise acquisition
[AD-A156817] N86-10699

ANALYSIS (MATHEMATICS)
Nonlinear methods for spacecraft attitude maneuvers
[AD-A156956] N86-10275
Progressive damage, fracture predictions and post mortem correlations for fiber composites
[NASA-TM-87101] N86-10290
Freezer model using a population balance approach for steady-state, direct-contact, secondary refrigerant, freeze desalination N86-10361
Analytical and experimental study of cracks emanating from an elliptical hole in unidirectional composite material N86-10567
A composite climatological study of the frequency and distribution of severe weather associated with spring season Colorado cyclogenesis
[AD-A156981] N86-10715

ANALYSIS OF VARIANCE
Robustness of multiple comparisons against variance heterogeneity
[COMP-CENT-NOTE-17] N86-10890
The power of weighted and ordinary least squares with estimated unequal variances in experimental design
[B8562446] N86-10894

ANALYTIC FUNCTIONS
Some remarks about cusp forms: Holomorphic and non-holomorphic
[CTH-MATH-1984-26] N86-10902

ANALYTIC GEOMETRY
Estimates for maximal functions along hypersurfaces
[CTH-MATH-1984-29] N86-10874

ANALYTICAL CHEMISTRY
New directions in chemical analysis
[DE85-012930] N86-10296

ANCHORS (FASTENERS)
Improved arresting and recovery system for test missiles
[AD-D011743] N86-10198

ANEMOMETERS
Velocities of gas and plasmas from real time holographic interograms
[DE85-014618] N86-10530

ANGLE OF ATTACK
Angle set-on apparatus
[AD-D011766] N86-10371

ANGLES (GEOMETRY)
Total internal reflection modulator/deflector
[AD-D011757] N86-10424
Angle of incidence effects for underwater shock using generic computational models
[DE85-012936] N86-10466
Angle of incidence effects for underwater shock using generic computational models, rev. 1
[DE85-012921] N86-10467
The effect of vegetation type, microrelief, and incidence angle on radar backscatter N86-10619

ANGULAR DISTRIBUTION
Joint research effort on vibrations of twisted plates, phase 1: Final results
[NASA-RP-1150] N86-10579
Angular distribution of neutral hydrogen following collisional electron detachment from H(-)
[DE85-014258] N86-10943

ANGULAR MOMENTUM
Local conservation laws for the Maxwell-Vlasov and collisionless kinetic guiding center theories
[DE85-013122] N86-11063
The dynamics and stellar content of globular star clusters N86-11131

ANGULAR RESOLUTION
Angle of incidence effects for underwater shock using generic computational models, rev. 1
[DE85-012921] N86-10467
Tunable acousto-optic filter with improved spectral resolution and increased aperture
[AD-D011758] N86-10915
Optical/IR telescope arrays: A study of their potential for satisfying observational requirements in astronomy for a large aperture system in the 1990s and beyond
[REPT-15] N86-11094
High angular resolution in the infrared: Prospects for space observations N86-11100

ANISOTROPIC MEDIA
Analytical and experimental study of cracks emanating from an elliptical hole in unidirectional composite material N86-10567

ANISOTROPIC SHELLS
Three-dimensional stress singularities in anisotropic materials and composites N86-10286

ANISOTROPY
Theory of dense molecular fluid equations of state with application to detonation products
[DE84-016822] N86-10927

ANNEALING
The interaction of small metal particles with refractory oxide supports
[NASA-CR-176228] N86-11047

ANNUAL VARIATIONS
Observations of the snow cover in the southern part of the Buryat Autonomous Soviet Socialist Republic
[NASA-TM-77910] N86-10613
Seasonal variations in atmospheric chemistry in the Adirondacks
[DE85-014227] N86-10719

ANNULAR DUCTS
Oscillations of subsonic flow in an abruptly expanding circular duct
[MPIS-16/1984] N86-10028

ANNULAR FLOW
Analysis of annular two-phase flow with liquid entrainment N86-10459

ANNULAR NOZZLES
On the method of characteristics and its application to the calculations of annular nozzle flowfields N86-10454

ANODIC COATINGS
Chemical/hydrogen energy systems
[DE85-012742] N86-10667

ANOMALIES
Local drift parameter, j/n sub e and resistivity anomaly measurements in CTX spheromaks
[DE85-012740] N86-10998

ANTARCTIC REGIONS
How Antarctica was unveiled. Masterpieces of Frankfurt topographic surveyors. A part of the German Antarctica research program N86-10181
Individual typological features of autonomic reactions during autogenic training in polar expedition members in period of wintering in Antarctica N86-10748
Adaptation of man to extreme conditions of Antarctica N86-10751

ANTENNA ARRAYS
Angle set-on apparatus
[AD-D011766] N86-10371
Method for tuning a phased array antenna
[AD-D011768] N86-10372
A dual frequency microstrip antenna for Ka band
[NASA-TM-87124] N86-10380
Planning for VLA/DSN arrayed support to the Voyager at Neptune N86-10395
A VLA experiment: Planning for Voyager at Neptune N86-10396

ANTENNA COMPONENTS
Signal analysis receiver with acousto-optic delay lines
[AD-D011761] N86-10427

ANTENNA DESIGN
Space antenna for gravitational wave astronomy N86-11123

ANTENNA FEEDS
A dual frequency microstrip antenna for Ka band
[NASA-TM-87124] N86-10380

ANTENNA RADIATION PATTERNS
A numerical method for approximating antenna surfaces defined by discrete surface points
[NASA-TM-87125] N86-10381

ANTHROPOMETRY
A graphic anthropometric aid for seating and workplace design
[AD-A156988] N86-10788
System integration report
[NASA-CR-171900] N86-10821

ANTIFERROELECTRICITY
Analysis of transitions between ferroelectric and antiferroelectric states under conditioning of uniaxial strain
[DE85-014468] N86-10350

ANTIFERROMAGNETISM
Fermi surface study of CeSb in the ferromagnetic and antiferromagnetic phases
[DE85-012122] N86-11052

ANTIMISSILE DEFENSE
An anthology: Rationale for a US ballistic missile defense (1969 - 1984)
[AD-A156781] N86-10199
Report of the ad hoc committee to review the program of the SDI Directorate on Innovative Science and Technology (IST)
[AD-A156668] N86-11071

ANTIMONY ALLOYS
Fermi surface study of CeSb in the ferromagnetic and antiferromagnetic phases
[DE85-012122] N86-11052

ANTIPARTICLES
Matter-antimatter transition operators: A manual for modeling N86-10921

ANTISUBMARINE WARFARE AIRCRAFT
A comparative analysis of a CV helicopter and a JVX (Joint Services Advanced Vertical Lift) tilt-rotor aircraft in an aircraft carrier based ASW (Anti-Submarine Warfare)
[AD-A156871] N86-10041

APERTURES
Tunable acousto-optic filter with improved spectral resolution and increased aperture
[AD-D011758] N86-10915
Optical testing of large telescopes using multiple subapertures N86-10971
Thermal and structural analysis of ring components by the finite element method
[DE85-013305] N86-11021
Tracking studies on the effects of magnet multipoles on the aperture of the RHIC heavy ion collider
[DE85-013282] N86-11023
Optical/IR telescope arrays: A study of their potential for satisfying observational requirements in astronomy for a large aperture system in the 1990s and beyond
[REPT-15] N86-11094

APPALACHIAN MOUNTAINS (NORTH AMERICA)
Dynamic lithostratigraphy and paleecology of upper Mississippi (Chesterian) strata of the northcentral Appalachian Basin N86-10693

APPROXIMATION
Second order approximation method for transonic flows over swept wings N86-10002
A fundamental study of smoldering with emphasis on experimental design for zero-g N86-10162
A numerical method for approximating antenna surfaces defined by discrete surface points
[NASA-TM-87125] N86-10381
Acceleration-invariant approximation method for recursive digital filters
[AD-A156655] N86-10865
Naive approximate realization of noisy data
[ER-83/10] N86-10880
Renormalization of an inverse scattering theory for inhomogeneous dielectrics
[AD-A156636] N86-11049
A study of the applicability of nucleation theory to quasi-thermodynamic transformations of second and higher Ehrenfest-order
[NASA-CR-176230] N86-11060

APTITUDE
Extended analysis of the structure of error scores in psychological aptitude tests
[DFVLR-FB-85-20] N86-10780

AQUEOUS SOLUTIONS
Separation of aqueous two-phase polymer systems in microgravity N66-10246
Streaming potentials in conductive and nonconductive tubing
[DE85-012984] N86-10438

AQUIFERS
Modeling groundwater flow into lakes N86-10598
Evaluating the ground-water resources of the high plains of Texas, Volume 4
[PB85-191625] N86-10641

ARC JET ENGINES
Experimental performance of a 1-kilowatt arcjet thruster
[NASA-TM-87131] N86-10281

ARCHITECTURE
Implementation issues for algorithmic VLSI (Very Large Scale Integration) processor arrays
[AD-A156699] N86-10432

ARCHITECTURE (COMPUTERS)
Special purpose hardware architectures for language recognition
[AD-A156634] N86-10793
Alternating direction methods on multiprocessors: An extended abstract
[AD-A156722] N86-10794
Efficient systolic arrays for the solution of toeplitz systems: An illustration of a methodology for the construction of systolic architectures in VLSI (Very Large Systems Integration)
[AD-A156767] N86-10795
Design of a multifunction Input-Output (I/O) controller
[EUT-84-E-143] N86-10802
The local disk controller
[REPT-1-68430-44(1985)01] N86-10806
An intelligent local disk control system
[REPT-051560-28(1984)08] N86-10808
USSR report: Cybernetics, computers and automation technology
[JPRS-UCC-85-006] N86-10809
Prospects for creation of optical digital high-performance computers N86-10810
Elektronika MS 1603 high-speed peripheral processor N86-10811
Diagnostics of peripheral processors and controllers N86-10812
An approach to implementing CAMAC microprocessor modules N86-10813
Compact, high-speed algorithm for laying out printed circuit board runs N86-10814
Fault-free behavior of reliable multiprocessor systems: FTMP experiments in AIRLAB
[NASA-CR-177967] N86-10848
Topological properties of hypercubes
[AD-A156777] N86-10850

ARCTIC OCEAN
Long term statistical measurements of environmental acoustics parameters in the arctic. AEAS report number 2. Low frequency transmission loss measurements in the central arctic ocean
[AD-A156576] N86-10727
ARID LANDS
Topographic interpretation of metric camera images: An example in Somalia --- Spacelab N86-10508
Representation of the distribution of the snow cover on the surface of the Earth's dry land
[NASA-TM-77909] N86-10612
Effect of inclusion of supplementary ascorbic acid in daily diet on degree of vitamin saturation of body and thermoresistance of erythrocytes while working in arid zone N86-10749
ARMED FORCES (UNITED STATES)
F-16X MSIP (Multi-national Staged Improvement Program) case example: Operating and support cost estimation using VAMOSC (Visibility And Management Of Operating and Support Costs)
[AD-A156893] N86-10006
Let's get serious about software
[AD-A156819] N86-10831
ARRAYS
An evaluation of the use of microphone arrays for studio recording
[BBC-RD-1985/8] N86-10366
P-N junction controlled field emitter array cathode
[AD-D011815] N86-10416
Signal analysis receiver with acousto-optic delay lines
[AD-D011761] N86-10427
Implementation issues for algorithmic VLSI (Very Large Scale Integration) processor arrays
[AD-A156699] N86-10432
Results and limitations of ground-based optical arrays --- stellar interferometry N86-11097
ARRESTING GEAR
Improved arresting and recovery system for test missiles
[AD-D011743] N86-10198
ARRIVALS
Angle set-on apparatus
[AD-D011766] N86-10371
ARTIFICIAL INTELLIGENCE
USSR report: Cybernetics, computers and automation technology
[JPRS-UCC-85-006] N86-10809
The DUCK manual
[AD-A156936] N86-10833
Generation of flight paths using hierarchical planning
[AD-A156905] N86-10900
ARTIFICIAL SATELLITES
Cryogenic equivalence principle experiment N86-10171
ASCORBIC ACID METABOLISM
Effect of inclusion of supplementary ascorbic acid in daily diet on degree of vitamin saturation of body and thermoresistance of erythrocytes while working in arid zone N86-10749
ASIA
Structural mapping of folded sedimentary environments from satellite images: An example from Central Asia N86-10607
ASPECT RATIO
Joint research effort on vibrations of twisted plates, phase 1: Final results
[NASA-RP-1150] N86-10579
ASSESS PROGRAM
The first German Spacelab mission D1 reports --- Spacelab payloads
[PR-2] N86-10188
ASSESSMENTS
Initial design of a relational database system for NPS computer asset identification and valuation for risk assessment
[AD-A156847] N86-10796
ASTEROID BELTS
Project VESTA, exploratory mission to the asteroids: Scientific objectives and technical specifications
[NASA-TM-77669] N86-10179
ASTEROID MISSIONS
Project VESTA, exploratory mission to the asteroids: Scientific objectives and technical specifications
[NASA-TM-77669] N86-10179
ASTRONAUT PERFORMANCE
The first German Spacelab mission D1 reports --- Spacelab payloads
[PR-2] N86-10188
ASTRONAUT TRAINING
The first German Spacelab mission D1 reports --- Spacelab payloads
[PR-3] N86-10189
ASTRONAUTICS
Space utilization N86-11067
DFVLR, strategic study of astronautics 1984, user requirements N86-11069
ASTRONOMICAL OBSERVATORIES
Activities report of the European Southern Observatory N86-11135
ASTRONOMICAL TELESCOPES
Planning for VLA/DSN arrayed support to the Voyager at Neptune N86-10395
Optical/IR telescope arrays: A study of their potential for satisfying observational requirements in astronomy for a large aperture system in the 1990s and beyond
[REPT-15] N86-11094
Results and limitations of ground-based optical arrays --- stellar interferometry N86-11097
Extragalactic observations with optical space arrays N86-11098
Strategy for the development of space arrays N86-11101
TRIO: A kilometric array stabilized by solar sails --- Spaceborne astronomy N86-11102
SAMSI: An orbiting spatial interferometer for micro-arc second astronomical observations --- Spacecraft Array for Michelson Spatial Interferometry (SAMSI) N86-11103
COSMIC: A high resolution, large collecting area telescope --- Coherent Optical System of Modular Imaging Collectors (COSMIC) N86-11104
A fiber-linked version of project TRIO --- telescope array N86-11105
OASIS: Optical Aperture Synthesis in Space N86-11106
Future space telescope design concepts N86-11107
TRIO optics --- spaceborne optical interferometer (TRIO) N86-11108
On line astronomical image processing using microcomputers N86-11121
The intensified multi CCD camera --- spaceborne interferometers N86-11122
Activities report of the European Southern Observatory N86-11135
ASTRONOMY
Activities report of the European Southern Observatory N86-11135
ASYMPTOTIC SERIES
The h, p and h-p versions of the finite element method in dimension. Part 1: The error analysis of the p-version
[AD-A156600] N86-10862
ATMOSPHERIC BOUNDARY LAYER
Simulation of the atmospheric boundary layer in the large wind tunnel of the TNO Institute for Building materials and Constructions (IBBC). Part 1: Theory
[BI-76-39/08.7.23100-PT-1] N86-10703
Simulation of the atmospheric boundary layer in the large wind tunnel of the TNO Institute for Building Materials and Construction (IBBC). Part 2: Experiments
[BI-76-39/08.7.23100-PT-2] N86-10704
List of publications on the 200 m meteorological mast at Cabauw, the Netherlands
[KNMI-FM-85-6] N86-10711
ATMOSPHERIC CHEMISTRY
Acoustic gravity wave chemistry model for the RAYTRACE code
[AD-A156850] N86-10405
Technical considerations in regional aerosol modeling
[PB85-193027] N86-10710
Seasonal variations in atmospheric chemistry in the Adirondacks
[DE85-014227] N86-10719
ATMOSPHERIC CIRCULATION
Computation of flow regimes in parameter space for the AGCE
[NASA-CR-178480] N86-10705
The Liu, Katsaros, and Businger (1979) bulk atmospheric flux computational iteration program in FORTRAN and BASIC
[AD-A156736] N86-10714
A composite climatological study of the frequency and distribution of severe weather associated with spring season Colorado cyclogenesis
[AD-A156981] N86-10715
Microphysical/mesoscale aspects of nuclear winter and new directions in assessments
[DE85-013479] N86-10718
ATMOSPHERIC MODELS
Simulation of the atmospheric boundary layer in the large wind tunnel of the TNO Institute for Building materials and Constructions (IBBC). Part 1: Theory
[BI-76-39/08.7.23100-PT-1] N86-10703
Simulation of the atmospheric boundary layer in the large wind tunnel of the TNO Institute for Building Materials and Construction (IBBC). Part 2: Experiments
[BI-76-39/08.7.23100-PT-2] N86-10704
Computation of flow regimes in parameter space for the AGCE
[NASA-CR-178480] N86-10705
Technical considerations in regional aerosol modeling
[PB85-193027] N86-10710
Smoke inputs to climate models: Optical properties and height distribution for nuclear winter studies
[DE85-011363] N86-10717
ATMOSPHERIC PRESSURE
Chemical kinetics and cellular structure of detonations in hydrogen sulphide and air
[DE85-009408] N86-10304
Reaction of rabbit respiration system to hypoxic stimulus in nitrogen-oxygen medium at elevated pressure N86-10760
ATMOSPHERIC SOUNDING
The air of life of the blue planet. Atmosphere research from space using data and facts against climate speculations N86-10184
ATMOSPHERIC TEMPERATURE
Monthly and Seasonal Weather Outlook for mid-April to mid-May 1985, Volume 39, Number 8
[PB85-195345] N86-10724
ATOMIC CLOCKS
A nanosecond or thirty centimeters: Why atomic clocks have to be synchronized. MITREX opens new dimensions for measuring accuracy N86-10185
ATOMIC ENERGY LEVELS
Theoretical investigation of electron-positive ion-atom interactions
[DE85-013019] N86-10939
ATOMIC EXCITATIONS
Theoretical investigation of electron-positive ion-atom interactions
[DE85-013019] N86-10939
ATOMIC INTERACTIONS
Evaluation and prediction of long-term environmental effects on non metallic materials
[NASA-CR-178495] N86-10340
ATOMIC PHYSICS
The 1984 bibliography of atomic and molecular processes
[DE85-010583] N86-10926
ATOMIC SPECTRA
Cooled ion frequency standard
[AD-A156813] N86-10295
Selected tables of atomic spectra. Atomic energy levels and multiplet table O3
[NBS/NSRDS-3/11] N86-10923
Cooperative emission by two different atoms into surface plasmons
[AD-A157033] N86-10925
The two micron spectrum of R Scuti N86-11092
ATOMIC STRUCTURE
Electronic and magnetic properties of noble-metal and transition-metal alloys, interfaces and overlayers
[DE85-014532] N86-10321
Non-empirical interatomic potentials for transition metals
[DE85-013448] N86-10440
ATOMIC WEIGHTS
Direct mass measurements in the light neutron-rich region using a combined energy and time-of-flight technique
[DE85-012758] N86-10963
ATOMIZING
The role of entrained surface oxides in RS-PM aluminum alloys on resultant structures and properties N86-10085
Modeling of engine sprays
[DE85-010020] N86-10559
ATTENUATION
Ultrasonic evaluation of mechanical properties of thick, multilayered, filament wound composites
[NASA-TM-87088] N86-10561
AUDITORY SIGNALS
Apparatus for locating passive intermodulation interference sources
[AD-D011798] N86-10435
Measurements of the acoustic interference between adjacent microphones
[AD-A156892] N86-10919
AUGER EFFECT
Mean life of the 2p(4)((1)S)3s (2)S state in fluorine
[DE85-012929] N86-10956
AURORAS
Potential structures and particle acceleration on auroral field lines
[AD-A156694] N86-10708
Activities report in geophysics
[KGI-188] N86-10709
AUTOCORRELATION
Periodic binary sequences with very good autocorrelation properties N86-10397
A binary sequence of period 60 with better autocorrelation properties than the Barker sequence of period 13 N86-10398

AUTOMATIC CONTROL
New directions in chemical analysis
[DE85-012930] N86-10296
Automated analysis of digital images generated by two-dimensional gel electrophoresis
[DE85-011906] N86-10526
Computer control of an electric hydraulic robot leg with proximity ranging system N86-10549
Framework for generating expert systems to perform computer security risk analysis
[DE85-014134] N86-10841

AUTOMATIC GAIN CONTROL
Constant rise AGC (Automatic Gain Control) device
[AD-D011744] N86-10421

AUTOMATION
USSR report: Cybernetics, computers and automation technology
[JPRS-UCC-85-006] N86-10809
An approach to implementing CAMAC microprocessor modules N86-10813
Compact, high-speed algorithm for laying out printed circuit board runs N86-10814
Collective use computer system for the Academy of Sciences KaSSR N86-10817

AUTOMOBILES
Studies on human vehicle control
[B8563352] N86-10775
Car driving as a supervisory control task
[B8563351] N86-10776
Path error-neglection in straight lane driving
[IZF-1984-32] N86-10783
Advanced vehicle systems assessment. Volume 2: Subsystems assessment
[NASA-CR-176205] N86-11083
Advanced vehicle systems assessment. Volume 3: Systems assessment
[NASA-CR-176206] N86-11084

AUTONOMIC NERVOUS SYSTEM
Individual typological features of autonomic reactions during autogenic training in polar expedition members in period of wintering in Antarctica N86-10748

AUTONOMOUS NAVIGATION
Digital control of the hydraulic actuators of an adaptive suspension vehicle N86-10548

AXES OF ROTATION
Multimode acoustic research N86-10167

AXIAL COMPRESSION LOADS
Effect of sequence of loading on interaction curves for buckling of stiffened shells
[TAE-536] N86-10583

AXIAL STRAIN
Analysis of transitions between ferroelectric and antiferroelectric states under conditioning of uniaxial strain
[DE85-014468] N86-10350
Inelastic analysis of frame structures including member and joint shears N86-10573
Experiments with tubular probes made of INCOLOY 800 H under uniaxial and multiaxial strain
[JUEL-1979] N86-10595

AXIAL STRESS
Defect identification in high-energy semiconductors
[DE85-014533] N86-10442

AXISYMMETRIC BODIES
Strength of shells under local transverse loads N86-10568

AXISYMMETRIC FLOW
Effect of a shear layer on the stability of an axisymmetrical external compression air intake N86-10010

B

BACKGROUND NOISE
Proposed aural nondetectability limits for Army materiel
[AD-A156704] N86-10917

BACKGROUND RADIATION
Extra-galactic X-ray sources and the diffuse X-ray background N86-11144

BACKSCATTERING
CV-990 L-band SAR: A calibration experiment N86-10617
The effect of vegetation type, microrelief, and incidence angle on radar backscatter N86-10619
Age-dating volcanic and alluvial surfaces with multipolarization data N86-10620
Mapping diverse forest cover with multipolarization airborne radar N86-10625
Modelling of vegetation volumes N86-10629

BACTERIA
Kinetics of biological ferrous iron oxidation
[DE85-014616] N86-10736

BAGS
The wearing comfort of the PVC: Combat back pack
[IZF-1984-34] N86-10789

BALLISTIC MISSILES
Improved arresting and recovery system for test missiles
[AD-D011743] N86-10198

BALLISTICS
Transient velocity assessment in gallium arsenide, and of other GaAs characteristics related to device functions
[AD-A156983] N86-11050

BANDPASS FILTERS
An active tracking band-pass filter
[AD-A156559] N86-10419

BANDWIDTH
Phase-coded pulse expander-compressor
[AD-D011812] N86-10375
Extended precision in video bandwidth analog to digital converter using optical techniques
[AD-D011745] N86-10422

BARIUM COMPOUNDS
Thermal expansion of glasses in the solid and liquid phases
[DE85-013953] N86-10351

BEACHES
Application of the dutch method for estimating storm-induced dune erosion
[AD-A156717] N86-10728

BEAM CURRENTS
Laser generation and transport of a relativistic electron beam
[DE85-011709] N86-10192
RFQ-funneling
[DE85-012483] N86-10194

BEAM INJECTION
RFQ-funneling
[DE85-012483] N86-10194
High-brightness photoemitter injector for electron accelerators
[DE85-012673] N86-10929
Method for determining the position, angle and other injection parameters of a short pulsed beam in the Brookhaven AGS
[DE85-012523] N86-10931
Proposed bunching scheme for a polarized H(-) injector
[DE85-012648] N86-10986
Noninterceptive techniques for the measurement of longitudinal parameters for intense H(-) beams
[DE85-012662] N86-10992
Effects of slots/holes in disks on frequencies of TM01 and EH11 waves in the disk-loaded waveguide
[DE85-013376] N86-11009
Generalized helicity and its time derivative
[DE85-012770] N86-11027

BEAM INTERACTIONS
Beam-beam deflections to measure size spot and offset at SLC IP
[DE85-014285] N86-10965
SLC positron damping ring optics design
[DE85-013054] N86-11014
RHIC lattice
[DE85-013289] N86-11026

BEAM WAVEGUIDES
The Netherlands Institute for Nuclear and High Energy Physics (NIKHEF) traveling wave monitor user guide
[LINO-121] N86-10969
Superconvergent tracking and invariant surfaces in phase space
[DE85-013051] N86-10995
Effects of slots/holes in disks on frequencies of TM01 and EH11 waves in the disk-loaded waveguide
[DE85-013376] N86-11009

BEAMS (RADIATION)
RFQ-funneling
[DE85-012483] N86-10194
Surface conditioning of synchrotron radiation source to improve beam lifetime
[DE84-012185] N86-10948
Wide dynamic range beam profile monitor
[DE85-012709] N86-10950
Beam-beam deflections to measure size spot and offset at SLC IP
[DE85-014285] N86-10965
Beam line windows at LAMPF
[DE85-012723] N86-10985
Proposed bunching scheme for a polarized H(-) injector
[DE85-012648] N86-10986
Applications of the second-order achromat concept to the design of particle accelerators
[DE85-013072] N86-10994
Effects of slots/holes in disks on frequencies of TM01 and EH11 waves in the disk-loaded waveguide
[DE85-013376] N86-11009

BEAMS (SUPPORTS)
Load-deflection tests and computer analyses of a high-precision adhesive-bonded antenna reflector panel N86-10389
An analytical and numerical study of the buckling behavior of fiber-reinforced beams N86-10566
Joint research effort on vibrations of twisted plates, phase 1: Final results
[NASA-RP-1150] N86-10579
Three-dimensional vibration analysis of a uniform beam with offset inertial masses at the ends
[NASA-TM-86393] N86-10580

BEARINGS
Precise bearing support ditherer with piezoelectric drive means
[AD-D011819] N86-10483
The generation and transmission of vibration in plain cylindrical bearings. Part 2. Experiment
[AD-A156577] N86-10553

BEHAVIOR
Contact effects in light activated GaAs switches
[AD-A156957] N86-10434
USSR report: Life sciences. Biomedical and behavioral sciences
[JPRS-UBB-85-023] N86-10738

BELLOWS
Method for compensating bellows pressure loads while accommodating thermal deformations
[DE85-013306] N86-10933

BENARD CELLS
Rayleigh-Benard instability in systems presenting a minimum in surface tension N86-10245

BENDING
Measurement and resulting first and second order approximations for a 9 deg bending magnet in LAMPF's 750-keV transport
[DE85-012691] N86-10930

BERYLLIUM
Work-hardening and effective viscosity in solid beryllium
[DE85-013978] N86-10323
Anelastic relaxation in irradiated Cu-Be
[DE85-013893] N86-11056

BERYLLIUM OXIDES
High efficiency heat transport and power conversion system for cascade
[DE85-012959] N86-10468

BETA FACTOR
Freezer model using a population balance approach for steady-state, direct-contact, secondary refrigerant, freeze desalination N86-10361

BETATRONS
Use of the MURA transformation to generate the fields and calculate the motion of protons in the designed Argonne Mini-ASPUN FFAG spiral sector accelerator
[DE85-011477] N86-10934
Theory of non-planar orbits
[DE85-013284] N86-11018

BIBLIOGRAPHIES
An anthology: Rationale for a US ballistic missile defense (1969 - 1984)
[AD-A156781] N86-10199
Aerospace medicine and biology: A continuing bibliography with indexes (supplement 275)
[NASA-SP-7011(275)] N86-10768
Computer codes: A bibliography, supplement 1
[DE85-008721] N86-10838
The 1984 bibliography of atomic and molecular processes
[DE85-010583] N86-10926
An annotated bibliography of abstracts on the use of simulators in technical training
[AD-A156792] N86-11065
Annotated bibliography of publications dealing with occupational health and medical information systems, cost analysis procedures, evaluation methodology and related legal issues
[AD-A156650] N86-11078
Publication of the Executive Office of the President, January 20, 1981 - December 31, 1984
[PB85-187110] N86-11082

BINARY ALLOYS
Stability of metallic dispersions --- microgravity N86-10258
Dendritic solidification in a binary alloy melt: Steady-state versus morphological stability theories N86-10261

BINARY CODES
Periodic binary sequences with very good autocorrelation properties N86-10397
A binary sequence of period 60 with better autocorrelation properties than the Barker sequence of period 13 N86-10398

BINARY FLUIDS
Cell partition in two polymer aqueous phases N86-10139

BINARY MIXTURES
New approach to multiphase equilibria: Application to high-pressure physics problems
[DE85-013820] N86-10907
BINARY SYSTEMS (MATERIALS)
Solutal convection and its effects on crystal growth and segregation in binary and pseudo-binary system with large liquidus-solidus separation N86-10056
Separation of aqueous two-phase polymer systems in microgravity N86-10246
Rationale for two phase polymer system microgravity separation experiments N86-10247
Application of the theory of Ostwald ripening to microgravity phase separation experiments N86-10248
Thermodynamics of polymer-supercritical solvent mixtures
[AD-A157038] N86-11061
BINOMIALS
Estimation by moments in a model of faulty inspection
[AD-A156754] N86-10886
BIOASSAY
Development and evaluation of multispecies test protocols for assessing chemical toxicity
[DE85-013526] N86-10679
BIOCHEMISTRY
Biochemical assays of cultured cells N86-10134
BIOCONTROL SYSTEMS
Individual typological self-regulation of cardio-vascular system N86-10752
BIOCONVERSION
Romanian plant produces protein concentrate from paraffin-nourished yeasts N86-10741
BIODEGRADATION
Evaluation of the 90-day inhalation toxicity of petroleum and oil shale JP-5 jet fuel
[AD-A156815] N86-10675
BIOELECTRICITY
Criteria for the design or selection of a bioelectromagnetics experiment
[AD-A156575] N86-10420
BIOENGINEERING
LSRO/ONR ad hoc review process
[AD-A156590] N86-10735
BIOGRAPHY
Study of one- and two-dimensional filtering and deconvolution algorithms for a streaming array computer
[NASA-CR-176226] N86-10827
BIOLOGICAL EFFECTS
Aerospace medicine and biology: A continuing bibliography with indexes (supplement 275)
[NASA-SP-7011(275)] N86-10768
BIOLOGICAL MODELS (MATHEMATICS)
Mathematical models of continuous flow electrophoresis N86-10143
Hemodynamics during gravitational overloads (mathematical modeling) N86-10739
BIOMASS
Potential applications of multipolarization SAR for pine plantation biomass estimation N86-10626
Vegetation canopy discrimination and biomass assessment using multipolarized airborne SAR N86-10628
BIOMEDICAL DATA
USSR report: Life sciences. Biomedical and behavioral sciences
[JPRS-UBB-85-023] N86-10738
Annotated bibliography of publications dealing with occupational health and medical information systems, cost analysis procedures, evaluation methodology and related legal issues
[AD-A156850] N86-11078
BIOMETRICS
Dynamics of changes of statistical indicators of heart rhythm of persons with different degree of motion sickness N86-10743
BIOREACTORS
Cell separations in microgravity and development of a space bioreactor N86-10141
Kinetics of biological ferrous iron oxidation
[DE85-014616] N86-10736
BIOTECHNOLOGY
Microgravity Science and Applications Program tasks
[NASA-TM-87568] N86-10053
Lambda point equipment N86-10118
Biotechnology regulation
[GPO-43-778] N86-10733
USSR report: Life sciences. Biomedical and behavioral sciences
[JPRS-UBB-85-023] N86-10738
Biotechnology: Science and practice N86-10742
BISMUTH
Study of eutectic formation N86-10070
Thermal and solutal convection damping using an applied magnetic field N86-10094
BLACK AND WHITE PHOTOGRAPHY
Thematic mapping of metric camera color infrared and black and white photographs for land use classification N86-10510
Topographic and thematic mapping: Analysis of metric camera black and white photographs of the Rhone Delta N86-10514
BLACK BODY RADIATION
Scaling studies of solar pumped lasers
[NASA-CR-176240] N86-10540
Initial data for N black holes N86-11128
BLAST LOADS
Angle of incidence effects for underwater shock using generic computational models
[DE85-012936] N86-10466
Angle of incidence effects for underwater shock using generic computational models, rev. 1
[DE85-012921] N86-10467
BLOOD
A study of blood flow and of aggregation of blood cells under conditions of zero gravity: Its relevance to the occlusive diseases and cancer N86-10137
Evaluation of the 90-day inhalation toxicity of petroleum and oil shale JP-5 jet fuel
[AD-A156815] N86-10675
BLOOD CIRCULATION
Vestibular resistance and blood circulation changes in orthostatic position during hyperthermia N86-10758
Reaction of rabbit respiration system to hypoxic stimulus in nitrogen-oxygen medium at elevated pressure N86-10760
Indices of blood oxygen transporting properties and erythropoiesis in rats after prolonged stay in nitrogen-oxygen mixture at elevated pressure N86-10761
BLOOD FLOW
Streaming potentials in conductive and nonconductive tubing
[DE85-012984] N86-10438
BLOOD PLASMA
Effect of emotional stress on hemostasis system of healthy persons N86-10745
BLOOD PRESSURE
Vestibular resistance and blood circulation changes in orthostatic position during hyperthermia N86-10758
BODY TEMPERATURE
Short term heat effect on adreno- and cholino-sensitivity of rat's small intestine N86-10754
Efficiency of muscular work in white rats during adaptation to cold N86-10763
Effect of increased body clothing insulation on hand temperature in a cold environment
[AD-A156597] N86-10786
BODY WEIGHT
Evaluation of the 90-day inhalation toxicity of petroleum and oil shale JP-5 jet fuel
[AD-A156815] N86-10675
BOLTS
Rusty bolt intermodulation interference reducer
[AD-D011748] N86-10313
Over-center toggle latch
[AD-D011753] N86-10556
BOLTZMANN-VLASOV EQUATION
Local conservation laws for the Maxwell-Vlasov and collisionless kinetic guiding center theories
[DE85-013122] N86-11063
BONDING
Properties of plastic-bonded nitroguanidine
[DE85-015316] N86-10358
BOOLEAN ALGEBRA
Partial evolution and omega completeness of algebraic specifications
[CWI-CS-R8501] N86-10884
Reaching approximate agreement in the presence of faults
[AD-A156541] N86-10898
BORANES
Boronising of iron and steel by ionic bombardment by diborane
[BLL-BISI-TRANS-23034-(9022.06)] N86-10307
BORATES
Thermal expansion of glasses in the solid and liquid phases
[DE85-013953] N86-10351
BOREHOLES
Geologic evaluation and reservoir properties of the PR Spring tar sand deposit, Uintah and Grand Counties, Utah
[DE85-013248] N86-10634
BORESIGHTS
Radome analysis and design capabilities of the RF and Microwave Technology Branch
[AD-A156862] N86-10404
BORIDES
Mechanism of the formation of boronised layers on high carbon steel
[BLL-BISI-TRANS-23036-(9022.06)] N86-10306
BORON
Magnetic properties of doped semiconductors
[DE85-012090] N86-11053
BORON NITRIDES
Development of a sheath for sensor protection in molten steel applications
[AD-A156764] N86-10315
BOROSILICATE GLASS
Recirculation within a glass mixture subjected to external and resistive heating
[DE85-010068] N86-10348
BOSON FIELDS
Polarization transfer in inelastic scattering and pionic models of the EMC effect
[DE85-010738] N86-10955
BOSONS
Proceedings of a Workshop on Electroweak Symmetry Breaking
[DE85-004444] N86-11008
Two-loop large Higgs mass corrections to vector boson self-couplings
[NIKHEF-H/84-15] N86-11038
BOUNDARIES
Correlation between vibrations and buckling of cylindrical shells stiffened by spot-welded and riveted stringers
[TAE-537] N86-10584
A study of methods to predict and measure the transmission of sound through the walls of light aircraft. Integration of certain singular boundary element integrals for applications in linear acoustics
[NASA-CR-176229] N86-10912
BOUNDARY ELEMENT METHOD
Advanced development of BEM for two and three dimensional nonlinear analysis N86-10855
BOUNDARY LAYER FLOW
Acta Aeronautica et Astronautica Sinica (selected articles)
[AD-A147304] N86-10001
Second order approximation method for transonic flows over swept wings N86-10002
Investigations on a supercritical airfoil with boundary layer suction through a perforated strip in the shock region
[DFVLR-FB-85-15] N86-10025
A boundary layer flow model for areas of complex terrain N86-10701
Simulation of the atmospheric boundary layer in the large wind tunnel of the TNO Institute for Building materials and Constructions (IBBC). Part 1: Theory
[BI-76-39/08.7.23100-PT-1] N86-10703
Simulation of the atmospheric boundary layer in the large wind tunnel of the TNO Institute for Building Materials and Construction (IBBC). Part 2: Experiments
[BI-76-39/08.7.23100-PT-2] N86-10704
BOUNDARY LAYER SEPARATION
The role of freestream turbulence scale in subsonic flow separation
[NASA-CR-176237] N86-10014
Three-dimensional inviscid analysis of radial turbine flow and a limited comparison with experimental data
[NASA-TM-87091] N86-10017
BOUNDARY LAYERS
Fuel and lubricant behavior in boundary layers analyzed by infrared emission Fourier transform spectrometry N86-10336
The effects of orography on land-atmosphere turbulent exchange processes N86-10702
BOUNDARY VALUE PROBLEMS
A mesh moving technique for time dependent partial differential equations in two space dimensions
[AD-A156663] N86-10866
Error estimates and automatic time step control for numerical methods for stiff ordinary differential equations
[CTH-MATH-1984-27] N86-10872
BRAGG ANGLE
Signal analysis receiver with acousto-optic delay lines
[AD-D011761] N86-10427
BRAIN
TV monitoring control system in electrophysiological studies N86-10765
BRAYTON CYCLE
High efficiency heat transport and power conversion system for cascade
[DE85-012959] N86-10468
BRAZING
Vacuum brazing under microgravity — Spacelab N86-10214
Metallurgy and metallography of braze joints
[DE85-014563] N86-10325
BREADBOARD MODELS
Advanced optical measurement techniques N86-10174

Advanced containerless processing technology N86-10176

BREMSSTRAHLUNG
Radiation field results from the SPEED triaxiode, a large area, high dose rate, short pulse 1MV bremsstrahlung source
[DE85-009438] N86-11005
Directionality of bremsstrahlung from relativistic electrons in solar flares
[NASA-TM-87509] N86-11141

BRIDGMAN METHOD
Microgravity Science and Applications Program tasks
[NASA-TM-87568] N86-10053
Fluid flow in crystal growth: Analysis of the verticle Bridgman and floating zone process N86-10055
Growth of solid solution crystals N86-10065
Heat flow and segregation in directional solidification N86-10072
Lead telluride crystals grown in microgravity: Experiment ES 318 — Spacelab N86-10220

BRIGHTNESS
Age-dating volcanic and alluvial surfaces with multipolarization data N86-10620
Mild hypoxia and visual performance with night vision goggles
[AD-A156969] N86-10787
High-brightness photoemitter injector for electron accelerators
[DE85-012673] N86-10929

BRIGHTNESS DISTRIBUTION
Improved mapping of radio sources from VLBI data by least-square fit N86-10402
Radio studies of a complete sample of quasars N86-11093
Cometary atmospheres: Modeling the spatial distribution of observed neutral radicals
[NASA-CR-176242] N86-11133

BRILLOUIN EFFECT
Real-time holography by stimulated Raman and Brillouin scattering N86-10479

BROADCASTING
An evaluation of the use of microphone arrays for studio recording
[BBC-RD-1985/8] N86-10366

BROKEN SYMMETRY
Proceedings of a Workshop on Electroweak Symmetry Breaking
[DE85-004444] N86-11008

BROMIDES
Laser Raman spectroscopy study of the zinc and bromide ion complex equilibrium in zinc/bromine battery electrolytes
[DE85-011820] N86-10301

BROMINE
Laser Raman spectroscopy study of the zinc and bromide ion complex equilibrium in zinc/bromine battery electrolytes
[DE85-011820] N86-10301

BRONZES
The mechanism of erosion of metallic materials under cavitation attack
[NASA-TM-87133] N86-10552
Fracture toughness testing of centrifugally cast nickel aluminium bronze
[REPT-MAT/720] N86-10575

BUBBLE TECHNIQUE
Theoretical modeling of the vapor cavitation in dynamically loaded journal bearings
[NASA-TM-87076] N86-10463

BUBBLES
Mass transport phenomena between bubbles and dissolved gases in liquids under reduced gravity conditions N86-10110
Thermocapillary and diffusocapillary migration of a fluid drop N86-10128
Fusion target technology N86-10156
Shrinking of a gas bubble in a glass melt under microgravity conditions — STS-11 N86-10254
Acoustic cavitation and bubble dynamics
[AD-A156888] N86-10918
Methane-bubble formation in hydrogen-charged Fe-30 ppM C
[DE85-012526] N86-10937

BUCKLING
An analytical and numerical study of the buckling behavior of fiber-reinforced beams N86-10566
Optimal design of portal frames against buckling N86-10572
Effect of sequence of loading on interaction curves for buckling of stiffened shells
[TAE-536] N86-10583
Correlation between vibrations and buckling of cylindrical shells stiffened by spot-welded and riveted stringers
[TAE-537] N86-10584

BUDGETS
Report of the ad hoc committee to review the program of the SDI Directorate on Innovative Science and Technology (IST)
[AD-A156668] N86-11071

BUILDINGS
Vibro-acoustic forecast for space shuttle launches at Vandenberg AFB: The payload changeout room and the administration building
[AD-A156944] N86-10269
Load space formulation of reliability for nonlinear random structural systems N86-10570

BUNCHING
Report on a visit to CERN in February 1985. Notes on bunch monitors, high-frequency systems, linacs, kickers, magnets, vacuum and bunch extraction
[LINO-119] N86-10967
Proposed bunching scheme for a polarized H(-) injector
[DE85-012648] N86-10986

BUOYANCY
Crystal melts under reduced gravity N86-10062
Float zone experiments in space N86-10067
Fluid dynamics and thermodynamics of vapor phase crystal growth N86-10068
Buoyancy effects upon vapor flame and explosion processes N86-10161
Fundamental studies of droplet combustion at reduced gravity N86-10165

BURKINA
With Argus eyes from space. Satellite Diagnosis for Upper Volta. Seven maps without mystery N86-10183

BURNERS
Design and calibration of a flat-flame burner using line reversal techniques
[AD-A156724] N86-10294
Effects of chemistry and swirl on the production of turbulence in a flame
[PB85-219632] N86-10305

BURNING RATE
A fundamental study of smoldering with emphasis on experimental design for zero-g N86-10162

BYPASSES
Digital control of the hydraulic actuators of an adaptive suspension vehicle N86-10548

C

CABLES (ROPES)
Guidance and control of a cable based payload pickup system N86-10046

CADMIUM TELLURIDES
Solution growth of cadmium telluride: Experiment ES 322 — Spacelab N86-10225
Sensor system
[AD-D011767] N86-10480

CALCIUM CARBONATES
High-pressure release-wave measurements and phase transformation in CaCO3
[DE85-012592] N86-11055

CALCIUM COMPOUNDS
Crystal growth from solution — Spacelab N86-10229
Characterization of cathodic corrosion products in the Ca/CaCrO4 thermal battery
[DE85-013442] N86-10644

CALCIUM PHOSPHATES
Growth and characterization of brushite and lead monetite, simulation and results — Spacelab N86-10230

CALIBRATING
Operating characteristics of the multiple critical Venturi System and secondary calibration nozzles used for weight-flow measurements in the Langley 16-foot transonic tunnel
[NASA-TM-86405] N86-10016
Design and calibration of a flat-flame burner using line reversal techniques
[AD-A156724] N86-10294
Comparison of the calibration of ionospheric delay in VLBI data by the methods of dual frequency and Faraday rotation N86-10384
A VLA experiment: Planning for Voyager at Neptune N86-10396
Mobile VLBI and GPS measurement of vertical crustal motion N86-10401
A comparison of swept frequency and FFT methods used to calibrate array test modules
[AD-A156629] N86-10430
Calibrated Faraday current and magnetic field sensor
[DE85-013438] N86-10439
Investigation of the uncertainties of the NBS (National Bureau of Standards) thermal voltage and current converters
[PB85-200178] N86-10453
Partial in-flight calibration of the metric camera --- Spacelab N86-10496
High flux calorimetry
[AD-A156852] N86-10524
CV-990 L-band SAR: A calibration experiment N86-10617
Calibration of the multispectral scanner (MSS) satellite data to evaluate change in the reflection of coniferous stocks
[DFVLR-FB-84-44] N86-10636
Harmonic distortion reduction technique for data acquisition
[AD-D011771] N86-10799
Fiber optic gradient hydrophone construction and calibration for sea trial
[AD-A156469] N86-10914
Secondary standards laboratories for ionizing radiation calibrations: The national laboratory interests
[DE85-007046] N86-10938

CALIFORNIA
Structural discontinuity within the southern California continental margin: Seismic and gravity models of the western Transverse Ranges N86-10699
Surface winds at NWC (Naval Weapons Center): 1964 - 1982
[AD-A156660] N86-10712

CALORIMETERS
High flux calorimetry
[AD-A156852] N86-10524
Guidelines for a thermochemical kinetics computer program
[DE85-014266] N86-10839

CAMERAS
Fall velocity indicator/viewer
[AD-D011789] N86-10482
OEEPE participation in testing metric camera photography — European Organization for Experimental Photogrammetric Investigations (OEEPE) N86-10507
Land evaluation successes with the metric camera --- Spacelab N86-10512
Type of new Chinese-produced high-speed camera and its utilization in detonation physics experiments
[DE85-015191] N86-10529

CANOPIES (VEGETATION)
Mapping diverse forest cover with multipolarization airborne radar N86-10625
Vegetation canopy discrimination and biomass assessment using multipolarized airborne SAR N86-10628

CANTILEVER PLATES
Joint research effort on vibrations of twisted plates, phase 1: Final results
[NASA-RP-1150] N86-10579

CAPACITORS
Intrinsic mechanisms of multilayer ceramic capacitor failure
[AD-A156638] N86-10431
Interdigital Schottky barrier capacitor apparatus
[AD-D011799] N86-10436

CAPILLARY FLOW
Thermocapillary flows and their stability: Effects of surface layers and contamination N86-10109
Energy stability of thermocapillary convection in models of the float zone process N86-10123
Thermocapillary and diffusocapillary migration of a fluid drop N86-10128
Miscibility gap systems
[NASA ORDER H-27954B] N86-10131
Capillary forces in a low gravity environment — Spacelab N86-10202
Liquid column stability: Experiment 1 ES-331 --- Spacelab N86-10205
The influence of thermocapillarity on the migration of droplets in a liquid possessing a uniform temperature gradient N86-10237
Measurements of the critical Marangoni number of the laminar-oscillatory transition of thermocapillary convection in floating zones N86-10242

CAPILLARY TUBES
Rapid analysis using capillary supercritical fluid chromatography
[DE85-012460] N86-10297

CARBON
Cometary atmospheres: Modeling the spatial distribution of observed neutral radicals
[NASA-CR-176242] N86-11133

CARBON DIOXIDE
Rapid analysis using capillary supercritical fluid chromatography
[DE85-012460] N86-10297
A superconducting tunnel junction receiver for millimeter-wave astronomy N86-11041

CARBON FIBER REINFORCED PLASTICS
Carbon fiber reinforced polymide filament wound tube manufacturing
[BR64172] N86-10339

CARBON FIBERS
Continuous fiberization of silicon-carbide-nitride precursor resin N86-10168
CARBON MONOXIDE
Catalytic activity of shock modified ZnO for CO oxidation and methanol synthesis
[DE85-014704] N86-10300
Effect of H2S and COS in the fuel gas on the performance of ambient pressure phosphoric acid fuel cells
[DE85-013913] N86-10446
The two micron spectrum of R Scuti N86-11092
CARBON STEELS
Mechanism of the formation of boronised layers on high carbon steel
[BLL-BISI-TRANS-23036-(9022.06)] N86-10306
Boronising of iron and steel by ionic bombardment by diborane
[BLL-BISI-TRANS-23034-(9022.06)] N86-10307
Study of statis and dynamic stress effects in nonlinear solids
[NASA-CR-176236] N86-10578
CARBON-CARBON COMPOSITES
Erosion-resistant nosetip construction
[AD-D011787] N86-10289
Process models for 3D composites
[AD-A156889] N86-10292
High temperature mechanical testing of a cylindrical weave carbon-carbon composite
[AD-A156639] N86-10591
CARBONATES
Effects of H2S on molten carbonate fuel cells
[DE85-014052] N86-10447
CARDIOVASCULAR SYSTEM
Capacity for work and hemodynamics in males residing at middle and high latitudes N86-10747
Individual typological self-regulation of cardio-vascular system N86-10752
Classification of changes in electrocardiogram during muscular exertion of healthy individuals N86-10755
CARRIER MOBILITY
Free carrier absorption from electrons in confined systems N86-11042
CARTRIDGES
Small cartridge heater
[AD-D011784] N86-10277
Specification for the performance, design, development and test requirements for a severe environment cartridge recorder. Issue 4
[AD-A156637] N86-10523
Optical disc transport system
[AD-D011779] N86-10974
CASSEGRAIN OPTICS
TRIO optics --- spaceborne optical interferometer (TRIO) N86-11108
CAST ALLOYS
Unidirectional solidification of cast iron: Experiment ES-325 — Spacelab N86-10212
CASTING
Skin casting of alloys and composites: Results of Spacelab (SL)-1 and TEXUS experiments N86-10213
CASTINGS
Control of cast iron microstructure N86-10084
Graphite formation in cast iron N86-10100
CATALOGS (PUBLICATIONS)
Catalog of Resources for Education in Ada (trademark) and Software Engineering (CREASE). Version 3.0
[AD-A156687] N86-10790
CATALYSIS
Surface science and catalysis
[DE85-013922] N86-11057
CATALYSTS
Physical and chemical properties of a nickel catalyst processed under microgravity — STS-7 N86-10255
Effects of H2S on molten carbonate fuel cells
[DE85-014052] N86-10447
Phosphoric and electric utility fuel technology development
[DE85-014741] N86-10651
Phosphoric and electric utility fuel cell technology development
[DE85-014552] N86-10652
CATALYTIC ACTIVITY
Catalytic activity of shock modified ZnO for CO oxidation and methanol synthesis
[DE85-014704] N86-10300
CATHODE RAY TUBES
Measurement of visual contrast sensitivity
[AD-D011776] N86-10973
CATHODES
P-N junction controlled field emitter array cathode
[AD-D011815] N86-10416
Effects of H2S on molten carbonate fuel cells
[DE85-014052] N86-10447
Characterization of cathodic corrosion products in the Ca/CaCrO4 thermal battery
[DE85-013442] N86-10644
CATIONS
Report on the engineering test of the LBL 30 second neutral beam source for the MFTF-B project
[DE85-013317] N86-10962
CAUCASUS MOUNTAINS (U.S.S.R.)
Laws of distribution of the snow cover on the greater Caucasus (Soviet Union)
[NASA-TM-77911] N86-10614
CAUCHY PROBLEM
A modified modified Korteweg-deVries equation
[PN-84/27] N86-10859
Initial data for N black holes N86-11128
CAVITATION FLOW
Theoretical modeling of the vapor cavitation in dynamically loaded journal bearings
[NASA-TM-87076] N86-10463
The mechanism of erosion of metallic materials under cavitation attack
[NASA-TM-87133] N86-10552
Acoustic cavitation and bubble dynamics
[AD-A156888] N86-10918
CAVITIES
Development of materials processing systems for use in space on low-g simulation devices N86-10166
CAVITY RESONATORS
Compact, low jitter, triggered spark gap
[DE85-012812] N86-10195
An experimental TE sub 12 - TE sub 11 circular waveguide mode converter N86-10387
Direct-coupled cavity filters with irises of arbitrary thickness
[DFVLR-FB-85-14] N86-10412
Beam-cavity interaction measurements in a DAW structure
[DE85-012660] N86-10987
Analytic evaluation of LAMPF 2 Booster Cavity design
[DE85-012680] N86-11002
Superconductors for pulsed RF accelerators
[DE85-013378] N86-11051
CELESTIAL REFERENCE SYSTEMS
A VLBI survey at 2.29 GHz N86-10383
CELL CATHODES
Advanced fuel cell development
[DE85-014550] N86-10659
CELL DIVISION
Cell partition in two polymer aqueous phases N86-10139
Purification and cultivation of human pituitary growth hormones secreting cells N86-10140
Cell separations in microgravity and development of a space bioreactor N86-10141
CELLS (BIOLOGY)
Biochemical assays of cultured cells N86-10134
Cell partition in two polymer aqueous phases N86-10136
Purification and cultivation of human pituitary growth hormones secreting cells N86-10140
Cell separations in microgravity and development of a space bioreactor N86-10141
Cell maintenance systems N86-10142
Kidney cell electrophoresis N86-10145
Somatic cell and molecular genetics approach to DNA repair and mutagenesis
[DE85-014181] N86-10737
Treatment planning with ion beams
[DE85-012661] N86-10990
CENTRAL NERVOUS SYSTEM
Homocarnosin in rat brain during adaptation to cold N86-10762
CENTRAL PROCESSING UNITS
Arithmetic pipeline for image processing
[AD-D011773] N86-10800
CENTRIFUGAL CASTING
Fracture toughness testing of centrifugally cast nickel aluminium bronze
[REPT-MAT/720] N86-10575
CERAMICS
Attachment method-ceramic radome to metal body
[AD-D011778] N86-10032
Microgravity Science and Applications Program tasks
[NASA-TM-87568] N86-10053
Lambda point equipment N86-10118
Gel precursors as glass and ceramic starting materials for space processing applications research N86-10150
Rapid solidification of magnetic oxides N86-10152
Glass research N86-10157
Microgravity Materials Science Laboratory N86-10173
Acoustic levitation containerless processing N86-10177
High-temperature controlled redox crystallization studies N86-10178
Small cartridge heater
[AD-D011784] N86-10277
Tribological properties of structural ceramics
[NASA-TM-87105] N86-10341
Mixed-mode fracture of ceramics
[DE85-014087] N86-10349
High efficiency heat transport and power conversion system for cascade
[DE85-012959] N86-10468
Characterization of mechanical damage mechanisms in ceramic composite materials
[AD-A156574] N86-10590
Advanced Gas Turbine (AGT) powertrain system development for automotive applications report
[NASA-CR-174886] N86-11087
CERIUM COMPOUNDS
Fermi surface study of CeSb in the ferromagnetic and antiferromagnetic phases
[DE85-012122] N86-11052
CESIUM 137
Sediment characterization. Task 2: Instream contaminant study. Volume 2: Appendices
[DE85-013503] N86-10680
CHAFF
AIRBOC (air rapid bloom offboard chaff) chaff deployment system
[AD-D011746] N86-10554
CHANGE DETECTION
Calibration of the multispectral scanner (MSS) satellite data to evaluate change in the reflection of coniferous stocks
[DFVLR-FB-84-44] N86-10636
CHANNEL FLOW
The development and prevention of channel segregation during alloy solidification N86-10086
Large eddy interactions in a turbulent channel flow
[NASA-TM-86757] N86-10464
CHANNELS (DATA TRANSMISSION)
Parallel local interface bus
[AD-D011742] N86-10792
An intelligent local disk control system
[REPT-051560-28(1984)08] N86-10808
CHARGE COUPLED DEVICES
The intensified multi CCD camera --- spaceborne interferometers N86-11122
CHARGE EXCHANGE
Charge exchange in slow collisions of atoms and molecules N86-10922
CHARGE TRANSFER
Polyacetylene polymerization, structure, and electrical transport properties N86-10334
Charge exchange in slow collisions of atoms and molecules N86-10922
CHARGED PARTICLES
Design and construction of a Faraday cup for measurement of small electronic currents
[NASA-TM-77915] N86-10418
Hyperon polarization: An unresolved problem
[DE85-012298] N86-10946
Lie algebraic methods for charged particle beams and light optics N86-10970
CHARPY IMPACT TEST
Fabrication and metallurgical properties of modified 9Cr-1 Mo steel
[DE85-012885] N86-10328
CHARRING
A fundamental study of smoldering with emphasis on experimental design for zero-g N86-10162
CHARTS
Vision test chart and method using Gaussians
[AD-D011756] N86-10778
CHEBYSHEV APPROXIMATION
Partial eigensolutions of large nonsymmetric matrices
[AD-A156711] N86-10867
Spectral methods in adapted curved grids N86-10878
CHECKOUT
Classification of real-time program testing tasks and methods N86-10815
Collective use computer system for the Academy of Sciences KaSSR N86-10817
CHELATES
Extraction of lanthanide ions by 2-methyl-8-quinolinol
[DE85-014277] N86-10303
CHELATION
Rusty bolt intermodulation interference reducer
[AD-D011748] N86-10313
CHEMICAL ANALYSIS
Biochemical assays of cultured cells N86-10134
New directions in chemical analysis
[DE85-012930] N86-10296
Theoretical comparison of classical (K-matrix) and inverse (P-matrix) least-squares methods for quantitative infrared spectroscopy
[DE85-012827] N86-10298

Weld metal hot-cracking of hastelloy alloys C-22 and C-276: A study by analytical electron microscopy
[DE85-009437] N86-10324
Development and evaluation of multispecies test protocols for assessing chemical toxicity
[DE85-013526] N86-10679

CHEMICAL BONDS
A procedure identifying a polyacetylene initiator of olefin metathesis. The reactivities of metal-carbenes toward alkenes and alkynes
[AD-A156997] N86-10283
Non-empirical interatomic potentials for transition metals
[DE85-013448] N86-10440

CHEMICAL CLEANING
Passivation of steel with aqueous amine solutions
[AD-D011749] N86-10314

CHEMICAL COMPOSITION
Fabrication and metallurgical properties of modified 9Cr-1 Mo steel
[DE85-012885] N86-10328
Development of new ammonium nitrate composite explosives
[DE85-014252] N86-10356
Evaluation of the 90-day inhalation toxicity of petroleum and oil shale JP-5 jet fuel
[AD-A156815] N86-10675
Microcomputer aided calculations of parameters for spray dryer operation
[DE85-013468] N86-10681
Radionuclide complexation in xylem exudates of plants
[DE85-013446] N86-10684

CHEMICAL ELEMENTS
Study of the reactive-element effect in oxidation of Fe-Cr alloys using transverse section analytical electron microscopy N86-10087

CHEMICAL ENGINEERING
Research needs for corrosion control and prevention in energy conservation systems
[DE85-014852] N86-10326
Acquaintance with on line literature research. An introduction for education at the Chemical Technology Section N86-11081

CHEMICAL EQUILIBRIUM
Laser Raman spectroscopy study of the zinc and bromide ion complex equilibrium in zinc/bromine battery electrolytes
[DE85-011820] N86-10301

CHEMICAL EXPLOSIONS
Development of new ammonium nitrate composite explosives
[DE85-014252] N86-10356
Type of new Chinese-produced high-speed camera and its utilization in detonation physics experiments
[DE85-015191] N86-10529
Guidelines for a thermochemical kinetics computer program
[DE85-014266] N86-10839

CHEMICAL LASERS
La Recherche Aerospatiale, bimonthly bulletin, no. 1984-5, September-October 1985
[ESA-TT-899] N86-10363

CHEMICAL PROPERTIES
Colloidal oxide properties and kinetic studies N86-10147
Crystallization, optical and chemical properties of fluoride glasses N86-10149
Fundamental studies of droplet combustion at reduced gravity N86-10165
Age-life prediction of nylon 66 parachute materials. Part 2: Changes in the chemical and physical properties of materials on aging
[AD-A156909] N86-10347

CHEMICAL REACTIONS
A procedure identifying a polyacetylene initiator of olefin metathesis. The reactivities of metal-carbenes toward alkenes and alkynes
[AD-A156997] N86-10283
Chemical kinetics and cellular structure of detonations in hydrogen sulphide and air
[DE85-009408] N86-10304
Investigation of metallic impurities introduced into SiO2 and silicon by various candidate VLSI metallization systems: Chemical reactions, diffusion, and electrical properties
[AD-A156609] N86-10429
Chemical kinetics and photochemical data for use in stratospheric modeling
[NASA-CR-176198] N86-10707
Surface science and catalysis
[DE85-013922] N86-11057

CHIPS (ELECTRONICS)
The VLSI design of error-trellis syndrome decoding for convolutional codes N86-10391
Making the right choice --- silicon photodiodes N86-10669
Prospects for creation of optical digital high-performance computers N86-10810

CHLORINE COMPOUNDS
Sediment characterization. Task 2: Instream contaminant study, volume 1
[DE85-013502] N86-10683

CHLOROFORM
Extraction of lanthanide ions by 2-methyl-8-quinolinol
[DE85-014277] N86-10303

CHOKES (FUEL SYSTEMS)
Operating characteristics of the multiple critical Venturi System and secondary calibration nozzles used for weight-flow measurements in the Langley 16-foot transonic tunnel
[NASA-TM-86405] N86-10016

CHOLINE
Short term heat effect on adreno- and cholino-sensitivity of rat's small intestine N86-10754

CHROMATES
Characterization of cathodic corrosion products in the Ca/CaCrO4 thermal battery
[DE85-013442] N86-10644

CHROMATOGRAPHY
New instrumentation for phase partitioning N86-10138
Rapid analysis using capillary supercritical fluid chromatography
[DE85-012460] N86-10297
Volatile organic compounds in indoor air: A survey of various structures
[PB85-198356] N86-10687
Applications of the second-order achromat concept to the design of particle accelerators
[DE85-013072] N86-10994

CHROMIUM
Environmental degradation of materials: Surface chemistry related to stress corrosion cracking N86-10099

CHROMIUM ALLOYS
Study of the reactive-element effect in oxidation of Fe-Cr alloys using transverse section analytical electron microscopy N86-10087
Electronic and magnetic properties of noble-metal and transition-metal alloys, interfaces and overlayers
[DE85-014532] N86-10321

CHROMIUM STEELS
Fabrication and metallurgical properties of modified 9Cr-1 Mo steel
[DE85-012885] N86-10328

CHROMOSOMES
Study of hypokinesia and acceleration effects on human chromosomes N86-10740

CIRCADIAN RHYTHMS
Intradiurnial organization of wakefulness-sleep sequence and energy metabolism in rats exposed to low ambient temperature N86-10764

CIRCUIT BOARDS
Multi-row connector with ground plane board
[AD-D011803] N86-10437

CIRCUITS
Miniature radar packaging
[DE85-014598] N86-10410

CIRCULATION
Effects of chemistry and swirl on the production of turbulence in a flame
[PB85-219632] N86-10305
Recirculation within a glass mixture subjected to external and resistive heating
[DE85-010068] N86-10348
Geothermal lost circulation zone mapping tool
[DE85-008696] N86-10531

CITIES
Metric camera image of Munich as additional means for urban cartography — Spacelab N86-10519

CIVIL AVIATION
A review of Australian investigations on aeronautical fatigue during the period April 1983 to March 1985
[AD-A156602] N86-10036

CLADDING
General-purpose heat source development: Safety Verification Test Program. Bullet/fragment test series
[DE85-014262] N86-10660

CLASSIFICATIONS
The effects of merging TM and A/C radar on wetland classification N86-10621
Classification of real-time program testing tasks and methods N86-10815

CLEANING
Impurity extraction by droplets N86-10122

CLIMATE
Observations of the snow cover in the southern part of the Buryat Autonomous Soviet Socialist Republic
[NASA-TM-77910] N86-10613
Smoke inputs to climate models: Optical properties and height distribution for nuclear winter studies
[DE85-011363] N86-10717
contemporary Aeolian processes on Mars: Local dust storms N86-11136

CLIMATOLOGY
The air of life of the blue planet. Atmosphere research from space using data and facts against climate speculations N86-10184
Laws of distribution of the snow cover on the greater Caucasus (Soviet Union)
[NASA-TM-77911] N86-10614
A composite climatological study of the frequency and distribution of severe weather associated with spring season Colorado cyclogenesis
[AD-A156981] N86-10715

CLINICAL MEDICINE
Annotated bibliography of publications dealing with occupational health and medical information systems, cost analysis procedures, evaluation methodology and related legal issues
[AD-A156650] N86-11078

CLOSED CIRCUIT TELEVISION
Geothermal lost circulation zone mapping tool
[DE85-008696] N86-10531

CLOSURES
Fundamental study of the closure property of joints N86-10698

CLOUD COVER
Applications for three-dimensional computer graphic cloud representations produced from satellite imagery
[AD-A156903] N86-10798

CLOUD GLACIATION
Comparative flight measurement of icing parameters for the propeller aircraft Do-28D2 of the test station 61 of the DFVLR and for the DFVLR aircraft Falon 20e in stratus clouds
[DFVLR-FB-85-16] N86-10720

CLOUD PHYSICS
Cloud microphysics by thermal wave methods N86-10103

CLOUDS
Cloud microphysics by thermal wave methods N86-10103
Particle cloud combustion experiment N86-10160
Applications for three-dimensional computer graphic cloud representations produced from satellite imagery
[AD-A156903] N86-10798
A modeling analysis program for the JPL table mountain lo sodium cloud
[NASA-CR-176241] N86-11139

CLUMPS
Supersonic metal cluster beams
[DE85-014321] N86-10966

COARSENESS
Undercooling, remelting, and coarsening N86-10080

COASTAL ECOLOGY
Utilization of satellite remote sensing for the monitoring of oil pollution and marine ecosystems in Indonesia. A Tropical Earth Resources Satellite program (TERS) case study implemented for the NLR, Delft N86-10640

COASTAL PLAINS
Cretaceous and cenozoic stratigraphy of the upper and middle coastal plain, Harnett County area, North Carolina N86-10690

COASTAL WATER
Long range translocations ashore to offshore using Spacelab-1 metric camera imagery in the perspective of integrated geophysical surveys N86-10499

COATINGS
Mechanics of coated fiber composites N86-10285
Steady state frictional behavior of thin film coatings N86-10335
The influence of the substrate on the practical machining applications of cutting edges coated with different materials
[BLL-RISLEY-TR-5039-(9091.9F)] N86-10546

COAXIAL CABLES
Miniature radar packaging
[DE85-014598] N86-10410

COAXIAL FLOW
Buoyancy effects upon vapor flame and explosion processes N86-10161

COBALT
Thermomigration of cobalt in liquid tin: Experiment 1 ES 320 --- Spacelab N86-10222

COBALT ALLOYS
Electronic and magnetic properties of noble-metal and transition-metal alloys, interfaces and overlayers
[DE85-014532] N86-10321

COCKPITS
Proposed modifications for the RAAF Airtrainer CT-4A cockpit
[AD-A156808] N86-10039

CODERS
Phase coded pulse expander-compressor
[AD-D011817] N86-10376
CODING
Progressive damage, fracture predictions and post mortem correlations for fiber composites
[NASA-TM-87101] N86-10290
Determining a physically appropriate neutron spectrum from multisphere data
[DE85-013045] N86-10299
High-rate convolutional code construction with the minimum required SNR criterion N86-10392
An analytical and numerical study of the buckling behavior of fiber-reinforced beams N86-10566
COGENERATION
Fuel Cell Technology Assessment Program, work element no. 6
[DE85-008228] N86-10444
COGNITION
Psychological Sciences Division 1984 programs
[AD-A156631] N86-10779
COGNITIVE PSYCHOLOGY
Risk propensity, action readiness and the roles of societal and individual decision makers
[IZF-1984-27] N86-11077
COHERENT LIGHT
Signal analysis receiver with acousto-optic delay lines
[AD-D011761] N86-10427
COSMIC: A high resolution, large collecting area telescope --- Coherent Optical System of Modular Imaging Collectors (COSMIC) N86-11104
COLD ACCLIMATIZATION
Individual typological features of autonomic reactions during autogenic training in polar expedition members in period of wintering in Antarctica N86-10748
Adaptation of man to extreme conditions of Antarctica N86-10751
Homocarnosin in rat brain during adaptation to cold N86-10762
Efficiency of muscular work in white rats during adaptation to cold N86-10763
Intradiurnal organization of wakefulness-sleep sequence and energy metabolism in rats exposed to low ambient temperature N86-10764
COLD TOLERANCE
Effect of cold on brain serotonin system and plasma corticosteroid level in different strains of mice N86-10766
COLD WEATHER
Microphysical/mesoscale aspects of nuclear winter and new directions in assessments
[DE85-013479] N86-10718
COLD WORKING
Formation and characterization of amorphous erbium-based alloys prepared by near-isothermal cold-rolling of elemental composites
[DE85-014853] N86-10327
COLLIMATION
Beam-beam deflections to measure size spot and offset at SLC IP
[DE85-014285] N86-10965
Tracking studies on the effects of magnet multipoles on the aperture of the RHIC heavy ion collider
[DE85-013282] N86-11023
COLLIMATORS
Applications of the second-order achromat concept to the design of particle accelerators
[DE85-013072] N86-10994
COLLISION PARAMETERS
Charge exchange in slow collisions of atoms and molecules N86-10922
COLLISION RATES
Rapid evaluation of ion thruster lifetime using optical emission spectroscopy
[NASA-TM-87103] N86-10280
COLLISIONAL PLASMAS
Time-implicity simulation of particle-fluid systems
[DE85-012944] N86-10471
COLLISIONLESS PLASMAS
Heating and generation of suprathermal particles at collisionless shocks
[DE85-014114] N86-11034
Local conservation laws for the Maxwell-Vlasov and collisionless kinetic guiding center theories
[DE85-013122] N86-11063
COLLISIONS
Hugoniot measurements in aluminum to 420 GPa using the LLNL two-stage light-gas gun
[DE85-013821] N86-10317
Electron momentum transfer collision frequency in N(2), O(2) and air
[AD-A157030] N86-10924
COLLOIDS
Colloidal oxide properties and kinetic studies N86-10147
COLOR
The synthesis and analysis of color images
[NASA-TM-86844] N86-10777
COLOR CENTERS
Defect identification in high-energy semiconductors
[DE85-014533] N86-10442
COLOR CODING
Report on a visit to England --- color and monochrome displays
[FOA-C5-85-0006-H2] N86-10364
COLOR INFRARED PHOTOGRAPHY
Erosion control and watershed management by Spacelab photography N86-10493
Thematic mapping of metric camera color infrared and black and white photographs for land use classification N86-10510
Remote sensing study project East Gelderland (Netherlands). Part 2: Remote sensing flights in 1982 and 1983; organization aspects N86-10639
COLORADO
Report of the Workshop on Geologic Applications of Remote Sensing to the Study of Sedimentary Basins
[E86-10002] N86-10599
Position paper: Workshop on Geologic Applications of Remote Sensing to the Study of Sedimentary Basins N86-10601
Tertiary and quaternary research with remote sensing methods N86-10603
Remote stratigraphic and structural analysis: Multisensor results in the Wind River/Bighorn Basin area, Wyoming N86-10606
Foreland basin structures and remote sensing N86-10608
A composite climatological study of the frequency and distribution of severe weather associated with spring season Colorado cyclogenesis
[AD-A156981] N86-10715
COLORIMETRY
Captive volume device as a safe life monitor
[AD-D011802] N86-10525
COLUMNS (SUPPORTS)
Passive damping concepts for slender columns in space structures
[NASA-CR-176234] N86-10577
COMBAT
The quest for a helicopter suitable for combat rescue, 1967 - 1983
[AD-A156842] N86-10040
COMBINATORIAL ANALYSIS
State assignment in sequential circuits
[EUT-85-E-146] N86-10846
COMBINED STRESS
Three-dimensional stress singularities in anisotropic materials and composites N86-10286
COMBUSTION
Microgravity Science and Applications Program tasks
[NASA-TM-87568] N86-10053
Lambda point equipment N86-10118
Buoyancy effects upon vapor flame and explosion processes N86-10161
Fundamental studies of droplet combustion at reduced gravity N86-10165
Effects of scale and geometry on hydrogen-air detonations
[DE85-006762] N86-10474
Type of new Chinese-produced high-speed camera and its utilization in detonation physics experiments
[DE85-015191] N86-10529
COMBUSTION PHYSICS
Solid surface combustion at reduced gravity N86-10159
Particle cloud combustion experiment N86-10160
Experimental investigations of thermal radiation from potassium atoms and design applications
[DE85-004086] N86-11036
COMBUSTION PRODUCTS
Radiative heat transfer in nonisothermal combustion products N86-10458
COMBUSTION TEMPERATURE
A fundamental study of smoldering with emphasis on experimental design for zero-g N86-10162
COMETARY ATMOSPHERES
Cometary atmospheres: Modeling the spatial distribution of observed neutral radicals
[NASA-CR-176242] N86-11133
COMETS
A sequential decoding performance analysis for International Comet Explorer N86-10390
Cometary atmospheres: Modeling the spatial distribution of observed neutral radicals
[NASA-CR-176242] N86-11133
COMFORT
The wearing comfort of the PVC: Combat back pack
[IZF-1984-34] N86-10789
COMMERCE
Space utilization N86-11067
COMMUNICATION NETWORKS
Methods for developing jam-resistant security communications networks at fixed-site facilities
[DE85-012032] N86-10408
COMMUNICATION SATELLITES
Discussion on the progress and future of satellite communication (Japan)
[NASA-TM-77672] N86-10378
COMPACTING
COMPACT: Compaction of hierarchial chip layouts based on a constraint graph method with double-sided constraints N86-10845
COMPARATORS
Investigation of the uncertainties of the NBS (National Bureau of Standards) thermal voltage and current converters
[PB85-200178] N86-10453
Nickel-cadmium battery conditioner and tester apparatus
[AD-D011770] N86-10642
COMPARISON
Theoretical comparison of classical (K-matrix) and inverse (P-matrix) least-squares methods for quantitative infrared spectroscopy
[DE85-012827] N86-10298
Advanced vehicle systems assessment. Volume 3: Systems assessment
[NASA-CR-176206] N86-11084
Advanced vehicle systems assessment. Volume 4: Supporting analyses
[NASA-CR-176207] N86-11085
Photographic catalog of selected planetary size comparisons
[NASA-TM-86207] N86-11138
COMPENSATORY TRACKING
The influence of tactual seat-motion cues on training and performance in a roll-axis compensatory tracking task setting N86-10784
COMPLETENESS
Partial evolution and omega completeness of algebraic specifications
[CWI-CS-R8501] N86-10884
COMPLEX VARIABLES
Coordinate axes, location of origin, and redundancy for the one and two-dimensional discrete Fourier transform
[NASA-CR-176225] N86-10826
COMPOSITE MATERIALS
Microgravity Science and Applications Program tasks
[NASA-TM-87568] N86-10053
Lambda point equipment N86-10118
First Spacelab Payload (FSLP) experiments on composite materials N86-10265
The mechanics of delamination in composite materials N86-10284
Evaluation and prediction of long-term environmental effects on non metallic materials
[NASA-CR-178495] N86-10340
Development of new ammonium nitrate composite explosives
[DE85-014252] N86-10356
Composite explosives for metal acceleration: The effect of detonation temperature
[DE85-013982] N86-10359
Analytical and experimental study of cracks emanating from an elliptical hole in unidirectional composite material N86-10567
Characterization of mechanical damage mechanisms in ceramic composite materials
[AD-A156574] N86-10590
Investigation of composite materials property requirements for sonic fatigue research
[NASA-TM-87601] N86-10913
COMPOSITE STRUCTURES
A review of Australian investigations on aeronautical fatigue during the period April 1983 to March 1985
[AD-A156602] N86-10036
The effect of debond growth on crack propagation in composite plates reinforced with adhesively bonded composite stringers N86-10287
COMPOSITE WRAPPING
Stiffened and prestressed composite overwrapped pressure vessels N86-10547
COMPOSITION (PROPERTY)
Glass formation in reluctant glass formers N86-10151
Oxidation behavior of glassy alloys N86-10158
COMPRESSIBLE BOUNDARY LAYER
A numerical solution of the shock-turbulent interaction over a compression corner for supersonic flow N86-10003
COMPRESSION LOADS
Catalytic activity of shock modified ZnO for CO oxidation and methanol synthesis
[DE85-014704] N86-10300

COMPRESSION TESTS
Hugoniot measurements in aluminum to 420 GPa using the LLNL two-stage light-gas gun
[DE85-013821] N86-10317
COMPRESSIVE STRENGTH
Characterization of mechanical damage mechanisms in ceramic composite materials
[AD-A156574] N86-10590
COMPUTATION
Progressive damage, fracture predictions and post mortem correlations for fiber composites
[NASA-TM-87101] N86-10290
Self-heating to ignition measurements and computation of critical size for solar energy collector materials
[DE85-011449] N86-10302
Computational techniques for the analysis and design of digital communication systems
[AD-A156945] N86-10407
New probabilistic modeling and simulation methods for complex time-dependent systems
[DE85-009575] N86-10835
Revision of and documentation for the standard version of the Poisson-Group codes
[DE85-012659] N86-10837
Guidelines for a thermochemical kinetics computer program
[DE85-014266] N86-10839
Kalman filter preprocessor
[AD-D011774] N86-10972
COMPUTATIONAL FLUID DYNAMICS
Numerical solution of hypersonic flow near leading edge of a flat plate N86-10008
Numerical simulation of unsteady thermal Marangoni flows N86-10238
Numerical simulation of convections in the microgravity environment N86-10239
Experiments and computations on unsteady separating flow in an expanding flume
[REPT-2-84] N86-10477
Spectral methods in adapted curved grids N86-10878
COMPUTATIONAL GRIDS
Inviscid flow field analysis of maneuvering hypersonic vehicles using the SCM formulation and parabolic grid generation
[DE85-013950] N86-10021
A mesh moving technique for time dependent partial differential equations in two space dimensions
[AD-A156663] N86-10866
The h, p and h-p versions of the finite element method in 1 dimension. Part 2. The error analysis of the H and h-p versions
[AD-A156835] N86-10869
Spectral methods in adapted curved grids N86-10878
COMPUTER AIDED DESIGN
COMPACT: Compaction of hierarchial chip layouts based on a constraint graph method with double-sided constraints N86-10845
COMPUTER ASSISTED INSTRUCTION
Catalog of Resources for Education in Ada (trademark) and Software Engineering (CREASE). Version 3.0
[AD-A156687] N86-10790
Computer-based training for the US Coast Guard standard terminal microcomputer: A basis for implementation utilizing the elaboration theory of instructional design
[AD-A156548] N86-10791
Development of IS2100: An information systems laboratory
[AD-A156848] N86-10797
COMPUTER COMPONENTS
A course on field programmable logic
[EUT-85-E-148] N86-10805
COMPUTER GRAPHICS
TEMPUS: Simulating personnel and tasks in a 3-D environment
[NASA-CR-171901] N86-10785
Applications for three-dimensional computer graphic cloud representations produced from satellite imagery
[AD-A156903] N86-10798
Arithmetic pipeline for image processing
[AD-D011773] N86-10800
USSR report: Cybernetics, computers and automation technology
[JPRS-UCC-85-006] N86-10809
Zero-gravity movement studies
[NASA-CR-171899] N86-10897
Infrared system with computerized image display
[AD-D011777] N86-10906
COMPUTER INFORMATION SECURITY
Initial design of a relational database system for NPS computer asset identification and valuation for risk assessment
[AD-A156847] N86-10796
Framework for generating expert systems to perform computer security risk analysis
[DE85-014134] N86-10841
COMPUTER NETWORKS
Methods for developing jam-resistant security communications networks at fixed-site facilities
[DE85-012032] N86-10408
COMPUTER PROGRAMMING
An analytical and numerical study of the buckling behavior of fiber-reinforced beams N86-10566
DBS/R database control system N86-10816
Let's get serious about software
[AD-A156819] N86-10831
The DUCK manual
[AD-A156936] N86-10833
NBSGSC: A FORTRAN program for quantitative X-ray fluorescence analysis
[PB85-206068] N86-10847
Test of a multilevel computational theory of stereoscopic visual image processing
[AD-A157011] N86-10870
COMPUTER PROGRAMS
Optimum design of an aircraft wing structure with multiple constraints by the direct-vision criteria method N86-10004
On the design of airfoils in transonic flow using the Euler equations N86-10013
Automatic processing of reactive polymers N86-10127
Progressive damage, fracture predictions and post mortem correlations for fiber composites
[NASA-TM-87101] N86-10290
High-rate convolutional code construction with the minimum required SNR criterion N86-10392
Radome analysis and design capabilities of the RF and Microwave Technology Branch
[AD-A156662] N86-10404
KRAK: A computer program for two-phase, two-component porous flow and fracture propagation, revision
[DE85-014264] N86-10469
Finite element analysis of metals at elevated temperature using unified constitutive theories N86-10569
Radar system description N86-10616
Analysis of edge detection algorithms on DIAL (Digital Image Analysis Laboratory)
[AD-A156735] N86-10630
Application of the ruthenium and technetium thermodynamic data bases used in the EQ3/6 geochemical codes
[DE85-013766] N86-10632
The Liu, Katsaros, and Businger (1979) bulk atmospheric flux computational iteration program in FORTRAN and BASIC
[AD-A156736] N86-10714
Application of the dutch method for estimating storm-induced dune erosion
[AD-A156717] N86-10728
TEMPUS: Simulating personnel and tasks in a 3-D environment
[NASA-CR-171901] N86-10785
Catalog of Resources for Education in Ada (trademark) and Software Engineering (CREASE). Version 3.0
[AD-A156687] N86-10790
Computer-based training for the US Coast Guard standard terminal microcomputer: A basis for implementation utilizing the elaboration theory of instructional design
[AD-A156548] N86-10791
Special purpose hardware architectures for language recognition
[AD-A156634] N86-10793
Dissecting the cow
[DE85-013369] N86-10801
USSR report: Cybernetics, computers and automation technology
[JPRS-UCC-85-006] N86-10809
Classification of real-time program testing tasks and methods N86-10815
System integration report
[NASA-CR-171900] N86-10821
Supervisory control of the right arm of the beam assembly teleoperator
[AD-A156856] N86-10832
Compexity of higher-order programs
[DE85-012776] N86-10834
Klystron control software in the SIC
[DE85-013068] N86-10836
Computer codes: A bibliography, supplement 1
[DE85-008721] N86-10838
Guidelines for a thermochemical kinetics computer program
[DE85-014266] N86-10839
Box method for finding intersections of a trajectory with axisymmetric flux surfaces
[DE85-013525] N86-10840
Software for an automated gaging system
[DE85-013322] N86-10842
HALFBREED: An extended capability version of the YAQUI code
[DE85-014237] N86-10843
Timing system control software in the SLC
[DE85-013380] N86-11024
COMPUTER SYSTEMS DESIGN
Shipboard non-tactical computer systems of the US Navy
[AD-A156769] N86-10849
On line astronomical image processing using microcomputers N86-11121
COMPUTER SYSTEMS PERFORMANCE
The Rhine-Meuse estuary hydraulic scale model. Experiences with computer configuration and software
[PUBL-335] N86-10637
Performance analysis of the IBM Direct Access Storage Device (DASD) subsystem, and some suggestions for improved systems
[REPT-1-68430-44(1985)02] N86-10807
Shipboard non-tactical computer systems of the US Navy
[AD-A156769] N86-10849
COMPUTER SYSTEMS PROGRAMS
Numerical simulation of convections in the microgravity environment N86-10239
The identification package SATER
[ER-83/08] N86-10844
COMPACT: Compaction of hierarchial chip layouts based on a constraint graph method with double-sided constraints N86-10845
Writer/editor and the computer
[DE85-011843] N86-11080
COMPUTER TECHNIQUES
Periodic binary sequences with very good autocorrelation properties N86-10397
Multisensor data integration techniques N86-10604
Collective use computer system for the Academy of Sciences KaSSR N86-10817
Study of one- and two-dimensional filtering and deconvolution algorithms for a streaming array computer
[NASA-CR-176221] N86-10822
Coordinate axes, location of origin, and redundancy for the one and two-dimensional discrete Fourier transform
[NASA-CR-176225] N86-10826
Revision of and documentation for the standard version of the Poisson-Group codes
[DE85-012659] N86-10837
An annotated bibliography of abstracts on the use of simulators in technical training
[AD-A156792] N86-11065
Writer/editor and the computer
[DE85-011843] N86-11080
COMPUTER VISION
Test of a multilevel computational theory of stereoscopic visual image processing
[AD-A157011] N86-10870
COMPUTERIZED SIMULATION
Automatic processing of reactive polymers N86-10127
Hormone purification by isoelectric focusing N86-10135
Work-hardening and effective viscosity in solid beryllium
[DE85-013978] N86-10323
Acoustic gravity wave chemistry model for the RAYTRACE code
[AD-A156850] N86-10405
Angle of incidence effects for underwater shock using generic computational models, rev. 1
[DE85-012921] N86-10467
KRAK: A computer program for two-phase, two-component porous flow and fracture propagation, revision
[DE85-014264] N86-10469
Dynamic analysis of robotic manipulations with flexible links N86-10545
Numerical simulation of crack arrest experiments on Araldite B using the finite difference method
[REPT-W-9/82] N86-10596
The Rhine-Meuse estuary hydraulic scale model. Experiences with computer configuration and software
[PUBL-335] N86-10637
Contribution of wind energy to the energy balance of a combined solar and wind energy system. Part 2: Computer-assisted investigations
[BMFT-FB-T-85-052-VOL-2] N86-10671
Strength modeling report
[NASA-CR-171896] N86-10770
TEMPUS: Simulating personnel and tasks in a 3-D environment
[NASA-CR-171901] N86-10785

Minimization of programmable logic arrays
[EUT-84-E-145] N86-10803
Digital processing of images in tracking a moving object N86-10818
LANES 1 Users' Guide
[NASA-CR-177334] N86-10819
User interface enhancement report
[NASA-CR-171898] N86-10820
SUTRA (Saturated-unsaturated transport). A finite-element simulation model for saturated-unsaturated, Fluid-Density-Dependent ground-water flow with energy transport or chemically-reactive single-species solute transport
[AD-A156779] N86-10830
New probabilistic modeling and simulation methods for complex time-dependent systems
[DE85-009575] N86-10835
Framework for generating expert systems to perform computer security risk analysis
[DE85-014134] N86-10841
Regression analysis: Assumptions, alternatives, applications N86-10895
Motion analysis report
[NASA-CR-171897] N86-10896
Zero-gravity movement studies
[NASA-CR-171899] N86-10897
Infrared system with computerized image display
[AD-D011777] N86-10906
Impact of long-lived radionuclides on waste classification for fusion
[DE85-013205] N86-10959
Analytic evaluation of LAMPF 2 Booster Cavity design
[DE85-012680] N86-11002
Engineering high reliability, low-jitter Marx generators
[DE85-012811] N86-11013

COMPUTERS
New directions in chemical analysis
[DE85-012930] N86-10296
Initial design of a relational database system for NPS computer asset identification and valuation for risk assessment
[AD-A156847] N86-10796
User interface enhancement report
[NASA-CR-171898] N86-10820
Computer control of rf at SLAC
[DE85-013065] N86-11015
Beam steering in the SLC linac
[DE85-013370] N86-11025

CONCENTRATION (COMPOSITION)
Evaluation of the 90-day inhalation toxicity of petroleum and oil shale JP-5 jet fuel
[AD-A156815] N86-10675

CONCENTRATORS
Research on solar pumped liquid lasers
[NASA-CR-176235] N86-10539
Time resolved flow velocity and concentration measurements using a travelling thermal lens
[AD-A156706] N86-10541
Identification of chemical and physical phenomena affecting the durability of silvered polymer (PMMA) mirrors
[DE85-012131] N86-10645
Theory of advanced, high-efficience concentrator cells
[DE85-008821] N86-10655
Photovoltaic concentrator array evaluation
[DE85-013789] N86-10665

CONCENTRIC CYLINDERS
Mechanics of coated fiber composites N86-10285

CONDITIONS
Analysis of transitions between ferroelectric and antiferroelectric states under conditioning of uniaxial strain
[DE85-014468] N86-10350

CONDUCTIVE HEAT TRANSFER
Determination of thermophysical characteristics of solid materials by electrical modelling of the solutions to the inverse problems in nonsteady heat conduction
[NASA-TM-77907] N86-10293

CONDUCTORS
Conducting wall and pressure profile effect on MHD stabilization of axisymmetric mirror
[DE85-013647] N86-11020

CONFERENCES
Fifth European symposium on Material Sciences under Microgravity. Results of Spacelab 1
[ESA-SP-222] N86-10200
Report on a visit to England — color and monochrome displays
[FOA-C5-85-0006-H2] N86-10364
Metric Camera Workshop — Spacelab
[ESA-SP-209] N86-10485
Report of the Workshop on Geologic Applications of Remote Sensing to the Study of Sedimentary Basins
[E86-10002] N86-10599
NASA/JPL Aircraft SAR Workshop Proceedings
[NASA-CR-176204] N86-10615
Proceedings: First Annual Acid Deposition Emissions Inventory Symposium
[PB85-200004] N86-10686
Ada (trademark) Programming Support Environment (APSE) Evaluation and Validation (E and V) workshop report held at Airlie, Virginia on 2-6 April 1984
[AD-A156667] N86-10629
Proceedings of a Workshop on Electroweak Symmetry Breaking
[DE85-004444] N86-11008
Colloquium on Kilometric Optical Arrays in Space
[ESA-SP-226] N86-11096

CONFORMAL MAPPING
On the design of airfoils in transonic flow using the Euler equations N86-10013

CONGRESSIONAL REPORTS
Biotechnology regulation
[GPO-43-778] N86-10733

CONICAL BODIES
Explosive initiation by very small conical shaped charge jets
[DE85-009443] N86-10357

CONIFERS
Potential applications of multipolarization SAR for pine plantation biomass estimation N86-10626
Calibration of the multispectral scanner (MSS) satellite data to evaluate change in the reflection of coniferous stocks
[DFVLR-FB-84-44] N86-10636

CONSERVATION EQUATIONS
Freezer model using a population balance approach for steady-state, direct-contact, secondary refrigerant, freeze desalination N86-10361
Laminar film condensation in vertical closed two-phase thermosiphons
[IKE-5-220] N86-10476

CONSERVATION LAWS
Local conservation laws for the Maxwell-Vlasov and collisionless kinetic guiding center theories
[DE85-013122] N86-11063

CONSTITUTIVE EQUATIONS
Finite element analysis of metals at elevated temperature using unified constitutive theories N86-10569

CONSTRAINTS
Thermodynamic constraints on ion beam mixing of metals on insulators
[DE85-013628] N86-10448
National perspective on environmental constraints to hydroelectric development
[DE85-013111] N86-10678
Always-convergent iterative noise removal and deconvolution for image data
[NASA-CR-176223] N86-10824

CONSTRUCTION
Erosion-resistant nosetip construction
[AD-D011787] N86-10289

CONTAINERLESS MELTS
Fluid flow in crystal growth: Analysis of the verticle Bridgman and floating zone process N86-10055
Crystal growth research in space N86-10057
Crystal melts under reduced gravity N86-10062
Effect of undercooling in a low-gravity containerless environment on the structure and properties of alloys N86-10073
Convection during unidirectional solidification N86-10077
Solidification fundamentals N86-10090
Containerless high temperature property measurements by atomic fluorescence N86-10092
Containerless processing of undercooled melts N86-10093
Containerless studies of nucleation and undercooling N86-10102
Containerless processing of glass forming melts in space N86-10148
Gel precursors as glass and ceramic starting materials for space processing applications research N86-10150
Sol-gel glasses N86-10153
Physical phenomena in containerless glass processing N86-10155
Levitating furnance for containerless processing in space N86-10169
Electric field containerless processing technology N86-10170
Advanced containerless processing technology N86-10176
Acoustic levitation containerless processing N86-10177
Undercooling investigations on the easy glass former Pd-Cu-Si N86-10259
Containerless undercooling of Ni N86-10260

CONTAINERS
Marginal terrain straddle-lift container handler
[AD-D011752] N86-10555

CONTAMINANTS
Compatibility of grain-stabilized platinum with candidate propellants for resistojets
[NASA-TM-87118] N86-10279
Effects of H2S on molten carbonate fuel cells
[DE85-014052] N86-10447
Volatile organic compounds in indoor air: A survey of various structures
[PB85-198356] N86-10687
Emissions of NOx, SOx and VOC from Antropogenic sources
[PB85-193530] N86-10688
Evaluation of Passive Sampling Devices (PSDs)
[PB85-198418] N86-10689

CONTAMINATION
A fundamental study of the sticking of insect residues to aircraft wings
[NASA-CR-176231] N86-10033
Thermocapillary flows and their stability: Effects of surface layers and contamination N86-10109

CONTINUOUS WAVE RADAR
On the use of X-band CW nanosecond airborne radar for terrain profiling
[AD-A156886] N86-10406

CONTINUUM FLOW
Mathematical models of continuous flow electrophoresis N86-10143

CONTINUUM MODELING
Design sensitivity analysis and optimization of built-up structures N86-10565

CONTOURS
Evaluation of the accuracy of the metric camera images for the production of line maps and orthophotos N86-10490
Line mapping and resolution tests with metric camera data — Spacelab N86-10500

CONTRACT MANAGEMENT
LSRO/ONR ad hoc review process
[AD-A156590] N86-10735

CONTRACTS
LSRO/ONR ad hoc review process
[AD-A156590] N86-10735

CONTRAST
Vision test chart and method using Gaussians
[AD-D011756] N86-10778
Measurement of visual contrast sensitivity
[AD-D011776] N86-10973

CONTROL
Collective use computer system for the Academy of Sciences KaSSR N86-10817

CONTROL EQUIPMENT
Dissecting the cow
[DE85-013369] N86-10801
Klystron control software in the SIC
[DE85-013068] N86-10836
Beam stability in a 6 GeV synchrotron light source
[DE85-013850] N86-10979
Computer control of rf at SLAC
[DE85-013065] N86-11015
Beam steering in the SLC linac
[DE85-013370] N86-11025
Programmable delay unit incorporating a semi-custom integrated circuit
[DE85-013379] N86-11033

CONTROL SIMULATION
Control concepts for in-flight simulation including actuator nonlinearities and time delays
[DFVLR-FB-85-24] N86-10047

CONTROL STICKS
Proposed modifications for the RAAF Airtrainer CT-4A cockpit
[AD-A156808] N86-10039

CONTROL SYSTEMS DESIGN
Modeling and control of nonlinear systems N86-10362
Design of a multifunction Input-Output (I/O) controller
[EUT-84-E-143] N86-10802
The local disk controller
[REPT-1-68430-44(1985)01] N86-10806
An approach to implementing CAMAC microprocessor modules N86-10813
The identification package SATER
[ER-83/08] N86-10844

CONTROL THEORY
Guidance and control of a cable based payload pickup system N86-10046
Car driving as a supervisory control task
[B8563351] N86-10776
The influence of tactual seat-motion cues on training and performance in a roll-axis compensatory tracking task setting N86-10784
Spillover minimization in self-adjoint distributed-parameter systems with direct output feedback N86-10852
Optimal control modeling of lower extremity musculoskeletal motion N86-10853

Identification of a plant's weighting sequence --- self-tuning control
[OUEL-1534/84] N86-10854

CONTROL UNITS (COMPUTERS)
Design of a multifunction Input-Output (I/O) controller
[EUT-84-E-143] N86-10802
Minimization of programmable logic arrays
[EUT-84-E-145] N86-10803
Realization of a multifunction Input/Output (I/O) controller by means of a gate array
[EUT-85-E-147] N86-10804
An intelligent local disk control system
[REPT-051560-28(1984)08] N86-10808

CONTROLLABILITY
System modeling and identification of equivalent systems with and without compensating time delay for control-augmented aircraft
[ESA-TT-852] N86-10043

CONTROLLED ATMOSPHERES
Dynamics of general resistance of rats during readaptation period after training in altered gas environment N86-10767

CONTROLLERS
Modeling and control of nonlinear systems N86-10362

CONVECTION
Solutal convection and its effects on crystal growth and segregation in binary and pseudo-binary system with large liquidus-solidus separation N86-10056
The influence of low frequency mechanical vibrations on the growth of single crystals N86-10059
Solution growth of crystals in zero-gravity N86-10064
Fluid dynamics and thermodynamics of vapor phase crystal growth N86-10068
Vapor growth of alloy-type semiconductor crystals N86-10069
Study of eutectic formation N86-10070
Suppression of Marangoni convection in float zones N86-10111
Surface tension induced instabilities in reduced gravity: The Benard problem N86-10117
Recirculation within a glass mixture subjected to external and resistive heating
[DE85-010068] N86-10348

CONVECTIVE FLOW
Convection during unidirectional solidification N86-10077
Thermal and solutal convection damping using an applied magnetic field N86-10094
Role of convection in grain refining N86-10133

CONVECTIVE HEAT TRANSFER
Ignition and flame spread above liquid fuel pools N86-10163
The TEXUS flight results on convective flows and heat transfer in simulated floating zones N86-10235
Nucleate pool boiling in subcooled liquid under microgravity: Results of TEXUS experimental investigations N86-10250

CONVERGENCE
Comment on Determination of Aerodynamic Coefficients for a Reentry Body by Means of the Kalman Filter Method N86-10011
Determining a physically appropriate neutron spectrum from multisphere data
[DE85-013045] N86-10299
A study of Morrison's iterative noise removal method
[NASA-CR-176222] N86-10823
Always-convergent iterative noise removal and deconvolution for image data
[NASA-CR-176223] N86-10824
A modified Successive Over-Relaxation (SOR) method for the Poisson equation in unsteady free-surface flow calculations
[TW-264] N86-10881
Superconvergent tracking and invariant surfaces in phase space
[DE85-013051] N86-10995

CONVERTERS
An experimental TE sub 12 - TE sub 11 circular waveguide mode converter N86-10387

CONVOLUTION INTEGRALS
A simple method of obtaining concentration depth-profiles from X-ray diffraction
[NASA-CR-176262] N86-10310
The VLSI design of error-trellis syndrome decoding for convolutional codes N86-10391
Study of one- and two-dimensional filtering and deconvolution algorithms for a streaming array computer
[NASA-CR-176221] N86-10822
A study of Morrison's iterative noise removal method
[NASA-CR-176222] N86-10823
Coordinate axes, location of origin, and redundancy for the one and two-dimensional discrete Fourier transform
[NASA-CR-176225] N86-10826

COOLING
Effect of undercooling in a low-gravity containerless environment on the structure and properties of alloys N86-10073
The influence of containerless undercooling and rapid solid-state quenching on the superconductive and magnetic properties of some clustering alloy systems N86-10076
Undercooling, remelting, and coarsening N86-10080
Liquid phase miscibility gap materials N86-10081
Dendritic growth in undercooled melts N86-10082
Containerless processing of undercooled melts N86-10093
Containerless studies of nucleation and undercooling N86-10102
Fusion target technology N86-10156
Acoustic levitation containerless processing N86-10177
Test and evaluate passive orbital disconnect struts (PODS 3)
[NASA-CR-177368] N86-10274
Beam line windows at LAMPF
[DE85-012723] N86-10985

COOLING SYSTEMS
High efficiency heat transport and power conversion system for cascade
[DE85-012959] N86-10468

COORDINATES
Coordinate axes, location of origin, and redundancy for the one and two-dimensional discrete Fourier transform
[NASA-CR-176225] N86-10826
Supervisory control of the right arm of the beam assembly teleoperator
[AD-A156856] N86-10832

COPOLYMERS
Synthesis of arylene siloxanylene polymers and copolymers
[AD-D011780] N86-10338

COPPER
The mechanism of erosion of metallic materials under cavitation attack
[NASA-TM-87133] N86-10552
Initial increase, peaking effect, in the internal friction of copper following pulsed neutron and electron irradiation
[DE85-012767] N86-10932

COPPER ALLOYS
Electronic and magnetic properties of noble-metal and transition-metal alloys, interfaces and overlayers
[DE85-014532] N86-10321
Anelastic relaxation in irradiated Cu-Be
[DE85-013893] N86-11056

COPPER CHLORIDES
Rusty bolt intermodulation interference reducer
[AD-D011748] N86-10313

COPPER OXIDES
Rusty bolt intermodulation interference reducer
[AD-D011748] N86-10313

CORIOLIS EFFECT
Elastic wave gyrometer. Experiments with a parametric wave device
[REPT-26/5005/HF/AR] N86-10533
Dynamics of changes of statistical indicators of heart rhythm of persons with different degree of motion sickness N86-10743

CORRECTION
Applications of the second-order achromat concept to the design of particle accelerators
[DE85-013072] N86-10994

CORRELATION
Correlation between vibrations and buckling of cylindrical shells stiffened by spot-welded and riveted stringers
[TAE-537] N86-10584

CORRELATORS
Instantaneous frequency measurement receiver with digital processing
[AD-D011759] N86-10425
A compact bulk acousto-optic time integrating correlator
[AD-A156608] N86-10428

CORROSION
Characterization of cathodic corrosion products in the Ca/CaCrO4 thermal battery
[DE85-013442] N86-10644

CORROSION PREVENTION
Rusty bolt intermodulation interference reducer
[AD-D011748] N86-10313
Passivation of steel with aqueous amine solutions
[AD-D011749] N86-10314
Research needs for corrosion control and prevention in energy conservation systems
[DE85-014852] N86-10326

CORROSION RESISTANCE
Mechanism of the formation of boronised layers on high carbon steel
[BLL-BISI-TRANS-23036-(9022.06)] N86-10306
Development of a sheath for sensor protection in molten steel applications
[AD-A156764] N86-10315
Aluminum ion plating for corrosion protection of uranium, revision 1
[DE85-012419] N86-10330

CORROSION TESTS
Nondestructive corrosion test of aluminum alloy structures
[PV-43-954/F/2] N86-10594

CORTICOSTEROIDS
Effect of cold on brain serotonin system and plasma corticosteroid level in different strains of mice N86-10766

COSMIC RAYS
Solar modulation of galactic cosmic rays: Techniques and applications N86-11143

COSMIC X RAYS
Extra-galactic X-ray sources and the diffuse X-ray background N86-11144

COST ANALYSIS
Field-independent normalization of SSC Collider Ring costs
[DE85-012425] N86-10997
Annotated bibliography of publications dealing with occupational health and medical information systems, cost analysis procedures, evaluation methodology and related legal issues
[AD-A156650] N86-11078
Advanced vehicle systems assessment. Volume 3: Systems assessment
[NASA-CR-176206] N86-11084

COST EFFECTIVENESS
Retrofit of SAC EC-135C and RC-135 aircraft with CFM-56 engines
[AD-A156688] N86-10038
Test on mapping application of metric camera imagery --- Spacelab N86-10505
Editors rattle space N86-10586
An annotated bibliography of abstracts on the use of simulators in technical training
[AD-A156792] N86-11065

COST ESTIMATES
F-16X MSIP (Multi-national Staged Improvement Program) case example: Operating and support cost estimation using VAMOSC (Visibility And Management Of Operating and Support Costs)
[AD-A156893] N86-10006

COST REDUCTION
Nondestructive corrosion test of aluminum alloy structures
[PV-43-954/F/2] N86-10594

COSTS
Report of the ad hoc committee to review the program of the SDI Directorate on Innovative Science and Technology (IST)
[AD-A156668] N86-11071

COULOMB POTENTIAL
Relativistic wavefunction at the origin and the pion decay constant
[DE85-012392] N86-11062

COUPLING COEFFICIENTS
Evaluation of surface exchange coefficients from mildex ocean/atmosphere mixed layer data
[AD-A156765] N86-10729

CRACK ARREST
Numerical simulation of crack arrest experiments on Araldite B using the finite difference method
[REPT-W-9/82] N86-10596

CRACK INITIATION
Fracture toughness testing of centrifugally cast nickel aluminium bronze
[REPT-MAT/720] N86-10575

CRACK PROPAGATION
A review of Australian investigations on aeronautical fatigue during the period April 1983 to March 1985
[AD-A156602] N86-10036
Report on an overseas visit
[AD-A156603] N86-10037
The effect of debond growth on crack propagation in composite plates reinforced with adhesively bonded composite stringers N86-10287
Creep-fatigue behavior of NiCoCrAlY coated PWA 1480 superalloy single crystals
[NASA-TM-87110] N86-10311
Fabrication and metallurgical properties of modified 9Cr-1 Mo steel
[DE85-012885] N86-10328
Finite deformation crack-line fields in a thin elasto-plastic sheet
[AD-A156757] N86-10346
Analytical and experimental study of cracks emanating from an elliptical hole in unidirectional composite material N86-10567
The use of new path indepedent integrals in elastic-plastic and creep fracture N86-10574

Fatigue of graphite/epoxy buffer strip panels with center cracks
[NASA-TM-87595] N86-10581
Resistance curves for crack growth under plane-stress conditions in an elastic perfectly-plastic material
[AD-A156778] N86-10593

CRACK TIPS
Fatigue of graphite/epoxy buffer strip panels with center cracks
[NASA-TM-87595] N86-10581

CRACKS
Metallurgy and metallography of braze joints
[DE85-014563] N86-10325
Mixed-mode fracture of ceramics
[DE85-014087] N86-10349
Microwave evaluation of materials
[DE85-013183] N86-10409

CREEP PROPERTIES
Creep-fatigue behavior of NiCoCrAlY coated PWA 1480 superalloy single crystals
[NASA-TM-87110] N86-10311

CREEP RUPTURE STRENGTH
Fabrication and metallurgical properties of modified 9Cr-1 Mo steel
[DE85-012885] N86-10328
High temperature properties of SiC materials
[BMFT-FB-T-85-047] N86-10353

CREEP STRENGTH
The use of new path indepedent integrals in elastic-plastic and creep fracture N86-10574

CREEP TESTS
Constitutive modeling for isotropic materials (HOST)
[NASA-CR-174980] N86-10589
Experiments with tubular probes made of INCOLOY 800 H under uniaxial and multiaxial strain
[JUEL-1979] N86-10595

CRITICAL MASS
Self-heating to ignition measurements and computation of critical size for solar energy collector materials
[DE85-011449] N86-10302

CRITICAL POINT
Critical transport phenomena in fluid helium under low gravity N86-10119
Precise viscosity measurements very close to critical points
[NASA ORDER C-86129D] N86-10120
Holographic interferometry near gas/liquid critical points: Ground-based study of a D1 experiment — Spacelab N86-10249
Isochoric specific heat of sulfur hexafluoride at the critical point. A Spacelab experiment for the German D1-mission in 1985 N86-10251

CRITICAL TEMPERATURE
Self-heating to ignition measurements and computation of critical size for solar energy collector materials
[DE85-011449] N86-10302
Development of new ammonium nitrate composite explosives
[DE85-014252] N86-10356

CRITICAL VELOCITY
Transport processes in directional solidification during space shuttle flight N86-10257

CROP IDENTIFICATION
On the use of L-band multipolarization airborne SAR for surveys of crops, vineyards, and orchards in a California irrigated agricultural region N86-10627
Vegetation canopy discrimination and biomass assessment using multipolarized airborne SAR N86-10628

CRUDE OIL
Evaluation of the 90-day inhalation toxicity of petroleum and oil shale JP-5 jet fuel
[AD-A156815] N86-10675

CRUSTAL FRACTURES
Formation of waves by ground motion
[PM/84/09] N86-10706

CRYOGENIC FLUID STORAGE
Test and evaluate passive orbital disconnect struts (PODS 3)
[NASA-CR-177368] N86-10274

CRYOGENIC MAGNETS
Cryogenic equivalence principle experiment N86-10171
Cryogenic structural materials for superconducting magnets
[DE85-008026] N86-10908

CRYOGENICS
Volatile organic compounds in indoor air: A survey of various structures
[PB85-198356] N86-10687

CRYSTAL DEFECTS
The control of float zone interfaces by the use of selected boundary conditions N86-10060
Microgravity silicon zoning investigation N86-10063
Hgl sub 2 crystal growth for nuclear detectors N86-10066
Defect identification in high-energy semiconductors
[DE85-014533] N86-10442

CRYSTAL DISLOCATIONS
Low temperature plastic deformation mechanisms of alpha-titanium single crystals
[ESA-TT-871] N86-10332

CRYSTAL GROWTH
Fluid flow in crystal growth: Analysis of the verticle Bridgman and floating zone process N86-10055
Solutal convection and its effects on crystal growth and segregation in binary and pseudo-binary system with large liquidus-solidus separation N86-10056
Crystal growth research in space N86-10057
Growth of organic crystals by Ostwald ripening N86-10058
The influence of low frequency mechanical vibrations on the growth of single crystals N86-10059
The control of float zone interfaces by the use of selected boundary conditions N86-10060
Crystal growth of device quality GaAs in space N86-10061
Crystal melts under reduced gravity N86-10062
Microgravity silicon zoning investigation N86-10063
Solution growth of crystals in zero-gravity N86-10064
Hgl sub 2 crystal growth for nuclear detectors N86-10066
Fluid dynamics and thermodynamics of vapor phase crystal growth N86-10068
Vapor growth of alloy-type semiconductor crystals N86-10069
Study of eutectic formation N86-10070
Heat flow and segregation in directional solidification N86-10072
Dendritic growth in undercooled melts N86-10082
Orbital processing of aligned magnetic composites N86-10089
Thermal and solutal convection damping using an applied magnetic field N86-10094
Extension of Ostwald ripening theory N86-10104
Transport processes in solution crystal growth N86-10107
Surface tensions and their variations with temperature and impurities
[NASA ORDER H-27954B] N86-10115
Energy stability of thermocapillary convection in models of the float zone process N86-10123
Morphological stability and fluid dynamics of vapor crystal growth N86-10126
Experimental and theoretical analysis of chemical vapor deposition with prediction of gravity effects N86-10132
Glass formation in reluctant glass formers N86-10151
Microgravity Materials Science Laboratory N86-10173
High-temperature controlled redox crystallization studies N86-10178
Satellite use for men — West German space program N86-10180
Growth of larger single crystals N86-10186
GaS-semiconductor crystals under microgravity: Experiment ES 323 — Spacelab N86-10224
Solution growth of cadmium telluride: Experiment ES 322 — Spacelab N86-10225
Crystal growth from solution — Spacelab N86-10229
Crystal growth from solutions and nucleation from the vapor phase — Spacelab N86-10267
Preliminary reports, memoranda and technical notes of the Materials Research Council Summer Conference, La Jolla, California
[AD-A156776] N86-10291
The interaction of small metal particles with refractory oxide supports
[NASA-CR-176228] N86-11047

CRYSTAL STRUCTURE
Crystal growth research in space N86-10057
High-temperature controlled redox crystallization studies N86-10178
Growth and characterization of brushite and lead monetite, simulation and results — Spacelab N86-10230
A preliminary report on floating zone experiments with germanium crystals in a sounding rocket N86-10256
Cellular morphologies in lead-thallium alloys — gravitational effects N86-10262

CRYSTALLITES
Extension of Ostwald ripening theory N86-10104

CRYSTALLIZATION
Convection during unidirectional solidification N86-10077
Crystallization, optical and chemical properties of fluoride glasses N86-10149
Glass formation in reluctant glass formers N86-10151
Glass research N86-10157
High-temperature controlled redox crystallization studies N86-10178
Crystal nucleation and glass formation in metallic alloy melts N86-10233
Experimental facility for materials research in space (CSK-1) N86-10263
Formation and characterization of amorphous erbium-based alloys prepared by near-isothermal cold-rolling of elemental composites
[DE85-014853] N86-10327
Elastic properties and thermal stability characterization of metallic glasses by guided wave techniques N86-10337
Thermal expansion of glasses in the solid and liquid phases
[DE85-013953] N86-10351
Freezer model using a population balance approach for steady-state, direct-contact, secondary refrigerant, freeze desalination N86-10361

CRYSTALLOGRAPHY
Protein single crystal growth under microgravity — Spacelab N86-10228
Growth and characterization of brushite and lead monetite, simulation and results — Spacelab N86-10230

CUBES (MATHEMATICS)
On the analytical evaluation of the partition function for unit hypercubes in four dimensions — lattice theory
[NIKHEF-H/84-12] N86-10882

CULTURE TECHNIQUES
Purification and cultivation of human pituitary growth hormones secreting cells N86-10140
Cell separations in microgravity and development of a space bioreactor N86-10141
Cell maintenance systems N86-10142
Kidney cell electrophoresis N86-10145

CURRENT DENSITY
Improved blue response and efficiency of A-Si:H solar cells deposited from disilane using a dual-chamber plasma system
[DE85-013269] N86-10649
Noninterceptive techniques for the measurement of longitudinal parameters for intense H(-) beams
[DE85-012662] N86-10992

CURRENT REGULATORS
High output programmable signal current source for low output impedance applications
[AD-D011751] N86-10423

CURVATURE
Charge exchange in slow collisions of atoms and molecules N86-10922

CURVES
Resistance curves for crack growth under plane-stress conditions in an elastic perfectly-plastic material
[AD-A156778] N86-10593

CUSPS (MATHEMATICS)
Some remarks about cusp forms: Holomorphic and non-holomorphic
[CTH-MATH-1984-26] N86-10902

CUTTING
The influence of the substrate on the practical machining applications of cutting edges coated with different materials
[BLL-RISLEY-TR-5039-(9091.9F)] N86-10546

CYBERNETICS
USSR report: Cybernetics, computers and automation technology
[JPRS-UCC-85-006] N86-10809

CYCLES
Advanced absorption heat pump cycles
[DE85-003914] N86-10654

CYCLIC ACCELERATORS
Ion sources for high-frequency accelerators
[DE85-012992] N86-11006

CYCLIC HYDROCARBONS
A procedure identifying a polyacetylene initiator of olefin metathesis. The reactivities of metal-carbenes toward alkenes and alkynes
[AD-A156997] N86-10283

CYCLIC LOADS
Inelastic analysis of frame structures including member and joint shears N86-10573

CYCLOGENESIS
A composite climatological study of the frequency and distribution of severe weather associated with spring season Colorado cyclogenesis
[AD-A156981] N86-10715

CYCLONES
A composite climatological study of the frequency and distribution of severe weather associated with spring season Colorado cyclogenesis
[AD-A156981] N86-10715

CYCLOTRON RESONANCE
Two-dimensional electrons
[AD-A156894] N86-10982

CYCLOTRONS
Supersonic metal cluster beams
[DE85-014321] N86-10966

CYGNUS CONSTELLATION
A superconducting tunnel junction receiver for millimeter-wave astronomy N86-11041
CYLINDRICAL BODIES
Electromagnetic resonances of cylinders and aircraft model with resistive wires
[NASA-CR-176250] N86-10042
Analysis of combined natural and forced convection around cylinders and spheres N86-10456
Stiffened and prestressed composite overwrapped pressure vessels N86-10547
CYLINDRICAL SHELLS
Strength of shells under local transverse loads N86-10568
Effect of sequence of loading on interaction curves for buckling of stiffened shells
[TAE-536] N86-10583
Correlation between vibrations and buckling of cylindrical shells stiffened by spot-welded and riveted stringers
[TAE-537] N86-10584

D

DAMAGE
Progressive damage, fracture predictions and post mortem correlations for fiber composites
[NASA-TM-87101] N86-10290
Evaluation of the 90-day inhalation toxicity of petroleum and oil shale JP-5 jet fuel
[AD-A156815] N86-10675
DAMPING
Thermal and solutal convection damping using an applied magnetic field N86-10094
Passive damping concepts for slender columns in space structures
[NASA-CR-176234] N86-10577
SLC positron damping ring optics design
[DE85-013054] N86-11014
DATA ACQUISITION
Simulated direct-strike lightning testing at Sandia National Laboratories
[DE85-012033] N86-10049
Development of new ammonium nitrate composite explosives
[DE85-014252] N86-10356
The Telecommunications and Data Acquisition Report
[NASA-CR-176203] N86-10382
Soudan 2 data acquisition and trigger electronics
[DE85-013864] N86-10443
Laboratory experiments of heat pump dynamic losses
[DE85-013931] N86-10473
ELCAP instrumentation
[DE85-013042] N86-10527
Measurement of the density of base fluids at pressures 0.422 to 2.20 GPa
[NASA-TM-87114] N86-10551
Remote sensing
[NOTA-1535] N86-10638
Harmonic distortion reduction technique for data acquisition
[AD-D011771] N86-10799
Advances in data acquisition system technology for PBFA 2
[DE85-012860] N86-11011
Academic Research Equipment in selected science-engineering fields, 1982-83. An analysis of findings from the Baseline National Survey of academic research instruments and instrumentation needs N86-11088
DATA BASE MANAGEMENT SYSTEMS
DBS/R database control system N86-10816
Stock-taking of data base management systems choice considerations for the Eindhoven Technical University Computing Center (THE-RC)
[COMP-CENT-NOTE-18] N86-10851
DATA BASES
SARSAT LUC (Local user terminal) to CMCC (Canadian Mission Control Centre) alert data interface: A critical review
[AD-A156881] N86-10276
Microcircuit device reliability field experience database. Volume 1. Field data. Volume 2. Failure Event/Analysis data
[AD-A156836] N86-10433
Vegetation and soils field research data base: Experiment summaries
[E85-10110] N86-10610
Application of the ruthenium and technetium thermodynamic data bases used in the EQ3/6 geochemical codes
[DE85-013766] N86-10632
Examples of regional environmental assessment using acid deposition data
[DE85-012903] N86-10677
Initial design of a relational database system for NPS computer asset identification and valuation for risk assessment
[AD-A156847] N86-10796
DBS/R database control system N86-10816
System integration report
[NASA-CR-171900] N86-10821
Ada (trademark) Programming Support Environment (APSE) Evaluation and Validation (E and V) workshop report held at Airlie, Virginia on 2-6 April 1984
[AD-A156667] N86-10829
The DUCK manual
[AD-A156936] N86-10833
Stock-taking of data base management systems choice considerations for the Eindhoven Technical University Computing Center (THE-RC)
[COMP-CENT-NOTE-18] N86-10851
US superconducting magnet data base assessment for INTOR
[DE85-013648] N86-11000
Acquaintance with on line literature research. An introduction for education at the Chemical Technology Section N86-11081
Academic Research Equipment in selected science-engineering fields, 1982-83. An analysis of findings from the Baseline National Survey of academic research instruments and instrumentation needs N86-11088
DATA LINKS
LANES 1 Users' Guide
[NASA-CR-177334] N86-10819
DATA PROCESSING
Automated analysis of digital images generated by two-dimensional gel electrophoresis
[DE85-011906] N86-10526
Multisensor data integration techniques N86-10604
USSR report: Cybernetics, computers and automation technology
[JPRS-UCC-85-006] N86-10809
LANES 1 Users' Guide
[NASA-CR-177334] N86-10819
Solar flares and magnetospheric particles: Investigations based upon the ONR-602 experiment
[AD-A156583] N86-11142
DATA RECORDERS
Advances in data acquisition system technology for PBFA 2
[DE85-012860] N86-11011
DATA RECORDING
Simulated direct-strike lightning testing at Sandia National Laboratories
[DE85-012033] N86-10049
DATA REDUCTION
Harmonic distortion reduction technique for data acquisition
[AD-D011771] N86-10799
DATA SAMPLING
Sample data phase locked loop for adaptive Doppler tracker
[AD-D011788] N86-10374
Nonparametric comparison of several mean values with mild adaptation to some sample characteristics
[COMP-CENT-NOTE-20] N86-10891
DATA SMOOTHING
Determining a physically appropriate neutron spectrum from multisphere data
[DE85-013045] N86-10299
DATA SYSTEMS
Methods for developing jam-resistant security communications networks at fixed-site facilities
[DE85-012032] N86-10408
DATA TRANSMISSION
A sequential decoding performance analysis for International Comet Explorer N86-10390
The GCF Mark 4 implementation and beyond N86-10399
Methods for developing jam-resistant security communications networks at fixed-site facilities
[DE85-012032] N86-10408
DAYGLOW
Ultraviolet spectroscopy of the Earth's dayglow and magnetosphere cleft N86-10696
DAYTIME
A composite climatological study of the frequency and distribution of severe weather associated with spring season Colorado cyclogenesis
[AD-A156981] N86-10715
DECAY
Matter-antimatter transition operators: A manual for modeling N86-10921
Mean life of the 2p(4)((1)S)3s (2)S state in fluorine
[DE85-012929] N86-10956
DECAY RATES
Rapid evaluation of ion thruster lifetime using optical emission spectroscopy
[NASA-TM-87103] N86-10280
DECISION MAKING
Psychological Sciences Division 1984 programs
[AD-A156631] N86-10779
Extended analysis of the structure of error scores in psychological aptitude tests
[DFVLR-FB-85-20] N86-10780
Path error-neglection in straight lane driving
[IZF-1984-32] N86-10783
Derivational analogy: A theory of reconstructive problem solving and expertise acquisition
[AD-A156817] N86-10899
Risk propensity, action readiness and the roles of societal and individual decision makers
[IZF-1984-27] N86-11077
DECODERS
A sequential decoding performance analysis for International Comet Explorer N86-10390
High-rate convolutional code construction with the minimum required SNR criterion N86-10392
DECODING
A sequential decoding performance analysis for International Comet Explorer N86-10390
The VLSI design of error-trellis syndrome decoding for convolutional codes N86-10391
High-rate convolutional code construction with the minimum required SNR criterion N86-10392
Digital decoding of in-line holograms N86-10478
DECOMPOSITION
Large eddy interactions in a turbulent channel flow
[NASA-TM-86757] N86-10464
Guidelines for a thermochemical kinetics computer program
[DE85-014266] N86-10839
DEEP SPACE NETWORK
The Telecommunications and Data Acquisition Report
[NASA-CR-176203] N86-10382
A VLBI survey at 2.29 GHz N86-10383
DSN frequency and timing system, Mark 4-85 N86-10393
JPL emergency support of TDRSS and compatible satellites N86-10394
Planning for VLA/DSN arrayed support to the Voyager at Neptune N86-10395
The GCF Mark 4 implementation and beyond N86-10399
DEFECTS
Mixed-mode fracture of ceramics
[DE85-014087] N86-10349
Defect identification in high-energy semiconductors
[DE85-014533] N86-10442
Exploratory development for a high reliability flaw characterization module
[AD-A156632] N86-10916
ORR core re-configuration measurements to increase the fast neutron flux in the Magnetic Fusion Energy (MFE) experiments
[DE85-013520] N86-10958
DEFENSE PROGRAM
Report of the ad hoc committee to review the program of the SDI Directorate on Innovative Science and Technology (IST)
[AD-A156668] N86-11071
DEFLECTION
Beam-beam deflections to measure size spot and offset at SLC IP
[DE85-014285] N86-10965
DEFLECTORS
Total internal reflection modulator/deflector
[AD-D011757] N86-10424
DEFORMATION
Fundamental studies of low velocity impact resistance of graphite fiber reinforced polymer matrix composites N86-10288
Binder-filler interaction in energetic polymers
[AD-A156752] N86-10345
Resistance curves for crack growth under plane-stress conditions in an elastic perfectly-plastic material
[AD-A156778] N86-10593
Neogene compressional deformation and possible thrust faulting in southwest Dominican Republic N86-10618
Bounding solutions of geometrically nonlinear viscoelastic problems
[NASA-CR-176219] N86-10860
DEFROSTING
Laboratory experiments of heat pump dynamic losses
[DE85-013931] N86-10473
DEGRADATION
Intrinsic mechanisms of multilayer ceramic capacitor failure
[AD-A156638] N86-10431
DELAMINATING
The mechanics of delamination in composite materials N86-10284
The effect of debond growth on crack propagation in composite plates reinforced with adhesively bonded composite stringers N86-10287

DELAY
Comparison of the calibration of ionospheric delay in VLBI data by the methods of dual frequency and Faraday rotation N86-10384
DELAY CIRCUITS
Programmable delay unit incorporating a semi-custom integrated circuit
[DE85-013379] N86-11033
DELAY LINES
Signal analysis receiver with acousto-optic delay lines
[AD-D011761] N86-10427
DENDRITIC CRYSTALS
Dendritic growth in undercooled melts N86-10082
The development and prevention of channel segregation during alloy solidification N86-10086
Theoretical problems in materials science N86-10088
Dendritic solidification in a binary alloy melt: Steady-state versus morphological stability theories N86-10261
DENSITY
Computational techniques for the analysis and design of digital communication systems
[AD-A156945] N86-10407
DENSITY (MASS/VOLUME)
Light scattering tests of fundamental theories of transport properties in the critical region N86-10113
DENSITY DISTRIBUTION
Investigation of density gradient fluctuations in a turbulent free jet by means of the laser schlieren crossed-beam method
[DFVLR-FB-85-19] N86-10027
Flammability limits of gases under low gravity conditions N86-10164
DEOXYRIBONUCLEIC ACID
Somatic cell and molecular genetics approach to DNA repair and mutagenesis
[DE85-014181] N86-10737
DEPLOYMENT
AIRBOC (air rapid bloom offboard chaff) chaff deployment system
[AD-D011746] N86-10554
DEPOLARIZATION
Chemical/hydrogen energy systems
[DE85-012742] N86-10667
DEPOSITION
Dust deposition in regions of separated flow
[JUEL-1985] N86-10475
Examples of regional environmental assessment using acid deposition data
[DE85-012903] N86-10677
Application of the dutch method for estimating storm-induced dune erosion
[AD-A156717] N86-10728
DEPOSITS
Metals electroprocessing in molten salts N86-10098
DEPRIVATION
Mild hypoxia and visual performance with night vision goggles
[AD-A156969] N86-10787
DEPTH MEASUREMENT
A simple method of obtaining concentration depth-profiles from X-ray diffraction
[NASA-CR-176262] N86-10310
DERIVATION
A study of derivative filters using the discrete Fourier transform
[NASA-CR-176224] N86-10825
DESALINIZATION
Freezer model using a population balance approach for steady-state, direct-contact, secondary refrigerant, freeze desalination N86-10361
DESIGN
Collective use computer system for the Academy of Sciences KaSSR N86-10817
DESIGN ANALYSIS
Geothermal lost circulation zone mapping tool
[DE85-008696] N86-10531
Design sensitivity analysis and optimization of built-up structures N86-10565
Design of a multifunction Input-Output (I/O) controller
[EUT-84-E-143] N86-10802
Evolution of the fusion power demonstration tandem mirror reactor configuration
[DE85-012889] N86-10960
Advanced Gas Turbine (AGT) powertrain system development for automotive applications report
[NASA-CR-174886] N86-11087
DESORPTION
Surface conditioning of synchrotron radiation source to improve beam lifetime
[DE84-012185] N86-10948
DESTABILIZATION
Mephisto: Interfacial destabilization in metal alloys N86-10079
DESTRUCTIVE TESTS
Evaluation of the International Atomic Energy Agency (IAEA) Safeguards Analytical Laboratory quality assurance program
[DE85-012078] N86-10953
DETECTION
Robust failure detection filters
[NASA-CR-176232] N86-10271
Analysis of edge detection algorithms on DIAL (Digital Image Analysis Laboratory)
[AD-A156735] N86-10630
Volatile organic compounds in indoor air: A survey of various structures
[PB85-196356] N86-10687
Proposed aural nondetectability limits for Army materiel
[AD-A156704] N86-10917
Understanding and improving acoustic to seismic coupling as it pertains to Sandia's helicopter detector
[DE85-009440] N86-10920
New particle searches
[DE85-014073] N86-10942
Wide dynamic range beam profile monitor
[DE85-012709] N86-10950
Optical detection of photoacoustic pulses in thin silicon wafers
[AD-A156705] N86-10977
DETECTORS
Instantaneous frequency measurement receiver with digital processing
[AD-D011759] N86-10425
DETONATION
Chemical kinetics and cellular structure of detonations in hydrogen sulphide and air
[DE85-009408] N86-10304
Development of new ammonium nitrate composite explosives
[DE85-014252] N86-10356
Explosive initiation by very small conical shaped charge jets
[DE85-009443] N86-10357
Composite explosives for metal acceleration: The effect of detonation temperature
[DE85-013982] N86-10359
Effects of scale and geometry on hydrogen-air detonations
[DE85-006762] N86-10474
Type of new Chinese-produced high-speed camera and its utilization in detonation physics experiments
[DE85-015191] N86-10529
Theory of dense molecular fluid equations of state with application to detonation products
[DE84-016822] N86-10927
DEVELOPMENT
Collective use computer system for the Academy of Sciences KaSSR N86-10817
DEXTRANS
Separation of aqueous two-phase polymer systems in microgravity N86-10246
Application of the theory of Ostwald ripening to microgravity phase separation experiments N86-10248
DIAGNOSIS
Test, measurement, and diagnostic equipment (system peculiar)
[AD-A156669] N86-10563
DIATOMIC MOLECULES
Cooperative emission by two different atoms into surface plasmons
[AD-A157033] N86-10925
DIBORANE
Boronising of iron and steel by ionic bombardment by diborane
[BLL-BISI-TRANS-23034-(9022.06)] N86-10307
DIELECTRIC PROPERTIES
Polymer engineering: Polymeric and molecular electronic, dielectric and optical properties for device applications
[AD-A156671] N86-10344
Microwave evaluation of materials
[DE85-013183] N86-10409
DIELECTRICS
Thermodynamic constraints on ion beam mixing of metals on insulators
[DE85-013628] N86-10448
Renormalization of an inverse scattering theory for inhomogeneous dielectrics
[AD-A156836] N86-11049
DIFFERENCES
A study of derivative filters using the discrete Fourier transform
[NASA-CR-176224] N86-10825
DIFFERENTIAL EQUATIONS
Three-dimensional stress singularities in anisotropic materials and composites N86-10286
Theoretical and numerical investigation of dipole radiation over a flat earth N86-10369
Analysis of annular two-phase flow with liquid entrainment N86-10459
Computing the structural index
[DE85-014370] N86-10871
DIFFERENTIAL PRESSURE
Cryogenic equivalence principle experiment N86-10171
DIFFRACTION PATTERNS
A simple method of obtaining concentration depth-profiles from X-ray diffraction
[NASA-CR-176262] N86-10310
Fringe drift compensation in computer memory --- Michelson interferometry N86-11112
DIFFUSION
Colloidal oxide properties and kinetic studies N86-10147
Investigation of metallic impurities introduced into SiO2 and silicon by various candidate VLSI metallization systems: Chemical reactions, diffusion, and electrical properties
[AD-A156809] N86-10429
Smoke inputs to climate models: Optical properties and height distribution for nuclear winter studies
[DE85-011363] N86-10717
DIFFUSION COEFFICIENT
Diffusion in immiscible melts N86-10096
Interdiffusion in the glass melt system (Na2O+Rb2O).3SiO2 --- Spacelab N86-10216
Self diffusion of Sn112 and Sn124 in liquid tin N86-10231
Transport processes in directional solidification during space shuttle flight N86-10257
The measurement and application of transport properties of ion swarms in gases N86-10370
DIFFUSION FLAMES
Buoyancy effects upon vapor flame and explosion processes N86-10161
DIGITAL COMMAND SYSTEMS
Digital control of the hydraulic actuators of an adaptive suspension vehicle N86-10548
DIGITAL COMPUTERS
USSR report: Cybernetics, computers and automation technology
[JPRS-UCC-85-006] N86-10809
Prospects for creation of optical digital high-performance computers N86-10810
DIGITAL FILTERS
Digital decoding of in-line holograms N86-10478
Acceleration-invariant approximation method for recursive digital filters
[AD-A156655] N86-10865
DIGITAL SIMULATION
Evaluating the ground-water resources of the high plains of Texas, Volume 4
[PB85-191625] N86-10641
Imaging speckle interferometer in space: Digital simulations of image reconstruction and photon noise N86-11120
DIGITAL SPACECRAFT TELEVISION
Digital transmission experiments with the Orbital Test Satellite
[EUT-84-E-144] N86-10270
DIGITAL SYSTEMS
The interpolation of signals sampled at less than the Nyquist rate N86-10368
Specification for the performance, design, development and test requirements for a severe environment cartridge recorder. Issue 4
[AD-A156637] N86-10523
Automated analysis of digital images generated by two-dimensional gel electrophoresis
[DE85-011906] N86-10526
Digital processing of images in tracking a moving object N86-10818
Study of one- and two-dimensional filtering and deconvolution algorithms for a streaming array computer
[NASA-CR-176221] N86-10822
DIGITAL TECHNIQUES
The interpolation of signals sampled at less than the Nyquist rate N86-10368
Digital radio link: Method and a measuring system for studying the radio channel during frequency selective fading
[FOA-C-30386-E2] N86-10411
Extended precision in video bandwidth analog to digital converter using optical techniques
[AD-D011745] N86-10422
Sound radiation from repetitive transient vibrations using multi-channel digital signal processing with application to impact machinery N86-10910
DIMENSIONLESS NUMBERS
A fundamental study of smoldering with emphasis on experimental design for zero-g N86-10162
DIMENSIONS
Two-dimensional electrons
[AD-A156894] N86-10982

DIODES
Investigation of metallic impurities introduced into SiO2 and silicon by various candidate VLSI metallization systems: Chemical reactions, diffusion, and electrical properties
[AD-A156609] N86-10429
DIRECT CURRENT
Total internal reflection modulator/deflector
[AD-D011757] N86-10424
Investigation of the uncertainties of the NBS (National Bureau of Standards) thermal voltage and current converters
[PB85-200178] N86-10453
DIRECTIONAL SOLIDIFICATION (CRYSTALS)
Modeling directional solidification N86-10071
Effect of undercooling in a low-gravity containerless environment on the structure and properties of alloys N86-10073
Unidirectional solidification of cast iron: Experiment ES-325 --- Spacelab N86-10212
Gradient heating facility behavior --- Spacelab N86-10217
Directional solidification of an aluminum-zinc vapor emulsion in microgravity --- Spacelab N86-10218
Directional solidification of eutectic alloys --- Spacelab N86-10219
Crystallization of a silicon sphere --- Spacelab N86-10226
Crystal growth of silicon in Spacelab 1: Experiment ES-321 N86-10227
Transport processes in directional solidification during space shuttle flight N86-10257
Stability of metallic dispersions --- microgravity N86-10258
Dendritic solidification in a binary alloy melt: Steady-state versus morphological stability theories N86-10261
Cellular morphologies in lead-thallium alloys --- gravitational effects N86-10262
DIRICHLET PROBLEM
On the absolute continuity of elliptic measures
[CTH-MATH-1984-28] N86-10873
Poisson semigroups and singular integrals
[CTH-MATH-1985-05] N86-10876
DISCONNECT DEVICES
AIRBOC (air rapid bloom offboard chaff) chaff deployment system
[AD-D011746] N86-10554
DISCRETE FUNCTIONS
Phase-coded pulse expander-compressor
[AD-D011812] N86-10375
Phase coded pulse expander-compressor
[AD-D011817] N86-10376
Acceleration-invariant approximation method for recursive digital filters
[AD-A156655] N86-10865
DISKS (SHAPES)
Effects of slots/holes in disks on frequencies of TM01 and EH11 waves in the disk-loaded waveguide
[DE85-013376] N86-11009
DISORDERS
Topics in the electronic theory of disordered semiconductors N86-11045
DISPERSIONS
Production of large-particle-size monodisperse latexes in microgravity N86-10146
DISPLAY DEVICES
Report on a visit to England --- color and monochrome displays
[FOA-C5-85-0008-H2] N86-10364
Guidelines for a thermochemical kinetics computer program
[DE85-014266] N86-10839
Infrared system with computerized image display
[AD-D011777] N86-10906
DISSOLVED GASES
Mass transport phenomena between bubbles and dissolved gases in liquids under reduced gravity conditions N86-10110
DISTORTION
Harmonic distortion reduction technique for data acquisition
[AD-D011771] N86-10799
DISTRIBUTED PARAMETER SYSTEMS
Spillover minimization in self-adjoint distributed-parameter systems with direct output feedback N86-10852
DISTRIBUTED PROCESSING
Parallel local interface bus
[AD-D011742] N86-10792
DITHERS
Precise bearing support ditherer with piezoelectric drive means
[AD-D011819] N86-10483
DIURNAL VARIATIONS
Intradiurnial organization of wakefulness-sleep sequence and energy metabolism in rats exposed to low ambient temperature N86-10764
DIVERTERS
GA Theory News, January-March 1985
[DE85-012572] N86-11007
DOCUMENTATION
Let's get serious about software
[AD-A156819] N86-10831
DOCUMENTS
Study of one- and two-dimensional filtering and deconvolution algorithms for a streaming array computer
[NASA-CR-176226] N86-10827
DOGS
Evaluation of the 90-day inhalation toxicity of petroleum and oil shale JP-5 jet fuel
[AD-A156815] N86-10675
DOMAINS
Digital control of the hydraulic actuators of an adaptive suspension vehicle N86-10548
DOMESTIC ENERGY
Contribution of wind energy to the energy balance of a combined solar and wind energy system. Part 1: System description, data acquisition and system performance
[BMFT-FB-T-85-051-VOL-1] N86-10670
Contribution of wind energy to the energy balance of a combined solar and wind energy system. Part 2: Computer-assisted investigations
[BMFT-FB-T-85-052-VOL-2] N86-10671
DOPED CRYSTALS
A preliminary report on floating zone experiments with germanium crystals in a sounding rocket N86-10256
DOPPLER EFFECT
Cooled ion frequency standard
[AD-A156813] N86-10295
DOSAGE
Effect of various doses of some vitamins on non-specific mechanisms of adaptation of man N86-10750
DOSIMETERS
Development and application of the electrochemical etching technique
[DE85-010302] N86-10957
DRAG CHUTES
AIRBOC (air rapid bloom offboard chaff) chaff deployment system
[AD-D011746] N86-10554
DRAG REDUCTION
A study of the aerodynamic performance of Weis-Fogh wings N86-10012
DRAINAGE
Kinetics of biological ferrous iron oxidation
[DE85-014616] N86-10736
DRIFT RATE
Local drift parameter, j/n sub e and resistivity anomaly measurements in CTX spheromaks
[DE85-012740] N86-10998
DROP SIZE
Cloud microphysics by thermal wave methods N86-10103
Freezer model using a population balance approach for steady-state, direct-contact, secondary refrigerant, freeze desalination N86-10361
DROP TESTS
Ignition and flame spread above liquid fuel pools N86-10163
DROP TOWERS
Effect of undercooling in a low-gravity containerless environment on the structure and properties of alloys N86-10073
The influence of containerless undercooling and rapid solid-state quenching on the superconductive and magnetic properties of some clustering alloy systems N86-10076
Development of materials processing systems for use in space on low-g simulation devices N86-10166
DROPS (LIQUIDS)
Cloud microphysics by thermal wave methods N86-10103
Extension of Ostwald ripening theory N86-10104
Surface tensions and their variations with temperature and impurities
[NASA ORDER H-27954B] N86-10115
Fundamental studies of droplet combustion at reduced gravity N86-10165
Kinetics of spreading of liquids in microgravity: Experiment 1 ES 327 --- Spacelab N86-10207
The influence of thermocapillarity on the migration of droplets in a liquid possessing a uniform temperature gradient N86-10237
Oscillations of a viscoelastic liquid drop in zero-gravity N86-10240
DRUGS
Mechanism of adaptogenic action of prickly eleuterococcus on man during heat stress N86-10757
DRYING APPARATUS
Microcomputer aided calculations of parameters for spray dryer operation
[DE85-013468] N86-10681
DUCTED FLOW
Oscillations of subsonic flow in an abruptly expanding circular duct
[MPIS-16/1984] N86-10028
Dust deposition in regions of separated flow
[JUEL-1985] N86-10475
DUCTILITY
Fabrication and metallurgical properties of modified 9Cr-1 Mo steel
[DE85-012885] N86-10328
Strength of shells under local transverse loads N86-10568
DUNES
Application of the dutch method for estimating storm-induced dune erosion
[AD-A156717] N86-10728
DUOPLASMATRONS
Ion sources for high-frequency accelerators
[DE85-012992] N86-11006
DURABILITY
Identification of chemical and physical phenomena affecting the durability of silvered polymer (PMMA) mirrors
[DE85-012131] N86-10645
DUST
Dust deposition in regions of separated flow
[JUEL-1985] N86-10475
DUST STORMS
contemporary Aeolian processes on Mars: Local dust storms N86-11136
DYNAMIC CHARACTERISTICS
Dynamic analysis of a sled traveling along a rough rail
[AD-A156589] N86-10191
Inelastic analysis of frame structures including member and joint shears N86-10573
Acoustic cavitation and bubble dynamics
[AD-A156888] N86-10918
DYNAMIC LOADS
Dynamic analysis of a sled traveling along a rough rail
[AD-A156589] N86-10191
Theoretical modeling of the vapor cavitation in dynamically loaded journal bearings
[NASA-TM-87076] N86-10463
DYNAMIC MODELS
Dynamic analysis of robotic manipulations with flexible links N86-10545
DYNAMIC RESPONSE
Design, fabrication and testing of an experimental apparatus for determining particle behavior under very low intergranular stresses N86-10175
Determination of symmetry and phase in human visual response functions: Theory and experiments N86-10769
DYNAMIC STRUCTURAL ANALYSIS
Acta Aeronautica et Astronautica Sinica (selected articles)
[AD-A147304] N86-10001
Optimum design of an aircraft wing structure with multiple constraints by the direct-vision criteria method N86-10004
Seismic analysis of the large 70-meter antenna, part 1: Earthquake response spectra versus full transient analysis N86-10386
Finite element analysis of statics and dynamic structural engineering problems using semi-explicit methods N86-10571
DYNAMICAL SYSTEMS
Large eddy interactions in a turbulent channel flow
[NASA-TM-86757] N86-10464
DYSPROSIUM ISOTOPES
Information on continuum states from feeding times and total (GAMMA) spectra measured with BGO suppressed detectors
[DE85-013868] N86-10961

E

E GLASS
Undercooling investigations on the easy glass former Pd-Cu-Si N86-10259
EARTH (PLANET)
Theoretical and numerical investigation of dipole radiation over a flat earth N86-10369
EARTH ATMOSPHERE
The air of life of the blue planet. Atmosphere research from space using data and facts against climate speculations N86-10184
EARTH CRUST
Mobile VLBI and GPS measurement of vertical crustal motion N86-10401

Time-term analysis of upper crustal structure in the Columbia Basin, Washington
[DE85-012390] N86-10633
Crustal structure of the southern Rio Grande rift determined from seismic refraction, surface wave dispersion, and gravity data N86-10700
In-situ geophysical investigations into the nature of the oceanic crust N86-10725

EARTH MOVEMENTS
Mobile VLBI and GPS measurement of vertical crustal motion N86-10401

EARTH ORBITS
User's guide for Langley Research Center Orbital Lifetime program
[NASA-TM-87587] N86-10828

EARTH RESOURCES
The dirigible: A catalyst for resource exploitation in remote areas?
[AD-A156518] N86-10034
Geologic evaluation and reservoir properties of the PR Spring tar sand deposit, Uintah and Grand Counties, Utah
[DE85-013248] N86-10634
Remote sensing
[NOTA-1535] N86-10638

EARTH SURFACE
Representation of the distribution of the snow cover on the surface of the Earth's dry land
[NASA-TM-77909] N86-10612

EARTHQUAKE RESISTANCE
Seismic analysis of the large 70-meter antenna, part 1: Earthquake response spectra versus full transient analysis N86-10386

EARTHQUAKE RESISTANT STRUCTURES
Seismic analysis of the large 70-meter antenna, part 1: Earthquake response spectra versus full transient analysis N86-10386

EARTHQUAKES
Design, fabrication and testing of an experimental apparatus for determining particle behavior under very low intergranular stresses N86-10175

ECCENTRICITY
Lumped geopotential harmonics of order 14, from the orbit of 1967-11G
[AD-A156627] N86-10190

ECOLOGY
Sediment characterization. Task 2: Instream contaminant study, volume 1
[DE85-013502] N86-10683
Adaptation of man to extreme conditions of Antarctica N86-10751
Mission orientation in science N86-11066

ECONOMIC ANALYSIS
Fuel Cell Technology Assessment Program, work element no. 6
[DE85-008228] N86-10444

EDGES
The influence of the substrate on the practical machining applications of cutting edges coated with different materials
[BLL-RISLEY-TR-5039-(9091.9F)] N86-10546

EDUCATION
Methods for developing jam-resistant security communications networks at fixed-site facilities
[DE85-012032] N86-10408
Catalog of Resources for Education in Ada (trademark) and Software Engineering (CREASE). Version 3.0
[AD-A156687] N86-10790
NASA/American Society for Engineering Education (ASEE) Summer Faculty Fellowship Program, 1985
[NASA-CR-177972] N86-11064

EFFICIENCY
Aluminum battery alloys
[DE85-011599] N86-10445
Analyses of advanced residential abosrption heat pump cycles
[DE85-005244] N86-10664
Photovoltaic concentrator array evaluation
[DE85-013789] N86-10665
Energy efficiency of the CTX magnetized coaxial plasma source
[DE85-012735] N86-11003

EFFLUENTS
Membrane research in energy and solvent recovery from industrial effluent streams
[DE85-014583] N86-10682

EGYPT
Report of the Workshop on Geologic Applications of Remote Sensing to the Study of Sedimentary Basins
[E86-10002] N86-10599
Analysis of remote sensing data N86-10605

EIGENVALUES
Design sensitivity analysis and optimization of built-up structures N86-10565
Optimal design of portal frames against buckling N86-10572
Partial eigensolutions of large nonsymmetric matrices
[AD-A156711] N86-10867
Conducting wall and pressure profile effect on MHD stabilization of axisymmetric mirror
[DE85-013647] N86-11020

EINSTEIN EQUATIONS
Initial data for N black holes N86-11128
Gravitational collapse of a scalar field N86-11129

ELASTIC DEFORMATION
Finite deformation crack-line fields in a thin elasto-plastic sheet
[AD-A156757] N86-10346
Analysis of large, non-isothermal elastic-visco-plastic deformations
[NASA-CR-176220] N86-10588

ELASTIC PROPERTIES
Elastic properties and thermal stability characterization of metallic glasses by guided wave techniques N86-10337
A transformation method for the evaluation of the response moments of elastic structures with random properties
[AD-A156882] N86-10557
Analytical and experimental study of cracks emanating from an elliptical hole in unidirectional composite material N86-10567

ELASTIC WAVES
Nonlinear propagation of elastoplastic waves in Ke penetrators (excerpts)
[DE85-011450] N86-10318
Elastic wave gyrometer. Experiments with a parametric wave device
[REPT-26/5005/HF/AR] N86-10533

ELASTOHYDRODYNAMICS
Measurement of the density of base fluids at pressures 0.422 to 2.20 GPa
[NASA-TM-87114] N86-10551

ELASTOPLASTICITY
Nonlinear propagation of elastoplastic waves in Ke penetrators (excerpts)
[DE85-011450] N86-10318
The use of new path indepedent integrals in elastic-plastic and creep fracture N86-10574
Advanced development of BEM for two and three dimensional nonlinear analysis N86-10855

ELECTRIC BATTERIES
Laser Raman spectroscopy study of the zinc and bromide ion complex equilibrium in zinc/bromine battery electrolytes
[DE85-011820] N86-10301
Aluminum battery alloys
[DE85-011599] N86-10445
Nickel-cadmium battery conditioner and tester apparatus
[AD-D011770] N86-10642
Phosphoric and electric utility fuel cell technology development
[DE85-014552] N86-10652
Advanced vehicle systems assessment. Volume 2: Subsystems assessment
[NASA-CR-176205] N86-11083
Advanced vehicle systems assessment. Volume 4: Supporting analyses
[NASA-CR-176207] N86-11085

ELECTRIC CONDUCTORS
Electrically conducting polymers N86-10333
Polymer engineering: Polymeric and molecular electronic, dielectric and optical properties for device applications
[AD-A156671] N86-10344

ELECTRIC CONNECTORS
Multi-row connector with ground plane board
[AD-D011803] N86-10437

ELECTRIC CONTACTS
Development of metallization process
[NASA-CR-176209] N86-10312
Contact effects in light activated GaAs switches
[AD-A156957] N86-10434

ELECTRIC CURRENT
Signal analysis of gas tungsten arc welds N86-10078
Protection circuitry for high voltage drivers
[AD-D011781] N86-10414

ELECTRIC DISCHARGES
Nickel-cadmium battery conditioner and tester apparatus
[AD-D011770] N86-10642

ELECTRIC EQUIPMENT
Photovoltaic systems in remote locations: An experience summary
[NASA-TM-87106] N86-10643

ELECTRIC FIELDS
Mathematical models of continuous flow electrophoresis N86-10143
Electric field containerless processing technology N86-10170
Amplitude and phase modulation in fin-lines electrical tuning
[AD-D011813] N86-10415
Total internal reflection modulator/deflector
[AD-D011757] N86-10424
Photoionization technique for growth of metallic films
[AD-D011760] N86-10426
Computation of flow regimes in parameter space for the AGCE
[NASA-CR-178480] N86-10705
Fiber optic system for measuring electric fields
[AD-D011830] N86-10976
Electron wind in strong wave guide fields
[DE85-013062] N86-11004
A study of the applicability of nucleation theory to quasi-thermodynamic transformations of second and higher Ehrenfest-order
[NASA-CR-176230] N86-11060

ELECTRIC FURNACES
Recirculation within a glass mixture subjected to external and resistive heating
[DE85-010068] N86-10348

ELECTRIC GENERATORS
Photovoltaic systems in remote locations: An experience summary
[NASA-TM-87106] N86-10643

ELECTRIC HYBRID VEHICLES
Advanced vehicle systems assessment. Volume 2: Subsystems assessment
[NASA-CR-176205] N86-11083
Advanced vehicle systems assessment. Volume 3: Systems assessment
[NASA-CR-176206] N86-11084
Advanced vehicle systems assessment. Volume 5: Appendices
[NASA-CR-176208] N86-11086

ELECTRIC MOTOR VEHICLES
Advanced vehicle systems assessment. Volume 4: Supporting analyses
[NASA-CR-176207] N86-11085

ELECTRIC POTENTIAL
Signal analysis of gas tungsten arc welds N86-10078
Intrinsic mechanisms of multilayer ceramic capacitor failure
[AD-A156638] N86-10431
Interdigital Schottky barrier capacitor apparatus
[AD-D011799] N86-10436
Increased particle confinement with the use of external dc bias field in the CTX spheromak
[DE85-012744] N86-10988

ELECTRIC PROPULSION
Experimental performance of a 1-kilowatt arcjet thruster
[NASA-TM-87131] N86-10281

ELECTRICAL ENGINEERING
Report on the engineering test of the LBL 30 second neutral beam source for the MFTF-B project
[DE85-013317] N86-10962

ELECTRICAL FAULTS
Contact effects in light activated GaAs switches
[AD-A156957] N86-10434

ELECTRICAL GROUNDING
Multi-row connector with ground plane board
[AD-D011803] N86-10437

ELECTRICAL IMPEDANCE
High output programmable signal current source for low output impedance applications
[AD-D011751] N86-10423

ELECTRICAL INSULATION
Numerical methods for analyzing electromagnetic scattering
[NASA-CR-176141] N86-10377
High voltage instrument transformers for outdoor service with an insulation of low pressure SF6 gas and plastic foils
[BMFT-FB-T-85-034] N86-10449

ELECTRICAL PROPERTIES
Miniature radar packaging
[DE85-014598] N86-10410

ELECTRICAL RESISTIVITY
Electrically conducting polymers N86-10333
A simplified method of estimation of the specular components of radar cross section for some re-entrant conductors
[AD-A156573] N86-10403
Theoretical aspects of magnetic helicity
[DE85-011846] N86-10984
Local drift parameter, j/n sub e and resistivity anomaly measurements in CTX spheromaks
[DE85-012740] N86-10996
Electron tunneling in metal/tunnel-oxide/degenerate silicon junctions N86-11043

ELECTRO-OPTICS
Levitating furnance for containerless processing in space N86-10169

Extended precision in video bandwidth analog to digital converter using optical techniques
[AD-D011745] N86-10422
Information technique 1985: Optical technology and electro-optics, a defense technical component review
[FOA-A-30037-E] N86-10980
ELECTROACOUSTIC TRANSDUCERS
Precise bearing support ditherer with piezoelectric drive means
[AD-D011819] N86-10483
ELECTROCARDIOGRAPHY
Assessment of state of chronotropic and inotropic heart function at different degrees of physical fitness N86-10746
Individual typological self-regulation of cardio-vascular system N86-10752
ELECTROCHEMICAL CELLS
Metals electroprocessing in molten salts N86-10098
A compact bulk acousto-optic time integrating correlator
[AD-A156608] N86-10428
Aluminum battery alloys
[DE85-011599] N86-10445
ELECTRODEPOSITION
Metals electroprocessing in molten salts N86-10098
ELECTRODES
Phosphoric and electric utility fuel cell technology development
[DE85-014552] N86-10652
Introduction to the m = 1 helicity source
[DE85-012771] N86-10999
ELECTROENCEPHALOGRAPHY
TV monitoring control system in electrophysiological studies N86-10765
Variability analysis of visually induced responses in the midst of noise
[B8564052] N86-10774
ELECTROHYDRODYNAMICS
Electrohydrodynamics N86-10130
ELECTROLYSIS
Chemical/hydrogen energy systems
[DE85-012742] N86-10667
ELECTROLYTES
Laser Raman spectroscopy study of the zinc and bromide ion complex equilibrium in zinc/bromine battery electrolytes
[DE85-011820] N86-10301
Streaming potentials in conductive and nonconductive tubing
[DE85-012984] N86-10438
Phosphoric and electric utility fuel technology development
[DE85-014741] N86-10651
ELECTROMAGNETIC ABSORPTION
Free carrier absorption from electrons in confined systems N86-11042
ELECTROMAGNETIC FIELDS
Modification of the electromagnetic levitator (EML) hardware N86-10172
Criteria for the design or selection of a bioelectromagnetics experiment
[AD-A156575] N86-10420
Effect of single actions of weak electromagnetic fields of ultralow frequency on indices of endocrine system N86-10744
ELECTROMAGNETIC INTERACTIONS
Proceedings of a Workshop on Electroweak Symmetry Breaking
[DE85-004444] N86-11008
ELECTROMAGNETIC INTERFERENCE
Apparatus for locating passive intermodulation interference sources
[AD-D011798] N86-10435
Experimental investigations of pulse-pulse interference in heterodyne detection
[DFVLR-FB-85-26] N86-10544
Measurements of the acoustic interference between adjacent microphones
[AD-A156892] N86-10919
ELECTROMAGNETIC PROPERTIES
Electromagnetic resonances of cylinders and aircraft model with resistive wires
[NASA-CR-176250] N86-10042
ELECTROMAGNETIC PROPULSION
Overpulse railgun energy recovery circuit
[DE85-011607] N86-10197
ELECTROMAGNETIC PULSES
Experimental investigations of pulse-pulse interference in heterodyne detection
[DFVLR-FB-85-26] N86-10544
Method for determining the position, angle and other injection parameters of a short pulsed beam in the Brookhaven AGS
[DE85-012523] N86-10931
Optical detection of photoacoustic pulses in thin silicon wafers
[AD-A156705] N86-10977
Beam-cavity interaction measurements in a DAW structure
[DE85-012660] N86-10987
ELECTROMAGNETIC RADIATION
Theoretical and numerical investigation of dipole radiation over a flat earth N86-10369
Remote sensing
[NOTA-1535] N86-10638
USSR report: Life sciences. Biomedical and behavioral sciences
[JPRS-UBB-85-023] N86-10738
Analytic evaluation of LAMPF 2 Booster Cavity design
[DE85-012680] N86-11002
ELECTROMAGNETIC SCATTERING
Numerical methods for analyzing electromagnetic scattering
[NASA-CR-176141] N86-10377
ELECTROMAGNETIC WAVE TRANSMISSION
Integrating sphere measurements of directional-hemispherical transmittance of window systems
[DE85-013926] N86-10978
ELECTROMAGNETISM
Measurement of high temperature thermophysical properties N86-10074
ELECTROMAGNETS
Revision of and documentation for the standard version of the Poisson-Group codes
[DE85-012659] N86-10837
Report on a visit to CERN in February 1985. Notes on bunch monitors, high-frequency systems, linacs, kickers, magnets, vacuum and bunch extraction
[LINO-119] N86-10967
ELECTROMECHANICAL DEVICES
Levitating furnance for containerless processing in space N86-10169
ELECTRON ACCELERATORS
High-brightness photoemitter injector for electron accelerators
[DE85-012673] N86-10929
The MEA vacuum system
[LINO-120] N86-10968
ELECTRON BEAMS
Compact, low jitter, triggered spark gap
[DE85-012812] N86-10195
An experimental TE sub 12 - TE sub 11 circular waveguide mode converter N86-10387
Potential structures and particle acceleration on auroral field lines
[AD-A156694] N86-10708
Initial increase, peaking effect, in the internal friction of copper following pulsed neutron and electron irradiation
[DE85-012767] N86-10932
Beam profile monitor for the NSLS VUV ring employing linear photodiode arrays
[DE85-012184] N86-10947
Beam stability in a 6 GeV synchrotron light source
[DE85-013850] N86-10979
Beam-cavity interaction measurements in a DAW structure
[DE85-012660] N86-10987
Effects of slots/holes in disks on frequencies of TM01 and EH11 waves in the disk-loaded waveguide
[DE85-013376] N86-11009
Computer control of rf at SLAC
[DE85-013065] N86-11015
ELECTRON BUNCHING
The MEA vacuum system
[LINO-120] N86-10968
High-resolution phosphor screen beam profile monitor
[DE85-013074] N86-11012
ELECTRON CAPTURE
Volatile organic compounds in indoor air: A survey of various structures
[PB85-198356] N86-10687
ELECTRON DISTRIBUTION
Electron momentum transfer collision frequency in N(2), O(2) and air
[AD-A157030] N86-10924
Electron wind in strong wave guide fields
[DE85-013062] N86-11004
ELECTRON EMISSION
Electron wind in strong wave guide fields
[DE85-013062] N86-11004
ELECTRON ENERGY
Angular distribution of neutral hydrogen following collisional electron detachment from H(-)
[DE85-014258] N86-10943
Electron-ion recombination studies of planetary ionospheric and astrophysical ions N86-11132
ELECTRON IMPACT
Ultraviolet spectroscopy of the Earth's dayglow and magnetosphere cleft N86-10696
ELECTRON IRRADIATION
Evaluation and prediction of long-term environmental effects on non metallic materials
[NASA-CR-178495] N86-10340
Experimental studies of transition radiation and optical bremsstrahlung
[DE85-0135637] N86-10949
ELECTRON MICROSCOPY
A fundamental study of the sticking of insect residues to aircraft wings
[NASA-CR-176231] N86-10033
Study of the reactive-element effect in oxidation of Fe-Cr alloys using transverse section analytical electron microscopy N86-10087
Simulating the CTR environment in the HVBM
[DE85-011745] N86-10193
Weld metal hot-cracking of hastelloy alloys C-22 and C-276: A study by analytical electron microscopy
[DE85-009437] N86-10324
Metastable phase formation in Ni-implanted Al: An analytical electron microscope investigation
[DE85-009105] N86-10331
ELECTRON OPTICS
Superconvergent tracking and invariant surfaces in phase space
[DE85-013051] N86-10995
ELECTRON RECOMBINATION
Electron-ion recombination studies of planetary ionospheric and astrophysical ions N86-11132
ELECTRON SCATTERING
Electron momentum transfer collision frequency in N(2), O(2) and air
[AD-A157030] N86-10924
ELECTRON TRANSFER
Electron momentum transfer collision frequency in N(2), O(2) and air
[AD-A157030] N86-10924
ELECTRON TRANSITIONS
Selected tables of atomic spectra. Atomic energy levels and multiplet table O3
[NBS/NSRDS-3/11] N86-10923
Cooperative emission by two different atoms into surface plasmons
[AD-A157033] N86-10925
Mean life of the 2p(4)((1)S)3s (2)S state in fluorine
[DE85-012929] N86-10956
A superconducting tunnel junction receiver for millimeter-wave astronomy N86-11041
ELECTRON TUNNELING
Electron tunneling in metal/tunnel-oxide/degenerate silicon junctions N86-11043
ELECTRONIC CONTROL
Renovated cooling at PIMU
[LINO-122] N86-10452
ELECTRONIC COUNTERMEASURES
Submerged ram air inlets for ECM (electronic countermeasures) pods
[AD-D011801] N86-10020
Angle set-on apparatus
[AD-D011766] N86-10371
ELECTRONIC EQUIPMENT
Simulated direct-strike lightning testing at Sandia National Laboratories
[DE85-012033] N86-10049
Soudan 2 data acquisition and trigger electronics
[DE85-013864] N86-10443
ELECTRONIC PACKAGING
Increase of the packaging density of Very Large Scale Integration (VLSI) circuits using automatic alignment
[BMFT-FB-T-85-020] N86-10451
ELECTRONIC TRANSDUCERS
Fiber optic system for measuring electric fields
[AD-D011830] N86-10976
ELECTRONS
Theoretical studies of the surface tension of liquid metal system N86-10101
Theoretical investigation of electron-positive ion-atom interactions
[DE85-013019] N86-10939
The 20 keV undulators for a 6-GeV storage ring
[DE85-013867] N86-10941
Two-dimensional electrons
[AD-A156894] N86-10982
Local drift parameter, j/n sub e and resistivity anomaly measurements in CTX spheromaks
[DE85-012740] N86-10998
SLC positron damping ring optics design
[DE85-013054] N86-11014
Beam steering in the SLC linac
[DE85-013370] N86-11025
Symmetric Tandem Mirror Program
[DE85-012352] N86-11032

Free carrier absorption from electrons in confined systems N86-11042
ELECTROPHORESIS
Mathematical models of continuous flow electrophoresis N86-10143
Electrophoresis technology N86-10144
Kidney cell electrophoresis N86-10145
Automated analysis of digital images generated by two-dimensional gel electrophoresis
[DE85-011906] N86-10526
ELECTROPHYSIOLOGY
TV monitoring control system in electrophysiological studies N86-10765
ELECTROSTATIC CHARGE
Design and construction of a Faraday cup for measurement of small electronic currents
[NASA-TM-77915] N86-10418
ELECTROSTATIC PROBES
Polymer engineering: Polymeric and molecular electronic, dielectric and optical properties for device applications
[AD-A156671] N86-10344
ELECTROSTATICS
Electric field containerless processing technology N86-10170
ELEMENTARY EXCITATIONS
A superconducting tunnel junction receiver for millimeter-wave astronomy N86-11041
ELEVATION
A graphic anthropometric aid for seating and workplace design
[AD-A156988] N86-10788
ELEVATION ANGLE
Guidance and control of a cable based payload pickup system N86-10046
ELLIPTIC FUNCTIONS
Acceleration-invariant approximation method for recursive digital filters
[AD-A156655] N86-10865
EMBRITTLEMENT
Simulating the CTR environment in the HVBM
[DE85-011745] N86-10193
EMISSION
Emissions of NOx, SOx and VOC from Antropogenic sources
[PB85-193530] N86-10688
Cooperative emission by two different atoms into surface plasmons
[AD-A157033] N86-10925
EMISSION SPECTRA
Selected tables of atomic spectra. Atomic energy levels and multiplet table O3
[NBS/NSRDS-3/11] N86-10923
Experimental studies of transition radiation and optical bremsstrahlung
[DE85-013563?] N86-10949
Mean life of the 2p(4)((1)S)3s (2)S state in fluorine
[DE85-012929] N86-10956
Dynamics of imploding neon gas puff plasmas. 1
[AD-A156916] N86-10983
Directionality of bremsstrahlung from relativistic electrons in solar flares
[NASA-TM-87509] N86-11141
EMITTERS
P-N junction controlled field emitter array cathode
[AD-D011815] N86-10416
ENDOCRINE SYSTEMS
Effect of single actions of weak electromagnetic fields of ultralow frequency on indices of endocrine system N86-10744
ENERGY ABSORPTION
Advanced absorption heat pump cycles
[DE85-003914] N86-10654
ENERGY BUDGETS
Energy balance in a deep Colorado valley: ASCOT 84
[DE85-012441] N86-10631
ENERGY CONSERVATION
Research needs for corrosion control and prevention in energy conservation systems
[DE85-014852] N86-10326
ENERGY CONSUMPTION
Laboratory experiments of heat pump dynamic losses
[DE85-013931] N86-10473
ENERGY CONVERSION
Membrane research in energy and solvent recovery from industrial effluent streams
[DE85-014583] N86-10682
Ocean energy technology program summary
[DE85-013102] N86-10731
ENERGY CONVERSION EFFICIENCY
Theory of advanced, high-efficience concentrator cells
[DE85-008821] N86-10655
ENERGY DISSIPATION
Float zone experiments in space N86-10067
Laboratory experiments of heat pump dynamic losses
[DE85-013931] N86-10473
Photoactivation of PBFA-2
[DE85-013439] N86-11019
ENERGY LEVELS
Selected tables of atomic spectra. Atomic energy levels and multiplet table O3
[NBS/NSRDS-3/11] N86-10923
Nature of photoemission into dielectric fluids
[DE85-013017] N86-10945
Fermi surface study of CeSb in the ferromagnetic and antiferromagnetic phases
[DE85-012122] N86-11052
ENERGY METHODS
On the method of characteristics and its application to the calculations of annular nozzle flowfields N86-10454
ENERGY POLICY
Contribution of wind energy to the energy balance of a combined solar and wind energy system. Part 1: System description, data acquisition and system performance
[BMFT-FB-T-85-051-VOL-1] N86-10670
Contribution of wind energy to the energy balance of a combined solar and wind energy system. Part 2: Computer-assisted investigations
[BMFT-FB-T-85-052-VOL-2] N86-10671
Wind energy in agriculture, a promise
[SS-45] N86-10672
Wind energy, a feasibility investigation for wind mills in agriculture
[SS-45A] N86-10673
ENERGY SPECTRA
Polarization transfer in inelastic scattering and pionic models of the EMC effect
[DE85-010738] N86-10955
Information on continuum states from feeding times and total (GAMMA) spectra measured with BGO suppressed detectors
[DE85-013868] N86-10961
ENERGY STORAGE
Counterpulse railgun energy recovery circuit
[DE85-011603] N86-10196
Overpulse railgun energy recovery circuit
[DE85-011607] N86-10197
Advanced vehicle systems assessment. Volume 2: Subsystems assessment
[NASA-CR-176205] N86-11083
ENERGY TECHNOLOGY
LANDSAT TM image data quality analysis for energy-related applications
[E85-10109] N86-10597
Ground-coupled heat pump research at the University of Tennessee Washington, D.C., 10 Dec. 1984
[DE85-005357] N86-10650
Phosphoric and electric utility fuel cell technology development
[DE85-014552] N86-10652
Chemical/hydrogen energy systems
[DE85-012742] N86-10667
Ocean energy technology program summary
[DE85-013102] N86-10731
Computer codes: A bibliography, supplement 1
[DE85-008721] N86-10838
ENERGY TRANSFER
SUTRA (Saturated-unsaturated transport). A finite-element simulation model for saturated-unsaturated, Fluid-Density-Dependent ground-water flow with energy transport or chemically-reactive single-species solute transport
[AD-A156779] N86-10830
Recent helicity source and power supply improvements in CTX
[DE85-012741] N86-11028
ENGINE MONITORING INSTRUMENTS
Trials on the asperity counting monitoring system --- helicopter gearboxes
[RES-PAPER-670] N86-10550
ENGINEERING
NASA/American Society for Engineering Education (ASEE) Summer Faculty Fellowship Program, 1985
[NASA-CR-177972] N86-11064
ENGINES
Simplified analysis of Stirling engines and heat pumps
[DE85-005366] N86-10647
Stirling-engine-driven heat pump program overview
[DE85-004796] N86-10661
ENTHALPY
Thermodynamic constraints on ion beam mixing of metals on insulators
[DE85-013628] N86-10448
ENTRAINMENT
Analysis of annular two-phase flow with liquid entrainment N86-10459
ENVIRONMENT EFFECTS
Evaluation and prediction of long-term environmental effects on non metallic materials
[NASA-CR-178495] N86-10340
Approaches to cumulative impact assessment
[DE85-013891] N86-10635
Examples of regional environmental assessment using acid deposition data
[DE85-012903] N86-10677
ENVIRONMENT MANAGEMENT
Erosion control and watershed management by Spacelab photography N86-10493
ENVIRONMENT MODELS
Process models for 3D composites
[AD-A156889] N86-10292
ENVIRONMENT POLLUTION
Chemical kinetics and photochemical data for use in stratospheric modeling
[NASA-CR-176198] N86-10707
ENVIRONMENTAL CHEMISTRY
Preliminary reports, memoranda and technical notes of the Materials Research Council Summer Conference, La Jolla, California
[AD-A156776] N86-10291
Mission orientation in science N86-11066
ENVIRONMENTAL MONITORING
Specification for the performance, design, development and test requirements for a severe environment cartridge recorder. Issue 4
[AD-A156837] N86-10523
Utilization of satellite remote sensing for the monitoring of oil pollution and marine ecosystems in Indonesia. A Tropical Earth Resources Satellite program (TERS) case study implemented for the NLR, Delft N86-10640
ENVIRONMENTAL TESTS
Test, measurement, and diagnostic equipment (system peculiar)
[AD-A156669] N86-10563
Fracture toughness of hydrogen-embrittled precipitation-hardened stainless steels
[AD-A156664] N86-10592
ENVIRONMENTS
National perspective on environmental constraints to hydroelectric development
[DE85-013111] N86-10678
ENZYME ACTIVITY
Romanian plant produces protein concentrate from paraffin-nourished yeasts N86-10741
Biotechnology: Science and practice N86-10742
EOSS
Mathematical simulation of disturbing forces and material science processes under low gravity N86-10236
EPINEPHRINE
Short term heat effect on adreno- and cholino-sensitivity of rat's small intestine N86-10754
EPITAXY
W-shaped diffused stripe GaAs/AlGaAs laser
[AD-D011818] N86-10538
EPOXY COMPOUNDS
Investigation of composite materials property requirements for sonic fatigue research
[NASA-TM-87601] N86-10913
EPOXY RESINS
The preparation and testing of titanium and zirconium coupling agents
[SJ70] N86-10576
EQUATIONS OF MOTION
Theory of non-planar orbits
[DE85-013284] N86-11018
EQUATIONS OF STATE
Work-hardening and effective viscosity in solid beryllium
[DE85-013978] N86-10323
KRAK: A computer program for two-phase, two-component porous flow and fracture propagation, revision
[DE85-014264] N86-10469
Improved particle-velocity transducer for equation-of-state experiments
[DE85-013204] N86-10532
New approach to multiphase equilibria: Application to high-pressure physics problems
[DE85-013820] N86-10907
Theory of dense molecular fluid equations of state with application to detonation products
[DE84-016822] N86-10927
EQUIVALENCE
Cryogenic equivalence principle experiment N86-10171
ERBIUM ALLOYS
Formation and characterization of amorphous erbium-based alloys prepared by near-isothermal cold-rolling of elemental composites
[DE85-014853] N86-10327
EROS (SATELLITES)
Utilization of satellite remote sensing for the monitoring of oil pollution and marine ecosystems in Indonesia. A Tropical Earth Resources Satellite program (TERS) case study implemented for the NLR, Delft N86-10640

EROSION
Rapid evaluation of ion thruster lifetime using optical emission spectroscopy
[NASA-TM-87103] N86-10280
Erosion-resistant nosetip construction
[AD-D011787] N86-10289
The mechanism of erosion of metallic materials under cavitation attack
[NASA-TM-87133] N86-10552
Introduction to the m = 1 helicity source
[DE85-012771] N86-10999

ERROR ANALYSIS
Extended analysis of the structure of error scores in psychological aptitude tests
[DFVLR-FB-85-20] N86-10780
Classification of real-time program testing tasks and methods N86-10815
A study of Morrison's iterative noise removal method
[NASA-CR-176222] N86-10823
Fault-free behavior of reliable multiprocessor systems: FTMP experiments in AIRLAB
[NASA-CR-177967] N86-10848
The h, p and h-p versions of the finite element method in dimension. Part 1: The error analysis of the p-version
[AD-A156600] N86-10862
The h, p and h-p versions of the finite element method in 1 dimension. Part 3. The adaptive h-p version
[AD-A156626] N86-10864
The h, p and h-p versions of the finite element method in 1 dimension. Part 2. The error analysis of the H and h-p versions
[AD-A156835] N86-10869
Error estimates and automatic time step control for numerical methods for stiff ordinary differential equations
[CTH-MATH-1984-27] N86-10872
On the numerical determination of the dimension of an attractor --- strange attractors
[ZW-8415] N86-10892

ERROR FUNCTIONS
Acceleration-invariant approximation method for recursive digital filters
[AD-A156655] N86-10865
Superefficient estimation of power functions in simulation experiments
[B8562445] N86-10893

ERRORS
The VLSI design of error-trellis syndrome decoding for convolutional codes N86-10391
A mesh moving technique for time dependent partial differential equations in two space dimensions
[AD-A156663] N86-10866

ERYTHROCYTES
A study of blood flow and of aggregation of blood cells under conditions of zero gravity: Its relevance to the occlusive diseases and cancer N86-10137
Effect of inclusion of supplementary ascorbic acid in daily diet on degree of vitamin saturation of body and thermoresistance of erythrocytes while working in arid zone N86-10749
Indices of blood oxygen transporting properties and erythropoiesis in rats after prolonged stay in nitrogen-oxygen mixture at elevated pressure N86-10761

ESCAPE VELOCITY
The two micron spectrum of R Scuti N86-11092

ESTIMATES
A numerical model for the estimation of solar radiation on rugged terrain N86-10694
Estimation by moments in a model of faulty inspection
[AD-A156754] N86-10886

ESTIMATING
Application of the dutch method for estimating storm-induced dune erosion
[AD-A156717] N86-10728

ESTUARIES
The Rhine-Meuse estuary hydraulic scale model. Experiences with computer configuration and software
[PUBL-335] N86-10637

ETHYL ALCOHOL
Recovery of alcohol from a fermentation source by separation rather than distillation
[AD-D011782] N86-10282

ETHYLENE COMPOUNDS
Rusty bolt intermodulation interference reducer
[AD-D011748] N86-10313

EULER EQUATIONS OF MOTION
On the design of airfoils in transonic flow using the Euler equations N86-10013

EUROPE
Tendencies toward liberalization in European air traffic control
[DFVLR-FB-85-23] N86-10030
Maximum water reserves in the snow cover in the European territory of the USSR according to data for 1892-1960
[NASA-TM-77901] N86-10611

EUROPEAN SPACE PROGRAMS
Satellite use for men --- West German space program N86-10180

EUROPIUM
Extraction of lanthanide ions by 2-methyl-8-quinolinol
[DE85-014277] N86-10303

EUTECTIC ALLOYS
Study of eutectic formation N86-10070
Thermal and solutal convection damping using an applied magnetic field N86-10094
Melting and solidification in O-g of sintered alloys: Experiments ES 311 A and B bubble reinforced materials --- Spacelab N86-10215
Directional solidification of eutectic alloys --- Spacelab N86-10219
Directional solidification of InSb-NiSb eutectic --- Spacelab N86-10221

EUTECTIC COMPOSITES
Orbital processing of aligned magnetic composites N86-10089

EUTECTICS
Development of new ammonium nitrate composite explosives
[DE85-014252] N86-10356

EVALUATION
Test and evaluate passive orbital disconnect struts (PODS 3)
[NASA-CR-177368] N86-10274
Theoretical comparison of classical (K-matrix) and inverse (P-matrix) least-squares methods for quantitative infrared spectroscopy
[DE85-012827] N86-10298
Ultrasonic evaluation of mechanical properties of thick, multilayered, filament wound composites
[MASA-TM-87088] N86-10561
Photovoltaic concentrator array evaluation
[DE85-013789] N86-10665

EVAPORATION
Cloud microphysics by thermal wave methods N86-10103
The development of a neutron evaporation theory code for the thermal fission of Uranium-235
[AD-A156593] N86-10951

EXCITATION
Rapid evaluation of ion thruster lifetime using optical emission spectroscopy
[NASA-TM-87103] N86-10280

EXHAUST GASES
Airborne measurements of the border-crossing air pollution in the area between Weiden and Hof/Bavaria
[DFVLR-FB-85-25] N86-10685

EXHAUST SYSTEMS
The Shock and Vibration Digest, volume 17, no. 3
[AD-A154144] N86-10585
Recent advances in the analysis of exhaust mufflers N86-10587

EXHAUST VELOCITY
Acta Aeronautica et Astronautica Sinica (selected articles)
[AD-A147304] N86-10001
Theoretical specific impulse for two-phase flow in nozzle of rocket-ramjet engine: A simple estimation method N86-10005

EXOBIOLOGY
Life sciences research on the space station: An introduction
[NASA-TM-86836] N86-10734
Aerospace medicine and biology: A continuing bibliography with indexes (supplement 275)
[NASA-SP-7011(275)] N86-10768

EXPERIMENT DESIGN
Ignition and flame spread above liquid fuel pools N86-10163
Rationale for two phase polymer system microgravity separation experiments N86-10247
Space experiment on thermal diffusion. Preparation and theoretical analysis N86-10253
The power of weighted and ordinary least squares with estimated unequal variances in experimental design
[B8562446] N86-10894

EXPERIMENTAL BREEDER REACTOR 2
Swelling and tensile properties of EBR-2-irradiated tantalum alloys for space reactor applications
[DE85-012887] N86-10329

EXPERIMENTATION
Progressive damage, fracture predictions and post mortem correlations for fiber composites
[NASA-TM-87101] N86-10290
Laboratory experiments of heat pump dynamic losses
[DE85-013931] N86-10473
Measurement of the density of base fluids at pressures 0.422 to 2.20 GPa
[NASA-TM-87114] N86-10551
Analytical and experimental study of cracks emanating from an elliptical hole in unidirectional composite material N86-10567
Experimental X-ray scattering cross sections for H2 and rare atomic gases
[DE85-011572] N86-10936

EXPERT SYSTEMS
Framework for generating expert systems to perform computer security risk analysis
[DE85-014134] N86-10841

EXPIRED AIR
Conditioning potentialities of respiratory apparatus N86-10753

EXPLOSIONS
Angle of incidence effects for underwater shock using generic computational models, rev. 1
[DE85-012921] N86-10467

EXPLOSIVES
Development of new ammonium nitrate composite explosives
[DE85-014252] N86-10356
Explosive initiation by very small conical shaped charge jets
[DE85-009443] N86-10357
Properties of plastic-bonded nitroguanidine
[DE85-015316] N86-10358
Composite explosives for metal acceleration: The effect of detonation temperature
[DE85-013982] N86-10359
Guidelines for a thermochemical kinetics computer program
[DE85-014266] N86-10839

EXPONENTIAL FUNCTIONS
A modified repair strategy for two-component systems with revealed and unrevealed faults
[AD-A156715] N86-10885

EXPOSURE
Approaches to quantitative expression of dose response
[DE85-013498] N86-10772

EXTINCTION
A fundamental study of smoldering with emphasis on experimental design for zero-g N86-10162
Flammability limits of gases under low gravity conditions N86-10164
Fundamental studies of droplet combustion at reduced gravity N86-10165

EXTRACTION
Recovery of alcohol from a fermentation source by separation rather than distillation
[AD-D011782] N86-10282
Beam line windows at LAMPF
[DE85-012723] N86-10985

EXTRAGALACTIC RADIO SOURCES
Physical conditions in giant extragalactic H2 regions N86-11130

EXTRATERRESTRIAL INTELLIGENCE
SETI radio spectrum surveillance system N86-10400

EXTREMELY HIGH FREQUENCIES
An experimental TE sub 12 - TE sub 11 circular waveguide mode converter N86-10387
Propagation and radiation characteristics of a multimode corrugated waveguide feedhorn N86-10388

EXTRUDING
Continuous fiberization of silicon-carbide-nitride precursor resin N86-10168
Reduction of noble metal stock and noble metal loss during wire production with the Conform extrusion process
[BMFT-FB-T-85-049] N86-10560

EYE (ANATOMY)
A graphic anthropometric aid for seating and workplace design
[AD-A156988] N86-10788

F

F REGION
Acoustic gravity wave chemistry model for the RAYTRACE code
[AD-A156850] N86-10405

FABRICATION
Fabrication and metallurgical properties of modified 9Cr-1 Mo steel
[DE85-012885] N86-10328
Device for cryogenically fabricating source material for plasma X-ray lasers
[AD-D011814] N86-10537

FAILURE
Intrinsic mechanisms of multilayer ceramic capacitor failure
[AD-A156638] N86-10431

FAILURE ANALYSIS
Robust failure detection filters
[NASA-CR-176232] N86-10271
Analytical investigation of solid rocket nozzle failure
[NASA-TM-86513] N86-10278
Metallurgy and metallography of braze joints
[DE85-014563] N86-10325
Load space formulation of reliability for nonlinear random structural systems N86-10570
New probabilistic modeling and simulation methods for complex time-dependent systems
[DE85-009575] N86-10835
Investigation of composite materials property requirements for sonic fatigue research
[NASA-TM-87601] N86-10913
Failures and successes of quantitative methods in management
[ARW-03-THE-BDK/ORS/83-06] N86-11076

FAILURE MODES
New probabilistic modeling and simulation methods for complex time-dependent systems
[DE85-009575] N86-10835
Investigation of composite materials property requirements for sonic fatigue research
[NASA-TM-87601] N86-10913

FALLING SPHERES
Fall velocity indicator/viewer
[AD-D011789] N86-10482

FAR FIELDS
Summary of work on jet noise prediction
[ESDU-BR-82636] N86-10909

FAR INFRARED RADIATION
The DUO: Far infrared heterodyne concept for space interferometry N86-11125

FAR ULTRAVIOLET RADIATION
Determination of optical properties by third-harmonic generation in noble gases in unfocused laser beams N86-10535

FARADAY EFFECT
Comparison of the calibration of ionospheric delay in VLBI data by the methods of dual frequency and Faraday rotation N86-10384
Calibrated Faraday current and magnetic field sensor
[DE85-013438] N86-10439

FARM CROPS
Vegetation and soils field research data base: Experiment summaries
[E85-10110] N86-10610

FAST FOURIER TRANSFORMATIONS
A comparison of swept frequency and FFT methods used to calibrate array test modules
[AD-A156629] N86-10430
An improved FFT (Fast fourier transform) for a four parallel pipe SIMD arithmetic processor
[AD-A156625] N86-10863

FAST NEUTRONS
ORR core re-configuration measurements to increase the fast neutron flux in the Magnetic Fusion Energy (MFE) experiments
[DE85-013520] N86-10958

FATIGUE (BIOLOGY)
Eye-movement activity as index of functional state of brain N86-10756

FATIGUE (MATERIALS)
A review of Australian investigations on aeronautical fatigue during the period April 1983 to March 1985
[AD-A156602] N86-10036
Report on an overseas visit
[AD-A156603] N86-10037
Review of investigations on aeronautical fatigue in the Federal Republic of Germany
[LBF-S-173] N86-10044
Fatigue, static tensile strength and stress corrosion of aircraft materials and structures
[VTH-LR-360-PT-1] N86-10045
Fatigue of graphite/epoxy buffer strip panels with center cracks
[NASA-TM-87595] N86-10581

FATIGUE LIFE
A review of Australian investigations on aeronautical fatigue during the period April 1983 to March 1985
[AD-A156602] N86-10036

FATIGUE TESTS
Creep-fatigue behavior of NiCoCrAlY coated PWA 1480 superalloy single crystals
[NASA-TM-87110] N86-10311

FAULT TOLERANCE
Diagnostics of peripheral processors and controllers N86-10812
Fault-free behavior of reliable multiprocessor systems: FTMP experiments in AIRLAB
[NASA-CR-177967] N86-10848
Reaching approximate agreement in the presence of faults
[AD-A156541] N86-10898

FAULT TREES
New probabilistic modeling and simulation methods for complex time-dependent systems
[DE85-009575] N86-10835

FAULTS
A modified repair strategy for two-component systems with revealed and unrevealed faults
[AD-A156715] N86-10885

FEASIBILITY ANALYSIS
Wind energy in agriculture, a promise
[SS-45] N86-10672
Wind energy, a feasibility investigation for wind mills in agriculture
[SS-45A] N86-10673
A logistics scenario for an early lunar base
[ILR-MITT-143] N86-11140

FEED SYSTEMS
Continuous fiberization of silicon-carbide-nitride precursor resin N86-10168

FEEDBACK
Levitating furnance for containerless processing in space N86-10169

FEEDBACK CONTROL
Digital control of the hydraulic actuators of an adaptive suspension vehicle N86-10548
Studies on human vehicle control
[B8563352] N86-10775
Spillover minimization in self-adjoint distributed-parameter systems with direct output feedback N86-10852
Identification of a plant's weighting sequence --- self-tuning control
[OUEL-1534/84] N86-10854
High-power rf controls for the NBS-Los Alamos racetrack microtron
[DE85-012658] N86-10993

FEMALES
Evaluation of the 90-day inhalation toxicity of petroleum and oil shale JP-5 jet fuel
[AD-A156815] N86-10675

FERMENTATION
Recovery of alcohol from a fermentation source by separation rather than distillation
[AD-D011782] N86-10282
Biotechnology: Science and practice N86-10742

FERMI SURFACES
Fermi surface study of CeSb in the ferromagnetic and antiferromagnetic phases
[DE85-012122] N86-11052

FERRITES
Amplitude and phase modulation in fin-lines electrical tuning
[AD-D011813] N86-10415

FERROELECTRICITY
Analysis of transitions between ferroelectric and antiferroelectric states under conditioning of uniaxial strain
[DE85-014468] N86-10350

FERROMAGNETIC RESONANCE
Amplitude and phase modulation in fin-lines electrical tuning
[AD-D011813] N86-10415

FERROUS METALS
Liquid crystal non-destructive inspection of metals
[AD-D011772] N86-10316

FIBER COMPOSITES
Directional solidification of InSb-NiSb eutectic --- Spacelab N86-10221
Mechanics of coated fiber composites N86-10285
Stiffened and prestressed composite overwrapped pressure vessels N86-10547

FIBER OPTICS
Acoustic levitation containerless processing N86-10177
Multiple site laser excited pollution monitoring system
[AD-D011769] N86-10674
LANES 1 Users' Guide
[NASA-CR-177334] N86-10819
Fiber optic gradient hydrophone construction and calibration for sea trial
[AD-A156469] N86-10914
Fiber optic system for measuring electric fields
[AD-D011830] N86-10976
A fiber-linked version of project TRIO --- telescope array N86-11105

FIBER REINFORCED COMPOSITES
Fundamental studies of low velocity impact resistance of graphite fiber reinforced polymer matrix composites N86-10288
Erosion-resistant nosetip construction
[AD-D011787] N86-10289
An analytical and numerical study of the buckling behavior of fiber-reinforced beams N86-10566
Characterization of mechanical damage mechanisms in ceramic composite materials
[AD-A156574] N86-10590

FIBERS
Continuous fiberization of silicon-carbide-nitride precursor resin N86-10168
Acoustic levitation containerless processing N86-10177

FIELD EFFECT TRANSISTORS
Test results for 20-GHz GaAs FET spacecraft power amplifier
[NASA-TM-87072] N86-10379
Transient velocity assessment in gallium arsenide, and of other GaAs characteristics related to device functions
[AD-A156983] N86-11050

FIELD STRENGTH
Electrohydrodynamics N86-10130

FIELD THEORY (PHYSICS)
Gravitational collapse of a scalar field N86-11129

FIGHTER AIRCRAFT
System modeling and identification of equivalent systems with and without compensating time delay for control-augmented aircraft
[ESA-TT-852] N86-10043
Let's get serious about software
[AD-A156819] N86-10831

FILAMENT WINDING
Carbon fiber reinforced polymide filament wound tube manufacturing
[BR64172] N86-10339
Ultrasonic evaluation of mechanical properties of thick, multilayered, filament wound composites
[MASA-TM-87088] N86-10561

FILE MAINTENANCE (COMPUTERS)
DBS/R database control system N86-10816

FILLERS
Binder-filler interaction in energetic polymers
[AD-A156752] N86-10345

FILM CONDENSATION
Laminar film condensation in vertical closed two-phase thermosiphons
[IKE-5-220] N86-10476

FILM COOLING
Film cooling on a convex wall: Heat transfer and hydrodynamic measurements for full and partial coverage
[NASA-CR-174964] N86-10461

FILTERS
Robust failure detection filters
[NASA-CR-176232] N86-10271

FILTRATION
Recovery of alcohol from a fermentation source by separation rather than distillation
[AD-D011782] N86-10282
Multipurpose pan development
[DE85-012326] N86-10319

FINANCIAL MANAGEMENT
Space research expenses of the Federal Ministry of Research and Technology (BMFT) in the period 1983-1985 N86-11070

FINITE DIFFERENCE THEORY
Second order approximation method for transonic flows over swept wings N86-10002
Numerical simulation of crack arrest experiments on Araldite B using the finite difference method
[REPT-W-9/82] N86-10596
Arithmetic pipeline for image processing
[AD-D011773] N86-10800
A mesh moving technique for time dependent partial differential equations in two space dimensions
[AD-A156863] N86-10866

FINITE ELEMENT METHOD
Process models for 3D composites
[AD-A156889] N86-10292
Finite element solution of the Navier-Stokes equations for 3-D turbulent free shear flows N86-10457
Finite element analysis of metals at elevated temperature using unified constitutive theories N86-10569
Finite element analysis of statics and dynamic structural engineering problems using semi-explicit methods N86-10571
Joint research effort on vibrations of twisted plates, phase 1: Final results
[NASA-RP-1150] N86-10579
Recent advances in the analysis of exhaust mufflers N86-10587
Modeling groundwater flow into lakes N86-10598
SUTRA (Saturated-unsaturated transport). A finite-element simulation model for saturated-unsaturated, Fluid-Density-Dependent ground-water flow with energy transport or chemically-reactive single-species solute transport
[AD-A156779] N86-10830
The h, p and h-p versions of the finite element method in dimension. Part 1: The error analysis of the p-version
[AD-A156600] N86-10862

The h, p and h-p versions of the finite element method in 1 dimension. Part 3. The adaptive h-p version [AD-A156626] N86-10864
A mesh moving technique for time dependent partial differential equations in two space dimensions [AD-A156663] N86-10866
The h, p and h-p versions of the finite element method in 1 dimension. Part 2. The error analysis of the H and h-p versions [AD-A156835] N86-10869
Thermal and structural analysis of ring components by the finite element method [DE85-013305] N86-11021

FIRE PREVENTION
Ignition and flame spread above liquid fuel pools N86-10163
Self-heating to ignition measurements and computation of critical size for solar energy collector materials [DE85-011449] N86-10302

FISHERIES
National perspective on environmental constraints to hydroelectric development [DE85-013111] N86-10678

FISSION
The development of a neutron evaporation theory code for the thermal fission of Uranium-235 [AD-A156593] N86-10951

FISSION PRODUCTS
The development of a neutron evaporation theory code for the thermal fission of Uranium-235 [AD-A156593] N86-10951
Scoping studies of vapor behavior during a severe accident in a metal-fueling reactor [DE85-011474] N86-10952
On-line gamma-ray data acquisition at the Power Burst facility [DE85-011957] N86-10954

FLAME IONIZATION
Volatile organic compounds in indoor air: A survey of various structures [PB85-198356] N86-10687

FLAME PROPAGATION
Particle cloud combustion experiment N86-10160
A fundamental study of smoldering with emphasis on experimental design for zero-g N86-10162
Ignition and flame spread above liquid fuel pools N86-10163
Flammability limits of gases under low gravity conditions N86-10164
Effects of scale and geometry on hydrogen-air detonations [DE85-006762] N86-10474

FLAME STABILITY
Buoyancy effects upon vapor flame and explosion processes N86-10161
Flammability limits of gases under low gravity conditions N86-10164

FLAME TEMPERATURE
Design and calibration of a flat-flame burner using line reversal techniques [AD-A156724] N86-10294

FLAMES
Effects of chemistry and swirl on the production of turbulence in a flame [PB85-219632] N86-10305

FLAMMABILITY
Flammability limits of gases under low gravity conditions N86-10164

FLAMMABLE GASES
Flammability limits of gases under low gravity conditions N86-10164

FLANGES
Over-center toggle latch [AD-D011753] N86-10556

FLAPS (CONTROL SURFACES)
AIRBOC (air rapid bloom offboard chaff) chaff deployment system [AD-D011746] N86-10554

FLASHOVER
Delay times and jitter in triggered vacuum spark gaps using metal vapor and surface flashover types of triggers [DE85-013966] N86-10441

FLAT PLATES
Three articles on new calculation methods in aeronautics (selected articles) [AD-A145745] N86-10007
Numerical solution of hypersonic flow near leading edge of a flat plate N86-10008
Self-heating to ignition measurements and computation of critical size for solar energy collector materials [DE85-011449] N86-10302

FLEXIBILITY
Dynamic analysis of robotic manipulations with flexible links N86-10545

FLEXIBLE SPACECRAFT
Evaluation of a pulse control law for flexible spacecraft [NASA-CR-176233] N86-10272
Three-dimensional vibration analysis of a uniform beam with offset inertial masses at the ends [NASA-TM-86393] N86-10580

FLEXING
Geothermal influences on the long-term thickness of the mechanical lithosphere during flexure N86-10697

FLIGHT ALTITUDE
Mild hypoxia and visual performance with night vision goggles [AD-A156969] N86-10787

FLIGHT PATHS
Generation of flight paths using hierarchical planning [AD-A156905] N86-10900

FLIGHT SIMULATION
Manned flight simulation: Challenge and response [NASA-TM-86827] N86-10048

FLOAT ZONES
Microgravity Science and Applications Program tasks [NASA-TM-87568] N86-10053
Fluid flow in crystal growth: Analysis of the verticle Bridgman and floating zone process N86-10055
The influence of low frequency mechanical vibrations on the growth of single crystals N86-10059
The control of float zone interfaces by the use of selected boundary conditions N86-10060
Microgravity silicon zoning investigation N86-10063
Hgl sub 2 crystal growth for nuclear detectors N86-10066
Float zone experiments in space N86-10067
Thermocapillary flows and their stability: Effects of surface layers and contamination N86-10109
Suppression of Marangoni convection in float zones N86-10111
The TEXUS flight results on convective flows and heat transfer in simulated floating zones N86-10235
Measurements of the critical Marangoni number of the laminar-oscillatory transition of thermocapillary convection in floating zones N86-10242
A preliminary report on floating zone experiments with germanium crystals in a sounding rocket N86-10256

FLOORS
Modeling groundwater flow into lakes N86-10598

FLOW DISTRIBUTION
Inviscid flow field analysis of maneuvering hypersonic vehicles using the SCM formulation and parabolic grid generation [DE85-013950] N86-10021
Experimental and theoretical investigations of the flow around airfoil systems with ground effect [DFVLR-FB-85-17] N86-10026
On the method of characteristics and its application to the calculations of annular nozzle flowfields N86-10454

FLOW GEOMETRY
The rubber tube test section of the DFVLR in Goettingen, West Germany — wind tunnel walls [DFVLR-FB-85-18] N86-10051

FLOW MEASUREMENT
Experiments and computations on unsteady separating flow in an expanding flume [REPT-2-84] N86-10477

FLOW RESISTANCE
Precise viscosity measurements very close to critical points [NASA ORDER C-86129D] N86-10120

FLOW VELOCITY
Mean turbulence structure in strongly heating air flows N86-10455
Time resolved flow velocity and concentration measurements using a travelling thermal lens [AD-A156706] N86-10541
HALFBREED: An extended capability version of the YAQUI code [DE85-014237] N86-10843

FLUE GASES
Microcomputer aided calculations of parameters for spray dryer operation [DE85-013468] N86-10681

FLUID BOUNDARIES
Liquids and interfaces — Spacelab N86-10268
New approach to multiphase equilibria: Application to high-pressure physics problems [DE85-013820] N86-10907

FLUID DYNAMICS
Microgravity Science and Applications Program tasks [NASA-TM-87568] N86-10053
Fluid dynamics and thermodynamics of vapor phase crystal growth N86-10068
Surface tension induced instabilities in reduced gravity: The Benard problem N86-10117
Lambda point equipment N86-10118
Critical transport phenomena in fluid helium under low gravity N86-10119
Morphological stability and fluid dynamics of vapor crystal growth N86-10126
Miscibility gap systems [NASA ORDER H-27954B] N86-10131
Experimental and theoretical analysis of chemical vapor deposition with prediction of gravity effects N86-10132
Measurement of the density of base fluids at pressures 0.422 to 2.20 GPa [NASA-TM-87114] N86-10551

FLUID FLOW
Fluid flow in crystal growth: Analysis of the verticle Bridgman and floating zone process N86-10055
Convection during unidirectional solidification N86-10077
Metals electroprocessing in molten salts N86-10098
Transport processes in solution crystal growth N86-10107
Surface tensions and their variations with temperature and impurities [NASA ORDER H-27954B] N86-10115
Surface-tension driven convection N86-10124
Role of convection in grain refining N86-10133
Electrophoresis technology N86-10144
Flammability limits of gases under low gravity conditions N86-10164
Modification of the electromagnetic levitator (EML) hardware N86-10172
Process models for 3D composites [AD-A156889] N86-10292
KRAK: A computer program for two-phase, two-component porous flow and fracture propagation, revision [DE85-014264] N86-10469
Time-implicity simulation of particle-fluid systems [DE85-012944] N86-10471
Physical acoustics: Investigation of chemical kinetic and thermodynamic properties of fluids N86-10911

FLUID MECHANICS
Surface-tension driven convection N86-10124
Thermocapillary motion research N86-10125
Transport processes research N86-10129
The fluid physics module: A technical description — Spacelab N86-10201
HALFBREED: An extended capability version of the YAQUI code [DE85-014237] N86-10843

FLUID PRESSURE
SUTRA (Saturated-unsaturated transport). A finite-element simulation model for saturated-unsaturated, Fluid-Density-Dependent ground-water flow with energy transport or chemically-reactive single-species solute transport [AD-A156779] N86-10830

FLUORESCENCE
Containerless high temperature property measurements by atomic fluorescence N86-10092
Automated analysis of digital images generated by two-dimensional gel electrophoresis [DE85-011906] N86-10526

FLUORIDES
Crystallization, optical and chemical properties of fluoride glasses N86-10149

FLUX (RATE)
ORR core re-configuration measurements to increase the fast neutron flux in the Magnetic Fusion Energy (MFE) experiments [DE85-013520] N86-10958

FLUXES
Metallurgy and metallography of braze joints [DE85-014563] N86-10325

FLYING SPOT SCANNERS
Stereoscopic video imagery generation [AD-D011785] N86-10481

FOCUSING
Beam-beam deflections to measure size spot and offset at SLC IP [DE85-014285] N86-10965
Applications of the second-order achromat concept to the design of particle accelerators [DE85-013072] N86-10994

FOILS (MATERIALS)
Formation and characterization of amorphous erbium-based alloys prepared by near-isothermal cold-rolling of elemental composites [DE85-014853] N86-10327
Development and application of the electrochemical etching technique [DE85-010302] N86-10957

FOLDS (GEOLOGY)
Tectonic analysis of typical fold structures in the Zagros Mountains (Iran) by the application of quantitative photogrammetric methods on metric camera data — Spacelab N86-10521
Structural mapping of folded sedimentary environments from satellite images: An example from Central Asia N86-10607

FORBIDDEN TRANSITIONS
Mean life of the 2p(4)((1)S)3s (2)S state in fluorine [DE85-012929] N86-10956
FORCED CONVECTION
Analysis of combined natural and forced convection around cylinders and spheres N86-10456
FORECASTING
The air traffic demand in passenger travel of the Federal Republic of Germany 1990 - 2000. Update of the DFVLR air traffic forecast [DFVLR-MITT-85-06] N86-10031
FOREST MANAGEMENT
Requirements and possibilities of Spacelab metric camera photos usage for inventories of large areas of extensively managed forests N86-10513
FORESTS
Thematic investigations in France based on metric camera imagery — Spacelab N86-10509
Analysis of remote sensing data N86-10605
Mapping diverse forest cover with multipolarization airborne radar N86-10625
Potential applications of multipolarization SAR for pine plantation biomass estimation N86-10626
FORMING TECHNIQUES
Formation and characterization of amorphous erbium-based alloys prepared by near-isothermal cold-rolling of elemental composites [DE85-014853] N86-10327
FORMULAS (MATHEMATICS)
Estimation by moments in a model of faulty inspection [AD-A156754] N86-10886
FORTRAN
User's guide for Langley Research Center Orbital Lifetime program [NASA-TM-87587] N86-10828
SUTRA (Saturated-unsaturated transport). A finite-element simulation model for saturated-unsaturated, Fluid-Density-Dependent ground-water flow with energy transport or chemically-reactive single-species solute transport [AD-A156779] N86-10830
NBSGSC: A FORTRAN program for quantitative X-ray fluorescence analysis [PB85-206068] N86-10847
FOSSILS
Paleogene vertebrate paleontology, geology and remote sensing in the Wind River Basin N86-10609
Paleontology and stratigraphy of Lower Cambrian and upper Proterozoic sediments, Caborca region, northwestern Sonora, Mexico N86-10692
FOURIER ANALYSIS
A study of Morrison's iterative noise removal method [NASA-CR-176222] N86-10823
FOURIER TRANSFORMATION
Process models for 3D composites [AD-A156889] N86-10292
Fuel and lubricant behavior in boundary layers analyzed by infrared emission Fourier transform spectrometry N86-10336
Phase-coded pulse expander-compressor [AD-D011812] N86-10375
Phase coded pulse expander-compressor [AD-D011817] N86-10376
A study of derivative filters using the discrete Fourier transform [NASA-CR-176224] N86-10825
Coordinate axes, location of origin, and redundancy for the one and two-dimensional discrete Fourier transform [NASA-CR-176225] N86-10826
Spatial frequency multiplexed coherent optical processor for calculating generalized moments [AD-D011816] N86-10975
Numerical experiments in image reconstruction — stellar interferometry N86-11116
FRACTURE MECHANICS
Progressive damage, fracture predictions and post mortem correlations for fiber composites [NASA-TM-87101] N86-10290
Preliminary reports, memoranda and technical notes of the Materials Research Council Summer Conference, La Jolla, California [AD-A156776] N86-10291
Fracture toughness and stress relief response of irradiated type 347/348 stainless steel N86-10320
Finite deformation crack-line fields in a thin elasto-plastic sheet [AD-A156757] N86-10346
Fracture toughness testing of centrifugally cast nickel aluminium bronze [REPT-MAT/720] N86-10575
Numerical simulation of crack arrest experiments on Araldite B using the finite difference method [REPT-W-9/82] N86-10596
Recent development in the Hot Dry Rock Geothermal Energy Program [DE85-009562] N86-10663
FRACTURE STRENGTH
Application of the unloading compliance methods in fracture toughness measurements of a quenched and tempered steel [BLL-BISI-TRANS-21628-(9022.06)] N86-10308
Fracture toughness and stress relief response of irradiated type 347/348 stainless steel N86-10320
The use of new path indepedent integrals in elastic-plastic and creep fracture N86-10574
Fracture toughness testing of centrifugally cast nickel aluminium bronze [REPT-MAT/720] N86-10575
Fatigue of graphite/epoxy buffer strip panels with center cracks [NASA-TM-87595] N86-10581
Characterization of mechanical damage mechanisms in ceramic composite materials [AD-A156574] N86-10590
Fracture toughness of hydrogen-embrittled precipitation-hardened stainless steels [AD-A156664] N86-10592
FRACTURES (MATERIALS)
Fundamental studies of low velocity impact resistance of graphite fiber reinforced polymer matrix composites N86-10288
Mixed-mode fracture of ceramics [DE85-014087] N86-10349
FRACTURING
Progressive damage, fracture predictions and post mortem correlations for fiber composites [NASA-TM-87101] N86-10290
FRAMES
Optimal design of portal frames against buckling N86-10572
FREE BOUNDARIES
Free surface phenomena under low- and zero-gravity conditions N86-10108
Suppression of Marangoni convection in float zones N86-10111
On the method of characteristics and its application to the calculations of annular nozzle flowfields N86-10454
FREE CONVECTION
Energy stability of thermocapillary convection in models of the float zone process N86-10123
Some results of the Marangoni free convection experiment — Spacelab N86-10203
Analysis of combined natural and forced convection around cylinders and spheres N86-10456
FREE ELECTRON LASERS
Soviet free-electron laser research [AD-A156898] N86-10542
High-brightness photoemitter injector for electron accelerators [DE85-012673] N86-10929
FREE ELECTRONS
Photoactivation of PBFA-2 [DE85-013439] N86-11019
FREE FLOW
The role of freestream turbulence scale in subsonic flow separation [NASA-CR-176237] N86-10014
FREE JETS
Investigation of density gradient fluctuations in a turbulent free jet by means of the laser schlieren crossed-beam method [DFVLR-FB-85-19] N86-10027
FREEZING
Freezer model using a population balance approach for steady-state, direct-contact, secondary refrigerant, freeze desalination N86-10361
FREON
Transient heat transfer in zero gravity environment [NASA ORDER H-27954B] N86-10114
FREQUENCY DISTRIBUTION
A composite climatological study of the frequency and distribution of severe weather associated with spring season Colorado cyclogenesis [AD-A156981] N86-10715
FREQUENCY HOPPING
An active tracking band-pass filter [AD-A156559] N86-10419
FREQUENCY STANDARDS
Cooled ion frequency standard [AD-A156813] N86-10295
DSN frequency and timing system, Mark 4-85 N86-10393
FREQUENCY SYNCHRONIZATION
DSN frequency and timing system, Mark 4-85 N86-10393
FRICTION
Tribological properties of structural ceramics [NASA-TM-87105] N86-10341
FROST
Laboratory experiments of heat pump dynamic losses [DE85-013931] N86-10473
FROUDE NUMBER
Laminar film condensation in vertical closed two-phase thermosiphons [IKE-5-220] N86-10476
FUEL CELL POWER PLANTS
Fuel Cell Technology Assessment Program, work element no. 6 [DE85-008228] N86-10444
FUEL CELLS
Fuel Cell Technology Assessment Program, work element no. 6 [DE85-008228] N86-10444
Effects of H2S on molten carbonate fuel cells [DE85-014052] N86-10447
Phosphoric and electric utility fuel technology development [DE85-014741] N86-10651
Phosphoric and electric utility fuel cell technology development [DE85-014552] N86-10652
Advanced fuel cell development [DE85-014550] N86-10659
FUEL CONTAMINATION
Method for determining elemental sulfur in jet fuel — differential pulse polarography [FOA-C-40211-B4] N86-10360
FUEL FLOW
Gas generator fuel flow throttle control system [AD-D011797] N86-10355
FUEL INJECTION
Modeling of engine sprays [DE85-010020] N86-10559
FUEL-AIR RATIO
Design and calibration of a flat-flame burner using line reversal techniques [AD-A156724] N86-10294
Effects of chemistry and swirl on the production of turbulence in a flame [PB85-219632] N86-10305
FUELS
Retrofit of SAC EC-135C and RC-135 aircraft with CFM-56 engines [AD-A156688] N86-10038
Remote stratigraphic and structural analysis: Multisensor results in the Wind River/Bighorn Basin area, Wyoming N86-10606
FUNCTIONS (MATHEMATICS)
Arithmetic pipeline for image processing [AD-D011773] N86-10800
FURNACES
Graphite formation in cast iron N86-10100
Development of materials processing systems for use in space on low-g simulation devices N86-10166
Levitating furnance for containerless processing in space N86-10169
High-temperature controlled redox crystallization studies N86-10178
FUSELAGES
Proposed modifications for the RAAF Airtrainer CT-4A cockpit [AD-A156808] N86-10039
FUSION (MELTING)
Fusion target technology N86-10156
Revision of and documentation for the standard version of the Poisson-Group codes [DE85-012659] N86-10837
Scoping studies of vapor behavior during a severe accident in a metal-fueling reactor [DE85-011474] N86-10952
Photoactivation of PBFA-2 [DE85-013439] N86-11019
FUSION REACTORS
Providing automated control for PBFA-2 [DE85-012867] N86-10928
Impact of long-lived radionuclides on waste classification for fusion [DE85-013205] N86-10959
Evolution of the fusion power demonstration tandem mirror reactor configuration [DE85-012889] N86-10960
Alternative fusion concepts and the prospects for improved reactors [DE85-009622] N86-11031
Hot cell facility design for large fusion devices [DE85-012893] N86-11037

G

GALACTIC RADIATION
Solar modulation of galactic cosmic rays: Techniques and applications N86-11143
Extra-galactic X-ray sources and the diffuse X-ray background N86-11144

GALAXIES
A superconducting tunnel junction receiver for millimeter-wave astronomy N86-11041
GALERKIN METHOD
Error estimates and automatic time step control for numerical methods for stiff ordinary differential equations
[CTH-MATH-1984-27] N86-10872
GALILEO PROJECT
Galileo: Exploration of Jupiter's system
[NASA-SP-479] N86-11137
GALLIUM ANTIMONIDES
GaS-semiconductor crystals under microgravity: Experiment ES 323 — Spacelab N86-10224
GALLIUM ARSENIDE LASERS
W-shaped diffused stripe GaAs/AlGaAs laser
[AD-D011818] N86-10538
GALLIUM ARSENIDES
Crystal growth of device quality GaAs in space N86-10061
Crystal growth of GaAs in space N86-10234
Test results for 20-GHz GaAs FET spacecraft power amplifier
[NASA-TM-87072] N86-10379
Contact effects in light activated GaAs switches
[AD-A156957] N86-10434
Theory of advanced, high-efficience concentrator cells
[DE85-008821] N86-10655
Transient velocity assessment in gallium arsenide, and of other GaAs characteristics related to device functions
[AD-A156983] N86-11050
GAMMA RAY SPECTRA
Parallel pulse processing for mercuric iodide gamma-ray detectors
[DE85-013391] N86-10528
Directionality of bremsstrahlung from relativistic electrons in solar flares
[NASA-TM-87509] N86-11141
GAMMA RAYS
The development of a neutron evaporation theory code for the thermal fission of Uranium-235
[AD-A156593] N86-10951
Information on continuum states from feeding times and total (GAMMA) spectra measured with BGO suppressed detectors
[DE85-013868] N86-10961
GAPS
Liquid phase miscibility gap materials N86-10081
GAS DYNAMICS
La Recherche Aerospatiale, bimonthly bulletin, no. 1984-5, September-October 1985
[ESA-TT-899] N86-10363
GAS FLOW
Design and calibration of a flat-flame burner using line reversal techniques
[AD-A156724] N86-10294
Gas generator fuel flow throttle control system
[AD-D011797] N86-10355
GAS GENERATORS
Gas generator fuel flow throttle control system
[AD-D011797] N86-10355
GAS INJECTION
Mass transport phenomena between bubbles and dissolved gases in liquids under reduced gravity conditions N86-10110
GAS JETS
Suppression of Marangoni convection in float zones N86-10111
GAS MIXTURES
Scaling studies of solar pumped lasers
[NASA-CR-176240] N86-10540
GAS PRESSURE
Effect of H2S and COS in the fuel gas on the performance of ambient pressure phosphoric acid fuel cells
[DE85-013913] N86-10446
GAS TUNGSTEN ARC WELDING
Signal analysis of gas tungsten arc welds N86-10078
Measurement of workpiece temperature during welding for welding robot control N86-10534
GAS TURBINE ENGINES
Constitutive modeling for isotropic materials (HOST)
[NASA-CR-174980] N86-10589
Advanced Gas Turbine (AGT) powertrain system development for automotive applications report
[NASA-CR-174886] N86-11087
GASES
KRAK: A computer program for two-phase, two-component porous flow and fracture propagation, revision
[DE85-014264] N86-10469
Velocities of gas and plasmas from real time holographic interograms
[DE85-014618] N86-10530
GATES (CIRCUITS)
Investigation of metallic impurities introduced into SiO2 and silicon by various candidate VLSI metallization systems: Chemical reactions, diffusion, and electrical properties
[AD-A156609] N86-10429
Realization of a multifunction Input/Output (I/O) controller by means of a gate array
[EUT-85-E-147] N86-10804
GAUGE THEORY
On the analytical evaluation of the partition function for unit hypercubes in four dimensions — lattice theory
[NIKHEF-H/84-12] N86-10882
Variational estimates for the mass gap of SU(2) Euclidean lattice gauge theory
[NIKHEF-H/84-13] N86-10883
GAUSS EQUATION
A study of methods to predict and measure the transmission of sound through the walls of light aircraft. Integration of certain singular boundary element integrals for applications in linear acoustics
[NASA-CR-176229] N86-10912
GEARS
Trials on the asperity counting monitoring system — helicopter gearboxes
[RES-PAPER-670] N86-10550
GELS
Gel precursors as glass and ceramic starting materials for space processing applications research N86-10150
Sol-gel glasses N86-10153
Glass research N86-10157
Growth and characterization of brushite and lead monetite, simulation and results — Spacelab N86-10230
Automated analysis of digital images generated by two-dimensional gel electrophoresis
[DE85-011906] N86-10526
GENETIC ENGINEERING
Biotechnology regulation
[GPO-43-778] N86-10733
Somatic cell and molecular genetics approach to DNA repair and mutagenesis
[DE85-014181] N86-10737
GENETICS
Somatic cell and molecular genetics approach to DNA repair and mutagenesis
[DE85-014181] N86-10737
GEOCHEMISTRY
Applica.ion of the ruthenium and technetium thermodynamic data bases used in the EQ3/6 geochemical codes
[DE85-013766] N86-10632
GEOCHRONOLOGY
Report of the Workshop on Geologic Applications of Remote Sensing to the Study of Sedimentary Basins
[E86-10002] N86-10599
Chronologic analysis of terrestrial sediments and basin evolution N86-10602
Remote stratigraphic and structural analysis: Multisensor results in the Wind River/Bighorn Basin area, Wyoming N86-10606
Foreland basin structures and remote sensing N86-10608
Age-dating volcanic and alluvial surfaces with multipolarization data N86-10620
GEODESY
Mobile VLBI and GPS measurement of vertical crustal motion N86-10401
GEODETIC SURVEYS
How Antarctica was unveiled. Masterpieces of Frankfurt topographic surveyors. A part of the German Antarctica research program N86-10181
GEOLOGICAL FAULTS
Structural mapping of folded sedimentary environments from satellite images: An example from Central Asia N86-10607
Neogene compressional deformation and possible thrust faulting in southwest Dominican Republic N86-10618
Structural discontinuity within the southern California continental margin: Seismic and gravity models of the western Transverse Ranges N86-10699
Crustal structure of the southern Rio Grande rift determined from seismic refraction, surface wave dispersion, and gravity data N86-10700
GEOLOGICAL SURVEYS
Metric Camera Workshop — Spacelab
[ESA-SP-209] N86-10485
A geological structural analysis of the southeastern Zagros (Iran) ranges based on metric camera photos N86-10492
The role of very small scale metric images in modern geology — Spacelab metric camera N86-10502
Geological mapping of remote mountainous regions using metric camera imagery — Spacelab N86-10503
Thematic investigations in France based on metric camera imagery — Spacelab N86-10509
Time-term analysis of upper crustal structure in the Columbia Basin, Washington
[DE85-012390] N86-10633
GEOMETRICAL THEORY OF DIFFRACTION
Numerical methods for analyzing electromagnetic scattering
[NASA-CR-176141] N86-10377
GEOMETRY
Effects of scale and geometry on hydrogen-air detonations
[DE85-006762] N86-10474
Topological properties of hypercubes
[AD-A156777] N86-10850
GEOPHYSICAL OBSERVATORIES
Activities report in geophysics
[KGI-188] N86-10709
GEOPHYSICS
Report of the Workshop on Geologic Applications of Remote Sensing to the Study of Sedimentary Basins
[E86-10002] N86-10599
Formation of waves by ground motion
[PM/84/09] N86-10706
In-situ geophysical investigations into the nature of the oceanic crust N86-10725
GEOPOTENTIAL HEIGHT
Lumped geopotential harmonics of order 14, from the orbit of 1967-11G
[AD-A156627] N86-10190
GEOTEMPERATURE
Geothermal influences on the long-term thickness of the mechanical lithosphere during flexure N86-10697
GEOTHERMAL ENERGY EXTRACTION
Recent development in the Hot Dry Rock Geothermal Energy Program
[DE85-009562] N86-10663
GEOTHERMAL ENERGY UTILIZATION
Ocean energy technology program summary
[DE85-013102] N86-10731
GEOTHERMAL RESOURCES
Geothermal lost circulation zone mapping tool
[DE85-008696] N86-10531
Geothermal Energy Technology Program summary
[DE85-013101] N86-10646
Recent development in the Hot Dry Rock Geothermal Energy Program
[DE85-009562] N86-10663
GEOTHERMAL TECHNOLOGY
Geothermal Energy Technology Program summary
[DE85-013101] N86-10646
GERMANIUM
A preliminary report on floating zone experiments with germanium crystals in a sounding rocket N86-10256
Defect identification in high-energy semiconductors
[DE85-014533] N86-10442
GERMANIUM ALLOYS
Effect of undercooling and modified microstructure on the physical properties of material synthesized in the drop tube and drop tower N86-10075
GEYSERS
KRAK: A computer program for two-phase, two-component porous flow and fracture propagation, revision
[DE85-014264] N86-10469
GIANT STARS
Physical conditions in giant extragalactic H2 regions N86-11130
GIRDERS
Load-deflection tests and computer analyses of a high-precision adhesive-bonded antenna reflector panel N86-10389
GLASS
Lambda point equipment N86-10118
Containerless processing of glass forming melts in space N86-10148
Gel precursors as glass and ceramic starting materials for space processing applications research N86-10150
Glass formation in reluctant glass formers N86-10151
Sol-gel glasses N86-10153
Physical phenomena in containerless glass processing N86-10155
Glass research N86-10157
Microgravity Materials Science Laboratory N86-10173
Acoustic levitation containerless processing N86-10177
Shrinking of a gas bubble in a glass melt under microgravity conditions — STS-11 N86-10254
Calculation of the glass transition temperatures of linear polymers. Part 1: Rules for hierarchical ordering of the data set
[AD-A156584] N86-10343
Thermal expansion of glasses in the solid and liquid phases
[DE85-013953] N86-10351

Fatigue of graphite/epoxy buffer strip panels with center cracks
[NASA-TM-87595] N86-10581
Fundamental study of the closure property of joints N86-10698
A study of the applicability of nucleation theory to quasi-thermodynamic transformations of second and higher Ehrenfest-order
[NASA-CR-176230] N86-11060

GLOBAL POSITIONING SYSTEM
Mobile VLBI and GPS measurement of vertical crustal motion N86-10401

GLOBULAR CLUSTERS
The dynamics and stellar content of globular star clusters N86-11131

GLOVES
Effect of increased body clothing insulation on hand temperature in a cold environment
[AD-A156597] N86-10786

GLOW DISCHARGES
Surface conditioning of synchrotron radiation source to improve beam lifetime
[DE84-012185] N86-10948

GLYCEROLS
Rapid analysis using capillary supercritical fluid chromatography
[DE85-012460] N86-10297

GLYCOLS
Separation of aqueous two-phase polymer systems in microgravity N86-10246
Application of the theory of Ostwald ripening to microgravity phase separation experiments N86-10248

GNOMONIC PROJECTION
Stereo-orthophotos in various map projections N86-10488

GOLD ALLOYS
Effect of undercooling and modified microstructure on the physical properties of material synthesized in the drop tube and drop tower N86-10075

GOVERNMENT PROCUREMENT
F-16X MSIP (Multi-national Staged Improvement Program) case example: Operating and support cost estimation using VAMOSC (Visibility And Management Of Operating and Support Costs)
[AD-A156893] N86-10006

GRAIN BOUNDARIES
Design, fabrication and testing of an experimental apparatus for determining particle behavior under very low intergranular stresses N86-10175
Compatibility of grain-stabilized platinum with candidate propellants for resistojets
[NASA-TM-87118] N86-10279
Intrinsic mechanisms of multilayer ceramic capacitor failure
[AD-A156638] N86-10431

GRANITE
Altitudinal distribution of granitic landforms in the south central Sierra Nevada, California N86-10695

GRANTS
Study of one- and two-dimensional filtering and deconvolution algorithms for a streaming array computer
[NASA-CR-176226] N86-10827

GRANULAR MATERIALS
Compatibility of grain-stabilized platinum with candidate propellants for resistojets
[NASA-TM-87118] N86-10279
High efficiency heat transport and power conversion system for cascade
[DE85-012959] N86-10468

GRAPHIC ARTS
A graphic anthropometric aid for seating and workplace design
[AD-A156988] N86-10788

GRAPHITE
Graphite formation in cast iron N86-10100
Fundamental studies of low velocity impact resistance of graphite fiber reinforced polymer matrix composites N86-10288
High temperature mechanical testing of a cylindrical weave carbon-carbon composite
[AD-A156639] N86-10591
Investigation of composite materials property requirements for sonic fatigue research
[NASA-TM-87601] N86-10913

GRAPHITE-EPOXY COMPOSITES
Progressive damage, fracture predictions and post mortem correlations for fiber composites
[NASA-TM-87101] N86-10290
Ultrasonic evaluation of mechanical properties of thick, multilayered, filament wound composites
[MASA-TM-87088] N86-10561
Fatigue of graphite/epoxy buffer strip panels with center cracks
[NASA-TM-87595] N86-10581

GRAVELS
Cretaceous and cenozoic stratigraphy of the upper and middle coastal plain, Harnett County area, North Carolina N86-10690

GRAVITATIONAL COLLAPSE
A method for numerical relativity: Simulation of axisymmetric gravitational collapse and gravitational radiation generation N86-11127
Gravitational collapse of a scalar field N86-11129

GRAVITATIONAL EFFECTS
Thermal and solutal convection damping using an applied magnetic field N86-10094
Metallic foams N86-10095
Cell partition in two polymer aqueous phases N86-10139
Colloidal oxide properties and kinetic studies N86-10147
Fusion target technology N86-10156
Cryogenic equivalence principle experiment N86-10171
Design, fabrication and testing of an experimental apparatus for determining particle behavior under very low intergranular stresses N86-10175
Fifth European symposium on Material Sciences under Microgravity. Results of Spacelab 1
[ESA-SP-222] N86-10200
The fluid physics module: A technical description — Spacelab N86-10201
Influences affecting separation in monotectic alloys under microgravity N86-10209
Melting and solidification of metal matrix composites under microgravity — Spacelab N86-10211
Unidirectional solidification of cast iron: Experiment ES-325 — Spacelab N86-10212
Vacuum brazing under microgravity — Spacelab N86-10214
Directional solidification of an aluminum-zinc vapor emulsion in microgravity — Spacelab N86-10218
Crystal growth of silicon in Spacelab 1: Experiment ES-321 N86-10227
Mathematical simulation of disturbing forces and material science processes under low gravity N86-10236
Experimental study on Marangoni convection N86-10243
Rationale for two phase polymer system microgravity separation experiments N86-10247
Application of the theory of Ostwald ripening to microgravity phase separation experiments N86-10248
Nucleate pool boiling in subcooled liquid under microgravity: Results of TEXUS experimental investigations N86-10250
Shrinking of a gas bubble in a glass melt under microgravity conditions — STS-11 N86-10254
Physical and chemical properties of a nickel catalyst processed under microgravity — STS-7 N86-10255
A preliminary report on floating zone experiments with germanium crystals in a sounding rocket N86-10256
Cellular morphologies in lead-thallium alloys — gravitational effects N86-10262
Computation of flow regimes in parameter space for the AGCE
[NASA-CR-178480] N86-10705
User's guide for Langley Research Center Orbital Lifetime program
[NASA-TM-87587] N86-10828
Space antenna for gravitational wave astronomy N86-11123

GRAVITATIONAL FIELDS
Lumped geopotential harmonics of order 14, from the orbit of 1967-11G
[AD-A156627] N86-10190

GRAVITATIONAL WAVE ANTENNAS
Space antenna for gravitational wave astronomy N86-11123

GRAVITATIONAL WAVES
A method for numerical relativity: Simulation of axisymmetric gravitational collapse and gravitational radiation generation N86-11127

GREAT PLAINS CORRIDOR (NORTH AMERICA)
Vegetation and soils field research data base: Experiment summaries
[E85-10110] N86-10610

GROUND BASED CONTROL
Construction and use of a radio controlled model helicopter for research
[AD-A156547] N86-10035
Optical/IR telescope arrays: A study of their potential for satisfying observational requirements in astronomy for a large aperture system in the 1990s and beyond
[REPT-15] N86-11094

GROUND EFFECT (AERODYNAMICS)
Experimental and theoretical investigations of the flow around airfoil systems with ground effect
[DFVLR-FB-85-17] N86-10026

GROUND STATIONS
JPL emergency support of TDRSS and compatible satellites N86-10394
The GCF Mark 4 implementation and beyond N86-10399

GROUND TRUTH
Creation of Ground Control Points (GCP) library using ESA Spacelab metric camera imagery — ground control point (gcp) N86-10516
Vegetation and soils field research data base: Experiment summaries
[E85-10110] N86-10610

GROUND WATER
Modeling groundwater flow into lakes N86-10598
Evaluating the ground-water resources of the high plains of Texas, Volume 4
[PB85-191625] N86-10641

GROUP THEORY
On class groups of lattices
[CTH-MATH-1985-08] N86-10903

GROWTH
Cell maintenance systems N86-10142

GUN PROPELLANTS
Binder-filler interaction in energetic polymers
[AD-A156752] N86-10345

GUSTS
Forced response analysis of an aerodynamically detuned supersonic turbomachine rotor
[NASA-TM-87093] N86-10019

GYROCOMPASSES
Elastic wave gyrometer. Experiments with a parametric wave device
[REPT-26/5005/HF/AR] N86-10533

H

HADRONS
Microwave instability across the transition energy
[DE85-013304] N86-11010

HALF LIFE
Information on continuum states from feeding times and total (GAMMA) spectra measured with BGO suppressed detectors
[DE85-013868] N86-10961
Relativistic wavefunction at the origin and the pion decay constant
[DE85-012392] N86-11062

HALIDES
Photoionization technique for growth of metallic films
[AD-D011760] N86-10426

HAMILTONIAN FUNCTIONS
Lie algebraic methods for charged particle beams and light optics N86-10970

HAND (ANATOMY)
Effect of increased body clothing insulation on hand temperature in a cold environment
[AD-A156597] N86-10786

HANDBOOKS
Solar thermal technical information guide
[DE85-002941] N86-10657

HARDNESS
Fabrication and metallurgical properties of modified 9Cr-1 Mo steel
[DE85-012885] N86-10328

HARMONIC GENERATIONS
Determination of optical properties by third-harmonic generation in noble gases in unfocused laser beams N86-10535

HARMONIC MOTION
Theoretical study of the unsteady linear problem for a rectangular wing with a pitching movement
[ONERA-RT-17/1841-RY-010-R] N86-10022

HARMONIC RADIATION
The 20 keV undulators for a 6-GeV storage ring
[DE85-013867] N86-10941

HARMONICS
Harmonic distortion reduction technique for data acquisition
[AD-D011771] N86-10799

HASTELLOY (TRADEMARK)
Weld metal hot-cracking of hastelloy alloys C-22 and C-276: A study by analytical electron microscopy
[DE85-009437] N86-10324

HAZARDS
Development of the Multi-Attribute Hazard Assessment System (MAHAS) and its application to energy-related waste streams
[DE85-010278] N86-10676
Biotechnology regulation
[GPO-43-778] N86-10733

HEARING
Proposed aural nondetectability limits for Army materiel
[AD-A156704] N86-10917

HEART FUNCTION
Assessment of state of chronotropic and inotropic heart function at different degrees of physical fitness N86-10746
HEART RATE
Dynamics of changes of statistical indicators of heart rhythm of persons with different degree of motion sickness N86-10743
Assessment of state of chronotropic and inotropic heart function at different degrees of physical fitness N86-10746
HEAT
Advanced absorption heat pump cycles [DE85-003914] N86-10654
HEAT ACCLIMATIZATION
Mechanism of adaptogenic action of prickly eleuterococcus on man during heat stress N86-10757
HEAT BALANCE
Freezer model using a population balance approach for steady-state, direct-contact, secondary refrigerant, freeze desalination N86-10361
HEAT EXCHANGERS
Submerged ram air inlets for ECM (electronic countermeasures) pods [AD-D011801] N86-10020
High efficiency heat transport and power conversion system for cascade [DE85-012959] N86-10468
Ground-coupled heat pump research at the University of Tennessee Washington, D.C., 10 Dec. 1984 [DE85-005357] N86-10650
HEAT FLUX
Nucleate pool boiling in subcooled liquid under microgravity: Results of TEXUS experimental investigations N86-10250
Radiative heat transfer in nonisothermal combustion products N86-10458
Energy balance in a deep Colorado valley: ASCOT 84 [DE85-012441] N86-10631
HEAT MEASUREMENT
Thermal expansion of glasses in the solid and liquid phases [DE85-013953] N86-10351
High flux calorimetry [AD-A156852] N86-10524
HEAT OF COMBUSTION
Guidelines for a thermochemical kinetics computer program [DE85-014266] N86-10839
HEAT OF FUSION
Measurement of the properties of tungsten at high temperatures N86-10091
HEAT PIPES
Development of materials processing systems for use in space on low-g simulation devices N86-10165
HEAT PUMPS
Engine-driven and absorption heat pump programs [DE85-013930] N86-10472
Laboratory experiments of heat pump dynamic losses [DE85-013931] N86-10473
Simplified analysis of Stirling engines and heat pumps [DE85-005366] N86-10647
Ground-coupled heat pump research at the University of Tennessee Washington, D.C., 10 Dec. 1984 [DE85-005357] N86-10650
Comparative analysis of single and continuously variable-capacity heat pump concepts [DE85-004089] N86-10653
Advanced absorption heat pump cycles [DE85-003914] N86-10654
Stirling-engine-driven heat pump program overview [DE85-004796] N86-10661
Analyses of advanced residential abosrption heat pump cycles [DE85-005244] N86-10664
HEAT RESISTANT ALLOYS
Oxidation behavior of glassy alloys N86-10158
Experiments with tubular probes made of INCOLOY 800 H under uniaxial and multiaxial strain [JUEL-1979] N86-10595
HEAT SOURCES
General-purpose heat source development: Safety Verification Test Program. Bullet/fragment test series [DE85-014262] N86-10660
HEAT STORAGE
Passive solar design handbook [DE85-014263] N86-10656
HEAT TOLERANCE
Effect of inclusion of supplementary ascorbic acid in daily diet on degree of vitamin saturation of body and thermoresistance of erythrocytes while working in arid zone N86-10749
HEAT TRANSFER
Modelling of laser-enhanced chemical vapor deposition N86-10105
Transient heat transfer in zero gravity environment [NASA ORDER H-27954B] N86-10114
Solid surface combustion at reduced gravity N86-10159
Fundamental studies of droplet combustion at reduced gravity N86-10165
Analytical investigation of solid rocket nozzle failure [NASA-TM-86513] N86-10278
Film cooling on a convex wall: Heat transfer and hydrodynamic measurements for full and partial coverage [NASA-CR-174964] N86-10461
High efficiency heat transport and power conversion system for cascade [DE85-012959] N86-10468
KRAK: A computer program for two-phase, two-component porous flow and fracture propagation, revision [DE85-014264] N86-10469
Laminar film condensation in vertical closed two-phase thermosiphons [IKE-5-220] N86-10476
The boundary condition in a numerical model of atmospheric flows over fixed interfaces [GKSS-85-E-10] N86-10722
Heat transfer mechanism in human extremities N86-10759
Physical acoustics: Investigation of chemical kinetic and thermodynamic properties of fluids N86-10911
Heat transfer in condensing and evaporating two-component, two-phase flow inside a horizontal tube N86-11058
HEAT TRANSFER COEFFICIENTS
Freezer model using a population balance approach for steady-state, direct-contact, secondary refrigerant, freeze desalination N86-10361
HEAT TRANSMISSION
The control of float zone interfaces by the use of selected boundary conditions N86-10060
Heat flow and segregation in directional solidification N86-10072
HEATERS
Small cartridge heater [AD-D011784] N86-10277
HEATING
Efficiency of muscular work in white rats during adaptation to cold N86-10763
HEATING EQUIPMENT
Small cartridge heater [AD-D011784] N86-10277
HEAVY IONS
Microwave instability across the transition energy [DE85-013304] N86-11010
Unicell structure for superconducting storage rings [DE85-013303] N86-11022
Tracking studies on the effects of magnet multipoles on the aperture of the RHIC heavy ion collider [DE85-013282] N86-11023
HEIGHT
Digital elevation model from Spacelab metric camera photographs N86-10486
HELICAL FLOW
Theoretical aspects of magnetic helicity [DE85-011846] N86-10984
HELICAL INDUCERS
Generalized helicity and its time derivative [DE85-012770] N86-11027
HELICOPTERS
Construction and use of a radio controlled model helicopter for research [AD-A156547] N86-10035
The quest for a helicopter suitable for combat rescue, 1967 - 1983 [AD-A156842] N86-10040
A comparative analysis of a CV helicopter and a JVX (Joint Services Advanced Vertical Lift) tilt-rotor aircraft in an aircraft carrier based ASW (Anti-Submarine Warfare) [AD-A156871] N86-10041
Trials on the asperity counting monitoring system — helicopter gearboxes [RES-PAPER-670] N86-10550
Understanding and improving acoustic to seismic coupling as it pertains to Sandia's helicopter detector [DE85-009440] N86-10920
HELIUM
Cryogenic equivalence principle experiment N86-10171
Simulating the CTR environment in the HVBM [DE85-011745] N86-10193
Experimental X-ray scattering cross sections for H2 and rare atomic gases [DE85-011572] N86-10936
Magnetic properties of doped semiconductors [DE85-012090] N86-11053
HELIUM ISOTOPES
An investigation of vortex dynamics in 2-dimensional superfluid films of helium-4 N86-11040
HEMATOPOIESIS
Indices of blood oxygen transporting properties and erythropoiesis in rats after prolonged stay in nitrogen-oxygen mixture at elevated pressure N86-10761
HEMODYNAMIC RESPONSES
Hemodynamics during gravitational overloads (mathematical modeling) N86-10739
Capacity for work and hemodynamics in males residing at middle and high latitudes N86-10747
HETERODYNING
A superconducting tunnel junction receiver for millimeter-wave astronomy N86-11041
HEURISTIC METHODS
State assignment in sequential circuits [EUT-85-E-146] N86-10846
HIERARCHIES
Calculation of the glass transition temperatures of linear polymers. Part 1: Rules for hierarchical ordering of the data set [AD-A156584] N86-10343
Generation of flight paths using hierarchical planning [AD-A156905] N86-10900
HIGH ENERGY INTERACTIONS
Proceedings of a Workshop on Electroweak Symmetry Breaking [DE85-004444] N86-11008
Search for heavy neutrinos produced in e(+)e(-) annihilation [DE85-013372] N86-11035
HIGH FREQUENCIES
Report on a visit to CERN in February 1985. Notes on bunch monitors, high-frequency systems, linacs, kickers, magnets, vacuum and bunch extraction [LINO-119] N86-10967
HIGH PASS FILTERS
On the use of X-band CW nanosecond airborne radar for terrain profiling [AD-A156886] N86-10406
HIGH PRESSURE
Spontaneous Raman spectroscopy of shocked H2O [DE85-014557] N86-10470
Measurement of the density of base fluids at pressures 0.422 to 2.20 GPa [NASA-TM-87114] N86-10551
Liquid to gas leak ratios with liquid nitrogen and liquid helium [DE85-012950] N86-11030
High-pressure release-wave measurements and phase transformation in CaCO3 [DE85-012592] N86-11055
Thermodynamics of polymer-supercritical solvent mixtures [AD-A157036] N86-11061
HIGH RESOLUTION
Cooled ion frequency standard [AD-A156813] N86-10295
HIGH SPEED
Type of new Chinese-produced high-speed camera and its utilization in detonation physics experiments [DE85-015191] N86-10529
Elektronika MS 1603 high-speed peripheral processor N86-10811
Diagnostics of peripheral processors and controllers N86-10812
Transient velocity assessment in gallium arsenide, and of other GaAs characteristics related to device functions [AD-A156983] N86-11050
HIGH TEMPERATURE
Measurement of the properties of tungsten at high temperatures N86-10091
Containerless high temperature property measurements by atomic fluorescence N86-10092
Advanced containerless processing technology N86-10176
Acoustic levitation containerless processing N86-10177
High-temperature controlled redox crystallization studies N86-10178
Multipurpose pan development [DE85-012326] N86-10319
Swelling and tensile properties of EBR-2-irradiated tantalum alloys for space reactor applications [DE85-012887] N86-10329
Spontaneous Raman spectroscopy of shocked H2O [DE85-014557] N86-10470
Dust deposition in regions of separated flow [JUEL-1985] N86-10475
Finite element analysis of metals at elevated temperature using unified constitutive theories N86-10569
Constitutive modeling for isotropic materials (HOST) [NASA-CR-174980] N86-10589

Liquid to gas leak ratios with liquid nitrogen and liquid helium
[DE85-012950] N86-11030

HIGH TEMPERATURE ENVIRONMENTS
Dynamic thermophysical measurements in space
[NASA ORDER H-27954-B] N86-10106

HIGH TEMPERATURE PLASMAS
Potential structures and particle acceleration on auroral field lines
[AD-A156694] N86-10708
Symmetric Tandem Mirror Program
[DE85-012352] N86-11032

HIGH TEMPERATURE RESEARCH
Measurement of high temperature thermophysical properties N86-10074

HIGH TEMPERATURE TESTS
High temperature properties and characterization of S3-N4 materials
[BMFT-FB-T-85-046] N86-10352
High temperature properties of SiC materials
[BMFT-FB-T-85-047] N86-10353
High temperature mechanical testing of a cylindrical weave carbon-carbon composite
[AD-A156639] N86-10591
Experiments with tubular probes made of INCOLOY 800 H under uniaxial and multiaxial strain
[JUEL-1979] N86-10595

HIGH VOLTAGES
Calibrated Faraday current and magnetic field sensor
[DE85-013438] N86-10439
High voltage instrument transformers for outdoor service with an insulation of low pressure SF6 gas and plastic foils
[BMFT-FB-T-85-034] N86-10449

HIMALAYAS
Test on mapping application of metric camera imagery — Spacelab N86-10505
Report of the Workshop on Geologic Applications of Remote Sensing to the Study of Sedimentary Basins
[E86-10002] N86-10599

HOLE GEOMETRY (MECHANICS)
Analytical and experimental study of cracks emanating from an elliptical hole in unidirectional composite material N86-10567

HOLMIUM
Extraction of lanthanide ions by 2-methyl-8-quinolinol
[DE85-014277] N86-10303

HOLMIUM ISOTOPES
Information on continuum states from feeding times and total (GAMMA) spectra measured with BGO suppressed detectors
[DE85-013868] N86-10961

HOLOGRAPHIC INTERFEROMETRY
Holographic interferometry near gas/liquid critical points: Ground-based study of a D1 experiment — Spacelab N86-10249

HOLOGRAPHY
Advanced optical measurement techniques N86-10174
Digital decoding of in-line holograms N86-10478
Velocities of gas and plasmas from real time holographic interograms
[DE85-014618] N86-10530
Spatial frequency multiplexed coherent optical processor for calculating generalized moments
[AD-D011816] N86-10975

HOMEOSTASIS
Effect of emotional stress on hemostasis system of healthy persons N86-10745

HOMOLOGY
Galois descent and class groups of orders
[CTH-MATH-1985-09] N86-10904

HORMONES
Hormone purification by isoelectric focusing N86-10135
Effect of single actions of weak electromagnetic fields of ultralow frequency on indices of endocrine system N86-10744

HORN ANTENNAS
Propagation and radiation characteristics of a multimode corrugated waveguide feedhorn N86-10388

HOT CORROSION
Weld metal hot-cracking of hastelloy alloys C-22 and C-276: A study by analytical electron microscopy
[DE85-009437] N86-10324

HOT PRESSING
Containerless processing of glass forming melts in space N86-10148

HOUSINGS
Small cartridge heater
[AD-D011784] N86-10277

HUGONIOT EQUATION OF STATE
Hugoniot measurements in aluminum to 420 GPa using the LLNL two-stage light-gas gun
[DE85-013821] N86-10317

HUMAN BEHAVIOR
Individual typological features of autonomic reactions during autogenic training in polar expedition members in period of wintering in Antarctica N86-10748

HUMAN BODY
Motion analysis report
[NASA-CR-171897] N86-10896

HUMAN FACTORS ENGINEERING
Proposed modifications for the RAAF Airtrainer CT-4A cockpit
[AD-A156808] N86-10039
The synthesis and analysis of color images
[NASA-TM-86844] N86-10777
LANES 1 Users' Guide
[NASA-CR-177334] N86-10819

HUMAN PERFORMANCE
The effects of age, sleep deprivation, and altitude on complex performance
[AD-A156987] N86-10771
Studies on human vehicle control
[B8563352] N86-10775
Car driving as a supervisory control task
[B8563351] N86-10776
Standardization of tasks: Approach planning — human performance assessment
[IZF-1984-19] N86-10782

HUMAN TOLERANCES
Effect of various doses of some vitamins on non-specific mechanisms of adaptation of man N86-10750

HUMIDITY
Laboratory experiments of heat pump dynamic losses
[DE85-013931] N86-10473

HUYGENS PRINCIPLE
A simplified method of estimation of the specular components of radar cross section for some re-entrant conductors
[AD-A156573] N86-10403

HYDRAULIC CONTROL
Digital control of the hydraulic actuators of an adaptive suspension vehicle N86-10548

HYDRAULIC EQUIPMENT
Computer control of an electric hydraulic robot leg with proximity ranging system N86-10549

HYDRAULIC FLUIDS
The Rhine-Meuse estuary hydraulic scale model. Experiences with computer configuration and software
[PUBL-335] N86-10637

HYDRIDES
Development of metallization process
[NASA-CR-176209] N86-10312

HYDROBROMIC ACID
Laser Raman spectroscopy study of the zinc and bromide ion complex equilibrium in zinc/bromine battery electrolytes
[DE85-011820] N86-10301

HYDRODYNAMICS
Streaming potentials in conductive and nonconductive tubing
[DE85-012984] N86-10438
Time-implicity simulation of particle-fluid systems
[DE85-012944] N86-10471
The generation and transmission of vibration in plain cylindrical bearings. Part 2. Experiment
[AD-A156577] N86-10553
Dynamics of imploding neon gas puff plasmas. 1
[AD-A156916] N86-10983

HYDROELECTRIC POWER STATIONS
Ultrasonic inspection of weldments in large size spiral box for hydroelectric plant
[AS-701/85] N86-10562
National perspective on environmental constraints to hydroelectric development
[DE85-013111] N86-10678

HYDROELECTRICITY
National perspective on environmental constraints to hydroelectric development
[DE85-013111] N86-10678

HYDROGEN
Effects of scale and geometry on hydrogen-air detonations
[DE85-006762] N86-10474
Experimental X-ray scattering cross sections for H2 and rare atomic gases
[DE85-011572] N86-10936
Angular distribution of neutral hydrogen following collisional electron detachment from H(-)
[DE85-014258] N86-10943
Proposed bunching scheme for a polarized H(-) injector
[DE85-012648] N86-10986
Noninterceptive techniques for the measurement of longitudinal parameters for intense H(-) beams
[DE85-012662] N86-10992

HYDROGEN EMBRITTLEMENT
Fracture toughness of hydrogen-embrittled precipitation-hardened stainless steels
[AD-A156664] N86-10592
Chemical/hydrogen energy systems
[DE85-012742] N86-10667
Methane-bubble formation in hydrogen-charged Fe-30 ppM C
[DE85-012526] N86-10937

HYDROGEN IONS
AGS polarized H(-) source
[DE85-013296] N86-10935
Performance of the H(-) ion source for the intense pulsed neutron source
[DE85-012368] N86-10991

HYDROGEN PRODUCTION
Chemical/hydrogen energy systems
[DE85-012742] N86-10667

HYDROGEN SULFIDE
Chemical kinetics and cellular structure of detonations in hydrogen sulphide and air
[DE85-009408] N86-10304
Method for determining elemental sulfur in jet fuel — differential pulse polarography
[FOA-C-40211-B4] N86-10360

HYDROLOGY
Interpretation of metric camera concerning hydrologic structures of the Rhone Delta — Spacelab N86-10504

HYDROLOGY MODELS
Modeling groundwater flow into lakes N86-10598

HYDROMECHANICS
Recent development in the Hot Dry Rock Geothermal Energy Program
[DE85-009562] N86-10663

HYDROPHONES
A comparison of swept frequency and FFT methods used to calibrate array test modules
[AD-A156629] N86-10430
Fiber optic gradient hydrophone construction and calibration for sea trial
[AD-A156469] N86-10914

HYDROTHERMAL SYSTEMS
Geothermal Energy Technology Program summary
[DE85-013101] N86-10646

HYDROXYL COMPOUNDS
Extraction of lanthanide ions by 2-methyl-8-quinolinol
[DE85-014277] N86-10303

HYDROXYL EMISSION
The two micron spectrum of R Scuti N86-11092

HYPERBOLIC FUNCTIONS
La Recherche Aerospatiale, bimonthly bulletin, no. 1984-5, September-October 1985
[ESA-TT-899] N86-10363

HYPERCAPNIA
Dynamics of general resistance of rats during readaptation period after training in altered gas environment N86-10767

HYPERONS
Hyperon polarization: An unresolved problem
[DE85-012298] N86-10946

HYPERSONIC FLOW
Three articles on new calculation methods in aeronautics (selected articles)
[AD-A145745] N86-10007
Numerical solution of hypersonic flow near leading edge of a flat plate N86-10008
Numerical procedure for three-dimensional hypersonic viscous flow over aerobrake configuration
[NASA-TM-58269] N86-10018
Inviscid flow field analysis of maneuvering hypersonic vehicles using the SCM formulation and parabolic grid generation
[DE85-013950] N86-10021

HYPERSONIC VEHICLES
Inviscid flow field analysis of maneuvering hypersonic vehicles using the SCM formulation and parabolic grid generation
[DE85-013950] N86-10021

HYPERSONIC WAKES
Numerical procedure for three-dimensional hypersonic viscous flow over aerobrake configuration
[NASA-TM-58269] N86-10018

HYPERSPACES
On the analytical evaluation of the partition function for unit hypercubes in four dimensions — lattice theory
[NIKHEF-H/84-12] N86-10882

HYPERTHERMIA
Short term heat effect on adreno- and cholino-sensitivity of rat's small intestine N86-10754
Vestibular resistance and blood circulation changes in orthostatic position during hyperthermia N86-10758

HYPERVELOCITY GUNS
EMACK railgun firing test report number 9
[AD-A156661] N86-10354

HYPERVELOCITY LAUNCHERS
EMACK railgun firing test report number 9
[AD-A156661] N86-10354
HYPOKINESIA
Study of hypokinesia and acceleration effects on human chromosomes N86-10740
HYPOTHERMIA
Intradiurnial organization of wakefulness-sleep sequence and energy metabolism in rats exposed to low ambient temperature N86-10764
HYPOXIA
Reaction of rabbit respiration system to hypoxic stimulus in nitrogen-oxygen medium at elevated pressure N86-10760
Indices of blood oxygen transporting properties and erythropoiesis in rats after prolonged stay in nitrogen-oxygen mixture at elevated pressure N86-10761
Dynamics of general resistance of rats during readaptation period after training in altered gas environment N86-10767
Mild hypoxia and visual performance with night vision goggles
[AD-A156969] N86-10787

I

IBM 370 COMPUTER
The local disk controller
[REPT-1-68430-44(1985)01] N86-10806
Performance analysis of the IBM Direct Access Storage Device (DASD) subsystem, and some suggestions for improved systems
[REPT-1-68430-44(1985)02] N86-10807
An intelligent local disk control system
[REPT-051560-28(1984)08] N86-10808
IDEAL GAS
On the method of characteristics and its application to the calculations of annular nozzle flowfields N86-10454
IDENTIFYING
Defect identification in high-energy semiconductors
[DE85-014533] N86-10442
IGNITION
Solid surface combustion at reduced gravity N86-10159
Ignition and flame spread above liquid fuel pools N86-10163
Self-heating to ignition measurements and computation of critical size for solar energy collector materials
[DE85-011449] N86-10302
IGNITION SYSTEMS
Fundamental studies of droplet combustion at reduced gravity N86-10165
IGNITION TEMPERATURE
A fundamental study of smoldering with emphasis on experimental design for zero-g N86-10162
ILLUMINATING
Methods for developing jam-resistant security communications networks at fixed-site facilities
[DE85-012032] N86-10408
Passive and hybrid solar technologies program summary
[DE85-013100] N86-10648
IMAGE ANALYSIS
Satellite data even for a poultry farm. A development for Tanzania. Image evaluation following new ways N86-10182
LANDSAT TM image data quality analysis for energy-related applications
[E85-10109] N86-10597
Multisensor data integration techniques N86-10604
Analysis of edge detection algorithms on DIAL (Digital Image Analysis Laboratory)
[AD-A156735] N86-10630
IMAGE CORRELATORS
The OASIS correlator — Optical Aperture Synthesis in Space (OASIS) N86-11119
On line astronomical image processing using microcomputers N86-11121
IMAGE FURNACES
The mirror heating facility: Performance and experiences — Spacelab N86-10223
IMAGE PROCESSING
Real-time holography by stimulated Raman and Brillouin scattering N86-10479
Evaluation of metric camera images at the University of London — Spacelab N86-10495
Digital image processing of metric camera imagery — Spacelab N86-10511
Creation of Ground Control Points (GCP) library using ESA Spacelab metric camera imagery — ground control point (gcp) N86-10516
Automated analysis of digital images generated by two-dimensional gel electrophoresis
[DE85-011906] N86-10526
Remote sensing
[NOTA-1535] N86-10638
Applications for three-dimensional computer graphic cloud representations produced from satellite imagery
[AD-A156903] N86-10798
Arithmetic pipeline for image processing
[AD-D011773] N86-10800
Digital processing of images in tracking a moving object N86-10818
Always-convergent iterative noise removal and deconvolution for image data
[NASA-CR-176223] N86-10824
Test of a multilevel computational theory of stereoscopic visual image processing
[AD-A157011] N86-10870
Kalman filter preprocessor
[AD-D011774] N86-10972
Spatial frequency multiplexed coherent optical processor for calculating generalized moments
[AD-D011816] N86-10975
Fringe drift compensation in computer memory — Michelson interferometry N86-11112
Numerical experiments in image reconstruction — stellar interferometry N86-11116
On line astronomical image processing using microcomputers N86-11121
A modeling analysis program for the JPL table mountain lo sodium cloud
[NASA-CR-176241] N86-11139
IMAGE RECONSTRUCTION
Digital decoding of in-line holograms N86-10478
Real-time holography by stimulated Raman and Brillouin scattering N86-10479
Restitution of Spacelab photography by analog stereoplotter N86-10489
Problems in image reconstruction with optical arrays — spaceborne astronomy N86-11115
Numerical experiments in image reconstruction — stellar interferometry N86-11116
Radio astronomy experience in image reconstruction. A history lesson for optical astronomers N86-11117
COSMIC image reconstruction — Coherent Optical System of Modular Imaging Collectors (COSMIC) N86-11118
The OASIS correlator — Optical Aperture Synthesis in Space (OASIS) N86-11119
Imaging speckle interferometer in space: Digital simulations of image reconstruction and photon noise N86-11120
Aperture synthesis with or without phase information for kilometric arrays interpolation algorithms for stabilized image reconstruction N86-11124
IMAGE RESOLUTION
SAR image quality: A review
[DFVLR-MITT-85-07] N86-10413
Line mapping and resolution tests with metric camera data — Spacelab N86-10500
IMAGERY
Stereoscopic video imagery generation
[AD-D011785] N86-10481
IMAGES
Radar system description N86-10616
IMAGING TECHNIQUES
Digital decoding of in-line holograms N86-10478
The synthesis and analysis of color images
[NASA-TM-86844] N86-10777
Information technique 1985: Optical technology and electro-optics, a defense technical component review
[FOA-A-30037-E] N86-10980
Physical conditions in giant extragalactic H2 regions N86-11130
IMPACT LOADS
The mechanics of delamination in composite materials N86-10284
Fundamental studies of low velocity impact resistance of graphite fiber reinforced polymer matrix composites N86-10288
Explosive initiation by very small conical shaped charge jets
[DE85-009443] N86-10357
IMPACT RESISTANCE
Fundamental studies of low velocity impact resistance of graphite fiber reinforced polymer matrix composites N86-10288
IMPACT STRENGTH
Fabrication and metallurgical properties of modified 9Cr-1 Mo steel
[DE85-012885] N86-10328
IMPLOSIONS
Preliminary investigation of changes in X-ray multilayer optics subjected to high radiation flux
[DE85-014074] N86-10944
IMPURITIES
Surface tensions and their variations with temperature and impurities
[NASA ORDER H-27954B] N86-10115
Impurity extraction by droplets N86-10122
Investigation of metallic impurities introduced into SiO2 and silicon by various candidate VLSI metallization systems: Chemical reactions, diffusion, and electrical properties
[AD-A156609] N86-10429
IN-FLIGHT MONITORING
Partial in-flight calibration of the metric camera — Spacelab N86-10496
INCIDENCE
Angle of incidence effects for underwater shock using generic computational models
[DE85-012936] N86-10466
Angle of incidence effects for underwater shock using generic computational models, rev. 1
[DE85-012921] N86-10467
The effect of vegetation type, microrelief, and incidence angle on radar backscatter N86-10619
INCLUSIONS
Three-dimensional stress singularities in anisotropic materials and composites N86-10286
INCOMPRESSIBLE FLOW
A root-mean-square pressure fluctuations model for internal flow applications
[NASA-CR-3928] N86-10460
INDEPENDENT VARIABLES
The Liu, Katsaros, and Businger (1979) bulk atmospheric flux computational iteration program in FORTRAN and BASIC
[AD-A156736] N86-10714
INDEXES (DOCUMENTATION)
The 1984 bibliography of atomic and molecular processes
[DE85-010583] N86-10926
Advanced vehicle systems assessment. Volume 5: Appendices
[NASA-CR-176208] N86-11086
INDIA
Report of the Workshop on Geologic Applications of Remote Sensing to the Study of Sedimentary Basins
[E86-10002] N86-10599
Chronologic analysis of terrestrial sediments and basin evolution N86-10602
INDIUM ALLOYS
Directional solidification of monotectic and hypermonotectic aluminum-indium alloys under micron-g N86-10097
Space shuttle experiments on Al-In liquid phase miscibility gap (LPMG) alloys N86-10264
INDOOR AIR POLLUTION
Volatile organic compounds in indoor air: A survey of various structures
[PB85-198356] N86-10687
INDUCTANCE
Compact, low jitter, triggered spark gap
[DE85-012812] N86-10195
INDUCTORS
Overpulse railgun energy recovery circuit
[DE85-011607] N86-10197
INDUSTRIAL PLANTS
Identification of a plant's weighting sequence — self-tuning control
[OUEL-1534/84] N86-10854
INDUSTRIAL SAFETY
Effect of various doses of some vitamins on non-specific mechanisms of adaptation of man N86-10750
Report on the research activities on whole-body vibrations. Human strain due to mechanical vibrations
[ISBN-3-88383-107-7] N86-10773
Annotated bibliography of publications dealing with occupational health and medical information systems, cost analysis procedures, evaluation methodology and related legal issues
[AD-A156650] N86-11078
INDUSTRIAL WASTES
Membrane research in energy and solvent recovery from industrial effluent streams
[DE85-014583] N86-10682
INDUSTRIES
Research needs for corrosion control and prevention in energy conservation systems
[DE85-014852] N86-10326
Biotechnology: Science and practice N86-10742
INELASTIC SCATTERING
Polarization transfer in inelastic scattering and pionic models of the EMC effect
[DE85-010738] N86-10955
INELASTIC STRESS
Inelastic analysis of frame structures including member and joint shears N86-10573
Analysis of large, non-isothermal elastic-visco-plastic deformations
[NASA-CR-176220] N86-10588

INERTIAL CONFINEMENT FUSION
High efficiency heat transport and power conversion system for cascade
[DE85-012959] N86-10468
INERTIAL UPPER STAGE
Analytical investigation of solid rocket nozzle failure
[NASA-TM-86513] N86-10278
INFORMATION DISSEMINATION
Project VESTA, exploratory mission to the asteroids: Scientific objectives and technical specifications
[NASA-TM-77669] N86-10179
Solar thermal technical information guide
[DE85-002941] N86-10657
Publication of the Executive Office of the President, January 20, 1981 - December 31, 1984
[PB85-187110] N86-11082
INFORMATION FLOW
Editors rattle space N86-10586
INFORMATION RETRIEVAL
Publication of the Executive Office of the President, January 20, 1981 - December 31, 1984
[PB85-187110] N86-11082
INFORMATION SYSTEMS
Development of IS2100: An information systems laboratory
[AD-A156848] N86-10797
Annotated bibliography of publications dealing with occupational health and medical information systems, cost analysis procedures, evaluation methodology and related legal issues
[AD-A156650] N86-11078
Publication of the Executive Office of the President, January 20, 1981 - December 31, 1984
[PB85-187110] N86-11082
INFRARED ASTRONOMY
Optical/IR telescope arrays: A study of their potential for satisfying observational requirements in astronomy for a large aperture system in the 1990s and beyond
[REPT-15] N86-11094
High angular resolution in the infrared: Prospects for space observations N86-11100
The DUO: Far infrared heterodyne concept for space interferometry N86-11125
INFRARED DETECTORS
Sensor system
[AD-D011767] N86-10480
INFRARED IMAGERY
Infrared system with computerized image display
[AD-D011777] N86-10906
INFRARED PHOTOGRAPHY
Neogene compressional deformation and possible thrust faulting in southwest Dominican Republic N86-10618
INFRARED SCANNERS
Infrared system with computerized image display
[AD-D011777] N86-10906
INFRARED SPECTROPHOTOMETERS
Fuel and lubricant behavior in boundary layers analyzed by infrared emission Fourier transform spectrometry N86-10336
INFRARED SPECTROSCOPY
Theoretical comparison of classical (K-matrix) and inverse (P-matrix) least-squares methods for quantitative infrared spectroscopy
[DE85-012827] N86-10298
INHOMOGENEITY
Mechanics of coated fiber composites N86-10285
INITIATION
Explosive initiation by very small conical shaped charge jets
[DE85-009443] N86-10357
INLET PRESSURE
Effect of a shear layer on the stability of an axisymmetrical external compression air intake N86-10010
INPUT
Signal analysis of gas tungsten arc welds N86-10078
Phase-coded pulse expander-compressor
[AD-D011812] N86-10375
INPUT/OUTPUT ROUTINES
Design of a multifunction Input-Output (I/O) controller
[EUT-84-E-143] N86-10802
Realization of a multifunction Input/Output (I/O) controller by means of a gate array
[EUT-85-E-147] N86-10804
The local disk controller
[REPT-1-68430-44(1985)01] N86-10806
Performance analysis of the IBM Direct Access Storage Device (DASD) subsystem, and some suggestions for improved systems
[REPT-1-68430-44(1985)02] N86-10807
INSECTS
A fundamental study of the sticking of insect residues to aircraft wings
[NASA-CR-176231] N86-10033
INSPECTION
Nondestructive control of thick structures made without disassembling
[PV-43-954/F/3] N86-10564
INSTRUMENT TRANSFORMERS
High voltage instrument transformers for outdoor service with an insulation of low pressure SF6 gas and plastic foils
[BMFT-FB-T-85-034] N86-10449
INSULATION
Transient velocity assessment in gallium arsenide, and of other GaAs characteristics related to device functions
[AD-A156983] N86-11050
INSULATORS
Thermodynamic constraints on ion beam mixing of metals on insulators
[DE85-013628] N86-10448
INTEGRALS
The use of new path indepedent integrals in elastic-plastic and creep fracture N86-10574
A study of methods to predict and measure the transmission of sound through the walls of light aircraft. Integration of certain singular boundary element integrals for applications in linear acoustics
[NASA-CR-176229] N86-10912
INTEGRATED CIRCUITS
Investigation of metallic impurities introduced into SiO2 and silicon by various candidate VLSI metallization systems: Chemical reactions, diffusion, and electrical properties
[AD-A156609] N86-10429
Efficient systolic arrays for the solution of toeplitz systems: An illustration of a methodology for the construction of systolic architectures in VLSI (Very Large Systems Integration)
[AD-A156767] N86-10795
COMPACT: Compaction of hierarchial chip layouts based on a constraint graph method with double-sided constraints N86-10845
Transient velocity assessment in gallium arsenide, and of other GaAs characteristics related to device functions
[AD-A156983] N86-11050
INTERATOMIC FORCES
Non-empirical interatomic potentials for transition metals
[DE85-013448] N86-10440
INTERFACE STABILITY
Mephisto: Interfacial destabilization in metal alloys N86-10079
Dendritic solidification in a binary alloy melt: Steady-state versus morphological stability theories N86-10261
INTERFACES
Thermodynamic constraints on ion beam mixing of metals on insulators
[DE85-013628] N86-10448
Design sensitivity analysis and optimization of built-up structures N86-10565
Parallel local interface bus
[AD-D011742] N86-10792
LANES 1 Users' Guide
[NASA-CR-177334] N86-10819
User interface enhancement report
[NASA-CR-171898] N86-10820
System integration report
[NASA-CR-171900] N86-10821
INTERFACIAL TENSION
Theoretical studies of the surface tension of liquid metal system N86-10101
Suppression of Marangoni convection in float zones N86-10111
Surface tensions and their variations with temperature and impurities
[NASA ORDER H-27954B] N86-10115
Surface tension induced instabilities in reduced gravity: The Benard problem N86-10117
Surface-tension driven convection N86-10124
Thermocapillary motion research N86-10125
Thermocapillary and diffusocapillary migration of a fluid drop N86-10128
Cell partition in two polymer aqueous phases N86-10136
The influence of thermocapillarity on the migration of droplets in a liquid possessing a uniform temperature gradient N86-10237
Rayleigh-Benard instability in systems presenting a minimum in surface tension N86-10245
Surface forces in contacting solids --- microgravity rocket experiment N86-10252
INTERFEROMETERS
Imaging speckle interferometer in space: Digital simulations of image reconstruction and photon noise N86-11120
INTERFEROMETRY
Experimental and theoretical studies of wetting and multilayer adsorption
[NASA ORDER H-27954B] N86-10121
Signal analysis receiver with acousto-optic delay lines
[AD-D011761] N86-10427
Velocities of gas and plasmas from real time holographic interograms
[DE85-014618] N86-10530
NASA/JPL Aircraft SAR Workshop Proceedings
[NASA-CR-176204] N86-10615
Topographic mapping from interferometric synthetic aperture radar observations N86-10622
Imaging speckle interferometer in space: Digital simulations of image reconstruction and photon noise N86-11120
INTERGALACTIC MEDIA
Extragalactic observations with optical space arrays N86-11098
INTERMETALLICS
Metallurgy and metallography of braze joints
[DE85-014563] N86-10325
INTERMODULATION
Rusty bolt intermodulation interference reducer
[AD-D011748] N86-10313
Apparatus for locating passive intermodulation interference sources
[AD-D011798] N86-10435
INTERNAL COMBUSTION ENGINES
Modeling of engine sprays
[DE85-010020] N86-10559
INTERNAL FRICTION
Initial increase, peaking effect, in the internal friction of copper following pulsed neutron and electron irradiation
[DE85-012767] N86-10932
INTERNAL PRESSURE
Acoustic cavitation and bubble dynamics
[AD-A156888] N86-10918
INTERNATIONAL COOPERATION
Project VESTA, exploratory mission to the asteroids: Scientific objectives and technical specifications
[NASA-TM-77669] N86-10179
INTERPOLATION
The interpolation of signals sampled at less than the Nyquist rate N86-10368
A numerical method for approximating antenna surfaces defined by discrete surface points
[NASA-TM-87125] N86-10381
A sequential decoding performance analysis for International Comet Explorer N86-10390
Aperture synthesis with or without phase information for kilometric arrays interpolation algorithms for stabilized image reconstruction N86-11124
INTERSTELLAR GAS
A superconducting tunnel junction receiver for millimeter-wave astronomy N86-11041
INVERSE SCATTERING
Renormalization of an inverse scattering theory for inhomogeneous dielectrics
[AD-A156636] N86-11049
INVERSIONS
Well-posed questions and exploration of the space of parameters in linear and non linear inversion
[PN-84/13] N86-10858
INVISCID FLOW
Three-dimensional inviscid analysis of radial turbine flow and a limited comparison with experimental data
[NASA-TM-87091] N86-10017
Inviscid flow field analysis of maneuvering hypersonic vehicles using the SCM formulation and parabolic grid generation
[DE85-013950] N86-10021
IO
A modeling analysis program for the JPL table mountain Io sodium cloud
[NASA-CR-176241] N86-11139
IODIDES
Parallel pulse processing for mercuric iodide gamma-ray detectors
[DE85-013391] N86-10528
ION ACCELERATORS
Microwave instability across the transition energy
[DE85-013304] N86-11010
Tracking studies on the effects of magnet multipoles on the aperture of the RHIC heavy ion collider
[DE85-013282] N86-11023
ION BEAMS
Simulating the CTR environment in the HVBM
[DE85-011745] N86-10193
RFQ-funneling
[DE85-012483] N86-10194
Thermodynamic constraints on ion beam mixing of metals on insulators
[DE85-013628] N86-10448

Supersonic metal cluster beams
[DE85-014321] N86-10966
Treatment planning with ion beams
[DE85-012661] N86-10990

ION IMPLANTATION
Metastable phase formation in Ni-implanted Al: An analytical electron microscope investigation
[DE85-009105] N86-10331

ION IRRADIATION
Boronising of iron and steel by ionic bombardment by diborane
[BLL-BISI-TRANS-23034-(9022.06)] N86-10307
Thermodynamic constraints on ion beam mixing of metals on insulators
[DE85-013528] N86-10448

ION MOTION
The measurement and application of transport properties of ion swarms in gases N86-10370

ION PROPULSION
Rapid evaluation of ion thruster lifetime using optical emission spectroscopy
[NASA-TM-87103] N86-10280

ION RECOMBINATION
Electron-ion recombination studies of planetary ionospheric and astrophysical ions N86-11132

ION SOURCES
AGS polarized H(-) source
[DE85-013296] N86-10935
Report on the engineering test of the LBL 30 second neutral beam source for the MFTF-B project
[DE85-013317] N86-10962
Performance of the H(-) ion source for the intense pulsed neutron source
[DE85-012368] N86-10991
Ion sources for high-frequency accelerators
[DE85-012992] N86-11006

ION STORAGE
Cooled ion frequency standard
[AD-A156813] N86-10295

IONIC COLLISIONS
The measurement and application of transport properties of ion swarms in gases N86-10370
Charge exchange in slow collisions of atoms and molecules N86-10922
Angular distribution of neutral hydrogen following collisional electron detachment from H(-)
[DE85-014258] N86-10943

IONIC MOBILITY
Electrohydrodynamics N86-10130
The measurement and application of transport properties of ion swarms in gases N86-10370

IONIZING RADIATION
Criteria for the design or selection of a bioelectromagnetics experiment
[AD-A156575] N86-10420

IONOSPHERE
Comparison of the calibration of ionospheric delay in VLBI data by the methods of dual frequency and Faraday rotation N86-10384
Potential structures and particle acceleration on auroral field lines
[AD-A156694] N86-10708
Activities report in geophysics
[KGI-188] N86-10709
Electron-ion recombination studies of planetary ionospheric and astrophysical ions N86-11132

IONS
Laser Raman spectroscopy study of the zinc and bromide ion complex equilibrium in zinc/bromine battery electrolytes
[DE85-011820] N86-10301
Extraction of lanthanide ions by 2-methyl-8-quinolinol
[DE85-014277] N86-10303
Potential structures and particle acceleration on auroral field lines
[AD-A156694] N86-10708
Theoretical investigation of electron-positive ion-atom interactions
[DE85-013019] N86-10939

IRAN
A geological structural analysis of the southeastern Zagros (Iran) ranges based on metric camera photos N86-10492
Tectonic analysis of typical fold structures in the Zagros Mountains (Iran) by the application of quantitative photogrammetric methods on metric camera data --- Spacelab N86-10521

IRIDIUM
General-purpose heat source development: Safety Verification Test Program. Bullet/fragment test series
[DE85-014262] N86-10660

IRISES (MECHANICAL APERTURES)
Direct-coupled cavity filters with irises of arbitrary thickness
[DFVLR-FB-85-14] N86-10412

IRON
Control of cast iron microstructure N86-10084
Study of the reactive-element effect in oxidation of Fe-Cr alloys using transverse section analytical electron microscopy N86-10087
Graphite formation in cast iron N86-10100
The mechanism of erosion of metallic materials under cavitation attack
[NASA-TM-87133] N86-10552
Advanced fuel cell development
[DE85-014550] N86-10659
Kinetics of biological ferrous iron oxidation
[DE85-014616] N86-10736
Methane-bubble formation in hydrogen-charged Fe-30 ppM C
[DE85-012526] N86-10937

IRON ALLOYS
Unidirectional solidification of cast iron: Experiment ES-325 --- Spacelab N86-10212
Skin casting of alloys and composites: Results of Spacelab (SL)-1 and TEXUS experiments N86-10213
Electronic and magnetic properties of noble-metal and transition-metal alloys, interfaces and overlayers
[DE85-014532] N86-10321

IRRADIATION
Swelling and tensile properties of EBR-2-irradiated tantalum alloys for space reactor applications
[DE85-012887] N86-10329
Approaches to quantitative expression of dose response
[DE85-013498] N86-10772
Initial increase, peaking effect, in the internal friction of copper following pulsed neutron and electron irradiation
[DE85-012767] N86-10932

IRRIGATION
On the use of L-band multipolarization airborne SAR for surveys of crops, vineyards, and orchards in a California irrigated agricultural region N86-10627

ISLANDS
Analysis of remote sensing data N86-10605

ISOCHORIC PROCESSES
Isochoric specific heat of sulfur hexafluoride at the critical point. A Spacelab experiment for the German D1-mission in 1985 N86-10251

ISOTHERMAL PROCESSES
The isothermal heating facility --- Spacelab N86-10208

ISOTOPE SEPARATION
Beam line windows at LAMPF
[DE85-012723] N86-10985

ISOTROPIC MEDIA
Stiffened and prestressed composite overwrapped pressure vessels N86-10547
Constitutive modeling for isotropic materials (HOST)
[NASA-CR-174980] N86-10589

ITERATION
Second order approximation method for transonic flows over swept wings N86-10002
Determining a physically appropriate neutron spectrum from multisphere data
[DE85-013045] N86-10299

ITERATIVE SOLUTION
Improved mapping of radio sources from VLBI data by least-square fit N86-10402
A study of Morrison's iterative noise removal method
[NASA-CR-176222] N86-10823
Always-convergent iterative noise removal and deconvolution for image data
[NASA-CR-176223] N86-10824

J

J INTEGRAL
Application of the unloading compliance methods in fracture toughness measurements of a quenched and tempered steel
[BLL-BISI-TRANS-21628-(9022.06)] N86-10308

JAMMING
Methods for developing jam-resistant security communications networks at fixed-site facilities
[DE85-012032] N86-10408

JET AIRCRAFT NOISE
Summary of work on jet noise prediction
[ESDU-BR-62636] N86-10909

JET BOUNDARIES
On the method of characteristics and its application to the calculations of annular nozzle flowfields N86-10454

JET ENGINE FUELS
Method for determining elemental sulfur in jet fuel --- differential pulse polarography
[FOA-C-40211-B4] N86-10360

JET ENGINES
Retrofit of SAC EC-135C and RC-135 aircraft with CFM-56 engines
[AD-A156688] N86-10038
The Shock and Vibration Digest, volume 17, no. 3
[AD-A154144] N86-10585

JET FLOW
Buoyancy effects upon vapor flame and explosion processes N86-10161
Confined swirling jet predictions using a multiple-scale turbulence model
[NASA-CR-178484] N86-10462

JET MIXING FLOW
Summary of work on jet noise prediction
[ESDU-BR-62636] N86-10909

JET THRUST
Experimental performance of a 1-kilowatt arcjet thruster
[NASA-TM-87131] N86-10281

JOINTS (JUNCTIONS)
Metallurgy and metallography of braze joints
[DE85-014563] N86-10325
Inelastic analysis of frame structures including member and joint shears N86-10573
Improved stud configurations for attaching laminated wood wind turbine blades
[NASA-TM-87109] N86-10582
Fundamental study of the closure property of joints N86-10698

JOURNAL BEARINGS
Theoretical modeling of the vapor cavitation in dynamically loaded journal bearings
[NASA-TM-87076] N86-10463

JP-5 JET FUEL
Evaluation of the 90-day inhalation toxicity of petroleum and oil shale JP-5 jet fuel
[AD-A156815] N86-10675

JUPITER ATMOSPHERE
Galileo: Exploration of Jupiter's system
[NASA-SP-479] N86-11137

K

KALMAN FILTERS
Comment on Determination of Aerodynamic Coefficients for a Reentry Body by Means of the Kalman Filter Method N86-10011
SARSAT LUC (Local user terminal) to CMCC (Canadian Mission Control Centre) alert data interface: A critical review
[AD-A156881] N86-10276
Kalman filter preprocessor
[AD-D011774] N86-10972

KAONS
Separated K(-) beams (10 GeV and above)
[DE85-012527] N86-10989

KEVLAR (TRADEMARK)
Fatigue of graphite/epoxy buffer strip panels with center cracks
[NASA-TM-87595] N86-10581

KIDNEYS
Biochemical assays of cultured cells N86-10134
Kidney cell electrophoresis N86-10145

KINEMATICS
Design sensitivity analysis and optimization of built-up structures N86-10585
Analysis of large, non-isothermal elastic-visco-plastic deformations
[NASA-CR-176220] N86-10588
The two micron spectrum of R Scuti N86-11092

KINETIC ENERGY
The effects of orography on land-atmosphere turbulent exchange processes N86-10702
The development of a neutron evaporation theory code for the thermal fission of Uranium-235
[AD-A156593] N86-10951
Dynamics of imploding neon gas puff plasmas. 1
[AD-A156916] N86-10983

KINETIC FRICTION
Steady state frictional behavior of thin film coatings N86-10335

KINETICS
Environmental degradation of materials: Surface chemistry related to stress corrosion cracking N86-10099
Colloidal oxide properties and kinetic studies N86-10147
Crystallization, optical and chemical properties of fluoride glasses N86-10149
Glass formation in reluctant glass formers N86-10151
Kinetics of spreading of liquids in microgravity: Experiment 1 ES 327 --- Spacelab N86-10207

Rapid evaluation of ion thruster lifetime using optical emission spectroscopy
[NASA-TM-87103] N86-10280
Type of new Chinese-produced high-speed camera and its utilization in detonation physics experiments
[DE85-015191] N86-10529
Chemical kinetics and photochemical data for use in stratospheric modeling
[NASA-CR-176198] N86-10707

KLYSTRONS
An experimental TE sub 12 - TE sub 11 circular waveguide mode converter N86-10387
Klystron control software in the SIC
[DE85-013068] N86-10836
The MEA vacuum system
[LINO-120] N86-10968
High-power rf controls for the NBS-Los Alamos racetrack microtron
[DE85-012658] N86-10993

KNEE (ANATOMY)
A graphic anthropometric aid for seating and workplace design
[AD-A156988] N86-10788

KORTEWEG-DEVRIES EQUATION
A modified modified Korteweg-deVries equation
[PN-84/27] N86-10859

KRYPTON
Thermodynamic constraints on ion beam mixing of metals on insulators
[DE85-013628] N86-10448

L

LABORATORIES
Microgravity Materials Science Laboratory N86-10173
Laboratory experiments of heat pump dynamic losses
[DE85-013931] N86-10473
Secondary standards laboratories for ionizing radiation calibrations: The national laboratory interests
[DE85-007046] N86-10938

LABORATORY EQUIPMENT
Continuous fiberization of silicon-carbide-nitride precursor resin N86-10168
The fluid physics module: A technical description — Spacelab N86-10201
The isothermal heating facility — Spacelab N86-10208
The mirror heating facility: Performance and experiences — Spacelab N86-10223
Experimental facility for materials research in space (CSK-1) N86-10263

LAKES
Examples of regional environmental assessment using acid deposition data
[DE85-012903] N86-10677

LAMELLA (METALLURGY)
Study of eutectic formation N86-10070

LAMINAR FLOW
Measurements of the critical Marangoni number of the laminar-oscillatory transition of thermocapillary convection in floating zones N86-10242

LAMINATES
Three-dimensional stress singularities in anisotropic materials and composites N86-10286
Ultrasonic evaluation of mechanical properties of thick, multilayered, filament wound composites
[MASA-TM-87088] N86-10561

LAND
The effects of orography on land-atmosphere turbulent exchange processes N86-10702

LAND MANAGEMENT
Land evaluation successes with the metric camera — Spacelab N86-10512

LAND USE
Thematic investigations in France based on metric camera imagery — Spacelab N86-10509
Thematic mapping of metric camera color infrared and black and white photographs for land use classification N86-10510
Approaches to cumulative impact assessment
[DE85-013891] N86-10635

LANDAU DAMPING
Microwave instability across the transition energy
[DE85-013304] N86-11010

LANDFORMS
Altitudinal distribution of granitic landforms in the south central Sierra Nevada, California N86-10695

LANDSAT SATELLITES
The effects of merging TM and A/C radar on wetland classification N86-10621
Lithologic mapping in a sedimentary environment using multipolarization SAR images N86-10624

LANGUAGES
Special purpose hardware architectures for language recognition
[AD-A156634] N86-10793

LANTHANUM
Extraction of lanthanide ions by 2-methyl-8-quinolinol
[DE85-014277] N86-10303

LARGE SPACE STRUCTURES
Passive damping concepts for slender columns in space structures
[NASA-CR-176234] N86-10577

LASER ANNEALING
W-shaped diffused stripe GaAs/AlGaAs laser
[AD-D011818] N86-10538

LASER APPLICATIONS
Containerless high temperature property measurements by atomic fluorescence N86-10092
Scaling studies of solar pumped lasers
[NASA-CR-176240] N86-10540
Information technique 1985: Optical technology and electro-optics, a defense technical component review
[FOA-A-30037-E] N86-10980

LASER DOPPLER VELOCIMETERS
Velocities of gas and plasmas from real time holographic interograms
[DE85-014618] N86-10530

LASER HEATING
Modelling of laser-enhanced chemical vapor deposition N86-10105
Characterization of vapor and aerosol flows by photothermal methods
[AD-A156601] N86-10465

LASER INTERFEROMETRY
Optical detection of photoacoustic pulses in thin silicon wafers
[AD-A156705] N86-10977

LASER MATERIALS
Device for cryogenically fabricating source material for plasma X-ray lasers
[AD-D011814] N86-10537

LASER OUTPUTS
Laser generation and transport of a relativistic electron beam
[DE85-011709] N86-10192
Laser Raman spectroscopy study of the zinc and bromide ion complex equilibrium in zinc/bromine battery electrolytes
[DE85-011820] N86-10301
Contact effects in light activated GaAs switches
[AD-A156957] N86-10434
Laser target speckle eliminator
[AD-D011775] N86-10536
Research on solar pumped liquid lasers
[NASA-CR-176235] N86-10539
Scaling studies of solar pumped lasers
[NASA-CR-176240] N86-10540
Multiple site laser excited pollution monitoring system
[AD-D011769] N86-10674

LASER PUMPING
Device for cryogenically fabricating source material for plasma X-ray lasers
[AD-D011814] N86-10537
Research on solar pumped liquid lasers
[NASA-CR-176235] N86-10539

LASER TARGET INTERACTIONS
Laser target speckle eliminator
[AD-D011775] N86-10536

LASING
Research on solar pumped liquid lasers
[NASA-CR-176235] N86-10539

LATCHES
Over-center toggle latch
[AD-D011753] N86-10556

LATERAL CONTROL
Car driving as a supervisory control task
[B8563351] N86-10776

LATEX
Production of large-particle-size monodisperse latexes in microgravity N86-10146

LATITUDE
Capacity for work and hemodynamics in males residing at middle and high latitudes N86-10747

LATTICES (MATHEMATICS)
On the analytical evaluation of the partition function for unit hypercubes in four dimensions — lattice theory
[NIKHEF-H/84-12] N86-10882
Variational estimates for the mass gap of SU(2) Euclidean lattice gauge theory
[NIKHEF-H/84-13] N86-10883

LAVA
Age-dating volcanic and alluvial surfaces with multipolarization data N86-10620

LAW (JURISPRUDENCE)
Annotated bibliography of publications dealing with occupational health and medical information systems, cost analysis procedures, evaluation methodology and related legal issues
[AD-A156850] N86-11078

LAYOUTS
COMPACT: Compaction of hierarchial chip layouts based on a constraint graph method with double-sided constraints N86-10845

LEAD (METAL)
Diffusion in immiscible melts N86-10096

LEAD ALLOYS
Particle coarsening in immiscible zinc-lead alloys under microgravity — Spacelab N86-10210
Cellular morphologies in lead-thallium alloys — gravitational effects N86-10262

LEAD OXIDES
Thermal expansion of glasses in the solid and liquid phases
[DE85-013953] N86-10351

LEAD TELLURIDES
Lead telluride crystals grown in microgravity: Experiment ES 318 — Spacelab N86-10220

LEADING EDGES
Three articles on new calculation methods in aeronautics (selected articles)
[AD-A145745] N86-10007
Numerical solution of hypersonic flow near leading edge of a flat plate N86-10008

LEAKAGE
Liquid to gas leak ratios with liquid nitrogen and liquid helium
[DE85-012950] N86-11030

LEARNING
NASA/American Society for Engineering Education (ASEE) Summer Faculty Fellowship Program, 1985
[NASA-CR-177972] N86-11064

LEAST SQUARES METHOD
Theoretical comparison of classical (K-matrix) and inverse (P-matrix) least-squares methods for quantitative infrared spectroscopy
[DE85-012827] N86-10298
Improved mapping of radio sources from VLBI data by least-square fit N86-10402
Radome analysis and design capabilities of the RF and Microwave Technology Branch
[AD-A156662] N86-10404
Rank revealing QR-Factorizations
[AD-A156756] N86-10887
The power of weighted and ordinary least squares with estimated unequal variances in experimental design
[B8562446] N86-10894
Regression analysis: Assumptions, alternatives, applications N86-10895

LEGENDRE FUNCTIONS
The h, p and h-p versions of the finite element method in dimension. Part 1: The error analysis of the p-version
[AD-A156600] N86-10862

LENSES
Time resolved flow velocity and concentration measurements using a travelling thermal lens
[AD-A156706] N86-10541

LEVITATION
Measurement of high temperature thermophysical properties N86-10074
Undercooling, remelting, and coarsening N86-10080
Role of convection in grain refining N86-10133
Modification of the electromagnetic levitator (EML) hardware N86-10172

LEVITATION MELTING
Multimode acoustic research N86-10167
Levitating furnance for containerless processing in space N86-10169
Containerless undercooling of Ni N86-10260

LIBRARIES
A systems development life cycle study of the information center
[AD-A156977] N86-11079

LIE GROUPS
Lie algebraic methods for charged particle beams and light optics N86-10970

LIFE (DURABILITY)
Compatibility of grain-stabilized platinum with candidate propellants for resistojets
[NASA-TM-87118] N86-10279
High temperature properties and characterization of S3-N4 materials
[BMFT-FB-T-85-046] N86-10352

LIFE CYCLE COSTS
Advanced vehicle systems assessment. Volume 3: Systems assessment
[NASA-CR-176206] N86-11084

LIFE SCIENCES
Life sciences research on the space station: An introduction
[NASA-TM-86836] N86-10734
USSR report: Life sciences. Biomedical and behavioral sciences
[JPRS-UBB-85-023] N86-10738
LIFT AUGMENTATION
Aerodynamics of hyperlift systems
[SNIAS-443.501/85] N86-10023
Analysis of hyperlift systems. Study of a singularities method
[SNIAS-443.529/84] N86-10024
LIFT DEVICES
Aerodynamics of hyperlift systems
[SNIAS-443.501/85] N86-10023
Analysis of hyperlift systems. Study of a singularities method
[SNIAS-443.529/84] N86-10024
LIGANDS
Cell partition in two polymer aqueous phases N86-10139
LIGHT (VISIBLE RADIATION)
Optical/IR telescope arrays: A study of their potential for satisfying observational requirements in astronomy for a large aperture system in the 1990s and beyond
[REPT-15] N86-11094
LIGHT EMISSION
Photonic diagnostics and pulsed power research
[DE85-013752] N86-10940
LIGHT MODULATION
Extended precision in video bandwidth analog to digital converter using optical techniques
[AD-D011745] N86-10422
LIGHT SCATTERING
Light scattering tests of fundamental theories of transport properties in the critical region N86-10113
A study of the applicability of nucleation theory to quasi-thermodynamic transformations of second and higher Ehrenfest-order
[NASA-CR-176230] N86-11060
LIGHTNING
Electromagnetic resonances of cylinders and aircraft model with resistive wires
[NASA-CR-176250] N86-10042
Simulated direct-strike lightning testing at Sandia National Laboratories
[DE85-012033] N86-10049
LIMBS (ANATOMY)
Heat transfer mechanism in human extremities N86-10759
LINE OF SIGHT
Mild hypoxia and visual performance with night vision goggles
[AD-A156969] N86-10787
LINEAR ACCELERATORS
RFQ-funneling
[DE85-012483] N86-10194
Klystron control software in the SIC
[DE85-013068] N86-10836
High-brightness photoemitter injector for electron accelerators
[DE85-012673] N86-10929
Beam-cavity interaction measurements in a DAW structure
[DE85-012660] N86-10987
Radiation field results from the SPEED triaxiode, a large area, high dose rate, short pulse 1MV bremsstrahlung source
[DE85-009438] N86-11005
High-resolution phosphor screen beam profile monitor
[DE85-013074] N86-11012
Beam steering in the SLC linac
[DE85-013370] N86-11025
Programmable delay unit incorporating a semi-custom integrated circuit
[DE85-013379] N86-11033
LINEAR EQUATIONS
Well-posed questions and exploration of the space of parameters in linear and non linear inversion
[PN-84/13] N86-10858
LINEAR FILTERS
Always-convergent iterative noise removal and deconvolution for image data
[NASA-CR-176223] N86-10824
LINEAR INTEGRATED CIRCUITS
Microcircuit device reliability field experience database. Volume 1. Field data. Volume 2. Failure Event/Analysis data
[AD-A156836] N86-10433
LINEAR SYSTEMS
Digital decoding of in-line holograms N86-10478
On the lanczos method for solving symmetric linear systems with several right-hand-sides
[AD-A156816] N86-10868
Multivariable partial realization and the aspect of uniqueness
[ER-83/09] N86-10879
Naive approximate realization of noisy data
[ER-83/10] N86-10880
LINEARITY
Finite deformation crack-line fields in a thin elasto-plastic sheet
[AD-A156757] N86-10346
Determination of symmetry and phase in human visual response functions: Theory and experiments N86-10769
LINEARIZATION
A study of methods to predict and measure the transmission of sound through the walls of light aircraft. Integration of certain singular boundary element integrals for applications in linear acoustics
[NASA-CR-176229] N86-10912
LININGS
Explosive initiation by very small conical shaped charge jets
[DE85-009443] N86-10357
LIPSCHITZ CONDITION
Poisson semigroups and singular integrals
[CTH-MATH-1985-05] N86-10876
LIQUID COOLING
Renovated cooling at PIMU
[LINO-122] N86-10452
LIQUID CRYSTALS
Liquid crystal non-destructive inspection of metals
[AD-D011772] N86-10316
LIQUID FLOW
Capillary forces in a low gravity environment --- Spacelab N86-10202
Some results of the Marangoni free convection experiment --- Spacelab N86-10203
Oscillations of semi-free liquids in microgravity: Spacelab 1 experiment ES 326 N86-10204
Kinetics of spreading of liquids in microgravity: Experiment 1 ES 327 --- Spacelab N86-10207
The influence of thermocapillarity on the migration of droplets in a liquid possessing a uniform temperature gradient N86-10237
Liquids and interfaces --- Spacelab N86-10268
LIQUID FUELS
Ignition and flame spread above liquid fuel pools N86-10163
LIQUID HELIUM
Liquid to gas leak ratios with liquid nitrogen and liquid helium
[DE85-012950] N86-11030
An investigation of vortex dynamics in 2-dimensional superfluid films of helium-4 N86-11040
Critical dynamics in superfluid helium N86-11046
LIQUID LASERS
Research on solar pumped liquid lasers
[NASA-CR-176235] N86-10539
LIQUID METAL FAST BREEDER REACTORS
Scoping studies of vapor behavior during a severe accident in a metal-fueling reactor
[DE85-011474] N86-10952
LIQUID METALS
Undercooling, remelting, and coarsening N86-10080
Measurement of the properties of tungsten at high temperatures N86-10091
Theoretical studies of the surface tension of liquid metal system N86-10101
Multimode acoustic research N86-10167
Development of a sheath for sensor protection in molten steel applications
[AD-A156764] N86-10315
LIQUID NITROGEN
Liquid to gas leak ratios with liquid nitrogen and liquid helium
[DE85-012950] N86-11030
LIQUID PHASE EPITAXY
Processing of complex compound semiconductors in space N86-10054
LIQUID PHASES
Mephisto: Interfacial destabilization in metal alloys N86-10079
Liquid phase miscibility gap materials N86-10081
Diffusion in immiscible melts N86-10096
Verification of turbulence developing from the oscillatory Marangoni convection in a liquid column --- rocket flight N86-10241
Space shuttle experiments on Al-In liquid phase miscibility gap (LPMG) alloys N86-10264
First Spacelab Payload (FSLP) experiments on composite materials N86-10265
Thermal expansion of glasses in the solid and liquid phases
[DE85-013953] N86-10351
LIQUID SURFACES
Free surface phenomena under low- and zero-gravity conditions N86-10108
Suppression of Marangoni convection in float zones N86-10111
Axisymmetric free surface behavior of moving liquid in a cylinder in microgravity --- Spacelab N86-10206
LIQUID-LIQUID INTERFACES
The influence of thermocapillarity on the migration of droplets in a liquid possessing a uniform temperature gradient N86-10237
Rationale for two phase polymer system microgravity separation experiments N86-10247
Application of the theory of Ostwald ripening to microgravity phase separation experiments N86-10248
LIQUID-SOLID INTERFACES
Liquid phase miscibility gap materials N86-10081
Influence of melt convection on solid-liquid interface under terrestrial and reduced gravity environments N86-10083
The development and prevention of channel segregation during alloy solidification N86-10086
Thermal and solutal convection damping using an applied magnetic field N86-10094
Liquid column stability: Experiment 1 ES-331 --- Spacelab N86-10205
Stability of long liquid columns N86-10244
LIQUID-VAPOR INTERFACES
Experimental and theoretical studies of wetting and multilayer adsorption
[NASA ORDER H-27954B] N86-10121
Impurity extraction by droplets N86-10122
Holographic interferometry near gas/liquid critical points: Ground-based study of a D1 experiment --- Spacelab N86-10249
LIQUIDS
Dynamic thermophysical measurements in space
[NASA ORDER H-27954-B] N86-10106
Mass transport phenomena between bubbles and dissolved gases in liquids under reduced gravity conditions N86-10110
Light scattering tests of fundamental theories of transport properties in the critical region N86-10113
Surface tensions and their variations with temperature and impurities
[NASA ORDER H-27954B] N86-10115
Acoustic cavitation and bubble dynamics
[AD-A156888] N86-10918
LITHIUM
Advanced fuel cell development
[DE85-014550] N86-10659
LITHIUM OXIDES
Thermal expansion of glasses in the solid and liquid phases
[DE85-013953] N86-10351
High efficiency heat transport and power conversion system for cascade
[DE85-012959] N86-10468
LITHOLOGY
Remote stratigraphic and structural analysis: Multisensor results in the Wind River/Bighorn Basin area, Wyoming N86-10606
Lithologic mapping in a sedimentary environment using multipolarization SAR images N86-10624
Geologic evaluation and reservoir properties of the PR Spring tar sand deposit, Uintah and Grand Counties, Utah
[DE85-013248] N86-10634
LITHOSPHERE
Stratigraphy, petrology, depositional and post-depositional histories and their effects upon reservoir properties of the Parkman Formation of the Mesa Verde group, Powder River Basin, Wyoming N86-10691
Paleontology and stratigraphy of Lower Cambrian and upper Proterozoic sediments, Caborca region, northwestern Sonora, Mexico N86-10692
Geothermal influences on the long-term thickness of the mechanical lithosphere during flexure N86-10697
LOAD DISTRIBUTION (FORCES)
Stiffened and prestressed composite overwrapped pressure vessels N86-10547
LOADS (FORCES)
Mechanics of coated fiber composites N86-10285
Application of the unloading compliance methods in fracture toughness measurements of a quenched and tempered steel
[BLL-BISI-TRANS-21628-(9022.06)] N86-10308
Load-deflection tests and computer analyses of a high-precision adhesive-bonded antenna reflector panel N86-10389
Termination load carrying device
[AD-D011800] N86-10558
Strength of shells under local transverse loads N86-10568
Optimal design of portal frames against buckling N86-10572
Effect of sequence of loading on interaction curves for buckling of stiffened shells
[TAE-536] N86-10583

LOGARITHMS
Arithmetic pipeline for image processing
[AD-D011773] N86-10800
LOGIC CIRCUITS
Minimization of programmable logic arrays
[EUT-84-E-145] N86-10803
A course on field programmable logic
[EUT-85-E-148] N86-10805
LOGIC DESIGN
Realization of a multifunction Input/Output (I/O) controller by means of a gate array
[EUT-85-E-147] N86-10804
A course on field programmable logic
[EUT-85-E-148] N86-10805
Compexity of higher-order programs
[DE85-012776] N86-10834
LOGIC PROGRAMMING
A course on field programmable logic
[EUT-85-E-148] N86-10805
LOGICAL ELEMENTS
Minimization of programmable logic arrays
[EUT-84-E-145] N86-10803
A course on field programmable logic
[EUT-85-E-148] N86-10805
LONG TERM EFFECTS
Evaluation and prediction of long-term environmental effects on non metallic materials
[NASA-CR-178495] N86-10340
LOOPS
Sample data phase locked loop for adaptive Doppler tracker
[AD-D011788] N86-10374
LOSSES
Geothermal lost circulation zone mapping tool
[DE85-008696] N86-10531
Surface conditioning of synchrotron radiation source to improve beam lifetime
[DE84-012185] N86-10948
Parasitic mode losses versus signal sensitivity in beam position monitors
[DE85-014367] N86-10964
The two micron spectrum of R Scuti N86-11092
LOW FREQUENCIES
The influence of low frequency mechanical vibrations on the growth of single crystals N86-10059
LOW GRAVITY MANUFACTURING
Effect of undercooling and modified microstructure on the physical properties of material synthesized in the drop tube and drop tower N86-10075
The influence of containerless undercooling and rapid solid-state quenching on the superconductive and magnetic properties of some clustering alloy systems N86-10076
Liquid phase miscibility gap materials N86-10081
Orbital processing of aligned magnetic composites N86-10089
Metallic foams N86-10095
Graphite formation in cast iron N86-10100
Containerless studies of nucleation and undercooling N86-10102
Suppression of Marangoni convection in float zones N86-10111
LOW PASS FILTERS
An active tracking band-pass filter
[AD-A156559] N86-10419
A study of derivative filters using the discrete Fourier transform
[NASA-CR-176224] N86-10825
LOW SPEED
Fundamental studies of low velocity impact resistance of graphite fiber reinforced polymer matrix composites N86-10288
LOW SPEED WIND TUNNELS
Activities report of the German-Dutch wind tunnel N86-10029
Activities report of the German-Dutch wind tunnel N86-10052
LOW TEMPERATURE
Adsorption of oxygen on single crystal tin at liquid helium temperatures N86-11044
LOW TEMPERATURE ENVIRONMENTS
Effect of increased body clothing insulation on hand temperature in a cold environment
[AD-A156597] N86-10786
LOW VOLTAGE
Total internal reflection modulator/deflector
[AD-D011757] N86-10424
LUBRICANT TESTS
Trials on the asperity counting monitoring system --- helicopter gearboxes
[RES-PAPER-670] N86-10550
LUBRICANTS
Steady state frictional behavior of thin film coatings N86-10335
LUBRICATION
Measurement of the density of base fluids at pressures 0.422 to 2.20 GPa
[NASA-TM-87114] N86-10551
LUMINANCE
Vision test chart and method using Gaussians
[AD-D011756] N86-10778
LUMINOSITY
Beam-beam deflections to measure size spot and offset at SLC IP
[DE85-014285] N86-10985
LUMINOUS INTENSITY
A simple method of obtaining concentration depth-profiles from X-ray diffraction
[NASA-CR-176262] N86-10310
Mild hypoxia and visual performance with night vision goggles
[AD-A156969] N86-10787
LUNAR BASES
A logistics scenario for an early lunar base
[ILR-MITT-143] N86-11140
LUNAR LOGISTICS
A logistics scenario for an early lunar base
[ILR-MITT-143] N86-11140
LYMPHOCYTES
Study of hypokinesia and acceleration effects on human chromosomes N86-10740

M

MACH-ZEHNDER INTERFEROMETERS
Advanced optical measurement techniques N86-10174
Fiber optic gradient hydrophone construction and calibration for sea trial
[AD-A156469] N86-10914
MACHINERY
Sound radiation from repetitive transient vibrations using multi-channel digital signal processing with application to impact machinery N86-10910
MACHINING
The influence of the substrate on the practical machining applications of cutting edges coated with different materials
[BLL-RISLEY-TR-5039-(9091.9F)] N86-10546
MAGNET COILS
Improved particle-velocity transducer for equation-of-state experiments
[DE85-013204] N86-10532
MAGNETIC DIPOLES
Theoretical and numerical investigation of dipole radiation over a flat earth N86-10369
Tracking studies on the effects of magnet multipoles on the aperture of the RHIC heavy ion collider
[DE85-013282] N86-11023
MAGNETIC DISKS
The local disk controller
[REPT-1-68430-44(1985)01] N86-10806
Performance analysis of the IBM Direct Access Storage Device (DASD) subsystem, and some suggestions for improved systems
[REPT-1-68430-44(1985)02] N86-10807
An intelligent local disk control system
[REPT-051560-28(1984)08] N86-10808
MAGNETIC FIELD CONFIGURATIONS
Box method for finding intersections of a trajectory with axisymmetric flux surfaces
[DE85-013525] N86-10840
Evolution of the fusion power demonstration tandem mirror reactor configuration
[DE85-012889] N86-10960
Theoretical aspects of magnetic helicity
[DE85-011846] N86-10984
Increased particle confinement with the use of external dc bias field in the CTX spheromak
[DE85-012744] N86-10988
GA Theory News, January-March 1985
[DE85-012572] N86-11007
Generalized helicity and its time derivative
[DE85-012770] N86-11027
Equilibrium of the kink source experiment
[DE85-012764] N86-11029
MAGNETIC FIELD INVERSIONS
Theoretical aspects of magnetic helicity
[DE85-011846] N86-10984
MAGNETIC FIELDS
Thermal and solutal convection damping using an applied magnetic field N86-10094
Calibrated Faraday current and magnetic field sensor
[DE85-013438] N86-10439
Measurement and resulting first and second order approximations for a 9 deg bending magnet in LAMPF's 750-keV transport
[DE85-012691] N86-10930
Use of the MURA transformation to generate the fields and calculate the motion of protons in the designed Argonne Mini-ASPUN FFAG spiral sector accelerator
[DE85-011477] N86-10934
Two-dimensional electrons
[AD-A156894] N86-10982
US superconducting magnet data base assessment for INTOR
[DE85-013648] N86-11000
A study of the applicability of nucleation theory to quasi-thermodynamic transformations of second and higher Ehrenfest-order
[NASA-CR-176230] N86-11060
MAGNETIC FLUX
Box method for finding intersections of a trajectory with axisymmetric flux surfaces
[DE85-013525] N86-10840
Local drift parameter, j/n sub e and resistivity anomaly measurements in CTX spheromaks
[DE85-012740] N86-10998
MAGNETIC MATERIALS
Rapid solidification of magnetic oxides N86-10152
MAGNETIC MIRRORS
Conducting wall and pressure profile effect on MHD stabilization of axisymmetric mirror
[DE85-013647] N86-11020
Symmetric Tandem Mirror Program
[DE85-012352] N86-11032
MAGNETIC MOMENTS
Hyperon polarization: An unresolved problem
[DE85-012298] N86-10946
MAGNETIC PROPERTIES
Orbital processing of aligned magnetic composites N86-10089
Electronic and magnetic properties of noble-metal and transition-metal alloys, interfaces and overlayers
[DE85-014532] N86-10321
Cryogenic structural materials for superconducting magnets
[DE85-008026] N86-10908
Topics in the electronic theory of disordered semiconductors N86-11045
Magnetic properties of doped semiconductors
[DE85-012090] N86-11053
MAGNETIC RECORDING
An evaluation of the use of microphone arrays for studio recording
[BBC-RD-1985/8] N86-10366
Specification for the performance, design, development and test requirements for a severe environment cartridge recorder. Issue 4
[AD-A156637] N86-10523
MAGNETIC SIGNALS
Amplitude and phase modulation in fin-lines electrical tuning
[AD-D011813] N86-10415
MAGNETOHYDRODYNAMIC FLOW
Velocities of gas and plasmas from real time holographic interograms
[DE85-014618] N86-10530
MAGNETOHYDRODYNAMICS
GA Theory News, January-March 1985
[DE85-012572] N86-11007
Conducting wall and pressure profile effect on MHD stabilization of axisymmetric mirror
[DE85-013647] N86-11020
MAGNETOMETERS
Calibrated Faraday current and magnetic field sensor
[DE85-013438] N86-10439
MAGNETORESISTIVITY
Two-dimensional electrons
[AD-A156894] N86-10982
MAGNETOSPHERE
Potential structures and particle acceleration on auroral field lines
[AD-A156694] N86-10708
Activities report in geophysics
[KGI-188] N86-10709
Solar flares and magnetospheric particles: Investigations based upon the ONR-602 experiment
[AD-A156583] N86-11142
MAGNETS
Ferrite kicker magnet for the IAMPF switchyard upgrade
[DE85-012857] N86-10996
MAINTENANCE
A modified repair strategy for two-component systems with revealed and unrevealed faults
[AD-A156715] N86-10885
MAN ENVIRONMENT INTERACTIONS
Adaptation of man to extreme conditions of Antarctica N86-10751
Individual typological self-regulation of cardio-vascular system N86-10752

MANAGEMENT ANALYSIS
Management of organizational operations in dynamic environments. Towards a frame of reference.
[FOA-C5-85-0003-H2] N86-11072
MANAGEMENT METHODS
Management of organizational operations in dynamic environments. Towards a frame of reference.
[FOA-C5-85-0003-H2] N86-11072
Failures and successes of quantitative methods in management
[ARW-03-THE-BDK/ORS/83-06] N86-11076
MANAGEMENT PLANNING
Land evaluation successes with the metric camera --- Spacelab N86-10512
Operations research applications
[ARW-03-THE-BDK/ORS/83-08] N86-10901
Management of organizational operations in dynamic environments. Towards a frame of reference.
[FOA-C5-85-0003-H2] N86-11072
On the structure of manpower planning, a contribution of simulation experiments with decomposition methods
[MANPOWER-PLANNING-28] N86-11073
Aspects of manpower planning at a Dutch university, an example of aggregation and decomposition methods in manpower planning
[MANPOWER-PLANNING-29] N86-11074
On the structure of manpower planning, a contribution of simulation experiments with aggregation methods
[MANPOWER-PLANNING-30] N86-11075
A systems development life cycle study of the information center
[AD-A156977] N86-11079
MANEUVERABILITY
Marginal terrain straddle-lift container handler
[AD-D011752] N86-10555
MANGANESE
Study of eutectic formation N86-10070
Theoretical problems in materials science N86-10088
Thermal and solutal convection damping using an applied magnetic field N86-10094
Advanced fuel cell development
[DE85-014550] N86-10659
MANIFOLDS (MATHEMATICS)
Estimates for maximal functions along hypersurfaces
[CTH-MATH-1984-29] N86-10874
A note on the differenciability of center manifolds
[ZW-8414] N86-10905
MANIPULATORS
Dynamic analysis of robotic manipulations with flexible links N86-10545
Supervisory control of the right arm of the beam assembly teleoperator
[AD-A156856] N86-10832
MANNED ORBITAL RESEARCH LABORATORIES
The first German Spacelab mission D1 reports --- Spacelab payloads
[PR-3] N86-10189
The fluid physics module: A technical description --- Spacelab N86-10201
MANNED SPACE FLIGHT
Manned flight simulation: Challenge and response
[NASA-TM-86827] N86-10048
A logistics scenario for an early lunar base
[ILR-MITT-143] N86-11140
MANPOWER
On the structure of manpower planning, a contribution of simulation experiments with decomposition methods
[MANPOWER-PLANNING-28] N86-11073
Aspects of manpower planning at a Dutch university, an example of aggregation and decomposition methods in manpower planning
[MANPOWER-PLANNING-29] N86-11074
On the structure of manpower planning, a contribution of simulation experiments with aggregation methods
[MANPOWER-PLANNING-30] N86-11075
MANUALS
User manual for the Falcon system --- Falcon research aircraft
[DFVLR-MITT-85-08] N86-10721
The DUCK manual
[AD-A156936] N86-10833
The Netherlands Institute for Nuclear and High Energy Physics (NIKHEF) traveling wave monitor user guide
[LINO-121] N86-10969
MAPPING
Improved mapping of radio sources from VLBI data by least-square fit N86-10402
Maximum water reserves in the snow cover in the European territory of the USSR according to data for 1892-1960
[NASA-TM-77901] N86-10611
Geologic evaluation and reservoir properties of the PR Spring tar sand deposit, Uintah and Grand Counties, Utah
[DE85-013248] N86-10634
MARANGONI CONVECTION
Some results of the Marangoni free convection experiment --- Spacelab N86-10203
Crystallization of a silicon sphere --- Spacelab N86-10226
The TEXUS flight results on convective flows and heat transfer in simulated floating zones N86-10235
Numerical simulation of unsteady thermal Marangoni flows N86-10238
Numerical simulation of convections in the microgravity environment N86-10239
Verification of turbulence developing from the oscillatory Marangoni convection in a liquid column --- rocket flight N86-10241
Measurements of the critical Marangoni number of the laminar-oscillatory transition of thermocapillary convection in floating zones N86-10242
Experimental study on Marangoni convection N86-10243
Rayleigh-Benard instability in systems presenting a minimum in surface tension N86-10245
MARINE ENVIRONMENTS
Evaluation of surface exchange coefficients from mildex ocean/atmosphere mixed layer data
[AD-A156765] N86-10729
MARINE TECHNOLOGY
LSRO/ONR ad hoc review process
[AD-A156590] N86-10735
MARKET RESEARCH
The air traffic demand in passenger travel of the Federal Republic of Germany 1990 - 2000. Update of the DFVLR air traffic forecast
[DFVLR-MITT-85-06] N86-10031
MARKOV PROCESSES
New probabilistic modeling and simulation methods for complex time-dependent systems
[DE85-009575] N86-10835
Multivariable partial realization and the aspect of uniqueness
[ER-83/09] N86-10879
Naive approximate realization of noisy data
[ER-83/10] N86-10880
MARS ATMOSPHERE
contemporary Aeolian processes on Mars: Local dust storms N86-11136
MASS DISTRIBUTION
Freezer model using a population balance approach for steady-state, direct-contact, secondary refrigerant, freeze desalination N86-10361
Representation of the distribution of the snow cover on the surface of the Earth's dry land
[NASA-TM-77909] N86-10612
Observations of the snow cover in the southern part of the Buryat Autonomous Soviet Socialist Republic
[NASA-TM-77910] N86-10613
Laws of distribution of the snow cover on the greater Caucasus (Soviet Union)
[NASA-TM-77911] N86-10614
MASS FLOW
The control of float zone interfaces by the use of selected boundary conditions N86-10060
The two micron spectrum of R Scuti N86-11092
MASS SPECTRA
Direct mass measurements in the light neutron-rich region using a combined energy and time-of-flight technique
[DE85-012758] N86-10963
Stellar s-process diagnostics
[DE85-012926] N86-11134
MASS TRANSFER
Solution growth of crystals in zero-gravity N86-10064
Modelling of laser-enhanced chemical vapor deposition N86-10105
Mass transport phenomena between bubbles and dissolved gases in liquids under reduced gravity conditions N86-10110
Fundamental studies of droplet combustion at reduced gravity N86-10165
Microphysical/mesoscale aspects of nuclear winter and new directions in assessments
[DE85-013479] N86-10718
MATERIALS HANDLING
Theoretical problems in materials science N86-10088
Development of materials processing systems for use in space on low-g simulation devices N86-10166
Microgravity Materials Science Laboratory N86-10173
Swelling and tensile properties of EBR-2-irradiated tantalum alloys for space reactor applications
[DE85-012887] N86-10329
Marginal terrain straddle-lift container handler
[AD-D011752] N86-10555
Hot cell facility design for large fusion devices
[DE85-012893] N86-11037
MATERIALS RECOVERY
Recovery of alcohol from a fermentation source by separation rather than distillation
[AD-D011782] N86-10282
MATHEMATICAL MODELS
Acta Aeronautica et Astronautica Sinica (selected articles)
[AD-A147304] N86-10001
A numerical solution of the shock-turbulent interaction over a compression corner for supersonic flow N86-10003
Impurity extraction by droplets N86-10122
Role of convection in grain refining N86-10133
Ignition and flame spread above liquid fuel pools N86-10163
Mathematical simulation of disturbing forces and material science processes under low gravity N86-10236
Dendritic solidification in a binary alloy melt: Steady-state versus morphological stability theories N86-10261
Nonlinear methods for spacecraft attitude maneuvers
[AD-A156956] N86-10275
The mechanics of delamination in composite materials N86-10284
Determination of thermophysical characteristics of solid materials by electrical modelling of the solutions to the inverse problems in nonsteady heat conduction
[NASA-TM-77907] N86-10293
Analysis of transitions between ferroelectric and antiferroelectric states under conditioning of uniaxial strain
[DE85-014468] N86-10350
Freezer model using a population balance approach for steady-state, direct-contact, secondary refrigerant, freeze desalination N86-10361
Radiative heat transfer in nonisothermal combustion products N86-10458
Analysis of annular two-phase flow with liquid entrainment N86-10459
Confined swirling jet predictions using a multiple-scale turbulence model
[NASA-CR-178484] N86-10462
Angle of incidence effects for underwater shock using generic computational models
[DE85-012936] N86-10466
Experiments with tubular probes made of INCOLOY 800 H under uniaxial and multiaxial strain
[JUEL-1979] N86-10595
Contribution of wind energy to the energy balance of a combined solar and wind energy system. Part 2: Computer-assisted investigations
[BMFT-FB-T-85-052-VOL-2] N86-10671
A numerical model for the estimation of solar radiation on rugged terrain N86-10694
Geothermal influences on the long-term thickness of the mechanical lithosphere during flexure N86-10697
Strength modeling report
[NASA-CR-171896] N86-10770
Applications for three-dimensional computer graphic cloud representations produced from satellite imagery
[AD-A156903] N86-10798
SUTRA (Saturated-unsaturated transport). A finite-element simulation model for saturated-unsaturated, Fluid-Density-Dependent ground-water flow with energy transport or chemically-reactive single-species solute transport
[AD-A156779] N86-10830
On maximal and distributional coupling
[CTH-MATH-1984-30] N86-10875
A modified repair strategy for two-component systems with revealed and unrevealed faults
[AD-A156715] N86-10885
Estimation by moments in a model of faulty inspection
[AD-A156754] N86-10886
Measurement and resulting first and second order approximations for a 9 deg bending magnet in LAMPF's 750-keV transport
[DE85-012691] N86-10930
Polarization transfer in inelastic scattering and pionic models of the EMC effect
[DE85-010738] N86-10955
Equilibrium of the kink source experiment
[DE85-012764] N86-11029
Experimental investigations of thermal radiation from potassium atoms and design applications
[DE85-004086] N86-11036
A method for numerical relativity: Simulation of axisymmetric gravitational collapse and gravitational radiation generation N86-11127
The dynamics and stellar content of globular star clusters N86-11131
Solar modulation of galactic cosmic rays: Techniques and applications N86-11143

MATHEMATICAL PROGRAMMING
Study of one- and two-dimensional filtering and deconvolution algorithms for a streaming array computer
[NASA-CR-176221] N86-10822
MATRICES (MATHEMATICS)
Theoretical comparison of classical (K-matrix) and inverse (P-matrix) least-squares methods for quantitative infrared spectroscopy
[DE85-012827] N86-10298
Coincidence densities and spectra of a class of substitution minimal sets N86-10857
Partial eigensolutions of large nonsymmetric matrices
[AD-A156711] N86-10867
Computing the structural index
[DE85-014370] N86-10871
Rank revealing QR-Factorizations
[AD-A156756] N86-10887
MATRIX THEORY
Variational estimates for the mass gap of SU(2) Euclidean lattice gauge theory
[NIKHEF-H/84-13] N86-10883
MAXIMUM LIKELIHOOD ESTIMATES
On the numerical determination of the dimension of an attractor — strange attractors
[ZW-8415] N86-10892
MAXWELL EQUATION
Geothermal influences on the long-term thickness of the mechanical lithosphere during flexure N86-10697
Electron momentum transfer collision frequency in N(2), O(2) and air
[AD-A157030] N86-10924
MEAN
Mean turbulence structure in strongly heating air flows N86-10455
Nonparametric comparison of several mean values with mild adaptation to some sample characteristics
[COMP-CENT-NOTE-20] N86-10891
MEASURE AND INTEGRATION
On the absolute continuity of elliptic measures
[CTH-MATH-1984-28] N86-10873
MEASURING INSTRUMENTS
High sensitivity millimeter-wave measurement apparatus
[AD-D011786] N86-10373
ELCAP instrumentation
[DE85-013042] N86-10527
Velocities of gas and plasmas from real time holographic interograms
[DE85-014618] N86-10530
Software for an automated gaging system
[DE85-013322] N86-10842
MECHANICAL DEVICES
Mathematical models of continuous flow electrophoresis N86-10143
MECHANICAL DRIVES
Termination load carrying device
[AD-D011800] N86-10558
MECHANICAL MEASUREMENT
Portevin-Le Chatelier effect. 1: Model for the type-E serrations
[DE85-006879] N86-10322
MECHANICAL PROPERTIES
Ultrasonic evaluation of mechanical properties of thick, multilayered, filament wound composites
[MASA-TM-87088] N86-10561
MECHANICAL SHOCK
The Shock and Vibration Digest, volume 17, no. 3
[AD-A154144] N86-10585
MEDICAL SCIENCE
USSR report: Life sciences. Biomedical and behavioral sciences
[JPRS-UBB-85-023] N86-10738
MEDICAL SERVICES
Annotated bibliography of publications dealing with occupational health and medical information systems, cost analysis procedures, evaluation methodology and related legal issues
[AD-A156650] N86-11078
MELTING
Undercooling, remelting, and coarsening N86-10080
Metallic foams N86-10095
Melting and solidification in O-g of sintered alloys: Experiments ES 311 A and B bubble reinforced materials — Spacelab N86-10215
Interdiffusion in the glass melt system (Na2O+Rb2O).3SiO2 — Spacelab N86-10216
Recirculation within a glass mixture subjected to external and resistive heating
[DE85-010068] N86-10348
Maximum water reserves in the snow cover in the European territory of the USSR according to data for 1892-1960
[NASA-TM-77901] N86-10611
MELTS (CRYSTAL GROWTH)
Growth of solid solution crystals N86-10065
Dendritic growth in undercooled melts N86-10082
Influence of melt convection on solid-liquid interface under terrestrial and reduced gravity environments N86-10083
Solidification fundamentals N86-10090
Containerless processing of undercooled melts N86-10093
Metallic foams N86-10095
Morphological stability and fluid dynamics of vapor crystal growth N86-10126
Bulk formation of metallic glasses and amorphous silicon from the melt N86-10154
Crystal growth of GaAs in space N86-10234
Dendritic solidification in a binary alloy melt: Steady-state versus morphological stability theories N86-10261
MEMBRANES
Streaming potentials in conductive and nonconductive tubing
[DE85-012984] N86-10438
Membrane research in energy and solvent recovery from industrial effluent streams
[DE85-014583] N86-10682
MEMORY (COMPUTERS)
Elektronika MS 1603 high-speed peripheral processor N86-10811
MENTAL PERFORMANCE
The effects of age, sleep deprivation, and altitude on complex performance
[AD-A156987] N86-10771
Derivational analogy: A theory of reconstructive problem solving and expertise acquisition
[AD-A156817] N86-10899
MERCURY (METAL)
Sediment characterization. Task 2: Instream contaminant study. Volume 2: Appendices
[DE85-013503] N86-10680
Sediment characterization. Task 2: Instream contaminant study, volume 1
[DE85-013502] N86-10683
MERCURY COMPOUNDS
Sensor system
[AD-D011767] N86-10480
Parallel pulse processing for mercuric iodide gamma-ray detectors
[DE85-013391] N86-10528
MESOSCALE PHENOMENA
The boundary condition in a numerical model of atmospheric flows over fixed interfaces
[GKSS-85-E-10] N86-10722
METABOLISM
Intradiurnial organization of wakefulness-sleep sequence and energy metabolism in rats exposed to low ambient temperature N86-10764
METAL BONDING
Metallurgy and metallography of braze joints
[DE85-014563] N86-10325
The preparation and testing of titanium and zirconium coupling agents
[SJ70] N86-10576
METAL COATINGS
The role of entrained surface oxides in RS-PM aluminum alloys on resultant structures and properties N86-10085
METAL CRYSTALS
Transport processes in directional solidification during space shuttle flight N86-10257
Stability of metallic dispersions — microgravity N86-10258
Surface science and catalysis
[DE85-013922] N86-11057
METAL FATIGUE
Fabrication and metallurgical properties of modified 9Cr-1 Mo steel
[DE85-012885] N86-10328
METAL FILMS
Photoionization technique for growth of metallic films
[AD-D011760] N86-10426
Thermodynamic constraints on ion beam mixing of metals on insulators
[DE85-013628] N86-10448
METAL FINISHING
Multipurpose pan development
[DE85-012326] N86-10319
METAL FOAMS
Metallic foams N86-10095
METAL MATRIX COMPOSITES
Melting and solidification of metal matrix composites under microgravity — Spacelab N86-10211
Preliminary reports, memoranda and technical notes of the Materials Research Council Summer Conference, La Jolla, California
[AD-A156776] N86-10291
METAL PARTICLES
Particle coarsening in immiscible zinc-lead alloys under microgravity — Spacelab N86-10210
METAL PLATES
Nondestructive control of thick structures made without disassembling
[PV-43-954/F/3] N86-10564
METAL PROPELLANTS
Compatibility of grain-stabilized platinum with candidate propellants for resistojets
[NASA-TM-87118] N86-10279
METAL SURFACES
Mechanism of the formation of boronised layers on high carbon steel
[BLL-BISI-TRANS-23036-(9022.06)] N86-10306
Boronising of iron and steel by ionic bombardment by diborane
[BLL-BISI-TRANS-23034-(9022.06)] N86-10307
Fuel and lubricant behavior in boundary layers analyzed by infrared emission Fourier transform spectrometry N86-10336
Surface science and catalysis
[DE85-013922] N86-11057
METAL-NITRIDE-OXIDE-SEMICONDUCTORS
The VLSI design of error-trellis syndrome decoding for convolutional codes N86-10391
METALLIC GLASSES
Crystallization, optical and chemical properties of fluoride glasses N86-10149
Bulk formation of metallic glasses and amorphous silicon from the melt N86-10154
Fusion target technology N86-10156
Oxidation behavior of glassy alloys N86-10158
Crystal nucleation and glass formation in metallic alloy melts N86-10233
Formation and characterization of amorphous erbium-based alloys prepared by near-isothermal cold-rolling of elemental composites
[DE85-014853] N86-10327
Elastic properties and thermal stability characterization of metallic glasses by guided wave techniques N86-10337
METALLIZING
Development of metallization process
[NASA-CR-176209] N86-10312
Investigation of metallic impurities introduced into SiO2 and silicon by various candidate VLSI metallization systems: Chemical reactions, diffusion, and electrical properties
[AD-A156609] N86-10429
The mechanism of erosion of metallic materials under cavitation attack
[NASA-TM-87133] N86-10552
METALLOGRAPHY
Fracture toughness of hydrogen-embrittled precipitation-hardened stainless steels
[AD-A156664] N86-10592
METALLURGY
First Spacelab Payload (FSLP) experiments in metallurgy N86-10266
Metallurgy and metallography of braze joints
[DE85-014563] N86-10325
METALS
Attachment method-ceramic radome to metal body
[AD-D011778] N86-10032
Microgravity Science and Applications Program tasks
[NASA-TM-87568] N86-10053
Undercooling, remelting, and coarsening N86-10080
Microgravity Materials Science Laboratory N86-10173
Weld metal hot-cracking of hastelloy alloys C-22 and C-276: A study by analytical electron microscopy
[DE85-009437] N86-10324
Research needs for corrosion control and prevention in energy conservation systems
[DE85-014852] N86-10326
Composite explosives for metal acceleration: The effect of detonation temperature
[DE85-013982] N86-10359
Thermodynamic constraints on ion beam mixing of metals on insulators
[DE85-013628] N86-10448
Finite element analysis of metals at elevated temperature using unified constitutive theories N86-10569
Preliminary investigation of changes in X-ray multilayer optics subjected to high radiation flux
[DE85-014074] N86-10944
Surface science and catalysis
[DE85-013922] N86-11057
METASTABLE STATE
High-pressure release-wave measurements and phase transformation in CaCO3
[DE85-012592] N86-11055
METEOROLOGICAL CHARTS
Monthly Bulletin North Sea: Volume 2, January 1985
[KNMI-167-VOL-2] N86-10732

METEOROLOGICAL FLIGHT
Comparative flight measurement of icing parameters for the propeller aircraft Do-28D2 of the test station 61 of the DFVLR and for the DFVLR aircraft Falon 20e in stratus clouds
[DFVLR-FB-85-16] N86-10720
User manual for the Falcon system --- Falcon research aircraft
[DFVLR-MITT-85-08] N86-10721
METEOROLOGICAL INSTRUMENTS
Fall velocity indicator/viewer
[AD-D011789] N86-10482
METEOROLOGICAL PARAMETERS
ELCAP instrumentation
[DE85-013042] N86-10527
Surface winds at NWC (Naval Weapons Center): 1964 - 1982
[AD-A156660] N86-10712
Monthly Bulletin North Sea: Volume 2, January 1985
[KNMI-167-VOL-2] N86-10732
METEOROLOGICAL SERVICES
List of publications on the 200 m meteorological mast at Cabauw, the Netherlands
[KNMI-FM-85-6] N86-10711
METHANE
Flammability limits of gases under low gravity conditions N86-10164
Design and calibration of a flat-flame burner using line reversal techniques
[AD-A156724] N86-10294
Catalytic activity of shock modified ZnO for CO oxidation and methanol synthesis
[DE85-014704] N86-10300
Methane-bubble formation in hydrogen-charged Fe-30 ppM C
[DE85-012526] N86-10937
METHOD OF CHARACTERISTICS
On the method of characteristics and its application to the calculations of annular nozzle flowfields N86-10454
METHOD OF MOMENTS
A transformation method for the evaluation of the response moments of elastic structures with random properties
[AD-A156882] N86-10557
METRIC PHOTOGRAPHY
Metric Camera Workshop --- Spacelab
[ESA-SP-209] N86-10485
Digital elevation model from Spacelab metric camera photographs N86-10486
Orthophotomapping from metric camera imagery --- Spacelab N86-10487
Restitution of Spacelab photography by analog stereoplotter N86-10489
Evaluation of the accuracy of the metric camera images for the production of line maps and orthophotos N86-10490
Photomapping in different climatic zones --- Spacelab metric camera N86-10491
A geological structural analysis of the southeastern Zagros (Iran) ranges based on metric camera photos N86-10492
Erosion control and watershed management by Spacelab photography N86-10493
High-resolution image data from the Space Shuttle N86-10494
Evaluation of metric camera images at the University of London --- Spacelab N86-10495
Partial in-flight calibration of the metric camera --- Spacelab N86-10496
Identification of planimetric features from the metric camera --- Spacelab N86-10497
Analysis of metric camera images from the USA and their suitability for topographic and thematic mapping --- Spacelab N86-10498
Long range translocations ashore to offshore using Spacelab-1 metric camera imagery in the perspective of integrated geophysical surveys N86-10499
Line mapping and resolution tests with metric camera data --- Spacelab N86-10500
Role of the Economic Commission for Africa as a principal investigator in the metric camera experiment and reports of the result of the assessment for topographic and revision of maps in populated and developed areas of the world N86-10501
The role of very small scale metric images in modern geology --- Spacelab metric camera N86-10502
Geological mapping of remote mountainous regions using metric camera imagery --- Spacelab N86-10503
Interpretation of metric camera concerning hydrologic structures of the Rhone Delta --- Spacelab N86-10504
Test on mapping application of metric camera imagery --- Spacelab N86-10505
Status of preparation activities for metric camera reflight on EOM-1/2 N86-10506
OEEPE participation in testing metric camera photography --- European Organization for Experimental Photogrammetric Investigations (OEEPE) N86-10507
Topographic interpretation of metric camera images: An example in Somalia --- Spacelab N86-10508
Thematic investigations in France based on metric camera imagery --- Spacelab N86-10509
Thematic mapping of metric camera color infrared and black and white photographs for land use classification N86-10510
Digital image processing of metric camera imagery --- Spacelab N86-10511
Land evaluation successes with the metric camera --- Spacelab N86-10512
Requirements and possibilities of Spacelab metric camera photos usage for inventories of large areas of extensively managed forests N86-10513
Evaluation of metric camera photos --- Spacelab; alpine snow cover N86-10515
Creation of Ground Control Points (GCP) library using ESA Spacelab metric camera imagery --- ground control point (gcp) N86-10516
Updating of topographic maps by means of metric camera photos example: Hallertau (Bavaria) N86-10517
Interpretation of Spacelab-1 photographs for the generation of 1:200000 topographic map N86-10518
Metric camera image of Munich as additional means for urban cartography --- Spacelab N86-10519
An example of single model orientation of metric camera stereophotographs --- Spacelab N86-10520
Tectonic analysis of typical fold structures in the Zagros Mountains (Iran) by the application of quantitative photogrammetric methods on metric camera data --- Spacelab N86-10521
Test results using metric camera photography for 1:250,000 mapping --- Spacelab N86-10522
METRIC SPACE
Gravitational collapse of a scalar field N86-11129
MICHELSON INTERFEROMETERS
Colloquium on Kilometric Optical Arrays in Space
[ESA-SP-226] N86-11096
Results and limitations of ground-based optical arrays --- stellar interferometry N86-11097
Extragalactic observations with optical space arrays N86-11098
Astronomical criteria for interferometric arrays --- Spacecraft design N86-11099
TRIO: A kilometric array stabilized by solar sails --- Spaceborne astronomy N86-11102
SAMSI: An orbiting spatial interferometer for micro-arc second astronomical observations --- Spacecraft Array for Michelson Spatial Interferometry (SAMSI) N86-11103
COSMIC: A high resolution, large collecting area telescope --- Coherent Optical System of Modular Imaging Collectors (COSMIC) N86-11104
TRIO optics --- spaceborne optical interferometer (TRIO) N86-11108
Solar propulsion for the TRIO interferometer N86-11109
Preliminary studies of a spinning tether-connected TRIO concept --- spaceborne interferometer (TRIO) N86-11110
TRIO interferometer positioning --- spaceborne interferometers (TRIO) N86-11111
Fringe drift compensation in computer memory --- Michelson interferometry N86-11112
TRIANGLE: A different design for a three satellite interferometer in space N86-11113
Mission analysis aspects --- spaceborne interferometry N86-11114
Problems in image reconstruction with optical arrays --- spaceborne astronomy N86-11115
Numerical experiments in image reconstruction --- stellar interferometry N86-11116
On line astronomical image processing using microcomputers N86-11121
The DUO: Far infrared heterodyne concept for space interferometry N86-11125
VLBI at optical and radio wavelengths: Congruences and contrasts N86-11126
MICROBIOLOGY
Biotechnology: Science and practice N86-10742
MICROCOMPUTERS
Radar system description N86-10616
Microcomputer aided calculations of parameters for spray dryer operation
[DE85-013468] N86-10681
Computer-based training for the US Coast Guard standard terminal microcomputer: A basis for implementation utilizing the elaboration theory of instructional design
[AD-A156548] N86-10791
Development of IS2100: An information systems laboratory
[AD-A156848] N86-10797
Dissecting the cow
[DE85-013369] N86-10801
Klystron control software in the SIC
[DE85-013068] N86-10836
Software for an automated gaging system
[DE85-013322] N86-10842
A systems development life cycle study of the information center
[AD-A156977] N86-11079
On line astronomical image processing using microcomputers N86-11121
MICROELECTRONICS
Microcircuit device reliability field experience database. Volume 1. Field data. Volume 2. Failure Event/Analysis data
[AD-A156836] N86-10433
Prospects for creation of optical digital high-performance computers N86-10810
MICROORGANISMS
Development and evaluation of multispecies test protocols for assessing chemical toxicity
[DE85-013526] N86-10679
Biotechnology: Science and practice N86-10742
MICROPHONES
An evaluation of the use of microphone arrays for studio recording
[BBC-RD-1985/8] N86-10366
Measurements of the acoustic interference between adjacent microphones
[AD-A156892] N86-10919
MICROPROCESSORS
Periodic binary sequences with very good autocorrelation properties N86-10397
Soudan 2 data acquisition and trigger electronics
[DE85-013864] N86-10443
ELCAP instrumentation
[DE85-013042] N86-10527
Digital control of the hydraulic actuators of an adaptive suspension vehicle N86-10548
Parallel local interface bus
[AD-D011742] N86-10792
USSR report: Cybernetics, computers and automation technology
[JPRS-UCC-85-006] N86-10809
Elektronika MS 1603 high-speed peripheral processor N86-10811
Diagnostics of peripheral processors and controllers N86-10812
An approach to implementing CAMAC microprocessor modules N86-10813
MICROSCOPY
Advanced optical measurement techniques N86-10174
MICROSTRIP TRANSMISSION LINES
A dual frequency microstrip antenna for Ka band
[NASA-TM-87124] N86-10380
MICROSTRUCTURE
Study of eutectic formation N86-10070
Modeling directional solidification N86-10071
Effect of undercooling and modified microstructure on the physical properties of material synthesized in the drop tube and drop tower N86-10075
The influence of containerless undercooling and rapid solid-state quenching on the superconductive and magnetic properties of some clustering alloy systems N86-10076
Liquid phase miscibility gap materials N86-10081
Control of cast iron microstructure N86-10084
The role of entrained surface oxides in RS-PM aluminum alloys on resultant structures and properties N86-10085
The development and prevention of channel segregation during alloy solidification N86-10086
Environmental degradation of materials: Surface chemistry related to stress corrosion cracking N86-10099
Rapid solidification of magnetic oxides N86-10152
Sol-gel glasses N86-10153
Acoustic levitation containerless processing N86-10177
Progressive damage, fracture predictions and post mortem correlations for fiber composites
[NASA-TM-87101] N86-10290
Fabrication and metallurgical properties of modified 9Cr-1 Mo steel
[DE85-012885] N86-10328
Aluminum ion plating for corrosion protection of uranium, revision 1
[DE85-012419] N86-10330
Theoretical analysis of Wolter/LSM X-ray telescope systems
[NASA-CR-176244] N86-11095
MICROWAVE ANTENNAS
A new 70-meter antenna quadripod with reduced RF blockage N86-10385

MICROWAVE EQUIPMENT
Miniature radar packaging
[DE85-014598] N86-10410
MICROWAVE TRANSMISSION
Radome analysis and design capabilities of the RF and Microwave Technology Branch
[AD-A156662] N86-10404
MICROWAVES
Microwave evaluation of materials
[DE85-013183] N86-10409
Potential applications of multipolarization SAR for pine plantation biomass estimation N86-10626
Compact torus compression of microwaves
[DE85-012919] N86-11016
MIGRATION
The influence of thermocapillarity on the migration of droplets in a liquid possessing a uniform temperature gradient N86-10237
MILITARY PSYCHOLOGY
Standardization of tasks: Approach planning --- human performance assessment
[IZF-1984-19] N86-10782
MILITARY TECHNOLOGY
USSR report: Life sciences. Biomedical and behavioral sciences
[JPRS-UBB-85-023] N86-10738
Information technique 1985: Optical technology and electro-optics, a defense technical component review
[FOA-A-30037-E] N86-10980
MILLIMETER WAVES
High sensitivity millimeter-wave measurement apparatus
[AD-D011786] N86-10373
A superconducting tunnel junction receiver for millimeter-wave astronomy N86-11041
MINERAL DEPOSITS
Remote stratigraphic and structural analysis: Multisensor results in the Wind River/Bighorn Basin area, Wyoming N86-10606
MINERAL OILS
The mechanism of erosion of metallic materials under cavitation attack
[NASA-TM-87133] N86-10552
MINES (EXCAVATIONS)
Kinetics of biological ferrous iron oxidation
[DE85-014616] N86-10736
MINICOMPUTERS
Compact, high-speed algorithm for laying out printed circuit board runs N86-10814
MINKOWSKI SPACE
Gravitational collapse of a scalar field N86-11129
MIRAGE AIRCRAFT
Report on an overseas visit
[AD-A156603] N86-10037
MIRROR FUSION
Evolution of the fusion power demonstration tandem mirror reactor configuration
[DE85-012889] N86-10960
Application of structural-mechanics methods to the design of large tandem-mirror fusion devices (MFTF-B)
[DE85-008960] N86-11017
MIRRORS
Identification of chemical and physical phenomena affecting the durability of silvered polymer (PMMA) mirrors
[DE85-012131] N86-10645
Optical/IR telescope arrays: A study of their potential for satisfying observational requirements in astronomy for a large aperture system in the 1990s and beyond
[REPT-15] N86-11094
Theoretical analysis of Wolter/LSM X-ray telescope systems
[NASA-CR-176244] N86-11095
MISSION PLANNING
A comparative analysis of a CV helicopter and a JVX (Joint Services Advanced Vertical Lift) tilt-rotor aircraft in an aircraft carrier based ASW (Anti-Submarine Warfare)
[AD-A156871] N86-10041
The first German Spacelab mission D1 reports --- Spacelab payloads
[PR-1] N86-10187
Status of preparation activities for metric camera reflight on EOM-1/2 N86-10506
Mission analysis aspects --- spaceborne interferometry N86-11114
Galileo: Exploration of Jupiter's system
[NASA-SP-479] N86-11137
MISSOURI
Analysis of remote sensing data N86-10605
MIXING
The influence of low frequency mechanical vibrations on the growth of single crystals N86-10059
Particle cloud combustion experiment N86-10160
Recirculation within a glass mixture subjected to external and resistive heating
[DE85-010068] N86-10348
Thermodynamic constraints on ion beam mixing of metals on insulators
[DE85-013628] N86-10448
MIXTURES
Effects of scale and geometry on hydrogen-air detonations
[DE85-006762] N86-10474
MODELS
Thermocapillary motion research N86-10125
Electrohydrodynamics N86-10130
Experimental and theoretical analysis of chemical vapor deposition with prediction of gravity effects N86-10132
Theoretical modeling of the vapor cavitation in dynamically loaded journal bearings
[NASA-TM-87076] N86-10463
Constitutive modeling for isotropic materials (HOST)
[NASA-CR-174980] N86-10589
Evaluation of surface exchange coefficients from mildex ocean/atmosphere mixed layer data
[AD-A156765] N86-10729
TEMPUS: Simulating personnel and tasks in a 3-D environment
[NASA-CR-171901] N86-10785
Optimal control modeling of lower extremity musculoskeletal motion N86-10853
New approach to multiphase equilibria: Application to high-pressure physics problems
[DE85-013820] N86-10907
MODEMS
A nanosecond or thirty centimeters: Why atomic clocks have to be synchronized. MITREX opens new dimensions for measuring accuracy N86-10185
MODULARITY
Realization of a multifunction Input/Output (I/O) controller by means of a gate array
[EUT-85-E-147] N86-10804
MODULATION
Solar modulation of galactic cosmic rays: Techniques and applications N86-11143
MODULATORS
Total internal reflection modulator/deflector
[AD-D011757] N86-10424
MODULES
An approach to implementing CAMAC microprocessor modules N86-10813
MOISTURE CONTENT
Microwave evaluation of materials
[DE85-013183] N86-10409
MOLDING MATERIALS
Automatic processing of reactive polymers N86-10127
MOLECULAR BIOLOGY
LSRO/ONR ad hoc review process
[AD-A156590] N86-10735
MOLECULAR CLOUDS
A superconducting tunnel junction receiver for millimeter-wave astronomy N86-11041
MOLECULAR SPECTRA
The two micron spectrum of R Scuti N86-11092
MOLECULAR STRUCTURE
Synthesis of arylene siloxanylene polymers and copolymers
[AD-D011780] N86-10338
MOLECULAR WEIGHT
Polyacetylene polymerization, structure, and electrical transport properties N86-10334
Automated analysis of digital images generated by two-dimensional gel electrophoresis
[DE85-011906] N86-10526
MOLECULES
Theory of dense molecular fluid equations of state with application to detonation products
[DE84-016822] N86-10927
MOLTEN SALT ELECTROLYTES
Metals electroprocessing in molten salts N86-10098
MOLTEN SALTS
Crystal growth from solution --- Spacelab N86-10229
MOLYBDENUM
Rapid evaluation of ion thruster lifetime using optical emission spectroscopy
[NASA-TM-87103] N86-10280
Development of metallization process
[NASA-CR-176209] N86-10312
The mechanism of erosion of metallic materials under cavitation attack
[NASA-TM-87133] N86-10552
MOLYBDENUM ALLOYS
Fabrication and metallurgical properties of modified 9Cr-1 Mo steel
[DE85-012885] N86-10328
MOMENTUM TRANSFER
Electron momentum transfer collision frequency in N(2), O(2) and air
[AD-A157030] N86-10924
MONITORS
Specification for the performance, design, development and test requirements for a severe environment cartridge recorder. Issue 4
[AD-A156637] N86-10523
Captive volume device as a safe life monitor
[AD-D011802] N86-10525
TV monitoring control system in electrophysiological studies N86-10765
Providing automated control for PBFA-2
[DE85-012867] N86-10928
Wide dynamic range beam profile monitor
[DE85-012709] N86-10950
Advances in data acquisition system technology for PBFA 2
[DE85-012860] N86-11011
High-resolution phosphor screen beam profile monitor
[DE85-013074] N86-11012
MONOTECTIC ALLOYS
Studies of model immiscible systems N86-10112
Influences affecting separation in monotectic alloys under microgravity N86-10209
Particle coarsening in immiscible zinc-lead alloys under microgravity --- Spacelab N86-10210
MONOTONE FUNCTIONS
Strength of shells under local transverse loads N86-10568
MONTE CARLO METHOD
Time-implicity simulation of particle-fluid systems
[DE85-012944] N86-10471
New probabilistic modeling and simulation methods for complex time-dependent systems
[DE85-009575] N86-10835
Superefficient estimation of power functions in simulation experiments
[B8562445] N86-10893
MOON
Photographic catalog of selected planetary size comparisons
[NASA-TM-86207] N86-11138
MORPHOLOGY
Morphological stability and fluid dynamics of vapor crystal growth N86-10126
Dendritic solidification in a binary alloy melt: Steady-state versus morphological stability theories N86-10261
MOTION SICKNESS
Dynamics of changes of statistical indicators of heart rhythm of persons with different degree of motion sickness N86-10743
MOTION SIMULATORS
Motion analysis report
[NASA-CR-171897] N86-10896
Zero-gravity movement studies
[NASA-CR-171899] N86-10897
MOUNTAINS
A geological structural analysis of the southeastern Zagros (Iran) ranges based on metric camera photos N86-10492
Geological mapping of remote mountainous regions using metric camera imagery --- Spacelab N86-10503
Tectonic analysis of typical fold structures in the Zagros Mountains (Iran) by the application of quantitative photogrammetric methods on metric camera data --- Spacelab N86-10521
MUFFLERS
The Shock and Vibration Digest, volume 17, no. 3
[AD-A154144] N86-10585
Recent advances in the analysis of exhaust mufflers N86-10587
MULTIPLEXING
Wide dynamic range beam profile monitor
[DE85-012709] N86-10950
MULTIPROCESSING (COMPUTERS)
Alternating direction methods on multiprocessors: An extended abstract
[AD-A156722] N86-10794
Efficient systolic arrays for the solution of toeplitz systems: An illustration of a methodology for the construction of systolic architectures in VLSI (Very Large Systems Integration)
[AD-A156767] N86-10795
Fault-free behavior of reliable multiprocessor systems: FTMP experiments in AIRLAB
[NASA-CR-177967] N86-10848
Topological properties of hypercubes
[AD-A156777] N86-10850
MULTISPECTRAL BAND SCANNERS
Multisensor data integration techniques N86-10604
Lithologic mapping in a sedimentary environment using multipolarization SAR images N86-10624
Calibration of the multispectral scanner (MSS) satellite data to evaluate change in the reflection of coniferous stocks
[DFVLR-FB-84-44] N86-10636

MULTIVARIATE STATISTICAL ANALYSIS
Theoretical comparison of classical (K-matrix) and inverse (P-matrix) least-squares methods for quantitative infrared spectroscopy
[DE85-012827] N86-10298
MUON SPIN ROTATION
Polarization transfer in inelastic scattering and pionic models of the EMC effect
[DE85-010738] N86-10955
MUSCLES
Strength modeling report
[NASA-CR-171896] N86-10770
MUSCULAR FUNCTION
Assessment of state of chronotropic and inotropic heart function at different degrees of physical fitness N86-10746
Heat transfer mechanism in human extremities N86-10759
Strength modeling report
[NASA-CR-171896] N86-10770
MUSCULAR STRENGTH
Efficiency of muscular work in white rats during adaptation to cold N86-10763
Strength modeling report
[NASA-CR-171896] N86-10770
MUSCULOSKELETAL SYSTEM
Optimal control modeling of lower extremity musculoskeletal motion N86-10853
MUTAGENS
Somatic cell and molecular genetics approach to DNA repair and mutagenesis
[DE85-014181] N86-10737
MYOCARDIUM
Classification of changes in electrocardiogram during muscular exertion of healthy individuals N86-10755

N

N-TYPE SEMICONDUCTORS
W-shaped diffused stripe GaAs/AlGaAs laser
[AD-D011818] N86-10538
NASA PROGRAMS
NASA/American Society for Engineering Education (ASEE) Summer Faculty Fellowship Program, 1985
[NASA-CR-177972] N86-11064
NATURAL GAS
Analyses of advanced residential absorption heat pump cycles
[DE85-005244] N86-10664
NAVIER-STOKES EQUATION
Numerical solution of hypersonic flow near leading edge of a flat plate N86-10008
Numerical procedure for three-dimensional hypersonic viscous flow over aerobrake configuration
[NASA-TM-58269] N86-10018
Numerical simulation of unsteady thermal Marangoni flows N86-10238
Finite element solution of the Navier-Stokes equations for 3-D turbulent free shear flows N86-10457
NEODYMIUM
Research on solar pumped liquid lasers
[NASA-CR-176235] N86-10539
NEODYMIUM LASERS
Design, fabricate and test a 1.06(MU) repetitively pulsed laser
[DE85-014439] N86-10543
NEON
Dynamics of imploding neon gas puff plasmas. 1
[AD-A156916] N86-10983
NEON ISOTOPES
Direct mass measurements in the light neutron-rich region using a combined energy and time-of-flight technique
[DE85-012758] N86-10963
NEPTUNE (PLANET)
Planning for VLA/DSN arrayed support to the Voyager at Neptune N86-10395
A VLA experiment: Planning for Voyager at Neptune N86-10396
NERVOUS SYSTEM
Eye-movement activity as index of functional state of brain N86-10756
NETHERLANDS
Wind energy in agriculture, a promise
[SS-45] N86-10672
Wind energy, a feasibility investigation for wind mills in agriculture
[SS-45A] N86-10673
Activities report of the Space Flight Laboratory N86-11090
Activities Report of the Space Flight Laboratory N86-11091
NETWORK ANALYSIS
LANES 1 Users' Guide
[NASA-CR-177334] N86-10619
NETWORK SYNTHESIS
Spectral methods in adapted curved grids N86-10878
NEUTRAL BEAMS
Report on the engineering test of the LBL 30 second neutral beam source for the MFTF-B project
[DE85-013317] N86-10962
Noninterceptive techniques for the measurement of longitudinal parameters for intense H(-) beams
[DE85-012662] N86-10992
NEUTRAL GASES
Cometary atmospheres: Modeling the spatial distribution of observed neutral radicals
[NASA-CR-176242] N86-11133
NEUTRINOS
Matter-antimatter transition operators: A manual for modeling N86-10921
Search for heavy neutrines produced in e(+)e(-) annihilation
[DE85-013372] N86-11035
NEUTRON BEAMS
Initial increase, peaking effect, in the internal friction of copper following pulsed neutron and electron irradiation
[DE85-012767] N86-10932
NEUTRON IRRADIATION
Anelastic relaxation in irradiated Cu-Be
[DE85-013893] N86-11056
NEUTRON SOURCES
Use of the MURA transformation to generate the fields and calculate the motion of protons in the designed Argonne Mini-ASPUN FFAG spiral sector accelerator
[DE85-011477] N86-10934
Performance of the H(-) ion source for the intense pulsed neutron source
[DE85-012368] N86-10991
Beginnings of remote handling at the RAL Spallation Neutron Source
[DE85-012681] N86-11001
NEUTRON SPECTRA
Determining a physically appropriate neutron spectrum from multisphere data
[DE85-013045] N86-10299
The development of a neutron evaporation theory code for the thermal fission of Uranium-235
[AD-A156593] N86-10951
NEUTRON SPECTROMETERS
Determining a physically appropriate neutron spectrum from multisphere data
[DE85-013045] N86-10299
NEUTRONS
The development of a neutron evaporation theory code for the thermal fission of Uranium-235
[AD-A156593] N86-10951
Development and application of the electrochemical etching technique
[DE85-010302] N86-10957
Photoactivation of PBFA-2
[DE85-013439] N86-11019
NEW MEXICO
Remote stratigraphic and structural analysis: Multisensor results in the Wind River/Bighorn Basin area, Wyoming N86-10606
NICKEL
Physical and chemical properties of a nickel catalyst processed under microgravity --- STS-7 N86-10255
Containerless undercooling of Ni N86-10260
NICKEL ALLOYS
Undercooling, remelting, and coarsening N86-10080
Small cartridge heater
[AD-D011784] N86-10277
Electronic and magnetic properties of noble-metal and transition-metal alloys, interfaces and overlayers
[DE85-014532] N86-10321
Formation and characterization of amorphous erbium-based alloys prepared by near-isothermal cold-rolling of elemental composites
[DE85-014853] N86-10327
Metastable phase formation in Ni-implanted Al: An analytical electron microscope investigation
[DE85-009105] N86-10331
NICKEL CADMIUM BATTERIES
Nickel-cadmium battery conditioner and tester apparatus
[AD-D011770] N86-10642
NIGHT VISION
Mild hypoxia and visual performance with night vision goggles
[AD-A156969] N86-10787
NITRIC OXIDE
Emissions of NOx, SOx and VOC from Antropogenic sources
[PB85-193530] N86-10688
NITRIDES
Continuous fiberization of silicon-carbide-nitride precursor resin N86-10168
NITRO COMPOUNDS
Development of new ammonium nitrate composite explosives
[DE85-014252] N86-10356
Composite explosives for metal acceleration: The effect of detonation temperature
[DE85-013982] N86-10359
NITROGEN
Membrane research in energy and solvent recovery from industrial effluent streams
[DE85-014583] N86-10682
NITROGUANIDINE
Properties of plastic-bonded nitroguanidine
[DE85-015316] N86-10358
NOISE POLLUTION
Recent advances in the analysis of exhaust mufflers N86-10587
NOISE PREDICTION
Recent advances in the analysis of exhaust mufflers N86-10587
NOISE PREDICTION (AIRCRAFT)
Summary of work on jet noise prediction
[ESDU-BR-62636] N86-10909
NOISE PROPAGATION
A study of derivative filters using the discrete Fourier transform
[NASA-CR-176224] N86-10825
NOISE REDUCTION
A study of Morrison's iterative noise removal method
[NASA-CR-176222] N86-10823
Always-convergent iterative noise removal and deconvolution for image data
[NASA-CR-176223] N86-10824
A study of derivative filters using the discrete Fourier transform
[NASA-CR-176224] N86-10825
A superconducting tunnel junction receiver for millimeter-wave astronomy N86-11041
NONDESTRUCTIVE TESTS
Report on an overseas visit
[AD-A156603] N86-10037
Liquid crystal non-destructive inspection of metals
[AD-D011772] N86-10316
Nondestructive control of thick structures made without disassembling
[PV-43-954/F/3] N86-10564
Study of statis and dynamic stress effects in nonlinear solids
[NASA-CR-176236] N86-10578
Nondestructive corrosion test of aluminum alloy structures
[PV-43-954/F/2] N86-10594
Exploratory development for a high reliability flaw characterization module
[AD-A156632] N86-10916
NONFERROUS METALS
Liquid crystal non-destructive inspection of metals
[AD-D011772] N86-10316
NONISOTHERMAL PROCESSES
Analysis of large, non-isothermal elastic-visco-plastic deformations
[NASA-CR-176220] N86-10588
NONLINEAR EQUATIONS
Topics in nonlinear wave theory with applications N86-10367
Three-dimensional vibration analysis of a uniform beam with offset inertial masses at the ends
[NASA-TM-86393] N86-10580
Well-posed questions and exploration of the space of parameters in linear and non linear inversion
[PN-84/13] N86-10858
A modified modified Korteweg-deVries equation
[PN-84/27] N86-10859
NONLINEAR EVOLUTION EQUATIONS
On the absolute continuity of elliptic measures
[CTH-MATH-1984-28] N86-10873
NONLINEAR FILTERS
Computational techniques for the analysis and design of digital communication systems
[AD-A156945] N86-10407
NONLINEAR SYSTEMS
Control concepts for in-flight simulation including actuator nonlinearities and time delays
[DFVLR-FB-85-24] N86-10047
Modeling and control of nonlinear systems N86-10362
Large eddy interactions in a turbulent channel flow
[NASA-TM-86757] N86-10464
Constitutive modeling for isotropic materials (HOST)
[NASA-CR-174980] N86-10589
Superconvergent tracking and invariant surfaces in phase space
[DE85-013051] N86-10995
NONLINEARITY
A study of the aerodynamic performance of Weis-Fogh wings N86-10012

Nonlinear methods for spacecraft attitude maneuvers [AD-A156956] N86-10275
Nonlinear propagation of elastoplastic waves in Ke penetrators (excerpts) [DE85-011450] N86-10318
Topics in nonlinear wave theory with applications N86-10367
An analytical and numerical study of the buckling behavior of fiber-reinforced beams N86-10566
Load space formulation of reliability for nonlinear random structural systems N86-10570
Analysis of large, non-isothermal elastic-visco-plastic deformations [NASA-CR-176220] N86-10588
Always-convergent iterative noise removal and deconvolution for image data [NASA-CR-176223] N86-10824
Advanced development of BEM for two and three dimensional nonlinear analysis N86-10855
Bounding solutions of geometrically nonlinear viscoelastic problems [NASA-CR-176219] N86-10860

NONSTABILIZED OSCILLATION
Oscillations of a viscoelastic liquid drop in zero-gravity N86-10240

NORTH SEA
Monthly Bulletin North Sea: Volume 2, January 1985 [KNMI-167-VOL-2] N86-10732

NOSE TIPS
Erosion-resistant nosetip construction [AD-D011787] N86-10289

NOTCH STRENGTH
Three-dimensional stress singularities in anisotropic materials and composites N86-10286

NOZZLE DESIGN
Operating characteristics of the multiple critical Venturi System and secondary calibration nozzles used for weight-flow measurements in the Langley 16-foot transonic tunnel [NASA-TM-86405] N86-10016

NOZZLE EFFICIENCY
Experimental performance of a 1-kilowatt arcjet thruster [NASA-TM-87131] N86-10281

NOZZLE FLOW
Theoretical specific impulse for two-phase flow in nozzle of rocket-ramjet engine: A simple estimation method N86-10005
Operating characteristics of the multiple critical Venturi System and secondary calibration nozzles used for weight-flow measurements in the Langley 16-foot transonic tunnel [NASA-TM-86405] N86-10016

NUCLEAR CHEMISTRY
Evaluation of the International Atomic Energy Agency (IAEA) Safeguards Analytical Laboratory quality assurance program [DE85-012078] N86-10953

NUCLEAR EXPLOSION EFFECT
Microphysical/mesoscale aspects of nuclear winter and new directions in assessments [DE85-013479] N86-10718

NUCLEAR EXPLOSIONS
Smoke inputs to climate models: Optical properties and height distribution for nuclear winter studies [DE85-011363] N86-10717
Microphysical/mesoscale aspects of nuclear winter and new directions in assessments [DE85-013479] N86-10718

NUCLEAR FUEL ELEMENTS
On-line gamma-ray data acquisition at the Power Burst facility [DE85-011957] N86-10954

NUCLEAR FUSION
ORR core re-configuration measurements to increase the fast neutron flux in the Magnetic Fusion Energy (MFE) experiments [DE85-013520] N86-10958

NUCLEAR PHYSICS
The 1984 bibliography of atomic and molecular processes [DE85-010563] N86-10926
Report on the engineering test of the LBL 30 second neutral beam source for the MFTF-B project [DE85-013317] N86-10962

NUCLEAR POWER PLANTS
Methods for developing jam-resistant security communications networks at fixed-site facilities [DE85-012032] N86-10408

NUCLEAR RADIATION
Hgl sub 2 crystal growth for nuclear detectors N86-10066

NUCLEAR RESEARCH AND TEST REACTORS
Activities report in safety N86-10365

NUCLEAR SCATTERING
Charge exchange in slow collisions of atoms and molecules N86-10922

NUCLEAR WARFARE
An anthology: Rationale for a US ballistic missile defense (1969 - 1984) [AD-A156781] N86-10199

NUCLEAR WEAPONS
Microphysical/mesoscale aspects of nuclear winter and new directions in assessments [DE85-013479] N86-10718

NUCLEATE BOILING
Nucleate pool boiling in subcooled liquid under microgravity: Results of TEXUS experimental investigations N86-10250

NUCLEATION
Theoretical problems in materials science N86-10088
Containerless studies of nucleation and undercooling N86-10102
Extension of Ostwald ripening theory N86-10104
Bulk formation of metallic glasses and amorphous silicon from the melt N86-10154
Glass research N86-10157
Crystal nucleation and glass formation in metallic alloy melts N86-10233
Undercooling investigations on the easy glass former Pd-Cu-Si N86-10259
Crystal growth from solutions and nucleation from the vapor phase — Spacelab N86-10267
A study of the applicability of nucleation theory to quasi-thermodynamic transitions of second and higher Ehrenfest-order [NASA-CR-176238] N86-11059
A study of the applicability of nucleation theory to quasi-thermodynamic transformations of second and higher Ehrenfest-order [NASA-CR-176230] N86-11060

NUCLEI (NUCLEAR PHYSICS)
Direct mass measurements in the light neutron-rich region using a combined energy and time-of-flight technique [DE85-012758] N86-10963

NUCLEONICS
Information on continuum states from feeding times and total (GAMMA) spectra measured with BGO suppressed detectors [DE85-013868] N86-10961

NUCLEONS
Soudan 2 data acquisition and trigger electronics [DE85-013864] N86-10443

NULL HYPOTHESIS
Superefficient estimation of power functions in simulation experiments [B8562445] N86-10893

NUMBER THEORY
Freezer model using a population balance approach for steady-state, direct-contact, secondary refrigerant, freeze desalination N86-10361
Some remarks about cusp forms: Holomorphic and non-holomorphic [CTH-MATH-1984-26] N86-10902
Galois descent and class groups of orders [CTH-MATH-1985-09] N86-10904

NUMERICAL ANALYSIS
Numerical procedure for three-dimensional hypersonic viscous flow over aerobrake configuration [NASA-TM-58269] N86-10018
Analysis of transitions between ferroelectric and antiferroelectric states under conditioning of uniaxial strain [DE85-014468] N86-10350
An analytical and numerical study of the buckling behavior of fiber-reinforced beams N86-10566

NUMERICAL CONTROL
Dissecting the cow [DE85-013369] N86-10601
Providing automated control for PBFA-2 [DE85-012867] N86-10928
Timing system control software in the SLC [DE85-013380] N86-11024

NUMERICAL WEATHER FORECASTING
The boundary condition in a numerical model of atmospheric flows over fixed interfaces [GKSS-85-E-10] N86-10722

NUTS (FASTENERS)
Over-center toggle latch [AD-D011753] N86-10556
Termination load carrying device [AD-D011800] N86-10558

NYLON (TRADEMARK)
Age-life prediction of nylon 66 parachute materials. Part 2: Changes in the chemical and physical properties of materials on aging [AD-A156909] N86-10347

NYQUIST FREQUENCIES
The interpolation of signals sampled at less than the Nyquist rate N86-10368

O

OCEAN BOTTOM
In-situ geophysical investigations into the nature of the oceanic crust N86-10725
A quantitative method for analyzing the roughness of the seafloor N86-10726
Long term statistical measurements of environmental acoustics parameters in the arctic. AEAS report number 2. Low frequency transmission loss measurements in the central arctic ocean [AD-A156576] N86-10727

OCEAN CURRENTS
Ocean energy technology program summary [DE85-013102] N86-10731

OCEAN DYNAMICS
Formation of waves by ground motion [PM/84/09] N86-10706
A processor for the study of ocean fine-scale patches [AD-A157019] N86-10730

OCEAN MODELS
Formation of waves by ground motion [PM/84/09] N86-10706

OCEAN THERMAL ENERGY CONVERSION
Ocean energy technology program summary [DE85-013102] N86-10731

OCEANOGRAPHIC PARAMETERS
A processor for the study of ocean fine-scale patches [AD-A157019] N86-10730
Monthly Bulletin North Sea: Volume 2, January 1985 [KNMI-167-VOL-2] N86-10732

OCEANS
In-situ geophysical investigations into the nature of the oceanic crust N86-10725

OIL POLLUTION
Utilization of satellite remote sensing for the monitoring of oil pollution and marine ecosystems in Indonesia. A Tropical Earth Resources Satellite program (TERS) case study implemented for the NLR, Delft N86-10640

OILS
Surface tension induced instabilities in reduced gravity: The Benard problem N86-10117
Heat transfer in condensing and evaporating two-component, two-phase flow inside a horizontal tube N86-11058

ON-LINE SYSTEMS
Acquaintance with on line literature research. An introduction for education at the Chemical Technology Section N86-11081
On line astronomical image processing using microcomputers N86-11121

ONE DIMENSIONAL FLOW
Time-implicity simulation of particle-fluid systems [DE85-012944] N86-10471

OPEN CHANNEL FLOW
Experiments and computations on unsteady separating flow in an expanding flume [REPT-2-84] N86-10477

OPENINGS
Optimal design of portal frames against buckling N86-10572

OPERATING COSTS
F-16X MSIP (Multi-national Staged Improvement Program) case example: Operating and support cost estimation using VAMOSC (Visibility And Management Of Operating and Support Costs) [AD-A156893] N86-10006

OPERATIONAL AMPLIFIERS
High output programmable signal current source for low output impedance applications [AD-D011751] N86-10423

OPERATIONS RESEARCH
Operations research applications [ARW-03-THE-BDK/ORS/83-06] N86-10901
Failures and successes of quantitative methods in management [ARW-03-THE-BDK/ORS/83-06] N86-11076

OPERATOR PERFORMANCE
Effect of various doses of some vitamins on non-specific mechanisms of adaptation of man N86-10750

OPERATORS (MATHEMATICS)
Lie algebraic methods for charged particle beams and light optics N86-10970

OPTICAL COMPUTERS
Spatial frequency multiplexed coherent optical processor for calculating generalized moments [AD-D011816] N86-10975

OPTICAL COUPLING
A fiber-linked version of project TRIO --- telescope array N86-11105

OPTICAL DATA PROCESSING
Prospects for creation of optical digital high-performance computers N86-10810
OPTICAL DISKS
Optical disc transport system
[AD-D011779] N86-10974
OPTICAL EMISSION SPECTROSCOPY
Rapid evaluation of ion thruster lifetime using optical emission spectroscopy
[NASA-TM-87103] N86-10280
OPTICAL EQUIPMENT
Always-convergent iterative noise removal and deconvolution for image data
[NASA-CR-176223] N86-10824
OPTICAL HETERODYNING
Experimental investigations of pulse-pulse interference in heterodyne detection
[DFVLR-FB-85-26] N86-10544
The DUO: Far infrared heterodyne concept for space interferometry N86-11125
OPTICAL MEASUREMENT
Advanced optical measurement techniques N86-10174
Time resolved flow velocity and concentration measurements using a travelling thermal lens
[AD-A156706] N86-10541
Optical detection of photoacoustic pulses in thin silicon wafers
[AD-A156705] N86-10977
OPTICAL MEASURING INSTRUMENTS
Photonic diagnostics and pulsed power research
[DE85-013752] N86-10940
OPTICAL MEMORY (DATA STORAGE)
Optical disc transport system
[AD-D011779] N86-10974
OPTICAL PROPERTIES
Crystallization, optical and chemical properties of fluoride glasses N86-10149
Polymer engineering: Polymeric and molecular electronic, dielectric and optical properties for device applications
[AD-A156671] N86-10344
Determination of optical properties by third-harmonic generation in noble gases in unfocused laser beams N86-10535
OPTICAL PUMPING
Scaling studies of solar pumped lasers
[NASA-CR-176240] N86-10540
OPTICAL TRANSFER FUNCTION
Always-convergent iterative noise removal and deconvolution for image data
[NASA-CR-176223] N86-10324
OPTICAL WAVEGUIDES
Extended precision in video bandwidth analog to digital converter using optical techniques
[AD-D011745] N86-10422
Fiber optic system for measuring electric fields
[AD-D011830] N86-10976
OPTIMAL CONTROL
Optimal control modeling of lower extremity musculoskeletal motion N86-10853
OPTIMIZATION
Optimum design of an aircraft wing structure with multiple constraints by the direct-vision criteria method N86-10004
High temperature properties of SiC materials
[BMFT-FB-T-85-047] N86-10353
Modeling and control of nonlinear systems N86-10362
Design sensitivity analysis and optimization of built-up structures N86-10565
Strength of shells under local transverse loads N86-10568
Harmonic distortion reduction technique for data acquisition
[AD-D011771] N86-10799
Minimization of programmable logic arrays
[EUT-84-E-145] N86-10803
State assignment in sequential circuits
[EUT-85-E-146] N86-10846
OPTOMETRY
Measurement of visual contrast sensitivity
[AD-D011776] N86-10973
ORBITAL ASSEMBLY
Test and evaluate passive orbital disconnect struts (PODS 3)
[NASA-CR-177368] N86-10274
ORBITAL LIFETIME
User's guide for Langley Research Center Orbital Lifetime program
[NASA-TM-87567] N86-10828
ORBITAL MECHANICS
User's guide for Langley Research Center Orbital Lifetime program
[NASA-TM-87567] N86-10828
ORBITS
Lumped geopotential harmonics of order 14, from the orbit of 1967-11G
[AD-A156627] N86-10190
ORCHARDS
On the use of L-band multipolarization airborne SAR for surveys of crops, vineyards, and orchards in a California irrigated agricultural region N86-10627
ORGANIC CHEMISTRY
Growth of organic crystals by Ostwald ripening N86-10058
ORGANIC COMPOUNDS
Volatile organic compounds in indoor air: A survey of various structures
[PB85-198356] N86-10687
Emissions of NOx, SOx and VOC from Antropogenic sources
[PB85-193530] N86-10688
Evaluation of Passive Sampling Devices (PSDs)
[PB85-196418] N86-10689
ORGANIZING
Remote sensing study project East Gelderland (Netherlands). Part 2: Remote sensing flights in 1982 and 1983; organization aspects N86-10639
OROGRAPHY
Observations of the snow cover in the southern part of the Buryat Autonomous Soviet Socialist Republic
[NASA-TM-77910] N86-10613
Laws of distribution of the snow cover on the greater Caucasus (Soviet Union)
[NASA-TM-77911] N86-10614
The effects of orography on land-atmosphere turbulent exchange processes N86-10702
ORTHOGONAL FUNCTIONS
Large eddy interactions in a turbulent channel flow
[NASA-TM-86757] N86-10464
ORTHOPHOTOGRAPHY
Orthophotomapping from metric camera imagery --- Spacelab N86-10487
Stereo-orthophotos in various map projections N86-10488
Evaluation of the accuracy of the metric camera images for the production of line maps and orthophotos N86-10490
ORTHOSTATIC TOLERANCE
Study of hypokinesia and acceleration effects on human chromosomes N86-10740
Vestibular resistance and blood circulation changes in orthostatic position during hyperthermia N86-10758
ORTHOTROPIC SHELLS
Stiffened and prestressed composite overwrapped pressure vessels N86-10547
OSCILLATING FLOW
Oscillations of subsonic flow in an abruptly expanding circular duct
[MPIS-16/1984] N86-10028
Measurements of the critical Marangoni number of the laminar-oscillatory transition of thermocapillary convection in floating zones N86-10242
OSCILLATIONS
Theory of non-planar orbits
[DE85-013284] N86-11018
OTS (ESA)
Digital transmission experiments with the Orbital Test Satellite
[EUT-84-E-144] N86-10270
OUTPUT
Phase-coded pulse expander-compressor
[AD-D011812] N86-10375
OXIDATION
Study of the reactive-element effect in oxidation of Fe-Cr alloys using transverse section analytical electron microscopy N86-10087
Oxidation behavior of glassy alloys N86-10158
Catalytic activity of shock modified ZnO for CO oxidation and methanol synthesis
[DE85-014704] N86-10300
Chemical kinetics and cellular structure of detonations in hydrogen sulphide and air
[DE85-009408] N86-10304
Evaluation and prediction of long-term environmental effects on non metallic materials
[NASA-CR-178495] N86-10340
Kinetics of biological ferrous iron oxidation
[DE85-014616] N86-10736
OXIDATION RESISTANCE
High temperature properties and characterization of S3-N4 materials
[BMFT-FB-T-85-046] N86-10352
OXIDES
The role of entrained surface oxides in RS-PM aluminum alloys on resultant structures and properties N86-10085
Environmental degradation of materials: Surface chemistry related to stress corrosion cracking N86-10099
Rapid solidification of magnetic oxides N86-10152
OXYGEN
High-temperature controlled redox crystallization studies N86-10178
Mild hypoxia and visual performance with night vision goggles
[AD-A156969] N86-10787
Adsorption of oxygen on single crystal tin at liquid helium temperatures N86-11044
OXYGEN CONSUMPTION
Reaction of rabbit respiration system to hypoxic stimulus in nitrogen-oxygen medium at elevated pressure N86-10760
OXYGEN METABOLISM
Indices of blood oxygen transporting properties and erythropoiesis in rats after prolonged stay in nitrogen-oxygen mixture at elevated pressure N86-10761
OXYGEN SPECTRA
Selected tables of atomic spectra. Atomic energy levels and multiplet table O3
[NBS/NSRDS-3/11] N86-10923
OZONE
Chemical kinetics and photochemical data for use in stratospheric modeling
[NASA-CR-176198] N86-10707

P

P WAVES
Structural discontinuity within the southern California continental margin: Seismic and gravity models of the western Transverse Ranges N86-10699
P-N JUNCTIONS
P-N junction controlled field emitter array cathode
[AD-D011815] N86-10416
P-TYPE SEMICONDUCTORS
W-shaped diffused stripe GaAs/AlGaAs laser
[AD-D011818] N86-10538
PACKAGING
Miniature radar packaging
[DE85-014598] N86-10410
PAIR PRODUCTION
Search for heavy neutrinos produced in e(+)e(-) annihilation
[DE85-013372] N86-11035
PAKISTAN
Report of the Workshop on Geologic Applications of Remote Sensing to the Study of Sedimentary Basins
[E86-10002] N86-10599
Chronologic analysis of terrestrial sediments and basin evolution N86-10602
PALEONTOLOGY
Paleogene vertebrate paleontology, geology and remote sensing in the Wind River Basin N86-10609
Paleontology and stratigraphy of Lower Cambrian and upper Proterozoic sediments, Caborca region, northwestern Sonora, Mexico N86-10692
PALLADIUM
The interaction of small metal particles with refractory oxide supports
[NASA-CR-176228] N86-11047
PANELS
Load-deflection tests and computer analyses of a high-precision adhesive-bonded antenna reflector panel N86-10389
Inelastic analysis of frame structures including member and joint shears N86-10573
Fatigue of graphite/epoxy buffer strip panels with center cracks
[NASA-TM-87595] N86-10581
PANT PROGRAM
Erosion-resistant nosetip construction
[AD-D011787] N86-10289
PARABOLIC FLIGHT
Advanced optical measurement techniques N86-10174
PARACHUTE FABRICS
Age-life prediction of nylon 66 parachute materials. Part 2: Changes in the chemical and physical properties of materials on aging
[AD-A156909] N86-10347
PARAFFINS
Romanian plant produces protein concentrate from paraffin-nourished yeasts N86-10741
PARALLEL PROCESSING (COMPUTERS)
An improved FFT (Fast fourier transform) for a four parallel pipe SIMD arithmetic processor
[AD-A156625] N86-10863
PARALLEL PROGRAMMING
Soudan 2 data acquisition and trigger electronics
[DE85-013864] N86-10443

PARAMETER IDENTIFICATION
Comment on Determination of Aerodynamic Coefficients for a Reentry Body by Means of the Kalman Filter Method N86-10011
System modeling and identification of equivalent systems with and without compensating time delay for control-augmented aircraft
[ESA-TT-852] N86-10043
Spillover minimization in self-adjoint distributed-parameter systems with direct output feedback N86-10852
Multivariable partial realization and the aspect of uniqueness
[ER-83/09] N86-10879
PARAMETERIZATION
Theoretical specific impulse for two-phase flow in nozzle of rocket-ramjet engine: A simple estimation method N86-10005
Field-independent normalization of SSC Collider Ring costs
[DE85-012425] N86-10997
PARAMETRIC AMPLIFIERS
Elastic wave gyrometer. Experiments with a parametric wave device
[REPT-26/5005/HF/AR] N86-10533
PARTIAL DIFFERENTIAL EQUATIONS
Alternating direction methods on multiprocessors: An extended abstract
[AD-A156722] N86-10794
A modified modified Korteweg-deVries equation
[PN-84/27] N86-10859
A mesh moving technique for time dependent partial differential equations in two space dimensions
[AD-A156663] N86-10866
A note on the differenciability of center manifolds
[ZW-8414] N86-10905
PARTICLE ACCELERATION
Potential structures and particle acceleration on auroral field lines
[AD-A156694] N86-10708
PARTICLE ACCELERATORS
Revision of and documentation for the standard version of the Poisson-Group codes
[DE85-012659] N86-10837
Providing automated control for PBFA-2
[DE85-012867] N86-10928
AGS polarized H(-) source
[DE85-013296] N86-10935
New particle searches
[DE85-014073] N86-10942
Separated K(-) beams (10 GeV and above)
[DE85-012527] N86-10989
Beginnings of remote handling at the RAL Spallation Neutron Source
[DE85-012681] N86-11001
Proceedings of a Workshop on Electroweak Symmetry Breaking
[DE85-004444] N86-11008
Advances in data acquisition system technology for PBFA 2
[DE85-012860] N86-11011
Engineering high reliability, low-jitter Marx generators
[DE85-012811] N86-11013
SLC positron damping ring optics design
[DE85-013054] N86-11014
Computer control of rf at SLAC
[DE85-013065] N86-11015
Theory of non-planar orbits
[DE85-013284] N86-11018
Photoactivation of PBFA-2
[DE85-013439] N86-11019
Unicell structure for superconducting storage rings
[DE85-013303] N86-11022
Timing system control software in the SLC
[DE85-013380] N86-11024
RHIC lattice
[DE85-013289] N86-11026
PARTICLE BEAMS
Revision of and documentation for the standard version of the Poisson-Group codes
[DE85-012659] N86-10837
Providing automated control for PBFA-2
[DE85-012867] N86-10928
Parasitic mode losses versus signal sensitivity in beam position monitors
[DE85-014367] N86-10964
Separated K(-) beams (10 GeV and above)
[DE85-012527] N86-10989
Noninterceptive techniques for the measurement of longitudinal parameters for intense H(-) beams
[DE85-012662] N86-10992
Ferrite kicker magnet for the IAMPF switchyard upgrade
[DE85-012657] N86-10996
Advances in data acquisition system technology for PBFA 2
[DE85-012860] N86-11011
High-resolution phosphor screen beam profile monitor
[DE85-013074] N86-11012
Photoactivation of PBFA-2
[DE85-013439] N86-11019
RHIC lattice
[DE85-013289] N86-11026
PARTICLE EMISSION
Ultraviolet spectroscopy of the Earth's dayglow and magnetosphere cleft N86-10696
PARTICLE INTERACTIONS
Improved particle-velocity transducer for equation-of-state experiments
[DE85-013204] N86-10532
Cooperative emission by two different atoms into surface plasmons
[AD-A157033] N86-10925
Supersonic metal cluster beams
[DE85-014321] N86-10966
PARTICLE MASS
Variational estimates for the mass gap of SU(2) Euclidean lattice gauge theory
[NIKHEF-H/84-13] N86-10883
Two-loop large Higgs mass corrections to vector boson self-couplings
[NIKHEF-H/84-15] N86-11038
PARTICLE MOTION
Electrophoresis technology N86-10144
Measurement and resulting first and second order approximations for a 9 deg bending magnet in LAMPF's 750-keV transport
[DE85-012691] N86-10930
PARTICLE SIZE DISTRIBUTION
Production of large-particle-size monodisperse latexes in microgravity N86-10146
Binder-filler interaction in energetic polymers
[AD-A156752] N86-10345
PARTICLE TELESCOPES
The intensified multi CCD camera --- spaceborne interferometers N86-11122
PARTICLE TRACKS
Tracking studies on the effects of magnet multipoles on the aperture of the RHIC heavy ion collider
[DE85-013282] N86-11023
PARTICLE TRAJECTORIES
Lie algebraic methods for charged particle beams and light optics N86-10970
PARTICLES
Particle cloud combustion experiment N86-10160
New particle searches
[DE85-014073] N86-10942
Solar flares and magnetospheric particles: Investigations based upon the ONR-602 experiment
[AD-A156583] N86-11142
PARTITIONS (MATHEMATICS)
On the analytical evaluation of the partition function for unit hypercubes in four dimensions --- lattice theory
[NIKHEF-H/84-12] N86-10882
PASSENGERS
The air traffic demand in passenger travel of the Federal Republic of Germany 1990 - 2000. Update of the DFVLR air traffic forecast
[DFVLR-MITT-85-06] N86-10031
PASSIVITY
Passivation of steel with aqueous amine solutions
[AD-D011749] N86-10314
PATTERN RECOGNITION
Analysis of edge detection algorithms on DIAL (Digital Image Analysis Laboratory)
[AD-A156735] N86-10630
Special purpose hardware architectures for language recognition
[AD-A156634] N86-10793
PAYLOAD INTEGRATION PLAN
The first German Spacelab mission D1 reports --- Spacelab payloads
[PR-2] N86-10188
PAYLOADS
Guidance and control of a cable based payload pickup system N86-10046
PEPTIDES
Homocarnosin in rat brain during adaptation to cold N86-10762
PERCHLORATES
Composite explosives for metal acceleration: The effect of detonation temperature
[DE85-013982] N86-10359
PERFORMANCE PREDICTION
A comparative analysis of a CV helicopter and a JVX (Joint Services Advanced Vertical Lift) tilt-rotor aircraft in an aircraft carrier based ASW (Anti-Submarine Warfare)
[AD-A156871] N86-10041
High temperature mechanical testing of a cylindrical weave carbon-carbon composite
[AD-A156639] N86-10591
Optical testing of large telescopes using multiple subapertures N86-10971
PERFORMANCE TESTS
Test and evaluate passive orbital disconnect struts (PODS 3)
[NASA-CR-177368] N86-10274
Explosive initiation by very small conical shaped charge jets
[DE85-009443] N86-10357
Test results for 20-GHz GaAs FET spacecraft power amplifier
[NASA-TM-87072] N86-10379
Implementation issues for algorithmic VLSI (Very Large Scale Integration) processor arrays
[AD-A156699] N86-10432
Type of new Chinese-produced high-speed camera and its utilization in detonation physics experiments
[DE85-015191] N86-10529
Advanced Gas Turbine (AGT) powertrain system development for automotive applications report
[NASA-CR-174886] N86-11087
PERIPHERAL EQUIPMENT (COMPUTERS)
Elektronika MS 1603 high-speed peripheral processor N86-10611
Diagnostics of peripheral processors and controllers N86-10612
Shipboard non-tactical computer systems of the US Navy
[AD-A156769] N86-10849
PERMEABILITY
KRAK: A computer program for two-phase, two-component porous flow and fracture propagation, revision
[DE85-014264] N86-10469
PERSIAN GULF
A geological structural analysis of the southeastern Zagros (Iran) ranges based on metric camera photos N86-10492
PERSONNEL MANAGEMENT
Psychological Sciences Division 1984 programs
[AD-A156631] N86-10779
On the structure of manpower planning, a contribution of simulation experiments with decomposition methods
[MANPOWER-PLANNING-28] N86-11073
Aspects of manpower planning at a Dutch university, an example of aggregation and decomposition methods in manpower planning
[MANPOWER-PLANNING-29] N86-11074
On the structure of manpower planning, a contribution of simulation experiments with aggregation methods
[MANPOWER-PLANNING-30] N86-11075
PERSONNEL SELECTION
Standardization of tasks: Approach planning --- human performance assessment
[IZF-1984-19] N86-10782
PERTURBATION
Nonlinear methods for spacecraft attitude maneuvers
[AD-A156956] N86-10275
Computation of flow regimes in parameter space for the AGCE
[NASA-CR-178480] N86-10705
PETROLEUM PRODUCTS
Evaluation of the 90-day inhalation toxicity of petroleum and oil shale JP-5 jet fuel
[AD-A156815] N86-10675
PETROLOGY
Stratigraphy, petrology, depositional and post-depositional histories and their effects upon reservoir properties of the Parkman Formation of the Mesa Verde group, Powder River Basin, Wyoming N86-10691
PH
Hormone purification by isoelectric focusing N86-10135
PH FACTOR
Hormone purification by isoelectric focusing N86-10135
Automated analysis of digital images generated by two-dimensional gel electrophoresis
[DE85-011906] N86-10526
PHARMACOLOGY
Mechanism of adaptogenic action of prickly eleutercoccus on man during heat stress N86-10757
PHASE CHANGE MATERIALS
Metastable phase formation in Ni-implanted Al: An analytical electron microscope investigation
[DE85-009105] N86-10331
PHASE DEVIATION
Aperture synthesis with or without phase information for kilometric arrays interpolation algorithms for stabilized image reconstruction N86-11124

PHASE DIAGRAMS
Weld metal hot-cracking of hastelloy alloys C-22 and C-276: A study by analytical electron microscopy
[DE85-009437] N86-10324
PHASE LOCKED SYSTEMS
High sensitivity millimeter-wave measurement apparatus
[AD-D011786] N86-10373
Sample data phase locked loop for adaptive Doppler tracker
[AD-D011788] N86-10374
PHASE MODULATION
Phase-coded pulse expander-compressor
[AD-D011812] N86-10375
Phase coded pulse expander-compressor
[AD-D011817] N86-10376
Amplitude and phase modulation in fin-lines electrical tuning
[AD-D011813] N86-10415
PHASE SHIFT
Method for tuning a phased array antenna
[AD-D011768] N86-10372
Determination of symmetry and phase in human visual response functions: Theory and experiments N86-10769
High-power rf controls for the NBS-Los Alamos racetrack microtron
[DE85-012658] N86-10993
PHASE SHIFT CIRCUITS
Pulse compression system
[AD-D011833] N86-10417
PHASE SWITCHING INTERFEROMETERS
Radio astronomy experience in image reconstruction. A history lesson for optical astronomers N86-11117
PHASE TRANSFORMATIONS
Experimental and theoretical studies of wetting and multilayer adsorption
[NASA ORDER H-27954B] N86-10121
Impurity extraction by droplets N86-10122
Analysis of transitions between ferroelectric and antiferroelectric states under conditioning of uniaxial strain
[DE85-014468] N86-10350
Measurement of the density of base fluids at pressures 0.422 to 2.20 GPa
[NASA-TM-87114] N86-10551
New approach to multiphase equilibria: Application to high-pressure physics problems
[DE85-013820] N86-10907
High-pressure release-wave measurements and phase transformation in CaCO3
[DE85-012592] N86-11055
PHASED ARRAYS
Angle set-on apparatus
[AD-D011766] N86-10371
Method for tuning a phased array antenna
[AD-D011768] N86-10372
Optical/IR telescope arrays: A study of their potential for satisfying observational requirements in astronomy for a large aperture system in the 1990s and beyond
[REPT-15] N86-11094
PHENOLS
Sediment characterization. Task 2: Instream contaminant study, volume 1
[DE85-013502] N86-10683
PHOSPHATES
Thermal expansion of glasses in the solid and liquid phases
[DE85-013953] N86-10351
PHOSPHORIC ACID FUEL CELLS
Effect of H2S and COS in the fuel gas on the performance of ambient pressure phosphoric acid fuel cells
[DE85-013913] N86-10446
PHOSPHORUS
The mechanism of erosion of metallic materials under cavitation attack
[NASA-TM-87133] N86-10552
Magnetic properties of doped semiconductors
[DE85-012090] N86-11053
PHOTOACOUSTIC SPECTROSCOPY
Optical detection of photoacoustic pulses in thin silicon wafers
[AD-A156705] N86-10977
PHOTOCHEMICAL REACTIONS
Chemical kinetics and photochemical data for use in stratospheric modeling
[NASA-CR-176198] N86-10707
PHOTODECOMPOSITION
Age-life prediction of nylon 66 parachute materials. Part 2: Changes in the chemical and physical properties of materials on aging
[AD-A156909] N86-10347
Photoionization technique for growth of metallic films
[AD-D011760] N86-10426
PHOTODIODES
Making the right choice --- silicon photodiodes N86-10669
PHOTOELECTRIC EMISSION
Nature of photoemission into dielectric fluids
[DE85-013017] N86-10945
PHOTOELECTRIC MATERIALS
High-brightness photoemitter injector for electron accelerators
[DE85-012673] N86-10929
PHOTOELECTRONS
Ultraviolet spectroscopy of the Earth's dayglow and magnetosphere cleft N86-10696
PHOTOGEOLOGY
LANDSAT TM image data quality analysis for energy-related applications
[E85-10109] N86-10597
Report of the Workshop on Geologic Applications of Remote Sensing to the Study of Sedimentary Basins
[E86-10002] N86-10599
Some opinions on remote sensing and geologic studies N86-10600
Position paper: Workshop on Geologic Applications of Remote Sensing to the Study of Sedimentary Basins N86-10601
Chronologic analysis of terrestrial sediments and basin evolution N86-10602
Tertiary and quaternary research with remote sensing methods N86-10603
Multisensor data integration techniques N86-10604
Foreland basin structures and remote sensing N86-10608
PHOTOGRAMMETRY
Metric Camera Workshop --- Spacelab
[ESA-SP-209] N86-10485
High-resolution image data from the Space Shuttle N86-10494
Evaluation of metric camera images at the University of London --- Spacelab N86-10495
OEEPE participation in testing metric camera photography --- European Organization for Experimental Photogrammetric Investigations (OEEPE) N86-10507
An example of single model orientation of metric camera stereophotographs --- Spacelab N86-10520
Tectonic analysis of typical fold structures in the Zagros Mountains (Iran) by the application of quantitative photogrammetric methods on metric camera data --- Spacelab N86-10521
PHOTOGRAPHY
Fundamental studies of droplet combustion at reduced gravity N86-10165
Type of new Chinese-produced high-speed camera and its utilization in detonation physics experiments
[DE85-015191] N86-10529
PHOTOINTERPRETATION
Metric Camera Workshop --- Spacelab
[ESA-SP-209] N86-10485
Erosion control and watershed management by Spacelab photography N86-10493
Topographic interpretation of metric camera images: An example in Somalia --- Spacelab N86-10508
Thematic investigations in France based on metric camera imagery --- Spacelab N86-10509
Evaluation of metric camera photos --- Spacelab; alpine snow cover N86-10515
Interpretation of Spacelab-1 photographs for the generation of 1:200000 topographic map N86-10518
The effect of vegetation type, microrelief, and incidence angle on radar backscatter N86-10619
Age-dating volcanic and alluvial surfaces with multipolarization data N86-10620
The effects of merging TM and A/C radar on wetland classification N86-10621
Strategies for analyzing mixed pixels in remotely sensed imagery N86-10623
Mapping diverse forest cover with multipolarization airborne radar N86-10625
Remote sensing
[NOTA-1535] N86-10638
PHOTOIONIZATION
Photoionization technique for growth of metallic films
[AD-D011760] N86-10426
Theoretical investigation of electron-positive ion-atom interactions
[DE85-013019] N86-10939
Nature of photoemission into dielectric fluids
[DE85-013017] N86-10945
PHOTOMAPPING
Satellite use for men --- West German space program N86-10180
How Antarctica was unveiled. Masterpieces of Frankfurt topographic surveyors. A part of the German Antarctica research program N86-10181
Satellite data even for a poultry farm. A development for Tanzania. Image evaluation following new ways N86-10182
With Argus eyes from space. Satellite Diagnosis for Upper Volta. Seven maps without mystery N86-10183
Metric Camera Workshop --- Spacelab
[ESA-SP-209] N86-10485
Digital elevation model from Spacelab metric camera photographs N86-10486
Orthophotomapping from metric camera imagery --- Spacelab N86-10487
Stereo-orthophotos in various map projections N86-10488
Restitution of Spacelab photography by analog stereoplotter N86-10489
Evaluation of the accuracy of the metric camera images for the production of line maps and orthophotos N86-10490
Photomapping in different climatic zones --- Spacelab metric camera N86-10491
High-resolution image data from the Space Shuttle N86-10494
Evaluation of metric camera images at the University of London --- Spacelab N86-10495
Identification of planimetric features from the metric camera --- Spacelab N86-10497
Analysis of metric camera images from the USA and their suitability for topographic and thematic mapping --- Spacelab N86-10498
Line mapping and resolution tests with metric camera data --- Spacelab N86-10500
Role of the Economic Commission for Africa as a principal investigator in the metric camera experiment and reports of the result of the assessment for topographic and revision of maps in populated and developed areas of the world N86-10501
The role of very small scale metric images in modern geology --- Spacelab metric camera N86-10502
Geological mapping of remote mountainous regions using metric camera imagery --- Spacelab N86-10503
Interpretation of metric camera concerning hydrologic structures of the Rhone Delta --- Spacelab N86-10504
Test on mapping application of metric camera imagery --- Spacelab N86-10505
Status of preparation activities for metric camera reflight on EOM-1/2 N86-10506
Thematic mapping of metric camera color infrared and black and white photographs for land use classification N86-10510
Digital image processing of metric camera imagery --- Spacelab N86-10511
Topographic and thematic mapping: Analysis of metric camera black and white photographs of the Rhone Delta N86-10514
Updating of topographic maps by means of metric camera photos example: Hallertau (Bavaria) N86-10517
Interpretation of Spacelab-1 photographs for the generation of 1:200000 topographic map N86-10518
Metric camera image of Munich as additional means for urban cartography --- Spacelab N86-10519
Test results using metric camera photography for 1:250,000 mapping --- Spacelab N86-10522
Report of the Workshop on Geologic Applications of Remote Sensing to the Study of Sedimentary Basins
[E86-10002] N86-10599
Chronologic analysis of terrestrial sediments and basin evolution N86-10602
Tertiary and quaternary research with remote sensing methods N86-10603
Analysis of remote sensing data N86-10605
Structural mapping of folded sedimentary environments from satellite images: An example from Central Asia N86-10607
Foreland basin structures and remote sensing N86-10608
Topographic mapping from interferometric synthetic aperture radar observations N86-10622
Lithologic mapping in a sedimentary environment using multipolarization SAR images N86-10624
PHOTOMAPS
Structural mapping of folded sedimentary environments from satellite images: An example from Central Asia N86-10607
PHOTOMETERS
Signal analysis receiver with acousto-optic delay lines
[AD-D011761] N86-10427
Semiconductor superlattic photodetectors
[NASA-CR-176249] N86-10484
Making the right choice --- silicon photodiodes N86-10669
PHOTOMULTIPLIER TUBES
Semiconductor superlattic photodetectors
[NASA-CR-176249] N86-10484
PHOTON BEAMS
The 20 keV undulators for a 6-GeV storage ring
[DE85-013867] N86-10941
Beam stability in a 6 GeV synchrotron light source
[DE85-013850] N86-10979

Thermal and structural analysis of ring components by the finite element method
[DE85-013305] N86-11021

PHOTON DENSITY
The intensified multi CCD camera --- spaceborne interferometers N86-11122

PHOTONICS
Photonic diagnostics and pulsed power research
[DE85-013752] N86-10940

PHOTONS
Ultraviolet spectroscopy of the Earth's dayglow and magnetosphere cleft N86-10696
Photonic diagnostics and pulsed power research
[DE85-013752] N86-10940
Surface conditioning of synchrotron radiation source to improve beam lifetime
[DE84-012185] N86-10948

PHOTONUCLEAR REACTIONS
Experimental X-ray scattering cross sections for H2 and rare atomic gases
[DE85-011572] N86-10936

PHOTOOXIDATION
Age-life prediction of nylon 66 parachute materials. Part 2: Changes in the chemical and physical properties of materials on aging
[AD-A156909] N86-10347

PHOTOTHERMAL CONVERSION
Time resolved flow velocity and concentration measurements using a travelling thermal lens
[AD-A156706] N86-10541

PHOTOVOLTAIC CELLS
Photovoltaic systems in remote locations: An experience summary
[NASA-TM-87106] N86-10643
Photovoltaic concentrator array evaluation
[DE85-013789] N86-10665

PHOTOVOLTAIC EFFECT
Sensor system
[AD-D011767] N86-10480
Photovoltaic systems in remote locations: An experience summary
[NASA-TM-87106] N86-10643
Some aspects of long-range, high-risk photovoltaic research at SERI
[DE85-012144] N86-10662

PHYSICAL EXERCISE
Assessment of state of chronotropic and inotropic heart function at different degrees of physical fitness N86-10746
Classification of changes in electrocardiogram during muscular exertion of healthy individuals N86-10755

PHYSICAL FACTORS
Identification of chemical and physical phenomena affecting the durability of silvered polymer (PMMA) mirrors
[DE85-012131] N86-10645

PHYSICAL OPTICS
Scattering by complicated structures: Calculation of the radar properties of metallic targets by means of physical optics
[DFVLR-FB-85-22] N86-10981

PHYSICAL WORK
Efficiency of muscular work in white rats during adaptation to cold N86-10763

PHYSIOLOGICAL EFFECTS
Effect of emotional stress on hemostasis system of healthy persons N86-10745
Short term heat effect on adreno- and cholino-sensitivity of rat's small intestine N86-10754
Indices of blood oxygen transporting properties and erythropoiesis in rats after prolonged stay in nitrogen-oxygen mixture at elevated pressure N86-10761
Homocarnosin in rat brain during adaptation to cold N86-10762
The effects of age, sleep deprivation, and altitude on complex performance
[AD-A156987] N86-10771
Report on the research activities on whole-body vibrations. Human strain due to mechanical vibrations
[ISBN-3-88383-107-7] N86-10773

PHYSIOLOGICAL RESPONSES
Effect of single actions of weak electromagnetic fields of ultralow frequency on indices of endocrine system N86-10744
Individual typological features of autonomic reactions during autogenic training in polar expedition members in period of wintering in Antarctica N86-10748
Individual typological self-regulation of cardio-vascular system N86-10752
TV monitoring control system in electrophysiological studies N86-10765
Effect of cold on brain serotonin system and plasma corticosteroid level in different strains of mice N86-10766
Variability analysis of visually induced responses in the midst of noise
[B8564052] N86-10774

PHYSIOLOGICAL TESTS
The wearing comfort of the PVC: Combat back pack
[IZF-1984-34] N86-10789

PHYSIOLOGY
USSR report: Life sciences. Biomedical and behavioral sciences
[JPRS-UBB-85-023] N86-10738

PIEZOELECTRIC TRANSDUCERS
Precise bearing support ditherer with piezoelectric drive means
[AD-D011819] N86-10483

PIEZOELECTRICITY
Precise bearing support ditherer with piezoelectric drive means
[AD-D011819] N86-10483
Fiber optic system for measuring electric fields
[AD-D011830] N86-10976

PIEZOMETERS
Modeling groundwater flow into lakes N86-10596

PILOT ERROR
Extended analysis of the structure of error scores in psychological aptitude tests
[DFVLR-FB-85-20] N86-10780
Speed of work and error rate: Analyses of individual differences in a choice reaction series with a cognitive component
[DFVLR-FB-85-21] N86-10781

PILOT PERFORMANCE
Mild hypoxia and visual performance with night vision goggles
[AD-A156969] N86-10787

PILOT TRAINING
Proposed modifications for the RAAF Airtrainer CT-4A cockpit
[AD-A156808] N86-10039

PIONS
Relativistic wavefunction at the origin and the pion decay constant
[DE85-012392] N86-11062

PIPELINING (COMPUTERS)
Arithmetic pipeline for image processing
[AD-D011773] N86-10800

PIPES (TUBES)
Carbon fiber reinforced polymide filament wound tube manufacturing
[BR64172] N86-10339
Streaming potentials in conductive and nonconductive tubing
[DE85-012984] N86-10438

PITCH (INCLINATION)
Theoretical study of the unsteady linear problem for a rectangular wing with a pitching movement
[ONERA-RT-17/1841-RY-010-R] N86-10022

PITUITARY HORMONES
Purification and cultivation of human pituitary growth hormones secreting cells N86-10140

PLAINS
Observations of the snow cover in the southern part of the Buryat Autonomous Soviet Socialist Republic
[NASA-TM-77910] N86-10613

PLANE WAVES
Topics in nonlinear wave theory with applications N86-10367
Measurements of the acoustic interference between adjacent microphones
[AD-A153892] N86-10919

PLANETS
Photographic catalog of selected planetary size comparisons
[NASA-TM-86207] N86-11138

PLANNING
F-16X MSIP (Multi-national Staged Improvement Program) case example: Operating and support cost estimation using VAMOSC (Visibility And Management Of Operating and Support Costs)
[AD-A156893] N86-10006
Research needs for corrosion control and prevention in energy conservation systems
[DE85-014852] N86-10326
Generation of flight paths using hierarchical planning
[AD-A156905] N86-10900
Application of structural-mechanics methods to the design of large tandem-mirror fusion devices (MFTF-B)
[DE85-006960] N86-11017

PLANT ROOTS
Radionuclide complexation in xylem exudates of plants
[DE85-013446] N86-10684

PLANTS (BOTANY)
Radionuclide complexation in xylem exudates of plants
[DE85-013446] N86-10684
Romanian plant produces protein concentrate from paraffin-nourished yeasts N86-10741

PLASMA ACCELERATORS
Theoretical aspects of magnetic helicity
[DE85-011846] N86-10984
Introduction to the m = 1 helicity source
[DE85-012771] N86-10999
Energy efficiency of the CTX magnetized coaxial plasma source
[DE85-012735] N86-11003

PLASMA COMPRESSION
Compact torus compression of microwaves
[DE85-012919] N86-11016

PLASMA CONTROL
Increased particle confinement with the use of external dc bias field in the CTX spheromak
[DE85-012744] N86-10988
Compact torus compression of microwaves
[DE85-012919] N86-11016
Symmetric Tandem Mirror Program
[DE85-012352] N86-11032

PLASMA CURRENTS
Recent helicity source and power supply improvements in CTX
[DE85-012741] N86-11028

PLASMA DENSITY
Local drift parameter, j/n sub e and resistivity anomaly measurements in CTX spheromaks
[DE85-012740] N86-10998

PLASMA DIAGNOSTICS
Activities report in geophysics
[KGI-188] N86-10709
Activities report in plasma physics N86-11039

PLASMA DYNAMICS
Dynamics of imploding neon gas puff plasmas. 1
[AD-A156916] N86-10963

PLASMA EQUILIBRIUM
Conducting wall and pressure profile effect on MHD stabilization of axisymmetric mirror
[DE85-013647] N86-11020

PLASMA GUNS
Theoretical aspects of magnetic helicity
[DE85-011846] N86-10984

PLASMA HEATING
Heating and generation of suprathermal particles at collisionless shocks
[DE85-014114] N86-11034

PLASMA JETS
Velocities of gas and plasmas from real time holographic interograms
[DE85-014618] N86-10530

PLASMA PHYSICS
Activities report in plasma physics N86-11039

PLASMA PINCH
Introduction to the m = 1 helicity source
[DE85-012771] N86-10999
Activities report in plasma physics N86-11039

PLASMA SHEATHS
Generalized helicity and its time derivative
[DE85-012770] N86-11027

PLASMA SPRAYING
Creep-fatigue behavior of NiCoCrAlY coated PWA 1480 superalloy single crystals
[NASA-TM-87110] N86-10311

PLASMAS (PHYSICS)
Improved blue response and efficiency of A-Si:H solar cells deposited from disilane using a dual-chamber plasma system
[DE85-013289] N86-10649
Dynamics of imploding neon gas puff plasmas. 1
[AD-A156916] N86-10963

PLASMONS
Dielectric properties of silicon surfaces and silver thin films
[JUEL-1968] N86-10450
Cooperative emission by two different atoms into surface plasmons
[AD-A157033] N86-10925

PLASTIC DEFORMATION
Low temperature plastic deformation mechanisms of alpha-titanium single crystals
[ESA-TT-871] N86-10332

PLASTIC PROPERTIES
Nonlinear propagation of elastoplastic waves in Ke penetrators (excerpts)
[DE85-011450] N86-10318
Swelling and tensile properties of EBR-2-irradiated tantalum alloys for space reactor applications
[DE85-012887] N86-10329
Finite deformation crack-line fields in a thin elasto-plastic sheet
[AD-A156757] N86-10346
Resistance curves for crack growth under plane-stress conditions in an elastic perfectly-plastic material
[AD-A156778] N86-10593

PLASTICIZERS
Binder-filler interaction in energetic polymers
[AD-A156752] N86-10345
PLASTICS
Automatic processing of reactive polymers N86-10127
Properties of plastic-bonded nitroguanidine
[DE85-015316] N86-10358
PLATINUM
Multipurpose pan development
[DE85-012326] N86-10319
PLATINUM COMPOUNDS
Compatibility of grain-stabilized platinum with candidate propellants for resistojets
[NASA-TM-87118] N86-10279
PLOTTERS
Restitution of Spacelab photography by analog stereoplotter N86-10489
PLUMES
Vibro-acoustic forecast for space shuttle launches at Vandenberg AFB: The payload changeout room and the administration building
[AD-A156944] N86-10269
PLUTONIUM FLUORIDES
Multipurpose pan development
[DE85-012326] N86-10319
PODS (EXTERNAL STORES)
Test and evaluate passive orbital disconnect struts (PODS 3)
[NASA-CR-177368] N86-10274
POISONING (REACTION INHIBITION)
Effect of H2S and COS in the fuel gas on the performance of ambient pressure phosphoric acid fuel cells
[DE85-013913] N86-10446
Effects of H2S on molten carbonate fuel cells
[DE85-014052] N86-10447
POISSON EQUATION
Analysis of combined natural and forced convection around cylinders and spheres N86-10456
Poisson semigroups and singular integrals
[CTH-MATH-1985-05] N86-10876
A modified Successive Over-Relaxation (SOR) method for the Poisson equation in unsteady free-surface flow calculations
[TW-264] N86-10881
POLARIZATION
Electric field containerless processing technology N86-10170
POLARIZATION (CHARGE SEPARATION)
AGS polarized H(-) source
[DE85-013296] N86-10935
Beam steering in the SLC linac
[DE85-013370] N86-11025
POLARIZATION (WAVES)
Charge exchange in slow collisions of atoms and molecules N86-10922
POLARIZED RADIATION
Polarization transfer in inelastic scattering and pionic models of the EMC effect
[DE85-010738] N86-10955
Proposed bunching scheme for a polarized H(-) injector
[DE85-012648] N86-10986
POLAROGRAPHY
Method for determining elemental sulfur in jet fuel — differential pulse polarography
[FOA-C-40211-B4] N86-10360
POLICE
Methods for developing jam-resistant security communications networks at fixed-site facilities
[DE85-012032] N86-10408
POLICIES
Tendencies toward liberalization in European air traffic control
[DFVLR-FB-85-23] N86-10030
An anthology: Rationale for a US ballistic missile defense (1969 - 1984)
[AD-A156781] N86-10199
POLLUTION CONTROL
Proceedings: First Annual Acid Deposition Emissions Inventory Symposium
[PB85-200004] N86-10686
POLLUTION MONITORING
Utilization of satellite remote sensing for the monitoring of oil pollution and marine ecosystems in Indonesia. A Tropical Earth Resources Satellite program (TERS) case study implemented for the NLR, Delft N86-10640
Multiple site laser excited pollution monitoring system
[AD-D011769] N86-10674
POLLUTION TRANSPORT
Sediment characterization. Task 2: Instream contaminant study, volume 1
[DE85-013502] N86-10683
POLYACETYLENE
Electrically conducting polymers N86-10333
Polyacetylene polymerization, structure, and electrical transport properties N86-10334
POLYAMIDE RESINS
Age-life prediction of nylon 66 parachute materials. Part 2: Changes in the chemical and physical properties of materials on aging
[AD-A156909] N86-10347
POLYCRYSTALS
The mechanism of erosion of metallic materials under cavitation attack
[NASA-TM-87133] N86-10552
POLYETHYLENES
Cell partition in two polymer aqueous phases N86-10139
Passive damping concepts for slender columns in space structures
[NASA-CR-176234] N86-10577
POLYIMIDES
Carbon fiber reinforced polymide filament wound tube manufacturing
[BR64172] N86-10339
POLYMER CHEMISTRY
Cell partition in two polymer aqueous phases N86-10139
Calculation of the glass transition temperatures of linear polymers. Part 1: Rules for hierarchical ordering of the data set
[AD-A156584] N86-10343
Polymer engineering: Polymeric and molecular electronic, dielectric and optical properties for device applications
[AD-A156671] N86-10344
Thermodynamics of polymer-supercritical solvent mixtures
[AD-A157038] N86-11061
POLYMER PHYSICS
Polymer engineering: Polymeric and molecular electronic, dielectric and optical properties for device applications
[AD-A156671] N86-10344
POLYMERIC FILMS
Evaluation and prediction of long-term environmental effects on non metallic materials
[NASA-CR-178495] N86-10340
High voltage instrument transformers for outdoor service with an insulation of low pressure SF6 gas and plastic foils
[BMFT-FB-T-85-034] N86-10449
POLYMERIZATION
Polyacetylene polymerization, structure, and electrical transport properties N86-10334
Synthesis of arylene siloxanylene polymers and copolymers
[AD-D011780] N86-10338
POLYNOMIALS
Partial eigensolutions of large nonsymmetric matrices
[AD-A156711] N86-10867
POLYPHENYLS
Electrically conducting polymers N86-10333
POLYSTATION DOPPLER TRACKING SYSTEM
Sample data phase locked loop for adaptive Doppler tracker
[AD-D011788] N86-10374
POLYSTYRENE
Production of large-particle-size monodisperse latexes in microgravity N86-10146
POLYURETHANE FOAM
Self-heating to ignition measurements and computation of critical size for solar energy collector materials
[DE85-011449] N86-10302
POLYVINYL CHLORIDE
The wearing comfort of the PVC: Combat back pack
[IZF-1984-34] N86-10789
POROSITY
Metallurgy and metallography of braze joints
[DE85-014563] N86-10325
POROUS MATERIALS
KRAK: A computer program for two-phase, two-component porous flow and fracture propagation, revision
[DE85-014264] N86-10469
POSITION (LOCATION)
Long range translocations ashore to offshore using Spacelab-1 metric camera imagery in the perspective of integrated geophysical surveys N86-10499
Capacity for work and hemodynamics in males residing at middle and high latitudes N86-10747
Supervisory control of the right arm of the beam assembly teleoperator
[AD-A156856] N86-10832
POSITION ERRORS
Path error-neglection in straight lane driving
[IZF-1984-32] N86-10783
POSITIONING
User interface enhancement report
[NASA-CR-171898] N86-10820
Parasitic mode losses versus signal sensitivity in beam position monitors
[DE85-014367] N86-10964
Beam stability in a 6 GeV synchrotron light source
[DE85-013850] N86-10979
TRIO interferometer positioning — spaceborne interferometers (TRIO) N86-11111
POSITRON ANNIHILATION
Search for heavy neutrinos produced in e(+)e(-) annihilation
[DE85-013372] N86-11035
POSITRONS
Methane-bubble formation in hydrogen-charged Fe-30 ppM C
[DE85-012526] N86-10937
SLC positron damping ring optics design
[DE85-013054] N86-11014
Computer control of rf at SLAC
[DE85-013065] N86-11015
Beam steering in the SLC linac
[DE85-013370] N86-11025
POTASSIUM
Experimental investigations of thermal radiation from potassium atoms and design applications
[DE85-004086] N86-11036
POTASSIUM NITRATES
Development of new ammonium nitrate composite explosives
[DE85-014252] N86-10356
POTENTIAL FIELDS
Potential structures and particle acceleration on auroral field lines
[AD-A156694] N86-10708
POWDER METALLURGY
The role of entrained surface oxides in RS-PM aluminum alloys on resultant structures and properties N86-10085
Mechanism of the formation of boronised layers on high carbon steel
[BLL-BISI-TRANS-23036-(9022.06)] N86-10306
POWER AMPLIFIERS
Test results for 20-GHz GaAs FET spacecraft power amplifier
[NASA-TM-87072] N86-10379
POWER SERIES
Multivariable partial realization and the aspect of uniqueness
[ER-83/09] N86-10879
POWER SPECTRA
Computational techniques for the analysis and design of digital communication systems
[AD-A156945] N86-10407
POWER SUPPLY CIRCUITS
Protection circuitry for high voltage drivers
[AD-D011781] N86-10414
PRASEODYMIUM
Extraction of lanthanide ions by 2-methyl-8-quinolinol
[DE85-014277] N86-10303
PRECIPITATION (CHEMISTRY)
Growth of organic crystals by Ostwald ripening N86-10058
Theoretical problems in materials science N86-10088
Growth and characterization of brushite and lead monetite, simulation and results — Spacelab N86-10230
PRECIPITATION (METEOROLOGY)
Observations of the snow cover in the southern part of the Buryat Autonomous Soviet Socialist Republic
[NASA-TM-77910] N86-10613
Monthly and Seasonal Weather Outlook for mid-April to mid-May 1985, Volume 39, Number 8
[PB85-195345] N86-10724
PRECIPITATION HARDENING
Fracture toughness of hydrogen-embrittled precipitation-hardened stainless steels
[AD-A156664] N86-10592
PREDICTION ANALYSIS TECHNIQUES
Evaluation of an aerodynamic-load prediction method on a STOL fighter configuration
[NASA-TM-86782] N86-10015
Dynamic analysis of a sled traveling along a rough rail
[AD-A156589] N86-10191
Process models for 3D composites
[AD-A156889] N86-10292
Approaches to cumulative impact assessment
[DE85-013891] N86-10635
Evaluation of surface exchange coefficients from mildex ocean/atmosphere mixed layer data
[AD-A156765] N86-10729
PREDICTIONS
Manned flight simulation: Challenge and response
[NASA-TM-86827] N86-10048
Progressive damage, fracture predictions and post mortem correlations for fiber composites
[NASA-TM-87101] N86-10290

Scaling studies of solar pumped lasers
[NASA-CR-176240] N86-10540

PREPROCESSING
Kalman filter preprocessor
[AD-D011774] N86-10972

PRESIDENTIAL REPORTS
Publication of the Executive Office of the President, January 20, 1981 - December 31, 1984
[PB85-187110] N86-11082

PRESSURE
Effect of sequence of loading on interaction curves for buckling of stiffened shells
[TAE-536] N86-10583

PRESSURE BREATHING
Reaction of rabbit respiration system to hypoxic stimulus in nitrogen-oxygen medium at elevated pressure N86-10760

PRESSURE DEPENDENCE
Rapid analysis using capillary supercritical fluid chromatography
[DE85-012460] N86-10297
Chemical kinetics and cellular structure of detonations in hydrogen sulphide and air
[DE85-009408] N86-10304

PRESSURE DISTRIBUTION
Experimental and theoretical investigations of the flow around airfoil systems with ground effect
[DFVLR-FB-85-17] N86-10026

PRESSURE DROP
Effect of a shear layer on the stability of an axisymmetrical external compression air intake N86-10010

PRESSURE EFFECTS
Conducting wall and pressure profile effect on MHD stabilization of axisymmetric mirror
[DE85-013647] N86-11020

PRESSURE GRADIENTS
A root-mean-square pressure fluctuations model for internal flow applications
[NASA-CR-3928] N86-10460

PRESSURE VESSELS
Stiffened and prestressed composite overwrapped pressure vessels N86-10547

PRESTRESSING
Stiffened and prestressed composite overwrapped pressure vessels N86-10547

PREVENTION
Report on the research activities on whole-body vibrations. Human strain due to mechanical vibrations
[ISBN-3-88383-107-7] N86-10773

PRINTED CIRCUITS
Multi-row connector with ground plane board
[AD-D011803] N86-10437
Soudan 2 data acquisition and trigger electronics
[DE85-013864] N86-10443
Increase of the packaging density of Very Large Scale Integration (VLSI) circuits using automatic alignment
[BMFT-FB-T-85-020] N86-10451
Compact, high-speed algorithm for laying out printed circuit board runs N86-10814

PRINTING
Development of metallization process
[NASA-CR-176209] N86-10312

PRISMS
Tunable acousto-optic filter with improved spectral resolution and increased aperture
[AD-D011758] N86-10915

PROBABILITY DISTRIBUTION FUNCTIONS
Superefficient estimation of power functions in simulation experiments
[B8562445] N86-10893

PROBABILITY THEORY
Computational techniques for the analysis and design of digital communication systems
[AD-A156945] N86-10407
New probabilistic modeling and simulation methods for complex time-dependent systems
[DE85-009575] N86-10835
On maximal and distributional coupling
[CTH-MATH-1984-30] N86-10675

PROBLEM SOLVING
The effects of age, sleep deprivation, and altitude on complex performance
[AD-A156987] N86-10771
Extended analysis of the structure of error scores in psychological aptitude tests
[DFVLR-FB-85-20] N86-10780
Well-posed questions and exploration of the space of parameters in linear and non linear inversion
[PN-84/13] N86-10858
On the lanczos method for solving symmetric linear systems with several right-hand-sides
[AD-A156816] N86-10868
Computing the structural index
[DE85-014370] N86-10871
Derivational analogy: A theory of reconstructive problem solving and expertise acquisition
[AD-A156817] N86-10899

PROCESS CONTROL (INDUSTRY)
Automatic processing of reactive polymers N86-10127

PROCUREMENT POLICY
Making the right choice — silicon photodiodes N86-10669

PRODUCT DEVELOPMENT
Carbon fiber reinforced polymide filament wound tube manufacturing
[BR64172] N86-10339
Phosphoric and electric utility fuel technology development
[DE85-014741] N86-10651
Strategy for the development of space arrays N86-11101

PROFILOMETERS
On the use of X-band CW nanosecond airborne radar for terrain profiling
[AD-A156886] N86-10406

PROGRAMMING LANGUAGES
Catalog of Resources for Education in Ada (trademark) and Software Engineering (CREASE). Version 3.0
[AD-A156687] N86-10790
User interface enhancement report
[NASA-CR-171898] N86-10820
The DUCK manual
[AD-A156936] N86-10833
Compexity of higher-order programs
[DE85-012776] N86-10834

PROJECT PLANNING
The first German Spacelab mission D1 reports — Spacelab payloads
[PR-3] N86-10189

PROJECT SETI
SETI radio spectrum surveillance system N86-10400

PROJECTILES
Counterpulse railgun energy recovery circuit
[DE85-011603] N86-10196

PROJECTIVE GEOMETRY
Brauer-Severi schemes of orders
[CTH-MATH-1985-06] N86-10877
Some remarks about cusp forms: Holomorphic and non-holomorphic
[CTH-MATH-1984-26] N86-10902
Galois descent and class groups of orders
[CTH-MATH-1985-09] N86-10904

PROPAGATION (EXTENSION)
The mechanics of delamination in composite materials N86-10284

PROPELLANT GRAINS
Gas generator fuel flow throttle control system
[AD-D011797] N86-10355

PROPORTIONAL COUNTERS
Soudan 2 data acquisition and trigger electronics
[DE85-013864] N86-10443

PROPULSION
Compatibility of grain-stabilized platinum with candidate propellants for resistojets
[NASA-TM-87118] N86-10279

PROPULSION SYSTEM PERFORMANCE
Experimental performance of a 1-kilowatt arcjet thruster
[NASA-TM-87131] N86-10281

PROTECTION
Development of a sheath for sensor protection in molten steel applications
[AD-A156764] N86-10315
Protection circuitry for high voltage drivers
[AD-D011781] N86-10414

PROTECTIVE COATINGS
Passivation of steel with aqueous amine solutions
[AD-D011749] N86-10314
Aluminum ion plating for corrosion protection of uranium, revision 1
[DE85-012419] N86-10330

PROTEIN METABOLISM
Growth of larger single crystals N86-10186

PROTEINS
Protein single crystal growth under microgravity — Spacelab N86-10228
Automated analysis of digital images generated by two-dimensional gel electrophoresis
[DE85-011906] N86-10526
Romanian plant produces protein concentrate from paraffin-nourished yeasts N86-10741
Biotechnology: Science and practice N86-10742

PROTON BEAMS
Use of the MURA transformation to generate the fields and calculate the motion of protons in the designed Argonne Mini-ASPUN FFAG spiral sector accelerator
[DE85-011477] N86-10934
Treatment planning with ion beams
[DE85-012661] N86-10990
Microwave instability across the transition energy
[DE85-013304] N86-11010

PROTON IRRADIATION
Beam line windows at LAMPF
[DE85-012723] N86-10985

PROTONS
Matter-antimatter transition operators: A manual for modeling N86-10921
Method for determining the position, angle and other injection parameters of a short pulsed beam in the Brookhaven AGS
[DE85-012523] N86-10931
Development and application of the electrochemical etching technique
[DE85-010302] N86-10957

PSYCHOACOUSTICS
Proposed aural nondetectability limits for Army materiel
[AD-A156704] N86-10917

PSYCHOLOGICAL EFFECTS
Report on the research activities on whole-body vibrations. Human strain due to mechanical vibrations
[ISBN-3-88383-107-7] N86-10773

PSYCHOLOGICAL FACTORS
Effect of emotional stress on hemostasis system of healthy persons N86-10745

PSYCHOLOGICAL TESTS
Extended analysis of the structure of error scores in psychological aptitude tests
[DFVLR-FB-85-20] N86-10780
Speed of work and error rate: Analyses of individual differences in a choice reaction series with a cognitive component
[DFVLR-FB-85-21] N86-10781
Standardization of tasks: Approach planning — human performance assessment
[IZF-1984-19] N86-10782

PSYCHOLOGY
Psychological Sciences Division 1984 programs
[AD-A156631] N86-10779

PUBLIC HEALTH
Development of the Multi-Attribute Hazard Assessment System (MAHAS) and its application to energy-related waste streams
[DE85-010278] N86-10676
Biotechnology regulation
[GPO-43-778] N86-10733

PULLEYS
Improved arresting and recovery system for test missiles
[AD-D011743] N86-10198

PULSE AMPLITUDE MODULATION
Apparatus for locating passive intermodulation interference sources
[AD-D011798] N86-10435

PULSE CODE MODULATION
Phase coded pulse expander-compressor
[AD-D011817] N86-10376
Pulse compression system
[AD-D011833] N86-10417

PULSE COMMUNICATION
High-rate convolutional code construction with the minimum required SNR criterion N86-10392
The GCF Mark 4 implementation and beyond N86-10399
Computational techniques for the analysis and design of digital communication systems
[AD-A156945] N86-10407

PULSE COMPRESSION
Phase-coded pulse expander-compressor
[AD-D011812] N86-10375
Pulse compression system
[AD-D011833] N86-10417

PULSE DURATION
Timing system control software in the SLC
[DE85-013380] N86-11024
Recent helicity source and power supply improvements in CTX
[DE85-012741] N86-11028

PULSE GENERATORS
Overpulse railgun energy recovery circuit
[DE85-011607] N86-10197
Calibrated Faraday current and magnetic field sensor
[DE85-013438] N86-10439
Ferrite kicker magnet for the IAMPF switchyard upgrade
[DE85-012657] N86-10996
Engineering high reliability, low-jitter Marx generators
[DE85-012811] N86-11013
Recent helicity source and power supply improvements in CTX
[DE85-012741] N86-11028
Programmable delay unit incorporating a semi-custom integrated circuit
[DE85-013379] N86-11033

PULSE RADAR
Topographic mapping from interferometric synthetic aperture radar observations N86-10622
PULSE RATE
Dynamics of changes of statistical indicators of heart rhythm of persons with different degree of motion sickness N86-10743
PULSE REPETITION RATE
Overpulse railgun energy recovery circuit
[DE85-011607] N86-10197
PULSED LASERS
Contact effects in light activated GaAs switches
[AD-A156957] N86-10434
Time resolved flow velocity and concentration measurements using a travelling thermal lens
[AD-A156706] N86-10541
Design, fabricate and test a 1.06(MU) repetitively pulsed laser
[DE85-014439] N86-10543
Optical detection of photoacoustic pulses in thin silicon wafers
[AD-A156705] N86-10977
PULSED RADIATION
Radiation field results from the SPEED triaxiode, a large area, high dose rate, short pulse 1MV bremsstrahlung source
[DE85-009438] N86-11005
PULSES
Parallel pulse processing for mercuric iodide gamma-ray detectors
[DE85-013391] N86-10528
PURIFICATION
New instrumentation for phase partitioning N86-10138
Purification and cultivation of human pituitary growth hormones secreting cells N86-10140
PYROLYSIS
Modelling of laser-enhanced chemical vapor deposition N86-10105

Q

Q FACTORS
SAR image quality: A review
[DFVLR-MITT-85-07] N86-10413
Q SWITCHED LASERS
Characterization of vapor and aerosol flows by photothermal methods
[AD-A156601] N86-10465
QUADRATURES
A study of methods to predict and measure the transmission of sound through the walls of light aircraft. Integration of certain singular boundary element integrals for applications in linear acoustics
[NASA-CR-176229] N86-10912
QUADRUPOLE NETWORKS
RFQ-funneling
[DE85-012483] N86-10194
QUALITY CONTROL
Reduction of noble metal stock and noble metal loss during wire production with the Conform extrusion process
[BMFT-FB-T-85-049] N86-10560
Software for an automated gaging system
[DE85-013322] N86-10842
QUANTITATIVE ANALYSIS
Theoretical comparison of classical (K-matrix) and inverse (P-matrix) least-squares methods for quantitative infrared spectroscopy
[DE85-012827] N86-10298
QUANTUM EFFICIENCY
Improved blue response and efficiency of A-Si:H solar cells deposited from disilane using a dual-chamber plasma system
[DE85-013289] N86-10649
QUARTZ
Shock loading and release behavior of x-cut quartz
[DE85-013954] N86-11054
QUASARS
A VLBI survey at 2.29 GHz N86-10383
Radio studies of a complete sample of quasars N86-11093
QUASI-STEADY STATES
Strength of shells under local transverse loads N86-10568
QUATERNARY ALLOYS
Laser Raman spectroscopy study of the zinc and bromide ion complex equilibrium in zinc/bromine battery electrolytes
[DE85-011820] N86-10301
QUATERNIONS
Brauer-Severi schemes of orders
[CTH-MATH-1985-06] N86-10677
QUENCHING (COOLING)
Theoretical problems in materials science N86-10088
Application of the unloading compliance methods in fracture toughness measurements of a quenched and tempered steel
[BLL-BISI-TRANS-21628-(9022.06)] N86-10308
QUINOLINE
Extraction of lanthanide ions by 2-methyl-8-quinolinol
[DE85-014277] N86-10303

R

RADAR
Periodic binary sequences with very good autocorrelation properties N86-10397
A binary sequence of period 60 with better autocorrelation properties than the Barker sequence of period 13 N86-10398
Miniature radar packaging
[DE85-014598] N86-10410
RADAR CROSS SECTIONS
A simplified method of estimation of the specular components of radar cross section for some re-entrant conductors
[AD-A156573] N86-10403
RADAR IMAGERY
SAR image quality: A review
[DFVLR-MITT-85-07] N86-10413
Multisensor data integration techniques N86-10604
NASA/JPL Aircraft SAR Workshop Proceedings
[NASA-CR-176204] N86-10615
Radar system description N86-10616
The effect of vegetation type, microrelief, and incidence angle on radar backscatter N86-10619
Age-dating volcanic and alluvial surfaces with multipolarization data N86-10620
Strategies for analyzing mixed pixels in remotely sensed imagery N86-10623
Mapping diverse forest cover with multipolarization airborne radar N86-10625
RADAR MAPS
High-resolution image data from the Space Shuttle N86-10494
RADAR RANGE
Guidance and control of a cable based payload pickup system N86-10046
On the use of X-band CW nanosecond airborne radar for terrain profiling
[AD-A156886] N86-10406
RADAR RESOLUTION
SAR image quality: A review
[DFVLR-MITT-85-07] N86-10413
RADAR SCATTERING
Modelling of vegetation volumes N86-10629
Scattering by complicated structures: Calculation of the radar properties of metallic targets by means of physical optics
[DFVLR-FB-85-22] N86-10981
RADAR SIGNATURES
La Recherche Aerospatiale, bimonthly bulletin, no. 1984-5, September-October 1985
[ESA-TT-899] N86-10363
Strategies for analyzing mixed pixels in remotely sensed imagery N86-10623
RADAR TARGETS
Scattering by complicated structures: Calculation of the radar properties of metallic targets by means of physical optics
[DFVLR-FB-85-22] N86-10981
RADAR TRACKING
On the use of X-band CW nanosecond airborne radar for terrain profiling
[AD-A156886] N86-10406
RADAR TRANSMISSION
Propagation and radiation characteristics of a multimode corrugated waveguide feedhorn N86-10388
RADIAL FLOW
Three-dimensional inviscid analysis of radial turbine flow and a limited comparison with experimental data
[NASA-TM-87091] N86-10017
SUTRA (Saturated-unsaturated transport). A finite-element simulation model for saturated-unsaturated, Fluid-Density-Dependent ground-water flow with energy transport or chemically-reactive single-species solute transport
[AD-A156779] N86-10830
RADIANT FLUX DENSITY
Solar modulation of galactic cosmic rays: Techniques and applications N86-11143
RADIANT HEATING
Levitating furnance for containerless processing in space N86-10169
RADIATION DISTRIBUTION
Radiation field results from the SPEED triaxiode, a large area, high dose rate, short pulse 1MV bremsstrahlung source
[DE85-009438] N86-11005
RADIATION DOSAGE
Effect of single actions of weak electromagnetic fields of ultralow frequency on indices of endocrine system N86-10744
Approaches to quantitative expression of dose response
[DE85-013498] N86-10772
Development and application of the electrochemical etching technique
[DE85-010302] N86-10957
Treatment planning with ion beams
[DE85-012661] N86-10990
RADIATION EFFECTS
Swelling and tensile properties of EBR-2-irradiated tantalum alloys for space reactor applications
[DE85-012887] N86-10329
Criteria for the design or selection of a bioelectromagnetics experiment
[AD-A156575] N86-10420
RADIATION HAZARDS
Approaches to quantitative expression of dose response
[DE85-013498] N86-10772
Hot cell facility design for large fusion devices
[DE85-012893] N86-11037
RADIATION MEASUREMENT
Secondary standards laboratories for ionizing radiation calibrations: The national laboratory interests
[DE85-007046] N86-10938
On-line gamma-ray data acquisition at the Power Burst facility
[DE85-011957] N86-10954
Energy efficiency of the CTX magnetized coaxial plasma source
[DE85-012735] N86-11003
RADIATION MEASURING INSTRUMENTS
On-line gamma-ray data acquisition at the Power Burst facility
[DE85-011957] N86-10954
RADIATION PRESSURE
A modeling analysis program for the JPL table mountain lo sodium cloud
[NASA-CR-176241] N86-11139
RADIATION PYROMETERS
Measurement of workpiece temperature during welding for welding robot control N86-10534
RADIATION SOURCES
Sound radiation from repetitive transient vibrations using multi-channel digital signal processing with application to impact machinery N86-10910
RADIATIVE HEAT TRANSFER
Radiative heat transfer in nonisothermal combustion products N86-10458
RADICALS
Cometary atmospheres: Modeling the spatial distribution of observed neutral radicals
[NASA-CR-176242] N86-11133
RADIO ANTENNAS
Seismic analysis of the large 70-meter antenna, part 1: Earthquake response spectra versus full transient analysis N86-10386
Load-deflection tests and computer analyses of a high-precision adhesive-bonded antenna reflector panel N86-10389
Planning for VLA/DSN arrayed support to the Voyager at Neptune N86-10395
A VLA experiment: Planning for Voyager at Neptune N86-10396
RADIO ASTRONOMY
Radio studies of a complete sample of quasars N86-11093
Radio astronomy experience in image reconstruction. A history lesson for optical astronomers N86-11117
VLBI at optical and radio wavelengths: Congruences and contrasts N86-11126
RADIO CONTROL
Construction and use of a radio controlled model helicopter for research
[AD-A156547] N86-10035
RADIO EMISSION
Radio studies of a complete sample of quasars N86-11093
RADIO EQUIPMENT
Methods for developing jam-resistant security communications networks at fixed-site facilities
[DE85-012032] N86-10408
RADIO FREQUENCIES
RFQ-funneling
[DE85-012483] N86-10194

Apparatus for locating passive intermodulation interference sources
[AD-D011798] N86-10435
High-power rf controls for the NBS-Los Alamos racetrack microtron
[DE85-012658] N86-10993
Superconductors for pulsed RF accelerators
[DE85-013378] N86-11051

RADIO FREQUENCY DISCHARGE
High-resolution phosphor screen beam profile monitor
[DE85-013074] N86-11012

RADIO FREQUENCY INTERFERENCE
SETI radio spectrum surveillance system N86-10400

RADIO SOURCES (ASTRONOMY)
Improved mapping of radio sources from VLBI data by least-square fit N86-10402
A superconducting tunnel junction receiver for millimeter-wave astronomy N86-11041

RADIO SPECTRA
SETI radio spectrum surveillance system N86-10400

RADIO TELESCOPES
Planning for VLA/DSN arrayed support to the Voyager at Neptune N86-10395
A VLA experiment: Planning for Voyager at Neptune N86-10396

RADIO TRANSMISSION
Digital radio link: Method and a measuring system for studying the radio channel during frequency selective fading
[FOA-C-30386-E2] N86-10411

RADIO TRANSMITTERS
An experimental TE sub 12 - TE sub 11 circular waveguide mode converter N86-10387

RADIOACTIVE DECAY
Relativistic wavefunction at the origin and the pion decay constant
[DE85-012392] N86-11062

RADIOACTIVE ISOTOPES
General-purpose heat source development: Safety Verification Test Program. Bullet/fragment test series
[DE85-014262] N86-10660
Impact of long-lived radionuclides on waste classification for fusion
[DE85-013205] N86-10959

RADIOACTIVE MATERIALS
Hot cell facility design for large fusion devices
[DE85-012893] N86-11037

RADIOACTIVE WASTES
Recirculation within a glass mixture subjected to external and resistive heating
[DE85-010068] N86-10348
Impact of long-lived radionuclides on waste classification for fusion
[DE85-013205] N86-10959
Hot cell facility design for large fusion devices
[DE85-012893] N86-11037

RADIOACTIVITY
Automated analysis of digital images generated by two-dimensional gel electrophoresis
[DE85-011906] N86-10526

RADIOMETERS
Mobile VLBI and GPS measurement of vertical crustal motion N86-10401

RADOMES
Attachment method-ceramic radome to metal body
[AD-D011778] N86-10032
Radome analysis and design capabilities of the RF and Microwave Technology Branch
[AD-A156662] N86-10404

RAIL TRANSPORTATION
Study of statis and dynamic stress effects in nonlinear solids
[NASA-CR-176236] N86-10578

RAILGUN ACCELERATORS
Counterpulse railgun energy recovery circuit
[DE85-011603] N86-10196
Overpulse railgun energy recovery circuit
[DE85-011607] N86-10197
EMACK railgun firing test report number 9
[AD-A156661] N86-10354

RAILS
Study of statis and dynamic stress effects in nonlinear solids
[NASA-CR-176236] N86-10578

RAMAN SPECTRA
Spontaneous Raman spectroscopy of shocked H2O
[DE85-014557] N86-10470
Real-time holography by stimulated Raman and Brillouin scattering N86-10479

RAMAN SPECTROSCOPY
Design and calibration of a flat-flame burner using line reversal techniques
[AD-A156724] N86-10294
Laser Raman spectroscopy study of the zinc and bromide ion complex equilibrium in zinc/bromine battery electrolytes
[DE85-011820] N86-10301

RAMJET ENGINES
Theoretical specific impulse for two-phase flow in nozzle of rocket-ramjet engine: A simple estimation method N86-10005

RANDOM NOISE
A study of Morrison's iterative noise removal method
[NASA-CR-176222] N86-10823

RANDOM SAMPLING
Adaptive distribution-free test for the K random sampling problem, part 1
[COMP-CENT-NOTE-14-PT-1] N86-10888
Adaptive distribution free test for the K random sampling problem, part 2
[COMP-CENT-NOTE-15-PT-2] N86-10889

RANGE (EXTREMES)
An active tracking band-pass filter
[AD-A156559] N86-10419

RANGE FINDERS
Satellite use for men --- West German space program N86-10180
A nanosecond or thirty centimeters: Why atomic clocks have to be synchronized. MITREX opens new dimensions for measuring accuracy N86-10185

RANGEFINDING
Phase coded pulse expander-compressor
[AD-D011817] N86-10376

RANK TESTS
Adaptive distribution-free test for the K random sampling problem, part 1
[COMP-CENT-NOTE-14-PT-1] N86-10888
Adaptive distribution free test for the K random sampling problem, part 2
[COMP-CENT-NOTE-15-PT-2] N86-10889
Nonparametric comparison of several mean values with mild adaptation to some sample characteristics
[COMP-CENT-NOTE-20] N86-10891

RANKINE CYCLE
Fuel Cell Technology Assessment Program, work element no. 6
[DE85-008228] N86-10444

RANKING
Rank revealing QR-Factorizations
[AD-A156756] N86-10887

RARE GASES
Determination of optical properties by third-harmonic generation in noble gases in unfocused laser beams N86-10535
Experimental X-ray scattering cross sections for H2 and rare atomic gases
[DE85-011572] N86-10936

RATES (PER TIME)
Study of one- and two-dimensional filtering and deconvolution algorithms for a streaming array computer
[NASA-CR-176221] N86-10822

RATS
Evaluation of the 90-day inhalation toxicity of petroleum and oil shale JP-5 jet fuel
[AD-A156615] N86-10675

RAY TRACING
Theoretical analysis of Wolter/LSM X-ray telescope systems
[NASA-CR-176244] N86-11095

RAYLEIGH NUMBER
Rayleigh-Benard instability in systems presenting a minimum in surface tension N86-10245

REACTION KINETICS
Fundamental studies of droplet combustion at reduced gravity N86-10165
A procedure identifying a polyacetylene initiator of olefin metathesis. The reactivities of metal-carbenes toward alkenes and alkynes
[AD-A156997] N86-10283
Catalytic activity of shock modified ZnO for CO oxidation and methanol synthesis
[DE85-014704] N86-10300
Self-heating to ignition measurements and computation of critical size for solar energy collector materials
[DE85-011449] N86-10302
Chemical kinetics and cellular structure of detonations in hydrogen sulphide and air
[DE85-009408] N86-10304
Kinetics of biological ferrous iron oxidation
[DE85-014616] N86-10736
Physical acoustics: Investigation of chemical kinetic and thermodynamic properties of fluids N86-10911

REACTIVITY
The role of entrained surface oxides in RS-PM aluminum alloys on resultant structures and properties N86-10085
Study of the reactive-element effect in oxidation of Fe-Cr alloys using transverse section analytical electron microscopy N86-10087

REACTOR DESIGN
Alternative fusion concepts and the prospects for improved reactors
[DE85-009622] N86-11031

REACTOR MATERIALS
ORR core re-configuration measurements to increase the fast neutron flux in the Magnetic Fusion Energy (MFE) experiments
[DE85-013520] N86-10958

REACTOR PHYSICS
Report on a visit to CERN in February 1985. Notes on bunch monitors, high-frequency systems, linacs, kickers, magnets, vacuum and bunch extraction
[LINO-119] N86-10967

REACTOR SAFETY
Activities report in safety N86-10365

REACTORS
Dust deposition in regions of separated flow
[JUEL-1985] N86-10475

READOUT
Soudan 2 data acquisition and trigger electronics
[DE85-013864] N86-10443

REAL GASES
On the method of characteristics and its application to the calculations of annular nozzle flowfields N86-10454

REAL TIME OPERATION
Velocities of gas and plasmas from real time holographic interograms
[DE85-014618] N86-10530
Computer control of an electric hydraulic robot leg with proximity ranging system N86-10549
Efficient systolic arrays for the solution of toeplitz systems: An illustration of a methodology for the construction of systolic architectures in VLSI (Very Large Systems Integration)
[AD-A156767] N86-10795
Classification of real-time program testing tasks and methods N86-10815

REAL VARIABLES
Coordinate axes, location of origin, and redundancy for the one and two-dimensional discrete Fourier transform
[NASA-CR-176225] N86-10826

RECEIVERS
Instantaneous frequency measurement receiver with digital processing
[AD-D011759] N86-10425
Fiber optic gradient hydrophone construction and calibration for sea trial
[AD-A156469] N86-10914

RECIRCULATIVE FLUID FLOW
Confined swirling jet predictions using a multiple-scale turbulence model
[NASA-CR-178484] N86-10462

RECOMMENDATIONS
Research needs for corrosion control and prevention in energy conservation systems
[DE85-014852] N86-10326

RECORDING
Fall velocity indicator/viewer
[AD-D011789] N86-10482

RECOVERABILITY
Improved arresting and recovery system for test missiles
[AD-D011743] N86-10198

RECTANGULAR WINGS
Experimental and theoretical investigations of the flow around airfoil systems with ground effect
[DFVLR-FB-85-17] N86-10026

RECURSIVE FUNCTIONS
Acceleration-invariant approximation method for recursive digital filters
[AD-A156655] N86-10865

RED SEA
Report of the Workshop on Geologic Applications of Remote Sensing to the Study of Sedimentary Basins
[E86-10002] N86-10599
Analysis of remote sensing data N86-10605

RED SHIFT
Radio studies of a complete sample of quasars N86-11093

REDOX CELLS
High-temperature controlled redox crystallization studies N86-10178

REDUCED GRAVITY
Microgravity Science and Applications Program tasks
[NASA-TM-87568] N86-10053
Solutal convection and its effects on crystal growth and segregation in binary and pseudo-binary system with large liquidus-solidus separation N86-10056
Crystal growth research in space N86-10057
Growth of organic crystals by Ostwald ripening N86-10058
The influence of low frequency mechanical vibrations on the growth of single crystals N86-10059
The control of float zone interfaces by the use of selected boundary conditions N86-10060

Crystal growth of device quality GaAs in space N86-10061
Crystal melts under reduced gravity N86-10062
Microgravity silicon zoning investigation N86-10063
Solution growth of crystals in zero-gravity N86-10064
Growth of solid solution crystals N86-10065
HgI sub 2 crystal growth for nuclear detectors N86-10066
Fluid dynamics and thermodynamics of vapor phase crystal growth N86-10068
Vapor growth of alloy-type semiconductor crystals N86-10069
Modeling directional solidification N86-10071
Heat flow and segregation in directional solidification N86-10072
Effect of undercooling in a low-gravity containerless environment on the structure and properties of alloys N86-10073
Control of cast iron microstructure N86-10084
Solidification fundamentals N86-10090
Diffusion in immiscible melts N86-10096
Directional solidification of monotectic and hypermonotectic aluminum-indium alloys under micron-g N86-10097
Environmental degradation of materials: Surface chemistry related to stress corrosion cracking N86-10099
Graphite formation in cast iron N86-10100
Theoretical studies of the surface tension of liquid metal system N86-10101
Cloud microphysics by thermal wave methods N86-10103
Extension of Ostwald ripening theory N86-10104
Dynamic thermophysical measurements in space [NASA ORDER H-27954-B] N86-10106
Transport processes in solution crystal growth N86-10107
Free surface phenomena under low- and zero-gravity conditions N86-10108
Thermocapillary flows and their stability: Effects of surface layers and contamination N86-10109
Mass transport phenomena between bubbles and dissolved gases in liquids under reduced gravity conditions N86-10110
Suppression of Marangoni convection in float zones N86-10111
Studies of model immiscible systems N86-10112
Light scattering tests of fundamental theories of transport properties in the critical region N86-10113
Transient heat transfer in zero gravity environment [NASA ORDER H-27954B] N86-10114
Surface tensions and their variations with temperature and impurities [NASA ORDER H-27954B] N86-10115
Direct observation of critical point wetting in microgravity N86-10116
Surface tension induced instabilities in reduced gravity: The Benard problem N86-10117
Critical transport phenomena in fluid helium under low gravity N86-10119
Surface-tension driven convection N86-10124
Thermocapillary motion research N86-10125
Thermocapillary and diffusocapillary migration of a fluid drop N86-10128
Transport processes research N86-10129
Experimental and theoretical analysis of chemical vapor deposition with prediction of gravity effects N86-10132
Hormone purification by isoelectric focusing N86-10135
Cell partition in two polymer aqueous phases N86-10136
A study of blood flow and of aggregation of blood cells under conditions of zero gravity: Its relevance to the occlusive diseases and cancer N86-10137
New instrumentation for phase partitioning N86-10138
Cell separations in microgravity and development of a space bioreactor N86-10141
Cell maintenance systems N86-10142
Kidney cell electrophoresis N86-10145
Production of large-particle-size monodisperse latexes in microgravity N86-10146
Containerless processing of glass forming melts in space N86-10148
Sol-gel glasses N86-10153
Physical phenomena in containerless glass processing N86-10155
Fusion target technology N86-10156
Solid surface combustion at reduced gravity N86-10159
Buoyancy effects upon vapor flame and explosion processes N86-10161
A fundamental study of smoldering with emphasis on experimental design for zero-g N86-10162
Ignition and flame spread above liquid fuel pools N86-10163
Flammability limits of gases under low gravity conditions N86-10164
Fundamental studies of droplet combustion at reduced gravity N86-10165
Development of materials processing systems for use in space on low-g simulation devices N86-10166
Multimode acoustic research N86-10167
Levitating furnance for containerless processing in space N86-10169
Microgravity Materials Science Laboratory N86-10173
High-temperature controlled redox crystallization studies N86-10178
Fifth European symposium on Material Sciences under Microgravity. Results of Spacelab 1 [ESA-SP-222] N86-10200
The fluid physics module: A technical description — Spacelab N86-10201
Capillary forces in a low gravity environment — Spacelab N86-10202
Oscillations of semi-free liquids in microgravity: Spacelab 1 experiment ES 326 N86-10204
Axisymmetric free surface behavior of moving liquid in a cylinder in microgravity — Spacelab N86-10206
Kinetics of spreading of liquids in microgravity: Experiment 1 ES 327 — Spacelab N86-10207
Influences affecting separation in monotectic alloys under microgravity N86-10209
Particle coarsening in immiscible zinc-lead alloys under microgravity — Spacelab N86-10210
Melting and solidification of metal matrix composites under microgravity — Spacelab N86-10211
Unidirectional solidification of cast iron: Experiment ES-325 — Spacelab N86-10212
Vacuum brazing under microgravity — Spacelab N86-10214
Melting and solidification in O-g of sintered alloys: Experiments ES 311 A and B bubble reinforced materials — Spacelab N86-10215
Directional solidification of an aluminum-zinc vapor emulsion in microgravity — Spacelab N86-10218
Protein single crystal growth under microgravity — Spacelab N86-10228
Mathematical simulation of disturbing forces and material science processes under low gravity N86-10236
Numerical simulation of convections in the microgravity environment N86-10239
Verification of turbulence developing from the oscillatory Marangoni convection in a liquid column — rocket flight N86-10241
Measurements of the critical Marangoni number of the laminar-oscillatory transition of thermocapillary convection in floating zones N86-10242
Experimental study on Marangoni convection N86-10243
Stability of long liquid columns N86-10244
Separation of aqueous two-phase polymer systems in microgravity N86-10246
Rationale for two phase polymer system microgravity separation experiments N86-10247
Application of the theory of Ostwald ripening to microgravity phase separation experiments N86-10248
Nucleate pool boiling in subcooled liquid under microgravity: Results of TEXUS experimental investigations N86-10250
Surface forces in contacting solids — microgravity rocket experiment N86-10252
Shrinking of a gas bubble in a glass melt under microgravity conditions — STS-11 N86-10254
Physical and chemical properties of a nickel catalyst processed under microgravity — STS-7 N86-10255
Cellular morphologies in lead-thallium alloys — gravitational effects N86-10262
Motion analysis report [NASA-CR-171897] N86-10896
Zero-gravity movement studies [NASA-CR-171899] N86-10897
Space sciences: Perspectives of commercial utilization for the German industry N86-11068

REDUNDANCY
Coordinate axes, location of origin, and redundancy for the one and two-dimensional discrete Fourier transform [NASA-CR-176225] N86-10826

REENTRY VEHICLES
Three articles on new calculation methods in aeronautics (selected articles) [AD-A145745] N86-10007

REFINING
Glass research N86-10157

REFLECTANCE
Vision test chart and method using Gaussians [AD-D011756] N86-10778
Preliminary investigation of changes in X-ray multilayer optics subjected to high radiation flux [DE85-014074] N86-10944

REFLECTION
Total internal reflection modulator/deflector [AD-D011757] N86-10424
Laser target speckle eliminator [AD-D011775] N86-10536

REFLECTORS
A numerical method for approximating antenna surfaces defined by discrete surface points [NASA-TM-87125] N86-10381
Theoretical analysis of Wolter/LSM X-ray telescope systems [NASA-CR-176244] N86-11095

REFRACTION
Crustal structure of the southern Rio Grande rift determined from seismic refraction, surface wave dispersion, and gravity data N86-10700

REFRACTORIES
Swelling and tensile properties of EBR-2-irradiated tantalum alloys for space reactor applications [DE85-012887] N86-10329

REFRACTORY MATERIALS
Development of a sheath for sensor protection in molten steel applications [AD-A156764] N86-10315

REFRIGERANTS
Freezer model using a population balance approach for steady-state, direct-contact, secondary refrigerant, freeze desalination N86-10361
Heat transfer in condensing and evaporating two-component, two-phase flow inside a horizontal tube N86-11058

REFRIGERATING MACHINERY
Engine-driven and absorption heat pump programs [DE85-013930] N86-10472

REGRESSION ANALYSIS
Regression analysis: Assumptions, alternatives, applications N86-10895

REGULATIONS
Tendencies toward liberalization in European air traffic control [DFVLR-FB-85-23] N86-10030
Biotechnology regulation [GPO-43-778] N86-10733

RELATIVISTIC EFFECTS
Relativistic wavefunction at the origin and the pion decay constant [DE85-012392] N86-11062
A method for numerical relativity: Simulation of axisymmetric gravitational collapse and gravitational radiation generation N86-11127

RELATIVISTIC ELECTRON BEAMS
Laser generation and transport of a relativistic electron beam [DE85-011709] N86-10192
Directionality of bremsstrahlung from relativistic electrons in solar flares [NASA-TM-87509] N86-11141

RELATIVITY
Initial data for N black holes N86-11128

RELAXATION (MECHANICS)
Anelastic relaxation in irradiated Cu-Be [DE85-013893] N86-11056

RELAXATION METHOD (MATHEMATICS)
A modified Successive Over-Relaxation (SOR) method for the Poisson equation in unsteady free-surface flow calculations [TW-264] N86-10881

RELIABILITY
Microcircuit device reliability field experience database. Volume 1. Field data. Volume 2. Failure Event/Analysis data [AD-A156836] N86-10433
Load space formulation of reliability for nonlinear random structural systems N86-10570
Elektronika MS 1603 high-speed peripheral processor N86-10811

REMOTE CONSOLES
SARSAT LUC (Local user terminal) to CMCC (Canadian Mission Control Centre) alert data interface: A critical review [AD-A156681] N86-10276

REMOTE CONTROL
Construction and use of a radio controlled model helicopter for research [AD-A156547] N86-10035

REMOTE HANDLING
Beginnings of remote handling at the RAL Spallation Neutron Source [DE85-012681] N86-11001

REMOTE REGIONS
The dirigible: A catalyst for resource exploitation in remote areas? [AD-A156518] N86-10034
Geological mapping of remote mountainous regions using metric camera imagery — Spacelab N86-10503

Photovoltaic systems in remote locations: An experience summary
[NASA-TM-87106] N86-10643

REMOTE SENSING
Discussion on the progress and future of satellite communication (Japan)
[NASA-TM-77672] N86-10378
Remote sensing
[NOTA-1535] N86-10638
Remote sensing study project East Gelderland (Netherlands). Part 2: Remote sensing flights in 1982 and 1983; organization aspects N86-10639
Life sciences research on the space station: An introduction
[NASA-TM-86836] N86-10734

REMOTE SENSORS
Multiple site laser excited pollution monitoring system
[AD-D011769] N86-10674

REPORTS
X-ray satellite
[NASA-TM-77923] N86-10273
Photovoltaics: Report, 1984
[DE85-014713] N86-10658

REQUIREMENTS
Specification for the performance, design, development and test requirements for a severe environment cartridge recorder. Issue 4
[AD-A156637] N86-10523
Test, measurement, and diagnostic equipment (system peculiar)
[AD-A156669] N86-10563

RESCUE OPERATIONS
The quest for a helicopter suitable for combat rescue, 1967 - 1983
[AD-A156842] N86-10040
SARSAT LUC (Local user terminal) to CMCC (Canadian Mission Control Centre) alert data interface: A critical review
[AD-A156881] N86-10276

RESEARCH
Psychological Sciences Division 1984 programs
[AD-A156631] N86-10779
Study of one- and two-dimensional filtering and deconvolution algorithms for a streaming array computer
[NASA-CR-176226] N86-10827

RESEARCH AIRCRAFT
User manual for the Falcon system — Falcon research aircraft
[DFVLR-MITT-85-08] N86-10721

RESEARCH AND DEVELOPMENT
Research needs for corrosion control and prevention in energy conservation systems
[DE85-014852] N86-10326
Soviet free-electron laser research
[AD-A156898] N86-10542
Phosphoric and electric utility fuel technology development
[DE85-014741] N86-10651
Alternative fusion concepts and the prospects for improved reactors
[DE85-009622] N86-11031
Space research expenses of the Federal Ministry of Research and Technology (BMFT) in the period 1983-1985 N86-11070
Academic Research Equipment in selected science-engineering fields, 1982-83. An analysis of findings from the Baseline National Survey of academic research instruments and instrumentation needs N86-11088
Aerospace research at NLR N86-11089

RESEARCH FACILITIES
Collective use computer system for the Academy of Sciences KaSSR N86-10817
Academic Research Equipment in selected science-engineering fields, 1982-83. An analysis of findings from the Baseline National Survey of academic research instruments and instrumentation needs N86-11088

RESEARCH MANAGEMENT
LSRO/ONR ad hoc review process
[AD-A156590] N86-10735
Mission orientation in science N86-11066
Space utilization N86-11067
Space research expenses of the Federal Ministry of Research and Technology (BMFT) in the period 1983-1985 N86-11070
Report of the ad hoc committee to review the program of the SDI Directorate on Innovative Science and Technology (IST)
[AD-A156668] N86-11071
Activities report of the Space Flight Laboratory N86-11090
Activities Report of the Space Flight Laboratory N86-11091

RESERVES
Maximum water reserves in the snow cover in the European territory of the USSR according to data for 1892-1960
[NASA-TM-77901] N86-10611

RESERVOIRS
Geologic evaluation and reservoir properties of the PR Spring tar sand deposit, Uintah and Grand Counties, Utah
[DE85-013248] N86-10634

RESIDENTIAL ENERGY
Comparative analysis of single and continuously variable-capacity heat pump concepts
[DE85-004089] N86-10653
Analyses of advanced residential absorption heat pump cycles
[DE85-005244] N86-10664
Contribution of wind energy to the energy balance of a combined solar and wind energy system. Part 1: System description, data acquisition and system performance
[BMFT-FB-T-85-051-VOL-1] N86-10670
Contribution of wind energy to the energy balance of a combined solar and wind energy system. Part 2: Computer-assisted investigations
[BMFT-FB-T-85-052-VOL-2] N86-10671

RESIDUAL STRENGTH
Fatigue of graphite/epoxy buffer strip panels with center cracks
[NASA-TM-87595] N86-10581

RESIDUES
A fundamental study of the sticking of insect residues to aircraft wings
[NASA-CR-176231] N86-10033

RESIN BONDING
The preparation and testing of titanium and zirconium coupling agents
[SJ70] N86-10576

RESINS
Continuous fiberization of silicon-carbide-nitride precursor resin N86-10168
Carbon fiber reinforced polymide filament wound tube manufacturing
[BR64172] N86-10339

RESISTANCE
Resistance curves for crack growth under plane-stress conditions in an elastic perfectly-plastic material
[AD-A156778] N86-10593

RESISTOJET ENGINES
Compatibility of grain-stabilized platinum with candidate propellants for resistojets
[NASA-TM-87118] N86-10279

RESONANCE
Supersonic metal cluster beams
[DE85-014321] N86-10966
Analytic evaluation of LAMPF 2 Booster Cavity design
[DE85-012680] N86-11002

RESONANCE TESTING
Test and evaluate passive orbital disconnect struts (PODS 3)
[NASA-CR-177368] N86-10274

RESONANT FREQUENCIES
Electromagnetic resonances of cylinders and aircraft model with resistive wires
[NASA-CR-176250] N86-10042

RESPIRATION
Evaluation of the 90-day inhalation toxicity of petroleum and oil shale JP-5 jet fuel
[AD-A156815] N86-10675

RESPIRATORS
Conditioning potentialities of respiratory apparatus N86-10753

RESPIRATORY RATE
Dynamics of general resistance of rats during readaptation period after training in altered gas environment N86-10767

RESPIRATORY SYSTEM
Classification of changes in electrocardiogram during muscular exertion of healthy individuals N86-10755
Reaction of rabbit respiration system to hypoxic stimulus in nitrogen-oxygen medium at elevated pressure N86-10760

RESPONSE TIME (COMPUTERS)
Study of one- and two-dimensional filtering and deconvolution algorithms for a streaming array computer
[NASA-CR-176221] N86-10822

RESPONSES
Determining a physically appropriate neutron spectrum from multisphere data
[DE85-013045] N86-10299
A transformation method for the evaluation of the response moments of elastic structures with random properties
[AD-A156882] N86-10557
A study of Morrison's iterative noise removal method
[NASA-CR-176222] N86-10823
Always-convergent iterative noise removal and deconvolution for image data
[NASA-CR-176223] N86-10824

RETARDING
Suppression of Marangoni convection in float zones N86-10111

RETROFITTING
Retrofit of SAC EC-135C and RC-135 aircraft with CFM-56 engines
[AD-A156688] N86-10038

REYNOLDS STRESS
Large eddy interactions in a turbulent channel flow
[NASA-TM-86757] N86-10464

RHEOELECTRICAL SIMULATION
Determination of thermophysical characteristics of solid materials by electrical modelling of the solutions to the inverse problems in nonsteady heat conduction
[NASA-TM-77907] N86-10293

RHEOLOGY
A study of blood flow and of aggregation of blood cells under conditions of zero gravity: Its relevance to the occlusive diseases and cancer N86-10137
Geothermal influences on the long-term thickness of the mechanical lithosphere during flexure N86-10697

RHONE DELTA (FRANCE)
Interpretation of metric camera concerning hydrologic structures of the Rhone Delta — Spacelab N86-10504
Topographic and thematic mapping: Analysis of metric camera black and white photographs of the Rhone Delta N86-10514

RIO GRANDE (NORTH AMERICA)
Crustal structure of the southern Rio Grande rift determined from seismic refraction, surface wave dispersion, and gravity data N86-10700

RISK
Development of the Multi-Attribute Hazard Assessment System (MAHAS) and its application to energy-related waste streams
[DE85-010278] N86-10676
Initial design of a relational database system for NPS computer asset identification and valuation for risk assessment
[AD-A156847] N86-10796
Framework for generating expert systems to perform computer security risk analysis
[DE85-014134] N86-10841
Risk propensity, action readiness and the roles of societal and individual decision makers
[IZF-1984-27] N86-11077

RIVER BASINS
Tertiary and quaternary research with remote sensing methods N86-10603
Paleogene vertebrate paleontology, geology and remote sensing in the Wind River Basin N86-10609

RIVERS
Report of the Workshop on Geologic Applications of Remote Sensing to the Study of Sedimentary Basins
[E86-10002] N86-10599

RIVETED JOINTS
Correlation between vibrations and buckling of cylindrical shells stiffened by spot-welded and riveted stringers
[TAE-537] N86-10584

ROBOTICS
Dynamic analysis of robotic manipulations with flexible links N86-10545
Computer control of an electric hydraulic robot leg with proximity ranging system N86-10549

ROBOTS
Measurement of workpiece temperature during welding for welding robot control N86-10534
USSR report: Cybernetics, computers and automation technology
[JPRS-UCC-85-006] N86-10809

ROBUSTNESS (MATHEMATICS)
Robust failure detection filters
[NASA-CR-176232] N86-10271
Robustness of multiple comparisons against variance heterogeneity
[COMP-CENT-NOTE-17] N86-10890

ROCKET ENGINE CASES
Ultrasonic evaluation of mechanical properties of thick, multilayered, filament wound composites
[MASA-TM-87088] N86-10561

ROCKET ENGINES
Analytical investigation of solid rocket nozzle failure
[NASA-TM-86513] N86-10278

ROCKET EXHAUST
Vibro-acoustic forecast for space shuttle launches at Vandenberg AFB: The payload changeout room and the administration building
[AD-A156944] N86-10269

ROCKET FLIGHT
Skin casting of alloys and composites: Results of Spacelab (SL)-1 and TEXUS experiments N86-10213
The TEXUS flight results on convective flows and heat transfer in simulated floating zones N86-10235

Verification of turbulence developing from the oscillatory Marangoni convection in a liquid column --- rocket flight N86-10241
A preliminary report on floating zone experiments with germanium crystals in a sounding rocket N86-10256

ROCKET LAUNCHING
Vibro-acoustic forecast for space shuttle launches at Vandenberg AFB: The payload changeout room and the administration building
[AD-A156944] N86-10269

ROCKET NOZZLES
High temperature mechanical testing of a cylindrical weave carbon-carbon composite
[AD-A156639] N86-10591

ROCKET PROPELLED SLEDS
Dynamic analysis of a sled traveling along a rough rail
[AD-A156589] N86-10191

ROCKS
Analysis of remote sensing data N86-10605
Remote stratigraphic and structural analysis: Multisensor results in the Wind River/Bighorn Basin area, Wyoming N86-10606
Geothermal influences on the long-term thickness of the mechanical lithosphere during flexure N86-10697
Fundamental study of the closure property of joints N86-10698

ROCKY MOUNTAINS (NORTH AMERICA)
Report of the Workshop on Geologic Applications of Remote Sensing to the Study of Sedimentary Basins
[E86-10002] N86-10599
Foreland basin structures and remote sensing N86-10608

ROLL
The influence of tactual seat-motion cues on training and performance in a roll-axis compensatory tracking task setting N86-10784

ROOM TEMPERATURE
Liquid to gas leak ratios with liquid nitrogen and liquid helium
[DE85-012950] N86-11030

ROOT-MEAN-SQUARE ERRORS
A root-mean-square pressure fluctuations model for internal flow applications
[NASA-CR-3928] N86-10460

ROTARY WINGS
Theoretical study of the unsteady linear problem for a rectangular wing with a pitching movement
[ONERA-RT-17/1841-RY-010-R] N86-10022

ROTATION
Theoretical modeling of the vapor cavitation in dynamically loaded journal bearings
[NASA-TM-87076] N86-10463
A superconducting tunnel junction receiver for millimeter-wave astronomy N86-11041

ROTOR BLADES (TURBOMACHINERY)
Forced response analysis of an aerodynamically detuned supersonic turbomachine rotor
[NASA-TM-87093] N86-10019

ROTORS
Three-dimensional inviscid analysis of radial turbine flow and a limited comparison with experimental data
[NASA-TM-87091] N86-10017

ROUGHNESS
A quantitative method for analyzing the roughness of the seafloor N86-10726

RUBBER
The rubber tube test section of the DFVLR in Goettingen, West Germany --- wind tunnel walls
[DFVLR-FB-85-18] N86-10051
Whole plant utilization of sunflowers as a renewable source of strategic materials (rubber)
[AD-A155833] N86-10342
Membrane research in energy and solvent recovery from industrial effluent streams
[DE85-014583] N86-10682

RUSTING
Rusty bolt intermodulation interference reducer
[AD-D011748] N86-10313
Passivation of steel with aqueous amine solutions
[AD-D011749] N86-10314

RUTHENIUM
Application of the ruthenium and technetium thermodynamic data bases used in the EQ3/6 geochemical codes
[DE85-013766] N86-10632

S

S CURVES
Stellar s-process diagnostics
[DE85-012926] N86-11134

SACCADIC EYE MOVEMENTS
Eye-movement activity as index of functional state of brain N86-10756

SAFETY DEVICES
Evaluation of the International Atomic Energy Agency (IAEA) Safeguards Analytical Laboratory quality assurance program
[DE85-012078] N86-10953

SAFETY MANAGEMENT
Activities report in safety N86-10365
Evaluation of the International Atomic Energy Agency (IAEA) Safeguards Analytical Laboratory quality assurance program
[DE85-012078] N86-10953

SANDSTONES
Tertiary and quaternary research with remote sensing methods N86-10603

SARSAT
SARSAT LUC (Local user terminal) to CMCC (Canadian Mission Control Centre) alert data interface: A critical review
[AD-A156881] N86-10276

SATELLITE ANTENNAS
A dual frequency microstrip antenna for Ka band
[NASA-TM-87124] N86-10380

SATELLITE ATTITUDE CONTROL
Nonlinear methods for spacecraft attitude maneuvers
[AD-A156956] N86-10275

SATELLITE IMAGERY
Satellite use for men --- West German space program N86-10180
Satellite data even for a poultry farm. A development for Tanzania. Image evaluation following new ways N86-10182
With Argus eyes from space. Satellite Diagnosis for Upper Volta. Seven maps without mystery N86-10183
LANDSAT TM image data quality analysis for energy-related applications
[E85-10109] N86-10597
Applications for three-dimensional computer graphic cloud representations produced from satellite imagery
[AD-A156903] N86-10798

SATELLITE NETWORKS
JPL emergency support of TDRSS and compatible satellites N86-10394

SATELLITE OBSERVATION
The air of life of the blue planet. Atmosphere research from space using data and facts against climate speculations N86-10184
Calibration of the multispectral scanner (MSS) satellite data to evaluate change in the reflection of coniferous stocks
[DFVLR-FB-84-44] N86-10636

SATELLITE TRANSMISSION
Digital transmission experiments with the Orbital Test Satellite
[EUT-84-E-144] N86-10270

SATELLITE-BORNE PHOTOGRAPHY
With Argus eyes from space. Satellite Diagnosis for Upper Volta. Seven maps without mystery N86-10183

SATELLITES
Lumped geopotential harmonics of order 14, from the orbit of 1967-11G
[AD-A156627] N86-10190

SCALARS
Gravitational collapse of a scalar field N86-11129

SCALE EFFECT
Freezer model using a population balance approach for steady-state, direct-contact, secondary refrigerant, freeze desalination N86-10361

SCALE MODELS
The Rhine-Meuse estuary hydraulic scale model. Experiences with computer configuration and software
[PUBL-335] N86-10637

SCALING LAWS
Ignition and flame spread above liquid fuel pools N86-10163
Design, fabricate and test a 1.06(MU) repetitively pulsed laser
[DE85-014439] N86-10543
Critical dynamics in superfluid helium N86-11046

SCATTERING
Ultrasonic evaluation of mechanical properties of thick, multilayered, filament wound composites
[MASA-TM-87088] N86-10561

SCATTERING CROSS SECTIONS
Dielectric properties of silicon surfaces and silver thin films
[JUEL-1968] N86-10450
Charge exchange in slow collisions of atoms and molecules N86-10922
Experimental X-ray scattering cross sections for H2 and rare atomic gases
[DE85-011572] N86-10936

SCATTEROMETERS
CV-990 L-band SAR: A calibration experiment N86-10617

SCHLIEREN PHOTOGRAPHY
Investigation of density gradient fluctuations in a turbulent free jet by means of the laser schlieren crossed-beam method
[DFVLR-FB-85-19] N86-10027
Advanced optical measurement techniques N86-10174

SCHOTTKY DIODES
Interdigital Schottky barrier capacitor apparatus
[AD-D011799] N86-10436
Realization of a multifunction Input/Output (I/O) controller by means of a gate array
[EUT-85-E-147] N86-10804

SCIENCE
Collective use computer system for the Academy of Sciences KaSSR N86-10817

SCIENTIFIC SATELLITES
X-ray satellite
[NASA-TM-77923] N86-10273

SCREWS
Termination load carrying device
[AD-D011800] N86-10558

SEA LEVEL
Mild hypoxia and visual performance with night vision goggles
[AD-A156969] N86-10787

SEATS
The influence of tactual seat-motion cues on training and performance in a roll-axis compensatory tracking task setting N86-10784
A graphic anthropometric aid for seating and workplace design
[AD-A156988] N86-10788

SECURITY
Methods for developing jam-resistant security communications networks at fixed-site facilities
[DE85-012032] N86-10408

SEDIMENT TRANSPORT
Dust deposition in regions of separated flow
[JUEL-1985] N86-10475

SEDIMENTARY ROCKS
Structural mapping of folded sedimentary environments from satellite images: An example from Central Asia N86-10607
Cretaceous and cenozoic stratigraphy of the upper and middle coastal plain, Harnett County area, North Carolina N86-10690
Stratigraphy, petrology, depositional and post-depositional histories and their effects upon reservoir properties of the Parkman Formation of the Mesa Verde group, Powder River Basin, Wyoming N86-10691

SEDIMENTS
Report of the Workshop on Geologic Applications of Remote Sensing to the Study of Sedimentary Basins
[E86-10002] N86-10599
Some opinions on remote sensing and geologic studies N86-10600
Position paper: Workshop on Geologic Applications of Remote Sensing to the Study of Sedimentary Basins N86-10601
Chronologic analysis of terrestrial sediments and basin evolution N86-10602
Tertiary and quaternary research with remote sensing methods N86-10603
Analysis of remote sensing data N86-10605
Remote stratigraphic and structural analysis: Multisensor results in the Wind River/Bighorn Basin area, Wyoming N86-10606
Structural mapping of folded sedimentary environments from satellite images: An example from Central Asia N86-10607
Foreland basin structures and remote sensing N86-10608
Neogene compressional deformation and possible thrust faulting in southwest Dominican Republic N86-10618
Lithologic mapping in a sedimentary environment using multipolarization SAR images N86-10624
Sediment characterization. Task 2: Instream contaminant study. Volume 2: Appendices
[DE85-013503] N86-10680
Application of the dutch method for estimating storm-induced dune erosion
[AD-A156717] N86-10728

SEISMIC ENERGY
Structural discontinuity within the southern California continental margin: Seismic and gravity models of the western Transverse Ranges N86-10699
Crustal structure of the southern Rio Grande rift determined from seismic refraction, surface wave dispersion, and gravity data N86-10700

SEISMIC WAVES
Cryogenic equivalence principle experiment N86-10171
Design, fabrication and testing of an experimental apparatus for determining particle behavior under very low intergranular stresses N86-10175

Formation of waves by ground motion
[PM/84/09] N86-10706
Understanding and improving acoustic to seismic coupling as it pertains to Sandia's helicopter detector
[DE85-009440] N86-10920

SEISMOLOGY
Seismic analysis of the large 70-meter antenna, part 1: Earthquake response spectra versus full transient analysis N86-10386
Remote stratigraphic and structural analysis: Multisensor results in the Wind River/Bighorn Basin area, Wyoming N86-10606
Time-term analysis of upper crustal structure in the Columbia Basin, Washington
[DE85-012390] N86-10633
In-situ geophysical investigations into the nature of the oceanic crust N86-10725

SELECTIVE FADING
Digital radio link: Method and a measuring system for studying the radio channel during frequency selective fading
[FOA-C-30386-E2] N86-10411

SELF ADAPTIVE CONTROL SYSTEMS
Identification of a plant's weighting sequence --- self-tuning control
[OUEL-1534/84] N86-10854

SELF ALIGNMENT
Increase of the packaging density of Very Large Scale Integration (VLSI) circuits using automatic alignment
[BMFT-FB-T-85-020] N86-10451

SELF DIFFUSION (SOLID STATE)
Self diffusion of Sn112 and Sn124 in liquid tin N86-10231

SEMANTICS
Compexity of higher-order programs
[DE85-012776] N86-10834

SEMICONDUCTOR DEVICES
Magnetic properties of doped semiconductors
[DE85-012090] N86-11053

SEMICONDUCTOR JUNCTIONS
Rusty bolt intermodulation interference reducer
[AD-D011748] N86-10313
P-N junction controlled field emitter array cathode
[AD-D011815] N86-10416
Sensor system
[AD-D011767] N86-10480
Some aspects of long-range, high-risk photovoltaic research at SERI
[DE85-012144] N86-10662
Electron tunneling in metal/tunnel-oxide/degenerate silicon junctions N86-11043

SEMICONDUCTORS (MATERIALS)
Processing of complex compound semiconductors in space N86-10054
Crystal growth of device quality GaAs in space N86-10061
Growth of solid solution crystals N86-10065
Vapor growth of alloy-type semiconductor crystals N86-10069
Energy stability of thermocapillary convection in models of the float zone process N86-10123
Directional solidification of InSb-NiSb eutectic --- Spacelab N86-10221
GaS-semiconductor crystals under microgravity: Experiment ES 323 --- Spacelab N86-10224
Preliminary reports, memoranda and technical notes of the Materials Research Council Summer Conference, La Jolla, California
[AD-A156776] N86-10291
Electrically conducting polymers N86-10333
Polymer engineering: Polymeric and molecular electronic, dielectric and optical properties for device applications
[AD-A156671] N86-10344
Interdigital Schottky barrier capacitor apparatus
[AD-D011799] N86-10436
Non-empirical interatomic potentials for transition metals
[DE85-013448] N86-10440
Parallel pulse processing for mercuric iodide gamma-ray detectors
[DE85-013391] N86-10528
Free carrier absorption from electrons in confined systems N86-11042
Electron tunneling in metal/tunnel-oxide/degenerate silicon junctions N86-11043

SENSITIVITY
High sensitivity millimeter-wave measurement apparatus
[AD-D011786] N86-10373
Elastic wave gyrometer. Experiments with a parametric wave device
[REPT-26/5005/HF/AR] N86-10533
Design sensitivity analysis and optimization of built-up structures N86-10565
Measurement of visual contrast sensitivity
[AD-D011776] N86-10973

SEPARATED FLOW
Experiments and computations on unsteady separating flow in an expanding flume
[REPT-2-84] N86-10477

SEPARATION
Weld metal hot-cracking of hastelloy alloys C-22 and C-276: A study by analytical electron microscopy
[DE85-009437] N86-10324

SEPARATORS
Impurity extraction by droplets N86-10122
Electrophoresis technology N86-10144
Phosphoric and electric utility fuel cell technology development
[DE85-014552] N86-10652
Membrane research in energy and solvent recovery from industrial effluent streams
[DE85-014583] N86-10682

SEQUENCING
Periodic binary sequences with very good autocorrelation properties N86-10397
A binary sequence of period 60 with better autocorrelation properties than the Barker sequence of period 13 N86-10398
Effect of sequence of loading on interaction curves for buckling of stiffened shells
[TAE-536] N86-10583

SEQUENTIAL COMPUTERS
Study of one- and two-dimensional filtering and deconvolution algorithms for a streaming array computer
[NASA-CR-176221] N86-10822

SEQUENTIAL CONTROL
Dynamic analysis of robotic manipulations with flexible links N86-10545

SEROTONIN
Effect of cold on brain serotonin system and plasma corticosteroid level in different strains of mice N86-10766

SERVICE LIFE
Captive volume device as a safe life monitor
[AD-D011802] N86-10525

SET THEORY
Principal bundles on the affine line N86-10856
Two algorithms for weighted matroid intersection
[AD-A156525] N86-10861

SETTLING
High-temperature controlled redox crystallization studies N86-10178

SHAPE CONTROL
Skin casting of alloys and composites: Results of Spacelab (SL)-1 and TEXUS experiments N86-10213
Design sensitivity analysis and optimization of built-up structures N86-10565

SHAPED CHARGES
Explosive initiation by very small conical shaped charge jets
[DE85-009443] N86-10357

SHAPES
Vision test chart and method using Gaussians
[AD-D011756] N86-10778
Conducting wall and pressure profile effect on MHD stabilization of axisymmetric mirror
[DE85-013847] N86-11020

SHEAR FLOW
Finite element solution of the Navier-Stokes equations for 3-D turbulent free shear flows N86-10457

SHEAR LAYERS
Three articles on new calculation methods in aeronautics (selected articles)
[AD-A145745] N86-10007
Effect of a shear layer on the stability of an axisymmetrical external compression air intake N86-10010

SHEAR PROPERTIES
Fabrication and metallurgical properties of modified 9Cr-1 Mo steel
[DE85-012885] N86-10328

SHEAR STRENGTH
Ultrasonic evaluation of mechanical properties of thick, multilayered, filament wound composites
[MASA-TM-87088] N86-10561

SHEAR STRESS
Inelastic analysis of frame structures including member and joint shears N86-10573

SHEATHS
Development of a sheath for sensor protection in molten steel applications
[AD-A156764] N86-10315

SHELLS (STRUCTURAL FORMS)
Attachment method-ceramic radome to metal body
[AD-D011778] N86-10032
Joint research effort on vibrations of twisted plates, phase 1: Final results
[NASA-RP-1150] N86-10579

SHOCK LOADS
Shock loading and release behavior of x-cut quartz
[DE85-013954] N86-11054

SHOCK WAVE INTERACTION
A numerical solution of the shock-turbulent interaction over a compression corner for supersonic flow N86-10003
Heating and generation of suprathermal particles at collisionless shocks
[DE85-014114] N86-11034

SHOCK WAVE PROPAGATION
Heating and generation of suprathermal particles at collisionless shocks
[DE85-014114] N86-11034
Shock loading and release behavior of x-cut quartz
[DE85-013954] N86-11054

SHOCK WAVES
Second order approximation method for transonic flows over swept wings N86-10002
Catalytic activity of shock modified ZnO for CO oxidation and methanol synthesis
[DE85-014704] N86-10300
On the method of characteristics and its application to the calculations of annular nozzle flowfields N86-10454
Angle of incidence effects for underwater shock using generic computational models, rev. 1
[DE85-012921] N86-10467
Spontaneous Raman spectroscopy of shocked H2O
[DE85-014557] N86-10470
Improved particle-velocity transducer for equation-of-state experiments
[DE85-013204] N86-10532
High-pressure release-wave measurements and phase transformation in CaCO3
[DE85-012592] N86-11055

SHORT TAKEOFF AIRCRAFT
Evaluation of an aerodynamic-load prediction method on a STOL fighter configuration
[NASA-TM-86782] N86-10015

SHORT WAVE RADIO TRANSMISSION
Acoustic gravity wave chemistry model for the RAYTRACE code
[AD-A156850] N86-10405

SHRINKAGE
Shrinking of a gas bubble in a glass melt under microgravity conditions --- STS-11 N86-10254

SHUTTLE IMAGING RADAR
High-resolution image data from the Space Shuttle N86-10494
Vegetation canopy discrimination and biomass assessment using multipolarized airborne SAR N86-10628

SIDELOBE REDUCTION
A binary sequence of period 60 with better autocorrelation properties than the Barker sequence of period 13 N86-10398

SIDELOBES
Periodic binary sequences with very good autocorrelation properties N86-10397
A binary sequence of period 60 with better autocorrelation properties than the Barker sequence of period 13 N86-10398

SIERRA NEVADA MOUNTAINS (CA)
Altitudinal distribution of granitic landforms in the south central Sierra Nevada, California N86-10695

SIGNAL ANALYSIS
The role of freestream turbulence scale in subsonic flow separation
[NASA-CR-176237] N86-10014
Signal analysis of gas tungsten arc welds N86-10078
Signal analysis receiver with acousto-optic delay lines
[AD-D011761] N86-10427

SIGNAL DETECTION
Apparatus for locating passive intermodulation interference sources
[AD-D011798] N86-10435
Proposed aural nondetectability limits for Army materiel
[AD-A156704] N86-10917
Optical detection of photoacoustic pulses in thin silicon wafers
[AD-A156705] N86-10977

SIGNAL DETECTORS
Constant rise AGC (Automatic Gain Control) device
[AD-D011744] N86-10421
Fiber optic gradient hydrophone construction and calibration for sea trial
[AD-A156469] N86-10914

SIGNAL ENCODING
Computational techniques for the analysis and design of digital communication systems
[AD-A156945] N86-10407

SIGNAL FADING
Digital radio link: Method and a measuring system for studying the radio channel during frequency selective fading
[FOA-C-30386-E2] N86-10411
SIGNAL MEASUREMENT
Optical detection of photoacoustic pulses in thin silicon wafers
[AD-A156705] N86-10977
SIGNAL PROCESSING
The interpolation of signals sampled at less than the Nyquist rate N86-10368
Amplitude and phase modulation in fin-lines electrical tuning
[AD-D011813] N86-10415
Pulse compression system
[AD-D011833] N86-10417
A compact bulk acousto-optic time integrating correlator
[AD-A156608] N86-10428
Multiple site laser excited pollution monitoring system
[AD-D011769] N86-10674
Parallel local interface bus
[AD-D011742] N86-10792
Efficient systolic arrays for the solution of toeplitz systems: An illustration of a methodology for the construction of systolic architectures in VLSI (Very Large Systems Integration)
[AD-A156767] N86-10795
An improved FFT (Fast fourier transform) for a four parallel pipe SIMD arithmetic processor
[AD-A156625] N86-10863
Sound radiation from repetitive transient vibrations using multi-channel digital signal processing with application to impact machinery N86-10910
Method for determining the position, angle and other injection parameters of a short pulsed beam in the Brookhaven AGS
[DE85-012523] N86-10931
Kalman filter preprocessor
[AD-D011774] N86-10972
SIGNAL TO NOISE RATIOS
Sample data phase locked loop for adaptive Doppler tracker
[AD-D011788] N86-10374
A sequential decoding performance analysis for International Comet Explorer N86-10390
High-rate convolutional code construction with the minimum required SNR criterion N86-10392
Pulse compression system
[AD-D011833] N86-10417
Variability analysis of visually induced responses in the midst of noise
[B8564052] N86-10774
A study of derivative filters using the discrete Fourier transform
[NASA-CR-176224] N86-10825
Naive approximate realization of noisy data
[ER-83/10] N86-10880
SIGNAL TRANSMISSION
Mobile VLBI and GPS measurement of vertical crustal motion N86-10401
SILANES
Modelling of laser-enhanced chemical vapor deposition N86-10105
Photovoltaic devices using a Si:H from higher order silanes
[DE85-008804] N86-10668
SILICA GLASS
Interdiffusion in the glass melt system (Na2O+Rb2O).3SiO2 --- Spacelab N86-10216
SILICATES
High-temperature controlled redox crystallization studies N86-10178
SILICON
Microgravity silicon zoning investigation N86-10063
Modelling of laser-enhanced chemical vapor deposition N86-10105
Surface tension induced instabilities in reduced gravity: The Benard problem N86-10117
Bulk formation of metallic glasses and amorphous silicon from the melt N86-10154
Crystallization of a silicon sphere --- Spacelab N86-10226
Crystal growth of silicon in Spacelab 1: Experiment ES-321 N86-10227
Development of metallization process
[NASA-CR-176209] N86-10312
Defect identification in high-energy semiconductors
[DE85-014533] N86-10442
Dielectric properties of silicon surfaces and silver thin films
[JUEL-1968] N86-10450
Making the right choice --- silicon photodiodes N86-10669
Optical detection of photoacoustic pulses in thin silicon wafers
[AD-A156705] N86-10977
Magnetic properties of doped semiconductors
[DE85-012090] N86-11053
SILICON CARBIDES
Continuous fiberization of silicon-carbide-nitride precursor resin N86-10168
High temperature properties of SiC materials
[BMFT-FB-T-85-047] N86-10353
Characterization of mechanical damage mechanisms in ceramic composite materials
[AD-A156574] N86-10590
SILICON DIOXIDE
Investigation of metallic impurities introduced into SiO2 and silicon by various candidate VLSI metallization systems: Chemical reactions, diffusion, and electrical properties
[AD-A156609] N86-10429
SILICON FILMS
Improved blue response and efficiency of A-Si:H solar cells deposited from disilane using a dual-chamber plasma system
[DE85-013289] N86-10649
SILICON JUNCTIONS
Investigation of metallic impurities introduced into SiO2 and silicon by various candidate VLSI metallization systems: Chemical reactions, diffusion, and electrical properties
[AD-A156609] N86-10429
SILICON NITRIDES
Mixed-mode fracture of ceramics
[DE85-014087] N86-10349
High temperature properties and characterization of S3-N4 materials
[BMFT-FB-T-85-046] N86-10352
SILICON OXIDES
Colloidal oxide properties and kinetic studies N86-10147
SILVER
Dielectric properties of silicon surfaces and silver thin films
[JUEL-1968] N86-10450
SILVER ALLOYS
Reduction of noble metal stock and noble metal loss during wire production with the Conform extrusion process
[BMFT-FB-T-85-049] N86-10560
SIMULATION
Cryogenic equivalence principle experiment N86-10171
Time-implicity simulation of particle-fluid systems
[DE85-012944] N86-10471
High flux calorimetry
[AD-A156852] N86-10524
Simulation of the atmospheric boundary layer in the large wind tunnel of the TNO Institute for Building materials and Constructions (IBBC). Part 1: Theory
[BI-76-39/08.7.23100-PT-1] N86-10703
Simulation of the atmospheric boundary layer in the large wind tunnel of the TNO Institute for Building Materials and Construction (IBBC). Part 2: Experiments
[BI-76-39/08.7.23100-PT-2] N86-10704
Optical testing of large telescopes using multiple subapertures N86-10971
A method for numerical relativity: Simulation of axisymmetric gravitational collapse and gravitational radiation generation N86-11127
SIMULATORS
Simulated direct-strike lightning testing at Sandia National Laboratories
[DE85-012033] N86-10049
SINGLE CRYSTALS
Processing of complex compound semiconductors in space N86-10054
Growth of solid solution crystals N86-10065
Fluid dynamics and thermodynamics of vapor phase crystal growth N86-10068
Environmental degradation of materials: Surface chemistry related to stress corrosion cracking N86-10099
Growth of larger single crystals N86-10186
Lead telluride crystals grown in microgravity: Experiment ES 318 --- Spacelab N86-10220
GaS-semiconductor crystals under microgravity: Experiment ES 323 --- Spacelab N86-10224
Solution growth of cadmium telluride: Experiment ES 322 --- Spacelab N86-10225
Protein single crystal growth under microgravity --- Spacelab N86-10228
Growth and characterization of brushite and lead monetite, simulation and results --- Spacelab N86-10230
Creep-fatigue behavior of NiCoCrAlY coated PWA 1480 superalloy single crystals
[NASA-TM-87110] N86-10311
Low temperature plastic deformation mechanisms of alpha-titanium single crystals
[ESA-TT-871] N86-10332
Extended precision in video bandwidth analog to digital converter using optical techniques
[AD-D011745] N86-10422
Adsorption of oxygen on single crystal tin at liquid helium temperatures N86-11044
High-pressure release-wave measurements and phase transformation in CaCO3
[DE85-012592] N86-11055
SINGULARITY (MATHEMATICS)
Theoretical specific impulse for two-phase flow in nozzle of rocket-ramjet engine: A simple estimation method N86-10005
Analysis of hyperlift systems. Study of a singularities method
[SNIAS-443.529/84] N86-10024
Estimates for maximal functions along hypersurfaces
[CTH-MATH-1984-29] N86-10874
SINTERED ALUMINUM POWDER
Melting and solidification in O-g of sintered alloys: Experiments ES 311 A and B bubble reinforced materials --- Spacelab N86-10215
SINTERING
Melting and solidification in O-g of sintered alloys: Experiments ES 311 A and B bubble reinforced materials --- Spacelab N86-10215
SIPHONS
Laminar film condensation in vertical closed two-phase thermosiphons
[IKE-5-220] N86-10476
SITE SELECTION
LANDSAT TM image data quality analysis for energy-related applications
[E85-10109] N86-10597
Overview of wind turbine siting research: Prospecting to micrositing
[DE85-013496] N86-10666
SITES
Methods for developing jam-resistant security communications networks at fixed-site facilities
[DE85-012032] N86-10408
SIZE (DIMENSIONS)
Self-heating to ignition measurements and computation of critical size for solar energy collector materials
[DE85-011449] N86-10302
Photographic catalog of selected planetary size comparisons
[NASA-TM-86207] N86-11138
SKIN TEMPERATURE (BIOLOGY)
Heat transfer mechanism in human extremities N86-10759
SKY BRIGHTNESS
Mobile VLBI and GPS measurement of vertical crustal motion N86-10401
Optical/IR telescope arrays: A study of their potential for satisfying observational requirements in astronomy for a large aperture system in the 1990s and beyond
[REPT-15] N86-11094
SLEEP
Intradiurnal organization of wakefulness-sleep sequence and energy metabolism in rats exposed to low ambient temperature N86-10764
SLEEP DEPRIVATION
The effects of age, sleep deprivation, and altitude on complex performance
[AD-A156987] N86-10771
SLOPES
Marginal terrain straddle-lift container handler
[AD-D011752] N86-10555
SLOTS
Effects of slots/holes in disks on frequencies of TM01 and EH11 waves in the disk-loaded waveguide
[DE85-013376] N86-11009
SLOTTED WIND TUNNELS
Investigations to improve the slotted-wall test section of the F+W transonic wind tunnel
[F+W-FO-1752] N86-10050
SMELTING
Multimode acoustic research N86-10167
SMOKE
Methods for developing jam-resistant security communications networks at fixed-site facilities
[DE85-012032] N86-10408
SNOW COVER
Evaluation of metric camera photos --- Spacelab; alpine snow cover N86-10515
Maximum water reserves in the snow cover in the European territory of the USSR according to data for 1892-1960
[NASA-TM-77901] N86-10611
Representation of the distribution of the snow cover on the surface of the Earth's dry land
[NASA-TM-77909] N86-10612

Observations of the snow cover in the southern part of the Buryat Autonomous Soviet Socialist Republic
[NASA-TM-77910] N86-10613
Laws of distribution of the snow cover on the greater Caucasus (Soviet Union)
[NASA-TM-77911] N86-10614

SODIUM
Design and calibration of a flat-flame burner using line reversal techniques
[AD-A156724] N86-10294
A modeling analysis program for the JPL table mountain lo sodium cloud
[NASA-CR-176241] N86-11139

SODIUM SULFATES
Environmental degradation of materials: Surface chemistry related to stress corrosion cracking N86-10099

SOFTWARE TOOLS
Ada (trademark) Programming Support Environment (APSE) Evaluation and Validation (E and V) workshop report held at Airlie, Virginia on 2-6 April 1984
[AD-A156667] N86-10829

SOIL EROSION
Erosion control and watershed management by Spacelab photography N86-10493
Application of the dutch method for estimating storm-induced dune erosion
[AD-A156717] N86-10728

SOIL MAPPING
Examples of regional environmental assessment using acid deposition data
[DE85-012903] N86-10677

SOIL MOISTURE
The effect of vegetation type, microrelief, and incidence angle on radar backscatter N86-10619
The boundary condition in a numerical model of atmospheric flows over fixed interfaces
[GKSS-85-E-10] N86-10722

SOIL SCIENCE
Development and evaluation of multispecies test protocols for assessing chemical toxicity
[DE85-013526] N86-10679

SOILS
Design, fabrication and testing of an experimental apparatus for determining particle behavior under very low intergranular stresses N86-10175
Marginal terrain straddle-lift container handler
[AD-D011752] N86-10555
Vegetation and soils field research data base: Experiment summaries
[E85-10110] N86-10610

SOLAR ARRAYS
Photovoltaics: Report, 1984
[DE85-014713] N86-10658
Photovoltaic concentrator array evaluation
[DE85-013789] N86-10665

SOLAR CELLS
Development of metallization process
[NASA-CR-176209] N86-10312
Improved blue response and efficiency of A-Si:H solar cells deposited from disilane using a dual-chamber plasma system
[DE85-013289] N86-10649
Theory of advanced, high-efficience concentrator cells
[DE85-008821] N86-10655
Photovoltaics: Report, 1984
[DE85-014713] N86-10658
Some aspects of long-range, high-risk photovoltaic research at SERI
[DE85-012144] N86-10662
Photovoltaic devices using a Si:H from higher order silanes
[DE85-008804] N86-10668
Cooperative emission by two different atoms into surface plasmons
[AD-A157033] N86-10925

SOLAR COLLECTORS
Self-heating to ignition measurements and computation of critical size for solar energy collector materials
[DE85-011449] N86-10302
Solar thermal technical information guide
[DE85-002941] N86-10657
Photovoltaics: Report, 1984
[DE85-014713] N86-10658

SOLAR COOLING
Passive and hybrid solar technologies program summary
[DE85-013100] N86-10648

SOLAR ELECTRIC PROPULSION
Solar propulsion for the TRIO interferometer N86-11109

SOLAR ENERGY
Passive solar design handbook
[DE85-014263] N86-10656
Solar thermal technical information guide
[DE85-002941] N86-10657
Contribution of wind energy to the energy balance of a combined solar and wind energy system. Part 1: System description, data acquisition and system performance
[BMFT-FB-T-85-051-VOL-1] N86-10670

SOLAR ENERGY CONVERSION
Passive and hybrid solar technologies program summary
[DE85-013100] N86-10648
Solar thermal technical information guide
[DE85-002941] N86-10657

SOLAR FLARES
Directionality of bremsstrahlung from relativistic electrons in solar flares
[NASA-TM-87509] N86-11141
Solar flares and magnetospheric particles: Investigations based upon the ONR-602 experiment
[AD-A156583] N86-11142

SOLAR FLUX
Integrating sphere measurements of directional-hemispherical transmittance of window systems
[DE85-013926] N86-10978

SOLAR GENERATORS
Research on solar pumped liquid lasers
[NASA-CR-176235] N86-10539
Passive and hybrid solar technologies program summary
[DE85-013100] N86-10648

SOLAR HEATING
Passive and hybrid solar technologies program summary
[DE85-013100] N86-10648
Passive solar design handbook
[DE85-014263] N86-10656
Contribution of wind energy to the energy balance of a combined solar and wind energy system. Part 1: System description, data acquisition and system performance
[BMFT-FB-T-85-051-VOL-1] N86-10670

SOLAR HOUSES
Passive and hybrid solar technologies program summary
[DE85-013100] N86-10648

SOLAR RADIATION
Energy balance in a deep Colorado valley: ASCOT 84
[DE85-012441] N86-10631
Identification of chemical and physical phenomena affecting the durability of silvered polymer (PMMA) mirrors
[DE85-012131] N86-10645
A numerical model for the estimation of solar radiation on rugged terrain N86-10694
A modeling analysis program for the JPL table mountain lo sodium cloud
[NASA-CR-176241] N86-11139

SOLAR REFLECTORS
Identiiication of chemical and physical phenomena affecting the durability of silvered polymer (PMMA) mirrors
[DE85-012131] N86-10645

SOLAR SAILS
TRIO: A kilometric array stabilized by solar sails --- Spaceborne astronomy N86-11102
Solar propulsion for the TRIO interferometer N86-11109

SOLAR SYSTEM
Stellar s-process diagnostics
[DE85-012926] N86-11134
Photographic catalog of selected planetary size comparisons
[NASA-TM-86207] N86-11138

SOLDERS
Reduction of noble metal stock and noble metal loss during wire production with the Conform extrusion process
[BMFT-FB-T-85-049] N86-10560

SOLID PHASES
Thermal expansion of glasses in the solid and liquid phases
[DE85-013953] N86-10351

SOLID PROPELLANTS
Analytical investigation of solid rocket nozzle failure
[NASA-TM-86513] N86-10278

SOLID ROCKET BINDERS
Binder-filler interaction in energetic polymers
[AD-A156752] N86-10345

SOLID STATE DEVICES
Fluid dynamics and thermodynamics of vapor phase crystal growth N86-10068
Preliminary reports, memoranda and technical notes of the Materials Research Council Summer Conference, La Jolla, California
[AD-A156776] N86-10291
Semiconductor superlattic photodetectors
[NASA-CR-176249] N86-10484

SOLID STATE LASERS
Design, fabricate and test a 1.06(MU) repetitively pulsed laser
[DE85-014439] N86-10543

SOLID SURFACES
Solid surface combustion at reduced gravity N86-10159

SOLID-SOLID INTERFACES
Surface forces in contacting solids --- microgravity rocket experiment N86-10252

SOLIDIFICATION
Microgravity Science and Applications Program tasks
[NASA-TM-87568] N86-10053
Fluid flow in crystal growth: Analysis of the verticle Bridgman and floating zone process N86-10055
Solutal convection and its effects on crystal growth and segregation in binary and pseudo-binary system with large liquidus-solidus separation N86-10056
The influence of containerless undercooling and rapid solid-state quenching on the superconductive and magnetic properties of some clustering alloy systems N86-10076
Convection during unidirectional solidification N86-10077
Mephisto: Interfacial destabilization in metal alloys N86-10079
Undercooling, remelting, and coarsening N86-10080
Dendritic growth in undercooled melts N86-10082
Influence of melt convection on solid-liquid interface under terrestrial and reduced gravity environments N86-10083
Control of cast iron microstructure N86-10084
The development and prevention of channel segregation during alloy solidification N86-10086
Orbital processing of aligned magnetic composites N86-10089
Solidification fundamentals N86-10090
Containerless processing of undercooled melts N86-10093
Thermal and solutal convection damping using an applied magnetic field N86-10094
Directional solidification of monotectic and hypermonotectic aluminum-indium alloys under micron-g N86-10097
Graphite formation in cast iron N86-10100
Studies of model immiscible systems N86-10112
Rapid solidification of magnetic oxides N86-10152
Oxidation behavior of glassy alloys N86-10158
Modification of the electromagnetic levitator (EML) hardware N86-10172
Microgravity Materials Science Laboratory N86-10173
Melting and solidification of metal matrix composites under microgravity --- Spacelab N86-10211
Melting and solidification in O-g of sintered alloys: Experiments ES 311 A and B bubble reinforced materials --- Spacelab N86-10215
Directional solidification of InSb-NiSb eutectic --- Spacelab N86-10221
Experimental facility for materials research in space (CSK-1) N86-10263
Measurement of the density of base fluids at pressures 0.422 to 2.20 GPa
[NASA-TM-87114] N86-10551

SOLIDS
Directional solidification of monotectic and hypermonotectic aluminum-indium alloys under micron-g N86-10097
Dynamic thermophysical measurements in space
[NASA ORDER H-27954-B] N86-10106
Determination of thermophysical characteristics of solid materials by electrical modelling of the solutions to the inverse problems in nonsteady heat conduction
[NASA-TM-77907] N86-10293

SOLITARY WAVES
Topics in nonlinear wave theory with applications N86-10367

SOLUBILITY
Liquid phase miscibility gap materials N86-10081
Influences affecting separation in monotectic alloys under microgravity N86-10209
Particle coarsening in immiscible zinc-lead alloys under microgravity --- Spacelab N86-10210
Stability of metallic dispersions --- microgravity N86-10258
Space shuttle experiments on Al-In liquid phase miscibility gap (LPMG) alloys N86-10264

SOLUTES
Electrohydrodynamics N86-10130

SOLVATION
Rapid analysis using capillary supercritical fluid chromatography
[DE85-012460] N86-10297

SOLVENT EXTRACTION
Extraction of lanthanide ions by 2-methyl-8-quinolinol
[DE85-014277] N86-10303

SOLVENTS
Recovery of alcohol from a fermentation source by separation rather than distillation
[AD-D011782] N86-10282
Rusty bolt intermodulation interference reducer
[AD-D011748] N86-10313
Thermodynamics of polymer-supercritical solvent mixtures
[AD-A157038] N86-11061
SONDES
Satellite use for men --- West German space program N86-10180
SONIC ANEMOMETERS
Field comparison of in situ meteorological sensors
[PB85-196988] N86-10723
SOOT
Microphysical/mesoscale aspects of nuclear winter and new directions in assessments
[DE85-013479] N86-10718
SORET COEFFICIENT
Thermomigration of cobalt in liquid tin: Experiment 1 ES 320 --- Spacelab N86-10222
Space experiment on thermal diffusion. Preparation and theoretical analysis N86-10253
SOUND TRANSMISSION
Proposed aural nondetectability limits for Army materiel
[AD-A156704] N86-10917
SOUND WAVES
Multimode acoustic research N86-10167
Advanced containerless processing technology N86-10176
Elastic properties and thermal stability characterization of metallic glasses by guided wave techniques N86-10337
Tunable acousto-optic filter with improved spectral resolution and increased aperture
[AD-D011758] N86-10915
SOUTHERN HEMISPHERE
Representation of the distribution of the snow cover on the surface of the Earth's dry land
[NASA-TM-77909] N86-10612
SPACE CAPSULES
Guidance and control of a cable based payload pickup system N86-10046
SPACE COMMERCIALIZATION
Space utilization N86-11067
Space sciences: Perspectives of commercial utilization for the German industry N86-11068
SPACE INDUSTRIALIZATION
Space sciences: Perspectives of commercial utilization for the German industry N86-11068
SPACE MAINTENANCE
Cell maintenance systems N86-10142
SPACE MANUFACTURING
Thermocapillary and diffusocapillary migration of a fluid drop N86-10128
Development of materials processing systems for use in space on low-g simulation devices N86-10166
SPACE OBSERVATIONS (FROM EARTH)
Results and limitations of ground-based optical arrays --- stellar interferometry N86-11097
SPACE POWER REACTORS
Swelling and tensile properties of EBR-2-irradiated tantalum alloys for space reactor applications
[DE85-012887] N86-10329
SPACE PROBES
A sequential decoding performance analysis for International Comet Explorer N86-10390
SPACE PROCESSING
Microgravity Science and Applications Program tasks
[NASA-TM-87568] N86-10053
Processing of complex compound semiconductors in space N86-10054
Fluid flow in crystal growth: Analysis of the verticle Bridgman and floating zone process N86-10055
Solutal convection and its effects on crystal growth and segregation in binary and pseudo-binary system with large liquidus-solidus separation N86-10056
Crystal growth research in space N86-10057
Crystal melts under reduced gravity N86-10062
Solution growth of crystals in zero-gravity N86-10064
Float zone experiments in space N86-10067
Modeling directional solidification N86-10071
Heat flow and segregation in directional solidification N86-10072
Measurement of high temperature thermophysical properties N86-10074
Effect of undercooling and modified microstructure on the physical properties of material synthesized in the drop tube and drop tower N86-10075
Production of large-particle-size monodisperse latexes in microgravity N86-10146
Containerless processing of glass forming melts in space N86-10148
Gel precursors as glass and ceramic starting materials for space processing applications research N86-10150
Glass formation in reluctant glass formers N86-10151
Sol-gel glasses N86-10153
Physical phenomena in containerless glass processing N86-10155
Glass research N86-10157
Electric field containerless processing technology N86-10170
Fifth European symposium on Material Sciences under Microgravity. Results of Spacelab 1
[ESA-SP-222] N86-10200
Unidirectional solidification of cast iron: Experiment ES-325 --- Spacelab N86-10212
Skin casting of alloys and composites: Results of Spacelab (SL)-1 and TEXUS experiments N86-10213
Crystal growth of GaAs in space N86-10234
Mathematical simulation of disturbing forces and material science processes under low gravity N86-10236
Physical and chemical properties of a nickel catalyst processed under microgravity --- STS-7 N86-10255
Stability of metallic dispersions --- microgravity N86-10258
First Spacelab Payload (FSLP) experiments on composite materials N86-10265
First Spacelab Payload (FSLP) experiments in metallurgy N86-10266
SPACE PROGRAMS
Space research expenses of the Federal Ministry of Research and Technology (BMFT) in the period 1983-1985 N86-11070
SPACE SHUTTLE MISSION 41-G
High-resolution image data from the Space Shuttle N86-10494
SPACE SHUTTLE ORBITERS
Physical and chemical properties of a nickel catalyst processed under microgravity --- STS-7 N86-10255
Transport processes in directional solidification during space shuttle flight N86-10257
Stability of metallic dispersions --- microgravity N86-10258
SPACE SHUTTLE PAYLOADS
Modification of the electromagnetic levitator (EML) hardware N86-10172
SPACE SHUTTLES
Vibro-acoustic forecast for space shuttle launches at Vandenberg AFB: The payload changeout room and the administration building
[AD-A156944] N86-10269
SPACE STATIONS
Compatibility of grain-stabilized platinum with candidate propellants for resistojets
[NASA-TM-87118] N86-10279
Life sciences research on the space station: An introduction
[NASA-TM-86836] N86-10734
SPACE SURVEILLANCE (GROUND BASED)
SETI radio spectrum surveillance system N86-10400
SPACEBORNE ASTRONOMY
Colloquium on Kilometric Optical Arrays in Space
[ESA-SP-226] N86-11096
Extragalactic observations with optical space arrays N86-11098
Astronomical criteria for interferometric arrays --- Spacecraft design N86-11099
High angular resolution in the infrared: Prospects for space observations N86-11100
Strategy for the development of space arrays N86-11101
TRIO: A kilometric array stabilized by solar sails --- Spaceborne astronomy N86-11102
SAMSI: An orbiting spatial interferometer for micro-arc second astronomical observations --- Spacecraft Array for Michelson Spatial Interferometry (SAMSI) N86-11103
COSMIC: A high resolution, large collecting area telescope --- Coherent Optical System of Modular Imaging Collectors (COSMIC) N86-11104
A fiber-linked version of project TRIO --- telescope array N86-11105
OASIS: Optical Aperture Synthesis in Space N86-11106
Future space telescope design concepts N86-11107
TRIO optics --- spaceborne optical interferometer (TRIO) N86-11108
Mission analysis aspects --- spaceborne interferometry N86-11114
Problems in image reconstruction with optical arrays --- spaceborne astronomy N86-11115
Space antenna for gravitational wave astronomy N86-11123
The DUO: Far infrared heterodyne concept for space interferometry N86-11125
SPACEBORNE EXPERIMENTS
Orbital processing of aligned magnetic composites N86-10089
Purification and cultivation of human pituitary growth hormones secreting cells N86-10140
Cell separations in microgravity and development of a space bioreactor N86-10141
Electrophoresis technology N86-10144
Space experiment on thermal diffusion. Preparation and theoretical analysis N86-10253
Shrinking of a gas bubble in a glass melt under microgravity conditions --- STS-11 N86-10254
Experimental facility for materials research in space (CSK-1) N86-10263
Space shuttle experiments on Al-In liquid phase miscibility gap (LPMG) alloys N86-10264
SPACEBORNE PHOTOGRAPHY
Metric Camera Workshop --- Spacelab
[ESA-SP-209] N86-10485
Digital elevation model from Spacelab metric camera photographs N86-10486
Orthophotomapping from metric camera imagery --- Spacelab N86-10487
Restitution of Spacelab photography by analog stereoplotter N86-10489
Evaluation of the accuracy of the metric camera images for the production of line maps and orthophotos N86-10490
Photomapping in different climatic zones --- Spacelab metric camera N86-10491
A geological structural analysis of the southeastern Zagros (Iran) ranges based on metric camera photos N86-10492
Erosion control and watershed management by Spacelab photography N86-10493
Identification of planimetric features from the metric camera --- Spacelab N86-10497
Analysis of metric camera images from the USA and their suitability for topographic and thematic mapping --- Spacelab N86-10498
Long range translocations ashore to offshore using Spacelab-1 metric camera imagery in the perspective of integrated geophysical surveys N86-10499
Role of the Economic Commission for Africa as a principal investigator in the metric camera experiment and reports of the result of the assessment for topographic and revision of maps in populated and developed areas of the world N86-10501
The role of very small scale metric images in modern geology --- Spacelab metric camera N86-10502
Geological mapping of remote mountainous regions using metric camera imagery --- Spacelab N86-10503
Interpretation of metric camera concerning hydrologic structures of the Rhone Delta --- Spacelab N86-10504
OEEPE participation in testing metric camera photography --- European Organization for Experimental Photogrammetric Investigations (OEEPE) N86-10507
Topographic interpretation of metric camera images: An example in Somalia --- Spacelab N86-10508
Thematic investigations in France based on metric camera imagery --- Spacelab N86-10509
Photographic catalog of selected planetary size comparisons
[NASA-TM-86207] N86-11138
SPACEBORNE TELESCOPES
Extragalactic observations with optical space arrays N86-11098
Astronomical criteria for interferometric arrays --- Spacecraft design N86-11099
Strategy for the development of space arrays N86-11101
TRIO: A kilometric array stabilized by solar sails --- Spaceborne astronomy N86-11102
SAMSI: An orbiting spatial interferometer for micro-arc second astronomical observations --- Spacecraft Array for Michelson Spatial Interferometry (SAMSI) N86-11103
COSMIC: A high resolution, large collecting area telescope --- Coherent Optical System of Modular Imaging Collectors (COSMIC) N86-11104
A fiber-linked version of project TRIO --- telescope array N86-11105
Future space telescope design concepts N86-11107
TRIO optics --- spaceborne optical interferometer (TRIO) N86-11108
Solar propulsion for the TRIO interferometer N86-11109
Preliminary studies of a spinning tether-connected TRIO concept --- spaceborne interferometer (TRIO) N86-11110
TRIO interferometer positioning --- spaceborne interferometers (TRIO) N86-11111
TRIANGLE: A different design for a three satellite interferometer in space N86-11113
Problems in image reconstruction with optical arrays --- spaceborne astronomy N86-11115

COSMIC image reconstruction — Coherent Optical System of Modular Imaging Collectors (COSMIC) N86-11118
The OASIS correlator — Optical Aperture Synthesis in Space (OASIS) N86-11119
Imaging speckle interferometer in space: Digital simulations of image reconstruction and photon noise N86-11120
The intensified multi CCD camera — spaceborne interferometers N86-11122

SPACECRAFT ANTENNAS
A numerical method for approximating antenna surfaces defined by discrete surface points [NASA-TM-87125] N86-10381

SPACECRAFT COMMUNICATION
SARSAT LUC (Local user terminal) to CMCC (Canadian Mission Control Centre) alert data interface: A critical review [AD-A156881] N86-10276
Discussion on the progress and future of satellite communication (Japan) [NASA-TM-77672] N86-10378

SPACECRAFT COMPONENTS
X-ray satellite [NASA-TM-77923] N86-10273

SPACECRAFT CONFIGURATIONS
Preliminary studies of a spinning tether-connected TRIO concept — spaceborne interferometer (TRIO) N86-11110

SPACECRAFT CONTROL
Evaluation of a pulse control law for flexible spacecraft [NASA-CR-176233] N86-10272

SPACECRAFT DESIGN
Manned flight simulation: Challenge and response [NASA-TM-86827] N86-10048
Astronomical criteria for interferometric arrays — Spacecraft design N86-11099
SAMSI: An orbiting spatial interferometer for micro-arc second astronomical observations — Spacecraft Array for Michelson Spatial Interferometry (SAMSI) N86-11103
Preliminary studies of a spinning tether-connected TRIO concept — spaceborne interferometer (TRIO) N86-11110
TRIANGLE: A different design for a three satellite interferometer in space N86-11113

SPACECRAFT MANEUVERS
Nonlinear methods for spacecraft attitude maneuvers [AD-A156956] N86-10275

SPACECRAFT POWER SUPPLIES
General-purpose heat source development: Safety Verification Test Program. Bullet/fragment test series [DE85-014262] N86-10660

SPACECRAFT STABILITY
TRIO: A kilometric array stabilized by solar sails — Spaceborne astronomy N86-11102

SPACELAB
The first German Spacelab mission D1 reports — Spacelab payloads [PR-1] N86-10187

SPACELAB PAYLOADS
Growth of larger single crystals N86-10186
The first German Spacelab mission D1 reports — Spacelab payloads [PR-1] N86-10187
The first German Spacelab mission D1 reports — Spacelab payloads [PR-2] N86-10188
The first German Spacelab mission D1 reports — Spacelab payloads [PR-3] N86-10189
Fifth European symposium on Material Sciences under Microgravity. Results of Spacelab 1 [ESA-SP-222] N86-10200
The fluid physics module: A technical description — Spacelab N86-10201
Capillary forces in a low gravity environment — Spacelab N86-10202
Some results of the Marangoni free convection experiment — Spacelab N86-10203
Oscillations of semi-free liquids in microgravity: Spacelab 1 experiment ES 326 N86-10204
Liquid column stability: Experiment 1 ES-331 — Spacelab N86-10205
Axisymmetric free surface behavior of moving liquid in a cylinder in microgravity — Spacelab N86-10206
Kinetics of spreading of liquids in microgravity: Experiment 1 ES 327 — Spacelab N86-10207
The isothermal heating facility — Spacelab N86-10208
Influences affecting separation in monotectic alloys under microgravity N86-10209
Melting and solidification of metal matrix composites under microgravity — Spacelab N86-10211
Unidirectional solidification of cast iron: Experiment ES-325 — Spacelab N86-10212
Skin casting of alloys and composites: Results of Spacelab (SL)-1 and TEXUS experiments N86-10213
Vacuum brazing under microgravity — Spacelab N86-10214
Melting and solidification in O-g of sintered alloys: Experiments ES 311 A and B bubble reinforced materials — Spacelab N86-10215
Interdiffusion in the glass melt system (Na2O+Rb2O).3SiO2 — Spacelab N86-10216
Gradient heating facility behavior — Spacelab N86-10217
Directional solidification of an aluminum-zinc vapor emulsion in microgravity — Spacelab N86-10218
Directional solidification of eutectic alloys — Spacelab N86-10219
Lead telluride crystals grown in microgravity: Experiment ES 318 — Spacelab N86-10220
Directional solidification of InSb-NiSb eutectic — Spacelab N86-10221
Thermomigration of cobalt in liquid tin: Experiment 1 ES 320 — Spacelab N86-10222
The mirror heating facility: Performance and experiences — Spacelab N86-10223
GaS-semiconductor crystals under microgravity: Experiment ES 323 — Spacelab N86-10224
Solution growth of cadmium telluride: Experiment ES 322 — Spacelab N86-10225
Crystallization of a silicon sphere — Spacelab N86-10226
Crystal growth of silicon in Spacelab 1: Experiment ES-321 N86-10227
Protein single crystal growth under microgravity — Spacelab N86-10228
Crystal growth from solution — Spacelab N86-10229
Growth and characterization of brushite and lead monetite, simulation and results — Spacelab N86-10230
Self diffusion of Sn112 and Sn124 in liquid tin N86-10231
Adhesion of metals: Experiment 1 ES-340 — Spacelab N86-10232
Holographic interferometry near gas/liquid critical points: Ground-based study of a D1 experiment — Spacelab N86-10249
Isochoric specific heat of sulfur hexafluoride at the critical point. A Spacelab experiment for the German D1-mission in 1985 N86-10251
First Spacelab Payload (FSLP) experiments on composite materials N86-10265
First Spacelab Payload (FSLP) experiments in metallurgy N86-10266
Crystal growth from solutions and nucleation from the vapor phase — Spacelab N86-10267
Liquids and interfaces — Spacelab N86-10268
Metric Camera Workshop — Spacelab [ESA-SP-209] N86-10485
Digital elevation model from Spacelab metric camera photographs N86-10486
Orthophotomapping from metric camera imagery — Spacelab N86-10487
Evaluation of the accuracy of the metric camera images for the production of line maps and orthophotos N86-10490
Photomapping in different climatic zones — Spacelab metric camera N86-10491
A geological structural analysis of the southeastern Zagros (Iran) ranges based on metric camera photos N86-10492
Erosion control and watershed management by Spacelab photography N86-10493
Evaluation of metric camera images at the University of London — Spacelab N86-10495
Partial in-flight calibration of the metric camera — Spacelab N86-10496
Identification of planimetric features from the metric camera — Spacelab N86-10497
Analysis of metric camera images from the USA and their suitability for topographic and thematic mapping — Spacelab N86-10498
Long range translocations ashore to offshore using Spacelab-1 metric camera imagery in the perspective of integrated geophysical surveys N86-10499
Line mapping and resolution tests with metric camera data — Spacelab N86-10500
Role of the Economic Commission for Africa as a principal investigator in the metric camera experiment and reports of the result of the assessment for topographic and revision of maps in populated and developed areas of the world N86-10501
The role of very small scale metric images in modern geology — Spacelab metric camera N86-10502
Geological mapping of remote mountainous regions using metric camera imagery — Spacelab N86-10503
Interpretation of metric camera concerning hydrologic structures of the Rhone Delta — Spacelab N86-10504
Test on mapping application of metric camera imagery — Spacelab N86-10505
Status of preparation activities for metric camera reflight on EOM-1/2 N86-10506
OEEPE participation in testing metric camera photography — European Organization for Experimental Photogrammetric Investigations (OEEPE) N86-10507
Topographic interpretation of metric camera images: An example in Somalia — Spacelab N86-10508
Thematic investigations in France based on metric camera imagery — Spacelab N86-10509
Thematic mapping of metric camera color infrared and black and white photographs for land use classification N86-10510
Digital image processing of metric camera imagery — Spacelab N86-10511
Land evaluation successes with the metric camera — Spacelab N86-10512
Requirements and possibilities of Spacelab metric camera photos usage for inventories of large areas of extensively managed forests N86-10513
Topographic and thematic mapping: Analysis of metric camera black and white photographs of the Rhone Delta N86-10514
Evaluation of metric camera photos — Spacelab; alpine snow cover N86-10515
Creation of Ground Control Points (GCP) library using ESA Spacelab metric camera imagery — ground control point (gcp) N86-10516
Updating of topographic maps by means of metric camera photos example: Hallertau (Bavaria) N86-10517
Interpretation of Spacelab-1 photographs for the generation of 1:200000 topographic map N86-10518
Metric camera image of Munich as additional means for urban cartography — Spacelab N86-10519
An example of single model orientation of metric camera stereophotographs — Spacelab N86-10520
Tectonic analysis of typical fold structures in the Zagros Mountains (Iran) by the application of quantitative photogrammetric methods on metric camera data — Spacelab N86-10521
Test results using metric camera photography for 1:250,000 mapping — Spacelab N86-10522

SPALLATION
Beginnings of remote handling at the RAL Spallation Neutron Source [DE85-012681] N86-11001

SPARK GAPS
Compact, low jitter, triggered spark gap [DE85-012812] N86-10195
Delay times and jitter in triggered vacuum spark gaps using metal vapor and surface flashover types of triggers [DE85-013966] N86-10441

SPATIAL DISTRIBUTION
Cometary atmospheres: Modeling the spatial distribution of observed neutral radicals [NASA-CR-176242] N86-11133

SPATIAL RESOLUTION
Time resolved flow velocity and concentration measurements using a travelling thermal lens [AD-A156706] N86-10541

SPECIFIC HEAT
Isochoric specific heat of sulfur hexafluoride at the critical point. A Spacelab experiment for the German D1-mission in 1985 N86-10251

SPECIFICATIONS
Specification for the performance, design, development and test requirements for a severe environment cartridge recorder. Issue 4 [AD-A156637] N86-10523
Partial evolution and omega completeness of algebraic specifications [CWI-CS-R8501] N86-10884
Application of structural-mechanics methods to the design of large tandem-mirror fusion devices (MFTF-B) [DE85-008960] N86-11017
RHIC lattice [DE85-013289] N86-11026

SPECKLE PATTERNS
Laser target speckle eliminator [AD-D011775] N86-10536
Imaging speckle interferometer in space: Digital simulations of image reconstruction and photon noise N86-11120

SPECTRAL METHODS
Spectral methods in adapted curved grids N86-10878

SPECTRAL REFLECTANCE
Vegetation and soils field research data base: Experiment summaries [E85-10110] N86-10610

Integrating sphere measurements of directional-hemispherical transmittance of window systems
[DE85-013926] N86-10978

SPECTRAL RESOLUTION
Parallel pulse processing for mercuric iodide gamma-ray detectors
[DE85-013391] N86-10528

SPECTROMETERS
Lithologic mapping in a sedimentary environment using multipolarization SAR images N86-10624
NBSGSC: A FORTRAN program for quantitative X-ray fluorescence analysis
[PB85-206068] N86-10847

SPECTROSCOPY
Light scattering tests of fundamental theories of transport properties in the critical region N86-10113

SPECTRUM ANALYSIS
A superconducting tunnel junction receiver for millimeter-wave astronomy N86-11041
Theoretical analysis of Wolter/LSM X-ray telescope systems
[NASA-CR-176244] N86-11095

SPHERES
Analysis of combined natural and forced convection around cylinders and spheres N86-10456

SPHERICAL SHELLS
Fusion target technology N86-10156
Strength of shells under local transverse loads N86-10568

SPHEROIDS
Mechanics of coated fiber composites N86-10285

SPHEROMAKS
Theoretical aspects of magnetic helicity
[DE85-011846] N86-10984
Increased particle confinement with the use of external dc bias field in the CTX spheromak
[DE85-012744] N86-10988
Local drift parameter, j/n sub e and resistivity anomaly measurements in CTX spheromaks
[DE85-012740] N86-10998
Energy efficiency of the CTX magnetized coaxial plasma source
[DE85-012735] N86-11003
Generalized helicity and its time derivative
[DE85-012770] N86-11027
Recent helicity source and power supply improvements in CTX
[DE85-012741] N86-11028
Equilibrium of the kink source experiment
[DE85-012764] N86-11029

SPIN EXCHANGE
Polarization transfer in inelastic scattering and pionic models of the EMC effect
[DE85-010738] N86-10955

SPIN STABILIZATION
Preliminary studies of a spinning tether-connected TRIO concept --- spaceborne interferometer (TRIO) N86-11110

SPIN TESTS
Axisymmetric free surface behavior of moving liquid in a cylinder in microgravity --- Spacelab N86-10206

SPIN-SPIN COUPLING
Two-loop large Higgs mass corrections to vector boson self-couplings
[NIKHEF-H/84-15] N86-11038

SPINOR GROUPS
On class groups of lattices
[CTH-MATH-1985-08] N86-10903

SPONTANEOUS COMBUSTION
Self-heating to ignition measurements and computation of critical size for solar energy collector materials
[DE85-011449] N86-10302

SPONTANEOUS EMISSION
Spontaneous Raman spectroscopy of shocked H2O
[DE85-014557] N86-10470

SPOT WELDS
Correlation between vibrations and buckling of cylindrical shells stiffened by spot-welded and riveted stringers
[TAE-537] N86-10584

SPRAY NOZZLES
Modeling of engine sprays
[DE85-010020] N86-10559

SPRAYERS
Microcomputer aided calculations of parameters for spray dryer operation
[DE85-013468] N86-10681

SPRING (SEASON)
A composite climatological study of the frequency and distribution of severe weather associated with spring season Colorado cyclogenesis
[AD-A156981] N86-10715

SPUTTERING
Rapid evaluation of ion thruster lifetime using optical emission spectroscopy
[NASA-TM-87103] N86-10280
Identification of chemical and physical phenomena affecting the durability of silvered polymer (PMMA) mirrors
[DE85-012131] N86-10645

STABILITY
Topics in nonlinear wave theory with applications N86-10367
Beam stability in a 6 GeV synchrotron light source
[DE85-013850] N86-10979

STAINLESS STEELS
Adhesion of metals: Experiment 1 ES-340 --- Spacelab N86-10232
Fracture toughness and stress relief response of irradiated type 347/348 stainless steel N86-10320
Fracture toughness of hydrogen-embrittled precipitation-hardened stainless steels
[AD-A156664] N86-10592

STANDARDIZATION
Standardization of tasks: Approach planning --- human performance assessment
[IZF-1984-19] N86-10782

STANDARDS
Secondary standards laboratories for ionizing radiation calibrations: The national laboratory interests
[DE85-007046] N86-10938

STANDING WAVES
Multimode acoustic research N86-10167

STAR CLUSTERS
The dynamics and stellar content of globular star clusters N86-11131

STARS
Radio studies of a complete sample of quasars N86-11093
Stellar s-process diagnostics
[DE85-012926] N86-11134

STARTING
Gel precursors as glass and ceramic starting materials for space processing applications research N86-10150

STATISTICAL ANALYSIS
Dynamic analysis of a sled traveling along a rough rail
[AD-A156589] N86-10191
A quantitative method for analyzing the roughness of the seafloor N86-10726

STATISTICAL DISTRIBUTIONS
A modified repair strategy for two-component systems with revealed and unrevealed faults
[AD-A156715] N86-10885
Adaptive distribution-free test for the K random sampling problem, part 1
[COMP-CENT-NOTE-14-PT-1] N86-10888
Adaptive distribution free test for the K random sampling problem, part 2
[COMP-CENT-NOTE-15-PT-2] N86-10889

STATISTICAL MECHANICS
Theoretical studies of the surface tension of liquid metal system N86-10101
New approach to multiphase equilibria: Application to high-pressure physics problems
[DE85-013820] N86-10907

STATISTICAL TESTS
Robustness of multiple comparisons against variance heterogeneity
[COMP-CENT-NOTE-17] N86-10890

STEADY STATE
Mephisto: Interfacial destabilization in metal alloys N86-10079
Dendritic solidification in a binary alloy melt: Steady-state versus morphological stability theories N86-10261
Rapid evaluation of ion thruster lifetime using optical emission spectroscopy
[NASA-TM-87103] N86-10280
Steady state frictional behavior of thin film coatings N86-10335

STEAM
KRAK: A computer program for two-phase, two-component porous flow and fracture propagation, revision
[DE85-014264] N86-10469

STEELS
Application of the unloading compliance methods in fracture toughness measurements of a quenched and tempered steel
[BLL-BISI-TRANS-21628-(9022.06)] N86-10308
Passivation of steel with aqueous amine solutions
[AD-D011749] N86-10314
Development of a sheath for sensor protection in molten steel applications
[AD-A156764] N86-10315
Chemical/hydrogen energy systems
[DE85-012742] N86-10667

STEERING
Path error-neglection in straight lane driving
[IZF-1984-32] N86-10783

STELLAR ENVELOPES
The two micron spectrum of R Scuti N86-11092

STELLAR EVOLUTION
Project VESTA, exploratory mission to the asteroids: Scientific objectives and technical specifications
[NASA-TM-77669] N86-10179

STELLAR ROTATION
The dynamics and stellar content of globular star clusters N86-11131

STEPPES
Observations of the snow cover in the southern part of the Buryat Autonomous Soviet Socialist Republic
[NASA-TM-77910] N86-10613

STEREOPHOTOGRAPHY
Stereoscopic video imagery generation
[AD-D011785] N86-10481
Stereo-orthophotos in various map projections N86-10488
Restitution of Spacelab photography by analog stereoplotter N86-10489
Land evaluation successes with the metric camera --- Spacelab N86-10512
An example of single model orientation of metric camera stereophotographs --- Spacelab N86-10520

STEREOSCOPIC VISION
Test of a multilevel computational theory of stereoscopic visual image processing
[AD-A157011] N86-10870

STIFFNESS
Finite element analysis of statics and dynamic structural engineering problems using semi-explicit methods N86-10571

STIRLING CYCLE
Simplified analysis of Stirling engines and heat pumps
[DE85-005366] N86-10647
Stirling-engine-driven heat pump program overview
[DE85-004796] N86-10661

STOCHASTIC PROCESSES
A quantitative method for analyzing the roughness of the seafloor N86-10726
On maximal and distributional coupling
[CTH-MATH-1984-30] N86-10875

STOICHIOMETRY
Crystal growth of GaAs in space N86-10234

STORAGE RINGS (PARTICLE ACCELERATORS)
Method for compensating bellows pressure loads while accommodating thermal deformations
[DE85-013306] N86-10933
The 20 keV undulators for a 6-GeV storage ring
[DE85-013867] N86-10941
Beam profile monitor for the NSLS VUV ring employing linear photodiode arrays
[DE85-012184] N86-10947
Surface conditioning of synchrotron radiation source to improve beam lifetime
[DE84-012185] N86-10948
Parasitic mode losses versus signal sensitivity in beam position monitors
[DE85-014367] N86-10964
Superconvergent tracking and invariant surfaces in phase space
[DE85-013051] N86-10995
Ferrite kicker magnet for the IAMPF switchyard upgrade
[DE85-012657] N86-10996
Field-independent normalization of SSC Collider Ring costs
[DE85-012425] N86-10997
Thermal and structural analysis of ring components by the finite element method
[DE85-013305] N86-11021
Unicell structure for superconducting storage rings
[DE85-013303] N86-11022
Tracking studies on the effects of magnet multipoles on the aperture of the RHIC heavy ion collider
[DE85-013282] N86-11023

STORMS
A composite climatological study of the frequency and distribution of severe weather associated with spring season Colorado cyclogenesis
[AD-A156981] N86-10715
Application of the dutch method for estimating storm-induced dune erosion
[AD-A156717] N86-10728

STRAIN HARDENING
Portevin-Le Chatelier effect. 1: Model for the type-E serrations
[DE85-006879] N86-10322

STRANGENESS
Hyperon polarization: An unresolved problem
[DE85-012298] N86-10946

STRATA
Dynamic lithostratigraphy and paleecology of upper Mississippi (Chesterian) strata of the northcentral Appalachian Basin N86-10693

STRATEGIC MATERIALS
Whole plant utilization of sunflowers as a renewable source of strategic materials (rubber)
[AD-A155833] N86-10342
STRATEGY
DFVLR, strategic study of astronautics 1984, user requirements N86-11069
Report of the ad hoc committee to review the program of the SDI Directorate on Innovative Science and Technology (IST)
[AD-A156668] N86-11071
STRATIGRAPHY
Report of the Workshop on Geologic Applications of Remote Sensing to the Study of Sedimentary Basins
[E86-10002] N86-10599
Chronologic analysis of terrestrial sediments and basin evolution N86-10602
Multisensor data integration techniques N86-10604
Paleogene vertebrate paleontology, geology and remote sensing in the Wind River Basin N86-10609
Cretaceous and cenozoic stratigraphy of the upper and middle coastal plain, Harnett County area, North Carolina N86-10690
Stratigraphy, petrology, depositional and post-depositional histories and their effects upon reservoir properties of the Parkman Formation of the Mesa Verde group, Powder River Basin, Wyoming N86-10691
Paleontology and stratigraphy of Lower Cambrian and upper Proterozoic sediments, Caborca region, northwestern Sonora, Mexico N86-10692
Dynamic lithostratigraphy and paleecology of upper Mississippi (Chesterian) strata of the northcentral Appalachian Basin N86-10693
In-situ geophysical investigations into the nature of the oceanic crust N86-10725
STRATOSPHERE
Chemical kinetics and photochemical data for use in stratospheric modeling
[NASA-CR-176198] N86-10707
STRATUS CLOUDS
Comparative flight measurement of icing parameters for the propeller aircraft Do-28D2 of the test station 61 of the DFVLR and for the DFVLR aircraft Falon 20e in stratus clouds
[DFVLR-FB-85-16] N86-10720
STREAM FUNCTIONS (FLUIDS)
Analysis of combined natural and forced convection around cylinders and spheres N86-10456
STREAMS
Development of the Multi-Attribute Hazard Assessment System (MAHAS) and its application to energy-related waste streams
[DE85-010278] N86-10676
STRESS (PHYSIOLOGY)
Classification of changes in electrocardiogram during muscular exertion of healthy individuals N86-10755
Mechanism of adaptogenic action of prickly eleuterococcus on man during heat stress N86-10757
Report on the research activities on whole-body vibrations. Human strain due to mechanical vibrations
[ISBN-3-88383-107-7] N86-10773
STRESS (PSYCHOLOGY)
Effect of emotional stress on hemostasis system of healthy persons N86-10745
Eye-movement activity as index of functional state of brain N86-10756
STRESS ANALYSIS
Finite element analysis of metals at elevated temperature using unified constitutive theories N86-10569
STRESS CONCENTRATION
Mechanics of coated fiber composites N86-10285
Analytical and experimental study of cracks emanating from an elliptical hole in unidirectional composite material N86-10567
Strength of shells under local transverse loads N86-10568
STRESS CORROSION
Fatigue, static tensile strength and stress corrosion of aircraft materials and structures
[VTH-LR-360-PT-1] N86-10045
Design, fabrication and testing of an experimental apparatus for determining particle behavior under very low intergranular stresses N86-10175
STRESS CORROSION CRACKING
Environmental degradation of materials: Surface chemistry related to stress corrosion cracking N86-10099
STRESS INTENSITY FACTORS
Analytical and experimental study of cracks emanating from an elliptical hole in unidirectional composite material N86-10567
Numerical simulation of crack arrest experiments on Araldite B using the finite difference method
[REPT-W-9/82] N86-10596
STRESS MEASUREMENT
Study of statis and dynamic stress effects in nonlinear solids
[NASA-CR-176236] N86-10578
STRESS RELAXATION
Constitutive modeling for isotropic materials (HOST)
[NASA-CR-174980] N86-10589
STRESS WAVES
Ultrasonic evaluation of mechanical properties of thick, multilayered, filament wound composites
[MASA-TM-87088] N86-10561
STRESS-STRAIN-TIME RELATIONS
High temperature properties and characterization of S3-N4 materials
[BMFT-FB-T-85-046] N86-10352
High temperature properties of SiC materials
[BMFT-FB-T-85-047] N86-10353
STRESSES
Resistance curves for crack growth under plane-stress conditions in an elastic perfectly-plastic material
[AD-A156778] N86-10593
Fundamental study of the closure property of joints N86-10698
Shock loading and release behavior of x-cut quartz
[DE85-013954] N86-11054
STRINGERS
The effect of debond growth on crack propagation in composite plates reinforced with adhesively bonded composite stringers N86-10287
Effect of sequence of loading on interaction curves for buckling of stiffened shells
[TAE-536] N86-10583
Correlation between vibrations and buckling of cylindrical shells stiffened by spot-welded and riveted stringers
[TAE-537] N86-10584
STRUCTURAL ANALYSIS
Load-deflection tests and computer analyses of a high-precision adhesive-bonded antenna reflector panel N86-10389
Marginal terrain straddle-lift container handler
[AD-D011752] N86-10555
A transformation method for the evaluation of the response moments of elastic structures with random properties
[AD-A156882] N86-10557
Load space formulation of reliability for nonlinear random structural systems N86-10570
Three-dimensional vibration analysis of a uniform beam with offset inertial masses at the ends
[NASA-TM-86393] N86-10580
Constitutive modeling for isotropic materials (HOST)
[NASA-CR-174980] N86-10589
Thermal and structural analysis of ring components by the finite element method
[DE85-013305] N86-11021
STRUCTURAL BASINS
Report of the Workshop on Geologic Applications of Remote Sensing to the Study of Sedimentary Basins
[E86-10002] N86-10599
Some opinions on remote sensing and geologic studies N86-10600
Position paper: Workshop on Geologic Applications of Remote Sensing to the Study of Sedimentary Basins N86-10601
Chronologic analysis of terrestrial sediments and basin evolution N86-10602
Analysis of remote sensing data N86-10605
Remote stratigraphic and structural analysis: Multisensor results in the Wind River/Bighorn Basin area, Wyoming N86-10606
Foreland basin structures and remote sensing N86-10608
Lithologic mapping in a sedimentary environment using multipolarization SAR images N86-10624
Time-term analysis of upper crustal structure in the Columbia Basin, Washington
[DE85-012390] N86-10633
Dynamic lithostratigraphy and paleecology of upper Mississippi (Chesterian) strata of the northcentral Appalachian Basin N86-10693
STRUCTURAL DESIGN
Design sensitivity analysis and optimization of built-up structures N86-10565
Application of structural-mechanics methods to the design of large tandem-mirror fusion devices (MFTF-B)
[DE85-008960] N86-11017
STRUCTURAL DESIGN CRITERIA
Optimum design of an aircraft wing structure with multiple constraints by the direct-vision criteria method N86-10004
Optimal design of portal frames against buckling N86-10572
Application of structural-mechanics methods to the design of large tandem-mirror fusion devices (MFTF-B)
[DE85-008960] N86-11017
Astronomical criteria for interferometric arrays — Spacecraft design N86-11099
STRUCTURAL ENGINEERING
Finite element analysis of statics and dynamic structural engineering problems using semi-explicit methods N86-10571
STRUCTURAL FAILURE
Progressive damage, fracture predictions and post mortem correlations for fiber composites
[NASA-TM-87101] N86-10290
STRUCTURAL PROPERTIES (GEOLOGY)
A geological structural analysis of the southeastern Zagros (Iran) ranges based on metric camera photos N86-10492
Geologic evaluation and reservoir properties of the PR Spring tar sand deposit, Uintah and Grand Counties, Utah
[DE85-013248] N86-10634
Structural discontinuity within the southern California continental margin: Seismic and gravity models of the western Transverse Ranges N86-10699
STRUCTURAL STABILITY
Application of structural-mechanics methods to the design of large tandem-mirror fusion devices (MFTF-B)
[DE85-008960] N86-11017
STRUCTURAL VIBRATION
Evaluation of a pulse control law for flexible spacecraft
[NASA-CR-176233] N86-10272
STRUTS
Test and evaluate passive orbital disconnect struts (PODS 3)
[NASA-CR-177368] N86-10274
STUDS (STRUCTURAL MEMBERS)
Improved stud configurations for attaching laminated wood wind turbine blades
[NASA-TM-87109] N86-10582
SUBMARINES
Angle of incidence effects for underwater shock using generic computational models
[DE85-012936] N86-10466
Angle of incidence effects for underwater shock using generic computational models, rev. 1
[DE85-012921] N86-10467
SUBROUTINES
The development of a neutron evaporation theory code for the thermal fission of Uranium-235
[AD-A156593] N86-10951
SUBSONIC FLOW
The role of freestream turbulence scale in subsonic flow separation
[NASA-CR-176237] N86-10014
Oscillations of subsonic flow in an abruptly expanding circular duct
[MPIS-16/1984] N86-10028
SUBSONIC SPEED
Summary of work on jet noise prediction
[ESDU-BR-82636] N86-10909
SUBSTITUTES
Coincidence densities and spectra of a class of substitution minimal sets N86-10657
SUBSTRATES
Modelling of laser-enhanced chemical vapor deposition N86-10105
Thermodynamic constraints on ion beam mixing of metals on insulators
[DE85-013628] N86-10448
The influence of the substrate on the practical machining applications of cutting edges coated with different materials
[BLL-RISLEY-TR-5039-(9091.9F)] N86-10546
The interaction of small metal particles with refractory oxide supports
[NASA-CR-176228] N86-11047
SUCTION
Investigations on a supercritical airfoil with boundary layer suction through a perforated strip in the shock region
[DFVLR-FB-85-15] N86-10025
SULFUR
Method for determining elemental sulfur in jet fuel — differential pulse polarography
[FOA-C-40211-B4] N86-10360
SULFUR DIOXIDES
Emissions of NOx, SOx and VOC from Antropogenic sources
[PB85-193530] N86-10688
Seasonal variations in atmospheric chemistry in the Adirondacks
[DE85-014227] N86-10719
SULFUR FLUORIDES
Isochoric specific heat of sulfur hexafluoride at the critical point. A Spacelab experiment for the German D1-mission in 1985 N86-10251

High voltage instrument transformers for outdoor service with an insulation of low pressure SF6 gas and plastic foils
[BMFT-FB-T-85-034] N86-10449

SUNFLOWERS
Whole plant utilization of sunflowers as a renewable source of strategic materials (rubber)
[AD-A155833] N86-10342

SUPERCONDUCTING MAGNETS
Cryogenic equivalence principle experiment N86-10171
Cryogenic structural materials for superconducting magnets
[DE85-008026] N86-10908
Field-independent normalization of SSC Collider Ring costs
[DE85-012425] N86-10997
US superconducting magnet data base assessment for INTOR
[DE85-013648] N86-11000
Unicell structure for superconducting storage rings
[DE85-013303] N86-11022

SUPERCONDUCTORS
A superconducting tunnel junction receiver for millimeter-wave astronomy N86-11041
Superconductors for pulsed RF accelerators
[DE85-013378] N86-11051

SUPERCOOLING
Glass formation in reluctant glass formers N86-10151
Bulk formation of metallic glasses and amorphous silicon from the melt N86-10154

SUPERCRITICAL FLUIDS
Rapid analysis using capillary supercritical fluid chromatography
[DE85-012460] N86-10297

SUPERCRITICAL WINGS
Investigations on a supercritical airfoil with boundary layer suction through a perforated strip in the shock region
[DFVLR-FB-85-15] N86-10025

SUPERFLUIDITY
An investigation of vortex dynamics in 2-dimensional superfluid films of helium-4 N86-11040
Critical dynamics in superfluid helium N86-11046

SUPERHIGH FREQUENCIES
On the use of X-band CW nanosecond airborne radar for terrain profiling
[AD-A156886] N86-10406
Digital radio link: Method and a measuring system for studying the radio channel during frequency selective fading
[FOA-C-30386-E2] N86-10411

SUPERLATTICES
Semiconductor superlattic photodetectors
[NASA-CR-176249] N86-10484

SUPERNOVA REMNANTS
Physical conditions in giant extragalactic H2 regions N86-11130

SUPERSONIC FLOW
A numerical solution of the shock-turbulent interaction over a compression corner for supersonic flow N86-10003
A new method for calculating unsteady supersonic aerodynamic forces and its application N86-10009
Forced response analysis of an aerodynamically detuned supersonic turbomachine rotor
[NASA-TM-87093] N86-10019

SUPERSONIC FLUTTER
A new method for calculating unsteady supersonic aerodynamic forces and its application N86-10009

SUPERSONIC INLETS
Effect of a shear layer on the stability of an axisymmetrical external compression air intake N86-10010

SUPERSONIC SPEEDS
Supersonic metal cluster beams
[DE85-014321] N86-10966

SUPPLEMENTS
Advanced vehicle systems assessment. Volume 5: Appendices
[NASA-CR-176208] N86-11086

SUPPORTS
A new 70-meter antenna quadripod with reduced RF blockage N86-10385
Cryogenic structural materials for superconducting magnets
[DE85-008026] N86-10908

SURFACE COOLING
Undercooling investigations on the easy glass former Pd-Cu-Si N86-10259

SURFACE DEFECTS
Liquid crystal non-destructive inspection of metals
[AD-D011772] N86-10316

SURFACE ENERGY
Surface forces in contacting solids — microgravity rocket experiment N86-10252

SURFACE FINISHING
Mechanism of the formation of boronised layers on high carbon steel
[BLL-BISI-TRANS-23036-(9022.06)] N86-10306
Boronising of iron and steel by ionic bombardment by diborane
[BLL-BISI-TRANS-23034-(9022.06)] N86-10307
Pre-bond treatment for titanium alloys
[BAE-AL/MAT/3864] N86-10309
Fuel and lubricant behavior in boundary layers analyzed by infrared emission Fourier transform spectrometry N86-10336

SURFACE LAYERS
Thermocapillary flows and their stability: Effects of surface layers and contamination N86-10109
Mechanism of the formation of boronised layers on high carbon steel
[BLL-BISI-TRANS-23036-(9022.06)] N86-10306

SURFACE PROPERTIES
Mixed-mode fracture of ceramics
[DE85-014087] N86-10349
Fundamental study of the closure property of joints N86-10698

SURFACE REACTIONS
Environmental degradation of materials: Surface chemistry related to stress corrosion cracking N86-10099
Compatibility of grain-stabilized platinum with candidate propellants for resistojets
[NASA-TM-87118] N86-10279

SURFACE ROUGHNESS
Age-dating volcanic and alluvial surfaces with multipolarization data N86-10620

SURFACE ROUGHNESS EFFECTS
Laser target speckle eliminator
[AD-D011775] N86-10536

SURFACE TEMPERATURE
LANDSAT TM image data quality analysis for energy-related applications
[E85-10109] N86-10597

SWEEP FREQUENCY
A comparison of swept frequency and FFT methods used to calibrate array test modules
[AD-A156629] N86-10430

SWELLING
Swelling and tensile properties of EBR-2-irradiated tantalum alloys for space reactor applications
[DE85-012887] N86-10329

SWEPT WINGS
Second order approximation method for transonic flows over swept wings N86-10002

SWIRLING
Confined swirling jet predictions using a multiple-scale turbulence model
[NASA-CR-178484] N86-10462

SWITCHING CIRCUITS
Counterpulse railgun energy recovery circuit
[DE85-011603] N86-10196
Contact effects in light activated GaAs switches
[AD-A156957] N86-10434
A course on field programmable logic
[EUT-85-E-148] N86-10805
State assignment in sequential circuits
[EUT-85-E-146] N86-10846

SWITCHING THEORY
Theoretical modeling of the vapor cavitation in dynamically loaded journal bearings
[NASA-TM-87076] N86-10463

SYMMETRY
Determination of symmetry and phase in human visual response functions: Theory and experiments N86-10769
Charge exchange in slow collisions of atoms and molecules N86-10922
Conducting wall and pressure profile effect on MHD stabilization of axisymmetric mirror
[DE85-013647] N86-11020

SYNCHRONISM
Reaching approximate agreement in the presence of faults
[AD-A156541] N86-10898
Engineering high reliability, low-jitter Marx generators
[DE85-012811] N86-11013

SYNCHRONIZERS
Programmable delay unit incorporating a semi-custom integrated circuit
[DE85-013379] N86-11033

SYNCHROTRON RADIATION
Method for determining the position, angle and other injection parameters of a short pulsed beam in the Brookhaven AGS
[DE85-012523] N86-10931
Beam profile monitor for the NSLS VUV ring employing linear photodiode arrays
[DE85-012184] N86-10947
Surface conditioning of synchrotron radiation source to improve beam lifetime
[DE84-012185] N86-10948
Beam stability in a 6 GeV synchrotron light source
[DE85-013850] N86-10979
Noninterceptive techniques for the measurement of longitudinal parameters for intense H(-) beams
[DE85-012662] N86-10992

SYNCHROTRONS
Use of the MURA transformation to generate the fields and calculate the motion of protons in the designed Argonne Mini-ASPUN FFAG spiral sector accelerator
[DE85-011477] N86-10934
Report on a visit to CERN in February 1985. Notes on bunch monitors, high-frequency systems, linacs, kickers, magnets, vacuum and bunch extraction
[LINO-119] N86-10967
Performance of the H(-) ion source for the intense pulsed neutron source
[DE85-012368] N86-10991

SYNOPTIC METEOROLOGY
A composite climatological study of the frequency and distribution of severe weather associated with spring season Colorado cyclogenesis
[AD-A156981] N86-10715

SYNTHESIS (CHEMISTRY)
Catalytic activity of shock modified ZnO for CO oxidation and methanol synthesis
[DE85-014704] N86-10300
Synthesis of arylene siloxanylene polymers and copolymers
[AD-D011780] N86-10338

SYNTHETIC APERTURE RADAR
SAR image quality: A review
[DFVLR-MITT-85-07] N86-10413
Multisensor data integration techniques N86-10604
NASA/JPL Aircraft SAR Workshop Proceedings
[NASA-CR-176204] N86-10615
Radar system description N86-10616
CV-990 L-band SAR: A calibration experiment N86-10617
Neogene compressional deformation and possible thrust faulting in southwest Dominican Republic N86-10618
The effect of vegetation type, microrelief, and incidence angle on radar backscatter N86-10619
Age-dating volcanic and alluvial surfaces with multipolarization data N86-10620
Topographic mapping from interferometric synthetic aperture radar observations N86-10622
Strategies for analyzing mixed pixels in remotely sensed imagery N86-10623
Lithologic mapping in a sedimentary environment using multipolarization SAR images N86-10624
Mapping diverse forest cover with multipolarization airborne radar N86-10625
Potential applications of multipolarization SAR for pine plantation biomass estimation N86-10626
On the use of L-band multipolarization airborne SAR for surveys of crops, vineyards, and orchards in a California irrigated agricultural region N86-10627
Vegetation canopy discrimination and biomass assessment using multipolarized airborne SAR N86-10628

SYNTHETIC APERTURES
Optical/IR telescope arrays: A study of their potential for satisfying observational requirements in astronomy for a large aperture system in the 1990s and beyond
[REPT-15] N86-11094
OASIS: Optical Aperture Synthesis in Space N86-11106
COSMIC image reconstruction — Coherent Optical System of Modular Imaging Collectors (COSMIC) N86-11118
The OASIS correlator — Optical Aperture Synthesis in Space (OASIS) N86-11119
Aperture synthesis with or without phase information for kilometric arrays interpolation algorithms for stabilized image reconstruction N86-11124
VLBI at optical and radio wavelengths: Congruences and contrasts N86-11126

SYNTHETIC ARRAYS
Optical/IR telescope arrays: A study of their potential for satisfying observational requirements in astronomy for a large aperture system in the 1990s and beyond
[REPT-15] N86-11094
Colloquium on Kilometric Optical Arrays in Space
[ESA-SP-226] N86-11096
Extragalactic observations with optical space arrays N86-11098
Astronomical criteria for interferometric arrays — Spacecraft design N86-11099
Strategy for the development of space arrays N86-11101

TRIO: A kilometric array stabilized by solar sails — Spaceborne astronomy N86-11102
SAMSI: An orbiting spatial interferometer for micro-arc second astronomical observations — Spacecraft Array for Michelson Spatial Interferometry (SAMSI) N86-11103
COSMIC: A high resolution, large collecting area telescope — Coherent Optical System of Modular Imaging Collectors (COSMIC) N86-11104
A fiber-linked version of project TRIO — telescope array N86-11105
OASIS: Optical Aperture Synthesis in Space N86-11106
Problems in image reconstruction with optical arrays — spaceborne astronomy N86-11115
The OASIS correlator — Optical Aperture Synthesis in Space (OASIS) N86-11119
Aperture synthesis with or without phase information for kilometric arrays interpolation algorithms for stabilized image reconstruction N86-11124

SYSTEM EFFECTIVENESS
An annotated bibliography of abstracts on the use of simulators in technical training
[AD-A156792] N86-11065
Advanced vehicle systems assessment. Volume 2: Subsystems assessment
[NASA-CR-176205] N86-11083

SYSTEM IDENTIFICATION
The identification package SATER
[ER-83/08] N86-10844
Naive approximate realization of noisy data
[ER-83/10] N86-10880

SYSTEMS ANALYSIS
Annotated bibliography of publications dealing with occupational health and medical information systems, cost analysis procedures, evaluation methodology and related legal issues
[AD-A156650] N86-11078
A systems development life cycle study of the information center
[AD-A156977] N86-11079

SYSTEMS ENGINEERING
New directions in chemical analysis
[DE85-012930] N86-10296
Initial design of a relational database system for NPS computer asset identification and valuation for risk assessment
[AD-A156847] N86-10796
System integration report
[NASA-CR-171900] N86-10821
Ada (trademark) Programming Support Environment (APSE) Evaluation and Validation (E and V) workshop report held at Airlie, Virginia on 2-6 April 1984
[AD-A156667] N86-10829
Fault-free behavior of reliable multiprocessor systems: FTMP experiments in AIRLAB
[NASA-CR-177967] N86-10848
A systems development life cycle study of the information center
[AD-A156977] N86-11079
Future space telescope design concepts N86-11107

SYSTEMS INTEGRATION
Efficient systolic arrays for the solution of toeplitz systems: An illustration of a methodology for the construction of systolic architectures in VLSI (Very Large Systems Integration)
[AD-A156767] N86-10795
System integration report
[NASA-CR-171900] N86-10821

SYSTEMS MANAGEMENT
Development of IS2100: An information systems laboratory
[AD-A156848] N86-10797

SYSTEMS STABILITY
Stability of long liquid columns N86-10244

T

TABLES (DATA)
Monthly and Seasonal Weather Outlook for mid-April to mid-May 1985, Volume 39, Number 8
[PB85-195345] N86-10724

TANTALUM ALLOYS
Swelling and tensile properties of EBR-2-irradiated tantalum alloys for space reactor applications
[DE85-012887] N86-10329

TANZANIA
Satellite data even for a poultry farm. A development for Tanzania. Image evaluation following new ways N86-10182

TAPE RECORDERS
Specification for the performance, design, development and test requirements for a severe environment cartridge recorder. Issue 4
[AD-A156637] N86-10523

TARGET ACQUISITION
Guidance and control of a cable based payload pickup system N86-10046

TARS
A fundamental study of smoldering with emphasis on experimental design for zero-g N86-10162

TASKS
Standardization of tasks: Approach planning — human performance assessment
[IZF-1984-19] N86-10782

TATB
Composite explosives for metal acceleration: The effect of detonation temperature
[DE85-013982] N86-10359

TAYLOR INSTABILITY
Equilibrium of the kink source experiment
[DE85-012764] N86-11029

TDR SATELLITES
JPL emergency support of TDRSS and compatible satellites N86-10394

TECHNETIUM
Application of the ruthenium and technetium thermodynamic data bases used in the EQ3/6 geochemical codes
[DE85-013766] N86-10632

TECHNICAL WRITING
Writer/editor and the computer
[DE85-011843] N86-11080

TECHNOLOGICAL FORECASTING
Evaluation and prediction of long-term environmental effects on non metallic materials
[NASA-CR-178495] N86-10340
Report of the ad hoc committee to review the program of the SDI Directorate on Innovative Science and Technology (IST)
[AD-A156668] N86-11071

TECHNOLOGY ASSESSMENT
New directions in chemical analysis
[DE85-012930] N86-10296
Fuel Cell Technology Assessment Program, work element no. 6
[DE85-008228] N86-10444
Photomapping in different climatic zones — Spacelab metric camera N86-10491
Analysis of metric camera images from the USA and their suitability for topographic and thematic mapping — Spacelab N86-10498
Role of the Economic Commission for Africa as a principal investigator in the metric camera experiment and reports of the result of the assessment for topographic and revision of maps in populated and developed areas of the world N86-10501
The role of very small scale metric images in modern geology — Spacelab metric camera N86-10502
OEEPE participation in testing metric camera photography — European Organization for Experimental Photogrammetric Investigations (OEEPE) N86-10507
Requirements and possibilities of Spacelab metric camera photos usage for inventories of large areas of extensively managed forests N86-10513
Updating of topographic maps by means of metric camera photos example: Hallertau (Bavaria) N86-10517
Improved particle-velocity transducer for equation-of-state experiments
[DE85-013204] N86-10532
Stock-taking of data base management systems choice considerations for the Eindhoven Technical University Computing Center (THE-RC)
[COMP-CENT-NOTE-18] N86-10851
US superconducting magnet data base assessment for INTOR
[DE85-013648] N86-11000
Advanced vehicle systems assessment. Volume 3: Systems assessment
[NASA-CR-176206] N86-11084
Advanced vehicle systems assessment. Volume 4: Supporting analyses
[NASA-CR-176207] N86-11085
Results and limitations of ground-based optical arrays — stellar interferometry N86-11097

TECHNOLOGY TRANSFER
Editors rattle space N86-10586
Solar thermal technical information guide
[DE85-002941] N86-10657
Publication of the Executive Office of the President, January 20, 1981 - December 31, 1984
[PB85-187110] N86-11082

TECHNOLOGY UTILIZATION
The dirigible: A catalyst for resource exploitation in remote areas?
[AD-A156518] N86-10034
Wind energy in agriculture, a promise
[SS-45] N86-10672
Wind energy, a feasibility investigation for wind mills in agriculture
[SS-45A] N86-10673
Advanced vehicle systems assessment. Volume 5: Appendices
[NASA-CR-176208] N86-11086

TECTONICS
A geological structural analysis of the southeastern Zagros (Iran) ranges based on metric camera photos N86-10492
Tectonic analysis of typical fold structures in the Zagros Mountains (Iran) by the application of quantitative photogrammetric methods on metric camera data — Spacelab N86-10521
Chronologic analysis of terrestrial sediments and basin evolution N86-10602
Remote stratigraphic and structural analysis: Multisensor results in the Wind River/Bighorn Basin area, Wyoming N86-10606

TELECOMMUNICATION
Construction and use of a radio controlled model helicopter for research
[AD-A156547] N86-10035
The Telecommunications and Data Acquisition Report
[NASA-CR-176203] N86-10382
DFVLR, strategic study of astronautics 1984, user requirements N86-11069

TELEMETRY
A sequential decoding performance analysis for International Comet Explorer N86-10390

TELEOPERATORS
Supervisory control of the right arm of the beam assembly teleoperator
[AD-A156856] N86-10832

TELEPHONES
Methods for developing jam-resistant security communications networks at fixed-site facilities
[DE85-012032] N86-10408

TELEPHONY
Digital transmission experiments with the Orbital Test Satellite
[EUT-84-E-144] N86-10270

TELESCOPES
Optical testing of large telescopes using multiple subapertures N86-10971

TELEVISION CAMERAS
The intensified multi CCD camera — spaceborne interferometers N86-11122

TEMPERATURE
Mathematical models of continuous flow electrophoresis N86-10143

TEMPERATURE CONTROL
Renovated cooling at PIMU
[LINO-122] N86-10452

TEMPERATURE DEPENDENCE
Surface tensions and their variations with temperature and impurities
[NASA ORDER H-27954B] N86-10115
Miscibility gap systems
[NASA ORDER H-27954B] N86-10131
Chemical kinetics and cellular structure of detonations in hydrogen sulphide and air
[DE85-009408] N86-10304
Portevin-Le Chatelier effect. 1: Model for the type-E serrations
[DE85-006879] N86-10322
Recirculation within a glass mixture subjected to external and resistive heating
[DE85-010068] N86-10348
Laminar film condensation in vertical closed two-phase thermosiphons
[IKE-5-220] N86-10476
Conditioning potentialities of respiratory apparatus N86-10753
Experimental investigations of thermal radiation from potassium atoms and design applications
[DE85-004086] N86-11036
Critical dynamics in superfluid helium N86-11046
Anelastic relaxation in irradiated Cu-Be
[DE85-013893] N86-11056

TEMPERATURE DISTRIBUTION
Design and calibration of a flat-flame burner using line reversal techniques
[AD-A156724] N86-10294

TEMPERATURE EFFECTS
Composite explosives for metal acceleration: The effect of detonation temperature
[DE85-013982] N86-10359
Mean turbulence structure in strongly heating air flows N86-10455
Short term heat effect on adreno- and cholino-sensitivity of rat's small intestine N86-10754
Efficiency of muscular work in white rats during adaptation to cold N86-10763
Beam line windows at LAMPF
[DE85-012723] N86-10985

TEMPERATURE GRADIENTS
Graphite formation in cast iron N86-10100
Thermocapillary motion research N86-10125
Miscibility gap systems
[NASA ORDER H-27954B] N86-10131
Advanced containerless processing technology N86-10176
Gradient heating facility behavior --- Spacelab N86-10217
Thermomigration of cobalt in liquid tin: Experiment 1 ES 320 --- Spacelab N86-10222
The influence of thermocapillarity on the migration of droplets in a liquid possessing a uniform temperature gradient N86-10237
Analysis of large, non-isothermal elastic-visco-plastic deformations
[NASA-CR-176220] N86-10588
Smoke inputs to climate models: Optical properties and height distribution for nuclear winter studies
[DE85-011363] N86-10717
A processor for the study of ocean fine-scale patches
[AD-A157019] N86-10730

TEMPERATURE MEASUREMENT
Containerless high temperature property measurements by atomic fluorescence N86-10092
Measurement of workpiece temperature during welding for welding robot control N86-10534

TEMPERATURE MEASURING INSTRUMENTS
Development of a sheath for sensor protection in molten steel applications
[AD-A156764] N86-10315

TEMPERATURE PROFILES
Float zone experiments in space N86-10067
Flammability limits of gases under low gravity conditions N86-10164

TEMPERING
Application of the unloading compliance methods in fracture toughness measurements of a quenched and tempered steel
[BLL-BISI-TRANS-21628-(9022.06)] N86-10308

TENNESSEE
Ground-coupled heat pump research at the University of Tennessee Washington, D.C., 10 Dec. 1984
[DE85-005357] N86-10650

TENSILE PROPERTIES
Swelling and tensile properties of EBR-2-irradiated tantalum alloys for space reactor applications
[DE85-012887] N86-10329

TENSILE STRENGTH
Fatigue, static tensile strength and stress corrosion of aircraft materials and structures
[VTH-LR-360-PT-1] N86-10045
Age-life prediction of nylon 66 parachute materials. Part 2: Changes in the chemical and physical properties of materials on aging
[AD-A156909] N86-10347

TENSILE TESTS
Constitutive modeling for isotropic materials (HOST)
[NASA-CR-174980] N86-10589

TENSOR ANALYSIS
Gravitational collapse of a scalar field N86-11129

TERRAIN
On the use of X-band CW nanosecond airborne radar for terrain profiling
[AD-A156886] N86-10406
Marginal terrain straddle-lift container handler
[AD-D011752] N86-10555
A numerical model for the estimation of solar radiation on rugged terrain N86-10694
A boundary layer flow model for areas of complex terrain N86-10701

TERRAIN ANALYSIS
Multisensor data integration techniques N86-10604

TEST CHAMBERS
Fundamental studies of droplet combustion at reduced gravity N86-10165

TEST EQUIPMENT
Academic Research Equipment in selected science-engineering fields, 1982-83. An analysis of findings from the Baseline National Survey of academic research instruments and instrumentation needs N86-11088

TEST FACILITIES
Test, measurement, and diagnostic equipment (system peculiar)
[AD-A156669] N86-10563
Evaluation of the International Atomic Energy Agency (IAEA) Safeguards Analytical Laboratory quality assurance program
[DE85-012078] N86-10953

TEST FIRING
EMACK railgun firing test report number 9
[AD-A156661] N86-10354

TETHERED SATELLITES
Preliminary studies of a spinning tether-connected TRIO concept --- spaceborne interferometer (TRIO) N86-11110

TEXTBOOKS
Catalog of Resources for Education in Ada (trademark) and Software Engineering (CREASE). Version 3.0
[AD-A156687] N86-10790

THALLIUM ALLOYS
Cellular morphologies in lead-thallium alloys --- gravitational effects N86-10262

THEMATIC MAPPING
Photomapping in different climatic zones --- Spacelab metric camera N86-10491
Analysis of metric camera images from the USA and their suitability for topographic and thematic mapping --- Spacelab N86-10498
Thematic investigations in France based on metric camera imagery --- Spacelab N86-10509
Thematic mapping of metric camera color infrared and black and white photographs for land use classification N86-10510
Topographic and thematic mapping: Analysis of metric camera black and white photographs of the Rhone Delta N86-10514
Multisensor data integration techniques N86-10604
The effects of merging TM and A/C radar on wetland classification N86-10621
Lithologic mapping in a sedimentary environment using multipolarization SAR images N86-10624

THEOREM PROVING
Principal bundles on the affine line N86-10856
Coincidence densities and spectra of a class of substitution minimal sets N86-10857

THERMAL ANALYSIS
Thermal and structural analysis of ring components by the finite element method
[DE85-013305] N86-11021

THERMAL BATTERIES
Characterization of cathodic corrosion products in the Ca/CaCrO4 thermal battery
[DE85-013442] N86-10644

THERMAL CONDUCTIVITY
Recirculation within a glass mixture subjected to external and resistive heating
[DE85-010068] N86-10348

THERMAL CONTROL COATINGS
Steady state frictional behavior of thin film coatings N86-10335

THERMAL DEGRADATION
Age-life prediction of nylon 66 parachute materials. Part 2: Changes in the chemical and physical properties of materials on aging
[AD-A156909] N86-10347

THERMAL DIFFUSION
Space experiment on thermal diffusion. Preparation and theoretical analysis N86-10253
HALFBREED: An extended capability version of the YAQUI code
[DE85-014237] N86-10843

THERMAL DIFFUSIVITY
Recirculation within a glass mixture subjected to external and resistive heating
[DE85-010068] N86-10348

THERMAL EMISSION
Investigation of the uncertainties of the NBS (National Bureau of Standards) thermal voltage and current converters
[PB85-200178] N86-10453

THERMAL ENERGY
Time resolved flow velocity and concentration measurements using a travelling thermal lens
[AD-A156706] N86-10541
Solar thermal technical information guide
[DE85-002941] N86-10657

THERMAL EXPANSION
Thermal expansion of glasses in the solid and liquid phases
[DE85-013953] N86-10351
Method for compensating bellows pressure loads while accommodating thermal deformations
[DE85-013306] N86-10933

THERMAL INSULATION
Effect of increased body clothing insulation on hand temperature in a cold environment
[AD-A156597] N86-10786

THERMAL MAPPING
LANDSAT TM image data quality analysis for energy-related applications
[E85-10109] N86-10597

THERMAL NEUTRONS
Anelastic relaxation in irradiated Cu-Be
[DE85-013893] N86-11056

THERMAL PROTECTION
Analytical investigation of solid rocket nozzle failure
[NASA-TM-86513] N86-10278

THERMAL RADIATION
Experimental investigations of thermal radiation from potassium atoms and design applications
[DE85-004086] N86-11036

THERMAL STABILITY
Elastic properties and thermal stability characterization of metallic glasses by guided wave techniques N86-10337

THERMAL STRESSES
Fracture toughness and stress relief response of irradiated type 347/348 stainless steel N86-10320

THERMOCHEMICAL PROPERTIES
Guidelines for a thermochemical kinetics computer program
[DE85-014266] N86-10839

THERMOCHEMISTRY
Process models for 3D composites
[AD-A156889] N86-10292

THERMOCLINES
A processor for the study of ocean fine-scale patches
[AD-A157019] N86-10730

THERMODYNAMIC CYCLES
Engine-driven and absorption heat pump programs
[DE85-013930] N86-10472
Analyses of advanced residential abosrption heat pump cycles
[DE85-005244] N86-10664

THERMODYNAMIC PROPERTIES
Application of the ruthenium and technetium thermodynamic data bases used in the EQ3/6 geochemical codes
[DE85-013766] N86-10632
The effects of orography on land-atmosphere turbulent exchange processes N86-10702

THERMODYNAMICS
Thermocapillary flows and their stability: Effects of surface layers and contamination N86-10109
Thermodynamic constraints on ion beam mixing of metals on insulators
[DE85-013628] N86-10448
Simplified analysis of Stirling engines and heat pumps
[DE85-005366] N86-10647
Thermodynamics of polymer-supercritical solvent mixtures
[AD-A157038] N86-11061

THERMOELECTRIC GENERATORS
General-purpose heat source development: Safety Verification Test Program. Bullet/fragment test series
[DE85-014262] N86-10660

THERMOELECTRIC MATERIALS
Magnetic properties of doped semiconductors
[DE85-012090] N86-11053

THERMOMECHANICAL TREATMENT
The influence of containerless undercooling and rapid solid-state quenching on the superconductive and magnetic properties of some clustering alloy systems N86-10076

THERMOMIGRATION
Thermomigration of cobalt in liquid tin: Experiment 1 ES 320 --- Spacelab N86-10222

THERMONUCLEAR REACTIONS
ORR core re-configuration measurements to increase the fast neutron flux in the Magnetic Fusion Energy (MFE) experiments
[DE85-013520] N86-10958

THERMOPHYSICAL PROPERTIES
Measurement of high temperature thermophysical properties N86-10074
Measurement of the properties of tungsten at high temperatures N86-10091
Dynamic thermophysical measurements in space
[NASA ORDER H-27954-B] N86-10106
Determination of thermophysical characteristics of solid materials by electrical modelling of the solutions to the inverse problems in nonsteady heat conduction
[NASA-TM-77907] N86-10293
Age-life prediction of nylon 66 parachute materials. Part 2: Changes in the chemical and physical properties of materials on aging
[AD-A156909] N86-10347
A study of the applicability of nucleation theory to quasi-thermodynamic transitions of second and higher Ehrenfest-order
[NASA-CR-176238] N86-11059

THERMOREGULATION
Mechanism of adaptogenic action of prickly eleuterococcus on man during heat stress N86-10757
Vestibular resistance and blood circulation changes in orthostatic position during hyperthermia N86-10758
Heat transfer mechanism in human extremities N86-10759

THERMOVISCOELASTICITY
Oscillations of a viscoelastic liquid drop in zero-gravity N86-10240

THESES
Study of one- and two-dimensional filtering and deconvolution algorithms for a streaming array computer [NASA-CR-176226] N86-10827
THICK PLATES
The effect of debond growth on crack propagation in composite plates reinforced with adhesively bonded composite stringers N86-10287
THICKNESS
Explosive initiation by very small conical shaped charge jets [DE85-009443] N86-10357
Geothermal influences on the long-term thickness of the mechanical lithosphere during flexure N86-10697
Ion beam sputter deposited zinc telluride films [NASA-TM-87119] N86-11048
THICKNESS RATIO
Joint research effort on vibrations of twisted plates, phase 1: Final results [NASA-RP-1150] N86-10579
THIN FILMS
Modelling of laser-enhanced chemical vapor deposition N86-10105
Capillary forces in a low gravity environment — Spacelab N86-10202
Steady state frictional behavior of thin film coatings N86-10335
Fuel and lubricant behavior in boundary layers analyzed by infrared emission Fourier transform spectrometry N86-10336
Dielectric properties of silicon surfaces and silver thin films [JUEL-1968] N86-10450
Experimental studies of transition radiation and optical bremsstrahlung [DE85-0135637] N86-10949
An investigation of vortex dynamics in 2-dimensional superfluid films of helium-4 N86-11040
Ion beam sputter deposited zinc telluride films [NASA-TM-87119] N86-11048
THIN WALLED SHELLS
Stiffened and prestressed composite overwrapped pressure vessels N86-10547
Strength of shells under local transverse loads N86-10568
THIN WALLS
An analytical and numerical study of the buckling behavior of fiber-reinforced beams N86-10566
THOMSON SCATTERING
Design, fabricate and test a 1.06(MU) repetitively pulsed laser [DE85-014439] N86-10543
THREE DIMENSIONAL COMPOSITES
Mechanics of coated fiber composites N86-10285
THREE DIMENSIONAL FLOW
Three-dimensional inviscid analysis of radial turbine flow and a limited comparison with experimental data [NASA-TM-87091] N86-10017
Mathematical models of continuous flow electrophoresis N86-10143
Finite element solution of the Navier-Stokes equations for 3-D turbulent free shear flows N86-10457
THREE DIMENSIONAL MOTION
Motion analysis report [NASA-CR-171897] N86-10896
THRESHOLDS (PERCEPTION)
Dynamics of changes of statistical indicators of heart rhythm of persons with different degree of motion sickness N86-10743
Determination of symmetry and phase in human visual response functions: Theory and experiments N86-10769
THROMBOCYTES
Effect of emotional stress on hemostasis system of healthy persons N86-10745
THRUST BEARINGS
Termination load carrying device [AD-D011800] N86-10558
THRUST CHAMBERS
Rapid evaluation of ion thruster lifetime using optical emission spectroscopy [NASA-TM-87103] N86-10280
TILT ROTOR AIRCRAFT
A comparative analysis of a CV helicopter and a JVX (Joint Services Advanced Vertical Lift) tilt-rotor aircraft in an aircraft carrier based ASW (Anti-Submarine Warfare) [AD-A156871] N86-10041
TIMBER INVENTORY
Requirements and possibilities of Spacelab metric camera photos usage for inventories of large areas of extensively managed forests N86-10513
TIME CONSTANT
Timing system control software in the SLC [DE85-013380] N86-11024
TIME DEPENDENCE
Portevin-Le Chatelier effect. 1: Model for the type-E serrations [DE85-006879] N86-10322
Time-implicity simulation of particle-fluid systems [DE85-012944] N86-10471
New probabilistic modeling and simulation methods for complex time-dependent systems [DE85-009575] N86-10835
A mesh moving technique for time dependent partial differential equations in two space dimensions [AD-A156663] N86-10866
TIME LAG
Control concepts for in-flight simulation including actuator nonlinearities and time delays [DFVLR-FB-85-24] N86-10047
Signal analysis receiver with acousto-optic delay lines [AD-D011761] N86-10427
TIME MEASUREMENT
Time resolved flow velocity and concentration measurements using a travelling thermal lens [AD-A156706] N86-10541
TIME OF FLIGHT SPECTROMETERS
Direct mass measurements in the light neutron-rich region using a combined energy and time-of-flight technique [DE85-012758] N86-10963
TIME SIGNALS
DSN frequency and timing system, Mark 4-85 N86-10393
TIMING DEVICES
DSN frequency and timing system, Mark 4-85 N86-10393
TIN
Self diffusion of Sn112 and Sn124 in liquid tin N86-10231
Development of metallization process [NASA-CR-176209] N86-10312
Adsorption of oxygen on single crystal tin at liquid helium temperatures N86-11044
TIN ALLOYS
Thermomigration of cobalt in liquid tin: Experiment 1 ES 320 — Spacelab N86-10222
TIN ISOTOPES
Self diffusion of Sn112 and Sn124 in liquid tin N86-10231
TIN OXIDES
Float zone experiments in space N86-10067
TITANIUM
Low temperature plastic deformation mechanisms of alpha-titanium single crystals [ESA-TT-871] N86-10332
TITANIUM ALLOYS
Pre-bond treatment for titanium alloys [BAE-AL/MAT/3864] N86-10309
TITANIUM COMPOUNDS
Development of metallization process [NASA-CR-176209] N86-10312
TOKAMAK DEVICES
GA Theory News, January-March 1985 [DE85-012572] N86-11007
Activities report in plasma physics N86-11039
TOPOGRAPHY
How Antarctica was unveiled. Masterpieces of Frankfurt topographic surveyors. A part of the German Antarctica research program N86-10181
On the use of X-band CW nanosecond airborne radar for terrain profiling [AD-A156886] N86-10406
Analysis of metric camera images from the USA and their suitability for topographic and thematic mapping — Spacelab N86-10498
Line mapping and resolution tests with metric camera data — Spacelab N86-10500
Topographic and thematic mapping: Analysis of metric camera black and white photographs of the Rhone Delta N86-10514
Updating of topographic maps by means of metric camera photos example: Hallertau (Bavaria) N86-10517
Interpretation of Spacelab-1 photographs for the generation of 1:200000 topographic map N86-10518
Multisensor data integration techniques N86-10604
Representation of the distribution of the snow cover on the surface of the Earth's dry land [NASA-TM-77909] N86-10612
Topographic mapping from interferometric synthetic aperture radar observations N86-10622
Analysis of edge detection algorithms on DIAL (Digital Image Analysis Laboratory) [AD-A156735] N86-10630
Fundamental study of the closure property of joints N86-10698
A boundary layer flow model for areas of complex terrain N86-10701
Applications for three-dimensional computer graphic cloud representations produced from satellite imagery [AD-A156903] N86-10798
contemporary Aeolian processes on Mars: Local dust storms N86-11136
TOPOLOGY
Topological properties of hypercubes [AD-A156777] N86-10850
TOROIDAL PLASMAS
Box method for finding intersections of a trajectory with axisymmetric flux surfaces [DE85-013525] N86-10840
Compact torus compression of microwaves [DE85-012919] N86-11016
Recent helicity source and power supply improvements in CTX [DE85-012741] N86-11028
TOUGHNESS
Application of the unloading compliance methods in fracture toughness measurements of a quenched and tempered steel [BLL-BISI-TRANS-21628-(9022.06)] N86-10308
TOWED BODIES
A processor for the study of ocean fine-scale patches [AD-A157019] N86-10730
TOWERS
List of publications on the 200 m meteorological mast at Cabauw, the Netherlands [KNMI-FM-85-6] N86-10711
TOXICITY
Evaluation of the 90-day inhalation toxicity of petroleum and oil shale JP-5 jet fuel [AD-A156815] N86-10675
Development and evaluation of multispecies test protocols for assessing chemical toxicity [DE85-013526] N86-10679
TRACKING (POSITION)
Digital processing of images in tracking a moving object N86-10818
TRACKING FILTERS
An active tracking band-pass filter [AD-A156559] N86-10419
TRACKING PROBLEM
Superconvergent tracking and invariant surfaces in phase space [DE85-013051] N86-10995
TRAINING AIRCRAFT
Proposed modifications for the RAAF Airtrainer CT-4A cockpit [AD-A156808] N86-10039
TRAINING DEVICES
The influence of tactual seat-motion cues on training and performance in a roll-axis compensatory tracking task setting N86-10784
An annotated bibliography of abstracts on the use of simulators in technical training [AD-A156792] N86-11065
TRAINING SIMULATORS
The first German Spacelab mission D1 reports — Spacelab payloads [PR-3] N86-10189
The influence of tactual seat-motion cues on training and performance in a roll-axis compensatory tracking task setting N86-10784
An annotated bibliography of abstracts on the use of simulators in technical training [AD-A156792] N86-11065
TRAJECTORIES
Lumped geopotential harmonics of order 14, from the orbit of 1967-11G [AD-A156627] N86-10190
TRAJECTORY ANALYSIS
Box method for finding intersections of a trajectory with axisymmetric flux surfaces [DE85-013525] N86-10840
TRANSDUCERS
Levitating furnance for containerless processing in space N86-10169
Elastic properties and thermal stability characterization of metallic glasses by guided wave techniques N86-10337
Improved particle-velocity transducer for equation-of-state experiments [DE85-013204] N86-10532
TRANSFER FUNCTIONS
Advanced containerless processing technology N86-10176
Digital control of the hydraulic actuators of an adaptive suspension vehicle N86-10548
Acceleration-invariant approximation method for recursive digital filters [AD-A156655] N86-10865

TRANSFORMATIONS (MATHEMATICS)
A transformation method for the evaluation of the response moments of elastic structures with random properties
[AD-A156882] N86-10557
Well-posed questions and exploration of the space of parameters in linear and non linear inversion
[PN-84/13] N86-10858
Bounding solutions of geometrically nonlinear viscoelastic problems
[NASA-CR-176219] N86-10860
Measurement and resulting first and second order approximations for a 9 deg bending magnet in LAMPF's 750-keV transport
[DE85-012691] N86-10930
TRANSIENT RESPONSE
Mephisto: Interfacial destabilization in metal alloys N86-10079
A fundamental study of smoldering with emphasis on experimental design for zero-g N86-10162
TRANSITION METALS
Non-empirical interatomic potentials for transition metals
[DE85-013448] N86-10440
TRANSITION TEMPERATURE
Experimental and theoretical studies of wetting and multilayer adsorption
[NASA ORDER H-27954B] N86-10121
Calculation of the glass transition temperatures of linear polymers. Part 1: Rules for hierarchical ordering of the data set
[AD-A156584] N86-10343
A study of the applicability of nucleation theory to quasi-thermodynamic transitions of second and higher Ehrenfest-order
[NASA-CR-176238] N86-11059
TRANSLATIONAL MOTION
Multimode acoustic research N86-10167
TRANSMISSION
The generation and transmission of vibration in plain cylindrical bearings. Part 2. Experiment
[AD-A156577] N86-10553
TRANSMISSION LINES
Method for tuning a phased array antenna
[AD-D011768] N86-10372
TRANSMISSION LOSS
Long term statistical measurements of environmental acoustics parameters in the arctic. AEAS report number 2. Low frequency transmission loss measurements in the central arctic ocean
[AD-A156576] N86-10727
TRANSMISSIVITY
Particle cloud combustion experiment N86-10160
Radome analysis and design capabilities of the RF and Microwave Technology Branch
[AD-A156662] N86-10404
TRANSMITTERS
High sensitivity millimeter-wave measurement apparatus
[AD-D011786] N86-10373
TRANSONIC FLOW
Acta Aeronautica et Astronautica Sinica (selected articles)
[AD-A147304] N86-10001
Second order approximation method for transonic flows over swept wings N86-10002
On the design of airfoils in transonic flow using the Euler equations N86-10013
TRANSONIC WIND TUNNELS
Investigations to improve the slotted-wall test section of the F+W transonic wind tunnel
[F+W-FO-1752] N86-10050
The rubber tube test section of the DFVLR in Goettingen, West Germany — wind tunnel walls
[DFVLR-FB-85-18] N86-10051
TRANSPORT AIRCRAFT
The dirigible: A catalyst for resource exploitation in remote areas?
[AD-A156518] N86-10034
Retrofit of SAC EC-135C and RC-135 aircraft with CFM-56 engines
[AD-A156688] N86-10038
TRANSPORT PROPERTIES
Light scattering tests of fundamental theories of transport properties in the critical region N86-10113
Critical transport phenomena in fluid helium under low gravity N86-10119
Transport processes research N86-10129
Advanced containerless processing technology N86-10176
Laser generation and transport of a relativistic electron beam
[DE85-011709] N86-10192
Polyacetylene polymerization, structure, and electrical transport properties N86-10334
The measurement and application of transport properties of ion swarms in gases N86-10370
Radionuclide complexation in xylem exudates of plants
[DE85-013446] N86-10684
Technical considerations in regional aerosol modeling
[PB85-193027] N86-10710
Indices of blood oxygen transporting properties and erythropoiesis in rats after prolonged stay in nitrogen-oxygen mixture at elevated pressure N86-10761
Beam line windows at LAMPF
[DE85-012723] N86-10985
Applications of the second-order achromat concept to the design of particle accelerators
[DE85-013072] N86-10994
TRANSPORT THEORY
Transport processes in solution crystal growth N86-10107
Lambda point equipment N86-10118
Critical transport phenomena in fluid helium under low gravity N86-10119
Transport processes research N86-10129
TRANSPORTATION NETWORKS
Research needs for corrosion control and prevention in energy conservation systems
[DE85-014852] N86-10326
TRANSVERSE ACCELERATION
Strength of shells under local transverse loads N86-10568
TRAVELING WAVE TUBES
The Netherlands Institute for Nuclear and High Energy Physics (NIKHEF) traveling wave monitor user guide
[LINO-121] N86-10969
TREES (PLANTS)
Vegetation and soils field research data base: Experiment summaries
[E85-10110] N86-10610
TRIBOLOGY
Steady state frictional behavior of thin film coatings N86-10335
Tribological properties of structural ceramics
[NASA-TM-87105] N86-10341
TRIGGER CIRCUITS
Compact, low jitter, triggered spark gap
[DE85-012812] N86-10195
Delay times and jitter in triggered vacuum spark gaps using metal vapor and surface flashover types of triggers
[DE85-013966] N86-10441
Soudan 2 data acquisition and trigger electronics
[DE85-013864] N86-10443
Timing system control software in the SLC
[DE85-013380] N86-11024
TROPOSPHERE
The Liu, Katsaros, and Businger (1979) bulk atmospheric flux computational iteration program in FORTRAN and BASIC
[AD-A156736] N86-10714
TRYPTOPHAN
Effect of cold on brain serotonin system and plasma corticosteroid level in different strains of mice N86-10766
TSUNAMI WAVES
Formation of waves by ground motion
[PM/84/09] N86-10706
TUNGSTEN
Measurement of the properties of tungsten at high temperatures N86-10091
TUNING
Effects of slots/holes in disks on frequencies of TM01 and EH11 waves in the disk-loaded waveguide
[DE85-013376] N86-11009
TURBINE BLADES
Three-dimensional inviscid analysis of radial turbine flow and a limited comparison with experimental data
[NASA-TM-87091] N86-10017
Film cooling on a convex wall: Heat transfer and hydrodynamic measurements for full and partial coverage
[NASA-CR-174964] N86-10461
Joint research effort on vibrations of twisted plates, phase 1: Final results
[NASA-RP-1150] N86-10579
Improved stud configurations for attaching laminated wood wind turbine blades
[NASA-TM-87109] N86-10582
TURBINE ENGINES
Film cooling on a convex wall: Heat transfer and hydrodynamic measurements for full and partial coverage
[NASA-CR-174964] N86-10461
TURBULENCE
Acta Aeronautica et Astronautica Sinica (selected articles)
[AD-A147304] N86-10001
A numerical solution of the shock-turbulent interaction over a compression corner for supersonic flow N86-10003
The role of freestream turbulence scale in subsonic flow separation
[NASA-CR-176237] N86-10014
Role of convection in grain refining N86-10133
Effects of chemistry and swirl on the production of turbulence in a flame
[PB85-219632] N86-10305
Mean turbulence structure in strongly heating air flows N86-10455
A root-mean-square pressure fluctuations model for internal flow applications
[NASA-CR-3928] N86-10460
Film cooling on a convex wall: Heat transfer and hydrodynamic measurements for full and partial coverage
[NASA-CR-174964] N86-10461
The effects of orography on land-atmosphere turbulent exchange processes N86-10702
GA Theory News, January-March 1985
[DE85-012572] N86-11007
TURBULENCE EFFECTS
Buoyancy effects upon vapor flame and explosion processes N86-10161
Large eddy interactions in a turbulent channel flow
[NASA-TM-86757] N86-10464
TURBULENT BOUNDARY LAYER
Evaluation of surface exchange coefficients from mildex ocean/atmosphere mixed layer data
[AD-A156765] N86-10729
TURBULENT FLOW
Verification of turbulence developing from the oscillatory Marangoni convection in a liquid column — rocket flight N86-10241
Finite element solution of the Navier-Stokes equations for 3-D turbulent free shear flows N86-10457
A root-mean-square pressure fluctuations model for internal flow applications
[NASA-CR-3928] N86-10460
Large eddy interactions in a turbulent channel flow
[NASA-TM-86757] N86-10464
TURBULENT JETS
Investigation of density gradient fluctuations in a turbulent free jet by means of the laser schlieren crossed-beam method
[DFVLR-FB-85-19] N86-10027
Confined swirling jet predictions using a multiple-scale turbulence model
[NASA-CR-178484] N86-10462
TURBULENT WAKES
Effects of chemistry and swirl on the production of turbulence in a flame
[PB85-219632] N86-10305
TWISTING
Joint research effort on vibrations of twisted plates, phase 1: Final results
[NASA-RP-1150] N86-10579
TWO DIMENSIONAL BODIES
Automated analysis of digital images generated by two-dimensional gel electrophoresis
[DE85-011906] N86-10526
An analytical and numerical study of the buckling behavior of fiber-reinforced beams N86-10566
TWO DIMENSIONAL FLOW
Numerical solution of hypersonic flow near leading edge of a flat plate N86-10008
Aerodynamics of hyperlift systems
[SNIAS-443.501/85] N86-10023
Spectral methods in adapted curved grids N86-10878
TWO PHASE FLOW
Theoretical specific impulse for two-phase flow in nozzle of rocket-ramjet engine: A simple estimation method N86-10005
Analysis of annular two-phase flow with liquid entrainment N86-10459
KRAK: A computer program for two-phase, two-component porous flow and fracture propagation, revision
[DE85-014264] N86-10469
Heat transfer in condensing and evaporating two-component, two-phase flow inside a horizontal tube N86-11058

U

U.S.S.R.
Soviet free-electron laser research
[AD-A156898] N86-10542
Report of the Workshop on Geologic Applications of Remote Sensing to the Study of Sedimentary Basins
[E86-10002] N86-10599

Structural mapping of folded sedimentary environments from satellite images: An example from Central Asia N86-10607
Maximum water reserves in the snow cover in the European territory of the USSR according to data for 1892-1960
[NASA-TM-77901] N86-10611
Observations of the snow cover in the southern part of the Buryat Autonomous Soviet Socialist Republic
[NASA-TM-77910] N86-10613

ULTRAHIGH VACUUM
Report on a visit to CERN in February 1985. Notes on bunch monitors, high-frequency systems, linacs, kickers, magnets, vacuum and bunch extraction
[LINO-119] N86-10967
The MEA vacuum system
[LINO-120] N86-10968

ULTRALOW TEMPERATURES
Magnetic properties of doped semiconductors
[DE85-012090] N86-11053

ULTRAPURE METALS
Defect identification in high-energy semiconductors
[DE85-014533] N86-10442

ULTRASONIC FLAW DETECTION
Ultrasonic inspection of weldments in large size spiral box for hydroelectric plant
[AS-701/85] N86-10562

ULTRASONIC SPECTROSCOPY
Characterization of vapor and aerosol flows by photothermal methods
[AD-A156601] N86-10465

ULTRASONIC TESTS
Ultrasonic evaluation of mechanical properties of thick, multilayered, filament wound composites
[MASA-TM-87088] N86-10561

ULTRASONIC WAVE TRANSDUCERS
Ultrasonic evaluation of mechanical properties of thick, multilayered, filament wound composites
[MASA-TM-87088] N86-10561

ULTRASONICS
Exploratory development for a high reliability flaw characterization module
[AD-A156632] N86-10916

ULTRAVIOLET RADIATION
Identification of chemical and physical phenomena affecting the durability of silvered polymer (PMMA) mirrors
[DE85-012131] N86-10645
Somatic cell and molecular genetics approach to DNA repair and mutagenesis
[DE85-014181] N86-10737

ULTRAVIOLET SPECTROSCOPY
Ultraviolet spectroscopy of the Earth's dayglow and magnetosphere cleft N86-10696

UNDERGROUND ACOUSTICS
Geothermal lost circulation zone mapping tool
[DE85-008696] N86-10531

UNDERWATER ACOUSTICS
Long term statistical measurements of environmental acoustics parameters in the arctic. AEAS report number 2. Low frequency transmission loss measurements in the central arctic ocean
[AD-A156576] N86-10727

UNDERWATER EXPLOSIONS
Angle of incidence effects for underwater shock using generic computational models
[DE85-012936] N86-10466

UNIQUENESS
Multivariable partial realization and the aspect of uniqueness
[ER-83/09] N86-10879

UNITED STATES
An anthology: Rationale for a US ballistic missile defense (1969 - 1984)
[AD-A156781] N86-10199

UNIVERSITIES
NASA/American Society for Engineering Education (ASEE) Summer Faculty Fellowship Program, 1985
[NASA-CR-177972] N86-11064
Academic Research Equipment in selected science-engineering fields, 1982-83. An analysis of findings from the Baseline National Survey of academic research instruments and instrumentation needs N86-11088

UNSTEADY FLOW
A new method for calculating unsteady supersonic aerodynamic forces and its application N86-10009
A study of the aerodynamic performance of Weis-Fogh wings N86-10012
Theoretical study of the unsteady linear problem for a rectangular wing with a pitching movement
[ONERA-RT-17/1841-RY-010-R] N86-10022
Numerical simulation of unsteady thermal Marangoni flows N86-10238
Experiments and computations on unsteady separating flow in an expanding flume
[REPT-2-84] N86-10477
A modified Successive Over-Relaxation (SOR) method for the Poisson equation in unsteady free-surface flow calculations
[TW-264] N86-10881

UPGRADING
Computer control of rf at SLAC
[DE85-013065] N86-11015

URANIUM
Aluminum ion plating for corrosion protection of uranium, revision 1
[DE85-012419] N86-10330

URANIUM 235
The development of a neutron evaporation theory code for the thermal fission of Uranium-235
[AD-A156593] N86-10951

UREAS
Growth of organic crystals by Ostwald ripening N86-10058

USER MANUALS (COMPUTER PROGRAMS)
User's guide for Langley Research Center Orbital Lifetime program
[NASA-TM-87587] N86-10828

USER REQUIREMENTS
Computer-based training for the US Coast Guard standard terminal microcomputer: A basis for implementation utilizing the elaboration theory of instructional design
[AD-A156548] N86-10791
DFVLR, strategic study of astronautics 1984, user requirements N86-11069

UTILITIES
Photovoltaic systems in remote locations: An experience summary
[NASA-TM-87106] N86-10643
Phosphoric and electric utility fuel technology development
[DE85-014741] N86-10651

UTILIZATION
Operations research applications
[ARW-03-THE-BDK/ORS/83-08] N86-10901

V

VACUUM CHAMBERS
Adhesion of metals: Experiment 1 ES-340 — Spacelab N86-10232

VACUUM FURNACES
The isothermal heating facility — Spacelab N86-10208
Vacuum brazing under microgravity — Spacelab N86-10214
Gradient heating facility behavior — Spacelab N86-10217

VACUUM MELTING
Melting and solidification of metal matrix composites under microgravity — Spacelab N86-10211
Shrinking of a gas bubble in a glass melt under microgravity conditions — STS-11 N86-10254

VACUUM SYSTEMS
Delay times and jitter in triggered vacuum spark gaps using metal vapor and surface flashover types of triggers
[DE85-013968] N86-10441
Method for compensating bellows pressure loads while accommodating thermal deformations
[DE85-013306] N86-10933
The MEA vacuum system
[LINO-120] N86-10968

VALVES
Digital control of the hydraulic actuators of an adaptive suspension vehicle N86-10548

VANADIUM
Fabrication and metallurgical properties of modified 9Cr-1 Mo steel
[DE85-012885] N86-10328

VAPOR DEPOSITION
Modelling of laser-enhanced chemical vapor deposition N86-10105
Morphological stability and fluid dynamics of vapor crystal growth N86-10126
Experimental and theoretical analysis of chemical vapor deposition with prediction of gravity effects N86-10132
Preliminary reports, memoranda and technical notes of the Materials Research Council Summer Conference, La Jolla, California
[AD-A156776] N86-10291
The influence of the substrate on the practical machining applications of cutting edges coated with different materials
[BLL-RISLEY-TR-5039-(9091.9F)] N86-10546
Improved blue response and efficiency of A-Si:H solar cells deposited from disilane using a dual-chamber plasma system
[DE85-013289] N86-10649
Photovoltaic devices using a Si:H from higher order silanes
[DE85-006804] N86-10668

VAPOR PHASE EPITAXY
Hgl sub 2 crystal growth for nuclear detectors N86-10066
Fluid dynamics and thermodynamics of vapor phase crystal growth N86-10068
Vapor growth of alloy-type semiconductor crystals N86-10069
Experimental and theoretical analysis of chemical vapor deposition with prediction of gravity effects N86-10132
Directional solidification of an aluminum-zinc vapor emulsion in microgravity — Spacelab N86-10218

VAPOR PHASES
Modelling of laser-enhanced chemical vapor deposition N86-10105
Fundamental studies of droplet combustion at reduced gravity N86-10165
Crystal growth from solutions and nucleation from the vapor phase — Spacelab N86-10267

VAPORS
Test and evaluate passive orbital disconnect struts (PODS 3)
[NASA-CR-177368] N86-10274
Characterization of vapor and aerosol flows by photothermal methods
[AD-A156601] N86-10465
Scoping studies of vapor behavior during a severe accident in a metal-fueling reactor
[DE85-011474] N86-10952

VARIABILITY
A quantitative method for analyzing the roughness of the seafloor N86-10726
Variability analysis of visually induced responses in the midst of noise
[B8564052] N86-10774

VARIABLE STARS
The two micron spectrum of R Scuti N86-11092

VARIATIONAL PRINCIPLES
Variational estimates for the mass gap of SU(2) Euclidean lattice gauge theory
[NIKHEF-H/84-13] N86-10883

VECTOR ANALYSIS
Study of one- and two-dimensional filtering and deconvolution algorithms for a streaming array computer
[NASA-CR-176221] N86-10822
A mesh moving technique for time dependent partial differential equations in two space dimensions
[AD-A156663] N86-10866

VECTOR MESONS
Two-loop large Higgs mass corrections to vector boson self-couplings
[NIKHEF-H/84-15] N86-11038

VEGETATION
Vegetation and soils field research data base: Experiment summaries
[E85-10110] N86-10610
The effect of vegetation type, microrelief, and incidence angle on radar backscatter N86-10619
The effects of merging TM and A/C radar on wetland classification N86-10621
Modelling of vegetation volumes N86-10629

VEHICLES
Marginal terrain straddle-lift container handler
[AD-D011752] N86-10555

VELOCITY
Chemical kinetics and cellular structure of detonations in hydrogen sulphide and air
[DE85-009408] N86-10304
Velocities of gas and plasmas from real time holographic interograms
[DE85-014618] N86-10530
Ultrasonic evaluation of mechanical properties of thick, multilayered, filament wound composites
[MASA-TM-87088] N86-10561

VELOCITY DISTRIBUTION
Large eddy interactions in a turbulent channel flow
[NASA-TM-86757] N86-10464
Strength of shells under local transverse loads N86-10568

VELOCITY MEASUREMENT
Fall velocity indicator/viewer
[AD-D011789] N86-10482
Time resolved flow velocity and concentration measurements using a travelling thermal lens
[AD-A156706] N86-10541
Structural discontinuity within the southern California continental margin: Seismic and gravity models of the western Transverse Ranges N86-10699

VERTEBRATES
Paleogene vertebrate paleontology, geology and remote sensing in the Wind River Basin N86-10609
VERTICAL DISTRIBUTION
Field comparison of in situ meteorological sensors [PB85-196988] N86-10723
VERTICAL MOTION
System modeling and identification of equivalent systems with and without compensating time delay for control-augmented aircraft [ESA-TT-852] N86-10043
VERY LARGE SCALE INTEGRATION
The VLSI design of error-trellis syndrome decoding for convolutional codes N86-10391
Investigation of metallic impurities introduced into SiO2 and silicon by various candidate VLSI metallization systems: Chemical reactions, diffusion, and electrical properties [AD-A156609] N86-10429
Implementation issues for algorithmic VLSI (Very Large Scale Integration) processor arrays [AD-A156699] N86-10432
Microcircuit device reliability field experience database. Volume 1. Field data. Volume 2. Failure Event/Analysis data [AD-A156836] N86-10433
Increase of the packaging density of Very Large Scale Integration (VLSI) circuits using automatic alignment [BMFT-FB-T-85-020] N86-10451
Efficient systolic arrays for the solution of toeplitz systems: An illustration of a methodology for the construction of systolic architectures in VLSI (Very Large Systems Integration) [AD-A156767] N86-10795
Design of a multifunction Input-Output (I/O) controller [EUT-84-E-143] N86-10802
VERY LONG BASE INTERFEROMETRY
A VLBI survey at 2.29 GHz N86-10383
Comparison of the calibration of ionospheric delay in VLBI data by the methods of dual frequency and Faraday rotation N86-10384
Mobile VLBI and GPS measurement of vertical crustal motion N86-10401
Improved mapping of radio sources from VLBI data by least-square fit N86-10402
Optical/IR telescope arrays: A study of their potential for satisfying observational requirements in astronomy for a large aperture system in the 1990s and beyond [REPT-15] N86-11094
Colloquium on Kilometric Optical Arrays in Space [ESA-SP-226] N86-11096
Radio astronomy experience in image reconstruction. A history lesson for optical astronomers N86-11117
VLBI at optical and radio wavelengths: Congruences and contrasts N86-11126
VESTIBULAR TESTS
Vestibular resistance and blood circulation changes in orthostatic position during hyperthermia N86-10758
VIBRATION
The influence of low frequency mechanical vibrations on the growth of single crystals N86-10059
Compact, low jitter, triggered spark gap [DE85-012812] N86-10195
Vibro-acoustic forecast for space shuttle launches at Vandenberg AFB: The payload changeout room and the administration building [AD-A156944] N86-10269
Specification for the performance, design, development and test requirements for a severe environment cartridge recorder. Issue 4 [AD-A156637] N86-10523
Passive damping concepts for slender columns in space structures [NASA-CR-176234] N86-10577
Three-dimensional vibration analysis of a uniform beam with offset inertial masses at the ends [NASA-TM-86393] N86-10580
The Shock and Vibration Digest, volume 17, no. 3 [AD-A154144] N86-10585
Sound radiation from repetitive transient vibrations using multi-channel digital signal processing with application to impact machinery N86-10910
VIBRATION DAMPING
Evaluation of a pulse control law for flexible spacecraft [NASA-CR-176233] N86-10272
VIBRATION EFFECTS
Oscillations of semi-free liquids in microgravity: Spacelab 1 experiment ES 326 N86-10204
Numerical simulation of convections in the microgravity environment N86-10239
Report on the research activities on whole-body vibrations. Human strain due to mechanical vibrations [ISBN-3-88383-107-7] N86-10773
VIBRATION ISOLATORS
Cryogenic equivalence principle experiment N86-10171
VIBRATION MEASUREMENT
Test and evaluate passive orbital disconnect struts (PODS 3) [NASA-CR-177368] N86-10274
Joint research effort on vibrations of twisted plates, phase 1: Final results [NASA-RP-1150] N86-10579
Correlation between vibrations and buckling of cylindrical shells stiffened by spot-welded and riveted stringers [TAE-537] N86-10584
VIBRATION SIMULATORS
The generation and transmission of vibration in plain cylindrical bearings. Part 2. Experiment [AD-A156577] N86-10553
VIBRATIONAL SPECTRA
The generation and transmission of vibration in plain cylindrical bearings. Part 2. Experiment [AD-A156577] N86-10553
VIDEO DATA
Extended precision in video bandwidth analog to digital converter using optical techniques [AD-D011745] N86-10422
Stereoscopic video imagery generation [AD-D011785] N86-10481
Fall velocity indicator/viewer [AD-D011789] N86-10482
Catalog of Resources for Education in Ada (trademark) and Software Engineering (CREASE). Version 3.0 [AD-A156687] N86-10790
VIEWING
Fall velocity indicator/viewer [AD-D011789] N86-10482
VINYL POLYMERS
Electrically conducting polymers N86-10333
VISCOELASTICITY
Bounding solutions of geometrically nonlinear viscoelastic problems [NASA-CR-176219] N86-10860
VISCOPLASTICITY
Advanced development of BEM for two and three dimensional nonlinear analysis N86-10855
VISCOSITY
Precise viscosity measurements very close to critical points [NASA ORDER C-86129D] N86-10120
A study of blood flow and of aggregation of blood cells under conditions of zero gravity: Its relevance to the occlusive diseases and cancer N86-10137
Work-hardening and effective viscosity in solid beryllium [DE85-013978] N86-10323
Recirculation within a glass mixture subjected to external and resistive heating [DE85-010068] N86-10348
On the method of characteristics and its application to the calculations of annular nozzle flowfields N86-10454
Physical acoustics: Investigation of chemical kinetic and thermodynamic properties of fluids N86-10911
Acoustic cavitation and bubble dynamics [AD-A156888] N86-10918
VISCOUS DAMPING
Inelastic analysis of frame structures including member and joint shears N86-10573
VISCOUS FLOW
A study of the aerodynamic performance of Weis-Fogh wings N86-10012
Numerical procedure for three-dimensional hypersonic viscous flow over aerobrake configuration [NASA-TM-58269] N86-10018
Precise viscosity measurements very close to critical points [NASA ORDER C-86129D] N86-10120
On the method of characteristics and its application to the calculations of annular nozzle flowfields N86-10454
VISION
Vision test chart and method using Gaussians [AD-D011756] N86-10778
VISUAL ACUITY
Mild hypoxia and visual performance with night vision goggles [AD-A156969] N86-10787
VISUAL DISCRIMINATION
Speed of work and error rate: Analyses of individual differences in a choice reaction series with a cognitive component [DFVLR-FB-85-21] N86-10781
VISUAL PERCEPTION
Determination of symmetry and phase in human visual response functions: Theory and experiments N86-10769
The synthesis and analysis of color images [NASA-TM-86844] N86-10777
Mild hypoxia and visual performance with night vision goggles [AD-A156969] N86-10787
Test of a multilevel computational theory of stereoscopic visual image processing [AD-A157011] N86-10870
Measurement of visual contrast sensitivity [AD-D011776] N86-10973
VISUAL STIMULI
Variability analysis of visually induced responses in the midst of noise [B8564052] N86-10774
VITAMINS
Effect of various doses of some vitamins on non-specific mechanisms of adaptation of man N86-10750
VLASOV EQUATIONS
Local conservation laws for the Maxwell-Vlasov and collisionless kinetic guiding center theories [DE85-013122] N86-11063
VOIDS
Binder-filler interaction in energetic polymers [AD-A156752] N86-10345
VOLATILITY
Volatile organic compounds in indoor air: A survey of various structures [PB85-198356] N86-10687
Emissions of NOx, SOx and VOC from Antropogenic sources [PB85-193530] N86-10688
Evaluation of Passive Sampling Devices (PSDs) [PB85-196418] N86-10689
VOLTAGE CONVERTERS (AC TO AC)
Investigation of the uncertainties of the NBS (National Bureau of Standards) thermal voltage and current converters [PB85-200178] N86-10453
VOLTAGE CONVERTERS (DC TO DC)
Investigation of the uncertainties of the NBS (National Bureau of Standards) thermal voltage and current converters [PB85-200178] N86-10453
VOLUME
Captive volume device as a safe life monitor [AD-D011802] N86-10525
VOLUMETRIC ANALYSIS
Measurement of the density of base fluids at pressures 0.422 to 2.20 GPa [NASA-TM-87114] N86-10551
VORTICES
Large eddy interactions in a turbulent channel flow [NASA-TM-86757] N86-10464
VORTICITY
Analysis of combined natural and forced convection around cylinders and spheres N86-10456
VOYAGER PROJECT
Planning for VLA/DSN arrayed support to the Voyager at Neptune N86-10395
A VLA experiment: Planning for Voyager at Neptune N86-10396

W

WAFERS
Contact effects in light activated GaAs switches [AD-A156957] N86-10434
Optical detection of photoacoustic pulses in thin silicon wafers [AD-A156705] N86-10977
Transient velocity assessment in gallium arsenide, and of other GaAs characteristics related to device functions [AD-A156983] N86-11050
WAKEFULNESS
Intradiurnial organization of wakefulness-sleep sequence and energy metabolism in rats exposed to low ambient temperature N86-10764
WALKING MACHINES
Digital control of the hydraulic actuators of an adaptive suspension vehicle N86-10548
WALL FLOW
Mean turbulence structure in strongly heating air flows N86-10455
WALL PRESSURE
Conducting wall and pressure profile effect on MHD stabilization of axisymmetric mirror [DE85-013647] N86-11020
WARFARE
The quest for a helicopter suitable for combat rescue, 1967 - 1983 [AD-A156842] N86-10040
WASTE DISPOSAL
Hot cell facility design for large fusion devices [DE85-012893] N86-11037

WASTE WATER
Development of the Multi-Attribute Hazard Assessment System (MAHAS) and its application to energy-related waste streams
[DE85-010278] N86-10676
Membrane research in energy and solvent recovery from industrial effluent streams
[DE85-014583] N86-10682
WATER
Passivation of steel with aqueous amine solutions
[AD-D011749] N86-10314
KRAK: A computer program for two-phase, two-component porous flow and fracture propagation, revision
[DE85-014264] N86-10469
Spontaneous Raman spectroscopy of shocked H2O
[DE85-014557] N86-10470
Application of the dutch method for estimating storm-induced dune erosion
[AD-A156717] N86-10728
WATER FLOW
Modeling groundwater flow into lakes N86-10598
The Rhine-Meuse estuary hydraulic scale model. Experiences with computer configuration and software
[PUBL-335] N86-10637
SUTRA (Saturated-unsaturated transport). A finite-element simulation model for saturated-unsaturated, Fluid-Density-Dependent ground-water flow with energy transport or chemically-reactive single-species solute transport
[AD-A156779] N86-10830
WATER POLLUTION
Sediment characterization. Task 2: Instream contaminant study. Volume 2: Appendices
[DE85-013503] N86-10680
Sediment characterization. Task 2: Instream contaminant study, volume 1
[DE85-013502] N86-10683
WATER RESOURCES
Maximum water reserves in the snow cover in the European territory of the USSR according to data for 1892-1960
[NASA-TM-77901] N86-10611
WATER RUNOFF
Maximum water reserves in the snow cover in the European territory of the USSR according to data for 1892-1960
[NASA-TM-77901] N86-10611
WATER TABLES
Evaluating the ground-water resources of the high plains of Texas, Volume 4
[PB85-191625] N86-10641
WATER TEMPERATURE
LANDSAT TM image data quality analysis for energy-related applications
[E85-10109] N86-10597
WATER VAPOR
Mobile VLBI and GPS measurement of vertical crustal motion N86-10401
Chemical/hydrogen energy systems
[DE85-012742] N86-10667
WATER WAVES
Formation of waves by ground motion
[PM/84/09] N86-10706
WATERSHEDS
Erosion control and watershed management by Spacelab photography N86-10493
WAVE ATTENUATION
Numerical methods for analyzing electromagnetic scattering
[NASA-CR-176141] N86-10377
WAVE DISPERSION
Phase-coded pulse expander-compressor
[AD-D011812] N86-10375
WAVE EQUATIONS
Recent advances in the analysis of exhaust mufflers N86-10587
WAVE FRONTS
A mesh moving technique for time dependent partial differential equations in two space dimensions
[AD-A156663] N86-10866
WAVE FUNCTIONS
Experimental X-ray scattering cross sections for H2 and rare atomic gases
[DE85-011572] N86-10936
Relativistic wavefunction at the origin and the pion decay constant
[DE85-012392] N86-11062
WAVE INTERACTION
Large eddy interactions in a turbulent channel flow
[NASA-TM-86757] N86-10464
WAVE PROPAGATION
Nonlinear propagation of elastoplastic waves in Ke penetrators (excerpts)
[DE85-011450] N86-10318
An experimental TE sub 12 - TE sub 11 circular waveguide mode converter N86-10387
Propagation and radiation characteristics of a multimode corrugated waveguide feedhorn N86-10388
A simplified method of estimation of the specular components of radar cross section for some re-entrant conductors
[AD-A156573] N86-10403
Formation of waves by ground motion
[PM/84/09] N86-10706
WAVE REFLECTION
Radome analysis and design capabilities of the RF and Microwave Technology Branch
[AD-A156662] N86-10404
WAVE SCATTERING
Renormalization of an inverse scattering theory for inhomogeneous dielectrics
[AD-A156636] N86-11049
WAVEFORMS
Signal analysis of gas tungsten arc welds N86-10078
Periodic binary sequences with very good autocorrelation properties N86-10397
WAVEGUIDE FILTERS
Direct-coupled cavity filters with irises of arbitrary thickness
[DFVLR-FB-85-14] N86-10412
WAVEGUIDES
Numerical methods for analyzing electromagnetic scattering
[NASA-CR-176141] N86-10377
An experimental TE sub 12 - TE sub 11 circular waveguide mode converter N86-10387
Propagation and radiation characteristics of a multimode corrugated waveguide feedhorn N86-10388
High-power rf controls for the NBS-Los Alamos racetrack microtron
[DE85-012658] N86-10993
Electron wind in strong wave guide fields
[DE85-013062] N86-11004
WEAR
Tribological properties of structural ceramics
[NASA-TM-87105] N86-10341
WEAR INHIBITORS
Steady state frictional behavior of thin film coatings N86-10335
WEATHER
ELCAP instrumentation
[DE85-013042] N86-10527
WEATHER FORECASTING
Monthly and Seasonal Weather Outlook for mid-April to mid-May 1985, Volume 39, Number 8
[PB85-195345] N86-10724
WEATHERING
Altitudinal distribution of granitic landforms in the south central Sierra Nevada, California N86-10695
WEDGE FLOW
A numerical solution of the shock-turbulent interaction over a compression corner for supersonic flow N86-10003
WEIGHT (MASS)
Operating characteristics of the multiple critical Venturi System and secondary calibration nozzles used for weight-flow measurements in the Langley 16-foot transonic tunnel
[NASA-TM-86405] N86-10016
WEIGHTING FUNCTIONS
Identification of a plant's weighting sequence --- self-tuning control
[OUEL-1534/84] N86-10854
Two algorithms for weighted matroid intersection
[AD-A156525] N86-10861
WEIGHTLESSNESS
Microgravity Science and Applications Program tasks
[NASA-TM-87568] N86-10053
Solutal convection and its effects on crystal growth and segregation in binary and pseudo-binary system with large liquidus-solidus separation N86-10056
Effect of undercooling and modified microstructure on the physical properties of material synthesized in the drop tube and drop tower N86-10075
The influence of containerless undercooling and rapid solid-state quenching on the superconductive and magnetic properties of some clustering alloy systems N86-10076
Influence of melt convection on solid-liquid interface under terrestrial and reduced gravity environments N86-10083
Orbital processing of aligned magnetic composites N86-10089
Metallic foams N86-10095
Growth of larger single crystals N86-10186
Oscillations of a viscoelastic liquid drop in zero-gravity N86-10240
WEIGHTLESSNESS SIMULATION
The first German Spacelab mission D1 reports --- Spacelab payloads
[PR-2] N86-10188
The first German Spacelab mission D1 reports --- Spacelab payloads
[PR-3] N86-10189
Mathematical simulation of disturbing forces and material science processes under low gravity N86-10236
Nucleate pool boiling in subcooled liquid under microgravity: Results of TEXUS experimental investigations N86-10250
A preliminary report on floating zone experiments with germanium crystals in a sounding rocket N86-10256
WELDED JOINTS
Ultrasonic inspection of weldments in large size spiral box for hydroelectric plant
[AS-701/85] N86-10562
WELDING
Weld metal hot-cracking of hastelloy alloys C-22 and C-276: A study by analytical electron microscopy
[DE85-009437] N86-10324
WELDING MACHINES
Measurement of workpiece temperature during welding for welding robot control N86-10534
WELLS
Geothermal lost circulation zone mapping tool
[DE85-008696] N86-10531
Evaluating the ground-water resources of the high plains of Texas, Volume 4
[PB85-191625] N86-10641
WEST GERMANY
The air traffic demand in passenger travel of the Federal Republic of Germany 1990 - 2000. Update of the DFVLR air traffic forecast
[DFVLR-MITT-85-06] N86-10031
Satellite use for men --- West German space program N86-10180
Airborne measurements of the border-crossing air pollution in the area between Weiden and Hof/Bavaria
[DFVLR-FB-85-25] N86-10685
Space research expenses of the Federal Ministry of Research and Technology (BMFT) in the period 1983-1985 N86-11070
WETLANDS
The effects of merging TM and A/C radar on wetland classification N86-10621
Approaches to cumulative impact assessment
[DE85-013891] N86-10635
WETTING
Direct observation of critical point wetting in microgravity N86-10116
WIGGLER MAGNETS
Thermal and structural analysis of ring components by the finite element method
[DE85-013305] N86-11021
WIND (METEOROLOGY)
Surface winds at NWC (Naval Weapons Center): 1964 - 1982
[AD-A156660] N86-10712
Estimating wind speed as a function of height above ground: An analysis of data obtained at the Southwest Residential Experiment Station, Las Cruces, New Mexico
[DE85-013262] N86-10716
Field comparison of in situ meteorological sensors
[PB85-196988] N86-10723
Evaluation of surface exchange coefficients from mildex ocean/atmosphere mixed layer data
[AD-A156765] N86-10729
WIND DIRECTION
Overview of wind turbine siting research: Prospecting to micrositing
[DE85-013496] N86-10666
Surface winds at NWC (Naval Weapons Center): 1964 - 1982
[AD-A156660] N86-10712
Field comparison of in situ meteorological sensors
[PB85-196988] N86-10723
WIND EFFECTS
contemporary Aeolian processes on Mars: Local dust storms N86-11136
WIND MEASUREMENT
Overview of wind turbine siting research: Prospecting to micrositing
[DE85-013496] N86-10666
Contribution of wind energy to the energy balance of a combined solar and wind energy system. Part 1: System description, data acquisition and system performance
[BMFT-FB-T-85-051-VOL-1] N86-10670
WIND SHEAR
Rotary-wing operations in a microburst environment
[AD-A156695] N86-10713
WIND TUNNEL APPARATUS
Activities report of the German-Dutch wind tunnel N86-10029

The rubber tube test section of the DFVLR in Goettingen, West Germany — wind tunnel walls
[DFVLR-FB-85-18] N86-10051
Activities report of the German-Dutch wind tunnel N86-10052

WIND TUNNEL MODELS
Simulation of the atmospheric boundary layer in the large wind tunnel of the TNO Institute for Building materials and Constructions (IBBC). Part 1: Theory
[BI-76-39/08.7.23100-PT-1] N86-10703

WIND TUNNEL TESTS
Second order approximation method for transonic flows over swept wings N86-10002
Evaluation of an aerodynamic-load prediction method on a STOL fighter configuration
[NASA-TM-86782] N86-10015
Operating characteristics of the multiple critical Venturi System and secondary calibration nozzles used for weight-flow measurements in the Langley 16-foot transonic tunnel
[NASA-TM-86405] N86-10016
Activities report of the German-Dutch wind tunnel N86-10029
Investigations to improve the slotted-wall test section of the F+W transonic wind tunnel
[F+W-FO-1752] N86-10050
Activities report of the German-Dutch wind tunnel N86-10052
Simulation of the atmospheric boundary layer in the large wind tunnel of the TNO Institute for Building Materials and Construction (IBBC). Part 2: Experiments
[BI-76-39/08.7.23100-PT-2] N86-10704

WIND TUNNEL WALLS
Investigations to improve the slotted-wall test section of the F+W transonic wind tunnel
[F+W-FO-1752] N86-10050
The rubber tube test section of the DFVLR in Goettingen, West Germany — wind tunnel walls
[DFVLR-FB-85-18] N86-10051

WIND TURBINES
Improved stud configurations for attaching laminated wood wind turbine blades
[NASA-TM-87109] N86-10582

WIND VANES
Field comparison of in situ meteorological sensors
[PB85-196988] N86-10723

WIND VELOCITY
Surface winds at NWC (Naval Weapons Center): 1964 - 1982
[AD-A156660] N86-10712
Estimating wind speed as a function of height above ground: An analysis of data obtained at the Southwest Residential Experiment Station, Las Cruces, New Mexico
[DE85-013262] N86-10716
Field comparison of in situ meteorological sensors
[PB85-196988] N86-10723

WIND VELOCITY MEASUREMENT
Overview of wind turbine siting research: Prospecting to micrositing
[DE85-013496] N86-10666
The boundary condition in a numerical model of atmospheric flows over fixed interfaces
[GKSS-85-E-10] N86-10722

WINDMILLS (WINDPOWERED MACHINES)
Wind energy in agriculture, a promise
[SS-45] N86-10672
Wind energy, a feasibility investigation for wind mills in agriculture
[SS-45A] N86-10673

WINDOWS (APERTURES)
Integrating sphere measurements of directional-hemispherical transmittance of window systems
[DE85-013926] N86-10978
Beam line windows at LAMPF
[DE85-012723] N86-10985

WINDPOWER UTILIZATION
Overview of wind turbine siting research: Prospecting to micrositing
[DE85-013496] N86-10666
Contribution of wind energy to the energy balance of a combined solar and wind energy system. Part 1: System description, data acquisition and system performance
[BMFT-FB-T-85-051-VOL-1] N86-10670
Contribution of wind energy to the energy balance of a combined solar and wind energy system. Part 2: Computer-assisted investigations
[BMFT-FB-T-85-052-VOL-2] N86-10671
Wind energy in agriculture, a promise
[SS-45] N86-10672

WINDPOWERED GENERATORS
Wind energy, a feasibility investigation for wind mills in agriculture
[SS-45A] N86-10673

WING PANELS
Optimum design of an aircraft wing structure with multiple constraints by the direct-vision criteria method N86-10004

WING PROFILES
A study of the aerodynamic performance of Weis-Fogh wings N86-10012
Aerodynamics of hyperlift systems
[SNIAS-443.501/85] N86-10023

WINTER
Smoke inputs to climate models: Optical properties and height distribution for nuclear winter studies
[DE85-011363] N86-10717
Microphysical/mesoscale aspects of nuclear winter and new directions in assessments
[DE85-013479] N86-10718

WIRE
Reduction of noble metal stock and noble metal loss during wire production with the Conform extrusion process
[BMFT-FB-T-85-049] N86-10560

WOOD
Self-heating to ignition measurements and computation of critical size for solar energy collector materials
[DE85-011449] N86-10302
Improved stud configurations for attaching laminated wood wind turbine blades
[NASA-TM-87109] N86-10582

WORK CAPACITY
Adaptation of man to extreme conditions of Antarctica N86-10751

WORKING FLUIDS
Simplified analysis of Stirling engines and heat pumps
[DE85-005366] N86-10647
Analyses of advanced residential absorption heat pump cycles
[DE85-005244] N86-10664

WORKLOADS (PSYCHOPHYSIOLOGY)
Capacity for work and hemodynamics in males residing at middle and high latitudes N86-10747
Effect of inclusion of supplementary ascorbic acid in daily diet on degree of vitamin saturation of body and thermoresistance of erythrocytes while working in arid zone N86-10749
Effect of various doses of some vitamins on non-specific mechanisms of adaptation of man N86-10750
The effects of age, sleep deprivation, and altitude on complex performance
[AD-A156987] N86-10771
Report on the research activities on whole-body vibrations. Human strain due to mechanical vibrations
[ISBN-3-88383-107-7] N86-10773

WYOMING
Report of the Workshop on Geologic Applications of Remote Sensing to the Study of Sedimentary Basins
[E86-10002] N86-10599
Paleogene vertebrate paleontology, geology and remote sensing in the Wind River Basin N86-10609

X

X RAY ABSORPTION
NBSGSC: A FORTRAN program for quantitative X-ray fluorescence analysis
[PB85-206068] N86-10847

X RAY ANALYSIS
La Recherche Aerospatiale, bimonthly bulletin, no. 1984-5, September-October 1985
[ESA-TT-899] N86-10363

X RAY ASTRONOMY
X-ray satellite
[NASA-TM-77923] N86-10273
Theoretical analysis of Wolter/LSM X-ray telescope systems
[NASA-CR-176244] N86-11095

X RAY DENSITY MEASUREMENT
Extra-galactic X-ray sources and the diffuse X-ray background N86-11144

X RAY DIFFRACTION
A simple method of obtaining concentration depth-profiles from X-ray diffraction
[NASA-CR-176262] N86-10310

X RAY FLUORESCENCE
NBSGSC: A FORTRAN program for quantitative X-ray fluorescence analysis
[PB85-206068] N86-10847

X RAY IRRADIATION
Preliminary investigation of changes in X-ray multilayer optics subjected to high radiation flux
[DE85-014074] N86-10944

X RAY SCATTERING
Experimental X-ray scattering cross sections for H2 and rare atomic gases
[DE85-011572] N86-10936

X RAY SOURCES
Device for cryogenically fabricating source material for plasma X-ray lasers
[AD-D011814] N86-10537

X RAY SPECTRA
NBSGSC: A FORTRAN program for quantitative X-ray fluorescence analysis
[PB85-206068] N86-10847

X RAY TELESCOPES
Theoretical analysis of Wolter/LSM X-ray telescope systems
[NASA-CR-176244] N86-11095

X RAYS
Dynamics of imploding neon gas puff plasmas. 1
[AD-A156916] N86-10983
Photoactivation of PBFA-2
[DE85-013439] N86-11019

XENON
Light scattering tests of fundamental theories of transport properties in the critical region N86-10113
Thermodynamic constraints on ion beam mixing of metals on insulators
[DE85-013628] N86-10448
Determination of optical properties by third-harmonic generation in noble gases in unfocused laser beams N86-10535

Y

YAG LASERS
Contact effects in light activated GaAs switches
[AD-A156957] N86-10434

YEAST
Romanian plant produces protein concentrate from paraffin-nourished yeasts N86-10741

YTTERBIUM
Extraction of lanthanide ions by 2-methyl-8-quinolinol
[DE85-014277] N86-10303

YTTRIUM
Study of the reactive-element effect in oxidation of Fe-Cr alloys using transverse section analytical electron microscopy N86-10087
Characterization of mechanical damage mechanisms in ceramic composite materials
[AD-A156574] N86-10590

Z

ZETA PINCH
Equilibrium of the kink source experiment
[DE85-012764] N86-11029

ZINC
Diffusion in immiscible melts N86-10096
Environmental degradation of materials: Surface chemistry related to stress corrosion cracking N86-10099
Laser Raman spectroscopy study of the zinc and bromide ion complex equilibrium in zinc/bromine battery electrolytes
[DE85-011820] N86-10301
W-shaped diffused stripe GaAs/AlGaAs laser
[AD-D011818] N86-10538

ZINC ALLOYS
Particle coarsening in immiscible zinc-lead alloys under microgravity — Spacelab N86-10210

ZINC COMPOUNDS
Directional solidification of an aluminum-zinc vapor emulsion in microgravity — Spacelab N86-10218
Laser Raman spectroscopy study of the zinc and bromide ion complex equilibrium in zinc/bromine battery electrolytes
[DE85-011820] N86-10301

ZINC OXIDES
Catalytic activity of shock modified ZnO for CO oxidation and methanol synthesis
[DE85-014704] N86-10300

ZINC TELLURIDES
Ion beam sputter deposited zinc telluride films
[NASA-TM-87119] N86-11048

ZIRCONIUM TITANATES
The preparation and testing of titanium and zirconium coupling agents
[SJ70] N86-10576

ZONE MELTING
Float zone experiments in space N86-10067

Typical Personal Author Index Listing

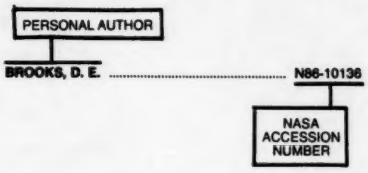

Listings in this index are arranged alphabetically by personal author. The NASA accession number denotes the number by which the citation is identified.

A

ABOLFADL, M. A. N86-10459
ABRAMOVICH, H. N86-10583
N86-10584
ACHENBACH, J. D. N86-10348
N86-10593
ACKERMANN, F. N86-10486
ACOSTA, R. N86-10381
ADAMS, J. N86-10623
ADAMSKA, H. N86-11042
ADHIKARY, K. R. N86-10505
AERTS, N. N86-11074
AGARKOV, F. T. N86-10753
AGRAWALA, M. N86-10897
AHLBORN, H. N86-10209
AHMAD, I. N86-10961
AHRENS, L. N86-10931
AKSENOV, V. V. N86-10746
ALBERTZ, J. N86-10508
ALBRECHT, J. N86-10308
ALDRICH, B. R. N86-10166
ALESSI, J. G. N86-10935
ALFORQUE, R. N86-11021
ALI, A. W. N86-10924
ALLAN, J. A. N86-10495
ALLARD, R. N86-11072
ALLEN, G. N86-10940
ALLISON, L. J. N86-10677
ALPATOV, B. A. N86-10818
ALSEM, W. H. M. N86-10212
ALTENKIRCH, R. A. N86-10159
ANDERSON, B. J. N86-10103
ANDERSON, C. M. N86-10829
ANDERSON, E. C. N86-10694
ANDERSON, K. W. N86-10030
N86-10788
ANDRESEN, U. N86-10183
ANDREWS, G. W. N86-10410
ANITLLON, A. N86-11018
AOKI, H. N86-11052
APPLETON, B. R. N86-10448
ARAKAWA, E. T. N86-10949
ARAM, S. N86-11116
ARKHANGELSKIY, D. Y. N86-10739
ARNBAK, J. C. N86-10270
ARNEY, D. C. N86-10866
ARP, V. D. N86-10114
ARVIDSON, R. E. N86-10605
ASSARD, G. L. N86-10483
ATCHLEY, A. A. N86-10918
ATHALE, R. N86-10975
ATHERTON, P. D. N86-11106
N86-11119
ATTENBERGER, S. E. N86-10840
ATZMON, M. N86-10327
AUBRON, R. N86-10217
AUDU, M. L. N86-10853
AUTHIER, A. N86-10230
AUTHIER, B. N86-11102
N86-11108
N86-11111
AXLER, K. M. N86-10660
AYRES, A. N86-11065
AZQUI, N. N86-10961

B

BABUSKA, I. N86-10862
N86-10864
N86-10869
BACHMANN, K. N86-10031
N86-10054
BACKES, U. N86-10450
BADDOUR, M. F. N86-10380
BADLER, N. I. N86-10770
N86-10785
N86-10820
N86-10821
N86-10896
N86-10897
BAEHR, H. P. N86-10489
BAGLIN, J. E. F. N86-10448
BAILEY, G. B. N86-10600
BAIRD, J. N86-10104
BAIRD, J. K. N86-10248
BAKER, M. S. N86-10656
BAKER, R. W. N86-10682
BALACHANDRAN, V. N86-10573
BALANDRIN, M. F. N86-10342
BALKO, B. N86-11071
BALUDA, M. V. N86-10745
BAMBADE, P. N86-10965
BAMBERGER, S. B. N86-10246
N86-10247
BANE, K. L. N86-10964
BANGERT, L. S. N86-10016
BARBIER, F. N86-10215
BARISAS, S. G. N86-10676
BARKER, D. S. N86-10852
BARKER, R. E., JR. N86-11059
N86-11060
BARLOW, G. H. N86-10134
BARMATZ, M. N86-10167
BARNARD, J. C. N86-10597
BARNES, C. W. N86-10988
N86-10998
N86-11003
N86-11028
BARNES, H. M. N86-10710
BARNETT, C. F. N86-10926
BARNETT, R. J. N86-10014
BARR, B. N86-10821
BARRETT, R. J. N86-11037
BARRETT, T. W. N86-10344
BARTA, C. N86-10263
BARTHOLOMEW, R. J. N86-10835
BATTEN, A. L. N86-10275
BATZER, T. H. N86-11030
BAUDOIN, A. N86-10497
BAUER, H. F. N86-10240
BAUER, M. E. N86-10610
BAUGH, R. N. N86-10650
BAUMAN, T. J. N86-10531
BAYUZICK, R. J. N86-10073
BAZARNYY, Y. M. N86-10813
BEALE, J. N86-10821
BEHRINGER, R. P. N86-10119
BENCUYA, I. N86-11043
BENDER, P. L. N86-11123
BENNETT, I. F. N86-10195
BENNETT, R. H. N86-10557
BENOIT, J. N86-10217
BENZ, K. W. N86-10224
BERG, B. N86-10120
BERGGRUND, U. N86-10364
BERGSTROEM, S. I. N86-10551
BERLAD, A. L. N86-10160
BERMAN, M. N86-10474
BERNHARD, R. J. N86-10912
BERRIER, B. L. N86-10016
BERT, J. N86-10253
BERTHEL, R. O. N86-10482
BERTOLA, E. N86-11098
BEYERLE, A. N86-10528
BHASAVANICH, D. N86-10441
BIDDLE, R. S. N86-10993
BIEHL, L. L. N86-10610
BIER, M. N86-10135
BIERIG N86-10436
BIGELOW, C. A. N86-10287
N86-10581
BIGLIERI, E. N86-10407
BIJLEVELD, J. N86-10964
BILLIA, B. N86-10262
BILSKIE, J. R. N86-10950
BIRKEMEIER, W. A. N86-10728
BIRNBAUM N86-10424
BISCH, C. N86-10204
BLAAUW, G. J. N86-10776
BLAKE, P. L. N86-10601
N86-10604
BLAKE, R. L. N86-10944
BLAKEMORE, J. S. N86-11050
BLANC, T. V. N86-10714
BLAYLOCK, B. G. N86-10679
BLAZIT, A. N86-11122
BLODGETT, J. A. N86-10975
BLOOMFIELD, D. N86-10444
BOATNER, L. A. N86-10448
BOBB, L. C. N86-10976
BOBKOVA, N. N. N86-10740
BODDAERT, M. N86-10217
BODECHTEL, J. N86-10521
BODINE, F. R. N86-10481
BODNER, S. R. N86-10589
BOER, L. C. N86-10782
BOHMAN, L. N86-10980
BOICOURT, G. P. N86-10837
N86-10992
BOIT, J. L. N86-11109
BOLLEN, R. N86-10844
BONDARENKO, T. I. N86-10762
BONNELL, D. W. N86-10074
BONNET, C. N86-10023
BORGARDT N86-10525
BORQUE, R. F. N86-10468
BORTNOVSKIY, V. N. N86-10750
BOTTA, E. F. F. N86-10881
BOTTEGA, W. J. N86-10284
BOUCHIER, F. A. N86-11011
BOUDREAULT, R. N86-10239
BOUSSOUF, M. D. N86-10547
BOUTEMY, O. N86-10217
BOUTENKO, O. N86-10306
BOUWMANS, J. M. M. N86-10638
BOWDLE, D. A. N86-10103
BOWLES, K. J. N86-10288
BOYER, W. B. N86-11011
BRACCO, F. V. N86-10559
BRACEY, J. T. N86-10953
BRACKENBUSH, L. W. N86-10299
BRADBURY, K. A. N86-10366
BRAEDT, M. N86-10216
BRAETSCH, V. N86-10216
BRAND, U. N86-10449
BREAULT, R. D. N86-10651
N86-10652
BREITHAUPT, D. N86-10323
BREWE, D. E. N86-10463
BREZINSKI, D. K. N86-10693
BREZOVEC, C. N86-10861
BRIGGS, T. A. N86-10651
N86-10652
BROCKWELL, J. L. N86-10110
BROOKS, D. E. N86-10136
N86-10246
N86-10247
BROOMAN, E. W. N86-10326
BROWMAN, A. A. N86-10986
BROWN, D. N86-10950
BROWN, D. W. N86-10395
BROWN, J. M. N86-10630
BROWN, K. L. N86-10994
BROWN, R. A. N86-10055
N86-10056
N86-10105
BROWN, R. D. N86-10985

BROWN, S. R. N86-10698
BROWN, W. E. N86-10616
BRUCKENTHAL, E. N86-10601
BRUNING, T. H. N86-10851
BRUST, F. W., JR. N86-10574
BRYANT, G. G. N86-10315
BRYANT, J. N86-10554
BRZEZINSKI, J. N86-10877
N86-10903
BUCH, Y. I. N86-10765
BUCHENAUER, C. J. N86-10998
BUCHROITHNER, M. F. N86-10503
BUCK, B. M. N86-10727
BUCKLEY, D. H. N86-10341
N86-10552
BULAKH, M. A. N86-10817
BUNCE, G. M. N86-10989
BUNNER, A. N. N86-11107
BURBANK, D. N86-10602
BURGDORF, K. N86-11088
BURKE, B. F. N86-11126
BURTON, L. C. N86-10431
BUSSELL, G. T. N86-11037
BUTLER, G. W. N86-10963
BUTTRAM, M. T. N86-10441
BUXBAUM, O. N86-10044
BYRD, L. W. N86-10361

C

CABE, S. N86-10690
CADA, G. F. N86-10678
CAHN, J. W. N86-10121
CAI, J. N86-10011
CALDECOTT, S. J. N86-10523
CALL, W. R. N86-11030
CALOGERO, F. N86-10859
CALVERT, P. D. N86-10576
CAMBIAGHI, D. N86-10252
CAMBON, G. N86-10217
CAMEL, D. N86-10262
CAMPBELL, G. W. N86-10938
CAMPBELL, K. W. N86-11059
CAMPISI, I. E. N86-11051
CAPBERN, P. N86-10023
CAPITAINE, G. N86-10050
CARBONELL, J. G. N86-10899
CARLBERG, T. N86-10256
CARLETON, N. P. N86-11104
CARLSON, R. L. N86-10588
CARLSSON, H. N86-10874
CARNEY, K. S. N86-10579
CASADESUS, P. N86-10307
CASSENTI, B. N. N86-10589
CASTETS, B. N86-10217
CASTOR, V. L. N86-10829
CATALDO, D. A. N86-10684
CATHEY, W. N. N86-10644
CATTROLL, S. W. N86-10786
CAVALLO, J. M. N86-11044
CEZAIRLIYAN, A. N86-10106
CHABILDAS, L. C. N86-11054
CHAI, A. T. N86-10107
N86-10117
N86-10125
CHAN, K. S. N86-10589
CHAN, T. F. N86-10887
CHANG, I. C. N86-10915
CHANG, J. N86-10439
N86-10540
N86-10940
CHANG, J. P. N86-10569
CHANG, L. W. N86-10545
CHAO, S. N86-11095
CHEN, C. P. N86-10462
CHEN, D. T. N86-10406
CHEN, F. C. N86-10661
CHEN, H. H. N86-10012
CHEN, I. W. N86-10147
CHEN, M. H. N86-10956
CHEN, N. C. J. N86-10647
CHEN, X. N86-10358
CHEN, Y. S. N86-10460
CHENG, K. T. N86-10956
CHIAN, C. T. N86-10386
N86-10389
CHING, L. N86-10400
CHIU, S. Y. N86-10676
CHO, Y. N86-10941
CHOINSKI, T. C. N86-10863
CHOO, Y. K. N86-10017
CHOU, T. S. N86-10948
CHOW, L. S. H. N86-11036
CHOWDHURY, P. N86-10961
CHRISTIANSEN, W. H. N86-10540
CHU, C. W. N86-10075
CHUANG, S. L. N86-10377
N86-10484
CHUN, C. H. N86-10241
CHUZEVILLE, G. N86-10253
CIESLAK, M. J. N86-10324
CIVINSKAS, K. C. N86-10017
CLARK, G. J. N86-10448
CLARK, R. W. N86-10983
CLARKE, D. W. N86-10854
CLAUS, J. N86-11026
CLAUSSEN, M. N86-10722
CLUNE, E. N86-10848
COHRT, H. N86-10353
COLE, R. N86-10155
COLEMAN, J. J. N86-10484
COLEMAN, R. B. N86-10910
COLES, D. N86-10108
COLIN, L. N86-11137
COLLINGS, E. W. N86-10076
COLLINS, W. E. N86-10771
COMBI, M. R. N86-11133
CONCUS, P. N86-10108
CONEIM, C. N86-10022
CONEL, J. E. N86-10603
N86-10604
N86-10606
CONGDON, J. V. N86-10651
N86-10652
CONNES, P. N86-11105
CONTI, R. N86-10438
COOPER, J. C. N86-10313
COPPLESTONE, R. W. N86-10919
CORDERMAN, R. R. N86-10649
CORIELL, S. R. N86-10077
CORNUEJOLS, G. N86-10861
CORTEZ, J. H. N86-10992
COSTES, N. N86-10175
COTTINGAME, W. B. N86-10992
COURANT, E. D. N86-11026
COUTANT, R. W. N86-10689
COX, J. D. N86-10539
CRABTREE, G. W. N86-11052
CRAWFORD, E. A. N86-10543
CREEDON, R. I. N86-10468
CRELLIN, E. B. N86-11110
CREMERS, P. N86-10894
CRIST, C. E. N86-10192
CROSBIE, E. A. N86-10934
CROUCH, R. K. N86-10057
CROW, B. N86-10400
CROWE, R. A. N86-10399
CROWLEY, F. A. N86-10269
CRUM, L. A. N86-10918
CUCCHISSI, J. J. N86-10385
CUNNINGHAM, J. C. N86-10437
CURRERI, P. A. N86-10246
CZANDERNA, A. W. N86-10645

D

DABKOWSKI, F. N86-10234
DAHLBERG, B. E. J. N86-10873
N86-10876
DALDER, E. N. C. N86-10908
DALGITY, G. G. N86-10522
DAMEN, A. N86-10879
N86-10880
DANBY, G. N86-11022
DAPKUS, D. N86-10538
DASS, N. D. H. N86-10882
N86-10883
DAUGHTRY, C. S. T. N86-10610
DAVIDSON, J. M. N86-10401
DAVIS, A. H. N86-10469
DAVIS, J. N86-10983
DAVIS, S. H. N86-10109
DAWSON, J. N86-10443
DAY, D. D. N86-10148
DEASON, V. A. N86-10530
DEB, S. K. N86-10662
DECARLO, J. L. N86-10094
DEGASPERIS, A. N86-10859
DEGOER, J. N86-10219
DEGRAAUW, T. N86-11102
DEGROEN, P. N86-10452
DEGUIRE, M. R. N86-10152
DELAHAYE, J. P. N86-11014
DELAHOY, A. E. N86-10668
DELITZSCH, V. N86-10237
DELL, G. F. N86-11023
DELOSME, J. M. N86-10795
DEMORE, W. B. N86-10707
DEMOULIN, P. D. N86-10655
DENARD, J. C. N86-10964
DENAVIT, J. N86-10471
DEPURY, P. N86-10493
DEREFELDT, G. N86-10364
DERITO, R. F. N86-10697
DERMER, C. D. N86-11141
DEROQUEFORT, T. A. N86-10878
DERRICK, M. N86-10942
DERUYTTERE, A. N86-10211
DEUPREE, R. G. N86-10469
DEVITO, B. N86-11022
DEWITT, A. N86-10991
DEWITT, K. J. N86-10110
DIAN, R. N86-10225
DIEM, W. N86-10560
DIETZ, K. R. N86-10498
DIJK, J. N86-10270
DIJKSTRA, J. B. N86-10888
N86-10889
N86-10890
N86-10891
DINTENFASS, L. N86-10137
DIVSALAR, D. N86-10390
DIXON, R. H. N86-10537
DIXON, T. H. N86-10618
DOBSON, M. C. N86-10628
DOGAN, A. U. N86-10691
DOLEV, D. N86-10898
DOLGANYUK, I. N. N86-10815
DONG, H. N86-10358
DONINA, Z. A. N86-10760
DONOVAN, N. N86-10615
DOORNBOS, R. N86-10888
N86-10889
DOREMUS, R. H. N86-10149
DOWNMAN, I. J. N86-10495
N86-10507
DOWNS, R. L. N86-10150
DOWO, J. F. N86-10598
DOYLE, F. J. N86-10494
DRESSLER, R. F. N86-10111
DRIEDONKS, A. G. M. N86-10711
DRIGERT, M. W. N86-10961
DRISCOLL, J. F. N86-10305
DROTNING, W. D. N86-10351
DRUMM, D. M. N86-10788
DRUMMOND, C. J. N86-10681
DUBOIS, M. V. N86-10719
DUFF, I. S. N86-10871
DUGAN, J. P. N86-10730
DUNN, S. A. N86-10168
N86-10169
DUPUIS, H. N86-10773
DUPUY, J. N86-10253
DURKIN, P. S. N86-10434
DUSTERBERRY, J. C. N86-10048
DUVAL, W. M. B. N86-11058
DWORAK, J. A. N86-10548
DYBDAL, R. B. N86-10373
DYBOY, V. A. N86-10811
N86-10812

E

EAGAR, T. W. N86-10078
EASTES, R. W. N86-10696
ECKELMANN, H. N86-10237
EDELMAN, R. B. N86-10161
EDEN, J. G. N86-10426
EGBERT, W. N86-10058
EGERT, C. M. N86-10330
EGGLESTON, J. M. N86-10543
EGGLESTONE, G. T. N86-10347
EISS, N. S., JR. N86-10033
EKHELIKAR, R. K. N86-10577
EKLUND, R. C. N86-10554
EL-AASSER, M. S. N86-10146
EL-KADDAH, N. N86-10133
ELACHI, C. N86-10629
ELIASON, J. R. N86-10597
ELLEMAN, D. D. N86-10170
ELLENBROEK, M. H. M. N86-10881
ELLIOTT, G. N86-10920
ELTON, R. C. N86-10537
ELWELL, D. N86-10059
EMBLING, L. V. N86-10553
EMLING, H. N86-10961
ENG, C. N86-10366
ENGEL, H. N86-10487
ENGHETA, N. N86-10629
ENGSTROEM, O. N86-10980
ENYA, S. N86-10243
ERAMUS, D. A. N86-10701
ERDOES, P. N86-10182
ESHLEMAN, R. E. N86-10586
ETCHEVERRY, R. D. N86-10373

ETHRIDGE, E. C. N86-10087
N86-10151
EVANS, C. R., II N86-11127
EVANS, D. C. N86-11005
EVANS, D. L. N86-10604
N86-10615
N86-10624
EVANS, R. A. N86-10793
EVANS, W. P. N86-10799
EVERITT, C. W. F. N86-10171
EVERT, R. W. N86-10712
EYER, A. N86-10227
EZELL, T. F. N86-11011

F

FACEMIRE, B. R. N86-10112
FACO, P. N86-11105
FADOUL, J. R. N86-10582
FAIRBANK, W. M. N86-10118
FALA, G. N86-10820
FALICOV, L. M. N86-10321
FALIN, B. W. N86-10393
FALLER, J. E. N86-11123
FANALE, F. P. N86-11137
FANELLI, N. A. N86-10394
FANNING, U. N86-10112
FARCY, A. N86-10878
FARLOW, G. C. N86-10448
FARR, T. G. N86-10620
FAUCHERRE, M. N86-11116
FAULKNER, J. N86-10383
FAVIER, J. J. N86-10079
N86-10219
N86-10262
N86-10266
FAY, J. F. N86-10013
FEHLERT, G. P. N86-10636
FEHLING, H. N86-10451
FEIGELSON, R. S. N86-10059
FELDMAN, G. J. N86-11035
FERGER, R. N86-10670
FERGUSON, G. L. N86-10191
FERKO, P. N86-10554
FERNANDEZ-PELLO, A. C. N86-10162
FERNANDEZ, J. C. N86-10988
N86-11003
FERRELL, W. R. N86-10535
FEZER, F. E. N86-10491
FIGUROVA, M. Y. N86-10766
FILTER, W. F. N86-10940
FINE, J. N86-10115
FINGER, M. N86-10359
FINGLETON, D. J. N86-10676
FINKELSTEIN, P. L. N86-10723
FINN, R. N86-10108
FINSTERWALDER, R. N86-10518
FISCHER, M. N86-10294
FISCHER, S. K. N86-10653
FISCHMEISTER, H. N86-10210
FISHER, A. L. N86-10432
FISHER, C. E. N86-10014
FISHWICK, P. N86-10897
FLAHERTY, J. E. N86-10866
FLEETER, S. N86-10019
FLEMING, E. A. N86-10522
FLEMINGS, M. C. N86-10080
N86-10133
FOGG, D. A. B. N86-10428
FOGLER, R. J. N86-10920
FOKIN, A. A. N86-10811
N86-10812
FOLLSTAEDT, D. M. N86-10331
FOOTE, H. P. N86-10597
FORD, J. L. N86-10537
FORD, J. P. N86-10625
FOREST, J. C. E. P. E. N86-10970
FORSTREUTER, W. N86-10513
FOSS, M. H. N86-10990
FOSTER, L. M. N86-10060
FOX, C. G. N86-10726
FOXWELL N86-10020
FRANCO, N. N86-10084
FRANK, G. H. N86-10414
FRANK, L. N86-11137
FRANKE, P. R. N86-10663
FRANKLIN, T. L. N86-10195
FRANTZ, C. N86-10307
FRANZKE, K. N86-10595
FRASER, J. S. N86-10929
FRAZIER, D. O. N86-10112
FREISER, H. N86-10303
FREKERS, D. N86-10961
FRIANT, C. L. N86-10337
FRIEDRICHS, C. C. N86-11002
FRIELER, K. N86-10214
FRIPP, A. L. N86-10057
FRISCHAT, G. H. N86-10216
N86-10254
FRITSCHEN, L. J. N86-10631
FRITZE, G. N86-10488
FROEHLY, C. N86-11105
FROHBERG, G. N86-10231
FROST, C. A. N86-10192
FROST, R. T. N86-10172
FROYEN, L. N86-10211
FU, D. N86-10008
FUERST, M. N86-10492
FUNG, A. N86-10438
FURSHCHIK, A. B. N86-10813
FURUHAMA, K. N86-10461

G

GAILLARD, A. W. K. N86-10782
GALAYDA, J. N86-10947
GALIBERT, G. N86-10499
GALIBOIS, A. N86-10306
GALSTER, G. N86-10229
GAMMON, R. W. N86-10113
GANGEL, D. J. N86-10408
GANGEL, J. N86-10820
GANGOPADHYAY, P. K. N86-10922
GANGULI, B. N86-11132
GARCIA, A., III N86-10312
GARDNER, C. N86-10931
GARDNER, E. C. N86-10401
GARINTHER, G. R. N86-10917
GARLAND, T. R. N86-10684
GARTEN, C. T., JR. N86-10679
GASKELL, P. S. N86-10366
GATHERS, G. R. N86-10317
GATOS, H. C. N86-10061
N86-10234
GAWORSKI, C. L. N86-10675
GAY, J. N86-11125
GAYDA, J. N86-10311
GAYNOR, J. E. N86-10723
GEAR, C. W. N86-10871
GELBWACHS, J. A. N86-10674
GELLES, S. H. N86-10081
N86-10264
GELTIG, R. L. N86-10651
GELTING, R. L. N86-10652
GEORGE, G. A. N86-10347
GEORGE, T. F. N86-10925
GEORGE, T. G. N86-10660
GERRISH, V. N86-10528
GEZARI, D. Y. N86-11103
GHERSINI, G. N86-10232
GIARRATANO, P. G. N86-10114
GICQUEL, J. P. N86-10217
GIERLOFF-EMDEN, H. G. N86-10510
GILBERT, E. S. N86-10772
GILBODY, H. B. N86-10926
GILES, C. L. N86-10975
GILES, M. K. N86-10972
GILLESSEN, F. N86-10259
N86-10260
GILLIAM, D. R. N86-10033
GILLMAN, G. B. N86-10430
GILSON, A. P. N86-10974
GINSBERG, J. H. N86-10466
N86-10467
GLICKSMAN, M. E. N86-10082
N86-10083
N86-10088
GLOVER, D. W. N86-10633
GLOVER, F. N86-10861
GODFREY, B. B. N86-10192
GODTHELP, H. N86-10775
GODTHELP, J. N86-10783
GOETERS, K. M. N86-10780
N86-10781
GOGLIA, G. N86-11064
GOKHALE, R. B. N86-10014
GOLDBERG, B. A. N86-11139
GOLDEN, D. M. N86-10707
GOLDSTEIN, R. M. N86-10622
GOLDSTONE, J. A. N86-10932
GOLIA, C. N86-10238
GOLLER, G. J. N86-10651
N86-10652
GOLOMBEK, M. P. N86-10618
GONFALONE, A. N86-10201
GONNDI, P. N86-10215
GOPALAN, A. K. S. N86-10516
GOREAU, P. N86-10618
GORMAN, J. G. N86-10441
GORNEY, D. J. N86-10708
GRADY, D. E. N86-11055
GRAFOVA, V. A. N86-10749
GRAHAM, J. N86-10084
GRAHAM, R. A. N86-10300
GRAHAM, W. B. N86-10470
GRANATO, A. V. N86-11056
GRANT, N. J. N86-10085
GRATHWOHL, G. N86-10352
GRATHWOLH, G. N86-10353
GRAVES, M. E. N86-10723
GRAY, E. R. N86-10929
GRAY, H. F. N86-10416
GRAY, R. P., JR. N86-10372
GREENAWAY, A. H. N86-11094
N86-11106
N86-11119
GREENE, R. F. N86-10416
GREENSPAN, H. P. N86-10062
GREGORY, D. C. N86-10926
GRIEMERT, R. N86-10475
GRIFFIN, F. P. N86-10647
GRIFFIN, P. M. N86-10926
GRIFFITH, W. A. N86-10650
GRIMES, P. G. N86-10301
GRINDELAND, R. N86-10140
GRISAFFE, S. J. N86-10173
GRISHAM, D. L. N86-10985
GRISNIK, S. P. N86-10279
GROSSBECK, M. I. N86-10329
GROSSO, J. S. N86-10944
GRUBER, G. J. N86-10916
GUI, W. N86-10862
N86-10864
N86-10869
GUIDOTT, R. A. N86-10644
GUINESS, E. A. N86-10605
GULAID, A. A. N86-10508
GULINO, D. A. N86-11048
GURTOVAYA, Y. Y. N86-10614
GUYENNE, T. D. N86-10200
N86-10485
GYORKE, D. F. N86-10681

H

HABEGGER, L. J. N86-10676
HAEFNER, H. N86-10515
HAGAFORS, R. N86-11072
HAGG, E. N86-11062
HAGGAG, F. M. N86-10320
HAHN, H. N86-11026
HAJDASINSKI, A. N86-10879
N86-10880
HALL, I. J. N86-10716
HALL, J. L. N86-11123
HALLER, E. E. N86-10442
HALM, K. N86-10504
HAMDAN, M. A. N86-10458
HAMMER, J. H. N86-10984
HAMMINGER, R. N86-10353
HAMPSON, R. F. N86-10707
HAMROCK, B. J. N86-10551
HAN, C. C. N86-10283
HARDEKOPF, R. A. N86-10950
N86-10996
HARDY, K. N86-11083
N86-11084
N86-11085
N86-11086
HARDY, S. C. N86-10115
HARRIS, J. M. N86-10138
N86-10139
N86-10246
N86-10247
HARSHA, P. T. N86-10161
HARTNETT, E. B. N86-10269
HARTWELL, J. K. N86-10954
HARVEY, B. N86-11007
HASELMAN, I. C., JR. N86-10717
HASS, K. C. N86-11045
HAUCK, C. A. N86-10962
HAUN, C. C. N86-10675
HAUPT, R. J. N86-10030
HAUSMAN, H. J. N86-11088
HAVENER, C. C. N86-10926
HAYES, D. C. N86-10554
HAYES, K. F. N86-10592
HAYNES, J. M. N86-10207
HAYS, R. T. N86-11065
HEADLEY, T. J. N86-10324
HEARST, P. J. N86-10314
HEATH, J. E. N86-10480
HEBSUR, M. G. N86-10311
HEDDERGOTT, A. N86-10051
HEDEMANN, M. A. N86-11005

HEERING, J. N86-10884
HEGLAND, J. R. N86-10831
HEINE, E. N86-10968
HEINEMANN, K. N86-11047
HEINICKE, M. N86-11065
HEJHAL, D. A. N86-10902
HELD, D. N. N86-10615
N86-10616
N86-10617
N86-10628
HELLAWELL, A. N86-10086
HEMSKY, J. W. N86-10932
HENDRIX, G. J. N86-10916
HENDY, K. C. N86-10039
N86-10788
HENINS, I. N86-10988
N86-10998
N86-11028
HENNINGER, W. C. N86-10274
HENRY, D. N86-10253
HENSCHEL, F. N86-10047
HEPPELMAN, S. N86-10443
HERCEQ, R. N86-10659
HERLACH, D. M. N86-10259
N86-10260
HERMACH, F. L. N86-10453
HESS, K. N86-10484
HESSELINK, L. N86-10108
HESTER, J. N86-10278
HEUSTESS, J. E. N86-10408
HEWETT, D. W. N86-11016
HIGGINS, E. F. N86-10996
HIGGINS, W. W. N86-10992
HILDEBRAND, S. G. N86-10678
HILS, D. N86-11123
HINCHLIFFE, I. N86-11008
HINDS, F. T. N86-10556
HINES, R. E. N86-10842
HINTZE, C. J. N86-10035
HIRSCHFELD, T. B. N86-10296
HIRST, J. N86-11001
HOBBS, R. W. N86-10958
HOCKADAY, M. P. N86-10944
HODGE, D. C. N86-10917
HOEFER, H. R. N86-10027
HOFMANN, K. H. N86-11120
HOIDA, H. W. N86-10988
N86-10998
HOLIAN, B. L. N86-10927
HOLLAND, L. R. N86-10065
HOLLEMAN, F. B. N86-10370
HOLMES, N. C. N86-10470
HOLTKAMP, D. N86-10943
HOLZMANN, R. N86-10961
HOMOLYA, J. B. N86-10686
HOMSEY, G. M. N86-10109
HONG, C. S. N86-10538
HONG, S. K. N86-10464
HONIG, E. M. N86-10196
N86-10197
HONODEL, C. N86-10323
HOPPE, D. N86-10387
N86-10388
HOULBERG, W. A. N86-10840
HOUTEKAMER, G. E. N86-10806
N86-10807
N86-10808
HOWARD, A. M. N86-10926
HOWARD, C. J. N86-10707
HOWARD, W. M. N86-11134
HOYNIAK, D. N86-10019
HSU, I. S. N86-10391
HUGENTOBLER, F. N86-10515
HULL, K. N86-10528
HULLIGER, F. N86-11052
HUMPHRIES, C. M. N86-11094
HUMPHRIES, W. N86-10554
HUNT, J. J. N86-10200
N86-10485
HUNTEN, D. M. N86-11137
HURD, J. W. N86-10930
HURWITCH, J. W. N86-10326
HUTH, H. N86-10044
HUTTON, A. M. N86-10964
HYMER, W. C. N86-10140
HYNES, T. V. N86-10315

I

IAIRD, R. N86-10443
ICE, G. E. N86-10936
IGREVSKIY, A. V. N86-10743
ILLEGRAMS, P. F. A. N86-10534
ILYALETDINOV, A. N86-10742
IOUP, G. E. N86-10822
N86-10823
N86-10824
N86-10825
N86-10826
N86-10827
IOUP, J. W. N86-10826
IPSEN, I. C. F. N86-10795
IRIE, K. N86-10378
ISHERWOOD, D. N86-10632
ISIHARA, A. N86-10982
ITALIANO, V. M. N86-10928
IWASHITA, Y. N86-10987

J

JABLONSKI, D. G. N86-10423
JACKSON, J. N86-11022
JACKSON, T. J. N86-10619
JACOBSON, B. O. N86-10551
JAHNKE, T. O. N86-10040
JAMGOTCHIAN, H. N86-10262
JANKOWSKI, D. F. N86-10123
JANNEY, J. I. N86-10839
JANSA, J. N86-10488
JANSSENS, R. V. F. N86-10961
JARBOE, T. R. N86-10988
N86-10998
N86-10999
N86-11003
N86-11027
N86-11028
JAUNCEY, D. L. N86-10383
JAVELLE, J. N86-10023
JAWAD, M. N86-10328
JENKINS, C. J. N86-10553
JENSEN, J. M. N86-10391
JESSER, W. A. N86-10193
JHA, S. N. N86-10516
JOBE, R. K. N86-10836
JOERGEN, P. N86-10874
JOHENNING, B. N86-11140
JOHN, C. N86-10228
JOHNSON, C. N86-10872
JOHNSON, J. D. N86-10927
JOHNSON, N. L. N86-10885
N86-10886
JOHNSON, S. E. N86-10791
JOHNSON, T. V. N86-11137
JOHNSON, W. L. N86-10327
JOHNSON, W. S. N86-10650
JOHNSTON, J. P. N86-10461
JOHNSTON, M. H. N86-10174
JONES, E. E. N86-10195
JONES, M. W. N86-10339
JONES, S. H. N86-10482
JORDAN, A. K. N86-11049
JORDAN, H. L. N86-11068
JORDAN, J. N86-10819
JOSS, W. N86-11052
JOST, G. S. N86-10036
JUN, Y. W. N86-10046
JUNGBLUTH, R. N86-10186
JUNGBLUTTH, R. N86-10181

K

KABIR, K. L. N86-10368
KAIMAL, J. C. N86-10723
KALB, J. T. N86-10917
KALDIS, E. N86-10267
KALONJI, G. N86-10152
KAMAT, D. S. N86-10516
KAMMERER, P. N86-10517
KAMOTANI, Y. N86-10124
KAMPAS, F. J. N86-10649
KARAWAS, G. K. N86-10369
KARPENKO, V. N. N86-11017
KARPOVSKIY, Y. Y. N86-10815
KASHTANOV, V. V. N86-10811
KASSEL, S. N86-10542
KATZ, J. N86-10015
KATZ, S. A. N86-10274
KATZ, T. J. N86-10283
KAUKLER, W. F. N86-10112
N86-10116
KAUTZ, H. E. N86-10561
KAYS, W. M. N86-10461
KAYSER, R. F. N86-10121
KEECH, M. A. N86-10512
KELLER, B. R. N86-10699
KELLER, R. N86-11006
KELLY, T. J. N86-10719
KELSO, A. R. N86-10712
KENNEDY, A. N86-10309
KENNEDY, R. E. N86-10198
KEOHANE, G. N86-11022
KEREN, G. B. N86-11077
KERN, E. L. N86-10063
KESNER, J. N86-11020
KESSEL, J. N86-10978
KEYANG, S. N86-10002
KHALIL, S. A. M. N86-10567
KHOMSKAYA, Y. D. N86-10756
KHOO, T. L. N86-10961
KHOVANSKAYA, T. P. N86-10745
KIBBLEWHITE, E. N86-11099
N86-11102
KIEDRON, K. N86-10386
KIEKEL, P. D. N86-10192
KIELB, R. E. N86-10579
KILLIAN, E. W. N86-10954
KIM, M. N86-11040
KIM, S. H. N86-10941
KINCAID, J. M. N86-10122
KING-HELE, D. G. N86-10190
KING, J. D. N86-10943
KING, R. J. N86-10409
KING, W. E. N86-10087
KINNEY, D. C. N86-10642
KIRKPATRICK, M. I. N86-10926
KLEIJNEN, J. P. C. N86-10893
N86-10894
N86-10895
KLEIN, H. N86-10249
N86-10257
KLEIN, M. M. N86-10944
KLEMENT, D. N86-10981
KLEMME, K. E. N86-10546
KLEMT, W. B. N86-10641
KLEY, M. N86-10521
KLINE, K. B. N86-10900
KNEISSEL, A. N86-10210
KNOTT, M. N86-10979
KNOWLES, T. N86-10641
KNOX, J. B. N86-10718
KNOX, S. O. N86-11003
N86-11028
KOECHLIN, L. N86-11112
KOEK, F. B. N86-10732
KOELBL, O. N86-10493
KOELKER, H. N86-10226
KOELLE, H. H. N86-11140
KOHLER, R. N86-10309
KOMAROV, V. D. N86-10611
KOMPENHANS, J. N86-10027
KONECNY, G. N86-10487
KONINGS, C. A. G. N86-11081
KONSTANTINOV, M. A. N86-10752
KOOPS, J. N86-10672
N86-10673
KOREIN, J. D. N86-10785
N86-10821
KOREVAAR, C. G. N86-10732
KORNFELD, M. N86-10146
KOROTKOV, Y. A. N86-10743
KORTH, M. S. N86-11046
KORYAKINA, L. A. N86-10766
KOSCHMIEDER, E. N86-10117
KOSHCHIY, G. N. N86-10762
KOSHELEV, V. N. N86-10759
KOSTSOV, E. G. N86-10810
KOTZ, S. N86-10885
N86-10886
KOZDOBA, L. A. N86-10293
KPONCU, A. N86-10935
KRAATZ, K. H. N86-10231
KRAKOWSKI, R. A. N86-11031
KRAMER, J. F., JR. N86-10829
KRATIN, Y. G. N86-10765
KRAUS, K. N86-10488
KREMER, R. E. N86-11050
KRICHEVSKAYA, A. A. N86-10762
KRIENEN, F. N86-11004
KRISHTALKA, L. N86-10609
KRIVOSHEI, F. A. N86-10293
KROES, E. B. N86-10967
KROES, R. L. N86-10064
KROGER, P. M. N86-10401
KROGMANN, P. N86-10025
KUCERA, G. H. N86-10659
KULIKOV, A. V. N86-10766
KULKARNI, A. D. N86-11128
KUMAKAWA, A. N86-10114
KUNKLE, T. D. N86-10469
KUPERMAN, G. G. N86-10481
KUPFER, G. N86-10496
KURYLO, M. J. N86-10707
KURZWEG, U. H. N86-10539
KUSCHER, G. F. N86-10318
KUWAHARA, K. N86-10243
KYR, P. N86-10221

L

LABBE, P. N86-10419
N86-10865
LABEYRIE, A. N86-11097
N86-11101
N86-11102
N86-11108
N86-11115
LACASSE, M. G. N86-11118
LACH, J. N86-10946
LADOUCEUR, H. D. N86-11049
LAGOWSKI, J. N86-10234
LAL, R. B. N86-10084
LALANANDHAM, R. N86-10576
LAMBERT, J. E. N86-10985
LAMBERT, R. F. N86-10909
LANE, B. N86-11020
LANG, H. R. N86-10599
N86-10604
N86-10606
LANGBEIN, D. N86-10268
LANGDON, A. B. N86-11016
LANGE, H. G. N86-10555
LANGE, R. N86-10251
LANGER, J. S. N86-10088
LANGNER, A. N86-10506
LANHAM, W. N86-10140
LANKFORD, J. N86-10590
LANNES, A. N86-11124
LARGER, N. N86-10023
N86-10024
LARRABEE, J. A. N86-10301
LARSON, D. J. N86-10089
LATORRE, V. R. N86-10409
LAXMANAN, V. N86-10090
LAYANI, P. N86-10253
LAYLAND, J. W. N86-10395
N86-10396
LAYMANAN, V. N86-10261
LAZAREV, V. O. N86-10811
LEAHY, H. F. N86-10675
LEAVITT, L. D. N86-10016
LEBEDEV, A. P. N86-10236
LEBER, L. L. N86-10787
LEBURTON, J. P. N86-10484
LECHLEITNER, M. L. N86-11079
LECORDIX, P. Y. N86-10509
LECURU, D. N86-10564
N86-10594
LEE, C. S. N86-10377
LEE, D. M. N86-10950
LEE, H. G. N86-10565
LEE, K. Y. N86-10356
LEE, M. J. N86-11025
LEE, P. N86-10770
LEE, P. J. N86-10392
LEE, R. Q. N86-10380
N86-10381
LEE, S. W. N86-10377
LEE, S. Y. N86-11010
N86-11026
LEE, W. A. N86-10343
LEE, Y. K. N86-10300
LEE, Y. Y. N86-11022
LEFAUCHEUX, F. N86-10230
LEHOCZKY, S. L. N86-10065
LEIFESTE, G. T. N86-10192
LEISSA, A. W. N86-10579
LEISTE, H. N86-10227
LEITH, W. N86-10607
LENA, P. N86-11100
LEVY, R. N86-10389
LEWIS, B. L. N86-10375
N86-10376
N86-10417
LI, C. J. N86-10234
LI, C. P. N86-10018
LI, X. Z. N86-11020
LI, Z. L. N86-10593
LICHTENSTEIN, S. N86-11077
LIEFELD, R. J. N86-10944
LILLYBECK, N. N86-10084
LIM, J. J. N86-10841
LIN, T. S. N86-10570
LINANG, L. N86-10004
LINDHOLM, U. S. N86-10589
LINDQUIST, T. E. N86-10829
LINSTADT, E. N86-10801
N86-11033
LIPA, J. A. N86-10118
LISKA, D. J. N86-11001
LISOWSKI, P. W. N86-10943
LITTKE, W. N86-10228
LIU, K. C. N86-10925
LIU, W. T. N86-10714
LIU, Y. Z. N86-10538
LIVINGSTONE, S. D. N86-10786
LO, Y. T. N86-10377
LOAR, J. M. N86-10678
LOCKHART, T. J. N86-10723
LOCKWOOD, G. J. N86-10439
N86-10940
N86-11013
LOEHBERG, K. N86-10209
LOFTSSON, J. N86-10397
N86-10398
LOFTUS, J. J. N86-10302
LOGAN, T. L. N86-10604
LOHMANN, P. N86-10511
LOKSHIN, A. N86-10400
LONGDON, N. N86-11096
LOUSTEAU, D. C. N86-10960
LUIJCKX, G. N86-10967
LUNDSTROM, M. S. N86-10655
LUNSFORD, J. S. N86-10996
LUOMA, W. L. N86-10651
N86-10652
LUPTON, R. H. N88-11131
LUYENDIJK, T. N86-10212
LYNCH, N. A. N86-10898
LYNN, K. G. N86-10937

M

MAAS, R. N86-10967
MAAT, L. N86-11081
MACBAIN, J. C. N86-10579
MACDONALD, G. E. N86-10914
MACE, E. E. N86-10713
MACEWEN, J. D. N86-10675
MACHENS, U. N86-10670
MACK, S. N86-10591
MACPHERSON, P. B. N86-10550
MAEKAWA, T. N86-10243
MAHAR, D. J. N86-10433
MAISH, A. B. N86-10665
MAITHREYAN, T. N86-11129
MALMEJAC, Y. N86-10079
N86-10222
MALONE, S. D. N86-10633
MALOTA, F. N86-10544
MANABAYEV, G. T. N86-10817
MANGANIELLO, A. J. N86-10832
MANINGER, R. C. N86-10959
MANN, R. C. N86-10526
MANNARA, G. N86-10235
MANOOCHEHRI, K. N86-10821
MANSFIELD, B. K. N86-10526
MANTENIEKS, M. A. N86-10280
MANTOVANI, J. C. N86-10435
MANUKHIN, B. N. N86-10754
MARCHATERRE, J. F. N86-10952
MARGITAN, J. J. N86-10707
MARGRAVE, J. L. N86-10091
MARGULIES, T. S. N86-10911
MARINA, M. N86-10400
MARKARYAN, S. S. N86-10743
MARKLIN, G. N86-11029
MARKLIN, G. J. N86-10988
N86-10998
N86-11027
MARKO, A. R. N86-10973
MARKWORTH, A. J. N86-10081
N86-10264
MARMORINO, G. O. N86-10730
MARTIN, E. A. N86-10784
MARTINEAU, J. R. N86-10342
MARTINEZ, T. N86-10205
MARTINSON, R. H. N86-10345
MASHBURN, J. B. N86-11019
MATHEWS, G. J. N86-11134
MATTHEWS, A. J. N86-10482
MATTSON, C. B. N86-11011
MATTSSON, S. N86-10411
MATUSKA, W., JR. N86-10944
MATUSOV, A. L. N86-10751
MATVEYEV, L. N. N86-10747
MAVROGENES, G. S. N86-10987
MAXAM, G. L. N86-10049
MAY, E. N86-10443
MAYA, I. N86-10468
MAZIAR, C. M. N86-10655
MCCLENNY, W. A. N86-10687
MCCLOSKE, M. W. N86-10651
MCCLOSKEY, M. W. N86-10652
MCCOY, K. E. N86-10278
MCDANIEL, E. W. N86-10926
MCDERMOTT, D. N86-10833
MCDONALD, M. M. N88-10325
MCDONNELL, M. N86-10524
MCFADDEN, D. M. N86-10684
MCFADDEN, G. B. N86-10077
MCGRAW, B. A. N86-10650
MCGUFFIE, B. A. N86-10604
MCGUIRE, R. R. N86-10359
MCHARGUE, C. J. N86-10448
MCHUGH, M. A. N86-11061
MCILWAIN, M. E. N86-10530
MCKENNA, K. F. N86-11003
MCLAREN, S. E. N86-10719
MCMENAMIN, M. A. S. N86-10692
MCMICAN, W. J. N86-10849
MCPHERSON, W. R. N86-10276
MEADE, A. C. N86-10798
MEIER, G. E. A. N66-10028
MELITA, O. N86-11096
MENEGUETTE, A. N86-10495
MENG, F. N86-10358
MENICUCCI, D. F. N86-10716
MENITSKIY, D. N. N86-10752
MENZEL, M. T. N86-10837
MERRITT, F. L. N86-10277
MERTENS, H. W. N86-10771
MESEGUER, J. N86-10244
MESZAROS, S. P. N86-11138
MEYER, C. N86-10821
MEYER, F. W. N86-10926
MEYER, H. N86-10119
MEYER, P. N86-10553
MEZIDOVA, K. A. N86-10754
MICALE, F. J. N86-10146
MIENTEK, A. P. N86-10651
N86-10652
MIKATA, Y. N86-10285
MILLER, A. P. N86-10106
MILLER, J. O. N86-10669
MILLER, W. A. N86-10473
MILLER, W. H. N86-10355
MILLER, W. J. N86-10150
MILUTINOVIC, J. N86-10921
MINER, R. V. N86-10311
MINH, N. Q. N86-10659
MITCHELL, A. C. N86-10317
MIYASHITA, K. N86-10520
MIYOSHI, K. N86-10341
MIZUSAWA, H. N86-10378
MOBLEY, J. D. N86-10688
MOEN, I. O. N86-10304
MOFFAT, R. J. N86-10461
MOHAMED-ALY, H. N. N86-10566
MOHSENI, S. N86-10362
MOLDOVER, M. R. N86-10113
N86-10120
N86-10121
MOLINA, M. J. N86-10707
MOMMADOV, I. M. N86-10749
MONDAL, N. N86-10443
MONTANARI, R. N86-10215
MONTGOMERY, D. B. N86-11000
MONTGOMERY, S. T. N86-10350
MONTH, M. N86-11018
MONTI, R. N86-10203
N86-10235
MOON, S. H. N86-10456
MOORCROFT, A. L. N86-10483
MOORE, C. E. N86-10923
MORABITO, D. D. N86-10383
MORESCHI, J. N86-10659
MORGAN, T. J. N86-10926
MORGAND, P. N86-10218
MORI, T. T. N86-10373
MORIN, A. N86-10419
N86-10865
MORIOKA, M. N86-10243
MORIONDO, A. N86-10490
MORISON, J. D. N86-10793
MOROSIN, B. N86-10300
MORRIS, J. W., JR. N86-10908
MORRISON, D. N86-10140
MORRISON, D. R. N86-10141
N86-10142
MORRISON, G. N86-10122
MORRISON, P. J. N86-11063
MORSE, M. S. N86-10106
MOSES, J. D. N86-10943
MOSS, J. M. N86-10955
MOZURKEWICH, D. N86-11092
MRAZEK, F. C. N86-10659
MSEZANE, A. Z. N88-10939
MUELLER, G. N86-10221
MUELLER, T. A. N86-10916
MUENZER, U. N86-10521
MUKHERJEE, S. P. N86-10153
MULLIGAN, P. J. N86-10621
MUNJAL, M. L. N86-10587

MURALIDHARAN, S. N86-10857
MURPHY, J. C. N86-10034

N

NAEHLE, R. N86-10257
NAGEL, G. N86-10224
NAGLE-ESHLEMAN, J. N86-10585
NAKA, S. N86-10332
NAKANISHI, S. N86-10281
NAMKUNG, M. N86-10578
NAPIER, P. J. N86-10396
NAPOLITANO, L. G. N86-10203
N86-10235
N86-10238
NAUMANN, R. N86-10058
N86-10104
NAWROCKY, R. J. N86-10947
NEEF, J. D. N86-10198
NEFEDEVA, Y. A. N86-10613
NEIDLINGER, H. H. N86-10645
NEITZEL, G. P. N86-10123
NELLIS, W. J. N86-10470
NEPOMUCENO, L. X. N86-10562
NEWCOM, C. C. N86-11011
NEWMARK, R. L. N86-10725
NEYER, B. T. N86-10439
N86-10940
NG, D. S. N86-11017
NICHOLLS, L. A. N86-10403
NICKEL, H. N86-10595
NICOLSON, G. D. N86-10383
NIELSEN, K. F. N86-10229
NIESWAAG, H. N86-10212
NIEUWENHUIS, G. J. A. N86-10638
N86-10639
NIKITIN, S. A. N86-10236
NISHIMURA, N. N86-10346
NITSCHE, K. N86-10251
NITSCHE, R. N86-10223
N86-10225
N86-10227
NOACK, R. W. N86-10021
NOLAN, R. W. N86-10786
NOOMEN, J. N86-10967
NOORDAM, J. E. N86-11106
N86-11119
NORDINE, P. C. N86-10092
NORDSTROM, P. N86-10641
NOREM, J. N86-10979
NOVIKOV, I. V. N86-10745
NOVIKOV, V. S. N86-10750
NOVOZHILOV, G. N. N86-10757
NOWICKI, C. M. N86-10792
NUNZ, G. J. N86-10663

O

OBRIEN, J. J. N86-10651
N86-10652
OCHIAI, J. N86-10243
OGATA, M. N86-10378
OLD, T. E. N86-10405
OLEM, H. N86-10736
OLIVER, K. N86-10687
OLOFSSON, B. N86-10360
OLSON, N. N86-10524
OLSON, R. J. N86-10677
OLUJOHUNGBE, O. N86-10501
ONEILL, P. E. N86-10619
ONURAL, L. N86-10478
ORGILL, M. M. N86-10631
ORMSBY, J. P. N86-10621
ORR, L. H. N86-10828
OSHIMA, T. N86-10520
OSTRACH, S. N86-10124
OTOOLE, J. A. N86-10960
OTTO, H. N86-10258
OVERFELT, P. L. N86-10404
OWE, M. N86-10619
OWEN, R. B. N86-10174

P

PADDAY, J. E. N86-10202
PAFFRATH, D. N86-10685
PAGANO, N. J. N86-10292
PAGNI, P. J. N86-10162
PAK, I. T. N86-10817
PALATUCCI, G. J. N86-10792
PALETS, B. L. N86-10739
PALMER, M. A. N86-10944
PAN, S. K. N86-11041
PANAYAPPAN, R. N86-10313
PAPAS, C. H. N86-10629
PAPAZIAN, H. N86-10340
PAPPAS, J. A. N86-10354
PAPTHEODOROU, T. N86-10071
PARIS, J. F. N86-10627
PARK, C. N86-11047
PARK, J. E. N86-10843
PARKAS, Z. D. N86-11051
PARKIN, D. M. N86-10932
PARMLEY, R. T. N86-10274
PARSONS, M. L. N86-10280
PARZEN, G. N86-11023
N86-11026
PASTUKHOV, Y. F. N86-10764
PATRIARCA, P. N86-10328
PATRICK, H. V. L. N86-10913
PATUELLI, C. N86-10215
PAUT, A. J. N86-10023
PAWLOWICZ, L. M. N86-10234
PAYLOR, E. D. N86-10604
N86-10606
N86-10608
PECH, G. J. N86-10316
PELLA, P. A. N86-10847
PELLEGRIN, J. I. N86-10964
PELLETIER, D. H. N86-10457
PENG, C. N86-10010
PENKALLA, H. J. N86-10595
PENNER, J. E. N86-10717
PENNLINE, H. W. N86-10681
PENTECOST, E. N86-10053
PEPPER, D. W. N86-10348
PEREPEZKO, J. H. N86-10093
PERKO, J. S. N86-11143
PERRY, J. S. N86-10032
PERTSOV, O. L. N86-10759
PETERFREUND, A. R. N86-11136
PETERS, J. H. N86-10715
PETERSEN, R. H. N86-10676
PETERSON, T. T. N86-10125
PETRIE, G. M. N86-10597
PETROVA, L. A. N86-10612
PETROVIC, J. J. N86-10349
PFIRSCH, D. N86-11063
PHILLIPS, B. A. N86-10664
PHILLIPS, R. N86-11022
PHILLIS, N. J. N86-10523
PHINNEY, N. N86-10836
N86-11024
PICKARD, W. F. N86-10420
PIERCE, R. D. N86-10659
PIETRI, C. E. N86-10953
PIKE, T. K. N86-10413
PILLAI, C. N86-10963
PINCOSY, P. A. N86-10962
PINTER, S. S. N86-10898
PIPEROPOULOU, H. N86-10444
PIRICH, R. G. N86-10094
PLANK, V. G. N86-10482
PLATE, S. N86-11022
PLATTEN, J. K. N86-10245
PLATTS, D. A. N86-10999
N86-11003
PLEIL, J. D. N86-10687
PODSIADLY, C. N86-10058
POEPPEL, R. B. N86-10659
POLETTI, G. N86-10252
POLEZHAEV, V. I. N86-10236
POND, R. B. N86-10095
N86-10096
POPECHITELEV, Y. P. N86-10765
POPOV, A. A. N86-10739
POPOVA, N. K. N86-10766
PORZ, F. N86-10352
POSEY, L. D. N86-11005
POSNER, E. C. N86-10382
POSOSHENKO, L. Z. N86-10813
POTARD, C. N86-10097
N86-10218
POTASH, R. I. N86-11093
POTTER, J. L. N86-10014
POTTER, J. M. N86-10987
POUKEY, J. W. N86-10192
PRAIZEY, J. P. N86-10222
PREGENZER, A. L. N86-11005
PRESTON, R. A. N86-10383
PRICE, G. R. N86-10917
PRIVON, G. T. N86-10472
PURASINGHE, R. N86-10571
PYLE, R. V. N86-10962

Q

QIPENG, C. N86-10003

R

RAALAND, D. M. N86-10298
RABBIA, Y. N86-11125
RABOUT, P. N86-11108
RADFORD, D. C. N86-10961
RAGHUNATHAN, M. S. N86-10856
RAJESWARAN, G. N86-10649
RAMANTHAN, A. N86-10856
RAMATY, R. N86-11141
RANDALL, S. A. N86-10651
N86-10652
RANNENBERG, S. N86-10027
RAO, B. C. S. N86-10552
RATAJCZAK, A. F. N86-10643
RAUBENHEIMER, T. N86-10995
RAUCHAS, A. N86-10979
RAVEENDRA, S. T. N86-10855
RAVISHANKARA, A. R. N86-10707
RAYGORODSKAYA, T. G. N86-10759
RAZZAQ, Z. N86-10577
REBER, G. N86-10195
REDDISH, V. C. N86-11094
REDEEN, W. C. N86-10006
REE, F. H. N86-10907
REED, I. S. N86-10391
REGEL, L. L. N86-10263
REHN, L. E. N86-11056
REIMANN, R. C. N86-10654
REINHARDT, F. W. N86-10644
REISCHEL, M. N86-10103
REMICK, R. J. N86-10447
REMSBERG, I. P. N86-10963
RENHORN, I. N86-10980
REPETA, L. N86-11022
REX, J. D. N86-10906
REY, C. A. N86-10177
REYNOLDS, J. R. N86-10333
REYNOLDS, L. D. N86-10530
REZAIE-KEYVAN, N. N86-10572
REZTSOV, V. P. N86-10813
RHIM, W. K. N86-10170
RICE, C. K. N86-10653
RICHARDS, J. J. N86-10849
RIEPL, H. N86-10255
RIFF, R. N86-10588
RIKHTER, G. D. N86-10612
RIVKIN, I. N86-11014
RIVKIN, L. N86-10964
ROBERSON, P. I. N86-10938
ROBERT, M. C. N86-10230
ROBERTS, G. O. N86-10705
ROBERTSON, D. K. N86-10580
ROCK, B. A. N86-10280
RODEMICH, E. R. N86-10402
RODENZ, G. W. N86-10837
N86-10929
RODOT, H. N86-10204
N86-10220
RODRIGUES, G. C. N86-10319
ROEDER, A. W. N86-10374
ROEDIG, M. N86-10595
ROFFEY, R. N86-10360
ROGERS, J. W., JR. N86-10644
ROGERS, R. B. N86-10972
ROHAY, A. C. N86-10633
ROKNI, S. H. N86-10963
ROMIG, A. D., JR. N86-10324
N86-10331
ROOIJAKKERS, R. V. H. N86-10889
ROSENBERG, H. N86-10338
ROSENBERGER, F. N86-10126
ROSENBLUM, L. J. N86-10730
ROSENER, T. J. N86-10951
ROSENKILDE, C. E. N86-10466
N86-10467
ROSENKRANZ, V. N86-10254
ROSNER, H. S. N86-10729
ROSS, M. C. N86-11025
ROSS, P. N., JR. N86-10446
ROSSI, M. J. N86-10433
ROSSITTO, F. N86-10232
ROTH, E. A. N86-11114
ROUSSEAU, R. M. N86-10847
ROUTHORT, J. N86-10659
ROUX, B. N86-10253
ROVINS, J. N86-10821
ROY, S. N86-10479
ROYLANCE, D. N86-10127
ROZENDAAL, L. T. N86-10804
RUGGLES, L. E. N86-10439
RUSSEL, W. B. N86-10129
RUSSO, G. N86-10203
RUSZKAY, J. N86-10438
RUTH, R. D. N86-10995

S

SAAD, Y. N86-10794
N86-10850
N86-10867
N86-10868
SABATIER, P. C. N86-10706
N86-10858
SABER, A. J. N86-10304
SADOWAY, D. R. N86-10098
SALBERGER, P. N86-10904
SALE, M. J. N86-10678
SANDER, O. R. N86-10992
SANDERS, M. E. N86-10957
SANDOVAL, D. P. N86-10992
SANG, Y. N86-10529
SANI, R. L. N86-10128
SANMARTIN, A. M. N86-10271
SARACHIK, M. P. N86-11053
SARGENT, F. E. N86-10728
SAVILLE, D. A. N86-10129
N86-10130
N86-10143
SAYLES, D. C. N86-10282
SAZONOV, V. S. N86-10764
SCALA, C. M. N86-10037
SCHAEFER, R. J. N86-10077
SCHARMANN, A. N86-10242
SCHEID, J. A. N86-10384
SCHEMPP, A. N86-10194
SCHEN, M. A. N86-10334
SCHENCK, L. R. N86-10604
N86-10624
SCHERPELZ, R. I. N86-10299
SCHICKEL, K. P. N86-10720
SCHIJVE, J. N86-10045
SCHISSEL, P. N86-10645
SCHLERETH, J. N86-10443
SCHMID, L. A. N86-10106
N86-10131
SCHMIDT, J. W. N86-10121
SCHMUGGE, T. J. N86-10619
SCHNEIDER, L. X. N86-11013
SCHNEIDER, R. T. N86-10539
SCHNEPPLE, W. F. N86-10066
SCHOENHOLZ, R. N86-10225
SCHOLTEN, W. N86-10637
SCHRIBER, S. O. N86-10987
SCHROEDER, M. N86-10500
SCHUBERT, F. N86-10595
SCHUERING, A. N86-10500
SCHUHR, W. N86-10500
SCHULTZ, J. H. N86-11000
SCHULTZ, K. R. N86-10468
SCHULTZ, M. H. N86-10794
N86-10850
SCHUMMERS, J. H. N86-10906
SCHUSTER, G. J. N86-10527
SCHWAB, D. N86-10184
SCHWABE, D. N86-10242
SCHWARTZ, R. J. N86-10655
SCHWARZ, H. D. N86-11015
SCHWARZ, J. A. N86-10099
SCHWARZ, R. B. N86-10322
SCHWEBEKE, H. N86-10968
SCOTT, D. H. N86-10445
SCULLY, C. N. N86-10536
SEEBAUGH, W. R. N86-10014
SEEMAN, J. T. N86-11025
SEGALL, Z. N86-10848
SEIGNEUR, C. N86-10710
SELEROWICZ, W. C. N86-10028
SELKIRK, J. K. N86-10526
SELKOWITZ, S. N86-10978
SELPH, M. M. N86-10944
SELYAYEV, A. A. N86-10818
SEMENOVA, O. S. N86-10812
SERVRANCKX, R. V. N86-10994
SEVESTRE, C. N86-10363
SEZAKI, K. N86-10243
SGAVETTI, M. N86-10502
SHALKHAUSER, K. A. N86-10379
SHARITZ, R. R. N86-10625
SHARMA, S. N86-11021
SHARR, Y. N86-10816
SHAW, M. S. N86-10927
SHEALY, D. L. N86-11095
SHEFFIELD, R. L. N86-10929
SHEHATA, A. M. T. M. N86-10455
SHEPHERD, J. E. N86-10304
SHEPPARD, J. C. N86-11025
SHIELDS, G. N86-10820
SHIGUAN, B. N86-10005
SHIH, W. H. N86-10101
SHIMAZAKI, Y. N86-10335
SHIOHARA, Y. N86-10080
N86-10133
SHISONG, M. N86-10886
SHOPE, S. L. N86-10192
SHRADER, C. R. N86-11144
SHU, D. M. N86-10947
SHULTIS, J. N86-10834
SHUMILOVA, T. Y. N86-10761
SIDOROV, Y. A. N86-10748
N86-10751
SIEGFRIED, E. N86-10214
SIEWIOREK, D. N86-10848
SIGMON, T. W. N86-10429
SIKKA, V. K. N86-10328
SILCHENKO, K. K. N86-10757
SIMITSES, G. J. N86-10588
N86-10860
SIMMONS, J. E. N86-10943
SIMMONS, T. N. N86-11019
SIMPSON, H. M. N86-10932
SIMPSON, J. R. N86-10631
SIMS, T. M. N86-10958
SINEGUB, Y. S. N86-10611
SINES, G. N86-10591
SINGER, J. N86-10584
SINGER, M. J. N86-11065
SINGER, R. B. N86-10601
N86-10604
SINKS, D. J. N86-10634
SINNO, Y. A. N86-10700
SINNOTT, M. J. N86-10291
SIOCHI, E. J. N86-10033
SIRIGNANO, W. A. N86-10163
SKAALEN, C. I. N86-10555
SKARITKA, J. N86-11022
SKILLMAN, E. D. N86-11130
SKUDRIDAKIS, J. N86-10043
SLACK, R. A. N86-10421
SLINKER, S. N86-10924
SLINN, S. Y. N86-10276
SLUIJK, I. N86-10969
SLUYTERS, T. N86-10935
SMALLEY, R. E. N86-10966
SMEULDERS, T. N86-10888
SMITH, B. R. N86-11080
SMITH, J. L. N86-10659
SMITH, L. N86-11022
SMITH, M. N86-10623
SMITH, R. D. N86-10297
SMITH, S. T. N86-10841
SMYTH, W. H. N86-11139
SNEAD, C. L., JR. N86-10937
SNELL, M. K. N86-10408
SNELLING, D. R. N86-10294
SNYDER, R. S. N86-10143
N86-10144
SOBOLEVSKIY, V. I. N86-10758
SOKOLOV, Y. I. N86-10745
SOLOMEY, N. N86-10443
SOLOVYEV, A. N. N86-10765
SOMARATNA, N. N86-10286
SOMORJAI, G. A. N86-11057
SONI, S. R. N86-10292
SONTAG, H. N86-10465
N86-10541
N86-10977
SOROKO, S. I. N86-10751
SPAEPEN, F. N86-10154
N86-10233
SPATARO, S. J. N86-10532
SPEAR, K. E. N86-10132
SPENCE, P. W. N86-11005
SPENCER, B. W. N86-10952
SPENDEL, T. N86-10476
SPRADLEY, I. N86-10274
SPRENGER, H. N86-10213
SPRINGSTON, P. S. N86-10555
SRINIVASAN, M. A. N86-10568
SRIVASTAVA, P. K. N86-10516
STACHNIK, R. V. N86-11103
N86-11116
STAPASHKIN, A. I. N86-10818
STAPAY, J. R. N86-10659
STARK, E. N86-10486
STARK, E. W. N86-10898
STEFANESCU, D. M. N86-10084
N86-10100
STEINBACH, D. N86-10026
STEINBERG, D. N86-10323
STEINER, W. R. N86-10800
STELLING, G. S. N86-10477
STEVENS, M. P. J. N86-10802
N86-10804
STICKLER, R. N86-10214
STIENING, R. F. N86-11025
STINESPRING, C. D. N86-10132
STINNETT, R. M. N86-10958
STIPP, V. N86-10991
STOECKL, H. N86-10596
STOLZ, W. N86-10514
STONE, G. A. N86-10342
STOOKE, W. N., JR. N86-10038
STORK, D. G. N86-10769
STRATHMANN, F. W. N86-10519
STRAUB, J. N86-10250
N86-10251
STREHLOW, R. A. N86-10164
STROO, R. N86-10968
STROUD, D. G. N86-10101
STUBSTAD, J. M. N86-10860
STUCKY, R. K. N86-10609
STUHLINGER, T. W. N86-10971
STURE, S. N86-10175
SUBRAMANIAN, R. S. N86-10155
SUENAGA, M. N86-10937
SUGIURA, T. N86-10520
SULAKVELIDZE, G. K. N86-10614
SULMISTRAS, A. N86-10304
SULTAN, M. N86-10605
SULTANGAZIN, U. M. N86-10817
SULTANOV, F. F. N86-10754
SUTER, G. W., JR. N86-10679
SUURA, H. N86-11062
SVENSSON, S. N86-10980
SWAB, J. J. N86-10315
SWAIN, G. R. N86-10986
SWANSON, R. M. N86-10429
SWENSON, D. A. N86-10987
SWENSON, H. W. N86-10480
SWENSON, I. W. N86-10963
SYNDER, S. N86-10246
SZEKELY, J. N86-10133
SZOFRAN, F. R. N86-10065
SZU, H. H. N86-10975
SZUMOWSKI, A. P. N86-10028

T

TAFT, N. N86-10897
TAGUCHI, S. N86-10303
TAKAHASHI, K. N86-11134
TAKENS, F. N86-10892
N86-10905
TAM, A. C. N86-10465
N86-10541
N86-10977
TANAKA, S. N86-10520
TANASAWA, I. N86-10243
TANNER, R. L. N86-10719
TAO, G. Y. N86-10847
TASK, H. L. N86-10778
TATE, R. E. N86-10660
TAVERNA, A. R. N86-10289
TAYLOR, C. H. N86-10277
TAYLOR, H. F. N86-10422
TAZETDINOV, I. G. N86-10746
TERVO, J. N. N86-10558
THEON, J. S. N86-10702
THOEMING, G. H. N86-10838
THOM, C. N86-11121
THOMPSON, A. R. N86-10396
THOMPSON, D. S. N86-10445
THOMPSON, F. W. N86-10796
THOMPSON, K. N86-10836
N86-11024
THOMPSON, L. H. N86-10737
THOMPSON, W. S. N86-10289
THOMSEN, M. F. N86-11034
THORISSON, H. N86-10875
THRON, J. N86-10443
TIAN, Y. N86-10358
TIKHONOV, M. A. N86-10739
TILANUS, C. B. N86-10901
N86-11076
TIMMERMANS, X. I. M. N86-10845
TIRCUIT, E. C. N86-10199
TKACHENKO, Y. Y. N86-10763
TODD, P. N86-10140
N86-10145
TOGLIATTI, G. N86-10490
TOLCOTT, M. A. N86-10779
TOMICH, S. D. N86-10527
TOOHIG, T. E. N86-10997
TOOTHMAN, D. A. N86-10688
TOTTEREAU, O. N86-10220
TRACY, E. R. N86-10367
TRAUB, W. A. N86-11104
N86-11118
TRAVIS, B. J. N86-10469
TRINH, E. H. N86-10102
TRINKA, J. N86-10263

TRISKA, A. N86-10263
TROSHIKHIN, G. V. N86-10761
TROST, T. F. N86-10042
TRUONG, T. K. N86-10391
TSAI, C. K. N86-10549
TSAI, T. T. N86-10338
TSAY, V. A. N86-10817
TSUI, J. B. Y. N86-10425
N86-10427
TUCKER, W. K. N86-10195
TUPIKOVA, G. A. N86-10749
TURNER, R. S. N86-10677
TYLASKA, T. T. N86-10863
TYLER, S. N86-10397
N86-10398

U

UDANI, P. M. N86-10516
ULABY, F. T. N86-10628
ULIANA, E. A. N86-10406
UNNAM, J. N86-10310
UNRUH, K. M. N86-10327
UTTAL, W. R. N86-10870
UWIRA, K. N86-10720

V

VAKILI, F. N86-11113
VANALSTINE, J. N86-10247
VANALSTINE, J. M. N86-10246
VANBELLE, F. N86-10894
VANDENBERG, L. N86-10066
VANDENBOOM, A. J. W. N86-10844
VANDENDAELE, W. N86-11066
VANDENEIJNDEN, P. M. C. M. N86-10804
N86-10805
VANDENHOF, P. N86-10879
N86-10880
VANDENHONDEL, M. N86-11081
VANDERBIJ, J. D. N86-11073
N86-11074
N86-11075
VANDERBIJ, J. J. N86-11038
VANDERHOFF, J. W. N86-10146
VANDERLINDE, F. J. G. N86-10789
VANDERSCHAAF, T. W. N86-11077
VANDYCK, O. B. V. N86-10950
VANIER, P. E. N86-10649
VANLOON, M. F. N86-10774
VANLOON, M. P. M. N86-10802
VANMIDDENDORP, H. N86-10789
VANMOERKERKEN, R. A. N86-10732
VANWEERT, M. J. M. N86-10803
VANZYL, J. J. N86-10629
VASHCHILLO, Y. G. N86-10752
VASQUEZ, M. C. N86-10837
VAZIRI, K. N86-10963
VELLA, M. C. N86-10962
VENDETTI, A. N86-10562
VENTURINI, E. L. N86-10644
VERHOEVEN, J. D. N86-10067
VERLIJSDONK, A. P. N86-10270
VERMEULEN, P. N86-10703
N86-10704
VERNOT, E. H. N86-10675
VEYSSIERE, A. N86-10418
VIEIRA, D. J. N86-10963
VIGIL, M. G. N86-10357
VILLERS, D. N86-10245
VINCENT, M. A. N86-11123
VITTORIA, C. N86-10415
VIVIANI, A. N86-10238
VOGEL, P. N86-10336
VOLZHSKAYA, A. M. N86-10761
VONGIERKE, H. E. N86-10973
VOSHALL, R. E. N86-10441
VOSS, C. I. N86-10830
VOYZELLE, B. N86-10306
VREEBURG, J. P. B. N86-10206
VYSTAVKIN, A. N. N86-10813

W

WAEGEL, K. H. N86-10412
WAGENFAR, W. A. N86-11077
WALKER, K. P. N86-10589
WALKER, R. P. N86-10906
WALLACE, J. F. N86-10090
WALRAFEN, G. E. N86-10470
WALSHAW, D. J. N86-11094
WALTER, H. U. N86-10265
WALTON, D. R. M. N86-10576
WALZ, D. R. N86-11012
WANDELL, B. A. N86-10777
WANDERS, K. N86-10249
N86-10257
WANG, B. N. N86-10454
WANG, C. S. N86-11036
WANG, J. M. N86-11010
WANG, L. X. N86-10477
WANG, P. N86-10964
WANG, Q. N86-10358
WANG, T. G. N86-10156
N86-10176
WANG, X. N86-10009
WARD, R. A. N86-11134
WARNER, P. J. N86-11117
WARNOCK, R. L. N86-10995
WARREN, J. L. N86-10837
WATKINS, J. N86-10398
WATKINS, R. W. N86-10423
WATSON, R. T. N86-10707
WEAVER, J. N. N86-10964
WEBER, P. J. N86-10030
WEBER, R. M. N86-10589
WEDEMEYER, E. N86-10051
WEFEL, J. P. N86-11142
WEIGELT, G. N86-11102
N86-11120
WEIHL, W. E. N86-10898
WEINBERG, M. C. N86-10157
WEINSTEIN, N. H. N86-10539
WEINZIERL, A. N86-10250
WEISSER, M. N86-10412
WELLER, T. N86-10583
N86-10584
WENDELL, L. L. N86-10666
WENSIERSKI, P. W. N86-10671
WERNER, C. N86-10617
WESSELS, J. N86-11073
N86-11074
N86-11075
WEST, C. D. N86-10647
WEVER, H. N86-10231
WHALEN, M. V. N86-10279
WHITE, C. W. N86-10448
WHITEHORN, M. A. N86-10824
WHITEMAN, C. D. N86-10631
WHITSEL, R. N86-10792
WHITT, W. D. N86-10166
WHYMARK, R. R. N86-10177
WICHLACZ, P. L. N86-10736
WICKLAND, D. E. N86-10625
WIEDEMANN, K. E. N86-10310
WIEDEMEIER, H. N86-10068
N86-10069
WIEDERSICH, H. N86-11056
WIESNER, K. P. N86-10491
WIFFEN, F. W. N86-10329
WIGHTMAN, J. P. N86-10033
WIJNGAARD, J. N86-11073
N86-11075
WILCOX, W. R. N86-10070
N86-10071
WILDE, R. L. N86-10041
WILDUNG, R. R. N86-10684
WILKEN, D. N86-10031
WILLIAMS, F. A. N86-10165
WILLIAMS, F. L. N86-10300
WILLIAMS, J. G. N86-10383
WILLIAMS, R. J. N86-10178
WILLIAMS, W. N86-10354
WILLMORE, R. R. N86-10371
WILLNECKER, R. N86-10259
N86-10260
WINDSOR, M. F. N86-10695
WINELAND, D. J. N86-10295
WITHEROW, W. K. N86-10112
N86-10174
WITMER, G. W. N86-10635
WITT, A. F. N86-10056
N86-10072
WITTEN, C. S. D. N86-10797
WITTMANN, K. N86-10208
WOLZ, H. D. N86-10185
WONG, S. N86-10770
WOOD, G. W. N86-10042
WOODLE, M. H. N86-10933
WOODLEY, M. D. N86-11025
WOODS, S. N86-10524
WORDEN, P. W. N86-10171
WORDSWORTH, R. N86-10550
WOUTES, J. M. N86-10963
WRIGHT, B. L. N86-10999
WRIGHT, B. W. N86-10297
WRIGHT, K. A. R. N86-10823
WU, S. T. N86-10626
WUEST, W. N86-10237
WUETHRICH, C. N86-10308
WUKELIC, G. E. N86-10597

Y

YAKIMENKO, M. A. N86-10763
YAO, C. G. N86-11009
YASHINA, A. V. N86-10614
YEATES, C. M. N86-11137
YEFIMOVA, I. V. N86-10756
YEGOROV, V. M. N86-10810
YEH, J. T. N86-10681
YENCHO, S. N86-11012
YOSHIMURA, M. N86-10520
YOUNG, I. M. N86-10993
YU, L. H. N86-10947
YU, S. N86-10010
YUREK, G. N86-10158

Z

ZAGORSKAYA, Y. A. N86-10744
ZAPOLOTSKIY, D. Y. N86-10814
ZAVYALOV, A. I. N86-10755
ZEBKER, H. A. N86-10622
ZELL, M. N86-10250
ZERLETT, G. N86-10773
ZHANG, K. N86-10010
ZIELINSKI, A. E. N86-10354
ZIMMERLE, D. N86-10912
ZSIDISIN, G. N86-10354
ZVERKOVA, Y. Y. N86-10767

Typical Corporate Source Index Listing

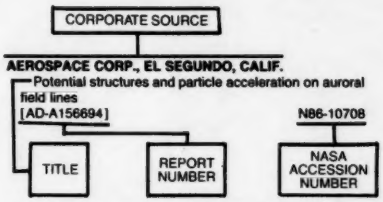

Listings in this index are arranged alphabetically by corporate source. The title of the document provides the user with a brief description of the subject matter. The report number helps to indicate the type of document cited (e.g., NASA report, translation, NASA contractor report). The NASA accession number denotes the number by which the citation is identified. The titles are arranged under each corporate source in ascending accession number order.

A

ACADEMY OF SCIENCES (USSR), MOSCOW.
Mathematical simulation of disturbing forces and material science processes under low gravity N86-10236

ADMIRALTY MARINE TECHNOLOGY ESTABLISHMENT, TEDDINGTON (ENGLAND).
The generation and transmission of vibration in plain cylindrical bearings. Part 2. Experiment
[AD-A156577] N86-10553

ADVANCED ENGINEERING LAB., ADELAIDE (AUSTRALIA).
Specification for the performance, design, development and test requirements for a severe environment cartridge recorder. Issue 4
[AD-A156637] N86-10523

AERODYNE RESEARCH, INC., BILLERICA, MASS.
Experimental and theoretical analysis of chemical vapor deposition with prediction of gravity effects N86-10132

AERONAUTICAL RESEARCH LABS., MELBOURNE (AUSTRALIA).
A review of Australian investigations on aeronautical fatigue during the period April 1983 to March 1985
[AD-A156602] N86-10036
Report on an overseas visit
[AD-A156603] N86-10037
Proposed modifications for the RAAF Airtrainer CT-4A cockpit
[AD-A156808] N86-10039
A graphic anthropometric aid for seating and workplace design
[AD-A156988] N86-10788

AEROSPACE CORP., EL SEGUNDO, CALIF.
Potential structures and particle acceleration on auroral field lines
[AD-A156694] N86-10708

AIR COMMAND AND STAFF COLL., MAXWELL AFB, ALA.
The dirigible: A catalyst for resource exploitation in remote areas?
[AD-A156518] N86-10034
Retrofit of SAC EC-135C and RC-135 aircraft with CFM-56 engines
[AD-A156688] N86-10038
The quest for a helicopter suitable for combat rescue, 1967 - 1983
[AD-A156842] N86-10040
An anthology: Rationale for a US ballistic missile defense (1969 - 1984)
[AD-A156781] N86-10199
Rotary-wing operations in a microburst environment
[AD-A156695] N86-10713
Let's get serious about software
[AD-A156819] N86-10831

AIR FORCE INST. OF TECH., WRIGHT-PATTERSON AFB, OHIO.
Nonlinear methods for spacecraft attitude maneuvers
[AD-A156956] N86-10275
Contact effects in light activated GaAs switches
[AD-A156957] N86-10434
A transformation method for the evaluation of the response moments of elastic structures with random properties
[AD-A156882] N86-10557
A composite climatological study of the frequency and distribution of severe weather associated with spring season Colorado cyclogenesis
[AD-A156981] N86-10715
Mild hypoxia and visual performance with night vision goggles
[AD-A156969] N86-10787
Applications for three-dimensional computer graphic cloud representations produced from satellite imagery
[AD-A156903] N86-10798
Generation of flight paths using hierarchical planning
[AD-A156905] N86-10900

AIR FORCE SYSTEMS COMMAND, WRIGHT-PATTERSON AFB, OHIO.
Acta Aeronautica et Astronautica Sinica (selected articles)
[AD-A147304] N86-10001
Second order approximation method for transonic flows over swept wings N86-10002
A numerical solution of the shock-turbulent interaction over a compression corner for supersonic flow N86-10003
Optimum design of an aircraft wing structure with multiple constraints by the direct-vision criteria method N86-10004
Theoretical specific impulse for two-phase flow in nozzle of rocket-ramjet engine: A simple estimation method N86-10005
Three articles on new calculation methods in aeronautics (selected articles)
[AD-A145745] N86-10007
Numerical solution of hypersonic flow near leading edge of a flat plate N86-10008
A new method for calculating unsteady supersonic aerodynamic forces and its application N86-10009
Effect of a shear layer on the stability of an axisymmetrical external compression air intake N86-10010
Comment on Determination of Aerodynamic Coefficients for a Reentry Body by Means of the Kalman Filter Method N86-10011

AKRON UNIV., OHIO.
Finite element analysis of metals at elevated temperature using unified constitutive theories N86-10569

ALABAMA A & M UNIV., NORMAL.
Solution growth of crystals in zero-gravity N86-10064

ALABAMA UNIV., BIRMINGHAM.
Theoretical analysis of Wolter/LSM X-ray telescope systems
[NASA-CR-176244] N86-11095

ALABAMA UNIV., HUNTSVILLE.
Graphite formation in cast iron N86-10100
Direct observation of critical point wetting in microgravity N86-10116
New instrumentation for phase partitioning N86-10138
Cell partition in two polymer aqueous phases N86-10139
Application of the theory of Ostwald ripening to microgravity phase separation experiments N86-10248

ALLIED BENDIX AEROSPACE, KANSAS CITY, MO.
Miniature radar packaging
[DE85-014598] N86-10410
Software for an automated gaging system
[DE85-013322] N86-10842

AMES LAB., IOWA.
Float zone experiments in space N86-10067

AMSTERDAM UNIV. (NETHERLANDS).
Variability analysis of visually induced responses in the midst of noise
[B8564052] N86-10774
Mission orientation in science N86-11066

ANALYTICAL SERVICES AND MATERIALS, INC., TABB, VA.
A simple method of obtaining concentration depth-profiles from X-ray diffraction
[NASA-CR-176262] N86-10310

ARGONNE NATIONAL LAB., ILL.
Portevin-Le Chatelier effect. 1: Model for the type-E serrations
[DE85-006879] N86-10322
Soudan 2 data acquisition and trigger electronics
[DE85-013864] N86-10443
Approaches to cumulative impact assessment
[DE85-013891] N86-10635
Advanced fuel cell development
[DE85-014550] N86-10659
Chemical/hydrogen energy systems
[DE85-012742] N86-10667
Development of the Multi-Attribute Hazard Assessment System (MAHAS) and its application to energy-related waste streams
[DE85-010278] N86-10676
Computing the structural index
[DE85-014370] N86-10871
Use of the MURA transformation to generate the fields and calculate the motion of protons in the designed Argonne Mini-ASPUN FFAG spiral sector accelerator
[DE85-011477] N86-10934
The 20 keV undulators for a 6-GeV storage ring
[DE85-013867] N86-10941
New particle searches
[DE85-014073] N86-10942
Scoping studies of vapor behavior during a severe accident in a metal-fueling reactor
[DE85-011474] N86-10952
Information on continuum states from feeding times and total (GAMMA) spectra measured with BGO suppressed detectors
[DE85-013868] N86-10961
Beam stability in a 6 GeV synchrotron light source
[DE85-013850] N86-10979
Performance of the H(-) ion source for the intense pulsed neutron source
[DE85-012368] N86-10991
Experimental investigations of thermal radiation from potassium atoms and design applications
[DE85-004086] N86-11036
Fermi surface study of CeSb in the ferromagnetic and antiferromagnetic phases
[DE85-012122] N86-11052
Anelastic relaxation in irradiated Cu-Be
[DE85-013893] N86-11056

ARIZONA STATE UNIV., TEMPE.
Energy stability of thermocapillary convection in models of the float zone process N86-10123
contemporary Aeolian processes on Mars: Local dust storms N86-11136

ARIZONA UNIV., TUCSON.
Hormone purification by isoelectric focusing N86-10135
Extraction of lanthanide ions by 2-methyl-8-quinolinol
[DE85-004277] N86-10303
Mean turbulence structure in strongly heating air flows N86-10455
Optical testing of large telescopes using multiple subapertures N86-10971

ARMAMENT DEVELOPMENT AND TEST CENTER, EGLIN AFB, FLA.
Dynamic analysis of a sled traveling along a rough rail
[AD-A156589] N86-10191

ARMY ARMAMENT RESEARCH AND DEVELOPMENT COMMAND, DOVER, N. J.
EMACK railgun firing test report number 9
[AD-A156661] N86-10354

ARMY ENGINEER TOPOGRAPHIC LABS., FORT BELVOIR, VA.
Analysis of edge detection algorithms on DIAL (Digital Image Analysis Laboratory)
[AD-A156735] N86-10630

ARMY MATERIALS AND MECHANICS RESEARCH CENTER, WATERTOWN, MASS.
Development of a sheath for sensor protection in molten steel applications
[AD-A156764] N86-10315
ARMY MILITARY PERSONNEL CENTER, ALEXANDRIA, VA.
Supervisory control of the right arm of the beam assembly teleoperator
[AD-A156856] N86-10832
The development of a neutron evaporation theory code for the thermal fission of Uranium-235
[AD-A156593] N86-10951
ARMY TEST AND EVALUATION COMMAND, ABERDEEN PROVING GROUND, MD.
Test, measurement, and diagnostic equipment (system peculiar)
[AD-A156669] N86-10563
ATLANTA UNIV., GA.
Theoretical investigation of electron-positive ion-atom interactions
[DE85-013019] N86-10939
ATMOSPHERIC AND ENVIRONMENTAL RESEARCH, INC., CAMBRIDGE, MASS.
Cometary atmospheres: Modeling the spatial distribution of observed neutral radicals
[NASA-CR-176242] N86-11133

B

BATTELLE COLUMBUS LABS., OHIO.
Research needs for corrosion control and prevention in energy conservation systems
[DE85-014852] N86-10326
Evaluation of Passive Sampling Devices (PSDs)
[PB85-196418] N86-10689
BATTELLE INST., FRANKFURT AM MAIN (WEST GERMANY).
Liquids and interfaces N86-10268
BATTELLE MEMORIAL INST., COLUMBUS, OHIO.
The influence of containerless undercooling and rapid solid-state quenching on the superconductive and magnetic properties of some clustering alloy systems N86-10076
BJORKSTEN RESEARCH LABS., INC., MADISON, WIS.
Continuous fiberization of silicon-carbide-nitride precursor resin N86-10168
Levitating furnance for containerless processing in space N86-10169
Electric field containerless processing technology N86-10170
BOLOGNA UNIV. (ITALY).
Melting and solidification in O-g of sintered alloys: Experiments ES 311 A and B bubble reinforced materials N86-10215
BONN UNIV. (WEST GERMANY).
Partial in-flight calibration of the metric camera N86-10496
BONNEVILLE POWER ADMINISTRATION, PORTLAND, OREG.
Passive solar design handbook
[DE85-014263] N86-10656
BOSTON UNIV., MASS.
Gravitational collapse of a scalar field N86-11129
BRANDEIS UNIV., WALTHAM, MASS.
Radio studies of a complete sample of quasars N86-11093
BRISTOL UNIV. (ENGLAND).
Kinetics of spreading of liquids in microgravity: Experiment 1 ES 327 N86-10207
BRITISH AEROSPACE AIRCRAFT GROUP, BRISTOL (ENGLAND).
Pre-bond treatment for titanium alloys
[BAE-AL/MAT/3864] N86-10309
BRITISH BROADCASTING CORP., KINGSWOOD (ENGLAND).
An evaluation of the use of microphone arrays for studio recording
[BBC-RD-1985/8] N86-10366
BROOKHAVEN NATIONAL LAB., UPTON, N. Y.
Streaming potentials in conductive and nonconductive tubing
[DE85-012984] N86-10438
Improved blue response and efficiency of A-Si:H solar cells deposited from disilane using a dual-chamber plasma system
[DE85-013289] N86-10649
Seasonal variations in atmospheric chemistry in the Adirondacks
[DE85-014227] N86-10719
Method for determining the position, angle and other injection parameters of a short pulsed beam in the Brookhaven AGS
[DE85-012523] N86-10931
Method for compensating bellows pressure loads while accommodating thermal deformations
[DE85-013306] N86-10933
AGS polarized H(-) source
[DE85-013296] N86-10935
Methane-bubble formation in hydrogen-charged Fe-30 ppM C
[DE85-012526] N86-10937
Beam profile monitor for the NSLS VUV ring employing linear photodiode arrays
[DE85-012184] N86-10947
Surface conditioning of synchrotron radiation source to improve beam lifetime
[DE84-012185] N86-10948
Separated K(-) beams (10 GeV and above)
[DE85-012527] N86-10989
Microwave instability across the transition energy
[DE85-013304] N86-11010
Theory of non-planar orbits
[DE85-013284] N86-11018
Thermal and structural analysis of ring components by the finite element method
[DE85-013305] N86-11021
Unicell structure for superconducting storage rings
[DE85-013303] N86-11022
Tracking studies on the effects of magnet multipoles on the aperture of the RHIC heavy ion collider
[DE85-013282] N86-11023
RHIC lattice
[DE85-013289] N86-11026
BUNDESMINISTERIUM FUER FORSCHUNG UND TECHNOLOGIE, BONN (WEST GERMANY).
Satellite use for men N86-10180
How Antarctica was unveiled. Masterpieces of Frankfurt topographic surveyors. A part of the German Antarctica research program N86-10181
Satellite data even for a poultry farm. A development for Tanzania. Image evaluation following new ways N86-10182
With Argus eyes from space. Satellite Diagnosis for Upper Volta. Seven maps without mystery N86-10183
The air of life of the blue planet. Atmosphere research from space using data and facts against climate speculations N86-10184
A nanosecond or thirty centimeters: Why atomic clocks have to be synchronized. MITREX opens new dimensions for measuring accuracy N86-10185
Growth of larger single crystals N86-10186
Space utilization N86-11067
Space sciences: Perspectives of commercial utilization for the German industry N86-11068
DFVLR, strategic study of astronautics 1984, user requirements N86-11069
Space research expenses of the Federal Ministry of Research and Technology (BMFT) in the period 1983-1985 N86-11070
BURNS AND ROE, INC., ORADELL, N. J.
Hot cell facility design for large fusion devices
[DE85-012893] N86-11037

C

CALIFORNIA INST. OF TECH., PASADENA.
Formation and characterization of amorphous erbium-based alloys prepared by near-isothermal cold-rolling of elemental composites
[DE85-014853] N86-10327
VLBI at optical and radio wavelengths: Congruences and contrasts N86-11126
CALIFORNIA UNIV., BERKELEY.
Free surface phenomena under low- and zero-gravity conditions N86-10108
A fundamental study of smoldering with emphasis on experimental design for zero-g N86-10162
CALIFORNIA UNIV., BERKELEY. LAWRENCE BERKELEY LAB.
Electronic and magnetic properties of noble-metal and transition-metal alloys, interfaces and overlayers
[DE85-014532] N86-10321
Defect identification in high-energy semiconductors
[DE85-014533] N86-10442
Effect of H2S and COS in the fuel gas on the performance of ambient pressure phosphoric acid fuel cells
[DE85-013913] N86-10446
Report on the engineering test of the LBL 30 second neutral beam source for the MFTF-B project
[DE85-013317] N86-10962
Integrating sphere measurements of directional-hemispherical transmittance of window systems
[DE85-013926] N86-10978
Superconvergent tracking and invariant surfaces in phase space
[DE85-013051] N86-10995
Proceedings of a Workshop on Electroweak Symmetry Breaking
[DE85-004444] N86-11008
Surface science and catalysis
[DE85-013922] N86-11057
CALIFORNIA UNIV., IRVINE, DAYTON, OHIO.
Evaluation of the 90-day inhalation toxicity of petroleum and oil shale JP-5 jet fuel
[AD-A156815] N86-10675
CALIFORNIA UNIV., LIVERMORE. LAWRENCE LIVERMORE LAB.
New directions in chemical analysis
[DE85-012930] N86-10296
Hugoniot measurements in aluminum to 420 GPa using the LLNL two-stage light-gas gun
[DE85-013821] N86-10317
Nonlinear propagation of elastoplastic waves in Ke penetrators (excerpts)
[DE85-011450] N86-10318
Work-hardening and effective viscosity in solid beryllium
[DE85-013978] N86-10323
Composite explosives for metal acceleration: The effect of detonation temperature
[DE85-013982] N86-10359
Microwave evaluation of materials
[DE85-013183] N86-10409
Angle of incidence effects for underwater shock using generic computational models
[DE85-012936] N86-10466
Angle of incidence effects for underwater shock using generic computational models, rev. 1
[DE85-012921] N86-10467
Spontaneous Raman spectroscopy of shocked H2O
[DE85-014557] N86-10470
Time-implicity simulation of particle-fluid systems
[DE85-012944] N86-10471
Improved particle-velocity transducer for equation-of-state experiments
[DE85-013204] N86-10532
Application of the ruthenium and technetium thermodynamic data bases used in the EQ3/6 geochemical codes
[DE85-013766] N86-10632
Smoke inputs to climate models: Optical properties and height distribution for nuclear winter studies
[DE85-011363] N86-10717
Microphysical/mesoscale aspects of nuclear winter and new directions in assessments
[DE85-013479] N86-10718
Somatic cell and molecular genetics approach to DNA repair and mutagenesis
[DE85-014181] N86-10737
New approach to multiphase equilibria: Application to high-pressure physics problems
[DE85-013820] N86-10907
Cryogenic structural materials for superconducting magnets
[DE85-008026] N86-10908
Mean life of the 2p(4)((1)S)3s (2)S state in fluorine
[DE85-012929] N86-10956
Impact of long-lived radionuclides on waste classification for fusion
[DE85-013205] N86-10959
Theoretical aspects of magnetic helicity
[DE85-011846] N86-10984
Compact torus compression of microwaves
[DE85-012919] N86-11016
Application of structural-mechanics methods to the design of large tandem-mirror fusion devices (MFTF-B)
[DE85-008960] N86-11017
Liquid to gas leak ratios with liquid nitrogen and liquid helium
[DE85-012950] N86-11030
Writer/editor and the computer
[DE85-011843] N86-11080
Stellar s-process diagnostics
[DE85-012926] N86-11134
CALIFORNIA UNIV., LOS ANGELES.
High temperature mechanical testing of a cylindrical weave carbon-carbon composite
[AD-A156639] N86-10591
CALIFORNIA UNIV., SAN DIEGO, LA JOLLA.
Particle cloud combustion experiment N86-10160
CALIFORNIA UNIV., SANTA BARBARA.
Theoretical problems in materials science N86-10088
Paleontology and stratigraphy of Lower Cambrian and upper Proterozoic sediments, Caborca region, northwestern Sonora, Mexico N86-10692
Structural discontinuity within the southern California continental margin: Seismic and gravity models of the western Transverse Ranges N86-10699
CAMBRIDGE UNIV. (ENGLAND).
Astronomical criteria for interferometric arrays N86-11099

CANADIAN ASTRONAUTICS LTD., OTTAWA (ONTARIO).
Numerical simulation of convections in the microgravity environment N86-10239
CARNEGIE-MELLON INST. OF RESEARCH, PITTSBURGH, PA.
Implementation issues for algorithmic VLSI (Very Large Scale Integration) processor arrays [AD-A156699] N86-10432
CARNEGIE-MELLON UNIV., PITTSBURGH, PA.
Ignition and flame spread above liquid fuel pools N86-10163
Fault-free behavior of reliable multiprocessor systems: FTMP experiments in AIRLAB [NASA-CR-177967] N86-10848
Two algorithms for weighted matroid intersection [AD-A156525] N86-10861
Derivational analogy: A theory of reconstructive problem solving and expertise acquisition [AD-A156817] N86-10899
CARNEGIE MUSEUM OF NATURAL HISTORY, PITTSBURGH, PA.
Paleogene vertebrate paleontology, geology and remote sensing in the Wind River Basin N86-10609
CARRIER CORP., SYRACUSE, N.Y.
Advanced absorption heat pump cycles [DE85-003914] N86-10654
CASE WESTERN RESERVE UNIV., CLEVELAND, OHIO.
Solidification fundamentals N86-10090
Surface-tension driven convection N86-10124
Fundamental studies of low velocity impact resistance of graphite fiber reinforced polymer matrix composites N86-10288
Theoretical and numerical investigation of dipole radiation over a flat earth N86-10369
Finite element analysis of statics and dynamic structural engineering problems using semi-explicit methods N86-10571
Optimal control modeling of lower extremity musculoskeletal motion N86-10853
CENTER FOR MATHEMATICS AND COMPUTER SCIENCE, AMSTERDAM (NETHERLANDS).
Partial evolution and omega completeness of algebraic specifications [CWI-CS-R8501] N86-10884
CENTRE D'ETUDES AERODYNAMIQUES ET THERMIQUES, POITIERS (FRANCE).
Spectral methods in adapted curved grids N86-10878
CENTRE D'ETUDES ET DE RECHERCHES GEODYNAMIQUES ET ASTRONOMIQUES, ST. VALLIER DE THIEY (FRANCE).
Results and limitations of ground-based optical arrays N86-11097
Strategy for the development of space arrays N86-11101
TRIO: A kilometric array stabilized by solar sails N86-11102
Fringe drift compensation in computer memory N86-11112
TRIANGLE: A different design for a three satellite interferometer in space N86-11113
Problems in image reconstruction with optical arrays N86-11115
On line astronomical image processing using microcomputers N86-11121
The intensified multi CCD camera N86-11122
The DUO: Far infrared heterodyne concept for space interferometry N86-11125
CENTRE NATIONAL D'ETUDES SPATIALES, TOULOUSE (FRANCE).
Gradient heating facility behavior N86-10217
CENTRE NATIONAL DE LA RECHERCHE SCIENTIFIQUE, MARSEILLES (FRANCE).
TRIO optics N86-11108
Solar propulsion for the TRIO interferometer N86-11109
TRIO interferometer positioning N86-11111
CENTRE NATIONAL DE LA RECHERCHE SCIENTIFIQUE, MEUDON-BELLEVUE (FRANCE).
Oscillations of semi-free liquids in microgravity: Spacelab 1 experiment ES 326 N86-10204
Lead telluride crystals grown in microgravity: Experiment ES 318 N86-10220
CENTRE NATIONAL DE LA RECHERCHE SCIENTIFIQUE, TOULOUSE (FRANCE).
Aperture synthesis with or without phase information for kilometric arrays interpolation algorithms for stabilized image reconstruction N86-11124
CENTRE NATIONAL DE LA RECHERCHE SCIENTIFIQUE, VERRIERES-LE BUISSON (FRANCE).
A fiber-linked version of project TRIO N86-11105
CENTRONIC LTD., CROYDON (ENGLAND).
Making the right choice N86-10669
CESKOSLOVENSKA AKADEMIE VED, PRAGUE.
Experimental facility for materials research in space (CSK-1) N86-10263
CHALMERS UNIV. OF TECHNOLOGY, GOTEBORG (SWEDEN).
Error estimates and automatic time step control for numerical methods for stiff ordinary differential equations [CTH-MATH-1984-27] N86-10872
On the absolute continuity of elliptic measures [CTH-MATH-1984-28] N86-10873
Estimates for maximal functions along hypersurfaces [CTH-MATH-1984-29] N86-10874
On maximal and distributional coupling [CTH-MATH-1984-30] N86-10875
Poisson semigroups and singular integrals [CTH-MATH-1985-05] N86-10876
Brauer-Severi schemes of orders [CTH-MATH-1985-06] N86-10877
Some remarks about cusp forms: Holomorphic and non-holomorphic [CTH-MATH-1984-26] N86-10902
On class groups of lattices [CTH-MATH-1985-08] N86-10903
Galois descent and class groups of orders [CTH-MATH-1985-09] N86-10904
CHRONAR CORP., PRINCETON, N.J.
Photovoltaic devices using a Si:H from higher order silanes [DE85-008804] N86-10668
CITY UNIV. OF NEW YORK, N.Y.
Magnetic properties of doped semiconductors [DE85-012090] N86-11053
CLARKSON COLL. OF TECHNOLOGY, POTSDAM, N.Y.
Study of eutectic formation N86-10070
Modeling directional solidification N86-10071
Physical phenomena in containerless glass processing N86-10155
CLEMSON UNIV., S.C.
An analytical and numerical study of the buckling behavior of fiber-reinforced beams N86-10566
COASTAL ENGINEERING RESEARCH CENTER, VICKSBURG, MISS.
Application of the dutch method for estimating storm-induced dune erosion [AD-A156717] N86-10728
COLLEGE OF WILLIAM AND MARY, WILLIAMSBURG, VA.
Study of statis and dynamic stress effects in nonlinear solids [NASA-CR-176236] N86-10578
COLORADO UNIV., BOULDER.
Thermocapillary and diffusocapillary migration of a fluid drop N86-10128
Compexity of higher-order programs [DE85-012776] N86-10834
COLUMBIA UNIV., NEW YORK.
A procedure identifying a polyacetylene initiator of olefin metathesis. The reactivities of metal-carbenes toward alkenes and alkynes [AD-A156997] N86-10283
Fundamental study of the closure property of joints N86-10698
In-situ geophysical investigations into the nature of the oceanic crust N86-10725
A quantitative method for analyzing the roughness of the seafloor N86-10726
A superconducting tunnel junction receiver for millimeter-wave astronomy N86-11041
COMMISSARIAT A L'ENERGIE ATOMIQUE, GRENOBLE (FRANCE).
Mephisto: Interfacial destabilization in metal alloys N86-10079
Directional solidification of monotectic and hypermonotectic aluminum-indium alloys under micron-g N86-10097
Directional solidification of an aluminum-zinc vapor emulsion in microgravity N86-10218
Directional solidification of eutectic alloys N86-10219
Thermomigration of cobalt in liquid tin: Experiment 1 ES 320 N86-10222
Cellular morphologies in lead-thallium alloys N86-10262
First Spacelab Payload (FSLP) experiments in metallurgy N86-10266
COMMITTEE ON ENERGY AND COMMERCE (U. S. HOUSE).
Biotechnology regulation [GPO-43-778] N86-10733
CONCORDIA UNIV., MONTREAL (QUEBEC).
Chemical kinetics and cellular structure of detonations in hydrogen sulphide and air [DE85-009408] N86-10304
CONSERVATION AND RENEWABLE ENERGY INQUIRY AND REFERRAL SERVICE, SILVER SPRING, MD.
Geothermal Energy Technology Program summary [DE85-013101] N86-10646
Passive and hybrid solar technologies program summary [DE85-013100] N86-10648
Ocean energy technology program summary [DE85-013102] N86-10731

D

DARTMOUTH COLL., HANOVER, N.H.
Analysis of annular two-phase flow with liquid entrainment N86-10459
DAYTON UNIV., OHIO.
Process models for 3D composites [AD-A156889] N86-10292
DEERE AND CO., MOLINE, ILL.
Control of cast iron microstructure N86-10084
DEFENCE RESEARCH ESTABLISHMENT, OTTAWA. (ONTARIO).
SARSAT LUC (Local user terminal) to CMCC (Canadian Mission Control Centre) alert data interface: A critical review [AD-A156881] N86-10276
Design and calibration of a flat-flame burner using line reversal techniques [AD-A156724] N86-10294
Effect of increased body clothing insulation on hand temperature in a cold environment [AD-A156597] N86-10786
DEFENCE RESEARCH ESTABLISHMENT VALCARTIER (QUEBEC).
An active tracking band-pass filter [AD-A156559] N86-10419
Acceleration-invariant approximation method for recursive digital filters [AD-A156655] N86-10865
DELAWARE UNIV., NEWARK.
Mechanics of coated fiber composites N86-10285
The interpolation of signals sampled at less than the Nyquist rate N86-10368
DELFT HYDRAULICS LAB. (NETHERLANDS).
The Rhine-Meuse estuary hydraulic scale model. Experiences with computer configuration and software [PUBL-335] N86-10637
DEPARTMENT OF ENERGY, ARGONNE, ILL.
Evaluation of the International Atomic Energy Agency (IAEA) Safeguards Analytical Laboratory quality assurance program [DE85-012078] N86-10953
DEPARTMENT OF ENERGY, OAK RIDGE, TENN.
Computer codes: A bibliography, supplement 1 [DE85-008721] N86-10838
DEPARTMENT OF ENERGY, PITTSBURGH, PA.
Microcomputer aided calculations of parameters for spray dryer operation [DE85-013468] N86-10681
DEPARTMENT OF ENERGY, WASHINGTON, D. C.
Counterpulse railgun energy recovery circuit [DE85-011603] N86-10196
Overpulse railgun energy recovery circuit [DE85-011607] N86-10197
Aluminum battery alloys [DE85-011599] N86-10445
DEPARTMENT OF THE AIR FORCE, WASHINGTON, D.C.
Submerged ram air inlets for ECM (electronic countermeasures) pods [AD-D011801] N86-10020
Attachment method-ceramic radome to metal body [AD-D011778] N86-10032
Small cartridge heater [AD-D011784] N86-10277
Erosion-resistant nosetip construction [AD-D011787] N86-10289
Liquid crystal non-destructive inspection of metals [AD-D011772] N86-10316
Synthesis of arylene siloxanylene polymers and copolymers [AD-D011780] N86-10338
Gas generator fuel flow throttle control system [AD-D011797] N86-10355
Angle set-on apparatus [AD-D011766] N86-10371
Method for tuning a phased array antenna [AD-D011768] N86-10372
High sensitivity millimeter-wave measurement apparatus [AD-D011786] N86-10373
Sample data phase locked loop for adaptive Doppler tracker [AD-D011788] N86-10374
Protection circuitry for high voltage drivers [AD-D011781] N86-10414
Total internal reflection modulator/deflector [AD-D011757] N86-10424

Instantaneous frequency measurement receiver with digital processing
[AD-D011759] N86-10425
Photoionization technique for growth of metallic films
[AD-D011760] N86-10426
Signal analysis receiver with acousto-optic delay lines
[AD-D011761] N86-10427
Apparatus for locating passive intermodulation interference sources
[AD-D011798] N86-10435
Interdigital Schottky barrier capacitor apparatus
[AD-D011799] N86-10436
Multi-row connector with ground plane board
[AD-D011803] N86-10437
Sensor system
[AD-D011767] N86-10480
Stereoscopic video imagery generation
[AD-D011785] N86-10481
Fall velocity indicator/viewer
[AD-D011789] N86-10482
Captive volume device as a safe life monitor
[AD-D011802] N86-10525
Laser target speckle eliminator
[AD-D011775] N86-10536
Over-center toggle latch
[AD-D011753] N86-10556
Termination load carrying device
[AD-D011800] N86-10558
Nickel-cadmium battery conditioner and tester apparatus
[AD-D011770] N86-10642
Multiple site laser excited pollution monitoring system
[AD-D011769] N86-10674
Vision test chart and method using Gaussians
[AD-D011756] N86-10778
Harmonic distortion reduction technique for data acquisition
[AD-D011771] N86-10799
Arithmetic pipeline for image processing
[AD-D011773] N86-10800
Infrared system with computerized image display
[AD-D011777] N86-10906
Tunable acousto-optic filter with improved spectral resolution and increased aperture
[AD-D011758] N86-10915
Kalman filter preprocessor
[AD-D011774] N86-10972
Measurement of visual contrast sensitivity
[AD-D011776] N86-10973
Optical disc transport system
[AD-D011779] N86-10974

DEPARTMENT OF THE ARMY, WASHINGTON, D. C.
Recovery of alcohol from a fermentation source by separation rather than distillation
[AD-D011782] N86-10282

DEPARTMENT OF THE NAVY, WASHINGTON, D. C.
Improved arresting and recovery system for test missiles
[AD-D011743] N86-10198
Rusty bolt intermodulation interference reducer
[AD-D011748] N86-10313
Passivation of steel with aqueous amine solutions
[AD-D011749] N86-10314
Phase-coded pulse expander-compressor
[AD-D011812] N86-10375
Phase coded pulse expander-compressor
[AD-D011817] N86-10376
Amplitude and phase modulation in fin-lines electrical tuning
[AD-D011813] N86-10415
P-N junction controlled field emitter array cathode
[AD-D011815] N86-10416
Pulse compression system
[AD-D011833] N86-10417
Constant rise AGC (Automatic Gain Control) device
[AD-D011744] N86-10421
Extended precision in video bandwidth analog to digital converter using optical techniques
[AD-D011745] N86-10422
High output programmable signal current source for low output impedance applications
[AD-D011751] N86-10423
Precise bearing support ditherer with piezoelectric drive means
[AD-D011819] N86-10483
Device for cryogenically fabricating source material for plasma X-ray lasers
[AD-D011814] N86-10537
W-shaped diffused stripe GaAs/AlGaAs laser
[AD-D011818] N86-10538
AIRBOC (air rapid bloom offboard chaff) chaff deployment system
[AD-D011746] N86-10554
Marginal terrain straddle-lift container handler
[AD-D011752] N86-10555
Parallel local interface bus
[AD-D011742] N86-10792
Spatial frequency multiplexed coherent optical processor for calculating generalized moments
[AD-D011816] N86-10975
Fiber optic system for measuring electric fields
[AD-D011830] N86-10976

DEUTSCHE FORSCHUNGS- UND VERSUCHSANSTALT FUER LUFT- UND RAUMFAHRT, BRUNSWICK (WEST GERMANY).
Control concepts for in-flight simulation including actuator nonlinearities and time delays
[DFVLR-FB-85-24] N86-10047

DEUTSCHE FORSCHUNGS- UND VERSUCHSANSTALT FUER LUFT- UND RAUMFAHRT, COLOGNE (WEST GERMANY).
Tendencies toward liberalization in European air traffic control
[DFVLR-FB-85-23] N86-10030
The air traffic demand in passenger travel of the Federal Republic of Germany 1990 - 2000. Update of the DFVLR air traffic forecast
[DFVLR-MITT-85-06] N86-10031
The first German Spacelab mission D1 reports
[PR-1] N86-10187
The first German Spacelab mission D1 reports
[PR-2] N86-10188
The first German Spacelab mission D1 reports
[PR-3] N86-10189
The isothermal heating facility N86-10208
Holographic interferometry near gas/liquid critical points: Ground-based study of a D1 experiment N86-10249
Transport processes in directional solidification during space shuttle flight N86-10257
Stability of metallic dispersions N86-10258
Undercooling investigations on the easy glass former Pd-Cu-Si N86-10259
Containerless undercooling of Ni N86-10260
Status of preparation activities for metric camera reflight on EOM-1/2 N86-10506

DEUTSCHE FORSCHUNGS- UND VERSUCHSANSTALT FUER LUFT- UND RAUMFAHRT, GOETTINGEN (WEST GERMANY).
Investigations on a supercritical airfoil with boundary layer suction through a perforated strip in the shock region
[DFVLR-FB-85-15] N86-10025
Experimental and theoretical investigations of the flow around airfoil systems with ground effect
[DFVLR-FB-85-17] N86-10026
Investigation of density gradient fluctuations in a turbulent free jet by means of the laser schlieren crossed-beam method
[DFVLR-FB-85-19] N86-10027
The rubber tube test section of the DFVLR in Goettingen, West Germany
[DFVLR-FB-85-18] N86-10051

DEUTSCHE FORSCHUNGS- UND VERSUCHSANSTALT FUER LUFT- UND RAUMFAHRT, HAMBURG (WEST GERMANY).
Extended analysis of the structure of error scores in psychological aptitude tests
[DFVLR-FB-85-20] N86-10780
Speed of work and error rate: Analyses of individual differences in a choice reaction series with a cognitive component
[DFVLR-FB-85-21] N86-10781

DEUTSCHE FORSCHUNGS- UND VERSUCHSANSTALT FUER LUFT- UND RAUMFAHRT, OBERPFAFFENHOFEN (WEST GERMANY).
Direct-coupled cavity filters with irises of arbitrary thickness
[DFVLR-FB-85-14] N86-10412
SAR image quality: A review
[DFVLR-MITT-85-07] N86-10413
Line mapping and resolution tests with metric camera data N86-10500
Experimental investigations of pulse-pulse interference in heterodyne detection
[DFVLR-FB-85-26] N86-10544
Calibration of the multispectral scanner (MSS) satellite data to evaluate change in the reflection of coniferous stocks
[DFVLR-FB-84-44] N86-10636
Airborne measurements of the border-crossing air pollution in the area between Weiden and Hof/Bavaria
[DFVLR-FB-85-25] N86-10685
Comparative flight measurement of icing parameters for the propeller aircraft Do-28D2 of the test station 61 of the DFVLR and for the DFVLR aircraft Falon 20e in stratus clouds
[DFVLR-FB-85-16] N86-10720
User manual for the Falcon system
[DFVLR-MITT-85-08] N86-10721
Scattering by complicated structures: Calculation of the radar properties of metallic targets by means of physical optics
[DFVLR-FB-85-22] N86-10981

DEUTSCHE GOLD- UND SILBER-SCHEIDEANSTALT, FRANKFURT AM MAIN (WEST GERMANY).
Reduction of noble metal stock and noble metal loss during wire production with the Conform extrusion process
[BMFT-FB-T-85-049] N86-10560

DU PONT DE NEMOURS (E. I.) AND CO., AIKEN, S.C.
Multipurpose pan development
[DE85-012326] N86-10319
Recirculation within a glass mixture subjected to external and resistive heating
[DE85-010068] N86-10348

DUKE UNIV., DURHAM, N. C.
Critical transport phenomena in fluid helium under low gravity N86-10119

E

ECOLE POLYTECHNIQUE FEDERALE DE LAUSANNE (SWITZERLAND).
Erosion control and watershed management by Spacelab photography N86-10493

EDGERTON, GERMESHAUSEN AND GRIER, INC., GOLETA, CALIF.
Hgl sub 2 crystal growth for nuclear detectors N86-10066
Parallel pulse processing for mercuric iodide gamma-ray detectors
[DE85-013391] N86-10528

EDGERTON, GERMESHAUSEN AND GRIER, INC., IDAHO FALLS, IDAHO.
Fracture toughness and stress relief response of irradiated type 347/348 stainless steel N86-10320
Velocities of gas and plasmas from real time holographic interograms
[DE85-014618] N86-10530
Kinetics of biological ferrous iron oxidation
[DE85-014616] N86-10736

EIDGENOESSISCHE TECHNISCHE HOCHSCHULE, ZURICH (SWITZERLAND).
Crystal growth from solutions and nucleation from the vapor phase N86-10267

EIDGENOESSISCHES FLUGZEUGWERK, EMMEN (SWITZERLAND).
Investigations to improve the slotted-wall test section of the F+W transonic wind tunnel
[F+W-FO-1752] N86-10050

ELECTRONICS RESEARCH LAB., ADELAIDE (AUSTRALIA).
A compact bulk acousto-optic time integrating correlator
[AD-A156608] N86-10428

ELORET CORP., SUNNYVALE, CALIF.
The interaction of small metal particles with refractory oxide supports
[NASA-CR-176228] N86-11047

ENGINEERING-SCIENCE, INC., FAIRFAX, VA.
Emissions of NOx, SOx and VOC from Antropogenic sources
[PB85-193530] N86-10688

ENVIRONMENTAL PROTECTION AGENCY, RESEARCH TRIANGLE PARK, N.C.
Volatile organic compounds in indoor air: A survey of various structures
[PB85-198356] N86-10687

ERLANGEN-NUREMBERG UNIV. (WEST GERMANY).
Directional solidification of InSb-NiSb eutectic N86-10221
Imaging speckle interferometer in space: Digital simulations of image reconstruction and photon noise N86-11120

ESDU INTERNATIONAL LTD., LONDON (ENGLAND).
Summary of work on jet noise prediction
[ESDU-BR-82636] N86-10909

EUROPEAN ORGANIZATION FOR NUCLEAR RESEARCH, GENEVA (SWITZERLAND).
Applications of the second-order achromat concept to the design of particle accelerators
[DE85-013072] N86-10994

EUROPEAN SOUTHERN OBSERVATORY, MUNICH (WEST GERMANY).
Activities report of the European Southern Observatory N86-11135

EUROPEAN SPACE AGENCY, PARIS (FRANCE).
System modeling and identification of equivalent systems with and without compensating time delay for control-augmented aircraft
[ESA-TT-852] N86-10043
Fifth European symposium on Material Sciences under Microgravity. Results of Spacelab 1
[ESA-SP-222] N86-10200

First Spacelab Payload (FSLP) experiments on composite materials N86-10265
Low temperature plastic deformation mechanisms of alpha-titanium single crystals
[ESA-TT-871] N86-10332
Metric Camera Workshop
[ESA-SP-209] N86-10485
Colloquium on Kilometric Optical Arrays in Space
[ESA-SP-226] N86-11096

EUROPEAN SPACE AGENCY. EUROPEAN SPACE OPERATIONS CENTER, DARMSTADT (WEST GERMANY).
Mission analysis aspects N86-11114

EUROPEAN SPACE AGENCY. EUROPEAN SPACE RESEARCH AND TECHNOLOGY CENTER, ESTEC, NOORDWIJK (NETHERLANDS).
The fluid physics module: A technical description N86-10201
Preliminary studies of a spinning tether-connected TRIO concept N86-11110

EXECUTIVE OFFICE OF THE PRESIDENT, WASHINGTON, D. C.
Publication of the Executive Office of the President, January 20, 1981 - December 31, 1984
[PB85-187110] N86-11082

EXXON RESEARCH AND ENGINEERING CO., ANNANDALE, N.J.
Laser Raman spectroscopy study of the zinc and bromide ion complex equilibrium in zinc/bromine battery electrolytes
[DE85-011820] N86-10301

F

FACHHOCHSCHULE, GIESSEN (WEST GERMANY).
Contribution of wind energy to the energy balance of a combined solar and wind energy system. Part 1: System description, data acquisition and system performance
[BMFT-FB-T-85-051-VOL-1] N86-10670

FEDERAL AVIATION ADMINISTRATION, WASHINGTON, D.C.
The effects of age, sleep deprivation, and altitude on complex performance
[AD-A156987] N86-10771

FEDERATION OF AMERICAN SOCIETIES FOR EXPERIMENTAL BIOLOGY, BETHESDA, MD.
LSRO/ONR ad hoc review process
[AD-A156590] N86-10735

FERMI NATIONAL ACCELERATOR LAB., BATAVIA, ILL.
Hyperon polarization: An unresolved problem
[DE85-012298] N86-10946
Field-independent normalization of SSC Collider Ring costs
[DE85-012425] N86-10997

FLORIDA UNIV., GAINESVILLE.
Research on solar pumped liquid lasers
[NASA-CR-176235] N86-10539
Analytical and experimental study of cracks emanating from an elliptical hole in unidirectional composite material N86-10567
Inelastic analysis of frame structures including member and joint shears N86-10573

FOM-INST. VOOR PLASMAFYSICA, RIJNHUIZEN, JUTPHAAS (NETHERLANDS).
Activities report in plasma physics N86-11039

FRAUNHOFER-INST. FUER BETRIEBSFESTIGKEIT, DARMSTADT (WEST GERMANY).
Review of investigations on aeronautical fatigue in the Federal Republic of Germany
[LBF-S-173] N86-10044

FRAUNHOFER INST. FUER WERKSTOFFMECHANIK, FREIBURG (WEST GERMANY).
Numerical simulation of crack arrest experiments on Araldite B using the finite difference method
[REPT-W-9/82] N86-10596

FREIBURG UNIV. (WEST GERMANY).
The mirror heating facility: Performance and experiences N86-10223
Solution growth of cadmium telluride: Experiment ES 322 N86-10225
Crystal growth of silicon in Spacelab 1: Experiment ES-321 N86-10227
Protein single crystal growth under microgravity N86-10228
Requirements and possibilities of Spacelab metric camera photos usage for inventories of large areas of extensively managed forests N86-10513

G

GA TECHNOLOGIES, INC., SAN DIEGO, CALIF.
High efficiency heat transport and power conversion system for cascade
[DE85-012959] N86-10468
GA Theory News, January-March 1985
[DE85-012572] N86-11007

GARRETT MFG. LTD., REXDALE (ONTARIO).
Advanced Gas Turbine (AGT) powertrain system development for automotive applications report
[NASA-CR-174886] N86-11087

GELLES (S. H.) ASSOCIATES, COLUMBUS, OHIO.
Liquid phase miscibility gap materials N86-10081
Space shuttle experiments on Al-In liquid phase miscibility gap (LPMG) alloys N86-10264

GENERAL ELECTRIC CO., PHILADELPHIA, PA.
Modification of the electromagnetic levitator (EML) hardware N86-10172

GEOLOGICAL SURVEY, RESTON, VA.
High-resolution image data from the Space Shuttle N86-10494
SUTRA (Saturated-unsaturated transport). A finite-element simulation model for saturated-unsaturated, Fluid-Density-Dependent ground-water flow with energy transport or chemically-reactive single-species solute transport
[AD-A156779] N86-10830

GEOLOGICAL SURVEY, SIOUX FALLS, S. DAK.
Some opinions on remote sensing and geologic studies N86-10600

GEOLOGICAL SURVEY OF CANADA, OTTAWA (ONTARIO).
NBSGSC: A FORTRAN program for quantitative X-ray fluorescence analysis
[PB85-206068] N86-10847

GEORGE MASON UNIV., FAIRFAX, VA.
An annotated bibliography of abstracts on the use of simulators in technical training
[AD-A156792] N86-11065

GEORGE WASHINGTON UNIV., WASHINGTON, D.C.
Suppression of Marangoni convection in float zones N86-10111

GEORGIA INST. OF TECH., ATLANTA.
A study of the aerodynamic performance of Weis-Fogh wings N86-10012
The effect of debond growth on crack propagation in composite plates reinforced with adhesively bonded composite stringers N86-10287
Steady state frictional behavior of thin film coatings N86-10335
The measurement and application of transport properties of ion swarms in gases N86-10370
Angle of incidence effects for underwater shock using generic computational models
[DE85-012936] N86-10466
Angle of incidence effects for underwater shock using generic computational models, rev. 1
[DE85-012921] N86-10467
The use of new path indepedent integrals in elastic-plastic and creep fracture N86-10574
Analysis of large, non-isothermal elastic-visco-plastic deformations
[NASA-CR-176220] N86-10588
Bounding solutions of geometrically nonlinear viscoelastic problems
[NASA-CR-176219] N86-10860
Development and application of the electrochemical etching technique
[DE85-010302] N86-10957

GERMAN-DUTCH WIND TUNNEL, NORTH EAST POLDER (NETHERLANDS).
Activities report of the German-Dutch wind tunnel N86-10029
Activities report of the German-Dutch wind tunnel N86-10052

GESAMTHOCHSCHULE, ESSEN (WEST GERMANY).
Verification of turbulence developing from the oscillatory Marangoni convection in a liquid column N86-10241

GESELLSCHAFT FUER SCHWERIONENFORSCHUNG M.B.H., DARMSTADT (WEST GERMANY).
Information on continuum states from feeding times and total (GAMMA) spectra measured with BGO suppressed detectors
[DE85-013868] N86-10961

GIESSEN UNIV. (WEST GERMANY).
Measurements of the critical Marangoni number of the laminar-oscillatory transition of thermocapillary convection in floating zones N86-10242

GKSS-FORSCHUNGSZENTRUM GEESTHACHT (WEST GERMANY).
The boundary condition in a numerical model of atmospheric flows over fixed interfaces
[GKSS-85-E-10] N86-10722

GOETTINGEN UNIV. (WEST GERMANY).
The influence of thermocapillarity on the migration of droplets in a liquid possessing a uniform temperature gradient N86-10237

GRONINGEN RIJKSUNIVERSITEIT (NETHERLANDS).
Wind energy in agriculture: a promise
[SS-45] N86-10672

Wind energy, a feasibility investigation for wind mills in agriculture
[SS-45A] N86-10673
A modified Successive Over-Relaxation (SOR) method for the Poisson equation in unsteady free-surface flow calculations
[TW-264] N86-10881
On the numerical determination of the dimension of an attractor
[ZW-8415] N86-10892
A note on the differenciability of center manifolds
[ZW-8414] N86-10905
The OASIS correlator N86-11119

GRUMMAN AEROSPACE CORP., BETHPAGE, N.Y.
Orbital processing of aligned magnetic composites N86-10089
Thermal and solutal convection damping using an applied magnetic field N86-10094

H

HAMBURG UNIV. (WEST GERMANY).
Influences affecting separation in monotectic alloys under microgravity N86-10209

HARVARD-SMITHSONIAN CENTER FOR ASTROPHYSICS, CAMBRIDGE, MASS.
COSMIC: A high resolution, large collecting area telescope N86-11104
Numerical experiments in image reconstruction N86-11116
COSMIC image reconstruction N86-11118

HARVARD UNIV., CAMBRIDGE, MASS.
Bulk formation of metallic glasses and amorphous silicon from the melt N86-10154
Crystal nucleation and glass formation in metallic alloy melts N86-10233
Topics in the electronic theory of disordered semiconductors N86-11045

HASKONING, CONSULTING ENGINEERS, NIJMEGEN (NETHERLANDS).
Utilization of satellite remote sensing for the monitoring of oil pollution and marine ecosystems in Indonesia. A Tropical Earth Resources Satellite program (TERS) case study implemented for the NLR, Delft N86-10640

HAUPTVERBAND DER GEWERBLICHEN BERUFSGENOSSENSCHAFTEN, E. V., BONN (WEST GERMANY).
Report on the research activities on whole-body vibrations. Human strain due to mechanical vibrations
[ISBN-3-88383-107-7] N86-10773

HAWAII UNIV., HONOLULU.
Position paper: Workshop on Geologic Applications of Remote Sensing to the Study of Sedimentary Basins N86-10601
A boundary layer flow model for areas of complex terrain N86-10701

HEIDELBERG UNIV. (WEST GERMANY).
Photomapping in different climatic zones N86-10491

HELLER (JEAN), LOS ALAMOS, N. MEX.
Properties of plastic-bonded nitroguanidine
[DE85-015316] N86-10358
Type of new Chinese-produced high-speed camera and its utilization in detonation physics experiments
[DE85-015191] N86-10529

HOCHSCHULE DER BUNDESWEHR, MUNICH (WEST GERMANY).
Oscillations of a viscoelastic liquid drop in zero-gravity N86-10240

HOSEI UNIV., TOKYO (JAPAN).
An example of single model orientation of metric camera stereophotographs N86-10520

HOUSTON UNIV., TEX.
Effect of undercooling and modified microstructure on the physical properties of material synthesized in the drop tube and drop tower N86-10075

HUMAN ENGINEERING LABS., ABERDEEN PROVING GROUND, MD.
Proposed aural nondetectability limits for Army materiel
[AD-A156704] N86-10917

I

IBM RESEARCH LAB., SAN JOSE, CALIF.
Characterization of vapor and aerosol flows by photothermal methods
[AD-A156601] N86-10465
Time resolved flow velocity and concentration measurements using a travelling thermal lens
[AD-A156706] N86-10541
Optical detection of photoacoustic pulses in thin silicon wafers
[AD-A156705] N86-10977

IBM RESEARCH LAB., YORKTOWN HEIGHTS, N. Y.
Thermodynamic constraints on ion beam mixing of metals on insulators
[DE85-013628] N86-10448
IDAHO NATIONAL ENGINEERING LAB., IDAHO FALLS.
On-line gamma-ray data acquisition at the Power Burst facility
[DE85-011957] N86-10954
IIT RESEARCH INST., ROME, N.Y.
Catalog of Resources for Education in Ada (trademark) and Software Engineering (CREASE). Version 3.0
[AD-A156687] N86-10790
ILLINOIS INST. OF TECH., CHICAGO.
Free carrier absorption from electrons in confined systems N86-11042
ILLINOIS UNIV., CHICAGO.
Three-dimensional stress singularities in anisotropic materials and composites N86-10286
Optimal design of portal frames against buckling N86-10572
ILLINOIS UNIV., URBANA.
Flammability limits of gases under low gravity conditions N86-10164
Numerical methods for analyzing electromagnetic scattering
[NASA-CR-176141] N86-10377
Anelastic relaxation in irradiated Cu-Be
[DE85-013893] N86-11056
ILLINOIS UNIV., URBANA-CHAMPAIGN.
Semiconductor superlattic photodetectors
[NASA-CR-176249] N86-10484
IMPERIAL METAL INDUSTRIES LTD., KIDDERMINSTER (ENGLAND).
Carbon fiber reinforced polymide filament wound tube manufacturing
[BR64172] N86-10339
INDIAN INST. OF SCIENCE, BANGALORE.
Recent advances in the analysis of exhaust mufflers N86-10587
INDIAN SPACE RESEARCH ORGANIZATION, AHMEDABAD.
Creation of Ground Control Points (GCP) library using ESA Spacelab metric camera imagery N86-10516
INFORMATICS, INC., PALO ALTO, CALIF.
LANES 1 Users' Guide
[NASA-CR-177334] N86-10819
INFORMATION SPECTRUM, INC., ARLINGTON, VA.
F-16X MSIP (Multi-national Staged Improvement Program) case example: Operating and support cost estimation using VAMOSC (Visibility And Management Of Operating and Support Costs)
[AD-A156893] N86-10006
INSTITUT GEOGRAPHIQUE NATIONAL, PARIS (FRANCE).
Identification of planimetric features from the metric camera N86-10497
Thematic investigations in France based on metric camera imagery N86-10509
INSTITUTE FOR DEFENSE ANALYSES, ALEXANDRIA, VA.
Ada (trademark) Programming Support Environment (APSE) Evaluation and Validation (E and V) workshop report held at Airlie, Virginia on 2-6 April 1984
[AD-A156667] N86-10829
Report of the ad hoc committee to review the program of the SDI Directorate on Innovative Science and Technology (IST)
[AD-A156668] N86-11071
INSTITUTE FOR PERCEPTION RVO-TNO, SOESTERBERG (NETHERLANDS).
Studies on human vehicle control
[B8563352] N86-10775
Car driving as a supervisory control task
[B8563351] N86-10776
Standardization of tasks: Approach planning
[IZF-1984-19] N86-10782
Path error-neglection in straight lane driving
[IZF-1984-32] N86-10783
The wearing comfort of the PVC: Combat back pack
[IZF-1984-34] N86-10789
Risk propensity, action readiness and the roles of societal and individual decision makers
[IZF-1984-27] N86-11077
INSTITUTE OF GAS TECHNOLOGY, CHICAGO, ILL.
Effects of H2S on molten carbonate fuel cells
[DE85-014052] N86-10447
INSTITUUT TNO VOOR BOUWMATERIALEN EN BOUWCONSTRUCTIES, DELFT (NETHERLANDS).
Simulation of the atmospheric boundary layer in the large wind tunnel of the TNO Institute for Building materials and Constructions (IBBC). Part 1: Theory
[BI-76-39/08.7.23100-PT-1] N86-10703
Simulation of the atmospheric boundary layer in the large wind tunnel of the TNO Institute for Building Materials and Construction (IBBC). Part 2: Experiments
[BI-76-39/08.7.23100-PT-2] N86-10704
INSTITUUT VOOR CULTURRTECHNIEK EN WATERHUISHOUDING, WAGENINGEN (NETHERLANDS).
Remote sensing
[NOTA-1535] N86-10638
Remote sensing study project East Gelderland (Netherlands). Part 2: Remote sensing flights in 1982 and 1983; organization aspects N86-10639
INTERSONICS, INC., NORTHBROOK, ILL.
Acoustic levitation containerless processing N86-10177
IOWA UNIV., IOWA CITY.
Design sensitivity analysis and optimization of built-up structures N86-10565
Stratigraphy, petrology, depositional and post-depositional histories and their effects upon reservoir properties of the Parkman Formation of the Mesa Verde group, Powder River Basin, Wyoming N86-10691
ISHIKAWAJIMA-HARIMA HEAVY INDUSTRIES CO. LTD., YOKOHAMA (JAPAN).
Experimental study on Marangoni convection N86-10243

J

JET PROPULSION LAB., CALIFORNIA INST. OF TECH., PASADENA.
Containerless studies of nucleation and undercooling N86-10102
Sol-gel glasses N86-10153
Fusion target technology N86-10156
Glass research N86-10157
Multimode acoustic research N86-10167
Advanced containerless processing technology N86-10176
The Telecommunications and Data Acquisition Report
[NASA-CR-176203] N86-10382
A VLBI survey at 2.29 GHz N86-10383
Comparison of the calibration of ionospheric delay in VLBI data by the methods of dual frequency and Faraday rotation N86-10384
A new 70-meter antenna quadripod with reduced RF blockage N86-10385
Seismic analysis of the large 70-meter antenna, part 1: Earthquake response spectra versus full transient analysis N86-10386
An experimental TE sub 12 - TE sub 11 circular waveguide mode converter N86-10387
Propagation and radiation characteristics of a multimode corrugated waveguide feedhorn N86-10388
Load-deflection tests and computer analyses of a high-precision adhesive-bonded antenna reflector panel N86-10389
A sequential decoding performance analysis for International Comet Explorer N86-10390
The VLSI design of error-trellis syndrome decoding for convolutional codes N86-10391
High-rate convolutional code construction with the minimum required SNR criterion N86-10392
DSN frequency and timing system, Mark 4-85 N86-10393
JPL emergency support of TDRSS and compatible satellites N86-10394
Planning for VLA/DSN arrayed support to the Voyager at Neptune N86-10395
A VLA experiment: Planning for Voyager at Neptune N86-10396
Periodic binary sequences with very good autocorrelation properties N86-10397
A binary sequence of period 60 with better autocorrelation properties than the Barker sequence of period 13 N86-10398
The GCF Mark 4 implementation and beyond N86-10399
SETI radio spectrum surveillance system N86-10400
Mobile VLBI and GPS measurement of vertical crustal motion N86-10401
Improved mapping of radio sources from VLBI data by least-square fit N86-10402
Report of the Workshop on Geologic Applications of Remote Sensing to the Study of Sedimentary Basins
[E86-10002] N86-10599
Tertiary and quaternary research with remote sensing methods N86-10603
Multisensor data integration techniques N86-10604
Remote stratigraphic and structural analysis: Multisensor results in the Wind River/Bighorn Basin area, Wyoming N86-10606
Foreland basin structures and remote sensing N86-10608
NASA/JPL Aircraft SAR Workshop Proceedings
[NASA-CR-176204] N86-10615
Radar system description N86-10616
CV-990 L-band SAR: A calibration experiment N86-10617
Neogene compressional deformation and possible thrust faulting in southwest Dominican Republic N86-10618
Age-dating volcanic and alluvial surfaces with multipolarization data N86-10620
Topographic mapping from interferometric synthetic aperture radar observations N86-10622
Lithologic mapping in a sedimentary environment using multipolarization SAR images N86-10624
Mapping diverse forest cover with multipolarization airborne radar N86-10625
On the use of L-band multipolarization airborne SAR for surveys of crops, vineyards, and orchards in a California irrigated agricultural region N86-10627
Vegetation canopy discrimination and biomass assessment using multipolarized airborne SAR N86-10628
Modelling of vegetation volumes N86-10629
Chemical kinetics and photochemical data for use in stratospheric modeling
[NASA-CR-176198] N86-10707
Advanced vehicle systems assessment. Volume 2: Subsystems assessment
[NASA-CR-176205] N86-11083
Advanced vehicle systems assessment. Volume 3: Systems assessment
[NASA-CR-176206] N86-11084
Advanced vehicle systems assessment. Volume 4: Supporting analyses
[NASA-CR-176207] N86-11085
Advanced vehicle systems assessment. Volume 5: Appendices
[NASA-CR-176208] N86-11086
Galileo: Exploration of Jupiter's system
[NASA-SP-479] N86-11137
A modeling analysis program for the JPL table mountain lo sodium cloud
[NASA-CR-176241] N86-11139
JOHNS HOPKINS UNIV., BALTIMORE, MD.
Metallic foams N86-10095
Diffusion in immiscible melts N86-10096
Elastic properties and thermal stability characterization of metallic glasses by guided wave techniques N86-10337
Stiffened and prestressed composite overwrapped pressure vessels N86-10547
Load space formulation of reliability for nonlinear random structural systems N86-10570
Ultraviolet spectroscopy of the Earth's dayglow and magnetosphere cleft N86-10696
Physical acoustics: Investigation of chemical kinetic and thermodynamic properties of fluids N86-10911
Thermodynamics of polymer-supercritical solvent mixtures
[AD-A157038] N86-11061
JOINT INST. FOR LAB. ASTROPHYSICS, BOULDER, COLO.
Space antenna for gravitational wave astronomy N86-11123
JOINT PUBLICATIONS RESEARCH SERVICE, ARLINGTON, VA.
USSR report: Life sciences. Biomedical and behavioral sciences
[JPRS-UBB-85-023] N86-10738
Hemodynamics during gravitational overloads (mathematical modeling) N86-10739
Study of hypokinesia and acceleration effects on human chromosomes N86-10740
Romanian plant produces protein concentrate from paraffin-nourished yeasts N86-10741
Biotechnology: Science and practice N86-10742
Dynamics of changes of statistical indicators of heart rhythm of persons with different degree of motion sickness N86-10743
Effect of single actions of weak electromagnetic fields of ultralow frequency on indices of endocrine system N86-10744
Effect of emotional stress on hemostasis system of healthy persons N86-10745
Assessment of state of chronotropic and inotropic heart function at different degrees of physical fitness N86-10746
Capacity for work and hemodynamics in males residing at middle and high latitudes N86-10747
Individual typological features of autonomic reactions during autogenic training in polar expedition members in period of wintering in Antarctica N86-10748
Effect of inclusion of supplementary ascorbic acid in daily diet on degree of vitamin saturation of body and thermoresistance of erythrocytes while working in arid zone N86-10749
Effect of various doses of some vitamins on non-specific mechanisms of adaptation of man N86-10750
Adaptation of man to extreme conditions of Antarctica N86-10751
Individual typological self-regulation of cardio-vascular system N86-10752

Conditioning potentialities of respiratory apparatus N86-10753
Short term heat effect on adreno- and cholino-sensitivity of rat's small intestine N86-10754
Classification of changes in electrocardiogram during muscular exertion of healthy individuals N86-10755
Eye-movement activity as index of functional state of brain N86-10756
Mechanism of adaptogenic action of prickly eleuterococcus on man during heat stress N86-10757
Vestibular resistance and blood circulation changes in orthostatic position during hyperthermia N86-10758
Heat transfer mechanism in human extremities N86-10759
Reaction of rabbit respiration system to hypoxic stimulus in nitrogen-oxygen medium at elevated pressure N86-10760
Indices of blood oxygen transporting properties and erythropoiesis in rats after prolonged stay in nitrogen-oxygen mixture at elevated pressure N86-10761
Homocarnosin in rat brain during adaptation to cold N86-10762
Efficiency of muscular work in white rats during adaptation to cold N86-10763
Intradiurnial organization of wakefulness-sleep sequence and energy metabolism in rats exposed to low ambient temperature N86-10764
TV monitoring control system in electrophysiological studies N86-10765
Effect of cold on brain serotonin system and plasma corticosteroid level in different strains of mice N86-10766
Dynamics of general resistance of rats during readaptation period after training in altered gas environment N86-10767
USSR report: Cybernetics, computers and automation technology
[JPRS-UCC-85-006] N86-10809
Prospects for creation of optical digital high-performance computers N86-10810
Elektronika MS 1603 high-speed peripheral processor N86-10811
Diagnostics of peripheral processors and controllers N86-10812
An approach to implementing CAMAC microprocessor modules N86-10813
Compact, high-speed algorithm for laying out printed circuit board runs N86-10814
Classification of real-time program testing tasks and methods N86-10815
DBS/R database control system N86-10816
Collective use computer system for the Academy of Sciences KaSSR N86-10817
Digital processing of images in tracking a moving object N86-10818

K

KANNER (LEO) ASSOCIATES, REDWOOD CITY, CALIF.
RFQ-funneling
[DE85-012483] N86-10194
Ion sources for high-frequency accelerators
[DE85-012992] N86-11006
KARLSRUHE UNIV. (WEST GERMANY).
High temperature properties and characterization of S3-N4 materials
[BMFT-FB-T-85-046] N86-10352
High temperature properties of SiC materials
[BMFT-FB-T-85-047] N86-10353
Restitution of Spacelab photography by analog stereoplotter N86-10489
KATHOLIEKE UNIVERSITEIT TE LEUVEN (BELGIUM).
Melting and solidification of metal matrix composites under microgravity N86-10211
KENTUCKY UNIV., LEXINGTON.
Solid surface combustion at reduced gravity N86-10159
KERNFORSCHUNGSANLAGE, JUELICH (WEST GERMANY).
Dielectric properties of silicon surfaces and silver thin films
[JUEL-1968] N86-10450
Dust deposition in regions of separated flow
[JUEL-1985] N86-10475
Experiments with tubular probes made of INCOLOY 800 H under uniaxial and multiaxial strain
[JUEL-1979] N86-10595
Contribution of wind energy to the energy balance of a combined solar and wind energy system. Part 2: Computer-assisted investigations
[BMFT-FB-T-85-052-VOL-2] N86-10671
KIRUNA GEOPHYSICAL INST. (SWEDEN).
Activities report in geophysics
[KGI-188] N86-10709
KMS FUSION, INC., ANN ARBOR, MICH.
Gel precursors as glass and ceramic starting materials for space processing applications research N86-10150
KODAK LTD., LONDON (ENGLAND).
Capillary forces in a low gravity environment N86-10202

L

LABORATORIO DE ACUSTICA E SONICA, SAO PAULO (BRAZIL).
Ultrasonic inspection of weldments in large size spiral box for hydroelectric plant
[AS-701/85] N86-10562
LAMONT-DOHERTY GEOLOGICAL OBSERVATORY, PALISADES, N. Y.
Structural mapping of folded sedimentary environments from satellite images: An example from Central Asia N86-10607
LAPPEENRANNAN TEKNILLINEN, KORKEAKOULU (FINALAND).
Information on continuum states from feeding times and total (GAMMA) spectra measured with BGO suppressed detectors
[DE85-013868] N86-10981
LOCKHEED MISSILES AND SPACE CO., PALO ALTO, CALIF.
Test and evaluate passive orbital disconnect struts (PODS 3)
[NASA-CR-177368] N86-10274
Binder-filler interaction in energetic polymers
[AD-A156752] N86-10345
LOS ALAMOS NATIONAL LAB., N. MEX.
Mixed-mode fracture of ceramics
[DE85-014087] N86-10349
Revision of and documentation for the standard version of the Poisson-Group codes
[DE85-012659] N86-10837
Theory of dense molecular fluid equations of state with application to detonation products
[DE84-016822] N86-10927
High-brightness photoemitter injector for electron accelerators
[DE85-012673] N86-10929
Measurement and resulting first and second order approximations for a 9 deg bending magnet in LAMPF's 750-keV transport
[DE85-012691] N86-10930
Wide dynamic range beam profile monitor
[DE85-012709] N86-10950
Ferrite kicker magnet for the LAMPF switchyard upgrade
[DE85-012657] N86-10996
Local drift parameter, j/n sub e and resistivity anomaly measurements in CTX spheromaks
[DE85-012740] N86-10998
Introduction to the m = 1 helicity source
[DE85-012771] N86-10999
Beginnings of remote handling at the RAL Spallation Neutron Source
[DE85-012681] N86-11001
Analytic evaluation of LAMPF 2 Booster Cavity design
[DE85-012680] N86-11002
LOS ALAMOS SCIENTIFIC LAB., N. MEX.
RFQ-funneling
[DE85-012483] N86-10194
Development of new ammonium nitrate composite explosives
[DE85-014252] N86-10356
KRAK: A computer program for two-phase, two-component porous flow and fracture propagation, revision
[DE85-014264] N86-10469
General-purpose heat source development: Safety Verification Test Program. Bullet/fragment test series
[DE85-014262] N86-10660
Recent development in the Hot Dry Rock Geothermal Energy Program
[DE85-009562] N86-10663
New probabilistic modeling and simulation methods for complex time-dependent systems
[DE85-009575] N86-10835
Guidelines for a thermochemical kinetics computer program
[DE85-014266] N86-10839
Framework for generating expert systems to perform computer security risk analysis
[DE85-014134] N86-10841
Initial increase, peaking effect, in the internal friction of copper following pulsed neutron and electron irradiation
[DE85-012767] N86-10932
Angular distribution of neutral hydrogen following collisional electron detachment from H(-)
[DE85-014258] N86-10943

Preliminary investigation of changes in X-ray multilayer optics subjected to high radiation flux
[DE85-014074] N86-10944
Polarization transfer in inelastic scattering and pionic models of the EMC effect
[DE85-010738] N86-10955
Direct mass measurements in the light neutron-rich region using a combined energy and time-of-flight technique
[DE85-012758] N86-10963
Beam line windows at LAMPF
[DE85-012723] N86-10985
Proposed bunching scheme for a polarized H(-) injector
[DE85-012648] N86-10986
Beam-cavity interaction measurements in a DAW structure
[DE85-012660] N86-10987
Increased particle confinement with the use of external dc bias field in the CTX spheromak
[DE85-012744] N86-10988
Treatment planning with ion beams
[DE85-012661] N86-10990
Noninterceptive techniques for the measurement of longitudinal parameters for intense H(-) beams
[DE85-012662] N86-10992
High-power rf controls for the NBS-Los Alamos racetrack microtron
[DE85-012658] N86-10993
Energy efficiency of the CTX magnetized coaxial plasma source
[DE85-012735] N86-11003
Generalized helicity and its time derivative
[DE85-012770] N86-11027
Recent helicity source and power supply improvements in CTX
[DE85-012741] N86-11028
Equilibrium of the kink source experiment
[DE85-012764] N86-11029
Alternative fusion concepts and the prospects for improved reactors
[DE85-009622] N86-11031
Heating and generation of suprathermal particles at collisionless shocks
[DE85-014114] N86-11034
LOUISIANA STATE UNIV., BATON ROUGE.
Solar flares and magnetospheric particles: Investigations based upon the ONR-602 experiment
[AD-A156583] N86-11142
LYON-1 UNIV. (FRANCE).
Space experiment on thermal diffusion. Preparation and theoretical analysis N86-10253

M

MAINZ UNIV. (WEST GERMANY).
A geological structural analysis of the southeastern Zagros (Iran) ranges based on metric camera photos N86-10492
MAPPING AND CHARTING ESTABLISHMENT, OTTAWA (ONTARIO).
Test results using metric camera photography for 1:250,000 mapping N86-10522
MARTIN MARIETTA AEROSPACE, DENVER, COLO.
Evaluation and prediction of long-term environmental effects on non metallic materials
[NASA-CR-178495] N86-10340
MARTIN MARIETTA ENERGY SYSTEMS, INC., PADUCAH, KY.
Evaluation of the International Atomic Energy Agency (IAEA) Safeguards Analytical Laboratory quality assurance program
[DE85-012078] N86-10953
MARYLAND UNIV., COLLEGE PARK.
Light scattering tests of fundamental theories of transport properties in the critical region N86-10113
Topics in nonlinear wave theory with applications N86-10367
Analysis of combined natural and forced convection around cylinders and spheres N86-10456
Determination of symmetry and phase in human visual response functions: Theory and experiments N86-10769
The h, p and h-p versions of the finite element method in dimension. Part 1: The error analysis of the p-version
[AD-A156600] N86-10862
The h, p and h-p versions of the finite element method in 1 dimension. Part 3. The adaptive h-p version
[AD-A156626] N86-10864
The h, p and h-p versions of the finite element method in 1 dimension. Part 2. The error analysis of the H and h-p versions
[AD-A156835] N86-10869

A modified repair strategy for two-component systems with revealed and unrevealed faults
[AD-A156715] N86-10885
Estimation by moments in a model of faulty inspection
[AD-A156754] N86-10886
Matter-anti-matter transition operators: A manual for modeling N86-10921
Lie algebraic methods for charged particle beams and light optics N86-10970
Adsorption of oxygen on single crystal tin at liquid helium temperatures N86-11044
Critical dynamics in superfluid helium N86-11046

MASCHINENFABRIK AUGSBURG-NUERNBERG A.G., MUNICH (WEST GERMANY).
Skin casting of alloys and composites: Results of Spacelab (SL)-1 and TEXUS experiments N86-10213

MASSACHUSETTS INST. OF TECH., CAMBRIDGE.
Fluid flow in crystal growth: Analysis of the verticle Bridgman and floating zone process N86-10055
Solutal convection and its effects on crystal growth and segregation in binary and pseudo-binary system with large liquidus-solidus separation N86-10056
Crystal growth of device quality GaAs in space N86-10061
Crystal melts under reduced gravity N86-10062
Heat flow and segregation in directional solidification N86-10072
Signal analysis of gas tungsten arc welds N86-10078
Undercooling, remelting, and coarsening N86-10080
The role of entrained surface oxides in RS-PM aluminum alloys on resultant structures and properties N86-10085
Metals electroprocessing in molten salts N86-10098
Modelling of laser-enhanced chemical vapor deposition N86-10105
Automatic processing of reactive polymers N86-10127
Role of convection in grain refining N86-10133
Colloidal oxide properties and kinetic studies N86-10147
Rapid solidification of magnetic oxides N86-10152
Oxidation behavior of glassy alloys N86-10158
Crystal growth of GaAs in space N86-10234
Robust failure detection filters
[NASA-CR-176232] N86-10271
Reaching approximate agreement in the presence of faults
[AD-A156541] N86-10898
US superconducting magnet data base assessment for INTOR
[DE85-013648] N86-11000
Conducting wall and pressure profile effect on MHD stabilization of axisymmetric mirror
[DE85-013647] N86-11020

MASSACHUSETTS UNIV., AMHERST.
Electricaily conducting polymers N86-10333
Polyacetylene polymerization, structure, and electrical transport properties N86-10334
Relativistic wavefunction at the origin and the pion decay constant
[DE85-012392] N86-11062

MATERIALS RESEARCH LABS., ASCOT VALE (AUSTRALIA).
Age-life prediction of nylon 66 parachute materials. Part 2: Changes in the chemical and physical properties of materials on aging
[AD-A156909] N86-10347

MAX-PLANCK-INST. FUER METALLFORSCHUNG, STUTTGART (WEST GERMANY).
Particle coarsening in immiscible zinc-lead alloys under microgravity N86-10210

MAX-PLANCK-INSTITUT FUER STROEMUNGSFORSCHUNG, GOETTINGEN (WEST GERMANY).
Oscillations of subsonic flow in an abruptly expanding circular duct
[MPIS-16/1984] N86-10028

MCELROY (RALPH) CO., AUSTIN, TEX.
Nonlinear propagation of elastoplastic waves in Ke penetrators (excerpts)
[DE85-011450] N86-10318

MEMBRANE TECHNOLOGY AND RESEARCH, INC., MENLO PARK, CALIF.
Membrane research in energy and solvent recovery from industrial effluent streams
[DE85-014583] N86-10682

MESSWANDLER-BAU G.M.B.H., BAMBERG (WEST GERMANY).
High voltage instrument transformers for outdoor service with an insulation of low pressure SF6 gas and plastic foils
[BMFT-FB-T-85-034] N86-10449

METALS SOCIETY, LONDON (ENGLAND).
Mechanism of the formation of boronised layers on high carbon steel
[BLL-BISI-TRANS-23036-(9022.06)] N86-10306
Boronising of iron and steel by ionic bombardment by diborane
[BLL-BISI-TRANS-23034-(9022.06)] N86-10307
Application of the unloading compliance methods in fracture toughness measurements of a quenched and tempered steel
[BLL-BISI-TRANS-21628-(9022.06)] N86-10308

MICHAEL REESE RESEARCH FOUNDATION, CHICAGO, ILL.
Biochemical assays of cultured cells N86-10134

MICHIGAN TECHNOLOGICAL UNIV., HOUGHTON.
The development and prevention of channel segregation during alloy solidification N86-10086

MICHIGAN UNIV., ANN ARBOR.
Preliminary reports, memoranda and technical notes of the Materials Research Council Summer Conference, La Jolla, California
[AD-A156776] N86-10291
Effects of chemistry and swirl on the production of turbulence in a flame
[PB85-219632] N86-10305
Test of a multilevel computational theory of stereoscopic visual image processing
[AD-A157011] N86-10870

MIDWEST RESEARCH INST., GOLDEN, COLO.
Identification of chemical and physical phenomena affecting the durability of silvered polymer (PMMA) mirrors
[DE85-012131] N86-10645
Solar thermal technical information guide
[DE85-002941] N86-10657
Photovoltaics: Report, 1984
[DE85-014713] N86-10658
Some aspects of long-range, high-risk photovoltaic research at SERI
[DE85-012144] N86-10662

MIDWEST RESEARCH INST., KANSAS CITY, MO.
Containerless high temperature property measurements by atomic fluorescence N86-10092

MILAN UNIV. (ITALY).
Surface forces in contacting solids N86-10252

MISSION RESEARCH CORP., ALBUQUERQUE, N. MEX.
Laser generation and transport of a relativistic electron beam
[DE85-011709] N86-10192

MISSION RESEARCH CORP., SANTA BARBARA, CALIF.
Acoustic gravity wave chemistry model for the RAYTRACE code
[AD-A156850] N86-10405

MISSISSIPPI STATE UNIV., STATE COLLEGE.
Guidance and control of a cable based payload pickup system N86-10046

MISSISSIPPI UNIV., UNIVERSITY.
Acoustic cavitation and bubble dynamics
[AD-A156888] N86-10918

MISSOURI UNIV., ROLLA.
Containerless processing of glass forming melts in space N86-10148

MONS UNIV. (BELGIUM).
Rayleigh-Benard instability in systems presenting a minimum in surface tension N86-10245

MULLARD RADIO ASTRONOMY OBSERVATORY, CAMBRIDGE (ENGLAND).
Radio astronomy experience in image reconstruction. A history lesson for optical astronomers N86-11117

N

NANJING UNIV. (CHINA).
Effects of slots/holes in disks on frequencies of TM01 and EH11 waves in the disk-loaded waveguide
[DE85-013376] N86-11009

NAPLES UNIV. (ITALY).
Some results of the Marangoni free convection experiment N86-10203
The TEXUS flight results on convective flows and heat transfer in simulated floating zones N86-10235
Numerical simulation of unsteady thermal Marangoni flows N86-10238

NATIONAAL INST. VOOR KERNFYSICA EN HOGE ENERGIEFYSICA, AMSTERDAM (NETHERLANDS).
Activities report in safety N86-10365
Renovated cooling at PIMU
[LINO-122] N86-10452
On the analytical evaluation of the partition function for unit hypercubes in four dimensions
[NIKHEF-H/84-12] N86-10882
Variational estimates for the mass gap of SU(2) Euclidean lattice gauge theory
[NIKHEF-H/84-13] N86-10883
Report on a visit to CERN in February 1985. Notes on bunch monitors, high-frequency systems, linacs, kickers, magnets, vacuum and bunch extraction
[LINO-119] N86-10967
The MEA vacuum system
[LINO-120] N86-10968
The Netherlands Institute for Nuclear and High Energy Physics (NIKHEF) traveling wave monitor user guide
[LINO-121] N86-10969
Two-loop large Higgs mass corrections to vector boson self-couplings
[NIKHEF-H/84-15] N86-11038

NATIONAL ACADEMY OF SCIENCES - NATIONAL RESEARCH COUNCIL, WASHINGTON, D. C.
Confined swirling jet predictions using a multiple-scale turbulence model
[NASA-CR-178484] N86-10462

NATIONAL AERONAUTICS AND SPACE ADMINISTRATION, WASHINGTON, D. C.
Microgravity Science and Applications Program tasks
[NASA-TM-87568] N86-10053
Project VESTA, exploratory mission to the asteroids: Scientific objectives and technical specifications
[NASA-TM-77669] N86-10179
X-ray satellite
[NASA-TM-77923] N86-10273
Determination of thermophysical characteristics of solid materials by electrical modelling of the solutions to the inverse problems in nonsteady heat conduction
[NASA-TM-77907] N86-10293
Discussion on the progress and future of satellite communication (Japan)
[NASA-TM-77672] N86-10378
Design and construction of a Faraday cup for measurement of small electronic currents
[NASA-TM-77915] N86-10418
Maximum water reserves in the snow cover in the European territory of the USSR according to data for 1892-1960
[NASA-TM-77901] N86-10611
Representation of the distribution of the snow cover on the surface of the Earth's dry land
[NASA-TM-77909] N86-10612
Observations of the snow cover in the southern part of the Buryat Autonomous Soviet Socialist Republic
[NASA-TM-77910] N86-10613
Laws of distribution of the snow cover on the greater Caucasus (Soviet Union)
[NASA-TM-77911] N86-10614
Aerospace medicine and biology: A continuing bibliography with indexes (supplement 275)
[NASA-SP-7011(275)] N96-10768

NATIONAL AERONAUTICS AND SPACE ADMINISTRATION. AMES RESEARCH CENTER, MOFFETT FIELD, CALIF.
Evaluation of an aerodynamic-load prediction method on a STOL fighter configuration
[NASA-TM-86782] N86-10015
Manned flight simulation: Challenge and response
[NASA-TM-86827] N86-10048
Large eddy interactions in a turbulent channel flow
[NASA-TM-86757] N86-10464
Life sciences research on the space station: An introduction
[NASA-TM-86836] N86-10734
The synthesis and analysis of color images
[NASA-TM-86844] N86-10777

NATIONAL AERONAUTICS AND SPACE ADMINISTRATION. GODDARD SPACE FLIGHT CENTER, GREENBELT, MD.
The effect of vegetation type, microrelief, and incidence angle on radar backscatter N86-10619
The effects of merging TM and A/C radar on wetland classification N86-10621
SAMSI: An orbiting spatial interferometer for micro-arc second astronomical observations N86-11103
Photographic catalog of selected planetary size comparisons
[NASA-TM-86207] N86-11138
Directionality of bremsstrahlung from relativistic electrons in solar flares
[NASA-TM-87509] N86-11141

NATIONAL AERONAUTICS AND SPACE ADMINISTRATION. JOHNSON (LYNDON B.) SPACE CENTER,
Numerical procedure for three-dimensional hypersonic viscous flow over aerobrake configuration
[NASA-TM-58269] N86-10018
Purification and cultivation of human pituitary growth hormones secreting cells N86-10140
Cell separations in microgravity and development of a space bioreactor N86-10141
Cell maintenance systems N86-10142
High-temperature controlled redox crystallization studies N86-10178

NATIONAL AERONAUTICS AND SPACE ADMINISTRATION. LANGLEY RESEARCH CENTER, HAMPTON, VA.
Operating characteristics of the multiple critical Venturi System and secondary calibration nozzles used for weight-flow measurements in the Langley 16-foot transonic tunnel
[NASA-TM-86405] N86-10016
Crystal growth research in space N86-10057
Three-dimensional vibration analysis of a uniform beam with offset inertial masses at the ends
[NASA-TM-86393] N86-10580
Fatigue of graphite/epoxy buffer strip panels with center cracks
[NASA-TM-87595] N86-10581
User's guide for Langley Research Center Orbital Lifetime program
[NASA-TM-87587] N86-10828
Investigation of composite materials property requirements for sonic fatigue research
[NASA-TM-87601] N86-10913

NATIONAL AERONAUTICS AND SPACE ADMINISTRATION. LEWIS RESEARCH CENTER, CLEVELAND, OHIO.
Three-dimensional inviscid analysis of radial turbine flow and a limited comparison with experimental data
[NASA-TM-87091] N86-10017
Forced response analysis of an aerodynamically detuned supersonic turbomachine rotor
[NASA-TM-87093] N86-10019
Transport processes in solution crystal growth N86-10107
Surface tension induced instabilities in reduced gravity: The Benard problem N86-10117
Thermocapillary motion research N86-10125
Microgravity Materials Science Laboratory N86-10173
Dendritic solidification in a binary alloy melt: Steady-state versus morphological stability theories N86-10261
Compatibility of grain-stabilized platinum with candidate propellants for resistojets
[NASA-TM-87118] N86-10279
Rapid evaluation of ion thruster lifetime using optical emission spectroscopy
[NASA-TM-87103] N86-10280
Experimental performance of a 1-kilowatt arcjet thruster
[NASA-TM-87131] N86-10281
Progressive damage, fracture predictions and post mortem correlations for fiber composites
[NASA-TM-87101] N86-10290
Creep-fatigue behavior of NiCoCrAlY coated PWA 1480 superalloy single crystals
[NASA-TM-87110] N86-10311
Tribological properties of structural ceramics
[NASA-TM-87105] N86-10341
Test results for 20-GHz GaAs FET spacecraft power amplifier
[NASA-TM-87072] N86-10379
A dual frequency microstrip antenna for Ka band
[NASA-TM-87124] N86-10380
A numerical method for approximating antenna surfaces defined by discrete surface points
[NASA-TM-87125] N86-10381
Theoretical modeling of the vapor cavitation in dynamically loaded journal bearings
[NASA-TM-87076] N86-10463
Measurement of the density of base fluids at pressures 0.422 to 2.20 GPa
[NASA-TM-87114] N86-10551
The mechanism of erosion of metallic materials under cavitation attack
[NASA-TM-87133] N86-10552
Ultrasonic evaluation of mechanical properties of thick, multilayered, filament wound composites
[MASA-TM-87088] N86-10561
Joint research effort on vibrations of twisted plates, phase 1: Final results
[NASA-RP-1150] N86-10579
Improved stud configurations for attaching laminated wood wind turbine blades
[NASA-TM-87109] N86-10582
Photovoltaic systems in remote locations: An experience summary
[NASA-TM-87106] N86-10643
Ion beam sputter deposited zinc telluride films
[NASA-TM-87119] N86-11048

NATIONAL AERONAUTICS AND SPACE ADMINISTRATION. MARSHALL SPACE FLIGHT CENTER, HUNTSVILLE, ALA.
Growth of organic crystals by Ostwald ripening N86-10058
Growth of solid solution crystals N86-10065
Study of the reactive-element effect in oxidation of Fe-Cr alloys using transverse section analytical electron microscopy N86-10087
Cloud microphysics by thermal wave methods N86-10103
Extension of Ostwald ripening theory N86-10104
Studies of model immiscible systems N86-10112
Mathematical models of continuous flow electrophoresis N86-10143
Electrophoresis technology N86-10144
Production of large-particle-size monodisperse latexes in microgravity N86-10146
Glass formation in reluctant glass formers N86-10151
Development of materials processing systems for use in space on low-g simulation devices N86-10166
Advanced optical measurement techniques N86-10174
Design, fabrication and testing of an experimental apparatus for determining particle behavior under very low intergranular stresses N86-10175
Separation of aqueous two-phase polymer systems in microgravity N86-10246
Rationale for two phase polymer system microgravity separation experiments N86-10247
Analytical investigation of solid rocket nozzle failure
[NASA-TM-86513] N86-10278

NATIONAL AERONAUTICS AND SPACE ADMINISTRATION. NATIONAL SPACE TECHNOLOGY LABS., BAY SAINT LOUIS, MISS.
Potential applications of multipolarization SAR for pine plantation biomass estimation N86-10626

NATIONAL AEROSPACE LAB., AMSTERDAM (NETHERLANDS).
Axisymmetric free surface behavior of moving liquid in a cylinder in microgravity N86-10206
Aerospace research at NLR N86-11089
Activities report of the Space Flight Laboratory N86-11090
Activities Report of the Space Flight Laboratory N86-11091

NATIONAL BUREAU OF STANDARDS, BOULDER, COLO.
Transient heat transfer in zero gravity environment
[NASA ORDER H-27954B] N86-10114
Cooled ion frequency standard
[AD-A156813] N86-10295
Space antenna for gravitational wave astronomy N86-11123

NATIONAL BUREAU OF STANDARDS, GAITHERSBURG, MD.
Investigation of the uncertainties of the NBS (National Bureau of Standards) thermal voltage and current converters
[PB85-200178] N86-10453
NBSGSC: A FORTRAN program for quantitative X-ray fluorescence analysis
[PB85-206068] N86-10847
Selected tables of atomic spectra. Atomic energy levels and multiplet table O3
[NBS/NSRDS-3/11] N86-10923

NATIONAL BUREAU OF STANDARDS, WASHINGTON, D.C.
Measurement of high temperature thermophysical properties N86-10074
Convection during unidirectional solidification N86-10077
Dynamic thermophysical measurements in space
[NASA ORDER H-27954-B] N86-10106
Surface tensions and their variations with temperature and impurities
[NASA ORDER H-27954B] N86-10115
Precise viscosity measurements very close to critical points
[NASA ORDER C-86129D] N86-10120
Experimental and theoretical studies of wetting and multilayer adsorption
[NASA ORDER H-27954B] N86-10121
Impurity extraction by droplets N86-10122
Miscibility gap systems
[NASA ORDER H-27954B] N86-10131
Self-heating to ignition measurements and computation of critical size for solar energy collector materials
[DE85-011449] N86-10302

NATIONAL OCEANIC AND ATMOSPHERIC ADMINISTRATION, BOULDER, COLO.
Field comparison of in situ meteorological sensors
[PB85-196988] N86-10723

NATIONAL WEATHER SERVICE, WASHINGTON, D.C.
Monthly and Seasonal Weather Outlook for mid-April to mid-May 1985, Volume 39, Number 8
[PB85-195345] N86-10724

NAVAL AIR SYSTEMS COMMAND, WASHINGTON, D. C.
Polymer engineering: Polymeric and molecular electronic, dielectric and optical properties for device applications
[AD-A156671] N86-10344

NAVAL MEDICAL RESEARCH AND DEVELOPMENT COMMAND, BETHESDA, MD.
Evaluation of the 90-day inhalation toxicity of petroleum and oil shale JP-5 jet fuel
[AD-A156815] N86-10675

NAVAL POSTGRADUATE SCHOOL, MONTEREY, CALIF.
Construction and use of a radio controlled model helicopter for research
[AD-A156547] N86-10035
A comparative analysis of a CV helicopter and a JVX (Joint Services Advanced Vertical Lift) tilt-rotor aircraft in an aircraft carrier based ASW (Anti-Submarine Warfare)
[AD-A156871] N86-10041
Evaluation of surface exchange coefficients from mildex ocean/atmosphere mixed layer data
[AD-A156765] N86-10729
Computer-based training for the US Coast Guard standard terminal microcomputer: A basis for implementation utilizing the elaboration theory of instructional design
[AD-A156548] N86-10791
Initial design of a relational database system for NPS computer asset identification and valuation for risk assessment
[AD-A156847] N86-10796
Development of IS2100: An information systems laboratory
[AD-A156848] N86-10797
Shipboard non-tactical computer systems of the US Navy
[AD-A156789] N86-10849
Fiber optic gradient hydrophone construction and calibration for sea trial
[AD-A156469] N86-10914
A systems development life cycle study of the information center
[AD-A156977] N86-11079

NAVAL RESEARCH LAB., WASHINGTON, D. C.
On the use of X-band CW nanosecond airborne radar for terrain profiling
[AD-A156886] N86-10406
The Liu, Katsaros, and Businger (1979) bulk atmospheric flux computational iteration program in FORTRAN and BASIC
[AD-A156736] N86-10714
A processor for the study of ocean fine-scale patches
[AD-A157019] N86-10730
Selected tables of atomic spectra. Atomic energy levels and multiplet table O3
[NBS/NSRDS-3/11] N86-10923
Electron momentum transfer collision frequency in N(2), O(2) and air
[AD-A157030] N86-10924
Dynamics of imploding neon gas puff plasmas. 1
[AD-A156916] N86-10983
Renormalization of an inverse scattering theory for inhomogeneous dielectrics
[AD-A156636] N86-11049

NAVAL UNDERWATER SYSTEMS CENTER, NEW LONDON, CONN.
An improved FFT (Fast fourier transform) for a four parallel pipe SIMD arithmetic processor
[AD-A156625] N86-10863

NAVAL WEAPONS CENTER, CHINA LAKE, CALIF.
Radome analysis and design capabilities of the RF and Microwave Technology Branch
[AD-A156662] N86-10404
Fracture toughness of hydrogen-embrittled precipitation-hardened stainless steels
[AD-A156664] N86-10592
Surface winds at NWC (Naval Weapons Center): 1964 - 1982
[AD-A156660] N86-10712

NEVADA UNIV., RENO.
Characterization of cathodic corrosion products in the Ca/CaCrO4 thermal battery
[DE85-013442] N86-10644

NEW HAMPSHIRE UNIV., DURHAM.
Solar modulation of galactic cosmic rays: Techniques and applications N86-11143

NEW MEXICO STATE UNIV., LAS CRUCES.
Preliminary investigation of changes in X-ray multilayer optics subjected to high radiation flux
[DE85-014074] N86-10944

NEW MEXICO UNIV., ALBUQUERQUE.
Catalytic activity of shock modified ZnO for CO oxidation and methanol synthesis
[DE85-014704] N86-10300

NEW ORLEANS UNIV., LA.
Study of one- and two-dimensional filtering and deconvolution algorithms for a streaming array computer [NASA-CR-176221] N86-10822
A study of Morrison's iterative noise removal method [NASA-CR-176222] N86-10823
Always-convergent iterative noise removal and deconvolution for image data [NASA-CR-176223] N86-10824
A study of derivative filters using the discrete Fourier transform [NASA-CR-176224] N86-10825
Coordinate axes, location of origin, and redundancy for the one and two-dimensional discrete Fourier transform [NASA-CR-176225] N86-10826
Study of one- and two-dimensional filtering and deconvolution algorithms for a streaming array computer [NASA-CR-176226] N86-10827
NOOTER CORP., ST. LOUIS, MO.
Fabrication and metallurgical properties of modified 9Cr-1 Mo steel [DE85-012885] N86-10328
NORTH CAROLINA STATE UNIV., RALEIGH.
Processing of complex compound semiconductors in space N86-10054
Freezer model using a population balance approach for steady-state, direct-contact, secondary refrigerant, freeze desalination N86-10361
Sound radiation from repetitive transient vibrations using multi-channel digital signal processing with application to impact machinery N86-10910
NORTH CAROLINA UNIV., CHAPEL HILL.
Cretaceous and cenozoic stratigraphy of the upper and middle coastal plain, Harnett County area, North Carolina N86-10690
NORTH CAROLINA UNIV., CHARLOTTE.
Initial increase, peaking effect, in the internal friction of copper following pulsed neutron and electron irradiation [DE85-012767] N86-10932
NORTHROP SERVICES, INC., RESEARCH TRIANGLE PARK, N. C.
Volatile organic compounds in indoor air: A survey of various structures [PB85-198356] N86-10687
NORTHWESTERN UNIV., EVANSTON, ILL.
Thermocapillary flows and their stability: Effects of surface layers and contamination N86-10109
Finite deformation crack-line fields in a thin elasto-plastic sheet [AD-A156757] N86-10346
Resistance curves for crack growth under plane-stress conditions in an elastic perfectly-plastic material [AD-A156778] N86-10593
NOTRE DAME UNIV., IND.
Information on continuum states from feeding times and total (GAMMA) spectra measured with BGO suppressed detectors [DE85-013868] N86-10961

O

OAK RIDGE GASEOUS DIFFUSION PLANT, TENN.
HALFBREED: An extended capability version of the YAQUI code [DE85-014237] N86-10843
OAK RIDGE NATIONAL LAB., TENN.
Fabrication and metallurgical properties of modified 9Cr-1 Mo steel [DE85-012885] N86-10328
Swelling and tensile properties of EBR-2-irradiated tantalum alloys for space reactor applications [DE85-012887] N86-10329
Engine-driven and absorption heat pump programs [DE85-013930] N86-10472
Laboratory experiments of heat pump dynamic losses [DE85-013931] N86-10473
Automated analysis of digital images generated by two-dimensional gel electrophoresis [DE85-011906] N86-10526
Simplified analysis of Stirling engines and heat pumps [DE85-005366] N86-10647
Comparative analysis of single and continuously variable-capacity heat pump concepts [DE85-004089] N86-10653
Stirling-engine-driven heat pump program overview [DE85-004796] N86-10661
Examples of regional environmental assessment using acid deposition data [DE85-012903] N86-10677
National perspective on environmental constraints to hydroelectric development [DE85-013111] N86-10678
Development and evaluation of multispecies test protocols for assessing chemical toxicity [DE85-013526] N86-10679
Box method for finding intersections of a trajectory with axisymmetric flux surfaces [DE85-013525] N86-10840
The 1984 bibliography of atomic and molecular processes [DE85-010583] N86-10926
Experimental X-ray scattering cross sections for H2 and rare atomic gases [DE85-011572] N86-10936
Experimental studies of transition radiation and optical bremsstrahlung [DE85-0135637] N86-10949
ORR core re-configuration measurements to increase the fast neutron flux in the Magnetic Fusion Energy (MFE) experiments [DE85-013520] N86-10958
Evolution of the fusion power demonstration tandem mirror reactor configuration [DE85-012889] N86-10960
Hot cell facility design for large fusion devices [DE85-012893] N86-11037
OAK RIDGE Y-12 PLANT, TENN.
Aluminum ion plating for corrosion protection of uranium, revision 1 [DE85-012419] N86-10330
OFFICE NATIONAL D'ETUDES ET DE RECHERCHES AEROSPATIALES, PARIS (FRANCE).
Theoretical study of the unsteady linear problem for a rectangular wing with a pitching movement [ONERA-RT-17/1841-RY-010-R] N86-10022
La Recherche Aerospatiale, bimonthly bulletin, no. 1984-5, September-October 1985 [ESA-TT-899] N86-10363
OFFICE OF NAVAL RESEARCH, ARLINGTON, VA.
Psychological Sciences Division 1984 programs [AD-A156631] N86-10779
OHIO STATE UNIV., COLUMBUS.
Theoretical studies of the surface tension of liquid metal system N86-10101
Digital control of the hydraulic actuators of an adaptive suspension vehicle N86-10548
Computer control of an electric hydraulic robot leg with proximity ranging system N86-10549
A numerical model for the estimation of solar radiation on rugged terrain N86-10694
The influence of tactual seat-motion cues on training and performance in a roll-axis compensatory tracking task setting N86-10784
OLD DOMINION UNIV., NORFOLK, VA.
Passive damping concepts for slender columns in space structures [NASA-CR-176234] N86-10577
NASA/American Society for Engineering Education (ASEE) Summer Faculty Fellowship Program, 1985 [NASA-CR-177972] N86-11064
OREGON GRADUATE CENTER FOR STUDY AND RESEARCH, BEAVERTON.
Transient velocity assessment in gallium arsenide, and of other GaAs characteristics related to device functions [AD-A156983] N86-11050
OREGON HEALTH SCIENCES UNIV., PORTLAND.
Cell partition in two polymer aqueous phases N86-10136
OREGON STATE UNIV., CORVALLIS.
Direct mass measurements in the light neutron-rich region using a combined energy and time-of-flight technique [DE85-012758] N86-10963
OXFORD UNIV. (ENGLAND).
Identification of a plant's weighting sequence [OUEL-1534/84] N86-10854

P

PACIFIC NORTHWEST LAB., RICHLAND, WASH.
Rapid analysis using capillary supercritical fluid chromatography [DE85-012460] N86-10297
Determining a physically appropriate neutron spectrum from multisphere data [DE85-013045] N86-10299
ELCAP instrumentation [DE85-013042] N86-10527
LANDSAT TM image data quality analysis for energy-related applications [E85-10109] N86-10597
Energy balance in a deep Colorado valley: ASCOT 84 [DE85-012441] N86-10631
Overview of wind turbine siting research: Prospecting to micrositing [DE85-013496] N86-10666
Radionuclide complexation in xylem exudates of plants [DE85-013446] N86-10684
Approaches to quantitative expression of dose response [DE85-013498] N86-10772
Secondary standards laboratories for ionizing radiation calibrations: The national laboratory interests [DE85-007046] N86-10938
PADUA UNIV. (ITALY).
Extragalactic observations with optical space arrays N86-11098
PARIS VI UNIV. (FRANCE).
Growth and characterization of brushite and lead monetite, simulation and results N86-10230
PARIS VII UNIV. (FRANCE).
High angular resolution in the infrared: Prospects for space observations N86-11100
PARMA UNIV. (ITALY).
The role of very small scale metric images in modern geology N86-10502
PENNSYLVANIA STATE UNIV., UNIVERSITY PARK.
Kidney cell electrophoresis N86-10145
PENNSYLVANIA UNIV., PHILADELPHIA.
Strength modeling report [NASA-CR-171896] N86-10770
TEMPUS: Simulating personnel and tasks in a 3-D environment [NASA-CR-171901] N86-10785
User interface enhancement report [NASA-CR-171898] N86-10820
System integration report [NASA-CR-171900] N86-10821
Motion analysis report [NASA-CR-171897] N86-10896
Zero-gravity movement studies [NASA-CR-171899] N86-10897
PERKIN-ELMER CORP., DANBURY, CONN.
Future space telescope design concepts N86-11107
PHILLIPS ENGINEERING CO., ST. JOSEPH, MICH.
Analyses of advanced residential abosrption heat pump cycles [DE85-005244] N86-10664
PHYSICAL SCIENCES, INC., ANDOVER, MASS.
Fuel Cell Technology Assessment Program, work element no. 6 [DE85-008228] N86-10444
PITTSBURGH UNIV., PA.
Dynamic lithostratigraphy and paleecology of upper Mississippi (Chesterian) strata of the northcentral Appalachian Basin N86-10693
Charge exchange in slow collisions of atoms and molecules N86-10922
Electron-ion recombination studies of planetary ionospheric and astrophysical ions N86-11132
PLANT RESOURCES INST., SALT LAKE CITY, UTAH.
Whole plant utilization of sunflowers as a renewable source of strategic materials (rubber) [AD-A155833] N86-10342
POLAR RESEARCH LAB., INC., CARPINTERIA, CALIF.
Long term statistical measurements of environmental acoustics parameters in the arctic. AEAS report number 2. Low frequency transmission loss measurements in the central arctic ocean [AD-A156576] N86-10727
POLITECNICO DI MILANO (ITALY).
Adhesion of metals: Experiment 1 ES-340 N86-10232
Evaluation of the accuracy of the metric camera images for the production of line maps and orthophotos N86-10490
POLITECNICO DI TORINO (ITALY).
Computational techniques for the analysis and design of digital communication systems [AD-A156945] N86-10407
PRINCETON UNIV., N. J.
On the design of airfoils in transonic flow using the Euler equations N86-10013
Transport processes research N86-10129
Electrohydrodynamics N86-10130
Fundamental studies of droplet combustion at reduced gravity N86-10165
Modeling of engine sprays [DE85-010020] N86-10559
The dynamics and stellar content of globular star clusters N86-11131
PULSE SCIENCES, INC., SAN LEANDRO, CALIF.
Radiation field results from the SPEED triaxiode, a large area, high dose rate, short pulse 1MV bremsstrahlung source [DE85-009438] N86-11005
PURDUE UNIV., LAFAYETTE, IND.
On the method of characteristics and its application to the calculations of annular nozzle flowfields N86-10454
Dynamic analysis of robotic manipulations with flexible links N86-10545

Vegetation and soils field research data base: Experiment summaries
[E85-10110] N86-10610
Theory of advanced, high-efficience concentrator cells
[DE85-008821] N86-10655
A study of methods to predict and measure the transmission of sound through the walls of light aircraft. Integration of certain singular boundary element integrals for applications in linear acoustics
[NASA-CR-176229] N86-10912
Information on continuum states from feeding times and total (GAMMA) spectra measured with BGO suppressed detectors
[DE85-013868] N86-10961

R

R-K RESEARCH AND SYSTEM DESIGN, MALIBU, CALIF.
Annotated bibliography of publications dealing with occupational health and medical information systems, cost analysis procedures, evaluation methodology and related legal issues
[AD-A156650] N86-11078
RADIAN CORP., MORRISVILLE, N.C.
Proceedings: First Annual Acid Deposition Emissions Inventory Symposium
[PB85-200004] N86-10686
RAND CORP., SANTA MONICA, CALIF.
Soviet free-electron laser research
[AD-A156898] N86-10542
RELIABILITY ANALYSIS CENTER, GRIFFISS AFB, N. Y.
Microcircuit device reliability field experience database. Volume 1. Field data. Volume 2. Failure Event/Analysis data
[AD-A156836] N86-10433
RENNES UNIV. (FRANCE).
Long range translocations ashore to offshore using Spacelab-1 metric camera imagery in the perspective of integrated geophysical surveys N86-10499
RENSSELAER POLYTECHNIC INST., TROY, N. Y.
Fluid dynamics and thermodynamics of vapor phase crystal growth N86-10068
Vapor growth of alloy-type semiconductor crystals N86-10069
Dendritic growth in undercooled melts N86-10082
Influence of melt convection on solid-liquid interface under terrestrial and reduced gravity environments N86-10083
Crystallization, optical and chemical properties of fluoride glasses N86-10149
Fuel and lubricant behavior in boundary layers analyzed by infrared emission Fourier transform spectrometry N86-10336
Modeling and control of nonlinear systems N86-10362
A mesh moving technique for time dependent partial differential equations in two space dimensions
[AD-A156663] N86-10866
Heat transfer in condensing and evaporating two-component, two-phase flow inside a horizontal tube N86-11058
RESEARCH INST. OF NATIONAL DEFENCE, LINKOEPING (SWEDEN).
Digital radio link: Method and a measuring system for studying the radio channel during frequency selective fading
[FOA-C-30386-E2] N86-10411
Information technique 1985: Optical technology and electro-optics, a defense technical component review
[FOA-A-30037-E] N86-10980
RESEARCH INST. OF NATIONAL DEFENCE, STOCKHOLM (SWEDEN).
Report on a visit to England
[FOA-C5-85-0006-H2] N86-10364
Management of organizational operations in dynamic environments. Towards a frame of reference.
[FOA-C5-85-0003-H2] N86-11072
RESEARCH INST. OF NATIONAL DEFENCE, UMEA (SWEDEN).
Method for determining elemental sulfur in jet fuel
[FOA-C-40211-B4] N86-10360
RICE UNIV., HOUSTON, TEX.
Measurement of the properties of tungsten at high temperatures N86-10091
Supersonic metal cluster beams
[DE85-014321] N86-10966
ROBERTS ASSOCIATES, INC., VIENNA, VA.
Computation of flow regimes in parameter space for the AGCE
[NASA-CR-178480] N86-10705
ROCHESTER UNIV., N. Y.
Cooperative emission by two different atoms into surface plasmons
[AD-A157033] N86-10925
ROCKWELL INTERNATIONAL CORP., GOLDEN, COLO.
Metallurgy and metallography of braze joints
[DE85-014563] N86-10325
Secondary standards laboratories for ionizing radiation calibrations: The national laboratory interests
[DE85-007046] N86-10938
ROCKWELL INTERNATIONAL CORP., RICHLAND, WASH.
Time-term analysis of upper crustal structure in the Columbia Basin, Washington
[DE85-012390] N86-10633
ROYAL AIRCRAFT ESTABLISHMENT, FARNBOROUGH (ENGLAND).
Lumped geopotential harmonics of order 14, from the orbit of 1967-11G
[AD-A156627] N86-10190
Calculation of the glass transition temperatures of linear polymers. Part 1: Rules for hierarchical ordering of the data set
[AD-A156584] N86-10343
Measurements of the acoustic interference between adjacent microphones
[AD-A156892] N86-10919
ROYAL GREENWICH OBSERVATORY, HERSTMONCEUX (ENGLAND).
OASIS: Optical Aperture Synthesis in Space N86-11106
ROYAL INST. OF TECH., STOCKHOLM (SWEDEN).
A preliminary report on floating zone experiments with germanium crystals in a sounding rocket N86-10256
ROYAL NETHERLANDS METEOROLOGICAL INST., DE BILT.
List of publications on the 200 m meteorological mast at Cabauw, the Netherlands
[KNMI-FM-85-6] N86-10711
Monthly Bulletin North Sea: Volume 2, January 1985
[KNMI-167-VOL-2] N86-10732
ROYAL OBSERVATORY, EDINBURGH (SCOTLAND).
Optical/IR telescope arrays: A study of their potential for satisfying observational requirements in astronomy for a large aperture system in the 1990s and beyond
[REPT-15] N86-11094
ROYAL SIGNALS AND RADAR ESTABLISHMENT, MALVERN (ENGLAND).
Special purpose hardware architectures for language recognition
[AD-A156634] N86-10793
RUTGERS - THE STATE UNIV., NEW BRUNSWICK, N. J.
An investigation of vortex dynamics in 2-dimensional superfluid films of helium-4 N86-11040
Extra-galactic X-ray sources and the diffuse X-ray background N86-11144

S

SANDIA LABS., ALBUQUERQUE, N. MEX.
Inviscid flow field analysis of maneuvering hypersonic vehicles using the SCM formulation and parabolic grid generation
[DE85-013950] N86-10021
Simulated direct-strike lightning testing at Sandia National Laboratories
[DE85-012033] N86-10049
Laser generation and transport of a relativistic electron beam
[DE85-011709] N86-10192
Compact, low jitter, triggered spark gap
[DE85-012812] N86-10195
Theoretical comparison of classical (K-matrix) and inverse (P-matrix) least-squares methods for quantitative infrared spectroscopy
[DE85-012827] N86-10298
Chemical kinetics and cellular structure of detonations in hydrogen sulphide and air
[DE85-009408] N86-10304
Weld metal hot-cracking of hastelloy alloys C-22 and C-276: A study by analytical electron microscopy
[DE85-009437] N86-10324
Metastable phase formation in Ni-implanted Al: An analytical electron microscope investigation
[DE85-009105] N86-10331
Analysis of transitions between ferroelectric and antiferroelectric states under conditioning of uniaxial strain
[DE85-014468] N86-10350
Thermal expansion of glasses in the solid and liquid phases
[DE85-013953] N86-10351
Explosive initiation by very small conical shaped charge jets
[DE85-009443] N86-10357
Methods for developing jam-resistant security communications networks at fixed-site facilities
[DE85-012032] N86-10408
Calibrated Faraday current and magnetic field sensor
[DE85-013438] N86-10439
Effects of scale and geometry on hydrogen-air detonations
[DE85-006762] N86-10474
Geothermal lost circulation zone mapping tool
[DE85-008696] N86-10531
Characterization of cathodic corrosion products in the Ca/CaCrO4 thermal battery
[DE85-013442] N86-10644
Photovoltaic concentrator array evaluation
[DE85-013789] N86-10665
Estimating wind speed as a function of height above ground: An analysis of data obtained at the Southwest Residential Experiment Station, Las Cruces, New Mexico
[DE85-013262] N86-10716
Understanding and improving acoustic to seismic coupling as it pertains to Sandia's helicopter detector
[DE85-009440] N86-10920
Providing automated control for PBFA-2
[DE85-012867] N86-10928
Photonic diagnostics and pulsed power research
[DE85-013752] N86-10940
Preliminary investigation of changes in X-ray multilayer optics subjected to high radiation flux
[DE85-014074] N86-10944
Radiation field results from the SPEED triaxiode, a large area, high dose rate, short pulse 1MV bremsstrahlung source
[DE85-009438] N86-11005
Advances in data acquisition system technology for PBFA 2
[DE85-012860] N86-11011
Engineering high reliability, low-jitter Marx generators
[DE85-012811] N86-11013
Photoactivation of PBFA-2
[DE85-013439] N86-11019
Shock loading and release behavior of x-cut quartz
[DE85-013954] N86-11054
High-pressure release-wave measurements and phase transformation in CaCO3
[DE85-012592] N86-11055
SASKATCHEWAN UNIV., SASKATOON.
Applications of the second-order achromat concept to the design of particle accelerators
[DE85-013072] N86-10994
SCIENCE APPLICATIONS, INC., CHATSWORTH, CALIF.
Buoyancy effects upon vapor flame and explosion processes N86-10161
SCIENCE APPLICATIONS, INC., HUNTSVILLE, ALA.
The control of float zone interfaces by the use of selected boundary conditions N86-10060
SCIENCE APPLICATIONS INTERNATIONAL CORP., MCLEAN, VA.
High flux calorimetry
[AD-A156852] N86-10524
SHOCK AND VIBRATION INFORMATION CENTER (DEFENSE), WASHINGTON, D. C.
The Shock and Vibration Digest, volume 17, no. 3
[AD-A154144] N86-10585
Editors rattle space N86-10586
SILSOE COLL., BEDFORD (ENGLAND).
Land evaluation successes with the metric camera N86-10512
SOCIETE CROUZET, VALENCE (FRANCE).
Elastic wave gyrometer. Experiments with a parametric wave device
[REPT-26/5005/HF/AR] N86-10533
SOCIETE NATIONALE INDUSTRIELLE AEROSPATIALE, SURESNES (FRANCE).
Nondestructive control of thick structures made without disassembling
[PV-43-954/F/3] N86-10564
Nondestructive corrosion test of aluminum alloy structures
[PV-43-954/F/2] N86-10594
SOCIETE NATIONALE INDUSTRIELLE AEROSPATIALE, TOULOUSE (FRANCE).
Aerodynamics of hyperlift systems
[SNIAS-443.501/85] N86-10023
Analysis of hyperlift systems. Study of a singularities method
[SNIAS-443.529/84] N86-10024
SOUTHWEST RESEARCH INST., SAN ANTONIO, TEX.
Constitutive modeling for isotropic materials (HOST)
[NASA-CR-174980] N86-10589
Characterization of mechanical damage mechanisms in ceramic composite materials
[AD-A156574] N86-10590
Exploratory development for a high reliability flaw characterization module
[AD-A156632] N86-10916
SPECTRA TECHNOLOGY, INC., BELLEVUE, WASH.
Design, fabricate and test a 1.06(MU) repetitively pulsed laser
[DE85-014439] N86-10543

SPECTROLAB, INC., SYLMAR, CALIF.
Development of metallization process
[NASA-CR-176209] N86-10312
STANFORD LINEAR ACCELERATOR CENTER, CALIF.
Dissecting the cow
[DE85-013369] N86-10801
Klystron control software in the SIC
[DE85-013068] N86-10836
Parasitic mode losses versus signal sensitivity in beam position monitors
[DE85-014367] N86-10964
Beam-beam deflections to measure size spot and offset at SLC IP
[DE85-014285] N86-10965
Applications of the second-order achromat concept to the design of particle accelerators
[DE85-013072] N86-10994
Superconvergent tracking and invariant surfaces in phase space
[DE85-013051] N86-10995
Electron wind in strong wave guide fields
[DE85-013062] N86-11004
Effects of slots/holes in disks on frequencies of TM01 and EH11 waves in the disk-loaded waveguide
[DE85-013376] N86-11009
High-resolution phosphor screen beam profile monitor
[DE85-013074] N86-11012
SLC positron damping ring optics design
[DE85-013054] N86-11014
Timing system control software in the SLC
[DE85-013380] N86-11024
Beam steering in the SLC linac
[DE85-013370] N86-11025
Programmable delay unit incorporating a semi-custom integrated circuit
[DE85-013379] N86-11033
Search for heavy neutrines produced in e(+)e(-) annihilation
[DE85-013372] N86-11035
Superconductors for pulsed RF accelerators
[DE85-013378] N86-11051
STANFORD UNIV., CALIF.
The influence of low frequency mechanical vibrations on the growth of single crystals N86-10059
Lambda point equipment N86-10118
Cryogenic equivalence principle experiment N86-10171
Investigation of metallic impurities introduced into SiO2 and silicon by various candidate VLSI metallization systems: Chemical reactions, diffusion, and electrical properties
[AD-A156609] N86-10429
Film cooling on a convex wall: Heat transfer and hydrodynamic measurements for full and partial coverage
[NASA-CR-174964] N86-10461
Computer control of rf at SLAC
[DE85-013065] N86-11015
STATE UNIV. COLL. OF NEW YORK, BUFFALO.
Geothermal influences on the long-term thickness of the mechanical lithosphere during flexure N86-10697
STATE UNIV. OF NEW YORK, ALBANY.
Seasonal variations in atmospheric chemistry in the Adirondacks
[DE85-014227] N86-10719
STATE UNIV. OF NEW YORK, BUFFALO.
Digital decoding of in-line holograms N86-10478
Advanced development of BEM for two and three dimensional nonlinear analysis N86-10855
Cooperative emission by two different atoms into surface plasmons
[AD-A157033] N86-10925
STATE UNIV. OF NEW YORK AT BUFFALO, AMHERST.
Two-dimensional electrons
[AD-A156894] N86-10982
STONE AND WEBSTER ENGINEERING CORP., BOSTON, MASS.
Hot cell facility design for large fusion devices
[DE85-012893] N86-11037
STUTTGART UNIV. (WEST GERMANY).
GaS-semiconductor crystals under microgravity: Experiment ES 323 N86-10224
Laminar film condensation in vertical closed two-phase thermosiphons
[IKE-5-220] N86-10476
Digital elevation model from Spacelab metric camera photographs N86-10486
SUSSEX UNIV., BRIGHTON (ENGLAND).
The preparation and testing of titanium and zirconium coupling agents
[SJ70] N86-10576
SYDNEY UNIV. (AUSTRALIA).
A study of blood flow and of aggregation of blood cells under conditions of zero gravity: Its relevance to the occlusive diseases and cancer N86-10137
SYRACUSE UNIV., N. Y.
Environmental degradation of materials: Surface chemistry related to stress corrosion cracking N86-10099
SYSTEMS APPLICATIONS, INC., SAN RAFAEL, CALIF.
Technical considerations in regional aerosol modeling
[PB85-193027] N86-10710

T

TATA INST. OF FUNDAMENTAL RESEARCH, BOMBAY (INDIA).
Principal bundles on the affine line N86-10856
Coincidence densities and spectra of a class of substitution minimal sets N86-10857
TECHNICAL UNIV. OF DENMARK, LYNGBY.
Crystal growth from solution N86-10229
TECHNION - ISRAEL INST. OF TECH., HAIFA.
Effect of sequence of loading on interaction curves for buckling of stiffened shells
[TAE-536] N86-10583
Correlation between vibrations and buckling of cylindrical shells stiffened by spot-welded and riveted stringers
[TAE-537] N86-10584
TECHNISCHE HOCHSCHULE, GRAZ (AUSTRIA).
Geological mapping of remote mountainous regions using metric camera imagery N86-10503
TECHNISCHE HOGESCHOOL, DELFT (NETHERLANDS).
Fatigue, static tensile strength and stress corrosion of aircraft materials and structures
[VTH-LR-360-PT-1] N86-10045
Unidirectional solidification of cast iron: Experiment ES-325 N86-10212
Experiments and computations on unsteady separating flow in an expanding flume
[REPT-2-84] N86-10477
The local disk controller
[REPT-1-68430-44(1985)01] N86-10806
Performance analysis of the IBM Direct Access Storage Device (DASD) subsystem, and some suggestions for improved systems
[REPT-1-68430-44(1985)02] N86-10807
An intelligent local disk control system
[REPT-051560-28(1984)08] N86-10808
Acquaintance with on line literature research. An introduction for education at the Chemical Technology Section N86-11081
TECHNISCHE HOGESCHOOL, EINDHOVEN (NETHERLANDS).
Digital transmission experiments with the Orbital Test Satellite
[EUT-84-E-144] N86-10270
Measurement of workpiece temperature during welding for welding robot control N86-10534
Design of a multifunction Input-Output (I/O) controller
[EUT-84-E-143] N86-10802
Minimization of programmable logic arrays
[EUT-84-E-145] N86-10803
Realization of a multifunction Input/Output (I/O) controller by means of a gate array
[EUT-85-E-147] N86-10804
A course on field programmable logic
[EUT-85-E-148] N86-10805
The identification package SATER
[ER-83/08] N86-10844
COMPACT: Compaction of hierarchial chip layouts based on a constraint graph method with double-sided constraints N86-10845
State assignment in sequential circuits
[EUT-85-E-146] N86-10846
Stock-taking of data base management systems choice considerations for the Eindhoven Technical University Computing Center (THE-RC)
[COMP-CENT-NOTE-18] N86-10851
Multivariable partial realization and the aspect of uniqueness
[ER-83/09] N86-10879
Naive approximate realization of noisy data
[ER-83/10] N86-10880
Adaptive distribution-free test for the K random sampling problem, part 1
[COMP-CENT-NOTE-14-PT-1] N86-10888
Adaptive distribution free test for the K random sampling problem, part 2
[COMP-CENT-NOTE-15-PT-2] N86-10889
Robustness of multiple comparisons against variance heterogeneity
[COMP-CENT-NOTE-17] N86-10890
Nonparametric comparison of several mean values with mild adaptation to some sample characteristics
[COMP-CENT-NOTE-20] N86-10891
Operations research applications
[ARW-03-THE-BDK/ORS/83-08] N86-10901
On the structure of manpower planning, a contribution of simulation experiments with decomposition methods
[MANPOWER-PLANNING-28] N86-11073
Aspects of manpower planning at a Dutch university, an example of aggregation and decomposition methods in manpower planning
[MANPOWER-PLANNING-29] N86-11074
On the structure of manpower planning, a contribution of simulation experiments with aggregation methods
[MANPOWER-PLANNING-30] N86-11075
Failures and successes of quantitative methods in management
[ARW-03-THE-BDK/ORS/83-06] N86-11076
TECHNISCHE UNIV., BERLIN (WEST GERMANY).
Self diffusion of Sn112 and Sn124 in liquid tin N86-10231
Topographic interpretation of metric camera images: An example in Somalia N86-10508
A logistics scenario for an early lunar base
[ILR-MITT-143] N86-11140
TECHNISCHE UNIV., CLAUSTHAL-ZELLERFELD (WEST GERMANY).
Interdiffusion in the glass melt system (Na2O+Rb2O).3SiO2 N86-10216
Shrinking of a gas bubble in a glass melt under microgravity conditions N86-10254
TECHNISCHE UNIV., HANOVER (WEST GERMANY).
Orthophotomapping from metric camera imagery N86-10487
Digital image processing of metric camera imagery N86-10511
TECHNISCHE UNIV., MUNICH (WEST GERMANY).
Nucleate pool boiling in subcooled liquid under microgravity: Results of TEXUS experimental investigations N86-10250
Isochoric specific heat of sulfur hexafluoride at the critical point. A Spacelab experiment for the German D1-mission in 1985 N86-10251
Physical and chemical properties of a nickel catalyst processed under microgravity N86-10255
Analysis of metric camera images from the USA and their suitability for topographic and thematic mapping N86-10498
Interpretation of metric camera concerning hydrologic structures of the Rhone Delta N86-10504
Thematic mapping of metric camera color infrared and black and white photographs for land use classification N86-10510
Topographic and thematic mapping: Analysis of metric camera black and white photographs of the Rhone Delta N86-10514
Updating of topographic maps by means of metric camera photos example: Hallertau (Bavaria) N86-10517
Interpretation of Spacelab-1 photographs for the generation of 1:200000 topographic map N86-10518
Metric camera image of Munich as additional means for urban cartography N86-10519
Tectonic analysis of typical fold structures in the Zagros Mountains (Iran) by the application of quantitative photogrammetric methods on metric camera data N86-10521
TECHNISCHE UNIV., VIENNA (AUSTRIA).
Vacuum brazing under microgravity N86-10214
Stereo-orthophotos in various map projections N86-10488
TENNESSEE UNIV., KNOXVILLE.
Thermodynamic constraints on ion beam mixing of metals on insulators
[DE85-013628] N86-10448
Determination of optical properties by third-harmonic generation in noble gases in unfocused laser beams N86-10535
Ground-coupled heat pump research at the University of Tennessee Washington, D.C., 10 Dec. 1984
[DE85-005357] N86-10650
The effects of orography on land-atmosphere turbulent exchange processes N86-10702
TENNESSEE VALLEY AUTHORITY, CHATTANOOGA.
Kinetics of biological ferrous iron oxidation
[DE85-014616] N86-10736
TENNESSEE VALLEY AUTHORITY, KNOXVILLE.
Sediment characterization. Task 2: Instream contaminant study. Volume 2: Appendices
[DE85-013503] N86-10680
Sediment characterization. Task 2: Instream contaminant study, volume 1
[DE85-013502] N86-10683
TESTWELL LTD., DAVENTRY (ENGLAND).
Fracture toughness testing of centrifugally cast nickel aluminium bronze
[REPT-MAT/720] N86-10575
TEXAS CHRISTIAN UNIV., FORT WORTH.
Real-time holography by stimulated Raman and Brillouin scattering N86-10479

TEXAS DEPT. OF WATER RESOURCES, AUSTIN.
Evaluating the ground-water resources of the high plains of Texas, Volume 4
[PB85-191625] N86-10641
TEXAS TECHNOLOGICAL UNIV., LUBBOCK.
Electromagnetic resonances of cylinders and aircraft model with resistive wires
[NASA-CR-176250] N86-10042
TEXAS UNIV., AUSTIN.
Nature of photoemission into dielectric fluids
[DE85-013017] N86-10945
Local conservation laws for the Maxwell-Vlasov and collisionless kinetic guiding center theories
[DE85-013122] N86-11063
A method for numerical relativity: Simulation of axisymmetric gravitational collapse and gravitational radiation generation N86-11127
Initial data for N black holes N86-11128
TEXAS UNIV., EL PASO.
Crustal structure of the southern Rio Grande rift determined from seismic refraction, surface wave dispersion, and gravity data N86-10700
TILBURG UNIV. (NETHERLANDS).
Superefficient estimation of power functions in simulation experiments
[B8562445] N86-10893
The power of weighted and ordinary least squares with estimated unequal variances in experimental design
[B8562446] N86-10894
Regression analysis: Assumptions, alternatives, applications N86-10895
TOLEDO UNIV., OHIO.
Mass transport phenomena between bubbles and dissolved gases in liquids under reduced gravity conditions N86-10110
TOPOGRAPHICAL SURVEY BRANCH, KATHMANDU (NEPAL).
Test on mapping application of metric camera imagery N86-10505
TRW SPACE TECHNOLOGY LABS., REDONDO BEACH, CALIF.
Symmetric Tandem Mirror Program
[DE85-012352] N86-11032

U

UNITED KINGDOM ATOMIC ENERGY AUTHORITY, RISLEY (ENGLAND).
The influence of the substrate on the practical machining applications of cutting edges coated with different materials
[BLL-RISLEY-TR-5039-(9091.9F)] N86-10546
UNITED NATIONS ECONOMIC COMMISSION FOR AFRICA, ADDIS ABABA (ETHIOPIA).
Role of the Economic Commission for Africa as a principal investigator in the metric camera experiment and reports of the result of the assessment for topographic and revision of maps in populated and developed areas of the world N86-10501
UNITED TECHNOLOGIES CORP., SOUTH WINDSOR, CONN.
Phosphoric and electric utility fuel technology development
[DE85-014741] N86-10651
Phosphoric and electric utility fuel cell technology development
[DE85-014552] N86-10652
UNIVERSIDAD POLITECNICA DE MADRID (SPAIN).
Liquid column stability: Experiment 1 ES-331 N86-10205
Stability of long liquid columns N86-10244
UNIVERSITE DES SCIENCES ET TECHNIQUES DU LANGUEDOC, MONTPELLIER (FRANCE).
Formation of waves by ground motion
[PM/84/09] N86-10706
Well-posed questions and exploration of the space of parameters in linear and non linear inversion
[PN-84/13] N86-10858
A modified modified Korteweg-deVries equation
[PN-84/27] N86-10859
UNIVERSITIES SPACE RESEARCH ASSOCIATION, COLUMBIA, MD.
A root-mean-square pressure fluctuations model for internal flow applications
[NASA-CR-3928] N86-10460
UNIVERSITY COLL., LONDON (ENGLAND).
Evaluation of metric camera images at the University of London N86-10495
OEEPE participation in testing metric camera photography N86-10507
UNIVERSITY OF SOUTHERN CALIFORNIA, LOS ANGELES.
Evaluation of a pulse control law for flexible spacecraft
[NASA-CR-176233] N86-10272
Chronologic analysis of terrestrial sediments and basin evolution N86-10602
UTAH UNIV., SALT LAKE CITY.
Morphological stability and fluid dynamics of vapor crystal growth N86-10126

V

VALVO ROEHREN- UND HALBLEITERWERKE DER PHILIPS G.M.B.H., HAMBURG (WEST GERMANY).
Increase of the packaging density of Very Large Scale Integration (VLSI) circuits using automatic alignment
[BMFT-FB-T-85-020] N86-10451
VANDERBILT UNIV., NASHVILLE, TENN.
The role of freestream turbulence scale in subsonic flow separation
[NASA-CR-176237] N86-10014
Effect of undercooling in a low-gravity containerless environment on the structure and properties of alloys N86-10073
VIRGINIA POLYTECHNIC INST., BLACKSBURG.
Intrinsic mechanisms of multilayer ceramic capacitor failure
[AD-A156638] N86-10431
VIRGINIA POLYTECHNIC INST. AND STATE UNIV., BLACKSBURG.
A fundamental study of the sticking of insect residues to aircraft wings
[NASA-CR-176231] N86-10033
Finite element solution of the Navier-Stokes equations for 3-D turbulent free shear flows N86-10457
VIRGINIA UNIV., CHARLOTTESVILLE.
Simulating the CTR environment in the HVBM
[DE85-011745] N86-10193
A study of the applicability of nucleation theory to quasi-thermodynamic transitions of second and higher Ehrenfest-order
[NASA-CR-176238] N86-11059
A study of the applicability of nucleation theory to quasi-thermodynamic transformations of second and higher Ehrenfest-order
[NASA-CR-176230] N86-11060

W

WACKER-CHEMIE G.M.B.H. BURGHAUSEN (WEST GERMANY).
Crystallization of a silicon sphere N86-10226
WASHINGTON UNIV., SEATTLE.
Radiative heat transfer in nonisothermal combustion products N86-10458
Scaling studies of solar pumped lasers
[NASA-CR-176240] N86-10540
Strategies for analyzing mixed pixels in remotely sensed imagery N86-10623
Energy balance in a deep Colorado valley: ASCOT 84
[DE85-012441] N86-10631
Physical conditions in giant extragalactic H2 regions N86-11130
WASHINGTON UNIV., ST. LOUIS, MO.
Criteria for the design or selection of a bioelectromagnetics experiment
[AD-A156575] N86-10420
Non-empirical interatomic potentials for transition metals
[DE85-013448] N86-10440
Analysis of remote sensing data N86-10605
WEAPONS SYSTEMS RESEARCH LAB., ADELAIDE (AUSTRALIA).
A simplified method of estimation of the specular components of radar cross section for some re-entrant conductors
[AD-A156573] N86-10403
A comparison of swept frequency and FFT methods used to calibrate array test modules
[AD-A156629] N86-10430
WESTAT RESEARCH, INC., ROCKVILLE, MD.
Academic Research Equipment in selected science-engineering fields, 1982-83. An analysis of findings from the Baseline National Survey of academic research instruments and instrumentation needs N86-11088
WESTECH SYSTEMS, INC., PHOENIX, ARIZ.
Microgravity silicon zoning investigation N86-10063
WESTERN RESEARCH INST., LARAMIE, WYO.
Geologic evaluation and reservoir properties of the PR Spring tar sand deposit, Uintah and Grand Counties, Utah
[DE85-013248] N86-10634
WESTINGHOUSE RESEARCH AND DEVELOPMENT CENTER, PITTSBURGH, PA.
Delay times and jitter in triggered vacuum spark gaps using metal vapor and surface flashover types of triggers
[DE85-013966] N86-10441
WESTLAND HELICOPTERS LTD., YEOVIL (ENGLAND).
Trials on the asperity counting monitoring system
[RES-PAPER-670] N86-10550
WESTON OBSERVATORY, MASS.
Vibro-acoustic forecast for space shuttle launches at Vandenberg AFB: The payload changeout room and the administration building
[AD-A156944] N86-10269
WISCONSIN UNIV., MADISON.
Containerless processing of undercooled melts N86-10093
WISCONSIN UNIV., MILWAUKEE.
Altitudinal distribution of granitic landforms in the south central Sierra Nevada, California N86-10695
WRIGHT STATE UNIV., DAYTON, OHIO.
Initial increase, peaking effect, in the internal friction of copper following pulsed neutron and electron irradiation
[DE85-012767] N86-10932
WYOMING UNIV., LARAMIE.
Spillover minimization in self-adjoint distributed-parameter systems with direct output feedback N86-10852
The two micron spectrum of R Scuti N86-11092

Y

YALE UNIV., NEW HAVEN, CONN.
The mechanics of delamination in composite materials N86-10284
Strength of shells under local transverse loads N86-10568
Modeling groundwater flow into lakes N86-10598
Alternating direction methods on multiprocessors: An extended abstract
[AD-A156722] N86-10794
Efficient systolic arrays for the solution of toeplitz systems: An illustration of a methodology for the construction of systolic architectures in VLSI (Very Large Systems Integration)
[AD-A156767] N86-10795
The DUCK manual
[AD-A156936] N86-10833
Topological properties of hypercubes
[AD-A156777] N86-10850
Rank revealing QR-Factorizations
[AD-A156756] N86-10887
Electron tunneling in metal/tunnel-oxide/degenerate silicon junctions N86-11043
YALE UNIV. OBSERVATORY, NEW HAVEN, CONN.
Partial eigensolutions of large nonsymmetric matrices
[AD-A156711] N86-10867
On the lanczos method for solving symmetric linear systems with several right-hand-sides
[AD-A156816] N86-10868

Z

ZURICH UNIV. (SWITZERLAND).
Evaluation of metric camera photos N86-10515

Typical Contract Number Index Listing

DE-AC06-77RL-01030 ..... N86-10633

CONTRACT NUMBER — NASA ACCESSION NUMBER

Listings in this index are arranged alphanumerically by contract number. Under each contract number the NASA accession numbers denoting documents that have been produced as a result of research done under that contract are arranged in ascending order. The NASA accession number denotes the number by which the citation is identified.

AF PROJ. TKSI N86-10191
AF PROJ. 2103 ..... N86-10830
AF-AFOSR-0192-80 ..... N86-10866
AF-AFOSR-0193-81 ..... N86-10868
AF-AFOSR-0290-82 ..... N86-11060
AMTE-NSM42D/1611 ..... N86-10575
ARPA ORDER 4395 ..... N86-10924
ARPA ORDER 5020 ..... N86-11050
A12/1347 ..... N86-10550
A79/KL/097 ..... N86-10789
A83/K/045 ..... N86-10782
BMFT-01-QV-148-ZA-SN-SLN-7786 ..... N86-10242
CNR-PSN-83-070 ..... N86-10203
N86-10238
DA PROJ. RR0-3302 ..... N86-11049
DA PROJ. W05-270 ..... N86-10406
DA PROJ. 1L1-61102-BH-57 ..... N86-10407
DA PROJ. 4A7-62707-A-855 ..... N86-10630
DA PROJ. 376-3 ..... N86-10042
DAAG29-82-K-0197 ..... N86-10866
DAAG29-83-C-0016 ..... N86-10342
DAAG29-83-K-0177 ..... N86-10887
DAJA37-80-C-0011 ..... N86-10407
DARPA ORDER A04541 ..... N86-10429
DARPA ORDER 4000 ..... N86-10291
DE-AC01-83CE-30780 ..... N86-10646
N86-10648
N86-10731
DE-AC02-76CH-00016 ..... N86-10438
N86-10649
N86-10667
N86-10719
N86-10931
N86-10933
N86-10935
N86-10937
N86-10947
N86-10948
N86-10989
N86-11010
N86-11018
N86-11021
N86-11022
N86-11023
N86-11026
DE-AC02-76CH-03000 ..... N86-10946
N86-10997
DE-AC02-76ER-04073 ..... N86-10303
DE-AC02-78ET-51013 ..... N86-11000
N86-11020
DE-AC02-81ER-10996 ..... N86-10868
N86-10887
DE-AC02-83CH-10093 ..... N86-10645
N86-10655
N86-10657
N86-10658
N86-10668
DE-AC02-83CH-100983 ..... N86-10662
DE-AC02-83ER-40105 ..... N86-11062
DE-AC03-76SF-00098 ..... N86-10321
N86-10442
N86-10446
N86-10962
N86-10978
N86-10995
N86-11008
N86-11057
DE-AC03-76SF-00515 ..... N86-10801
N86-10836
N86-10964
N86-10965
N86-10994
N86-10995
N86-11004
N86-11009
N86-11012
N86-11014
N86-11015
N86-11024
N86-11025
N86-11033
N86-11035
N86-11051
DE-AC03-79ET-51017 ..... N86-11032
DE-AC03-81ER-40050 ..... N86-11014
DE-AC04-76DP-00613 ..... N86-10410
N86-10842
DE-AC04-76DP-00789 ..... N86-10021
N86-10049
N86-10192
N86-10195
N86-10298
N86-10300
N86-10301
N86-10304
N86-10324
N86-10331
N86-10350
N86-10351
N86-10357
N86-10408
N86-10439
N86-10441
N86-10474
N86-10531
N86-10644
N86-10716
N86-10920
N86-10928
N86-10940
N86-11005
N86-11011
N86-11013
N86-11019
N86-11054
N86-11055
DE-AC04-76DP-03533 ..... N86-10325
DE-AC04-81AL-16338 ..... N86-10559
DE-AC05-84CR-21400 ..... N86-10328
N86-10958
DE-AC05-84CT-21400 ..... N86-10843
DE-AC05-84OR-21400 ..... N86-10329
N86-10448
N86-10472
N86-10473
N86-10526
N86-10647
N86-10650
N86-10653
N86-10654
N86-10661
N86-10664
N86-10677
N86-10678
N86-10679
N86-10840
N86-10926
N86-10936
N86-10949
N86-10960
N86-11037
DE-AC05-84OS-21400 ..... N86-10330
DE-AC05-84OU-21400 ..... N86-10953
DE-AC06-76RL-01830 ..... N86-10297
N86-10299
N86-10326
N86-10527
N86-10631
N86-10666
N86-10684
N86-10772
N86-10938
DE-AC06-77RL-01030 ..... N86-10633
DE-AC06-83FR-53157 ..... N86-10543
DE-AC07-76ID-01570 ..... N86-10320
N86-10530
N86-10736
N86-10954
DE-AC07-83ID-12379 ..... N86-10682
DE-AC08-83NV-10282 ..... N86-10528
DE-AC09-76SF-00001 ..... N86-10348
DE-AC09-76SR-00001 ..... N86-10319
DE-AC21-81FE-15078 ..... N86-10444
DE-AC21-83FE-60338 ..... N86-10651
N86-10652
DE-AC21-83MC-20212 ..... N86-10447
DE-AC79-83BP-13795 ..... N86-10527
DE-AI01-76ET-20320 ..... N86-10582
DE-AI01-78CS-54209 ..... N86-11083
N86-11084
N86-11085
N86-11086
DE-AI01-79ET-20485 ..... N86-10643
DE-AI05-84CR-21444 ..... N86-10680
DE-AS05-76ET-52023 ..... N86-10193
DE-AS05-76FV-04814 ..... N86-10957
DE-AS05-78ER-06035 ..... N86-10966
DE-AT01-77DP-70032 ..... N86-10302
DE-AT03-81ER-10870 ..... N86-10327
DE-AT03-84ER-53158 ..... N86-11007
DE-FC21-83FE-60177 ..... N86-10634
DE-FG02-84ER-13283 ..... N86-10834
DE-FG02-84ER-45130 ..... N86-10440
DE-FG02-84ER-45153 ..... N86-11053
DE-FG05-80ET-53088 ..... N86-11063
DE-FG05-84ER-45064 ..... N86-10945
DE-FG05-84FR-13266 ..... N86-10939
DFVLR-01-QV-698 ..... N86-10224
DNA001-80-C-0022 ..... N86-10405
DNA001-82-C-0185 ..... N86-10524
DRET-81-668 ..... N86-10878
DRET-83-34-051-00-470-75-01 ..... N86-10023
DRET-83-34-135 ..... N86-10022
DRET-83-058 ..... N86-10533
EPA-68-02-3487 ..... N86-10689
EPA-68-02-3994 ..... N86-10686
EPA-68-02-3996 ..... N86-10688
EPA-68-02-4076 ..... N86-10710
F04701-83-C-0064 ..... N86-10708
F19628-84-C-0011 ..... N86-10269
F30602-84-C-0162 ..... N86-10433
F33600-82-C-0543 ..... N86-10006
F33615-80-C-0512 ..... N86-10675
F33615-81-C-5056 ..... N86-10292
F33615-81-C-5066 ..... N86-10916
F33615-81-K-1539 ..... N86-10432
JPL PROJ. 5030-573 ..... N86-11083
N86-11084
N86-11085
N86-11086
JPL-955057 ..... N86-10118
JPL-955870 ..... N86-10149
JPL-956205 ..... N86-10312
LFP-955147 ..... N86-10050
MDA903-82-K-0412 ..... N86-10429
MDA903-83-C-0306 ..... N86-10790
MDA903-83-M-2646 ..... N86-11065
MDA903-84-C-0031 ..... N86-10829
N86-11071
MDA903-84-K-0232 ..... N86-10291
MDA903-84-K-0374 ..... N86-11050
MDA903-85-C-0030 ..... N86-10542
MIN-DEF-A93B/1034 ..... N86-10309
MIN-DEF-ERC/9/4/2120/034 ..... N86-10576
MIN-DEF-K80B/33 ..... N86-10339
MIPR-N-83-18 ..... N86-10830
NAG-483 ..... N86-10101

NAGW-466 ..... N86-10099
NAGW-469 ..... N86-10100
NAG1-28 ..... N86-10042
NAG1-58 ..... N86-10912
NAG1-126 ..... N86-10271
NAG1-135 ..... N86-10539
NAG1-176 ..... N86-10540
NAG1-190 ..... N86-10848
NAG1-300 ..... N86-10033
NAG1-336 ..... N86-10577
NAG1-354 ..... N86-10054
NAG1-419 ..... N86-11059
N86-11060
NAG1-471 ..... N86-10272
NAG1-483 ..... N86-10014
NAG1-500 ..... N86-10484
NAG2-62 ..... N86-10118
NAG3-3 ..... N86-10461
NAG3-34 ..... N86-10110
NAG3-147 ..... N86-10108
NAG3-259 ..... N86-10130
NAG3-303 ..... N86-10117
NAG3-333 ..... N86-10083
NAG3-380 ..... N86-10165
NAG3-381 ..... N86-10160
NAG3-404 ..... N86-10163
NAG3-417 ..... N86-10090
NAG3-436 ..... N86-10093
NAG3-443 ..... N86-10162
NAG3-447 ..... N86-10129
NAG3-470 ..... N86-10113
NAG3-475 ..... N86-10377
NAG3-493 ..... N86-10128
NAG3-534 ..... N86-10588
N86-10860
NAG3-560 ..... N86-10086
NAG3-568 ..... N86-10123
NAG3-570 ..... N86-10124
NAG4-379 ..... N86-10119
NASA ORDER H-27954-B N86-10074
N86-10077
NASA ORDER H-34328-B N86-10067
NASA ORDER H-73830-B N86-10066
NASA ORDER H-78181-B N86-10705
NASA ORDER H-78183-B N86-11095
NASA ORDER R05-030-001 ..... N86-11047
NASA ORDER S-12402-C N86-10597
NASW-3458 ..... N86-10462
NASW-3755 ..... N86-11103
NASW-3949 ..... N86-11139
NASW-3950 ..... N86-11133
NASW-4004 ..... N86-10418
NASW-4005 ..... N86-10293
N86-10611
N86-10612
N86-10613
N86-10614
NASW-4006 ..... N86-10179
N86-10273
N86-10378
NAS2-11555 ..... N86-10819
NAS2-11948 ..... N86-10274
NAS3-22822 ..... N86-10161
NAS3-23770 ..... N86-10164
NAS3-23925 ..... N86-10589
NAS3-23934 ..... N86-10132
NAS7-100 ..... N86-10150
N86-10312
NAS7-918 ..... N86-10102
N86-10167
N86-10382
N86-10599
N86-10615
N86-10707
N86-11083
N86-11084
N86-11085
N86-11086
NAS8-32614 ..... N86-10143
NAS8-32936 ..... N86-10069
NAS8-32945 ..... N86-10064
NAS8-32950 ..... N86-10135
NAS8-32951 ..... N86-10146
NAS8-32952 ..... N86-10081
N86-10264
NAS8-33021 ..... N86-10095
NAS8-33199 ..... N86-10091
NAS8-33513 ..... N86-10169
NAS8-33562 ..... N86-10068
NAS8-33742 ..... N86-10177
NAS8-33881 ..... N86-10109
NAS8-34321 ..... N86-10172
NAS8-34648 ..... N86-10168
NAS8-34676 ..... N86-10073
NAS8-34758 ..... N86-10148
NAS8-34872 ..... N86-10059
NAS8-34887 ..... N86-10070
NAS8-34891 ..... N86-10071
NAS8-34920 ..... N86-10063
NAS8-35108 ..... N86-10060
NAS8-35145 ..... N86-10076
NAS8-35161 ..... N86-10075
NAS8-35333 ..... N86-10136
N86-10246
NAS8-35334 ..... N86-10138
N86-10248
NAS8-35362 ..... N86-10139
N86-10246
NAS8-35412 ..... N86-10062
NAS8-35416 ..... N86-10154
NAS8-35483 ..... N86-10089
NAS8-35620 ..... N86-10096
NAS8-35668 ..... N86-10175
NAS8-35918 ..... N86-10460
NAS8-36516 ..... N86-10233
NAS9-15566 ..... N86-10140
NAS9-15584 ..... N86-10145
NAS9-16389 ..... N86-10134
NAS9-16528 ..... N86-10610
NAS9-16634 ..... N86-10770
N86-10785
N86-10820
N86-10821
N86-10896
N86-10897
NCC1-75 ..... N86-10578
NCC2-248 ..... N86-11047
NGT-47-003-029 ..... N86-11064
NSF DCR-84-07077 ..... N86-10833
NSF DMS-83-15216 ..... N86-10862
N86-10864
N86-10869
NSF ECS-82-05425 ..... N86-10861
NSF PHY-77-27084 ..... N86-10088
NSF PHY-84-01063 ..... N86-11008
NSF SRS-80-17873 ..... N86-11088
NSG-1468 ..... N86-10827
NSG-1534 ..... N86-10126
NSG-1648 ..... N86-10822
N86-10823
N86-10824
N86-10825
N86-10826
NSG-7176 ..... N86-11103
N86-11104
N86-11118
NSG-7331 ..... N86-10061
NSG-7645 ..... N86-10055
N86-10056
N86-10072
N86-10078
N86-10080
N86-10085
N86-10098
N86-10105
N86-10127
N86-10133
N86-10147
N86-10152
N86-10158
N00014-76-C-0063 ..... N86-10346
N86-10593
N00014-76-C-0370 ..... N86-10432
N00014-77-C-0505 ..... N86-10591
N00014-79-C-0661 ..... N86-10899
N00014-79-C-0683 ..... N86-10283
N00014-80-C-0236 ..... N86-10432
N00014-80-C-0472 ..... N86-10925
N00014-82-C-5076 ..... N86-10899
N00014-82-K-0184 ..... N86-10794
N86-10795
N86-10850
N86-10867
N86-10868
N86-10887
N00014-82-K-0329 ..... N86-10861
N00014-83-C-0170 ..... N86-10465
N86-10541
N86-10977
N00014-83-C-0196 ..... N86-10735
N00014-83-C-0271 ..... N86-10345
N00014-83-K-0125 ..... N86-10898
N00014-83-K-0168 ..... N86-10431
N00014-83-K-0281 ..... N86-10833
N00014-83-K-0365 ..... N86-11142
N00014-83-K-0613 ..... N86-11061
N00014-84-C-0123 ..... N86-10590
N00014-84-C-0193 ..... N86-10918
N00014-84-C-0394 ..... N86-10727
N00014-84-C-0601 ..... N86-11078
N00014-84-K-0092 ..... N86-10795
N00014-84-K-0301 ..... N86-10885
N86-10886
N00014-84-K-0387 ..... N86-10982
N00014-84-K-0457 ..... N86-10420
N00014-85-F-0004 ..... N86-10295
N00014-85-K-0131 ..... N86-10870
N00014-85-K-0169 ..... N86-10862
N86-10864
N86-10869
RR0-1103 ..... N86-10295
RR0-3302 ..... N86-10714
RR0-4209 ..... N86-10870
STPA-82-96-006 ..... N86-10564
STPA-82-96006 ..... N86-10594
S14-40 ..... N86-10863
T99-QMXL N86-10983
USPN-HL-23374 ..... N86-10247
W-31-109-ENG-38 ..... N86-10322
N86-10443
N86-10635
N86-10659
N86-10676
N86-10871
N86-10934
N86-10941
N86-10942
N86-10952
N86-10961
N86-10979
N86-10991
N86-11036
N86-11052
N86-11056
W-7405-ENG-26 ..... N86-10985
W-7405-ENG-36 ..... N86-10194
N86-10349
N86-10356
N86-10358
N86-10469
N86-10529
N86-10660
N86-10663
N86-10835
N86-10837
N86-10839
N86-10841
N86-10927
N86-10929
N86-10930
N86-10932
N86-10943
N86-10944
N86-10950
N86-10963
N86-10986
N86-10987
N86-10988
N86-10990
N86-10992
N86-10993
N86-10996
N86-10998
N86-10999
N86-11001
N86-11002
N86-11003
N86-11006
N86-11027
N86-11028
N86-11029
N86-11031
N86-11034
W-7405-ENG-48 ..... N86-10296
N86-10317
N86-10318
N86-10323
N86-10359
N86-10409
N86-10445
N86-10466
N86-10467
N86-10468
N86-10470
N86-10471
N86-10532
N86-10632
N86-10717
N86-10718
N86-10737
N86-10907
N86-10908
N86-10956
N86-10959
N86-10984
N86-11016
N86-11017
N86-11030

	N86-11080
	N86-11134
W-7503-ENG-36	N86-10955
147-51-02-40-00	N86-10707
199-80-42	N86-10734
446-01-01-01-00	N86-10615
503-56-11	N86-11047
504-64-23	N86-10828
505-31-01	N86-10464
505-31-04	N86-10017
	N86-10461
505-33-1A	N86-10290
	N86-10311
505-33-53-03	N86-10913
505-33-78	N86-10579
505-34-13-32	N86-10848
505-35-31	N86-10048
505-40-90-01	N86-10016
505-43-01	N86-10015
506-53-1A	N86-10561
506-53-1B	N86-10552
506-53-23-05	N86-10581
506-54-21	N86-10274
506-55-22	N86-10279
	N86-10281
506-55-72	N86-11048
506-57-13-01	N86-10580
506-57-21	N86-10777
506-57-27-36	N86-10770
	N86-10785
	N86-10820
	N86-10821
	N86-10896
	N86-10897
506-58-22	N86-10380
	N86-10381
533-04-1A	N86-10589
776-33-41	N86-10582
776-52-41	N86-10643
778-36-05-01	N86-11083
	N86-11084
	N86-11085
	N86-11086
953-36-00-00-72	N86-10018
999-43-02	N86-10819

Typical Report Number Index Listing

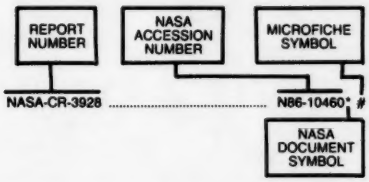

Listings in this index are arranged alphanumerically by report number. The NASA accession number denotes the number by which the citation is identified. An asterisk (*) indicates that the item is a NASA report. A pound sign (#) indicates that the item is available on microfiche.

ACSC-85-1130 ..... N86-10831 #
ACSC-85-1330 ..... N86-10040 #
ACSC-85-1670 ..... N86-10713 #
ACSC-85-1950 ..... N86-10034 #
ACSC-85-2630 ..... N86-10038 #
ACSC-85-2715 ..... N86-10199 #

AD-A145745 ..... N86-10007 #
AD-A147304 ..... N86-10001 #
AD-A154144 ..... N86-10585 #
AD-A155833 ..... N86-10342 #
AD-A156469 ..... N86-10914 #
AD-A156518 ..... N86-10034 #
AD-A156525 ..... N86-10861 #
AD-A156541 ..... N86-10898 #
AD-A156547 ..... N86-10035 #
AD-A156548 ..... N86-10791 #
AD-A156559 ..... N86-10419 #
AD-A156573 ..... N86-10403 #
AD-A156574 ..... N86-10590 #
AD-A156575 ..... N86-10420 #
AD-A156576 ..... N86-10727 #
AD-A156577 ..... N86-10553 #
AD-A156583 ..... N86-11142 #
AD-A156584 ..... N86-10343 #
AD-A156589 ..... N86-10191 #
AD-A156590 ..... N86-10735 #
AD-A156593 ..... N86-10951 #
AD-A156597 ..... N86-10786 #
AD-A156600 ..... N86-10862 #
AD-A156601 ..... N86-10465 #
AD-A156602 ..... N86-10036 #
AD-A156603 ..... N86-10037 #
AD-A156608 ..... N86-10428 #
AD-A156609 ..... N86-10429 #
AD-A156625 ..... N86-10863 #
AD-A156626 ..... N86-10864 #
AD-A156627 ..... N86-10190 #
AD-A156629 ..... N86-10430 #
AD-A156631 ..... N86-10779 #
AD-A156632 ..... N86-10916 #
AD-A156634 ..... N86-10793 #
AD-A156636 ..... N86-11049 #
AD-A156637 ..... N86-10523 #
AD-A156638 ..... N86-10431 #
AD-A156639 ..... N86-10591 #
AD-A156650 ..... N86-11078 #
AD-A156655 ..... N86-10865 #
AD-A156660 ..... N86-10712 #
AD-A156661 ..... N86-10354 #
AD-A156662 ..... N86-10404 #
AD-A156663 ..... N86-10866 #
AD-A156664 ..... N86-10592 #
AD-A156667 ..... N86-10829 #
AD-A156668 ..... N86-11071 #
AD-A156669 ..... N86-10563 #
AD-A156671 ..... N86-10344 #
AD-A156687 ..... N86-10790 #
AD-A156688 ..... N86-10038 #
AD-A156694 ..... N86-10708 #
AD-A156695 ..... N86-10713 #
AD-A156699 ..... N86-10432 #
AD-A156704 ..... N86-10917 #
AD-A156705 ..... N86-10977 #
AD-A156706 ..... N86-10541 #
AD-A156711 ..... N86-10867 #
AD-A156715 ..... N86-10885 #
AD-A156717 ..... N86-10728 #
AD-A156722 ..... N86-10794 #
AD-A156724 ..... N86-10294 #
AD-A156735 ..... N86-10630 #
AD-A156736 ..... N86-10714 #
AD-A156752 ..... N86-10345 #
AD-A156754 ..... N86-10886 #
AD-A156756 ..... N86-10887 #
AD-A156757 ..... N86-10346 #
AD-A156764 ..... N86-10315 #
AD-A156765 ..... N86-10729 #
AD-A156767 ..... N86-10795 #
AD-A156769 ..... N86-10849 #
AD-A156776 ..... N86-10291 #
AD-A156777 ..... N86-10850 #
AD-A156778 ..... N86-10593 #
AD-A156779 ..... N86-10830 #
AD-A156781 ..... N86-10199 #
AD-A156792 ..... N86-11065 #
AD-A156808 ..... N86-10039 #
AD-A156813 ..... N86-10295 #
AD-A156815 ..... N86-10675 #
AD-A156816 ..... N86-10868 #
AD-A156817 ..... N86-10899 #
AD-A156819 ..... N86-10831 #
AD-A156835 ..... N86-10869 #
AD-A156836 ..... N86-10433 #
AD-A156842 ..... N86-10040 #
AD-A156847 ..... N86-10796 #
AD-A156848 ..... N86-10797 #
AD-A156850 ..... N86-10405 #
AD-A156852 ..... N86-10524 #
AD-A156856 ..... N86-10832 #
AD-A156871 ..... N86-10041 #
AD-A156881 ..... N86-10276 #
AD-A156882 ..... N86-10557 #
AD-A156886 ..... N86-10406 #
AD-A156888 ..... N86-10918 #
AD-A156889 ..... N86-10292 #
AD-A156892 ..... N86-10919 #
AD-A156893 ..... N86-10006 #
AD-A156894 ..... N86-10982 #
AD-A156898 ..... N86-10542 #
AD-A156903 ..... N86-10798 #
AD-A156905 ..... N86-10900 #
AD-A156909 ..... N86-10347 #
AD-A156916 ..... N86-10983 #
AD-A156936 ..... N86-10833 #
AD-A156944 ..... N86-10269 #
AD-A156945 ..... N86-10407 #
AD-A156956 ..... N86-10275 #
AD-A156957 ..... N86-10434 #
AD-A156960 ..... N86-10042* #
AD-A156969 ..... N86-10787 #
AD-A156977 ..... N86-11079 #
AD-A156981 ..... N86-10715 #
AD-A156983 ..... N86-11050 #
AD-A156987 ..... N86-10771 #
AD-A156988 ..... N86-10788 #
AD-A156997 ..... N86-10283 #
AD-A157011 ..... N86-10870 #
AD-A157019 ..... N86-10730 #
AD-A157030 ..... N86-10924 #
AD-A157033 ..... N86-10925 #
AD-A157038 ..... N86-11061 #

AD-D011742 ..... N86-10792 #
AD-D011743 ..... N86-10198 #
AD-D011744 ..... N86-10421 #
AD-D011745 ..... N86-10422 #
AD-D011746 ..... N86-10554 #
AD-D011748 ..... N86-10313 #
AD-D011749 ..... N86-10314 #
AD-D011751 ..... N86-10423 #
AD-D011752 ..... N86-10555 #
AD-D011753 ..... N86-10556 #
AD-D011756 ..... N86-10778 #
AD-D011757 ..... N86-10424 #
AD-D011758 ..... N86-10915 #
AD-D011759 ..... N86-10425 #
AD-D011760 ..... N86-10426 #
AD-D011761 ..... N86-10427 #
AD-D011766 ..... N86-10371
AD-D011767 ..... N86-10480
AD-D011768 ..... N86-10372
AD-D011769 ..... N86-10674
AD-D011770 ..... N86-10642
AD-D011771 ..... N86-10799 #
AD-D011772 ..... N86-10316 #
AD-D011773 ..... N86-10800 #
AD-D011774 ..... N86-10972
AD-D011775 ..... N86-10536
AD-D011776 ..... N86-10973
AD-D011777 ..... N86-10906
AD-D011778 ..... N86-10032
AD-D011779 ..... N86-10974
AD-D011780 ..... N86-10338
AD-D011781 ..... N86-10414
AD-D011782 ..... N86-10282
AD-D011784 ..... N86-10277
AD-D011785 ..... N86-10481
AD-D011786 ..... N86-10373
AD-D011787 ..... N86-10289
AD-D011788 ..... N86-10374
AD-D011789 ..... N86-10482
AD-D011797 ..... N86-10355 #
AD-D011798 ..... N86-10435 #
AD-D011799 ..... N86-10436 #
AD-D011800 ..... N86-10558 #
AD-D011801 ..... N86-10020 #
AD-D011802 ..... N86-10525 #
AD-D011803 ..... N86-10437 #
AD-D011812 ..... N86-10375
AD-D011813 ..... N86-10415
AD-D011814 ..... N86-10537
AD-D011815 ..... N86-10416
AD-D011816 ..... N86-10975
AD-D011817 ..... N86-10376
AD-D011818 ..... N86-10538
AD-D011819 ..... N86-10483
AD-D011830 ..... N86-10976
AD-D011833 ..... N86-10417

AD-E301723 ..... N86-10040 #
AD-E301723 ..... N86-10405 #
AD-E301723 ..... N86-10433 #
AD-E301723 ..... N86-10796 #
AD-E301723 ..... N86-10797 #
AD-E301723 ..... N86-10869 #
AD-E301731 ..... N86-10524 #
AD-E401349 ..... N86-10354 #
AD-E440287 ..... N86-10866 #
AD-E500720 ..... N86-11071 #
AD-E500721 ..... N86-10829 #
AD-E750985 ..... N86-10407 #
AD-E900456 ..... N86-10712 #
AD-E900472 ..... N86-10592 #
AD-E900475 ..... N86-10404 #
AD-E950724 ..... N86-10283 #
AD-E950724 ..... N86-10715 #
AD-E950724 ..... N86-10771 #
AD-E950724 ..... N86-10787 #
AD-E950724 ..... N86-10788 #
AD-E950724 ..... N86-11050 #
AD-E950724 ..... N86-11079 #

AD-TR-85-39 ..... N86-10191 #

AEAS-2 ..... N86-10727 #

AEL-0125-SD ..... N86-10523 #

AFAMRL-TR-85-035 ..... N86-10675 #

AFESC/ESL-TR-85-10 ..... N86-10830 #

AFGL-TR-84-0322 ..... N86-10269 #

AFIT/CI/NR-85-35T ..... N86-10787 #
AFIT/CI/NR-85-37T ..... N86-10900 #

AFIT/CI/NR-85-40T ..... N86-10434 #
AFIT/CI/NR-85-46D ..... N86-10557 #
AFIT/CI/NR-85-50T ..... N86-10798 #
AFIT/CI/NR-85-51D ..... N86-10275 #
AFIT/CI/NR-85-52T ..... N86-10715 #

AFWAL-TR-84-4172 ..... N86-10916 #
AFWAL-TR-85-4002 ..... N86-10292 #

AFWL-TR-84-90 ..... N86-10042* #

AIAA-85-2011 ..... N86-10280* #
AIAA-85-2014 ..... N86-10279* #

AMMRC-TR-85-9 ..... N86-10315 #

AMTE(N)/R84009-PT-2 ..... N86-10553 #

ANL-HEP-CP-85-34 ..... N86-10934 #
ANL-HEP-CP-85-44 ..... N86-10942 #

ANL-85-7 ..... N86-10659 #

ANL/MCS-TM-50 ..... N86-10871 #

ARI-RP-84-21 ..... N86-11065 #

ARL/MAT-TM-388 ..... N86-10037 #

ARL/STRUC-TM-399 ..... N86-10036 #

ARL/SYS-R-29 ..... N86-10788 #

ARL/SYS-TM-75 ..... N86-10039 #

ARLCB-TR-85016 ..... N86-10866 #

ARLCD-TR-85009 ..... N86-10354 #

ARO-20679.1-MS-S ..... N86-10342 #

ARW-03-THE-BDK/ORS/83-06 ..... N86-11076 #
ARW-03-THE-BDK/ORS/83-08 ..... N86-10901 #

AS-701/85 ..... N86-10562 #

ASR-2 ..... N86-10589* #

BAE-AL/MAT/3864 ..... N86-10309

BAO-6 ..... N86-10723 #

BBC-RD-1985/8 ..... N86-10366

BDX-613-3266 ..... N86-10410 #
BDX-613-3268 ..... N86-10842 #

BI-76-39/08.7.23100-PT-1 ..... N86-10703
BI-76-39/08.7.23100-PT-2 ..... N86-10704

BLL-BISI-TRANS-21628-(9022.06) N86-10308
BLL-BISI-TRANS-23034-(9022.06) N86-10307
BLL-BISI-TRANS-23036-(9022.06) N86-10306

BLL-RISLEY-TR-5039-(9091.9F) N86-10546

BMFT-FB-T-85-020 ..... N86-10451 #
BMFT-FB-T-85-034 ..... N86-10449 #
BMFT-FB-T-85-046 ..... N86-10352 #
BMFT-FB-T-85-047 ..... N86-10353 #
BMFT-FB-T-85-049 ..... N86-10560 #
BMFT-FB-T-85-051-VOL-1 ..... N86-10670 #
BMFT-FB-T-85-052-VOL-2 ..... N86-10671 #

BN-1036 ..... N86-10862 #
BN-1037-PT-2 ..... N86-10869 #
BN-1038 ..... N86-10864 #

BNL-36414 ..... N86-10937 #
BNL-36450 ..... N86-10989 #
BNL-36486 ..... N86-10935 #
BNL-36490 ..... N86-10931 #
BNL-36495 ..... N86-11018 #
BNL-36497 ..... N86-10947 #
BNL-36546 ..... N86-10948 #
BNL-36559 ..... N86-11022 #
BNL-36564 ..... N86-11010 #
BNL-36566 ..... N86-11023 #
BNL-36572 ..... N86-10933 #
BNL-36573 ..... N86-11021 #
BNL-36577 ..... N86-10649 #
BNL-36671 ..... N86-10719 #
BNL-51865 ..... N86-10667 #
BNL-51875 ..... N86-10438 #

BR64172 ..... N86-10339

BR91279 ..... N86-10576
BR91991 ..... N86-10309
BR93962 ..... N86-10550
BR94518 ..... N86-10575

B8475856 ..... N86-10673 #
B8476135 ..... N86-10672 #
B8561677 ..... N86-10883 #
B8561680 ..... N86-11038 #
B8562445 ..... N86-10893 #
B8562446 ..... N86-10894 #
B8562871 ..... N86-10890 #
B8562872 ..... N86-10851 #
B8562873 ..... N86-10891 #
B8563351 ..... N86-10776
B8563352 ..... N86-10775
B8564052 ..... N86-10774 #

CEA-R-3276 ..... N86-10418* #

CERC-IR-85-2 ..... N86-10728 #

CMU-CS-85-115 ..... N86-10899 #

COMP-CENT-NOTE-14-PT-1 ..... N86-10888 #
COMP-CENT-NOTE-15-PT-2 ..... N86-10889 #
COMP-CENT-NOTE-17 ..... N86-10890 #
COMP-CENT-NOTE-18 ..... N86-10851 #
COMP-CENT-NOTE-20 ..... N86-10891 #

CONF-840817-3 ..... N86-10978 #
CONF-841231-5 ..... N86-10647 #
CONF-841231-7 ..... N86-10650 #
CONF-841231-10 ..... N86-10661 #
CONF-841231-17 ..... N86-10664 #
CONF-841231-20 ..... N86-10654 #
CONF-841231-21 ..... N86-10472 #
CONF-841231-22 ..... N86-10473 #
CONF-841231-23 ..... N86-10653 #
CONF-841267-1 ..... N86-10330 #
CONF-850103-10 ..... N86-10329 #
CONF-850137-4 ..... N86-10530 #
CONF-850169-13 ..... N86-10937 #
CONF-850175-1 ..... N86-10527 #
CONF-850211-10 ..... N86-10321 #
CONF-850211-12 ..... N86-10736 #
CONF-850266-6 ..... N86-10471 #
CONF-850286-1 ..... N86-11057 #
CONF-850310-104 ..... N86-11037 #
CONF-850310-109 ..... N86-10960 #
CONF-850310-110 ..... N86-10468 #
CONF-850310-112 ..... N86-11030 #
CONF-850315-2 ..... N86-10955 #
CONF-850375-1 ..... N86-10946 #
CONF-850375-4 ..... N86-11035 #
CONF-850375-5 ..... N86-11134 #
CONF-850410-47 ..... N86-10952 #
CONF-850421-01 ..... N86-10442 #
CONF-850421-10 ..... N86-10448 #
CONF-850473-3 ..... N86-10684 #
CONF-850484-1 ..... N86-10949 #
CONF-850504-30 ..... N86-10192 #
CONF-850504-48 ..... N86-10986 #
CONF-850504-53 ..... N86-10992 #
CONF-850504-54 ..... N86-10990 #
CONF-850504-56 ..... N86-10987 #
CONF-850504-60 ..... N86-10996 #
CONF-850504-61 ..... N86-10993 #
CONF-850504-62 ..... N86-10837 #
CONF-850504-67 ..... N86-11051 #
CONF-850504-69 ..... N86-10801 #
CONF-850504-70 ..... N86-11025 #
CONF-850504-72 ..... N86-11033 #
CONF-850504-75 ..... N86-10995 #
CONF-850504-77 ..... N86-10994 #
CONF-850504-79 ..... N86-10836 #
CONF-850504-83 ..... N86-11012 #
CONF-850504-87 ..... N86-11024 #
CONF-850504-98 ..... N86-10929 #
CONF-850504-99 ..... N86-11014 #
CONF-850504-108 ..... N86-11002 #
CONF-850504-109 ..... N86-11001 #
CONF-850504-110 ..... N86-11004 #
CONF-850504-113 ..... N86-10985 #
CONF-850504-117 ..... N86-10991 #
CONF-850504-118 ..... N86-10930 #
CONF-850504-134 ..... N86-10950 #
CONF-850504-135 ..... N86-10931 #
CONF-850504-142 ..... N86-10935 #
CONF-850504-144 ..... N86-10933 #
CONF-850504-145 ..... N86-11021 #
CONF-850504-146 ..... N86-11010 #
CONF-850504-147 ..... N86-11022 #
CONF-850504-150 ..... N86-11009 #
CONF-850504-157 ..... N86-11023 #
CONF-850504-160 ..... N86-11018 #

CONF-850504-170 ..... N86-10948 #
CONF-850504-172 ..... N86-10947 #
CONF-850504-175 ..... N86-10979 #
CONF-850504-177 ..... N86-10941 #
CONF-850504-190 ..... N86-10964 #
CONF-850507-40 ..... N86-10963 #
CONF-850533-5 ..... N86-10954 #
CONF-850533-9 ..... N86-10528 #
CONF-850560-5 ..... N86-10956 #
CONF-850577-1 ..... N86-10772 #
CONF-850579-3 ..... N86-10443 #
CONF-850581-3 ..... N86-10631 #
CONF-850604-6 ..... N86-10665 #
CONF-850610-30 ..... N86-10959 #
CONF-850612-2 ..... N86-10676 #
CONF-850612-4 ..... N86-10681 #
CONF-850612-5 ..... N86-10719 #
CONF-850616-1D ..... N86-10928 #
CONF-850616-18 ..... N86-10195 #
CONF-850616-30 ..... N86-11011 #
CONF-850616-35 ..... N86-11019 #
CONF-850616-38 ..... N86-10439 #
CONF-850616-44 ..... N86-10940 #
CONF-850616-46 ..... N86-10441 #
CONF-850617-1 ..... N86-10351 #
CONF-850706-1 ..... N86-10927 #
CONF-850706-9 ..... N86-10357 #
CONF-850706-21 ..... N86-10359 #
CONF-850711-7 ..... N86-11005 #
CONF-850717-1 ..... N86-10021 #
CONF-850723-2 ..... N86-10835 #
CONF-850726-1 ..... N86-10938 #
CONF-850736-2 ..... N86-11055 #
CONF-850736-4 ..... N86-10317 #
CONF-850736-6 ..... N86-11054 #
CONF-850736-14 ..... N86-10350 #
CONF-850736-19 ..... N86-10300 #
CONF-850745-8 ..... N86-10348 #
CONF-850753-2 ..... N86-10325 #
CONF-850759-1 ..... N86-10907 #
CONF-850759-2 ..... N86-10323 #
CONF-850759-3 ..... N86-10470 #
CONF-850801-7 ..... N86-10531 #
CONF-850801-24 ..... N86-10663 #
CONF-850808-3 ..... N86-11031 #
CONF-850809-19 ..... N86-10908 #
CONF-850809-29 ..... N86-11017 #
CONF-850810-3 ..... N86-11036 #
CONF-850810-6 ..... N86-10474 #
CONF-850823-3 ..... N86-10322 #
CONF-850830-2 ..... N86-10304 #
CONF-850840-2 ..... N86-10324 #
CONF-850840-3 ..... N86-10331 #
CONF-850864-1 ..... N86-11080 #
CONF-850884-1 ..... N86-10049 #
CONF-850885-1 ..... N86-10408 #
CONF-850885-2 ..... N86-10841 #
CONF-850887-4 ..... N86-10944 #
CONF-851043-1 ..... N86-10649 #
CONF-851048-2 ..... N86-10301 #
CONF-8406190 ..... N86-11008 #
CONF-8408121-4 ..... N86-11034 #
CONF-8408122-3 ..... N86-10717 #
CONF-8408122-5 ..... N86-10718 #
CONF-8410159-2 ..... N86-10466 #
CONF-8410159-2-REV-1 ..... N86-10467 #
CONF-8503137-1 ..... N86-10984 #
CONF-8504109-2 ..... N86-10662 #
CONF-8504115-4 ..... N86-11052 #
CONF-8504133-2 ..... N86-10989 #
CONF-8504136-1 ..... N86-10936 #
CONF-8504138-1 ..... N86-10296 #
CONF-8504151-1 ..... N86-10633 #
CONF-8504155-2 ..... N86-10942 #
CONF-8505100-2 ..... N86-11003 #
CONF-8505100-4 ..... N86-11028 #
CONF-8505100-5 ..... N86-10988 #
CONF-8505100-6 ..... N86-11016 #
CONF-8505100-11 ..... N86-10999 #
CONF-8505100-12 ..... N86-10998 #
CONF-8505100-14 ..... N86-11029 #
CONF-8505100-15 ..... N86-11027 #
CONF-8505103-3 ..... N86-10299 #
CONF-8505139-2 ..... N86-10319 #
CONF-8505145-1 ..... N86-10328 #
CONF-8505148-1 ..... N86-10678 #
CONF-8505149-1 ..... N86-10677 #
CONF-8505151-1 ..... N86-10297 #
CONF-8505171-1 ..... N86-10666 #
CONF-8506115-1 ..... N86-10526 #
CONF-8506118-1 ..... N86-10298 #
CONF-8506125-2 ..... N86-10932 #
CONF-8506125-3 ..... N86-11056 #
CONF-8506128-2 ..... N86-10349 #
CONF-8506131-1 ..... N86-10532 #
CONF-8506137-4 ..... N86-10737 #

CONF-8506146-1 ..... N86-10635 #

COO-1764-408 ..... N86-11062 #

CTH-MATH-1984-26 ..... N86-10902 #
CTH-MATH-1984-27 ..... N86-10872 #
CTH-MATH-1984-28 ..... N86-10873 #
CTH-MATH-1984-29 ..... N86-10874 #
CTH-MATH-1984-30 ..... N86-10875 #
CTH-MATH-1985-05 ..... N86-10876 #
CTH-MATH-1985-06 ..... N86-10877 #
CTH-MATH-1985-08 ..... N86-10903 #
CTH-MATH-1985-09 ..... N86-10904 #

CWI-CS-R8501 ..... N86-10884 #

D-82 ..... N86-10450 #

DE84-012185 ..... N86-10948 #
DE84-016822 ..... N86-10927 #
DE85-002941 ..... N86-10657 #
DE85-003914 ..... N86-10654 #
DE85-004086 ..... N86-11036 #
DE85-004089 ..... N86-10653 #
DE85-004444 ..... N86-11008 #
DE85-004796 ..... N86-10661 #
DE85-005244 ..... N86-10664 #
DE85-005357 ..... N86-10650 #
DE85-005366 ..... N86-10647 #
DE85-006762 ..... N86-10474 #
DE85-006879 ..... N86-10322 #
DE85-007046 ..... N86-10938 #
DE85-008026 ..... N86-10908 #
DE85-008228 ..... N86-10444 #
DE85-008696 ..... N86-10531 #
DE85-008721 ..... N86-10838 #
DE85-008804 ..... N86-10668 #
DE85-008821 ..... N86-10655 #
DE85-008960 ..... N86-11017 #
DE85-009105 ..... N86-10331 #
DE85-009408 ..... N86-10304 #
DE85-009437 ..... N86-10324 #
DE85-009438 ..... N86-11005 #
DE85-009440 ..... N86-10920 #
DE85-009443 ..... N86-10357 #
DE85-009562 ..... N86-10663 #
DE85-009575 ..... N86-10835 #
DE85-009622 ..... N86-11031 #
DE85-010020 ..... N86-10559 #
DE85-010068 ..... N86-10348 #
DE85-010278 ..... N86-10676 #
DE85-010302 ..... N86-10957 #
DE85-010583 ..... N86-10926 #
DE85-010738 ..... N86-10955 #
DE85-011363 ..... N86-10717 #
DE85-011449 ..... N86-10302 #
DE85-011450 ..... N86-10318 #
DE85-011474 ..... N86-10952 #
DE85-011477 ..... N86-10934 #
DE85-011572 ..... N86-10936 #
DE85-011599 ..... N86-10445 #
DE85-011603 ..... N86-10196 #
DE85-011607 ..... N86-10197 #
DE85-011709 ..... N86-10192 #
DE85-011745 ..... N86-10193 #
DE85-011820 ..... N86-10301 #
DE85-011843 ..... N86-11080 #
DE85-011846 ..... N86-10984 #
DE85-011906 ..... N86-10526 #
DE85-011957 ..... N86-10954 #
DE85-012032 ..... N86-10408 #
DE85-012033 ..... N86-10049 #
DE85-012078 ..... N86-10953 #
DE85-012090 ..... N86-11053 #
DE85-012122 ..... N86-11052 #
DE85-012131 ..... N86-10645 #
DE85-012144 ..... N86-10662 #
DE85-012184 ..... N86-10947 #
DE85-012298 ..... N86-10946 #
DE85-012326 ..... N86-10319 #
DE85-012352 ..... N86-11032 #
DE85-012368 ..... N86-10991 #
DE85-012390 ..... N86-10633. #
DE85-012392 ..... N86-11062 #
DE85-012419 ..... N86-10330 #
DE85-012425 ..... N86-10997 #
DE85-012441 ..... N86-10631 #
DE85-012460 ..... N86-10297 #
DE85-012483 ..... N86-10194 #
DE85-012523 ..... N86-10931 #
DE85-012526 ..... N86-10937 #
DE85-012527 ..... N86-10989 #
DE85-012572 ..... N86-11007 #
DE85-012592 ..... N86-11055 #
DE85-012648 ..... N86-10986 #
DE85-012657 ..... N86-10996 #
DE85-012658 ..... N86-10993 #
DE85-012659 ..... N86-10837 #
DE85-012660 ..... N86-10987 #
DE85-012661 ..... N86-10990 #
DE85-012662 ..... N86-10992 #
DE85-012673 ..... N86-10929 #
DE85-012680 ..... N86-11002 #
DE85-012681 ..... N86-11001 #
DE85-012691 ..... N86-10930 #
DE85-012709 ..... N86-10950 #
DE85-012723 ..... N86-10985 #
DE85-012735 ..... N86-11003 #
DE85-012740 ..... N86-10998 #
DE85-012741 ..... N86-11028 #
DE85-012742 ..... N86-10667 #
DE85-012744 ..... N86-10988 #
DE85-012758 ..... N86-10963 #
DE85-012764 ..... N86-11029 #
DE85-012767 ..... N86-10932 #
DE85-012770 ..... N86-11027 #
DE85-012771 ..... N86-10999 #
DE85-012776 ..... N86-10834 #
DE85-012811 ..... I-36-11013 #
DE85-012812 ..... N86-10195 #
DE85-012827 ..... N86-10298 #
DE85-012860 ..... N86-11011 #
DE85-012867 ..... N86-10928 #
DE85-012885 ..... N86-10328 #
DE85-012887 ..... N86-10329 #
DE85-012889 ..... N86-10960 #
DE85-012893 ..... N86-11037 #
DE85-012903 ..... N86-10677 #
DE85-012919 ..... N86-11016 #
DE85-012921 ..... N86-10467 #
DE85-012926 ..... N86-11134 #
DE85-012929 ..... N86-10956 #
DE85-012930 ..... N86-10296 #
DE85-012936 ..... N86-10466 #
DE85-012944 ..... N86-10471 #
DE85-012950 ..... N86-11030 #
DE85-012959 ..... N86-10468 #
DE85-012984 ..... N86-10438 #
DE85-012992 ..... N86-11006 #
DE85-013017 ..... N86-10945 #
DE85-013019 ..... N86-10939 #
DE85-013042 ..... N86-10527 #
DE85-013045 ..... N86-10299 #
DE85-013051 ..... N86-10995 #
DE85-013054 ..... N86-11014 #
DE85-013062 ..... N86-11004 #
DE85-013065 ..... N86-11015 #
DE85-013068 ..... N86-10836 #
DE85-013072 ..... N86-10994 #
DE85-013074 ..... N86-11012 #
DE85-013100 ..... N86-10648 #
DE85-013101 ..... N86-10646 #
DE85-013102 ..... N86-10731 #
DE85-013111 ..... N86-10678 #
DE85-013122 ..... N86-11063 #
DE85-013183 ..... N86-10409 #
DE85-013204 ..... N86-10532 #
DE85-013205 ..... N86-10959 #
DE85-013248 ..... N86-10634 #
DE85-013262 ..... N86-10716 #
DE85-013282 ..... N86-11023 #
DE85-013284 ..... N86-11018 #
DE85-013289 ..... N86-10649 #
DE85-013289 ..... N86-11026 #
DE85-013296 ..... N86-10935 #
DE85-013303 ..... N86-11022 #
DE85-013304 ..... N86-11010 #
DE85-013305 ..... N86-11021 #
DE85-013306 ..... N86-10933 #
DE85-013317 ..... N86-10962 #
DE85-013322 ..... N86-10842 #
DE85-013369 ..... N86-10801 #
DE85-013370 ..... N86-11025 #
DE85-013372 ..... N86-11035 #
DE85-013376 ..... N86-11009 #
DE85-013378 ..... N86-11051 #
DE85-013379 ..... N86-11033 #
DE85-013380 ..... N86-11024 #
DE85-013391 ..... N86-10528 #
DE85-013438 ..... N86-10439 #
DE85-013439 ..... N86-11019 #
DE85-013442 ..... N86-10644 #
DE85-013446 ..... N86-10684 #
DE85-013448 ..... N86-10440 #
DE85-013468 ..... N86-10681 #
DE85-013479 ..... N86-10718 #
DE85-013496 ..... N86-10666 #
DE85-013498 ..... N86-10772 #
DE85-013502 ..... N86-10683 #
DE85-013503 ..... N86-10680 #
DE85-013520 ..... N86-10958 #
DE85-013525 ..... N86-10840 #
DE85-013526 ..... N86-10679 #
DE85-013585 ..... N86-10312* #
DE85-013628 ..... N86-10448 #
DE85-013647 ..... N86-11020 #
DE85-013648 ..... N86-11000 #
DE85-013752 ..... N86-10940 #
DE85-013766 ..... N86-10832 #
DE85-013789 ..... N86-10865 #
DE85-013820 ..... N86-10907 #
DE85-013821 ..... N86-10317 #
DE85-013850 ..... N86-10979 #
DE85-013864 ..... N86-10443 #
DE85-013867 ..... N86-10941 #
DE85-013868 ..... N86-10961 #
DE85-013891 ..... N86-10835 #
DE85-013893 ..... N86-11056 #
DE85-013913 ..... N86-10446 #
DE85-013922 ..... N86-11057 #
DE85-013926 ..... N86-10978 #
DE85-013930 ..... N86-10472 #
DE85-013931 ..... N86-10473 #
DE85-013950 ..... N86-10021 #
DE85-013953 ..... N86-10351 #
DE85-013954 ..... N86-11054 #
DE85-013966 ..... N86-10441 #
DE85-013978 ..... N86-10323 #
DE85-013982 ..... N86-10359 #
DE85-014052 ..... N86-10447 #
DE85-014073 ..... N86-10942 #
DE85-014074 ..... N86-10944 #
DE85-014087 ..... N86-10349 #
DE85-014114 ..... N86-11034 #
DE85-014134 ..... N86-10841 #
DE85-014181 ..... N86-10737 #
DE85-014227 ..... N86-10719 #
DE85-014237 ..... N86-10843 #
DE85-014252 ..... N86-10356 #
DE85-014258 ..... N86-10943 #
DE85-014262 ..... N86-10660 #
DE85-014263 ..... N86-10656 #
DE85-014264 ..... N86-10469 #
DE85-014266 ..... N86-10839 #
DE85-014277 ..... N86-10303 #
DE85-014285 ..... N86-10965 #
DE85-014321 ..... N86-10966 #
DE85-014367 ..... N86-10964 #
DE85-014370 ..... N86-10871 #
DE85-014439 ..... N86-10543 #
DE85-014468 ..... N86-10350 #
DE85-014532 ..... N86-10321 #
DE85-014533 ..... N86-10442 #
DE85-014550 ..... N86-10659 #
DE85-014552 ..... N86-10652 #
DE85-014557 ..... N86-10470 #
DE85-014563 ..... N86-10325 #
DE85-014583 ..... N86-10682 #
DE85-014598 ..... N86-10410 #
DE85-014616 ..... N86-10736 #
DE85-014618 ..... N86-10530 #
DE85-014704 ..... N86-10300 #
DE85-014713 ..... N86-10658 #
DE85-014741 ..... N86-10651 #
DE85-014852 ..... N86-10326 #
DE85-014853 ..... N86-10327 #
DE85-015191 ..... N86-10529 #
DE85-015316 ..... N86-10358 #
DE85-0135637 ..... N86-10949 #

DFVLR-FB-83-36 ..... N86-10043 #
DFVLR-FB-84-44 ..... N86-10636 #
DFVLR-FB-85-14 ..... N86-10412 #
DFVLR-FB-85-15 ..... N86-10025 #
DFVLR-FB-85-16 ..... N86-10720 #
DFVLR-FB-85-17 ..... N86-10026 #
DFVLR-FB-85-18 ..... N86-10051 #
DFVLR-FB-85-19 ..... N86-10027 #
DFVLR-FB-85-20 ..... N86-10780 #
DFVLR-FB-85-21 ..... N86-10781 #
DFVLR-FB-85-22 ..... N86-10981 #
DFVLR-FB-85-23 ..... N86-10030 #
DFVLR-FB-85-24 ..... N86-10047 #
DFVLR-FB-85-25 ..... N86-10685 #
DFVLR-FB-85-26 ..... N86-10544 #

DFVLR-MITT-85-06 ..... N86-10031 #
DFVLR-MITT-85-07 ..... N86-10413 #
DFVLR-MITT-85-08 ..... N86-10721 #

DFVLR-WF2/8734 ..... N86-10273* #

DNA-TR-84-127 ..... N86-10405 #
DNA-TR-84-183 ..... N86-10524 #

DOE/AL-16338/T1 ..... N86-10559 #

DOE/BP-2 ..... N86-10656 #

DOE/CE-0109 ..... N86-10648 #
DOE/CE-0111 ..... N86-10646 #
DOE/CE-0114 ..... N86-10731 #
DOE/CE-0128 ..... N86-10658 #

DOE/CS-54209/22-VOL-2 ..... N86-11083* #
DOE/CS-54209/22-VOL-3 ..... N86-11084* #
DOE/CS-54209/22-VOL-4 ..... N86-11085* #
DOE/CS-54209/22-VOL-5 ..... N86-11086* #

DOE/ER-04073/18 ..... N86-10303 #
DOE/ER-06035/7 ..... N86-10966 #
DOE/ER-10870/156 ..... N86-10327 #
DOE/ER-13266/T1 ..... N86-10939 #
DOE/ER-13283/2 ..... N86-10834 #
DOE/ER-40105/T3 ..... N86-11062 #
DOE/ER-40561/1 ..... N86-10945 #
DOE/ER-45130/T1 ..... N86-10440 #
DOE/ER-45153/1 ..... N86-11053 #
DOE/ER-53157/T1 ..... N86-10543 #

DOE/ET-51013/135 ..... N86-11020 #
DOE/ET-51013/139 ..... N86-11000 #
DOE/ET-51017/T2 ..... N86-11032 #
DOE/ET-52023/34 ..... N86-10193 #
DOE/ET-53088/177 ..... N86-11063 #

DOE/EV-04814/T2 ..... N86-10957 #

DOE/FE-15078/6-1 ..... N86-10444 #
DOE/FE-60177/1883 ..... N86-10634 #

DOE/ID-12379/T2 ..... N86-10682 #

DOE/JPL/956205-85/8 ..... N86-10312* #

DOE/MC-20212/1850 ..... N86-10447 #

DOE/NASA/0167-9 ..... N86-11087* #
DOE/NASA/20320-66 ..... N86-10582* #
DOE/NASA/20485-20 ..... N86-10643* #

DOE/NBM-5013868 ..... N86-10961 #

DOE/OR-21444/T2-VOL-1 ..... N86-10683 #
DOE/OR-21444/T2-VOL-2 ..... N86-10680 #

DOE/TIC-3386-SUPPL-1 ..... N86-10838 #

DP-MS-85-29 ..... N86-10348 #
DP-MS-85-57 ..... N86-10319 #

DREO-TN-84-24 ..... N86-10276 #
DREO-TN-84-26 ..... N86-10786 #
DREO-TN-85-4 ..... N86-10294 #

DREV-4347/85 ..... N86-10419 #
DREV-4371/85 ..... N86-10865 #

DRIC-BR-94287-PT-1 ..... N86-10343 #
DRIC-BR-94556 ..... N86-10919 #
DRIC-BR-95198 ..... N86-10190 #
DRIC-BR-95691-PT-2 ..... N86-10553 #
DRIC-BR-95704 ..... N86-10793 #

DRL-175 ..... N86-10312* #

E-2573 ..... N86-10379* #
E-2576 ..... N86-10579* #
E-2649 ..... N86-10341* #
E-2650 ..... N86-10551* #
E-2651 ..... N86-10463* #
E-2676 ..... N86-10561* #
E-2679 ..... N86-10017* #
E-2684 ..... N86-10552* #
E-2685 ..... N86-10019* #
E-2695 ..... N86-10290* #
E-2700 ..... N86-10280* #
E-2703 ..... N86-10643* #
E-2709 ..... N86-10582* #
E-2710 ..... N86-10311* #
E-2725 ..... N86-10279* #
E-2726 ..... N86-11048* #
E-2737 ..... N86-10380* #
E-2738 ..... N86-10381* #
E-2744 ..... N86-10281* #

EEB-W-84-22 ..... N86-10978 #

EGG-M-08985 ..... N86-10954 #
EGG-M-27084 ..... N86-10530 #
EGG-M-27484 ..... N86-10736 #

EGG/10282-2055 ..... N86-10528 #

ENVIRON-SCI-DIV-2354 ..... N86-10679 #

EPA-600/D-85-083 ..... N86-10710 #
EPA-600/D-85-100 ..... N86-10687 #
EPA-600/D-85-106 ..... N86-10688 #
EPA-600/4-85-034 ..... N86-10689 #
EPA-600/9-85-015 ..... N86-10686 #

ER-83/08 ..... N86-10844 #
ER-83/09 ..... N86-10879 #
ER-83/10 ..... N86-10880 #

ERL-0323-TR ..... N86-10428 #

ESA-SP-209 ..... N86-10485 #
ESA-SP-222 ..... N86-10200 #
ESA-SP-226 ..... N86-11096 #

ESA-TT-852 ..... N86-10043 #
ESA-TT-871 ..... N86-10332 #
ESA-TT-899 ..... N86-10363 #

ESDU-AN-36B N86-10909

ESDU-BR-62636 ..... N86-10909

ETL-0371 ..... N86-10630 #

EUT-84-E-143 ..... N86-10802 #
EUT-84-E-144 ..... N86-10270 #
EUT-84-E-145 ..... N86-10803 #
EUT-85-E-146 ..... N86-10846 #
EUT-85-E-147 ..... N86-10804 #
EUT-85-E-148 ..... N86-10805 #

E85-10109 ..... N86-10597*
E85-10110 ..... N86-10610* #
E86-10002 ..... N86-10599* #

F+W-FO-1752 ..... N86-10050 #

FAA-AM-85-3 ..... N86-10771 #

FCR-6948P ..... N86-10651 #
FCR-6956P ..... N86-10652 #

FNAL-TM-1306 ..... N86-10997 #

FNAL/C-85/65 ..... N86-10946 #

FOA-A-30037-E ..... N86-10980 #

FOA-C-30386-E2 ..... N86-10411 #
FOA-C-40211-B4 ..... N86-10360 #

FOA-C5-85-0003-H2 ..... N86-11072 #
FOA-C5-85-0006-H2 ..... N86-10364 #

FTD-ID(RS)T-0910-84 ..... N86-10007 #
FTD-ID(RS)T-1120-84 ..... N86-10001 #

GA-A-17995 ..... N86-11007 #

GKSS-85-E-10 ..... N86-10722 #

GPO-43-778 ..... N86-10733 #

GRI-85/0064 ..... N86-10305 #

HEL-TM-3-85 ..... N86-10917 #

HL-85-21 ..... N86-10912* #

IA-UR-85-1620 ..... N86-10996 #

IDA-M-34 ..... N86-10829 #
IDA-M-83 ..... N86-11071 #

IDA/HQ-84-29295 ..... N86-10829 #
IDA/HQ-85-29861 ..... N86-11071 #

IFSR-177 ..... N86-11063 #

IKE-5-220 ..... N86-10476 #

ILR-MITT-143 ..... N86-11140 #

IPR-2 ..... N86-10014* #

ISBN-3-88383-107-7 ..... N86-10773 #
ISBN-90-6144-143-9 ..... N86-10802 #
ISBN-90-6144-144-7 ..... N86-10270 #
ISBN-90-6144-145-5 ..... N86-10803 #
ISBN-90-6144-146-3 ..... N86-10846 #
ISBN-90-6144-147-1 ..... N86-10804 #
ISBN-90-6144-148-X ..... N86-10805 #

ISI-V-4859-02 ..... N86-10006 #

ISPO-232 ..... N86-10953 #

ISSN-0167-9708 ..... N86-10270 #
ISSN-0167-9708 ..... N86-10802 #
ISSN-0167-9708 ..... N86-10803 #
ISSN-0167-9708 ..... N86-10804 #
ISSN-0167-9708 ..... N86-10805 #
ISSN-0167-9708 ..... N86-10846 #
ISSN-0168-8332 ..... N86-10732 #
ISSN-0171-1342 ..... N86-10025 #
ISSN-0171-1342 ..... N86-10026 #
ISSN-0171-1342 ..... N86-10027 #
ISSN-0171-1342 ..... N86-10030 #
ISSN-0171-1342 ..... N86-10047 #
ISSN-0171-1342 ..... N86-10051 #
ISSN-0171-1342 ..... N86-10412 #
ISSN-0171-1342 ..... N86-10544 #
ISSN-0171-1342 ..... N86-10636 #
ISSN-0171-1342 ..... N86-10685 #
ISSN-0171-1342 ..... N86-10720 #
ISSN-0171-1342 ..... N86-10780 #
ISSN-0171-1342 ..... N86-10781 #
ISSN-0171-1342 ..... N86-10981 #
ISSN-0173-6892 ..... N86-10476 #
ISSN-0176-7739 ..... N86-10031 #
ISSN-0176-7739 ..... N86-10413 #
ISSN-0176-7739 ..... N86-10721 #
ISSN-0281-0212 ..... N86-10980 #
ISSN-0309-099X ..... N86-11094 #
ISSN-0336-0885 ..... N86-10475 #
ISSN-0340-7608 ..... N86-10352 #
ISSN-0340-7608 ..... N86-10353 #
ISSN-0340-7608 ..... N86-10449 #
ISSN-0340-7608 ..... N86-10451 #
ISSN-0340-7608 ..... N86-10560 #
ISSN-0340-7608 ..... N86-10670 #
ISSN-0340-7608 ..... N86-10671 #
ISSN-0344-9629 ..... N86-10722 #
ISSN-0347-2124 ..... N86-10360 #
ISSN-0347-2809 ..... N86-10872 #
ISSN-0347-2809 ..... N86-10873 #
ISSN-0347-2809 ..... N86-10874 #
ISSN-0347-2809 ..... N86-10875 #
ISSN-0347-2809 ..... N86-10876 #
ISSN-0347-2809 ..... N86-10877 #
ISSN-0347-2809 ..... N86-10902 #
ISSN-0347-2809 ..... N86-10903 #
ISSN-0347-2809 ..... N86-10904 #
ISSN-0347-3708 ..... N86-10411 #
ISSN-0347-6405 ..... N86-10709 #
ISSN-0347-7665 ..... N86-10364 #
ISSN-0347-7665 ..... N86-11072 #
ISSN-0366-0885 ..... N86-10450 #
ISSN-0366-0885 ..... N86-10595 #
ISSN-0379-6566 ..... N86-10200 #
ISSN-0379-6566 ..... N86-10485 #
ISSN-0379-6566 ..... N86-11096 #
ISSN-0436-1199 ..... N86-10028 #
ISSN-0721-5320 ..... N86-10044 #

IZF-1984-19 ..... N86-10782 #
IZF-1984-27 ..... N86-11077 #
IZF-1984-32 ..... N86-10783 #
IZF-1984-34 ..... N86-10789 #

JPL-PUB-84-79-VOL-2 ..... N86-11083* #
JPL-PUB-84-79-VOL-3 ..... N86-11084* #
JPL-PUB-84-79-VOL-4 ..... N86-11085* #
JPL-PUB-84-79-VOL-5 ..... N86-11086* #
JPL-PUB-85-37 ..... N86-10707* #
JPL-PUB-85-39 ..... N86-10615* #
JPL-PUB-85-44 ..... N86-10599* #

JPL-5030-573-VOL-2 ..... N86-11083* #
JPL-5030-573-VOL-3 ..... N86-11084* #
JPL-5030-573-VOL-4 ..... N86-11085* #
JPL-5030-573-VOL-5 ..... N86-11086* #

JPRS-UBB-85-023 ..... N86-10738 #

JPRS-UCC-85-006 ..... N86-10809 #

JUEL-1968 ..... N86-10450 #
JUEL-1979 ..... N86-10595 #
JUEL-1985 ..... N86-10475 #

K/CSD/INF-85/4 ..... N86-10843 #

KGI-188 ..... N86-10709 #

KNMI-FM-85-6 ..... N86-10711

KNMI-167-VOL-2 ..... N86-10732 #

L-15960 ..... N86-10016* #

LA-TR-85-16 ..... N86-11006 #
LA-TR-85-21 ..... N86-10194 #
LA-TR-85-30 ..... N86-10358 #
LA-TR-85-31 ..... N86-10529 #

LA-UR-84-2753 ..... N86-10927 #
LA-UR-85-828 ..... N86-10835 #
LA-UR-85-934 ..... N86-10663 #
LA-UR-85-1035 ..... N86-11031 #
LA-UR-85-1450 ..... N86-10955 #
LA-UR-85-1528 ..... N86-10930 #
LA-UR-85-1585 ..... N86-11001 #
LA-UR-85-1586 ..... N86-11002 #
LA-UR-85-1615 ..... N86-10992 #
LA-UR-85-1616 ..... N86-10990 #
LA-UR-85-1618 ..... N86-10837 #
LA-UR-85-1619 ..... N86-10993 #
LA-UR-85-1632 ..... N86-10929 #
LA-UR-85-1640 ..... N86-10986 #
LA-UR-85-1651 ..... N86-10950 #
LA-UR-85-1737 ..... N86-10985 #
LA-UR-85-1789 ..... N86-10988 #
LA-UR-85-1791 ..... N86-10998 #
LA-UR-85-1818 ..... N86-11003 #
LA-UR-85-1820 ..... N86-10999 #
LA-UR-85-1821 ..... N86-11027 #
LA-UR-85-1829 ..... N86-10932 #
LA-UR-85-1837 ..... N86-11029 #
LA-UR-85-1923 ..... N86-10963 #
LA-UR-85-1933 ..... N86-10841 #
LA-UR-85-2073 ..... N86-11034 #
LA-UR-85-2195 ..... N86-10349 #
LA-UR-85-2265 ..... N86-10944 #
LA-UR-1790 ..... N86-11028 #

LA-74-85-1617 ..... N86-10987 #
LA-9703-REV ..... N86-10489 #
LA-10276 ..... N86-10356 #
LA-10326-ML ..... N86-10943 #
LA-10361-MS ..... N86-10839 #
LA-10364-MS ..... N86-10660 #

LARS-TR-042382 ..... N86-10610* #

LBF-S-173 ..... N86-10044 #

LBL-17284 ..... N86-10978 #
LBL-17550 ..... N86-10962 #
LBL-18001 ..... N86-10446 #
LBL-18571 ..... N86-11008 #
LBL-19139 ..... N86-11057 #
LBL-19218 ..... N86-10442 #
LBL-19695 ..... N86-10321 #

LC-64-60074 ..... N86-10923 #

LINO-119 ..... N86-10967 #
LINO-120 ..... N86-10968 #
LINO-121 ..... N86-10969 #
LINO-122 ..... N86-10452 #

LMSC/F035789 ..... N86-10345 #

MANPOWER-PLANNING-28 ..... N86-11073 #
MANPOWER-PLANNING-29 ..... N86-11074 #
MANPOWER-PLANNING-30 ..... N86-11075 #

MASA-TM-87088 ..... N86-10561* #

MCR-85-506-ADDN ..... N86-10340* #

MDR-21A-VOL-1/2 ..... N86-10433 #

MIT/BNL-84-4 ..... N86-10438 #

MIT/LCS/TM-276 ..... N86-10898 #

MPIS-16/1984 ..... N86-10028 #

MRC-R-815 ..... N86-10405 #

MRL-R-950-PT-2 ..... N86-10347 #

MSRR-517 ..... N86-10861 #

NAS 1.12/6:479 ..... N86-11137* #
NAS 1.15:58269 ..... N86-10018* #
NAS 1.15:77669 ..... N86-10179* #
NAS 1.15:77672 ..... N86-10378* #
NAS 1.15:77901 ..... N86-10611* #
NAS 1.15:77907 ..... N86-10293* #
NAS 1.15:77909 ..... N86-10612* #
NAS 1.15:77910 ..... N86-10613* #
NAS 1.15:77911 ..... N86-10614* #
NAS 1.15:77915 ..... N86-10418* #
NAS 1.15:77923 ..... N86-10273* #
NAS 1.15:86207 ..... N86-11138* #
NAS 1.15:86393 ..... N86-10580* #
NAS 1.15:86405 ..... N86-10016* #
NAS 1.15:86513 ..... N86-10278* #
NAS 1.15:86757 ..... N86-10464* #
NAS 1.15:86782 ..... N86-10015* #
NAS 1.15:86827 ..... N86-10048* #
NAS 1.15:86836 ..... N86-10734* #
NAS 1.15:86844 ..... N86-10777* #
NAS 1.15:87072 ..... N86-10379* #
NAS 1.15:87076 ..... N86-10463* #
NAS 1.15:87088 ..... N86-10561* #
NAS 1.15:87091 ..... N86-10017* #
NAS 1.15:87093 ..... N86-10019* #
NAS 1.15:87101 ..... N86-10290* #
NAS 1.15:87103 ..... N86-10280* #
NAS 1.15:87105 ..... N86-10341* #
NAS 1.15:87106 ..... N86-10643* #
NAS 1.15:87109 ..... N86-10582* #
NAS 1.15:87110 ..... N86-10311* #
NAS 1.15:87114 ..... N86-10551* #
NAS 1.15:87118 ..... N86-10279* #
NAS 1.15:87119 ..... N86-11048* #
NAS 1.15:87124 ..... N86-10380* #
NAS 1.15:87125 ..... N86-10381* #
NAS 1.15:87131 ..... N86-10281* #
NAS 1.15:87133 ..... N86-10552* #
NAS 1.15:87509 ..... N86-11141* #
NAS 1.15:87568 ..... N86-10053* #
NAS 1.15:87587 ..... N86-10828* #
NAS 1.15:87595 ..... N86-10581* #
NAS 1.15:87601 ..... N86-10913* #
NAS 1.21:7011(275) N86-10768*
NAS 1.26:3928 ..... N86-10460* #
NAS 1.26:171894 ..... N86-10610* #
NAS 1.26:171896 ..... N86-10770* #
NAS 1.26:171897 ..... N86-10896* #
NAS 1.26:171898 ..... N86-10820* #
NAS 1.26:171899 ..... N86-10897* #
NAS 1.26:171900 ..... N86-10821* #
NAS 1.26:171901 ..... N86-10785* #
NAS 1.26:174886 ..... N86-11087* #
NAS 1.26:174964 ..... N86-10461* #
NAS 1.26:174980 ..... N86-10589* #
NAS 1.26:176141 ..... N86-10377* #
NAS 1.26:176198 ..... N86-10707* #
NAS 1.26:176203 ..... N86-10382* #
NAS 1.26:176204 ..... N86-10615* #
NAS 1.26:176205 ..... N86-11083* #
NAS 1.26:176206 ..... N86-11084* #
NAS 1.26:176207 ..... N86-11085* #
NAS 1.26:176208 ..... N86-11086* #
NAS 1.26:176209 ..... N86-10312* #
NAS 1.26:176211 ..... N86-10599* #
NAS 1.26:176219 ..... N86-10860* #
NAS 1.26:176220 ..... N86-10588* #
NAS 1.26:176221 ..... N86-10822* #
NAS 1.26:176222 ..... N86-10823* #
NAS 1.26:176223 ..... N86-10824* #
NAS 1.26:176224 ..... N86-10825* #
NAS 1.26:176225 ..... N86-10826* #
NAS 1.26:176226 ..... N86-10827* #
NAS 1.26:176228 ..... N86-11047* #
NAS 1.26:176229 ..... N86-10912* #
NAS 1.26:176230 ..... N86-11060* #
NAS 1.26:176231 ..... N86-10033* #
NAS 1.26:176232 ..... N86-10271* #
NAS 1.26:176233 ..... N86-10272* #
NAS 1.26:176234 ..... N86-10577* #
NAS 1.26:176235 ..... N86-10539* #
NAS 1.26:176236 ..... N86-10578* #
NAS 1.26:176237 ..... N86-10014* #
NAS 1.26:176238 ..... N86-11059* #
NAS 1.26:176240 ..... N86-10540* #
NAS 1.26:176241 ..... N86-11139* #
NAS 1.26:176242 ..... N86-11133* #
NAS 1.26:176244 ..... N86-11095* #
NAS 1.26:176249 ..... N86-10484* #
NAS 1.26:176250 ..... N86-10042* #
NAS 1.26:176262 ..... N86-10310* #
NAS 1.26:176268 ..... N86-10597*
NAS 1.26:177334 ..... N86-10819* #
NAS 1.26:177368 ..... N86-10274* #
NAS 1.26:177967 ..... N86-10848* #
NAS 1.26:177972 ..... N86-11064* #
NAS 1.26:178480 ..... N86-10705* #
NAS 1.26:178484 ..... N86-10462* #
NAS 1.26:178495 ..... N86-10340* #
NAS 1.61:1150 ..... N86-10579* #

NASA ORDER C-86129D ..... N86-10120* #

NASA ORDER H-27954-B ..... N86-10106* #
NASA ORDER H-27954B ..... N86-10114* #
NASA ORDER H-27954B ..... N86-10115* #
NASA ORDER H-27954B ..... N86-10121* #
NASA ORDER H-27954B ..... N86-10131* #

NASA-CR-3928 ..... N86-10460* #
NASA-CR-171894 ..... N86-10610* #
NASA-CR-171896 ..... N86-10770* #
NASA-CR-171897 ..... N86-10896* #
NASA-CR-171898 ..... N86-10820* #
NASA-CR-171899 ..... N86-10897* #
NASA-CR-171900 ..... N86-10821* #
NASA-CR-171901 ..... N86-10785* #
NASA-CR-174886 ..... N86-11087* #
NASA-CR-174964 ..... N86-10461* #
NASA-CR-174980 ..... N86-10589* #
NASA-CR-176141 ..... N86-10377* #
NASA-CR-176198 ..... N86-10707* #
NASA-CR-176203 ..... N86-10382* #
NASA-CR-176204 ..... N86-10615* #
NASA-CR-176205 ..... N86-11083* #
NASA-CR-176206 ..... N86-11084* #
NASA-CR-176207 ..... N86-11085* #
NASA-CR-176208 ..... N86-11086* #
NASA-CR-176209 ..... N86-10312* #
NASA-CR-176211 ..... N86-10599* #
NASA-CR-176219 ..... N86-10860* #
NASA-CR-176220 ..... N86-10588* #
NASA-CR-176221 ..... N86-10822* #
NASA-CR-176222 ..... N86-10823* #
NASA-CR-176223 ..... N86-10824* #
NASA-CR-176224 ..... N86-10825* #
NASA-CR-176225 ..... N86-10826* #
NASA-CR-176226 ..... N86-10827* #
NASA-CR-176228 ..... N86-11047* #
NASA-CR-176229 ..... N86-10912* #
NASA-CR-176230 ..... N86-11060* #
NASA-CR-176231 ..... N86-10033* #
NASA-CR-176232 ..... N86-10271* #
NASA-CR-176233 ..... N86-10272* #
NASA-CR-176234 ..... N86-10577* #
NASA-CR-176235 ..... N86-10539* #
NASA-CR-176236 ..... N86-10578* #
NASA-CR-176237 ..... N86-10014* #
NASA-CR-176238 ..... N86-11059* #
NASA-CR-176240 ..... N86-10540* #
NASA-CR-176241 ..... N86-11139* #
NASA-CR-176242 ..... N86-11133* #
NASA-CR-176244 ..... N86-11095* #
NASA-CR-176249 ..... N86-10484* #
NASA-CR-176250 ..... N86-10042* #
NASA-CR-176262 ..... N86-10310* #
NASA-CR-176268 ..... N86-10597*
NASA-CR-177334 ..... N86-10819* #
NASA-CR-177368 ..... N86-10274* #
NASA-CR-177967 ..... N86-10848* #
NASA-CR-177972 ..... N86-11064* #
NASA-CR-178480 ..... N86-10705* #
NASA-CR-178484 ..... N86-10462* #
NASA-CR-178495 ..... N86-10340* #

NASA-RP-1150 ..... N86-10579* #

NASA-SP-479 ..... N86-11137* #
NASA-SP-7011(275) N86-10768*

NASA-TM-58269 ..... N86-10018* #
NASA-TM-77669 ..... N86-10179* #
NASA-TM-77672 ..... N86-10378* #
NASA-TM-77901 ..... N86-10611* #
NASA-TM-77907 ..... N86-10293* #
NASA-TM-77909 ..... N86-10612* #
NASA-TM-77910 ..... N86-10613* #
NASA-TM-77911 ..... N86-10614* #
NASA-TM-77915 ..... N86-10418* #
NASA-TM-77923 ..... N86-10273* #
NASA-TM-86207 ..... N86-11138* #
NASA-TM-86393 ..... N86-10580* #
NASA-TM-86405 ..... N86-10016* #
NASA-TM-86513 ..... N86-10278* #
NASA-TM-86757 ..... N86-10464* #
NASA-TM-86782 ..... N86-10015* #
NASA-TM-86827 ..... N86-10048* #
NASA-TM-86836 ..... N86-10734* #
NASA-TM-86844 ..... N86-10777* #
NASA-TM-87072 ..... N86-10379* #
NASA-TM-87076 ..... N86-10463* #
NASA-TM-87091 ..... N86-10017* #
NASA-TM-87093 ..... N86-10019* #
NASA-TM-87101 ..... N86-10290* #
NASA-TM-87103 ..... N86-10280* #
NASA-TM-87105 ..... N86-10341* #
NASA-TM-87106 ..... N86-10643* #
NASA-TM-87109 ..... N86-10582* #
NASA-TM-87110 ..... N86-10311* #
NASA-TM-87114 ..... N86-10551* #
NASA-TM-87118 ..... N86-10279* #
NASA-TM-87119 ..... N86-11048* #
NASA-TM-87124 ..... N86-10380* #

NASA-TM-87125 ..... N86-10381* #
NASA-TM-87131 ..... N86-10281* #
NASA-TM-87133 ..... N86-10552* #
NASA-TM-87509 ..... N86-11141* #
NASA-TM-87568 ..... N86-10053* #
NASA-TM-87587 ..... N86-10828* #
NASA-TM-87595 ..... N86-10581* #
NASA-TM-87601 ..... N86-10913* #

NBL-312 ..... N86-10953 #

NBS/NSRDS-3/11 ..... N86-10923 #

NBS/TN-1213 ..... N86-10847 #

NBSIR-84-2903 ..... N86-10453 #
NBSIR-85-3122 ..... N86-10302 #

NIKHEF-H/84-12 ..... N86-10882 #
NIKHEF-H/84-13 ..... N86-10883 #
NIKHEF-H/84-15 ..... N86-11038 #

NOTA-1535 ..... N86-10638 #

NRL-MR-5291 ..... N86-10714 #
NRL-MR-5573 ..... N86-10730 #
NRL-MR-5599 ..... N86-10406 #
NRL-MR-5613 ..... N86-10983 #
NRL-MR-5614 ..... N86-10924 #

NU-SML-TR-85-1 ..... N86-10593 #
NU-SML-TR-85-2 ..... N86-10346 #

NUSC-TR-7363 ..... N86-10863 #

NWC-TP-6488 ..... N86-10592 #
NWC-TP-6572 ..... N86-10712 #
NWC-TP-6636 ..... N86-10404 #

ONERA-NT-1983-7 ..... N86-10332 #

ONERA-RT-17/1841-RY-010-R ..... N86-10022 #

ORNL-6157 ..... N86-10926 #

ORNL/TM-9225 ..... N86-10679 #
ORNL/TM-9483 ..... N86-10840 #
ORNL/TM-9615 ..... N86-10958 #

OUEL-1534/84 ..... N86-10854 #

PB85-187110 ..... N86-11082 #
PB85-191625 ..... N86-10641 #
PB85-193027 ..... N86-10710 #
PB85-193530 ..... N86-10688 #
PB85-195345 ..... N86-10724 #
PB85-196418 ..... N86-10689 #
PB85-196988 ..... N86-10723 #
PB85-198356 ..... N86-10687 #
PB85-200004 ..... N86-10686 #
PB85-200178 ..... N86-10453 #
PB85-206068 ..... N86-10847 #
PB85-219632 ..... N86-10305 #

PERLAB-6 ..... N86-10870 #

PFC/RR-84-15 ..... N86-11020 #
PFC/RR-84-19 ..... N86-11000 #

PH-273 ..... N86-10366

PM/84/09 ..... N86-10706 #

PN-84/13 ..... N86-10858 #
PN-84/27 ..... N86-10859 #

PNL-SA-12423 ..... N86-10938 #
PNL-SA-12549 ..... N86-10684 #
PNL-SA-12698 ..... N86-10297 #
PNL-SA-12863 ..... N86-10527 #
PNL-SA-12888 ..... N86-10299 #
PNL-SA-12990 ..... N86-10631 #
PNL-SA-13032 ..... N86-10666 #
PNL-SA-13193 ..... N86-10772 #

PNL-5457 ..... N86-10326 #
PNL-5572 ..... N86-10597*

PR-1 ..... N86-10187 #
PR-2 ..... N86-10188 #
PR-3 ..... N86-10189 #

PRL-TR-55 ..... N86-10727 #

PSI-TR-451 ..... N86-10444 #

PUBL-335 ..... N86-10637 #

PV-43-954/F/2 ..... N86-10594 #
PV-43-954/F/3 ..... N86-10564 #

QPR-6 ..... N86-10339

RAE-TM-P-1030 ..... N86-10919 #

RAE-TR-84109-PT-1 ..... N86-10343 #
RAE-TR-85002 ..... N86-10190 #

RAI-84-AG-4 ..... N86-10705* #

RAND/R-3259-ARPA ..... N86-10542 #

REPT-MAT/720 ..... N86-10575

REPT-W-9/82 ..... N86-10596 #

REPT-1-68430-44(1985)01 ..... N86-10806 #
REPT-1-68430-44(1985)02 ..... N86-10807 #
REPT-2-84 ..... N86-10477 #
REPT-15 ..... N86-11094 #
REPT-26/5005/HF/AR ..... N86-10533 #
REPT-31-3725(9) ..... N86-11087* #
REPT-71-521-SA-1 ..... N86-11050 #
REPT-85B0346 ..... N86-11138* #
REPT-442-4 ..... N86-10779 #
REPT-0226-16 ..... N86-10912* #
REPT-85265 ..... N86-10464* #
REPT-85358 ..... N86-10015* #
REPT-85392 ..... N86-10048* #
REPT-85408 ..... N86-10734* #
REPT-85419 ..... N86-10777* #
REPT-051560-28(1984)08 ..... N86-10808 #

RES-PAPER-670 ..... N86-10550

RFP-3848 ..... N86-10325 #

RHO-BW-SA-435P ..... N86-10633 #

RSRE-MEMO-3806 ..... N86-10793 #

S-549 ..... N86-10018* #

SAIC-84/1104 ..... N86-10524 #

SAND-84-1098 ..... N86-10644 #
SAND-84-1775C ..... N86-10665 #
SAND-84-2342C ..... N86-10351 #
SAND-84-2395C ..... N86-10195 #
SAND-84-2434C ..... N86-10928 #
SAND-84-2498C ..... N86-11013 #
SAND-84-2500C ..... N86-10940 #
SAND-84-2530 ..... N86-10716 #
SAND-84-2544C ..... N86-10439 #
SAND-84-2576C ..... N86-11019 #
SAND-84-2670C ..... N86-10021 #
SAND-84-18440 ..... N86-10357 #
SAND-85-0042C ..... N86-10192 #
SAND-85-0063C ..... N86-10049 #
SAND-85-0098C ..... N86-10324 #
SAND-85-0148C ..... N86-11055 #
SAND-85-0149C ..... N86-11054 #
SAND-85-0171C ..... N86-10474 #
SAND-85-0200C ..... N86-10408 #
SAND-85-0258C ..... N86-10304 #
SAND-85-0262C ..... N86-10331 #
SAND-85-0459C ..... N86-11005 #
SAND-85-0554C ..... N86-10350 #
SAND-85-0721C ..... N86-10300 #
SAND-85-0841C ..... N86-10920 #
SAND-85-02980 ..... N86-10298 #
SAND-85-71960 ..... N86-10301 #
SAND-8402519C ..... N86-11011 #

SAPR-2 ..... N86-11060* #
SAPR-9 ..... N86-11087* #

SD-TR-85-12 ..... N86-10708 #

SERI/PR-255-2493 ..... N86-10645 #

SERI/SP-271-2511 ..... N86-10657 #

SERI/STR-211-2637 ..... N86-10668 #
SERI/STR-211-2687 ..... N86-10655 #

SERI/TP-212-2749 ..... N86-10662 #

SJ70 ..... N86-10576

SNIAS-443.501/85 ..... N86-10023 #
SNIAS-443.501/85 ..... N86-10024 #

SNIAS-443.529/84 ..... N86-10024 #

SR-2 ..... N86-10269 #

SS-45 ..... N86-10672 #
SS-45A ..... N86-10673 #

SSL-17-85 ..... N86-10271* #

SU-SLAC-CN-303 ..... N86-10965 #

SU-SLAC-PUB-3583 ..... N86-11025 #
SU-SLAC-PUB-3599 ..... N86-11009 #
SU-SLAC-PUB-3600 ..... N86-11015 #
SU-SLAC-PUB-3616 ..... N86-11004 #
SU-SLAC-PUB-3617 ..... N86-11051 #
SU-SLAC-PUB-3637 ..... N86-11033 #
SU-SLAC-PUB-3638 ..... N86-10801 #
SU-SLAC-PUB-3649 ..... N86-11014 #
SU-SLAC-PUB-3651 ..... N86-11024 #
SU-SLAC-PUB-3654 ..... N86-10964 #
SU-SLAC-PUB-3660 ..... N86-10995 #
SU-SLAC-PUB-3667 ..... N86-10836 #
SU-SLAC-PUB-3671 ..... N86-11012 #
SU-SLAC-PUB-3675 ..... N86-10994 #
SU-SLAC-PUB-3684 ..... N86-11035 #

SWRI-7576/30 ..... N86-10589* #

TAE-536 ..... N86-10583 #
TAE-537 ..... N86-10584 #

TDA-PR-42-82 ..... N86-10382* #

TDCK-79518 ..... N86-10782 #
TDCK-79524 ..... N86-11077 #
TDCK-79698 ..... N86-10783 #
TDCK-79782 ..... N86-10789 #

TDWR/R-288-VOL-4 ..... N86-10641 #

TEST-9 ..... N86-10354 #

THE-RC-51408-PT-1 ..... N86-10888 #
THE-RC-52082-PT-2 ..... N86-10889 #

TMS-PAPER-F8415 ..... N86-10310* #

TN-84-7104-925-46 ..... N86-10819* #

TOP-6-2-335 ..... N86-10563 #

TPR-20 ..... N86-10651 #
TPR-21 ..... N86-10652 #

TR-2-85 ..... N86-10918 #
TR-11 ..... N86-10283 #
TR-18 ..... N86-10541 #
TR-19 ..... N86-10465 #
TR-20 ..... N86-10977 #
TR-0084A(5940-05)-6 ..... N86-10708 #

TW-264 ..... N86-10881 #

UCID-20437 ..... N86-10409 #

UCLA-ENG-85-20 ..... N86-10591 #

UCRI-92523 ..... N86-10717 #

UCRL-TRANS-12061 ..... N86-10318 #

UCRL-15640 ..... N86-10468 #
UCRL-53594 ..... N86-10632 #
UCRL-91078-REV-1 ..... N86-10467 #
UCRL-91078-2 ..... N86-10466 #
UCRL-91359 ..... N86-10718 #
UCRL-91482 ..... N86-10359 #
UCRL-91642 ..... N86-10471 #
UCRL-91885 ..... N86-10959 #
UCRL-91892 ..... N86-10323 #
UCRL-91953 ..... N86-11030 #
UCRL-92121 ..... N86-10907 #
UCRL-92161 ..... N86-10908 #
UCRL-92204 ..... N86-10317 #
UCRL-92246 ..... N86-11017 #
UCRL-92525 ..... N86-11080 #
UCRL-92538 ..... N86-10984 #
UCRL-92648 ..... N86-10532 #
UCRL-92690 ..... N86-11016 #
UCRL-92713 ..... N86-10956 #
UCRL-92724 ..... N86-11134 #
UCRL-92731 ..... N86-10296 #
UCRL-92834 ..... N86-10737 #
UCRL-92895 ..... N86-10470 #

UMD-DMSS-85/5 ..... N86-10885 #
UMD-DMSS-85/6 ..... N86-10886 #

UROCHESTER/DC/85/TR-68 ..... N86-10925 #

US-PATENT-APPL-SN-143399 ..... N86-10417
US-PATENT-APPL-SN-329558 ..... N86-10374
US-PATENT-APPL-SN-343032 ..... N86-10338
US-PATENT-APPL-SN-347391 ..... N86-10674
US-PATENT-APPL-SN-347749 ..... N86-10371
US-PATENT-APPL-SN-361016 ..... N86-10481
US-PATENT-APPL-SN-377107 ..... N86-10376
US-PATENT-APPL-SN-387133 ..... N86-10975
US-PATENT-APPL-SN-388327 ..... N86-10373
US-PATENT-APPL-SN-388574 ..... N86-10972
US-PATENT-APPL-SN-403246 ..... N86-10906
US-PATENT-APPL-SN-403247 ..... N86-10973
US-PATENT-APPL-SN-415839 ..... N86-10538
US-PATENT-APPL-SN-420209 ..... N86-10375
US-PATENT-APPL-SN-421766 ..... N86-10416
US-PATENT-APPL-SN-431434 ..... N86-10642
US-PATENT-APPL-SN-431866 ..... N86-10480
US-PATENT-APPL-SN-442496 ..... N86-10482
US-PATENT-APPL-SN-442497 ..... N86-10976
US-PATENT-APPL-SN-452601 ..... N86-10536
US-PATENT-APPL-SN-455362 ..... N86-10282
US-PATENT-APPL-SN-471550 ..... N86-10372
US-PATENT-APPL-SN-486477 ..... N86-10974
US-PATENT-APPL-SN-486603 ..... N86-10032
US-PATENT-APPL-SN-500725 ..... N86-10537
US-PATENT-APPL-SN-505569 ..... N86-10415
US-PATENT-APPL-SN-529412 ..... N86-10414
US-PATENT-APPL-SN-577391 ..... N86-10277
US-PATENT-APPL-SN-591715 ..... N86-10355 #
US-PATENT-APPL-SN-617049 ..... N86-10483
US-PATENT-APPL-SN-637238 ..... N86-10198 #
US-PATENT-APPL-SN-640623 ..... N86-10556 #
US-PATENT-APPL-SN-643140 ..... N86-10289
US-PATENT-APPL-SN-655486 ..... N86-10445 #
US-PATENT-APPL-SN-655490 ..... N86-10196 #
US-PATENT-APPL-SN-655593 ..... N86-10197 #
US-PATENT-APPL-SN-677136 ..... N86-10792 #
US-PATENT-APPL-SN-693927 ..... N86-10778 #
US-PATENT-APPL-SN-708909 ..... N86-10437 #
US-PATENT-APPL-SN-715992 ..... N86-10421 #
US-PATENT-APPL-SN-717365 ..... N86-10422 #
US-PATENT-APPL-SN-718399 ..... N86-10554 #
US-PATENT-APPL-SN-718762 ..... N86-10555 #
US-PATENT-APPL-SN-719792 ..... N86-10435 #
US-PATENT-APPL-SN-722579 ..... N86-10313 #
US-PATENT-APPL-SN-726872 ..... N86-10424 #
US-PATENT-APPL-SN-727507 ..... N86-10915 #
US-PATENT-APPL-SN-729849 ..... N86-10314 #
US-PATENT-APPL-SN-731223 ..... N86-10436 #
US-PATENT-APPL-SN-732330 ..... N86-10423 #
US-PATENT-APPL-SN-738817 ..... N86-10426 #
US-PATENT-APPL-SN-739413 ..... N86-10425 #
US-PATENT-APPL-SN-741644 ..... N86-10800 #
US-PATENT-APPL-SN-742825 ..... N86-10427 #
US-PATENT-APPL-SN-743853 ..... N86-10799 #
US-PATENT-APPL-SN-744593 ..... N86-10316 #
US-PATENT-APPL-SN-746617 ..... N86-10558 #
US-PATENT-APPL-SN-749333 ..... N86-10020 #
US-PATENT-APPL-SN-749335 ..... N86-10525 #

US-PATENT-CLASS-17.2-PC N86-10376
US-PATENT-CLASS-118-724 ..... N86-10537
US-PATENT-CLASS-250-370 ..... N86-10480
US-PATENT-CLASS-310-323 ..... N86-10483
US-PATENT-CLASS-324-72 ..... N86-10976
US-PATENT-CLASS-324-433 ..... N86-10642
US-PATENT-CLASS-332-16R N86-10415
US-PATENT-CLASS-343-17.2PC N86-10375
US-PATENT-CLASS-343-17.2PC N86-10417
US-PATENT-CLASS-343-18 ..... N86-10371
US-PATENT-CLASS-343-372 ..... N86-10372
US-PATENT-CLASS-343-872 ..... N86-10032
US-PATENT-CLASS-350-162.13 ..... N86-10975
US-PATENT-CLASS-350-388 ..... N86-10972
US-PATENT-CLASS-350-403 ..... N86-10536
US-PATENT-CLASS-351-243 ..... N86-10973
US-PATENT-CLASS-356-437 ..... N86-10674
US-PATENT-CLASS-357-55 ..... N86-10416
US-PATENT-CLASS-358-88 ..... N86-10481
US-PATENT-CLASS-358-93 ..... N86-10482
US-PATENT-CLASS-361-58 ..... N86-10414
US-PATENT-CLASS-369-37 ..... N86-10974
US-PATENT-CLASS-372-45 ..... N86-10538
US-PATENT-CLASS-375-120 ..... N86-10374
US-PATENT-CLASS-382-1 ..... N86-10906
US-PATENT-CLASS-428-107 ..... N86-10289
US-PATENT-CLASS-455-67 ..... N86-10373
US-PATENT-CLASS-528-35 ..... N86-10338
US-PATENT-CLASS-568-923 ..... N86-10282

US-PATENT-4,505,544 ..... N86-10975
US-PATENT-4,506,234 ..... N86-10415
US-PATENT-4,508,055 ..... N86-10537
US-PATENT-4,508,929 ..... N86-10282
US-PATENT-4,509,051 ..... N86-10375
US-PATENT-4,510,377 ..... N86-10277
US-PATENT-4,510,525 ..... N86-10481
US-PATENT-4,510,622 ..... N86-10373
US-PATENT-4,511,219 ..... N86-10972
US-PATENT-4,511,220 ..... N86-10536
US-PATENT-4,511,228 ..... N86-10973
US-PATENT-4,513,308 ..... N86-10416
US-PATENT-4,513,429 ..... N86-10374
US-PATENT-4,514,758 ..... N86-10482
US-PATENT-4,515,847 ..... N86-10289
US-PATENT-4,516,858 ..... N86-10674
US-PATENT-4,517,464 ..... N86-10480
US-PATENT-4,517,517 ..... N86-10642
US-PATENT-4,517,568 ..... N86-10371
US-PATENT-4,517,570 ..... N86-10372
US-PATENT-4,517,618 ..... N86-10414
US-PATENT-4,518,759 ..... N86-10338
US-PATENT-4,519,055 ..... N86-10974
US-PATENT-4,520,364 ..... N86-10032
US-PATENT-4,520,504 ..... N86-10906
US-PATENT-4,521,779 ..... N86-10417
US-PATENT-4,521,887 ..... N86-10538
US-PATENT-4,523,120 ..... N86-10483
US-PATENT-4,524,322 ..... N86-10976
US-PATENT-4,524,362 ..... N86-10376

USAAVSCOM-TR-85-C-12 ..... N86-10017* #
USAAVSCOM-TR-85-C-15 ..... N86-10463* #

USGS/WRI/84-4369 ..... N86-10830 #

UVA/5-28230 ..... N86-11060* #
UVA/528230/MS86/101 ..... N86-11059* #

VTH-LR-360-PT-1 ..... N86-10045 #

WP-29-84-85 ..... N86-10861 #

WSRL-0383-TR ..... N86-10430 #
WSRL-0389-TM ..... N86-10403 #

Y/DV-404-REV-1 ..... N86-10330 #

YALEU/DCS/RR-370 ..... N86-10795 #
YALEU/DCS/RR-381 ..... N86-10794 #
YALEU/DCS/RR-389 ..... N86-10850 #
YALEU/DCS/RR-396 ..... N86-10868 #
YALEU/DCS/RR-397 ..... N86-10867 #
YALEU/DCS/RR-398 ..... N86-10887 #
YALEU/DCS/RR-399 ..... N86-10833 #

ZW-8414 ..... N86-10905 #
ZW-8415 ..... N86-10892 #

☆ U.S. GOVERNMENT PRINTING OFFICE: 1985-491-573/20024

FEDERAL DEPOSITORY LIBRARY PROGRAM

The Federal Depository Library Program provides Government publications to designated libraries throughout the United States. The Regional Depository Libraries listed below receive and retain at least one copy of nearly every Federal Government publication, either in printed or microfilm form, for use by the general public. These libraries provide reference services and inter-library loans; however, they are *not* sales outlets. You may wish to ask your local library to contact a Regional Depository to help you locate specific publications, or you may contact the Regional Depository yourself.

ARKANSAS STATE LIBRARY
One Capitol Mall
Little Rock, AR 72201
(501) 371-2326

AUBURN UNIV. AT MONTGOMERY LIBRARY
Documents Department
Montgomery, AL 36193
(205) 279-9110, ext. 253

UNIV. OF ALABAMA LIBRARY
Documents Dept.—Box S
University, AL 35486
(205) 348-7369

DEPT. OF LIBRARY, ARCHIVES AND PUBLIC RECORDS
Third Floor—State Cap.
1700 West Washington
Phoenix, AZ 85007
(602) 255-4121

UNIVERSITY OF ARIZONA LIB.
Government Documents Dept.
Tucson, AZ 85721
(602) 626-5233

CALIFORNIA STATE LIBRARY
Govt. Publications Section
P.O. Box 2037
Sacramento, CA 95809
(916) 322-4572

UNIV. OF COLORADO LIB.
Government Pub. Division
Campus Box 184
Boulder, CO 80309
(303) 492-8834

DENVER PUBLIC LIBRARY
Govt. Pub. Department
1357 Broadway
Denver, CO 80203
(303) 571-2131

CONNECTICUT STATE LIBRARY
Government Documents Unit
231 Capitol Avenue
Hartford, CT 06106
(203) 566-4971

UNIV. OF FLORIDA LIBRARIES
Library West
Documents Department
Gainesville, FL 32611
(904) 392-0367

UNIV. OF GEORGIA LIBRARIES
Government Reference Dept.
Athens, Ga 30602
(404) 542-8951

UNIV. OF HAWAII LIBRARY
Govt. Documents Collection
2550 The Mall
Honolulu, HI 96822
(808) 948-8230

UNIV. OF IDAHO LIBRARY
Documents Section
Moscow, ID 83843
(208) 885-6344

ILLINOIS STATE LIBRARY
Information Services Branch
Centennial Building
Springfield, IL 62706
(217) 782-5185

INDIANA STATE LIBRARY
Serials Documents Section
140 North Senate Avenue
Indianapolis, IN 46204
(317) 232-3686

UNIV. OF IOWA LIBRARIES
Govt. Documents Department
Iowa City, IA 52242
(319) 353-3318

UNIVERSITY OF KANSAS
Doc. Collect—Spencer Lib.
Lawrence, KS 66045
(913) 864-4662

UNIV. OF KENTUCKY LIBRARIES
Govt. Pub. Department
Lexington, KY 40506
(606) 257-3139

LOUISIANA STATE UNIVERSITY
Middleton Library
Govt. Docs. Dept.
Baton Rouge, LA 70803
(504) 388-2570

LOUISIANA TECHNICAL UNIV. LIBRARY
Documents Department
Ruston, LA 71272
(318) 257-4962

UNIVERSITY OF MAINE
Raymond H. Fogler Library
Tri-State Regional Documents Depository
Orono, ME 04469
(207) 581-1680

UNIVERSITY OF MARYLAND
McKeldin Lib.—Doc. Div.
College Park, MD 20742
(301) 454-3034

BOSTON PUBLIC LIBRARY
Government Docs. Dept.
Boston, MA 02117
(617) 536-5400 ext. 226

DETROIT PUBLIC LIBRARY
Sociology Department
5201 Woodward Avenue
Detroit, MI 48202
(313) 833-1409

MICHIGAN STATE LIBRARY
P.O. Box 30007
Lansing, MI 48909
(517) 373-0640

UNIVERSITY OF MINNESOTA
Government Pubs. Division
409 Wilson Library
309 19th Avenue South
Minneapolis, MN 55455
(612) 373-7813

UNIV. OF MISSISSIPPI LIB.
Documents Department
University, MS 38677
(601) 232-5857

UNIV. OF MONTANA
Mansfield Library
Documents Division
Missoula, MT 59812
(406) 243-6700

NEBRASKA LIBRARY COMM.
Federal Documents
1420 P Street
Lincoln, NE 68508
(402) 471-2045
In cooperation with University of Nebraska-Lincoln

UNIVERSITY OF NEVADA LIB.
Govt. Pub. Department
Reno, NV 89557
(702) 784-6579

NEWARK PUBLIC LIBRARY
5 Washington Street
Newark, NJ 07101
(201) 733-7812

UNIVERSITY OF NEW MEXICO
Zimmerman Library
Government Pub. Dept.
Albuquerque, NM 87131
(505) 277-5441

NEW MEXICO STATE LIBRARY
Reference Department
325 Don Gaspar Avenue
Santa Fe, NM 87501
(505) 827-2033, ext. 22

NEW YORK STATE LIBRARY
Empire State Plaza
Albany, NY 12230
(518) 474-5563

UNIVERSITY OF NORTH CAROLINA AT CHAPEL HILL
Wilson Library
BA/SS Documents Division
Chapel Hill, NC 27515
(919) 962-1321

UNIVERSITY OF NORTH DAKOTA
Chester Fritz Library
Documents Department
Grand Forks, ND 58202
(701) 777-2617, ext. 27
(In cooperation with North Dakota State Univ. Library)

STATE LIBRARY OF OHIO
Documents Department
65 South Front Street
Columbus, OH 43215
(614) 462-7051

OKLAHOMA DEPT. OF LIB.
Government Documents
200 NE 18th Street
Oklahoma City, OK 73105
(405) 521-2502

OKLAHOMA STATE UNIV. LIB.
Documents Department
Stillwater, OK 74078
(405) 624-6546

PORTLAND STATE UNIV. LIB.
Documents Department
P.O. Box 1151
Portland, OR 97207
(503) 229-3673

STATE LIBRARY OF PENN.
Government Pub. Section
P.O. Box 1601
Harrisburg, PA 17105
(717) 787-3752

TEXAS STATE LIBRARY
Public Services Department
P.O. Box 12927—Cap. Sta.
Austin, TX 78753
(512) 471-2996

TEXAS TECH UNIV. LIBRARY
Govt. Documents Department
Lubbock, TX 79409
(806) 742-2268

UTAH STATE UNIVERSITY
Merrill Library, U.M.C. 30
Logan, UT 84322
(801) 750-2682

UNIVERSITY OF VIRGINIA
Alderman Lib.—Public Doc.
Charlottesville, VA 22901
(804) 924-3133

WASHINGTON STATE LIBRARY
Documents Section
Olympia, WA 98504
(206) 753-4027

WEST VIRGINIA UNIV. LIB.
Documents Department
Morgantown, WV 26506
(304) 293-3640

MILWAUKEE PUBLIC LIBRARY
814 West Wisconsin Avenue
Milwaukee, WI 53233
(414) 278-3000

ST. HIST LIB. OF WISCONSIN
Government Pub. Section
816 State Street
Madison, WI 53706
(608) 262-4347

WYOMING STATE LIBRARY
Supreme Ct. & Library Bld.
Cheyenne, WY 82002
(307) 777-6344

National Aeronautics and
Space Administration
Code NIT-4
Washington, D.C.
20546

Official Business

Penalty for Private Use, $300

SPECIAL FOURTH-CLASS RATE
POSTAGE & FEES PAID
NASA
WASHINGTON, D.C.
PERMIT No. G 27

NASA

POSTMASTER: If Undeliverable (Section 158
Postal Manual) Do Not Return